Current Clinical Urology
Series Editor: Eric A. Klein

Thomas J. Polascik *Editor*

Imaging and Focal Therapy of Early Prostate Cancer

Second Edition

Springer

Current Clinical Urology

Eric A. Klein, MD, Series Editor
Professor of Surgery
Cleveland Clinic Lerner College of Medicine
Section of Urologic Oncology
Glickman Urological and Kidney Institute
Cleveland, OH

More information about this series at http://www.springer.com/series/7635

Thomas J. Polascik
Editor

Imaging and Focal Therapy of Early Prostate Cancer

Second Edition

Springer

Editor
Thomas J. Polascik, MD
Professor of Surgery
Department of Surgery
Duke Cancer Institute
Durham, NC, USA

ISSN 2197-7194 ISSN 2197-7208 (electronic)
Current Clinical Urology
ISBN 978-3-319-49910-9 ISBN 978-3-319-49911-6 (eBook)
DOI 10.1007/978-3-319-49911-6

Library of Congress Control Number: 2017931652

© Springer International Publishing AG 2017
This work is subject to copyright. All rights are reserved by the Publisher, whether the whole or part of the material is concerned, specifically the rights of translation, reprinting, reuse of illustrations, recitation, broadcasting, reproduction on microfilms or in any other physical way, and transmission or information storage and retrieval, electronic adaptation, computer software, or by similar or dissimilar methodology now known or hereafter developed.
The use of general descriptive names, registered names, trademarks, service marks, etc. in this publication does not imply, even in the absence of a specific statement, that such names are exempt from the relevant protective laws and regulations and therefore free for general use.
The publisher, the authors and the editors are safe to assume that the advice and information in this book are believed to be true and accurate at the date of publication. Neither the publisher nor the authors or the editors give a warranty, express or implied, with respect to the material contained herein or for any errors or omissions that may have been made. The publisher remains neutral with regard to jurisdictional claims in published maps and institutional affiliations.

Printed on acid-free paper

This Springer imprint is published by Springer Nature
The registered company is Springer International Publishing AG
The registered company address is: Gewerbestrasse 11, 6330 Cham, Switzerland

Foreword

The Best Is Still to Come

During the past decades, the age of men at prostate cancer detection has decreased by approximately 10 years, and men's life expectancy has increased by almost 4 years. Together with the increased diagnosis of low- and intermediate-risk prostate cancers, interest in minimally invasive focal treatment with its lower side-effect profile has grown. Consequently, focal therapy is a rapidly evolving field that covers several ablative techniques, energy sources, and treatment scenarios.

The rationale behind focal therapy sounds relatively simple, targeting the predefined cancerous part of the organ while sparing uninvolved tissue; hence, the execution in prostate cancer is somewhat more complicated. It is very difficult to predict the patient's individual clinical development or cancer progression. Selection of the appropriate patient takes into account factors such as prostate-specific antigen (PSA), biopsy results with histopathological parameters of the cancer foci, patients' life expectancy and quality of life, and most importantly the preferences of the patient. After selecting the patient, it remains challenging to localize, visualize, and characterize the significant tumor areas and to target the area accurately with the ablative modality most suitable. Finally, after the focal treatment, it is challenging to evaluate treatment efficacy by the interpretation of the serum PSA, imaging, and biopsy results during follow-up.

The establishment of focal therapies faces many challenges. While some ablative treatments have received approval from US Food and Drug Administration (FDA) authorities for application in prostate cancer, at present many other ablative techniques are being studied in early-phase trials. That research is taking place mainly to determine the safety of the technique and procedure and to evaluate the efficacy and adverse side effects. If the treatment is considered safe and feasible for targeted ablation of tumorous areas, research will proceed to the next phases. This will include prospective (randomized) controlled trials to determine efficiency, to compare the ablative techniques, and finally to test equivalence to current conventional treatments.

For focal therapy to evolve into an accepted segment of prostate cancer treatment, more research is needed directed at tissue-specific device settings, well-designed clinical trials with standardized ablation protocols, evaluation

of short-term ablation results, and long-term clinical benefit. This second edition edited by Thomas Polascik presents the current insights in imaging and focal therapy of early prostate cancer. The editor has to be complimented in spearheading this project and bringing together the thought leaders in this field. While a lot of progress has been achieved in the past decades, there is still a lot of work to do, and the best is yet to come: tailored treatment for each individual patient. This should be the focus for the third edition.

Amsterdam, The Netherlands Jean J.M.C.H. de la Rosette

Preface

For many decades, prostate cancer treatments have embraced radical whole-gland therapies, whether it be radical prostatectomy, radiation, or other whole-gland ablative modalities. A similar practice for the treatment of breast cancer also became commonplace after Dr. William Halsted described the radical mastectomy. Thereafter, the concept of breast-conserving therapy emerged, and the lumpectomy became commonly employed as an option to treat early and clinically localized breast cancer. This was feasible in the breast since the tumor could be easily imaged and subsequently surgically excised. We have witnessed the change in concept and surgical management of tumors in other organ systems that have attempted to only treat or remove the tumor yet preserve the remainder of uninvolved tissue. Indeed, in the field of urology, partial nephrectomy (excision of only the cancerous segment of the kidney) has become the standard of care for the small renal mass compared to radical nephrectomy (whole-gland removal) as described by Robson in 1963. Similar trends can be seen in the management of other organ systems as well.

In contrast, the prostate posed more challenges compared to other organs, given that most prostate cancers are very small, multifocal, and difficult to reliably image. For these reasons, whole-gland therapy has been the mainstay of prostate cancer treatment for decades, and changing this paradigm in the hearts and minds of physicians has been difficult. Focal therapy as a treatment option for clinically localized prostate cancer began to appear in the medical literature as recently as the turn of this century. In 2006, we entertained the idea of hosting an international focal therapy workshop at Duke University in an attempt to garner the best minds in academia and industry to discuss research and trials to propel the fledgling field forward. The First International Workshop on Imaging and Focal Therapy for Prostate Cancer was held in February 2008 and was an encouraging success. This international symposium has grown to an annual meeting alternating between the United States and Europe. Nearly every international meeting in urology today has a dedicated session on focal therapy for prostate cancer.

This book is the product of many of those same thought leaders who have been instrumental in the development of the focal therapy concept. These chapters highlight the state of the art on imaging and focal therapy for early stage prostate cancer, as we know it as of 2017. We continue to be humbled that much work still needs to be done to implement focal therapy in everyday practice. Today, there is much criticism regarding the over-detection and overtreatment of prostate cancer. However, along with these challenges

comes opportunity. Focal therapy presents a solution whereby in select men, aggressive lesions can be ablated and the remainder of the gland can be monitored, thereby preserving urinary continence and erectile function. Prostate cancer tends to be a slow-growing disease, allowing for periodic intervention such as focal therapy.

The authors of this textbook believe that with perseverance, further scientific inquiry, and new discoveries, the dogma of radical whole-gland therapy will be replaced by image-guided targeted therapy, ushering in a new era of precision medicine for our prostate cancer patients. I dedicate this second edition of *Imaging and Focal Therapy of Early Prostate Cancer* to those who dream and aspire to reach those ideals.

Durham, NC, USA Thomas J. Polascik, MD

Acknowledgements

I would like to acknowledge Ariel Schulman, MD; Efrat Tsivian, MD; and Kae Jack Tay, MBBS, for the manuscript editorial assistance.

Contents

Contributors

Hashim U. Ahmed Tissue and Energy, Division of Surgery and Interventional Science, University College London, London, UK

Mohamad E. Allaf Urology, Oncology, and Biomedical Engineering, Minimally Invasive and Robotic Surgery, Brady Urological Institute, Johns Hopkins Hospital, Baltimore, MD, USA

Mahul B. Amin Department of Pathology and Laboratory Medicine, Cedars-Sinai Medical Center, UCLA David Geffen School of Medicine, Los Angeles, CA, USA

Eric Barret Department of Urology, Institut Montsouris, Paris-Descartes University, Paris, France

John G. Baust UNESCO, Institute of Biomedical Technology, State University of New York at Binghamton, Binghamton, NY, USA

John M. Baust CPSI Biotech, Owego, NY, USA

Alberto Breda Department of Urology, University Autonoma of Barcelona, Fundaciò Puigvert, Barcelona, Spain

Paolo Capogrosso Department of Urology, IRCCS Ospedale San Raffaele/ Università Vita-Salute San Raffaele, Milan, Italy

Lina Maria Carmona Echeverria Tissue and Energy, Division of Surgery and Interventional Science, University College London, London, UK

Peter L. Choyke Molecular Imaging Program, National Cancer Institute, National Institutes of Health, Bethesda, MD, USA

E. David Crawford Surgery, Urology and Radiation Oncology, Urologic Oncology, University of Colorado, Denver, CO, USA

The University of Colorado Anschutz Campus, Aurora, CO, USA

Jean J.M.C.H. de la Rosette Department of Urology, Academic Medical Center (AMC) University Hospital, Amsterdam, The Netherlands

Theo M. de Reijke Department of Urology, Academic Medical Center, Amsterdam, The Netherlands

Behfar Ehdaie Urology Service, Department of Surgery, Memorial Sloan Kettering Cancer Center, New York, NY, USA

Scott Eggener Department of Surgery, Section of Urology, University of Chicago, Chicago, IL, USA

Mark Emberton Faculty of Medical Sciences, University College London, London, UK

Division of Surgery, Urology Department, University College London Hospitals Trust, London, UK

Andrew Evans Department of Laboratory Medicine and Pathology, University Health Network, Toronto General Hospital, Toronto, ON, Canada

John F. Feller Desert Medical Imaging, Indian Wells, CA, USA

Antonio Finelli Division of Urology/Uro-Oncology, Department of Surgical Oncology, Princess Margaret Cancer Centre, Toronto, ON, Canada

Stephen J. Freedland Division of Urology, Department of Surgery, Cedars-Sinai Medical Center, Los Angeles, CA, USA

Jurgen J. Fütterer Department of Radiology and Nuclear Medicine, Radboud University Medical Center, Nijmegen, Gelderland, The Netherlands

Isabel García-Fleury Mastology Section, Department of Obstetrics and Gynecology, Hospital Universitario de Caracas and Centro Médico de Caracas, Caracas, Venezuela

Sonia Gaur Molecular Imaging Program, National Cancer Institute, National Institutes of Health, Bethesda, MD, USA

Arvin K. George National Institutes of Health Clinical Center, Urologic Oncology Branch, National Cancer Institute, National Institutes of Health, Bethesda, MD, USA

Sangeet Ghai Department of Urologic Oncology, University of Toronto, Toronto, ON, Canada

Joint Department of Medical Imaging, University Health Network—Mount Sinai Hospital—Womens' College Hospital, Toronto General Hospital, Toronto, ON, Canada

Bernadette M. Greenwood Clinical Services, Desert Medical Imaging, Indian Wells, CA, USA

Thomas S. Griffith Department of Urology, University of Minnesota Medical Center, Minneapolis, MN, USA

Rajan T. Gupta Department of Radiology, Duke University Medical Center, Durham, NC, USA

Anouk E. Hentschel Department of Urology, Academic Medical Center (AMC) University Hospital, Amsterdam, The Netherlands

Markus Hohenfellner Department of Urology, Universitätsklinikum Heidelberg, Heidelberg, Baden-Württemberg, Germany

Jamie N. Holtz Department of Radiology, Duke University Medical Center, Durham, NC, USA

Shigeo Horie Department of Urology, Juntendo University, Graduate School of Medicine, Tokyo, Japan

R. Alex Hsi Department of Radiation Oncology, Peninsula Cancer Center, Poulsbo, WA, USA

Rafael E. Jimenez Division of Anatomic Pathology, Mayo Clinic, Rochester, MN, USA

J. Stephen Jones Regional Hospitals & Family Health Centers, Cleveland Clinic, Cleveland, OH, USA

James Kench Department of Tissue Pathology and Diagnostic Oncology, Royal Prince Alfred Hospital, Sydney, NSW, Australia

Masaki Kimura Department of Urology, Teikyo University School of Medicine, Tokyo, Japan

Alex Kirkham Department of Radiology, University College Hospital, London, UK

Laurence Klotz Department of Urology, Sunnybrook Health Sciences Centre, Toronto, ON, Canada

Badrinath R. Konety Department of Urology, University of Minnesota Medical Center, Minneapolis, MN, USA

Jaime Landman Department of Urology, University of California, Irvine, Orange, CA, USA

Marco Antonio López-Tovar Mastology Section, Department of Obstetrics and Gynecology, Hospital Universitario de Caracas and Centro Médico de Caracas, Caracas, Venezuela

Wesley W. Ludwig Department of Urology, The James Buchanan Brady Urological Institute, The Johns Hopkins University School of Medicine, Baltimore, MD, USA

Sherif Mehralivand Molecular Imaging Program, National Cancer Institute, National Institutes of Health, Bethesda, MD, USA

Rodolfo Montironi Department of Pathology, Genitourinary Cancer Program, Institute of Pathological Anatomy and Histopathology, Polytechnic University of the Marche Region Ancona, Italy

School of Medicine, United Hospitals, Torrette, Ancona, Italy

Caroline M. Moore Division of Surgical and Interventional Sciences, University College London, London, UK

Division of Surgery, Urology Department, University College London Hospitals Trust, London, UK

Judd W. Moul Division of Urology, Department of Surgery and Duke Cancer Institute, Duke University Medical Center, Durham, NC, USA

Vladimir Mouraviev Central Florida Cancer Institute, Davenport, FL, USA

Bladder Health and Reconstructive Institute, Memorial Hospital Miramar, South Broward Hospital District, Miramar, FL, USA

Akhil Muthigi National Institutes of Health Clinical Center, Urologic Oncology Branch, National Cancer Institute, National Institutes of Health, Bethesda, MD, USA

Satoru Muto Department of Urology, Teikyo University School of Medicine, Tokyo, Japan

Vikram Narayan Department of Urology, University of Minnesota Medical Center, Minneapolis, MN, USA

Pierre Nevoux Department of Urology, Regional University of Lille, Lille, France

Kathryn R. Nightingale Department of Biomedical Engineering, Duke University, Durham, NC, USA

Masakatsu Oishi Department of Urology, Kyoto Prefectural University of Medicine, Kyoto, Kyoto, Japan

Zhamshid Okhunov Department of Urology, University of California, Irvine, Orange, CA, USA

Aytekin Oto Department of Radiology, University of Chicago Medicine, Chicago, IL, USA

Mark L. Palmeri Department of Biomedical Engineering, Duke University, Durham, NC, USA

Roshan M. Patel Department of Urology, University of California, Irvine, Orange, CA, USA

Nathan Perlis Department of Urologic Oncology, University of Toronto, Toronto, ON, Canada

Division of Urology, Department of Surgical Oncology, University Health Network, Princess Margaret Cancer Centre, Toronto, ON, Canada

Adriana Pesci-Feltri Mastology Section, Department of Obstetrics and Gynecology, Hospital Universitario de Caracas, Centro Clínico de Maternidad Leopoldo Aguerrevere, Caracas, Venezuela

Peter A. Pinto Prostate Cancer Section, National Institutes of Health Clinical Center, Urologic Oncology Branch, National Cancer Institute, National Institutes of Health, Bethesda, MD, USA

Thomas J. Polascik, MD Professor of Surgery, Division of Urology, Department of Surgery, Duke Cancer Institute, Duke University School of Medicine, Durham, NC, USA

Arnoud W. Postema Department of Urology, Academic Medical Center, Amsterdam, The Netherlands

Robert Qi Division of Urology, Department of Surgery, Duke Cancer Institute, Duke University School of Medicine, Durham, NC, USA

Jan Philipp Radtke Department of Urology, Universitätsklinikum Heidelberg, Heidelberg, Baden-Württemberg, Germany

Department of Radiology, German Cancer Research Center, Heidelberg, Germany

Ardeshir R. Rastinehad Department of Urology and Radiology, Mount Sinai Hospital, New York, NY, USA

Anthony Robilotto Institute of Biomedical Technology, State University of New York at Binghamton, Binghamton, NY, USA

Rafael Sanchez-Salas Department of Urology, L'Institut Mutualiste Montsouris, Paris, France

Kimberly L. Santucci Institute of Biomedical Technology, State University of New York at Binghamton, Binghamton, NY, USA

Raj Satkunasivam Division of Urology, Department of Surgery, Sunnybrook Health Sciences Centre and University of Toronto, Toronto, ON, Canada

Matthijs J.V. Scheltema Department of Urology, Academic Medical Center (AMC) University Hospital, Amsterdam, The Netherlands

Ariel Schulman Duke Cancer Institute and Department of Surgery, Duke University Medical Center, Durham, NC, USA

Arjun Sivaraman Urology Service, Department of Surgery, Memorial Sloan Kettering Cancer Center, New York, NY, USA

Kristi K. Snyder CPSI Biotech, Owego, NY, USA

R. Jason Stafford Department of Imaging Physics, The University of Texas MD Anderson Cancer Center, Houston, TX, USA

Dan Stoianovici Brady Urological Institute, Johns Hopkins University, Baltimore, MD, USA

Nelson N. Stone Department of Urology and Radiation Oncology, The Icahn School of Medicine at Sinai, Mount Sinai Medical Center, New York, NY, USA

Kae Jack Tay Department of Urology, Duke University, Durham, NC, USA

Angelo Territo Department of Urology, University Autonoma of Barcelona, Fundaciò Puigvert, Barcelona, Spain

John Trachtenberg Division of Urology, Department of Surgical Oncology, University Health Network, Princess Margaret Cancer Centre, Toronto, ON, Canada

Igor Trilisky Department of Radiology, University of Chicago, Chicago, IL, USA

Efrat Tsivian Division of Urology, Department of Surgery, Duke University Medical Center, Durham, NC, USA

Baris Turkbey Molecular Imaging Program, National Cancer Institute, National Institutes of Health, Bethesda, MD, USA

Osamu Ukimura Department of Urology, University of Southern California Institute of Urology, Los Angeles, CA, USA

Robert G. VanBuskirk Institute of Biomedical Technology, State University of New York at Binghamton, Binghamton, NY, USA

Wulphert Venderink Department of Radiology and Nuclear Medicine, Radboud University Medical Center, Nijmegen, Gelderland, The Netherlands

Arnauld Villers Department of Urology, Hôpital Huriez, Centre Hospitalier Regional Universitaire, Université Lille Nord de France, Lille, France

Jochen Walz EAU Section of Urological Imaging (ESUI), Department of Urology, Institut Paoli-Calmettes Cancer Centre, Marseille, France

John F. Ward Department of Urology, M. D. Anderson Cancer Center, Houston, TX, USA

Thomas M. Wheeler Department of Pathology and Immunology, Baylor College of Medicine, Houston, TX, USA

Hayley Whitaker Tissue and Energy, Division of Surgery and Interventional Science, University College London, London, UK

Hessel Wijkstra Department of Urology, Academic Medical Center (AMC) University Hospital, Amsterdam, The Netherlands

Chi-hang Yee Department of Surgery, Prince of Wales Hospital, The Chinese University of Hong Kong, Shatin, China

Part I

Why Focal Therapy?

1 Evolution in the Concept of Focal Therapy: The Story of Breast Cancer and Prostate Cancer

Isabel García-Fleury, Chi-hang Yee, Marco Antonio López-Tovar, Adriana Pesci-Feltri, Arjun Sivaraman, and Rafael Sanchez-Salas

Introduction

Prostate cancer is characterized by a low mortality—incidence ratio partially due to the diagnosis of localized and low-risk disease. Focal therapy for prostate cancer has evolved in order to address the need for treatment of localized disease without exposing patients to the morbidities associated with radical therapy such as incontinence and erectile dysfunction and thus allowing them to maintain a good quality of life.

I. García-Fleury (✉) • M.A. López-Tovar
Mastology Section, Department of Obstetrics and Gynecology, Hospital Universitario de Caracas and Centro Médico de Caracas, Caracas, Venezuela
e-mail: igarciafleury@hotmail.com; isabelitagf@hotmail.com

C.-h. Yee
Department of Surgery, Prince of Wales Hospital, The Chinese University of Hong Kong, Shatin, China

A. Pesci-Feltri
Mastology Section, Department of Obstetrics and Gynecology, Hospital Universitario de Caracas, Centro Clínico de Maternidad Leopoldo Aguerrevere, Caracas, Venezuela

A. Sivaraman
Urology Service, Department of Surgery, Memorial Sloan Kettering Cancer Center, New York, NY, USA

R. Sanchez-Salas
Department of Urology, L'Institut Mutualiste Montsouris, Paris, France

In women, similarly to prostate cancer, the overdiagnosis of breast cancer due to improved imaging has induced the progression of surgical techniques from radical mastectomy to a more focal approach with individualized breast conservative strategies.

In the following chapter, we will be reviewing the evolution of focal therapy in breast and prostate cancer and will examine what were the factors that drove this evolution in time.

Breast Cancer

Introduction and Background

As the leading cause of cancer death in women all over the world, breast cancer is the most frequently diagnosed. It represents a growing and challenging problem for health services; currently its high incidence and mortality is considered a global public health problem [1]. It is also a systemic disease, with a heterogeneous behavior. It is mainly due to the tumors' biological characteristics, which are defined by different genetic profiles or immunohistochemistry. These characteristics are critical in determining the prognostic and predictive factors in each case.

In 1894 William Halsted published the results of his study "The results of operations for the cure of cancer of the breast performed at the Johns Hopkins Hospital from June 1889 to January

© Springer International Publishing AG 2017

T.J. Polascik (ed.), *Imaging and Focal Therapy of Early Prostate Cancer*, Current Clinical Urology, DOI 10.1007/978-3-319-49911-6_1

1894" [2]. In this study, a total of 50 patients underwent excision en bloc of the mammary gland, both pectoral muscles, and axillary lymph nodes. The procedure was justified on the Halsted theory, which argues that the tumor extends orderly and predictably, based on mechanical considerations. It also contemplates that the disease develops in stages: in the first one, the cancer develops in the organ in which it appears; the second regional stage in which it spreads to regional lymph nodes draining that circulation lymphatic; and finally, the systemic phase, which explains the metastasis. In this study there were no operative deaths, the local recurrence rate was 6 % (3 patients), and the 3-year survival rate was 45 % [2]. Patey and Dyson, of the Middlesex Hospital in London, experimented with a modified mastectomy, which preserves the pectoralis major muscle. In 1948, the group published the results of a cohort of mastectomies carried out between 1930 and 1943, comparing their modified mastectomy with the standard one [3]. In their publication of the first 118 surgeries, the patients were stratified according to the axillary lymph node status and the type of surgical procedure. They showed similar results in terms of survival at 3 years in patients with negative lymph nodes when compared with the Halsted mastectomy, 83 % vs. 78 % [3].

In view of the functional and psychological consequences of radical mastectomy, Mustakalio presented a more conservative treatment: removal of the tumor, preserving the breast tissue, and supplementing with radiation therapy. He recommended this procedure when the disease was not disseminated beyond the mammary gland. In 127 patients, the 5-year survival rate was 84 % [4]. Kennedy and Miller were the first to develop simple mastectomy, based on the fact that lymph nodes were not always involved in breast cancer. The procedure involves complete removal of the mammary gland and dissection of the pectoral fascia en bloc with the breast, preserving both pectoral muscles and axillary lymph nodes. Their series of cases from 1927 to 1956 showed a 5-year survival of 62 % in the group of tumors without local invasion [5]. In 1963 and 1965, Auchincloss and Madden described the modified radical mastectomy that consisted in total mastectomy preserving both pectorals plus axillary dissection; this provided satisfactory breast cancer control and better cosmetic results [6, 7].

In 1976, the National Surgical Adjuvant Breast and Bowel Project (NSABP) began to design a randomized trial, B-06, consisting of 2163 patients. They evaluated the efficacy of breast conservative surgery in women with stage I or II cancer, with tumors ≤4 cm in diameter. The patients underwent mastectomy, lumpectomy, or lumpectomy followed by radiation. All the patients underwent axillary dissection. The 20-year follow-up study showed that there was no difference in overall survival and disease-free survival between the treatment groups. These data showed a significant reduction in local recurrence in lumpectomy followed by radiotherapy (39.2 % vs. 14.3 %, $P < 0.01$) when compared with radical mastectomy [8].

The European Organization for Research and Treatment of the Cancer (EORTC) 10801, was a multicenter study [9]. It included breast cancer stage I–II patients treated with radical mastectomy, conservation mastectomy with lymph node dissection, and radiotherapy to the breast. Patients with metastases in lymph nodes received adjuvant chemotherapy. After 20 years of follow-up, the results showed that breast-conserving surgery group had no difference in overall survival [9]. When conservative treatment experienced a boom in the 1970s, contributions from the work of Mustakalio [4] and Hayward [10] provided references for Bernard Fisher in Pittsburgh [11] and Umberto Veronesi in Milan (QUART: quadrantectomy, axillary dissection, and radiotherapy) [12] to establish the preservative treatment guidelines.

As illustrated in Fig. 1.1, the data from these landmark studies laid the foundation of the concept for breast conservative surgery in the management of breast cancer.

Diagnostic and Imaging

The X-ray study of the breast can be performed for screening or diagnostic purposes. Screening mammography in an asymptomatic patient is

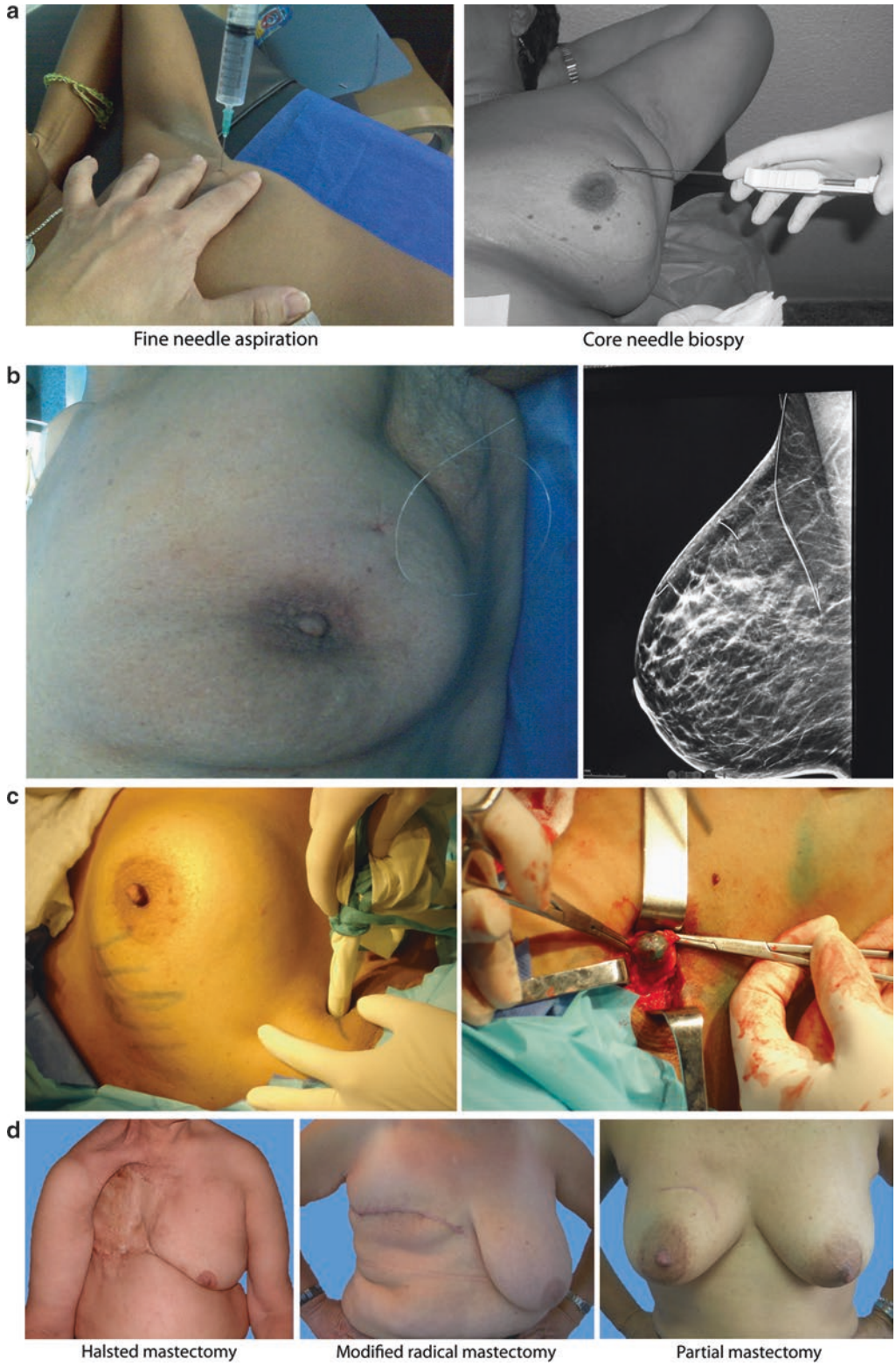

Fig. 1.1 Breast cancer treatment and evolution. (**a**) Diagnostic procedure: fine needle aspiration and core needle biopsy. (**b**) Radiolocalization using harpoon in a non-palpable lesion. (**c**) Sentinel node biopsy using gamma probe and blue dye. (**d**) Evolution of mastectomies. From Halsted to conservative surgery

confirmed by the usual projections as craniocaudal (CC) and medial-lateral oblique (MLO); diagnostic mammography occurs in a woman with signs and symptoms of breast disease or is ordered after the finding of pathology in the screening study, which may merit continuing with usual projections as focal compression with or without extension, exaggerated craniocaudal internal and external, strict side or side in 90° [13]. Mammography is the screening study of choice for breast cancer and has proven to be effective in the detection of lesions in very early stages, and its use has achieved a reduction in mortality from breast cancer by 30 %. The sensitivity has been reported to be 80–90 %, and specificity up to 97 % [14]. In the general population without risk factors for breast cancer, it is recommended that annual mammograms start at age 40. In patients with BRCA mutations, it should start earlier, between 25 and 30 years; in those patients with family history, screening should begin 10 years before the age of diagnosis of the affected family [15]. The American College of Radiology developed the Breast Imaging Reporting and Data System (BI-RADS) in 1992 to standardize the reporting of mammography, intending to develop a comprehensible and coherent language standardized internationally [16].

The image quality has evolved over time, from analogue mammography to breast tomosynthesis mammogram or three-dimensional (3D) mammogram, which was most recently approved by the US Food and Drug Administration (FDA). As for analogue mammography and digital or 2D mammography, both types of mammograms are made using the same technique. The difference is that analogue mammography obtained analogue files via photographic X-rays, while 2D mammography is processed by digital software. One of the disadvantages of analogue mammography is it is less sensitive in fibrous breasts. It is also operator dependent and not able to modify the images. Digital mammography overcomes these limitations of conventional mammography, allowing the electronic manipulation of the images. It also eliminates the taking of additional X-rays [17].

Digital 3D or breast tomosynthesis mammography is ideal for dense breasts. It consists of the acquisition of multiple screening exposures by a digital detector of an X-ray mammographic source moving along a limited angle arc, taking 0.5 mm images, which are then processed by software and read on a workstation similar to the studies of tomography and magnetic resonance (MR), where they are reconstructed in 2D images so you can navigate and view each slice. One of its advantages is that it allows physicians to evaluate better the superimposition of tissues, diminishing the recall rate [18].

Another effective and popular diagnostic tool for evaluating breast tissue is ultrasound [19]. In senology, ultrasound is indicated in the evaluation and characterization of palpable masses and other related signs or symptoms. It is also used in the evaluation of suspicious anomalies detected in other imaging studies, e.g., mammography or magnetic resonance imaging. It is used in the initial assessment of palpable masses in women under 30 years of age who do not have high risk for breast cancer or in pregnant women and nursing mothers as well. Another of its indications is in the evaluation of the problems associated with prosthetic breasts, evaluation of very dense fibroglandular tissue, or detecting an underlying mass that may be obscured in mammography. Ultrasound can also guide breast biopsies and other procedures of intervention or can be used in the identification and biopsy of suspicious lymph nodes [20].

Currently one of the advances of ultrasound is the development of elastography. The ultrasonic elastography was developed by Ophir et al. in 1991 [21]. It is a noninvasive method that allows the determination of the mechanical properties of tissue, providing information about its elasticity. It is very useful in evaluating breast tumors, allowing the differentiation between benign and malignant lesions: benign lesions are similar to the surrounding tissue elasticity, while malignant lesions are harder [22, 23].

Finally breast magnetic resonance imaging (MRI) has currently been a great contribution to senology. It is being employed as a screening tool in young patients with high risk of breast cancer.

It is also used in the assessment of local extension of the disease, since through this study multicentricity and multifocality are determined. Similarly, it can ascertain with great accuracy the relationship of the tumor with the fascia and the possible extension to pectoralis, serratus major muscle, or intercostal muscles. It is useful to evaluate residual disease in patients with a history of sparing mastectomy whose specimens have been reported as positive or close margins and to evaluate the response to neoadjuvant treatment. It also serves as a guide for carrying out breast biopsies and learning the location of the lesion prior to surgery [24].

Palpable or non-palpable breast lesions that have been categorized BI-RADS 4 by mammography, ultrasound, and/or kinetic curve suspicious in breast MRI require histological confirmation [25], either by fine needle aspiration (FNA) or core needle biopsy (CNB). The success rates of these procedures increase when they are performed under stereotactic guidance in the case of microcalcifications or parenchymal distortions, ultrasonographic for nodular lesions, or by MRI [26]. The CNB (14G) has reported sensitivity up to 88 % and a specificity of 90 % [27]. The procedure's sensitivity increases to 99.2 % if performed under ultrasound guidance [28] and up to 100 % with stereotactic guidance.

Surgical Treatment for Breast Cancer

Palpable Lesions

The decision to carry out a partial mastectomy before radiotherapy versus a total mastectomy is based on the proven concept of equal survival, low recurrence rate, and a remarkable benefit in cosmesis [11, 12].

Proper selection of patients is the most important issue to make the procedure successful. The American College of Surgeons, the American College of Radiology, the College of American Pathologists and the Society of Surgical Oncology have developed a consensus on standards of care for patients being offered conservative therapy [29]. The patient must have a biopsy that shows the presence of carcinoma. The histological study of the sample must be comprehensive. It includes assessment of hormonal receptors, which allows the attending physician to discuss with the multidisciplinary team about different treatment options that may follow. It also includes the possibility of neoadjuvant chemotherapy to reduce tumor size and the possibility of intraoperative radiotherapy planning. Radiological studies should be of good quality. Attention must be made to evaluate the possibility of the presence of more than one tumor or the presence of extensive areas of microcalcifications. These features would make the patients contraindicated for conservative therapy. A prior history of radiation therapy can also have the risk that makes the treatment process exceed the maximum dose allowable for the chest wall. It would make the patient unfit for a conservative breast procedure.

Regarding the surgical technique, the incision should be as close to the tumor as it can be, respecting the Langer's lines, avoiding any tunneling. Resection of skin depends on the proximity of the tumor, respecting negative margins but preserving, when it is possible, the subcutaneous fat that improves the cosmetic effect. The evaluation of the specimen by a pathologist at the time of the intervention gives us the negative margins safety and prevents the reoperation as a result of a positive margin reported in the final specimen. It is well known that the possibility of local recurrence in patients with positive margins is greater. It is considered a negative margin when the margin ranges from 0.5 to 1 cm. However, there are many studies that considered that having no ink on the tumor would be a margin good enough for breast conservative surgery. Resection of a greater margin should be considered in patients with lobular carcinoma and with extensive in situ disease.

Mastery of anatomy is vital to the realization of a mastectomy. The removal of all breast tissue is essential to prevent local recurrences. It will be performed in any patient who is not indicated to have a conservative surgery or prophylactically done to reduce the risk of breast cancer in patients with mutations of the breast cancer type 1 and 2 susceptibility genes (BRCA1

and BRCA2). Mastectomy is also indicated in patients with inflammatory carcinoma, extensive microcalcifications, or in the presence of multifocality or multicentricity. Finally, we should also respect the desire of the patient who wishes to undergo a total mastectomy. Tumor size in relation to a patient's breast size must also be considered in the decision to go for breast conservative surgery [30].

Non-palpable Lesions

The ability to detect smaller lesions allows us to know better the natural history of the disease. With the use of strict pathological criteria that define high-risk patients, the use of systemic and radiotherapy, coupled with the increased participation of patients in treatment decisions, has led to a radical change in behavior against breast cancer. We moved progressively from radical surgery to conserving surgery in the 1980s. Advances in diagnostic techniques—the transition from analogue mammography to digital and then to tomosynthesis, as well as breast ultrasound with greater precision and MRI—have allowed physicians to make more accurate diagnoses. Tumors being diagnosed are getting smaller and smaller, which significantly improves the morbidity and mortality of patients with breast cancer.

These advances have forced surgeons to develop surgical techniques that allow them to treat lesions that are not clinically identifiable. These are the lesions that are not tangible, namely, nodules, microcalcifications, or parenchymal distortions that are catalogued as BI-RADS 4 or 5. They can only be found in imaging studies, but normally physicians would not be able to identify them in the routine clinical evaluation.

A biopsy of any suspicious breast lesion should be done before the treatment decision can be made. Such biopsy allows the surgeon to decide if the lesion is appropriate for surgery and what surgical procedure is optimal. In view of these features of small tumors, surgery needs to be done with the aid of tumor localization by radiology. Placement of a guide in the lesion or adjacent to the lesion (e.g., a harpoon, radioactive decayed iodine 125 seed or technetium 99 bound to albumin macromolecule, or injection of liquid coal) allows surgeons to achieve a total excision of the tumor with adequate margins and at the same time keep as much healthy tissue as possible (Fig 1.1c). These surgeries give excellent results both from an oncological and an aesthetic point of view.

Sentinel Lymph Node and Axillar Dissection

The axillary status is one of the most important prognostic factors in breast cancer and is the decisive element for the implementation of systemic therapy. Previously, axillary dissection was always performed in any patient with breast cancer. In the last 15 years, the increasing number of patients with early stages (stage I and II) makes it more feasible to perform sentinel node biopsy (SNB) instead of the complete axillary node dissection. SNB is a minimally invasive technique that is used in patients with a confirmed diagnosis of breast cancer, in order to determine the presence of occult metastases in the axillary nodes. In accordance with the consensus on sentinel node biopsy in breast cancer, which was developed in Philadelphia in 2001, sentinel lymph node is defined as the first node that is oriented from breast cancer metastasis and lymphatic drainage [31, 32]. It is commonly found in the central portion of level I, but it can be found, in some cases, in level II or level III lymph nodes, as in Rotter nodes.

The axillary dissection as part of the treatment of breast carcinoma has a dual role: regional disease control and to provide forecast information in order to decide which is the appropriate adjuvant treatment. Only one-third of patients with clinically negative axilla would present metastasis in the final histopathological study. In the end, the goal of surgical intervention is not to perform extensive surgery or axillary dissection (overtreatment), which leads to increased and unnecessary morbidity. Numerous studies have shown that the information derived from SNB predicts what is going on in the remaining axillary nodes. Thanks to the validation of this technique, nowadays any patient with clinically negative axilla must undergo sentinel node biopsy.

The identification of sentinel node is called lymphatic mapping. The technique depends on multidisciplinary management, proper interaction with nuclear medicine colleagues, the use of technologically appropriate equipment, the use of a precise methodology, and the availability of a surgical team that has overcome the initial learning curve.

SNB is performed by peritumoral, tumor bedding, or subareolar injection of colloidal sulfur labeled with technetium 99 (6 to 12 h before surgery), vital blue (placed during surgery), or both. Often you can identify the sentinel node by the dye. When the combined technique is used, dissection is oriented with the gamma probe after the dye is identified. Through the radioactivity luminous and numerical signal, dissection is facilitated [33]. Sentinel lymph node can be assessed by the following criteria: blue lymph nodes, absence of blue nodes but stained afferent canaliculus, and nodes with radioactivity increased two to three times. According to the experience of the surgical team, either technique can be adopted. The identification rate varies between 92 and 98 %. The rate of false negatives, ranging from 0 to 15 %, is on average 8.8 %.

This technique of SNB is indicated in the following situations: infiltrating ductal carcinomas, extensive and/or high-degree intraductal carcinomas, candidate to mastectomy, or in T0, T1, and T2 stages (up to 5 cm in diameter) and with clinically negative axilla. There are special situations in which one could consider the implementation of the SNB, and these are post-adjuvant systemic therapy, during pregnancy, multicentric and multifocal disease, previous breast surgery, breast cancer in men, remapping of sentinel node, or risk reduction mastectomy. This technique is contraindicated when the axilla is clinically positive, when there is presence of distant metastasis or in inflammatory carcinoma [34].

Once the sentinel node biopsy is done, the sample should be sent to pathology; if it is confirmed as negative or there is absence of metastasis, axillary dissection is not indicated. If the biopsy reports positive for metastases, axillary dissection should be performed.

Conclusion

The presentation of breast cancer ranges from non-palpable disease to palpable disease and localized disease to systemic disease. It has come a long way since the initial universal approach with radical mastectomy, to the current individualized management option with the possibility of breast-conserving treatment. The availability of advanced imaging techniques, lesion localization techniques, and lymph node staging strategies together with different adjuvant therapies allows the possibility of a more focal treatment of breast cancer. While breast-conserving treatment is a surgical technique, preoperative patient assessment for suitability involves multiple facets of disease characterization. Advancement in genetics, radiology, radiation therapy, and chemotherapy are the necessary steps to make a focal surgical therapy for breast cancer possible, now and in the future.

Prostate Cancer

Introduction and Background

Prostate cancer is the most common malignancy in men in the United States [35], and the second most common malignancy in men in the world [36]. The established risk factors for prostate cancer are age, race, and family history. When a man has a first-degree relative being diagnosed with prostate cancer, his risk is about twice that for men in the general population [37]. Such risk would be doubled when the same relative is diagnosed with prostate cancer at an age younger than 60 years old [38]. Genetic studies in families with multiple cases of prostate cancer have suggested co-segregation of multiple genetic regions. Currently the homeobox gene HOXB13 has been identified as a prostate cancer predisposition gene [39]. Many other genetic regions are being studied for their role in prostate cancer occurrence.

The majority of men with prostate cancer have clinically localized disease [40]. In the past

few decades, much effort has been put into cancer awareness and screening, with the aim of early cancer diagnosis. Such effort significantly increases the diagnosis and incidence of early-stage prostate cancer [41]. Furthermore, prostate cancer covers a wide spectrum of prognoses, ranging from an indolent disease course to a lethal and metastatic state. All these facts challenge the traditional concept in management of localized prostate cancer, which groups all patients into either observation or radical whole-gland treatment. The Scandinavian Prostate Cancer Group 4 trial randomly assigned 695 men with localized prostate cancer to radical prostatectomy (RP) or watchful waiting between 1989 and 1999. The 18-year analysis reported a cumulative incidence of death was 56.1 % in the radical prostatectomy group and 68.9 % in the watchful waiting group (hazard ratio [HR] 0.71, 95 % CI, 0.59–0.86; $P < 0.001$) [42]. As most of the patients in this study had clinically palpable disease, some authors were skeptical about the generalization of this study's result to this era of mostly impalpable, prostate-specific antigen (PSA)-detected cancers [43]. On the other hand, a risk-stratified strategy in the proposition of RP to a specific group of patients was suggested, with respect to the study's findings that the benefit of surgery in preventing cancer-related mortality was largest in men younger than 65 years of age and in those with intermediate-risk prostate cancer.

Another study to assess the role of radical treatment in prostate cancer is the Prostate Cancer Intervention Versus Observation Trial (PIVOT) [44]. In the early era of PSA testing from 1994 to 2002, 731 men with localized prostate cancer were randomized into radical prostatectomy and watchful waiting. After 12 years, radical prostatectomy did not significantly reduce prostate cancer-specific or overall mortality. However, a reduction in overall mortality with radical prostatectomy was observed among patients with intermediate-risk disease in the subgroup analysis (HR 0.69, 95 % CI, 0.49–0.98). In the low-risk subgroup, though it was not statistically significant, the HR for overall mortality favored watchful waiting rather than radical prostatectomy (HR 1.15, 95 % CI, 0.81–1.66). Taken into account of the evidence from these two trials, as well as considering the morbidities associated with any radical treatment, a uniform radical approach to all localized prostate cancer calls for reconsideration.

To avoid the unnecessary harm brought upon by the overdiagnosis and the subsequent overtreatment of prostate cancer by radical means, a noninvasive option known as active surveillance was popularized by two groups from the University of Toronto and Johns Hopkins University in the mid-1990s [45, 46]. The results of such a treatment option demonstrated promising cancer-specific survival with minimal morbidity for men with low-risk, clinically localized prostate cancer.

However, this binary approach to prostate cancer still cannot fully match the spectrum of the disease. Active surveillance is infrequently used, and approximately a third of patients on active surveillance require treatment [47]. Lying between these two strategies of active surveillance and radical treatment of prostate cancer is focal therapy. Focal therapy is a therapeutic modality that seeks to treat the prostate gland under the principle of organ preservation. It is flexible in extent, and with the advantage of being tailored to the individual patient. In general, focal therapy is defined as ablation of the dominant or index lesion only [48]. In view of this, such therapeutic approach would require complementary diagnostic tools to accurately define and locate the lesion in order to achieve the best treatment outcome.

Diagnostic and Imaging

Systemic transrectal ultrasound (TRUS)-guided prostate biopsy has been the mainstay of prostate cancer diagnosis tools for several decades. Despite that the number of biopsy cores has increased when compared with that in the past, the sensitivity of TRUS-guided prostate biopsy remains low [49], and under-grading of cancer remains high [50].

A modification of TRUS-guided prostate biopsy is transperineal template-guided mapping

biopsy (TTMB). The Ginsburg Study Group's definition of TTMB is "exhaustive transperineal TRUS guided biopsies of the prostate performed with the patient in lithotomy position using a 5-mm brachytherapy grid, with at least one biopsy from each hole" [51]. While the cancer detection rate of 10- or 12-core TRUS-guided prostate biopsy from contemporary series is 20–35 %, Barqawi et al. reported a TTMB cancer detection rate of 68.8 % after an initial negative TRUS-guided biopsy [52]. Concerning primary TTMB, an even higher cancer detection rate up to 73.3 % was reported by Bittner et al. [53]. Furthermore, TTMB is more accurate in predicting tumor characteristics than TRUS-guided biopsy. Onik et al. reported a Gleason upgrade of 23 % with TTMB [54], and Crawford et al. reported that 72 % of the TTMB cores were identical in grade to RP specimens and 80 % accuracy in predicting laterality [55]. Authors have suggested that for TTMB, an easier access to transition zone and anterior region of the prostate, more tissue being sampled in each core, and the use of a uniform grid may account for such superior results [56].

Recently there has been a rapid development in prostate magnetic resonance imaging (MRI). Multiparametric MRI (mpMRI) encompassing diffusion-weighted imaging (DWI), magnetic resonance spectroscopy imaging, and dynamic contrast-enhanced MRI (DCE-MRI) is becoming more easily accessible. Its availability allows anatomical, functional, and metabolic assessment of the prostate and its lesions. Briefly, T2-weighted images demonstrate the anatomy of the prostate and identify any extraprostatic extension of the disease. Prostate cancer cells would take up and release contrast more rapidly in the DCE phase, and there is a correlation with tumor grading. DWI images show prostate cancer as high signal on longer b-value sequence and as low signal on the acquired diffusion coefficient (ADC) map due to the restricted diffusion of cancer cells. In addition, prostate cancer demonstrates an increased ratio of choline and creatinine to citrate on magnetic resonance spectroscopy. All these advances in MRI development make it a useful tool in prostate cancer detection. A systematic review reported sensitivities of 58–97 % and specificities of 23–87 % for detection of clinically significant prostate cancer using multiparametric MRI, with trends depending highly on the threshold used in the definition of clinically significant disease [57].

In view of the advances and popularity of MRI for prostate cancer assessment, the European Society of Urogenital Radiology (ESUR) published the Prostate Imaging Reporting and Data System (PI-RADS) to standardize the acquisition protocol and assessment of cancer suspicion level and location for lesions on MRI in 2012 [58]. A recent update with the collaboration of the American College of Radiology, ESUR, and AdMeTech Foundation brought forth PI-RADS version 2 [59]. The consensus expert opinion currently considers diagnostic quality T2W and DWI/ADC images to be the primary MRI sequences used for suspicion level assessment of lesions. However, DCE-MRI acquisition is still recommended in order not to miss small clinically significant cancers. A meta-analysis of 14 studies evaluating PI-RADS reported a pooled sensitivity of 78 % (95 % CI 70–84 %) and pooled specificity of 79 % (95 % CI 68–86 %) for detection of prostate cancer with multiparametric MRI [60].

MRI-guided prostate biopsy is becoming more and more available, but there is currently no consensus on the optimal technique. D'Amico et al. were among the first to report the use of MRI to guide prostate biopsy [61]. The initial report employed an open-source MRI scanner with a field strength of 0.5 T, and a transperineal biopsy of prostate was performed. Subsequently an MRI-compatible biopsy frame for performance of transrectal prostate biopsy within a closed MRI scanner was made available in the market. In general, in-bore MRI-guided biopsy is accurate, but it requires considerable technical support and has significant cost and logistic issues [62].

As an alternative to in-bore MRI-guided biopsy, cognitive fusion biopsy requires the TRUS operator to mentally integrate mpMRI findings with TRUS images to target the lesion. The cognitive fusion technique is relatively quick

and has a cost advantage. However, the accuracy is suboptimal when it comes to small lesions [63]. Such limitation may be overcome by the MRI/ultrasound (US) fusion technology, which employs the software fusion biopsy technique. With the MRI findings matched and registered to the real-time ultrasound images, targeted biopsy can be performed. Limitations of this technique include the errors in fusion due to spatial deformation of the prostate at TRUS compared to MRI [64]. Overall, mpMRI-guided biopsy has a higher prostate cancer detection rate and positive core rate as compared to standard random TRUS-guided biopsy or extended systematic biopsy, especially in patients with previous negative biopsy [62]. For the detection of clinically significant prostate cancer, Moore et al. concluded that both MRI-guided biopsy and standard biopsy are able to detect such an entity in an equivalent number of men. However, MRI-guided biopsy is able to achieve detection by using fewer biopsies in fewer men, with a reduction in the diagnosis of clinically insignificant cancers [65]. It is yet to be determined whether it is safe to exclusively biopsy the target lesion while abandoning additional routine systematic biopsy or whether the target lesion should only be biopsied at a higher sampling density as compared to the rest of the prostate tissue [62].

Focal Therapy Treatment and Its Evolution

The initial interest in focal therapy was ignited by interventional radiologists. In 2002, Onik et al. published the result of their pilot study, in which nine patients were treated with focal, unilateral nerve-sparing cryosurgery and had been followed up for 6 years [66]. All patients had stable PSA levels, six patients routinely biopsied had negative biopsies, and potency was maintained in seven of nine patients. In their more recently updated results of 48 men after hemispherical cryoablation, 94 % of the patients had stable PSA according to the original 1996 American Society for Therapeutic Radiology and Oncology (ASTRO) definition [67]. Twenty-four patients being routinely biopsied all turned out to be negative for prostate cancer. No local recurrences were noted in areas treated. All patients were continent, and potency was maintained to the satisfaction of the patients in 36 of 40 men who were potent preoperatively. This technique was coined as "male lumpectomy" in their published article.

A similar approach with cryoablation was also reported by Bahn et al. [68]. Thirty-one men with clinically organ-confined, unilateral tumor identified by color Doppler ultrasonography and confirmed by targeted and systematic biopsy underwent focal prostate cryoablation.

At a mean follow-up of 70 months, biochemical disease-free status according to the original 1996 ASTRO definition was 92.8 %, and a 96.0 % negative biopsy rate was observed. A total potency rate was 88.9 %, including patients on oral pharmaceutical assistance.

Urologists very soon reported their experience in cryoablation. Lambert et al. had a series of 25 patients with primary unifocal prostate cancer being treated with focal cryoablation between 2002 and 2005 [69]. After a median follow-up of 28 months, 84 % had not experienced biochemical failure, which was defined as a PSA nadir >50 % of the pretreatment PSA or a rise >2 above nadir. Seventeen patients remained potent, and no patients reported worsened lower urinary tract symptoms, incontinence, rectal pain, perineal discomfort, or fistula formation.

Besides cryoablation, high-intensity focused ultrasound (HIFU) was also employed as a modality of focal therapy, and the initial experience was reported by Ahmed et al. from the University College London [70]. Twenty patients were recruited into the trial after the diagnosis of prostate cancer by mpMRI and TTMB. Follow-up biopsy was performed on 19 patients, and 18 of them showed no local evidence of recurrence. PSA reduction was observed for 12 months, and 95 % of the patients had their potency maintained. As these focal therapy trials of cryoablation and HIFU provided encouraging results both in terms of oncological control and quality of life preservation, more interest has been observed in the research and development of focal therapy for prostate cancer.

Besides technology advancement, an area of constant evaluation and evolution in focal therapy is patient selection. In the initial phase of focal therapy development, focal therapy was thought to be an alternative to active surveillance in very low-risk disease. In 2007, the International Task Force on Prostate Cancer and the Focal Lesion Paradigm proposed selection criteria for focal therapy to include PSA <10 ng/ml, Gleason score ≤7, stage ≤T2a, PSA density <0.15 ng/ml/cm^3, PSA velocity less than 2 ng/ml, ≤20 % cancer involvement in any biopsy core, and ≤33 % of total cores containing cancer. Such conservative and restrictive criteria for focal therapy candidates are in big contrast to the initial focal therapy series. The cryoablation series by Onik et al. actually included 52 % of the patients at moderate or high risk according to D'Amico stratification [67]. Bahn et al. did not exclude patients based on their preoperative PSA level or Gleason score [68]. Ellis et al., who were among the first few groups reporting on the use of cryoablation for prostate cancer, included patients with intermediate-risk or high-risk disease characteristics [71].

In 2009, a consensus meeting on focal therapy in prostate cancer was held at the end of the 2nd International Workshop on Focal Therapy and Imaging in Prostate and Kidney Cancer in Amsterdam, Netherlands [72]. In light of the observation that many men with low-risk features on biopsy are found to have nondominant Gleason 4 disease at radical prostatectomy and ultimately with very little impact on the clinical course, the panel in the meeting considered the presence of Gleason pattern 4 disease a non-exclusionary condition. The perception on focal therapy has further shifted since then. In a more recent consensus meeting occurring in 2013, there was agreement, with a high level of consensus, that focal therapy should be recommended for intermediate-risk patients [48]. Concerning using focal therapy to treat men with low-risk disease, the agreement was with a lower level of consensus.

The concept of the index lesion and its impact on the prognosis of prostate cancer has increased the flexibility in the application of focal therapy (Fig. 1.2), and thus developed a novel approach in selecting the appropriate candidates. With time, there is a possibility that as long as localized prostate cancer is accurately staged and effective ablation of all targeted cancer is possible, the urology community may come to the consensus that the patient could be a potential candidate for focal therapy regardless of risk category.

Options of Focal Therapy

Cryotherapy

Cryotherapy uses extreme cold temperature to induce ice crystal formation, ischemic necrosis, and ultimately provoking cell death. With rapid freeze and thaw cycles, and the simultaneous application of multiple cryoprobes, the duration of treatment is reduced and the precision of the therapy is enhanced. Focal cryotherapy is delivered to the prostate with TRUS guidance, inserting cryoprobes transperineally using a brachytherapy grid or by a freehand fashion. Complication profile is minimized with the use of urethral warmer and thermocouples.

The treatment outcomes of cryotherapy were registered to the national Cryo On-Line Database (COLD) registry. In the 2011 report of the registry, Ward et al. reported 1160 men having been treated with focal cryoablation [73]. The 3-year biochemical disease-free survival was at 75.7 %. Prostate biopsy was performed in 164 patients whom were suspected of cancer recurrence, and 43 of them were found positive. Urinary continence, as defined by not needing any pad, was 98.4 %. Maintenance of spontaneous erections was 58.1 %. Rectourethral fistula was observed in one patient (0.1 %). While appreciating the effort of the registry, some authors criticized that the absence of entry criteria, of on-site quality control and traceability of data, as well as lack of patient-reported outcome measures made the registry not an ideal database to have a comprehensive assessment of cryoablation [74].

High-Intensity Focused Ultrasound

HIFU as a focal therapy for prostate cancer uses low frequencies of around 0.8–3.5 MHz to deliver high energy in a restricted space so as to destroy

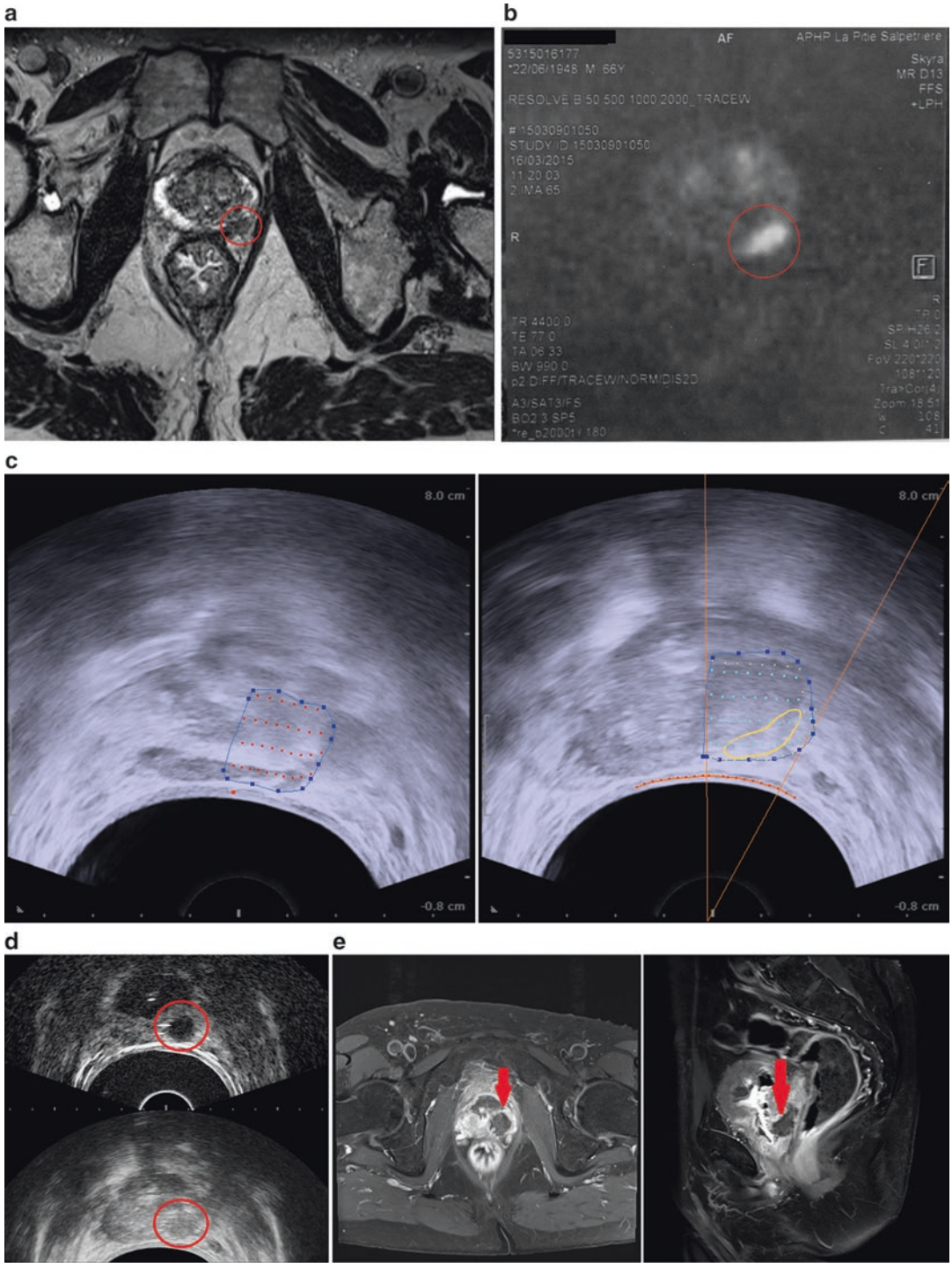

Fig. 1.2 The three pillars of focal therapy: planning, treatment, and control. (**a**) Coronal view: T2-weighted magnetic resonance images (MRI). *Red circle* indicates tumor outlines. (**b**) Coronal view: diffusion-weighted MRI. *Red circle* indicates region of interest (ROI) for ablation. (**c**) Coronal view (*left panel*): ultrasound images during ablation treatment. High-intensity focused ultrasound. Coronal view (*right panel*): ultrasound images during ablation treatment. *Yellow lines* delineate the region of interest (ROI). (**d**) Coronal view: real-time contrast-enhanced ultrasound during high-intensity focused ultrasound treatment. *Red circle* delineates hypoechoic devascularized ablated zone. (**e**) Coronal view (*left panel*): T2-weighted postoperative imaging. *Red arrow* shows the ablated zone. Sagittal view (*right panel*): T2-weighted postoperative imaging. *Red arrow* shows the ablated zone

a given area of tissue. By the mechanisms of coagulative necrosis and internal cavitation, therapeutic effect is achieved. Both transrectal and transurethral techniques have been described [75]. Localization of the lesion is by means of TRUS or MRI/US fusion. The procedure is performed under general or spinal anesthesia. Prior transurethral resection of prostate before HIFU focal therapy is no longer routine, considering the low risk of urinary retention [76].

A prospective study on HIFU by Ahmed et al. studied 42 men between 2007 and 2010 [77].

Of 35 men with good baseline function, 31 (89 %, 95 % CI 73–97) had erections sufficient for penetration at 12 months after focal therapy. No histological evidence of cancer was identified in 30 of 39 men biopsied at 6 months (77 %, 95 % CI 61–89). After retreatment in four men, 39 of 41 (95 %, 95 % CI 83–99) had no evidence of disease on mpMRI at 12 months.

So far, few prospective studies on HIFU are available. Trials to compare HIFU with standard-of-care treatment modality are awaited.

Photodynamic Therapy

Photodynamic therapy (PDT) uses reactive oxygen species to bring upon tissue damage. The interaction between light brought by a laser fiber, a photosensitive agent administrated orally or intravenously, and oxygen present in tissues leads to a chain reaction inducing the release of singlet oxygen and antioxidant enzymes. Azzouzi et al. reported their experience with 85 men having low- to intermediate-risk prostate cancer [78]. Sixty-eight patients had unilateral disease and underwent hemiablation. At 6 months, 17.4–38.1 % of patients had a positive biopsy. Currently, only phase II trial results are available concerning PDT.

Laser Interstitial Thermotherapy

Laser interstitial thermotherapy (LITT), or also known as focal laser ablation, uses laser fibers to raise the temperature of the treatment area in order to bring upon a therapeutic effect. Transperineal insertion of laser fiber to the target lesion is done under TRUS guidance or MRI guidance. In the phase I trial by Oto et al., it was shown to be a safe and feasible option [79]. Seven out of nine patients were found to be biopsy negative in the ablation zone. More data are needed to evaluate the oncological efficacy.

Irreversible Electroporation

In irreversible electroporation, cell homeostasis is disturbed by low-energy direct current resulting in tissue damage. Local thermal effect is avoided because of the low voltage. Energy is delivered to the target lesion via electrode needles. Treatment duration is relatively short, and preliminary assessment seems to demonstrate tissue selectivity [80], possibly allowing better nerve preservation during treatment. Valeria et al. reported their experience in 34 patients [81]. After a median follow-up of 6 months, mpMRI showed suspicious residual disease in six patients. All patients were continent and potency was preserved in 95 % of men. While the initial results are promising, the technology is still in its early stage of development and assessment.

Conclusion

To avoid the unnecessary complication associated with radical treatment, focal therapy is becoming more prominent as one of the potential options in the armamentarium of prostate cancer treatments (Fig. 1.3). Advancement in imaging and diagnostic techniques allows a more confident assessment before and after focal therapy. In general, phase III study of many focal therapy modalities is still lacking. However, preliminary data and initial results have demonstrated encouraging findings. With the aims of both oncological control and functional preservation, focal therapy is proving itself to be a promising treatment option for localized prostate cancer.

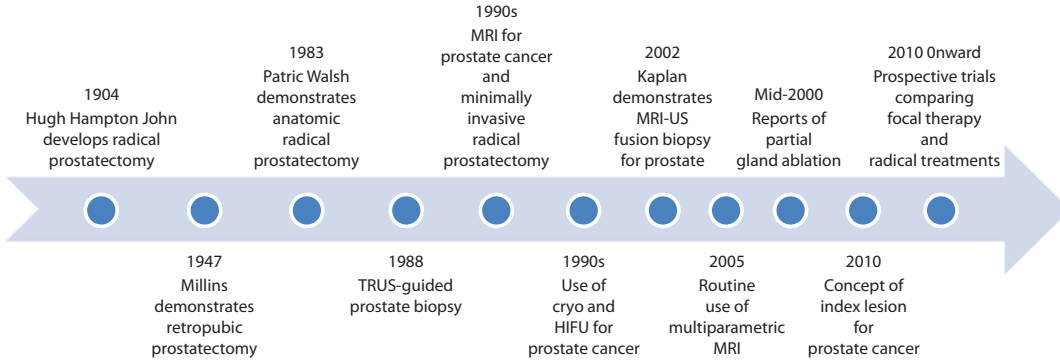

Fig. 1.3 Timeline for focal therapy of prostate cancer

References

1. GLOBOCAN 2012 (IARC), The World Bank Group 2014 Indicators. 2014. http://globocan.iarc.fr/; http://data.worldbank.org/indicator/NY.GDP.PCAP.CD.
2. Halsted W. The results of operation for the cure of the cancer breast performed at the John Hopkins Hospital, from June 1889 to January 1894. Bull Johns Hopkins Hosp. 1894;4:297–350.
3. Patey DH, Dyson WH. The prognosis of carcinoma of the breast in relation to the type of mastectomy performed. Br J Cancer. 1948;2:7–13.
4. Mustakalio S. Treatment of breast cancer by tumor extirpation and roentgen therapy instead of radical operation. J Fac Radiol. 1954;6:23–7.
5. Kennedy CS, Miller E. Simple mastectomy for mammary carcinoma. Ann Surg. 1963;157:161–2.
6. Auchincloss H. Significance of location and number of axillary metastases in carcinoma of the breast: a justification for a conservative operation. Ann Surg. 1963;158:37–46.
7. Madden JL. Modified radical mastectomy. Surg Gynecol Obstet. 1965;121(6):1221–30.
8. Fisher B, Anderson S, Bryant J, Margolese RG, Deutsch M, Fisher ER, et al. Twenty-year follow-up of a randomized trial comparing total mastectomy, lumpectomy, and lumpectomy plus irradiation for the treatment of invasive breast cancer. N Engl J Med. 2002;347(16):1233–41.
9. Black DM, Hunt KK, EA M, DM B, KK H. Long-term outcomes reporting the safety of breast conserving therapy compared to mastectomy: 20-year results of EORTC 10801. Gland Surg. 2013;2(3):120–3.
10. Hayward J. The conservative treatment of early breast cancer. Cancer. 1974;33(2):593–9.
11. Fisher B, Jeong JH, Anderson S, Bryant J, Fisher ER, Wolmark N. Twenty-five-year follow-up of a randomized trial comparing radical mastectomy, total mastectomy, and total mastectomy followed by irradiation. N Engl J Med. 2002;347(8):567–75.
12. Veronesi U, Cascinelli N, Mariani L, Greco M, Saccozzi R, Luini A, et al. Twenty-year follow-up of a randomized study comparing breast-conserving surgery with radical mastectomy for early breast cancer. N Engl J Med. 2002;347(16):1227–32.
13. American College of Radiology. ACR practice parameter for the performance of screening and diagnostic mammography. Amended 2014 (Resolution 39). http://www.acr.org/~/media/ACR/Documents/PGTS/guidelines/Image_Quality_Digital_Mammo.pdf. Accessed 12 Sept 2016.
14. Yang T-L, Liang H-L, Chou C-P, Huang J-S, Pan H-B. The adjunctive digital breast tomosynthesis in diagnosis of breast cancer. BioMed Res Int. 2013;2013:7, Article ID 597253.
15. Mainiero MB, Bailey L, D'Orsi C, Green ED, Holbrook AI, Lee S-J, et al. Breast cancer screening. American College of Radiology. ACR Appropriateness Criteria®. 2012. https://acsearch.acr.org/docs/70910/Narrative/. Accessed 12 Sept 2016.
16. D'Orsi CJ, Bassett LW, Feig SA, et al. Illustrated Breast Imaging Reporting and Data System: Illustrated BI-RADS. 5th ed. Reston: American College of Radiology; 2013.
17. Pilar Gazmuri P, Arturo EN. Mamografía "full digital" directa o en campo completo. Experiencia preliminar. Rev Chil Obstet Ginecol. 2002;67(5):343–8.
18. Helvie MA. Digital mammography imaging: breast tomosynthesis and advanced applications. Radiol Clin N Am. 2010;48(5):917–29.
19. Kim SA, Chang JM, Cho N, Yi A, Moon WK. Characterization of breast lesions: comparison of digital breast tomosynthesis and ultrasonography. Korean J Radiol. 2015;16(2):229–38.
20. American College of Radiology. ACR practice parameter for the performance of a breast ultrasound examination. Amended 2016 (Resolution 38). http://www.acr.org/~/media/ACR/Documents/PGTS/guidelines/US_Breast.pdf. Accessed 12 Sept 2016.
21. Ophir J, Céspedes I, Ponnekanti H, Yazdi Y, Li X. Elastography: a quantitative method for imaging

the elasticity of biological tissues. Ultrason Imaging. 1991;13(2):111–34.
22. Gong X, Wang Y, P X. Application of real-time ultrasound elastography for differential diagnosis of breast tumors. J Ultrasound Med. 2013;32:2171–6.
23. Gheonea IA, Stoica Z, Bondari S. Differential diagnosis of breast lesions using ultrasound elastography. Indian J Radiol Imaging. 2011;21(4):301–5.
24. American College of Radiology. ACR practice parameter for the performance of contrast enhanced magnetic resonance imaging (MRI) of the breast. Amended 2013 (Resolution 12). http://www.acr.org/~/media/2a0eb28eb59041e2825179afb72ef624.pdf
25. ACR BI-RADS Atlas. http://www.acr.org/Quality-Safety/Resources/BIRADS. Accessed 12 Sept 2016.
26. Heywang-Köbrunner SH, Heinig A, Pickuth D, Alberich T, Spielman RP. Interventional MRI of the breast: lesion localization and biopsy. Eur Radiol. 2000;10:36–45.
27. Westenend PJ, Sever AR, Beekman-De Volder HJ, Liem SJ. A comparison of aspiration cytology and core needle biopsy in the evaluation of breast lesions. Cancer. 2001;93:146–50.
28. Schoonjans JM, Brem RF. Fourteen-gauge ultrasonographically guided large-core needle biopsy of breast masses. J Ultrasound Med. 2001;20(9):967–72.
29. Morrow M, Strom EA, Bassett LW, Dershaw DD, Fowble B, Giuliano A, American College of Radiology, American College of Surgeons, Society of Surgical Oncology, College of American Pathology, et al. Standard for breast conservation therapy in the management of invasive breast carcinoma. CA Cancer J Clin. 2002;52(5):277–300.
30. Kwong A, Sabel M. Mastectomy: indications, types, and concurrent axillary lymph node management. http://www.uptodate.com/contents/mastectomy-indications-types-and-concurrent-axillary-lymph-node-management. Accessed 12 Sept 2016.
31. Schwartz GF, Giuliano AE, Veronesi U, Consensus Conference Committee. Proceedings of the consensus conference on the role of sentinel lymph node biopsy in carcinoma of the breast, April 19–22, 2001, Philadelphia, Pennsylvania. Cancer. 2002;94(10):2542–51.
32. Cabañas R. An approach for the treatment of penile carcinoma. Cancer. 1977;39:456–66.
33. Hernandez Muñoz G, Barros AC, et al. Ganglio Centinela en Mastología. Editorial Médica Panamericana SA. 2006;75–81.
34. Hernández G, Contreras A, Betancourt L, Acosta V, Pérez BR, Gómez A, et al. Reunión de consenso ganglio centinela en carcinoma de mama. Rev Venez Oncologia. 2010;22(2):133–41.
35. National Cancer Institute. http://www.cancer.gov. Accessed 20 Mar 2016.
36. GLOBOCAN 2012 v1.1, Cancer incidence and mortality worldwide: international agency for research on cancer. http://globocan.iarc.fr. Accessed 20 Mar 2016.
37. Goldgar DE, Easton DF, Cannon-Albright LA, Skolnick MH. Systematic population-based assessment of cancer risk in first-degree relatives of cancer probands. J Natl Cancer Inst. 1994;86(21):1600–8.
38. Johns LE, Houlston RS. A systematic review and meta-analysis of familial prostate cancer risk. BJU Int. 2003;91(9):789–94.
39. Ewing CM, Ray AM, Lange EM, Zuhlke KA, Robbins CM, Tembe WD, et al. Germline mutations in HOXB13 and prostate-cancer risk. N Engl J Med. 2012;366(2):141–9.
40. Eifler JB, Feng Z, Lin BM, Partin MT, Humphreys EB, Han M, et al. An updated prostate cancer staging nomogram (Partin tables) based on cases from 2006 to 2011. BJU Int. 2013;111(1):22–9.
41. Esserman LJ, Thompson Jr IM, Reid B. Overdiagnosis and overtreatment in cancer: an opportunity for improvement. JAMA. 2013;310(8):797–8.
42. Bill-Axelson A, Holmberg L, Garmo H, Rider JR, Taari K, Busch C, et al. Radical prostatectomy or watchful waiting in early prostate cancer. N Engl J Med. 2014;370(10):932–42.
43. Lucca I, Klatte T, Shariat SF. Words of wisdom. Re: radical prostatectomy or watchful waiting in early prostate cancer. Eur Urol. 2014;66(2):386–7.
44. Wilt TJ, Brawer MK, Jones KM, Barry MJ, Aronson WJ, Fox S, Prostate Cancer Intervention versus Observation Trial (PIVOT) Study Group, et al. Radical prostatectomy versus observation for localized prostate cancer. N Engl J Med. 2012;367(3):203–13.
45. Choo R, Klotz L, Danjoux C, Morton GC, DeBoer G, Szumacher E, et al. Feasibility study: watchful waiting for localized low to intermediate grade prostate carcinoma with selective delayed intervention based on prostate specific antigen, histological and/or clinical progression. J Urol. 2002;167(4):1664–9.
46. Carter HB, Kettermann A, Warlick C, Metter EJ, Landis P, Walsh PC, et al. Expectant management of prostate cancer with curative intent: an update of the Johns Hopkins experience. J Urol. 2007;178(6):2359–64.
47. Klotz L, Zhang L, Lam A, Nam R, Mamedov A, Loblaw A. Clinical results of long-term follow-up of a large, active surveillance cohort with localized prostate cancer. J Clin Oncol. 2010;28(1):126–31.
48. Donaldson IA, Alonzi R, Barratt D, Barret E, Berge V, Bott S, et al. Focal therapy: patients, interventions, and outcomes–a report from a consensus meeting. Eur Urol. 2015;67(4):771–7.
49. Shapiro RH, Johnstone PA. Risk of Gleason grade inaccuracies in prostate cancer patients eligible for active surveillance. Urology. 2012;80(3):661–6.
50. King CR, McNeal JE, Gill H, Presti Jr JC. Extended prostate biopsy scheme improves reliability of Gleason grading: implications for radiotherapy patients. Int J Radiat Oncol Biol Phys. 2004;59(2):386–91.
51. Kuru TH, Wadhwa K, Chang RT, Echeverria LM, Roethke M, Polson A, et al. Definitions of terms,

processes and a minimum dataset for transperineal prostate biopsies: a standardization approach of the Ginsburg Study Group for Enhanced Prostate Diagnostics. BJU Int. 2013;112(5):568–77.
52. Barqawi AB, Rove KO, Gholizadeh S, O'Donnell CI, Koul H, Crawford ED. The role of 3-dimensional mapping biopsy in decision making for treatment of apparent early stage prostate cancer. J Urol. 2011;186:80–5.
53. Bittner N, Merrick GS, Bennett A, Butler WM, Andreini HJ, Taubenslag W, et al. Diagnostic performance of initial transperineal template-guided mapping biopsy of the prostate gland. Am J Clin Oncol. 2015;38(3):300–3.
54. Onik G, Barzell W. Transperineal 3D mapping biopsy of the prostate: an essential tool in selecting patients for focal prostate cancer therapy. Urol Oncol. 2008; 26(5):506–10.
55. Crawford ED, Wilson SS, Torkko KC, Hirano D, Stewart JS, Brammell C, et al. Clinical staging of prostate cancer: a computer-simulated study of transperineal prostate biopsy. BJU Int. 2005;96(7): 999–1004.
56. Sivaraman A, Sanchez-Salas R, Barret E, Ahallal Y, Rozet F, Galiano M, et al. Transperineal template-guided mapping biopsy of the prostate. Int J Urol. 2015;22(2):146–51.
57. Fütterer JJ, Briganti A, De Visschere P, Emberton M, Giannarini G, Kirkham A, et al. Can clinically significant prostate cancer be detected with multiparametric magnetic resonance imaging? A systematic review of the literature. Eur Urol. 2015;68(6):1045–53.
58. Barentsz JO, Richenberg J, Clements R, Choyke P, Verma S, Villeirs G, et al. European society of urogenital radiology. ESUR prostate MR guidelines 2012. Eur Radiol. 2012;22(4):746–57.
59. Weinreb JC, Barentsz JO, Choyke PL, Cornud F, Haider MA, Macura KJ, et al. PI-RADS prostate imaging – reporting and data system: 2015, Version 2. Eur Urol. 2016;69(1):16–40.
60. Hamoen EH, de Rooij M, Witjes JA, Barentsz JO, Rovers MM. Use of the Prostate Imaging Reporting and Data System (PI-RADS) for prostate cancer detection with multiparametric magnetic resonance imaging: a diagnostic meta-analysis. Eur Urol. 2015;67(6):1112–21.
61. D'Amico AV, Tempany CM, Cormack R, Hata N, Jinzaki M, Tuncali K, et al. Transperineal magnetic resonance image guided prostate biopsy. J Urol. 2000;164(2):385–7.
62. De Visschere PJ, Briganti A, Fütterer JJ, Ghadjar P, Isbarn H, Massard C, et al. Role of multiparametric magnetic resonance imaging in early detection of prostate cancer. Insights Imaging. 2016;7(2):205–14.
63. Tonttila PP, Lantto J, Pääkkö E, Piippo U, Kauppila S, Lammentausta E, et al. Prebiopsy Multiparametric magnetic resonance imaging for prostate cancer diagnosis in biopsy-naive men with suspected prostate cancer based on elevated prostate-specific antigen values: results from a randomized prospective blinded controlled trial. Eur Urol. 2016;69(3):419–25.
64. Quon JS, Moosavi B, Khanna M, Flood TA, Lim CS, Schieda N. False positive and false negative diagnoses of prostate cancer at multi-parametric prostate MRI in active surveillance. Insights Imaging. 2015;6(4): 449–63.
65. Moore CM, Robertson NL, Arsanious N, Middleton T, Villers A, Klotz L, et al. Image-guided prostate biopsy using magnetic resonance imaging-derived targets: a systematic review. Eur Urol. 2013;63(1): 125–40.
66. Onik G, Narayan P, Vaughan D, Dineen M, Brunelle R. Focal "nerve-sparing" cryosurgery for treatment of primary prostate cancer: a new approach to preserving potency. Urology. 2002;60(1):109–14.
67. Onik G, Vaughan D, Lotenfoe R, Dineen M, Brady J. The "male lumpectomy": focal therapy for prostate cancer using cryoablation results in 48 patients with at least 2-year follow-up. Urol Oncol. 2008;26(5): 500–5.
68. Bahn DK, Silverman P, Lee Sr F, Badalament R, Bahn ED, Rewcastle JC. Focal prostate cryoablation: initial results show cancer control and potency preservation. J Endourol. 2006;20(9):688–92.
69. Lambert EH, Bolte K, Masson P, Katz AE. Focal cryosurgery: encouraging health outcomes for unifocal prostate cancer. Urology. 2007;69(6):1117–20.
70. Ahmed HU, Freeman A, Kirkham A, Sahu M, Scott R, Allen C, et al. Focal therapy for localized prostate cancer: a phase I/II trial. J Urol. 2011;185(4): 1246–54.
71. Ellis DS, Manny Jr TB, Rewcastle JC. Focal cryosurgery followed by penile rehabilitation as primary treatment for localized prostate cancer: initial results. Urology. 2007;70(6 Suppl):9–15.
72. de la Rosette J, Ahmed H, Barentsz J, Johansen TB, Brausi M, Emberton M, et al. Focal therapy in prostate cancer-report from a consensus panel. J Endourol. 2010;24(5):775–80.
73. Ward JF, Jones JS. Focal cryotherapy for localized prostate cancer: a report from the national Cryo On-Line Database (COLD) Registry. BJU Int. 2012;109(11):1648–54.
74. Valerio M, Emberton M, Barret E, Eberli D, Eggener SE, Ehdaie B, et al. Health technology assessment in evolution – focal therapy in localised prostate cancer. Expert Rev Anticancer Ther. 2014;14(11):1359–67.
75. Tempany CM, McDannold NJ, Hynynen K, Jolesz FA. Focused ultrasound surgery in oncology: overview and principles. Radiology. 2011;259(1):39–56.
76. Valerio M, Ahmed HU, Emberton M, Lawrentschuk N, Lazzeri M, Montironi R, et al. The role of focal therapy in the management of localised prostate cancer: a systematic review. Eur Urol. 2014;66(4):732–51.
77. Ahmed HU, Hindley RG, Dickinson L, Freeman A, Kirkham AP, Sahu M, et al. Focal therapy for localised unifocal and multifocal prostate cancer: a prospective development study. Lancet Oncol. 2012; 13(6):622–32.
78. Azzouzi AR, Barret E, Moore CM, Villers A, Allen C, Scherz A, et al. TOOKAD(®) Soluble vascular-targeted

photodynamic (VTP) therapy: determination of optimal treatment conditions and assessment of effects in patients with localised prostate cancer. BJU Int. 2013;112(6):766–74.
79. Oto A, Sethi I, Karczmar G, McNichols R, Ivancevic MK, Stadler WM, et al. MR imaging-guided focal laser ablation for prostate cancer: phase I trial. Radiology. 2013;267(3):932–40.
80. Li W, Fan Q, Ji Z, Qiu X, Li Z. The effects of irreversible electroporation (IRE) on nerves. PLoS One. 2011;6(4):e18831.
81. Valerio M, Stricker PD, Ahmed HU, Dickinson L, Ponsky L, Shnier R, et al. Initial assessment of safety and clinical feasibility of irreversible electroporation in the focal treatment of prostate cancer. Prostate Cancer Prostatic Dis. 2014;17(4):343–7.

Targeted Therapy for Localized Kidney Cancer

2

Zhamshid Okhunov, Roshan M. Patel, and Jaime Landman

Introduction

Kidney cancer is among the ten most common cancers in men and women, accounting for approximately 62,700 of new cases and 14,240 deaths per year in the United States [1]. Due to the increased use of cross-sectional imaging for abdominal imaging in recent decades, there has been a significant rise in the incidental detection and subsequent treatment of renal cortical neoplasms (RCN) [2]. The majority of RCN are discovered in early stages resulting in a paradigm shift in the management of small renal mass (SRM) (T1a). Historically, the standard treatment for all RCN, including SRM, was radical nephrectomy, although the management of RCN has evolved with the advancement of minimally invasive technology. The development of laparoscopic nephrectomy (LRN) in the 1990s—a technique first described by Clayman, Kavoussi, and colleagues—commenced a new era in treatment of RCN [3]. Consequently, LRN became the preferred treatment option for RCN. The pervasive use of LRN, however, led to two major sequelae. First, radical nephrectomy (RN) by any technique resulted in diminished renal function, which has been associated with poor cardiovascular outcomes, and decreased survival [4–7]. Second, insight into the natural history and progression of SRM was impeded due to the extensive use of RN.

Partial nephrectomy (PN) gradually emerged as a viable alternative to RN in the treatment of RCN, representing a nephron-sparing approach capable of averting chronic kidney disease (CKD) and cardiovascular sequelae associated with RN. Evidence of excellent outcomes following partial nephrectomy for SRM led the American Urological Association (AUA) to recommend that partial nephrectomy become the gold standard for all T1 ($\leq$7 cm) lesions when surgically feasible [8].

Recently, further advances in minimally invasive technology have expanded the spectrum of available treatment modalities for SRM. Treatments now include laparoscopic PN (LPN) and robot-assisted PN (RAPN), in addition to ablative modalities and active surveillance. While PN remains the current gold standard treatment for RCN [9], thermal ablation (TA) has emerged as a viable, less-invasive alternative to surgical extirpation, for patients who are poor surgical candidates, those with bilateral tumors or functioning solitary kidney. Cryoablation (CA), which may be delivered both laparoscopically (LCA) or percutaneously (PCA), and radiofrequency

Z. Okhunov • R.M. Patel • J. Landman (✉)
Department of Urology, University of California, Irvine, Orange, CA, USA
e-mail: landmanj@uci.edu

© Springer International Publishing AG 2017

T.J. Polascik (ed.), *Imaging and Focal Therapy of Early Prostate Cancer*, Current Clinical Urology, DOI 10.1007/978-3-319-49911-6_2

ablation (RFA) represent two TA modalities that have been best studied. Long-term retrospective studies regarding the efficacy of CA and RFA are emerging, allowing assessment of their viability as alternatives to PN. Several other TA technologies have also been developed, including high-intensity focused ultrasound (HIFU), laser interstitial thermal ablation, radiosurgery, and microwave ablation. In contrast to CA and RFA, few studies have addressed the efficacy of these approaches. This chapter will focus on LCA, PCA, and RFA, highlighting their indications, surgical approaches, and long-term oncological outcomes as therapeutic options for SRM.

The Small Renal Mass Dilemma

With the advancement of minimally invasive techniques, several treatment modalities are now available to patients for the treatment of RCN. While large RCN (> 4 cm lesions) are frequently extirpated by either PN or RN, determining the optimal approach for SRM (≤ 4 cm lesions) is more complex. In addition, considering factors such as patient age, patient preference, tumor size, and physician preference, among others, there may be a role for renal mass biopsy in influencing treatment decisions. In current AUA guidelines (updated 2011), active surveillance (AS), TA approaches (e.g., CA and RFA), and PN are all considered viable treatment options for T1a and T1b tumors, although PN remains the gold standard treatment.

As the literature on SRM has matured, the natural history of SRM is gradually being elucidated. It is now known that approximately 20 % of SRMs are benign, while another 50–60 % display low-grade features, and the remaining 20–30 % display aggressive features [10–12]. Given that a significant percentage of SRMs are benign or relatively indolent, surgical intervention may now be delayed or avoided following appropriate diagnostic workup.

A large series recently published by our group indicated that most SRMs grow slowly, with a growth rate of 0.34 cm/year and low metastatic rate (1.9 %), suggesting that AS is a reasonable treatment option for RCN in older patients [13]. Similarly, another study reported comparable findings with SRM having an annual tumor growth rate of 0.31 cm/year and 1.4 % metastatic rate [14]. The AUA guidelines panel concluded these rates of metastasis were sufficiently low and concluded that AS is a reasonable option in certain patient populations. Recent studies now point to expanding the use of AS. A study by Patel and colleagues suggested that AS appears to provide oncological efficacy equivalent to surgery, at least in the short- and intermediate-term management of SRM—a finding that requires confirmation in further studies [15]. It is now also thought that T1b and T2 renal tumors demonstrate similar growth rates compared to smaller T1a tumors. Growth rates for these tumors were found to be 0.58 cm/year, and this suggests AS may represent a viable treatment option even in larger renal tumors and should be considered in patients presenting with significant competing risks or limited life expectancy [16, 17].

Partial nephrectomy remains the current gold standard treatment of T1a renal cell carcinoma (RCC), although long-term follow-up data on CA and RFA and results from emerging studies involving AS may warrant reassessment of treatment indications. As data continues to emerge and the role of renal biopsy has been expanding, the algorithm of directing the urologist toward immediate nephron-sparing surgical extirpation may continue to be amended to support increased use of AS and ablative therapy. Patients seeking to avoid surgical resection can now be directed toward ablative therapy, given promising long-term data supporting its routine use. With the guidance of renal biopsy, AS also must be considered a viable alternative both as a strategy in initial management of non-aggressive SRM and in management of small recurrences following ablative or extirpative therapy. In the elderly, given the morbidity of active treatment, it is recommended that AS should be instituted followed by a minimalistic approach, such as ablation in those patients who progress or do not tolerate AS [18].

Renal Biopsy

Traditionally, most solid RCN were presumed to be malignant and treated with surgical extirpation. However, contemporary series have demonstrated that only 80 % of tumors less than 4 cm are malignant and that only a minority are high grade with potentially aggressive features [12]. Given the knowledge that at least 20 % of tumors are benign or relatively indolent, with proper diagnostic workup, there are many instances in which surgical intervention can be delayed or avoided completely [19]. The prediction of histopathology based on preoperative imaging such as computed tomography (CT) or magnetic resonance imaging (MRI) is limited and contemporary imaging modalities do not provide sufficient, reliable, and reproducible information for differential diagnosis of benign tumors, except for angiomyolipoma [20]. Percutaneous renal mass biopsy (RMB) has emerged as a reliable and safe diagnostic procedure to preoperatively characterize the histology and grade of SRMs. With a variety of treatment modalities available for SRMs, including AS, extirpative surgery, and TA technologies, indications for a RMB are expanding. Several studies have used RMB as a guide in treatment decisions in the management of patients with RCN [21–23].

The overview of contemporary series of RMB is provided in Table 2.1 [23–34]. Diagnostic rate and accuracy of SRM biopsy have steadily improved, and in contemporary series, it may be greater than 90 %. This is related to accumulating and growing experience with the procedure, continuous improvement in biopsy techniques, and facilitating technology [24]. Contemporary technology now allows the assessment of the histopathology of renal masses to properly counsel the patients and select the optimal treatment strategy [35]. Although minimally invasive treatment options for RCC have expanded, preoperative diagnosis is crucial for their proper use. According to meta-analysis performed by Kutikov and colleagues, only 75.8 % of patients who underwent CA had proven malignancy during intraoperative biopsy [36]. More than 20 % of patients who have had a benign histopathology with no potential threat to the patient still underwent ablative procedures. This and many other reports again raise a concern of an overtreatment of many indolent SRMs. Surgical resections or ablation may not be necessary for benign and certain indolent malignant RCN. In a study by Hu and colleagues, who evaluated the role of biopsy in the management of 206 patients with SRM, the diagnostic rate was 89 %. Of these, 84 % of patients who had biopsy-proven benign disease avoided any surgical intervention and were actively surveyed [35]. The consequences of indeterminate biopsy results are unknown and challenging to define. It is impossible to determine the relationship between the indeterminate and negative biopsy results if the patient did not undergo surgical extirpation. This topic is increasingly becoming one of concern [37]. Jewett and colleagues performed a repeat biopsy on patients with initially non-diagnostic biopsy results and demonstrated a malignancy diagnostic rate of 80 %, which was similar to initial biopsy rate [25]. This study has demonstrated that repeat RMB is feasible, safe, and can be expected to identify tumors with a similar success rate as the initial overall biopsy cohort.

Additionally, percutaneous RMB has been reported to be safe with the overall mean rate of minor and major complications of 5 % and 0.02 %, respectively (Table 2.1). In experienced centers, most complications are limited to local hematoma with minimal morbidity. With the contemporary facilitated ultrasound (US) technology and properly selected patients, the procedure can be performed in less than 15 minutes in an outpatient office setting [35].

Preoperative histopathological diagnosis of SRM with percutaneous biopsy along with other patient-related factors such as age, tumor size, and existing patient comorbidities is crucial in the decision-making process and selecting the most optimal treatment modality for patients with SRM. Beyond the fact that many SRMs are benign, there are major biologic differences between RCC subtypes, which may impact management strategies. As such, pretreatment biopsy should be considered for all RCN.

Table 2.1 Small renal mass biopsy series (2004–2015)

Authors	No. of patients	Mean size (cm)	Diagnostic rate (%)	Malignancy rate (%)	Complication rate (major/minor) (%)
Eshed et al. 2004 [26]	23	3.0	95.5	68.2	0/4.5
Neuzillet et al. 2004 [27]	88	2.8	96.6	75	0/0
Jaff et al. 2005 [34]	46	3.3	85.2	57.4	0/0
Shannon et al. 2008 [28]	222	2.9	78	75	0/0.9
Schmidbauer et al. 2008 [29]	78	4.0	97	79	0/3
Wang et al. 2009 [30]	106	2.7	90.9	65	0/7.5
Leveridge et al. 2011 [25]	294	2.5	80.6	79.4	0.3/10.1
Tan et al. 2012 [31]	78	2.9	93.6	89	N/A
Park et al. 2013 [32]	58	2.4	81	77	0/20.3
Menogue et al. 2013 [33]	250	2.5	80	74	0/0.7
Halverson et al. 2014 [23]	151	2.8	91.7	97.4	N/A
Hu et al. 2015 [24]	269	3.4	89	77	N/A
Overall	1663	2.9	88.3	76.1	0.02/5.22

Tumor seeding along the biopsy needle tract is exceedingly rare. There are only three documented events in the last three decades [38–41]. Akhavein and colleagues reported a case of an 84-year-old man with an asymptomatic 2.7 cm enhancing lower pole renal masses. Preoperative radiological evaluation demonstrated no evidence of metastases, and preoperative biopsy confirmed histopathological diagnosis of a clear cell renal cell carcinoma [41]. Due to the patient's comorbidities, percutaneous cryoablation was recommended. The patient underwent an uneventful percutaneous cryoablation with no evidence of residual disease at the termination of the procedure and at 5 and 12 months of follow-up. However, the patient underwent surveillance imaging at 15 months post-ablation, and while there was no evidence of local recurrence, he had numerous soft tissue nodules in the retroperitoneal fat posterior to the kidney, consistent with seeding in the cryoablation probe tract. Histopathological confirmation with biopsy was not possible due to an intraoperative complication, and the patient was managed with systemic therapy and close imaging surveillance. Sainani and colleagues reported another event of RCC seeding along the cryoablation probe tract [39]. A 61-year-old man with three bilateral masses on each side with a biopsy-proven RCC and oncocytoma underwent MRI-guided percutaneous cryoablation of three tumors and extirpative procedure for the remaining tumors that were not deemed amenable for an ablative procedure. In 4 years after the initial procedure, imaging revealed new enhancing soft tissue nodules up to 1.2 cm in the right retroperitoneum and paraspinal musculature. CT-guided biopsies revealed papillary RCC, and all enhancing lesions were managed with CT-guided cryoablation. At the follow-up imaging, there was no evidence of tumor. Mullins and Rodriguez reported a third case of RCC seeding of a percutaneous biopsy tract [38]. They reported a case of a 68-year-old man with papillary-type RCC who underwent a percutaneous biopsy. Local extension was detected at the time of partial nephrectomy, and biopsy confirmed papillary-type RCC. The patient underwent successful surgical excision of the tumor with no evidence of tumor recurrence on subsequent imaging surveillance.

These reports are very rare and should not discourage the use of percutaneous image-guided procedures such as biopsy or ablation. Proper actions can be taken to prevent these events [42].

Role, Indications, and Contraindications of Ablative Therapy

Given that most patients with SRM are elderly (>70 years) and present with significant comorbidities, it is important to balance the risks of surgical treatment with less-invasive ablative approaches and active surveillance.

The rationale for AT is to treat asymptomatic SRM in patients at high surgical risk with potentially reduced morbidity. Other potential indications include renal insufficiency, solitary kidney, transplant patients, and multiple or bilateral masses. With contemporary technology and techniques, these procedures can be performed in outpatient setting using image guidance with significantly reduced morbidity. The limitation for treating a renal lesion with CA is largely dependent upon obtaining an adequate ablation zone with the current technology. The larger the renal lesion, the more challenging it becomes to completely cover the lesion with the iceball while avoiding complications such as tumor cracking and bleeding. Patient preference plays an important role in selecting the choice of treatment. The less-invasive nature of renal ablation makes this modality very attractive for elderly patients with serious medical comorbidities who desire active treatment.

Contraindications to AT are tumors with a low chance of successful treatment, including tumor size greater than 3.5 cm. Location is another important factor to consider; posteriorly and laterally located tumors are more amenable for image-guided PCA. More anterior tumors are treated via laparoscopic approach. Hilar tumors close to the renal vasculature, ureter, and collecting system should avoid AT due to an increased risk of major complications and risk of recurrence.

Surgical Approach

CA and RFA are the most extensively characterized TA modalities. Both can be pursued laparoscopically or percutaneously under image guidance. The surgical approach is largely dependent on the location of the renal mass (Fig. 2.1). Lesions located on the anterior aspect of the kidney are more suitably approached laparoscopically via a transperitoneal approach, while posteriorly and laterally located tumors are best approached either percutaneously (CT or MRI guided) or via a retroperitoneal laparoscopic technique. Given the difficulties in approaching lateral tumors, they present a small challenge with the approach being based on surgeon preference. The majority of RFA is performed percutaneously, while CA has been well described both laparoscopically (trans- and retroperitoneally) and percutaneously. Another significant factor is the availability of CT ablation suites and having a good working relationship with an interventional radiology team. Interventional radiologists have extensive knowledge of image-guided ablation and can be outstanding partners for achieving optimal treatment outcome.

Patient Preparation

Preoperatively, patients should undergo a history and physical examination that includes a complete set of vitals, careful review of the past medical and surgical history, social history including smoking history, and a review of their medications. Laboratory examination should include a complete metabolic panel, complete blood count, and, when appropriate, a coagulation panel. All patients over the age of 40 should undergo a preoperative electrocardiogram and a

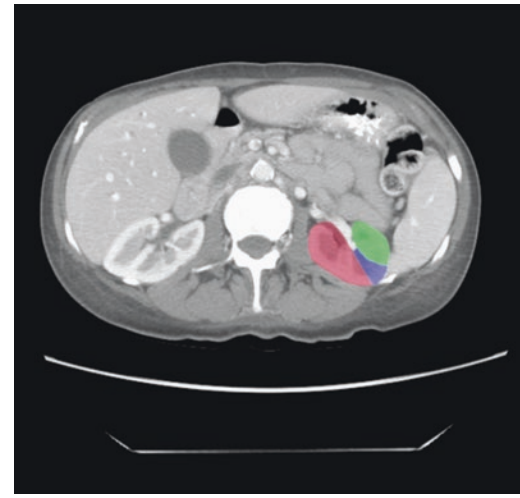

Fig. 2.1 Tumors located on the posterior aspect of the kidney (*red*) are ideally approached either percutaneously or via retroperitoneal laparoscopy. Tumors located on the anterior aspect of the kidney (*green*) are ideally approached by transperitoneal laparoscopy. Tumors located on the lateral aspect of the kidney (*blue*) can be approached by any technique

chest X-ray. Elevated liver enzymes may suggest either Stauffer's syndrome or, perhaps more ominous, metastasis to the liver. Careful reevaluation of the liver with axial imaging is warranted. Abnormal neurological findings or recent onset of headaches or blurred vision should prompt the surgeon to investigate the possibility of brain metastasis with a head CT or MRI. Similarly, complaints of bony pain, especially with concomitant elevations in serum alkaline phosphatase and/or calcium, could be indicative of bony metastasis, which should be evaluated with a nuclear bone scan. Finally, anticoagulants, including aspirin products, should be discontinued for an appropriate amount of time prior to treatment, and these patients should often be managed in conjunction with a medical team. The goal of this extensive preoperative routine is to identify potential obstacles that may affect surgical outcome. For example, vital signs may identify poorly controlled or previously unidentified hypertension, which places the patient at risk for intraoperative and postoperative bleeding, or labs that reveal a coagulopathy may increase bleeding diathesis. A thorough preoperative workup will stratify individual patients into the various management strategies mentioned earlier.

Recent high-quality axial imaging via CT or MRI with and without intravenous contrast is a key component to every preoperative routine. Poor quality or inadequate imaging may compromise surgical outcomes and should therefore be repeated prior to discussing management strategies. The surgeon should take special note of tumor characteristics such as size; location, especially in relation to the upper, lower, and interpolar regions, hilum and the collecting system (especially the ureter and ureteropelvic junction); and enhancement properties. Additionally, renal landmarks should be identified to aid in intraoperative location of the mass. Other metrics that should be recorded include whether the mass is exophytic ($\geq$ 50 % of mass extending beyond renal contour), mesophytic (20–50 % of mass beyond renal contour), cystic or solid, enhancement qualities, and abnormalities of shape or contour that may have to be accounted for during TA [43]. Additionally, recent evidence supports the use of the RENAL nephrometry score (Radius, Exophytic/endophytic properties, Nearness of the tumor to the collecting system or sinus, Anterior/posterior, Location relative to the polar lines) as a preoperative metric capable of predicting PN, LCA, and PCA complexity, complication rates, and outcomes [44–50]. Okhunov and colleagues demonstrated that tumors with RENAL nephrometry of higher than eight have significant risks for complications and local tumor recurrences after LCA [44]. Blute and colleagues also confirmed these findings in patients undergoing PCA. With each increase in RENAL nephrometry score, the risk of complications and recurrence increases 1.5-fold [51]. Additionally, skin-to-tumor distance has been shown to be an important factor in patients undergoing PCA. While the RENAL nephrometry score does not appear to be predictive of complications in RFA [52, 53], a modified RENAL score, using an adjusted size variable, R, may allow more accurate prediction and stratification of outcomes [54].

Occasionally, despite the use of high-quality axial imaging, the renal mass is difficult to discern from the surrounding normal renal parenchyma. This can be especially true with endophytic lesions. A preoperative ultrasound of the kidney may help characterize and further delineate the lesion. This may also prove useful since ultrasonography is the primary intraoperative imaging modality utilized in LCA. If the lesion is isoechoic on preoperative ultrasound, it may be difficult to accurately locate at the time of LCA, and options should be preoperatively discussed with the patient.

Principles of Ablation

As new technologies continue to shape the surgical landscape, it is the responsibility of the surgeon to fully understand the method of action, capabilities, and limitations of each new advancement in order to optimize outcomes. This is especially true of TA, which utilizes unique energy

delivery systems, different methods of action for tissue destruction, and different targeting and monitoring systems. A proper appreciation for the various treatment modalities improves efficacy and decreases the complication rate.

Cryoablation

Cryoablation was first described in 1995 by Uchida and colleagues [55], and it is currently the most studied of all ablative modalities in the treatment of SRM. CA exploits the Joule-Thomson principle to produce rapid temperature decreases at the probe tip [56]. At room temperature, with the exceptions of hydrogen, helium, and neon, all gases cool upon expansion. As gas molecules expand, collision rates between molecules decrease, thereby increasing potential energy and decreasing kinetic energy and therefore temperature. Specifically, the modern system utilizes highly pressurized liquid state argon gas that is allowed to expand into the gaseous state near the tip of the probe. The resulting expansion and phase change causes extreme drops in temperature, which induces iceball formation. Iceball dimensions and ablation zones are largely affected by the probe's design (at what point the gas is allowed to expand and changes in insulation) along with local tissue properties. The iceball does not extend appreciably beyond the tip of the probe but instead extends radially and proximally along the shaft of the probe.

There are several mechanisms that are ultimately responsible for cell death. The rapid cooling initially produces extracellular ice crystal formation followed by intracellular ice crystal formation. The intracellular crystals mechanically disrupt the cell membrane causing dramatic changes in intracellular pH and ionic composition, ultimately leading to protein denaturation. The extreme temperatures bring about local microcirculatory failure, which causes thrombosis, coagulation necrosis, and apoptosis. The dramatic fall in temperature additionally amplifies the extracellular osmotic force resulting in cellular crenation and dehydration. The sum of these effects is uniform cellular death within the ablation zone.

There is not one consistent temperature within the iceball but actually a gradient that extends from −140 to −190 °C at the cryoprobe tip to −3 °C at the edge of the iceball [57]. The phenomenon known as freezing point depression necessitates a temperature below 0 °C at the edge of the iceball. When solutes are added to a solvent, in this case the saline environment of tissue, these ions interfere with ice formation requiring a temperature below freezing in the periphery. This important property of the iceball is the main determinant in CA success and failures. While there is *extracellular* ice crystal formation at the iceball edge, there are no *intracellular* ice crystals, and it is the *intracellular* ice that causes cell lysis. Cellular death begins to occur at temperatures below −20 °C but is somewhat inconsistent [58]. Uniform and consistent cellular necrosis does not occur until temperatures fall below −40 °C. When the iceball temperature gradient is combined with the temperature requirements for cell death, three "zones" with different ablation properties are created within the iceball (Fig. 2.2). The central zone extends from the cryoprobe tip to the points within the iceball that are consistently below −40 °C. This central zone is characterized by consistent and uniform cellular necrosis. The intermediate zone comprises the iceball area that has reached temperatures between −40 °C and −20 °C and is characterized by both necrotic and viable tissue elements. The outer zone extends from −20 °C to the warmer iceball edge and is characterized by mostly viable tissue. It has been determined that temperatures of >−20 °C can be measured within 3.1 mm of the iceball edge [59]. Therefore, the standard practice in CA is to extend the iceball to 1 cm beyond the tumor edge to ensure uniform tissue ablation. One of the advantages of LCA is the ability to monitor iceball formation in real time using a laparoscopic ultrasound probe. The expanding iceball creates a readily visualized hyperechoic expanse that delineates the iceball edge (Fig. 2.3). After the freeze cycle is complete, helium is used to actively thaw the cryoprobe followed by a repeat freeze-thaw cycle to ensure complete ablation.

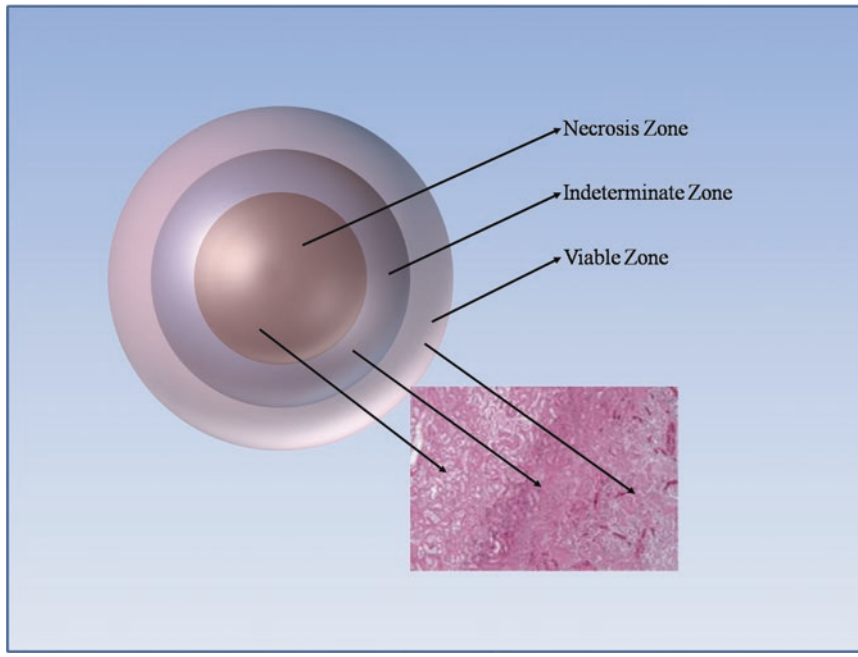

Fig. 2.2 Iceball ablation zones: The central/necrosis zone is characterized by uniform ablation and temperatures < −40 °C. Surrounding the central zone is the indeterminate zone, which has areas of cell death intermixed with viable cells and temperatures between −40 °C and −20 °C. The outermost zone is comprised of mostly viable cells with little to no necrosis and temperatures > −20 °C

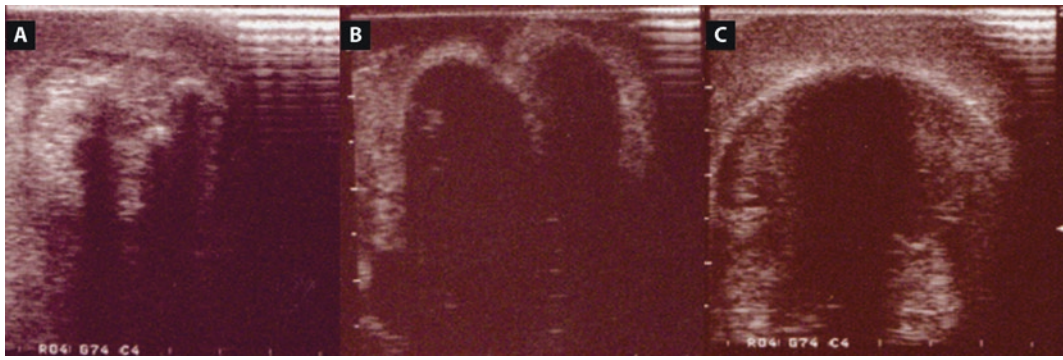

Fig. 2.3 (**a**) At the start of the freeze cycle, the iceball appears as an expanding hyperechoic region extending radially from the cryoprobes. (**b**) The hyperechoic regions begin to coalesce as the iceball expands. (**c**) At the completion of the freeze cycle, the iceball appears as a single hyperechoic mass that extends beyond the margin of the mass

Radiofrequency Ablation

The first report of RFA in the human kidney was in 1997 by Zlotta and colleagues, who utilized RFA in the treatment of exophytic renal masses in three patients [60]. After studies demonstrating safety and short- and intermediate-term efficacy, RFA has since gained significant popularity as a technique to ablate SRM. RFA induces thermal injury through a high-frequency, alternating electric current with a wavelength of 460–500 kHz that exploits the resistive properties of the kidney [61–63]. Probes introduced into the ablation zone deliver the electrical current to the target area, inducing the resistive heating of tissues adjacent to the electrode (Joule effect). The

local tissue's high resistance allows dramatic increases in temperature as the electrical current is transformed to heat, resulting in ionic agitation, denaturation of proteins, membrane damage, and vascular congestion [64]. Cellular injury does not typically occur until temperatures reach 50 °C for 4 to 6 min [65]. Instantaneous coagulative necrosis occurs as temperatures climb over 60 °C [66]. Given that temperatures over 105 °C induce tissue vaporization and ineffective ablation, RFA is optimally performed at temperatures 60–100 °C. To ensure adequate treatment, the ablation zone is extended to 1 cm beyond the tumor periphery. Because the ablation zone cannot be monitored in real time in RFA, temperature or impedance probes are placed near the area of interest to determine the extent of the effect.

Cryoablation Techniques

Maximizing the success of CA involves a combination of appropriate patient selection, understanding, and appropriately applying cryosurgical technology, adhering to the "imaging trifecta," precise initial probe placement, and accurate iceball management with a willingness to make intraoperative adjustments to any inconsistencies. Patient selection has been discussed elsewhere in this chapter, but in brief, the ideal patient has a mass ≤3.5 cm in size and has been preoperatively evaluated and counseled appropriately, and the approach has been tailored to the tumor location. The imaging trifecta refers mostly to the laparoscopic approach but certainly pertains to all TA modalities. The first part is the preoperative, high-quality imaging that allows the surgeon to accurately characterize the mass. The second is the liberal use of intraoperative imaging including laparoscopic ultrasound (LCA). Laparoscopic approach for renal ablation is used infrequently but still remains an option in selected patients with anteriorly located tumors. For image-guided PCA, US and CT or a combination of both is used during the tumor evaluation and probe placement. The final aspect is careful iceball monitoring during the freeze-thaw cycles to ensure that the iceball forms as expected with all of the expected margins extending beyond the mass. Correct initial probe placement might be among the most important determinants in success. Once the iceball begins to form, the probe cannot be repositioned, and furthermore, the expanding iceball creates a large acoustic shadow that makes targeting of the deep tissues difficult (Fig. 2.4). Occasionally, local tissue properties and/or poor initial probe placement creates an iceball that does not completely ablate the tumor. When this occurs, the surgeon should allow the probes to thaw, reassess, and reposition the probes and perform a repeat cycle to ensure complete tissue destruction.

Laparoscopic Cryoablation

After the patient is repositioned, trocars are placed in a standard nephrectomy template. The colon is reflected medially, and if on the right side, the duodenum is kocherized. The psoas muscle is identified as it courses posteromedial to the lower pole of the kidney. At this point, we usually place a laparoscopic retractor (Jarit® Padron Endoscopic Exposing Retractor

Fig. 2.4 The fully formed iceball obscures the deep margins due to a shadowing effect

(P.E.E.R.), Integra, Plainsboro, NJ) through a 5-mm port positioned in the midaxillary line or just anterior to it. This not only allows the kidney to be elevated for the remainder of the dissection but also for it to be positioned and stabilized in a manner that optimizes the renal mass' position during the actual ablation.

For lesions that are >3.5 cm or are exophytic, there is an increased risk for iceball cracking with subsequent major bleeding. In patients in whom this is a concern, the routine practice is to prepare the kidney as if a partial nephrectomy was going to be performed. The renal artery and vein are completely exposed, and Gerota's fascia is dissected away from the mass and the surrounding normal renal parenchyma. In this manner, should iceball cracking occur, clamping the renal artery can rapidly attain hemostasis, and the surgeon can proceed with partial nephrectomy without delay.

In order to maximize ablation efficacy, the cryoprobes should enter the intended ablation zone perpendicular to the mass. Tangentially placed probes are difficult to accurately position and often lead to viable residual tumor. First the kidney is manipulated to expose the renal mass to the anterolateral flank using the PEER to stabilize it. A BD™ Spinal Needle (BD Medical, Franklin Lakes, NJ) is used as a "finder needle" by passing it percutaneously until an ideal perpendicular trajectory is identified. A skin incision is then made adjacent to the spinal needle and several biopsies of the mass are taken using a Bard® MaxCore Disposable Core Biopsy Instrument (18G × 25 cm, Bard Peripheral Vascular, Inc./Bard Biopsy Systems, Tempe, AZ). The cryoprobes are then deployed at the predefined trajectory to sit at right angles to the mass. There are a variety of probes that are currently available; however, we prefer the IceRod cryoprobe (Galil Medical, Minneapolis, MN) due to its small size (1.47 mm) and consistently large ablation zone.

Of all the steps in renal ablation, accurate cryoprobe deployment ranks among the most important. It should be recognized that the iceball extends radially along the shaft of the probe, but does not extend appreciably beyond the tip [67]. To avoid deep margin recurrence, the probes should therefore be positioned 5 mm beyond the tumor. For solid masses, the probes are placed just within the tumor's margin. If the mass has cystic components, the cryoprobes are placed just outside the margin to avoid rupture and subsequent tumor spillage. Once the freeze cycle begins, the expanding iceball obscures the margins, making subsequent probe placement more challenging.

Tumor identification, especially endophytic tumors, probe deployment, and active iceball monitoring are all facilitated by the use of a laparoscopic ultrasound probe. Typically two freeze-thaw cycles are performed to ensure complete ablation, during which active ultrasonography ensures that the iceball extends 1 cm beyond the margins. In this manner, cryoablation is unique among other TA techniques in that the direct visualization of the growing iceball verifies complete ablation of the intended target. Following the second thaw cycle, the probes are removed, and the kidney is observed for a short period of time.

Percutaneous Cryoablation

Our team has found that optimizing successful outcomes with PCA requires close collaboration between interventional radiology (IR) and urology. The interventionist provides experience with percutaneous targeting and imaging modalities, while the urologist provides expertise and insight into the treatment of renal malignancies. As mentioned previously, PCA is usually reserved for tumors on the posterior and lateral aspect of the kidney. Because the probes are passed from the posterolateral flank into the kidney, performing PCA on an anterior renal mass requires traversing a significant portion of the kidney and is not recommended.

The "as low as reasonably achievable" (ALARA) principle states that the lowest dosage of ionizing radiation necessary should be used to achieve the desired therapeutic or diagnostic goal, without compromising quality of care. At University of California, Irvine we developed a

technique combining the use of US in conjunction with CT imaging for PCA of renal masses. This technique is used in an effort to reduce the total radiation dose per procedure.

The patient is placed prone on a CT scanner or, if the probes are MRI compatible, on an MRI scanner. Intravenous sedation utilizing midazolam and fentanyl is initiated with monitoring in accordance with the UC Irvine Moderate Sedation Policy. Local lidocaine 1 % is used for local anesthesia. In CT-guided cases, US is used to localize the tumor (Fig. 2.5a), and the intended initial access location is identified. Initial probe placement is performed under US (Fig. 2.5b). A focused non-contrast axial image is then obtained through the area of the kidney and compared to the preoperative contrast image (Fig. 2.5c, d). Based upon CT findings, the initial probe placement is optimized if necessary. If the tumor margins cannot be clearly identified, a repeat scan with a half bolus of intravenous contrast can be performed. Additional cryoprobes (up to a total of 3) are placed under US guidance, with limited axial CT acquisition used for final confirmation of optimal probe position. Probes are positioned one at a time, ensuring that the tips extend at least 5 mm beyond the deep margin. Careful attention should be paid when deploying multiple probes to avoid confusion in matching the intracorporeal cryoprobes as seen on axial imaging to the extracorporeal shafts as seen by the surgeon. Once desired cryoprobe deployment is achieved, a

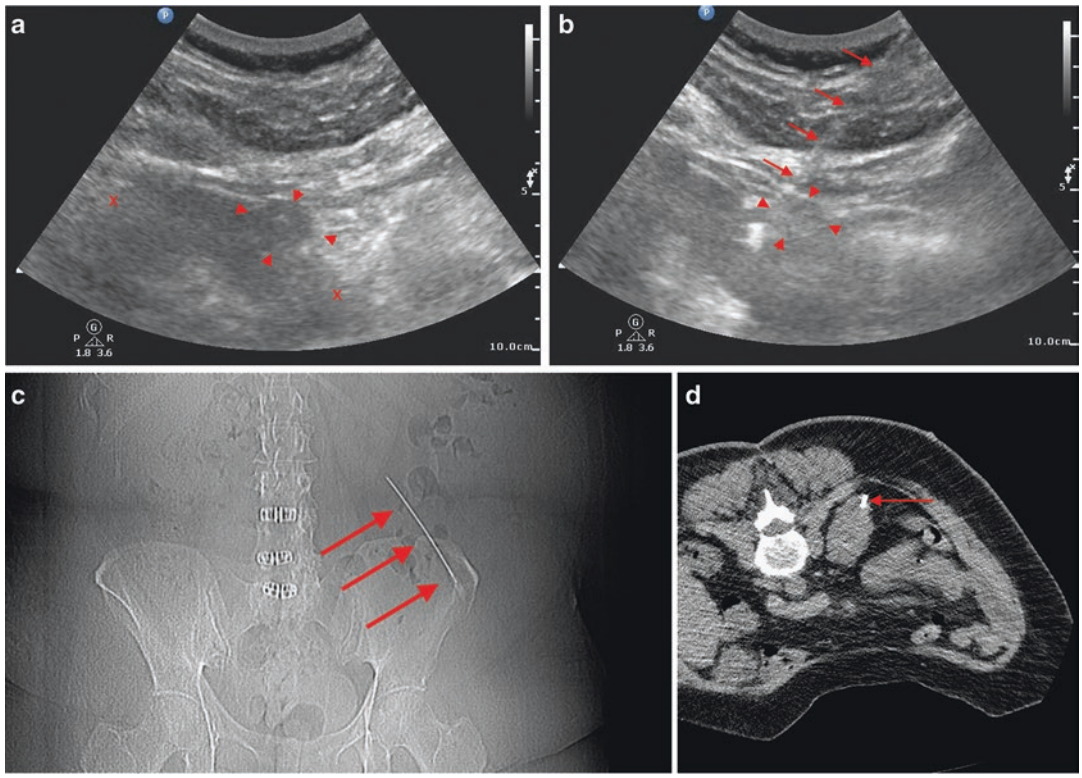

Fig. 2.5 Imaging of ultrasound-facilitated computed tomography-guided percutaneous cryoablation. (**a**) Long axis ultrasound image of the left kidney. Xs indicate superior and inferior poles of kidney. *Solid arrowheads* delineate borders of the cortical neoplasm. (**b**) Long axis ultrasound image of the left kidney. *Solid arrows* mark the cryoprobe traversing subcutaneous fat, muscle, and perirenal fat with tip of the first cryoprobe within the superior aspect of the neoplasm. *Solid arrowheads* mark the cortical neoplasm. (**c**) Scout computed tomography image demonstrates the presence of initial cryoprobe, placed under ultrasound guidance. *Solid arrows* mark cryoprobe. (**d**) Initial low-dose limited axial computed tomography images confirming cryoprobe location within the cortical neoplasm after initial ultrasound-guided placement. *Solid arrow* identifies cryoprobe tip within the neoplasm

standard double freeze-thaw cycle is performed with the goal of extending the iceball approximately 1 cm beyond the tumor margins in all directions. Toward the end of the first freeze cycle, limited axial CT images without contrast are obtained to assess iceball geometry and to ensure iceball extension beyond the margins of the tumor in all dimensions. Limited axial CT images without contrast are again obtained at the midpoint of the second freeze cycle to reassess adequacy of the iceball. Although seldom employed, active iceball formation can also be monitored using US. After completion of the double freeze-thaw cycles and removal of cryoprobes, a half-dose contrast-enhanced limited CT is obtained to confirm complete ablation of the SRM and to confirm the presence of a surrounding therapeutic margin and to identify possible viable tumor. Enhancement within or near the margin of the expected ablation zone is suggestive of residual tumor, which can be treated with the deployment of an additional cryoprobe and repeat ablation.

Oncological Outcomes and Follow-up

Successful outcomes of cryoablated tumors are characterized on CT imaging by significant shrinkage and loss of contrast enhancement [68]. Tumors successfully treated with RFA demonstrate no contrast enhancement with minimal shrinkage on CT [69]. On MRI, the imaging hallmark of successful renal tumor ablation is lack of tumor enhancement at gadolinium-enhanced imaging. Rim enhancement, believed to represent reactive change, may occasionally be seen at early post-procedural MR scanning after RFA or cryoablation, which later resolves.

Efficacy of Cryoablation

Longer-term follow-up studies (>60 months) assessing the efficacy of CA are beginning to emerge. Multiple long-term studies of LCA have demonstrated that this technique provides excellent oncological outcomes [70]. Although, there are fewer reports of longer-term follow-up after PCA in the literature, the limited data is similarly promising.

In a recent study of 138 patients undergoing LCA with mean follow-up of 98.8 months, Caputo and colleagues determined 5-year disease-free survival (DFS), cancer-specific survival (CSS), and overall survival (OS) of 86.5 %, 96.8 %, and 79.1 %, respectively. Ten-year DFS, CSS, and OS were 86.5 %, 92.6 %, and 53.8 %, while mean time to recurrence was 2.3 years post-ablation [71]. In another study of 112 T1 tumors including 92 RCC-confirmed tumors with the mean follow-up of 97.9 months post LCA, Johnson et al. determined OS, progression-free survival (PFS), and CSS of 98.5 %, 91.0 %, and 98.5 %, respectively [72]. Similarly, Tanagho and co-workers reported 76 months of follow-up data from 35 RCC-confirmed tumors treated with LCA, noting 6-year DFS, CSS, and OS of 80 %, 100 %, and 76.2 %, respectively, and excellent renal functional outcomes. The study demonstrated six patients (17 %) who experienced local recurrences after LCA [73]. Aron and colleagues reported their data on 80 patients who underwent LCA with median follow-up of 93 months [74]. The study reported 5-year OS, disease-specific survival (DSS), and RFS of 84 %, 92 %, and 81 %, respectively, and 10-year OS, DSS, and RFS of 51 %, 83 %, and 78 %, respectively. In this study, however, the ablation was performed using a single, large 4.8-mm probe; as this single probe technique has been largely supplanted by the use of multiple ultrathin (1.47 mm) probes, the continual evolution of technology and technique and its effect on outcomes remains to be seen.

Recent studies comparing CA and PN are also emerging. While perioperative outcomes in CA are superior, the data is unclear whether CA represents an increased risk of recurrence. Thompson and colleagues recently showed that recurrence rate was similar in patients who underwent PN and PCA for cT1 renal masses [75]. Overall survival was superior after PN, likely resulting from selection bias. A meta-analysis by Klatte and colleagues compared laparoscopic PN and LCA,

combining 13 studies. They found that patients treated with LCA demonstrated a shorter length of stay, less blood loss, and lower risk of complications, but that LCA was associated with an increased risk of recurrence (relative risk = 9.39) and metastatic progression (*RR* = 4.68) [76].

Studies comparing LCA vs PCA have found no difference in overall mortality or recurrence rates. Kim and colleagues compared 145 LCA and 118 PCA cases with mean follow-up 71.4 months for LCA and 38.6 months for PCA. The reported 5-year OS and RFS for LCA were 79.3 % and 85.5 %, respectively. Five-year OS and RFS for PCA were 86.3 % and 86.3 %, respectively. Cryoablation approach (LCA vs PCA) was not predictive of overall mortality or disease recurrence, although mean length of stay was shorter for PCA [77]. Similarly, Zargar and colleagues determined no significant difference in OS or RFS at 5 years between the patients undergoing LCA (n = 275) and PCA (n = 137). Tumor size and anterior location were predictive of higher local recurrence rates, while RENAL nephrometry score or type of cryoablation was not associated with tumor recurrence [78].

CA represents an alternative approach to the treatment of renal masses. The long-term oncological outcomes are promising, as are the improved renal functional outcomes, compared to PN. These findings make CA an ideal minimally invasive modality and support its use in a wider population. However, there is still an unclear risk of increased recurrence in CA, which balances the improved perioperative outcomes.

Salvage Cryoablation in the Setting of Recurrence Following Primary Cryoablation

Recurrence rate after focal TA is relatively higher when compared to extirpation. This increased oncological failure rate incites the potential need for salvage procedure. Currently there are no guidelines or recommendations regarding the management of recurrences following TA. This has led to controversy regarding the most appropriate salvage treatment therapy. The management of recurrent disease after PCA poses a great challenge to urologists and interventional radiologists. Extirpative management of locally recurrent RCC can be challenging due to the local fibrosis and eradication of anatomical surgical planes [79]. As thermal ablation of SRM emerges as a viable alternative to surgical extirpation, many patients are now treated with repeat PCA after recurrence following primary PCA. According to a literature review performed between 2000 and 2006 by Long and colleagues, repeat cryoablation is the most common treatment modality following failed prior cryoablation. Approximately 66 % to 73 % of patients who fail thermal ablation are managed by repeat focal therapy; overall, 0.9 % of all renal masses that underwent CA and fail receive salvage TA treatment [80]. The data is very limited regarding patient's characteristics, perioperative complications, and oncologic outcomes in those undergoing repeat ablation. Overall, repeat PCA has demonstrated an improved safety and convalescence profile compared to salvage LPN. Despite the technical challenges of the procedure, repeat PCA has gained increased popularity among urologists [81]. The advantages of using PCA in this patient population include faster convalescence, significantly shorter operative times, less pain, and the ability to perform the procedure under moderate sedation thus providing a viable treatment option for patients with significant comorbidities avoiding the risks associated with general anesthesia. Hegg and colleagues reported a major complication rate of 5.7 % in patients who underwent repeat PCA after local recurrence following LPN [82]. In our recent series, 8 % of 250 patients who underwent PCA for SRM underwent secondary ablation for biopsy-proven RCC recurrence. Our data demonstrated 86 % success rate with the mean follow-up of 30 months (Fig. 2.6). Only three patients were identified to have a second episode of local recurrence following PCA. All three patients were found to have biopsy-confirmed chromophobe-type RCC. One patient was reablated for a third time and two patients underwent laparoscopic partial nephrectomy. All three patients had no evidence of local or distant tumor progression at later follow-up visits. There were no complications, and no patients needed blood transfusions.

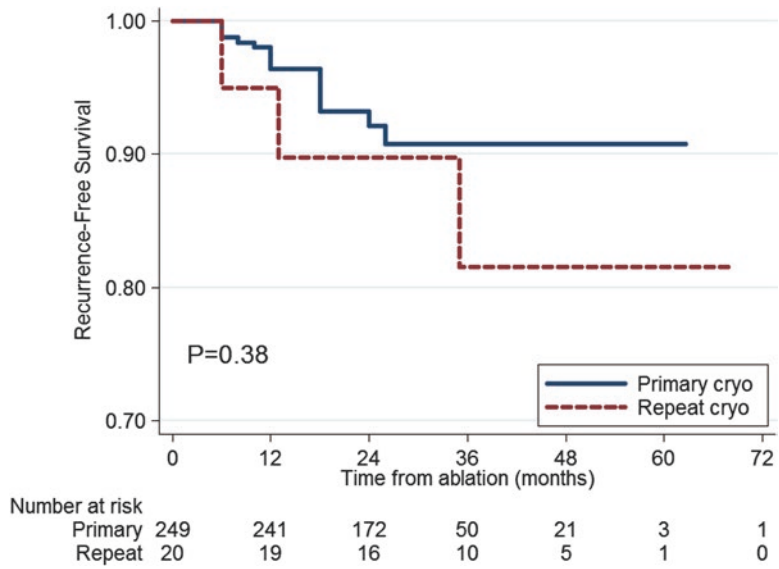

Fig. 2.6 Kaplan–Meier estimates of recurrence-free survival after primary and repeat cryoablation

All procedures were performed in less than 2 h with no patients needing general anesthesia [83]. Repeat PCA for locally recurrent disease is technically feasible, has a low complication rate, and demonstrates acceptable short-term oncologic outcomes in this challenging population.

Efficacy of Radiofrequency Ablation

The recent emergence of longer-term follow-up reports has demonstrated that RFA provides durable oncologic outcomes comparable to those reported following partial nephrectomy, in addition to improved renal functional outcomes. Multiple studies with follow-up > 60 months have demonstrated that RFA as a treatment of T1a RCCs provides long-term oncological control with survival rates comparable to those in PN [84–88].

A report by Olweny and colleagues compared patients with histologically confirmed T1a RCC treated by percutaneous RFA (n = 37) and PN (n = 37) with a median follow-up of 6.5 years. There were no significant differences in any of the survival rates between the two treatment groups: for RFA vs PN, the 5-year OS was 97.2 % vs 100 % (p = 0.31); CSS was 97.2 % vs 100 % (p = 0.31); DFS was 89.2 % vs 89.2 % (p = 0.78); local RFS was 91.7 % vs 94.6 % (p = 0.96); and metastasis-free survival (MFS) was 97.2 % vs 91.8 % (p = 0.35), respectively [89]. Chang and co-workers compared a propensity-matched cohort of T1a patients treated with RFA (n = 45) and LPN (n = 45), with a median follow-up 67.6 months. For RFA, the 5-year OS, CSS, DFS, RFS, and MFS were 90.2 %, 95.6 %, 86.7 %, 95.4 %, and 95.5 %, respectively. For LPN, these rates were 93.2 %, 97.7 %, 88.5 %, 97.7 %, and 95.5 %, respectively. The authors also found that RFA provided better renal functional preservation than PN [90].

Additional studies have similarly shown improved renal functional outcomes in RFA when compared to PN. A study of patients undergoing RFA (n = 21) and RN (n = 39) for T1b cancer determined that although OS was significantly lower in RFA vs RN, the RCC-related survival rate and disease-free survival rates were comparable between the two groups, and RFA was associated with less renal function decrease (12.5 %) compared to PN (32.5 %) [91]. Recently, Ji and colleagues found that for treatments of cT1a renal tumors, laparoscopic RFA provided excellent perioperative results, long-term functional and oncological outcomes. The decrease in glomerular filtration rate (GFR) was significantly lower in the LRFA group than the LPN group (p = 0.021) [92]. Faddegon and colleagues also determined that 5-year freedom from CKD stage progression for radiofrequency ablation and partial nephrectomy

was 85.4 % vs 82.1 % ($p = 0.06$), concluding that RFA provides similar long-term renal function preservation benefit as partial nephrectomy. [93].

In a study of 1424 cT1a patients comparing PN ($n = 1057$), CA ($n = 187$), and RFA ($n = 180$), Thompson and colleagues determined that while RFS was similar among the three treatments, metastasis-free survival (MFS) was superior for PN and CA patients when compared with RFA for cT1a patients ($p = 0.005$ and $p = 0.021$, respectively) [75].

Recent literature is promising and suggests that both CA and RFA are effective and durable treatment options for SRM. Like CA, RFA has undergone technological advancements that may continue to improve upon the emerging data. Additional prospective randomized studies may help further evaluate the efficacy and safety in relation to PN and CA.

Conclusion

The armamentarium in the treatment of the SRM continues to expand. Outcomes data on TA continue to mature, and recent longer-term follow-up results are very promising. These results suggest that CA and RFA may have a wider indication in the treatment of renal tumors. In order to effectively utilize the newer TA technologies, it is paramount to understand the technology being employed. The role of biopsy has been expanding and plays an important role in the decision-making process and patient counseling. Considering the myriad of options now afforded in the treatment of the SRM, a detailed discussion should be held with the patient prior to rendering any treatment, especially as the role of TA continues to expand.

References

1. Siegel RL, Miller KD, Jemal A. Cancer statistics, 2016. CA Cancer J Clin. 2016;66(1):7–30.
2. Hollingsworth JM, Miller DC, Daignault S, Hollenbeck BK. Rising incidence of small renal masses: a need to reassess treatment effect. J Natl Cancer Inst. 2006;98(18):1331–4.
3. Clayman RV, Kavoussi LR, Soper NJ, Dierks SM, Merety KS, Darcy MD, et al. Laparoscopic nephrectomy. N Engl J Med. 1991;324(19):1370–1.
4. Huang WC, Levey AS, Serio AM, Snyder M, Vickers AJ, Raj GV, et al. Chronic kidney disease after nephrectomy in patients with renal cortical tumours: a retrospective cohort study. Lancet Oncol. 2006;7(9):735–40.
5. McKiernan J, Simmons R, Katz J, Russo P. Natural history of chronic renal insufficiency after partial and radical nephrectomy. Urology. 2002;59(6):816–20.
6. Thompson RH, Boorjian SA, Lohse CM, Leibovich BC, Kwon ED, Cheville JC, et al. Radical nephrectomy for pt1a renal masses may be associated with decreased overall survival compared with partial nephrectomy. J Urol. 2008;179(2):468–71. discussion 472-463
7. Kim SP, Thompson RH, Boorjian SA, Weight CJ, Han LC, Murad MH, et al. Comparative effectiveness for survival and renal function of partial and radical nephrectomy for localized renal tumors: a systematic review and meta-analysis. J Urol. 2012;188(1):51–7.
8. Campbell SC, Novick AC, Belldegrun A, Blute ML, Chow GK, Derweesh IH, et al. Guideline for management of the clinical t1 renal mass. J Urol. 2009;182(4):1271–9.
9. Kutikov A, Kunkle DA, Uzzo RG. Focal therapy for kidney cancer: a systematic review. Curr Opin Urol. 2009;19(2):148–53.
10. Lane BR, Babineau D, Kattan MW, Novick AC, Gill IS, Zhou M, et al. A preoperative prognostic nomogram for solid enhancing renal tumors 7 cm or less amenable to partial nephrectomy. J Urol. 2007;178(2):429–34.
11. Frank I, Blute ML, Cheville JC, Lohse CM, Weaver AL, Zincke H. Solid renal tumors: An analysis of pathological features related to tumor size. J Urol. 2003;170(6 Pt 1):2217–20.
12. Volpe A, Mattar K, Finelli A, Kachura JR, Evans AJ, Geddie WR, et al. Contemporary results of percutaneous biopsy of 100 small renal masses: a single center experience. J Urol. 2008;180(6):2333–7.
13. Rosales JC, Haramis G, Moreno J, Badani K, Benson MC, McKiernan J, et al. Active surveillance for renal cortical neoplasms. J Urol. 2010;183(5):1698–702.
14. Graversen JA, Mues AC, de Lorca A P-L, Landman J. Active surveillance of renal cortical neoplasms: a contemporary review. Postgrad Med. 2011;123(1):105–13.
15. Patel N, Cranston D, Akhtar MZ, George C, Jones A, Leiblich A, et al. Active surveillance of small renal masses offers short-term oncological efficacy equivalent to radical and partial nephrectomy. BJU Int. 2012;110(9):1270–5.
16. Mehrazin R, Smaldone MC, Kutikov A, Li T, Tomaszewski JJ, Canter DJ, et al. Growth kinetics and short-term outcomes of ct1b and ct2 renal masses under active surveillance. J Urol. 2014;192(3):659–64.
17. Mues AC, Haramis G, Badani K, Gupta M, Benson MC, McKiernan JM, et al. Active surveillance for larger (ct1bn0m0 and ct2n0m0) renal cortical neoplasms. Urology. 2010;76(3):620–3.

18. Lane BR, Abouassaly R, Gao T, Weight CJ, Hernandez AV, Larson BT, et al. Active treatment of localized renal tumors may not impact overall survival in patients aged 75 years or older. Cancer. 2010;116(13):3119–26.
19. Ordon M, Landman J. Renal mass biopsy: "Just do it". J Urol. 2013;190(5):1638–40.
20. Lienert AR, Nicol D. Renal angiomyolipoma. BJU Int. 2012;110(Suppl 4):25–7.
21. Jewett MA, Mattar K, Basiuk J, Morash CG, Pautler SE, Siemens DR, et al. Active surveillance of small renal masses: progression patterns of early stage kidney cancer. Eur Urol. 2011;60(1):39–44.
22. Tsivian M, Rampersaud Jr EN, Del Pilar Laguna Pes M, Joniau S, RJ L, WB S, et al. Small renal mass biopsy – how, what and when: report from an international consensus panel. BJU Int. 2014;113(6): 854–63.
23. Halverson SJ, Kunju LP, Bhalla R, Gadzinski AJ, Alderman M, Miller DC, et al. Accuracy of determining small renal mass management with risk stratified biopsies: confirmation by final pathology. J Urol. 2013;189(2):441–6.
24. Hu R, Montemayor-Garcia C, Das K. Role of percutaneous needle core biopsy in diagnosis and clinical management of renal masses. Hum Pathol. 2015;46(4):570–6.
25. Leveridge MJ, Finelli A, Kachura JR, Evans A, Chung H, Shiff DA, et al. Outcomes of small renal mass needle core biopsy, nondiagnostic percutaneous biopsy, and the role of repeat biopsy. Eur Urol. 2011;60(3): 578–84.
26. Eshed I, Elias S, Sidi AA. Diagnostic value of CT-guided biopsy of indeterminate renal masses. Clin Radiol. 2004;59(3):262–7.
27. Neuzillet Y, Lechevallier E, Andre M, Daniel L, Coulange C. Accuracy and clinical role of fine needle percutaneous biopsy with computerized tomography guidance of small (less than 4.0 cm) renal masses. J Urol. 2004;171(5):1802–5.
28. Shannon BA, Cohen RJ, de Bruto H, Davies RJ. The value of preoperative needle core biopsy for diagnosing benign lesions among small, incidentally detected renal masses. J Urol. 2008;180(4):1257–61. discussion 1261
29. Schmidbauer J, Remzi M, Memarsadeghi M, Haitel A, Klingler HC, Katzenbeisser D, et al. Diagnostic accuracy of computed tomography-guided percutaneous biopsy of renal masses. Eur Urol. 2008;53(5): 1003–11.
30. Wang R, Wolf Jr JS, Wood Jr DP, Higgins EJ, Hafez KS. Accuracy of percutaneous core biopsy in management of small renal masses. Urology. 2009;73(3):586–90. discussion 590-581
31. Tan HJ, Jacobs BL, Hafez KS, Montgomery JS, Weizer AZ, Wood Jr DP, et al. Understanding the role of percutaneous biopsy in the management of patients with a small renal mass. Urology. 2012;79(2):372–7.
32. Park SY, Park BK, Kim CK, Kwon GY. Ultrasound-guided core biopsy of small renal masses: diagnostic rate and limitations. J Vasc Interv Radiol. 2013;24(1):90–6.
33. Menogue SR, O'Brien BA, Brown AL, Cohen RJ. Percutaneous core biopsy of small renal mass lesions: A diagnostic tool to better stratify patients for surgical intervention. BJU Int. 2013;111(4 Pt B):E146–151.
34. Jaff A, Molinie V, Mellot F, Guth A, Lebret T, Scherrer A. Evaluation of imaging-guided fine-needle percutaneous biopsy of renal masses. Eur Radiol. 2005;15(8):1721–6.
35. Menhadji AD, Nguyen V, Okhunov Z, Bucur P, Chu WH, Cho J, et al. Technique for office-based, ultrasound-guided percutaneous biopsy of renal cortical neoplasms using a novel transducer for facilitated ultrasound targeting. BJU Int. 2016;117(6):948–53.
36. Kunkle DA, Egleston BL, Uzzo RG. Excise, ablate or observe: the small renal mass dilemma–a meta-analysis and review. J Urol. 2008;179(4):1227–33. discussion 1233-1224
37. Babaian KN, Okhunov Z, Juncal S, Ordon M, Lusch A, Zand T, et al. Clinical outcomes of patients with nondiagnostic biopsy during cryoablation of small renal masses. Urology. 2015;85(3):605–9.
38. Mullins JK, Rodriguez R. Renal cell carcinoma seeding of a percutaneous biopsy tract. Can Urol Assoc J. 2013;7(3–4):E176–9.
39. Sainani NI, Tatli S, Anthony SG, Shyn PB, Tuncali K, Silverman SG. Successful percutaneous radiologic management of renal cell carcinoma tumor seeding caused by percutaneous biopsy performed before ablation. J Vasc Interv Radiol. 2013;24(9):1404–8.
40. Slywotzky C, Maya M. Needle tract seeding of transitional cell carcinoma following fine-needle aspiration of a renal mass. Abdom Imaging. 1994;19(2):174–6.
41. Akhavein A, Neuberger MM, Dahm P. Tumour-seeding: a rare complication of ablative therapy for clinically localised renal cell carcinoma. BMJ Case Rep. doi:10.1136/bcr-2012-006948.
42. Richard PO, Jewett MA, Bhatt JR, Kachura JR, Evans AJ, Zlotta AR, et al. Renal tumor biopsy for small renal masses: a single-center 13-year experience. Eur Urol. 2015;68:1007–13.
43. Kutikov A, Uzzo RG. The R.E.N.A.L. Nephrometry score: a comprehensive standardized system for quantitating renal tumor size, location and depth. J Urol. 2009;182(3):844–53.
44. Okhunov Z, Shapiro EY, Moreira DM, Lipsky MJ, Hillelsohn J, Badani K, et al. R.E.N.A.L. Nephrometry score accurately predicts complications following laparoscopic renal cryoablation. J Urol. 2012;188(5): 1796–800.
45. Sisul DM, Liss MA, Palazzi KL, Briles K, Mehrazin R, Gold RE, et al. Renal nephrometry score is associated with complications after renal cryoablation: a multicenter analysis. Urology. 2013;81(4):775–80.
46. Schmit GD, Thompson RH, Kurup AN, Weisbrod AJ, Boorjian SA, Carter RE, et al. Usefulness of R.E.N.A.L. Nephrometry scoring system for predicting outcomes and complications of percutaneous

ablation of 751 renal tumors. J Urol. 2013; 189(1):30–5.
47. Hayn MH, Schwaab T, Underwood W, Kim HL. Renal nephrometry score predicts surgical outcomes of laparoscopic partial nephrectomy. BJU Int. 2011;108(6): 876–81.
48. Gupta GN, Boris R, Chung P, Linehan WM, Pinto PA, Bratslavsky G. Robot-assisted laparoscopic partial nephrectomy for tumors greater than 4 cm and high nephrometry score: feasibility, renal functional, and oncological outcomes with minimum 1 year follow-up. Urol Oncol. 2013;31(1):51–6.
49. Hew MN, Baseskioglu B, Barwari K, Axwijk PH, Can C, Horenblas S, et al. Critical appraisal of the padua classification and assessment of the R.E.N.A.L. Nephrometry score in patients undergoing partial nephrectomy. J Urol. 2011;186(1):42–6.
50. Camacho JC, Kokabi N, Xing M, Master VA, Pattaras JG, Mittal PK, et al. R.E.N.A.L. (radius, exophytic/endophytic, nearness to collecting system or sinus, anterior/posterior, and location relative to polar lines) nephrometry score predicts early tumor recurrence and complications after percutaneous ablative therapies for renal cell carcinoma: a 5-year experience. J Vasc Interv Radiol. 2015;26(5):686–93.
51. Blute ML, Jr., Okhunov Z, Moreira DM, George AK, Sunday S, Lobko II, et al. Image-guided percutaneous renal cryoablation: Preoperative risk factors for recurrence and complications. BJU Int. 2013;111(4 Pt B):E181–185.
52. Seideman CA, Gahan J, Weaver M, Olweny EO, Richter M, Chan D, et al. Renal tumour nephrometry score does not correlate with the risk of radiofrequency ablation complications. BJU Int. 2013;112(8):1121–4.
53. Chang X, Liu T, Zhang F, Qian C, Ji C, Zhao X, et al. The comparison of r.E.N.A.L., padua and centrality index score in predicting perioperative outcomes and complications after laparoscopic radio frequency ablation of renal tumors. J Urol. 2015;194(4):897–902.
54. Gahan JC, Richter MD, Seideman CA, Trimmer C, Chan D, Weaver M, et al. The performance of a modified renal nephrometry score in predicting renal mass radiofrequency ablation success. Urology. 2015;85(1):125–9.
55. Uchida M, Imaide Y, Sugimoto K, Uehara H, Watanabe H. Percutaneous cryosurgery for renal tumours. Br J Urol. 1995;75(2):132–6. discussion 136-137
56. Rewcastle JC, Sandison GA, Saliken JC, Donnelly BJ, McKinnon JG. Considerations during clinical operation of two commercially available cryomachines. J Surg Oncol. 1999;71(2):106–11.
57. Gill W, Fraser J, Carter DC. Repeated freeze-thaw cycles in cryosurgery. Nature. 1968;219(5152):410–3.
58. Gill IS, Novick AC. Renal cryosurgery. Urology. 1999;54(2):215–9.
59. Campbell SC, Krishnamurthi V, Chow G, Hale J, Myles J, Novick AC. Renal cryosurgery: experimental evaluation of treatment parameters. Urology. 1998;52(1):29–33. discussion 33-24
60. Zlotta AR, Wildschutz T, Raviv G, Peny MO, van Gansbeke D, Noel JC, et al. Radiofrequency interstitial tumor ablation (rita) is a possible new modality for treatment of renal cancer: ex vivo and in vivo experience. J Endourol. 1997;11(4):251–8.
61. De Filippo M, Bozzetti F, Martora R, Zagaria R, Ferretti S, Macarini L, et al. Radiofrequency thermal ablation of renal tumors. La Radiol Med. 2014;119(7):499–511.
62. Ramanathan R, Leveillee RJ. Ablative therapies for renal tumors. Ther Adv Urol. 2010;2(2):51–68.
63. Gervais DA, Arellano RS, Mueller PR. Percutaneous radiofrequency ablation of renal cell carcinoma. Eur Radiol. 2005;15(5):960–7.
64. Aron M, Gill IS. Minimally invasive nephron-sparing surgery (minss) for renal tumours. Part II: probe ablative therapy. Eur Urol. 2007;51(2):348–57.
65. Goldberg SN, Gazelle GS, Mueller PR. Thermal ablation therapy for focal malignancy: a unified approach to underlying principles, techniques, and diagnostic imaging guidance. AJR Am J Roentgenol. 2000; 174(2):323–31.
66. Zagoria RJ, Hawkins AD, Clark PE, Hall MC, Matlaga BR, Dyer RB, et al. Percutaneous CT-guided radiofrequency ablation of renal neoplasms: factors influencing success. AJR Am J Roentgenol. 2004; 183(1):201–7.
67. Young JL, Kolla SB, Pick DL, Sountoulides P, Kaufmann OG, Ortiz-Vanderdys CG, et al. In vitro, ex vivo and in vivo isotherms for renal cryotherapy. J Urol. 2010;183(2):752–8.
68. Tsivian M, Kim CY, Caso JR, Rosenberg MD, Nelson RC, Polascik TJ. Contrast enhancement on computed tomography after renal cryoablation: an evidence of treatment failure? J Endourol. 2012;26(4):330–5.
69. Matsumoto ED, Watumull L, Johnson DB, Ogan K, Taylor GD, Josephs S, et al. The radiographic evolution of radio frequency ablated renal tumors. J Urol. 2004;172(1):45–8.
70. Rodriguez Faba O, Akdogan B, Marszalek M, Langenhuijsen JF, Brookman-May S, Stewart GD, et al. Current status of focal cryoablation for small renal masses. Urology. 2016;90:9–15.
71. Caputo PA, Ramirez D, Zargar H, Akca O, Andrade HS, O'Malley C, et al. Laparoscopic cryoablation for renal cell carcinoma: 100-month oncologic outcomes. J Urol. 2015;194(4):892–6.
72. Johnson S, Pham KN, See W, Begun FP, Langenstroer P. Laparoscopic cryoablation for clinical stage t1 renal masses: long-term oncologic outcomes at the medical college of wisconsin. Urology. 2014;84(3): 613–8.
73. Tanagho YS, Roytman TM, Bhayani SB, Kim EH, Benway BM, Gardner MW, et al. Laparoscopic cryoablation of renal masses: single-center long-term experience. Urology. 2012;80(2):307–14.
74. Aron M, Kamoi K, Remer E, Berger A, Desai M, Gill I. Laparoscopic renal cryoablation: 8-year, single surgeon outcomes. J Urol. 2010;183(3):889–95.
75. Thompson RH, Atwell T, Schmit G, Lohse CM, Kurup AN, Weisbrod A, et al. Comparison of partial

nephrectomy and percutaneous ablation for ct1 renal masses. Eur Urol. 2015;67(2):252–9.
76. Klatte T, Shariat SF, Remzi M. Systematic review and meta-analysis of perioperative and oncologic outcomes of laparoscopic cryoablation versus laparoscopic partial nephrectomy for the treatment of small renal tumors. J Urol. 2014;191(5):1209–17.
77. Kim EH, Tanagho YS, Saad NE, Bhayani SB, Figenshau RS. Comparison of laparoscopic and percutaneous cryoablation for treatment of renal masses. Urology. 2014;83(5):1081–7.
78. Zargar H, Samarasekera D, Khalifeh A, Remer EM, O'Malley C, Akca O, et al. Laparoscopic vs percutaneous cryoablation for the small renal mass: 15-year experience at a single center. Urology. 2015;85(4):850–5.
79. Breda A, Anterasian C, Belldegrun A. Management and outcomes of tumor recurrence after focal ablation renal therapy. J Endourol. 2010;24(5):749–52.
80. Kunkle DA, Uzzo RG. Cryoablation or radiofrequency ablation of the small renal mass: a meta-analysis. Cancer. 2008;113(10):2671–80.
81. Patel SR, Abel EJ, Hedican SP, Nakada SY. Ablation of small renal masses: practice patterns at academic institutions in the United States. J Endourol. 2013;27(2):158–61.
82. Hegg RM, Schmit GD, Boorjian SA, McDonald RJ, Kurup AN, Weisbrod AJ, et al. Percutaneous renal cryoablation after partial nephrectomy: technical feasibility, complications and outcomes. J Urol. 2013;189(4):1243–8.
83. Okhunov Z, Chamberlin J, Moreira DM, George A, Babaian K, Shah P, et al. Salvage percutaneous cryoablation for locally recurrent renal-cell carcinoma after primary cryoablation. J Endourol. 2016;30(6):632–7.
84. Lorber G, Glamore M, Doshi M, Jorda M, Morillo-Burgos G, Leveillee RJ. Long-term oncologic outcomes following radiofrequency ablation with real-time temperature monitoring for t1a renal cell cancer. Urol Oncol. 2014;32(7):1017–23.
85. Psutka SP, Feldman AS, McDougal WS, McGovern FJ, Mueller P, Gervais DA. Long-term oncologic outcomes after radiofrequency ablation for t1 renal cell carcinoma. Eur Urol. 2013;63(3):486–92.
86. Zagoria RJ, Pettus JA, Rogers M, Werle DM, Childs D, Leyendecker JR. Long-term outcomes after percutaneous radiofrequency ablation for renal cell carcinoma. Urology. 2011;77(6):1393–7.
87. Tracy CR, Raman JD, Donnally C, Trimmer CK, Cadeddu JA. Durable oncologic outcomes after radiofrequency ablation: experience from treating 243 small renal masses over 7.5 years. Cancer. 2010;116(13):3135–42.
88. Ma Y, Bedir S, Cadeddu JA, Gahan JC. Long-term outcomes in healthy adults after radiofrequency ablation of t1a renal tumours. BJU Int. 2014;113(1):51–5.
89. Olweny EO, Park SK, Tan YK, Best SL, Trimmer C, Cadeddu JA. Radiofrequency ablation versus partial nephrectomy in patients with solitary clinical t1a renal cell carcinoma: comparable oncologic outcomes at a minimum of 5 years of follow-up. Eur Urol. 2012;61(6):1156–61.
90. Chang X, Liu T, Zhang F, Ji C, Zhao X, Wang W, et al. Radiofrequency ablation versus partial nephrectomy for clinical t1a renal-cell carcinoma: long-term clinical and oncologic outcomes based on a propensity score analysis. J Endourol. 2015;29(5):518–25.
91. Takaki H, Soga N, Kanda H, Nakatsuka A, Uraki J, Fujimori M, et al. Radiofrequency ablation versus radical nephrectomy: clinical outcomes for stage t1b renal cell carcinoma. Radiology. 2014;270(1):292–9.
92. Ji C, Zhao X, Zhang S, Liu G, Li X, Zhang G, et al. Laparoscopic radiofrequency ablation versus partial nephrectomy for ct1a renal tumors: long-term outcome of 179 patients. Urol Int. 2016;96(3):345–53.
93. Faddegon S, Ju T, Olweny EO, Liu Z, Han WK, Yin G, et al. A comparison of long term renal functional outcomes following partial nephrectomy and radiofrequency ablation. Can J Urol. 2013;20(3):6785–9.

Focal Therapy for Prostate Cancer: A Guide for Patients

3

Kae Jack Tay and Thomas J. Polascik

Introduction

Prostate cancer has been traditionally treated with surgical removal or irradiation of the entire prostate gland. While effective at cancer treatment, damage to the delicate structures responsible for urinary control and erectile function can result in long-term side effects and reduced quality of life in prostate cancer survivors. In an effort to achieve cancer control and yet minimize damage to these structures, the urological community has been exploring the idea of treating just a specific portion of the prostate where the cancer is located and actively monitoring the untreated portion of the gland. This approach is known as "focal therapy."[1]

If chosen in the correct setting, *focal therapy* may allow one to maintain quality of life for as long as possible. With this strategy of treating only the areas of the prostate with aggressive cancer, additional treatments can be administered if new areas of aggressive cancer are identified. In order to do this, a close follow-up regime is necessary after treatment. We believe that the best outcomes are achieved when an appropriate treatment is matched to a suitable patient based on individual circumstances and needs. We wrote this chapter as a resource to help you better understand the concept of focal therapy, its benefits, possible side effects and risks so as to aid you in making an individualized treatment decision for your cancer. For a detailed description of specific topics of interest, please refer to the other chapters in this text. For any specifics regarding your personal health, please consult your physician.

Treatment Options for Prostate Cancer

Traditional Radical Therapies

Traditional treatment strategies for *localized prostate cancer*,[2] or cancer confined to the prostate only, are based on treating the entire gland. This involves *surgical excision* of the whole gland (radical prostatectomy), *radiation*

K.J. Tay (✉)
Department of Urology, Duke University, Durham, NC, USA
e-mail: kaejack.tay@gmail.com

T.J. Polascik, MD
Professor of Surgery, Division of Urology, Department of Surgery, Duke Cancer Institute, Duke University School of Medicine, Durham, NC, USA

[1] *Focal therapy* – treating only the area of the prostate where the cancer is located

[2] *Localized prostate cancer* – prostate cancer confined within the prostate gland only, with no evidence of outward spread

© Springer International Publishing AG 2017
T.J. Polascik (ed.), *Imaging and Focal Therapy of Early Prostate Cancer*, Current Clinical Urology, DOI 10.1007/978-3-319-49911-6_3

therapy (via direct placement of radioactive seeds/needles [brachytherapy] into the prostate or external beam radiation), or *ablation* (using various cold or heat methods such as cryotherapy, high-intensity focused ultrasound [HIFU] or laser, or nonthermal methods such as electric pulses [irreversible electroporation] to kill cancer).

These strategies have generally worked well in eliminating prostate cancer within the prostate gland but frequently are associated with side effects due to collateral damage to adjacent tissues. To help you understand this better, a sketch of basic male anatomy is shown in Fig. 3.1. As examples, damage to the erectile nerves cause inability to have a penile erection, resulting in

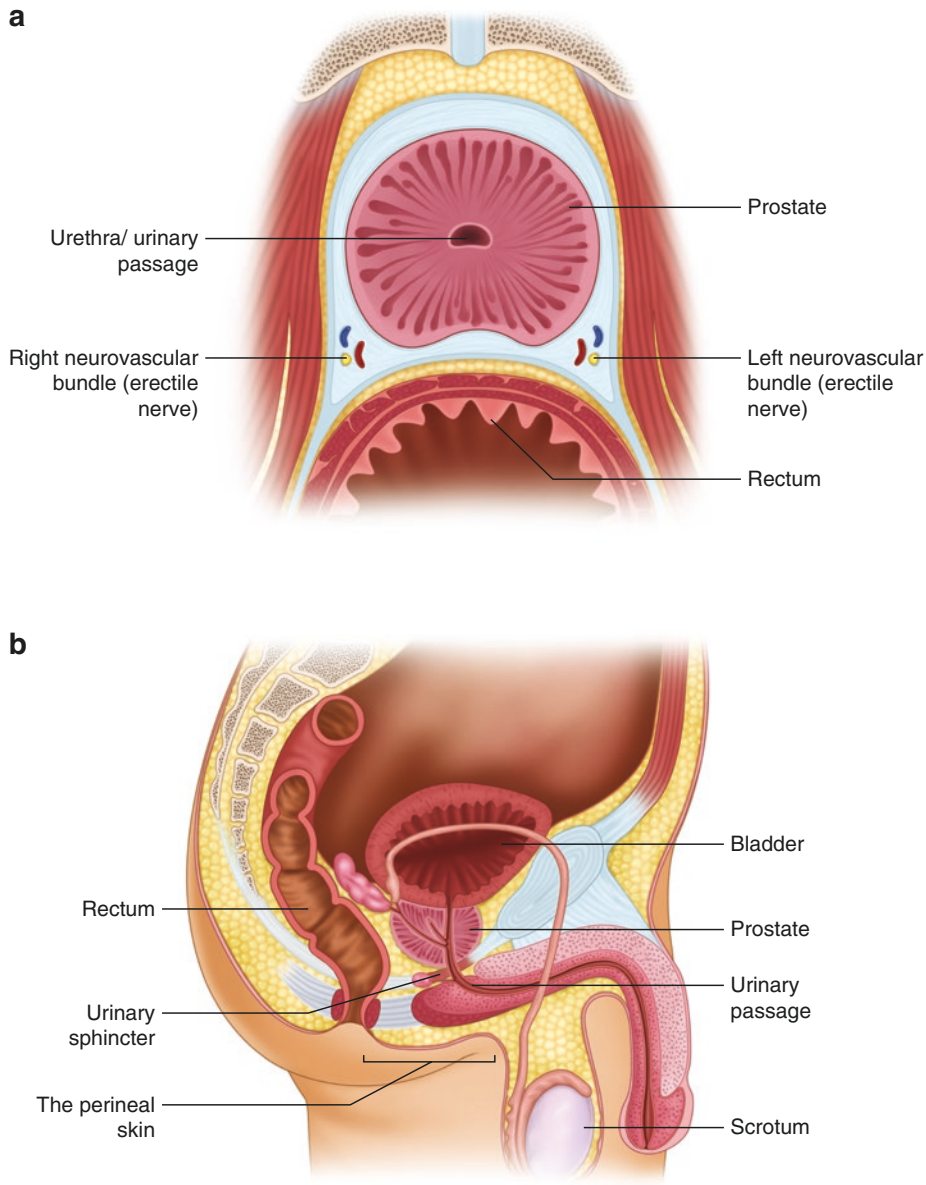

Fig. 3.1 Anatomy of the prostate and surrounding structures in (**a**) transverse view and (**b**) side view

impotence.[3] Damage to the urinary sphincter causes urinary leakage or *incontinence*.[4] Scarring to the urinary passage or *strictures*[5] result in difficulty with passage of urine. Radiation damage to the bladder (*cystitis*[6]) or rectum (*proctitis*[7]) can result in bleeding even years down the road.

The recognition that these side effects have a significant impact on the quality of life of prostate cancer survivors led the urological community to explore other, less morbid, ways of treating prostate cancer. One major development has been the recognition that men with low-risk[8] prostate cancer tend to have slow-growing, nonaggressive cancers. These cancers may have little or no impact on a man's life span, and this has led to many calling for not treating these cancers unless they grow and threaten a man's health. Potentially, these cancers can be monitored instead. However, this is complicated by the fact that up to 40 % of cancers thought to be low-risk initially are actually discovered later to be intermediate- or high-risk requiring treatment in order to avoid cancer growth and spread.

Active Surveillance

Active surveillance is an observation strategy of carefully monitoring men with low-risk prostate cancer with regular checkups using finger/digital exam of the prostate, blood tests (such as prostate-specific antigen [PSA]), imaging scans, and/or biopsies to periodically monitor the behavior of their cancer. At any time, if the cancer appears to behave in a more aggressive manner, these men would likely be advised to discontinue surveillance and receive standard treatment. In published reports, approximately 50 % of men remain treatment-free at 10–15 years of surveillance. The downside to this approach is that the frequent checks and biopsies are a healthcare burden to the patient. Prostate imaging and biopsies have an associated cost, and biopsy is not without discomfort and complications. There is still insufficient data and experience currently to support a reduced frequency of checks in men on active surveillance.

Focal Therapy

Focal therapy refers to a strategy of treating only the part of the prostate gland that contains cancer using an energy source such as cryotherapy (using very cold temperatures to freeze the tissue), HIFU (high-intensity ultrasound that heats up the tissue), or laser. This strategy is generally only suitable for men with one or two discrete areas of prostate cancer. This usually allows one to decrease the risk of collateral damage, reducing side effects and maintaining sexual and urinary function, while still eliminating the cancer. This technique, however, is still in the developmental phase, and long-term data is needed to demonstrate this. As long-term cancer recurrence rates are also unknown at this time, close follow-up after treatment is required to monitor for disease recurrence, similar to traditional treatments.

To take things one step further, one may treat the area of aggressive cancer within the prostate, leaving areas of slow-growing cancer untreated. In this approach, the remaining untreated part of the prostate gland is placed on active surveillance and closely followed to be sure no new tumors or aggressive ones develop. Focal therapy is also repeatable and can be applied to the same part of the prostate gland if cancer recurs here or other parts of the prostate gland as the need arises.

Another setting in which focal therapy may be applied is after other traditional treatments have failed. If cancer recurs after prostate irradiation or ablation, focal therapy can be used provided that the recurrence occurs in one well-defined part of the gland only. The use of focal therapy for prostate cancer that recurs following an initial

[3] *Impotence* – the inability to have an erection with the penis

[4] *Incontinence* – urinary leakage that cannot be controlled

[5] *Stricture* – narrowing of the urinary passage, usually due to scar tissue

[6] *Cystitis* – irritation/inflammation of the bladder

[7] *Proctitis* – irritation of the rectum

[8] The D'Amico low-risk criteria considers those with a prostate-specific antigen (PSA) <10, tumor involving less than half of one lobe of the prostate gland, and biopsy Gleason score of 3 + 3 or less.

treatment is called "salvage" and may carry with it a different side-effect profile.

Determining if Focal Therapy Is Suitable for You

Why Consider Focal Therapy?

Focal therapy can be considered if you wish to try to preserve your sexual and urinary function while achieving control of your cancer using a minimally invasive approach. However, focal therapy is a highly personalized approach that is suited to some, but not all, men. Here we discuss some factors that you should consider to help determine whether this is a treatment suitable for you.

Cancer Treatment Needs

The primary goal must be to eradicate any aggressive cancer within the prostate. Therefore, it is first important to determine whether your cancer can be sufficiently treated with focal therapy. It is currently thought that the majority of prostate cancers are low-grade and pose little threat to life, whereas a proportion of cancers are high grade, more aggressive, and more likely to impact one's life span. It is thus essential to map out the location of cancers within the three-dimensional (3D) space of the prostate with an emphasis on aggressive cancers. The most important principle is to get as accurate a cancer location map within the prostate as possible. The more accurate the map, the better the ability to target. As an example, if you were to invite someone to your house for dinner and told them to drive to Boston, well, Boston is a large city, and your guest would not be able to find you. In order for your guest to arrive at your exact house, you will need to provide directions that include the city, road, house or apartment number, etc. To date, there are two methods to identify and locate prostate cancer within the three-dimensional prostate gland: multiparametric magnetic resonance imaging (mpMRI) and biopsy. Cancer mapping can be accomplished using biopsy with or without the help of imaging such as mpMRI.

Biopsy of the Prostate

Standard 12-core transrectal ultrasound biopsy (TRUS biopsy), which is the usual biopsy that a man has in a urologist's office to detect cancer, is generally thought to be insufficient in terms of providing the precise "address" of the prostate cancer. Increasing the number of biopsy cores to 16, 18, or 24 may improve mapping prior to focal therapy but often marginally. Furthermore, this standard prostate biopsy procedure is usually performed in the office setting, and increasing the number of cores may result in a longer procedure and patient discomfort.

Three-dimensional transperineal[9] *mapping biopsy* (3D-TMB) is a biopsy usually performed under anesthesia obtaining anywhere from 40 to 80+ biopsies at close (5 mm) intervals using a grid to provide a 3D spatial record of the location (using x, y, and z coordinates) of each biopsy core. This is thought to be the gold standard for biopsy mapping of prostate cancer. While it is still possible to miss cancer within the 5 mm intervals, such a cancer focus would likely be very small and not be significant clinically.

Imaging

Multiparametric magnetic resonance imaging (mpMRI) is the best imaging modality available today for detecting prostate cancer. It preferentially detects larger and higher-grade or more aggressive cancers rather than low-grade cancers. When there is suspicion of a cancerous area seen on mpMRI, a *targeted biopsy*, where the biopsy needle is directed toward that specific area or target, may be performed to better characterize the cancer in terms of location and aggressiveness.

[9]The perineum refers to the skin between the scrotum and anus. The transperineal procedure thus uses this route and avoids going through the rectum.

Ultimately, your physician may recommend either a 3D-TMB or mpMRI (sometimes both) to locate your cancer and determine if you are a candidate for focal therapy. It also depends on how thorough an evaluation you desire pretreatment.

Personal Needs

In traditional whole-gland treatment, there is a moderate to high risk of damage to the erectile nerves, even when the surgeon tries to preserve them (nerve-sparing prostatectomy) (Fig. 3.1a). Focal therapy offers the potential to preserve or maintain sexual function. This is particularly the case where the cancerous area is located far away from both erectile nerves. Sexual function often carries a different importance to every individual. One's current and anticipated future level of sexual activity must thus be carefully considered in making the decision for focal therapy. For example, it would be of great interest to a man who is able to have erections and good sexual function. On the other hand, a man with already poor sexual function might not reap as much benefit from focal therapy and only assume the disadvantages (i.e., less certain cancer control). Such an individual might be better served with traditional whole-gland treatment.

Additionally, whole-gland treatment carries a real risk of posttreatment urinary leakage (incontinence) and narrowing of the urinary passage (urethral stricture) (Fig. 3.1b). Focal therapy directed on one specific part of the prostate away from the urethra or urinary sphincter[10] may theoretically help reduce the chance of these complications.

Mindset and Personality

The goal of focal therapy is to preserve urinary and sexual function, and it does so by selectively treating a part of the prostate gland. By not treating the entire prostate, aggressive cancer can occur later in other parts of the gland. This is opposed to traditional methods of treatment, which aim to eradicate the entire gland with the goal of a "one-step cure." As such, close follow-up is required after focal therapy, and the treatment itself can be seen as the first step in the journey of managing prostate cancer as a chronic disease.

While we believe that better outcomes can be achieved with this strategy in carefully selected patients, the patient himself must be willing to go along with the careful follow-up after treatment. If necessary, additional treatments will be administered as the condition evolves. This strategy would not be suitable for someone who is impatient, anxious, or would just like to get the problem "resolved." Such an individual might be better served with traditional whole-gland treatment methods.

Summary: Signs that Focal Therapy May Be a Good Fit for You

- Your PSA is less than 15.
- Your clinical stage of prostate cancer is T1c or T2a.
- The cancer appears to be clustered to one area of the prostate on 3D-TMB, mpMRI, or both.
- You understand and accept that the whole gland will not be treated.
- You understand the risks of undertreatment and progression and the potential need for further treatment.
- You understand the need for monitoring.
- You understand that while the goal is to maximize urinary and sexual function, there are no guarantees as to the results.

Types of Ablative Technology Available for Focal Therapy

While the concept of focal therapy remains constant, in real life there are many variations in its application. Put simply, it is the delivery of a

[10]A circular muscle around the urethra or urinary passage that tightens to prevent urinary leakage when the bladder is full and relaxes when it is time to pass urine (Figure 3.1)

Table 3.1 Various technologies for focal therapy

Energy	Energy type	Delivery mode	Guidance	Commercial example[a]
Heat	High intensity frequency ultrasound	Transrectal	Ultrasound	Ablatherm™ Sonablate™
	(HIFU)		MRI	InSightec
		Transurethral	Ultrasound	TULSA™
	Laser	Transperineal	Ultrasound	
			MRI	Visualase™
		Transrectal	Ultrasound, also MRI	
Cold	Cryotherapy	Transperineal needles	Ultrasound	Endocare Galil
			MRI	
Radiation	Gamma radiation	Extracorporeal[b]	Surgically placed gold markers	Stereotactic body radiation therapy (SBRT)
	Alpha radiation	Transperineal seed implants	Ultrasound	Seed brachytherapy
Nonthermal	Irreversible electroporation	Transperineal	Ultrasound	NanoKnife™
Light therapy	Photodynamic therapy	Transperineal	Ultrasound	Tookad™

[a]This list is not meant to be exhaustive
[b]From outside the body

toxic stimulus to kill a certain focus of cells within the prostate gland. The technical details of the various types of stimulus and how they can be delivered to the prostate are discussed in separate chapters of this book. It is important to understand that the risks and benefits of the proposed treatment are partly based on the technology used. Suffice it to say that there is currently insufficient evidence to conclude on the superiority of one technique over the other. Also, new developments are expected to occur in the future. Table 3.1 summarizes these various techniques.

What to Expect During the Treatment Process

The typical focal therapy procedure is an outpatient procedure, often performed under anesthesia. While it is usually short (approximately 1 h+ in duration), anesthesia is not without its risks. Therefore, standard preanesthetic workup including blood tests, chest X-ray, and an electrocardiogram may be performed. If you have other significant medical problems, you should visit your internist to make sure that you are medically optimized prior to scheduling the procedure. For example, if you are on anticoagulants,[11] these may need to be stopped or adjusted under the direction of your internist for several days prior to the procedure.

Fasting for several hours is required usually starting from the night prior to the procedure. You may also be required to undergo bowel preparation with laxatives. Occasionally, focal therapy may be performed under spinal anesthesia or simply with a local nerve block. This may be safer from an anesthetic standpoint, but there remains a possibility that partial anesthesia is insufficient and must be converted to general anesthesia. Prior to anesthesia, the anesthesiologist will meet with you to explain anesthetic considerations and risks in detail.

During the treatment, the patient will be positioned on the treatment table. The typical positions are on one's side for a transrectal treatment or on the back with the legs in the air supported by stirrups for a transperineal treatment. A targeting probe will typically be placed in the rectum, and the energy will be delivered transrectally or transperineally (Figs. 3.2 and 3.3). There may be

[11] Anticoagulant – a blood-thinning medication

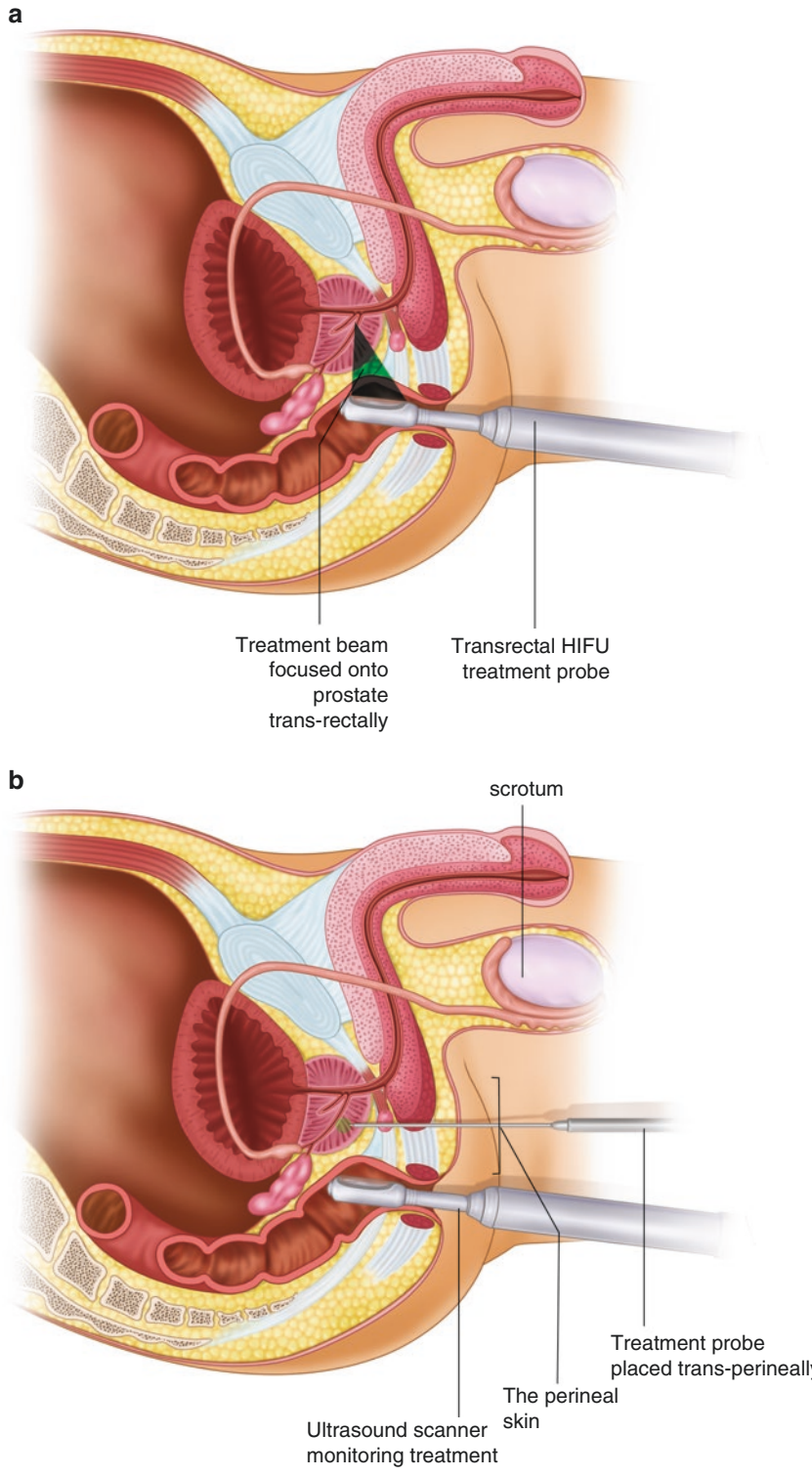

Fig. 3.2 (**a**) An example of transrectal treatment using a HIFU probe. The treatment beam passes through the rectal wall to focus on the prostate. (**b**) An example of transperineal treatment using a cryotherapy probe. The probe is placed through the perineal skin, and treatment is monitored by the ultrasound scanner in the rectum

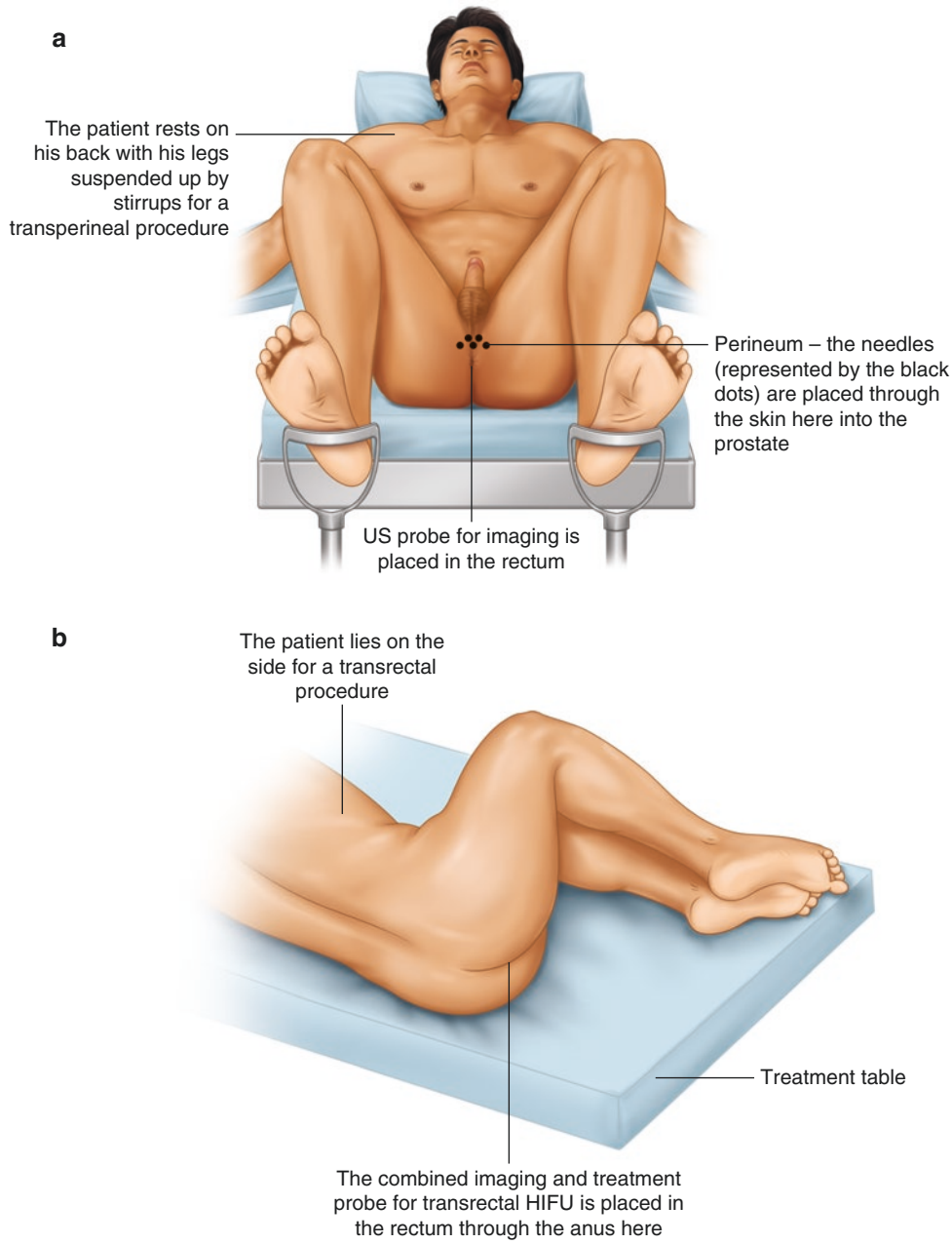

Fig. 3.3 Examples of patients receiving treatment in the (**a**) lithotomy position for transperineal treatment and (**b**) lateral position for transrectal treatment

transient rectal discomfort. When performed transperineally, there are usually small needle-prick wounds that may feel a little sore, or, less commonly, there may be bruising seen behind the scrotum. In some centers, real-time MRI is used to monitor the treatment, and the patient may be treated in the MRI "donut" itself.

What to Expect Immediately After Treatment

Some focal therapies cause swelling of the prostate that may make urination more difficult. At the end of the procedure, a urinary catheter may be temporarily placed via the urethra to allow

you to freely urinate. This is typically left in place for several days to allow any residual swelling caused by the therapy to resolve. Occasionally, a suprapubic catheter[12] may be used instead of a urethral catheter. A nurse will instruct you on care and management of the catheter if you have one. As focal therapy is usually performed as an outpatient procedure, one could reasonably expect to be sent home after a short period of observation.

Post-procedure, there is a small risk of bleeding or infection. It is not uncommon to have bruising of the skin where the treatment was applied. Some lightly blood-stained urine is normally seen in the days after the procedure and can persist or recur to some degree for several weeks. This is usually self-limiting and should not be cause for alarm. On the other hand, heavy (thick and red) bleeding may cause blockage to the catheter. Should this occur you will need to let your treating physician know. Persistent and high fevers may also signify infection and may need to be treated.

The urinary catheter, if you have one, is usually removed within several days to a few weeks after the procedure. You may be observed in a physician's office to ensure that you can urinate without difficulty. There may be a mild burning or painful sensation in your urethra upon urinating, but this should decrease and resolve over the subsequent days. If these sensations are persistent, worsening, or resulting in an inability to urinate, you should be assessed by your doctor.

Long-Term Functional and Oncological Outcomes after Focal Therapy

Functional Outcomes

The recovery of erections varies between individuals, depends on the prior ability to have and maintain erections, as well as one's desire (libido) and state of mind. When both erectile nerves are preserved, the rate of recovery of erections is approximately 90 % at 1 year. When only one erectile nerve is preserved, the rate of recovery is approximately 50–70 % at 1 year. During the recovery phase, it is sometimes helpful to undergo penile rehabilitation. This involves the stimulation of blood flow to the penis using medications such as Viagra, Cialis, or Levitra or the use of a vacuum pump. Put simply, the penis needs blood supply and penile massage is a great way to encourage this. In general, the earlier this is started, and the more persistently it is done, the better the chances of recovery. Erectile function can continue to improve over the course of a few years after treatment, particularly if you actively participate in an erection recovery program and penile stimulation, maintaining good blood supply to the penis.

The recovery of continence is usually early compared to traditional whole-gland treatments. Still, it is beneficial to strengthen the sphincter muscles by performing Kegel exercises.[13] Again, the earlier this is started and the more persistently it is done, the better the chances of recovery.

Cancer Treatment Outcomes and Posttreatment Surveillance

Focal therapy is a relatively new treatment strategy, and there is less experience with long-term outcomes in the urological community. Also, recurrence of cancer can occur within the treated zone, or a new cancer may be detected in a section of the prostate that was not treated. Cancer occurring outside the treated zone may be observed in small, low-grade tumors just as though they are on active surveillance. A large or high-grade cancer detected in or out of the treatment zone could potentially be treated with further focal therapy. Alternatively, one could consider switching to whole-gland treatment at this point.

While most physicians agree on the need for close follow-up, there has hitherto been no consensus on how intense this follow-up regimen will

[12] A suprapubic catheter is a urinary drainage tube placed into the bladder through the skin of the lower belly.

[13] An exercise where the pelvic floor muscles are squeezed and relaxed intermittently to strengthen the pelvic floor

be. International consensus panels` have recommended 6-month checkups with physical examination and PSA blood tests. As a good portion of the prostate gland likely remains untreated, one expects the PSA to be detectable after treatment. On average, the PSA drops by up to 80 % by the 3-month posttreatment visit. At present, there is insufficient evidence to guide the interpretation of PSA after focal therapy. Instead, we recommend repeat imaging with mpMRI and prostate biopsy of any suspicious lesions at 1 year and subsequently at the 2–3 year interval. However, if persistent elevation in PSA is observed, an earlier/additional biopsy or MRI should be considered.

Conclusion

Focal therapy is a cutting edge approach to prostate cancer treatment based on state-of-the-art understanding of the biology of prostate cancer. However, it is a relatively new approach to treating prostate cancer, and understanding its long-term outcomes requires a longer period of observation. In the right hands and applied to the right patients, it offers the potential to preserve urinary and erectile function, while achieving *eradication* of clinically significant prostate cancer. Close follow-up is recommended after treatment.

Part II

Global Perspective of Active Surveillance and Focal Therapy

4 Low-Risk Prostate Cancer in North America: Rationale, Uptake, and Limitations of Active Surveillance and Opportunities for Focal Therapy

Raj Satkunasivam and Laurence Klotz

Introduction

The Rationale for Active Surveillance of Low-Risk Prostate Cancer

The rapid uptake of prostate-specific antigen (PSA) testing in North America in the late 1990s was strongly associated with a nearly threefold increase in the incidence of prostate cancer over a half-decade [1]. During this period, the median volume of cancer in men with newly diagnosed prostate cancer also decreased, signaling a dramatic stage migration. A significant proportion of these men with newly diagnosed prostate cancer (approximately 50 %) have low-risk prostate cancer (Gleason score 6 and PSA <10) and do derive little benefit from active, radical treatment. The rationale for active surveillance (AS) hinges on a consideration of the molecular features and indolent clinical behavior of low-grade prostate cancer.

The wide disparity between prostate cancer prevalence and prostate cancer mortality underscores the fundamental molecular and genetic characteristics of Gleason grade 3 prostate cancer. Hallmarks of cancer include insensitivity to antigrowth signals, unlimited replicative potential, sustained angiogenesis, local tissue invasion, metastasis, self-sufficiency in growth signals, deregulation of cellular energetics, and avoidance of immune destruction [2]. These hallmarks are an important framework within which the contrasting genetic and molecular characteristics of Gleason grade 3 versus grade 4 cancers can be considered. Specifically, genes involved in cellular proliferation (*AKT, HER2*), which are overexpressed in Gleason grade 4, however, show normal levels in Gleason grade 3. The same is true of genes involved in cell-cycle regulation, cellular invasion, and metastasis. Lastly, genes that provide a survival advantage for cancer through apoptotic resistance, pro-angiogenesis, and deregulating cellular metabolomics are also abnormally overexpressed in Gleason grade 4, but not Gleason grade 3. More recently, deep sequencing of somatic mutations has shown that low-grade prostate cancer diverges early from high-grade cancer and that metastases share genetic homology with high-grade but not low-grade cancer [3].

The indolent behavior of Gleason score (GS) 6 is exemplified by large surgical series wherein this grade of cancer shows little or no metastatic potential. Surgical series are informative because pathological review of the resected prostate allows attribution of higher risk to those individuals concomitantly harboring higher-grade

R. Satkunasivam (✉) • L. Klotz
Division of Urology, Department of Surgery, Sunnybrook Health Sciences Centre and University of Toronto, Toronto, ON, Canada
e-mail: raj.satkunasivam@sunnybrook.ca

© Springer International Publishing AG 2017

T.J. Polascik (ed.), *Imaging and Focal Therapy of Early Prostate Cancer*, Current Clinical Urology, DOI 10.1007/978-3-319-49911-6_4

disease. It is estimated that approximately 30 % of cases with Gleason 6 on biopsy are upgraded after surgery and likely account for the prostate cancer mortality detected in series of "watchful waiting" based on biopsy pathology [4]. Although surgical extirpation may alter the natural history of cancer, large surgical series of pathologically homogeneous Gleason 6 demonstrate uniformly indolent behavior. In one study of approximately 14,000 men with pathological Gleason 6 cancer, only 22 had evidence of metastasis to lymph nodes [5]. When 19 of these 22 cases of lymphatic involvement were re-reviewed, they were all found to have higher-grade disease in the prostate than previously reported. In another series of approximately 24,000 patients treated by radical prostatectomy at four academic centers, the 15-year prostate cancer-specific mortality rate for 12,000 men with pathologically confirmed GS 6 or less was 0.2–1.2 % [6]. Only three patients out of 9557 with Gleason score 6 or less and organ-confined disease died of prostate cancer, and all of these had higher-grade cancer on re-review.

The substantial evidence that Gleason pattern 3 has little to no metastatic potential allows physicians to use terminology such as "pre-cancer" or "pseudo-cancer" when counselling patients. One significant limitation to this approach has been the apparent oxymoron of describing a "pseudo-cancer" using the term Gleason score 6 out of 10, which may be perceived by the patient as having an intermediate grade. The new International Society of Urological Pathology revised the scoring system [7], which uses Grade Groups 1–5 and will allow the clinician to ascribe indolence in the context of a congruent scoring system (Grade Group 1 = Gleason score 3+3). Widespread adoption of active surveillance for low-risk disease would preserve quality of life in many patients, avoiding the detrimental effects of treatment on erectile and voiding function. From a population health perspective, active surveillance represents a cogent response to the problem of overtreatment related to PSA-based screening. Public health agencies, such as the US Preventive Services Task Force (USPSTF), have recommended against PSA testing mainly because of harms caused by overtreatment compared to its relative benefits, summarized by a high number needed to treat (NNT) to avoid a single death. Using active surveillance for indolent cancers while selectively treating patients who need treatment (focusing on those at risk of prostate cancer-related mortality) has the potential to decrease the NNT. This has the potential to "rehabilitate" PSA-based screening, by matching the benefits of early diagnosis to those who need treatment, thereby leading to a reduction in prostate cancer-related mortality.

North American Uptake of Active Surveillance

There is substantial and mounting evidence of excellent oncological outcomes for patients managed with active surveillance, in terms of low metastatic events and favorable rates of prostate cancer death. These oncological outcomes, mostly from academic single-center experiences, have been reviewed extensively elsewhere [8, 9]. Over the past decade, wider acceptance of active surveillance has been reflected by several population-based studies. Data from the Cancer of the Prostate Strategic Urologic Research Endeavor (CaPSURE), a registry of 45 predominantly community-based urology practices in the United States, indicates that approximately 40 % of low-risk prostate cancer was managed by active surveillance or watchful waiting during the period of 2010–2013 [10]. This figure is nearly double in men aged 75 and over, who stand to benefit the most from this approach. By comparison, only 10 % of men with low-risk prostate cancer were managed with active surveillance or watchful waiting in 2004–2006 [11]. Ingimarsson et al. recently reported data from the New Hampshire State Cancer Registry, demonstrating that active surveillance for low-risk prostate cancer steadily increased from 17 % to 42 % over the study period (2004–2011) [12]. The Michigan Urologic Surgery Improvement Collaborative (MUSIC), which includes 42 urology practices, reported that approximately half utilized active surveillance for low-risk prostate cancer [13].

The Limitations of Active Surveillance

The strategy of active surveillance fundamentally hinges on the available technology and strategies to appropriately risk-stratify patients into low-risk disease, defined by grade and volume. Gleason grading involves judgment and thus is subject to variability in interpretation between observers. Despite this variability, it is remarkable that Gleason grade 3 assigned by the pathologist portends excellent prognosis and essentially little risk of metastasis based on the previously described clinical studies. However, Gleason scoring, despite its correlation with molecular phenotype, is imperfect. A recent report of detailed genetic analyses of multiple metastatic sites was performed on a single patient, initially treated by radical prostatectomy (pT3a, N1) at age 47, who eventually succumbed to metastatic castrate-resistant prostate cancer after multiple salvage therapies [14]. Whole genome analysis of anatomically separate metastases (lung, liver, and peri-gastric lymph node) showed closer molecular homology to a small focus of Gleason pattern 3 as opposed to the large volume of Gleason pattern 4 that was concomitantly present. The extent to which this finding is generalizable is unclear. It is possible that the genetic landscape of Gleason grade 3, which coexists with Gleason pattern 4, is more aggressive—a consideration that could not be further elucidated due a lack of high-quality DNA needed for evaluating the genetic relationship between different foci of cancers identified in the primary gland. Adverse genetic features of a low-grade cancer in a field of higher-grade cancer may reflect a field effect or the "phenocopying" influence of RNA-containing exosomes released by more malignant cells and taken up by lower-grade cells [15]. This case highlights a rare potential for Gleason grade 3 disease to metastasize, which must be weighed against the wealth of clinical data that supports the low metastatic potential of indolent prostate cancer and the further low likelihood of grade progression. It is estimated that the incidence of true biological grade progression (from pattern 3 to patterns 4–5) is on the order of 1 % per year and therefore relatively uncommon. Further, since it is likely the molecular markers of Gleason 3 that confer increased risk are infrequent, the yield of widespread screening to identify this small group of patients is unclear. This has to be balanced with the societally acceptable range of metastatic risk, which, depending on the inclusiveness of the active surveillance protocol, ranges from 0.5 to 5 % [16, 17].

Misattribution, or the failure to identify coexistent higher-grade disease, is a major limitation of active surveillance. This reflects the quality of prostate sampling. The practice of performing a confirmatory biopsy has been adopted to minimize this risk. In addition, predictive factors such as PSA density, race (African origin), and high volume Gleason pattern 3 (as signaled by significant core involvement) are used to identify men at risk of disease reclassification [18]. The ability to incorporate multiparametric magnetic resonance imaging (mpMRI) into the staging algorithm may allow for improved identification of coexistent, higher-risk disease prior to starting active surveillance. The negative predictive value of MRI is the key metric, which ranges from 58 to 100 % [19]. The combination of Gleason score 6 on biopsy with a negative MRI represents a novel low-risk class with a very low likelihood of harboring higher-grade disease [20, 21]. The Active Surveillance MRI Study (ASIST) trial, a randomized phase III study that recently completed accruement, is expected to provide information on whether MRI can improve the selection of patients for active surveillance [22].

Increased identification of low-risk disease (over-detection) has been driven by widespread PSA-based screening. While active surveillance addresses over-treatment, it cannot alter over-detection. It is, however, a reasonable solution to overtreatment and is cost-effective compared to definitive treatment [23, 24]. The burden of active surveillance is not zero. A proportion of men will eventually undergo treatment. In some patients, this is motivated by anxiety and/or worsening urinary symptoms, rather than objective evidence of cancer risk progression. These two phenomena

appear related. Anxiety in men on active surveillance is associated with intolerance to uncertainty and may be worsened by urinary symptoms [25]. Active surveillance also involves costs of long-term follow-up.

Thus, a corollary to this solution to overtreatment is to pursue novel methods to prevent detection of indolent prostate cancer in the first place [26]. Strategies to achieve this include targeted or individualized PSA-screening, use of multiparametric MRI and targeted biopsy for screening [27] and lastly, utilizing genetic and blood biomarkers in an integrated manner to decrease over-detection [28]. Reducing detection of indolent cancer, while appealing, requires proof that these strategies used to define individuals at little risk have robust negative predictive ability. While this remains to be achieved (MRI false-negative rate is 15 %), the likely sequela of this approach would lead to reducing the candidates who require active surveillance. A complementary strategy is the development of improved molecular biomarkers [29, 30] of truly indolent disease that would allow surveillance to be decreased in intensity and duration or altogether eliminated in appropriate individuals. Progression of Gleason score 6 to clinically significant cancer occurs rarely, and while this is a rare event that should not be viewed as a limitation to AS, biomarkers for progression are needed. Taken together, the proportion of candidates eligible for surveillance, and the nature of active surveillance, will evolve.

Boundary Between Active Surveillance and Focal Therapy

Focal therapy represents a strategy to target the location of the dominant disease in the prostate, thereby allowing significant tissue preservation and reduced negative effects to quality of life. Tissue preservation in active surveillance is inexorably linked to its quality of life benefits. Active surveillance represents an important step in matching the aggressiveness of the treatment strategy to that of the cancer, and focal therapy represents a middle ground, where some degree of tissue destruction is indicated to control the index cancer, but radical treatment to the whole gland represents overtreatment. Focal therapy will undoubtedly become an important strategy since diagnostic techniques that confer precise location such as mpMRI and template biopsy [31] are increasingly utilized. These identify index lesions that are clinically significant but occupy a small proportion of the prostate. These approaches have a high degree of concordance (approximately 95 %) between the risk at diagnosis by systematic biopsy and the assigned risk based on radical prostatectomy specimen or template mapping biopsy (5 mm) [32, 33]. A risk stratification model that takes into consideration both volume and grade, such as the "traffic-light" stratification model ("green," "yellow," and "red" disease), is compelling [8, 34].

Given the established role of active surveillance, candidates for aggressive treatment have been reduced. Specifically, Gleason 6, non-extensive disease, with a non-suspicious MRI and with low PSA density, represents ideal candidates for active surveillance. There exists a "gray zone" of patients wherein the selection of active surveillance versus more aggressive therapy is unclear. This may represent an opportunity to deploy focal therapy. This includes patients with very extensive Gleason score 6, Gleason 6 in men less than 50 years of age, and Gleason 7 with <10 % Gleason pattern 4. An additional group of patients are those with Prostate Imaging Reporting and Data System (PI-RADS) 4–5 with low-grade disease on targeted biopsy or a high PSA density. Lastly, African-American race should be given some consideration for more aggressive treatment. African-Americans on active surveillance have higher rates of disease reclassification and worse outcomes after treatment compared to Caucasians [35]. Emerging biomarkers, including genetic tests, could help further reclassify seemingly low-risk disease with greater metastatic potential that warrants more intensive therapy. In contrast, patients with Gleason ≥7 with >10 % Gleason grade 4 are clearly the traditional group of patients for aggressive therapy. The use of focal therapy in this group should remain selective.

Conclusion

Moving forward, the challenge focal therapy faces is in demonstrating long-term, durable disease control. There are several competing focal therapies such as high-intensity focused ultrasound, cryotherapy, and brachytherapy. The comparative effectiveness of these approaches remains to be elucidated. Studies of focal therapy should be carried out in patients with clinically significant cancer, not in men who would be better managed with surveillance. They are complementary. Without this focus, there remains a real risk of focal therapy being overutilized in low-risk prostate cancer.

References

1. Edwards BK, Noone AM, Mariotto AB, Simard EP, Boscoe FP, Henley SJ, et al. Annual report to the nation on the status of cancer, 1975–2010, featuring prevalence of comorbidity and impact on survival among persons with lung, colorectal, breast, or prostate cancer. Cancer. 2014;120:1290–314.
2. Hanahan D, Weinberg RA. Hallmarks of cancer: the next generation. Cell. 2011;144:646–74.
3. Vander Weele DJ, Brown CD, Taxy JB, Gillard M, Hatcher DM, Tom WR, et al. Low-grade prostate cancer diverges early from high grade and metastatic disease. Cancer Sci. 2014;105:1079–85.
4. Porten SP, Whitson JM, Cowan JE, Cooperberg MR, Shinohara K, Perez N, et al. Changes in prostate cancer grade on serial biopsy in men undergoing active surveillance. J Clin Oncol. 2011;29(20):2795–800.
5. Ross HM, Kryvenko ON, Cowan JE, Simko JP, Wheeler TM, Epstein JI. Do adenocarcinomas of the prostate with Gleason score (GS) ≤6 have the potential to metastasize to lymph nodes? Am J Surg Pathol. 2012;36(9):1346–52.
6. Eggener SE, Scardino PT, Walsh PC, Han M, Partin AW, Trock BJ, et al. Predicting 15-year prostate cancer specific mortality after radical prostatectomy. J Urol. 2011;185(3):869–75.
7. Epstein JI, Egevad L, Amin MB, Delahunt B, Srigley JR, PA H, Grading Committee. The 2014 International Society of Urological Pathology (ISUP) Consensus Conference on Gleason Grading of Prostatic Carcinoma: definition of grading patterns and proposal for a new grading system. Am J Surg Pathol. 2016;40(2):244–52.
8. Klotz L, Emberton M. Management of low risk prostate cancer—active surveillance and focal therapy. Nat Rev Clin Oncol. 2014;11:324–34.
9. Tosoian JJ, Carter HB, Lepor A, Loeb S. Active surveillance for prostate cancer: current evidence and contemporary state of practice. Nat Rev Urol. 2016;13(4):205–15.
10. Cooperberg MR, Carroll PR. Trends in management for patients with localized prostate. cancer, 1990–2013. JAMA. 2015;314:80–2.
11. Cooperberg MR, Broering JM, Kantoff PW, Carroll PR. Contemporary trends in low risk prostate cancer: risk assessment and treatment. JURO. 2007;178:S14–9.
12. Ingimarsson JP, Celaya MO, Laviolette M, Rees JR, Hyams ES. Trends in initial management of prostate cancer in New Hampshire. Cancer Causes Control. 2015;26:923–9.
13. Womble PR, Montie JE, Ye Z, Linsell SM, Lane BR, DC M, Michigan Urological Surgery Improvement Collaborative. Contemporary use of initial active surveillance among men in Michigan with low-risk prostate cancer. Eur Urol. 2015;67(1):44–50.
14. Haffner MC, Mosbruger T, Esopi DM, Fedor H, Heaphy CM, Walker DA, et al. Tracking the clonal origin of lethal prostate cancer. J Clin Invest. 2013;123(11):4918–22.
15. Zomer A, van Rheenen J. Implications of extracellular vesicle transfer on cellular heterogeneity in cancer: what are the potential clinical ramifications? Cancer Res. 2016;76(8):2071–5.
16. Klotz L, Vesprini D, Sethukavalan P, Jethava V, Zhang L, Jain S, et al. Long-term follow-up of a large active surveillance cohort of patients with prostate cancer. J Clin Oncol. 2015;33(3):272–7.
17. Tosoian JJ, Mamawala M, Epstein JI, Landis P, Wolf S, Trock BJ, et al. Intermediate and longer-term outcomes from a prospective active-surveillance program for favorable-risk prostate cancer. J Clin Oncol. 2015;33(30):3379–85.
18. Petrelli F, Vavassori I, Cabiddu M, Coinu A, Ghilardi M, Borgonovo K, et al. Predictive factors for reclassification and relapse in prostate cancer eligible for active surveillance: a systematic review and meta-analysis. Urology. 2016;91:136–42.
19. Hamoen EHJ, de Rooij M, Witjes JA, Barentsz JO, Rovers MM. Use of the Prostate Imaging Reporting and Data System (PI-RADS) for prostate cancer detection with multiparametric magnetic resonance imaging: a diagnostic meta-analysis. Eur Urol. 2015;67:1112–21.
20. Vargas HA, Akin O, Afaq A, Goldman D, Zheng J, Moskowitz CS, et al. Magnetic resonance imaging for predicting prostate biopsy findings in patients considered for active surveillance of clinically low risk prostate cancer. J Urol. 2012;188(5):1732–8.
21. Panebianco V, Barchetti F, Sciarra A, Ciardi A, Indino EL, Papalia R, et al. Multiparametric magnetic resonance imaging vs. standard care in men being evaluated for prostate cancer: a randomized study. Urol Oncol. 2015;33(1):17.e1–7.
22. Active Surveillance Magnetic Resonance Imaging Study (ASIST). NCT01354171. https://clinicaltrials.gov/ct2/show/NCT01354171?term=NCT01354171&rank=1.
23. Eldefrawy A, Katkoori D, Abramowitz M, Soloway MS, Manoharan M. Active surveillance vs. treatment

for low-risk prostate cancer: a cost comparison. Urol Oncologia. 2013;31:576–80.
24. Dragomir A, Cury FL, Aprikian AG. Active surveillance for low-risk prostate cancer compared with immediate treatment: a Canadian cost comparison. CMAJ Open. 2014;2(2):E60–8.
25. Tan HJ, Marks LS, Hoyt MA, Kwan L, Filson CP, Macairan M, et al. The relationship between intolerance of uncertainty and anxiety in men on active surveillance for prostate cancer. J Urol. 2016;195(6): 1724–30.
26. Gandaglia G, Briganti A, Fossati N, Salonia A, Mottrie A, Catto J, et al. The problem is not what to do with indolent and harmless prostate cancer-the problem is how to avoid finding these cancers. Eur Urol. 2016;70(4):547–8.
27. Nam RK, Wallis CJ, Stojcic-Bendavid J, Milot L, Sherman C, Sugar L, et al. A pilot study to evaluate the role of magnetic resonance imaging for prostate cancer screening in the general population. J Urol. 2016;196(2):361–6.
28. Grönberg H, Adolfsson J, Aly M, Nordström T, Wiklund P, Brandberg Y, et al. Prostate cancer screening in men aged 50-69 years (STHLM3): a prospective population-based diagnostic study. Lancet Oncol. 2015;16(16):1667–76.
29. Cullen J, Rosner IL, Brand TC, Zhang N, Tsiatis AC, Moncur J, et al. A biopsy-based 17-gene genomic prostate score predicts recurrence after radical prostatectomy and adverse surgical pathology in a racially diverse population of men with clinically low- and intermediate-risk prostate cancer. Eur Urol. 2015;68(1):123–31.
30. Lalonde E, Ishkanian AS, Sykes J, Fraser M, Ross-Adams H, Erho N, et al. Tumour genomic and microenvironmental heterogeneity for integrated prediction of 5-year biochemical recurrence of prostate cancer: a retrospective cohort study. Lancet Oncol. 2014;15(13):1521–32.
31. Barzell WE, Melamed MR. Appropriate patient selection in the focal treatment of prostate cancer: the role of transperineal 3-dimensional pathologic mapping of the prostate–a 4-year experience. Urology. 2007; 70:27–35.
32. Moore CM, Robertson NL, Arsanious N, Middleton T, Villers A, Klotz L, et al. Image-guided prostate biopsy using magnetic resonance imaging-derived targets: a systematic review. Eur Urol. 2013;63(1): 125–40.
33. Crawford ED, Rove KO, Barqawi AB, Maroni PD, Werahera PN, Baer CA, et al. Clinical-pathologic correlation between transperineal mapping biopsies of the prostate and three-dimensional reconstruction of prostatectomy specimens. Prostate. 2013;73(7): 778–87.
34. Ahmed HU, Hu Y, Carter T, Arumainayagam N, Lecornet E, Freeman A, et al. Characterizing clinically significant prostate cancer using template prostate mapping biopsy. J Urol. 2011;186(2):458–64.
35. Sundi D, Ross AE, Humphreys EB, Han M, Partin AW, Carter HB, et al. African American men with very low-risk prostate cancer exhibit adverse oncologic outcomes after radical prostatectomy: should active surveillance still be an option for them? J Clin Oncol. 2013;31(24):2991–7.

Focal Therapy and Active Surveillance in Europe

5

Jan Philipp Radtke, Angelo Territo, Markus Hohenfellner, and Alberto Breda

Introduction

Prostate cancer (PCa) is the most commonly diagnosed cancer in European men (382,000 new cases annually: 22.2 % of all male cancer cases), followed by lung (291,000, 17.0 %), colorectal (231,000, 13.5 %), bladder (110,000, 6.4 %), and stomach (89,000, 5.2 %) cancers [1]. The incidence of PCa is increasing dramatically (almost doubled from an age-standardized incidence of 47.4 per 100,000 in 1995 to 93.4 per 100,000 in 2008), especially in countries where prostate-specific antigen (PSA) testing of older men has become widespread. Mortality has, however, decreased in several countries, which may be related to improved outcome following early diagnosis [2]. Considering these epidemiological data, the diagnostic and therapeutic landscape of PCa is one of the most exciting areas of medical research in our modern age. The manner in which we currently diagnose and treat PCa seems to lead to an ever-increasing cost to the individual patient and to healthcare systems in general but with great uncertainty over the benefits.

While the incidence of PCa increased, the median volume of cancer in men with newly diagnosed PCa fell significantly [3]. These trends represented a classic stage migration of cancer associated with a new diagnostic test [3]. About half of newly diagnosed men are diagnosed with low-grade prostate cancer [3]. An emerging consensus is that most men with low-risk PCa do not derive any meaningful benefit from radical treatment and an initial conservative approach is warranted. Active surveillance (AS) and organ-sparing focal therapy (FT) have emerged as alternative treatment options for men with early-stage disease and continue to be intensely investigated. In Europe, the largest study for AS is the Prospective Validation of Active Surveillance in Prostate Cancer (PRIAS) study [4]. In the PRIAS cohort, more than 4500 men undergoing AS since 2009 have been followed up [5].

Focal therapy may possibly be offered to men with PCa within the lower ranges of intermediate-risk cancers. It has been emerging as a promising management strategy that ideally targets the cancer area selectively while sparing the rest of the gland, thereby leading to fewer adverse effects

J.P. Radtke (✉)
Department of Urology, Universitätsklinikum Heidelberg, Heidelberg, Baden-Württemberg, Germany

Department of Radiology, German Cancer Research Center, Heidelberg, Germany
e-mail: j.radtke@dkfz-heidelberg.de

A. Territo • A. Breda
Department of Urology, University Autonoma of Barcelona, Fundaciò Puigvert, Barcelona, Spain

M.R. Hohenfellner
Department of Urology, Universitätsklinikum Heidelberg, Heidelberg, Baden-Württemberg, Germany

© Springer International Publishing AG 2017

T.J. Polascik (ed.), *Imaging and Focal Therapy of Early Prostate Cancer*, Current Clinical Urology, DOI 10.1007/978-3-319-49911-6_5

than radical therapies. According to proponents of this approach, the so-called index lesion(s) represents the area where structural changes of the prostate by the tumor material reach a level of significant functional and metabolic modifications that can be designed for targeted biopsies and FT. Therefore, an index lesion is only one area of clinically significant disease in a patient. In case of no clinically significant disease, it is impossible to identify an index lesion [6]. According to the University College London definition, significant disease is "any lesion with a Gleason pattern of 4 and/or an estimated volume of 0.5 ml or greater" [6]. A maximum cancer core length of 6 mm or greater or a total cancer core length of 10 mm or greater in the transperineal template prostate mapping biopsy predicts a lesion of 0.5 ml or greater with more than 95 % accuracy [7]. Obviously, knowledge of the index lesion location is crucial to define the correct treatment plan. Although FT is not yet accepted as an alternative treatment for PCa, it has important potential. Any man with localized PCa suitable for curative therapy could potentially be considered as suitable for some form of FT intervention. Such a pragmatic approach would not entail a lower or upper age limit. However, FT has been seen by many, predominantly in the USA, as an alternative to AS, whereas others, mainly in Europe, have argued that FT should also be regarded as an alternative to radical therapies [8]. In European urological centers, several ablative energies have been applied in a focal manner for the treatment of PCa including cryotherapy, high-intensity focused ultrasound (HIFU), laser ablation therapy, radiofrequency ablation, irreversible electroporation, and photodynamic therapy. The optimal ablative modality to deliver FT is not clear. While cryoablation is recognized by the American Urological Association (AUA) guidelines as a valid method, the European Association of Urology (EAU) guidelines consider cryotherapy and HIFU as experimental options in the case of clinically localized PCa [9]. One of the primary tenets of surgery and medicine, referred to in the Hippocratic oath, is *primum non nocere*: First do no harm. It is mandatory to consider this injunction in the case of experimental therapy.

In this chapter we evaluate the role of AS and FT in men suffering from low-risk PCa. We report on different AS protocols and FT methods and analyze outcomes and follow-up of both approaches.

Active Surveillance in Europe

Criteria for Active Surveillance Inclusion

In Europe, three different protocols and programs are used to include patients into AS [4, 10, 11]. All protocols established criteria combining biopsy data (Gleason score [GS]) with clinical data to identify potentially low-risk tumors. According to the Epstein criteria, characteristics of "insignificance" incorporate clinical stage T1, Gleason pattern 3 in the biopsy specimen (no Gleason pattern 4), and either (1) prostate-specific antigen (PSA) density of 0.1 ng/ml/g, 2 or fewer positive biopsy cores (minimum of 6 cores taken), and no cores with >50 % involvement or (2) PSA density of 0.15 ng/ml/g and cancer <3 mm in only 1 biopsy core (minimum of 6 cores taken) [12, 13]. Based on the Epstein criteria, protocols incorporate Gleason grade ≤3+3 PCa, low clinical stage ≤cT2a, and low PSA values (<10 ng/ml) with biopsy-driven tumor volume estimates to select patients for AS eligibility [4, 10]. The use of more stringent criteria for entry will limit the number of men offered AS, and it remains debatable whether the most "conservative" selection criteria are optimal [14]. As most protocols limit AS to men with low-risk PCa, extending AS criteria under adherence to strict follow-up criteria might be debatable [15–17].

The most frequently used protocol is the PRIAS [4]. The PRIAS study was conducted from the European Randomized Study of Screening for Prostate Cancer (ERSPC) trial and initiated in 2009 [4]. Eligible patients had clinical stage T1/T2a PCa, prostate-specific antigen ≤10 ng/ml, PSA density <0.2 ng/ml/ml, 1 or 2 positive biopsy cores, and GS ≤ 6 [4]. Until 2015, a total of 4547 men with low-risk prostate cancer on AS were included and prospectively followed

[5]. Another protocol that is less strict histologically is the Royal Marsden Hospital protocol [10]. Eligible patients include those who have a clinical stage of T1/T2a, PSA ≤ 15 ng/ml, GS ≤ 3+4, and total number of involved cores ≤50 % [10]. The Göteborg randomized screening trial analyzed 341 men with very-low-risk and low-risk PCa according to Epstein criteria as well as 92 men with intermediate-risk and 6 men with high-risk PCa undergoing AS [11]. Follow-up included PSA monitoring every 3–6 months [11]. Rebiopsies were not regulated but were recommended at signs of PSA or T-stage progression; patients with stable disease were also recommended for rebiopsy typically every second to third year, but this referral depended on initial biopsy outcome, patient age, comorbidity, and preferences [11].

Repeat Prostate Biopsy Under Active Surveillance

Repeat prostate biopsies over time have been incorporated into most surveillance protocols [4, 10, 11]. As Gleason grade remains one of the most important predictors of prognosis for men with PCa, it is crucial to identify higher-grade disease that may not be best managed expectantly [14]. It has been recognized that many men undergoing immediate RP after cancer diagnosis are found to have higher-grade disease than known preoperatively [18, 19]. This risk of clinical undergrading with a 12-core biopsy is estimated to be 20–50 % [18–20]. Biopsy technique can affect both overall and clinically significant PCa detection [21–23].

It is unknown whether changes in histology over time represent tumor dedifferentiation and growth or simply tissue undersampling; however, it is likely a combination of the two [14, 24]. Serial prostate biopsy might identify both situations, with the early "confirmatory" and improved (magnetic resonance imaging [MRI]-targeted) biopsy minimizing the risk of undersampling [23, 25–27]. Within the PRIAS cohort, 79 % of men had either no PCa detected or PCa still meeting all AS criteria after confirmatory biopsy [28]. Nine percent of men had higher Gleason grade disease, while 17 % had higher-volume disease [28]. Overall, 21 % had adverse pathologic features after the first rebiopsy, rendering AS ineligibility [28]. Interim analyses of the PRIAS cohort showed that more positive cores at initial diagnosis (2 cores vs 1 core) and also at repeat biopsy were associated with higher grade or higher cancer volume at repeat biopsy and AS disqualification [5, 28]. Regarding the time interval between repeat biopsies, the PRIAS protocol recommends them at 1, 4, and 7 years after initial biopsy [4]. At the moment, no study available can demonstrate that repeat biopsies might be avoided. In particular, no robust data are available to support the use of MRI in place of repeat biopsy to detect progression over time [29]. The future role of MRI in selection of patients for repeat surveillance biopsy is discussed in Chap. 13.

The Role of Prostate-Specific Antigen and Serum Biomarkers

Bokhorst et al. focused on PSA, PSA density, and the PSA doubling time (PSA-DT) to determine upgrading from AS within the PRIAS trial [5]. They analyzed that the PSA doubling time (DT) at least once from 3 to 10 years ($p = 0.039$) as well as from 0 to 3 years ($p < 0.001$) were significant predictors of upgrading (Gleason >6 and/or 2 cores positive) [5]. In contrast, PSA-DT >10 years, PSA density at diagnosis, and PSA level at first or second repeat biopsy were not statistically significant predictors of upgrading [5].

Data from the Royal Marsden cohort suggest that PSA velocity (PSAV) may be more predictive than PSA-DT, showing that a PSAV >2.0 ng/ml/year was significantly associated with Gleason grade change from 3+3 to ≥3+4, more than half of the cores being positive for PCa or primary Gleason grade 4 [16].

When interpreting these data, it is important to consider the indications for repeat biopsy in the differing studies, as ascertainment bias can lead to stronger associations if men with rising PSA values were more likely to undergo frequent biopsy [14]. In fact, PSA changes are unlikely to justify treatment in isolation but may prompt an earlier repeat biopsy [14]. However, a

lack of histology progression with rising PSA may prompt intervention [14].

The discussion of the predictive value of PSA, PSA-DT, and PSAV leads to increasing interest in analyzing other serum markers and PSA isoforms to gain accuracy.

Tosoian et al. retrospectively related PSA isoforms to unfavorable findings (GS ≥7, 3 or more cores, >50 % involvement) on annual biopsy in AS patients ($n = 167$) [30]. In serum, free (fPSA) and bound forms of PSA as well as different PSA protein isoforms can be found. Biopsy reclassification was associated with baseline and longitudinally measured ratio of fPSA to total PSA (tPSA, %fPSA) and the Prostate Health Index (PHI) [31], defined as

$$([-2]\text{proPSA/free PSA}) \times \sqrt{\text{PSA}}$$

The mean baseline PHI for patients with and without biopsy reclassification was 37.45 versus 27.99 ($p = 0.0002$) [31]. In addition, Makarov et al. assessed PSA isoforms in serum and also in PCa and adjacent tissue areas with quantitative immunohistochemistry ($n = 71$) [32]. The results were analyzed with respect to unfavorable repeat biopsy findings during AS (GS ≥7, 3, or more cores, >50 % involvement) [32]. The ratio of [−2]proPSA to %fPSA in serum at diagnosis was higher in men developing unfavorable repeat biopsy [32]. The mean ratio of [−2]proPSA to %fPSA for favorable versus unfavorable repeat biopsy outcomes was 0.65 versus 0.87 ($p = 0.02$), respectively [32].

Two studies retrospectively focused on the value of fPSA in AS patients. Van As et al. found that T-stage and %fPSA remained significant predictors of transition to radical treatment during AS ($n = 326$) [10]. Classifying patients into groups using the median values as a threshold, patients with both favorable PSA and %fPSA, 1 favorable or both unfavorable, had an active treatment rate at 3 years of 0 %, 27 %, and 55 %, and histologic progression rates of 0 %, 28 %, and 35 %, respectively [10]. Receiver operating characteristic (ROC) for %fPSA as a predictor of radical treatment within 2 years was 0.83 [10]. Khan et al. found that besides tPSA and gland volume, %fPSA at diagnosis predicted unfavorable findings at repeat biopsy [33]. The diagnostic accuracy of combined variables ranged from 75 % to 84 %, and the area under the ROC curve was 0.83 [33].

Castro et al. recently investigated the association of germline BRCA1 and BRCA2 mutations with tumor features and outcomes in 2019 patients (18 BRCA1 carriers, 61 BRCA2 carriers, and 1940 noncarriers) with localized PCa [34]. PCa with germline BRCA1/2 mutations were more frequently associated with GS ≥ 8 ($p = 0.0003$), T3/T4 stage ($p = 0.003$), nodal involvement ($p = 0.00005$), and metastases at diagnosis ($p = 0.005$) than PCa in noncarriers [34]. For localized PCa, a 5-year cause-specific survival was significantly higher in noncarriers [34]. In conclusion, BRCA1/2 mutations confer a more aggressive PCa phenotype with a higher probability of nodal involvement and distant metastasis [34].

Within the IMPACT trial, Bancroft et al. analyzed data from 2481 men and found that the positive predictive value for biopsy using a PSA threshold of 3.0 ng/ml in BRCA2 mutation carriers was 48 %—double the positive predictive value reported in population screening studies [35]. To predict more aggressive and unfavorable PCa in the future, analyzing BRCA1/2 mutation carriers might be of gaining interest also in patients, in whom a GS 3+3 PCa was detected within biopsy and who might be appropriate for AS.

Klein et al. analyzed a 17-gene genomic classifier to predict PCa aggressiveness [36]. They analyzed 732 genes and found 288 that predicted clinical recurrence (defining aggressive PCa), GS, and clinical stage. Furthermore, 198 genes were predictive for aggressive disease. Eventually, 17 of the identified genes representing multiple biological pathways were combined into a genomic classifier algorithm. In a validation cohort, the genomic classifier predicted high-grade and high-stage at surgical pathology. After controlling for established clinical factors—for example, adjustment for the Cancer of the Prostate Risk Assessment (CAPRA) score—the classifier predicted high-grade and/or high-stage

disease [36]. They concluded that genes representing multiple biological pathways discriminate PCa aggressiveness in biopsy tissue despite tumor heterogeneity and multifocality. The biopsy-based 17-gene genomic classifier improves prediction of presence or absence of adverse pathology and may help men with PCa make more informed decisions between AS and immediate treatment [36].

Urinary and Tissue Markers

At the moment, no consensus exists regarding the optimal follow-up and dynamic progression criteria for AS [37]. Thus, novel biomarkers are gaining interest by potentially improving the prediction of tumor volume, tumor grade, and the natural history of PCa [38].

In this context, Berg et al. hypothesized that tissue biomarkers, in particular the gene fusion between TMPRSS2 and ERG, might improve individualized treatment regimens [39]. The gene fusion between TMPRSS2 and ERG, a consequence of chromosomal rearrangement or interstitial deletion, was identified as a common genetic alteration in PCa occurring in 40–70 % of tumors [40]. Consequently, ERG becomes androgen regulated and overexpressed in TMPRSS2-ERG-positive tumors [39]. TMPRSS2-ERG fusion is associated with an increased risk of PCa-specific death for patients managed conservatively and with higher tumor volume, stage, and grade [41–43]. Berg et al. retrospectively analyzed 265 ERG-positive and ERG-negative patients under AS. In a risk model, the ERG-positive group showed significantly higher incidences of overall AS progression ($p < 0.0001$), PSA progression ($p < 0.0001$), and histopathologic progression ($p < 0.0001$) [39]. The cumulative incidence in a 2-year follow-up of overall AS progression was 21.7 % in the ERG-negative group compared with 58.6 % in the ERG-positive group [39]. In addition, ERG positivity was a significant predictor of overall AS progression in multiple Cox regression (hazard ratio, 2.45; $p < 0.0001$) [39].

Ploussard et al. retrospectively tested the performance of PCA3 in 106 patients with low-risk PCa who underwent RP [44]. A PCA3 score threshold of 25 was significantly associated with tumor volume and improved on the predictive value of biopsy criteria (odds ratio for volume >0.5 ml was 3.19) [44]. Only 28 % of patients had a PCA3 score <25 [44].

However, van den Bergh et al. concluded that the value of PCA3 score seems limited due to the lack of a consistent association with disease stage or GS [38]. Only a minority of patients have the low PCA3 scores that show the best predictive accuracy [38]. If surveillance were restricted to those with such a low PCA3 score, many patients would be excluded from AS who may have in fact been suitable [38].

The Role of Imaging Utility of MRI and Targeted Biopsies Among Men Under Active Surveillance

Accurate risk stratification of patients undergoing active surveillance (AS) versus active treatment is crucial for a sound AS program with high patient safety and to reduce potential morbidities associated with radical treatment [45]. The most criticized part of AS is its dependence on the initial biopsy quality, since the GS of a high number of PCa is following RP [46, 47].

Accurate and safe stratification means to correctly rule in low-risk disease on the one hand and to rule out significant PCa on the other hand. With regard to AS candidacy, Vargas et al. demonstrated that multiparametric magnetic resonance imaging (mpMRI) can predict upstaging in rebiopsies of AS patients in up to 98 % [48, 49]. Similarly, the utility of MRI/transrectal ultrasound (TRUS)-fusion biopsies in AS cohorts has been demonstrated with encouraging results. Hu et al. have shown an upgrading in GS, core involvement, and targeted biopsy (TB) of 36 % compared to 12-core TRUS biopsy [50]. Best detection accuracy was demonstrated for the combination of targeted biopsy and systematic biopsy (SB), as TB alone led to underdetection of 10 % of significant PCa [50]. Radtke et al.

focused on the probability to stay on AS for men initially diagnosed by mpMRI and MRI/TRUS fusion biopsy compared to men, whose AS eligibility was confirmed based on a conventional 12-core TRUS biopsy [20]. They found a statistically significant higher probability to stay under AS for men whose eligibility was based on MRI/TRUS fusion biopsy over a period of 2 years of follow-up [20]. In addition, when AS was based or confirmed by MRI/TRUS fusion biopsy, only biopsying men, whose MRI showed Prostate Imaging Reporting and Data System (PI-RADS) score progression on the follow-up MRI, would not lead to miss AS disqualification [20].

A recently published systematic review focused on mpMRI in AS [29]. Schoots et al. found an overall reclassification rate of 33 % according to PRIAS criteria when TB are used after initial SB [29]. In AS follow-up, mpMRI using PI-RADS scoring has the potential to rule out significant PCa. Mullins et al., Vargas et al., and Da Rosa et al. showed a negative predictive value (NPV) of above 90 % for a pristine MRI to rule out significant PCa [48, 51, 52].

Going more into functional sequences (diffusion weight imaging [DWI] and apparent diffusion coefficient [ADC] maps on mpMRI), Van As et al. analyzed the ADC values of MRI lesions corresponding with positive biopsy in the same prostate region ($n = 86$) [53]. ADC was significantly related to adverse pathology on repeat biopsy, with area under the receiver operating characteristic (ROC) of 0.83 [53]. Interestingly, among those patients with a favorable ADC, none had adverse pathology at repeat biopsy, also suggesting that repeat biopsy might be unnecessary in men with a favorable MRI [53]. Somford et al. performed 3-T mpMRI with endorectal coil (including T2-weighted and DW images) in patients included in an AS protocol ($n = 54$) [54]. At least one suspicious region (two in most patients) was identified in 98 % of patients and biopsied [54]. Mean ADC was different between MRI-guided biopsies that showed no PCa (1.26), low-grade PCa (1.09), and high-grade PCa (0.84) [54].

In total, Schoots et al. concluded that MRI can detect clinically significant disease in one-third to half of men at the start of surveillance and in the follow-up course [29]. However, at the moment no robust data are available to support the use of MRI in place of repeat biopsy to detect progression over time [29]. In addition, Recabal et al. and Radtke et al. recently analyzed the potential of MRI-targeted biopsies compared to conventional 12-core TRUS and 24-core transperineal SB [20, 55]. Both described higher detection rates of pathological GS upgrading for MRI-targeted biopsies [20, 55]. However, at the moment, systematic biopsies cannot be omitted, due to a significant number of cores harboring unfavorable GS [20]. Van den Bergh et al. summarized in a systematic review that many studies are available on the value of MRI within AS, although none use MRI as an indication for treatment [38]. Multiparametric MRI generally shows a very high NPV for the intermediate end point of disease upgrading [38]. They concluded that favorable MRI findings on a good-quality mpMRI may therefore be used for selection and follow-up of patients during AS and might obviate the need for repeat biopsies in the future [38]. However, MRI was thought to be less useful after extensive biopsy protocols [38].

Expanding the Criteria of Active Surveillance

As one of the most conservative and secure AS protocols, the widespread use of the European PRIAS protocol has strict inclusion criteria for patients eligible for AS. It has become important to identify criteria to possibly expand the group of patients, who can be offered AS [14]. However, in order to expand the criteria of AS, both patient factors and tumor characteristics have to be taken into account [14]. Several studies have reported men with GS 7 PCa on AS, otherwise meeting AS criteria based on stage, PSA, and tumor volume estimates [5, 15, 56]. Van den Bergh et al. analyzed a cohort with GS 7 PCa with a median follow-up of 3.4 years and reported a 100 % PCa-specific and 68 % all-cause 6-year survival in 21 men [56]. In a multi-institutional trial, analyzing

2323 men with localized GS 3+4 PCa that subsequently underwent RP, Ploussard et al. reported that 46 % had unfavorable disease (upstaging or upgrading or both) [15]. However, only 19 % of patients without any risk factors (PSA up to 10 ng/ml, PSA density up to 0.15 ng/ml/g, T1c up to 2 positive cores) had unfavorable disease [15]. In contrast, Bokhorst et al. recently found that patients who continued AS with a GS >3+3 on the repeat biopsy had a 3.6-fold higher risk of unfavorable disease and consequently AS disqualification in the further follow-up [5]. Godtman et al. evaluated men within the Göteborg Randomized, Population-based Prostate Cancer Screening Trial and reported that those with intermediate-risk PCa on AS have a significant 3.7-fold higher risk of AS failure compared to men with very low-risk PCa [11].

In conclusion, expanding AS criteria to Gleason score 3+4 disease is controversial. Ploussard et al. conclude that expanding AS eligibility to patients with Gleason score 3+4 PCa might be acceptable, as long as there is adherence to strict selection criteria [15]. In contrast, the PRIAS and Göteborg Randomized, Population-based Prostate Cancer Screening Trial data suggest that AS should primarily be reserved for men with low-risk disease [5, 11]. In addition, Godtman et al. suggest that patients with intermediate-risk PCa should be carefully informed that delaying radical treatment is associated with a higher risk of developing incurable disease [11]. Dell'Era et al. and Ploussard et al. both conclude that future advances in mpMRI and biomarker discovery might allow inclusion criteria for AS to expand [14, 15].

Patient and Urologist Compliance on Active Surveillance

AS is a treatment option that aims to reduce the negative side effects of radical treatment while retaining the option for curative treatment, involving strict follow-up and only offering treatment to men who show signs of disease progression or reclassification [5]. However, optimal criteria for inclusion, exclusion, and follow-up are still discussed. Most protocols include criteria based on a combination of PSA tests, digital rectal examination, and repeated biopsies in order to define eligibility of patients and disease reclassification [57]. However, some men and their physicians might choose to deviate from these strict protocols, ignoring either the follow-up schedule or the advice to switch to curative treatment [5]. Bokhorst et al. studied compliance rates in the PRIAS protocol and found that protocol deviations occur especially in men who require yearly repeat biopsies due to fast-rising PSA [5]. In fact, in years 2 and 3 after diagnosis, approximately 30 % of men with a repeat biopsy because of PSA-DT between 3 and 10 years were upgraded [5]. Men who ignored the biopsy advice in year 2 or 3 seemed to have a similar rate of upgrading on biopsy in year 4 [5]. This indicates that upgrading is delayed by 1–2 years for 10–15 % of men ignoring the recommendation to have a repeat biopsy on the basis of PSA kinetics [5]. Despite the higher risk, which was reported before, many men do not have yearly biopsies [61]. Secondly, PSA kinetics such as PSA-DT were also regularly ignored as a recommendation to discontinue AS [5].

Bokhorst et al. also observed a decreased percentage of men receiving the standard repeat biopsies over time, from 81 % in year 1 to 60 % in year 4, 53 % in year 7, and 33 % at 10 years after diagnosis [5]. Compared to PSA testing, biopsies are considered uncomfortable. In addition, several complications are recorded, such as pain, hematuria, and even sepsis [58]. These complications will result in some men declining repeat biopsies [59]. However, in recent published results of the 1164 men within the PRIAS study, the infection rate was low (2.5 %) and only 1 of 5 men reported any form of complication [60]. The authors found no evidence that repeated prostate biopsies in itself pose a risk of infection [60].

Bokhorst et al. concluded that the development of follow-up schedules that are acceptable to those who follow them is crucial [5]. Less harmful ways of monitoring tumor progression, such as MRI, might be incorporated in the protocol design to improve compliance [5, 62]. In the PRIAS study, a side study was initiated to investigate if replacing yearly biopsies in men with fast-rising PSA by MRI with targeted biopsies in

the case of visible tumor progression could substantially reduce the number of biopsies (protocol available on www.prias-project.org) [5].

The quality of life for patients undergoing AS was studied in a European meta-analysis by Bellardita et al. [63]. High overall health-related quality of life (HRQoL) scores were reported in 70 % of the included AS studies, thus indicating good QoL [63]. No major differences were observed between the HRQoL scores of AS patients and their comparison groups [63]. There were also no major changes in HRQoL after 9 or 12 months on AS in two PRIAS cohorts [64, 65]. Finnish men in the PRIAS also reported higher scores than a sample population at baseline and follow-up assessments, which the authors suggested may result from men with favorable psychological characteristics choosing AS [65]. Vanagas et al. highlighted that men on AS reported significantly better HRQoL than men who underwent radical treatment in both functional and symptom scales [66].

Another issue is AS acceptance not only in university medical centers but also the widespread use in private practices. A German study analyzed 361 AS patients who were managed in an AS protocol by private practitioners [67]. The authors reported that only 15 % of all patients with localized PCa were treated with AS [67]. At baseline, 58 % of all AS patients met the PRIAS low-risk criteria [67]. After a median follow-up of 24 months, no systemic progression was observed, five patients died of non-disease-specific causes, and active treatment was delivered in 20.5 % of all patients [67]. Triggers for active therapy were progression at biopsy (42 %), rise in prostate-specific antigen level (27 %), medical advice (16 %), and patient's preference (10 %), respectively [67].

Focal Therapy in Europe

Definition, Possibilities, and Limits of Focal Therapy

FT is a tissue-preserving strategy with the aim to target the cancer and not the whole organ, reducing damage to collateral tissues. Therefore, any approach able to preserve part of prostatic tissue can be considered FT. According to it, target regions to treat with FT may include *index lesion target ablation* (a biopsy-confirmed cancer with a concordant radiographic lesion), *hemi-ablation* (one side of the prostate), *hockey-stick ablation* or *three-quarter ablation* (one side and a portion of the contralateral, considered an extended hemi-ablation), and *multifocal ablation* (when multifocal disease is present) [68, 69]. In Fig. 5.1 hemi-ablation using cryotherapy is shown.

The potential advantages of FT include (1) treatment of PCa with non-inferior rates of cancer progression or metastases risk compared to radical treatment (surgery or radiation), (2) reducing treatment-related morbidity, and (3) possibility to re-treat the prostate with focal or whole-gland treatment [70]. Despite these conceptually rational advantages, the main concern is the potential inadequate cancer control compared with whole-gland treatment. In fact, the limits of FT procedures are related to the possibility of inappropriate patient selection, inaccurate or incomplete tumor characterization (clinical staging, mapping, imaging), and suboptimal cancer ablation [70].

Risk Stratification System

A risk stratification model based on both volume and grade has recently been proposed [3]. This risk stratification system is exhaustive and is displayed as a traffic light system. *Green* indicates disease considered inconsequential, limited to small foci exclusively of Gleason pattern 3. *Yellow* represents a tumor focus with a volume greater than 0.2 cc but less than 0.5 cc as predicted by a maximum cancer core length of ≥4 mm. Alternatively, any secondary Gleason pattern 4 in a lower burden of cancer would trigger a "yellow" disease status, which is typically indeterminate. It is difficult to predict the outcome of this level of disease: These small lesions with a small component of secondary Gleason pattern 4 probably confer a very low risk of PCa-associated death if untreated. Therefore, in the older man or in the presence of comorbidities, observation may be considered. In young men,

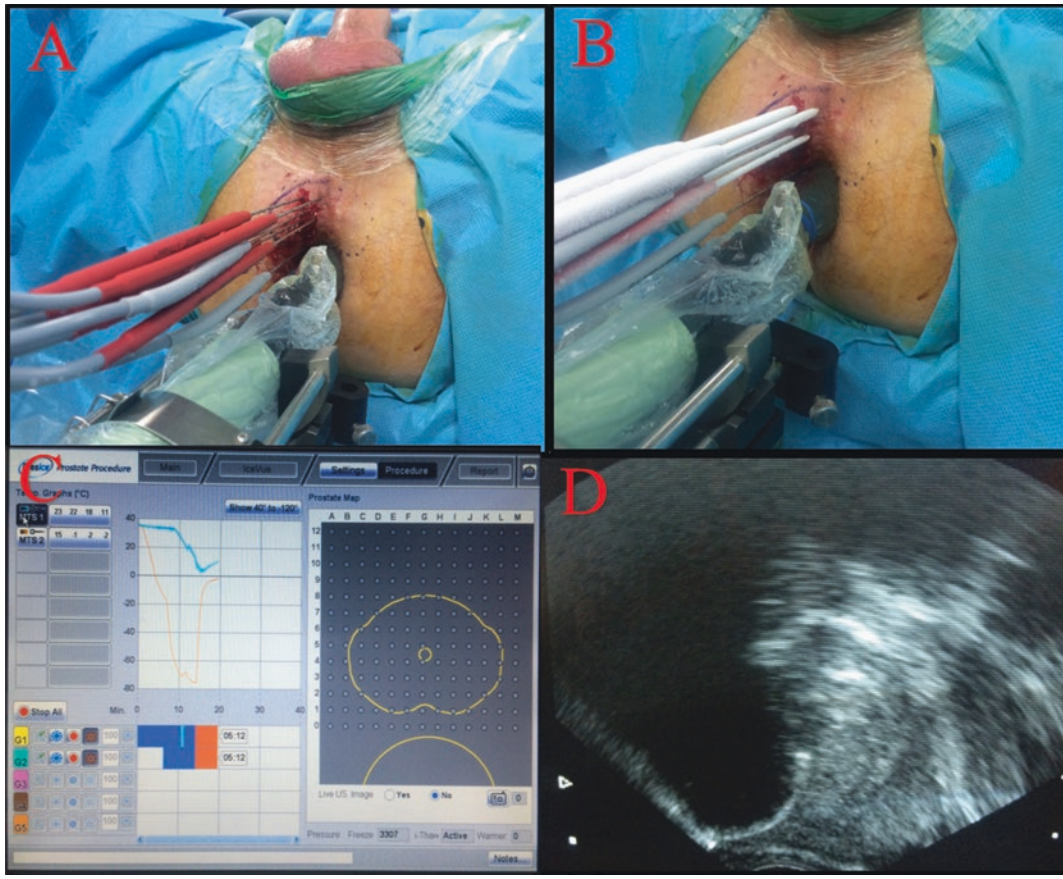

Fig. 5.1 Hemi-ablation using cryotherapy at Fundaciò Puigvert (Barcelona, Spain). (**a**) Needle placement in perineal area. (**b**) Needles during freezing cycle. (**c**) Monitor of temperature control. (**d**) Typical anechoic ultrasound image of hemi-ablation with cryotherapy

however, the potential benefits of treatment of these lesions must be taken into account. *Red* indicates a PCa that has a volume of at least 0.5 cc or is characterized by dominant Gleason pattern 4. The volume is derived from the presence of maximum cancer core lengths ≥6 mm. According to the data from the European Prostate Cancer Screening Study, tumor volumes below 1.3 cc and with a Gleason pattern 3 are clinically insignificant [7].

Inclusion and Exclusion Criteria for Focal Therapy

In Europe, no consensus exists on the ideal candidate for primary FT, despite several proposed consensus statements. Obviously, this reflects different European schools of thought about the role of FT in PCa. According to the International Multidisciplinary Consensus on FT in PCa, the percentage of positive samples should be taken into account when selecting patients [68]. Tumors with a GS 3+3 are eligible, containing at least 1 core with the presence of a substantial amount of cancer. FT should preferably not be offered to patients with clinically insignificant disease in whom FT could be considered overtreatment. Patients with a GS 3+4 locally confined to the prostate may also be considered as candidates for FT. For patient selection, nomograms may be used to minimize inclusion of patients with nodal disease, especially in patients with intermediate disease [71].

Regarding the age of the patients, an international consensus meeting of experts was convened to provide guidance on patient eligibility [69]. It was agreed that age should not be a primary determinant of eligibility for FT, although the panel was uncertain whether FT should be recommended for patients <40 or >80 years old. The panel was also asked to evaluate criteria other than age for selection of patients for FT. The panel agreed that patients with a World Health Organization performance status of 0 or 1 should be recommended for FT, while patients with a performance status of 3 or 4 should not [72]. There was uncertainty about the role of FT in patients with a performance status of 2. The group agreed that FT is best suited to patients with a life expectancy of >10 years and that it should not be applied in patients with a life expectancy of <5 years. While it is in general considered that there is no upper prostate volume limit for FT, focal use of HIFU is recommended only in patients with a prostate volume of up to 40 ml [73]. The consensus meeting panelists also agreed that 5-alpha-reductase inhibitors need not be stopped before a patient enters an FT trial [69]. Finally, it is not mandatory for MRI to display lesions concordant with biopsy before a patient is treated by FT. Renal failure, history of acute or chronic prostatitis, significant erectile dysfunction, and urinary incontinence are considered exclusion criteria. Exclusion of individual patients should be based on good clinical judgment, taking into consideration all comorbidities and performance status.

Oncological Outcomes

In European urological experience, a source of significant debate is how to assess the oncological success or failure of FT [74]. Established PSA follow-up criteria for whole-gland treatments, such as ASTRO, Phoenix, and the Stuttgart criteria, are difficult to apply following FT. PSA kinetics and PSA nadir may, however, play a role as PSA secretion from the healthy prostatic tissue, as shown by Ahmed et al. who reported an 80 % decrease in PSA at 3 months after focal HIFU, which remained stable at 12 months [75]. Also PSA density may play a determinant role. According to Stamey et al., who were the first to correlate PSA serum values and volume of prostatic tissue, PSA density may therefore be a good measure as it will allow for adjustment for residual tissue volume after FT [76].

Biopsies should be used to determine absence of disease in the treated areas, in order to verify FT success as well as untreated areas to detect recurrent and/or de novo disease. The key determination will be whether recurrence or de novo cancer found after FT is clinically significant to require further treatment [77]. According to an international consensus project, follow-up to focal therapy should include the performance of 12-core systematic TRUS biopsy combined with 4–6 target biopsy cores of the treated area and any suspicious lesion(s) after 1 year and subsequently only in case of suspicious imaging of PCa [78].

Multiparametric MRI seems to be the ideal imaging evaluation for detection of clinically significant cancer, thus potentially being used to drive the delivery of FT, demonstrating an accuracy of more than 85 % to 90 % for lesions that measure 0.2 or 0.5 cc in volume [79, 80]. Therefore, in medium- to long-term, surveillance MRI could be of significant help in detecting recurrence of clinically significant cancer. A negative MRI would imply absence of clinically significant disease that requires no treatment [80].

There have been several reports in the literature on the oncological efficacy of FT with different technologies. Cryotherapy and HIFU seem to be the two most used approaches in Europe [68].

Ward and Jones reported the results of about 1160 men treated with focal cryoablation [81]. The 3-year biochemical disease-free survival was at 75.7 % with a posttreatment positive biopsy rate of 26.3 % (considering only the patients who underwent biopsy due to biochemical failure) [81].

Barret et al. enrolled, in a prospective manner, 106 patients to undergo prostate hemi-ablation for unilateral PCa using different approaches: cryotherapy in 50, vascular-targeted photodynamic therapy in 23, HIFU in 21, and focal brachytherapy (iodine 125) in 12 cases [82].

The treatment modality was chosen depending on the patients' characteristics (cryotherapy and HIFU were used for smaller prostates and peripheral tumors; vascular-targeted photodynamic therapy was used for larger prostates). The median PSA level was 6.1 ng/ml and all the patients had a biopsy GS of 6 (3+3). At 3, 6, and 12 months after treatment, the median PSA was 3.1, 2.9, and 2.7 ng/ml, respectively [82]. This French pilot study showed encouraging results in terms of oncological outcomes [82].

HIFU relies on the focused conglomeration of ultrasound waves on a specific prostate point, leading to elevated temperatures (60–100 °C), protein denaturation, and coagulative necrosis [83]. Ahmed et al. reported oncological data for 20 men who underwent HIFU hemi-ablation [75]. Mean PSA decreased 80 % to 1.5 ng/ml at 12 months. In the 89 % of the men, there was no histological evidence of recurrence. Preliminary European data suggests, also, that contrast-enhanced ultrasound can reliably show, immediately after HIFU ablation, the location and amount of tissue that has not been destroyed after a first session of HIFU [84]. These results could allow immediate re-treatment of the incompletely destroyed areas after HIFU treatment.

Vascular-targeted photodynamic therapy uses the combination of a photosensitizing drug and light to damage target tissue. Generally, the photosensitizing agent is previous intravenous administered followed by irradiation of light at the target area at a wavelength that is absorbed by photosensitizer agent. In the gland, the photosensitizer generates reactive oxygen species resulting in vessel thrombosis of the treated area [85]. TOOKAD® Soluble (Steba Biotech, Luxembourg) was recently introduced as a novel photosensitizer with minimal extravasation from the vessels [86]. Azzouzi et al. evaluated the 6-month effects and oncological outcomes of focal vascular-targeted photodynamic therapy using TOOKAD® Soluble [87]. The treatment performed was a hemi-ablation in unilateral PCa or subtotal ablation in case of bilateral disease. At month 6, the negative biopsy rate was 68.4 % in the overall evaluable population (N = 114) and 80.6 % for patients treated by hemi-ablation with light density index ≥1 (N = 67) [87]. Mean prostate necroses at week 1 were 76.5 % and 86.3 %, respectively. PSA levels at month 6 decreased by 2.0 ng/ml in both groups [87].

Irreversible electroporation is a nonthermal energy source, used in the USA and in Europe by radiologists to treat liver, kidney, and pancreas tumors [88–90]. This novel approach leads to cell death by the formation of nanopores within the cell membrane [91]. In the European urological literature, there are only a few case reports of its use. In a study by Valerio et al., 34 patients were treated with a mean age of 65 years and a median PSA of 6.1 ng/ml [92]. The authors reported an ablation median volume of 12 ml, median PSA at month 6 of 3.4 ng/ml [92]. MRI showed suspicious residual disease in six patients, of whom 4 (17 %) underwent another local treatment [92]. According to these results, the authors concluded that it is difficult to establish rigorous oncological outcomes.

Functional Outcomes and Complications

The functional goal of FT is to minimize the damage to the neurovascular bundles, external sphincter, bladder neck, and rectum in order to preserve erectile potency, urinary continence, and rectal function [93].

Regarding the functional outcomes of focal cryotherapy, Ward and Jones in a series of 1160 patients reported urinary incontinence in 1.6 %, new erectile dysfunction in 41.9 %, and rectourethral fistula in 0.1 % of the cases [81].

Barret et al. evaluated the complications and morbidity in 106 patients who underwent FT for PCa, using hemi-ablation cryotherapy (50 patients), vascular-targeted photodynamic therapy (23 patients), hemi-ablation HIFU (21 patients), and focal brachytherapy (12 patients) [82]. They showed an acceptable morbidity for all FT approaches. The FT-related complication rate was 13 % (pelvic pain, urinary retention), with a <2 % rate of major complications (rectal fistula with perineal abscess, urethral stricture). The authors concluded that the complication rate

seems acceptable compared with the high incidence of complications related to radical treatment.

Ahmed et al. analyzed complications and functional outcomes in a total of 20 men (mean age 60.4 years) who underwent HIFU hemi-ablation, of whom 25 % had low-risk and 75 % had intermediate-risk PCa [75]. Return of erections sufficient for penetrative sex occurred in 95 % of men (19/20); 90 % of them (18/20) were pad-free, leak-free continent, while 95 % were pad-free [75].

Yap et al. pooled the functional data from three prospective, registered, ethics committee-approved studies on the use of FT in PCa that were conducted in the UK between 2009 and 2013 [94]. These three studies—a hemi-ablation trial, a focal lesion ablation trial, and an index lesion ablation trial—represent the largest set of prospectively collected data on erectile functional outcomes after FT using HIFU [75, 94–96]. Analysis of outcome with respect to erectile function showed that the proportion of men using phosphodiesterase-5 inhibitors was 10 % preoperatively, reached 43 % and 42 % at 6 and 9 months, and declined to 37 % at 1 year [94]. The only baseline determinants of postoperative erectile function were total International Index of Erectile Function (IIEF) and IIEF-erectile function scores ($p = 0.002$) [94]. Overall, these data suggest that a patient with a clinically localized PCa and no preoperative erectile dysfunction, if treated with FT, would completely recover erectile function 6 months after the treatment [94]. Gandaglia et al. observed that these excellent results regarding erectile dysfunction differ substantially from results observed in larger cohorts of men treated with surgery and radiotherapy [97]. This is because the favorable disease characteristics (PSA $\leq$ 15 ng/ml, Gleason score $\leq$4+3, stage $\leq$ T3aN0M0) reported in the article published by Yap et al. allowed treatment of the index lesion without damaging the neurovascular bundles (owing to maintenance of a minimum distance of 5 mm between the ablation zone and the neurovascular bundles) [94]. Recently, Van Velthoven et al. reported satisfactory functional outcomes in a prospective study on hemi-ablation HIFU in 50 patients with clinically localized unilateral, low- to intermediate-risk PCa [98]. All of the patients were continent preoperatively. Seven patients presented with transient incontinence during follow-up, of whom three had persistent incontinence at 12 months postoperatively [98]. The long-term pad-free continence rate was 94 %. Of 30 men who were sexually active preoperatively, 6 (20 %) developed postoperative erectile dysfunction [98].

Due to focal nature of target photodynamic therapy using TOOKAD® Soluble confined in the circulation system, the damage to surrounding tissue is really minimized. In their pooled analysis of 117 patients, Azzouzi et al. reported as adverse events dysuria (33.3 %), perineal pain (15.4 %), hematuria (13.7 %), urinary retention (11.1 %), and urgency (9.4 %) [87]. Regarding postoperative erectile dysfunction, it was reported in 16.2 % of the patients [87]. Moreover, the authors underlined that data about erectile dysfunction are difficult to analyze because many patients were not sexually active even before FT.

Valerio et al. evaluated functional results using irreversible electroporation of target area on 34 patients [92]. After a median follow-up of 6 months, potency was preserved in 95 %; urinary continence was in 100 % of cases (no pad usage after treatment) [92]. No rectal lesions or dysfunction was reported.

Therefore, these data show that the most frequent complications of FT are urinary retention, urinary stricture, and urinary tract infection. Rectal toxicity is a rare complication. Furthermore, preservation of sexual function and continence is a strong driver of patient choice regarding the treatment of PCa. Table 5.1 summarizes the complications and functional outcomes of patients undergoing FT in European centers [7, 82, 87, 94, 98].

Follow-Up After Focal Therapy

Currently, there is no evidence regarding the optimal form of follow-up in patients who have undergone FT for PCa. Most European urologists have to date commonly used PSA kinetics criteria and biopsy, with or without imaging

Table 5.1 Complication and functional outcomes of patients undergoing FT in European centers

Authors	Center	Number of patients	Energy modality for FT (number of patients)	Complications (%)	Functional outcomes	
					Urinary incontinence (%)	Erectile dysfunction (%)
Ahmed et al. (2011) [7]	London, UK	20	HIFU	Urinary retention: 0/20 (0)	Pad-free: 19/20 (95)	Postoperative ER: 1/20 (5)
				Urinary stricture: 1/20 (5)	Leak-free: 18/20 (90)	
				UTI: 0/20 (0)		
				Perineal pain: NR		
				Rectourethral fistula: 0/20 (0)		
Barret et al. (2013) [82]	Paris, France	106	Cryotherapy (50)	Urinary retention: 9/106 (8)	Pad-free: 106/106 (100)	NR
			VTP (23)	Urethral stricture: 1/106 (1)	Leak-free: NR	
			HIFU (21)	UTI: 0/106 (0)		
			Brachytherapy (12)	Perineal pain: 1/106 (1)		
				Rectourethral fistula: 1/106 (1)		
Yap et al. (2015) [94]	London, UK	118	HIFU	NR	NR	Men using PDE5 inhibitors: Preoperatively: 12/118 (10)
						6 months post-FT: 50/118 (42)
						1 year post-FT: 44/118 (37)
Van Velthoven et al. (2016) [98]	Brussels, Belgium	50	HIFU	Urinary retention: 4/50 (8)	Pad-free: 47/50 (94)	Postoperative ER: 6 (20)
				UTI: 3/50 (6)		
				LUTS: 9/50 (18)	Leak-free: NR	
				Urethral stricture: 2/50 (4)		
				Perineal pain: NR		
				Rectourethral fistula: NR		
Azzouzi et al. (2015) [87]	France, UK, Israel, USA	117	Photodynamic therapy using TOOKAD® Soluble	Urinary retention: 13/117 (11.1)	NR	Postoperative ER:19/117 (16.2)
Pooled analysis of three phase II studies				LUTS: 39/117 (33.3)		
				Perineal pain: 18/117 (15.4)		
				Hematuria: 16/117 (13.7)		

ER erectile dysfunction, *FT* focal therapy, *HIFU* high-intensity focused ultrasound, *LUTS* low urinary tract symptoms, *NR* not reported, *UTI* urinary tract infection, *VTP* vascular-targeted photodynamic therapy

evaluation [85]. It is important to assess the effectiveness of local cancer control after FT, bearing in mind that PSA is variable and of uncertain significance. Furthermore, there are no validated PSA criteria for measurement of failure after FT for PCa, even if the Phoenix or ASTRO criteria are often used [99]. Moreover, PSA kinetics should be interpreted with caution

because these criteria have not been validated for FT, taking into account the fact that cell death in FT is different from that in radiotherapy. Recently, an international multidisciplinary consensus meeting established that the minimum duration of follow-up after FT should be 5 years [78]. The following modalities should be included in assessment of posttreatment outcomes: mpMRI, biopsies, assessment of erectile function, QoL, urinary symptoms, and incontinence. A systematic 12-core TRUS biopsy combined with 4 to 6 targeted biopsy cores of the treated area and any suspicious lesion(s) should be performed after 1 year and thereafter only when there is suspicion on imaging. The ideal way to perform targeted biopsies is to use MRI/TRUS-fusion technology. PSA should be performed for research purposes, every 3 months during the first year and every 6 months thereafter. Multiparametric MRI is the optimal imaging modality for follow-up after FT. Imaging should be performed at 6 months and 1 year following FT and then annually until 5 years after treatment.

Conclusion

The increasing incidence of low- and intermediate-risk localized PCa indicates that demand for treatment interventions that are less aggressive than the established radical treatments will likely increase over the next decade in Europe.

AS is appropriate for most "true" low-risk PCa with promising long-term results regarding cancer-specific and overall survival. On the other hand, the patient is not compromised by possible side effects of radical treatment. Within this emerging field of AS, blood and urine biomarkers (PSA-DT, PHI, TMPRSS2 and ERG, and PCA3) and genomic classifiers will gain widespread use and may help to refine risk stratification of AS patients in the surveillance. In addition, the utility of mpMRI in AS will rapidly increase as well. In the future, favorable MRI findings on a good-quality mpMRI may be used for selection and follow-up of patients during AS and might obviate the need for repeat biopsies. However, at the moment, repeat biopsies are still necessary. Furthermore, expanding AS to patients with GS 3+4 PCa might be possible in strict follow-up protocols including novel markers and MRI. Nonetheless, the patient has to be counseled to elucidate about probably increased risk of unfavorable disease.

FT interventions include ablative therapy, which appears to be the ideal intervention because it actively treats cancer while being minimally invasive and potentially organ sparing. For primary ablative therapy, the currently available data are insufficiently robust to enable any definitive conclusions to be drawn regarding the clinical effectiveness, adverse impacts, or cost-effectiveness of either cryotherapy or HIFU in comparison with RP and external beam radiotherapy. On the other hand, FT is associated with low morbidity and can be considered a noninvasive, reproducible, tissue-preserving technique with a short learning curve. Currently, several phase II and III trials are in process in order to demonstrate FT to be a viable option in localized PCa. These studies include AS versus FT treatment using TOOKAD, HIFU versus brachytherapy, focal ablation versus extended ablation using IRE (conducted by the Clinical Research Office of the Endourological Society [CROES]), and hemi-ablation versus complete ablation using brachytherapy (conducted by the European Society for Therapeutic Radiology and Oncology [ESTRO]) [100]. The main focus should be on selecting the appropriate patients and demonstrating benefits of FT [101]. Further studies are needed in order to assess oncological and functional outcomes and to provide a sound basis for inclusion of this approach in European urology guidelines.

References

1. Ferlay J, Parkin DM, Steliarova-Foucher E. Estimates of cancer incidence and mortality in Europe in 2008. Eur J Cancer. 2010;46:765–81. doi:10.1016/j.ejca.2009.12.014.
2. Karim-Kos HE, de Vries E, Soerjomataram I, et al. Recent trends of cancer in Europe: a combined

approach of incidence, survival and mortality for 17 cancer sites since the 1990s. Eur J Cancer. 2008;44:1345–89.
3. Klotz L, Emberton M. Management of low risk prostate cancer-active surveillance and focal therapy. Nat Rev Clin Oncol. 2014;11:324–34. doi:10.1038/nrclinonc.2014.73.
4. van den Bergh RCN, Roemeling S, Roobol MJ, et al. Prospective validation of active surveillance in prostate cancer: the PRIAS Study. Eur Urol. 2007;52:1560–3. doi:10.1016/j.eururo.2007.05.011.
5. Bokhorst LP, Alberts AR, Rannikko A, et al. Compliance rates with the Prostate Cancer Research International Active Surveillance (PRIAS) protocol and disease reclassification in noncompliers. Eur Urol. 2015;68:814–21. doi:10.1016/j.eururo.2015.06.012.
6. Valerio M, Anele C, Freeman A, et al. Identifying the index lesion with template prostate mapping biopsies. J Urol. 2014;193:1185–90. doi:10.1016/j.juro.2014.11.015.
7. Ahmed HU, Hu Y, Carter T, et al. Characterizing clinically significant prostate cancer using template prostate mapping biopsy. J Urol. 2011;186:458–64. doi:10.1016/j.juro.2011.03.147.
8. Ahmed HU, Emberton M. Active surveillance and radical therapy in prostate cancer: can focal therapy offer the middle way? World J Urol. 2008;26:457–67. doi:10.1007/s00345-008-0317-5.
9. Heidenreich A, Bastian PJ, Bellmunt J, et al. EAU guidelines on prostate cancer. Part 1: screening, diagnosis, and local treatment with curative intent-update 2013. Eur Urol. 2014;65:124–37. doi:10.1016/j.eururo.2013.09.046.
10. van As NJ, Norman AR, Thomas K, et al. Predicting the probability of deferred radical treatment for localised prostate cancer managed by active surveillance. Eur Urol. 2008;54:1297–305. doi:10.1016/j.eururo.2008.02.039.
11. Arnsrud Godtman R, Holmberg E, Khatami A, et al. Outcome following active surveillance of men with goteborg screen-detected prostate cancer. Results from the go randomised population-based prostate cancer screening trial. Eur Urol. 2013;63:101–7.
12. Epstein JI, Walsh PC, Carmichael M, Brendler CB. Pathologic and clinical findings to predict tumor extent of nonpalpable (stage T1c) prostate cancer. JAMA. 1994;271:368–74. doi:10.1001/jama.271.5.368.
13. Bastian PJ, Mangold LA, Epstein JI, Partin AW. Characteristics of insignificant clinical T1c prostate tumors: a contemporary analysis. Cancer. 2004;101:2001–5. doi:10.1002/cncr.20586.
14. Dall'Era MA, Albertsen PC, Bangma C, et al. Active surveillance for prostate cancer: a systematic review of the literature. Eur Urol. 2012;62:976–83. doi:10.1016/j.eururo.2012.05.072.
15. Ploussard G, Isbarn H, Briganti A, et al. (2015) Can we expand active surveillance criteria to include biopsy Gleason 3+4 prostate cancer? A multi-institutional study of 2323 patients. Urol Oncol Semin Orig Investig 33:71.e1–71.e9. doi:10.1016/j.urolonc.2014.07.007.
16. Ng MK, Van As N, Thomas K, et al. Prostate-specific antigen (PSA) kinetics in untreated, localized prostate cancer: PSA velocity vs PSA doubling time. BJU Int. 2009;103:872–6. doi:10.1111/j.1464-410X.2008.08116.x.
17. Van Den Bergh RCN, Roemeling S, Roobol MJ, et al. Gleason score 7 screen-detected prostate cancers initially managed expectantly: outcomes in 50 men. BJU Int. 2009;103:1472–7. doi:10.1111/j.1464-410X.2008.08281.x.
18. Shaw GL, Thomas BC, Dawson SN, et al. (2014) Identification of pathologically insignificant prostate cancer is not accurate in unscreened men. Br Cournal Cancer. 110. doi:10.1038/bjc.2014.192.
19. Suardi N, Briganti A, Gallina A, et al. Testing the most stringent criteria for selection of candidates for active surveillance in patients with low-risk prostate cancer. BJU Int. 2010;105:1548–52. doi:10.1111/j.1464-410X.2009.09057.x.
20. Radtke JP, Kuru TH, Bonekamp D, et al. (2016). Further reduction of disqualification rates by additional MRI-targeted biopsy with transperineal saturation biopsy compared to standard 12-core systematic biopsies for selection of prostate cancer patients for active surveillance. Prostate Cancer Prostatic Dis. 2016 Sep;19(3):283–91. doi:10.1038/pcan.2016.16. Epub 2016 May 17.
21. Siddiqui MM, Rais-Bahrami S, Turkbey B, et al. Comparison of MR/ultrasound fusion–guided biopsy with ultrasound-guided biopsy for the diagnosis of prostate cancer. JAMA. 2015;313:390. doi:10.1001/jama.2014.17942.
22. Baco E, Ukimura O, Rud E, et al. magnetic resonance imaging – transrectal ultrasound image-fusion biopsies accurately characterize the index tumor: correlation with step-sectioned radical prostatectomy specimens in 135 patients. Eur Urol. 2015;67:787–94. doi:10.1016/j.eururo.2014.08.077.
23. Radtke JP, Schwab C, Wolf MB, et al. Multiparametric magnetic resonance imaging (MRI) and MRI – transrectal ultrasound fusion biopsy for index tumor detection: correlation with radical prostatectomy specimen. Eur Urol. 2016:6–13. doi:10.1016/j.eururo.2015.12.052.
24. Epstein JI, Walsh PC, Carter HB. Dedifferentiation of prostate cancer grade with time in men followed expectantly for stage T1c disease. J Urol. 2001;166:1688–91.
25. Soloway MS, Soloway CT, Eldefrawy A, et al. Careful selection and close monitoring of low-risk prostate cancer patients on active surveillance minimizes the need for treatment. Eur Urol. 2010;58:831–5. doi:10.1016/j.eururo.2010.08.027.
26. Ouzzane A, Renard-Penna R, Marliere F, et al. MRI-targeted biopsy improves selection of patients considered for active surveillance for clinically low-risk prostate cancer based on systematic biopsies. J Urol. 2015; doi:10.1016/j.juro.2015.02.2938.
27. Marliere F, Puech P, Benkirane A, et al. The role of MRI-targeted and confirmatory biopsies for cancer upstaging at selection in patients considered for

active surveillance for clinically low-risk prostate cancer. World J Urol. 2014;32:951–8. doi:10.1007/s00345-014-1314-5.
28. Bul M, Van Den Bergh RCN, Rannikko A, et al. Predictors of unfavourable repeat biopsy results in men participating in a prospective active surveillance program. Eur Urol. 2012;61:370–7. doi:10.1016/j.eururo.2011.06.027.
29. Schoots IG, Petrides N, Giganti F, et al. Magnetic resonance imaging in active surveillance of prostate cancer: a systematic review. Eur Urol. 2014:67–73. doi:10.1016/j.eururo.2014.10.050.
30. Tosoian JJ, JohnBull E, Trock BJ, et al. Pathological outcomes in men with low risk and very low risk prostate cancer: implications on the practice of active surveillance. J Urol. 2013;190:1218–22. doi:10.1016/j.juro.2013.04.071.
31. Tosoian JJ, Loeb S, Feng Z, et al. Association of [−2]proPSA with biopsy reclassification during active surveillance for prostate cancer. J Urol. 2012;188:1131–6. doi:10.1016/j.juro.2012.06.009.
32. Makarov DV, Isharwal S, Sokoll L, et al. Pro-prostate-specific anti- gen measurements in serum and tissue are associated with treatment necessity among men enrolled in expectant management for prostate cancer. Clin Cancer Res. 2009;15:7316–21. Clin Cancer Res 15:7316–7321
33. Khan MA, Carter HB, Epstein JI, et al. Can prostate specific antigen derivatives and pathological parameters predict significant change in expectant management criteria for prostate cancer? J Urol. 2003;170:2274–8. doi:10.1097/01.ju.0000097124.21878.6b.
34. Castro E, Goh C, Olmos D, et al. Germline BRCA mutations are associated with higher risk of nodal involvement, distant metastasis, and poor survival outcomes in prostate cancer. J Clin Oncol. 2013;31:1748–57. doi:10.1200/JCO.2012.43.1882.
35. Bancroft EK, Page EC, Castro E, et al. Targeted prostate cancer screening in BRCA1 and BRCA2 mutation carriers: Results from the initial screening round of the IMPACT study. Eur Urol. 2014;66:489–99. doi:10.1016/j.eururo.2014.01.003.
36. Klein EA, Cooperberg MR, Magi-Galluzzi C, et al. A 17-gene assay to predict prostate cancer aggressiveness in the context of gleason grade heterogeneity, tumor multifocality, and biopsy undersampling. Eur Urol. 2014;66:550–60. doi:10.1016/j.eururo.2014.05.004.
37. Lees K, Durve M, Parker C. Active surveillance in prostate cancer: patient selection and triggers for intervention. Curr Opin Urol. 2012;22:210–5.
38. Van Den Bergh RCN, Ahmed HU, Bangma CH, et al. Novel tools to improve patient selection and monitoring on active surveillance for low-risk prostate cancer: a systematic review. Eur Urol. 2014;65:1023–31. doi:10.1016/j.eururo.2014.01.027.
39. Berg KD, Vainer B, Thomsen FB, et al. ERG protein expression in diagnostic specimens is associated with increased risk of progression during active surveillance for prostate cancer. Eur Urol. 2014;66:851–60. doi:10.1016/j.eururo.2014.02.058.
40. Tomlins SA, Rhodes DR, Perner S, et al. Recurrent fusion of TMPRSS2 and ETS transcription factor genes in prostate cancer. Science. 2005;310:644–8. doi:10.1126/science.1117679.
41. Demichelis F, Fall K, Perner S, et al. TMPRSS2:ERG gene fusion associated with lethal prostate cancer in a watchful waiting cohort. Oncogene. 2007;26:4596–9. doi:10.1038/sj.onc.1210630.
42. Lin DW, Newcomb LF, Brown EC, et al. Urinary TMPRSS2:ERG and PCA3 in an active surveillance cohort: results from a baseline analysis in the canary prostate active surveillance study. Clin Cancer Res. 2013;19:2442–50. doi:10.1158/1078-0432.CCR-12-3283.
43. Leyten GHJM, Hessels D, Jannink SA, et al. Prospective multicentre evaluation of PCA3 and TMPRSS2-ERG gene fusions as diagnostic and prognostic urinary biomarkers for prostate cancer. Eur Urol. 2014;65:534–42. doi:10.1016/j.eururo.2012.11.014.
44. Ploussard G, Durand X, Xylinas E, et al. Prostate cancer antigen 3 score accurately predicts tumour volume and might help in selecting prostate cancer patients for active surveillance. Eur Urol. 2011;59:422–9. doi:10.1016/j.eururo.2010.11.044.
45. Loeb S, Bjurlin MA, Nicholson J, et al. Overdiagnosis and overtreatment of prostate cancer. Eur Urol. 2014;65:1046–55. doi:10.1016/j.eururo.2013.12.062.
46. Shaw GL, Thomas BC, Dawson SN, et al. Identification of pathologically insignificant prostate cancer is not accurate in unscreened men. Br J Cancer. 2014;110:2405–11. doi:10.1038/bjc.2014.192.
47. Epstein JI, Feng Z, Trock BJ, Pierorazio PM. Upgrading and downgrading of prostate cancer from biopsy to radical prostatectomy: Incidence and predictive factors using the modified gleason grading system and factoring in tertiary grades. Eur Urol. 2012;61:1019–24. doi:10.1016/j.eururo.2012.01.050.
48. Vargas HA, Akin O, Afaq A, et al. Magnetic resonance imaging for predicting prostate biopsy findings in patients considered for active surveillance of clinically low risk prostate cancer. J Urol. 2012;188:1732–8. doi:10.1016/j.juro.2012.07.024.
49. van den Bergh RCN, Roemeling S, Roobol MJ, et al. Outcomes of men with screen-detected prostate cancer eligible for active surveillance who were managed expectantly. Eur Urol. 2009;55:1–8. doi:10.1016/j.eururo.2008.09.007.
50. Hu JC, Chang E, Natarajan S, et al. Targeted prostate biopsy in select men for active surveillance: do the Epstein criteria still apply? J Urol. 2014;192:385–90. doi:10.1016/j.juro.2014.02.005.
51. Mullins JK, Bonekamp D, Landis P, et al. Multiparametric magnetic resonance imaging findings in men with low-risk prostate cancer followed using active surveillance. BJU Int. 2013;111:1037–45. doi:10.1111/j.1464-410X.2012.11641.x.
52. Da Rosa MR, Milot L, Sugar L, et al. A prospective comparison of MRI-US fused targeted biopsy versus systematic ultrasound-guided biopsy for detecting clinically significant prostate cancer in patients on

active surveillance. J Magn Reson Imaging. 2015;41:220–5. doi:10.1002/jmri.24710.
53. van As NJ, de Souza NM, Riches SF, et al. A study of diffusion-weighted magnetic resonance imaging in men with untreated localised prostate cancer on active surveillance. Eur Urol. 2009;56:981–8.
54. Somford DM, Hoeks CM, Hulsbergen-van de Kaa CA, et al. Evaluation of diffusion-weighted MR imaging at inclusion in an active surveillance protocol for low-risk prostate cancer. Invest Radiol. 2013;48:152–7. doi:10.1097/RLI.0b013e31827b711e.
55. Recabal P, Assel M, Sjoberg DD, et al. The efficacy of multiparametric magnetic resonance imaging and MRI-targeted biopsy in risk classification for patients with prostate cancer on active surveillance. J Urol. 2016; doi:10.1016/j.juro.2016.02.084.
56. Van Den Bergh RCN, Vasarainen H, Van Der Poel HG, et al. Short-term outcomes of the prospective multicentre "Prostate Cancer Research International: Active Surveillance" study. BJU Int. 2010;105:956–62. doi:10.1111/j.1464-410X.2009.08887.x.
57. Bul M, Zhu X, Valdagni R, et al. Active surveillance for low-risk prostate cancer worldwide: the PRIAS study. Eur Urol. 2013;63:597–603. doi:10.1016/j.juro.2012.12.080.
58. Loeb S, van den Heuvel S, Zhu X, et al. Infectious complications and hospital admissions after prostate biopsy in a European randomized trial. Eur Urol. 2012;61:1110–4. doi:10.1016/j.eururo.2011.12.058.
59. Mkinen T, Auvinen A, Hakama M, et al. Acceptability and complications of prostate biopsy in population-based PSA screening versus routine clinical practice: a prospective, controlled study. Urology. 2002;60:846–50. doi:10.1016/S0090-4295(02)01864-2.
60. Bokhorst LP, Lepistö I, Kakehi Y, et al. Complications after prostate biopsies in men on active surveillance and its effect on receiving further biopsies in the Prostate cancer Research International: Active Surveillance (PRIAS) study. BJU Int. 2016; doi:10.1111/bju.13410.
61. Bangma CH, Bul M, van der Kwast TH, et al. Active surveillance for low-risk prostate cancer. Crit Rev Oncol Hematol. 2013;85:295–302. doi:10.1016/j.critrevonc.2012.07.005.
62. Schoots IG, Roobol MJ, Nieboer D, et al. Magnetic resonance imaging–targeted biopsy may enhance the diagnostic accuracy of significant prostate cancer detection compared to standard transrectal ultrasound-guided biopsy: a systematic review and meta-analysis. Eur Urol. 2014:1–13. doi:10.1016/j.eururo.2014.11.037.
63. Bellardita L, Valdagni R, Van Den Bergh R, et al. How does active surveillance for prostate cancer affect quality of life? A systematic review. Eur Urol. 2015;67:637–45. doi:10.1016/j.eururo.2014.10.028.
64. van den Bergh RCN, Essink-Bot ML, Roobol MJ, et al. Do anxiety and distress increase during active surveillance for low risk prostate cancer? J Urol. 2010;183:1786–91. doi:10.1016/j.juro.2009.12.099.
65. Vasarainen H, Lokman U, Ruutu M, et al. Prostate cancer active surveillance and health-related quality of life: results of the Finnish arm of the prospective trial. BJU Int. 2012;109:1614–9. doi:10.1111/j.1464-410X.2011.10677.x.
66. Vanagas G, Mickeviciene A, Ulys A. Does quality of life of prostate cancer patients differ by stage and treatment? Scand J Public Health. 2013;41:58–64. doi:10.1177/1403494812467503.
67. Chun F, Becker A, Kluth L, et al. Patterns of care of patients with localized prostate cancer in Germany: a health care study with focus on active surveillance. Urol A. 2015;54:6–13.
68. Van Den Bos W, Muller BG, Ahmed H, et al. Focal therapy in prostate cancer: international multidisciplinary consensus on trial design. Eur Urol. 2014;65:1078–83. doi:10.1016/j.eururo.2014.01.001.
69. Donaldson IA, Alonzi R, Barratt D, et al. Focal therapy: patients, interventions, and outcomes – a report from a consensus meeting. Eur Urol. 2015;67:771–7. doi:10.1016/j.eururo.2014.09.018.
70. Eggener S, Salomon G, Scardino PT, et al. Focal therapy for prostate cancer: possibilities and limitations. Eur Urol. 2010;58:57–64. doi:10.1016/j.eururo.2010.03.034.
71. Eifler JB, Feng Z, Lin BM, et al. An updated prostate cancer staging nomogram (Partin tables) based on cases from 2006 to 2011. BJU Int. 2013;111:22–9. doi:10.1111/j.1464-410X.2012.11324.x.
72. Oken MMMD, Creech RHMDB, Tormey DCMDPDC, et al. Toxicity and response criteria of the Eastern Cooperative Oncology Group. Am J Clin Oncol. 1982;5:649–56. doi:10.1097/00000421-198212000-00014.
73. Cordeiro ER, Cathelineau X, Thüroff S, et al. High-intensity focused ultrasound (HIFU) for definitive treatment of prostate cancer. BJU Int. 2012;110:1228–42. doi:10.1111/j.1464-410X.2012.11262.x.
74. Ahmed HU, Zacharakis E, Dudderidge T, et al. High-intensity-focused ultrasound in the treatment of primary prostate cancer: the first UK series. Br J Cancer. 2009;101:19–26. doi:10.1038/sj.bjc.6605116.
75. Ahmed HU, Freeman A, Kirkham A, et al. Focal therapy for localized prostate cancer: a phase I/II trial. J Urol. 2011;185:1246–54. doi:10.1016/j.juro.2010.11.079.
76. Stamey TA, Yang N, Hay AR, et al. Prostate-specific antigen as a serum marker for adenocarcinoma of the prostate. N Engl J Med. 1987;317:909–16. doi:10.1056/NEJM198710083171501.
77. Ahmed HU, Moore C, Lecornet E, Emberton M. Focal therapy in prostate cancer: determinants of success and failure. J Endourol. 2010;24:819–25. doi:10.1089/end.2009.0665.
78. Muller BG, van den Bos W, Brausi M, et al. Follow-up modalities in focal therapy for prostate cancer: results from a Delphi consensus project. World J Urol. 2015;33:1503–9. doi:10.1007/s00345-014-1475-2.
79. Puech P, Potiron E, Lemaitre L, et al. Dynamic contrast-enhanced-magnetic resonance imaging evaluation of intraprostatic prostate cancer: correlation

with radical prostatectomy specimens. Urology. 2009;74:1094–9. doi:10.1016/j.urology.2009.04.102.
80. Villers A, Puech P, Mouton D, et al. Dynamic contrast enhanced, pelvic phased array magnetic resonance imaging of localized prostate cancer for predicting tumor volume: correlation with radical prostatectomy findings. J Urol. 2006;176:2432–7. doi:10.1016/j.juro.2006.08.007.
81. Ward JF, Jones JS. Focal cryotherapy for localized prostate cancer: a report from the national Cryo On-Line Database (COLD) Registry. BJU Int. 2012;109:1648–54. doi:10.1111/j.1464-410X.2011.10578.x.
82. Barret E, Ahallal Y, Sanchez-Salas R, et al. Morbidity of focal therapy in the treatment of localized prostate cancer. Eur Urol. 2013;63:618–22.
83. Tsakiris P, Thüroff S, de la Rosette J, Chaussy C. Transrectal high-intensity focused ultrasound devices: a critical appraisal of the available evidence. J Endourol. 2008;22:221–9. doi:10.1089/end.2007.9849.
84. Wink M, Frauscher F, Cosgrove D, et al. Contrast-enhanced ultrasound and prostate cancer; a multicentre European research coordination project. Eur Urol. 2008;54:982–93. doi:10.1016/j.eururo.2008.06.057.
85. Miano R, Asimakopoulos AD, Da Silva RD, et al. Focal therapy for prostate cancer: current status and future perspectives. Minerva Urol Nefrol. 2015;67:263–80.
86. Trachtenberg J, Bogaards A, Weersink RA, et al. Vascular targeted photodynamic therapy with palladium-bacteriopheophorbide photosensitizer for recurrent prostate cancer following definitive radiation therapy: assessment of safety and treatment response. J Urol. 2007;178:1974–9. doi:10.1016/j.juro.2007.07.036.
87. Azzouzi AR, Barret E, Bennet J, et al. TOOKAD® soluble focal therapy: pooled analysis of three phase II studies assessing the minimally invasive ablation of localized prostate cancer. World J Urol. 2015:945–53. doi:10.1007/s00345-015-1505-8.
88. Pech M, Janitzky A, Wendler JJ, et al. Irreversible electroporation of renal cell carcinoma: a first-in-man phase I clinical study. Cardiovasc Intervent Radiol. 2010;34:132–8. doi:10.1007/s00270-010-9964-1.
89. Martin RCG, McFarland K, Ellis S, Velanovich V. Irreversible electroporation therapy in the management of locally advanced pancreatic adenocarcinoma. J Am Coll Surg. 2012;215:361–9. doi:10.1016/j.jamcollsurg.2012.05.021.
90. Charpentier KP. Irreversible electroporation for the ablation of liver tumors: are we there yet? Arch Surg. 2012;147:1053–61. doi:10.1001/2013.jamasurg.100.
91. Rubinsky B, Onik G, Mikus P. Irreversible electroporation: a new ablation modality–clinical implications. Technol Cancer Res Treat. 2007;6:37–48.
92. Valerio M, Stricker PD, Ahmed HU, et al. Initial assessment of safety and clinical feasibility of irreversible electroporation in the focal treatment of prostate cancer. Prostate Cancer Prostatic Dis. 2014;17:343–7. doi:10.1038/pcan.2014.33.
93. Kasivisvanathan V, Emberton M, Ahmed HU. Focal therapy for prostate cancer: rationale and treatment opportunities. Clin Oncol (R Coll Radiol). 2013;25:461–73. doi:10.1016/j.clon. 2013.05.002.
94. Yap T, Ahmed HU, Hindley RG, et al. The effects of focal therapy for prostate cancer on sexual function: a combined analysis of three prospective trials. Eur Urol. 2015:1–8. doi:10.1016/j.eururo.2015.10.030.
95. Ahmed HU, Dickinson L, Charman S, et al. Focal ablation targeted to the index lesion in multifocal localised prostate cancer: a prospective development study. Eur Urol. 2015;68:927–36. doi:10.1016/j.eururo.2015.01.030.
96. Ahmed HU, Hindley RG, Dickinson L, et al. Focal therapy for localised unifocal and multifocal prostate cancer: a prospective development study. Lancet Oncol. 2012;13:622–32. doi:10.1016/S1470-2045(12)70121-3.
97. Gandaglia G, Briganti A, Salonia A, Montorsi F. Excellent erectile function recovery after focal therapy: is this enough. Eur Urol. 2015:S0302–2838.
98. van Velthoven R, Aoun F, Marcelis Q, et al. A prospective clinical trial of HIFU hemiablation for clinically localized prostate cancer. Prostate Cancer Prostatic Dis. 2016;19:79–83.
99. Roach M, Weinberg V, Nash M, et al. Defining high risk prostate cancer with risk groups and nomograms: implications for designing clinical trials. J Urol. 2006;176:S16–20. doi:10.1016/j.juro.2006.06.081.
100. van den Bos W, Muller BG, De La Rosette JJ. A randomized controlled trial on focal therapy for localized prostate carcinoma: hemiablation versus complete ablation with irreversible electroporation. J Endourol. 2013;27:262–4.
101. van den Bos W, Muller BG, Ehdaie B, et al. What is still needed to make focal therapy an accepted segment of standard therapy? Curr Opin Urol. 2014;24:247–55.

6 Focal Therapy and Active Surveillance of Prostate Cancer in East and Southeast Asia

Masaki Kimura, Kae Jack Tay, Satoru Muto, and Shigeo Horie

Introduction

Increasing recognition that a majority of prostate-specific antigen (PSA) screen-detected prostate cancers are indolent and slow growing has led to interest in gland-preserving strategies such as active surveillance (AS) and focal therapy (FT), which carry less morbidity and side effects than conventional radical treatments. Focal therapy is increasingly being seen for its potential as an active surveillance "extender" by periodically eradicating foci of clinically significant cancer so that the patient may go back on surveillance for the clinically insignificant cancers. With this strategy, overtreatment, which is one main harm of overdiagnosis, may be reduced.

M. Kimura • S. Muto
Department of Urology, Teikyo University School of Medicine, Tokyo, Japan

K.J. Tay (✉)
Department of Urology, Duke University, Durham, NC, USA
e-mail: Kaejack.tay@gmail.com

S. Horie
Department of Urology, Juntendo University, Graduate School of Medicine, Tokyo, Japan

This strategy is highly relevant today because of the high prevalence of low-grade, low-stage cancers discovered by PSA screening. On the other hand, in areas where there is a low incidence of screening, there may be a higher incidence of high-grade and high-stage prostate cancers that necessitate aggressive treatment. In an analysis of 50,066 men diagnosed with prostate cancer during an era where PSA testing was not widespread, investigators from the Thames Cancer Registry reported 20,181 deaths over an 8-year period, among which nearly half were attributed to prostate cancer [1]. Gland-preserving approaches must thus be judiciously and selectively applied with local population and patient characteristics in mind.

Asia, possibly derived from the Assyrian word *asu* meaning East, loosely comprises the part of the Eurasian continent east of an imaginary line following the Ural Mountains and River, the Black Sea with its Dardanelles and Bosporus outlets, the Caspian Sea, and the Caucasus Mountains, extending eastward to the Pacific Ocean, including 49 independent sovereignties and a heterogeneous multitude of ethnicities and cultures [2, 3]. In order to focus this chapter, we examine the present demographic trend in prostate cancer and developments favorable for focal therapy and active surveillance of prostate cancer, as well as published data from East and Southeast Asia.

© Springer International Publishing AG 2017

T.J. Polascik (ed.), *Imaging and Focal Therapy of Early Prostate Cancer*, Current Clinical Urology, DOI 10.1007/978-3-319-49911-6_6

Prostate Cancer Incidence and Mortality

The Globocan 2012 estimate for world prostate cancer incidence was 30.6 per 100,000 with a mortality rate of 7.8 per 100,000 [4]. In developed areas, the incidence rate was 68 per 100,000 with a mortality rate of 10 per 100,000 leading to a ratio of mortality to incidence at 15 %. In contrast, in less developed areas, the ratio of mortality to incidence was 46 % (Table 6.1). This may be attributed to less PSA testing in less developed areas as well as competing causes of mortality, resulting in the detection of only symptomatic, advanced cases of prostate cancer. An alternate explanation is that the less developed areas have reduced incidence of indolent or less aggressive prostate cancers, and a greater preponderance of aggressive cancers, though as early as 1977, a latent prostate cancer rate of 13–15 % was already noted in Hong Kong and Singapore among autopsy series [5]. In general, a rise in the incidence of prostate cancer has been observed in East and Southeast Asia over the last three to four decades [6]. According to Globocan, the mortality-to-incidence ratio for prostate cancer in East Asia is 30 %, and in Southeast Asia, it is as high as 60 % [4].

Among East and Southeast Asian countries, Japan, Korea, and Singapore appear to have mortality-to-incidence ratios similar to that of the West (Table 6.1). It is not clear whether these differences from other East and Southeast Asian counterparts are due to increases in incidence due to genetic and environmental differences or simply due to an increased prevalence of PSA testing. Environmental factors affecting the androgen receptor pathway or Westernization of diets

Table 6.1 Age-standardized incidence and mortality rates and mortality/incidence ratios of East and Southeast Asian countries

Population	ASR for incidence (per 100,000)	ASR for mortality (per 100,000)	Mortality/ incidence ratio
World	30.60	7.80	0.25
More developed regions	68.00	10.00	0.15
Less developed regions	14.50	6.60	0.46
Asia	9.40	3.80	0.40
Eastern Asia	10.50	3.10	0.30
China	5.30	2.50	0.47
Japan	30.40	5.00	0.16
Korea, Democratic Republic of	3.20	1.30	0.41
Korea, Republic of	30.30	4.60	0.15
Mongolia	3.40	2.10	0.62
Southeast Asia	11.20	6.70	0.60
Brunei	21.80	7.00	0.32
Cambodia	5.60	5.00	0.89
Indonesia	14.80	9.80	0.66
Lao PDR	3.50	2.70	0.77
Malaysia	10.80	4.60	0.43
Myanmar	4.30	3.40	0.79
Philippines	18.00	11.30	0.63
Singapore	33.10	4.50	0.14
Thailand	7.20	3.70	0.51
Timor-Leste	16.50	14.20	0.86
Vietnam	3.40	2.50	0.74

Adapted from Globocan 2012
ASR age-standardized rate

resulting in obesity and the gradual loss of "cultural protective factors" may also be implicit in these changes [7]. The observation that Asian immigrants to traditionally Western countries have been shown to have rates of prostate cancer nearer those of their adopted countries than their countries of birth lends support to this theory [8, 9]. In an analysis of global cancer registries, Bouchardy et al. observed an increasing incidence of prostate cancer mortality in China, Hong Kong, and Korea between the 1970s and early 2000s [10]. Comparatively, they found decreasing prostate cancer mortality trends in countries with a high penetrance of PSA screening. While it is possible that PSA screening or testing had an effect on mortality rate, it is difficult to estimate the penetrance of PSA testing in many communities, especially in Asia.

Prostate Cancer Screening and Detection

In the United States and Europe, a PSA cutoff of 4 ng/ml has traditionally been used to define a "positive" screen based on the original Hybritech assay calibrations [11]. Subsequently, with the recognition that the prevalence of benign prostatic hypertrophy increases with age, age-related cutoffs have been suggested [12]. PSA screening is currently opportunistic in Asia, with no established formal screening program. In a Malaysian report of 83 men undergoing transrectal biopsies from 2002 to 2008, median PSA was 574 ng/ml and 63 % were already stage 4 at diagnosis [13]. At the same time, there is little data as to whether the same PSA thresholds defined in Caucasian populations are directly applicable in Asia. In a multiethnic cross-sectional study of 1054 Malaysian men, Lim et al. reported that ethnicity independently influenced serum PSA level among Malay, Chinese, and Indians [14]. On the other hand, in a report from Singapore, Chia et al. reported that of a multiethnic group of 3486 men, 7.1 % had a PSA >4 ng/ml with no differences between ethnic groups [15].

Among reported Asian series from Korea, Japan, Singapore, Hong Kong, and Malaysia, the detection rate using standard biopsy techniques for a serum PSA of between 4 and 10 ng/ml ranges from 15 % to 22 %, and that for serum PSA between 10 and 20 ng/ml ranges from 35 % to 60 % [16–21]. These series likely represent areas where PSA testing is more prevalent compared to the rest of East and Southeast Asia. Many of these cancers are also likely to be low grade. In one study of 8236 men undergoing prostate needle biopsies, Kuo et al. reported a threefold increase in both low-grade and low-volume cancers over a 10-year period in Taiwan [22].

Patient Selection for Active Surveillance and Focal Therapy

Cancer Characterization/Localization

Patient selection is critical in both active surveillance and focal therapy. For the former, it is important to identify low-risk and low-volume intermediate-risk prostate cancer while excluding high-risk and high-volume intermediate-risk cancers. For the latter, it is important to localize cancer to a specific index lesion for the purposes of focal ablation. It is well recognized that standard extended transrectal ultrasound (TRUS) biopsy under-grades 30–50 % of prostate cancers [23]. Similar findings have been observed in series from Korea, Japan, and Singapore [24–26]. There now exist a plethora of methods such as multiparametric magnetic resonance imaging (mpMRI), advanced biopsy techniques (mapping or saturation prostate biopsies), and genomic markers that are available to aid in stratification of patients to gland-conserving strategies or radical interventions [27].

Prostate mpMRI preferentially detects higher-volume and higher-grade tumors [28, 29]. Correspondingly, there has been significant research and clinical interest in the use of mpMRI in Asia. Kitamura et al. reported on the effectiveness of mpMRI in characterizing prostate cancer in men with previous negative prostate biopsies [30]. Numao et al. combined extended prostate biopsies with diffusion-weighted MRI to achieve

a negative predictive value of 95.7 % for the absence of clinically significant prostate cancer in one lobe [31]. Extending this work further, the same group demonstrated negative and positive predictive values in excess of 91 % when identifying prostate quadrants containing significant prostate cancer [32]. On the other hand, Kan et al. reported that T1- and T2-weighted MRI alone without other parameters added only minimally to standard TRUS biopsy for localizing prostate cancers [33]. Similarly, Jeong et al. found that conventional MRI in addition to standard TRUS biopsy only had fair correlation with the laterality of prostate cancer [34]. Shoji and colleagues evaluated an MRI-TRUS fusion system on 20 Japanese men with a cancer detection rate of 31 % with targeted biopsies versus 6.7 % with systematic biopsies [35].

Transperineal mapping biopsy is considered the most accurate method of histologically characterizing prostate cancer with an accuracy of 95 %. A group in Singapore has developed a novel transperineal robot capable of performing mapping biopsy in a dual cone distribution via two transperineal punctures [36]. In characterizing men with low-risk prostate cancer thought to be suitable for active surveillance, the detection rate of Gleason >6 prostate cancer achieved using this robot was 20.7 % [37]. When this platform was used for combined MRI-targeted and mapping biopsy in men with low-risk prostate cancer about to go on active surveillance, the detection rate of clinically significant disease was 33.3 % [38].

Shared Decision-Making in Asia

Focal therapy and active surveillance for prostate cancer is a relatively novel concept and goes against the conventional grain of a radical approach to cancer treatment. Together with the expanding array of prostate cancer treatment options, decision-making in prostate cancer has become an intricate affair. To further complicate matters, decision-making in an Asian context tends to take on cultural hues. A focused group discussion of Malaysian urologists, exploring decision-making roles in localized prostate cancer treatment, showed that while many providers still preferred a more paternalistic role, others believed in attempting to build a consensus with patients [39]. An important theme that emerged was the involvement of the patient's family in decision-making. In a multicultural, multiracial survey conducted among patients in Singapore, two-thirds of patients, if diagnosed with cancer, would want their family to participate in decision-making [40]. Rhunke et al. found that Japanese physicians and patients placed far greater emphasis on the role of the family and physician recommendations compared to physicians and patients from the United States, where there was a greater emphasis on patient autonomy and individual decision-making [41]. The same study reported that these differences, while still present, were less pronounced in younger patients and such generational changes in thinking are also being observed elsewhere in East Asia [42]. Physicians in Asia will have to take into account the balance between cultural traditions and generational changes in thinking besides the cancer itself, to help guide the patient to making the appropriate treatment choice.

Patient Attitudes Toward Less Intervention in Asia

Focal therapy and/or active surveillance are strategies that convert suitable prostate cancers into chronic disease. This departs from traditional treatment paradigms and may be associated with an increased psychological burden on patients. In the Prostate Research International: Active Surveillance (PRIAS) study, 5 % of men discontinued surveillance at 18 months due to anxiety [43]. A neurotic personality score was associated with higher depression and prostate cancer-specific anxiety [44]. In a Malaysian study evaluating 193 men who were being followed for prostate cancer, the prevalence of anxiety was 25.4 %, and these men had a negatively impacted health-related quality of life [45]. In a study from Taiwan, Lin et al. reported that 31 % of men regretted undergoing radical prostatectomy and,

in a later study, found that a psychological support group reduced patient uncertainty regarding cancer treatment and complications [46, 47].

Active Surveillance and Focal Therapy in East/Southeast Asia: Current Practices and Outcomes

Based on published literature, Japan appears to have the most adoption of active surveillance compared to other Asian countries, with 33 institutions participating in the PRIAS study. In an interim report, 386 patients had been enrolled in PRIAS-JAPAN by the end of 2013, and of these, 216 underwent the first year re-biopsy with a 33.8 % reclassification rate [48]. Reasons for reclassification were increased core numbers (36 %), Gleason upgrading (25 %), or both (39 %). In a nationwide survey of Japanese urologists, 73 % had treated men with localized prostate cancer with active surveillance [49]. Ha et al. reported on a Korean series of 35 men treated with active surveillance over 4 years, with follow-up biopsies in 25 patients [50]. In all, 12 men underwent treatment, 5 of whom did so because of disease progression and 7 for anxiety. In a series of 108 Singaporean men with prostate cancer on active surveillance, 58 % remained stable with regard to serum PSA and biopsy findings [51]. However, a quarter of these men chose intervention despite stable disease. Overall, 70.5 % remained treatment-free at 24 months.

Muto et al. conducted the first focal therapy trial in Asia in 2008, treating 70 men with hemiablation using high-intensity focused ultrasound (HIFU) and achieving a negative biopsy in 76.5 % at 12 months [52]. A pilot series of 13 men with low-risk prostate cancer undergoing MRI-guided HIFU was reported from Singapore in 2011 [53]. More recently, in a Chinese study of 41 men undergoing primary focal cryoablation, Lian et al. reported a treatment failure rate of 10 % at a mean follow-up of 63 months [54]. Complete continence was achieved in 97.6 % of patients and potency sufficient for intercourse in 76.9 %.

Conclusion

Active surveillance is suitable for indolent prostate cancer, while focal therapy may be suitable for more aggressive but low-volume prostate cancer. These strategies are applicable in a setting where there are high rates of early prostate cancer diagnosis. With the present controversy about the role of systematic PSA screening, PSA testing is likely to be patient driven and thus more likely to occur in populations with greater longevity and better healthcare, such that mortality from prostate cancer becomes significant compared to other causes. As this scenario becomes increasingly common over time in East Asia and Southeast Asia, the role and relevance of active surveillance and focal therapy in addressing prostate cancer overdiagnosis and overtreatment will become more prominent. These treatment strategies will need to be supported by dissemination of advanced imaging, biopsy techniques, and ablative technologies, as well as trained urologists and radiologists.

References

1. Chowdhury S, Robinson D, Cahill D, Rodriguez-Vida A, Holmberg L, Moller H. Causes of death in men with prostate cancer: an analysis of 50,000 men from the thames cancer registry. BJU Int. 2013;112(2):182–9.
2. National Geographic S. National geographic atlas of the world. National Geographic Society. Washington, DC: National Geographic Society; 1999.
3. Reid TR. Confucius lives next door: what living in the east teaches us about living in the west. New York: Random House; 1999.
4. Ferlay J, Soerjomataram I, Ervik M, Dikshit R, Eser S, Mathers C, et al. Globocan 2012 v1.0, cancer incidence and mortality worldwide: Iarc cancerbase no. 11 [internet]. Lyon: International Agency for Research on Cancer; 2013 [3/2/2016]; Available from: http://globocan.iarc.fr.
5. Breslow N, Chan CW, Dhom G, Drury RA, Franks LM, Gellei B, et al. Latent carcinoma of prostate at autopsy in seven areas. The international agency for research on cancer, Lyons, France. Int J Cancer. 1977;20(5):680–8.
6. Cullen J, Elsamanoudi S, Brassell SA, Chen Y, Colombo M, Srivastava A, et al. The burden of prostate cancer in Asian nations. J Carcinog. 2012;11:7.

7. Sim HG, Cheng CW. Changing demography of prostate cancer in asia. Eur J Cancer. 2005;41(6):834–45.
8. Grulich AE, McCredie M, Coates M. Cancer incidence in asian migrants to new south wales, Australia. Br J Cancer. 1995;71(2):400–8.
9. Rastogi T, Devesa S, Mangtani P, Mathew A, Cooper N, Kao R, et al. Cancer incidence rates among South Asians in four geographic regions: India, Singapore, UK and US. Int J Epidemiol. 2008;37(1):147–60.
10. Bouchardy C, Fioretta G, Rapiti E, Verkooijen HM, Rapin CH, Schmidlin F, et al. Recent trends in prostate cancer mortality show a continuous decrease in several countries. Int J Cancer. 2008;123(2):421–9.
11. Myrtle J, Ivor L. Measurement of prostate-specific antigen (psa) in the serum by a two-site immunometric method (hybritech tandem-r/tandem-e psa). In: Catalona W, Coffey D, Karr J, editors. Clinical aspects of prostate cancer: assessment of new diagnostic and management procedures. New York: Elsevier; 1989. p. 161–71.
12. Oesterling JE, Jacobsen SJ, Chute CG, Guess HA, Girman CJ, Panser LA, et al. Serum prostate-specific antigen in a community-based population of healthy men. Establishment of age-specific reference ranges. JAMA. 1993;270(7):860–4.
13. Hong GE, Kong CH, Singam P, Cheok LB, Zainuddin ZM, Azrif M. Seven-year review of prostate carcinomas diagnosed by trus biopsy in a single malaysian institution. Asian Pac J Cancer Prev. 2010;11(5):1351–3.
14. Lim J, Bhoo-Pathy N, Sothilingam S, Malek R, Sundram M, Hisham Bahadzor B, et al. Ethnicity is an independent determinant of age-specific psa level: findings from a multiethnic asian setting. PLoS One. 2014;9(8):e104917.
15. Chia SE, Lau WK, Cheng C, Chin CM, Tan J, Ho SH. Prostate-specific antigen levels among Chinese, Malays and Indians in Singapore from a community-based study. Asian Pac J Cancer Prev. 2007;8(3):375–8.
16. Teo JK, Poh BK, Ng FC, Fong YK. Detection rate of prostate cancer on the basis of the vienna nomogram: a Singapore study. Korean J Urol. 2014;55(4):245–8.
17. Yang WJ, Lee DH, Chung BH, Cho JS, Choi YD, Kim SJ, et al. Detection rate of prostate cancer on biopsy according to serum prostate-specific antigen in Korean men: a multicenter study. Urology. 2006;67(2):333–6.
18. Ng LG, Yip S, Tan PH, Yuen J, Lau W, Cheng C. Improved detection rate of prostate cancer using the 10-core biopsy strategy in Singapore. Asian J Surg. 2002;25(3):238–43.
19. Egawa S, Matsumoto K, Yoshida K, Iwamura M, Kuwao S, Koshiba K. Results of transrectal ultrasound-guided biopsies and clinical significance of Japanese prostate cancer. Jpn J Clin Oncol. 1998;28(11):666–72.
20. Sothilingam S, Sundram M, Malek R, Sahabuddin RM. Prostate cancer screening perspective, Malaysia. Urol Oncol. 2010;28(6):670–2.
21. Teoh JY, Yuen SK, Tsu JH, Wong CK, Ho B, Ng AT, et al. Prostate cancer detection upon transrectal ultrasound-guided biopsy in relation to digital rectal examination and prostate-specific antigen level: what to expect in the Chinese population? Asian J Androl. 2015;17(5):821–5.
22. Kuo YJ, Lin SF, Chang YH, Pan CC. Trends in prostate needle biopsy diagnosis. A ten year experience of a medical center in Taiwan. Pathol Int. 2012;62(3):191–8.
23. Fu Q, Moul JW, Banez LL, Sun L, Mouraviev V, Xie D, et al. Association between percentage of tumor involvement and gleason score upgrading in low-risk prostate cancer. Med Oncol. 2012;29(5):3339–44.
24. Oh JJ, Hong SK, Lee JK, Lee BK, Lee S, Kwon OS, et al. Prostate-specific antigen vs prostate-specific antigen density as a predictor of upgrading in men diagnosed with gleason 6 prostate cancer by contemporary multicore prostate biopsy. BJU Int. 2012;110(11 Pt B):E494–9.
25. Imamoto T, Utsumi T, Takano M, Komaru A, Fukasawa S, Suyama T, et al. Development and external validation of a nomogram predicting the probability of significant gleason sum upgrading among Japanese patients with localized prostate cancer. Prostate Cancer. 2011;2011:754382. doi:10.1155/2011/754382.
26. Tan G, Ho H, Huang H, Cheng CWS, Lau WKO. Pathological outcome in men with prostate cancer suitable for active surveillance after radical prostatectomy. Proc Singapore Healthcare. 2012;21(2):102–8.
27. Tay KJ, Mendez M, Moul JW, Polascik TJ. Active surveillance for prostate cancer: can we modernize contemporary protocols to improve patient selection and outcomes in the focal therapy era? Curr Opin Urol. 2015;25(3):185–90.
28. Arumainayagam N, Ahmed HU, Moore CM, Freeman A, Allen C, Sohaib SA, et al. Multiparametric Mr imaging for detection of clinically significant prostate cancer: a validation cohort study with transperineal template prostate mapping as the reference standard. Radiology. 2013;268(3):761–9.
29. Rosenkrantz AB, Mendrinos S, Babb JS, Taneja SS. Prostate cancer foci detected on multiparametric magnetic resonance imaging are histologically distinct from those not detected. J Urol. 2012;187(6):2032–8.
30. Kitamura K, Muto S, Yokota I, Hoshimoto K, Kaminaga T, Noguchi T, et al. Feasibility of multiparametric prostate magnetic resonance imaging in the detection of cancer distribution: histopathological correlation with prostatectomy specimens. Prostate Int. 2014;2(4):188–95.
31. Matsuoka Y, Numao N, Saito K, Tanaka H, Kumagai J, Yoshida S, et al. Combination of diffusion-weighted magnetic resonance imaging and extended prostate biopsy predicts lobes without significant cancer: application in patient selection for hemiablative focal therapy. Eur Urol. 2014;65(1):186–92.
32. Matsuoka Y, Numao N, Saito K, Tanaka H, Kumagai J, Yoshida S, et al. Candidate selection for quadrant-based focal ablation through a combination of diffusion-weighted magnetic resonance imaging and prostate biopsy. BJU Int. 2016;117(1):94–101.

33. Kan RW, Kan CF, Ho LY, Chan SW. Pre-operative tumor localization and evaluation of extra-capsular extension of prostate cancer: how misleading can it be? Urol J. 2014;11(3):1615–9.
34. Jeong CW, Ku JH, Moon KC, Hong SK, Byun SS, Cho JY, et al. Can conventional magnetic resonance imaging, prostate needle biopsy, or their combination predict the laterality of clinically localized prostate cancer? Urology. 2012;79(6):1322–7.
35. Shoji S, Hiraiwa S, Endo J, Hashida K, Tomonaga T, Nakano M, et al. Manually controlled targeted prostate biopsy with real-time fusion imaging of multiparametric magnetic resonance imaging and transrectal ultrasound: an early experience. Int J Urol. 2015; 22(2):173–8.
36. Ho H, Yuen JS, Mohan P, Lim EW, Cheng CW. Robotic transperineal prostate biopsy: Pilot clinical study. Urology. 2011;78(5):1203–8.
37. Tay KJ, Ho H, Huang H, Law Z, Koh Z, Yuen J, et al. Robotic transperineal saturation biopsy approximates the "truth" in defining low-risk prostate cancer. Urology. 2013;82(3):S70.
38. Tay KJ, Chen K, Law YM, Ho H, Yuen J, Cheng C. Early outcomes of combination mri-targeted and saturation trans-perineal biopsy in restaging low-risk prostate cancer for active surveillance (mp48-08). J Urol. 2015;193(4):e597.
39. Lee YK, Lee PY, Cheong AT, Ng CJ, Abdullah KL, Ong TA, et al. To share or not to share: Malaysian healthcare professionals' views on localized prostate cancer treatment decision making roles. PLoS One. 2015;10(11):e0142812.
40. Tay KJ, Mohamad Zam NA, Cheng CW. Prevailing attitudes towards cancer: a multicultural survey in a tertiary outpatient setting. Ann Acad Med Singapore. 2013;42(10):492–8.
41. Ruhnke GW, Wilson SR, Akamatsu T, Kinoue T, Takashima Y, Goldstein MK, et al. Ethical decision making and patient autonomy: a comparison of physicians and patients in Japan and The United States. Chest. 2000;118(4):1172–82.
42. Dai Q. Informed consent in china: Status quo and its future. Med Law Int. 2003;6(1):53–71.
43. Venderbos LD, van den Bergh RC, Roobol MJ, Schroder FH, Essink-Bot ML, Bangma CH, et al. A longitudinal study on the impact of active surveillance for prostate cancer on anxiety and distress levels. Psychooncology. 2015;24(3):348–54.
44. van den Bergh RC, Essink-Bot ML, Roobol MJ, Wolters T, Schroder FH, Bangma CH, et al. Anxiety and distress during active surveillance for early prostate cancer. Cancer. 2009;115(17):3868–78.
45. Isa MR, Moy FM, Abdul Razack AH, Md Zainuddin Z, Zainal NZ. Anxiety status and its relationship with general health related quality of life among prostate cancer patients in two university hospitals in Kuala Lumpur, Malaysia. Iran J Public Health. 2013;42(3):240–8.
46. Lin YH. Treatment decision regret and related factors following radical prostatectomy. Cancer Nurs. 2011;34(5):417–22.
47. Lin YH, Yu TJ, Lin VC, Yang MS, Kao CC. Changes in quality of life among prostate cancer patients after surgery. Cancer Nurs. 2012;35(6):476–82.
48. Sugimoto M, Hirama H, Yamaguchi A, Koga H, Hashine K, Ninomiya I, et al. Should inclusion criteria for active surveillance for low-risk prostate cancer be more stringent? From an interim analysis of Prias-Japan. World J Urol. 2015;33(7):981–7.
49. Mitsuzuka K, Koga H, Sugimoto M, Arai Y, Ohyama C, Kakehi Y, et al. Current use of active surveillance for localized prostate cancer: a nationwide survey in Japan. Int J Urol. 2015;22(8):754–9.
50. Ha JY, Kim BH, Park CH, Kim CI. Early experience with active surveillance in low-risk prostate cancer treated. Korean J Urol. 2014;55(3):167–71.
51. Tay KJ, Huang HH, Lee LS, Cheng CWS, Yuen JSP. A treatment journey of 108 men on active surveillance for prostate cancer: why men change? BJU international. Hoboken: Wiley-Blackwell; 2014.
52. Muto S, Yoshii T, Saito K, Kamiyama Y, Ide H, Horie S. Focal therapy with high-intensity-focused ultrasound in the treatment of localized prostate cancer. Jpn J Clin Oncol. 2008;38(3):192–9.
53. Tay KJ, Cheng CW, Kwek JW, Thng CH, Lau WK, Ho HS, et al. Initial experience with MRGFUS focal therapy for low-risk prostate cancer. J Endourol. 2011;25(1):A99–100.
54. Lian H, Zhuang J, Yang R, Qu F, Wang W, Lin T, et al. Focal cryoablation for unilateral low-intermediate-risk prostate cancer: 63-month mean follow-up results of 41 patients. Int Urol Nephrol. 2016;48(1):85–90.

Part III

Scientific Foundation for the Focal Therapy Concept

7 Pathologic Rationale for Focal Therapy of Prostate Cancer: Elucidating Tumor Characteristics and Biology

Vladimir Mouraviev, Arnauld Villers, Thomas M. Wheeler, Rodolfo Montironi, Pierre Nevoux, Ariel Schulman, and Thomas J. Polascik

Introduction

The contemporary widespread detection of early-stage prostate cancer (PCa) has led to a dramatic shift in the treatment paradigm of localized disease toward nonaggressive and minimally invasive approaches such as active surveillance (AS) and focal therapy (FT) [1–3]. Quality of life outcomes, in particular urinary continence and erectile function, are particularly important to the relatively young cohort of men in their fifties and sixties who are candidates for PCa treatment. During the last several decades, pathologic and clinical studies have been done to better understand the role of prostate-preserving ablative technologies using targeted ablation as a "male lumpectomy" in appropriate candidates [4–8].

The recognition of the multifocality of the majority of cases of PCa, likelihood of synchronous cancer lesions, and lack of specific and sensitive imaging modalities to accurately identify the extent or contours of significant cancer foci remain major limitations to more broad implementation of FT [9–11]. Although, several recent studies based on unbiased genome-wide approaches demonstrated that anatomically distinct tumor metastases are derived from a single progenitor clone [12–15]. These data of the literature suggest that most commonly the driver lesion with potentially lethal clone is located inside of the index focus, which gives the bright prospects for focal ablation of this focus with potentially curable intent. However, currently, we still lack a reliable diagnostic tool to rule out an existence of this lethal clone in secondary (satellite) lesion(s) in some cohort of patients.

V. Mouraviev (✉)
Central Florida Cancer Institute, Davenport, FL, USA
e-mail: Vladimir.Mouraviev@flhosp.org

A. Villers
Department of Urology, Hôpital Huriez, Centre Hospitalier Regional Universitaire, Université Lille Nord de France, Lille, France

T.M. Wheeler
Department of Pathology and Immunology, Baylor College of Medicine, Houston, TX, USA

R. Montironi
Department of Pathology, Genitourinary Cancer Program, Institute of Pathological Anatomy and Histopathology, Polytechnic University of the Marche Region (Ancona), School of Medicine, United Hospitals, Torrette, Ancona, Italy

P. Nevoux
Department of Urology, Regional University of Lille, Lille, France

A. Schulman
Duke Cancer Institute and Department of Surgery, Duke University Medical Center, Durham, NC, USA

T.J. Polascik, MD
Professor of Surgery, Division of Urology, Department of Surgery, Duke Cancer Institute, Duke University School of Medicine, Durham, NC, USA

© Springer International Publishing AG 2017

T.J. Polascik (ed.), *Imaging and Focal Therapy of Early Prostate Cancer*, Current Clinical Urology, DOI 10.1007/978-3-319-49911-6_7

In this chapter we review the current literature on the pathologic significance of PCa including a number of tumors, location, aggressiveness, invasiveness, uni- vs. multifocality, and laterality along with genomic alterations. As we continue to understand the histologic and genomic biology of index and satellite lesions, we can better select candidates and predict those men most likely to benefit from an organ-preserving treatment approach.

The Pathological Parameters Defining Clinically Significant Prostate Cancer and Rationale for Focal Therapy

An international consensus panel of experts recently provided guidance on patient eligibility, interventions, and meaningful outcome measures for FT in clinical practice [16]. The panel noted a trend toward including FT for intermediate-risk disease compared to previously existing approaches treating only men with low-risk disease. This shift is based on growing confidence in the technique and promising medium-term follow-up results of multiple clinical trials [17–20]. Some critical definitions for patient selection were revised according to new data. For instance, prostate volume should no longer be a primary determinant of eligibility for FT. Other factors that require consideration include tumor grade and the boundaries and morphologic characteristics of the lesion. Furthermore, there are limitations in different ablative modalities that should be considered in planning focal therapy [16]. For example, high-intensity focused ultrasound (HIFU) may not have the required focal length to reach anterior lesions in larger glands.

The Index Lesion as a Driver of Cancer Progression

There are multiple factors including multifocality and varied histological, genomic, and molecular abnormalities that determine whether PCa will behave in an indolent or aggressive fashion. More than 80 % of prostatectomy specimens contain more than one disease focus [21, 22]. The index tumor, or dominant lesion, is defined as the largest volume lesion and presumed to be the main determinant for tumor progression and prognosis. Unifocal cancer has been identified in 13–33 % of radical prostatectomy (RP) specimens, and is generally associated with lower grade, stage, and recurrence rates than multifocal cancers [23–26]. In a review by Mouraviev et al., histologic features of the index lesion were linked to prostate cancer follow-up and generally were the main determinant of prognosis [4]. Karavitakis et al. reported that the largest lesion usually contains the worst histologic features on radical prostatectomy specimen [27]. This was confirmed by Huang et al. who analyzed 201 specimens and noted that the largest tumor volume, highest Gleason score (GS) and extraprostatic extension (if present) occurred within the same lesion in 88.7 % of cases with multifocal disease [28].

In the index lesion hypothesis, the satellite lesions, or secondary foci, are thus considered to be non-life-threatening. This is supported by a contemporary study by Mizuno et al. who reported that the largest tumor was a predictor of recurrence after treatment at multivariate analysis, alongside Gleason score and positive surgical margin [29]. Indeed, Liu et al. reported an autopsy series that noted a monoclonal cell precursor as the origin of metastasis [13]. Similarly, Mehra et al. described a single origin of metastasis [14]. Ding et al. found that some specific genetic alterations have implications in prostate cancer growth and metastatic progression [30]. Ultimately, Ahmed et al. formalized the concept of the index lesion according to data suggesting that genomic "signatures" of PCa and its metastases are all derived from a single clone in the prostate gland [31].

Based on 222 men with stage T1c PCa treated with RP, Noguchi et al. studied the prognostic value of secondary cancers in men having multifocal, localized PCa [32]. The cohort was divided into three groups including men with a single tumor (54 cases, 24 %), an index tumor with secondary cancers <0.5 cc (86 cases, 39 %), and an

index tumor with secondary cancers >0.5 cc (82 cases, 37 %). On multivariate analysis of the three groups, the investigators did not detect any differences in preoperative prostate-specific antigen (PSA), number of positive cores, percent of Gleason grade 4 or 5 in the needle biopsy, or histological features in RP specimens. However, when analyzing PSA failure rates among the three groups, the group with an index lesion and smaller secondary cancers had a better prognosis than the group with a single tumor. This study suggests that patients with multifocal PCa do not necessarily have a worse outcome than men with unifocal lesions. A report by Haffner et al. studying 108 RP specimens suggested that secondary cancers are rarely significant in volume [33]. Two simultaneous, significant volume cancers >0.5 cc were identified in only 11 of 152 (7 %) cases.

The Role of Small Satellite Lesions: Do They Need to be Treated?

Several reports contend that secondary, small-volume tumors do not significantly influence the survival of patients after RP [34–37]. A study by Liu et al. revealed support for a single aggressive lesion affecting the mortality of patients with advanced PCa [13]. This multi-institutional study using high-resolution, genome-wide single nucleotide polymorphism and copy number reported on 94 anatomically separate cancer sites in 30 men who died from metastatic PCa. These data in conjunction with a single-locus genetic study of advanced PCa evaluating the role of TMPRSS2-ETS in tumor progression demonstrated that in spite of common genetic heterogeneity in primary cancers, most metastatic cancers arise from a single clone of index lesion [13].

On the contrary, emerging data suggests that secondary tumors may grow and become clinically significant over time [38, 39]. The advanced genome-wide association studies (GWAS) have emerged as a new approach to identify alleles associated with prostate cancer risk in unbiased fashion; i.e., without prior knowledge of their position or function [40–43]. These GWASs can shed light to better understand tumor subclonality by using spatio-genomic approaches and sequencing multiple foci from each individual patient. All studies demonstrated the presence of multiple independent cancer clones both within and between (intrapatient heterogeneity) suggesting that FT for prostate cancer may be complicated by heterogeneous molecular aberrations.

Haffner et al. tracked the evolution of the lethal cell clone from primary PCa to metastases through samples collected during disease progression and at the time of death over a 17-year treatment course following primary radical prostatectomy [38, 39] (Fig. 7.1a, b). Despite being limited to one case, these analyses demonstrated that the lethal clone arose from a small, relatively low-grade cancer focus with a Gleason grade of 6 in the primary tumor, and not from the bulky, higher-grade primary cancer of Gleason grade 7 or from a lymph node metastasis resected at prostatectomy.

Taken together, the aforementioned studies reveal a series of unexpected characteristics of localized prostate cancer. First, they demonstrate the presence of widespread field effects, with mutational stress across the entire prostate gland superimposed with tumor evolution and selective pressures to produce substantial spatial heterogeneity. Second, they highlight the challenge of treating tumors composed of different subclones, some of which may respond to specific systemic or targeted therapies, and suggest a need for multimodal interventions. Finally, they suggest that genomic interrogation of a single biopsy specimen may be insufficient to generate robust predictions from molecular biomarkers, even if suspected trunk mutations are considered because of apparent multiple clonally independent tumors within a single individual. To date, these conclusions are based on a limited number of patient trials; therefore they cannot be used to make generalizations for all candidates for FT. More robust clinical observations are required. Furthermore, it is well known that these multiple genetic events may not always have an impact on the natural history of the disease.

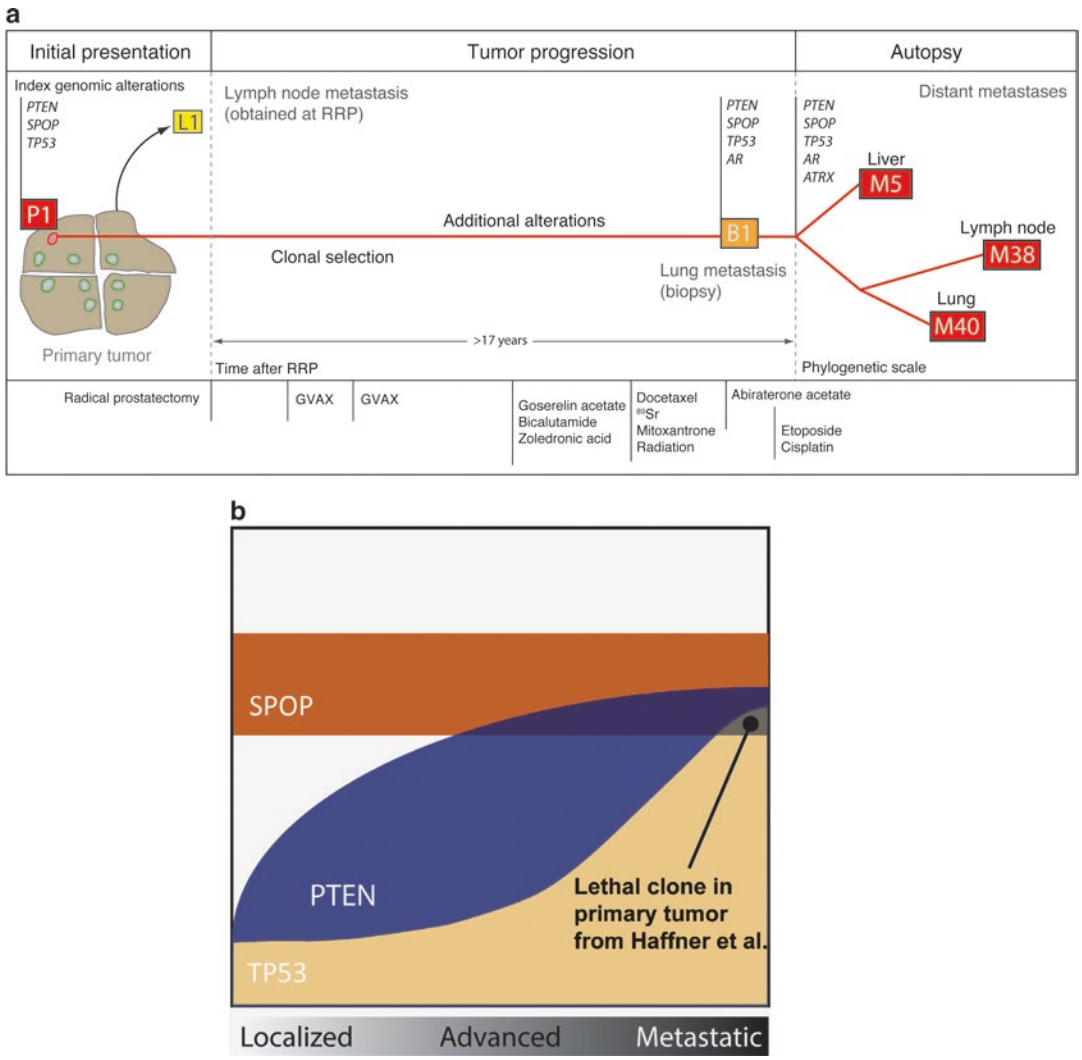

Fig. 7.1 Molecular and pathological findings in the primary tumor and their clonal relationship to the distant metastases. (**a**) Proposed model of disease progression in this index case, based on sequencing and molecular pathological analyses. Phylogenetic relationships of distant metastases were calculated based on structural rearrangements. (Reprinted with permission from Haffner MC, Mosbruger T, Esopi DM, Fedor H, Heaphy CM, Walker DA, et al. Tracking the clonal origin of lethal prostate cancer. J Clin Invest. 2013 Nov;123(11):4918–4922. [39]). (**b**) Speckle-type POZ protein (SPOP), phosphatase and tension homolog (PTEN), and tumor protein 53 (TP53) abnormalities across the spectrum of early and advanced prostate cancer. Reprinted with permission from Barbieri CE, Demichelis F, Rubin MA. The lethal clone in prostate cancer: Redefining the index. Eur Urol. 2014 Sep.;66(3): 395–397 [38]

If secondary cancers are initially left untreated, a stringent surveillance protocol including imaging and novel genomics tools should be followed. If significant growth of secondary lesions is noted during follow-up after index ablation, repeat ablation should be performed.

The index lesion may be considered the driving force of PCa progression and therefore should be identified and treated at an early stage. The majority of satellite lesions generally do not appear to be life threatening to the patient. Therefore, for patients considering FT, precise three-dimensional (3D) mapping biopsies and/or imaging studies should be done to identify and map the index tumor and ensure that potential clinically significant small-sized lesions are not inadvertently missed.

Cancer Laterality and Unifocality

Conventional PCa treatment, namely, whole-gland therapy, is dogmatically founded upon the principle of tumor heterogeneity and multifocality seen in 50–87 % of cases [4, 21, 22]. With prevalent PSA screening and early detection programs, investigators are now reporting an increased proportion of unifocal and/or unilateral disease.

Bostwick et al. demonstrated that multiple foci of prostatic intraepithelial neoplasia (PIN) may independently arise from various sites of the same prostate suggesting a field effect underlying the development of PCa [44]. Aurora et al. and Cheng et al. sequentially demonstrated that multifocal PCa is common (87 %) with extensive histological heterogeneity seen among foci within the same specimen even with very low total tumor volume [35]. These findings also support the "field effect" of carcinogenesis. Recently, the same group reviewed records of 184 patients with unifocal tumors [23]. They found that despite a number of patients with insignificant disease, the relative proportion of patients with a unifocal tumor increased from 13 % to 28 % in the overall cohort. Tumor focality failed to show an advantage in biochemical recurrence between unifocal and multifocal disease. There were not significant differences in 5-year biochemical recurrence-free survival (66 % and 61 %, respectively). However, these data suggest that unifocal lesions can be aggressive and require ablative therapy.

Some investigators found a significant difference in treatment outcome between unifocal and multifocal lesions [45], whereas others demonstrated that the number of tumor foci, index tumor volume, satellite tumor volume, or tumor unilaterality did not predict disease-free survival on multivariate analysis [32, 46, 47]. Such conflicting data suggest the limitations of single-institutional studies with specific geographic and demographic features along with variable follow-up. It also implies our incomplete knowledge about the natural history of early-stage disease, including the complexity of tumor biology and limited predictability of clinical behavior.

It has been noted that even within the same institution (Stanford, Colorado, and Indiana University, etc.) the incidence of unifocal PCa has fluctuated over time [25]. Some countries have shown a greater prevalence of unifocal lesions, such as Austria and France (30–33 %), and South Korea (67 %) based upon prostatectomy specimens [4]. This may reflect differences in selection factors, patient populations, and methods of tissue sampling, among other possible explanations.

From its onset, FT has encompassed the concept of hemi-ablation; e.g., ablating the side of the prostate containing the dominant or index tumor along with any other satellite lesions that are found on the same side of the prostate. Based upon this premise, the concept of the unilateral cancer may be a more practical approach than targeting the unifocal tumor. Mouraviev et al. analyzed 1186 prostatectomy specimens from patients with low- to low-intermediate risk, clinically localized PCa [48]. Pathologic assessment focused on cancer laterality, percentage of tumor involvement (PTI), and pathologic Gleason score. Unilateral cancer was identified in 227 (19.2 %) cases, suggesting that almost one of five candidates treated with surgery in contemporary series may be amenable to focal hemi-ablation of one side of the prostate.

It is important to recognize that there may be residual disease on the untreated side after hemi-ablation. Although small volume lesions are generally unilateral, some clinically significant tumors could be located on the contralateral side. Yoon et al. evaluated the contralateral gland in patients presumed to have unilateral prostate cancer on biopsy [49]. In this study of 100 low-risk patients, needle biopsy predicted what the authors defined as limited disease (less than 3 unilaterally positive cores, <50 % involvement of any positive core, Gleason score <6). Clinical stage T1c disease was diagnosed in 85 cases with cT2a disease in 15 with the palpable lesion located on the same side as the positive biopsies. In 66 cases, there was only one PCa focus identified in the contralateral lobe. Approximately 14 % of each positive core was involved with PCa. In 65 RP specimens, cancer was identified contralateral to the positive

biopsy side with a mean total tumor volume of 0.2 cm^3 (largest 1.3). There were 13 cases in which more than 0.5 cm^3 cancer was identified contralateral to the positive biopsy and seven with predominantly anteriorly located tumor. Overall, clinically significant cancer (Epstein definition) would have been missed in 20 % of cases in the contralateral lobe if hemi-ablation were performed based upon routine preoperative evaluation with *sextant* biopsy. This study underscores the limited accuracy of conventional, office-based transrectal ultrasound (TRUS)-guided prostate biopsy to select patients for hemi-ablation. In a study of 538 patients with biopsy-proven unilateral disease, analysis of the contralateral gland revealed pathologic features in 24 % of cases including extraprostatic extension (EPE) (14.9 %), PTI > 15 % (8.4 %), GS > 7 (4.7 %), seminal vesicle invasion (SVI, 2.5 %), or a combination of the aforementioned.

Bott et al. studied 100 prostatectomy specimens including men with intermediate- and high-risk disease and found multifocal disease in 84 patients, with 36 of them having had significant secondary tumors [50]. These clinically significant satellite cancers were defined by volume (≥0.5 ml), by grade (any Gleason pattern ≥4) in 19, and by stage (ECE) in six cases.

In the first prospective study from University College London, Ahmed et al. studied the feasibility of treating only the largest and highest-grade cancer in men with more than 1 known prostate tumor [51] (Fig. 7.2). They showed that the side effects of targeted ablation were low, with acceptable rates of early cancer control. The median PSA nadir decreased to 2.4 ng/ml (IQR 1.6–4.1). At 12 months, 42 of 52 (80.8 %) patients had histological absence of clinically significant cancer and 48 of 56 (85.7 %) patients had no measurable prostate cancer on rebiopsy or multiparametric magnetic resonance imaging (mpMRI). Despite an overall absence of clinically significant disease (primary end point) noted on follow-up, 43 % of men had persistent Gleason 6 disease at the study end. These cancers must be followed prospectively given the recent findings of Haffner et al. that noted distant metastasis originating from Gleason score 6 disease.

Gleason Grade

The Gleason grade reflects architectural patterns of groups of cancerous glands and has been established as an important predictor of biochemical and systemic failure as well as cancer-specific and overall survival. The new 2016 World Health Organization (WHO) Classification of PCa was recently introduced with a reorganized scoring system [52, 53] (Table 7.1). Gleason scores 2 to 6 are now condensed into a single prognostic grade group (PGG) 1, Gleason score 7 is divided into 2 groups based on primary score, and Gleason scores 9 and 10 are combined into group 5.

The international panel on FT agreed it was acceptable not to treat PGG 1 lesions up to a maximum cancer core length of 5 mm, although it has to be noted that the level of consensus was higher for not treating lesions with a smaller maximum cancer core length of 3 mm [16]. The panel agreed that PGG 2 (Gleason 3+4) lesions with a maximum cancer core length of 5 mm or PGG 3 (Gleason 4+3) disease of any length should be treated. However, the panel did not reach consensus on whether PGG 2 lesions with a maximum cancer core length of 3 mm could be left untreated.

In a contemporary series of patients who were selected for FT, most (85 %) had Gleason scores 5–7. Among these, Gleason 7 is of particular interest due to the controversy related to tumor biology and aggressiveness [17]. Some studies did not demonstrate a significant difference between clinical outcomes with histologically confirmed PGG 2 (GS 3+4) compared to PGG 3 (GS 4+3) disease [17]. However, other studies purport that cancers with primary Gleason pattern 4 have less favorable clinical behavior than those with primary Gleason pattern 3 [17]. Analyzing 1688 men 10 years after RP, Tollefson et al. demonstrated that a PGG 2 (GS 3+4) was associated with an increased biochemical disease-free survival (bDFS) (48 % vs. 38 %), lower systemic recurrence (8 % vs. 15 %), and higher cancer-specific survival (97 % vs. 83 %) compared to PGG 3 (GS 4+3), respectively [54]. Burdick et al. presented the results of 705 patients with Gleason

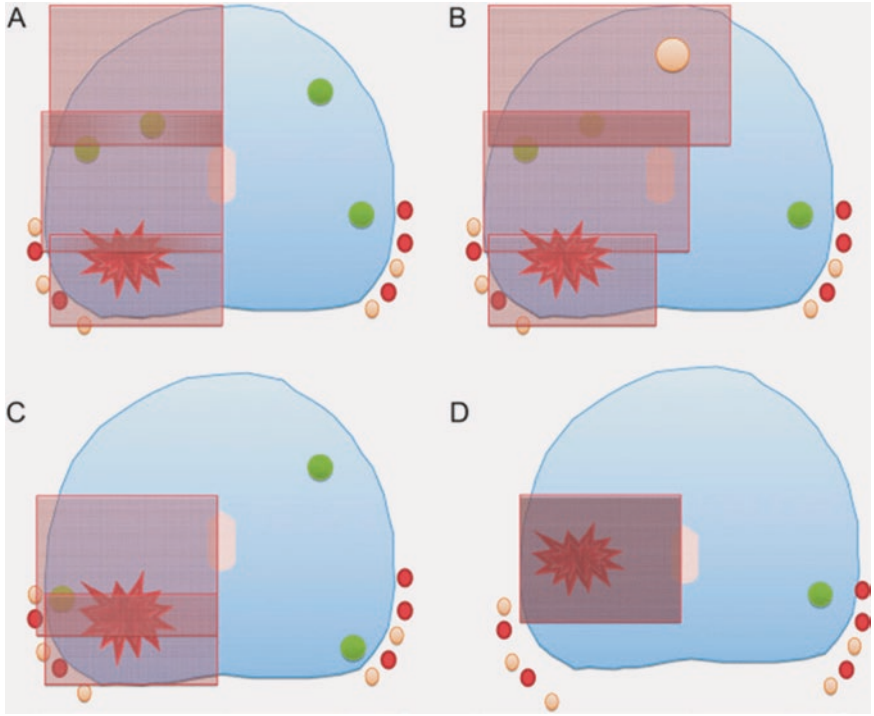

Fig. 7.2 Schematic diagrams demonstrating the types of focal therapy conducted in prospective development study on focal ablation of index lesion in multifocal localized prostate cancer. *Large red areas* represent dominant cancers (so-called index lesions), while *small green areas* represent small, low-grade, secondary lesions. *Red transparent boxes* represent ablation zones on the high-intensity focused ultrasound device: (**a**) hemi-ablation, (**b**) extended (dogleg) ablation, (**c**) quadrant ablation, (**d**) focal ablation. Reprinted with permission from Ahmed HU, Dickinson L, Charman S, Weir S, McCartan N, Hindley RG, et al. Focal ablation targeted to the index lesion in multifocal localized prostate cancer: a prospective development study. Eur Urol. 2015 Dec; 68(6):927–36

Table 7.1 World Health Organization (WHO) classification of prostate cancer

Prognostic grade group	Gleason score
1	3+3 = 6
2	3+4 = 7
3	4+3 = 7
4	8
5	9–10

7 prostate cancer treated with RP (n = 310), external beam radiotherapy (n = 268), or brachytherapy (n = 127) [55]. The 5-year bDFS rate was 78 % and 71 % (p = 0.0108) for PGG 2 (GS 3+4) and PGG 3 (GS 4+3), respectively [55]. The Physicians' Health Study and the Health Professionals Follow-Up Study reported on the mortality of PCa [56] suggesting that PGG 3 (GS 4+3) cancers were associated with a threefold increase in lethal PCa compared with PGG 2 (GS 3+4) cancers after RP.

Extraprostatic Extension Is Not an Absolute Contraindication to Focal Therapy

The risk of extraprostatic extension (EPE), which upgrades primary PCa to clinical stage T3a, should be considered in planning FT. EPE is a significant pathological parameter identified after RP that can influence disease-free recurrence. In a multivariate analysis by Ohori et al. the amount of EPE or prostate capsule invasion (PCI) was an independent prognostic factor of disease recurrence. These authors detected a strong correlation between the level of PCI and total tumor volume, Gleason grade, SVI, positive lymph node status

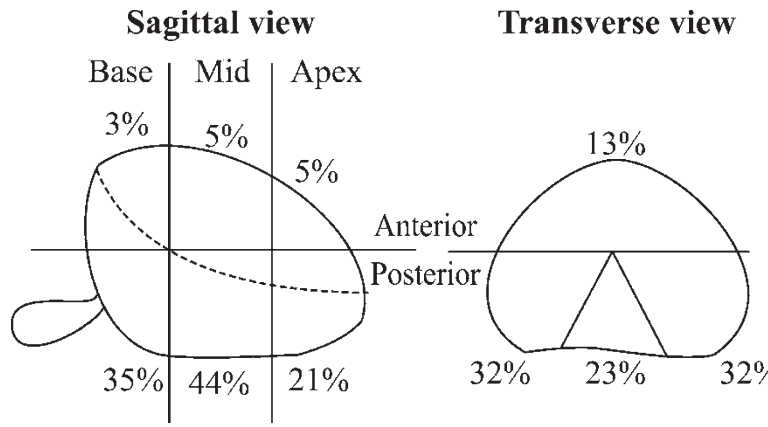

Fig. 7.3 Location and frequency of extraprostatic extension in radical prostatectomy specimens. Adapted from Ohori M, Scardino PT. Localized prostate cancer. Curr Probl Surg. 2002 Sep.;39(9):833–957 [57]

(+LN), and rate of biochemical recurrence after RP [57]. Of interest, PCa did not appear to metastasize in the absence of invasion into the prostate boundary regardless of the volume or grade of the intraprostatic tumor. Since EPE was identified as occurring more commonly on one side (85 % unilateral EPE vs. 15 % bilateral in this study), it is essential for optimal FT planning to understand the precise location of EPE. Unfortunately, EPE usually occurred near the neurovascular bundle (NVB) where it was exceedingly difficult to prevent collateral damage to this structure during thermal ablation. Figure 7.3 depicts the spatial location of EPE based on a large RP series from Baylor College of Medicine [57]. This map of possible locations of EPE is important and may guide treatment planning to preserve the contralateral NVB on the untreated side, thereby preserving erectile function.

Baylor and Memorial Sloan Kettering investigators studied the pathology of 1000 RP specimens of early-stage PCa patients [57]. The frequency of unifocal disease in men with baseline PSA <10 ng/ml was found to be 18 %. Generally, the largest (index) focus of cancer represented 80 % of the volume of all cancer present. They found that the index cancer was almost always the largest and highest-grade focus. However, in certain cases, larger lower-grade cancers were noted in the transition zone with smaller high-grade cancer in the peripheral zone. In these instances, the index cancer is defined as the one with the highest grade. Of 470 patients with PSA levels between 4 and 10 ng/ml, 30 % had EPE with 92 % of these derived from the index lesion, 5 % from more than one focus, and 3 % from smaller foci only. Of 126 patients with serum PSA ≤4 ng/ml, 20 % had EPE, 92 % of which emanated from the largest cancer and the remaining 8 % from other foci only. These data support the rationale to target the index lesion whereby the tumor burden would be reduced by 80 % and the focus giving rise to EPE would be controlled in >90 % of patients. Mouraviev et al. reported that among 1184 patients with low-risk PCa, EPE was noted in 19.2 % of RP specimens [48]. The majority of patients with EPE may still benefit from FT since several technologies such as cryoablation can extend beyond the capsule thereby treating EPE. However, this requires accurate identification of the location and extent of EPE and targeting the region accordingly during therapy.

Because EPE is a critical pathologic parameter of the natural history of carcinogenesis and prognosis, the curative intent to extend an ablative zone beyond the capsule is feasible, particularly when the index lesion is located near the capsule. Several ablative technologies can be used to safely destroy an index lesion with EPE with no collateral damage.

The Role of Spatial Distribution of Cancers According to Zone of Origin and Volume

An understanding of the modeling of cancer morphology such as the zonal origin and possibly intraprostatic patterns of cancer dissemination at histopathology is available for imaging interpretation and treatment planning. These models may help determine cancer volumes that can be followed as active surveillance or targeted by focal ablation. Additionally, planning may identify those cancers in which ablative therapy may affect areas of the prostate that are important for preservation of continence and potency. Combining histological data from RP sections, 12-core biopsy results, mpMRI data, and knowledge of the morphology of zonal prostate anatomy, it was possible to model PCa of different volumes and create graphical depictions of the likely shapes and sizes of tumors in different histological parts of the prostate, including modeling in axial versus coronal projections. Modeling studies estimate that approximately 30 % of low-volume cancers are located anteriorly. Anterior cancers originate in the transition zone (TZ) and may be compressed further anteriorly during benign prostatic hyperplastic (BPH) growth, giving rise to cancers located in the anterior fibromuscular stoma (AFMS).

A widely accepted tumor mapping strategy based on a 39-sector zone diagram from multiparametric MRI findings has been introduced by the recent European Society of Urogenital Radiology (ESUR) consensus meeting and modified by the American College of Radiology [58]. A prostate segmentation model defining each of the unique regions of the prostate for localization is depicted by Villers in chapter 28 of this book (see Fig. 28.2).

In a series of 108 RP specimens, Haffner et al. stated that of 188 peripheral zone (PZ) cancers, 179 were <4 cc and 168 were <2 cc [33]. PZ cancers tend to remain confined to their zone of origin for tumor volumes <2 cc. Between 2 cc and 4 cc, some cancers partly spread into the TZ or AFMS. In total, 64 % and 90 % of PZ cancers <4 cc were located in the lower and posterior half of the gland, respectively. Additionally, 10 % were located in the anterior horn of the PZ. Cancers <2 cc were confined to 1 lobe in 164 of 168 (98 %) cases and not confined in 3 of 11 (27 %) cancers measuring 2–4 cc in volume. Only cancer ≥2 cc involved both apex and base in the sagittal plane.

Bouye analyzed a series of 91 prostates with TZ/AFMS foci. Overall, 79 foci were <4 cc and 69 were <2 cc [59]. Additionally, 50 % and 70 % of cancers <4 cc were located in the anterior third and inferior half of the TZ and/or AFMS, respectively. The authors subclassified three varieties of the small cancers <2 cc according to their locations related to the boundaries of the histological zones: TZ type 1 (40 %) represented cancers confined to one TZ lobe; TZ type 2 (35 %) represented cancers mostly in one TZ lobe but crossing its anterior boundary; and type 3 AFMS (25 %) represented cancers confined to the AFMS.

Nevoux et al. analyzed a series of cystoprostatectomy specimens performed for bladder cancer from 345 consecutive patients without clinically manifested prostate cancer [60]. In the 96 prostates with prostate cancer, 215 cancer foci were identified (mean 2.24 cancers per prostate). Of the 215 cancers, 90 % were <0.5 cc and 79 % < 0.2 cc (Fig. 7.4). Overall, 88 % of cancer foci were clinically insignificant with a tumor volume <0.5 cc and no Gleason grades 4–5 (groups 4–5) (Fig. 7.5). Seventy-five percent of the cancer foci were located in the peripheral zone, while the remainder were within the transition zone. One-third of cancer foci were anteriorly located beyond the conventional area sampled by posterior biopsies. One-fifth of cancer foci were within 6 mm of the apex. Limitations include that cystoprostatectomy cancer foci are biologically at an earlier stage than screening-detected cancers. These results created the rationale for hypothesizing that AFMS cancers originate from anterior and medial TZ but become excluded from the TZ, anteriorly into the AFMS, due to growth of BPH. The TZ anterior limit would then function as a barrier to their posterior extension.

In summary, PZ (foci <2 cc), TZ/AFMS cancer contours and locations can be predictable and conform to histological zonal boundaries.

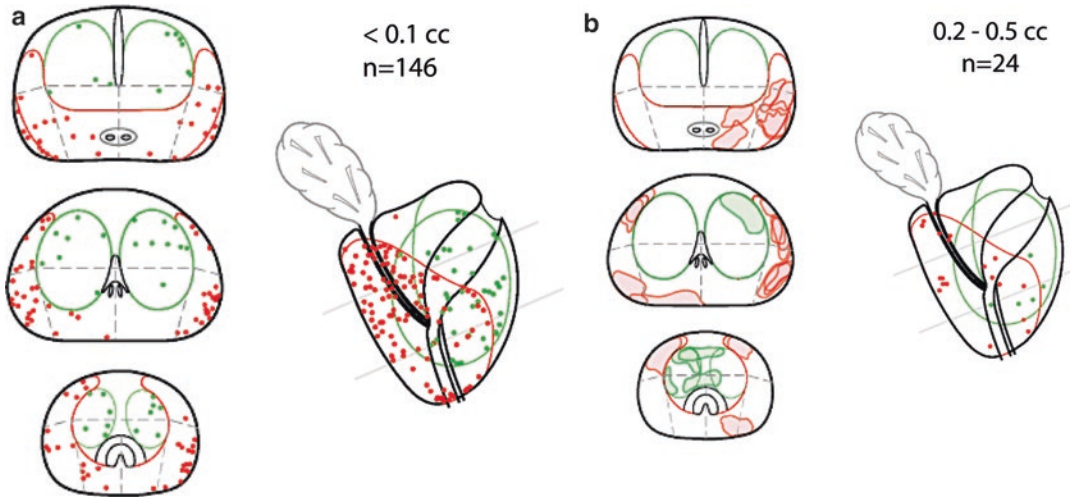

Fig. 7.4 Spatial distribution of (**a**) 146 prostate cancers <0.1 cc and (**b**) 24 prostate cancers 0.2–0.5 cc on sagittal and transverse prostate sections for an average 45 cc gland. *Dots* represent the center of each cancer focus. PZ cancers are in *red* and TZ/AFMS in *green*. Modified with permission from Nevoux P, Ouzzane A, Ahmed HU, Emberton M, Montironi R, Presti JC, Jr., et al. Quantitative tissue analyses of prostate cancer foci in an unselected cystoprostatectomy series. BJU Int. 2012 Aug;110(4):517–523 [60]

Knowledge of cancer origin and intraprostatic pattern of dissemination can be important for imaging, diagnosis, and guidance for biopsy and focal therapy. Additional study will be necessary to better understand the molecular events and potential intraprostatic spread of cancers within the prostate.

Accuracy of Novel Imaging-Guided Biopsies Validated by Final Pathology Assessment of Prostatectomy Specimens

To date, there is a lack of specific and sensitive imaging to accurately identify the extent or contours of significant cancer foci. In a milestone paper, Siddiqui et al. presented extensive experience from the National Cancer Institute (NCI) with fusion MRI/TRUS-guided biopsy [61]. Within the group of 170 who underwent prostatectomy, 17 patients were diagnosed only on standard biopsy, of whom 3 (18 %) had intermediate- or high-risk cancer on whole-mount pathology. By contrast, 20 patients were diagnosed with prostate cancer only on targeted biopsy, of whom 12 (60 %) had intermediate- or high-risk cancer on whole-mount pathology. When the ability of preoperative biopsy to predict whole-gland pathology was examined, the sensitivity of targeted biopsy was 77 % vs. 53 % for standard biopsy, while the specificities were similar (targeted, 68 %, vs. standard, 66 %). The area under the receiver operating curve (AUC) for targeted biopsy (0.73) was significantly greater than that of either standard biopsy (0.59, $P = 0.005$) or combined biopsy (0.67, $P = 0.04$) [61].

At the NCI, Turkbey et al. developed the customized mold and provided tissue blocks that permitted a direct one-to-one correlation with in vivo MRI [62, 63]. The use of the customized mold enabled more exact correlation between each MRI parameter and the histopathological specimen, without requiring a correction or an approximation approach to validate MRI with a more standardized, unbiased method. Whole-mount histopathological evaluation of 45 prostatectomy specimens revealed 342 tumor-positive regions: 281 (82 %) in the PZ and 61 (18 %) in the central zone (CZ) among 1746 regions. Of these 342 tumor positive regions, 90 (82 %) in the PZ and 20 (18 %) in the CZ contained tumors 5 mm or less in diameter, whereas 232 including 191 (82 %) in the PZ and 41 (18 %) in the CZ

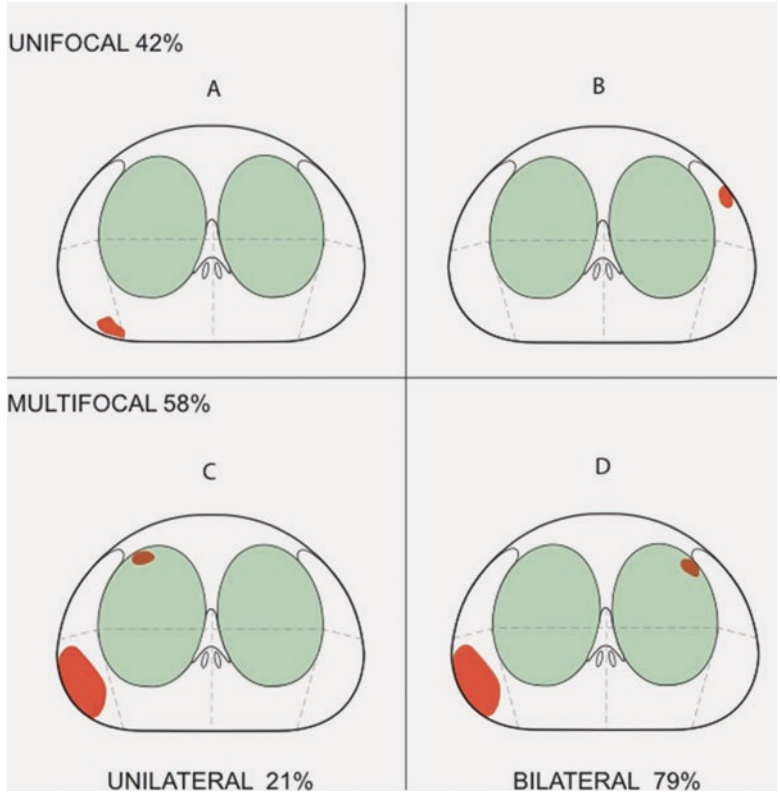

Fig. 7.5 Average transverse section of a 45 cc prostate at mid-gland depicting a model of distribution of 215 separate prostate cancers in 96 cystoprostatectomy specimens demonstrating unifocal (**a**, **b**) and multifocal (**c**, **d**), unilateral (**c**), and bilateral (**d**) tumors. Among the unilateral and multifocal cases (**c**), cancers were in the same anterior or posterior part of the gland in 50 % of cases. (**a**) Posterior insignificant cancer of 0.1 cc that could be detected by posterior systematic biopsies (SB). (**b**) Anterior insignificant cancer of 0.1 cc undetectable by posterior SB. (**c**, **d**) Unilateral (**c**) and bilateral (**d**) multifocal cancers with a large PZ cancer of 0.7 cc and a smaller TZ cancer of 0.1 cc. Modified with permission from Nevoux P, Ouzzane A, Ahmed HU, Emberton M, Montironi R, Presti JC, Jr., et al. Quantitative tissue analyses of prostate cancer foci in an unselected cystoprostatectomy series. BJU Int. 2012 Aug;110(4):517–523 [60]

contained tumors greater than 5 mm in diameter. Gleason scores were 7 or less in 235 regions: 194 (82.5 %) in the PZ and 41 (17.5 %) in the CZ regions and greater than 7 in 107 regions; 87 (81 %) in the PZ and 20 (19 %) in the CZ regions. On histopathological evaluation, extracapsular extension was detected in 20 regions in 12 prostatectomy specimens. Seminal vesicle invasion was detected in two patients. The positive predictive value of mpMRI to detect prostate cancer was 98 %, 98 %, and 100 % in the overall prostate, peripheral zone, and central gland, respectively. The sensitivity of MRI sequences was higher for tumors larger than 5 mm in diameter as well as for those with higher Gleason scores (greater than 7, $p < 0.05$) [63].

In prior studies to correct the mismatches between MRI and histopathology, several methods have been proposed. Scheidler et al. considered tumor sites detected on MRI and histopathology if they were in the same sextant within a range of 1 section (±3 to 4 mm craniocaudally) provided that they were in the same anterior or posterior prostatic hemisphere [64]. Villers et al. matched MRI with histopathology based on anatomical landmarks such as gland contours [65]. Other groups accepted a distance of 8 mm to 10 mm (approximately 2 sections) as evidence of a match between MRI and histopathology [66, 67].

Russo et al. presented results of 115 patients with biopsy-confirmed prostate cancer who

underwent mpMRI before radical prostatectomy [68]. Stained whole-mount histological sections were used as the reference standard. All lesions were contoured by an experienced uropathologist who assessed their volume and pathological Gleason score. All lesions with a volume of >0.5 ml and/or pathological Gleason score of > 6 were defined as clinically significant prostate cancer. In all, 104 of 115 index lesions were correctly diagnosed by mpMRI with sensitivity—90.4 % and 95 % confidence interval (CI) 83.5–95.1 %, including 98/105 clinically significant index lesions (93.3 %; 95 % CI 86.8–97.3 %), among which 3 of 3 lesions had a volume of <0.5 ml and Gleason score of >6. Overall, mpMRI detected 131/206 lesions, including 13 of 68 "insignificant" prostate cancers (Table 7.2) [68]. The multivariate logistic regression modeling showed that pathological Gleason score (odds ratio [OR] 11.7, 95 % CI 2.3–59.8; $P = 0.003$) and lesion volume (OR 4.24, 95 % CI 1.3–14.7; $P = 0.022$) were independently associated with the detection of index lesions at MRI.

In conclusion, fusion MRI/TRUS-targeted biopsy:

- Improves the cancer detection rate, especially Gleason score high-grade ≥7 tumors, but does not replace systematic biopsy making it complimentary.
- Undergrades 20–30 % of tumors particularly those with tertiary pattern grade.
- Misses (false-negative result) up to 30 % of clinically significant cancer lesions.
- Overall, mpMRI detects 80 % of index and 50 % of all prostate cancers.
- Significantly underestimates tumor diameter and volume for apex-base (longitudinal) dimension more than anterior-posterior and left-right (axial) dimension with large standard deviation that cannot predict in individual cases an actual tumor location.
- To date, results of fusion biopsy with spatial distribution of PCa are not reliable to plan a focal targeted therapy in case of switching patients from AS toward interventional therapy.

Ultimately, we believe that the 3DBiopsy™ System (3DBiopsy, Inc.) can potentially overcome the limitations of fusion biopsy.

There are several studies in the literature comparing the accuracy of transrectal and transperineal biopsy with computer simulation on reconstructed 3D computer models of radical whole-mount specimens [69]. Hu et al. determined the effectiveness of two sampling strategies: repeat TRUS biopsy and transperineal template-guided mapping biopsy (TTMB) to detect and exclude lesions of ≥0.2 ml or ≥0.5 ml [70].

Table 7.2 Per-index lesion sensitivity of mp-MRI according to pathological Gleason score and location

Sensitivity, % (*n/N*)					
	Gleason score ≤6	Gleason score 3+4	Gleason score 4+3	Gleason score ≥8	Total
All lesions					
PZ	28.1 (18/64)	85.1 (63/74)	100 (22/22)	93.7 (15/16)	67 (118/176)
TZ	30 (6/20)	71.4 (5/7)	50 (1/2)	100 (1/1)	43.3 (13/30)
Total	28.6 (24/84)	83.9 (68/81)	95.8 (23/24)	94.1 (16/17)	63.6 (131/206)
Clinically significant lesions (>0.5 ml or ≤0.5 ml and Gleason score ≥7)					
PZ	70 (7/10)	85.1 (63/74)	100 (22/22)	93.7 (15/16)	87.7 (107/122)
TZ	66.6 (4/6)	71.4 (5/7)	50 (1/2)	100 (1/1)	68.8 (11/16)
Total	68.7 (11/16)	83.9 (68/81)	95.8 (23/24)	94.1 (16/17)	85.5 (118/138)

Data are percentages, numerators indicate the number of detected lesions, and denominators represent the total number of lesions

PZ peripheral zone, *TZ* transitional zone

Reprinted with permission from Russo F, Regge D, Armando E, Giannini V, Vignati A, Mazzetti S, et al. Detection of prostate cancer index lesions with multiparametric magnetic resonance imaging (mp-mri) using whole-mount histological sections as the reference standard. BJU Int. 2016 Jul;118(1):84–94 [68]

In 107 consecutive cases that were analyzed with TTMB and five different TRUS biopsy strategies that were simulated, the latter involved a standard 12-core sampling and incorporated variable amounts of error, as well as the addition of anterior cores ≥0.5 ml. Overall, TTMB accuracy (AUC) was ≈0.90 compared with AUC 0.70–0.80 for TRUS biopsy. In addition, at best, TRUS biopsy missed 30–40 % of lesions of ≥0.2 ml and ≥0.5 ml, while TTMB missed 5 % of such lesions.

Muthuveloe et al. conducted a prospective study of 200 consecutive men who underwent template biopsy in a tertiary referral center, using a standard 24-region template prostate biopsy technique [71]. Overall detection rate was 47 %; 39.5 % of cases with previous negative transrectal biopsies were found to have prostate adenocarcinoma; and 47.5 % of cases on AS for Gleason 3+3 = 6 prostate adenocarcinoma were upgraded. The authors concluded that those considering AS for Gleason 3+3 = 6 disease should be offered template biopsy to confirm the grade of their disease.

Ayres et al. evaluated the role of TTMB in 101 men on active surveillance at a single center [72]. Criteria for active surveillance were ≤75 years, Gleason ≤3+3, PSA ≤ 15 ng/ml, clinical stage T1–2a, and ≤50 % TRUS guided transrectal biopsy cores positive for cancer with ≤10 mm of disease in a single core. The number of men with an increase in disease volume or Gleason grade on TTMB and the number of men who later underwent radical treatment were assessed. In all, 34 % of men had more significant prostate cancer on restaging transperineal template biopsies compared with their transrectal biopsies. Of these men, 44 % had disease predominantly in the anterior part of the gland, an area often undersampled by transrectal biopsies. In the group of men who had restaging TTMB within 6 months of commencing active surveillance, 38 % had more significant disease. In total, 33 % of men stopped active surveillance and had radical treatment. In conclusion, around one-third of men had more significant prostate cancer on TTMB. This probably reflects under-sampling by initial transrectal biopsies rather than disease progression.

Crawford et al. correlated the clinical-pathologic results of 1403 TTMB cores obtained from 25 men diagnosed with PCa with 64 cancer lesions found in their corresponding RP specimens [73]. Special computer models of 3D whole-mounted radical prostatectomy (3D–WMRP) specimens were generated and used as a gold standard to determine tumor morphometric data. Between-sample rates of upgrade and downgrade (highest GS and a novel cumulative GS) and upstage and downstage (laterality) were determined. Lesions ≥0.5 cm^3 or GS ≥ 7 were considered clinically significant. From 64 separate 3D–WMRP lesions, 25 had significant volume (mean 1.13 cm^3) and 39 were insignificant (mean 0.09 cm^3) ($P < 0.0001$); 18/64 lesions were missed by TTMB, but only 1 was clinically significant with GS-8 (0.02 cm^3). When comparing the cumulative GS of TTMB versus RP, 72 % ($n = 18$) had identical scores, 12 % ($n = 3$) were upgraded, and only 16 % ($n = 4$) were downgraded. Laterality of TTMB and RP was strongly correlated, 80 % same laterality, 4 % were upstaged, and 16 % downstaged. Finally, they demonstrated that TTMB using a 5 mm sampling frame had 95 % sensitivity and 30 % specificity to detect 0.5 ml lesions.

A number of clinical studies have shown that TTMB detects more cancer, identifies bilateral disease in men thought to have unilateral cancer, upgrades disease in approximately a third of patients, and provides localization information on individual lesions [72, 74, 75]. As a result, TTMB could be used to select men for active surveillance or focal therapy. This may decrease the 30–40 % delayed intervention rate currently seen in active surveillance cohorts and decrease the need for intensive biopsy surveillance.

The technique of TTMB is evolving to improve the outcomes of its diagnostic accuracy. Barzell and Melamed assessed 80 patients, in whom focal cryoablation was planned, with both TTMB and TRUS biopsy [76]. In their study, 47 % of patients found suitable by TRUS biopsy for focal therapy actually had high-risk cancer in TTMB. However, the technique used in that study is different from the present definition for mapping biopsy, and, according to the Ginsburg Study Group, Barzell's technique might be

termed as "transperineal template-guided saturation biopsy." Onik and Barzell used the Crawford model of TTMB to carry out mapping biopsy in 110 patients with TRUS biopsy-proven unilateral disease. They showed that TTMB found bilateral disease in 55 % and Gleason upgrading in 25 % of patients.

Sivaraman et al. carried out volume-based TTMB in 98 patients with low-risk PCa diagnosed by TRUS biopsy and found that 30.6 % of the patients were upstaged/upgraded (9.2 % had bilateral disease, 16.3 % had Gleason upgrade, and 5.1 % had both) [77]. According to present evidence, the cancer detection rate of TTMB after initial negative TRUS biopsy is 46–68 %. Diagnostic performance of TTMB in the initial biopsy setting is 73–76 %, which is superior to all the diagnostic modalities used for PCa to date. These data reflect the superior results of TTMB in detecting, grading, and mapping of PCa as compared with TRUS biopsy.

The results of TTMB are very encouraging, and it will potentially become an essential tool for the management of PCa. Future studies will broaden the indications of this excellent technique and define the limitations. Considering the exceptional cancer detection rate of TTMB, its use in the primary biopsy setting remains to be seen. However, the cost-benefit ratio of the procedure in this setting will determine the utility. Advances in image-guided mpMRI biopsies have enhanced TRUS biopsy cancer detection. Prebiopsy imaging or real-time image guidance can guide the clinician to cluster more high-quality cores with longer core distance covering a whole length. The differential clustering of cores within the prostate depending on image guidance could culminate in a superior cancer detection rate with exact spatial distribution of prostate cancer. Fusion of imaging with grid sampling will be an interesting advance in PCa diagnosis and can form the basis for future research in prostate biopsy techniques.

The definition of insignificant cancer for TTMB must be revisited and redefined. These attributes can potentially overcome most of the shortcomings of the present biopsy techniques. Huo et al., in their retrospective diagnostic accuracy study, compared the results of primary transperineal biopsies with the radical prostatectomy pathology of 414 consecutive patients treated at a single institution [78]. The average sensitivity and specificity for the detection of cancer in all prostates across all biopsy zones was 48 % (95 % CI 42.6–53.4) and 84.1 % (95 % CI 80–88.2), respectively. Interestingly, there was a statistically significant decrease in the sensitivity of transperineal biopsy in larger prostates. Grading concordance between biopsy and pathology specimens was achieved in 65.7 % of patients. Upgrading of Gleason scores occurred in 25.6 % of patients and downgrading occurred in 8.8 %. Thus, their transperineal biopsy method has demonstrated fair agreement with the histopathology findings of the corresponding radical prostatectomy specimens. The cancer detection rate was lower in larger prostates, suggesting an increase in the number of cores in larger prostates as a strategy to improve cancer detection.

A few randomized studies demonstrated that combined biopsy approach (fusion MRI/TRUS-targeted biopsy and transperineal multicore mapping biopsy) detects more significant PCa than fusion MRI/TRUS-targeted biopsy alone; however, it will double the detection rate of insignificant PCa [69]. For instance, Ting et al. performed a head-to-head comparison of 48 patients who underwent MRI/TRUS-targeted biopsy (TBx) and 80 patients underwent combined MRI/TRUS-targeted biopsy plus 24-core saturation TTMB [79]. In the MRI/TRUS-targeted biopsy versus combined biopsy strategy subgroup analysis ($n = 80$), there were 55 PCa and 38 significant PCa. The detection rate for the combined biopsy strategy versus MRI/TRUS-TBx for significant PCa was 49 % versus 40 % ($p = 0.02$) and for insignificant PCa was 20 % versus 10 % ($p = 0.04$), respectively. Eleven cases (14 %) of significant PCa were detected exclusively on MRI/TRUS-TBx and 7 cases (8.7 %) of significant PCa were detected exclusively on TTMB.

Radtke et al. reported a comparative analysis of 294 consecutive patients undergoing systematic transperineal biopsy and MRI/TRUS fusion TBx [80]. The authors reported that sampling efficiency was in favor of the second method,

with 46.0 % of MRI/TRUS fusion TB vs. 7.5 % of systematic biopsy cores detecting PCa with a Gleason score >7. However, there was still utility to perform systematic transperineal sampling, as 12.8 % Gleason score >7 were missed by the targeted approach. The opposite occurred in 20.9 %. The authors concluded that the gold standard for cancer detection is a combination of systematic and targeted cores.

In a recent review of the literature, Toner et al. demonstrated that mpMRI has an increasing role for PCa diagnosis, staging, and directing management toward improving patient outcomes [81]. Compared with radical prostatectomy RP and TTMB specimens, the sensitivity and specificity of mpMRI reported in the literature are approximately 80–90 % and 50–90 % (Table 7.3 [82–88] and Table 7.4 [82, 89–92]).

The Safety Margin of Focal Ablation Based on Concordance Between Baseline Multiparametric Magnetic Resonance Imaging and Final Pathology Assessment

Ideally, FT will completely treat all histologic malignancy, not just what is visible on imaging. At University of California, Los Angeles (UCLA), Priester et al. demonstrated that MRI consistently underestimates the size and extent of prostate tumors [93]. The study examined 114 men who had mpMRI before radical prostatectomy with patient-specific mold processing of the specimen. T2-weighted images were used to contour the prostate capsule and cancer-suspicious regions of interest (ROIs). The contours were used to design and 3D-print custom molds, which permitted alignment of excised prostates with MR images. Tumors were reconstructed in 3D from digitized whole-mount sections. Tumors were then matched with ROIs and their relative geometries were compared. At final pathology assessment, 222 tumors were evident on whole-mount sections, 118 of which had been identified on MRI. For the 118 ROIs, the mean volume was 0.8 cc and the longest 3D diameter was 17 mm. However, for matched pathologic tumors, most of which were GS ≥3+4, the mean volume was 2.5 cc and the longest 3D diameter was 28 mm. The median tumor had a 13.5 mm maximal extent beyond the MRI contour, and 80 % of cancer volume from matched tumors was outside of ROI boundaries. Size estimation was most accurate in the axial plane and least accurate along the base-apex axis. Prostate cancer foci had an average diameter 11 mm longer and a volume 3 times greater than T2-weighted MRI segmentations. These results may have important implications for improving accuracy, especially along the base-apex axis.

Table 7.3 Comparison data of multiparametric magnetic resonance imaging (mpMRI) with radical prostatectomy as a reference standard

Reference	*N*	Sensitivity (%)	Specificity (%)	NPV	PPV	Definition of significant PCa
Thompson et al. [82]	48	98	43	75	91	GS ≥ 7, GS = 6 CL ≥ 5 mm or 20 % cores positive
Chamie et al. [83]	115	96	46	92	66	pT3, GS ≥ 4+3, GS = 3+4 and ≥1.3 ml
Junker et al. [84]	50	97	79	NR	NR	Any PCa
Hoeks et al. [85]	63	65	67	NR	NR	Any PCa
Delongchamps et al. [86]	57	78	97	NR	NR	Any PCa
Yoschizako et al. [87]	35	69	94	NR	95	Any PCa
Villers et al. [88]	24	77	91	NR	NR	Any PCa

N number of radical prostatectomies, *NPV* negative predictive value, *PPV* positive predictive value, *PCa* prostate cancer, *GS* Gleason score, *CL* core length

Table 7.4 Comparison of multiparametric magnetic resonance imaging (mpMRI) with transperineal mapping biopsy (TPMB) as a reference control

Reference	*N*	Sensitivity (%)	Specificity (%)	NPV	PPV	Definition of significant PCa	Number of cores	Reporting system
Pepe et al. [89]	168	83	72	88	79	NR	6–35, median 28	NR
Thompson et al. [82]	150	93	53	52	98	GS ≥ 7, GS = 6 CL ≥ 5 mm or 20 % cores positive	median 30, two targeted	PI-RADS
Grey et al. [90]	201	97	60	98	49, 58, 84[a]	GS ≥ 7, GS = 6 CL ≥ 6 mm	24–40, two to four targeted	PI-RADS
Abd- Alazeez et al. [91]	54	90, 76	42, 42	95, 79	26, 38	UCL 1, UCL 2[b]	Minimum 10–12	PI-RADS
Arumainayagam et al. [92]	64	64–81, 58–73[c]	68–80, 71–83[c]	91–94, 84–89[c]	35–45, 49–63[c]	UCL 1, UCL 2[b]	29–41, median 34	Likert

N number of patients, *NPV* negative predictive value, *PPV* positive predictive value, *PCa* prostate cancer, *GS* Gleason score, *CL* core length, *PI-RADS* Prostate Imaging Reporting and Data System, *UCL* University College London

[a]PPV for PI-RADS 3, 4, and 5, respectively

[b]UCL 1, Gleason score of over 4+3 and/or maximum cancer core length (CCL_{max}) of 6 mm or more; UCL 2, Gleason score of 3+4 or more and/or CCL_{max} of 4 mm or more

[c]Range from different radiologists

The latest report of this group updated results showing an index PCa detection rate by mpMRI in 224 of 285 (78.6 %) tumors validated by whole-mount histopathology (WMHP) (Carroll P. Personal communication, 2016). The median maximal diameter of PCa index tumors on mpMRI was 1.3 cm while on WMHP measured as 2.0 cm with poor Pearson correlation coefficient of 0.45 ($p < 0.05$).

Le Nobin et al. examined the accuracy of 3 Tesla MRI before prostatectomy in 33 patients [11]. Concordance was conducted between lesion borders traced by a radiologist on MRI images and MRI and 3D reconstructions created from high-resolution digitalized slides of radical prostatectomy specimens and co-registered to imaging using advanced software. Tumors were compared between histology and imaging by the Hausdorff distance and stratified by the MRI suspicion score, Gleason score, and lesion diameter. The results showed a boundary underestimation in larger lesions with an imaging suspicion score 4 or greater (mean 3.49 ± 2.1 mm, $p < 0.001$) and a Gleason score of 7 or greater (mean 2.48 ± 2.8 mm, $p = 0.035$). A simulated treatment volume based on the MRI boundary missed an average 14.8 % of tumor volume compared to that based on the histological boundary (Fig. 7.6) [11]. Adjustment of simulated treatment volume to a 9 mm treatment margin achieved complete

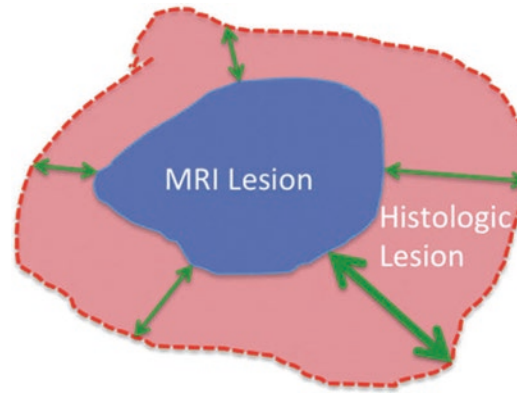

Fig. 7.6 Cartoon reconstruction of MRI-visible lesion (*blue boundary*) within actual histologic lesion (*pink boundary*). Note that the MRI-visible lesion underestimates the true histologic lesion. The *large two-headed arrow* indicates the maximum Hausdorff distance from the center of the lesion. Reprinted with permission from Le Nobin J, Rosenkrantz AB, Villers A, Orczyk C, Deng FM, Melamed J, et al. Image guided focal therapy for magnetic resonance imaging visible prostate cancer: Defining a 3-dimensional treatment margin based on magnetic resonance imaging histology co-registration analysis. J Urol. 2015 Aug;194(2):364–370 [11]

histological tumor destruction in 100 % of patients and should be incorporated into clinical ablation strategies.

Conclusion

The fast-growing implementation of organ-sparing approaches such as AS and FT has gained popularity in today's clinical practice both by patients and physicians alike due to the desire to avoid overtreatment and minimize the potential side effects of incontinence and impotence often associated with whole-gland therapy. The early detection of PCa with the introduction of advanced pathologic and genomics techniques has resulted in more frequent diagnoses of small tumors of lower volume and clinical stage that can be unifocal and/or unilateral, thus supporting the concept of AS and parenchyma-sparing FT. The several novel studies based on unbiased genome-wide approaches coupled with pathologic assessment demonstrated that anatomically distinct tumor metastases are derived from a single progenitor clone. These data of the literature suggest that most commonly the driver lesion with potentially lethal clone is located inside of index focus that gives the bright prospects for focal ablation of this focus with potentially curable intent. However, currently, we still lack a reliable diagnostic tool to rule out an existence of this lethal clone in secondary (satellite) lesion(s) in some cohort of patients.

References

1. Klotz L, Emberton M. Management of low risk prostate cancer: active surveillance and focal therapy. Curr Opin Urol. 2014;24(3):270–9.
2. Polascik TJ, Passoni NM, Villers A, Choyke PL. Modernizing the diagnostic and decision-making pathway for prostate cancer. Clin Cancer Res. 2014;20(24):6254–7.
3. van der Poel H, Klotz L, Andriole G, Azzouzi AR, Bjartell A, Cussenot O, et al. Role of active surveillance and focal therapy in low- and intermediate-risk prostate cancers. World J Urol. 2015;33(7):907–16.
4. Mouraviev V, Villers A, Bostwick DG, Wheeler TM, Montironi R, Polascik TJ. Understanding the pathological features of focality, grade and tumour volume of early-stage prostate cancer as a foundation for parenchyma-sparing prostate cancer therapies: active surveillance and focal targeted therapy. BJU Int. 2011;108(7):1074–85.
5. Muir G. Focal prostate therapy: will we ever know the best energy? BJU Int. 2014;113(1):8.
6. Polascik TJ, Mouraviev V. Focal therapy for prostate cancer is a reasonable treatment option in properly selected patients. Urology. 2009;74(4):726–30.
7. Sartor AO, Hricak H, Wheeler TM, Coleman J, Penson DF, Carroll PR, et al. Evaluating localized prostate cancer and identifying candidates for focal therapy. Urology. 2008;72(6 Suppl):S12–24.
8. Schmidt C. Focal therapy gains ground in low-risk prostate cancer. J Natl Cancer Inst. 2015;107(9).
9. Polascik TJ. Focal therapy of prostate cancer: making steady progress toward a first-line image-guided treatment modality. Curr Opin Urol. 2015;25(3):183–4.
10. Mendez MH, Joh DY, Gupta R, Polascik TJ. Current trends and new frontiers in focal therapy for localized prostate cancer. Curr Urol Rep. 2015;16(6):35.
11. Le Nobin J, Rosenkrantz AB, Villers A, Orczyk C, Deng FM, Melamed J, et al. Image guided focal therapy for magnetic resonance imaging visible prostate cancer: defining a 3-dimensional treatment margin based on magnetic resonance imaging histology co-registration analysis. J Urol. 2015;194(2):364–70.
12. Haffner MC, De Marzo AM, Yegnasubramanian S, Epstein JI, Carter HB. Diagnostic challenges of clonal heterogeneity in prostate cancer. J Clin Oncol. 2015;33(7):e38–40.
13. Liu W, Laitinen S, Khan S, Vihinen M, Kowalski J, Yu G, et al. Copy number analysis indicates monoclonal origin of lethal metastatic prostate cancer. Nat Med. 2009;15(5):559–65.
14. Mehra R, Tomlins SA, Yu J, Cao X, Wang L, Menon A, et al. Characterization of tmprss2-ets gene aberrations in androgen-independent metastatic prostate cancer. Cancer Res. 2008;68(10):3584–90.
15. Aryee MJ, Liu W, Engelmann JC, Nuhn P, Gurel M, Haffner MC, et al. DNA methylation alterations exhibit intraindividual stability and interindividual heterogeneity in prostate cancer metastases. Sci Transl Med. 2013;5(169):169ra110.
16. Postema AW, De Reijke TM, Ukimura O, Van den Bos W, Azzouzi AR, Barret E, et al. Standardization of definitions in focal therapy of prostate cancer: report from a delphi consensus project. World J Urol. 2016;34(10):1373–82.
17. Valerio M, Ahmed HU, Emberton M, Lawrentschuk N, Lazzeri M, Montironi R, et al. The role of focal therapy in the management of localised prostate cancer: a systematic review. Eur Urol. 2014;66(4):732–51.
18. Valerio M, Emberton M, Ahmed HU. Focal therapy will become a standard option for selected men with localized prostate cancer. J Clin Oncol. 2014;32(32):3680–1.
19. Eggener S, Salomon G, Scardino PT, De la Rosette J, Polascik TJ, Brewster S. Focal therapy for prostate

cancer: possibilities and limitations. Eur Urol. 2010;58(1):57–64.
20. Emberton M. Why focal therapy is a legitimate and necessary response to a changing world. J Urol. 2015;194(4):875–6.
21. Villers A, McNeal JE, Freiha FS, Stamey TA. Multiple cancers in the prostate. Morphologic features of clinically recognized versus incidental tumors. Cancer. 1992;70(9):2313–8.
22. Wolters T, Montironi R, Mazzucchelli R, Scarpelli M, Roobol MJ, van den Bergh RC, et al. Comparison of incidentally detected prostate cancer with screen-detected prostate cancer treated by prostatectomy. Prostate. 2012;72(1):108–15.
23. Masterson TA, Cheng L, Koch MO. Pathological characterization of unifocal prostate cancers in whole-mount radical prostatectomy specimens. BJU Int. 2011;107(10):1587–91.
24. Mouraviev V, Madden JF. Focal therapy for prostate cancer: pathologic basis. Curr Opin Urol. 2009;19(2):161–7.
25. Mouraviev V, Mayes JM, Polascik TJ. Pathologic basis of focal therapy for early-stage prostate cancer. Nat Rev Urol. 2009;6(4):205–15.
26. Karavitakis M, Ahmed HU, Abel PD, Hazell S, Winkler MH. Tumor focality in prostate cancer: implications for focal therapy. Nat Rev Clin Oncol. 2011;8(1):48–55.
27. Karavitakis M, Winkler M, Abel P, Livni N, Beckley I, Ahmed HU. Histological characteristics of the index lesion in whole-mount radical prostatectomy specimens: implications for focal therapy. Prostate Cancer Prostatic Dis. 2011;14(1):46–52.
28. Huang CC, Deng FM, Kong MX, Ren Q, Melamed J, Zhou M. Re-evaluating the concept of "dominant/index tumor nodule" in multifocal prostate cancer. Virchows Arch. 2014;464(5):589–94.
29. Mizuno R, Nakashima J, Mukai M, Ookita H, Nakagawa K, Oya M, et al. Maximum tumor diameter is a simple and valuable index associated with the local extent of disease in clinically localized prostate cancer. Int J Urol. 2006;13(7):951–5.
30. Ding Z, Wu CJ, Chu GC, Xiao Y, Ho D, Zhang J, et al. Smad4-dependent barrier constrains prostate cancer growth and metastatic progression. Nature. 2011;470(7333):269–73.
31. Ahmed HU. The index lesion and the origin of prostate cancer. N Engl J Med. 2009;361(17):1704–6.
32. Noguchi M, Stamey TA, McNeal JE, Nolley R. Prognostic factors for multifocal prostate cancer in radical prostatectomy specimens: lack of significance of secondary cancers. J Urol. 2003;170(2 Pt 1):459–63.
33. Haffner J, Potiron E, Bouye S, Puech P, Leroy X, Lemaitre L, et al. Peripheral zone prostate cancers: location and intraprostatic patterns of spread at histopathology. Prostate. 2009;69(3):276–82.
34. Algaba F, Montironi R. Impact of prostate cancer multifocality on its biology and treatment. J Endourol. 2010;24(5):799–804.
35. Arora R, Koch MO, Eble JN, Ulbright TM, Li L, Cheng L. Heterogeneity of gleason grade in multifocal adenocarcinoma of the prostate. Cancer. 2004;100(11):2362–6.
36. Andreoiu M, Cheng L. Multifocal prostate cancer: biologic, prognostic, and therapeutic implications. Hum Pathol. 2010;41(6):781–93.
37. Mai KT, Roustan Delatour NL, Assiri A, Al-Maghrabi H. Secondary prostatic adenocarcinoma: a cytopathological study of 50 cases. Diagn Cytopathol. 2007;35(2):91–5.
38. Barbieri CE, Demichelis F, Rubin MA. The lethal clone in prostate cancer: Redefining the index. Eur Urol. 2014;66(3):395–7.
39. Haffner MC, Mosbruger T, Esopi DM, Fedor H, Heaphy CM, Walker DA, et al. Tracking the clonal origin of lethal prostate cancer. J Clin Invest. 2013;123(11):4918–22.
40. Kumar A, White TA, MacKenzie AP, Clegg N, Lee C, Dumpit RF, et al. Exome sequencing identifies a spectrum of mutation frequencies in advanced and lethal prostate cancers. Proc Natl Acad Sci U S A. 2011;108(41):17087–92.
41. Grasso CS, Wu YM, Robinson DR, Cao X, Dhanasekaran SM, Khan AP, et al. The mutational landscape of lethal castration-resistant prostate cancer. Nature. 2012;487(7406):239–43.
42. Barbieri CE, Baca SC, Lawrence MS, Demichelis F, Blattner M, Theurillat JP, et al. Exome sequencing identifies recurrent spop, foxa1 and med12 mutations in prostate cancer. Nat Genet. 2012;44(6):685–9.
43. Fraser M, Berlin A, Bristow RG, van der Kwast T. Genomic, pathological, and clinical heterogeneity as drivers of personalized medicine in prostate cancer. Urol Oncol. 2015;33(2):85–94.
44. Bostwick DG, Shan A, Qian J, Darson M, Maihle NJ, Jenkins RB, et al. Independent origin of multiple foci of prostatic intraepithelial neoplasia: comparison with matched foci of prostate carcinoma. Cancer. 1998;83(9):1995–2002.
45. Djavan B, Susani M, Bursa B, Basharkhah A, Simak R, Marberger M. Predictability and significance of multifocal prostate cancer in the radical prostatectomy specimen. Tech Urol. 1999;5(3):139–42.
46. Ohori M, Kattan M, Scardino PT, Wheeler TM. Radical prostatectomy for carcinoma of the prostate. Mod Pathol. 2004;17(3):349–59.
47. Branca RT, Chen YM, Mouraviev V, Galiana G, Jenista ER, Kumar C, et al. Idqc anisotropy map imaging for tumor tissue characterization in vivo. Magn Reson Med. 2009;61(4):937–43.
48. Mouraviev V, Mayes JM, Sun L, Madden JF, Moul JW, Polascik TJ. Prostate cancer laterality as a rationale of focal ablative therapy for the treatment of clinically localized prostate cancer. Cancer. 2007;110(4):906–10.
49. Yoon GS, Wang W, Osunkoya AO, Lane Z, Partin AW, Epstein JI. Residual tumor potentially left behind after local ablation therapy in prostate adenocarcinoma. J Urol. 2008;179(6):2203–6. discussion 2206

50. Bott SR, Ahmed HU, Hindley RG, Abdul-Rahman A, Freeman A, Emberton M. The index lesion and focal therapy: an analysis of the pathological characteristics of prostate cancer. BJU Int. 2010;106(11):1607–11.
51. Ahmed HU, Freeman A, Kirkham A, Sahu M, Scott R, Allen C, et al. Focal therapy for localized prostate cancer: a phase I/II trial. J Urol. 2011;185(4):1246–54.
52. Epstein JI, Egevad L, Humphrey PA, Montironi R. Members of the IIiDUPG. Best practices recommendations in the application of immunohistochemistry in the prostate: report from the international society of urologic pathology consensus conference. Am J Surg Pathol. 2014;38(8):e6–e19.
53. Van der Kwast T. Gleason score 7: when qualitative change becomes quantitative change. J Urol. 2016;196(2):303–4.
54. Tollefson MK, Leibovich BC, Slezak JM, Zincke H, Blute ML. Long-term prognostic significance of primary Gleason pattern in patients with Gleason score 7 prostate cancer: impact on prostate cancer specific survival. J Urol. 2006;175(2):547–51.
55. Burdick MJ, Reddy CA, Ulchaker J, Angermeier K, Altman A, Chehade N, et al. Comparison of biochemical relapse-free survival between primary Gleason score 3 and primary Gleason score 4 for biopsy Gleason score 7 prostate cancer. Int J Radiat Oncol Biol Phys. 2009;73(5):1439–45.
56. Stark JR, Perner S, Stampfer MJ, Sinnott JA, Finn S, Eisenstein AS, et al. Gleason score and lethal prostate cancer: Does 3+4=4+3? J Clin Oncol. 2009;27(21):3459–64.
57. Ohori M, Scardino PT. Localized prostate cancer. Curr Probl Surg. 2002;39(9):833–957.
58. Weinreb JC, Barentsz JO, Choyke PL, Cornud F, Haider MA, Macura KJ, et al. PI-RADS prostate imaging – reporting and data system: 2015, version 2. Eur Urol. 2016;69(1):16–40.
59. Bouye S, Potiron E, Puech P, Leroy X, Lemaitre L, Villers A. Transition zone and anterior stromal prostate cancers: zone of origin and intraprostatic patterns of spread at histopathology. Prostate. 2009;69(1):105–13.
60. Nevoux P, Ouzzane A, Ahmed HU, Emberton M, Montironi R, Presti Jr JC, et al. Quantitative tissue analyses of prostate cancer foci in an unselected cystoprostatectomy series. BJU Int. 2012;110(4):517–23.
61. Siddiqui MM, Truong H, Rais-Bahrami S, Stamatakis L, Logan J, Walton-Diaz A, et al. Clinical implications of a multiparametric magnetic resonance imaging based nomogram applied to prostate cancer active surveillance. J Urol. 2015;193(6):1943–9.
62. Trivedi H, Turkbey B, Rastinehad AR, Benjamin CJ, Bernardo M, Pohida T, et al. Use of patient-specific MRI-based prostate mold for validation of multiparametric MRI in localization of prostate cancer. Urology. 2012;79(1):233–9.
63. Turkbey B, Mani H, Aras O, Rastinehad AR, Shah V, Bernardo M, et al. Correlation of magnetic resonance imaging tumor volume with histopathology. J Urol. 2012;188(4):1157–63.
64. Scheidler J, Weores I, Brinkschmidt C, Zeitler H, Panzer S, Scharf M, et al. Diagnosis of prostate cancer in patients with persistently elevated psa and tumor-negative biopsy in ambulatory care: performance of mr imaging in a multi-reader environment. Rofo. 2012;184(2):130–5.
65. Villers A, Lemaitre L, Haffner J, Puech P. Current status of mri for the diagnosis, staging and prognosis of prostate cancer: implications for focal therapy and active surveillance. Curr Opin Urol. 2009;19(3):274–82.
66. Eymerit-Morin C, Zidane M, Lebdai S, Triau S, Azzouzi AR, Rousselet MC. Histopathology of prostate tissue after vascular-targeted photodynamic therapy for localized prostate cancer. Virchows Arch. 2013;463(4):547–52.
67. Montironi R, Egevad L, Bjartell A, Berney DM. Role of histopathology and molecular markers in the active surveillance of prostate cancer. Acta Oncol. 2011;50(Suppl 1):56–60.
68. Russo F, Regge D, Armando E, Giannini V, Vignati A, Mazzetti S, et al. Detection of prostate cancer index lesions with multiparametric magnetic resonance imaging (MP-MRI) using whole-mount histological sections as the reference standard. BJU Int. 2016;118(1):84–94.
69. Sivaraman A, Sanchez-Salas R, Barret E, Ahallal Y, Rozet F, Galiano M, et al. Transperineal template-guided mapping biopsy of the prostate. Int J Urol. 2015;22(2):146–51.
70. Hu JC, Chang E, Natarajan S, Margolis DJ, Macairan M, Lieu P, et al. Targeted prostate biopsy in select men for active surveillance: do the Epstein criteria still apply? J Urol. 2014;192(2):385–90.
71. Muthuveloe D, Telford R, Viney R, Patel P. The detection and upgrade rates of prostate adenocarcinoma following transperineal template-guided prostate biopsy – a tertiary referral centre experience. Cent European J Urol. 2016;69(1):42–7.
72. Ayres BE, Montgomery BS, Barber NJ, Pereira N, Langley SE, Denham P, et al. The role of transperineal template prostate biopsies in restaging men with prostate cancer managed by active surveillance. BJU Int. 2012;109(8):1170–6.
73. Crawford ED, Rove KO, Barqawi AB, Maroni PD, Werahera PN, Baer CA, et al. Clinical-pathologic correlation between transperineal mapping biopsies of the prostate and three-dimensional reconstruction of prostatectomy specimens. Prostate. 2013;73(7):778–87.
74. Fernandez Gomez JM, Garcia RJ. Optimization of prostate biopsy in patients considered for active surveillance. The role of the confirmatory biopsy and transperineal techniques. Arch Esp Urol. 2014;67(5):409–18.
75. Bittner N, Merrick GS, Butler WM, Bennett A, Galbreath RW. Incidence and pathological features of prostate cancer detected on transperineal template guided mapping biopsy after negative transrectal ultrasound guided biopsy. J Urol. 2013;190(2):509–14.

76. Barzell WE, Melamed MR. Appropriate patient selection in the focal treatment of prostate cancer: the role of transperineal 3-dimensional pathologic mapping of the prostate–a 4-year experience. Urology. 2007;70(6 Suppl):27–35.
77. Sivaraman A, Sanchez-Salas R, Ahmed HU, Barret E, Cathala N, Mombet A, et al. Clinical utility of transperineal template-guided mapping biopsy of the prostate after negative magnetic resonance imaging-guided transrectal biopsy. Urol Oncol. 2015;33(7):329 e327–311.
78. Huo AS, Hossack T, Symons JL, PeBenito R, Delprado WJ, Brenner P, et al. Accuracy of primary systematic template guided transperineal biopsy of the prostate for locating prostate cancer: a comparison with radical prostatectomy specimens. J Urol. 2012;187(6):2044–9.
79. Ting F, van Leeuwen PJ, Delprado W, Haynes AM, Brenner P, Stricker PD. Tumor volume in insignificant prostate cancer: increasing the threshold is a safe approach to reduce over-treatment. Prostate. 2015;75(15):1768–73.
80. Radtke JP, Kuru TH, Boxler S, Alt CD, Popeneciu IV, Huettenbrink C, et al. Comparative analysis of transperineal template saturation prostate biopsy versus magnetic resonance imaging targeted biopsy with magnetic resonance imaging-ultrasound fusion guidance. J Urol. 2015;193(1):87–94.
81. Toner L, Weerakoon M, Bolton DM, Ryan A, Katelaris N, Lawrentschuk N. Magnetic resonance imaging for prostate cancer: comparative studies including radical prostatectomy specimens and template transperineal biopsy. Prostate Int. 2015;3(4):107–14.
82. Thompson JE, Moses D, Shnier R, Brenner P, Delprado W, Ponsky L, et al. Multiparametric magnetic resonance imaging guided diagnostic biopsy detects significant prostate cancer and could reduce unnecessary biopsies and over detection: a prospective study. J Urol. 2014;192(1):67–74.
83. Chamie K, Sonn GA, Finley DS, Tan N, Margolis DJ, Raman SS, et al. The role of magnetic resonance imaging in delineating clinically significant prostate cancer. Urology. 2014;83(2):369–75.
84. Junker D, Quentin M, Nagele U, Edlinger M, Richenberg J, Schaefer G, et al. Evaluation of the pirads scoring system for mpmri of the prostate: a whole-mount step-section analysis. World J Urol. 2015;33(7):1023–30.
85. Hoeks CM, Hambrock T, Yakar D, van de Hulsbergen-Kaa CA, Feuth T, Witjes JA, et al. Transition zone prostate cancer: detection and localization with 3-t multiparametric mr imaging. Radiology. 2013;266(1):207–17.
86. Delongchamps NB, Rouanne M, Flam T, Beuvon F, Liberatore M, Zerbib M, et al. Multiparametric magnetic resonance imaging for the detection and localization of prostate cancer: combination of t2-weighted, dynamic contrast-enhanced and diffusion-weighted imaging. BJU Int. 2011;107(9):1411–8.
87. Yoshizako T, Wada A, Uchida K, Hara S, Igawa M, Kitagaki H, et al. Apparent diffusion coefficient of line scan diffusion image in normal prostate and prostate cancer–comparison with single-shot echo planner image. Magn Reson Imaging. 2011;29(1):106–10.
88. Villers A, Puech P, Mouton D, Leroy X, Ballereau C, Lemaitre L. Dynamic contrast enhanced, pelvic phased array magnetic resonance imaging of localized prostate cancer for predicting tumor volume: correlation with radical prostatectomy findings. J Urol. 2006;176(6 Pt 1):2432–7.
89. Pepe P, Garufi A, Priolo G, Dibenedetto G, Salemi M, Pennisi M, et al. Accuracy of 3 tesla pelvic phased-array multiparametric mri in diagnosing prostate cancer at repeat biopsy. Arch Ital Urol Androl. 2014;86(4):336–9.
90. Grey AD, Chana MS, Popert R, Wolfe K, Liyanage SH, Acher PL. Diagnostic accuracy of magnetic resonance imaging (MRI) prostate imaging reporting and data system (PI-RADS) scoring in a transperineal prostate biopsy setting. BJU Int. 2015;115(5):728–35.
91. Abd-Alazeez M, Ahmed HU, Arya M, Charman SC, Anastasiadis E, Freeman A, et al. The accuracy of multiparametric MRI in men with negative biopsy and elevated PSA level–can it rule out clinically significant prostate cancer? Urol Oncol. 2014;32(1):45 e17–22.
92. Arumainayagam N, Ahmed HU, Moore CM, Freeman A, Allen C, Sohaib SA, et al. Multiparametric mr imaging for detection of clinically significant prostate cancer: a validation cohort study with transperineal template prostate mapping as the reference standard. Radiology. 2013;268(3):761–9.
93. Priester A, Natarajan S, Khoshnoodi P, Margolis DJ, Raman SS, Reiter RE, et al. MRI underestimation of prostate cancer geometry: use of patient-specific molds to correlate images with whole-mount pathology. J Urol. 2016; doi:10.1016/j.juro.2016.07.084.

8 Identifying and Characterizing the Index Lesion

Lina Maria Carmona Echeverria, Hayley Whitaker, and Hashim U. Ahmed

Introduction

Prostate cancer offers distinctive challenges. It can be diagnosed at a very early stage with little impact on the patient's life expectancy, and it can be extremely aggressive causing significant morbidity and mortality. In many other solid organ cancers (i.e., breast, kidney, bladder, thyroid, among others), tissue preservation is widely used, offering disease control and lower morbidity when compared to whole-organ therapy. Considering that traditional whole-gland treatment can cause long-term side effects [1], focal treatment is an attractive alternative that until recently had no place in prostate cancer management.

It is widely known that prostate cancer is multifocal. Certainly, ~80 % of prostate cancers contain more than one focus of disease [2]. However, in other organs in which the field effect concept is accepted, focal management of cancer is achieved along with adjuvant therapy to the remaining tissue (low-dose radiotherapy after wide local excision in breast cancer) and surveillance on a regular basis (mammography for breast cancer and computed tomography [CT] for kidney cancer). Sometimes, as in renal and thyroid tumors, adjuvant whole-gland therapy is not applied. In this chapter we will discuss the clinicopathological implications of multifocal prostate cancer and the role of the index lesion.

Definition of Multifocality

Attention to the definition of prostate cancer multifocality is required since the variability in rates of multifocality might be genuine cohort differences or differences in methodology. For example, in breast cancer in which multifocality is also a common finding (in between 7 % and 95 % of cases), multifocal disease is defined as two or more synchronous ipsilateral neoplasms that are separated by benign tissue in the same quadrant or different quadrants of the breast [3]. Currently, for prostate cancer, no precise definition has been established for focality, and institutional or investigator-specific criteria have been used. For instance, Wise et al. [4] considered a cancer to be spatially separate if it was 3 mm or greater from the closest cancer in any single section or 4 mm or greater from the closest cancer on the adjacent section above or below. Others have defined multifocality as a minimum separation of 4 mm between two malignant foci without further detail as to the distance between these foci on adjacent slides.

L.M.C. Echeverria (✉) • H. Whitaker • H.U. Ahmed
Tissue and Energy, Division of Surgery and Interventional Science, University College London, London, UK
e-mail: l.echeverria@ucl.ac.uk

© Springer International Publishing AG 2017

T.J. Polascik (ed.), *Imaging and Focal Therapy of Early Prostate Cancer*, Current Clinical Urology, DOI 10.1007/978-3-319-49911-6_8

This is clearly dependent on how radical prostatectomy specimens are processed, with different thresholds depending on the thickness of the slides (between 3 mm and 6 mm). Several issues arise from this processing bias. First, the variability between centers affects the definition of multifocality, with reported rates ranging anywhere between 60 % and 90 % [5–14]; therefore, tumors may be wrongly classified as unifocal (see Fig. 8.1), and small tumors may be missed, and this misclassification error would be even higher with thicker sections (>5 mm) as found by Noguchi et al. where 17 % of small cancers are missed when 6 mm step sections are performed [15]. Second, even when complete sectioning is performed, sampling error might occur. It has been estimated that generation of a single 5 μ(mu) m thick section from each 3 mm tissue block required for hematoxylin-eosin staining and microscopic evaluation provides an estimate of only 0.17 % of all embedded tissue [16]. A complete sampling of the prostate would need more than 2500 standard slides to be reviewed [17]. Third, the analysis of multifocality carries a great degree of subjectivity as the tumors are not discrete ovoid shapes but have areas that are solid and some areas that are less distinct. This is what some describe as the "octopus body and tentacles" phenomenon (others have used spiders or crabs for their description).

The Index and Non-index Lesion

The index lesion can be defined as the tumor foci that contains most of the cancer burden (Fig. 8.2); in the majority of cases, its volume ranges between 0.5 and 1.5 cm^3 in volume, and it comprises almost 90 % of the total tumor volume [17–20]. The index lesion is of paramount importance as it has been shown to be an independent predictor of prostate cancer progression along with Gleason grades 4 and 5 and lymphovascular invasion [4]. Indeed, we have previously shown that histopathological features of poor prognosis in the prostate are almost invariably determined by the index lesion [21]. As in other organs, tumor burden must be taken into account, and evidence has shown that tumors

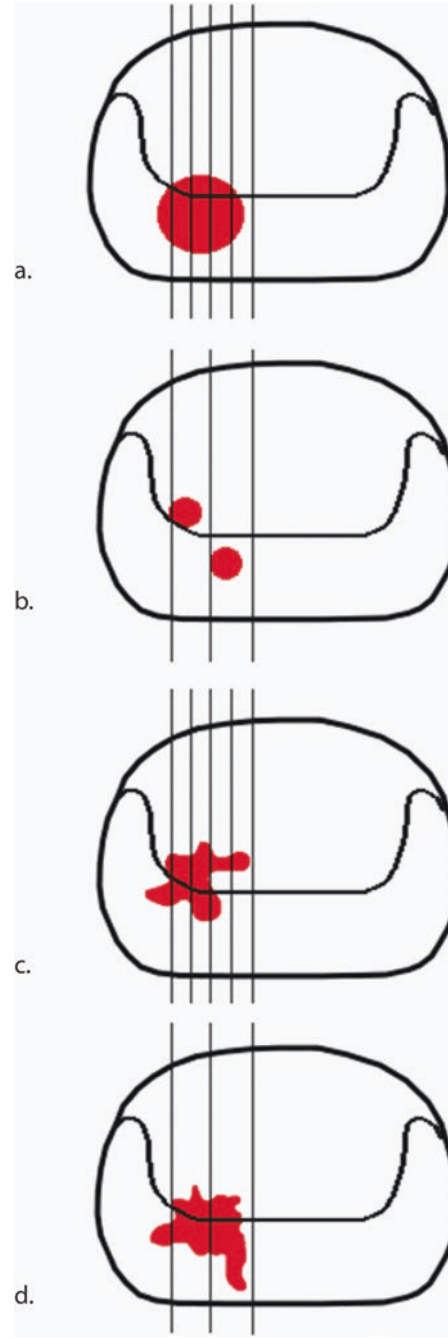

Fig. 8.1 Diagram showing the effect of different slicing techniques in the diagnosis of multifocality in prostate cancer. (**a**) 3 mm slices correctly identifying location and size of a prostate tumor. (**b**) Wider slicing (6 mm) can lead to misdiagnosis as it either misses the 2 lesions or incorrectly diagnoses the tumor as a large nodule. (**c**) 3 mm slicing showing the "octopus body and tentacles" phenomenon where the lesion is not ovoid in shape but rather irregular. (**d**) 6 mm slices would misdiagnose this tumor as it would miss the larger area of cancer

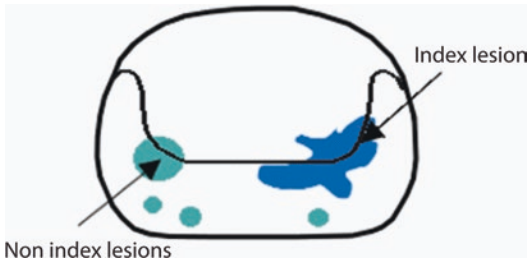

Fig. 8.2 Diagram depicting the index and non-index lesions or satellites. The index lesion is the tumor foci, which contain most of the cancer burden

smaller than 0.5 cm^3 can almost always be classified as insignificant due to their tumor volume doubling times when on active surveillance [22–25]. For instance, one study showed that 79 % of men with previously untreated prostate cancer of all clinical stages who had serial prostate-specific antigen (PSA) determination every 12 months had a PSA doubling time greater than 24 months [26]. Theoretically, lymph node metastasis can be found only when the primary tumor volume is higher than 4 cm^3 [23], and a 0.5 cm^3 cancer would take approximately 12 years to reach 4 cm^3 if its doubling time was 48 months and linear [26].

In addition, studies have shown the correlation between tumor volume and poorer pathological attributes. For instance, lesions ≥0.5 cm^3 have a 1-in-10 chance of capsular invasion, lesions ≥4 cm^3 have a 1-in-10 chance of seminal vesicle invasion, and lesions ≥10 cm^3 have a 1-in-10 chance of metastases [27]. It seems as well that tumor volume is also determinant of grade, as very rarely non-index lesions have Gleason pattern 4 or higher [2]. Mouraviev et al. found that a larger index lesion is associated with fewer satellite lesions, possibly due to the larger lesion integrating the smaller adjacent lesions, as well as a shift toward earlier diagnosis with lower tumor volume burden [19]. Broadly speaking, it has been stipulated that a prostatic lesion is significant when it reaches >0.5 cm^3 in size [22, 28]. Although tumors <0.1 cm^3 are thought to have a low biological potential [22, 29], these small tumors can also exhibit aggressive behavior, and non-index lesions have been found to harbor aggressive potential with extracapsular extension. Ruijter et al. described locally invasive tumors in up to 1-in-4 non-index lesions [30], and Hollman et al. found similar results, although 17 % of lesions with extracapsular extension (ECE) had a volume of >1.0 cm^3 [24].

Certain molecular alterations, such as TMPRSS-ERG gene fusions, have been found in lymph node metastases in concordance with the index lesion, but not on low-grade satellite lesions [31] or secondary high-grade and high-volume lesions [32]. Greene et al. assessed DNA ploidy status, which is an independent prognostic factor for localized prostate cancer. Of 141 separate cancers in 68 patients, the group discerned that 15 % of those 0.01–0.1 cm^3 and 31 % of those 0.1–1.0 cm^3 in volume were non-diploid [33]. This evidence supports the argument that, despite multifocality, prostate cancer disease progression is likely to be related to lesions that meet certain minimal grade and volume thresholds.

Furthermore, Schmidt et al. found men with circulating tumor cells and lymph node metastases in men with lesions of 0.2 cm^3 in volume [34]. Several groups have published data showing such aggressive behavior; in a series of 239 patients with tumor volume less than 0.5 cm^3, investigators demonstrated that 43 were poorly differentiated, 11 had extracapsular extension, 6 had positive surgical margins, 2 had positive lymph nodes, and 7 experienced progression within 5 years [35]. These observations point to the fact that volume alone cannot predict the biological behavior of such lesions and is therefore necessary to take other factors into account. This raises the critical issue that not all index lesions are clinically significant and not all clinically significant lesions are index lesions.

On the issue of clinical significance, it is increasingly clear that Gleason score 6 has very low metastatic potential. In relation to Gleason 6 disease and its biological potential, Eggener et al. demonstrated that of 9775 men who had only Gleason 6 low-risk disease in radical whole-mount prostatectomy specimens, only 3 died of prostate cancer in a 15-year period [36]. Such a small number cannot be fully accounted for by the success of surgery itself, and indeed these cases were found to harbor Gleason pattern 4

upon the second review. Another group showed similar findings with biochemical recurrence in a smaller cohort of men [37]. These clinical findings support the hypothesis that Gleason 6 disease could be considered nonmalignant and perhaps can be safely ignored [38]. Furthermore, Ross et al. reviewed 14,123 cases with initial diagnosis of Gleason ≤6 and found 22 patients with lymph node metastasis [39]. On review of the pathology, 19 of these had higher grade than initially graded (3 were not available for assessment). In conclusion there was not a single case of a Gleason score ≤6 tumor with lymph node metastases. As a result of these data, many [39] are now starting a debate as to whether Gleason 6 cases should be labeled as something other than malignant [38].

Is Multifocal Prostate Cancer Polyclonal or Monoclonal?

Cancerous cells can develop in a monoclonal or polyclonal fashion (Fig. 8.3). The monoclonal hypothesis suggests that a single precursor cell spreads through the prostate with the metastatic malignant cells sharing a common ancestor and therefore exhibiting some common early genetic alterations. A large number of genetic alterations are expressed in human cancers, and the majority of these changes are passenger events [40], which do not initiate cancer, but are a product of cancer evolution. Therefore, it is unlikely that all cancer subclones will harbor the same changes. Boyd et al. hypothesized that malignant cells may spread, giving rise to topographically distinct, yet genetically related tumor foci. They analyzed 48 microdissected cancers and high-grade prostatic intraepithelial neoplasia (HGPIN) foci from 18 cases and performed genome-wide copy-number analysis, finding that all tumors shared a common origin with a high degree of concordance with HGPIN foci [41]. Other researchers have also demonstrated a common cell of origin in metastatic prostate cancer [42, 43]. Lin et al. found that in primary prostate tumors metastatic potential can be confined to a minority of cancer cells. They used pieces of tissue from different foci of

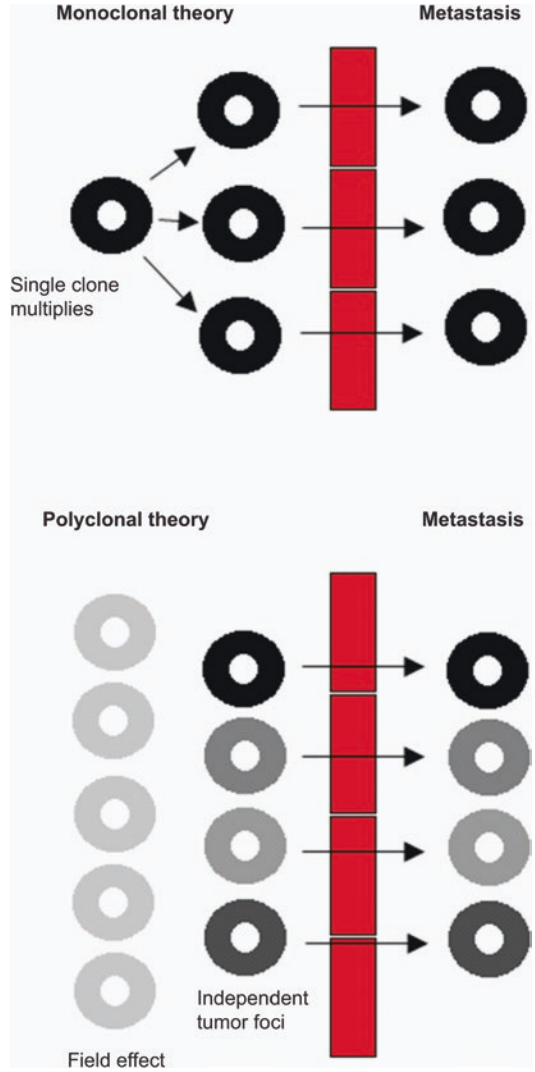

Fig. 8.3 Schematic representation of the monoclonal and polyclonal theory

a patient's primary prostate tumor that were grafted into subrenal capsules of nonobese diabetic/severe combined immunodeficiency (NOD/SCID) mice, and transplantable tumor sublines were established by serial passage. The metastatic ability of each subline was tested via orthotopic grafting into mice [44].

Liu et al. found that prostate cancer metastatic deposits in individual men have a monoclonal origin in most cases through an elegant autopsy study [42]. Although the question of whether the metastatic clone was derived from and situated in

the index lesion was not addressed by the authors, it seems likely that the precursor cells are found in the index lesion, considering the pathological characteristics.

The polyclonal hypothesis on the other side proposes a "field effect" [14] where early molecular changes may stimulate independent development of several tumor foci that will exhibit few similarities in their molecular profile. This proposition is supported by the genetic diversity observed in cancer foci from the same prostate [8, 9, 45–47] and premalignant lesions [14]. TMPRSS2-ERG fusion is detected in HGPIN, indicating it may be an early event [48], with different tumor foci exhibiting discordance in the fusion pattern and status suggesting different clonal origin [49] and intrahomogeneity in individual foci [50]. Nonetheless, the clonal origin of a tumor cell cannot be determined by a single fusion event, and several of the previous studies supporting the polyclonal origin of prostate cancer have studied a limited number of markers [9, 14, 49, 51] that cannot alone rule out the monoclonal hypothesis. Lindberg et al. analyzed intraprostatic tumor heterogeneity using whole-exome sequencing of multiple tumors from the same prostate in four men, targeting 180,000 protein-coding exomes on ten tumor samples [52]. Three patients displayed cancer in multiple foci with no apparent common somatic denominator [52].

New evidence has shown clonal expansions in morphologically normal prostate, providing evidence of a field effect where a background of genetic abnormalities provides a background against which prostate cancer develops [53]. In this study Cooper et al. analyzed three representative ERG mapped prostate cancers and performed parallel DNA sequencing on 12 cancer samples and three morphologically normal prostate areas. Remarkably, mutations were present at high levels in distant benign tissue, with some mutations shared between different ERG lineages indicating early or separate clonal expansions. Based on these findings, focal therapy has a place if normal tissue surrounding prostate cancer is also ablated.

Caution must be advised as so far the evidence regarding the origin of prostate cancer is conflicting. Therefore, one theory does not exclude the other. One proposition is that different patterns of allelic loss among multifocal tumors may simply be the result of clonal divergence after intraluminal spread rather than true oligoclonality [54]. Boutros et al. examined the genomic profile of 74 prostate cancer specimens derived from patients with Gleason 7 disease [55]. They confirmed known abnormalities in several cancer-associated genes such as the MYC oncogene. Those patients with MYC aberrations, specifically of the L-MYC family member, were associated with higher genomic instability. Interestingly, those aberrations may be preferentially localized to the index lesion [55].

It is possible that, at least in some cases, both field effect and monoclonal tumor expansion and intraglandular metastases may coexist. The monoclonal origin of metastatic prostate cancer has given fresh impetus to the idea of focal therapy for the majority of men who have multifocal, bilateral disease in which only the clinically significant lesion might be ablated [56]. Obviously, the concept of cancer that is "biologically unifocal" appears attractive when considering focal therapy. However, the previously mentioned studies underlying the potential clinical significance of satellite lesions suggest that even small secondary foci may require treatment in some patients. Therefore, advocacy of subtotal treatment with the knowledge that smaller secondary foci remain untreated continues to be controversial at present. At the very least, the only way to answer the questions is to set up natural history experiments (focal therapy cohorts) with surveillance strategies incorporating the fact that some untreated areas will show progression or de novo development of new lesions.

What Is the Clinical Significance of Multifocality?

While a small secondary lesion might be clinically insignificant, multifocality per se may constitute a surrogate prognostic factor independent of the volume of the index and secondary tumors. The presence of multiple tumors within the same

gland may reflect genetic instability that allows for accelerated disease progression. Rice et al. found that patients with a single focus adenocarcinoma had statistically higher rates of positive surgical margins, Gleason score 8–10 disease, and biochemical recurrence than those who had multifocal disease [57]. In an autopsy study of 264 prostates from men who died of diseases other than prostate cancer, another group found no significant difference with respect to total tumor volume, capsular penetration, and perineural or vascular invasion of multifocal compared with unifocal tumors [58].

In addition, several studies have shown that PSA-free survival is associated with only the index cancer and not with tumor multifocality [4, 59].

Treatment of such lesions by focal therapy might provide cure. However, in most cases where multifocality exists, close monitoring of the secondary tumors for early signs of progression may be the cornerstone of successful focal treatment. Much of the original evidence supporting the use of active surveillance might conceptually be applied to focal therapy. Clinical experience with active surveillance now suggests there is an estimated risk of metastasis of <1 % at 2–8 years [60–62], and disease-specific mortality is 1 % at 8 years while on surveillance.

There are several active ongoing surveillance cohorts in the literature, as of yet none of them offer >15 years follow-up, but preliminary results are encouraging enough for clinical guidelines to recommend active surveillance as standard care. Klotz et al. [63] reported a median follow-up of 6.8 years (range 1–13 years) of 450 patients with a reported 10-year cancer-specific survival rate of 97.2 %. Although there was no difference in overall survival between patients who remained on surveillance and those who were reclassified and treated radically, half of the men who underwent radical treatment experienced biochemical failure. This is likely as a result of selection bias of cases that progressed rather than demonstrating that selective delayed interventions confer less success. All prostate cancer-related mortality occurred in men who had been reclassified as higher risk and who were offered radical treatment. However, only one patient in this series who was treated after a relatively prolonged period of observation subsequently experienced progression to metastatic disease and death. Therefore, it is likely that reclassification of disease risk and subsequent radical treatment reflects under-sampling of the prostate rather than true progression. This observation highlights the necessity to incorporate innovative imaging tools such as magnetic resonance imaging (MRI) and template biopsy in the selection and monitoring of patients undergoing active surveillance [64, 65]. Warlick et al. found that delayed curative intent in patients under an active surveillance protocol for small, low-grade prostate cancer compared to immediate treatment was not associated with the risk of incurable cancer [66]. It seems that patients with small-volume, low-grade cancer monitored with a rigorous protocol for disease progression have the same risk of incurable prostate cancer for at least 2 years after diagnosis as patients who received immediate prostate cancer surgery. Therefore, one could argue that if it is safe to undergo surveillance in some carefully selected men (on the basis of repeat biopsy, PSA kinetics, and findings on digital rectal examination and MRI of the prostate), the same strategy could be applied to secondary tumors after index ablation.

Results from PIVOT (Prostate Cancer Intervention Versus Observation Trial) showed similar results after a 10-year follow-up in the early PSA era [67]. This is in contrast with findings by Bill-Axelson et al. who reported at 18 years of follow-up that approximately 60 % of men had disease progression (with or without confirmed metastases) on watchful waiting compared to 40 % in the radical prostatectomy group [68]. They also observed a significant absolute reduction in the rate of death from any cause and the rate of death from prostate cancer, and the risk of metastases in the radical prostatectomy group continued after up to 23.2 years of follow-up, with no evidence that these benefits diminished over time. It is important to note that this cohort was recruited from an era before the PSA screening and most of the patients in this cohort were high risk with likely locally advanced and even micrometastases at the time of diagnosis in contrast to the PIVOT trial.

Conclusion

Although the goal of focal therapy for prostate cancer is to selectively ablate known disease, it should be remembered that a field effect might occur; that is, neoplastic or paraneoplastic cells exist in the apparently histologically normal field adjacent to the tumor. Genetic alteration and molecular changes have been found in normal-appearing prostate tissue adjacent to tumor, consistent with the possibility of a field effect [53]. This finding seems to be dependent on the distance from the cancer focus but not in a linear fashion [69–71]. Although these studies theoretically suggest that the concept of focal ablation of the tumor area requires cautious robust study, current evidence suggests the field effect occurs in the immediate vicinity of the cancer focus and therefore an adequate margin around the cancer could be incorporated into treatment together with the lesion. The field effect concept is accepted in the treatment of other solid organ cancers with the use of adjuvant therapy to the remaining tissue (low-dose radiotherapy after wide local excision in breast cancer) and surveillance on a regular basis (mammography for breast cancer, CT for kidney cancer). Surveillance for untreated prostate cancer has been developed formally within active surveillance cohort studies, and similar principals may apply to untreated tissue harboring no clinically significant cancer.

References

1. Mohler J, Bahnson RR, Boston B, Busby JE, D'Amico A, Eastham JA, et al. NCCN clinical practice guidelines in oncology: prostate cancer. J Natl Compr Canc Netw. 2010;8(2):162–200.
2. Karavitakis M, Ahmed HU, Abel PD, Hazell S, Winkler MH. Tumor focality in prostate cancer: implications for focal therapy. Nat Rev Clin Oncol. 2011;8(1):48–55.
3. Zhou MR, Tang ZH, Li J, Fan JH, Pang Y, Yang HJ, et al. Clinical and pathologic features of multifocal and multicentric breast cancer in chinese women: a retrospective cohort study. J Breast Cancer. 2013;16(1):77–83.
4. Wise AM, Stamey TA, McNeal JE, Clayton JL. Morphologic and clinical significance of multifocal prostate cancers in radical prostatectomy specimens. Urology. 2002;60(2):264–9.
5. Bastacky SI, Wojno KJ, Walsh PC, Carmichael MJ, Epstein JI. Pathological features of hereditary prostate cancer. J Urol. 1995;153(3 Pt 2):987–92.
6. Cheng L, Poulos CK, Pan CX, Jones TD, Daggy JK, Eble JN, et al. Preoperative prediction of small volume cancer (less than 0.5 ml) in radical prostatectomy specimens. J Urol. 2005;174(3):898–902.
7. Cheng L, Jones TD, Pan CX, Barbarin A, Eble JN, Koch MO. Anatomic distribution and pathologic characterization of small-volume prostate cancer (<0.5 ml) in whole-mount prostatectomy specimens. Mod Pathol. 2005;18(8):1022–6.
8. Arora R, Koch MO, Eble JN, Ulbright TM, Li L, Cheng L. Heterogeneity of Gleason grade in multifocal adenocarcinoma of the prostate. Cancer. 2004;100(11):2362–6.
9. Cheng L, Song SY, Pretlow TG, Abdul-Karim FW, Kung HJ, Dawson DV, et al. Evidence of independent origin of multiple tumors from patients with prostate cancer. J Natl Cancer Inst. 1998;90(3):233–7.
10. Villers A, McNeal JE, Freiha FS, Stamey TA. Multiple cancers in the prostate. Morphologic features of clinically recognized versus incidental tumors. Cancer. 1992;70(9):2313–8.
11. Cheng L, Pisansky TM, Ramnani DM, Leibovich BC, Cheville JC, Slezak J, et al. Extranodal extension in lymph node-positive prostate cancer. Mod Pathol. 2000;13(2):113–8.
12. Miller GJ, Cygan JM. Morphology of prostate cancer: the effects of multifocality on histological grade, tumor volume and capsule penetration. J Urol. 1994;152(5 Pt 2):1709–13.
13. Aihara M, Wheeler TM, Ohori M, Scardino PT. Heterogeneity of prostate cancer in radical prostatectomy specimens. Urology. 1994;43(1):60–6. discussion 6–7
14. Bostwick DG, Shan A, Qian J, Darson M, Maihle NJ, Jenkins RB, et al. Independent origin of multiple foci of prostatic intraepithelial neoplasia: comparison with matched foci of prostate carcinoma. Cancer. 1998;83(9):1995–2002.
15. Noguchi M, Stamey TA, McNeal JE, Yemoto CE. Assessment of morphometric measurements of prostate carcinoma volume. Cancer. 2000;89(5):1056–64.
16. Hollenbeck BK, Bassily N, Wei JT, Montie JE, Hayasaka S, Taylor JM, et al. Whole mounted radical prostatectomy specimens do not increase detection of adverse pathological features. J Urol. 2000;164(5):1583–6.
17. Mouraviev V, Mayes JM, Sun L, Madden JF, Moul JW, Polascik TJ. Prostate cancer laterality as a rationale of focal ablative therapy for the treatment of clinically localized prostate cancer. Cancer. 2007;110(4):906–10.
18. Chen ME, Johnston DA, Tang K, Babaian RJ, Troncoso P. Detailed mapping of prostate carcinoma

foci: biopsy strategy implications. Cancer. 2000; 89(8):1800–9.
19. Mouraviev V, Villers A, Bostwick DG, Wheeler TM, Montironi R, Polascik TJ. Understanding the pathological features of focality, grade and tumour volume of early-stage prostate cancer as a foundation for parenchyma-sparing prostate cancer therapies: active surveillance and focal targeted therapy. BJU Int. 2011;108(7):1074–85.
20. Swanson GP, Epstein JI, Ha CS, Kryvenko ON. Pathological characteristics of low risk prostate cancer based on totally embedded prostatectomy specimens. Prostate. 2015;75(4):424–9.
21. Karavitakis M, Winkler M, Abel P, Livni N, Beckley I, Ahmed HU. Histological characteristics of the index lesion in whole-mount radical prostatectomy specimens: implications for focal therapy. Prostate Cancer Prostatic Dis. 2011;14(1):46–52.
22. Stamey TA, Freiha FS, McNeal JE, Redwine EA, Whittemore AS, Schmid HP. Localized prostate cancer. Relationship of tumor volume to clinical significance for treatment of prostate cancer. Cancer. 1993;71(3):933–8.
23. McNeal JE, Villers AA, Redwine EA, Freiha FS, Stamey TA. Histologic differentiation, cancer volume, and pelvic lymph node metastasis in adenocarcinoma of the prostate. Cancer. 1990;66(6):1225–33.
24. Hollmann BG, van Triest B, Ghobadi G, Groenendaal G, de Jong J, van der Poel HG, et al. Gross tumor volume and clinical target volume in prostate cancer: How do satellites relate to the index lesion. Radiother Oncol. 2015;115(1):96–100.
25. Nelson BA, Shappell SB, Chang SS, Wells N, Farnham SB, Smith Jr JA, et al. Tumour volume is an independent predictor of prostate-specific antigen recurrence in patients undergoing radical prostatectomy for clinically localized prostate cancer. BJU Int. 2006;97(6):1169–72.
26. Schmid HP, McNeal JE, Stamey TA. Observations on the doubling time of prostate cancer. The use of serial prostate-specific antigen in patients with untreated disease as a measure of increasing cancer volume. Cancer. 1993;71(6):2031–40.
27. Bostwick DG, Graham Jr SD, Napalkov P, Abrahamsson PA, di Sant'agnese PA, Algaba F, et al. Staging of early prostate cancer: a proposed tumor volume-based prognostic index. Urology. 1993;41(5):403–11.
28. Wolters T, Roobol MJ, van Leeuwen PJ, van den Bergh RC, Hoedemaeker RF, van Leenders GJ, et al. A critical analysis of the tumor volume threshold for clinically insignificant prostate cancer using a data set of a randomized screening trial. J Urol. 2011;185(1):121–5.
29. Dugan JA, Bostwick DG, Myers RP, Qian J, Bergstralh EJ, Oesterling JE. The definition and preoperative prediction of clinically insignificant prostate cancer. JAMA. 1996;275(4):288–94.
30. Ruijter ET, van de Kaa CA, Schalken JA, Debruyne FM, Ruiter DJ. Histological grade heterogeneity in multifocal prostate cancer. Biological and clinical implications. J Pathol. 1996;180(3):295–9.
31. Guo CC, Wang Y, Xiao L, Troncoso P, Czerniak BA. The relationship of TMPRSS2-ERG gene fusion between primary and metastatic prostate cancers. Hum Pathol. 2012;43(5):644–9.
32. Perner S, Svensson MA, Hossain RR, Day JR, Groskopf J, Slaughter RC, et al. ERG rearrangement metastasis patterns in locally advanced prostate cancer. Urology. 2010;75(4):762–7.
33. Greene DR, Rogers E, Wessels EC, Wheeler TM, Taylor SR, Santucci RA, et al. Some small prostate cancers are nondiploid by nuclear image analysis: correlation of deoxyribonucleic acid ploidy status and pathological features. J Urol. 1994;151(5):1301–7.
34. Schmidt H, DeAngelis G, Eltze E, Gockel I, Semjonow A, Brandt B. Asynchronous growth of prostate cancer is reflected by circulating tumor cells delivered from distinct, even small foci, harboring loss of heterozygosity of the PTEN gene. Cancer Res. 2006;66(18):8959–65.
35. Kikuchi E, Scardino PT, Wheeler TM, Slawin KM, Ohori M. Is tumor volume an independent prognostic factor in clinically localized prostate cancer? J Urol. 2004;172(2):508–11.
36. Eggener SE, Scardino PT, Walsh PC, Han M, Partin AW, Trock BJ, et al. Predicting 15-year prostate cancer specific mortality after radical prostatectomy. J Urol. 2011;185(3):869–75.
37. Lee EW, Laze J, Lepor H. Outcomes of extremely low risk prostate cancer following radical prostatectomy. Prostate Cancer Prostatic Dis. 2011;14(3):266–9.
38. Ahmed HU, Arya M, Freeman A, Emberton M. Do low-grade and low-volume prostate cancers bear the hallmarks of malignancy? Lancet Oncol. 2012;13(11):e509–17.
39. Ross HM, Kryvenko ON, Cowan JE, Simko JP, Wheeler TM, Epstein JI. Do adenocarcinomas of the prostate with Gleason score (GS) </=6 have the potential to metastasize to lymph nodes? Am J Surg Pathol. 2012;36(9):1346–52.
40. Greenman C, Stephens P, Smith R, Dalgliesh GL, Hunter C, Bignell G, et al. Patterns of somatic mutation in human cancer genomes. Nature. 2007;446(7132):153–8.
41. Boyd LK, Mao X, Xue L, Lin D, Chaplin T, Kudahetti SC, et al. High-resolution genome-wide copy-number analysis suggests a monoclonal origin of multifocal prostate cancer. Genes Chromosomes Cancer. 2012;51(6):579–89.
42. Liu W, Laitinen S, Khan S, Vihinen M, Kowalski J, Yu G, et al. Copy number analysis indicates monoclonal origin of lethal metastatic prostate cancer. Nat Med. 2009;15(5):559–65.
43. Grasso CS, Wu YM, Robinson DR, Cao X, Dhanasekaran SM, Khan AP, et al. The mutational landscape of lethal castration-resistant prostate cancer. Nature. 2012;487(7406):239–43.
44. Lin D, Bayani J, Wang Y, Sadar MD, Yoshimoto M, Gout PW, et al. Development of metastatic and non-

metastatic tumor lines from a patient's prostate cancer specimen-identification of a small subpopulation with metastatic potential in the primary tumor. Prostate. 2010;70(15):1636–44.
45. Kobayashi M, Ishida H, Shindo T, Niwa S, Kino M, Kawamura K, et al. Molecular analysis of multifocal prostate cancer by comparative genomic hybridization. Prostate. 2008;68(16):1715–24.
46. Ibeawuchi C, Schmidt H, Voss R, Titze U, Abbas M, Neumann J, et al. Genome-wide investigation of multifocal and unifocal prostate cancer-are they genetically different? Int J Mol Sci. 2013;14(6):11816–29.
47. Yoshimoto M, Ludkovski O, DeGrace D, Williams JL, Evans A, Sircar K, et al. PTEN genomic deletions that characterize aggressive prostate cancer originate close to segmental duplications. Genes Chromosomes Cancer. 2012;51(2):149–60.
48. Clark J, Attard G, Jhavar S, Flohr P, Reid A, De-Bono J, et al. Complex patterns of ETS gene alteration arise during cancer development in the human prostate. Oncogene. 2008;27(14):1993–2003.
49. Mehra R, Han B, Tomlins SA, Wang L, Menon A, Wasco MJ, et al. Heterogeneity of TMPRSS2 gene rearrangements in multifocal prostate adenocarcinoma: molecular evidence for an independent group of diseases. Cancer Res. 2007;67(17):7991–5.
50. Barry M, Perner S, Demichelis F, Rubin MA. TMPRSS2-ERG fusion heterogeneity in multifocal prostate cancer: clinical and biologic implications. Urology. 2007;70(4):630–3.
51. Ruijter ET, Miller GJ, van de Kaa CA, van Bokhoven A, Bussemakers MJ, Debruyne FM, et al. Molecular analysis of multifocal prostate cancer lesions. J Pathol. 1999;188(3):271–7.
52. Lindberg J, Klevebring D, Liu W, Neiman M, Xu J, Wiklund P, et al. Exome sequencing of prostate cancer supports the hypothesis of independent tumour origins. Eur Urol. 2013;63(2):347–53.
53. Cooper CS, Eeles R, Wedge DC, Loo P, Gundem G, Alexandrov LB, et al. Analysis of the genetic phylogeny of multifocal prostate cancer identifies multiple independent clonal expansions in neoplastic and morphologically normal prostate tissue. Nat Genet. 2015;47(4):367–72.
54. Jones TD, Wang M, Eble JN, MacLennan GT, Lopez-Beltran A, Zhang S, et al. Molecular evidence supporting field effect in urothelial carcinogenesis. Clin Cancer Res. 2005;11(18):6512–9.
55. Boutros PC, Fraser M, Harding NJ, de Borja R, Trudel D, Lalonde E, et al. Spatial genomic heterogeneity within localized, multifocal prostate cancer. Nat Genet. 2015;47(7):736–45.
56. Ahmed HU. The index lesion and the origin of prostate cancer. N Engl J Med. 2009;361(17):1704–6.
57. Rice KR, Furusato B, Chen Y, McLeod DG, Sesterhenn IA, Brassell SA. Clinicopathological behavior of single focus prostate adenocarcinoma. J Urol. 2009;182(6):2689–94.
58. Stamatiou KN, Dilernia GC, Ilias GK, Daskalopoulos GK, Koutelekos IK, Marianou SN, et al. The phenomenon of multifocality does not affect the biologic behavior of histologic prostate carcinoma. Med Sci Monit. 2009;15(2):BR61–3.
59. Fuchsjager MH, Pucar D, Zelefsky MJ, Zhang Z, Mo Q, Ben-Porat LS, et al. Predicting post-external beam radiation therapy PSA relapse of prostate cancer using pretreatment MRI. Int J Radiat Oncol Biol Phys. 2010;78(3):743–50.
60. Dall'Era MA, Konety BR, Cowan JE, Shinohara K, Stauf F, Cooperberg MR, et al. Active surveillance for the management of prostate cancer in a contemporary cohort. Cancer. 2008;112(12):2664–70.
61. van den Bergh RC, Roemeling S, Roobol MJ, Aus G, Hugosson J, Rannikko AS, et al. Outcomes of men with screen-detected prostate cancer eligible for active surveillance who were managed expectantly. Eur Urol. 2009;55(1):1–8.
62. Eggener SE, Mueller A, Berglund RK, Ayyathurai R, Soloway C, Soloway MS, et al. A multi-institutional evaluation of active surveillance for low risk prostate cancer. J Urol. 2009;181(4):1635–41. discussion 41
63. Klotz L, Zhang L, Lam A, Nam R, Mamedov A, Loblaw A. Clinical results of long-term follow-up of a large, active surveillance cohort with localized prostate cancer. J Clin Oncol. 2010;28(1):126–31.
64. Fedorov A, Penzkofer T, Hirsch MS, Flood TA, Vangel MG, Masry P, et al. The role of pathology correlation approach in prostate cancer index lesion detection and quantitative analysis with multiparametric MRI. Acad Radiol. 2015;22(5):548–55.
65. Le JD, Tan N, Shkolyar E, Lu DY, Kwan L, Marks LS, et al. multifocality and prostate cancer detection by multiparametric magnetic resonance imaging: correlation with whole-mount histopathology. Eur Urol. 2015;67(3):569–76.
66. Warlick C, Trock BJ, Landis P, Epstein JI, Carter HB. Delayed versus immediate surgical intervention and prostate cancer outcome. J Natl Cancer Inst. 2006;98(5):355–7.
67. Wilt TJ, Brawer MK, Jones KM, Barry MJ, Aronson WJ, Fox S, et al. Radical prostatectomy versus observation for localized prostate cancer. N Engl J Med. 2012;367(3):203–13.
68. Bill-Axelson A, Holmberg L, Garmo H, Rider JR, Taari K, Busch C, et al. Radical prostatectomy or watchful waiting in early prostate cancer. N Engl J Med. 2014;370(10):932–42.
69. Hanson JA, Gillespie JW, Grover A, Tangrea MA, Chuaqui RF, Emmert-Buck MR, et al. Gene promoter methylation in prostate tumor-associated stromal cells. J Natl Cancer Inst. 2006;98(4):255–61.
70. Mehrotra J, Varde S, Wang H, Chiu H, Vargo J, Gray K, et al. Quantitative, spatial resolution of the epigenetic field effect in prostate cancer. Prostate. 2008;68(2):152–60.
71. Uetsuki H, Tsunemori H, Taoka R, Haba R, Ishikawa M, Kakehi Y. Expression of a novel biomarker, EPCA, in adenocarcinomas and precancerous lesions in the prostate. J Urol. 2005;174(2):514–8.

Utilizing Biopsy-Based Genomic Assays to Risk-Stratify Patients

9

Robert Qi, Stephen J. Freedland, and Judd W. Moul

Introduction

Risk stratification is necessary for determining the proper management of prostate cancer. Current risk stratification of prostate cancer depends heavily on prostate-specific antigen (PSA) and Gleason scoring of biopsy cores. Nonetheless, such techniques may not distinguish true low-risk prostate cancer from the aggressive prostate cancers that are merely detected early in their course of disease in certain cases. Advances in molecular genetics have yielded multiple biopsy-based genomic assays that could supplement the diagnostic ability of these more commonly utilized methods. This chapter investigates the limitations of PSA and biopsy Gleason scoring, provides a conceptual overview of biopsy-based genomic markers and their inclusion in current guidelines, and reports the evidence and recommendations of the more common genomic tests available.

R. Qi
Division of Urology, Department of Surgery, Duke Cancer Institute, Duke University School of Medicine, Durham, NC, USA

S.J. Freedland
Division of Urology, Department of Surgery, Cedars-Sinai Medical Center, Los Angeles, CA, USA

J.W. Moul (✉)
Division of Urology, Department of Surgery and Duke Cancer Institute, Duke University Medical Center, Durham, NC, USA
e-mail: judd.moul@duke.edu

Current Risk-Stratification Methods

The Road to Risk Stratification: The Prostate-Specific Antigen Controversy and Aggressive Early-Stage Cancer

The incidence of prostate cancer dramatically increased with the advent of PSA screening from the late 1980s through early 1990s [1, 2]. Despite decreasing incidence of prostate cancer since peak incidence in 1992 [2], prostate cancer remains the most common type of cancer among men in the United States and is the second-leading cause of cancer-specific mortality in the country [3].

PSA screening has been criticized for overdiagnosing men with indolent prostate cancer, with different models reporting that 23 % to 84 % of prostate cancers previously diagnosed by routine PSA screening are overdiagnoses [4–6]. As such, the 2012 United States Preventive Services Task Force recommended against PSA screening (Grade D), citing that the harms from overdiagnosis and overtreatment outweigh potential benefits of earlier diagnoses [7]. Meanwhile, the American Urological Association (AUA), American Cancer Society, and American College

© Springer International Publishing AG 2017
T.J. Polascik (ed.), *Imaging and Focal Therapy of Early Prostate Cancer*, Current Clinical Urology, DOI 10.1007/978-3-319-49911-6_9

of Physicians all indicate patient-physician joint decision-making when considering PSA testing for men 55–69 years old, with emphasis on patient preferences and values [8–10].

However, evidence suggests that a specific subset of early-stage prostate cancer is aggressive. As early as 2002, a randomized controlled trial enlisting 695 patients with early-stage disease showed that patients undergoing radical prostatectomy (RP) had significantly reduced prostate cancer-specific mortality (PCSM) at median 6.2 years follow-up [11], which held true at 12.8 years follow-up compared to men treated with watchful waiting [12]. In another study with 223 men initially diagnosed with early-stage prostate cancer but not treated, 17 % eventually progressed to metastatic disease on long-term follow-up. While PCSM was 15 per 1000 person-years within 15 years of cancer diagnosis, it nearly tripled to 44 per 1000 person-years beyond 15-year follow-up [13]. Indeed, models have predicted that 22–66 % of prostate cancers in men ages 55–69 could possibly progress in Gleason scoring even during the indolent phase, with the risk of progression increasing with age [14].

As such, it is imperative to properly risk-stratify patients with prostate cancer to determine the optimal management course at the individual level. In the subset of patients whose prostate cancer is aggressive, early-stage diagnosis followed by treatment could spare the patient from the 20 % 10-year mortality risk that men initially diagnosed with high-risk prostate cancer face [15]. However, the morbidities of treatment are such that overtreatment is to be avoided [7].

The Limitations of Contemporary Biopsy Gleason Scoring

Modern prostate cancer risk stratification depends heavily on the biopsy Gleason score, a useful but imperfect system. As mentioned, a subset of patients with aggressive cancers will have disease progression after the initial biopsy diagnosis. While certain studies have shown that biopsy-diagnosed D'Amico low-risk diseases are at increased risk for biochemical recurrence if prostatectomy is delayed for more than 5 months compared with low-risk patients who chose immediate prostatectomy [16–18], other reports have not shown such a difference [19–21]. Given the lack of clear literature on disease progression, further information would be helpful when counseling individual patients.

Of patients initially diagnosed with Gleason ≤6 on biopsy who chose radical prostatectomy, between 16.9 % and 43.5 % of patients are upgraded to Gleason ≥7 on surgical pathology [22–26]. Certain studies report that patients whose pathology was upgraded from Gleason 3+3 on biopsy to Gleason 3+4 on surgical pathology had similar pathological characteristics and risk for biochemical recurrence, while those upgraded to Gleason 4+3 also had increased likelihood of adverse pathology and risk of biochemical recurrence [24]. Other studies report that any upgrading places men at higher risk of adverse pathology and biochemical recurrence [27]. These results suggest that a considerable number of patients currently on active surveillance after being risk-stratified actually have undergraded cancers that may render them not ideal candidates for surveillance. These patients are being undertreated and are at increased risk of mortality.

Biopsies may also underestimate the impact race has on prostate cancer prognosis. African-American men have more aggressive prostate cancer than men of other races. African-American men on active surveillance are more likely to have Gleason upgrading on repeated biopsies [28, 29] and discontinuation of surveillance for treatment [30]. African-American men who chose prostatectomy after being biopsy-diagnosed with Gleason 3+3 are more likely to have disease upgrading at prostatectomy (27.7 % vs 14.4 %) and adverse pathology on surgical specimen [29] than their Caucasian counterparts. Nonetheless, both studies show that African-American men who are undergraded at biopsy are still a (sizable) minority. Molecular markers could further individualize results for these men who may be genetically predisposed to aggressive cancer.

Finally, the changes to Gleason scoring made under the 2005 International Society of Urological Pathology (ISUP) modified Gleason system may be leading to overdiagnosis of prostate cancer. In general, the 2005 ISUP decreases diagnoses of Gleason pattern 3 while increasing the diagnoses of Gleason pattern 4 Consequently, there has been Gleason upgrading among both biopsy and surgical specimens. Biopsy-diagnosed Gleason 6 has decreased from 48–68 % of all diagnoses under pre-2005 classifications to 22–49 %, while biopsy-diagnosed Gleason 7 has increased from 25 % to 39–68 % [31]. This may be leading to certain men otherwise eligible for active surveillance being overtreated.

Contemporary Diagnostic Aids

Despite imperfections of PSA and biopsy Gleason scoring, current risk-stratification tools depend heavily on PSA and its derivatives (i.e., PSA velocity, % free PSA, PSA density), biopsy information (i.e., Gleason score, % positive biopsy cores, % cancer in cores), and clinical T-staging to determine management [32]. The numerous methods created to assist in predicting prostate cancer outcomes can be broadly classified as risk groupings, probability nomograms, probability graphs, and neural networks [32].

Among the more popular classification aids are the D'Amico criteria, the University of California San Francisco (UCSF) Cancer of the Prostate Risk Assessment (CAPRA) score, and the Kattan nomogram. The D'Amico criteria classify prostate cancer into low-, intermediate-, and high-risk groups using PSA, combined Gleason score, and clinical staging [33]. It has since become the standard of care for risk-stratifying prostate cancer and has been adopted and modified by the AUA, European Association of Urology (EAU), and the National Comprehensive Cancer Network (NCCN). The UCSF-CAPRA scores disease on a 0–10 scale to estimate cancer recurrence-free survival after prostatectomy using PSA, biopsy Gleason score, clinical T-stage, percent positive biopsy, and age [34]. There are multiple iterations of Kattan-type nomograms that incorporate biopsy Gleason grade, PSA, clinical stage, percent and amount of biopsy cores that are cancerous and noncancerous, prostate volume on ultrasound, and more to predict a variety of prostate cancer outcomes [35].

Genomic Biomarkers

Overview

Conceptually, a biomarker is an indicator of a physiological state. They serve as proxies when determining and monitoring normal physiologic states, disease states, and efficacy of treatment interventions. Because cancer cells have abnormally regulated cellular processes, there are many potential biomarkers to distinguish themselves from noncancerous cells. Potential genetic mutations include single nucleotide or oligonucleotide mutations, changes in gene expression, abnormal copy numbers, gene fusions, abnormal DNA methylation, and microRNA deregulation [36]. These abnormalities can trigger (1) continuous growth signaling, (2) defying apoptosis, (3) permanent replication ability, (4) ignoring growth inhibitors, (5) increased angiogenesis, and (6) metastasis from origin that define the "hallmark capabilities" of cancer [37].

Prostate cancer genomic biomarkers utilize mutations in DNA and RNA to differentiate cancer from noncancer and to determine the aggressiveness of cancer. Various methodologies include reverse transcription-polymerase chain reaction (RT-PCR), RNA microarray, immunohistochemistry (IHC), enzyme-linked immunosorbent assay (ELISA), and more.

Biopsy-based biomarkers can provide additional information to complement the use of PSA, biopsy Gleason scoring, and other traditional measurements. These markers could be useful when biopsy pathologies are unclear as to treatment recommendations, when more traditional variables have conflicting implications, or when patient preferences are indecisive. They can help appropriately risk-stratify patients, thereby aiding proper management.

Canfield et al. provides a convenient framework toward assessing molecular diagnostic assays [38]. There are four major aspects to assess biomarkers for:

1. The actual genetic paths or mutations that the test analyzes
2. The clinical requirements and indications of the test
3. The type of test, amount of tissue, and cost of test
4. That the test has been properly validated. There are three types of validation that must be addressed:
   (a) Analytic validation: The assay is repeatable, precise, and accurate.
   (b) Clinical validation: The assay results are strongly correlated with clinically important outcomes such as patient mortality, clinical recurrence, or adverse pathology.
   (c) Clinical utility: The assay profoundly impacts patient-physician decision-making and improves patient outcomes.

Clinical Guidelines

At the time of this writing (March 2016), biopsy-based molecular biomarkers are not incorporated as a standard-of-care diagnostic test for risk stratification of prostate cancer and will require more evidence before they are.

- NCCN Prostate Cancer guidelines state that "molecular (or biomarker) testing can be used with risk groups and nomograms to predict how aggressive prostate cancer will be." Only two molecular genetics tests are mentioned (Prolaris and Oncotype), citing that while they have been more researched and utilized than other tests, "more research is needed" [39].
- The AUA guidelines for prostate cancer detection only briefly mention molecular biomarkers and in a general sense [8]. Examples include "the literature supporting the efficacy of DRE and biomarkers other than PSA for screening average risk men provided minimal evidence to draw conclusions" and "in the future it is possible that individuals at high risk of developing a lethal prostate cancer phenotype may be identifiable at an early age through genetic testing and/or new biomarkers."
- The 2015 update to the EAU Prostate Cancer guidelines discusses PSA and prostate cancer antigen 3 (PCA3) urine biomarker but also states that "additional potential biomarkers have not been sufficiently studied to demonstrate their additional prognostic value and clinical usefulness outside the standard patient care setting" [40].

Regulatory Guidelines

The US Food and Drug Administration (FDA) and the Centers for Medicare & Medicaid Services (CMS) regulate all molecular genetics testing. Canfield et al. explain that "laboratory-developed assays (in vitro tests developed, validated, and performed in-house by a specific reference laboratory) are required to abide by the Clinical Laboratory Improvement Amendments of 1988, which are administered by CMS. CLIA aims to ensure reliability and accuracy of test results and establish quality standards for all laboratory testing" [38].

All three validation components (analytical validation, clinical validation, and clinical utility) are typically required for a test to be reimbursed by insurance payers [38]. Medicare reimbursement for services is done through Medicare Administrative Contractors (MAC) and private health insurers that process claims with geographic or treatment type authority [41, 42].

At the time of writing, the MAC responsible for molecular diagnostic tests has drafted determination for Medicare coverage for two biopsy-based molecular genetics tests that could be used to further clinically risk-stratify patients: Prolaris and Oncotype DX. Medicare reimburses both Prolaris [43] and Oncotype DX [44] in very low-risk and low-risk prostate cancer for determining active surveillance or immediate treatment.

In addition, Medicare also reimburses Decipher for postsurgical intermediate-risk and high-risk

specimen [45] as well as ConfirmMDx in negative biopsies. While not specifically utilized for risk stratification of men already diagnosed with prostate cancer, ConfirmMDx measures DNA methylation that could indicate the presence of nearby prostate cancer even if the biopsy sample is not cancerous and could potentially lead to more focused sampling on repeat biopsy or decreased repeat biopsy frequency [42].

Example Situations

The following are abstracted clinical situations in which a biopsy-based genomic assay may be useful in determining the aggressiveness of the cancer, thereby assisting the physician's recommendations and patient's decision on how to proceed with disease management.

- A 60-year-old PSA <10 ng/mL is diagnosed with Gleason 6 prostate cancer. Despite counseling that treatment does not significantly decrease mortality in patients diagnosed with Gleason 6 disease and PSA <10 ng/mL [46], the man remains very nervous if his prostate cancer is an aggressive variant. He states that if it is an aggressive cancer, he prefers treatment now at his current good health than if he waits and his health declines.
- A 60-year-old African-American man in good health with PSA <10 ng/mL is diagnosed with Gleason 6 prostate cancer. While he has a slight preference for active surveillance, he understands that African-Americans may have more aggressive disease and seriously questions if his risk is actually higher than his PSA and Gleason score suggests.
- A 70-year-old man with history of managed cardiovascular disease is diagnosed with Gleason 7 disease. He is unsure whether the prostate cancer or the cardiovascular disease poses the greater risk to his life. He is averse to radiation and is reluctant to proceed with radiation therapy unless it is absolutely necessary.
- An 80-year-old man with Gleason 7 cancer was previously recommended watchful waiting. His overall health suggests a life expectancy of approximately another 10 years. He is extremely anxious about his prostate cancer even after counseling, but would not like unnecessary treatment.

Commercial Biopsy-Based Risk-Stratification Assays

Multiple biopsy-based genomic assays are currently in use (Table 9.1) [47]. They utilize formalin-fixed, paraffin-embedded tissue samples that are the standard method for preserving biopsy cores.

Prolaris

Overview

Prolaris (Myriad, Salt Lake City, UT, USA) is an RT-PCR assay designed for assessing (1) biopsy tissue from men with any risk disease to help determine active surveillance status, immediate treatment, and treatment intensity and (2) prostatectomy

Table 9.1 Simplified table of biopsy-based molecular tests available for prostate cancer [47]

Test	Molecular type	Clinical recommendation	CMS approval
Prolaris	RT-PCR	Watchful waiting	Yes
Oncotype DX	RT-PCR	Active surveillance	Yes
Decipher	RNA microarray	Adjuvant treatment	Yes—adjuvant treatment only
ProMark	Proteomic	Active surveillance	No
Ki-67	IHC	Watchful waiting	No
PTEN	IHC	Active surveillance	No

RT-PCR reverse transcription-polymerase chain reaction, *IHC* immunohistochemistry, *PTEN* phosphatase and tensin homolog

specimen to help estimate the risk of biochemical recurrence. The assay measures the expression of cell cycle progression (CCP) genes, whose production levels reflect the rate of growth of tumors and indirectly tumor aggression. From 126 CCP genes, 31 genes that together represented the best correlation to the mean expression level of the entire 126 gene cohort were selected [48].

The CCP score correlates with the expected aggressiveness of the prostate cancer given its Gleason score [48]. In general, CCP scores less than −1.0 correlate with cancer that is less aggressive than expected given the biopsy Gleason score, CCP scores between −1.0 and 0 correlate cancer that is of expected aggressiveness with cancer of expected aggressiveness, and CCP scores greater than 0 correlate with cancer that is more aggressive than expected. Prolaris also measures the 10-year PCSM risk, with lower CCP scores corresponding to lower risk of 10-year PCSM [49].

Validation

Prolaris has been comparatively well studied (Table 9.2) [48, 50–53]. For its initial clinical validation, 336 men treated with prostatectomy between 1985 and 1995 and 337 men diagnosed with prostate cancer by transurethral resection of the prostate (TURP) between 1990 and 1996 were tested [48]. The CCP score predicted biochemical recurrence after prostatectomy (hazard ratio = 1.74, $p = 3.3 \times 10^{-6}$) and prostate cancer-specific mortality after TURP but without additional treatments (hazard ratio = 2.92, $p = 6.1 \times 10^{-22}$). Other studies have shown that each unit increase in CCP had hazard ratio for biochemical recurrence of 2.1 [50] and 1.60 [51] in prostatectomy patients. Prolaris is also the only test studied in biopsies to predict biochemical recurrence in patients treated with radiation therapy, with hazard ratio of 2.55 [52]. CCP score was also associated with 10-year prostate cancer-specific mortality ($p = 0.13$) [52] and metastatic disease (hazard ratio = 4.19, $p = 8.2 \times 10^{-6}$) [51].

Clinically, Prolaris was shown to change treatment in 47.8 % of patients. Of patients whose treatments were changed, 72.1 % were reductions and 26.9 % were increased treatment. The number of treatments per patient (i.e., prostatectomy, radiation therapy, androgen deprivation therapy) decreased with the test (1.72 to 1.16), and percent of treatment recommendations recommending multiple treatments decreased (31.6 % to 12.9 %). There was increase in primary and adjuvant androgen deprivation therapy, attributed to increased use in AUA high-risk categories [53].

Table 9.2 Select studies investigating Prolaris

Study	Major outcomes
Cuzick et al. (2011) [48]	31 genes combined into CCP score
	CCP predicts biochemical recurrence and PCSM
Cooperberg et al. (2013) [50]	CCP predicts biochemical recurrence
Bishoff et al. (2014) [51]	CCP associated with biochemical recurrence and metastatic disease
Freedland et al. (2013) [52]	CCP associated with biochemical recurrence and 10-year PCSM
Shore et al. (2015) [53]	CCP changed treatment decisions and generally decreased severity of interventions recommended

CCP cell cycle progression, *PCSM* prostate cancer-specific mortality

Recommendation

Prolaris has been CMS-approved for Medicare reimbursement in determining active surveillance or immediate treatment in low-risk and very low-risk disease. Expert opinion also suggests that Prolaris may be useful in determining watchful waiting in men with limited life expectancy to reduce anxiety and that treatment of certain intermediate-risk and high-risk disease could nonetheless prolong life [53].

Oncotype

Overview

Oncotype DX Genomic Prostate Score (GPS) (Genomic Health, Redwood City, CA, USA) is a RT-PCR assay designed for assessing biopsy tissue in men with low-risk or intermediate-risk disease considering active surveillance or treatment. From originally screening 772 genetic markers

for prostate cancer, Oncotype DX GPS ultimately chose 12 genes related to cancer and five genes for reference. These genes can be broadly classified into four categories: androgen response, stromal response, cellular organization, and proliferation [54].

The Oncotype DX GPS assay is scored on a 0–100 scale, with secondary correlations to NCCN risk stratification and to likelihood of favorable pathology. Thus, a lower GPS score would also correspond to higher chance of favorable pathology and likelihood of being stratified into the very low-risk or low-risk categories.

Validation

In 395 men with low-risk or intermediate-risk PC and underwent prostatectomy, a 20-point increase in GPS was associated with statistically significant increased adverse pathology on prostatectomy in an MVA model with CAPRA (odds ratio ~0.21, 95 % CI 1.4–3.2) (Table 9.3). Of this cohort, 31 % were diagnosed with high-grade (primary Gleason 4 or any Gleason 5) or non-organ confined disease at RP, and high GPS score was a predictor of such parameters [55].

Another study investigated biopsies from 402 men with low- or intermediate-risk cancer with the objective of predicting adverse pathology and biochemical recurrence after prostatectomy (Table 9.3). On multivariable analysis, GPS was associated with adverse pathology (odds ratio = 2.7, 95 % CI 1.77–4.36) and independently predictive of biochemical recurrence. Univariate analysis showed that a 20-point GPS correlated with increased hazard ratio of 2.9 for biochemical recurrence [56].

Clinically, Oncotype DX GPS was shown to change the risk stratification of 21 % of biopsy-diagnosed prostate cancer in a cohort of 115 men (Table 9.3). While 46 % of men diagnosed with NCCN low-risk disease were changed, 44 % of those changes were to NCCN very-low risk. Where risk stratification was changed, treatment recommendations were typically altered and were accepted by patients [57].

Table 9.3 Select studies investigating Oncotype DX GPS

Study	Major outcomes
Klein et al. (2014) [55]	17 genes combined into GPS algorithm GPS predicts high-grade and high-stage disease
Cullen et al. (2015) [56]	GPS predicts time to BCR and time to metastasis
Kartha et al. (2014) [57]	GPS changed risk stratification and impacted clinical management

GPS genomic prostate score, *BCR* biochemical recurrence

Recommendation

Oncotype DX GPS has been CMS-approved for Medicare reimbursement for patients with very low-risk or low-risk disease [44]. Expert opinion has suggested Oncotype DX could be used for stratifying patients with low- or intermediate-risk disease into either active surveillance or treatment cohorts depending on GPS score. It has also been suggested that Oncotype-detected less aggressive tumors could have less frequent surveillance biopsies [47].

Decipher

Overview

Decipher (GenomeDX Biosciences, San Diego, CA, USA, and Vancouver, British Columbia, Canada) is an RNA microarray assay currently utilized for determining risk of metastasis and the necessity of adjuvant or salvage treatment after prostatectomy for patients whose surgical pathology indicates intermediate- or high-risk Gleason score or has adverse pathology. Recent efforts have also focused on validating Decipher for biopsy sampling. From an initial 545 patients, RNA microarrays looked at 1.4 million "probe selection regions" to create a "genomic classifier" score predicting risk of metastasis and overall survival [58].

Decipher provides a 5-year metastatic probability after prostatectomy between 0 % and 100 %. Low risk of metastasis is considered <4 %, average risk of metastasis is 4–9 %, and high risk of metastasis is considered >9 %. Secondary correlation is a relative risk compared

with the average patient with adverse pathology (extracapsular extension, lymph node invasion, seminal vesicle invasion, positive margins, and biochemical recurrence), combined Gleason ≥7, or tertiary Gleason 5 pattern.

Validation

Decipher has been well-validated primarily in prostatectomy specimen for post-prostatectomy decision-making [58–60]. Multiple studies have shown Decipher to robustly correlate with biochemical recurrence, 5- and 10-year metastatic risk, and PCSM in post-prostatectomy patients and can be used in patients with biochemical recurrence to help discern those who most need salvage treatment [59]. Moreover, it is predictive of metastatic risk even after salvage radiation, with every 0.1 unit increase in Decipher score corresponding to a 1.58 hazard ratio for metastasis [60].

Recent efforts have begun to focus on its efficacy in biopsy specimen (Table 9.4). In its first Decipher biopsy validation study with 57 patients, 66.6 % of NCCN intermediate-risk pathologies were reclassified as lower or higher Decipher risk (48.1 % lower Decipher risk, 18.5 % higher Decipher risk). Decipher on biopsy specimen was a significant independent predictor of 10-year post-RP metastasis, and combined Decipher and NCCN guidelines had improved predictive ability of metastasis within 10 years of RP compared with NCCN guidelines alone (c-index 0.88 vs 0.75) [61]. This improvement in predictive accuracy is largest in Decipher compared with Prolaris or Oncotype DX GPS. Combined Prolaris and CAPRA-S score yielded c-index of 0.77 as compared to c-index of 0.73 for CAPRA-S alone for predicting 10-year biochemical recurrence after prostatectomy [50]. Combined Oncotype DX GPS and NCCN risk improved c-index from 0.59 to 0.68 compared with NCCN risk alone for predicting 5-year biochemical recurrence after prostatectomy [56].

Table 9.4 Select studies investigating Decipher

Study	Major outcomes
Erho et al. (2013) [58]	1.4 million RNA "probe selection regions" combine to form a "genomic classifier" that is predictive of risk of metastasis and overall survival
Klein et al. (2016) [61]	Decipher independently predicted 10-year post-RP metastasis and improved disease discrimination

RP radical prostatectomy

Recommendation

Decipher has been CMS-approved for Medicare reimbursement for post-prostatectomy patients whose specimens have adverse pathology, but has not been approved for use on biopsy cores to risk-stratify patients before intervention yet. Decipher is currently recommended only for analyzing biochemical, clinical, and metastatic recurrence after radical prostatectomy. As such, expert opinion indicates it may be useful for determining adjuvant radiation status at this time. However, efforts are being made to expand Decipher into biopsy-based risk stratification.

ProMark

Overview

ProMark (Metamark, Cambridge, MA, USA) is a proteomic assay designed to compensate for the sampling error inherent in all biopsy samples while also predicting prostate cancer aggressiveness. From 160 candidates, 12 genes were initially selected to predict surgical Gleason score, tumor-node-metastasis (TNM) staging, and mortality. These genes represented processes as diverse as protein degradation, cell proliferation, protein synthesis, apoptosis, and pre-mRNA splicing and were present in both high-Gleason and low-Gleason samples [62]. They were further refined to eight proteomic markers [63].

ProMark provides end point data on likelihood of favorable pathology (surgical Gleason ≤7 and ≤T2) and Gleason 6 (surgical Gleason 3+3 and ≤T3a). ProMark has a score range from 0 to 1. Scores <0.33 suggest increased likelihood of favorable pathology, while scores >0.80 suggest increased likelihood of non-favorable pathology.

Validation

In the initial validation cohort of 381 patients, cut-off values are at 0.33 for favorable pathology and 0.80 for non-favorable pathology (Table 9.5 [62–64]). Risk score ≤0.33 had predictive value for favorable pathology at 87.2 % for intermediate-risk cancer, 81.5 % for low-risk cancer, and 95 % for very low-risk cancer. Predictive percent for non-favorable pathology for risk-score >0.80 was 76.9 % across all risk groups [63].

In a second validation study, 276 cases were used to distinguish favorable vs. non-favorable pathology utilizing the cutoff values of 0.33 and 0.80. The study separated favorable from non-favorable pathology (OR = 20.9, $p < 0.0001$) and Gleason 6 vs. non-Gleason 6 pathology (odds ratio = 12.95, $P < 0.0001$) [63].

Recommendation

ProMark has not been CMS-approved for Medicare reimbursement at the time of writing. Expert opinion has recommended ProMark for stratifying low- and intermediate-risk disease patients into active surveillance or immediate treatment. Like other biomarkers, the majority of results would most likely be confirmatory and not change management decision [47].

Non-trademarked Individual Biomarkers

Ki-67

Overview

Among the many proteins associated with prostate cancer, Ki-67 is among the few that has been correlated with poor cancer outcomes based on biopsy needle samples. Ki-67 is nuclear protein associated with cell cycle proliferation, with the KIAA0101 gene closely associated with positive Ki-67 staining being included in the Prolaris test [48, 65]. It is present during active cell cycles phases (G1, S, G2, and mitosis) but is absent from G0 cells at rest. As such, it can be used to determine the proportion of cells growing in a sample. The MIB-1 monoclonal antibodies are typically used to determine the fraction of Ki-67 positive tumor cells in a cellular population sample (the Ki-67 labeling index), with higher indices suggesting more aggressive cancer.

Ki-67 was cited as an independent predictor of biochemical recurrence after prostatectomy as early as 1996 [66]. This test has not formally developed consensus for the cutoff values for the percent of Ki-67 staining, with different publications utilizing values from 6–10 % to define risk for outcomes.

Validation

RTOG 92-02 investigated the biopsies of 537 patients who received radiation therapy and androgen deprivation therapy [67] (Table 9.6 [68–70]). While Ki-67 staining index of 3.5 % was not significant, a staining index of 7.1 % was significantly correlated with distant metastasis ($p = 0.0008$) and PCSM ($p = 0.017$), borderline correlated with biochemical recurrence ($p = 0.0504$) and overall death ($p = 0.0551$), as well as greater percentage of Gleason 7–10 as compared with the 3.5 % staining index ($p = 0.0001$) [68]. The RTOG 92-02 follow-up conducted after 5 additional years showed that Ki-67 at 11.3 % staining index was correlated with metastasis (hazard ratio = 2.95, $p < 0.01$), PCSM (hazard

Table 9.5 Select studies investigating ProMark

Study	Major outcomes
Shipitsin et al. (2014) [62]	Twelve proteomic markers selected for ProMark
Blume-Jensen et al. (2015) [63]	Eight proteomic markers selected to determine favorable pathology
Roth et al. (2015) [64]	Using ProMark in Gleason 3+3 and 3+4 cancers decreases cost of care and slightly increases quality adjusted life-years

Table 9.6 Select studies investigating Ki-67

Study	Major outcomes
Pollack et al. (2004) [68]	Staining index of 7.1 % associated with metastasis and cancer-specific death
Tollefson et al. (2014) [69]	Each 1 % increase in Ki-67 expression associated with 12 % increase of cancer-specific death
Fisher et al. (2013) [70]	Staining index of 10 % associated with cancer-specific mortality

ratio = 2.35, $p = 0.0007$), and overall mortality (hazard ratio = 1.44, $p = 0.01$) [67].

Another study investigating biopsy specimen in 451 patients who underwent RP between 1995 and 1998 showed that Ki-67 expression was correlated with PCSM (Table 9.6). Each 1 % increase in Ki-67 expression was associated with a 12 % increased risk of PCSM ($p < 0.001$). Moreover, patients with Ki-67 labeling index >6 % were 5.8 times more likely to have PCSM than patients with labeling index ≤6 % [69]. When the threshold for Ki-67 was set at 10 %, Ki-67 was a predictor of prostate cancer-specific mortality in patients conservatively treated without intervention. Patients whose biopsy cores had labeling index >10 % had patient mortality hazard ratio of 3.13 in Gleason = 7 and 2.28 in Gleason >7 compared with patients whose biopsy cores had Ki-67 labeling index ≤10 % [70].

Recommendation

Although not as commonly used for risk stratification today as other biopsy-based genomic assays, Ki-67 was recommended for use in watchful waiting in men with limited life expectancy in light of research indicating it stratified PCSM and metastasis but not differentiation between risk-stratification groups. Concerns have been raised over the lack of standardized cutoff levels, which could further confuse patients and complicate clinical decision-making, as well as potential heterogeneous staining techniques among different laboratories. These concerns have potentially limited its applicability in modern diagnosis [47].

Phosphatase and Tensin Homolog (PTEN)

Overview

The phosphatase and tensin homolog (PTEN) is a lipid phosphatase tumor-suppressor gene commonly deleted or mutated in prostate cancer. It is implicated in proper functioning of cellular survival, growth and metabolism, migration and proliferation, and more. Biopsy-needle specimen can be stained for PTEN loss to help assess PCSM and Gleason upgrading on surgical pathology. The staining result is a binary yes or no for PTEN loss, with no direct cutoff values.

Validation

One study among 675 men undergoing conservative management showed that although only 3 % of men with low-risk disease had PTEN loss (Table 9.7). PTEN loss was highly correlated with PCSM in men with low-risk disease (defined using Gleason score, low PSA, low Ki-67 staining, and low extent of disease) (hazard ratio = 7.4, $p = 0.012$). Among patients with TURP diagnosed with Gleason <7 disease, PTEN loss had a hazard ratio of 8.13 (95 % CI 2.84–23.24) compared with non-PTEN loss. However, PTEN loss did not correlate with PCSM in high-risk disease [71].

In another study using needle biopsy cohort who eventually underwent prostatectomy, 174 men biopsy-diagnosed with Gleason 6, 11 % had PTEN loss (Table 9.7). Multivariable analysis showed that PTEN loss predicted Gleason upgrading on surgery (odds ratio = 3.04, $p = 0.035$) [72]. In addition, a study with 77 subjects who underwent prostatectomy showed that 12 % had PTEN loss (Table 9.7). On univariate analysis, PTEN loss is significantly associated with metastasis, metastatic castrate-resistant prostate cancer, and death [73].

Recommendation

Expert opinion has suggested PTEN could be used for stratifying patients into active surveillance. While not commonly used, there is growing interest. Because PTEN is less expensive than many other genomic assays, patients on active

Table 9.7 Select studies investigating PTEN

Study	Major outcomes
Cuzick et al. (2013) [71]	PTEN loss is highly correlated with cancer-specific mortality in men with low-risk disease
Lotan et al. (2015) [72]	PTEN loss predicts Gleason upgrading on surgical specimen
Mithal et al. (2014) [73]	PTEN loss is associated with post-prostatectomy metastasis and death

PTEN phosphatase and tensin homolog

surveillance could have serial PTEN testing to assess whether prostate cancer has increased in aggression. Moreover, the binary reporting of PTEN results eliminates ambiguity on the severity of prostate cancer disease [47].

Conclusion

Biopsy-based molecular biomarkers have great potential to distinguish the indolent, truly low-risk prostate cancers from highly aggressive prostate cancers that are merely detected early in their development. They are already becoming useful for counseling individual patients who are uncertain of an optimal management course. The multiple commercial assays all cite published literature validating their efficacy, and they are beginning to be reimbursed by insurance coverage. Overall, biopsy-based molecular biomarkers likely will have an increasing role in the management of prostate cancer in the future.

Acknowledgment Special acknowledgment goes to the following three articles for major contributions to the overall organization of this chapter:

- Ross AE, D'Amico AV, Freedland SJ. Which, when and why? Rational use of tissue-based molecular testing in localized prostate cancer. Prostate Cancer Prostatic Dis. 2016; 19 (1): 1–6.
- Canfield SE, Kibel AS, Kemeter MJ, Febbo PG, Lawrence HJ, Moul JW. A guide for clinicians in the evaluation of emerging molecular diagnostics for newly diagnosed prostate cancer. Rev. Urol. 2014; 16(4): 172–180.
- Falzarano SM, Ferro M, Bollito E, Klein EA, Carrieri G, Magi-Galluzzi C. Novel biomarkers and genomic tests in prostate cancer: a critical analysis. Minerva Urol Nefrol. 2015; 67(3): 211–231.

References

1. Potosky AL, Miller BA, Albertsen PC, Kramer BS. The role of increasing detection in the rising incidence of prostate cancer. JAMA. 1995;273(7):548–52.
2. Welch HG, Albertsen PC. Prostate cancer diagnosis and treatment after the introduction of prostate-specific antigen screening: 1986–2005. J Natl Cancer Inst. 2009;101(19):1325–9.
3. Siegel RL, Miller KD, Jemal A. Cancer statistics, 2015. CA Cancer J Clin. 2015;65(1):5–29.
4. Draisma G, Etzioni R, Tsodikov A, Mariotto A, Wever E, Gulati R, Feuer E, de Koning H. Lead time and overdiagnosis in prostate-specific antigen screening: importance of methods and context. J Natl Cancer Inst. 2009;101(6):374–83.
5. McGregor M, Hanley JA, Boivin JF, McLean RG. Screening for prostate cancer: estimating the magnitude of overdetection. CMAJ. 1998;159(11):1368–72.
6. Draisma G, Boer R, Otto SJ, van der Cruijsen IW, Damhuis RA, Schröder FH, de Koning HJ. Lead times and overdetection due to prostate-specific antigen screening: estimates from the european randomized study of screening for prostate cancer. J Natl Cancer Inst. 2003;95(12):868–78.
7. Moyer VA, US Preventive Services Task Force. Screening for prostate cancer: U.S. Preventive services task force recommendation statement. Ann Intern Med. 2012;157(2):120–34.
8. Carter HB, Albertsen PC, Barry MJ, Etzioni R, Freedland SJ, Greene KL, Holmberg L, Kantoff P, Konety BR, Murad MH, Penson DF, Zietman AL. Early detection of prostate cancer: Aua guideline. J Urol. 2013;190(2):419–26.
9. Wolf AM, Wender RC, Etzioni RB, Thompson IM, D'Amico AV, Volk RJ, Brooks DD, Dash C, Guessous I, Andrews K, DeSantis C, Smith RA, American Cancer Society Prostate Cancer Advisory Committee. American cancer society guideline for the early detection of prostate cancer: update 2010. CA Cancer J Clin. 2010;60(2):70–98.
10. Qaseem A, Barry MJ, Denberg TD, Owens DK, Shekelle P, Clinical Guidelines Committee of the American College of Physicians. Screening for prostate cancer: a guidance statement from the clinical guidelines committee of the american college of physicians. Ann Intern Med. 2013;158(10):761–9.
11. Holmberg L, Bill-Axelson A, Helgesen F, Salo JO, Folmerz P, Häggman M, Andersson SO, Spångberg A, Busch C, Nordling S, Palmgren J, Adami HO, Johansson JE, Norlén BJ, Scandinavian Prostatic Cancer Group Study Number 4. A randomized trial comparing radical prostatectomy with watchful waiting in early prostate cancer. N Engl J Med. 2002;347(11):781–9.
12. Bill-Axelson A, Holmberg L, Ruutu M, Garmo H, Stark JR, Busch C, Nordling S, Häggman M, Andersson SO, Bratell S, Spångberg A, Palmgren J, Steineck G, Adami HO, Johansson JE, SPCG-4 Investigators. Radical prostatectomy versus watchful waiting in early prostate cancer. N Engl J Med. 2011;364(18):1708–17.
13. Johansson JE, Andrén O, Andersson SO, Dickman PW, Holmberg L, Magnuson A, Adami HO. Natural history of early, localized prostate cancer. JAMA. 2004;291(22):2713–9.
14. Pashayan N, Pharoah P, Neal DE, Hamdy F, Donovan J, Martin RM, Greenberg D, Duffy SW. Psa-detected prostate cancer and the potential for dedifferentiation–estimating the proportion capable of progression. Int J Cancer. 2011;128(6):1462–70.

15. Cooperberg MR, Broering JM, Carroll PR. Risk assessment for prostate cancer metastasis and mortality at the time of diagnosis. J Natl Cancer Inst. 2009;101(12):878–87.
16. Berg WT, Danzig MR, Pak JS, Korets R, RoyChoudhury A, Hruby G, Benson MC, McKiernan JM, Badani KK. Delay from biopsy to radical prostatectomy influences the rate of adverse pathologic outcomes. Prostate. 2015;75(10):1085–91.
17. Nam RK, Jewett MA, Krahn MD, Robinette MA, Tsihlias J, Toi A, Ho M, Evans A, Sweet J, Trachtenberg J. Delay in surgical therapy for clinically localized prostate cancer and biochemical recurrence after radical prostatectomy. Can J Urol. 2003;10(3):1891–8.
18. O'Brien D, Loeb S, Carvalhal GF, McGuire BB, Kan D, Hofer MD, Casey JT, Helfand BT, Catalona WJ. Delay of surgery in men with low risk prostate cancer. J Urol. 2011;185(6):2143–7.
19. Graefen M, Chun KH, Schlomm T, Haese A, Huland H. Reasonable delay of surgical treatment in men with localized prostate cancer–impact on prognosis? Eur Urol. 2005;447(6):756–60.
20. van den Bergh RC, Steyerberg EW, Khatami A, Aus G, Pihl CG, Wolters T, van Leeuwen PJ, Roobol MJ, Schröder FH, Hugosson J, Swedish and Dutch sections of the European Randomized Study of Screening for Prostate Cancer. Is delayed radical prostatectomy in men with low-risk screen-detected prostate cancer associated with a higher risk of unfavorable outcomes? Cancer. 2010;116(5):1281–90.
21. Abern MR, Aronson WJ, Terris MK, Kane CJ, Presti Jr JC, Amling CL, Freedland SJ. Delayed radical prostatectomy for intermediate-risk prostate cancer is associated with biochemical recurrence: possible implications for active surveillance from the search database. Prostate. 2013;73(4):409–17.
22. Swanson GP, Epstein JI, Ha CS, Kryvenko ON. Pathological characteristics of low risk prostate cancer based on totally embedded prostatectomy specimens. Prostate. 2015;75(4):424–9.
23. Gofrit ON, Zorn KC, Taxy JB, Lin S, Zagaja GP, Steinberg GD, Shalhav AL. Predicting the risk of patients with biopsy gleason score 6 to harbor a higher grade cancer. J Urol. 2007;178(5):1925–8.
24. Corcoran NM, Hong MK, Casey RG, Hurtado-Coll A, Peters J, Harewood L, Goldenberg SL, Hovens CM, Costello AJ, Gleave ME. Upgrade in gleason score between prostate biopsies and pathology following radical prostatectomy significantly impacts upon the risk of biochemical recurrence. BJU Int. 2011;108(8):E202–10.
25. Thomas C, Pfirrmann K, Pieles F, Bogumil A, Gillitzer R, Wiesner C, Thüroff JW, Melchior SW. Predictors for clinically relevant gleason score upgrade in patients undergoing radical prostatectomy. BJU Int. 2012;109(2):214–9.
26. Isariyawongse BK, Sun L, Bañez LL, Robertson C, Polascik TJ, Maloney K, Donatucci C, Albala D, Mouraviev V, Madden JF, Moul JW. Significant discrepancies between diagnostic and pathologic gleason sums in prostate cancer: the predictive role of age and prostate-specific antigen. Urology. 2008;72(4):882–6.
27. Freedland SJ, Kane CJ, Aronson WJ, Terris MK, Presti Jr JC, SEARCH Database Study Group. Upgrading and downgrading of prostate needle biopsy specimens: risk factors and clinical implications. Urology. 2007;2007(69):3.
28. Sundi D, Faisal FA, Trock BJ, Landis PK, Feng Z, Ross AE, Carter HB, Schaeffer EM. Reclassification rates are higher among African American men than Caucasians on active surveillance. Urology. 2015; 85(1):155–60.
29. Sundi D, Ross AE, Humphreys EB, Han M, Partin AW, Carter HB, Schaeffer EM. African american men with very low-risk prostate cancer exhibit adverse oncologic outcomes after radical prostatectomy: should active surveillance still be an option for them? J Clin Oncol. 2013;31(24):2991–7.
30. Abern MR, Bassett MR, Tsivian M, Bañez LL, Polascik TJ, Ferrandino MN, Robertson CN, Freedland SJ, Moul JW. Race is associated with discontinuation of active surveillance of low-risk prostate cancer: results from the duke prostate center. Prostate Cancer Prostatic Dis. 2013;16(1):85–90.
31. Montironi R, Cheng L, Lopez-Beltran A, Scarpelli M, Mazzucchelli R, Mikuz G, Kirkali Z, Montorsi F. Original gleason system versus 2005 ISUP modified gleason system: the importance of indicating which system is used in the patient's pathology and clinical reports. Eur Urol. 2010;58(3):369–73.
32. Shariat SF, Karakiewicz PI, Roehrborn CG, Kattan MW. An updated catalog of prostate cancer predictive tools. Cancer. 2008;113(11):3075–99.
33. D'Amico AV, Whittington R, Malkowicz SB, Schultz D, Blank K, Broderick GA, Tomaszewski JE, Renshaw AA, Kaplan I, Beard CJ, Wein A. Biochemical outcome after radical prostatectomy, external beam radiation therapy, or interstitial radiation therapy for clinically localized prostate cancer. JAMA. 1998;280(11):969–74.
34. Cooperberg MR, Pasta DJ, Elkin EP, Litwin MS, Latini DM, Du Chane J, Carroll PR. The university of california, san francisco cancer of the prostate risk assessment score: a straightforward and reliable preoperative predictor of disease recurrence after radical prostatectomy. J Urol. 2005;173(6):1938–42.
35. Lughezzani G, Briganti A, Karakiewicz PI, Kattan MW, Montorsi F, Shariat SF, Vickers AJ. Predictive and prognostic models in radical prostatectomy candidates: a critical analysis of the literature. Eur Urol. 2010;58(5):687–700.
36. Spans L, Clinckemalie L, Helsen C, Vanderschueren D, Boonen S, Lerut E, Joniau S, Claessens F. The genomic landscape of prostate cancer. Int J Mol Sci. 2013;14(6):10822–51.
37. Hanahan D, Weinberg RA. Hallmarks of cancer: the next generation. Cell. 2011;144(5):646–74.
38. Canfield SE, Kibel AS, Kemeter MJ, Febbo PG, Lawrence HJ, Moul JW. A guide for clinicians in the

evaluation of emerging molecular diagnostics for newly diagnosed prostate cancer. Rev Urol. 2014;16(4):172–80.
39. Mohler JL, Armstrong AJ, Bahnson RR, D'Amico AV, Davis BJ, Eastham JA, Enke CA, Farrington TA, Higano CS, Horwitz EM, Hurwitz M, Kane CJ, Kawachi MH, Kuettel M, Lee RJ, Meeks JJ, Penson DF, Plimack ER, Pow-Sang JM, Raben D, Richey S, Roach M 3rd, Rosenfeld S, Schaeffer E, Skolarus TA, Small EJ, Sonpavde G, Srinivas S, Strope SA, Tward J, Shead DA, Freedman-Cass DA. Prostate cancer, version 1.2016. J Natl Compr Cancer Netw. 2016;14(1):19–30.
40. Mottet N, Bellmunt J, Briers E, van den Bergh RCN, Bolla M, van Casteren NJ, Cornford P, Culine S, Joniau S, Lam T, Mason MD, Matveev V, van der Poel H, van der Kwast TH, Rouviere O, Wiegel T. Guidelines on prostate cancer European Association of Urology; 2015. Available from: http://uroweb.org/wp-content/uploads/09-Prostate-Cancer_LR.pdf.
41. Services CfMM. What is a mac [Website] 2015; Available from: https://www.cms.gov/Medicare/Medicare-Contracting/Medicare-Administrative-Contractors/What-is-a-MAC.html. Accessed 18 Jan 2016.
42. Caffrey MK. Medicare reimburses 3 prostate cancer diagnostic tests. 2015; Available from: http://www.onclive.com/publications/oncology-business-news/2014/December-2014/Medicare-Reimburses-3-Prostate-Cancer-Diagnostic-Tests. Accessed 18 Jan 2016.
43. Myriad. Myriad receives draft medicare coverage for prolaris(r). 2014; Available from: http://investor.myriad.com/releasedetail.cfm?releaseid=876733.#sthash.xHYPA59N.dpuf. Accessed 18 Jan 2016.
44. Newswire P. Medicare initiates coverage for genomic health's oncotype dx® prostate cancer test effective immediately 2015; Available from: http://www.prnewswire.com/news-releases/medicare-initiates-coverage-for-genomic-healths-oncotype-dx-prostate-cancer-test-effective-immediately-300160776.html. Accessed 26 Feb 2016.
45. GenomeDx. Centers for medicare and medicaid services publishes draft coverage decision to reimburse the decipher® test for intermediate & high risk prostate cancer 2014; Available from: https://genomedx.com/press-releases/centers-medicare-medicaid-services-publishes-draft-coverage-decision-reimburse-decipher-test-intermediate-high-risk-prostate-cancer/. Accessed 18 Jan 2016.
46. Wilt TJ, Brawer MK, Jones KM, Barry MJ, Aronson WJ, Fox S, Gingrich JR, Wei JT, Gilhooly P, Grob BM, Nsouli I, Iyer P, Cartagena R, Snider G, Roehrborn C, Sharifi R, Blank W, Pandya P, Andriole GL, Culkin D, Wheeler T, Prostate Cancer Intervention versus Observation Trial (PIVOT) Study Group. Radical prostatectomy versus observation for localized prostate cancer. N Engl J Med. 2012;367(3):203–13.
47. Ross AE, D'Amico AV, Freedland SJ. Which, when and why? Rational use of tissue-based molecular testing in localized prostate cancer. Prostate Cancer Prostatic Dis. 2016;19(1):1–6.
48. Cuzick J, Swanson GP, Fisher G, Brothman AR, Berney DM, Reid JE, Mesher D, Speights VO, Stankiewicz E, Foster CS, Møller H, Scardino P, Warren JD, Park J, Younus A, Flake 2nd DD, Wagner S, Gutin A, Lanchbury JS, Stone S, Transatlantic Prostate Group. Prognostic value of an rna expression signature derived from cell cycle proliferation genes in patients with prostate cancer: a retrospective study. Lancet Oncol. 2011;12(3):245–55.
49. Myriad. What does a high prolaris score mean? 2015 [updated February 27]; Available from: https://prolaris.myriad.com/prolaris-for-physicians/physician-resources/talking-to-patients/.
50. Cooperberg MR, Simko JP, Cowan JE, Reid JE, Djalilvand A, Bhatnagar S, Gutin A, Lanchbury JS, Swanson GP, Stone S, Carroll PR. Validation of a cell-cycle progression gene panel to improve risk stratification in a contemporary prostatectomy cohort. J Clin Oncol. 2013;31(11):1428–34.
51. Bishoff JT, Freedland SJ, Gerber L, Tennstedt P, Reid J, Welbourn W, Graefen M, Sangale Z, Tikishvili E, Park J, Younus A, Gutin A, Lanchbury JS, Sauter G, Brawer M, Stone S, Schlomm T. Prognostic utility of the cell cycle progression score generated from biopsy in men treated with prostatectomy. J Urol. 2014;192(2):409–14.
52. Freedland SJ, Gerber L, Reid J, Welbourn W, Tikishvili E, Park J, Younus A, Gutin A, Sangale Z, Lanchbury JS, Salama JK, Stone S. Prognostic utility of cell cycle progression score in men with prostate cancer after primary external beam radiation therapy. Int J Radiat Oncol Biol Phys. 2013;86(5):848–53.
53. Shore ND, Kella N, Moran B, Boczko J, Bianco FJ, Crawford ED, Davis T, Roundy KM, Rushton K, Grier C, Kaldate R, Brawer MK, Gonzalgo ML. Impact of the cell cycle progression test on physician and patient treatment selection for localized prostate cancer. J Urol. 2016;195(3):612–8.
54. Falzarano SM, Ferro M, Bollito E, Klein EA, Carrieri G, Magi-Galluzzi C. Novel biomarkers and genomic tests in prostate cancer: a critical analysis. Minerva Urol Nefrol. 2015;67(3):211–31.
55. Klein EA, Cooperberg MR, Magi-Galluzzi C, Simko JP, Falzarano SM, Maddala T, Chan JM, Li J, Cowan JE, Tsiatis AC, Cherbavaz DB, Pelham RJ, Tenggara-Hunter I, Baehner FL, Knezevic D, Febbo PG, Shak S, Kattan MW, Lee M, Carroll PR. A 17-gene assay to predict prostate cancer aggressiveness in the context of gleason grade heterogeneity, tumor multifocality, and biopsy undersampling. Eur Urol. 2014;66(3):550–60.
56. Cullen J, Rosner IL, Brand TC, Zhang N, Tsiatis AC, Moncur J, Ali A, Chen Y, Knezevic D, Maddala T, Lawrence HJ, Febbo PG, Srivastava S, Sesterhenn IA, McLeod DG. A biopsy-based 17-gene genomic prostate score predicts recurrence after radical prostatectomy and adverse surgical pathology in a racially diverse population of men with clinically low- and

intermediate-risk prostate cancer. Eur Urol. 2015;68(1):123–31.
57. Kartha GK, Nyame Y, Klein EA. Evaluation of the oncotypedx genomic prostate score for risk stratification in prostate cancer patients considered candidates for active surveillance. J Clin Oncol. 2014;32(suppl 4):122.
58. Erho N, Crisan A, Vergara IA, Mitra AP, Ghadessi M, Buerki C, Bergstralh EJ, Kollmeyer T, Fink S, Haddad Z, Zimmermann B, Sierocinski T, Ballman KV, Triche TJ, Black PC, Karnes RJ, Klee G, Davicioni E, Jenkins RB. Discovery and validation of a prostate cancer genomic classifier that predicts early metastasis following radical prostatectomy. PLoS One. 2013;8(6):e66855.
59. Dalela D, Loppenberg B, Sood A, Sammon J, Abdollah F. Contemporary role of the decipher test in prostate cancer management: current practice and future perspectives. Rev Urol. 2016;18(1):1–9.
60. Freedland SJ, Choeurng V, Howard L, De Hoedt A, du Plessis M, Yousefi K, Lam LL, Buerki C, Ra S, Robbins B, Trabulsi EJ, Shah NL, Abdollah F, Feng FY, Davicioni E, Dicker AP, Karnes RJ, Den RB. Utilization of a genomic classifier for prediction of metastasis following salvage radiation therapy after radical prostatectomy. Eur Urol. 2016;70(4):588–96.
61. Klein EA, Haddad Z, Yousefi K, Lam LL, Wang Q, Choeurng V, Palmer-Aronsten B, Buerki C, Davicioni E, Li J, Kattan MW, Stephenson AJ, Magi-Galluzzi C. Decipher genomic classifier measured on prostate biopsy predicts metastasis risk. Urology. 2016;90:148–52.
62. Shipitsin M, Small C, Choudhury S, Giladi E, Friedlander S, Nardone J, Hussain S, Hurley AD, Ernst C, Huang YE, Chang H, Nifong TP, Rimm DL, Dunyak J, Loda M, Berman DM, Blume-Jensen P. Identification of proteomic biomarkers predicting prostate cancer aggressiveness and lethality despite biopsy-sampling error. Br J Cancer. 2014;111(6):1201–12.
63. Blume-Jensen P, Berman D, Rimm DL, Shipitsin M, Putzi M, Nifong TP, Small C, Choudhury S, Capela T, Coupal L, Ernst C, Hurley A, Kaprelyants A, Chang H, Giladi E, Nardone J, Dunyak J, Loda M, Klein EA, Magi-Galluzzi C, Latour M, Epstein JI, Kantoff P, Saad F. Development and clinical validation of an in situ biopsy-based multimarker assay for risk stratification in prostate cancer. Clin Cancer Res. 2015;21(11):2591–600.
64. Roth J, Ramsey SD, Carlson JJ. Cost-effectiveness of a biopsy-based 8-protein prostate cancer prognostic assay to optimize treatment decision making in gleason 3 + 3 and 3+4 early stage prostate cancer. Oncologist. 2015;20(12):1355–64.
65. Kais Z, Barsky SH, Mathsyaraja H, Zha A, Ransburgh DJ, He G, Pilarski RT, Shapiro CL, Huang K, Parvin JD. Kiaa0101 interacts with brca1 and regulates centrosome number. Mol Cancer Res. 2011;9(8):1091–9.
66. Bettencourt MC, Bauer JJ, Sesterhenn IA, Mostofi FK, McLeod DG, Moul JW. Ki-67 expression is a prognostic marker of prostate cancer recurrence after radical prostatectomy. J Urol. 1996;156(3):1064–8.
67. Khor LY, Bae K, Paulus R, Al-Saleem T, Hammond ME, Grignon DJ, Che M, Venkatesan V, Byhardt RW, Rotman M, Hanks GE, Sandler HM, Pollack A. Mdm2 and ki-67 predict for distant metastasis and mortality in men treated with radiotherapy and androgen deprivation for prostate cancer: Rtog 92-02. J Clin Oncol. 2009;27(19):3177–84.
68. Pollack A, DeSilvio M, Khor LY, Li R, Al-Saleem TI, Hammond ME, Venkatesan V, Lawton CA, Roach 3rd M, Shipley WU, Hanks GE, Sandler HM. Ki-67 staining is a strong predictor of distant metastasis and mortality for men with prostate cancer treated with radiotherapy plus androgen deprivation: radiation therapy oncology group trial 92-02. J Clin Oncol. 2004;22(11):2133–40.
69. Tollefson MK, Karnes RJ, Kwon ED, Lohse CM, Rangel LJ, Mynderse LA, Cheville JC, Sebo TJ. Prostate cancer ki-67 (mib-1) expression, perineural invasion, and gleason score as biopsy-based predictors of prostate cancer mortality: the mayo model. Mayo Clin Proc. 2014;89(3):308–18.
70. Fisher G, Yang ZH, Kudahetti S, Møller H, Scardino P, Cuzick J, Berney DM, Transatlantic Prostate Group. Prognostic value of ki-67 for prostate cancer death in a conservatively managed cohort. Br J Cancer. 2013;108(2):271–7.
71. Cuzick J, Yang ZH, Fisher G, Tikishvili E, Stone S, Lanchbury JS, Camacho N, Merson S, Brewer D, Cooper CS, Clark J, Berney DM, Møller H, Scardino P, Sangale Z, Transatlantic Prostate Group. Prognostic value of pten loss in men with conservatively managed localised prostate cancer. Br J Cancer. 2013;108(12):2585–9.
72. Lotan TL, Carvalho FL, Peskoe SB, Hicks JL, Good J, Fedor HL, Humphreys E, Han M, Platz EA, Squire JA, De Marzo AM, Berman DM. Pten loss is associated with upgrading of prostate cancer from biopsy to radical prostatectomy. Mod Pathol. 2015;28(1):128–37.
73. Mithal P, Allott E, Gerber L, Reid J, Welbourn W, Tikishvili E, Park J, Younus A, Sangale Z, Lanchbury JS, Stone S, Freedland SJ. Pten loss in biopsy tissue predicts poor clinical outcomes in prostate cancer. Int J Urol. 2014;21(12):1209–14.

Patient Selection for Focal Therapy of Prostate Cancer

10

Arjun Sivaraman and Rafael Sanchez-Salas

Introduction

The primary landscape of focal therapy (FT) in the management of prostate cancer (PCa) is rapidly evolving over the past decade. The process of defining an "ideal patient" for FT has been a dynamic process in accordance with the growing understanding and limitations of FT. The focus of FT has shifted from being an alternative for active surveillance (AS) to an acceptable middle ground therapeutic option between AS and radical treatment (surgery/radiation) [1]. The decision algorithm has seen a gradual shift over the years, and currently the focal therapist must answer the following questions before selecting patients for tissue preservation strategies: First, does this cancer need treatment? If not, they can be safely monitored with active surveillance. Second, if treatment is indicated, are tissue preservation strategies amenable? With this understanding, we are keen to avoid over-/undertreatment, and it is possible that most of the future FT patients will be a subset of those who underwent radical treatments in the past [2]. Although there is no high-level evidence to support the present trend of FT, phased evaluation of a number of retrospective and noncontrolled prospective studies has culminated in an eventual systematic review [3]. Moreover, an international panel of expert focal therapists convenes periodically to evaluate the recent literature and provide consensus statements for patient selection and guidance for future trials [4–7] (Table 10.1). The aim of this chapter is to present a brief review of factors that influence the patient selection for FT and also review the recent international consensus panel recommendations.

What Tumors Should We Treat with Focal Therapy?

The growing enthusiasm for tissue-preserving ablative strategies for prostate cancer and encouraging oncological and good functional results have resulted in increased acceptance of this treatment modality by patients and urologists worldwide. Theoretically, energies used for ablative therapies produce irreversible tissue destruction in the intended treatment zone. However, there are several factors to be considered in the appropriate case selection for focal therapy.

A. Sivaraman
Urology Service, Department of Surgery, Memorial Sloan Kettering Cancer Center, New York, NY, USA

R. Sanchez-Salas (✉)
Department of Urology, L'Institut Mutualiste Montsouris, Paris, France
e-mail: rafael.sanchez-salas@imm.fr

© Springer International Publishing AG 2017
T.J. Polascik (ed.), *Imaging and Focal Therapy of Early Prostate Cancer*, Current Clinical Urology, DOI 10.1007/978-3-319-49911-6_10

Table 10.1 Evolution of consensus and recommendations for focal therapy

2007	2010	2013	2015
Clinical Clinical stage T1 or T2a PSA <10 ng/ml PSA density <0.15 ng/ml/ml PSA velocity <2 ng/ml yearly in the year prior to diagnosis *Biopsy* Minimum 12 cores No Gleason 4 or 5 Maximum percentage of cancer in each core (e.g., 20 %) Maximum length of cancer in each core (e.g., 7 mm) Maximum percentage of total cores with cancer (e.g., 33 %) *Imaging* Single lesion with a maximum size (e.g., 12 mm) Maximum length of capsular contact (e.g., 10 mm) No evidence of extraprostatic extension or seminal vesicle invasion	(1) Candidates for focal therapy should ideally undergo transperineal template-mapping biopsies, although a state-of-the-art multifunctional MRI with TRUS biopsy at expert centers may be acceptable (2) Candidates for focal therapy should have a life expectancy of 10 or more years (3) Patients with previous prostate surgery should be counseled with caution (4) Patients with previous radiotherapy to the prostate or pelvis should not be treated until more data are available, although the panel accepts that focal salvage therapy may be a possibility in the future (5) The effects of focal therapy on men with lower urinary tract symptoms are not well known. These men should be counseled with caution (6) There will be specific attributes that are more related to the energy source than to focal therapy in general. Issues such as prostate size, presence of prostatic calcification, cysts, TUR cavity, access to rectum, and concurrent inflammation of rectal mucosa may need to be taken into consideration when selecting the optimal therapy (7) Focal therapy should be limited to patients of low to moderate risk (8) Focal therapy should be limited to men with clinical T2a or less N0M0 disease (9) Focal therapy should be limited to men with radiologic ≤T2b N0M0 disease (10) Defining the topography of the cancer is important. Disease that is predominantly apical or anterior in disposition may be technically difficult to manage with existing treatment modalities (11) The long-term effects of focal therapy on potency/erectile functions are not known. Men should be counseled in this regard before therapy	*Inclusion criteria* Serum PSA • PSA <15 ng/ml • PSA >15 ng/ml should be counseled with caution Clinical stage, T1c–T2a Pathology • Gleason score 3+3 • Gleason score 3+4 Life expectancy, >10 years Prostate volume, any; except in case of HIFU, <40 ml *Exclusion criteria* Previous treatment • Previous treatment of the primary cancer within the prostate • Previous hormone treatment for prostate cancer within 6 months before trial • Previous radiation to the pelvis • Active urinary tract infection Radiologic imaging • PI-RADS score <3; clinically significant cancer is equivocal • Extracapsular extension or seminal vesicle invasion Lymph node or bony metastasis	(1) Patients with intermediate risk and patients with unifocal and multifocal prostate cancer are eligible for focal treatment (2) MRI-targeted or template-mapping biopsy should be used to plan treatment (3) Planned treatment margins should be 5 mm from the known tumor (4) Prostate volume or age should not be a primary determinant of eligibility (5) Foci of indolent cancer can be left untreated when treating the dominant index lesion

PSA prostate-specific antigen, *MRI* magnetic resonance imaging, *TRUS* transrectal ultrasound, *TUR* transurethral resection, *HIFU* high-intensity focused ultrasound, *PI-RADS* Prostate Imaging Reporting and Data System

Patient Factors

Several clinical and social aspects of the patient need to be carefully considered during appropriate candidate selection. First, age and associated comorbidities of the patient should be evaluated when considering focal therapy. Ideally, healthier patients with a life expectancy of at least 10 years will be appropriate for providing tissue preservation treatment [8]. Older and sicker patients are more likely to die of other non-cancer-related causes. Providing FT for younger patients is often seen with skepticism, but with longer learning experience, focal therapists are more willing to ablate this cohort of patients with good cancer control and better preservation of genitourinary functions including orgasmic and ejaculatory potential. Second, patients not eligible for surgery due to non-cancer causes (prior pelvic surgery) are often treated with radiotherapy. FT ± adjuvant treatments can be a safe alternative in selected patients provided that the cancer characteristics are favorable. Third, FT is relatively a newer treatment modality, and our understanding of treatment principles and follow-up protocols is still evolving. Though early oncological outcomes are promising, long-term cancer control needs verification. Hence, patients should understand and be willing for posttreatment follow-up protocols. Fourth, most of the published series have reported up to 20 % residual cancer in the treated region and may also harbor insignificant cancer in the remaining prostate [9]. Patients should be aware of the re-treatment strategies, which include active surveillance, repeat FT, or radical treatment. Fifth, though patients can opt for radical prostatectomy (RP) at any point, they should be aware that the functional outcomes of salvage RP can be different from primary RP. Finally, FT is at different stages of approval by the governing bodies in different countries. Patients must realize that FT may be offered in a research setting or should have the knowledge of the local insurance policies.

Tumor Factors

A most interesting transition in the patient selection for FT was noted in the tumor characteristics that were recommended for focal ablation. As mentioned earlier, FT gradually shifted upstream from low-volume/low-grade cancers toward increasing volume and higher grade. There is no high-level evidence to support this transition except for the surgeon's learning curve and increasing confidence; promising results with the initial cases prompted this change.

Impact of Magnetic Resonance Imaging

Before discussing the various tumor factors that can influence the candidate selection for FT, we should understand the evolution of cancer localization strategies over the past decade. One of the major impacts in the patient selection process is the addition of prostate imaging to the diagnostic armamentarium. Earlier FT series were based on the cancer characteristics of transrectal ultrasound (TRUS)-guided and transperineal mapping biopsies [10]. Random and nontargeted biopsies have the inherent drawback of inaccuracies in tumor volume, grade, and localizations. Transperineal template-guided biopsies are extensive volume-based biopsy protocols that can overcome the limitations of random biopsies, but they are often elaborate, need anesthesia, and have slightly higher post-procedure morbidity [11]. Introduction of multiparametric magnetic resonance imaging (mpMRI) has revolutionized cancer detection and hence appropriateness of cancer selection [12]. Currently, mpMRI includes T2-weighted images with two functional images (perfusion and diffusion). Several MRI grading systems (Prostate Imaging Reporting and Data System [PI-RADS], Likert, European Society of Urogenital Radiology [ESUR], etc.) are being used to predict the probability of cancer in MRI-detected abnormalities. Sensitivity of MRI for cancer detection is 80 % in peripheral zone and 81 % in transitional zone. In biopsy-naïve patients, MRI increases the frequency of significant cancer detection to 50 % in low-risk and 71 % in high-risk patients. In previous negative biopsies, 72–87 % of MRI-guided biopsies show significant cancer. In low-risk patients, MRI has a negative predictive value up to 98 % to exclude clinically significant disease [13]. In addition to cancer identification, MRI also provides guidance for targeted biopsies. With most urologists adopting some form of MRI-targeted biopsies,

the overall accuracy of cancer localization and characterization is likely to improve. The most important message to be considered in this transition from random to targeted biopsies is the interpretation of cancer characteristics in the biopsy may vary.

Though we do not have any defined guidelines, there are several cancer characteristics to be considered when selecting a patient for focal treatment:

- *Cancer Size*: Currently, there is no definite limitation to FT based on cancer size. As mentioned earlier, the way we report and analyze cancer volume has changed dramatically. Conventionally, in the era of random biopsies, maximal cancer percentage in core <20 %, maximal cancer length in each core <7 mm, and maximal cores with cancer <33 % were used [4]. These criteria still hold for MRI-invisible cancers, but MRI visibility and the targeted biopsy have significantly replaced the older criteria, which was based on assumptions. Cancer volume can be effectively calculated using MR images, and any cancer less than 0.5 cc is more likely to represent insignificant disease and does not need treatment. Any cancer greater or equal to 5 mm in target biopsy is more likely to harbor clinically significant cancer and can be eligible for FT [14–16]. There is no strict upper limit of cancer volume in unifocal cancer in case selection for FT. However, Gleason grade, boundaries, and morphological distribution of cancer within prostate are important factors to be considered.
- *Cancer Grade*: Gleason grade is an important factor to be considered in the evaluation of the patient with PCa for FT. With routine use of MRI, grading systems, and guided biopsies, the Gleason grade of the biopsy is more likely to represent the actual score. In the earlier days of focal ablation, the presence of Gleason 4 in the biopsy was considered as an exclusion criterion for FT. However, many men with low-risk features on biopsy are found to have non-dominant Gleason 4 disease at radical prostatectomy with very little impact on the clinical course [17]. Hence, the presence of Gleason 4 disease was eventually considered amenable for FT. With longer experience, most urologists are currently comfortable to extend the indications for Gleason 7 cancer with dominant Gleason 4 glandular pattern. This transition again underlines the fact that the target cohort for treatment with FT is gradually shifting from low-risk to predominantly intermediate-risk disease. Routine treatment of Gleason 8 or more is currently not recommended for clinical practice. Several focal therapists are performing FT for carefully selected patients with Gleason score >7, and the results in the future will enlighten the clinical performance of FT in this cohort of patients.
- *Multifocality*: Multifocality is a known phenomenon in PCa, and the concept of the "index lesion" is firmly based on the postulate that in a background of multiple cancers with the prostate, the largest lesion is most likely to harbor the lethal clone with the highest Gleason grade and also influences the lethality and metastatic potential of the disease [18]. The congruous location of the large volume and highest Gleason grade had been demonstrated by several authors [19–21]. The multifocal tumors within the prostate can be monoclonal or polyclonal. Monoclonal hypothesis states that the transforming event leading to neoplasia originates in one particular cell and is spread by intraprostatic metastasis, while polyclonality arises from a field effect to a common inciting stimulus with several cells undergoing different transforming pathways. Most of the genetic analyses of multicentric prostate cancer suggest varying patterns of allelic losses on chromosomes indicating clonal diversity. But monoclonality cannot be ruled out completely since the clonal divergence can result after intraprostatic spread [22–24]. However, in the Project to Eliminate Lethal Prostate Cancer (PELICAN), Liu et al. analyzed 94

metastatic deposits from 30 men who died of prostate cancer. Copy number analysis and high-resolution genome-wide single nucleotide polymorphism were used to demonstrate that metastatic deposits had monoclonal origin. However, the authors did not trace the anatomic location of the lethal clone within the prostate [25]. These results are in conjunction with the single-locus genetic study evaluating the role of TMPRSS2-ETS in advanced PCa [26]. Despite tumor heterogeneity in primary cancers, the metastatic clones arose from a single source.

Currently, we do not have evidence to demonstrate the natural history on non-index lesions after the ablation of the primary index lesion. The relationship between the progression of the secondary lesion and the presence of large primary lesion in the vicinity is unknown. Most of the published literature on FT has specifically included unilateral and unifocal lesions for evaluation. In case of multifocal tumors, care should be taken to characterize all the visible foci to eliminate multifocal significant disease, and most of the focal therapists favor ablation of the index lesion alone.

- *MRI Visibility*: As mentioned earlier, routine use of MRI in FT has revolutionized the patient selection. The utility of MRI to accurately localize cancer lesion is shown in several studies and, more importantly, has a high negative predictive value (63–98 %) to exclude significant cancers in the absence of suspicious lesions [12]. Higher PI-RADS score in mpMRI correlated with the index lesion in more than 90 % of the cases, and the index lesions (<5 %) that were missed had low-volume (<0.4 ml) cancers. An ideal patient for FT can be described as one with a visible MRI lesion of significant cancer probability score (PI-RADS, Likert, etc.) and positive biopsy with significant cancer in the corresponding suspicious area and the absence of significant cancer in the random biopsy of nontargeted areas. FT for MRI-invisible cancers should be considered with caution, and saturation biopsy techniques such as transperineal mapping biopsy can be useful in accurately localizing the cancer.
- *Cancer Location*: Our understanding of the influence of topographic cancer location within the prostate on focal therapy is still evolving. The previous versions of consensus statements on patient selection have mentioned that the prostate volume can be a limiting factor for high-intensity focused ultrasound (HIFU) treatment [6]. This is due to the fact that during HIFU treatment, there can be dissipation of ultrasound (US) waves in longer focal points. The resulting prostatic edema can potentially displace the target from the firing zone during treatment [27]. This is particularly true when ablating an anterior zone cancer, the US waves need to travel a longer distance to reach the focal point, and after a few initial passages, the intervening prostatic tissue undergoes edema, resulting in pushing the target area farther away. Another critical cancer location is the apex close to the sphincters. Most of the FT experience worldwide was thermal-based energies (cryotherapy and HIFU), and both these energies are found to cause some degree of sphincteric dysfunction based on the whole-gland experience. However, brachytherapy, which can also be delivered focally, has demonstrated relatively low incontinence rates, and this observation may be due to the rapid falloff of the radiation within a few millimeters from the implantation seed. A model of personalizing FT energy based on intraprostatic cancer location has been proposed in the literature, and it needs verification in future prospective studies [28].

Posterior Cancers

HIFU is the least invasive of all the currently employed energies for FT and hence should be offered whenever feasible. PCa most commonly arises from the peripheral zone and more often below the level of the urethra. HIFU appears to

have more advantages in this cancer location considering the shorter focal point and more precise contouring of the target area.

Anterior Cancers

The efficacy of HIFU tends to decrease over longer focal points. However, cryotherapy, with ease of access to anterior zone, can be delivered through transperineal needles.

Apical Cancers

Both cryotherapy and HIFU tend to produce incontinence in apical cancers for reasons described earlier. Brachytherapy can be a potential treatment option in this location considering the rapid falloff of the radiation effect distal to the seeds.

Risk Group

Risk classification of PCa is one of the important factors to be considered when selecting patients for focal therapy. Most of the initial studies on FT were focused on low-risk category and with growing experience and confidence. Currently, focal therapists are aiming to treat mainly the intermediate-risk group to avoid overtreatment. Irrespective of the risk groups that will be discussed as follows, other cancer parameters should also be considered collectively in the decision-making process.

Low Risk

In the low-risk prostate cancer group, the first decision to be made is: Does this patient need treatment? If treatment is not required, he can be safely managed with active surveillance. However, FT can be offered at the patient's request to overcome the anxiety of harboring cancer and simultaneously avoiding radical surgery and preservation of optimal genitourinary function [29]. Selected patients with large volume, unifocal low risk can also be offered FT.

Intermediate Risk

The decision to treat intermediate-risk patients with FT also depends on the other cancer characteristics such as volume, MRI visibility, focality, etc. [7]. With a combination of these factors, it is important to decide if tissue preservation is amenable. MRI-invisible cancers, non-correspondence of MRI lesion and biopsy localization, and larger percent of Gleason 4 glands should be approached with caution to rule out multifocal significant disease.

High Risk

FT is not an optimal treatment option for high-risk patients, and radical treatment will address the disease more completely. However, selected patients with organ-confined, unifocal, small-volume disease and careful evaluation to rule out metastasis can be considered in a research setting with or without adjuvant treatment. Figure 10.1 shows a summary of today's indications for FT in PCa.

Consensus Panel Recommendations

Focal therapy experts around the world convene periodically to critically analyze the progress and the limitations of focal therapy. The published literature and personal experiences are discussed to set a pathway for future direction of research and clinical applications.

In 2007 [4], the first international panel started with urologic oncologists, radiotherapists, medical oncologists, epidemiologists, and pathologists all with interests in PCa management. The panel devised some practical selection criteria for FT and focused mainly on the low-volume, low-risk cancer group. This was a conservative beginning to FT and was logical since there was only a presumed but unproven oncological and functional advantage to FT. However, the panel encouraged for future trials to evaluate the clinical performance of FT.

The second panel convened in 2009 was more elaborate and addressed several issues after implementation of previous criteria into clinical use [5]. The panel was geared toward eradication of all known cancers in the prostate and made the presence of Gleason 4 gland as not a contraindication for FT. Much emphasis was placed on

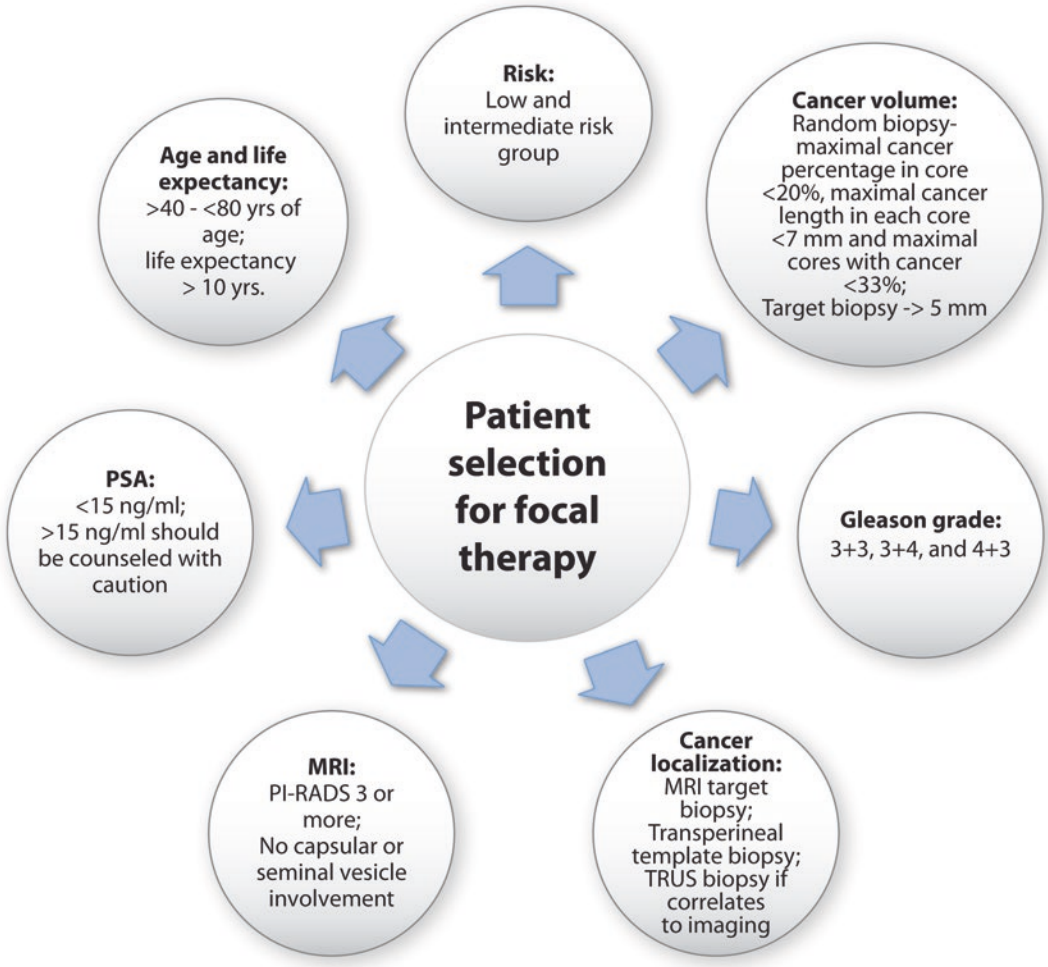

Fig. 10.1 Summary of patient selection criteria for focal therapy in 2016

selection process, and they agreed that transperineal mapping biopsy can be a standard technique for case selection to avoid missing other significant cancers. The role of MRI was also recognized as a potential tool for cancer localization.

Subsequently, in the third panel in 2013 [6], 48 experts participated, and a four-stage consensus project based on a modified Delphi process was conducted. Questionnaires were devised to address various issues of FT, including the candidate selection. Finally, 13 panelists discussed the acquired data, interpretation of results, and derived a conclusion for FT use: prostate-specific antigen (PSA) <15 ng/ml, clinical stage T1c–T2a, Gleason score 3+3 or 3+4, life expectancy of >10 years, and any prostate volume. This panel's decision was a significant move from the previous selection criteria, and the patients were more individually defined based on cancer characteristics.

More recently, the fourth panel convened in 2014 [7], and a similar questionnaire-based consensus approach was adopted to guide FT case selection. Though this mode of statements represents a low level of evidence for clinical practice, conducting a prospective randomized trial is very difficult for such newer innovations. Key points in this panel on patient selection were as follows:

- Patients with intermediate-risk PCa are eligible for focal treatment.
- Patients with unifocal and multifocal disease are eligible, and foci of indolent cancer can be left untreated when treating the dominant index lesion.
- MRI-targeted or template-mapping biopsy should be used to plan treatment.
- Prostate volume or age should not be a primary determinant of eligibility.

Conclusion

Focal therapy for prostate cancer is growing as an acceptable treatment option both by the patients and the physicians. One of the key factors for FT success is appropriate patient selection, and there are several patient-related and cancer-related factors to consider in the decision-making process. Patients should receive a thorough explanation about the advantages and the limitations of FT and be willing to undertake follow-up protocols. The routine use of MRI and guided biopsies has made a significant impact on accurate cancer localization. MRI-invisible and MRI discordant lesions should be approached with caution using mapping biopsies. Other cancer-related factors such as cancer volume, grade, location, and risk category should be carefully considered for a successful FT outcome. Overall, the focus of FT has shifted from low-risk patients to the intermediate-risk group, and with future research, we can further define the indications more accurately.

References

1. Marshall S, Taneja S. Focal therapy for prostate cancer: the current status. Prostate Int. 2015;3(2):35–41.
2. Emberton M. Why focal therapy is a legitimate and necessary response to a changing world. J Urol. 2015;194(4):875–6.
3. Valerio M, Ahmed HU, Emberton M, Lawrentschuk N, Lazzeri M, Montironi R, et al. The role of focal therapy in the management of localised prostate cancer: a systematic review. Eur Urol. 2014;66(4):732–51.
4. Eggener SE, Scardino PT, Carroll PR, Zelefsky MJ, Sartor O, Hricak H, et al. Focal therapy for localized prostate cancer: a critical appraisal of rationale and modalities. J Urol. 2007;178(6):2260–7.
5. de la Rosette J, Ahmed H, Barentsz J, Johansen TB, Brausi M, Emberton M, et al. Focal therapy in prostate cancer-report from a consensus panel. J Endourol. 2010;24(5):775–80.
6. van den Bos W, Muller BG, Ahmed H, Bangma CH, Barret E, Crouzet S, et al. Focal therapy in prostate cancer: international multidisciplinary consensus on trial design. Eur Urol. 2014;65(6):1078–83.
7. Donaldson IA, Alonzi R, Barratt D, Barret E, Berge V, Bott S, et al. Focal therapy: patients, interventions, and outcomes--a report from a consensus meeting. Eur Urol. 2015;67(4):771–7.
8. Passoni NM, Polascik TJ. How to select the right patients for focal therapy of prostate cancer? Curr Opin Urol. 2014;24(3):203–8.
9. Feijoo ERC, Sivaraman A, Barret E, Sanchez-Salas R, Galiano M, Rozet F, et al. Focal high-intensity focused ultrasound targeted hemiablation for unilateral prostate cancer: a prospective evaluation of oncologic and functional outcomes. Eur Urol. 2015;69:214–20.
10. Gravas S, Tzortzis V, de la Riva SIM, Laguna P, de la Rosette J. Focal therapy for prostate cancer: patient selection and evaluation. Expert Rev Anticancer Ther. 2012;12(1):77–86.
11. Sivaraman A, Sanchez-Salas R, Barret E, Ahallal Y, Rozet F, Galiano M, et al. Transperineal template-guided mapping biopsy of the prostate. Int J Urol. 2015;22(2):146–51.
12. Schoots IG, Roobol MJ, Nieboer D, Bangma CH, Steyerberg EW, Hunink MGM. Magnetic resonance imaging-targeted biopsy may enhance the diagnostic accuracy of significant prostate cancer detection compared to standard transrectal ultrasound-guided biopsy: a systematic review and meta-analysis. Eur Urol. 2014;68:438–50.
13. Bjurlin MA, Meng X, Le Nobin J, Wysock JS, Lepor H, Rosenkrantz AB, et al. Optimization of prostate biopsy: the role of magnetic resonance imaging targeted biopsy in detection, localization and risk assessment. J Urol. 2014;192(3):648–58.
14. Matsugasumi T, Baco E, Palmer S, Aron M, Sato Y, Fukuda N, et al. Prostate cancer volume estimation by combining magnetic resonance imaging and targeted biopsy proven cancer core length: correlation with cancer volume. J Urol. 2015;194(4):957–65.
15. Muller BG, van den Bos W, Pinto PA, de la Rosette JJ. Imaging modalities in focal therapy: patient selection, treatment guidance, and follow-up. Curr Opin Urol. 2014;24(3):218–24.
16. Toner L, Weerakoon M, Bolton DM, Ryan A, Katelaris N, Lawrentschuk N. Magnetic resonance imaging for prostate cancer: comparative studies including radical prostatectomy specimens and template transperineal biopsy. Prostate Int. 2015;3(4):107–14.
17. Ward JF, Pisters LL. Considerations for patient selection for focal therapy. Ther Adv Urol. 2013;5(6):330–7.
18. Ahmed HU. The index lesion and the origin of prostate cancer. N Engl J Med. 2009;361(17):1704–6.
19. Karavitakis M, Winkler M, Abel P, Livni N, Beckley I, Ahmed HU. Histological characteristics of the

index lesion in whole-mount radical prostatectomy specimens: implications for focal therapy. Prostate Cancer Prostatic Dis. 2011;14(1):46–52.
20. Arora R, Koch MO, Eble JN, Ulbright TM, Li L, Cheng L. Heterogeneity of Gleason grade in multifocal adenocarcinoma of the prostate. Cancer. 2004; 100(11):2362–6.
21. Wise AM, Stamey TA, McNeal JE, Clayton JL. Morphologic and clinical significance of multifocal prostate cancers in radical prostatectomy specimens. Urology. 2002;60(2):264–9.
22. Bostwick DG, Shan A, Qian J, Darson M, Maihle NJ, Jenkins RB, et al. Independent origin of multiple foci of prostatic intraepithelial neoplasia: comparison with matched foci of prostate carcinoma. Cancer. 1998;83(9):1995–2002.
23. Hügel A, Wernert N. Loss of heterozygosity (LOH), malignancy grade and clonality in microdissected prostate cancer. Br J Cancer. 1999;79(3–4):551–7.
24. Jones TD, Wang M, Eble JN, MacLennan GT, Lopez-Beltran A, Zhang S, et al. Molecular evidence supporting field effect in urothelial carcinogenesis. Clin Cancer Res. 2005;11(18):6512–9.
25. Liu W, Laitinen S, Khan S, Vihinen M, Kowalski J, Yu G, et al. Copy number analysis indicates monoclonal origin of lethal metastatic prostate cancer. Nat Med. 2009;15(5):559–65.
26. Mehra R, Tomlins SA, Yu J, Cao X, Wang L, Menon A, et al. Characterization of TMPRSS2-ETS gene aberrations in androgen-independent metastatic prostate cancer. Cancer Res. 2008;68(10):3584–90.
27. Clyne M. Prostate cancer: prostatic swelling and shift upon HIFU. Nat Rev Urol. 2013;10(6):306.
28. Sivaraman A, Barret E. Focal therapy for prostate cancer: an "À la Carte" approach. Eur Urol. 2016;69:973–5.
29. Klotz L. Active surveillance and focal therapy for low-intermediate risk prostate cancer. Transl Androl Urol. 2015;4(3):342–54.

Prostate Focal Therapy: Definitions and Common Terminology

11

John F. Ward

Introduction

The term "focal therapy" as applied to the treatment of localized prostate cancer is a blanket term that encompasses any treatment of the prostate with the intent to preserve some portion of the prostate gland. The intent behind this approach is generally to affect a curative prostate cancer treatment but with a reduced therapy-related morbidity profile. This concept of subtotal prostate therapy, or less than radical therapy for prostate cancer (radical radiation, radical surgery), is intended to allow a surgeon to provide a very personalized treatment of the prostate gland based upon the location and extent of the prostate cancer within the gland of the specific man. Rather than the brute, "one-size-fits-all" approach that has been the standard to prostate cancer for decades, focal therapy is a tailored approach to treating a cancer within the unique patient. Therefore, there is no one "focal therapy." Focal therapy by definition may involve the treatment and/or preservation of different proportions of the prostate gland or different regions of the prostate gland (apex, base, lateral, anterior) depending upon the extent and location of the disease. Focal therapy is tightly dependent upon the accuracy with which we can precisely identify the tumor.

Onik et al. in 2002 (updated in 2008), then Bahn et al. in 2006, were the first to report on patients with prostate cancer treated with a focal ablation of a single hemisphere of the prostate gland [1–3]. In total, these represent retrospective reports of only 79 patients; yet, they also demonstrate that both good oncologic outcomes and functional outcomes could be achieved with this approach. Despite the paucity of reports and lack of prospective studies involving subtotal prostate ablation, there has been a tremendous increase in the use of focal ablation within the urologic community. Ward and Jones looked at the number of patients captured within the Cryoablation On-Line Database (COLD) registry who were categorized as "subtotal" prostate cryoablation [4]. They observed a dramatic increase in the number of focal cryoablations performed per year from 46 in 1999 to 567 in 2005 ($p < 0.01$). However, a closer examination of the series reveals a lack of consistency or nomenclature employed to describe the volume and location of the prostate tissue targeted for destruction or preservation.

At this critical juncture in the development of truly a new paradigm for prostate cancer management, an understandable nomenclature that communicates the treatment intent is necessary [5]. As the approach and techniques for identifying the cancer and targeting the tissue for destruction advances, this common language is likely to grow.

J.F. Ward (✉)
Department of Urology, M. D. Anderson Cancer Center, Houston, TX, USA
e-mail: jfward@mdanderson.org

© Springer International Publishing AG 2017
T.J. Polascik (ed.), *Imaging and Focal Therapy of Early Prostate Cancer*, Current Clinical Urology, DOI 10.1007/978-3-319-49911-6_11

Focal therapy as it was initially performed was essentially a "blind" procedure. It was based upon the interpretation of a biopsy template, then applying that information to a region(s) of the prostate that seemed to contain the dominant cancer. To put it another way, focal therapy was initially being performed by treating a region of the prostate that encompassed both the predicted area of cancerous tissue and a varying amount of surrounding normal prostate tissue. Unlike organ-preserving therapies for other solid organ malignancies (liver, kidney), which are guided visually because the surgeon can visualize the tumor itself, prostate cancer has been relatively invisible to imaging techniques. Therefore, focal therapy of prostate cancer encompassed a region around which the cancer was identified, which itself was based upon a blind biopsy.

In developing a nomenclature for "focal therapy", the volume and location of the ablation region is what becomes important for us to communicate.

Multiparametric magnetic resonance imaging (mpMRI) of the prostate has begun to lift the veil that has hid prostate tumors in-situ [6]. Combined with in-bore or ultrasound fusion-targeted biopsy and targeted ablation, the possibility of truly conformal prostate cancer therapy has begun to seem a bit closer. However, limitations remain as we discover the inability of the current technology to accurately define cancer volume and margins [7]. Focal therapists continue to treat a margin around the identified tumor that essentially results in a zonal or regional ablation.

As focal therapy for prostate cancer is further studied we may find that it is possible to ablate the majority of the prostate in a specific region(s) of the gland (anterior region, for instance) and have no resulting effect upon urinary continence or erectile function. Alternatively, we may find that the same volume of tissue ablated in a different pattern or region of the prostate (e.g., the apex) may have a significantly different impact on treatment-related morbidity. A common nomenclature providing more information beyond the term "focal therapy" will continue to provide us with information we need to develop more personalized therapy for prostate cancer.

The nomenclature used to describe a treatment template is independent of the ablative energy employed; whether with cryoablation, high-intensity focused ultrasound, brachytherapy, interstitial laser ablation, or other energy sources, current techniques for focal ablation can be described using one of these terms with small modifiers (e.g., right dominant, left dominant, etc.).

Focal Therapy Nomenclature

Nerve Sparing (Unilateral or Bilateral)

Nerve-sparing ablation is the destruction of all prostate tissue from the base to the apex and from the anterior to the posterior, *excepting* the posterior lateral region on one or both sides near the expected location of the erectile neurovascular bundle(s) (Fig. 11.1).

With cryoablation as the destructive energy force, this template can be employed either with or without the use of a cryoprobe, which is warmed with pressurized helium, positioned near one or both erectile nerves. This template can also be achieved with high-intensity focused ultrasound (HIFU) wherein the energy is not directed laterally, near one or both neurovascular bundles.

It is well recognized that the posterior/lateral location is a common site for prostate cancer. Canine data has raised concerns about cancer

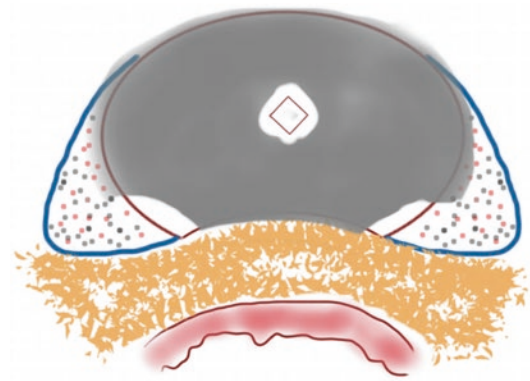

Fig. 11.1 Bilateral nerve-sparing ablation

control when this template is employed [8]. Additionally, the location of the erectile nerves is now better described and known to exist in a broad swath of periprostatic tissue, not in a single, posterior lateral location [9].

Hemi-ablation

Hemi-ablation is the unilateral (hemisphere) destruction of all prostate tissue that is present to the left or right of the urethra (dictated by the laterality of the targeted cancer) and from the apex to the base and anterior to posterior (Fig. 11.2).

The theoretical benefit is to maximally preserve the neurovascular bundle contralateral to the treated, cancerous side of the prostate. This can be thought of as a unilateral nerve bundle preservation; however, the functional outcomes in the reports by Bahn and Onik where this template was employed are significantly better than is observed with unilateral nerve bundle preservation at radical prostatectomy [2, 3, 10].

Anterior Hockey-Stick Ablation (Anterior Three-Fourth)

This is the extension of the hemi-ablation template across the midline only in the anterior region of the prostate, contralateral to the dominant cancer (Fig. 11.3).

Described first by Ward et al., this template has the theoretical benefits of treating potentially under-sampled, unrecognized cancers within the anterior region of the prostate contralateral to a dominant cancer that exists within the dominantly treated prostate hemisphere [11]. At a microscopic level, this template still provides preservation of the contralateral neurovascular bundle because of its delta shape in the periprostatic region, yet provides a significant amount of prostate gland ablation, especially in a region of the prostate that is under-sampled by standard transrectal prostate biopsy.

Posterior Hockey-Stick Ablation (Posterior Three-Fourth)

Posterior three-fourth ablation is the extension of the hemi-ablation to include the contralateral posterior region (Fig. 11.4). The template has the theoretical advantages of treating almost the entire prostate peripheral zone, while avoiding overlapping energy delivery to the urethra. However, the posterior peripheral zone of the prostate is better sampled than the anterior zone, and thus contralateral significant tumors are less likely un-sampled by standard prostate biopsy. Additionally, the delta-shaped neurovascular bundle is much more likely to receive lethal energy with this template, potentially negating the intent to preserve erectile function. In a prospective study that employed this

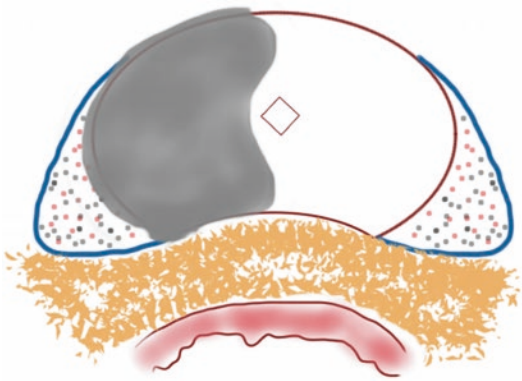

Fig. 11.2 Hemi-ablation

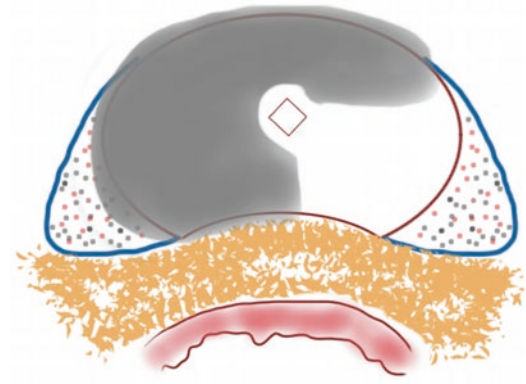

Fig. 11.3 Anterior hockey-stick ablation (right dominant with left wing)

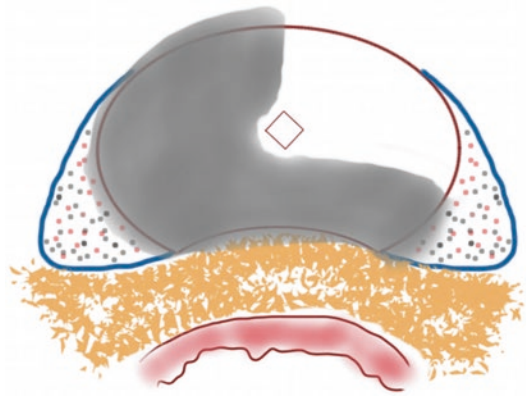

Fig. 11.4 Posterior hockey-stick ablation (right dominant with left wing)

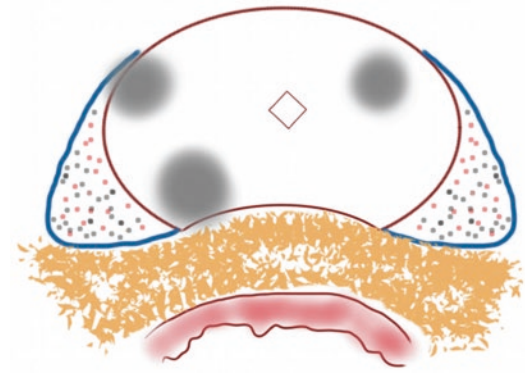

Fig. 11.5 Targeted focal therapy

template with HIFU as the ablative energy, it did result in decreased time of catheter bladder drainage than whole-gland HIFU. Thus, this template may offer an improvement in the urinary morbidity profile, especially when erectile function is not adequate at baseline [12].

Targeted Focal Therapy

Targeted focal therapy intends to minimize the collateral damage of surrounding normal prostate tissue and accurately target a volume of the prostate limited by the volume of the cancer (Fig. 11.5).

Because our current ability to visualize the prostate cancer within the prostate gland is not at the level of sensitivity or specificity that exists in other cancerous organ sites, this template requires very accurate prostate mapping—usually achieved through extensive prostate biopsy to create a three-dimensional (3D) model of the prostate and its contained tumors [13]. It is proposed that such definition of tumor location(s) may be achieved through a transperineal template-guided saturation biopsy schema followed by co-registering a three-dimensional image of the patient's prostate with the histology [14]. Technical limitations to a saturation, mapping biopsy—such as respiratory movement, needle deflection, deformation of the prostate with swelling, and contact of the needle upon the capsule—have all called into question the accuracy of the information obtained from this type of extensive saturation biopsy. Multiparametric MRI may provide an alternative approach to target acquisition. Studies using MRI to visualize the delivery of ablative energy are being conducted [15–17].

Eventually, it is expected that evolutions in prostate cancer imaging will allow real-time visualization of the tumor within the prostate and will be sufficiently sensitive and specific to guide and monitor ablative therapy in real time.

Quadrant (Zonal) Ablation

Zonal ablation is confining the treatment to a region allowing broad margins beyond known areas of cancer (Fig. 11.6). This form of focal therapy is similar to targeted focal therapy, except that it recognizes the inherent inaccuracies of current blinded biopsy strategies and thus ablates a zone of tissue that contains the cancer and a broader margin of normal tissue.

The limitation currently present in "knowing" the histology throughout the prostate due to spacing of the saturation biopsy needles, or the limitations placed by physics on prostate cancer imaging, has led to the concept of treating the prostate in up to 12 different regions. This concept allows the use of an accurate prostate biopsy mapping strategy that provides better assurance of an equal sampling of all

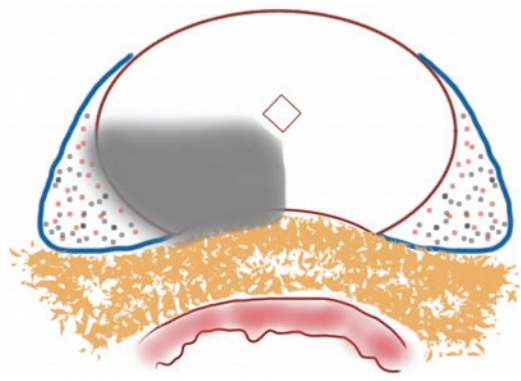

Fig. 11.6 Quadrant (zonal) ablation

regions of the prostate [18]. Conceptually, the prostate is divided into anterior and posterior zones consisting of the apex, middle, and base regions of the prostate. On the basis of the biopsy findings within each zone, ablation of the cancerous zone is performed. This pattern results in a greater rim or margin of regional tissue destruction than is achieved with targeted focal therapy, thereby allowing for the lack of precision that may occur using even the most aggressive saturation biopsy or imaging physics (i.e., ultrasound wavelength or voxel limitations of magnetic resonance spectroscopy).

Conclusion

As a concept supported by promising preliminary study, focal therapy for prostate cancer holds tremendous promise to balance the risks of prostate cancer treatments with the risks of the prostate cancer to the patient himself. Development of this field will take place at many centers throughout the world simultaneously. A nomenclature that describes what our intent is beyond the vagueness of just "focal therapy" is necessary. Our ideas and results will be better communicated with our peers through a common nomenclature. This enables an accurate level of knowledge transfer to thoughtfully move this therapy forward, thereby shifting the entire way we approach men with prostate cancer.

References

1. Onik G, Narayan P, Vaughan D, Dineen M, Brunelle R. Focal "nerve-sparing" cryosurgery for treatment of primary prostate cancer: a new approach to preserving potency. Urology. 2002;60:109–14.
2. Bahn DK, Silverman P, Lee Sr F, Badalament R, Bahn ED, Rewcastle JC. Focal prostate cryoablation: initial results show cancer control and potency preservation. J Endourol. 2006;20:688–92.
3. Onik G, Vaughan D, Iotenfoe R. The "male lumpectomy": focal therapy for prostate cancer using cryoablation results in 48 patients with a least 2-year follow-up. Urol Oncol. 2008;26:500–5.
4. Ward JF, Jones JS. Focal cryotherapy for localized prostate cancer: a report from the national Cryo On-Line Database (COLD) Registry. BJU Int. 2012;109:1648–54.
5. Ward JF, Jones JS. Classification system: organ preserving treatment for prostate cancer. Urology. 2010;75:1258–60.
6. Costa DN, Pedrosa I, Donato Jr F, Roehrborn CG, Rofsky NM. MR imaging–transrectal US fusion for targeted prostate biopsies: implications for diagnosis and clinical management. Radiographics. 2015;35:696–708.
7. Kirkham APS, Emberton M, Allen C. How good is MRI at detecting and characterising cancer within the prostate? Eur Urol. 2006;50:1163–74. discussion 1175
8. Janzen NK, Han KR, Perry KT, Said JW, Schulam PG, Belldegrun AS. Feasibility of nerve-sparing prostate cryosurgery: applications and limitations in a canine model. J Endourol. 2005;19:520–5.
9. Costello AJ, Dowdle BW, Namdarian B, Pedersen J, Murphy DG. Immunohistochemical study of the cavernous nerves in the periprostatic region. BJU Int. 2011;107:1210–5.
10. Davis JW, Chang DW, Chevray P, Wang R, Shen Y, Wen S, et al. Randomized phase II trial evaluation of erectile function after attempted unilateral cavernous nerve-sparing retropubic radical prostatectomy with versus without unilateral sural nerve grafting for clinically localized prostate cancer. Eur Urol. 2009;55:1135–43.
11. Ward JF, Nakanishi H, Pisters LL, Babaian RJ, Troncoso P. Cancer ablation with regional templates applied to prostatectomy specimens from men who were eligible for focal therapy. BJU Int. 2009;104:490–7.
12. Muto S, Yoshii T, Saito K. Focal therapy with high-intensity-focused ultrasound in the treatment of localized prostate cancer. Jpn J Clin Oncol. 2008;38:192–9.
13. Hou AH, Sullivan KF, Crawford ED. Targeted focal therapy for prostate cancer: a review. Curr Opin Urol. 2009;19:283–9.
14. Onik G, Barzell W. Transperineal 3D mapping biopsy of the prostate: an essential tool in selecting patients for focal prostate cancer therapy. Urol Oncol. 2008;26:506–10.

15. Raz O, Haider MA, Davidson SR, Lindner U, Hlasny E, Weersink R, et al. Real-time magnetic resonance imaging-guided focal laser therapy in patients with low-risk prostate cancer. Eur Urol. 2010;58:173–7.
16. Stafford RJ, Shetty A, Elliott AM, Klumpp SA, McNichols RJ, Gowda A, et al. Magnetic resonance guided, focal laser induced interstitial thermal therapy in a canine prostate model. J Urol. 2010;184: 1514–20.
17. Trachtenberg J, Weersink RA, Davidson SR, Haider MA, Bogaards A, Gertner MR, et al. Vascular-targeted photodynamic therapy (padoporfin, WST09) for recurrent prostate cancer after failure of external beam radiotherapy: a study of escalating light doses. BJU Int. 2008;102:556–62.
18. Megwalu II, Ferguson GG, Wei JT, Mouraviev V, Polascik TJ, Taneja S, et al. Evaluation of a novel precision template-guided biopsy system for detecting prostate cancer. BJU Int. 2008;102:546–50.

Part IV

Multiparametric MRI and ARFI Imaging of the Prostate

12 Reading and Reporting Standards: The Prostate Imaging Reporting and Data System—What Is It and What Can It Do?

Wulphert Venderink and Jurgen J. Fütterer

Introduction

To date, 10–12 core systematic transrectal ultrasound (TRUS)-guided biopsy is the standard to diagnose prostate cancer (PCa). TRUS-guided prostate biopsy is performed in men with raised prostate-specific antigen (PSA) blood levels or an aberrant digital rectal examination (DRE). However, TRUS-guided biopsy is not an appropriate tool for selecting patients suitable for focal therapy. In addition, TRUS-guided biopsy is associated with the underdiagnosis of PCa, and it often incorrectly classifies the aggressiveness of the disease [1]. Recently, multiparametric magnetic resonance imaging (mpMRI) has been introduced. In the early years of mpMRI practice for detecting and localizing PCa, a variety of reporting standards were used. Now reporting is more and more standardized by the use of the Prostate Imaging Reporting and Data System (PI-RADS) [2].

In this chapter we will outline the PI-RADS classification according to the more recent PI-RADS version 2 and the features PI-RADS offers. First, to place the PI-RADS classification in a framework, we will discuss the role of guidelines in general medical practice and the role of reporting standards in radiology. Then, the technique of mpMRI will be addressed. Thereafter, we will briefly describe the manner of prostate assessment before the introduction of the PI-RADS classification. Finally, the content of the PI-RADS classification and the features of it will be addressed.

Guidelines and Reporting Standards in Radiology

Clinical Practice Guidelines

Decision-making by medical doctors depends on many different factors. The current evidence of the potential benefit, the awareness of side effects of the intended treatment, and the wishes of patients are examples of such factors. To help clinicians and patients make complex decisions in the face of an ever-expanding amount of medical knowledge, clinical practice guidelines (CPGs) are increasingly used. CPGs aim to streamline processes according to a set routine, and they tend to make decision-making more uniform.

The definition of a CPG according to the Institute of Medicine (IoM) is as follows: “CPGs are statements that include recommendations intended to optimize patient care that are informed by a systematic review of evidence and

W. Venderink (✉) • J.J. Fütterer
Department of Radiology and Nuclear Medicine,
Radboud University Medical Center,
Nijmegen, Gelderland, The Netherlands
e-mail: wulphert.venderink@radboudumc.nl

© Springer International Publishing AG 2017
T.J. Polascik (ed.), *Imaging and Focal Therapy of Early Prostate Cancer*,
Current Clinical Urology, DOI 10.1007/978-3-319-49911-6_12

an assessment of the benefits and harms of alternative care options" [3].

For patients, the great advantage of CPGs is that their health outcomes may improve because CPGs promote effective treatments while discouraging ineffective interventions. Guidelines also standardize care, as patients suffering from the same disease will have the same treatments or diagnostic procedures.

Clinicians also benefit from the recommendations in CPGs in cases where the clinician is unsure of which decision to make. This increases the quality of the decision and, in some cases, guidelines can help clinicians to convince patients to agree to certain treatments. Another benefit for clinicians is the possibility to turn to guidelines for medicolegal protection, because acting in accordance with guidelines is mostly assumed to reflect good clinical practice [4].

Despite the benefits CPGs may offer, they come with limitations as well. Often a variety of guidelines addressing the same, or overlapping, subjects exists; therefore, the clinician facing a complex decision may have to decide which guideline to use. Further, the quality of CPGs differs tremendously as they often reflect expert opinion instead of evidence-based medicine [5]. A lack of supportive scientific evidence may lead to misleading or flawed recommendations. For this reason, the definition of a CPG used by the IoM includes the requirement of a systematic review of evidence. However, a pitfall of such a systematic review may be an improper study design causing inaccurate recommendations. As much value is attached to CPGs, inappropriate recommendations may have widespread consequences; for example, suboptimal or even harmful treatment decisions.

Another important limitation of CPGs is that they may become outdated quickly; updating CPGs is a time-consuming and costly process. The opposite is true for medical and scientific knowledge, which is evolving rapidly [6]. Also, guidelines provide uniform recommendations for the treatment or diagnostic procedures of a typical patient. Unfortunately, guidelines including recommendations for patients deviating from "normal" are often unclear and therefore not user-friendly.

Due to such limitations, clinicians who are about to make a decision should first carefully decide whether or not to use the guideline, as well as how to use it. Clinicians should be aware of the pitfalls of using a CPG, and they should be able to evaluate its quality. Most important is the attention that should be paid to whether or not the guideline covers the intended subject. Then, the quality of the supportive evidence and the quality of the recommendations derived from that evidence should be considered. Finally, the clinician should figure out whether the CPG recommendations can be applied to their individual patient [7].

Reporting Standards in Radiology and Structured Reporting

The radiology report is the most important product delivered by a radiologist after a diagnostic examination of a patient. It is the radiologist's tool to communicate to a referring physician, and it is an important part of a patient's medical record. Also, the report is an essential document in case a medicolegal problem arises [8].

Every diagnostic radiology report includes important identifying data, such as the name and birth date of the examined patient. Of course, imaging findings and a comparison with available prior examinations are included in the report. Based on clinical data and the imaging findings, a radiologist concludes which diagnosis is most likely to be present. If possible, recommendations are presented as well. Technical details and any limitations of the study may also be part of the report. It is important for a good report to be finished within a reasonable time so that the patient and the physician can proceed with a diagnostic and/or treatment procedure.

For physicians to efficiently extract key information from a radiology report, structured reports are preferred instead of free-text reports. However, free-text reports are still most used in daily practice despite the fact that they are criticized for their lack of structure and organization. Also, the content is not consistent as it is more easy to forget and skip a part of the report [9].

In Table 12.1, the requirements of a good radiology report are summarized [10]. For example, clarity, correctness, and completeness

are attributes of a good radiology report [9–11]. The best way to fulfill these requirements is by using a structured report. The Radiological Society of North America (RSNA) supports the use of structured reporting, and therefore in 2009, it created an online library of radiology report templates attempting to standardize and increase the quality of reporting. The templates in this online RSNA library are not intended as compelling guidelines, but they may be used by radiologists in their clinical practice to standardize the language and content of their reports [12]. At the time of writing, a template for assessing the prostate was not available.

Multiparametric Magnetic Resonance Imaging for Prostate Cancer

Today's most accurate imaging technique for the detection, localization, and local staging of PCa is mpMRI. Multiparametric MRI is a combination of anatomical and functional MR images that together allow for an accurate assessment of the prostate. To depict the anatomy of the prostate, T2-weighted images are used. The most used functional MR images are diffusion-weighted imaging (DWI) and dynamic contrast-enhanced imaging (DCE).

Table 12.1 A good radiology report according to the "6 C's" by Armas [10]

1	Clarity	Used nomenclature should be clear to avoid any misunderstanding by the referring physician
2	Correctness	Whenever possible, the radiology report should contain a precise diagnosis
3	Confidence	The level of certainty of a finding or a conclusion should be clarified
4	Concision	Findings should be reported with brevity
5	Completeness	All relevant clinical information should be reported
6	Consistency	Throughout the report, the included components should be the same

T2-Weighted Imaging

T2-weighted imaging is the cornerstone of prostate mpMRI. Due to the high spatial resolution and soft tissue contrast, T2-weighted imaging is ideal for differentiating between the high-signal-intensity peripheral zone (PZ) and the low-signal-intensity central and transition zone (TZ) (Figs. 12.1 and 12.2). In aging men, benign prostatic hypertrophy (BPH) commonly compresses the TZ whereby the remaining TZ is not recognizable anymore on mpMRI. Therefore, the prostate is mostly divided in a PZ and a TZ. The high signal intensity of the PZ may be disrupted due to the presence of PCa. However, benign conditions such as fibrosis, hemorrhage, atrophy, and prostatitis also frequently lower the signal intensity in the PZ and thus mimic PCa. However, based on morphologic features, commonly a differentiation can be made. A focal, round, or irregular structure is more likely to be PCa, whereas prostatitis, for example, is marked by a wedge-shaped and diffuse morphology.

The TZ is characterized by a low signal intensity. However, BPH obscures and mimics PCa in the TZ. BPH mostly appear as nodules with circumscribed margins. Regularly, BPH nodules are characterized by the mixture of hyper- and

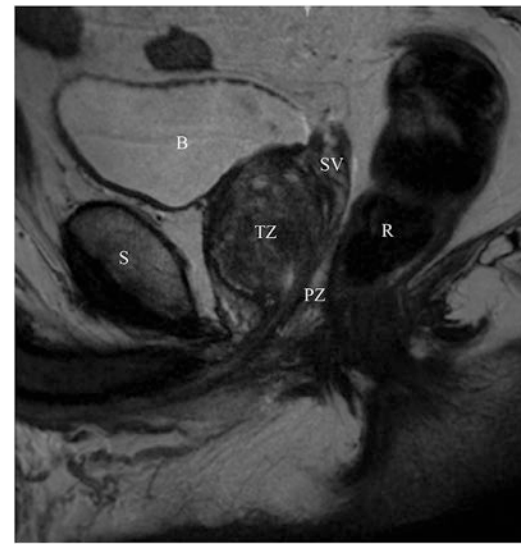

Fig. 12.1 Sagittal T2-weighted image of the prostate. *S* symphysis pubis, *B* bladder, *TZ* transition zone of the prostate, *PZ* peripheral zone of the prostate, *SV* seminal vesicle, *R* rectum

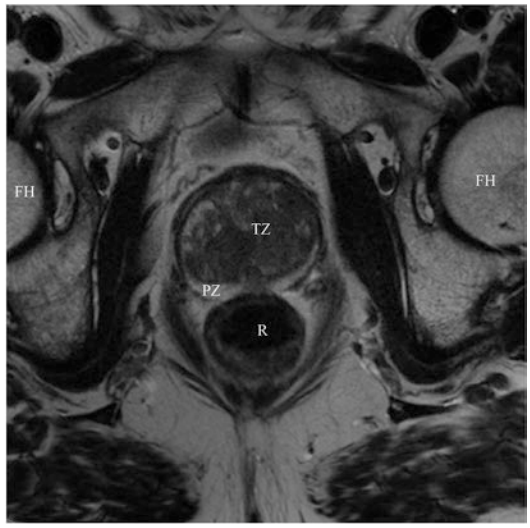

Fig. 12.2 Transversal or axial T2-weighted image of the prostate. *FH* femoral head, *TZ* transition zone of the prostate, *PZ* peripheral zone of the prostate, *R* rectum

hypo-signal intensity. Based on these characteristics, often a distinction can be made between a benign nodule or PCa [13]. To increase the diagnostic accuracy of MRI for PCa, T2-weighted images should be used along with functional imaging techniques.

Diffusion-Weighted Magnetic Resonance Imaging

The first functional imaging technique we will describe is diffusion-weighted imaging (DWI). In DWI, the Brownian motion of water protons is displayed. Brownian motion is the absolute random motion of water molecules in unrestricted tissue. To illustrate this motion in prostate tissue, spin-echo echoplanar T2-weighted images (EPI) are used most often.

DWI consists of two components: a *b*-value and an apparent diffusion coefficient (ADC). The *b*-value reflects the strength of the diffusion-sensitizing gradient. The *b*-value is measured in seconds per square millimeter, and it thus reflects the amount of diffusion weighting. In prostate DWI, different sensitizing gradients (*b*-values) are used for optimal evaluation of aberrant lesions in the prostate. Small *b*-values only result in signal loss of highly mobile water molecules (such as blood in a vessel). As water movement in highly

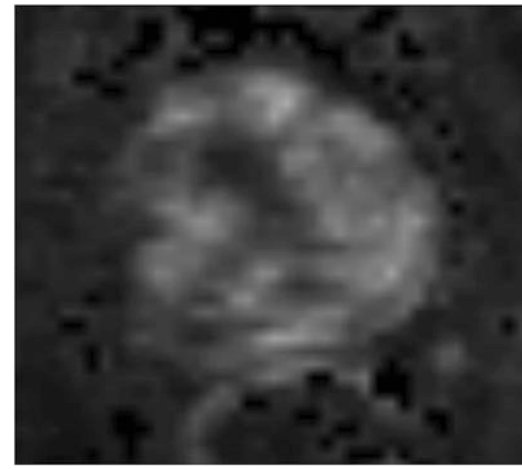

Fig. 12.3 High *b*-value image as part of the diffusion-weighted images of the prostate

cellular tissue is restricted, the water molecules retain their signal, even in high *b*-values. Cancer is highly cellular and thus restricts water movement; this is characterized by a high signal intensity on high *b*-value images (Fig. 12.3) [14].

An ADC map is calculated from at least two *b*-values. An ADC map is an automated calculation process from the MR scanner. The ADC map reflects differences of tissue density in different *b*-values [15]. In contrast to *b*-value, high cellular tissue is reflected by a low signal intensity on the ADC map (Fig. 12.4).

Unfortunately, not only PCa is characterized by high cellular tissue. BPH, prostatitis, and fibrosis are examples of benign tissue that may be marked by a high signal intensity on *b*-value imaging and a low signal intensity on the ADC map as well. These benign conditions often hamper the assessment of PCa with DWI, as it does with T2-weighted imaging. Further, DWI is very susceptible to artifacts (i.e., motion, bowel movement, and susceptibility).

Dynamic Contrast-Enhanced Magnetic Resonance Imaging

The second functional imaging technique that will be addressed in this chapter is dynamic contrast-enhanced MRI. DCE is an imaging technique representing the vascular properties of tissue. Repeatedly

Fig. 12.4 Calculated apparent diffusion coefficient (ADC) map as part of diffusion-weighted images of the prostate

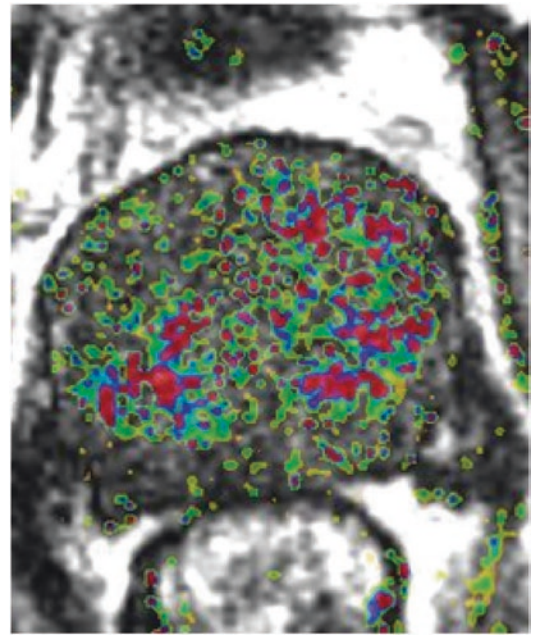

Fig. 12.5 Color map reflecting the dynamic contrast-enhanced MR images of the prostate

acquired fast T1-weighted sequences before, during, and after intravenous administration of a gadolinium-based contrast agent are used in DCE. Dedicated software is needed for post-processing the obtained images. Usually, color maps are extracted from the images for a simple understanding by both radiologists and non-radiologists. The colors used on those maps reflect a specific hemodynamic parameter, for example, the rate of wash-in and washout of the tissue (Fig. 12.5) [16].

Like other cancers, PCa is highly vascularized. The hemodynamic properties of PCa are characterized by an early and intense enhancement and subsequently a rapid washout. However, the assessment of DCE in the PZ is complicated by highly vascularized prostatitis. Within the TZ, the appreciation of DCE is difficult due to sometimes highly perfused BPH nodules. Corresponding T2-weighted images and DWI should be interpreted for a matched finding.

Spectroscopic Magnetic Resonance Imaging

The last functional sequence that we will describe is spectroscopy. As spectroscopic imaging is not often used anymore, we will only briefly describe the technique and its application. In the early days of prostate MR imaging, spectroscopic imaging was commonly used as part of mpMRI. Spectroscopic measurements provide biochemical information about prostate tissue. Choline and citrate are the metabolites most commonly measured in prostate MR spectroscopy. Compared with normal tissue, PCa usually shows increased choline levels and decreased citrate levels [17].

The major drawback of MR spectroscopy is that it is a time-consuming procedure. Furthermore, the interpretation is quite difficult, so it needs a high reader experience. These are some reasons that spectroscopy is not often used anymore.

Reporting Before the Use of the Prostate Imaging Reporting and Data System

About a decade ago, interest started to rise among radiologists in using MRI for the detection, localization, and characterization of PCa. Prior to this time, MRI was primarily used for local-regional staging. The growing interest was motivated by the introduction of functional MRI techniques that allowed for

more accurate detection and localization of PCa. Evidently, no agreement or guideline for prostate reporting was available at that time, resulting in the use of a variety of reporting methods. These methods were often based on an ordinal scale.

The easiest ordinal scale for oncologic imaging reporting is a binary scale allowing a radiologist to indicate whether a tumor is present or not. However, such a scale does not allow a radiologist to report equivocal findings. To overcome this gap, three-point and five-point scales were more used in prostate mpMRI [18].

Unfortunately, multiple problems arose with the varying scales used in prostate MR reading. Among scales, even in those with an equal range, different interpretations were being practiced. For example, a score of 5 (in a five-point scale) indicated "definitely cancer" in one system whereas it meant "likely malignant" in another [19, 20]. Another important dilemma was formed by the weighting of the different parameters used in mpMRI. The question arose whether all parameters should contribute in an equal way to a sum score or whether one parameter should be more important than the other. Before PI-RADS, a great amount of uncertainty existed relating to those difficulties. To standardize prostate MR assessment, following the example of the Breast Imaging Reporting and Data System (BI-RADS) in breast cancer, a scoring system was introduced for PCa [2].

The Prostate Imaging Reporting and Data System: What Is It?

PI-RADS Version 1

In 2012, Barentsz et al. [2] published the European Society of Urogenital Radiology (ESUR) clinical guidelines for mpMRI of the prostate. A mixture of technical and clinical recommendations was presented to "promulgate high-quality MRI in acquisition and evaluation with the correct indications for prostate cancer across the whole of Europe and eventually outside Europe." Along with these guidelines, the first version of the PI-RADS classification was introduced (PI-RADS v1).

The original published clinical guideline was not truly evidence based, but was rather an expert-opinion-based guideline. Formulating an evidence-based guideline was not possible at that time due to a lack of relevant literature. To compensate for this lack of supportive evidence, consensus among prostate MR experts was used to formulate "optimal" and "minimal" requirements.

The primary aims of the PI-RADS classification were to improve diagnostic quality and to simplify and standardize radiology reports. The introduction of PI-RADS v1 allowed radiologists to assess the prostate in a structured manner using a scoring system with predefined requirements that a lesion must satisfy in order to be given a certain level of suspicion for being PCa. PI-RADS v1 was (like version 2) based on a five-point Likert score because these were the most used reporting scales at that time. Every parameter (T2-weighted, DWI, DCE, and, as an option, spectroscopy) was rated on a score ranging from 1 to 5. Additionally, each lesion was given an overall score, also ranging from 1 to 5 (Table 12.2). PI-RADS v1 provided a separate scoring system for T2-weighted imaging for the PZ and the TZ. Version 2 also has an individual scoring for lesions located in the PZ or in the TZ.

Characteristic for PI-RADS v1 (which is not revisited in PI-RADS version 2) was the use of curve-type analysis in DCE imaging. Nowadays, a radiologist has to report whether the contrast enhancement pattern is positive or negative,

Table 12.2 Assessment categories of Prostate Imaging Reporting and Data System (PI-RADS) version 1 and version 2

Score 1	Clinically significant disease is highly unlikely to be present
Score 2	Clinically significant disease is unlikely to be present
Score 3	Clinically significant disease is equivocal
Score 4	Clinically significant disease is likely to be present
Score 5	Clinically significant disease is highly likely to be present

The higher the PI-RADS score, the higher the likelihood that clinically significant prostate cancer is present

while previously the radiologist had a choice between different types of enhancement curves (Fig. 12.6). Also, spectroscopic imaging is not included in version 2. Spectroscopic imaging is now considered a research sequence.

Since the introduction of PI-RADS v1, it has extensively been validated in clinical and research settings, resulting in a sensitivity of 0.78 (95% confidence interval [CI], 0.70–0.84) and a specificity of 0.79 (95% CI, 0.68–0.86) for PCa detection [21]. However, experience also revealed some limitations and therefore there was a need for a new version.

PI-RADS Version 2

PI-RADS version 2 (PI-RADS v2) was developed to further improve the accuracy and inter-observer agreement of the first version as that version was limited by variable interpretations [22]. PI-RADS v2 was developed by members of a steering committee using the best available evidence and expert consensus opinion [23].

We have already addressed some of the differences between version 1 and version 2. The other main novelties of version 2 include the use of a dominant sequence depending on the location of the lesion (PZ or TZ) and the employment of an overall score estimated from the individual scores of the used sequences. The overall PI-RADS score remains the same (Table 12.2).

In the appraisal of a lesion, first the location of the lesion has to be selected. This determines the dominant sequence of the overall PI-RADS score. Mainly, the overall PI-RADS score of a lesion located in the PZ follows the score of that lesion as determined with DWI. Only in case of a PI-RADS 3 score can a positive score on DCE upgrade the score to PI-RADS 4 (Table 12.3). T2-weighted imaging plays a minor role in lesions located in the PZ. The dominant sequence for lesions located in the TZ is T2-weighted imaging. Now, DWI can upgrade the overall PI-RADS score in case of an equivocal finding (PI-RADS 3) on T2-weighted imaging: a PI-RADS 5 on DWI may upgrade a PI-RADS 3 lesion to PI-RADS 4 (Table 12.4).

As the functional imaging techniques are susceptible to artifacts, it is not always possible to obtain adequate DWI or DCE data. The other modalities will then play a more important role in

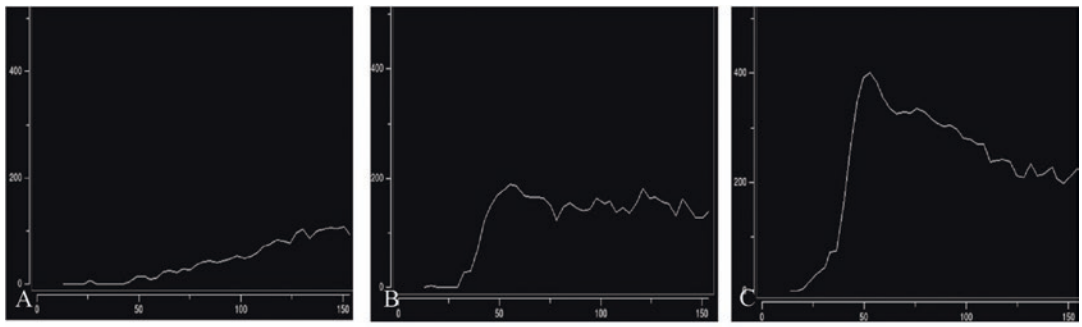

PI-RADS	Criteria	
1	Type 1 enhancement curve (A)	Slowly increasing enhancement
2	Type 2 enhancement curve (B)	Enhancement reaching a plateau phase
3	Type 3 enhancement curve (C)	Rapid enhancement and wash-out effect
+1	Focal enhancing with curve type 2 or 3	
+1	Assymetric lesion or a lesion at an unusual place with curve type 2 or 3	

Fig. 12.6 Types of enhancement curves used in the Prostate Imaging Reporting and Data System (PI-RADS) version 1

Table 12.3 Prostate Imaging Reporting and Data System (PI-RADS) version 2 classification of lesions located in the peripheral zone

DWI	T2-weighted imaging	DCE	Overall PI-RADS
1	1–5	−/+	1
2	1–5	−/+	2
3	1–5	−	3
3	1–5	+	4
4	1–5	−/+	4
5	1–5	−/+	5

DWI diffusion-weighted imaging, *DCE* dynamic contrast enhancement

Table 12.4 Prostate Imaging Reporting and Data System (PI-RADS) version 2 classification of lesions located in the transition zone

T2-weighted	DWI	DCE	Overall PI-RADS
1	1–5	−/+	1
2	1–5	−/+	2
3	1–4	−/+	3
3	5	−/+	4
4	1–5	−/+	4
5	1–5	−/+	5

DWI diffusion-weighted imaging, *DCE* dynamic contrast enhancement

Table 12.5 Prostate Imaging Reporting and Data System (PI-RADS) version 2 classification of lesions located in the transition zone in case an adequate DCE is not obtained. Lesions located within the peripheral zone are then solely determined by the DWI assessment category

T2-weighted	DWI	DCE	Overall PI-RADS
1	1–5	×	1
2	1–5	×	2
3	1–4	×	3
3	5	×	4
4	1–5	×	4
5	1–5	×	5

DWI diffusion-weighted imaging, *DCE* dynamic contrast enhancement

Table 12.6 Prostate Imaging Reporting and Data System (PI-RADS) version 2 classification of lesions located in the transition zone or the peripheral zone in case an adequate DWI is not obtained

T2-weighted imaging	DWI	DCE	Overall PI-RADS
1	X	−/+	1
2	X	−/+	2
3	X	−	3
3	X	+	4
4	X	−/+	4
5	X	−/+	5

DWI diffusion-weighted imaging, *DCE* dynamic contrast enhancement

the final PI-RADS score. In such a case, T2-weighted imaging is the dominant sequence and, depending on which functional imaging technique is missing, a PI-RADS 3 score may be upgraded to PI-RADS 4 (Tables 12.5 and 12.6).

T2-Weighted Imaging

On T2-weighted imaging, a normal PZ (PI-RADS 1 score) is characterized by a uniform hyperintense signal intensity. If a hypointense signal intensity is seen, the shape, the heterogeneity, and the size of that lesion are important features to establish the PI-RADS score. A circumscribed, homogeneous hypointensity is scored PI-RADS 4 or a PI-RADS 5 (in case the greatest dimension is at least 1.5 cm or definite extraprostatic extension [EPE] is present). Linear lesion, wedge-shaped lesion, and lesion with indistinct margins with a mild hypointensity are less suspected and thus scored PI-RADS 2. Equivocal lesions (PI-RADS 3) are often non-circumscribed but with a moderate hypointensity (Fig. 12.7). In contrast to the assessment of DWI and DCE, the appraisal of a lesion on T2-weighted imaging is slightly different between the TZ and the PZ.

The characteristics of a tumor located in the TZ include non-circumscribed homogeneous, moderately hypointense lesions (erased charcoal). Also, a lenticular shape, speculated margins, or invasion of the urethral sphincter or anterior fibromuscular stroma are features of PCa. The PI-RADS score increases with an increasing number of present characteristics. BPH nodules often mimic or obscure PCa lesions. However, BPH nodules are characterized by their well-defined margins (encapsulated nodules) and the heterogeneous signal intensity. BPH nodules are often described as “organized chaos” (Fig. 12.8).

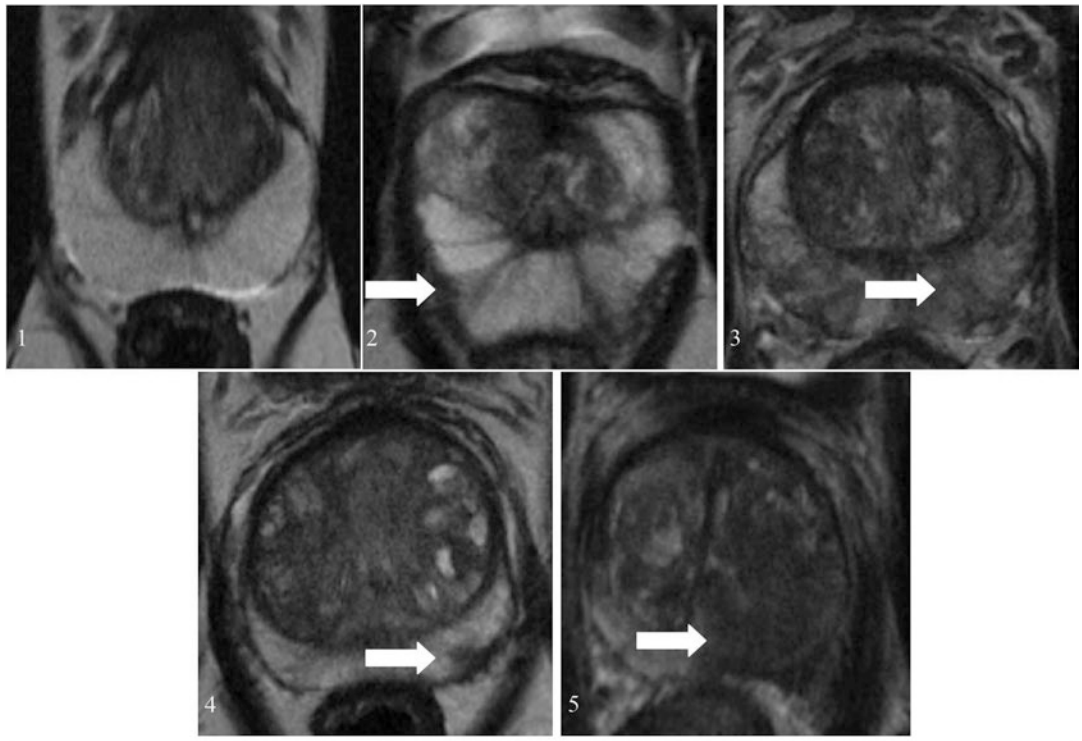

PI-RADS	
1	Uniform hyperintense signal intensity
2	Linear, wedge-shaped or diffuse mild hypointensity. Usually with indistinct margins
3	Heterogeneous signal intensity or non-circumscribed, rounded, moderate hypointensity
4	Circumscribed, homogenous moderate hypointense focus/mass confined to the prostate and < 1.5 cm in greatest dimension
5	Same as PI-RADS 4, but ≥ 1.5 cm in greatest dimension or definite extraprostatic extension or invasive behavior

Fig. 12.7 Prostate Imaging Reporting and Data System (PI-RADS) version 2 assessment for peripheral zone lesions on T2-weighted images

Diffusion-Weighted Magnetic Resonance Imaging

The assessment of DWI includes both the high *b*-value and the ADC. In a normal prostate, no abnormality is seen on *b*-value nor on ADC. A focal hypointensity on ADC and a focal hyperintensity on *b*-value are scored a PI-RADS 4 or 5. Again, a cut-off of 1.5 cm of the greatest dimension or a definite presence of EPE is used in order to make the difference between the two scores. A focal moderate hypointensity and a same hyperintensity on ADC and *b*-value, respectively, result in a PI-RADS 3 score, whereas a doubtful hypointensity on ADC alone should result in a PI-RADS 2 (Fig. 12.9).

Dynamic Contrast-Enhanced Magnetic Resonance Imaging

Since PI-RADS v2, DCE is a binary scale only including the decision of being either positive or negative. A positive enhancement pattern is

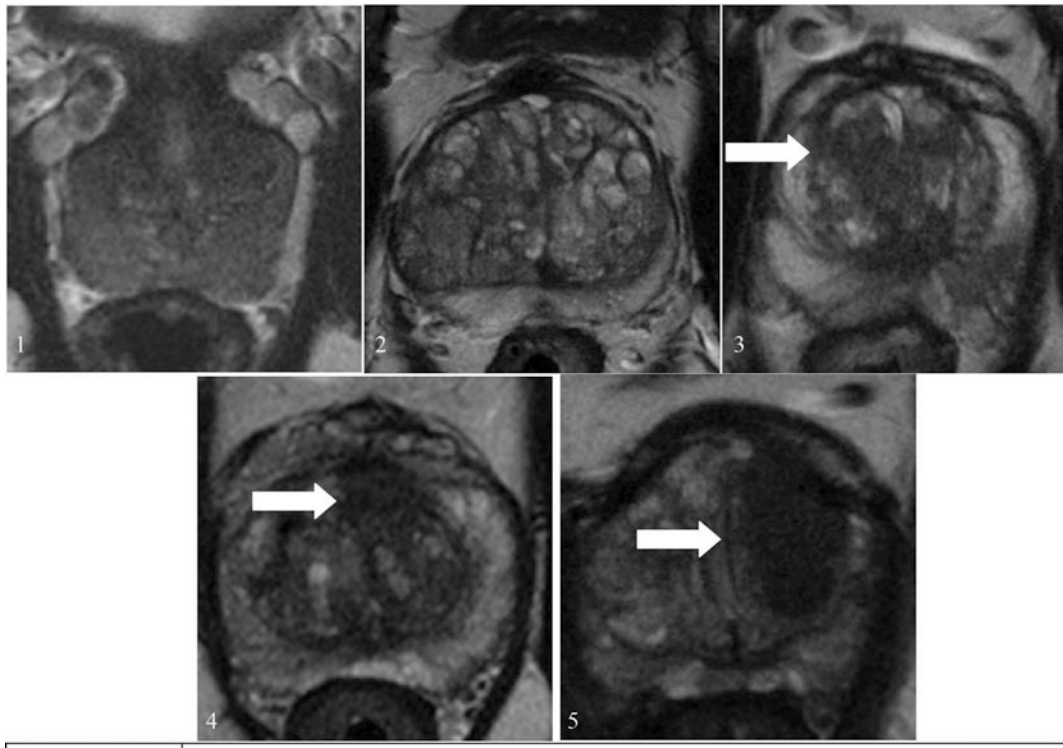

PI-RADS	
1	Homogeneous intermediate signal intensity
2	Circumscribed hypointense or heterogeneous encapsulated nodules "organized chaos"
3	Heterogeneous signal intensity with obscured margins.
4	Lenticular or non-circumscribed, homogeneous, moderately hypointensity and < 1.5 cm in greatest dimension
5	Same as Pi-RADS 4, but ≥ 1.5 cm in greatest dimension or definite extraprostatic extension or invasive behavior

Fig. 12.8 Prostate Imaging Reporting and Data System (PI-RADS) version 2 assessment for transition zone lesions on T2-weighted images

defined by a focal and earlier or contemporaneously enhancement compared to normal prostatic tissue. Additionally, the finding has to correspond to a suspicious finding on T2-weighted imaging or DWI, as often focal enhancement alone is seen in the prostate, which is not definitive for clinically significant PCa (Fig. 12.10). As with DWI, the assessment characteristics of DCE are the same for the PZ and the TZ.

The Prostate Imaging Reporting and Data System: What Can It Do?

The specific aims of the PI-RADS classification are quality guarding, simplifying and standardizing radiology reports for enhanced communications with referring clinicians, educating radiologists, collecting data for outcome monitoring and research, risk stratification of patients for tailored management, and guiding targeted biopsy.

High b-value DWI	ADC map	PI-RADS	
		1	No abnormality on both the high *b*-value and ADC
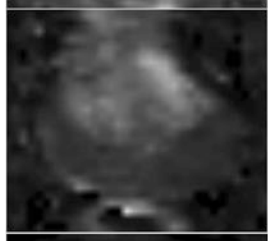	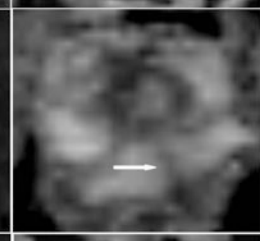	2	Doubtful or indistinct hypointensity on ADC
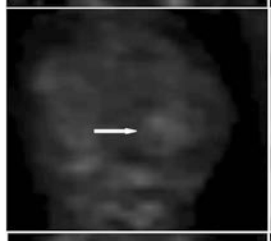	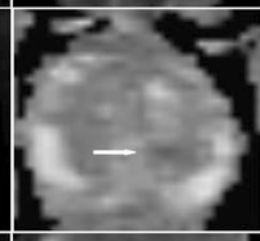	3	Focal moderate hyperintensity and a same hypointensity on high *b*-value and ADC respectively
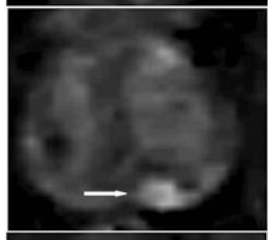	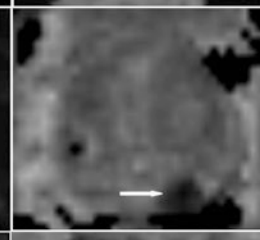	4	Focal hyperintensity on high *b*-value and a focal hypointensity on ADC < 1.5 cm on axial images
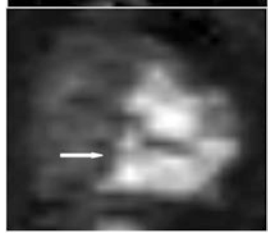	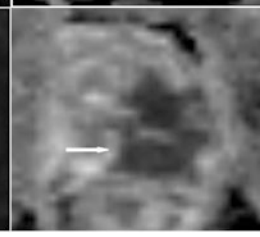	5	Same as PI-RADS 4, but ≥ 1.5 cm in greatest dimension or definite extraprostatic extension or invasive behavior

Fig. 12.9 Prostate Imaging Reporting and Data System (PI-RADS) version 2 assessment for transition and peripheral zone lesions on diffusion-weighted images

The PI-RADS score provides an effective framework for determining the likelihood of prostate cancer on mpMRI. The PI-RADS assessment uses a five-point scale based on the probability of the presence of clinically significant prostate cancer detected on the combined use of T2-weighted, DWI, and DCE MRI using a dominant sequence (Table 12.2). For mapping lesions, up to four findings with a PI-RADS score of ≥3 may be each assigned on the sector map. Further, the index lesion should be identified, which is the lesion with the highest PI-RADS score or the one that shows extracapsular extension. The identification of the index lesion is important in targeted biopsy.

By using PI-RADS v2, general body radiologists and prostate specialists can detect high-grade index prostate cancer lesions with

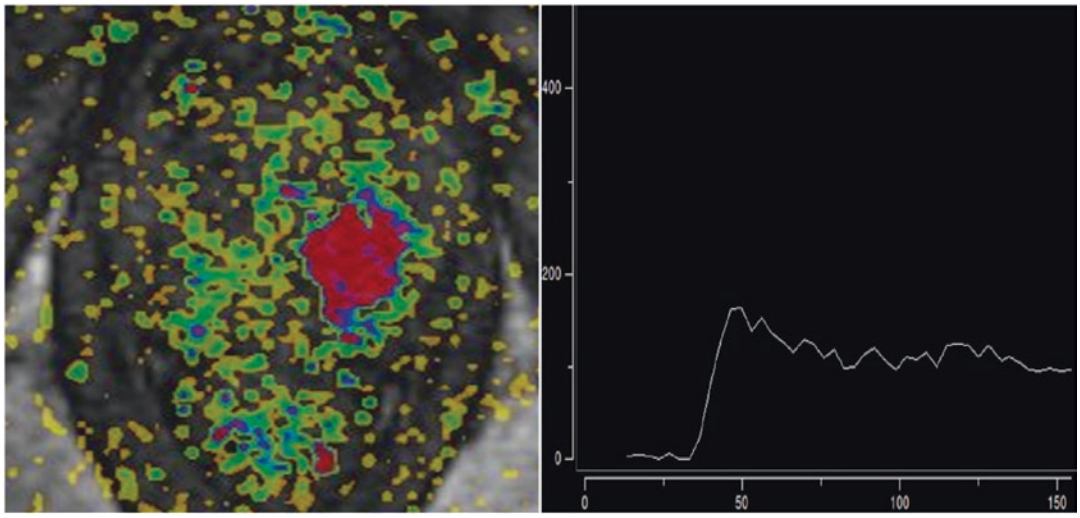

Fig. 12.10 Prostate Imaging Reporting and Data System (PI-RADS) version 2 assessment on dynamic contrast-enhanced images. On the *left*, a focal and early enhancement pattern with washout effect is depicted by a *red* spot on the color map. On the *right*, the curve type of the lesion corresponds to curve type 3 in PI-RADS version 1, which would result in a PI-RADS 5 score according to the then-used criteria (adding two points for focal and asymmetric enhancement)

high sensitivity and agreement [24]. However, experienced radiologists have achieved moderate reproducibility for PI-RADS v2, and neither required nor benefitted from a training session. Agreement tended to be better in PZ than TZ, although it was weak for DCE in PZ [25]. Other authors found an inter-reader agreement that was excellent for PI-RADS score of 4 or greater (weighted κ[kappa] = 0.801; 95% CI: 0.737, 0.865) [26].

Prostate lesions characterized on mpMRI as PIRADS 3, according to the current prevalent scoring systems, are associated with a low likelihood of the presence of clinically significant prostate cancer [27]. PI-RADS v2 showed moderate accuracy for the identification of clinically significant prostate cancer [28].

A visible lesion on mpMRI strongly predicts significant PCa in patients eligible for active surveillance (AS) according to PRIAS criteria (Prostate Cancer Research International: Active Surveillance), based on upstaging and unfavorable disease. Multiparametric MRI is an important tool and should be added to clinical selection criteria for AS [29]. In the latter study, multivariate logistic regression revealed that PIRADS 5 was a significant predictor of upstaging ($p = 0.05$, OR 16.12) and unfavorable disease ($p = 0.01$, OR 6.53). Furthermore, the presence of PI-RADS 4 or 5 lesions on men enrolled to AS programs for prostate cancer warrants concern [30].

References

1. Scattoni V, Zlotta A, Montironi R, Schulman C, Rigatti P, Montorsi F. Extended and saturation prostatic biopsy in the diagnosis and characterisation of prostate cancer: A critical analysis of the literature. Eur Urol. 2007;52(5):1309–22.
2. Barentsz JO, Richenberg J, Clements R, Choyke P, Verma S, Villeirs G, et al. Esur prostate mr guidelines 2012. Eur Radiol. 2012;22(4):746–57.
3. Graham RMM, Miller Wolman D, Greenfield S, Steinberg E. Clinical practice guidelines we can trust. Wahington, DC: National Academy Press; 2011.
4. Woolf SH, Grol R, Hutchinson A, Eccles M, Grimshaw J. Clinical guidelines: potential benefits, limitations, and harms of clinical guidelines. BMJ. 1999;318(7182):527–30.
5. Sniderman AD, Furberg CD. Why guideline-making requires reform. JAMA. 2009;301(4):429–31.
6. Kozlick D. Clinical practice guidelines and the legal standard of care: warnings, predictions, and interdisciplinary encounters. Health Law J. 2011;19:125–51.
7. Dahm P, Yeung LL, Gallucci M, Simone G, Schunemann HJ. How to use a clinical practice guideline. J Urol. 2009;181(2):472–9.
8. Dunnick NR, Langlotz CP. The radiology report of the future: a summary of the 2007 intersociety conference. J Am Coll Radiol JACR. 2008;5(5):626–9.

9. Sistrom CL, Langlotz CP. A framework for improving radiology reporting. J Am Coll Radiol JACR. 2005;2(2):159–67.
10. Armas RR. Qualities of a good radiology report. AJR Am J Roentgenol. 1998;170(4):1110.
11. American college of radiology. ACR standard for communication: diagnostic radiology. In: Standards 2000–2001. Reston, VA: American college of radiology; 2000. p. 1–3.
12. Morgan TA, Helibrun ME, Kahn Jr CE. Reporting initiative of the radiological society of north america: progress and new directions. Radiology. 2014;273(3): 642–5.
13. Hoeks CM, Barentsz JO, Hambrock T, Yakar D, Somford DM, Heijmink SW, et al. Prostate cancer: multiparametric MR imaging for detection, localization, and staging. Radiology. 2011;261(1):46–66.
14. Qayyum A. Diffusion-weighted imaging in the abdomen and pelvis: concepts and applications. Radiographics. 2009;29(6):1797–810.
15. Jacobs MA, Ouwerkerk R, Petrowski K, Macura KJ. Diffusion-weighted imaging with apparent diffusion coefficient mapping and spectroscopy in prostate cancer. Top Magn Reson Imaging TMRI. 2008; 19(6):261–72.
16. Cuenod CA, Balvay D. Perfusion and vascular permeability: basic concepts and measurement in dce-ct and dce-mri. Diagn Interv Imaging. 2013;94(12):1187–204.
17. Heerschap A, Jager GJ, van der Graaf M, Barentsz JO, de la Rosette JJ, Oosterhof GO, et al. In vivo proton MR spectroscopy reveals altered metabolite content in malignant prostate tissue. Anticancer Res. 1997;17(3A):1455–60.
18. Dickinson L, Ahmed HU, Allen C, Barentsz JO, Carey B, Futterer JJ, et al. Scoring systems used for the interpretation and reporting of multiparametric mri for prostate cancer detection, localization, and characterization: could standardization lead to improved utilization of imaging within the diagnostic pathway? J Magn Reson Imaging. 2013;37(1):48–58.
19. Mueller-Lisse U, Mueller-Lisse U, Scheidler J, Klein G, Reiser M. Reproducibility of image interpretation in MRI of the prostate: application of the sextant framework by two different radiologists. Eur Radiol. 2005;15(9):1826–33.
20. Jung JA, Coakley FV, Vigneron DB, Swanson MG, Qayyum A, Weinberg V, et al. Prostate depiction at endorectal mr spectroscopic imaging: investigation of a standardized evaluation system. Radiology. 2004;233(3):701–8.
21. Hamoen EH, de Rooij M, Witjes JA, Barentsz JO, Rovers MM. Use of the prostate imaging reporting and data system (PI-RADS) for prostate cancer detection with multiparametric magnetic resonance imaging: a diagnostic meta-analysis. Eur Urol. 2015;67(6):1112–21.
22. Renard-Penna R, Mozer P, Cornud F, Barry-Delongchamps N, Bruguiere E, Portalez D, et al. Prostate imaging reporting and data system and Likert scoring system: multiparametric MR imaging validation study to screen patients for initial biopsy. Radiology. 2015;275(2):458–68.
23. Weinreb JC, Barentsz JO, Choyke PL, Cornud F, Haider MA, Macura KJ, et al. PI-RADS prostate imaging – reporting and data system: 2015, version 2. Eur Urol. 2016;69(1):16–40.
24. Greer MD, Brown AM, Shih JH, Summers RM, Marko J, Law YM, et al. Accuracy and agreement of PIRADSV2 for prostate cancer mpMRI: a multireader study. J Magn Reson Imaging. 2016 Jul 8. doi: 10.1002/jmri.25372. [Epub ahead of print]
25. Rosenkrantz AB, Ginocchio LA, Cornfeld D, Froemming AT, Gupta RT, Turkbey B, et al. Interobserver reproducibility of the PI-RADS version 2 lexicon: a multicenter study of six experienced prostate radiologists. Radiology. 2016;280(3):152542.
26. Park SY, Jung DC, Oh YT, Cho NH, Choi YD, Rha KH, et al. Prostate cancer: Pi-rads version 2 helps preoperatively predict clinically significant cancers. Radiology. 2016;280(1):108–16.
27. Liddell H, Jyoti R, Haxhimolla HZ. mp-MRI prostate characterised pirads 3 lesions are associated with a low risk of clinically significant prostate cancer – a retrospective review of 92 biopsied PIRADS 3 lesions. Curr Urol. 2015;8(2):96–100.
28. Lin WC, Muglia VF, Silva GE, Chodraui Filho S, Reis RB, Westphalen AC. Multiparametric MRI of the prostate: diagnostic performance and interreader agreement of two scoring systems. Br J Radiol. 2016;89(1062):20151056.
29. Almeida GL, Petralia G, Ferro M, Ribas CA, Detti S, Jereczek-Fossa BA, et al. Role of multi-parametric magnetic resonance image and score in patients with prostate cancer eligible for active surveillance according PRIAS criteria. Urol Int. 2016;96(4):459–69.
30. Perera M, Katelaris N, Murphy DG, McGrath S, Lawrentschuk N. Prostate imaging reporting and data system score of four or more: active surveillance no more. BJU Int. 2016 Jun 22. doi: 10.1111/bju.13562. [Epub ahead of print].

Role of Magnetic Resonance Imaging in Prostate Cancer Assessment

13

Sonia Gaur, Sherif Mehralivand, Baris Turkbey, and Peter L. Choyke

Introduction

Prostate cancer is the most common solid organ malignancy and the second most common cause of cancer-related deaths among men in the United States. According to the Surveillance, Epidemiology, and End Results (SEER) database of the National Cancer Institute, approximately 180,890 men will be newly diagnosed in 2016, and 26,120 will die of prostate cancer [1]. Hence, it constitutes a major challenge for healthcare systems. Since 1994, when the US Food and Drug Administration (FDA) approved screening with serum prostate-specific antigen (PSA) in combination with digital rectal examination (DRE), there has been a dramatic surge in the number of newly diagnosed cases, resulting in treatment in the form of surgery or radiation therapy. However, it has become increasingly recognized that not all "tumors" require treatment. While many prostate tumors exhibit aggressive behavior leading to metastatic disease and death, even more have an indolent course such that men die *with* prostate cancer but not *of* prostate cancer. The recognition that not all prostate cancers require treatment has been revolutionary and has resulted in the increasing use of active surveillance rather than active intervention with its attendant side effects. However, despite these efforts to reduce the impact of overdiagnosis with active surveillance, the use of PSA for screening has decreased in the United States after the findings of the US Preventive Services Task Force (USPSTF) were reported in 2012, concluding that PSA screening was not justified [2, 3]. These findings were, in part, based on the results of two large prospective trials: one initiated in the United States (the Prostate, Lung, Colorectal and Ovarian Cancer Screening Trial or PLCO) and the other in Europe (the European Randomized Study of Screening for Prostate Cancer Trial or ERSPC). These studies reached different conclusions regarding PSA screening, with the PLCO trial showing no benefit in mortality reduction and the ERSPC trial showing only a small reduction in mortality in the screened arm [4, 5]. Recently, the PLCO trial has been criticized for allowing patients in the control arm to have intermittent PSA testing. Close to 90 % of the control group's patients had PSA testing done, thus bringing into question the evidence upon which the US Preventive Services Task Force recommendations were made [6]. The degree of contamination in the ERSPC trial has also been questioned, although it is undoubtedly less.

S. Gaur • S. Mehralivand • B. Turkbey (✉)
P.L. Choyke
Molecular Imaging Program, National Cancer Institute, National Institutes of Health, Bethesda, MD, USA
e-mail: turkbeyi@mail.nih.gov

© Springer International Publishing AG 2017

T.J. Polascik (ed.), *Imaging and Focal Therapy of Early Prostate Cancer*, Current Clinical Urology, DOI 10.1007/978-3-319-49911-6_13

Given the slow-growing nature of most prostate cancers, even one or two PSA tests during the study could have negated any benefits of PSA screening. Thus, there is reason to question the prudence of the USPSTF decision. Many observers believe this decision will need to be reversed as the percentage of men with advanced or metastatic disease at presentation increases, as has been suggested in some recent studies [7]. Meanwhile, European authorities continue to mainly endorse PSA screening.

Although overdiagnosis and overtreatment have received more attention during this controversy, somewhat neglected is the considerable amount of underdiagnosis of potentially lethal prostate cancer due to misses on systematic biopsies. The current standard of care in men suspected of having prostate cancer, based on elevated PSA and/or suspicious DRE, is a systematic 10–12 core biopsy (extended sextant biopsy) of the prostate—usually obtained transrectally through transrectal ultrasound (TRUS) guidance in the United States. However, systematic biopsies of the prostate often miss or undergrade tumors in up to 36 % of cases, when compared to prostatectomy specimens [8]. Despite the fact that these random biopsies are obtained with TRUS, ultrasound is generally insensitive to the detection of small tumors, and therefore biopsy needles are not necessarily directed into suspicious areas but rather are deployed in asymmetric patterns that do not take into consideration the location of the tumor. As many as 25–40 % of tumors show an isoechoic pattern on TRUS and are not visible unless they reach a larger size. Such errors can lead to missed diagnosis and delayed therapy. Thus, the current methods of PSA screening and random biopsy lead to underdiagnosis of clinically significant tumors.

The key to resolving both the overdiagnosis and the underdiagnosis dilemmas lies in improving the ability to detect prostate cancer locations and to provide a risk evaluation. To some extent, risk evaluation can be based on known risk factors such as age, PSA, and digital rectal exam status. These have been codified in several well-known nomograms. However, these nomograms also have several well-known problems. First, they provide no information regarding tumor location and therefore do not aid directly in guiding the biopsy. Moreover, they only provide a group risk estimate and do not individualize a particular patient's risk [9]. Several novel biomarkers have been introduced to improve individual risk assessment. For instance, the FDA approved the PCA3 and ProPSA assays in 2012. Although these improve on the accuracy and specificity of PSA with regard to predicting tumor aggressiveness and prognostic features, their eventual role in clinical routine is unclear, given the inability to localize tumors [10]. In order to both localize and stratify prostate cancer, magnetic resonance imaging (MRI) with image-guided biopsy has been introduced. A variety of alternative imaging methods including sonoelastography, HistoScanning, and contrast-enhanced ultrasound (CEUS) have been introduced, but do not perform as well as MRI.

MRI of the prostate and MRI-guided biopsy of the prostate were first described in the late 1980s [11]. In the early days of MRI, it was used strictly as a staging tool for biopsy-proven prostate cancers prior to surgery. It proved to have limited utility. It was not until the late 1990s that the potential of MRI to localize tumors within the prostate was recognized. In the last decade, MRI has evolved to include a combination of anatomical and functional MR sequences, creating the so-called multiparametric MRI (mpMRI). When used in combination with TRUS for MRI-fusion-guided targeted biopsies, this method has shown higher detection of clinically significant cancers and reduced detection of clinically insignificant cancers in patients after a prior negative systematic TRUS-guided biopsy [12, 13]. These promising results have led to increased application of mpMRI in the management of patients suspected of prostate cancer after negative systematic biopsies and in defining candidates for active surveillance.

The use of mpMRI has evolved rapidly in recent years and current treatment guidelines still do not incorporate the use of mpMRI. However, more centers are integrating mpMRI in their care

management workflows. Guidelines often lag practice, as a new method is often tested in academic centers before it is recommended for broad use. Meanwhile, prior to 2015, mpMRI was performed and interpreted in a variety of ways making it difficult to compare results. In 2015, the Prostate Imaging Reporting and Diagnosis System (PI-RADS) version 2 was published, which created standards for the performance and reporting of mpMRI. Here, we provide an overview of prostate mpMRI using PI-RADS version 2 nomenclature and describe the role of mpMRI in prostate cancer assessment.

Magnetic Resonance Imaging Acquisition

Multiparametric MRI consists of a combination of two anatomic sequences (T1-weighted [T1W] and T2-weighted [T2W]) and two functional sequences (diffusion-weighted imaging or DWI) and dynamic contrast-enhanced MRI (DCE-MRI). MR spectroscopic imaging, which had been a part of mpMRI, is no longer included in routine protocols as it provided minimal gain while requiring specialized expertise and substantial amounts of imaging time [14]. As mpMRI has begun to play a larger role in local staging, follow-up, and recurrence, emphasis has shifted to obtaining better images, with good spatial resolution, temporal resolution, and high signal-to-noise ratio [15]. In order to reach these goals, some key steps such as patient preparation and the correct use of proper MRI equipment with optimized protocols must be observed.

Patient Preparation

There is no consensus regarding patient preparation; however, PI-RADSv2 guidelines define several basic aspects of patient preparation. For instance, it is recommended that the patient's most recent PSA, PSA history, digital rectal exam findings, biopsy history, and family history be available prior to the MRI since this information can be helpful in tailoring the correct protocol. Additionally, labs should be drawn to obtain estimated glomerular filtration rate (GFR), in order to ensure the safe administration of gadolinium-based contrast media during the DCE portion of the exam [16].

Many patients who undergo mpMRI to evaluate prostate cancer are also patients who have undergone previous prostate biopsy. Hemorrhage from such biopsies is a source of artifact on MR images [17] and can mimic cancers on T2W imaging [18]. Generally, it is advised that mpMRI should be delayed at least 6 weeks post-biopsy, or as long as it takes for residual hemorrhage to resolve. A T1-weighted MRI can quickly check for the presence of hemorrhage, and, if present, the patient should be rescheduled. Bowel peristalsis and stool or air in the rectum can also compromise image quality due to movement (which causes image blurring) and due to susceptibility artifacts (which causes image distortion) mainly on DWI. In order to solve this challenge, the patient is advised to evacuate their rectum before imaging and can be offered an antispasmodic agent such as glucagon, scopolamine butylbromide, or sublingual hyoscyamine sulfate for inhibition of peristalsis [19]. However, evidence for the utility of antispasmodic agents is unconvincing, and such agents are usually not administered. Finally, for evaluating the seminal vesicles, we recommend that men avoid ejaculation for 3 days prior to the MRI so that the seminal vesicles will be optimally distended [20].

MRI Equipment

There are two important equipment issues relating to prostate MRI: the field strength of the MRI unit and the use of endorectal coils (ERCs). The minimum field strength advised for prostate cancer diagnosis is 1.5 tesla (T). 3 T scanners have better signal-to-noise ratios, and this allows higher-resolution images to be obtained in a shorter time [21]. Most expert centers utilize 3 T, although very acceptable images can be obtained at 1.5 T depending on the quality and age of the individual MRI unit and the care with which it is used.

All pulse sequences can be obtained with either external phased-array surface coils or an endorectal coil (ERC) [22, 23]. The ERC further improves signal-to-noise ratios (SNR), which can be used to obtain images with better resolution that are less prone to artifacts. Often ERC is recommended with 1.5 T MRI to overcome the SNR limitations of the latter. However, ERC also has been used with 3 T MRI to obtain maximal SNR [24]. While ERC provides clear benefits, there are also a number of drawbacks including increased cost and patient discomfort with insertion. Generally, the discomfort associated with ERC is overestimated, and most patients describe only low to moderate discomfort [25]. The use of the ERC may also be particularly helpful in certain clinical scenarios that require higher resolution, such as local staging, and for detection of recurrence after definitive treatment. However, the ERC may not be necessary in patients with small tumors or those who are followed on active surveillance. An important technical consideration is deciding what the balloon surrounding the actual ERC should be filled with. Simply putting air in the balloon, as suggested by the manufacturer, often leads to susceptibility artifacts, and therefore many centers have switched to using solutions such as dilute barium or perfluorocarbon. We find the latter to be particularly helpful in achieving high-quality images [26].

Pulse Sequences

Multiparametric MRI consists of four main pulse sequences, resulting in a combination of anatomical and functional data. High-resolution T2-weighted (T2W) images and T1-weighted (T1W) images are mainly used for review of morphology. In addition to these anatomical sequences, two functional sequences are also obtained. These are the diffusion-weighted imaging (DWI) sequences and dynamic contrast-enhanced (DCE) imaging, which requires the administration of intravenous contrast media. These four sequences work together to help define and confirm suspicious lesions within the prostate [27]. Details of acquisition for the main three sequences (T2W, DWI, DCE) are displayed in Table 13.1 [16].

T1W images are used to rule out the presence of biopsy-related residual hemorrhage and thus should be acquired prior to the other sequences. For T1W images, we use an axial image with the same thickness as the T2W images, which is usually 3 mm. The images can be obtained with or without fat suppression using spin echo or gradient echo (GRE) sequences. Fat suppression removes adipose hyperintensity that can interfere with interpretation of the image, but fat suppression is not critical. Since T1W MRI is mainly used for visualizing post-biopsy hemorrhage, image resolution is not critical. Residual hemorrhage can hinder accurate visualization of tumors within the prostate, so if a hyperintensity in the gland is seen, the patient should be rescheduled for mpMRI after waiting an appropriate period of time for the hemorrhage to resolve [16, 17].

T2W MRI is the main sequence used to delineate the prostate's zonal anatomy, to detect lesions, and to determine local staging; therefore, full coverage of the prostate and surrounding structures with high spatial resolution is essential. High image quality is particularly important for extraprostatic extension (EPE). To visualize the entirety of the prostate's anatomy, multiplanar images in axial, coronal, and sagittal are obtained. We perform T2-weighted MRI using fast-spin-echo images at 3 mm slice thickness with a field of view between 12 and 20 cm to allow visualization of the seminal vesicles as well as the entire prostate gland. Typically, images are obtained in two dimensions (2D); however three-dimensional (3D) images may also be obtained, and some consider 3D imaging more efficient and accurate [16, 28].

The most important functional sequence is DWI. DWI reflects the diffusion of free water molecules within the tissues and has much lower spatial resolution than the anatomical sequences. This sequence should be obtained in the axial plane at the same or similar geometry and slice thickness as the T2W images, for ease of comparison. DWI can be quantified by calculating apparent diffusion coefficient (ADC) maps voxel

Table 13.1 Acquisition parameters for T2W, DWI, DCE sequences of mpMRI. Adapted from [16]

	T2W	DWI	DCE
Image acquisition	2D RARE (rapid acquisition with relaxation enhancement) pulse sequences used. Avoid excessive echo train lengths to minimize blurring	Free-breathing spin echo EPI sequence combined with spectral fat saturation. ADC maps are calculated voxel by voxel. High *b*-value images may be acquired or calculated	Rapid 3D gradient echo T1W images obtained before, during, and after administration of contrast. Fat suppression recommended
Slice orientation	Axial, coronal, sagittal	Axial	Axial
TR/TE (ms)	2D RARE used	≤90 ms/≥3000 ms	<100 ms<5 ms
Slice thickness	3 mm, no gap. Should match other sequences	≤4 mm, no gap. Should match other sequences	3 mm, no gap. Should match other sequences
FOV (cm)	12–20 cm. Should be adjusted to cover entire prostate gland and seminal vesicles	16–22 cm	Should be adjusted to cover entire prostate gland and seminal vesicles
B-value (strength of magnetic field gradient applied)	–	ADC maps: ranging 50–100 s/min^3 to 800–1000 s/min^3. High *b*-value images: ≥ 1400-2000 s/min^3	–
In-plane resolution (phase × frequency)	≤0.7 × ≤0.4 mm	≤2.5 × ≤2.5 mm	≤2 × ≤2 mm
Temporal resolution	–	–	7 s preferred. Should be ≤10 s
Total observation rate	–	–	≥2 min
Contrast administration	–	–	*Dose*: 0.1 mmol/kg standard GBCA. *Injection rate*: 2–3 cc, with continuous image acquisition

*T2W*T2-weighted, *DWI* diffusion-weighted imaging, *DCE* dynamic contrast enhanced, *EPI* echo planar imaging, *T1W*T1-weighted, *TR/TE* repetition time/echo time, *FOV* field of view, *ADC* apparent diffusion coefficient, *GBCA* gadolinium-based contrast agent

by voxel using a signal decay model. ADC values are lower in areas of less diffusion, and vice versa. ADC values are calculated at various magnetic gradient strengths, referred to as *b*-values. DWI images are usually obtained using *b*-values ranging from 0 to 800 s/mm^3 [29]. At *b*-values >1000 s/mm^3, a "high b-value" image can be produced, which displays areas of decreased diffusion as regions of high signal [30]. However, high *b*-value imaging is compromised in signal-to-noise ratio, so another option is calculating a high *b*-value image based on lower *b*-value images [31]. The optimal high *b*-value for signal differentiation of tumors is 1500–2000 s/mm^3 [32]. Lower *b*-values are not as sensitive for tumor; higher values are associated with too much suppression of the background anatomy and loss of SNR [16, 33].

DCE-MRI consists of rapid 3D gradient echo (GRE) T1W images obtained before, during, and after administration of a gadolinium chelate-based contrast agent. The dynamic images should be acquired in the axial plane within the same slice width and geometry as the other sequences in the mpMRI set. This sequence reflects the leakage of the low-molecular-weight contrast agent into areas of pathology in the prostate. Due to tumors' increased vascular permeability as a result of angiogenesis, there is more rapid enhancement and wash-out after contrast administration, in comparison to the surrounding tissue. Before administration of contrast, the patient's

estimated glomerular filtration rate should be measured, as gadolinium-based contrast agents have been linked to nephrogenic systemic fibrosis in renal failure patients. Estimated GFR of at least 30 ml/min/1.73 m^3 is considered safe as per the FDA recommendations [16, 34].

Multiparametric MRI Interpretation

There are characteristic signal patterns on each sequence of the multiparametric MRI that are indicative of malignancy. Some are considered "dominant" depending on the location of the lesion within the gland; however, all data from every sequence should at least be considered when interpreting these studies. For instance, in the peripheral zone DWI is considered "dominant," whereas in the transition zone T2W is considered "dominant."

In interpreting T2W MRI, zonal anatomy can be appreciated immediately (Fig. 13.1). The peripheral zone is a hyperintense area on T2W bordering the iso-hypointense transition zone. The transition zone and peripheral zone are separated by the pseudocapsule or "surgical capsule," and the central zone, which is posteriorly and superiorly located in the gland, can sometimes be seen surrounding the ejaculatory ducts toward the base of the prostate. Ideally, one should also be able to identify the prostate capsule, neurovascular bundles at the 5 o'clock and 7 o'clock positions, and the seminal vesicles. Visualization of these structures is important for evaluating extraprostatic extension and for accurate locoregional staging. Suspicious lesions in the prostate tend to have shorter T2 relaxation time, causing them to be darker than surrounding tissue [35, 36]. In the peripheral zone (PZ), areas of suspicion appear hypointense, compared to the normally hyperintense PZ, and are often depicted as linear or heterogeneous regions with ill-defined borders or more homogenous regions with more defined borders. Because the normal PZ is relatively high in signal, most lesions can be seen on T2W. In the transition zone (TZ), the appearance of benign prostatic hyperplasia is more heterogeneous, often with well-circumscribed benign prostatic hyperplasia (BPH) nodules in older patients. In the TZ, a suspicious lesion may be similar in intensity or slightly less intense than the background tissue, and signal pattern may range from homogenous to heterogeneous. However, these findings are nonspecific for malignant changes on T2W imaging, as inflammation, atrophy, scarring, or hyperplasia may also cause the prostate tissue to have discrete low signal regions on T2W or be diffusely heterogeneous [37].

On DWI MRI, areas with restricted water diffusion are hypointense relative to the surrounding

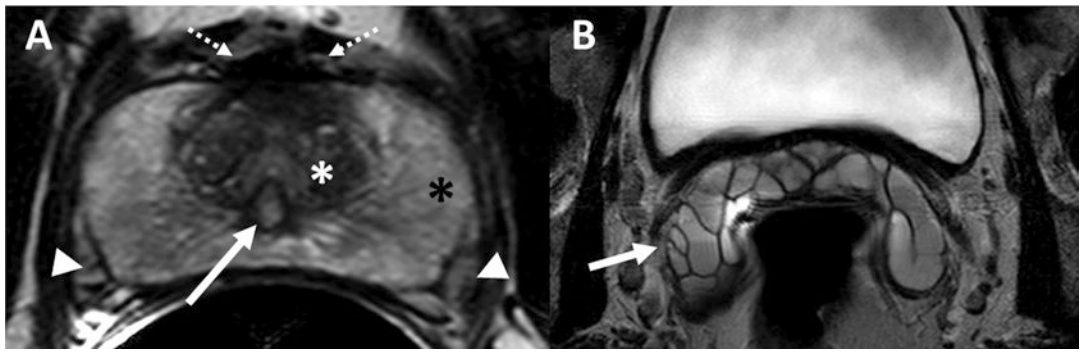

Fig. 13.1 Axial T2W MR scan of normal prostate anatomy is shown in (**a**). The transition zone (*white asterisk*) is separated from the peripheral zone (*black asterisk*) by the "surgical capsule" or pseudocapsule. The peripheral zone is surrounded by the prostatic capsule. The neurovascular bundles (*arrowheads*) can be visualized at the 5 o'clock and 7 o'clock positions. The urethra (*solid arrow*) is at the center. Anteriorly, the transition zone meets the anterior fibromuscular stroma (*dashed arrow*). In a superior axial slice from the same scan (**b**), the seminal vesicles (*arrow*) appear as well-dilated tubules

normal structures. Tumors, because of their tightly packed cellularity and increased stroma compared to the surrounding tissue, have more impeded water diffusion. The apparent diffusion coefficient is calculated on a voxel-by-voxel basis at varying gradient strengths ("b-values"). On the ADC map of DWI, areas with restricted diffusion will have lower ADC values and appear hypointense. ADC maps can be highly predictive. For instance, Faletti et al. demonstrated that a negative ADC map combined with a normal T2W MRI had a negative predictive value of 100 %. Thus, ADC maps can be a useful in differentiating benign and malignant lesions [38]. Additionally, ADC values inversely correlate with Gleason score of the lesion and can play a role in determining whether the cancer is low- or high-risk [39, 40]. Such information can help to determine whether a patient should be biopsied. ADC maps should always be interpreted with high *b*-value images acquired at *b*-values >1000 s/mm^3 or extrapolated from lower *b*-value images. These images display malignancy as high in signal making it easier to detect, in comparison to a relatively hypointense background in both the transition and the peripheral zones. High *b*-value imaging increases the sensitivity and specificity of prostate cancer detection on mpMRI [41]; *b*-values 1500–2500 s/mm^3 are ideal for detecting malignancy [33]. Tumor detection in the transition zone is especially improved with analysis of high *b*-value images [37]. Any suspected tumors on a high *b*-value image or an ADC map should be cross-checked with each other and also compared to the corresponding T2W image for confirmation that a suspicious area on the anatomical image is being evaluated.

DCE-MRI is another functional imaging method that also contributes to better detection of tumors. DCE-MRI takes advantage of enhanced capillary permeability of tumor vasculature. Normally, after contrast administration, a patient's prostate will show enhancement in the TZ with little enhancement in the PZ. In cases of BPH, there can be wide variation in enhancement. However, malignancies typically demonstrate increased vascular leakiness that leads to focal and rapid enhancement within the tumor. This is often accompanied by early wash-out of the enhancement due to increased blood flow and vessel leakiness. The combination of an early focal enhancement with early wash-out is strong evidence of a tumor. Thus, DCE-MRI adds confidence to the diagnosis, which is primarily based on the other sequences. DCE-MRI has proven to be most useful in the posttreatment setting when there is suspected recurrence, for which it exhibits high sensitivity and specificity [42].

Controversy remains regarding how best to analyze DCE-MRI data. The time-signal curve generated by a region of interest (ROI) in a suspected area can be evaluated qualitatively, semiquantitatively, or quantitatively. Qualitatively, early enhancing foci in the prostate can be visualized by scrolling the DCE-MRI in the cine mode. With experience, it is straightforward to recognize early, focal enhancement and early wash-out. Semiquantitative analysis extracts simple measurements from time-intensity curves, such as time of initial contrast uptake, time to peak enhancement, maximum slope, and wash-in and wash-out slopes. Qualitative and semiquantitative evaluation of DCE-MRI both improve detection of tumors, and the two interpretations perform similarly among readers [43]. However, they do not take into account factors such as gadolinium concentration is not directly related to MR signal intensity and the diffusion rate of contrast into tissues. Multiple attempts have been made to quantitate DCE-MRI in order to standardize measurements of enhancement across patients and scanners. In the quantitative approach, gadolinium concentration within the tissue is calculated based on relaxation rates of tissue, arterial input functions are measured, and the resulting curves are fit to a time-concentration curve from which rate constants such as K_{trans} and K_{ep} can be derived [44]. Although appealing in theory, there are several practical limitations. For instance, it is nearly impossible to measure actual input function to the tumor. Instead, approximations are made from adjacent large vessels such as the femoral artery. Moreover, estimating the T1 of tissue is fraught with error, and thus gadolinium concentration can be inaccurate. Also troubling is the plethora of different models, each

employing different assumptions that fill the literature. The value of such analyses when balanced against the difficulties encountered in obtaining them means that quantitative analysis of DCE-MRI is rarely employed. The weaknesses of DCE-MRI in general in the TZ reduce its value for a large part of the prostate gland [37]. Thus, T2W MRI and DWI have proven to be more robust than DCE-MRI. As a consequence, DCE-MRI plays a relatively minor role in PI-RADSv2 and is used primarily in increasing the score of lesions deemed to be PI-RADS 3 to PI-RADS 4 when classical tumor enhancement is seen.

In summary, a typical cancer within the prostate appears hypointense on T2W MRI, with low signal on the ADC map but high signal on high *b*-value DWI. The typical cancer enhances early after contrast administration on DCE-MRI (Fig. 13.2). There is some overlap between the imaging appearance of a malignancy and benign prostatic processes such as prostatitis and BPH; however, distinction is usually possible. The interpretation of mpMRI has been improved by the adoption of the PI-RADSv2 guidelines. In PI-RADSv2, a score ranging from 1 to 5 is assigned to each lesion. If the lesion is in the PZ the score is highly reliant on the DWI score and less on T2W and DCE-MRI; however, a positive DCE-MRI score can increase a PI-RADS 3 score to PI-RADS 4 thus communicating that a biopsy is indicated. In the TZ, the dominant pulse sequence is T2W, and DWI can be used in a similar manner as DCE-MRI in the PZ to increase a PI-RADS score of 3 to 4. Lesions scored as PI-RADS 4 or 5 suggest an increased likelihood of clinically significant malignancy, but the utility and reliability of PI-RADSv2 is still under investigation [16].

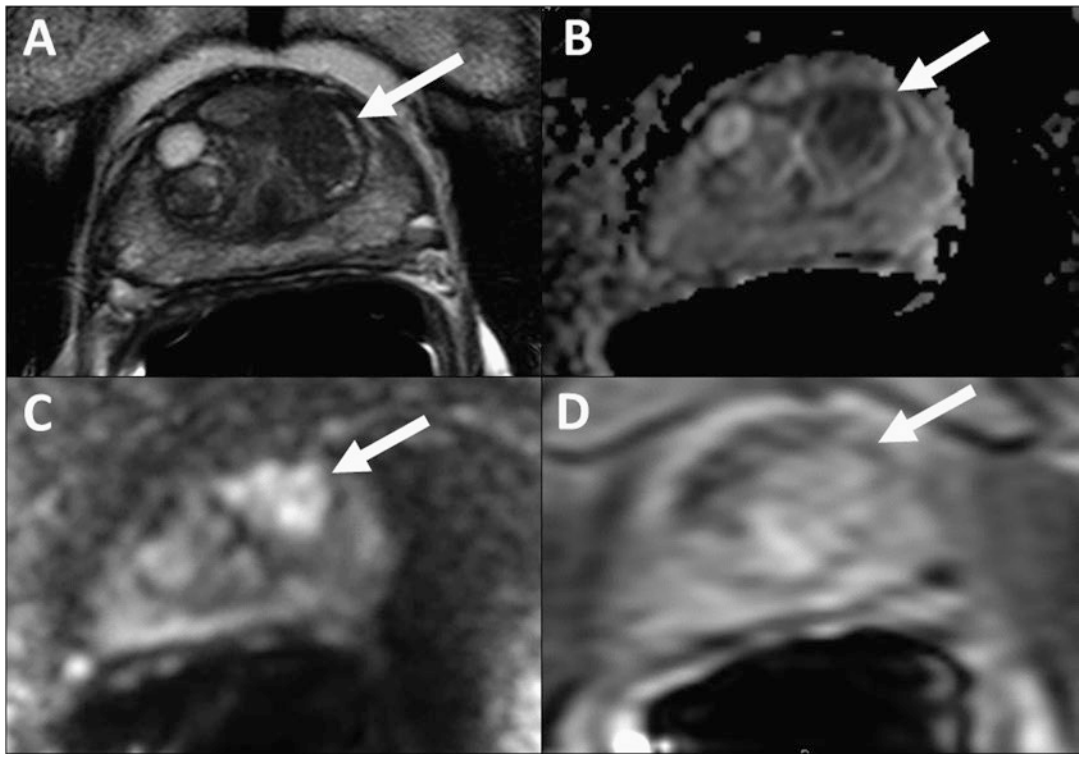

Fig. 13.2 A 64-year-old patient with a PSA = 6.10 ng/ml. Axial T2W MRI shows a hypointense lesion in the left mid-anterior transition zone, greatest diameter 1 cm (*arrow*) (**a**). The lesion is confirmed by hypointensity in the same location on ADC map (**b**), hyperintensity in the same location on b2000 DWI (**c**), and demonstration of hypervascularity within this location with early enhancement on DCE-MRI (**d**). Patient subsequently underwent MRI/fusion-guided biopsy, which resulted in a Gleason 3+4 disease diagnosis

Biopsy Guidance

By themselves, mpMRI findings are of little value. It is only after the mpMRI findings are used to obtain a tissue diagnosis that proper therapy can be instituted. Multiparametric MRI provides the opportunity for image-guided biopsy of suspected tumors. Common methods of using mpMRI during the biopsy procedure include cognitive fusion with real-time TRUS imaging, MRI/TRUS fusion devices, and in-bore MRI biopsy. In contrast, the standard 12-core systematic biopsy is not truly image-guided as the TRUS is unable to detect prostate cancers reliably. MRI-guided biopsies can reduce the need for biopsy by demonstrating a normal gland. MRI-guided biopsy also reduces the diagnosis of low-risk cancer and increases the diagnosis of intermediate/high-risk cancer [45–47].

With cognitive fusion-guided biopsy, the operator uses their prior review of the mpMRI images to guide the needle to the same region on the TRUS [48]. Because the planes of section between MRI and ultrasound are usually quite different, accurate knowledge of where an MRI finding appears on the TRUS can be very challenging. Cognitive biopsies require both experience and an understanding of the difference between axial MRI images and oblique ultrasound images. Therefore, the method is highly user dependent. Additionally, since there is no image taken while the biopsy is performed, location of the needle and biopsy site cannot be recorded [49]. This makes it impossible to confidently sample the same area on follow-up studies.

A relatively new alternative to cognitive biopsy is MRI/TRUS fusion biopsy. After the mpMRI is performed, the prostate gland is segmented and lesions are identified. The images are then transferred to the ultrasound suite where a software fusion system matches live transrectal ultrasound images to the acquired mpMRI images. The ultrasound is live-tracked using either a mechanical arm or a radiofrequency device. Once the two images are fused, the ultrasound can be tracked so that an updated MR image in the same plane as the TRUS is always displayed to the operator. With this method, accurate biopsies can be obtained, and the biopsy sites can be recorded [50]. Using this technique in more than 1000 patients, a 30 % higher detection rate of clinically significant cancer and a 17 % lower detection of indolent disease were found when compared to 12-core systematic biopsies [12]. Popular fusion systems include UroNav® (Invivo, Gainesville, FL), Artemis® (Eigen, Grass Valley, CA), Urostation® (Koelis, Meylan, France), and BiopSee® (Pi Medical, Athens, Greece), and each has a steep learning curve for operation [51].

Finally, in-bore MRI-guided biopsy is another possible method for image-guided biopsy. The biopsy takes place in the MR gantry after an initial mpMRI has detected suspicious lesions within the prostate. Biopsy needles can be introduced into the prostate either transrectally or transperineally, and MR images are obtained to ensure that the needles are in the correct location. Advantages of this approach include accurate detection of clinically significant cancer and good visualization of the needle [52]. However, patient discomfort is significant when they must be in the gantry for a long time, and the biopsy is highly user dependent and very difficult to teach to new operators. Moreover, the procedure is resource intense and thus also expensive compared to the other methods [53].

Indications for Magnetic Resonance Imaging

Detection of Prostate Cancer

The main purpose of mpMRI is to improve detection of prostate cancer compared to systematic biopsy, which is the current standard of care. Systematic biopsy is performed in patients either because of a suspicious digital rectal exam or an elevated PSA, but because TRUS is limited in its ability to detect prostate cancer, the biopsies are taken blindly from 10 to 12 different areas of the prostate. Significant cancer can be missed. Siddiqui et al. demonstrated that tumors detected with mpMRI can identify 30 % more clinically significant

cancers and 17 % fewer insignificant cancers compared with TRUS-guided biopsies [12].

Although mpMRI contributes to more accurate detection of prostate cancer, it has some limitations. Up to 18.7 % of MRIs can be false negative for prostate cancer [54]. One explanation could be that certain tumors do not grow focally but rather spread radially and discontinuously and are sometimes referred to as "sparse tumors." There is some evidence, however, that these MRI-negative cancers may represent a less aggressive form of the disease provided the mpMRI is truly negative. Additional potential reasons for a negative mpMRI in the setting of pathologic diagnosis of clinically significant prostate cancer include technically inadequate scans, interpretative errors, or failure to biopsy the correct target. For instance, the quality of an MRI scan may be insufficient to permit prostate cancer detection. This can arise from patient issues (motion, total hip replacement) or from machine issues (incorrect scanning parameters, misplacement of an endorectal coil, or other coil errors). Interpretive errors can occur from observer fatigue or from lack of training, both of which are correctable. Biopsy errors occur when the lesion is well identified, but the needle is placed in the wrong location. This can occur due to poor segmentation, inaccurate registration, or other user errors during the biopsy. Any of these factors in the "chain of quality" can result in diagnostic errors. Thus, in order to improve mpMRI, all aspects of the chain of quality must be maintained at a high level.

Staging of Prostate Cancer

Patients with prostate cancer can not only be diagnosed but can also be staged with mpMRI to determine the regional extent of disease. Conventional imaging techniques such as ultrasonography and computed tomography (CT) have insufficient soft tissue resolution to identify the extent of primary prostate cancer and their relation with the prostatic capsule and seminal vesicles, neurovascular bundles, or rectum. The most common staging system for prostate cancer is the T/N/M system: (T) tumor size, (N) presence of nodal involvement, and (M) presence of metastasis to local or distant structures [55]. Stages defined as T1–T2 are confined within the prostate, while extraprostatic extension upstages to T3A, seminal vesicle involvement upstages to T3B, and further organ involvement is T4 [56]. Axial T2W images are best for initially assessing extraprostatic extension. However, more complete assessment for staging includes making note of capsular shape and symmetry, of neurovascular bundle asymmetry, and of seminal vesicle involvement and pelvic nodal disease [57]. Subtle features indicative of extraprostatic extension include loss of the rectoprostatic angle, blurring of the prostatic capsule border, and unilateral change in the prostatic neurovascular bundle, which is found at the 5 o'clock or 7 o'clock position of the prostate in the axial plane. Seminal vesicle involvement can be evaluated by looking for focal hypointensity on the axial and coronal T2W [58]. The use of ERC is particularly helpful for extraprostatic extension and seminal vesicle invasion (SVI) [59]. The diagnosis of extraprostatic extension can be supplemented with DWI or DCE-MRI (Fig. 13.3). Addition of DWI with ADC mapping to the anatomical sequences has been shown to increase the accuracy of detecting extraprostatic extension [60]. However, staging using mpMRI has its limitations, especially in its ability to detect microscopic EPE. A meta-analysis conducted by de Rooij et al. regarding use of mpMRI for local staging revealed that the sensitivity of mpMRI for EPE/SVI is 57–61 %, whereas the specificity for detection of EPE/SVI was 88–96 % [61]. This study indicates the value of combining MRI findings with other clinicopathologic parameters.

MRI is also limited in differentiating malignant lymph nodes for staging since it mainly relies on size criteria and node shape, which are not sensitive or specific enough for nodal metastasis. In that respect, it performs very similarly to CT, which is notoriously insensitive for prostate cancer metastases.

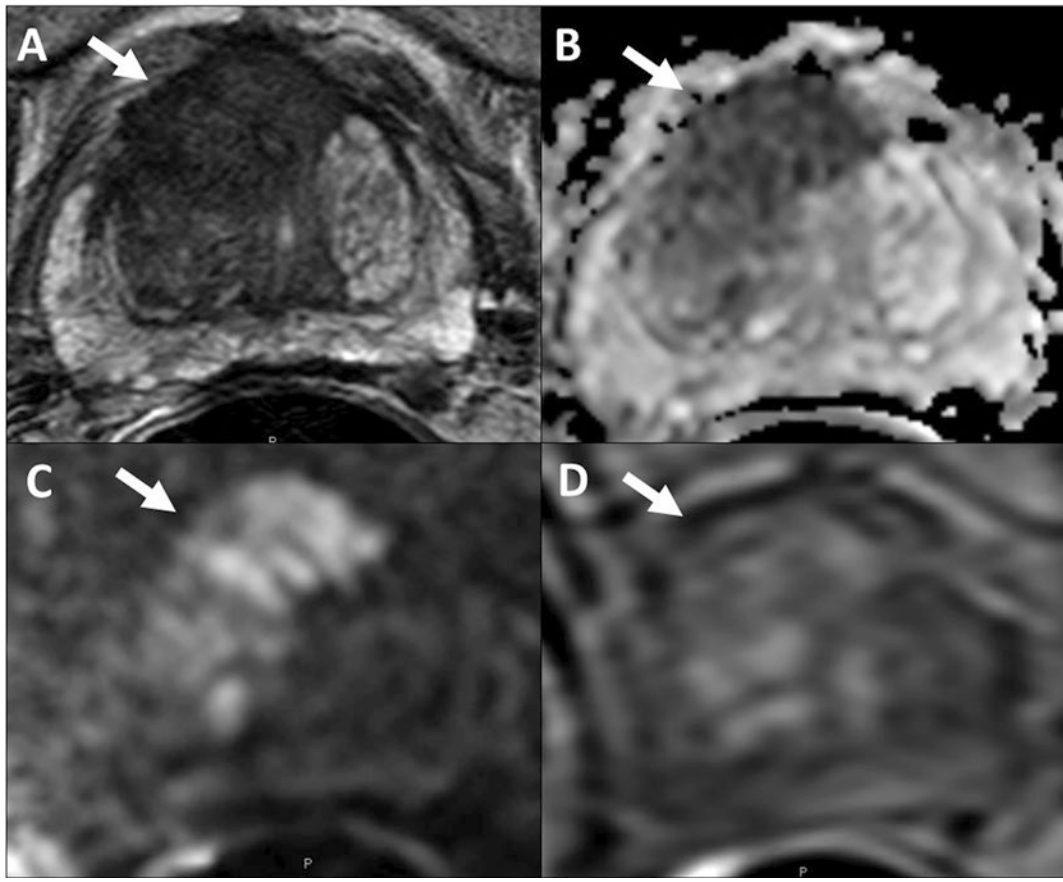

Fig. 13.3 A 79-year-old patient with a PSA = 11.12 ng/ml. Axial T2W MRI shows a 2.9 cm hypointense lesion in the midline to right apical-mid-anterior transition zone (*arrow*) with potential of extraprostatic extension toward the anterior of the gland, visualized as a capsular bulge (**a**). ADC maps of DWI identify the hypointense lesion in the same location (**b**) further confirmed with hyperintense signal pattern on b2000 DWI (**c**); the lesion shows focal hyperenhancement on DCE-MRI (**d**). Patient underwent MRI/TRUS fusion-guided biopsy, which resulted in a Gleason 4+5 disease diagnosis

Active Surveillance

Since the establishment of PSA screening in the 1990s, the detection and treatment of prostate cancer has significantly increased. Due to its slow-growing and progressing nature, many patients with prostate cancer die of other diseases, and therefore overtreatment is a real concern. Active treatment can have deleterious consequences on quality of life, and its effect on reduction of mortality is still controversial. Thus, active surveillance (AS) as an alternative has been discussed since the mid-1990s. Active surveillance is used for low-risk cancers and monitors patients with PSA and periodic re-biopsy. Current standard AS monitoring consists of PSA testing, DRE, and repeat standard biopsies. It is generally offered to patients who have prostate tumor that meets certain criteria: clinical stage ≤ T1c, Gleason grade ≤6, PSA density ≤0.15, tumor involving ≤2 cores, and ≤50 % involvement of any single core [62]. In case of progression or upgrading to a higher risk category, curative treatment is initiated.

However, these criteria can miss significant cancers lurking elsewhere within the gland. The strength of mpMRI for AS lies in the ability to detect lesions that were outside the initial biopsy template. Since a substantial number of men fall

out of AS due to continued rising PSA, mpMRI can be used to select out early men who are not appropriate candidates for AS. Meanwhile, because of its high negative predictive value for intermediate- and high-risk cancers, a negative mpMRI can support the choice of AS for appropriate patients [40, 62–64].

More controversial than its use in selecting patients for AS is the role of mpMRI in monitoring patients on AS. Multiparametric MRI has proven relatively insensitive to detecting upgrading of tumors from 3+3 to 3+4, which is the most common upgrading [62]. This apparent upgrading may be due to sampling different parts of the same stable tumor or it could represent real progression. In any case, the real implications of these minor increases in grade on serial biopsies during AS are still debated. In comparison to PSA, mpMRI has a lower sensitivity for progression but higher specificity [65]. It has been suggested that the combination of mpMRI and PSA density monitoring in AS may significantly improve prediction of pathological progression. Felker et al. suggested that adding mpMRI to traditional parameters such as PSA and grade carries incremental value; area under the receiver operating curve for PSA density or positive biopsy predicting progression was significantly increased from 0.87 to 0.91 with the addition of mpMRI results [66]. Finally, patients who choose AS over curative treatment may be concerned about any additional risks of AS and potential of undertreating disease. Two large prospective AS cohorts show a very low risk of prostate cancer-related mortality and metastatic disease [67, 68].

The utilization of mpMRI for AS is still evolving. Practice standards for its use in AS are just beginning to include mpMRI. Eligibility criteria and follow-up protocols demonstrate wide variability across institutions, and the best approach is still unclear. Ideal protocols should be able to identify eligible patients and detect progression of disease as early as possible in order to forestall disease progression. Additionally, monitoring methods for AS should be low cost and carry low morbidity. The morbidity of repeated biopsies during AS monitoring provides motivation to consider mpMRI as a substitute for routine biopsy, reserving biopsies instead for patients with rising PSA and/or changed mpMRI [69]. Finally, mpMRI's additional value in selecting AS patients is imperfect [70, 71]. In one study by Siddiqui et al., mpMRI misdirected 29 % of patients into AS, discovered by confirmatory biopsy [72]. Another study showed that up to 16 % of clinically significant cancers are missed by mpMRI [73]. Such limitations may explain why current guidelines are hesitant to integrate mpMRI into AS algorithms. The value of the inclusion of mpMRI in current nomograms has to be evaluated further through prospective trials [72]. However, since no perfect method exists for AS besides clinically validated molecular tests, prostate mpMRI has experienced increased use in monitoring of tumors.

Challenges and Limitations

Prostate mpMRI has utility in diagnosis, staging, and treatment planning. In addition to technical issues with the scans, mpMRI interpretation on the basis of PI-RADSv2 is still subject to variability among readers, despite attempts at standardization. In a multi-reader analysis, the average sensitivity for detecting all lesions across five readers was 63 %, and inter-reader agreement among readers was 58 % for scoring all lesions. This variability is especially pronounced in non-index lesions [74]. Secondly, image interpretation of mpMRI is challenging. It has been established that tumor size and grade are important predictors of tumor detection on imaging; however, as an example, in one study by Le et al., mpMRI failed to detect 28 % of tumors >1 cm and 28 % tumors ≥Gleason score 7 [75]. Finally, there are challenges faced in access to mpMRI as a standard modality for prostate imaging. While mpMRI followed by image-guided biopsy has been shown to be more cost effective compared to sextant biopsy, the price of obtaining the necessary resources to perform such biopsies can pose a challenge to centers that are not financially equipped [76]. The cost is further increased by the requirement for contrast media for DCE images, MRI supplies, and the ERC. ERC

reimbursement in particular is challenging, as there are conflicting studies regarding its utility [24, 25, 77, 78]. These limitations are important to consider when utilizing mpMRI for its multiple diagnostic capabilities. MRI of the prostate still has challenges that need to be overcome.

Conclusion

Multiparametric MRI has truly added to the evolution of prostate cancer detection, staging, and management. This modality's multiple pulse sequences can locate and characterize tumors in an in-depth manner, improving accuracy of imaging findings. Limitations include the cost of acquiring the images, and the skills required for reading and interpretation. The images obtained in mpMRI must be interpreted so as to provide uniform results across the world, and there are continued attempts to educate readers and to standardize image findings. However, accurate lesion visualization with MRI combined with novel image-guided biopsy enable a thorough method of lesion detection and treatment planning. Such advances suggest promise for the future of mpMRI and likely further exploration of its role and utilization in prostate cancer management.

References

1. Howlader N, Noone AM, Krapcho M, Miller D, Bishop K, Altekruse SF, Kosary CL, Yu M, Ruhl J, Tatalovich Z, Mariotto A, Lewis DR, Chen HS, Feuer EJ, Cronin KA (eds). SEER Cancer Statistics Review, 1975-2013, National Cancer Institute. Bethesda, MD, http://seer.cancer.gov/csr/1975_2013/, based on November 2015 SEER data submission, posted to the SEER web site, April 2016.
2. Heidenreich A, Bastian PJ, Bellmunt J, Bolla M, Joniau S, van der Kwast T, et al. Eau guidelines on prostate cancer. Part II: treatment of advanced, relapsing, and castration-resistant prostate cancer. Eur Urol. 2014;65(2):467–79.
3. Moyer VA. Force USPST. Screening for prostate cancer: U.S. Preventive services task force recommendation statement. Ann Intern Med. 2012;157(2):120–34.
4. Andriole GL, Crawford ED, Grubb 3rd RL, Buys SS, Chia D, Church TR, et al. Mortality results from a randomized prostate-cancer screening trial. N Engl J Med. 2009;360(13):1310–9.
5. Schroder FH, Hugosson J, Roobol MJ, Tammela TL, Ciatto S, Nelen V, et al. Screening and prostate-cancer mortality in a randomized European study. N Engl J Med. 2009;360(13):1320–8.
6. Shoag JE, Mittal S, Hu JC. Reevaluating psa testing rates in the PLCO trial. N Engl J Med. 2016;374(18):1795–6.
7. Weiner AB, Matulewicz RS, Eggener SE, Schaeffer EM. Increasing incidence of metastatic prostate cancer in the United States (2004–2013). Prostate Cancer Prostatic Dis. 2016; doi:10.1038/pcan.2016.30.
8. Epstein JI, Feng Z, Trock BJ, Pierorazio PM. Upgrading and downgrading of prostate cancer from biopsy to radical prostatectomy: incidence and predictive factors using the modified Gleason grading system and factoring in tertiary grades. Eur Urol. 2012;61(5):1019–24.
9. Caras RJ, Sterbis JR. Prostate cancer nomograms: a review of their use in cancer detection and treatment. Curr Urol Rep. 2014;15(3):391.
10. Cui Y, Cao W, Li Q, Shen H, Liu C, Deng J, et al. Evaluation of prostate cancer antigen 3 for detecting prostate cancer: a systematic review and meta-analysis. Sci Rep. 2016;6:25776.
11. Hricak H, Dooms GC, Jeffrey RB, Avallone A, Jacobs D, Benton WK, et al. Prostatic carcinoma: staging by clinical assessment, CT, and MR imaging. Radiology. 1987;162(2):331–6.
12. Siddiqui MM, Rais-Bahrami S, Turkbey B, George AK, Rothwax J, Shakir N, et al. Comparison of mr/ultrasound fusion-guided biopsy with ultrasound-guided biopsy for the diagnosis of prostate cancer. JAMA. 2015;313(4):390–7.
13. Filson CP, Natarajan S, Margolis DJ, Huang J, Lieu P, Dorey FJ, et al. Prostate cancer detection with magnetic resonance-ultrasound fusion biopsy: the role of systematic and targeted biopsies. Cancer. 2016;122(6):884–92.
14. Weinreb JC, Blume JD, Coakley FV, Wheeler TM, Cormack JB, Sotto CK, et al. Prostate cancer: sextant localization at mr imaging and mr spectroscopic imaging before prostatectomy–results of acrin prospective multi-institutional clinicopathologic study. Radiology. 2009;251(1):122–33.
15. Hoeks CM, Barentsz JO, Hambrock T, Yakar D, Somford DM, Heijmink SW, et al. Prostate cancer: multiparametric MR imaging for detection, localization, and staging. Radiology. 2011;261(1):46–66.
16. Weinreb JC, Barentsz JO, Choyke PL, Cornud F, Haider MA, Macura KJ, et al. PI-RADS prostate imaging – reporting and data system: 2015, version 2. Eur Urol. 2016;69(1):16–40.
17. Barrett T, Vargas HA, Akin O, Goldman DA, Hricak H. Value of the hemorrhage exclusion sign on t1-weighted prostate mr images for the detection of prostate cancer. Radiology. 2012;263(3):751–7.
18. Tamada T, Sone T, Jo Y, Yamamoto A, Yamashita T, Egashira N, et al. Prostate cancer: relationships

between postbiopsy hemorrhage and tumor detectability at MR diagnosis. Radiology. 2008; 248(2):531–9.
19. Zhao C, Gao G, Fang D, Li F, Yang X, Wang H, et al. The efficiency of multiparametric magnetic resonance imaging (mpMRI) using PI-RADS version 2 in the diagnosis of clinically significant prostate cancer. Clin Imaging. 2016;40(5):885–8.
20. Kabakus IM, Borofsky S, Mertan FV, Greer M, Daar D, Wood BJ, Pinto PA, Choyke PL, Turkbey B. Does abstinence from ejaculation before prostate MRI improve evaluation of the seminal vesicles? AJR Am J Roentgenol. 2016;207(6): 1205–9.
21. Johnston R, Wong LM, Warren A, Shah N, Neal D. The role of 1.5 tesla magnetic resonance imaging in staging prostate cancer. ANZ J Surg. 2013; 83(4):234–8.
22. Bloch BN, Lenkinski RE, Rofsky NM. The role of magnetic resonance imaging (MRI) in prostate cancer imaging and staging at 1.5 and 3 tesla: the Beth Israel Deaconess Medical Center (BIDMC) approach. Cancer Biomark. 2008;4(4–5):251–62.
23. Haider MA, Krieger A, Elliott C, Da Rosa MR, Milot L. Prostate imaging: evaluation of a reusable two-channel endorectal receiver coil for MR imaging at 1.5 t. Radiology. 2014;270(2):556–65.
24. Kim BS, Kim TH, Kwon TG, Yoo ES. Comparison of pelvic phased-array versus endorectal coil magnetic resonance imaging at 3 tesla for local staging of prostate cancer. Yonsei Med J. 2012;53(3):550–6.
25. Barth BK, Cornelius A, Nanz D, Eberli D, Donati OF. Comparison of image quality and patient discomfort in prostate MRI: pelvic phased array coil vs. Endorectal coil. Abdom Radiol (NY). 2016;41(11): 2218–26.
26. Rosen Y, Bloch BN, Lenkinski RE, Greenman RL, Marquis RP, Rofsky NM. 3t mr of the prostate: reducing susceptibility gradients by inflating the endorectal coil with a barium sulfate suspension. Magn Reson Med. 2007;57(5):898–904.
27. Fusco R, Sansone M, Petrillo M, Setola SV, Granata V, Botti G, et al. Multiparametric mri for prostate cancer detection: preliminary results on quantitative analysis of dynamic contrast enhanced imaging, diffusion-weighted imaging and spectroscopy imaging. Magn Reson Imaging. 2016;34(7):839–45.
28. Rosenkrantz AB, Neil J, Kong X, Melamed J, Babb JS, Taneja SS, et al. Prostate cancer: comparison of 3d t2-weighted with conventional 2d t2-weighted imaging for image quality and tumor detection. AJR Am J Roentgenol. 2010;194(2):446–52.
29. Hauth E, Hohmuth H, Cozub-Poetica C, Bernand S, Beer M, Jaeger H. Multiparametric MRI of the prostate with three functional techniques in patients with PSA elevation before initial TRUS-guided biopsy. Br J Radiol. 2015;88(1054):20150422.
30. Agarwal HK, Mertan FV, Sankineni S, Bernardo M, Senegas J, Keupp J, et al. Optimal high b-value for diffusion weighted mri in diagnosing high risk prostate cancers in the peripheral zone. J Magn Reson Imaging. 2016; doi:10.1002/jmri.25353.
31. Grant KB, Agarwal HK, Shih JH, Bernardo M, Pang Y, Daar D, et al. Comparison of calculated and acquired high b value diffusion-weighted imaging in prostate cancer. Abdom Imaging. 2015;40(3):578–86.
32. Metens T, Miranda D, Absil J, Matos C. What is the optimal b value in diffusion-weighted MR imaging to depict prostate cancer at 3 t? Eur Radiol. 2012;22(3):703–9.
33. Rosenkrantz AB, Parikh N, Kierans AS, Kong MX, Babb JS, Taneja SS, et al. Prostate cancer detection using computed very high b-value diffusion-weighted imaging: how high should we go? Acad Radiol. 2016;23(6):704–11.
34. Schlaudecker JD, Bernheisel CR. Gadolinium-associated nephrogenic systemic fibrosis. Am Fam Physician. 2009;80(7):711–4.
35. Wu LM, Zhou B, Lu Q, Suo ST, Liu Q, Hu J, et al. T2* relaxation time in the detection and assessment of aggressiveness of peripheral zone cancer in comparison with diffusion-weighted imaging. Clin Radiol. 2016;71(4):356–62.
36. Gibbs P, Tozer DJ, Liney GP, Turnbull LW. Comparison of quantitative t2 mapping and diffusion-weighted imaging in the normal and pathologic prostate. Magn Reson Med. 2001;46(6):1054–8.
37. Rosenkrantz AB, Kim S, Campbell N, Gaing B, Deng FM, Taneja SS. Transition zone prostate cancer: revisiting the role of multiparametric MRI at 3 t. AJR Am J Roentgenol. 2015;204(3):W266–72.
38. Faletti R, Battisti G, Discalzi A, Grognardi ML, Martinello S, Oderda M, et al. Can DW-MRI, with its adc values, be a reliable predictor of biopsy outcome in patients with suspected prostate cancer? Abdom Radiol (NY). 2016;41(5):926–33.
39. Salami SS, Ben-Levi E, Yaskiv O, Turkbey B, Villani R, Rastinehad AR. Risk stratification of prostate cancer utilizing apparent diffusion coefficient value and lesion volume on multiparametric mri. J Magn Reson Imaging. 2016; doi:10.1002/jmri.25363.
40. Hambrock T, Somford DM, Huisman HJ, van Oort IM, Witjes JA, van de Kaa Hulsbergen CA, et al. Relationship between apparent diffusion coefficients at 3.0-t MR imaging and Gleason grade in peripheral zone prostate cancer. Radiology. 2011;259(2):453–61.
41. Jambor I, Kahkonen E, Taimen P, Merisaari H, Saunavaara J, Alanen K, et al. Prebiopsy multiparametric 3 t prostate mri in patients with elevated PSA, normal digital rectal examination, and no previous biopsy. J Magn Reson Imaging. 2015;41(5):1394–404.
42. Yu T, Meng N, Chi D, Zhao Y, Wang Z, Luo Y. Diagnostic value of dynamic contrast-enhanced magnetic resonance imaging in detecting residual or recurrent prostate cancer after radical prostatectomy: a pooled analysis of 12 individual studies. Cell Biochem Biophys. 2015;72(3):687–94.
43. Tan CH, Hobbs BP, Wei W, Kundra V. Dynamic contrast-enhanced mri for the detection of prostate

cancer: meta-analysis. AJR Am J Roentgenol. 2015;204(4):W439–48.
44. Cho E, Chung DJ, Yeo DM, Sohn D, Son Y, Kim T, et al. Optimal cut-off value of perfusion parameters for diagnosing prostate cancer and for assessing aggressiveness associated with Gleason score. Clin Imaging. 2015;39(5):834–40.
45. Pokorny MR, de Rooij M, Duncan E, Schroder FH, Parkinson R, Barentsz JO, et al. Prospective study of diagnostic accuracy comparing prostate cancer detection by transrectal ultrasound-guided biopsy versus magnetic resonance (MR) imaging with subsequent MR-guided biopsy in men without previous prostate biopsies. Eur Urol. 2014;66(1):22–9.
46. Albertsen PC, Hanley JA, Gleason DF, Barry MJ. Competing risk analysis of men aged 55 to 74 years at diagnosis managed conservatively for clinically localized prostate cancer. JAMA. 1998;280(11):975–80.
47. Hong CW, Amalou H, Xu S, Turkbey B, Yan P, Kruecker J, et al. Prostate biopsy for the interventional radiologist. J Vasc Interv Radiol. 2014;25(5):675–84.
48. Robertson NL, Emberton M, Moore CM. MRI-targeted prostate biopsy: a review of technique and results. Nat Rev Urol. 2013;10(10):589–97.
49. Logan JK, Rais-Bahrami S, Turkbey B, Gomella A, Amalou H, Choyke PL, et al. Current status of magnetic resonance imaging (MRI) and ultrasonography fusion software platforms for guidance of prostate biopsies. BJU Int. 2014;114(5):641–52.
50. Miyagawa T, Ishikawa S, Kimura T, Suetomi T, Tsutsumi M, Irie T, et al. Real-time virtual sonography for navigation during targeted prostate biopsy using magnetic resonance imaging data. Int J Urol. 2010;17(10):855–60.
51. Brown AM, Elbuluk O, Mertan F, Sankineni S, Margolis DJ, Wood BJ, et al. Recent advances in image-guided targeted prostate biopsy. Abdom Imaging. 2015;40(6):1788–99.
52. Beyersdorff D, Winkel A, Hamm B, Lenk S, Loening SA, Taupitz M. MR imaging-guided prostate biopsy with a closed mr unit at 1.5 t: initial results. Radiology. 2005;234(2):576–81.
53. Overduin CG, Futterer JJ, Barentsz JO. MRI-guided biopsy for prostate cancer detection: a systematic review of current clinical results. Curr Urol Rep. 2013;14(3):209–13.
54. Wysock JS, Mendhiratta N, Zattoni F, Meng X, Bjurlin M, Huang WC, et al. Predictive value of negative 3 t multiparametric prostate MRI on 12 core biopsy results. BJU Int. 2016;118(4):515–20.
55. Clements R, Griffiths GJ, Peeling WB. Staging prostatic cancer. Clin Radiol. 1992;46(4):225–31.
56. Edge SB, Compton CC. The American joint committee on cancer: the 7th edition of the ajcc cancer staging manual and the future of tnm. Ann Surg Oncol. 2010;17(6):1471–4.
57. Wang L, Mullerad M, Chen HN, Eberhardt SC, Kattan MW, Scardino PT, et al. Prostate cancer: incremental value of endorectal MR imaging findings for prediction of extracapsular extension. Radiology. 2004;232(1):133–9.
58. Sala E, Akin O, Moskowitz CS, Eisenberg HF, Kuroiwa K, Ishill NM, et al. Endorectal MR imaging in the evaluation of seminal vesicle invasion: diagnostic accuracy and multivariate feature analysis. Radiology. 2006;238(3):929–37.
59. Rorvik J, Halvorsen OJ, Albrektsen G, Ersland L, Daehlin L, Haukaas S. MRI with an endorectal coil for staging of clinically localised prostate cancer prior to radical prostatectomy. Eur Radiol. 1999;9(1):29–34.
60. Lawrence EM, Gallagher FA, Barrett T, Warren AY, Priest AN, Goldman DA, et al. Preoperative 3-t diffusion-weighted MRI for the qualitative and quantitative assessment of extracapsular extension in patients with intermediate- or high-risk prostate cancer. AJR Am J Roentgenol. 2014;203(3):W280–6.
61. de Rooij M, Hamoen EH, Witjes JA, Barentsz JO, Rovers MM. Accuracy of magnetic resonance imaging for local staging of prostate cancer: a diagnostic meta-analysis. Eur Urol. 2016;70(2):233–45.
62. Walton Diaz A, Shakir NA, George AK, Rais-Bahrami S, Turkbey B, Rothwax JT, et al. Use of serial multiparametric magnetic resonance imaging in the management of patients with prostate cancer on active surveillance. Urol Oncol. 2015;33(5):202.e201–7.
63. Turkbey B, Mani H, Aras O, Ho J, Hoang A, Rastinehad AR, et al. Prostate cancer: can multiparametric MR imaging help identify patients who are candidates for active surveillance? Radiology. 2013;268(1):144–52.
64. Seiler D, Randazzo M, Leupold U, Zeh N, Isbarn H, Chun FK, et al. Protocol-based active surveillance for low-risk prostate cancer: anxiety levels in both men and their partners. Urology. 2012;80(3):564–9.
65. Rosenkrantz AB, Rice SL, Wehrli NE, Deng FM, Taneja SS. Association between changes in suspicious prostate lesions on serial mri examinations and follow-up biopsy results. Clin Imaging. 2015;39(2):264–9.
66. Felker ER, Wu J, Natarajan S, Margolis DJ, Raman SS, Huang J, et al. Serial magnetic resonance imaging in active surveillance of prostate cancer: incremental value. J Urol. 2016;195(5):1421–7.
67. Klotz L, Vesprini D, Sethukavalan P, Jethava V, Zhang L, Jain S, et al. Long-term follow-up of a large active surveillance cohort of patients with prostate cancer. J Clin Oncol. 2015;33(3):272–7.
68. Tosoian JJ, Mamawala M, Epstein JI, Landis P, Wolf S, Trock BJ, et al. Intermediate and longer-term outcomes from a prospective active-surveillance program for favorable-risk prostate cancer. J Clin Oncol. 2015;33(30):3379–85.
69. Bergman J, Litwin MS. Quality of life in men undergoing active surveillance for localized prostate cancer. J Natl Cancer Inst Monogr. 2012;2012(45):242–9.
70. Filippou P, Welty CJ, Cowan JE, Perez N, Shinohara K, Carroll PR. Immediate versus delayed radical prostatectomy: updated outcomes following active

surveillance of prostate cancer. Eur Urol. 2015; 68(3):458–63.
71. Tosoian JJ, Sundi D, Trock BJ, Landis P, Epstein JI, Schaeffer EM, et al. Pathologic outcomes in favorable-risk prostate cancer: comparative analysis of men electing active surveillance and immediate surgery. Eur Urol. 2016;69(4):576–81.
72. Stamatakis L, Siddiqui MM, Nix JW, Logan J, Rais-Bahrami S, Walton-Diaz A, et al. Accuracy of multiparametric magnetic resonance imaging in confirming eligibility for active surveillance for men with prostate cancer. Cancer. 2013;119(18):3359–66.
73. Serrao EM, Barrett T, Wadhwa K, Parashar D, Frey J, Koo BC, et al. Investigating the ability of multiparametric mri to exclude significant prostate cancer prior to transperineal biopsy. Can Urol Assoc J. 2015;9(11–12):E853–8.
74. Greer MD, Brown AM, Shih JH, Summers RM, Marko J, Law YM, et al. Accuracy and agreement of PIRADSV2 for prostate cancer mpMRI: a multireader study. J Magn Reson Imaging. 2016; doi:10.1002/jmri.25372.
75. Le JD, Tan N, Shkolyar E, Lu DY, Kwan L, Marks LS, et al. Multifocality and prostate cancer detection by multiparametric magnetic resonance imaging: correlation with whole-mount histopathology. Eur Urol. 2015;67(3):569–76.
76. Willis SR, Ahmed HU, Moore CM, Donaldson I, Emberton M, Miners AH, et al. Multiparametric MRI followed by targeted prostate biopsy for men with suspected prostate cancer: a clinical decision analysis. BMJ Open. 2014;4(6):e004895.
77. Turkbey B, Merino MJ, Gallardo EC, Shah V, Aras O, Bernardo M, et al. Comparison of endorectal coil and nonendorectal coil t2w and diffusion-weighted MRI at 3 tesla for localizing prostate cancer: correlation with whole-mount histopathology. J Magn Reson Imaging. 2014;39(6):1443–8.
78. Hoffner MK, Huebner F, Scholtz JE, Zangos S, Schulz B, Luboldt W, et al. Impact of an endorectal coil for 1 h-magnetic resonance spectroscopy of the prostate at 3.0 t in comparison to 1.5 t: do we need an endorectal coil? Eur J Radiol. 2016;85(8):1432–8.

14 Optimizing Multiparametric Magnetic Resonance Imaging for a Focal Therapy Practice: Quality Improvement

Jamie N. Holtz and Rajan T. Gupta

Introduction

Prostate magnetic resonance imaging (MRI) has been used for three decades, though it has only recently reached sufficient levels of quality to be reliably used in clinical applications. The main difference between the prostate MRI of yesterday and the prostate MRI of today is the multiparametric nature of the technique, consisting of high-resolution anatomical T2-weighted imaging (T2WI) and at least two functional parameters—most commonly diffusion-weighted imaging (DWI) and dynamic contrast-enhanced (DCE) sequences. This new form of prostate multiparametric MRI (mpMRI) can be used in the diagnosis, staging, treatment planning, and follow-up of prostate cancer. An expert panel of urologists and uroradiologists publishing in the field of focal therapy (FT) for prostate cancer and mpMRI has stated that mpMRI is the "ideal imaging tool for focal therapy of prostate cancer" [1].

Multiparametric MRI has multiple roles throughout the process of a patient receiving focal therapy: the initial diagnosis and evaluation for candidacy for focal therapy, image guidance for targeted biopsy and/or focal therapy, and follow-up imaging to detect treated tissue, potential residual disease, or disease recurrence. There are opportunities for the incorporation of quality improvement at each of these steps, which will be discussed further in this chapter.

Quality improvement (QI) is a relatively new term in healthcare and radiology, as the traditional term used is quality assurance (QA). The difference between these terms is not strictly semantic. QI aims at determining how one is currently performing and the areas in which one can improve; QA generally aims at determining where fault lies after medical errors. QI can be prospective or retrospective; QA is always retrospective. Perhaps most importantly, QI should be introspective. QI should be a vehicle to ensure delivery of quality care to patients while continuously iterating how that should best be done [2].

Optimal Image Acquisition

High-quality MR images are important to accurately detect and stage clinically significant prostate cancer and, ultimately, to appropriately select patients for focal therapy or direct them to another management plan. A detailed description of technical parameters of mpMRI is outside the scope of this chapter, but some key points will be

J.N. Holtz
Department of Radiology, Duke University Medical Center, Durham, NC, USA

R.T. Gupta (✉)
Department of Radiology, Duke Cancer Institute, Duke University Medical Center, Durham, NC, USA
e-mail: rajan.gupta@duke.edu

© Springer International Publishing AG 2017

T.J. Polascik (ed.), *Imaging and Focal Therapy of Early Prostate Cancer*, Current Clinical Urology, DOI 10.1007/978-3-319-49911-6_14

addressed. Current recommendations for parameters to include for prostate mpMRI are high-resolution, multiplanar T2WI for anatomic localization combined with at least two functional techniques, such as DWI and DCE-MRI, and/or magnetic resonance spectroscopy (MRS) [3].

T2-Weighted Imaging Guidelines

Most centers obtain T2WI of the prostate using two-dimensional rapid acquisition with relaxation enhancement (2D RARE) sequences (i.e., fast spin echo and turbo spin echo) in the orthogonal axial, sagittal, and coronal planes. This accounts for partial volume effects while allowing full visualization of the prostate morphology. Newer three-dimensional (3D) T2 sequences have been released by multiple vendors, and may be potential alternatives to obtaining sagittal images, as these sequences allow for the generation of a 3D dataset with high spatial resolution and voxel sizes of 1 mm or less that can be reformatted in any desired slice thickness or plane [4]. While the reformatted planes can decrease partial volume effects and produce subjectively comparable image quality to 2D RARE, they may also have more motion artifacts due to the typically longer acquisition times [5]. Thin sections of ≤3 mm each with no interslice gap and a field of view minimized to the extent possible while maintaining satisfactory signal-to-noise ratio (SNR) help to reduce the risk of missing small tumors on T2WI [6].

Diffusion-Weighted Imaging Guidelines

DWI is another sequence very important for detecting and characterizing prostate cancer, especially in the peripheral zone of the gland [6]. Arguably, DWI is as critical in mpMRI as the anatomic T2WI. Prostate cancer appears as areas of restricted diffusion in the gland, since malignant tissue typically restricts the random motion of water to a higher extent than healthy prostate tissue due to the higher cellular density of many tumors [3]. Guidelines recommend obtaining DWI with thin sections (≤4 mm) and a small field of view that still allows for adequate SNR [6]. Multiparametric MRI should also include an apparent diffusion coefficient (ADC) map created based on a monoexponential model using multiple *b* values ranging from 50 to 1000 s/mm^2, with at least two values required. Clinically significant prostate cancer is likely to be associated with lower ADC values and a hypointense appearance on ADC maps [7–9]. While additional *b* values can improve ADC calculation accuracy, this is associated with increased imaging. Ultrahigh *b* value (1400–2000 s/mm^2) imaging either estimated by extrapolating the data obtained from lower *b* values or obtained as a separate acquisition has been shown to increase detection of significant prostate cancer [10–14] and is a key addition to the Prostate Imaging Reporting and Data System (PI-RADS) version 2 [6].

Dynamic Contrast-Enhanced Magnetic Resonance Imaging Guidelines

The main role for DCE-MRI is in detecting recurrence of prostate cancer after treatment, which will be discussed later in this chapter. It should be noted that while DCE-MRI can also aid in prostate cancer detection and staging, its role has been de-emphasized in the latest PI-RADS version 2 recommendations [6]. To obtain DCE-MRI images, 0.1 mmol/kg of an extracellular gadolinium-based MR contrast agent is administered at 2–3 mL/s, and a 2D or 3D T1 gradient echo (GRE) sequence is acquired before and after the administration of contrast, typically with fat suppression and subtracted images. Prostate tumors are usually neovascular with highly permeable capillaries, and DCE-MRI takes advantage of these properties to detect cancer, which typically appears as earlier and more intense enhancement compared to surrounding prostate tissue [15, 16]. Temporal resolution of DCE images should ideally be less than 7 s and no more than 10 s to best ensure the point of peak enhancement is detected. The question of whether

to use quantitative or subjective models to interpret DCE-MRI has yet to be resolved, with some studies finding higher accuracy when quantitative or semiquantitative models are used, while others did not find a significant difference between approaches [17, 18].

Magnetic Resonance Spectroscopy Guidelines

Magnetic resonance spectroscopy uses elevated ratios of metabolites such as choline and creatine to citrate to identify areas suspicious for prostate cancer [19]. Despite its potential role in mpMRI, MR spectroscopy has significant disadvantages, including the high level of technical expertise required to acquire and interpret these images as well as a lack of apparent benefit over T1- and T2-weighted images alone [20]. As a result, this parameter is not included in prostate mpMRI at many centers or in the PI-RADS version 2 guidelines [6, 21].

General Acquisition Guidelines: Field Strength, Coils, Exam Timing, and Patient Preparation

In general, 3 T is the preferred field strength for prostate mpMRI when used for focal therapy [1] because of the higher SNR than at 1.5 T [22]. While pelvic phased array coils are considered a basic requirement in the acquisition of prostate mpMRI, the addition of an endorectal coil (ERC) can improve image quality, tumor localization, and prostate cancer staging by experienced radiologists [23, 24]. ERC is recommended when a field strength of 1.5 T is used, although many centers use endorectal coils with 3 T scanners as well [1]. One study by Bratan et al. found that the magnetic field strength of the scanner or whether an ERC was used did not significantly impact cancer detection rates on mpMRI [25], and experts have stated that while there are advantages to both 3 T scanners and ERCs, it is possible to obtain quality images at 1.5 T and without using an ERC if other acquisition parameters and patient characteristics are optimized [6]. The main advantage of the ERC is in the acquisition of high-quality DWI and DCE-MRI images as well as evaluation of the prostatic capsule and neurovascular bundles on T2WI [23, 26].

Other details that will affect image quality are timing of exam after biopsy and patient preparation. If the prostate has been biopsied, at least a 6-week delay before imaging is recommended since post-biopsy hemorrhage can interfere with cancer staging, though this may not significantly affect tumor detection [24, 27]. Post-biopsy hemorrhage can be differentiated from prostate cancer using pre-contrast T1 images; hemorrhage appears as T1 hyperintense signal, while prostate cancer will be isointense or hypointense on T1WI. With regard to patient preparation, air in the rectum can lead to susceptibility artifacts, which may substantially hinder image quality, especially of DWI. Rectal air can be minimized if using an ERC by removing the air from the coil balloon and filling the coil with material such as liquid perfluorocarbon or barium suspension [28]. If not using an ERC, options to minimize rectal air include instructing the patient to evacuate their rectum or using a small catheter to decompress and remove air from the rectum. Finally, motion artifact due to bowel peristalsis is another aspect of the exam that may inhibit image quality. While antiperistaltic agents such as glucagon may help reduce bowel motion in some patients, this is not required and is not used at many centers.

Opportunities for Quality Improvement in Image Acquisition

Recent research is promising for the continued improvement of mpMRI image quality. It is important for radiologists to not be complacent and to continue to assess acquisition parameters in order to continue to improve. Working directly with the MR scanner vendors and applications specialists from these companies can be invaluable in ensuring that the best sequences are being used at centers performing prostate mpMRI. Techniques have been developed with the goal of reducing motion

artifact of prostate T2WI. The BLADE technique (Siemens Healthcare, Erlangen, Germany) has been shown to help with the detection of extraprostatic extension, which may exclude patients from focal therapy, though this is done at the cost of reduced image contrast [29]. There are also techniques that have been demonstrated to improve the image quality of DCE-MRI [30] and DWI [31]. Radiologists in a prostate mpMRI practice used for focal therapy or other applications must stay abreast of recent developments and incorporate new technology into their practice as appropriate for prostate mpMRI to continue to improve.

Quality Improvement of Image Interpretation and Reporting

The demand for prostate mpMRI is outpacing the current capacity to perform high-quality mpMRI, which underscores the need to expand training and optimize image interpretation beyond a core group of academic and large-volume private/community centers. A consensus panel of expert radiologists and urologists agree that "the standardization of conduct and reporting protocols was of paramount importance" in prostate mpMRI for focal therapy [1].

The Value of the Prostate Imaging Reporting and Data System

PI-RADS version 2 provides standardized reporting guidelines for prostate mpMRI, and though these guidelines are not required, they are highly recommended [6]. PI-RADS version 2 recommends including the following in every prostate mpMRI report: PI-RADS score, lesion location based on gland segmentation scheme into a minimum of 16 divisions, maximum dimension of largest abnormal lesion, location and probability of extraprostatic extension (EPE), and pertinent incidental findings [6].

The PI-RADS score communicates the likelihood that a prostatic lesion represents a clinically significant cancer and can help guide whether a patient is recommended for biopsy or treatment, potentially including focal therapy. The lesion location based on a gland segmentation scheme into a minimum of 16 divisions is another aspect of the mpMRI report that may be important for focal therapy planning. For example, anterior tumors (Fig. 14.1) may be incompletely destroyed by focal therapy due to the inability to destroy tissue beyond a fixed focal point, so it is relevant for clinicians to know a tumor's location before deciding which treatment to recommend to their patient [32]. Another example of why lesion location is paramount to patient selection for focal therapy is a study by Rouviere et al., which found that "the location of cancer recurrence anterior to the urethra on MRI is an independent significant predictor of salvage HIFU failure for locally recurrent prostate cancer after EBRT" [33]. It is also critical for radiologists reporting prostate mpMRI to convey if the lesions extend across multiple anatomic divisions of the prostate; this information is vital for the treating clinician to determine the most appropriate treatment given the extent of the lesion(s).

The American College of Radiology (ACR) PI-RADS version 2 document also recommends reporting the maximum dimension of the largest abnormal lesion [6]. Focal therapy aims to treat the entire volume of a prostate tumor while minimizing the destruction of healthy prostate tissue; therefore lesion size is important information for treatment planning. Finally, patients with gross EPE or incidental findings, such as lymphadenopathy or bone metastases, may have prostate cancer that is too aggressive for treatment with focal therapy, so this information is also relevant for managing clinicians to know.

The Role of Education and Experience in Multiparametric Magnetic Resonance Imaging Interpretation

Another important aspect to the quality improvement of prostate mpMRI interpretation and reporting concerns reader experience level and how this relates to accuracy and inter-reader reliability across different radiologists. A study by Niaf et al. found that prostate mpMRI readers

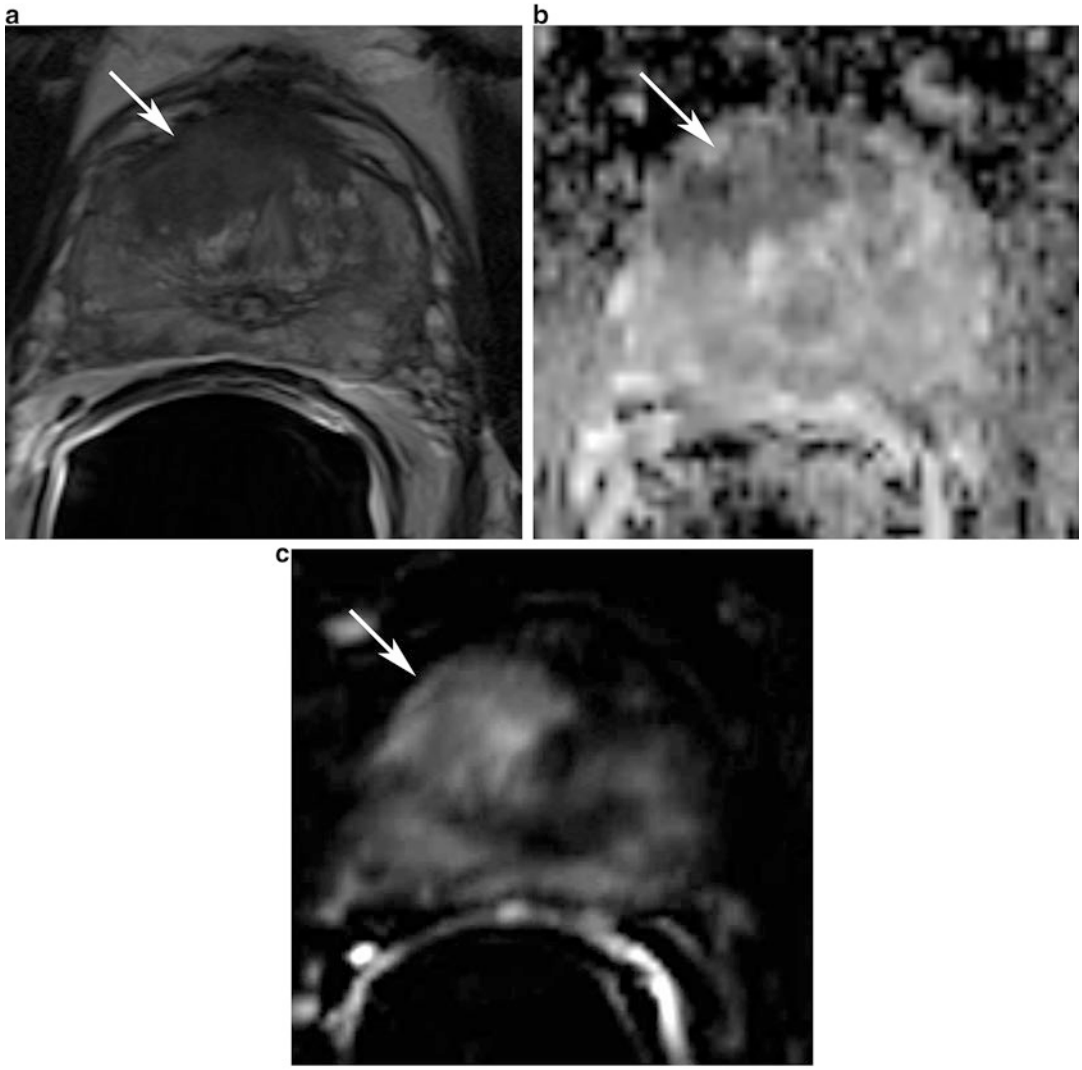

Fig. 14.1 A 58-year-old man on active surveillance with serum prostate-specific antigen (PSA) level of 8.4 ng/mL and transrectal ultrasound (TRUS)-guided biopsy showing Gleason 3 + 3 = 6 (5/12 cores) was referred for multiparametric magnetic resonance imaging (mpMRI). (**a**) Axial T2W images show a lesion with low T2 signal intensity in the right anterior transition zone (TZ) at the level of the mid-gland (*arrow*). (**b**) Axial apparent diffusion coefficient (ADC) map shows a corresponding area of low ADC value (*arrow*). The degree of restricted diffusion suggests the presence of a high-grade tumor in this location. (**c**) Perfusion images show early and focal enhancement of the lesion relative to the remainder of the gland. PI-RADS score is 5. The patient elected to undergo radical prostatectomy based on the mpMRI findings. Final pathologic analysis showed Gleason 4 + 3 = 7 prostate cancer. This case demonstrates how mpMRI and TRUS-guided systematic biopsy can have discordant assessments of prostate cancer grade and the potential influence mpMRI can have on treatment decisions

with less than 1 year experience had significantly lower areas under the curve (AUCs) for diagnostic accuracy when assessing the likelihood that focal prostate lesions represent clinically significant cancers than their more experienced colleagues [34]. That said, it has also been shown that accuracy of, and confidence in, prostate mpMRI interpretation can be significantly improved over the course of a fellowship year with a dedicated focus on education [35]. There

is no substitute for hands-on learning, repetition, and self-assessment in the forms of radiologic-pathologic correlation and peer review, both of which are critical to improve diagnostic performance with this technique. Radiologists first learning mpMRI should also aim to read key references in the field, some of which can be found in the PI-RADS version 2 document [6]. It is also very important to be aware of common pitfalls in mpMRI interpretation to avoid making these mistakes in your own clinical practice when interpreting prostate mpMRI. Rosenkrantz and Taneja have published an excellent article on the diagnostic challenges that may lead to mistakes when interpreting prostate mpMRI [36]. The radiologist learning mpMRI may quickly improve their skills interpreting prostate mpMRI by reading this article as it is as critical to be confident in the diagnosis of benign prostatic disease (to reduce morbidity related to unnecessary biopsy/treatment) as it is to be confident in diagnosis of clinically significant cancer (which can decrease mortality). The field of prostate mpMRI is evolving rapidly, so all radiologists using this technique should stay current with the literature and work to adapt their practice as new technologies and techniques become available.

In order for radiologists to be considered sufficiently experienced and adept at interpreting prostate mpMRI, experts recommend reading "at least 50 prostate mpMRI scans with pathological feedback per year" [1]. This is a difficult area to regulate, but the concepts of "double reads" within one's clinical practice or reading guided cases with experts at hands-on courses certainly have merit in improving one's skills and confidence with this modality. One study found that reader experience may lead to improved sensitivity, specificity, positive predictive value, negative predictive value, and accuracy for detecting extracapsular extension when interpreting prostate mpMRI [37]. While inter-reader variability between radiologists less experienced in prostate mpMRI interpretation may be reduced through dedicated reader education [35], others have found that radiologists experienced in prostate mpMRI "achieved moderate reproducibility for PI-RADS version 2, and neither required nor benefitted from a training session" [38]. This is likely related to a high baseline level of comfort and experience with this technique and reporting system across this group of highly experienced readers, and this may not be widely applicable to less experienced readers.

The Importance of Communication and Follow-Up to Quality Improvement

Quality improvement with regard to imaging interpretation of prostate mpMRI goes beyond having skills and experience; radiologists must have an open professional relationship with clinicians in other disciplines (e.g., pathology, urology, radiation oncology, medical oncology, etc.) to get feedback on their performance. By having an open door for input from other clinicians, radiologists may help to improve the value of prostate mpMRI to clinical practice. For example, there may be certain aspects of a prostate mpMRI not typically included in reports that a particular referrer may find more helpful to their practice, or referrers may not understand the nomenclature used in reports, and this may not come to light if the radiologist is not available and open for suggestions from their colleagues. An example of a more structured way that multidisciplinary collaboration can impact clinical outcomes is tumor board conferences, where multiple clinicians from different disciplines involved in the care of a particular group of patients (i.e., prostate cancer patients) meet and discuss specific diagnoses and management strategies. Tumor boards allow for clinicians from multiple disciplines to query each other and mutually learn from the others in order to best serve their patients. Tumor boards often also allow for more formalized quality improvement discussions as specific cases are often revisited after the patient has undergone biopsy or surgery, and the results are compared to initial diagnostic findings to assess for potential discordance and/or appropriate next steps in management.

It is also very important to quality improvement and research to compare imaging to histopathology

to ensure that correct diagnoses are made and to learn from any potential mistakes. While it is often difficult to compare images on mpMRI to histopathology because of shrinkage and freehand slicing of specimens, potential solutions have been developed [39]. One example of a potential solution is "deformable histopathology mpMRI fusion computer software based on 22 landmarks in the specimens," which has been shown to lead to improvement in matching accuracy of 32 % over traditional rigid comparison methods [40]. Another potential solution that has been suggested involves a "3D histopathology analysis tool using 3D printed customized molds based on preoperative mpMRI data, corrected for shrinkage, for slicing of the histopathological specimens in exactly the same plane as the mpMRI scanning" [41].

Technology like this will likely not be available at most centers and certainly not for every patient with a prostate mpMRI, but regardless, radiologists should aim to follow up the pathology in cases where the patient went on to transrectal ultrasound (TRUS)-guided biopsy, targeted biopsy, radical prostatectomy, etc. This will ideally help the radiologist to identify their blind spots and incorporate this knowledge for future application. This does require the radiologist to be willing to acknowledge their weaknesses and to learn from them. If multiple radiologists in a practice are reading prostate mpMRI, this practice may be done in a group so that everyone can learn from these mistakes together. This is not to say that all "misses" on biopsy represent mistakes on the radiologist's part; there may be discordant results on pathology, and radiologists should also be willing to suggest this if the imaging has highly suspicious characteristics. A strong professional relationship with colleagues in other specialties related to prostate cancer should help facilitate this kind of open discussion. Prostate imaging can and should consider following the example set in breast imaging with the review of biopsy results as concordant or discordant based on imaging findings. For example, if biopsy results of PI-RADS 4 or 5 lesions are negative, a repeat biopsy should be considered after review of the biopsy images to ensure that the specimen taken is reflective of the highly suspicious imaging findings. All of this said, more work is needed to determine what percent of PI-RADS 3, 4, and 5 lesions should represent clinically significant cancer as these numbers are critical to determine the performance of PI-RADS as well as the performance of those performing targeted biopsies.

Specific Considerations Regarding Multiparametric Magnetic Resonance Imaging in Focal Therapy

While the detection, characterization, and staging of prostate cancer are important in the evaluation of the general patient with prostate cancer, accurate tumor volumes are particularly important for focal therapy planning. Most experts in the field of prostate mpMRI and urology agreed that 0.5 mL is the "lower limit of a reliable detection rate in Gleason 6 tumors" [1]. Gleason 7 tumors may be possible to detect at smaller volumes, though this is not widely agreed upon [1]. While mpMRI accurately detects clinically significant prostate tumors, there is the risk of both underestimation and overestimation when using mpMRI to estimate tumor volume [42, 43]. There have been studies to determine which sequence is most accurate for tumor volume assessment, though there are some differences in results. For example, Bratan et al. have shown that no one mpMRI sequence is superior for accurately estimating tumor volumes; however, the "greatest volume determined on images from any of the individual MR pulse sequences" was least likely to lead to tumor volume underestimation [44]. Conversely, Mazaheri et al. found that DWI plus T2WI significantly improved the accuracy of prostate tumor volume measurement in the peripheral zone [45]. The issue of tumor volume underestimation may be mitigated by using a treatment margin of at least 9 mm around lesions visible on mpMRI [42]. Needless to say, a margin of 9 mm is very extensive, and more work is needed to ensure that mpMRI lesion sizes and treatment zones are better delineated, especially if this is to be used as a diagnostic modality for planning and monitoring focal therapy.

Quality Improvement Regarding Targeted Biopsy

The increased diagnostic quality of prostate mpMRI has made targeted biopsy possible. A landmark prospective study published in the *Journal of the American Medical Association* has established that targeted MRI/TRUS fusion biopsy can increase detection of high-risk prostate cancer while decreasing the detection of low-risk, clinically insignificant prostate cancer [46]. Again, the increased detection of clinically significant prostate cancer has the ability to decrease mortality, and the decreased detection of clinically insignificant prostate cancer can lead to decreased morbidity by avoidance of unnecessary or overtreatment. This and other studies have led many urology practices to begin performing targeted biopsy more in the diagnosis and evaluation of prostate cancer.

Most details of targeted biopsy are out of the scope of this chapter and are discussed in other chapters of this textbook, but it is important to note that the expansion of targeted biopsy requires even more collaboration between radiologists and their urology colleagues in the planning of these biopsies. For example, at the authors' institution, a dedicated abdominal radiologist highly experienced in prostate mpMRI regularly meets in person with the urologic oncologists who perform MRI/TRUS fusion biopsies to review the imaging for each patient prior to biopsy, including lesion segmentation and gland segmentation. This allows an extra level of planning to ensure that the patient is an appropriate candidate for MRI/TRUS fusion biopsy, as well as to categorize the biopsy targets in order of significance. At the authors' institution, it has been decided that lesions with a PI-RADS score of 4 or 5 and a volume of at least 0.5 mL are good candidates for MRI/TRUS fusion biopsy.

Radiologists interpreting prostate mpMRI for targeted biopsy planning must also learn how to maximize the use of third-party software and discover the best workflow to ensure this procedure runs smoothly for patients and clinicians alike. It is critical that radiologists bridge the potential communication gap with urologists by speaking the same language, utilizing agreed upon nomenclature, and releasing clinically relevant and actionable radiology reports.

Imaging Guidance for Focal Therapy

The main benefits of using mpMRI to guide focal therapy in real time are that it allows for accurate needle placement and thermometry or temperature mapping during the procedure to ensure adequate treatment is achieved [47]. Thermometry especially is an important benefit, as it can allow for adaptations to therapy to account for differences in the prostate size and anatomy for individual patients and can also help to protect surrounding tissues by monitoring temperature changes [48]. However, there are disadvantages to using MRI to guide focal therapy, including increased cost, limited space while working in the scanner, and the need for MR-compatible materials [47]. The role for mpMRI in image guidance for some of the various modalities of focal therapy will be discussed as follows:

Role of Multiparametric Magnetic Resonance Imaging in Focal Laser Therapy

Focal laser ablation has been identified as one of the more promising focal therapy modalities to be used with MRI guidance [47]. Stafford et al. studied an MRI-guided focal laser-induced interstitial thermal therapy system for prostate tissue ablation in a 1.5 T MRI scanner and found that the tissue destruction predicted by magnetic resonance-based thermal damage calculations had excellent correlation (r^2 = 0.94) with the damage observed on posttreatment imaging [49]. Posttreatment MRI after focal laser ablation (Fig. 14.2) has been shown to accurately depict treated tissue when defining necrosis as a "new confluent zone demonstrating <10% enhancement compared with the baseline pretreatment contrast-enhanced MRI" [50]. Cepek et al. developed a needle guidance system to be used within the

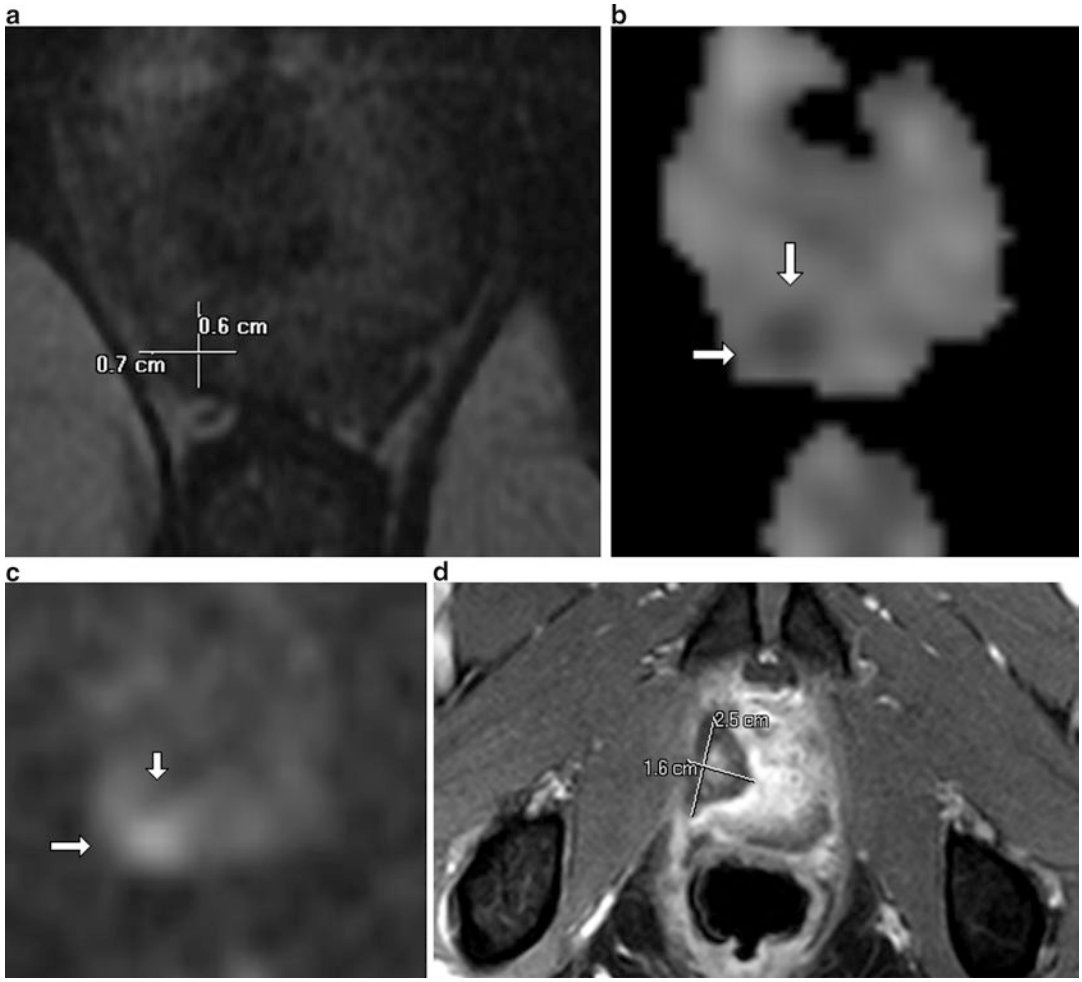

Fig. 14.2 A 60-year-old man with serum prostate-specific antigen (PSA) of 1.1 ng/mL underwent multiparametric magnetic resonance imaging (mpMRI) to assess for prostate cancer. (**a**) Axial T2WI shows a lesion with low T2 signal intensity in the right posterior peripheral zone (PZ) at the level of the apex (*arrow*). (**b**) Axial apparent diffusion coefficient (ADC) map shows a corresponding area of restricted diffusion (*arrows*). (**c**) Perfusion images show early and focal enhancement of the lesion relative to the remainder of the gland (*arrows*). PI-RADS score is 4. The diagnosis was confirmed with MRI-guided in-bore targeted biopsy, which showed Gleason score 4 + 3 = 7 disease. (**d**) Axial T2WI obtained during focal laser ablation (FLA) of the lesion shows posttreatment coagulation necrosis of the lesion and a margin of surrounding tissue. (**e**) Sagittal T2WI obtained during FLA of the lesion shows posttreatment coagulation necrosis (*arrow*). PSA level was 1.4 ng/mL 2 months after FLA, so the patient was referred for mpMRI to assess for residual disease versus recurrence. (**f**) Axial T2WI 3 months post-FLA shows a region of posttreatment necrosis in the right posterior PZ corresponding with treated area (*arrow*). (**g**) Colorized perfusion map created using post-processing software from DCE-MRI acquisition shows a corresponding perfusion defect (*arrow*). The patient continued to be followed. (**h**) Follow-up axial T2WI 6 months post-FLA again shows a region of necrosis in the right posterior PZ corresponding with treated area (*arrow*). (**i**) Colorized perfusion map from DCE-MRI acquisition shows a corresponding perfusion defect, though smaller than at 3 months posttreatment (*arrow*). There is no evidence of residual disease at 6 months post-FLA, and patient continued on follow-up with mpMRI. (Images courtesy of John Feller, MD and Bernadette Greenwood, Desert Medical Imaging, Palm Springs, California)

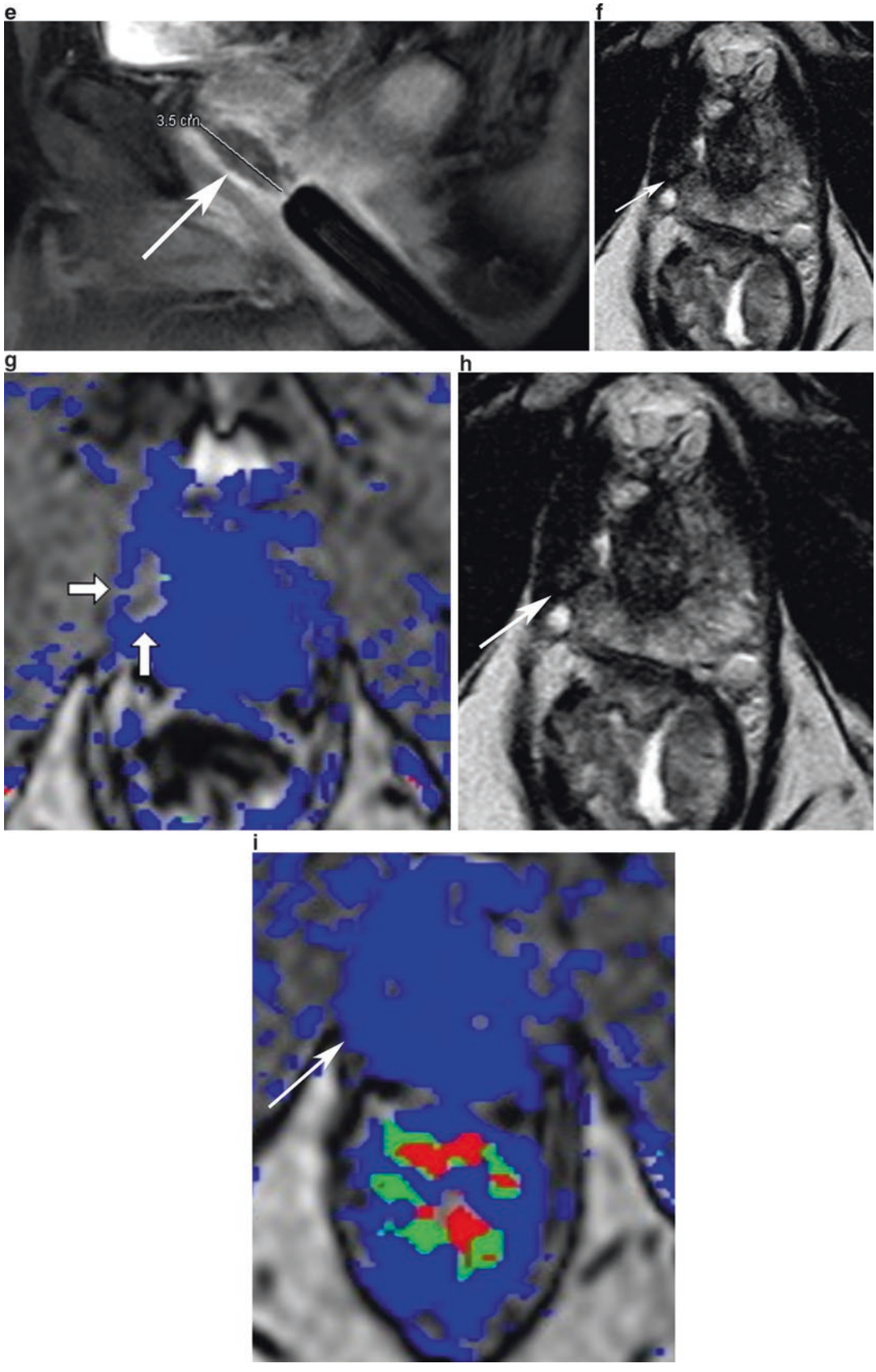

Fig. 14.2 (continued)

bore of an MRI scanner for use in focal laser thermal ablation of prostate tumors and found that the median needle guidance error was 3.5 mm [51, 52].

Role of Multiparametric Magnetic Resonance Imaging in Focal Ultrasound Therapy

Focused ultrasound therapy has also been deemed to be promising for use with MRI guidance [47]. A study by Chopra et al. found that the temperature information acquired with active MR temperature feedback during transurethral ultrasound therapy and the pattern of thermal damage measured on hematoxylin and eosin (H&E)-stained tissue sections of treated canine prostate tissue had excellent spatial agreement [53]. Another study by Siddiqui et al. helped to establish the feasibility of MRI-guided transurethral ultrasound therapy and demonstrated a "correlation of ≤3 mm between anatomical, thermal, and histologic images" [54]. Furthermore, gadolinium-enhanced MRI has been shown to accurately detect the degree of tissue damage caused by high-intensity focused ultrasound (HIFU) ablation [55].

Role of Multiparametric Magnetic Resonance Imaging in Focal Cryoablation Therapy

Some have stated that cryoablation is less suitable for MRI guidance because MRI thermometry is not feasible for temperatures below 0 °C [47] and because the volume mismatch of the ice ball on T1-weighted images obtained during the procedure and the volume of tissue necrosis observed on histopathologic analysis have occurred [56]. However, this same study found that DCE-MRI was the most accurate sequence (accuracy rate = 91 %) for the prediction of the area of tissue necrosis induced by cryoablation [56]. The tissue necrosis appeared as a nonenhancing region on DCE-MRI [56]. This finding was supported by another study by Larson et al., which found that areas of "gadolinium defects" on DCE-MRI could be matched with areas of necrosis on histopathologic evaluation after various minimally invasive treatments, including cryoablation and microwave thermotherapy [57]. DCE-MRI is a valuable tool in assessing post-treatment response to cryoablation and the absence of focal enhancement within the ablation bed after an appropriate time interval and in the absence of rising prostate-specific antigen (PSA) is an indicator of the lack of recurrent disease at the site (Fig. 14.3).

Role of Multiparametric Magnetic Resonance Imaging in Focal Radiofrequency and Microwave Therapy

MRI-guided radiofrequency ablation and microwave ablation have been demonstrated to be technically feasible, though there are significant drawbacks, namely, the "possible interference with the radiofrequency pulses of the MR system," which can cause noise in the MR images and with radiofrequency ablation, and "the large image artifact (up to eight times its original size) caused by the radiofrequency electrode...which makes temperature measurement at the vicinity of the electrode impossible" [47]. Nevertheless, mpMRI can be used after radiofrequency ablation to confirm adequate treatment [58].

Follow-Up Multiparametric Magnetic Resonance Imaging After Focal Therapy

Disease progression rates after focal therapy may be as high as 33 %, with recurrence potentially occurring in treated and/or untreated areas of the gland, according to a study of hemi-salvage HIFU in patients with unilateral radiorecurrent prostate cancer [59]. A study of 73 patients with clinically unilateral, low-intermediate risk prostate cancer found 25 % of patients had positive follow-up posttreatment biopsies, with the vast majority in the untreated contralateral lobe [60].

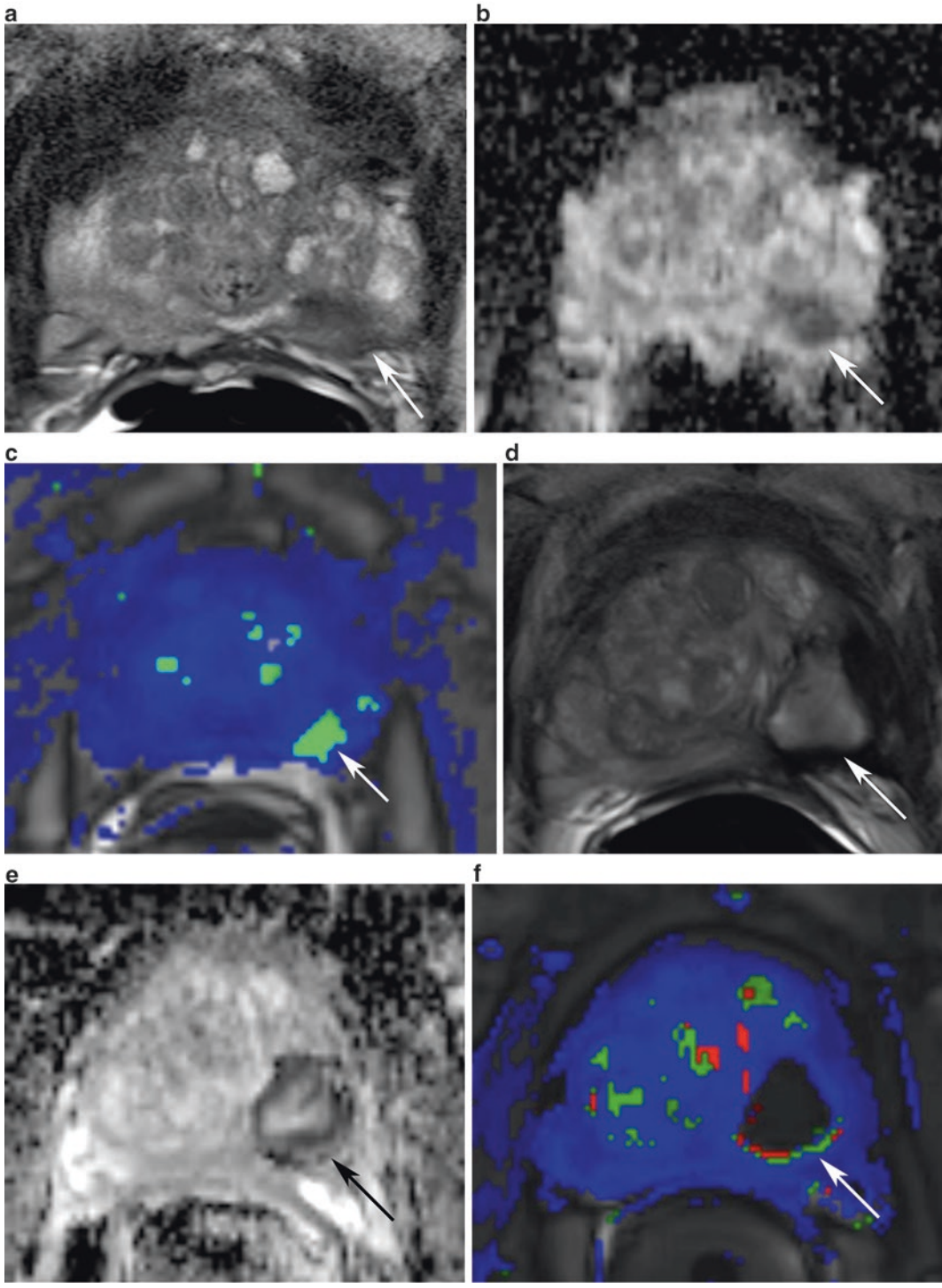

Fig. 14.3 A 72-year-old man with serum prostate-specific antigen (PSA) of 25 ng/mL and history of three negative systematic biopsies was referred for multiparametric magnetic resonance imaging (mpMRI) to assess for clinically significant prostate cancer. (**a**) Axial T2W images show a lesion with low T2 signal intensity in the left posterior medial and lateral peripheral zone (PZ) (*arrow*). There is also extensive benign prostatic hypertrophia (BPH). (**b**) Axial apparent diffusion coefficient (ADC) map shows a corresponding area of restricted diffusion (*arrow*). (**c**) Colorized perfusion images show suspicious enhancement of the lesion relative to the remainder of the gland. PI-RADS score is 4. The patient elected to undergo focal cryoablation. Serum PSA 3 months later was 9.9 ng/mL and 10.9 ng/mL at 7 months later. The patient was referred for mpMRI to assess for recurrence. (**d, e**) Axial T2W images and ADC maps in the same patient 7 months after focal therapy show post-cryoablation change in the left posterior PZ (*arrow*). (**f**) Colorized perfusion map created using post-processing software from DCE-MRI acquisition shows a perfusion defect corresponding to the treated area with no suspicious perfusion in the cryoablation cavity or in the remainder of the untreated prostate gland. The patient will continue on imaging surveillance

Furthermore, data from 279 patient's status/post-salvage cryoablation after failed radiation therapy found a biochemical disease-free rate of approximately 59 % [61]. This is all to illustrate that follow-up, preferably with imaging, is necessary after focal therapy treatment, especially if the focal therapy was a salvage procedure.

Prostate mpMRI has been considered the favored method of focal therapy follow-up by expert radiologists and urologists in the field [1]. A consensus was not reached regarding when follow-up mpMRI should be performed after focal therapy, though many recommend the first mpMRI be performed 6 months after FT and either biannually or annually thereafter [1]. Moreover, there are no universally accepted, validated criteria for biochemical failure with PSA after focal therapy [62].

Radiologists need to be able to distinguish residual disease from posttreatment effects after focal therapy. Litjens et al. compared pre- and post-laser interstitial thermotherapy MRI against ex vivo histology and found that there are imaging characteristics that may be used to distinguish posttreatment effects from residual disease, including DCE-MRI and T2WI texture features [63]. DWI was less relevant for detecting residual disease, as the changes in DWI features were similar for ablated tissue and residual disease [63].

Radiologists also need to be able to detect disease recurrence after focal therapy. Recurrent prostate cancer after focal therapies tends to appear as low signal intensity on T2WI, restricted diffusion on DWI, and rapid wash in and wash out of contrast on DCE-MRI [62]. Most of the evidence for the use of mpMRI to detect recurrence after focal therapy has focused on HIFU over the other focal therapy modalities. DCE-MRI has been found to be the best sequence to detect recurrence after transrectal HIFU. In fact, one study found it to have a sensitivity of 100 % and a specificity of 96 % [64–66]. However, another study by Punwani et al. found that DCE-MRI performed similarly to serial PSA in terms of sensitivity, specificity, and receiver operating characteristic (ROC) performance for the detection of recurrence after HIFU [67]; this is to say that, at this time, mpMRI results should be viewed in conjunction with serial PSA values to ensure appropriate mpMRI interpretations that are based in the current clinical context. Residual cancer is most likely in the prostatic apex after HIFU ablation, so radiologists may be able to improve the quality of mpMRI exams to detect recurrence by paying special attention to this region [68]. If signs of disease recurrence are seen on follow-up mpMRI after FT, targeted biopsy of the abnormality is warranted [1].

Conclusion

As the utilization of prostate mpMRI increases, the clinical roles for this diagnostic and evaluative modality will increase, and quality improvement must continue. Currently, prostate mpMRI may have value at multiple checkpoints throughout the process of a patient receiving focal therapy.

Multiple studies have demonstrated the value of prostate mpMRI in the initial detection and staging of prostate tumors. Prostate tumor characteristics such as estimated tumor volume are essential in the decision of whether a patient is an appropriate candidate for focal therapy. Prostate mpMRI also has a role as real-time image guidance for both targeted biopsies and certain forms of focal therapy, especially focal laser ablation and HIFU. Finally, prostate mpMRI can be used in the immediate follow-up after focal therapy to conclude whether treatment was successful or if there is residual disease, as well as long-term monitoring for disease recurrence.

There is room for quality improvement at each of these checkpoints. Image acquisition, interpretation, and reporting must be optimized for prostate mpMRI to realize its full potential for use in focal therapy. Radiologists new to prostate mpMRI must take the time to gain adequate education and experience, while radiologists experienced in mpMRI must maintain their expertise and pass their knowledge along to others. Both inexperienced and experienced radiologists can benefit from gaining feedback on their skills by following up pathology and establishing open professional relationships with their urology,

pathology, oncology, and radiation oncology colleagues. The process of quality improvement can be time consuming and requires an open mind, but it is absolutely essential if the field of prostate mpMRI is to continue to evolve and remain clinically relevant.

Financial Disclosures RTG—None relevant to this work. Outside of this work, Consultant, Invivo Corp.

JNH—None

References

1. Muller BG, van den Bos W, Brausi M, Cornud F, Gontero P, Kirkham A, et al. Role of multiparametric magnetic resonance imaging (MRI) in focal therapy for prostate cancer: a Delphi consensus project. BJU Int. 2014;114(5):698–707.
2. Kruskal JB, Eisenberg R, Sosna J, Yam CS, Kruskal JD, Boiselle PM. Quality initiatives: quality improvement in radiology: basic principles and tools required to achieve success. Radiographics. 2011;31(6):1499–509.
3. Gupta RT, Kauffman CR, Polascik TJ, Taneja SS, Rosenkrantz AB. The state of prostate MRI in 2013. Oncology (Williston Park). 2013;27(4):262–70.
4. Cornud F, Rouanne M, Beuvon F, Eiss D, Flam T, Liberatore M, et al. Endorectal 3D T2-weighted 1 mm-slice thickness MRI for prostate cancer staging at 1.5Tesla: should we reconsider the indirects signs of extracapsular extension according to the D'Amico tumor risk criteria? Eur J Radiol. 2012;81(4):e591–7.
5. Rosenkrantz AB, Neil J, Kong X, Melamed J, Babb JS, Taneja SS, et al. Prostate cancer: comparison of 3D T2-weighted with conventional 2D T2-weighted imaging for image quality and tumor detection. AJR Am J Roentgenol. 2010;194(2):446–52.
6. ACR. PI-RADS: prostate imaging – reporting and data system version 2 2015 [Available from: http://www.acr.org/~/media/ACR/Documents/PDF/QualitySafety/Resources/PIRADS/PIRADS.V2.pdf.
7. Turkbey B, Shah VP, Pang Y, Bernardo M, Xu S, Kruecker J, et al. Is apparent diffusion coefficient associated with clinical risk scores for prostate cancers that are visible on 3-T MR images? Radiology. 2011;258(2):488–95.
8. Somford DM, Hambrock T, van de Hulsbergen- KCA, Futterer JJ, van Oort IM, van Basten JP, et al. Initial experience with identifying high-grade prostate cancer using diffusion-weighted MR imaging (DWI) in patients with a Gleason score </= 3 + 3 = 6 upon schematic TRUS-guided biopsy: a radical prostatectomy correlated series. Investig Radiol. 2012;47(3):153–8.
9. Kim TH, Jeong JY, Lee SW, Kim CK, Park BK, Sung HH, et al. Diffusion-weighted magnetic resonance imaging for prediction of insignificant prostate cancer in potential candidates for active surveillance. Eur Radiol. 2015;25(6):1786–92.
10. Tamada T, Kanomata N, Sone T, Jo Y, Miyaji Y, Higashi H, et al. High b value (2000 s/mm^2) diffusion-weighted magnetic resonance imaging in prostate cancer at 3 Tesla: comparison with 1000 s/mm2 for tumor conspicuity and discrimination of aggressiveness. PLoS One. 2014;9(5):e96619.
11. Rosenkrantz AB, Hindman N, Lim RP, Das K, Babb JS, Mussi TC, et al. Diffusion-weighted imaging of the prostate: comparison of b1000 and b2000 image sets for index lesion detection. J Magn Reson Imaging. 2013;38(3):694–700.
12. Metens T, Miranda D, Absil J, Matos C. What is the optimal b value in diffusion-weighted MR imaging to depict prostate cancer at 3 T? Eur Radiol. 2012;22(3):703–9.
13. Kitajima K, Takahashi S, Ueno Y, Yoshikawa T, Ohno Y, Obara M, et al. Clinical utility of apparent diffusion coefficient values obtained using high b-value when diagnosing prostate cancer using 3 tesla MRI: comparison between ultra-high b-value (2000 s/mm(2)) and standard high b-value (1000 s/mm(2)). J Magn Reson Imaging. 2012;36(1):198–205.
14. Grant KB, Agarwal HK, Shih JH, Bernardo M, Pang Y, Daar D, et al. Comparison of calculated and acquired high b value diffusion-weighted imaging in prostate cancer. Abdom Imaging. 2015;40(3):578–86.
15. Nicholson B, Schaefer G, Theodorescu D. Angiogenesis in prostate cancer: biology and therapeutic opportunities. Cancer Metastasis Rev. 2001;20(3-4):297–319.
16. Engelbrecht MR, Huisman HJ, Laheij RJ, Jager GJ, van Leenders GJ, van de Hulsbergen- KCA, et al. Discrimination of prostate cancer from normal peripheral zone and central gland tissue by using dynamic contrast-enhanced MR imaging. Radiology. 2003;229(1):248–54.
17. Tan CH, Hobbs BP, Wei W, Kundra V. Dynamic contrast-enhanced MRI for the detection of prostate cancer: meta-analysis. AJR Am J Roentgenol. 2015;204(4):W439–48.
18. Rosenkrantz AB, Sabach A, Babb JS, Matza BW, Taneja SS, Deng FM. Prostate cancer: comparison of dynamic contrast-enhanced MRI techniques for localization of peripheral zone tumor. AJR Am J Roentgenol. 2013;201(3):W471–8.
19. Scheenen TW, Futterer J, Weiland E, van Hecke P, Lemort M, Zechmann C, et al. Discriminating cancer from noncancer tissue in the prostate by 3-dimensional proton magnetic resonance spectroscopic imaging: a prospective multicenter validation study. Investig Radiol. 2011;46(1):25–33.
20. Weinreb JC, Blume JD, Coakley FV, Wheeler TM, Cormack JB, Sotto CK, et al. Prostate cancer: sextant localization at MR imaging and MR spectroscopic

imaging before prostatectomy–results of ACRIN prospective multi-institutional clinicopathologic study. Radiology. 2009;251(1):122–33.
21. Leake JL, Hardman R, Ojili V, Thompson I, Shanbhogue A, Hernandez J, et al. Prostate MRI: access to and current practice of prostate MRI in the United States. J Am Coll Radiol. 2014;11(2):156–60.
22. Chang KJ, Kamel IR, Macura KJ, Bluemke DA. 3.0-T MR imaging of the abdomen: comparison with 1.5 T. Radiographics. 2008;28(7):1983–98.
23. Heijmink SW, Futterer JJ, Hambrock T, Takahashi S, Scheenen TW, Huisman HJ, et al. Prostate cancer: body-array versus endorectal coil MR imaging at 3 T--comparison of image quality, localization, and staging performance. Radiology. 2007;244(1):184–95.
24. Barentsz JO, Richenberg J, Clements R, Choyke P, Verma S, Villeirs G, et al. ESUR prostate MR guidelines 2012. Eur Radiol. 2012;22(4):746–57.
25. Bratan F, Niaf E, Melodelima C, Chesnais AL, Souchon R, Mege-Lechevallier F, et al. Influence of imaging and histological factors on prostate cancer detection and localisation on multiparametric MRI: a prospective study. Eur Radiol. 2013;23(7):2019–29.
26. Costa DN, Yuan Q, Xi Y, Rofsky NM, Lenkinski RE, Lotan Y, et al. Comparison of prostate cancer detection at 3-T MRI with and without an endorectal coil: a prospective, paired-patient study. Urol Oncol. 2016;34(6):255.e7–255.e13.
27. Rosenkrantz AB, Mussi TC, Hindman N, Lim RP, Kong MX, Babb JS, et al. Impact of delay after biopsy and post-biopsy haemorrhage on prostate cancer tumour detection using multi-parametric MRI: a multi-reader study. Clin Radiol. 2012;67(12):e83–90.
28. Rosen Y, Bloch BN, Lenkinski RE, Greenman RL, Marquis RP, Rofsky NM. 3T MR of the prostate: reducing susceptibility gradients by inflating the endorectal coil with a barium sulfate suspension. Magn Reson Med. 2007;57(5):898–904.
29. Rosenkrantz AB, Bennett GL, Doshi A, Deng FM, Babb JS, Taneja SS. T2-weighted imaging of the prostate: impact of the BLADE technique on image quality and tumor assessment. Abdom Imaging. 2015;40(3):552–9.
30. Rosenkrantz AB, Geppert C, Grimm R, Block TK, Glielmi C, Feng L, et al. Dynamic contrast-enhanced MRI of the prostate with high spatiotemporal resolution using compressed sensing, parallel imaging, and continuous golden-angle radial sampling: preliminary experience. J Magn Reson Imaging. 2015;41(5):1365–73.
31. Rosenkrantz AB, Chandarana H, Pfeuffer J, Triolo MJ, Shaikh MB, Mossa DJ, et al. Zoomed echo-planar imaging using parallel transmission: impact on image quality of diffusion-weighted imaging of the prostate at 3 T. Abdom Imaging. 2015;40(1):120–6.
32. Rouviere O. Imaging techniques for local recurrence of prostate cancer: for whom, why and how? Diagn Interv Imaging. 2012;93(4):279–90.
33. Rouviere O, Sbihi L, Gelet A, Chapelon JY. Salvage high-intensity focused ultrasound ablation for prostate cancer local recurrence after external-beam radiation therapy: prognostic value of prostate MRI. Clin Radiol. 2013;68(7):661–7.
34. Niaf E, Lartizien C, Bratan F, Roche L, Rabilloud M, Mege-Lechevallier F, et al. Prostate focal peripheral zone lesions: characterization at multiparametric MR imaging--influence of a computer-aided diagnosis system. Radiology. 2014;271(3):761–9.
35. Garcia-Reyes K, Passoni NM, Palmeri ML, Kauffman CR, Choudhury KR, Polascik TJ, et al. Detection of prostate cancer with multiparametric MRI (mpMRI): effect of dedicated reader education on accuracy and confidence of index and anterior cancer diagnosis. Abdom Imaging. 2015;40(1):134–42.
36. Rosenkrantz AB, Taneja SS. Radiologist, be aware: ten pitfalls that confound the interpretation of multiparametric prostate MRI. AJR Am J Roentgenol. 2014;202(1):109–20.
37. Latchamsetty KC, Borden Jr LS, Porter CR, Lacrampe M, Vaughan M, Lin E, et al. Experience improves staging accuracy of endorectal magnetic resonance imaging in prostate cancer: what is the learning curve? Can J Urol. 2007;14(1):3429–34.
38. Rosenkrantz AB, Ginocchio LA, Cornfeld D, Froemming AT, Gupta RT, Turkbey B, Westphalen AC, Babb JS, Margolis DJ. Interobserver Reproducibility of the PI-RADS Version 2 Lexicon: A Multicenter Study of Six Experienced Prostate Radiologists. Radiology. 2016 Sep;280(3):793–804.
39. Muller BG, van den Bos W, Pinto PA, de la Rosette JJ. Imaging modalities in focal therapy: patient selection, treatment guidance, and follow-up. Curr Opin Urol. 2014;24(3):218–24.
40. Orczyk C, Rusinek H, Rosenkrantz AB, Mikheev A, Deng FM, Melamed J, et al. Preliminary experience with a novel method of three-dimensional co-registration of prostate cancer digital histology and in vivo multiparametric MRI. Clin Radiol. 2013;68(12):e652–8.
41. Trivedi H, Turkbey B, Rastinehad AR, Benjamin CJ, Bernardo M, Pohida T, et al. Use of patient-specific MRI-based prostate mold for validation of multiparametric MRI in localization of prostate cancer. Urology. 2012;79(1):233–9.
42. Le Nobin J, Rosenkrantz AB, Villers A, Orczyk C, Deng FM, Melamed J, et al. Image guided focal therapy for magnetic resonance imaging visible prostate cancer: defining a 3-dimensional treatment margin based on magnetic resonance imaging histology co-registration analysis. J Urol. 2015;194(2):364–70.
43. Cornud F, Khoury G, Bouazza N, Beuvon F, Peyromaure M, Flam T, et al. Tumor target volume for focal therapy of prostate cancer-does multiparametric magnetic resonance imaging allow for a reliable estimation? J Urol. 2014;191(5):1272–9.
44. Bratan F, Melodelima C, Souchon R, Hoang Dinh A, Mege-Lechevallier F, Crouzet S, et al. How accurate is multiparametric MR imaging in evaluation of prostate cancer volume? Radiology. 2015;275(1):144–54.

45. Mazaheri Y, Hricak H, Fine SW, Akin O, Shukla-Dave A, Ishill NM, et al. Prostate tumor volume measurement with combined T2-weighted imaging and diffusion-weighted MR: correlation with pathologic tumor volume. Radiology. 2009;252(2):449–57.
46. Siddiqui MM, Rais-Bahrami S, Turkbey B, George AK, Rothwax J, Shakir N, et al. Comparison of MR/ultrasound fusion-guided biopsy with ultrasound-guided biopsy for the diagnosis of prostate cancer. JAMA. 2015;313(4):390–7.
47. Bomers JG, Sedelaar JP, Barentsz JO, Futterer JJ. MRI-guided interventions for the treatment of prostate cancer. AJR Am J Roentgenol. 2012;199(4):714–20.
48. Lindner U, Lawrentschuk N, Trachtenberg J. Image guidance for focal therapy of prostate cancer. World J Urol. 2010;28(6):727–34.
49. Stafford RJ, Shetty A, Elliott AM, Klumpp SA, McNichols RJ, Gowda A, et al. Magnetic resonance guided, focal laser induced interstitial thermal therapy in a canine prostate model. J Urol. 2010;184(4):1514–20.
50. Lindner U, Lawrentschuk N, Weersink RA, Davidson SR, Raz O, Hlasny E, et al. Focal laser ablation for prostate cancer followed by radical prostatectomy: validation of focal therapy and imaging accuracy. Eur Urol. 2010;57(6):1111–4.
51. Cepek J, Lindner U, Ghai S, Louis AS, Davidson SR, Gertner M, et al. Mechatronic system for in-bore MRI-guided insertion of needles to the prostate: an in vivo needle guidance accuracy study. J Magn Reson Imaging. 2015;42(1):48–55.
52. Cepek J, Chronik BA, Lindner U, Trachtenberg J, Davidson SR, Bax J, et al. A system for MRI-guided transperineal delivery of needles to the prostate for focal therapy. Med Phys. 2013;40(1):012304.
53. Chopra R, Tang K, Burtnyk M, Boyes A, Sugar L, Appu S, et al. Analysis of the spatial and temporal accuracy of heating in the prostate gland using transurethral ultrasound therapy and active MR temperature feedback. Phys Med Biol. 2009;54(9):2615–33.
54. Siddiqui K, Chopra R, Vedula S, Sugar L, Haider M, Boyes A, et al. MRI-guided transurethral ultrasound therapy of the prostate gland using real-time thermal mapping: initial studies. Urology. 2010;76(6):1506–11.
55. Rouviere O, Lyonnet D, Raudrant A, Colin-Pangaud C, Chapelon JY, Bouvier R, et al. MRI appearance of prostate following transrectal HIFU ablation of localized cancer. Eur Urol. 2001;40(3):265–74.
56. van den Bosch MA, Josan S, Bouley DM, Chen J, Gill H, Rieke V, et al. MR imaging-guided percutaneous cryoablation of the prostate in an animal model: in vivo imaging of cryoablation-induced tissue necrosis with immediate histopathologic correlation. J Vasc Interv Radiol. 2009;20(2):252–8.
57. Larson BT, Collins JM, Huidobro C, Corica A, Vallejo S, Bostwick DG. Gadolinium-enhanced MRI in the evaluation of minimally invasive treatments of the prostate: correlation with histopathologic findings. Urology. 2003;62(5):900–4.
58. Djavan B, Zlotta AR, Susani M, Heinz G, Shariat S, Silverman DE, et al. Transperineal radiofrequency interstitial tumor ablation of the prostate: correlation of magnetic resonance imaging with histopathologic examination. Urology. 1997;50(6):986–92. discussion 92–3
59. Baco E, Gelet A, Crouzet S, Rud E, Rouviere O, Tonoli-Catez H, et al. Hemi salvage high-intensity focused ultrasound (HIFU) in unilateral radiorecurrent prostate cancer: a prospective two-centre study. BJU Int. 2014;114(4):532–40.
60. Bahn D, de Castro Abreu AL, Gill IS, Hung AJ, Silverman P, Gross ME, et al. Focal cryotherapy for clinically unilateral, low-intermediate risk prostate cancer in 73 men with a median follow-up of 3.7 years. Eur Urol. 2012;62(1):55–63.
61. Pisters LL, Rewcastle JC, Donnelly BJ, Lugnani FM, Katz AE, Jones JS. Salvage prostate cryoablation: initial results from the cryo on-line data registry. J Urol. 2008;180(2):559–63. discussion 63-4
62. Panebianco V, Barchetti F, Grompone MD, Colarieti A, Salvo V, Cardone G, et al. Magnetic resonance imaging for localization of prostate cancer in the setting of biochemical recurrence. Urol Oncol. 2016;34(7):303–10.
63. Litjens GJ, Huisman HJ, Elliott RM, Shih NN, Feldman MD, Viswanath S, et al. Quantitative identification of magnetic resonance imaging features of prostate cancer response following laser ablation and radical prostatectomy. J Med Imaging (Bellingham). 2014;1(3):035001.
64. Rouviere O, Girouin N, Glas L, Ben Cheikh A, Gelet A, Mege-Lechevallier F, et al. Prostate cancer transrectal HIFU ablation: detection of local recurrences using T2-weighted and dynamic contrast-enhanced MRI. Eur Radiol. 2010;20(1):48–55.
65. Del Vescovo R, Pisanti F, Russo V, Battisti S, Cazzato RL, D'Agostino F, et al. Dynamic contrast-enhanced MR evaluation of prostate cancer before and after endorectal high-intensity focused ultrasound. Radiol Med. 2013;118(5):851–62.
66. Ben Cheikh A, Girouin N, Ryon-Taponnier P, Mege-Lechevallier F, Gelet A, Chapelon JY, et al. MR detection of local prostate cancer recurrence after transrectal high-intensity focused US treatment: preliminary results. J Radiol. 2008;89(5 Pt 1):571–7.
67. Punwani S, Emberton M, Walkden M, Sohaib A, Freeman A, Ahmed H, et al. Prostatic cancer surveillance following whole-gland high-intensity focused ultrasound: comparison of MRI and prostate-specific antigen for detection of residual or recurrent disease. Br J Radiol. 2012;85(1014):720–8.
68. Boutier R, Girouin N, Cheikh AB, Belot A, Rabilloud M, Gelet A, et al. Location of residual cancer after transrectal high-intensity focused ultrasound ablation for clinically localized prostate cancer. BJU Int. 2011;108(11):1776–81.

15 Acoustic Radiation Force Impulse Imaging for Targeting: Correlation with Histology

Mark L. Palmeri and Kathryn R. Nightingale

Introduction

B-mode ultrasound is the primary imaging tool used during prostate biopsy procedures, but its limited sensitivity and specificity for prostate cancer (PCa) lesion detection [1, 2] forces urologists to rely on systematic biopsy sampling methods for diagnosing cancer and making treatment decisions. Prostate cancer is commonly multifocal, which causes systematic sampling to only intersect a subset of clinically significant disease in the gland, complicating treatment decisions [3, 4]. Image-guided, targeted biopsy could improve diagnostic confidence by providing additional information for treatment decisions, improving confidence to use more focal therapies, and ultimately improving patient outcomes.

The past decade has seen the evolution of several non-acoustic radiation force impulse (ARFI)-based ultrasonic imaging modalities to improve ultrasonic visualization of PCa. In their studies, Hoyt et al. and Taylor et al. [5, 6] explored elasticity as a mechanism of delineating PCa using a sonoelastography crawling wave approach. Mahdavi et al. [7] have developed an ultrasonic vibro-elastography method that characterizes the viscoelastic properties of the prostate to delineate prostate anatomy, guide PCa diagnosis, and delineate regions of PCa suspicion. Vibro-elastography is also being studied in combination with prostate magnetic resonance imaging (MRI) to improve prostate cancer detection [8]. Shear wave elastography (SWE) [9] and strain-based elastography [10, 11] also have diagnostic value identifying PCa lesions based on their mechanical properties.

Preliminary studies have demonstrated that ARFI imaging, an ultrasonic, elasticity-based imaging modality, can delineate PCa and prostate anatomy with high fidelity [12–15]. ARFI imaging has short acquisition times, low cost, and portability that could be utilized to guide targeted biopsies in outpatient clinical settings. We recruited 29 patients with biopsy-confirmed PCa who were having radical prostatectomy treatments, and we identified regions in in vivo ARFI imaging that were suspicious for cancer (regions of suspicion [ROS]) and compared these ARFI image findings to whole-mount histopathology. Given the challenges associated with reconstructing imaged prostate volumes from whole-mount histology slides, we used a nearest-neighbor regional match approach to localize lesions and ROS to evaluate ARFI imaging's ability to identify clinically significant PCa lesions. Regions of atrophy and benign prostatic hyperplasia (BPH) were identified on histopathology and evaluated as potential confounders when identifying ROS in ARFI images.

M.L. Palmeri (✉) • K.R. Nightingale
Department of Biomedical Engineering, Duke University, Durham, NC, USA
e-mail: mark.palmeri@duke.edu

© Springer International Publishing AG 2017

T.J. Polascik (ed.), *Imaging and Focal Therapy of Early Prostate Cancer*, Current Clinical Urology, DOI 10.1007/978-3-319-49911-6_15

Methods

ARFI and B-mode Image Acquisition and Image Analysis

B-mode and ARFI prostate images were acquired in 29 patients with biopsy-confirmed PCa immediately prior to radical prostatectomy (RP) in an institutional review board (IRB)-approved study after obtaining written informed consent. Imaging was performed using a modified Siemens Acuson SC2000™ scanner (Siemens Medical Solutions, Ultrasound Division, Mountain View, CA) with an Acuson ER7B side-fire transrectal probe coupled to a mechanical rotation device (Fig. 15.1).

Images were acquired in the sagittal plane using a three focal zone ARFI excitation fired in rapid succession to create a virtual, extended acoustic radiation force excitation [14, 16, 17]. Raw baseband (in-phase and quadrature [IQ]) data were acquired at an 8 kHz pulse repetition frequency (PRF) for 5 ms using tracking beams focused at 60 mm at 5.0 MHz in an F/3 focal configuration with dynamic receive. Track beams were acquired using 4:1 parallel receive with 0.17 mm track beam spacing [18], and data were saved for offline displacement estimation. The ARFI data acquisition configuration has been described in detail in past studies [14].

High-resolution B-mode images were acquired in a subsequent data acquisition using 126 transmits spanning a 55 mm field of view with 7:1 parallel receive, coherent beamforming. These B-mode sequences used a 7.0 MHz transmit frequency with an F/3 focal configuration at a fixed focal depth dependent on the size of the prostate, which ranged from 10–60 mm across the subjects in this study. An F/1, dynamic receive focal configuration was used for receive beamforming.

Mechanical rotation of the ER7B probe was used to acquire three-dimensional (3D) prostate volumes in ~1 degree elevation increments between image acquisitions, sweeping an arc across the lateral extent of the prostate (Fig. 15.2). This rotation setup utilized a CIVCO Micro-Touch™ stabilizer (CIVCO Medical Solutions, Kalona, IA USA) with six axis degrees of freedom for manual positioning of the transducer to sweep through the entire prostate during imaging. A custom optical angular feedback transduction circuit utilizing a reflective linear strip with 212 lines-per-inch resolution (US Digital, Vancouver, WA, USA) was coupled to the transducer holding cradle (Fig. 15.1) and communicated with a QSB-S Quadrature-to-USB adapter to achieve 9-line/degree resolution.

The description of the post-processing of 3D ARFI imaging data has been previously described [14]. Briefly, ARFI image displacements were estimated, and a correlation coefficient threshold of 0.95 was applied to reject estimates corrupted by motion and noise. Displacement data from each focal depth were normalized to account for depth-dependent variations in ARFI amplitude [15]. The imaging planes of displacement data were scan-converted to an isotropic voxel size of $0.15 \times 0.15 \times 0.15$ mm^3 for image analysis in 3D

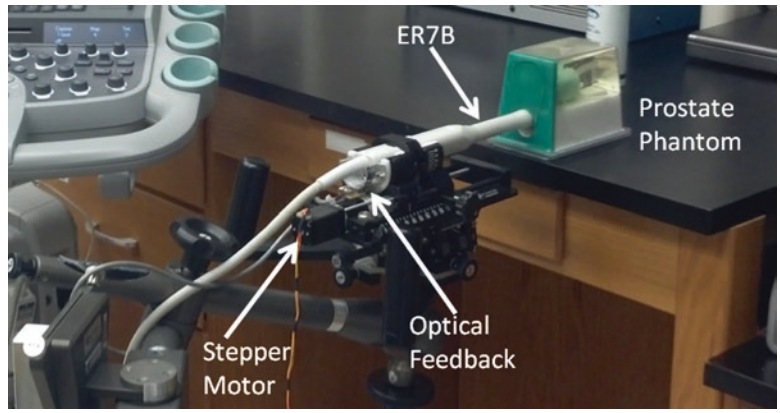

Fig. 15.1 B-mode/ARFI imaging setup with the ER7B ultrasound transducer integrated into a custom-rotating CIVCO transducer holder to obtain three-dimensional ultrasound datasets with the Siemens Acuson SC2000™ scanner

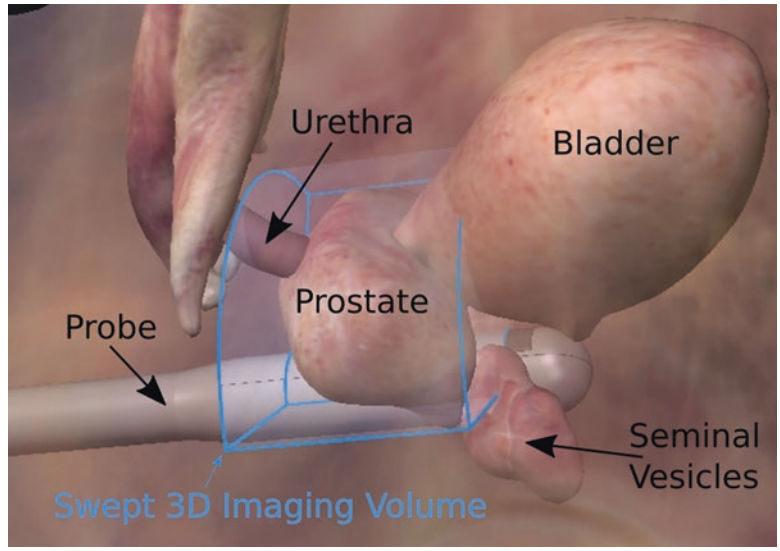

Fig. 15.2 Orientation of the swept imaging volume (*blue outline*) relative to the prostate and adjacent anatomy. B-mode and ARFI images were acquired in separate sweeps of this volume in ~1 degree increments

Table 15.1 Description of index-of-suspicion (IOS) scores for ARFI imaging regions of suspicion (ROS). Note that the healthy central gland exhibits heterogeneity in ARFI images that can confound the ability to identify ROS and, therefore, reduces this IOS in this scoring scheme

	ARFI imaging ROS characteristics			
IOS Score	Boundary	Contrast	Texture	Location
1	Variable	Low)	Variable	Peripheral zone or central gland
2	Variable	Medium	Smooth	Peripheral zone
3	Well defined	High	Smooth	Peripheral zone

Slicer [15, 19]. Prostate anatomic features, including the prostate capsule and central gland, were identified, segmented, modeled, and used for anatomic guidance during ROS identification [15]. ROS were identified, blinded to histopathology, and assigned an index of suspicion (IOS) based on a three-point scale (Table 15.1). Axial, coronal, and sagittal imaging planes were all used to assign IOS. ROS were segmented and modeled in 3D Slicer.

Histopathology Analysis

All ARFI-imaged prostates were radically excised and whole mounted for histologic evaluation with hematoxylin and eosin (H&E) stain. Two trained pathologists identified the outer capsule, verumontanum, and Gleason grade of PCa lesions, along with benign processes, including BPH and atrophy.

Histopathology slides were digitized and converted to Neuroimaging Informatics Technology Initiative (NIfTI) image stacks using ImageJ [14, 20].

Volume estimates were computed for all histology-identified PCa lesions using five steps:

1. Approximate prostate gland volume as an ellipsoid using pathology triaxial measurements from just after prostate excision [15].
2. Segment PCa lesion and prostate capsule outline on all slides using 3D Slicer.
3. Sum the total area of PCa lesion segmentations across all histology slides.
4. Divide the total area of PCa lesion by the total area of prostate capsule summed across slides to compute a total lesion area fraction.

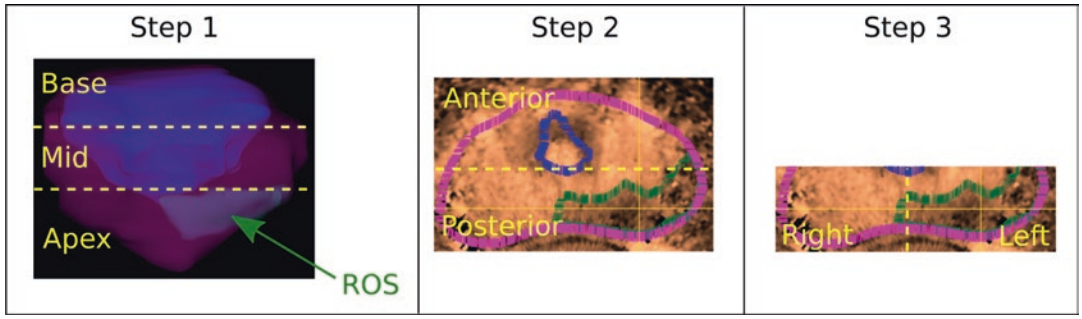

Fig. 15.3 Procedure for localizing ARFI image ROS. *Step 1*: Localize the ROS (*green sub-volume in model*) to the prostate base, mid, or apex region. *Step 2*: Localize the ROS (*green outline*, IOS = 3) to the prostate anterior or posterior region. The *magenta outline* represents the prostate capsule, and the *blue outline* represents the central gland outline. *Step 3*: Localize the ROS to the *right* or *left*. *Step 4* (not shown): Determine the single region that corresponds best to the bulk of the ROS burden

5. Multiply total lesion area fraction by approximated ellipsoid prostate volume to get approximated PCa lesion volume.

ARFI Imaging and Histopathology Correlation

The slice thickness and orientation of whole-mount histology slides were approximated during the slide registration process, making voxel-to-voxel comparisons between histology and imaging volumes challenging. For this reason, we chose to correlate ARFI image ROS to delineated histology lesions using a 27-region model of the prostate, where each region is defined by anatomic location in the prostate [21]. This regional localization procedure involved three steps:

1. Visual localization of ARFI image and histopathology models to a 27-region, standardized grid (Fig. 15.3) [21]
2. Approximation of the ARFI image ROS and histopathology lesion centers
3. Evaluating the matches between the centers of ARFI image ROS and histopathology lesions on the 27-region grid

ARFI image models (prostate capsule, central gland, ROS) and histopathology slides were visually registered to a standardized 27-region grid using anatomic features as fiducials [21]. The ARFI image ROS centers and histopathology lesions were then found by iteratively reducing the space of possible center locations on the 27-region grid to 1 center region using the following steps (Fig. 15.3):

1. Localize the ROS to the prostate base, mid, or apex region, reducing the number of possible regions from 27 down to 9.
2. Localize the ROS to the anterior/posterior region, reducing the number of possible regions to 5 (posterior) or 4 (anterior).
3. Localize the ROS to the prostate right/left side.
4. Determine the primary location of the tumor burden to localize the ROS to a single region.

ARFI-identified ROS that were either located in the same region or in the nearest-neighbor region as the histopathology PCa lesion center were scored as successfully identifying the histopathology lesion. ARFI ROS were also correlated with the presence of atrophy and BPH. Atrophy and BPH lesions were identified in all regions where present in the histopathology slides (not just a single center region as was done with the PCa) since these processes can be more diffuse, and ARFI ROS were deemed coincident with atrophy or BPH if the ROS intersected with any of the regions for these benign lesion types and did not match to a PCa region in histology.

Table 15.2 Clinical significance categories for histopathology-identified PCa [22, 24]. Lesions were also characterized by anterior or posterior location in the prostate

Clinically significant disease	Clinically insignificant disease
Lesion volume >=0.5 mL	Lesion volume <0.5 mL
And/or	And
Gleason score >6	Gleason score <=6

Histopathology Lesion Stratification and Calculations

Histopathology lesions were stratified into clinical significance categories (Table 15.2) [22]. Along with lesion size, Gleason score was used as a primary determinant of PCa clinical significance. ARFI imaging PCa detection rates and positive predictive values (PPV) were calculated for all PCa lesions in this study.

Results

Of all clinically significant lesions, 71.4 % were detected with ARFI imaging (Fig. 15.4a); 82.9 % of these clinically significant lesions were in the posterior prostate, and 17.1 % were in the anterior prostate. ARFI imaging was able to detect 79.3 % of all posterior and 33.3 % of all anterior clinically significant lesions.

Of ARFI-identified ROS, 79.3 % were clinically significant PCa with the majority having IOS scores ≥2 (Fig. 15.4b). One ARFI ROS was atrophy, and the others (IOS ≤2) corresponded to PCa lesions that were not clinically significant. No ARFI ROS were associated with BPH.

Higher-assigned ARFI imaging IOS values for lesions showed higher positive predictive value (PPV) for both clinically significant disease and clinically insignificant disease (Table 15.3).

Figure 15.5 shows examples of PCa lesion visibility in ARFI images scored with different indices of suspicion. Panel A shows two examples of PCa lesions that were identified as highly suspicious (IOS = 3) in ARFI imaging and corresponded to large, clinically significant, posterior PCa lesions. Panel B shows an example of a lower suspicion lesion (IOS = 1) that corresponded to a clinically insignificant PCa lesion. Panel C1 shows an example of an anterior, clinically significant PCa lesion that was not identified as an ROS in ARFI imaging, although in retrospect, this lesion is clearly visible. Panel C2 shows a small but clinically significant PCa lesion that was missed in ARFI imaging likely due to the high gland distortion introduced by the prevalent central gland BPH.

Figure 15.6 shows the characteristics of the clinically significant lesions that were detected and missed in ARFI images as a function of estimated histologic lesion volume and Gleason grade.

Discussion

ARFI imaging has proved to be very specific for clinically significant PCa, especially in the posterior region where 79.3 % of clinically significant lesions were detected (Fig. 15.4a). ARFI ROS scored with an IOS of 2–3 perfectly corresponded to PCa lesions (Table 15.3), and 100 % of ARFI IOS 3 lesions were clinically significant PCa lesions (Fig. 15.4, Table 15.3). The specificity of ARFI imaging is significantly greater than that of B-mode imaging alone [23]. The high specificity of ARFI imaging could have clinical utility in distinguishing aggressive PCa lesions that require treatment from indolent disease that could be focally treated or monitored for progression.

Larger lesions were more readily visualized in ARFI imaging. No clinically significant lesions with histology volume <0.4 mL (n = 5) were identified in ARFI (Fig. 15.6). ARFI imaging's greater sensitivity for larger lesions could be useful for diagnostic purposes to reduce the current overly aggressive treatment of small PCa lesions.

ARFI image lesion size does not, and was not expected, to match the size outlined in the histology slides (Fig. 15.5). The regions delineated with marker on the histology slides correspond to cellular patterns of dysplasia that are used to designate different Gleason grades, which

Fig. 15.4 (**a**) ARFI imaging detected 79.3 % of posterior and 33.3 % of anterior clinically significant lesions using the nearest-neighbor region match. The majority (82.9 %) of the clinically significant lesions were located in the posterior region. Lesions on whole-mount histology were classified as clinically significant/insignificant PCa, BPH, or atrophy. (**b**) 79.3 % of ARFI-identified lesions were clinically significant, with the majority having IOS ≥2 (sub-histogram). The clinically insignificant PCa lesions that were identified overall had lower IOS (sub-histogram), and one ARFI ROS (IOS = 1) corresponded to a region of atrophy. No ARFI ROS corresponded to BPH, and 1 ARFI ROS did not correspond to any histology-identified lesions

are not the features that we hypothesize generates contrast in ARFI images. We hypothesize that ARFI images have PCa lesion contrast due to increases in cellular density and intercellular connectivity that changes the more macrocellular mechanical properties. We expect these changes

to be greatest at the "center" of evolving PCa lesions, and therefore, we do not expect exact spatial correspondence between the outer areas outlined in histology and the outer extents of regions of decreased displacement in the ARFI images. Despite this discrepancy, an ARFI imaging system should be most sensitive to the center of PCa lesions, which is the most clinically useful feature when trying to target a biopsy needle.

Six of the prostates had multifocal disease with ≥4 discrete clinically significant PCa lesions. ARFI imaging was able to detect a PCa lesion in only 1/6 (16.7 %) of these cases due to the relatively small absolute size of any specific PCa focus (Fig. 15.6).

Atrophy was not a significant confounder when identifying PCa lesions. Across all ARFI-identified ROS, only one region of atrophy was identified as a region of low suspicion (IOS = 1) BPH and, however, can challenge the ability to identify peripheral PCa lesions, especially when

Table 15.3 Positive predictive value (PPV) and index of suspicion (IOS) for clinically significant disease (CSD) as well as the presence of any cancer (CSD or CINSD)

IOS score	PPV for CSD (%)	PPV for CSD or CINSD (%)
3	100	100
2	85	100
1	43	71

CSD clinically significant disease, *CINSD* clinically insignificant disease

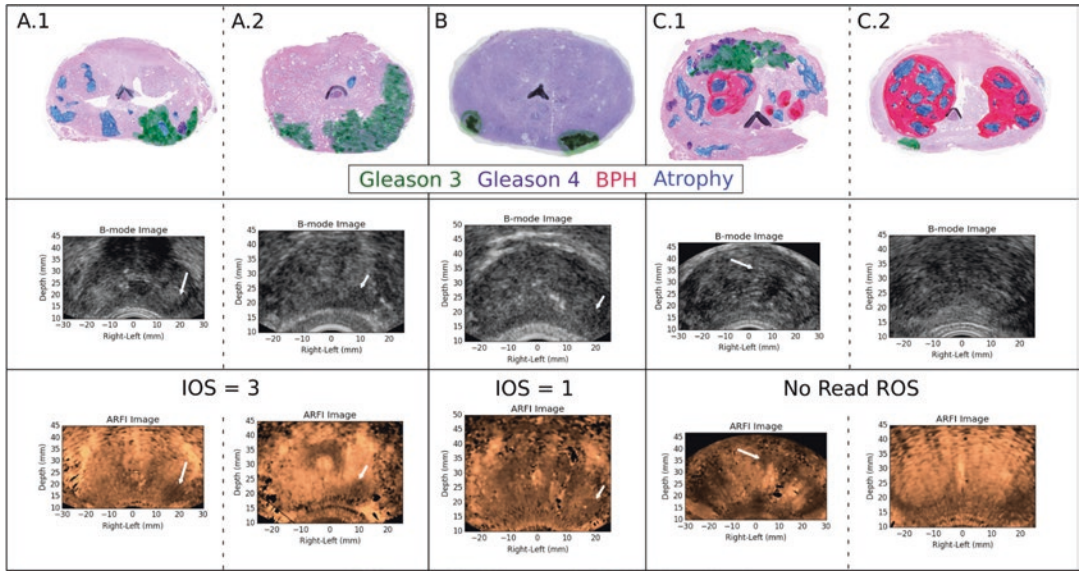

Fig. 15.5 Examples of PCa lesion appearance in histogram-normalized ARFI images. Panel (**a**) shows two examples of ARFI-identified IOS = 3 ROS that corresponded to large, posterior PCa index lesions that clearly appear as large regions of decreased displacement with contralateral contrast. Panel (**b**) shows an example of an ARFI-identified ROS (IOS = 1) that corresponded to a small, clinically insignificant posterior PCa lesion. This ROS was identified based on a small, localized region of decreased displacement. A second, smaller, clinically insignificant, posterior PCa lesion on the opposite side was not detected as a ROS in the ARFI images. Panel (**c**) shows two examples of PCa lesions that were not identified as ROS in ARFI imaging. Panel (*C1*) shows a PCa index lesion (*green* and *purple*) in the anterior stroma that was missed in ARFI imaging (no suspicious regions identified). The associated ARFI image from the mid-gland shows a bright central structure corresponding to the BPH/atrophy adjacent to midline on the patient right, but the anterior stroma of the prostate could not be reliably evaluated due to stiffness heterogeneity introduced by the BPH and atrophy. There is also shadowing and a region of decorrelation on the patient left due to a posterior calcification in the prostate (hypoechoic regions in the B-mode image) that can also complicate interpretation of the ARFI image. Panel (*C2*) is an example of a small but clinically significant PCa lesion in the patient right posterior region of the prostate that was missed in histogram-normalized ARFI imaging due to the dominant appearance of atrophy and BPH in the enlarged central gland. These large BPH nodules heavily distort the typical prostate anatomy and can confound identifying PCa lesions in ARFI images

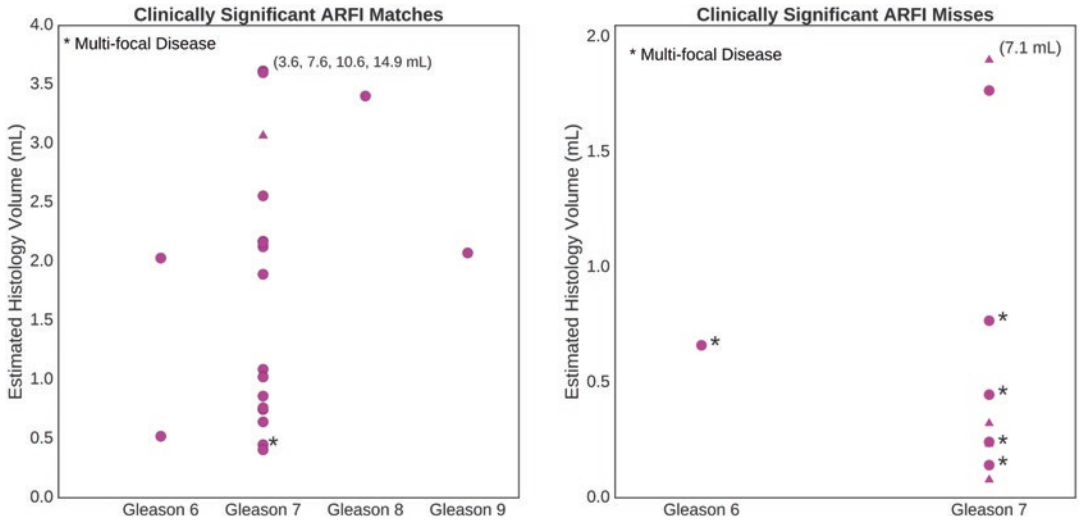

Fig. 15.6 Characteristics of the clinically significant lesions that ARFI imaging detected and missed as a function of estimated histologic lesion volume and Gleason grade. "Multifocal disease" is defined as a prostate having ≥4 cancerous foci. Notice that ARFI did not miss any of the highest Gleason grade lesions (Gleason 8 and 9), and the majority of the missed clinically significant lesions had volumes <1.0 mL or were located in the anterior region of the prostate. The numbers on the plots associated with some of the high-volume lesions indicate the absolute volumes of the lesions that fall off the scale of each plot

the BPH dominated the central gland and distorted the normal prostate anatomy visualized in ARFI images (Fig. 15.5) [15].

ARFI imaging is one of several novel ultrasonic imaging modalities being investigated to improve upon the poor performance of B-mode ultrasound imaging to delineate clinically significant PCa. Moradi et al. have used 3D vibroelastography and vector machine classification methods to identify PCa lesions based on image texture (e.g., contrast, homogeneity, standard deviation), which yielded an AUROC of 0.81 ± 0.1 [25]. Shear wave elasticity imaging (SWEI) of the prostate has also been studied in the prostate, with one study achieving a positive predictive value of 69.4 % using an absolute shear modulus threshold of 37 kPa [9]. Compressive strain elastography can also evaluate PCa lesions, with a specificity of 83–91 % and a positive predictive value of 69 % [26–28]. Other non-elasticity-based ultrasound methods using quantitative tissue characterization schemes are also being studied in the prostate [29, 30], along with contrast-based approaches [31–34].

ARFI imaging has several advantages over the other ultrasonic imaging modalities. Compressive strain elastography is dependent on applying uniform compression across the entire prostate gland, and relative strain ratios between different regions of interest and quality maps of strain confidence are used to overcome these challenges [27]. ARFI imaging does not depend on applying uniform compression, and in fact, after achieving adequate acoustic coupling to the rectal wall, additional compression was minimized to avoid any elastic nonlinearities in the tissue.

SWEI utilizes shear wave speed reconstruction kernels of finite spatial extent that can limit the achievable spatial resolution [35], but ARFI image spatial resolution is higher, since it is related to the displacement estimation kernel lengths and beam spacing (<1 mm). ARFI imaging is less susceptible to the shear wave reflection artifacts that can be present in SWEI images [35, 36].

The 71.4 % of clinically significant lesions that were detected in ARFI images across all of the prostates imaged in this study would be a

great improvement over the current transrectal ultrasound (TRUS) imaging used during biopsy procedures that simply guides the complete core sampling across the entire organ during a random biopsy procedure, without lesion targeting. Other imaging technologies are being studied to guide prostate biopsies, such as MR-ultrasound fusion, but these methods have yielded accuracy ranging from 60 to 70 % [37, 38] and are susceptible to modality registration errors due to prostate deformation and varying structural contrast between ultrasound and MR. The inherent co-registration between ARFI and B-mode ultrasound images provides a clear advantage over other multimodality imaging techniques.

Conclusion

ARFI imaging identified 79.3 % of posterior, clinically significant PCa lesions. All highly suspicious (IOS = 3) regions in ARFI images corresponded to clinically significant PCa lesions, and all moderately suspicious regions (IOS of 2–3) corresponded to PCa lesions. BPH can enlarge the central gland, causing peripheral zone distortion, and create stiffness heterogeneity in the prostate that confounds ARFI PCa lesion identification. Overall, ARFI imaging ROS did not coincide with benign atrophy and BPH pathologies. ARFI imaging has clinical value in identifying and differentiating clinically significant PCa lesion in the posterior region of the prostate. Future advances in transducer technology and modified ARFI imaging sequences should allow the anterior region of the prostate to be more reliably interrogated.

Acknowledgments This work was supported by NIH R01CA142824, NIH R41CA196565-01, NIH T32-EB001040, and the Duke Coulter Translational Grant program. The authors would like to thank Siemens Medical Solutions USA, Ultrasound Division, for their in-kind technical support and the Duke University Medical Center Pathology Assistants for whole-mount histology preparation. Additional thanks to Dr. Stephen Rosenzweig for ARFI image data acquisition, Tyler Glass for prostate lesion analysis, Dr. Andrew Buck for pathology analysis, and Dr. Thomas Polascik for clinical patient access.

References

1. Correas JM, Tissier AM, Khairoune A, Khoury G, Eiss D, Hélénon O. Ultrasound elastography of the prostate: state of the art. Diagn Interv Imaging. 2013;94(5):551–60.
2. Salomon G, Köllerman J, Thederan I, Chun FK, Budäus L, Schlomm T, et al. Evaluation of prostate cancer detection with ultrasound real-time elastography: a comparison with step section pathological analysis after radical prostatectomy. Eur Urol. 2008;54(6):1354–62.
3. Cornud F, Delongchamps NB, Mozer P, Beuvon F, Schull A, Muradyan N, et al. Value of multiparametric MRI in the work-up of prostate cancer. Curr Urol Rep. 2012;13(1):82–92.
4. Mufarrij P, Sankin A, Godoy G, Lepor H. Pathologic outcomes of candidates for active surveillance undergoing radical prostatectomy. Urology. 2010;76(3):689–92.
5. Hoyt K, Castaneda B, Zhang M, Nigwekar P, di Sant'agnese PA, Joseph JV, et al. Tissue elasticity properties as biomarkers for prostate cancer. Cancer Biother. 2008;4(4–5):213–25.
6. Taylor LS, Rubens DJ, Porter BC, Wu Z, Baggs RB, di Sant'Agnese PA, et al. Prostate cancer: three-dimensional sonoelastography for in vitro detection. Radiology. 2005;237(3):981–5.
7. Mahdavi SS, Moradi M, Wen X, Morris WJ, Salcudean SE. Evaluation of visualization of the prostate gland in vibro-elastography images. Med Image Anal. 2011;15(4):589–600.
8. Ashab HAD, Haq NF, Nir G, Kozlowski P, Black P, Jones EC, et al. Multimodal classification of prostate tissue: a feasibility study on combining multiparametric MRI and ultrasound. Proc SPIE. 2015;9414, 94141B.
9. Barr RG, Memo R, Schaub CR. Shear wave ultrasound elastography of the prostate: initial results. Ultrasound Q. 2012;28(1):13–20.
10. Pallwein L, Mitterberger M, Pinggera G, Aigner F, Pedross F, Gradl J, et al. Sonoelastography of the prostate: comparison with systematic biopsy findings in 492 patients. Eur J Radiol. 2008;65(2):304–10.
11. König K, Scheipers U, Pesavento A, Lorenz A, Ermert H, Senge T. Initial experiences with real-time elastography-guided biopsies of the prostate. J Urol. 2005;174(1):115–7.
12. Zhai L, Madden J, Foo WC, Palmeri ML, Mouraviev V, Polascik TJ, et al. Acoustic radiation force impulse imaging of human prostates ex vivo. Ultrasound Med Biol. 2010;36(4):576–88.
13. Zhai L, Polascik TJ, Foo WC, Rosenzweig S, Palmeri ML, Madden J, et al. Acoustic radiation force impulse imaging of human prostates: initial in vivo demonstration. Ultrasound Med Biol. 2012;38(1):50–61.
14. Palmeri ML, Glass TJ, Miller ZA, Rosenzweig SJ, Buck A, Polascik TJ, et al. Identifying clinically significant prostate cancers using 3-D in vivo acoustic radiation force impulse imaging with whole-mount

histology validation. Ultrasound Med Biol. 2016;42(6): 1251–62.
15. Palmeri ML, Miller ZA, Glass TJ, Garcia-Reyes K, Gupta RT, Rosenzweig SJ, et al. B-mode and acoustic radiation force impulse (ARFI) imaging of prostate zonal anatomy: comparison with 3tt2-weighted MR imaging. Ultrason Imaging. 2015;37(1):22–41.
16. Rosenzweig S, Palmeri M, Nightingale K. Analysis of rapid multi-focal-zone ARFI imaging. IEEE Trans Ultrason Ferroelectr Freq Control. 2015;62(2):280–9.
17. Bercoff J, Tanter M, Fink M. Supersonic shear imaging: a new technique for soft tissue elasticity mapping. IEEE Trans Ultrason Ferroelectr Freq Control. 2004;51(4):396–409.
18. Dahl JJ, Pinton GF, Mark L, Agrawal V, Nightingale KR, Trahey GE. A parallel tracking method for acoustic radiation force impulse imaging. IEEE Trans Ultrason Ferroelectr Freq Control. 2007;54(2):301–12.
19. Fedorov A, Beichel R, Kalpathy-Cramer J, Finet J, Fillion-Robin JC, Pujol S, et al. 3D slicer as an image computing platform for the quantitative imaging network. Magn Reson Imaging. 2012;30(9):1323–41.
20. Schneider CA, Rasband WS, Eliceiri KW. NIH Image to ImageJ: 25years of image analysis. Nat Methods. 2012;9(7):671–5.
21. Dickinson L, Ahmed HU, Allen C, Barentsz JO, Carey B, Futterer JJ, et al. Magnetic resonance imaging for the detection, localisation, and characterisation of prostate cancer: recommendations from a European consensus meeting. Eur Urol. 2011;59(4):477–94.
22. Mazzucchelli R, Barbisan F, Scarpelli M, Lopez-Beltran A, van der Kwast TH, Cheng L, et al. Is incidentally detected prostate cancer in patients undergoing radical cystoprostatectomy clinically significant? Am J Clin Pathol. 2009;131(2):279–83.
23. Eggert T, Khaled W, Wenske S, Ermert H, Noldus J. Impact of elastography in clinical diagnosis of prostate cancer. a comparison of cancer detection between b-mode sonography and elastography-guided 10-core biopsies. Urologe A. 2008;47(9):1212–7. German
24. Yang XJ, Lecksell K, Potter SR, Epstein JI. Significance of small foci of Gleason score 7 or greater prostate cancer on needle biopsy. Urology. 1999;54(3):528–32.
25. Moradi M, Mahdavi SS, Nir G, Mohareri O, Koupparis A, Gagnon LO, et al. Multiparametric 3D in vivo ultrasound vibroelastography imaging of prostate cancer: preliminary results. Med Phys. 2014;41(7):073505.
26. Zhang Y, Tang J, Li YM, Fei X, Lv FQ, He EH, et al. Differentiation of prostate cancer from benign lesions using strain index of transrectal real-time tissue elastography. Eur J Radiol. 2012;81(5):857–62.
27. Cosgrove D, Piscaglia F, Bamber J, Bojunga J, Correas JM, Gilja OH, et al. EFSUMB guidelines and recommendations on the clinical use of ultrasound elastography. Part 2: clinical applications. Ultraschall Med. 2013;34(3):238–53.
28. Walz J, Marcy M, Pianna JT, Brunelle S, Gravis G, Salem N, et al. Identification of the prostate cancer index lesion by real-time elastography: considerations for focal therapy of prostate cancer. World J Urol. 2011;29(5):589–94.
29. Braeckman J, Autier P, Garbar C, Marichal MP, Soviany C, Nir R, et al. Computer-aided ultrasonography (HistoScanning): a novel technology for locating and characterizing prostate cancer. BJU Int. 2008;101(3):293–8.
30. Feleppa EJ, Porter CR, Ketterling J, Lee P, Dasgupta S, Urban S, et al. Recent developments in tissue-type imaging (TTI) for planning and monitoring treatment of prostate cancer. Ultrason Imaging. 2004;26(3): 163–72.
31. Wink M, Frauscher F, Cosgrove D, Chapelon JY, Palwein L, Mitterberger M, et al. Contrast-enhanced ultrasound and prostate cancer; a multicentre European research coordination project. Eur Urol. 2008;54(5):982–92.
32. Kuenen MP, Mischi M, Wijkstra H. Contrast-ultrasound diffusion imaging for localization of prostate cancer. IEEE Trans Med Imaging. 2011;30(8):1493–502.
33. Ferrara KW, Merritt CR, Burns PN, Foster FS, Mattrey RF, Wickline SA. Evaluation of tumor angiogenesis with US: imaging, Doppler, and contrast agents. Acad Radiol. 2000;7(10):824–39.
34. Seitz M, Gratzke C, Schlenker B, Buchner A, Karl A, Roosen A, et al. Contrast-enhanced transrectal ultrasound (CE-TRUS) with cadence-contrast pulse sequence (CPS) technology for the identification of prostate cancer. Urol Oncol. 2011;29(3):295–301.
35. Rouze NC, Wang MH, Palmeri ML, Nightingale KR. Parameters affecting the resolution and accuracy of 2-D quantitative shear wave images. IEEE Trans Ultrason Ferroelectr Freq Control. 2012;59(8): 1729–40.
36. Deffieux T, Gennisson JL, Bercoff J, Tanter M. On the effects of reflected waves in transient shear wave elastography. IEEE Trans Ultrason Ferroelectr Freq Control. 2011;58(10):2032–5.
37. Siddiqui MM, Rais-Bahrami S, Turkbey B, George AK, Rothwax J, Shakir N, et al. Comparison of MR/ultrasound fusion-guided biopsy with ultrasound-guided biopsy for the diagnosis of prostate cancer. JAMA. 2015;313(4):390–7.
38. Fütterer JJ, Briganti A, De Visschere P, Emberton M, Giannarini G, Kirkham A, et al. Can clinically significant prostate cancer be detected with multiparametric magnetic resonance imaging? A systematic review of the literature. Eur Urol. 2015;68(6):1045–53.

Part V

Prostate Biopsy Techniques

In-Bore Magnetic Resonance Imaging-Targeted Prostate Biopsy

16

Igor Trilisky, Aytekin Oto, and Scott Eggener

Introduction

Over the last decade, multiparametric magnetic resonance imaging (mpMRI) of the prostate has evolved to be the preferred imaging modality for detecting and staging prostate cancer (PCa) [1]. MRI-guided prostate biopsy has become an established approach to sample the prostate in multiple clinical contexts [2–5]. Compared to transrectal ultrasound (TRUS)-guided systematic prostate biopsy (sPBx), MRI-guided prostate biopsy is more likely to detect clinically significant cancer with fewer cores [6–9], and Gleason scores obtained by MRI-guided biopsy correlate better with the Gleason scores of radical prostatectomy (RP) specimens. The precise identification of tumor location and aggressiveness allows for more confident selection of patients for active surveillance and focal ablation therapy. More accurate grading and staging of the tumor reduces the risk of inaccurate risk stratification and upgrading or upstaging the final diagnosis [6, 10, 11]. Moreover, MRI-guided prostate biopsy is less likely to diagnose clinically insignificant indolent PCa, therefore decreasing overdiagnosis, overtreatment, and the significant associated downstream costs and morbidity [12, 13].

I. Trilisky (✉) • A. Oto
Department of Radiology, University of Chicago, Chicago, IL, USA
e-mail: itrilisky@gmail.com

S. Eggener
Department of Surgery, Section of Urology, University of Chicago, Chicago, IL, USA

Magnetic Resonance Imaging-Guided Prostate Biopsy Technique Overview

The terms "MRI-guided" or "MRI-targeted" prostate biopsy have been used in the literature to describe several techniques that utilize MRI to biopsy selected targets in the prostate, including TRUS-MRI-guided prostate biopsy with cognitive registration, TRUS-MRI-guided fusion prostate biopsy, and in-bore MRI-targeted prostate biopsy.

In-Bore MRI-Targeted Prostate Biopsy

First described in 2000 [14–16], in-bore MRI-targeted prostate biopsy is performed under MRI guidance while the patient is in the magnet (in-bore) and allows for real-time direct visualization of the MRI abnormality as well as the needle. This approach has become technically feasible as MRI scanners have improved in speed and image quality, MRI-compatible equipment has been

© Springer International Publishing AG 2017

T.J. Polascik (ed.), *Imaging and Focal Therapy of Early Prostate Cancer*, Current Clinical Urology, DOI 10.1007/978-3-319-49911-6_16

developed, and advanced visualization software tools have become available to help guide the procedure.

Approaches Available for In-Bore MRI-Targeted Prostate Biopsy

Most commonly the procedure is performed via a transrectal approach. A trans-perineal approach is available to those patients who have undergone a proctectomy and have limiting perianal disease or anal stricture. Although other modalities have been reported for imaging guidance in this patient population—including trans-gluteal approach computed tomography (CT)-guided systematic biopsy [17], trans-perineal approach with trans-perineal ultrasound (US) guidance [18], and trans-perineal approach with transurethral US guidance [19]—the trans-perineal approach in-bore MRI-targeted prostate biopsy allows for best target lesion visualization in this subset of patients. A trans-gluteal approach in-bore MRI-targeted prostate biopsy has been described in the literature, potentially allowing for better access to the prostate gland apex in some cases [20].

Patient Preparation Prior to In-Bore MRI-Targeted Prostate Biopsy

Contraindications to MRI preclude a patient from MRI-guided prostate biopsy. A patient should undergo standard MRI screening to evaluate for devices (pacemaker, defibrillator, deep brain stimulator, cochlear implants, among others) or metal foreign bodies that can be absolute contraindications to MRI. Pre-procedural evaluation of a patient includes assessment for contraindications including serious bleeding diathesis, suspected acute bacterial prostatitis within 6 weeks of the procedure, or active perianal disease. Anticoagulation and anti-inflammatory medications should be appropriately managed. Minor complications following prostate biopsy are reported in 3–5 % of patients, including limited hematuria, hematochezia, hematospermia, urinary retention, and infection.

A diagnostic mpMRI of the prostate is performed where a suspicious or dominant lesion or lesions are identified. The diagnostic mpMRI may be performed immediately prior to the biopsy or on a different day. Prior to the biopsy, the patient is premedicated with an antibiotic regimen to decrease the risk of infection. The American Urological Association (AUA) recommends a 24 h course of a fluoroquinolone and cephalosporin in all patients. If this is not done beforehand, same-day intravenous antibiotics can be administered. In-bore MRI-targeted prostate biopsy requires MRI-compatible equipment. The technique has a steep learning curve and can be time-consuming initially; however, with experience with a transrectal or trans-perineal approach, a prostate can be sampled in approximately 30 min with an additional 10–15 min per additional target.

Transrectal Approach In-Bore MRI-Targeted Prostate Biopsy Technique

Transrectal approach is the most common technique used for in-bore MRI-targeted prostate biopsy. In our institution we use a 1.5 or 3 Tesla magnet, which allows for excellent visualization of the target lesion. Open MRI low magnetic field scanners have also been used for guidance. Although the open low-field-strength MRI approach may allow for easier access to the patient, the closed-bore high-field-strength magnet results in a significantly higher signal-to-noise ratio and thus better visualization of the target and the prostate. Table 16.1 outlines the steps of the protocol used at our institution.

MRI-compatible equipment is necessary and is available from several vendors. In our institution we use the DynaTRIM portable biopsy device (Fig. 16.1) and corresponding DynaCAD software (Invivo, Gainesville, Florida). The equipment comprises a fixed stable base placed underneath a prone patient. An adjustable needle guide is attached to the base once the patient is positioned. The needle guide is calibrated to its default neutral position settings. The needle sleeve is lubricated with lidocaine jelly, inserted into the rectum, and attached to the needle guide. The needle sleeve is filled with a gadolinium-based contrast agent to optimize

Table 16.1 Transrectal in-bore MRI-targeted biopsy technique

Pre-biopsy steps
1. Standard MRI safety precautions
2. Diagnostic multiparametric MRI performed with an endorectal coil to identify target lesions. Typically, high-field-strength MRI with small field-of-view T2-weighted, diffusion-weighted, and dynamic contrast-enhanced images
3. The patient is premedicated with oral antibiotics
4. Obtain an informed consent
Biopsy steps
1. The patient is placed prone on the table with the needle-guide base positioned at the level of the pelvis. Adjust patient position to minimize discomfort and motion
2. Phased-array coil is placed on the patient's lower back centered over the prostate
3. The needle guide is calibrated to its default neutral position settings
4. Needle sleeve is lubricated with lidocaine jelly
5. The needle guide is attached to the base, and the needle sleeve is inserted into the rectum and attached to the needle guide
6. A fast T2-weighted sagittal series is acquired and sent to the visualization workstation. The image that includes the distal tip and majority of the needle guide is identified. Calibrate the software to the needle sleeve location
7. Acquire a high-resolution T2-weighted axial image, transfer to workstation, and identify the target lesion. Use diagnostic mpMRI images as necessary to confirm location
8. Map and lock onto the lesion in the visualization software. The software generates adjustment parameters/coordinates to adjust the needle guide toward the target
9. Repeat the fast T2-weighted sagittal series and fast T2-weighted oblique axial series perpendicular to the needle sleeve
10. Adjust as necessary and repeat step 9 until needle sleeve is directed toward the target
11. Select the appropriate needle (15 or 17.5 cm) and remove the spacer device if necessary
12. Cock the needle and insert into the needle sleeve to the hub. Notify the patient about the sound and potential discomfort
13. Unlock and fire the needle. Leave the needle in position, and repeat the oblique axial T2-weighted series to document needle position within the lesion. Obtain two to three cores per lesion
14. If additional lesions are targeted, go back to step 8

MRI magnetic resonance imaging, *mpMRI* multiparametric MRI

visualization. The needle guide has a reasonable, yet limited, range of motion in the craniocaudal direction; therefore, we find it useful to consider the craniocaudal position of the lesion and the patient's body habitus in determining how far we initially place the needle sleeve. Specifically, for a base of the prostate lesion, we insert the needle sleeve up to the anal verge in contrast to an apex lesion where it may be partially inserted. The phased-array coil is placed on the patient's lower back.

A fast T2-weighted sagittal series is acquired. This series is used to identify the needle sleeve, which is subsequently mapped within the software to calibrate its neutral position. Subsequently, a high-resolution T2-weighted axial image is obtained in order to visualize the target lesion. Diffuse-weighted images (DWI) can also be used for visualization of the target. The lesion is mapped within the software, which "locks" onto the lesion and calculates the coordinates for adjusting the needle guide. In our experience, the generated coordinates slightly underestimate the necessary change in the lateral adjustments, and we tend to over-adjust by 2–5 degrees. This variability may be secondary to the patient's rectal tone and pelvis musculature. Following the adjustment, a fast T2-weighted oblique axial series is acquired parallel to the adjusted orientation of the needle sleeve to verify ideal positioning relative to the lesion. Additional fine adjustments are made as necessary to position the needle sleeve directly toward the target lesion. The software provides a recommended needle length (15 cm or 17.5 cm) and prescribes whether the spacer device within the needle sleeve should be removed, depending on the depth of the lesion relative to the needle sleeve hub. Once the needle sleeve tip is directed directly toward the target lesion, we fire the needle into the lesion and repeat the scan with the biopsy needle left in place to document intralesional needle position. We obtain two to three cores per lesion and frequently adjust the needle sleeve minimally between cores in order to sample a greater area of the lesion. Figures 16.2 and 16.3 illustrate a patient case.

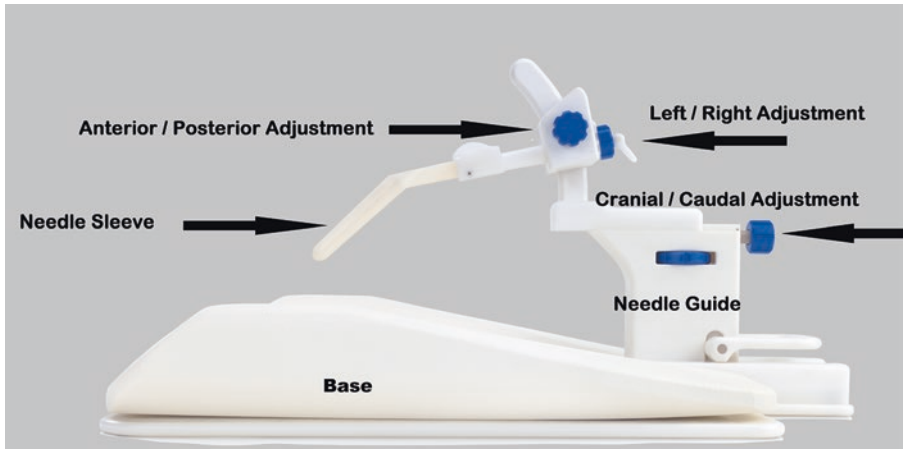

Fig. 16.1 DynaTRIM portable biopsy device. Figure courtesy of Invivo Corporation, Orlando, FL, USA

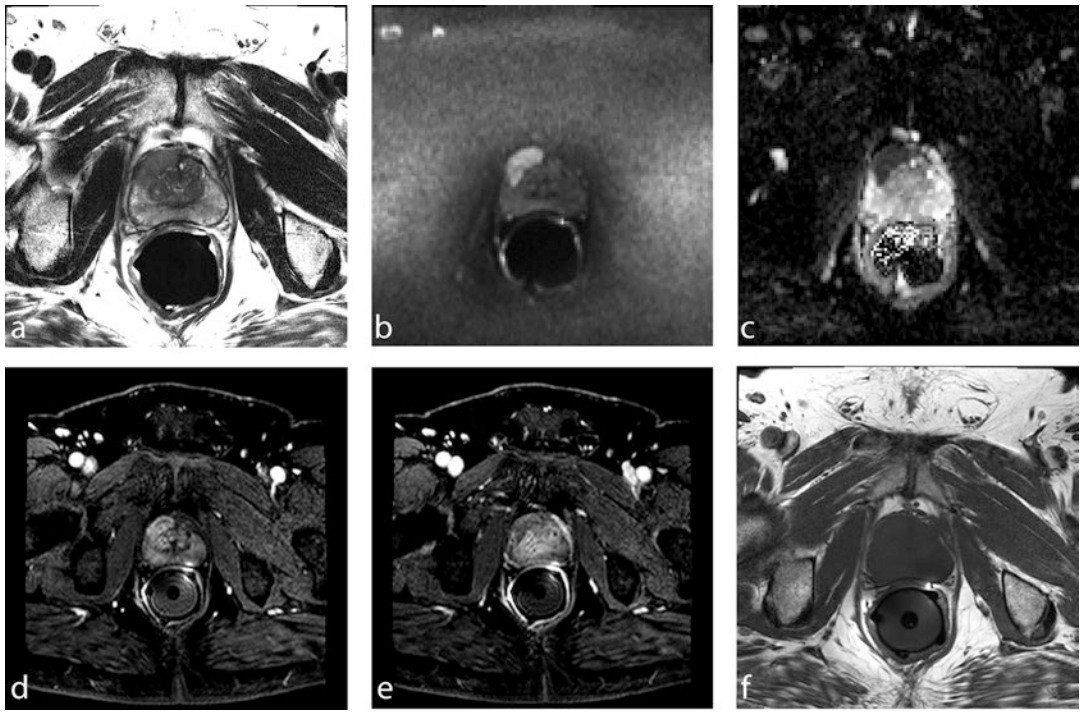

Fig. 16.2 Diagnostic multiparametric MRI of the prostate. A 56-year-old male with history of benign prostatic hyperplasia and elevated sPSA (7.5 in 2010, increased to 23.3 in 2014). Multiple negative previous conventional TRUS-guided systematic prostate biopsies, including saturation biopsies. A diagnostic multi-planar MRI was performed on a 3 T magnet with an endorectal coil. A dominant ovoid 2.7 × 1.6 cm lesion was identified in the anterior peripheral zone of the right mid-gland demonstrating decreased T2-weighted signal intensity ("charcoal" appearance) (**a**), marked restricted diffusion on high *B*-value ADC (*B* = 1550 ms) (**b**) and diffusion-weighted images (**c**), focal relative hyper-enhancement on early DCE images (**d**), and washout on delayed DCE images (**e**). No confounding T1-weighted (**f**) signal hyperintensity was present to suggest hemorrhage from prior biopsy. The lesion bulges the prostatic contour, suspicious for extra-prostatic tumor extension

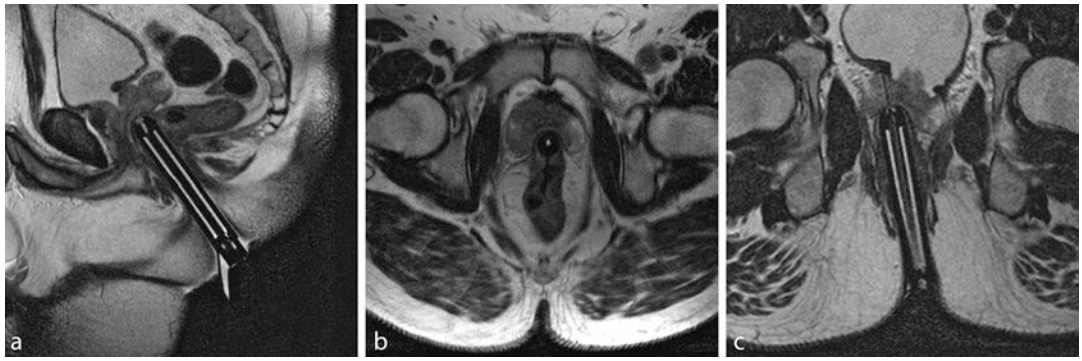

Fig. 16.3 Transrectal in-bore MRI-targeted prostate biopsy. The patient from Fig. 16.2 underwent a transrectal in-bore MRI-targeted prostate biopsy using a 1.5 T magnet and the DynaTRIM portable prostate biopsy device. The initial sagittal T2-weighted images (**a**) demonstrate the needle sleeve placed into the rectum. The axial T2-weighted images show the needle sleeve and lesion on the same image (**b**). Finally (**c**) shows an oblique coronal image that demonstrates intralesional location of the biopsy needle. Final pathology revealed Gleason grade 4+3 prostatic adenocarcinoma involving 50 % of the tissue volume of the three submitted core specimens

Trans-perineal Approach In-Bore MRI-Targeted Prostate Biopsy Technique

Patients without a rectum (prior proctectomy), limiting perianal disease, or an anal stricture may undergo a trans-perineal approach in-bore MRI-targeted prostate biopsy. Table 16.2 outlines the steps of the protocol used at our institution. In our institution we use a commercially available grid and software workstation for planning (Visualase, Inc., Houston, TX). This is performed with the patient in the supine position in our institution. Patients require moderate sedation and monitoring during the procedure to limit discomfort. A needle-guide template is secured flush against the perineum. A high-resolution axial T2-weighted sequence is obtained, which includes the template and the prostate. The template includes calibration markers, which are used by the software to identify the template's orientation and project the trajectory of the template holes onto the prostate. The target lesion is identified, and the appropriate template hole is chosen, and the depth of insertion is estimated by measuring the distance from the template to the target lesion (number of slices x slice thickness, assuming no slice gap was used). The perineum is anesthetized superficially and deeply with lidocaine and the trocar is inserted. Repeat imaging is performed to confirm the location. The depth of the trocar may be adjusted, or it may be withdrawn and repositioned through an appropriate adjacent template hole. Once adequate positioning is confirmed with repeat imaging, a core biopsy needle is inserted and fired. Additional images confirming intralesional needle placement are obtained. We typically obtain two to three cores per lesion.

Tokuda et al. described a custom-made in-bore setup and software to support MRI-targeted trans-perineal prostate biopsy in a wide-bore 3 Tesla MRI scanner without moving the patient out of the scanner [21]. A trans-perineal approach allows for better access of the anterior and apical regions of the prostate [22]. Computer-controlled robotic devices have been investigated and require safety validation [21, 23–26]. Automated technology may allow for more accurate needle placement and shorter procedure times. The limitations of a trans-perineal approach in-bore MRI-targeted prostate biopsy include the additional cost of sedation and monitoring during the procedure.

In-Bore MRI-Targeted Biopsy Performance

Schimmoller et al. retrospectively evaluated the detection rates of clinically significant prostate cancer using in-bore MRI-targeted prostate

Table 16.2 Trans-perineal in-bore MRI-targeted biopsy technique

Pre-biopsy steps
1. Standard MRI safety precautions
2. Diagnostic multiparametric MRI performed without an endorectal coil to identify target lesions. Typically, high-field-strength MRI with small field-of-view T2-weighted, diffusion-weighted, and dynamic contrast-enhanced images
3. The patient is premedicated with oral antibiotics
4. Obtain an informed consent
Biopsy steps
1. Moderate sedation and monitoring throughout the procedure to limit discomfort
2. The patient is placed supine on the table. Phased-array coil is placed on the patient's pelvis centered over the prostate
3. The needle-guide template is secured flush against the perineum
4. High-resolution axial T2-weighted sequence includes the template and the prostate. Images are sent to software for calibration of the template
5. The software projects the trajectory of the template holes onto the prostate. Once the target lesion is identified, the corresponding template hole is chosen. The depth of insertion is estimated by measuring the distance from the template to the target lesion
6. Local perineal anesthesia is performed through the chosen target template hole superficially and deeply
7. Trocar is inserted to estimated depth. Repeat imaging to confirm location
8. Once confirmed, cocked biopsy needle is inserted through trocar and fired. Repeat imaging to confirm intralesional needle placement. Obtain two to three cores per lesion
9. If additional lesions are targeted, go back to step 5 and select template hole and depth for additional lesions

MRI magnetic resonance imaging

biopsy in 297 consecutive biopsy-naive patients and patients with prior negative TRUS-guided sPBx [27] and reported a clinically significant (Gleason grade ≥4) PCa detection rate of 55.6 % and 43.1 %, respectively.

In 2006 Engelhard et al. reported a significant diagnostic yield of in-bore MRI-guided prostate biopsy among 37 patients with elevated serum prostate-specific antigen (sPSA) and negative prior TRUS-guided systematic prostate biopsies [28]. More recently, Hoeks et al. reported a clinically significant PCa detection rate of 41 % among 265 patients who underwent in-bore MRI-guided prostate biopsy of a suspicious MRI lesion in a cohort of 438 consecutive patients with a sPSA >4.0 ng/ml and one or more prior negative TRUS-guided sPBx [29]. Of the cancers detected, 87 % were clinically significant. Nine patients with a negative in-bore MRI-guided prostate biopsy had PCa detected during follow-up. In this clinical context, the 41 % PCa detection rate and 87 % clinically significant PCa detection rate were significantly higher than reported rates of cancer detection using repeated TRUS-guided systematic prostate biopsies <18 % [30, 31] and 56 % [32], respectively.

Pokorny et al. included a population of biopsy-naive men and reported a detection rate of TRUS-guided sPBx of 56.5 %, but a higher rate of detection for patients who underwent an in-bore MRI-guided prostate biopsy, 69.7 % [11]. Most of the tumors missed by in-bore MRI-guided prostate biopsy alone had a Gleason score of 3+3. Although approximately one fourth of patients with a non-suspicious MRI had PCa on TRUS-guided sPBx, the vast majority of these were clinically insignificant [6].

The Gleason grade correlates with tumor aggressiveness and is therefore a key factor in prognosis, risk stratification, and treatment decision-making. TRUS-guided prostate biopsy Gleason scores are very often discordant with radical prostatectomy specimens, with under-grading in up to 38 % of patients [33–35]. Hambrock et al. reported a concordance rate of 55 % for TRUS-guided sPBx in 64 patients and 88 % for transrectal approach in-bore MRI-targeted prostate biopsy of the most-suspicious lesion on DWI in 34 patients compared with radical prostatectomy [36]. This confirmed the findings of previous retrospective studies [37, 38], which supported the utility of mpMRI in predicting the highest Gleason grade tumor in radical prostatectomy specimens.

In-Bore MRI Versus TRUS-MRI-Guided Fusion Prostate Biopsy Performance

Several studies directly comparing in-bore MRI-targeted with TRUS-MRI-guided fusion prostate biopsy have been reported. Arsov et al. compared prostate cancer detection rates of in-bore MRI-targeted prostate biopsy alone and TRUS-MRI-guided fusion combined with TRUS-guided sPBx in patients with at least one prior negative TRUS-guided sPBx and a sPSA ≥4 ng/ml [39]. The trial demonstrated similar PCa detection rates, detection rates of clinically significant PCa, and highest percent tumor involvement per biopsy core.

Quentin et al. prospectively compared the in-bore MRI-guided and TRUS-guided sPBx in 128 biopsy-naive men with elevated sPSA levels and found equally high detection rates (53.1 %) [40]. The in-bore MRI-guided technique resulted in an 85.3 % rate of significant cancer detection, compared to 79.4 %. In most of the cases where a cancer was missed by the TRUS-guided sPBx, the lesions were located anteriorly and in the fibromuscular stroma—a significant known limitation as 21 % of all PCas are located in these regions [41]. In-bore MRI-guided prostate biopsy required significantly fewer cores and resulted in a higher length/percentage of tumor involvement per biopsy core. Combining the two biopsy methods resulted in a detection rate of 60.9 % and an 82.1 % incidence of clinically significant PCa.

Clinical Applications of MRI-Guided Prostate Biopsy

Role in Focal Ablation Therapy

Patients with clinically localized, clinically low-risk PCa can be considered for focal ablation therapy. In contradistinction to extensive whole-gland ablation, focal ablation therapy of the prostate treats only the portion of the prostate with documented PCa and has the potential of successfully treating the cancer in the long term while minimizing the risks associated with other treatment modalities. There are several ablative techniques, including high-intensity focused ultrasound (HIFU), cryotherapy, and brachytherapy, previously established in whole-gland ablations and modified for limited focal ablation therapy. Also, newer energy delivery modalities, electroporation and laser ablation, have been developed and are being investigated. Each approach has specific advantages and disadvantages, with some authors advocating a patient-tailored cancer-specific approach [42].

It is generally accepted that the target lesion should be confined to one lobe of the prostate and visible on the imaging modality guiding the treatment, most commonly mpMRI. It is critical to map the exact location of the dominant lesion and its borders for successful focal therapy. MRI-guided prostate biopsies together with systematic biopsies can be used for this purpose. Therefore, mpMRI and MRI-guided prostate biopsy play an integral role in patient selection for focal ablation therapy. Current areas of investigation include potential underestimation of the volume of tumor on mpMRI [43–45]. The ideal treatment "safety" margin around an MRI-visible index lesion has yet to be determined.

Prostate Cancer Screening

The essential features for a good screening tool include cost-effectiveness, reliability, validity, accessibility, and patient acceptance. Around a quarter of patients with no suspicious findings on mpMRI have PCa on TRUS-guided sPBx. However, a vast majority of these are low-grade, low-volume cancers. In patients with low risk (sPSA <10, digital rectal exam [DRE] normal, and no family history), the reported negative predictive value of mpMRI for clinically significant PCa is between 92 % and 100 %. mpMRI is reportedly negative in 18–33 % of patients with elevated sPSA. Given the generally indolent nature of PCa, continued monitoring with sPSA, DRE, and/or mpMRI while deferring or foregoing a biopsy in these patients may be a justifiable screening approach.

A negative pre-biopsy mpMRI in patients with high risk (sPSA > 10 and/or abnormal DRE) has a significantly lower negative predictive value (47–51 %) and should not preclude a biopsy. However, a subsequent MRI-guided prostate biopsy is significantly more likely to identify and accurately grade the PCa compared to a conventional TRUS-guided sPBx.

Although mpMRI has a significantly lower negative predictive value for low-grade clinically insignificant PCa, this results in a decreased rate of overdiagnosis and overtreatment [46].

Prior Negative TRUS-Guided Systematic Prostate Biopsies

The role of MRI-guided prostate biopsy in patients with prior negative TRUS-guided sPBx has been well supported and is included in several guidelines for this clinical context [47]. As mentioned previously, the rate of PCa detection for a first TRUS-guided sPBx is low, typically 30–50 % [48, 49]. Many patients with persistently elevated sPSA may harbor undetected PCa and are frequently advised to undergo repeated TRUS-guided sPBx. Historically, repeated TRUS-guided sPBx has shown unsatisfactorily low detection rates, 11–47 % [50], often missing clinically significant anteriorly located tumors [51, 52]. In patients with prior negative TRUS-guided sPBx with persistently elevated sPSA, PCa detection rates with MRI-guided prostate biopsy have been reported between 9.5 and 59 % [50]. Resnick et al. reported an increasing likelihood of diagnosing clinically insignificant disease in patients undergoing serial TRUS-guided sPBx [53]. However, there remained a significant risk of under-grading relative to the final radical prostatectomy specimen. In-bore MRI-targeted prostate biopsy outperforms serial TRUS-guided sPBx [36] in diagnostic yield and concordance with final pathology.

Active Surveillance

The significant disparity between cancer incidence (15–20 % lifetime) and mortality (3 % lifetime risk of death from PCa) reflects that many men may not benefit from aggressive definitive treatment of low-grade low-volume PCa. In recent years there has been a transition to individualized patient-tailored management decisions. Several studies have shown that patients with low-grade, localized PCa have a low risk for clinical progression within the first 10–15 years after diagnosis [54–61]. Watchful waiting with palliative treatment for local or metastatic progression, if and when it occurs, is one option that may be appropriate in specific clinical settings, such as patients with short life expectancy [58]. Alternatively, active surveillance (AS) attempts to provide definitive treatment to those with localized cancers that are likely to progress while reducing the risk of treatment-related complications for cancers not likely to progress. Patients diagnosed with low-grade, low-volume PCa are initially not treated but are followed. If there is tumor progression or threat of tumor progression, they can be treated with curative intent. Initial studies with short-term follow-up have been promising [62–65], such as the Prostate Cancer Research International Active Surveillance (PRIAS) study, which showed a disease-specific survival rate of 100 % of patients on AS in a median follow-up of 1.6 years, but more long-term date is needed to validate this approach [66]. Godtman et al. concluded that a large proportion of men with screening-detected PCa can be managed with AS after following 439 men for a median of 6 years from diagnosis [67]. AS typically consists of a combination of periodic physical examination and sPSA testing to assess for biochemical signs of progression and repeat periodic biopsies to assess for histopathologic progression. To date, an ideal surveillance regimen has not been agreed upon, with as many as 16 cohorts described in a systematic review in 2011, comprising different monitoring protocols. The most important factor in a successful AS program, minimizing the long-term risk-to-benefit ratio, is the initial selection of patients and the accuracy of the monitoring program. Gleason score, clinical stage, and sPSA are widely accepted clinical variables that predict the likelihood of tumor progression and eligibility criteria for AS; however, the ideal cutoffs are not fully validated [68]. Proposed eligibility criteria

include clinically confined PCa, a Gleason score ≤6, three or fewer cores involved with cancer, ≤50 % of each core involved with cancer, and sPSA <10 ng/ml [47, 69]. AS eligibility criteria to date have been shown to result in significant under-grading and under-staging [70]. Proposed clinical criteria for cancer progression include sPSA doubling time ≤2 or ≤4 years, Gleason score progression to ≥7, and sPSA progression >10 ng/ml; however, significant limitations have been noted [64, 66, 71, 72]. mpMRI has a potentially significant role in accurate initial staging and in the subsequent surveillance regimen. Several studies have investigated the added benefit of mpMRI and MRI-guided prostate biopsy among men on AS. Recabal et al. investigated the added benefit of MRI-guided prostate biopsy using cognitive registration and TRUS-MRI-guided fusion prostate biopsy in addition to a 14-core TRUS-guided sPBx in a prospective cohort of 206 consecutive men on AS with previously diagnosed Gleason 3+3 disease. The combined approach of MRI-guided with TRUS-guided sPBx resulted in the highest detection rate for higher-grade cancer [73].

Residual or Recurrent Prostate Cancer

Up to 25–33 % of patients experience tumor recurrence after radiation or surgery. Patients who have undergone radical prostatectomy routinely have their sPSA levels checked in addition to other potential tests to evaluate for residual tumor or recurrent disease. The sPSA level is expected to be very low or nearly undetectable within a few months following radical prostatectomy. PSA can remain in the bloodstream following surgery, and doctors often advise waiting 6–8 weeks prior to rechecking the sPSA level. Although uncommon, very low sPSA levels can potentially reflect normal residual prostate tissue—sometimes referred to as benign regeneration. Rising or elevated sPSA levels (commonly accepted as > 0.2 ng/mL) can reflect tumor recurrence. Initial evaluation requires differentiating local recurrence, systemic recurrence, or both, in order to assess appropriate second-line treatment. Previously, bone scintigraphy with technetium-99m medronic acid and contrast-enhanced abdominopelvic computed tomography have been the first-line modalities for detecting skeletal and lymph node metastases, respectively. More recently mpMRI and positron emission tomography/CT with choline-derivative tracers have demonstrated superior performance in depicting local recurrence and lymph node metastatic disease, respectively [74]. mpMRI is now frequently used in detecting local recurrence after radical prostatectomy or radiation therapy [75]. Dynamic contrast-enhanced imaging specifically has been reported to be the most reliable sequence in detecting local recurrence [76, 77], commonly seen at the vesicourethral anastomosis. In current guidelines, lack of imaging evidence for local recurrence does not preclude initiation of local salvage treatment in the presence of biochemical recurrence, given the limited sensitivity for detecting small-sized local recurrence. In the presence of suspicious imaging findings, a confirmatory MRI-guided prostate/lesion biopsy may be obtained. If focal ablation therapy is considered for suspected locally recurrent prostate cancer, a confirmatory MRI-guided prostate/lesion biopsy is typically warranted.

Proctectomy Patients

In patients with a proctectomy, limiting perianal disease, or an anal stricture, a TRUS-guided sPBx may not be possible. A trans-perineal or trans-gluteal approach in-bore MRI-targeted prostate biopsy may be performed to evaluate for suspected prostate cancer.

Other MRI-Guided Prostate Biopsy Techniques

TRUS-MRI-Guided Prostate Biopsy with Cognitive Registration

TRUS-MRI-guided prostate biopsy with cognitive (or "visual") registration ("fusion" or "estimation") requires the physician who will be performing the biopsy to review, be aware of,

and/or have before them the mpMRI findings in order to cognitively register the suspicious mpMRI target location onto the real-time TRUS images of the prostate and subsequently manually guide the needle to the anticipated corresponding site of the target. The accuracy of this technique is dependent on the operator's technical skill in addition to the accuracy of mpMRI to detect PCa. With the advancement of mpMRI, this method was described in the early 2000s and has subsequently become widely used [6, 78–80]. In experienced hands this approach has been shown to be up to 82 % accurate in sampling the correct target, with anterior tumors being the most challenging [81]. This may be the most widely used technique given its technological simplicity and no requirement for additional costly equipment. In addition to the complex technical and cognitive challenges of this technique, there are other constraints. Specifically, the mpMRI images may reflect a different geometric appearance of the prostate compared to the real-time TRUS images given the variable degree of mass effect from an endorectal coil, if present during the mpMRI, the degree of bladder and/or rectal distension, and the degree of distortion from the ultrasound probe, making spatial registration challenging. Experience, knowledge of zonal topography, and anatomical landmarks are fundamental to successful targeting [82].

TRUS-MRI-Guided Fusion Prostate Biopsy

The next technological iteration of MRI-guided prostate biopsy has been the advent of hardware and software fusion (or "registration") allowing real-time guidance by co-registering and overlaying the previously acquired mapped mpMRI images onto the TRUS images during the biopsy. Typically, this is done by outlining (or "mapping") the prostate margin and the suspicious lesion on the mpMRI images. These images are subsequently transferred to a specialized workstation. The entire volume of the prostate is imaged by TRUS, and the software fuses the mpMRI and ultrasound images of the prostate by using the boundaries as a guide (using a fixed and/or flexible approach, depending on the vendor's implementation). The hardware subsequently monitors the position of the TRUS probe relative to the prostate and can provide real-time imaging in order to align the biopsy to the co-registered site of the target lesion. Compared to cognitive registration, this technique potentially has improved reproducibility by decreasing dependence on the biopsy physician. However, this technique requires special hardware and software, training, and meticulous implementation. Rarely is there visualization of the lesion on the ultrasound images. Without an ultrasound imaging correlate for the mpMRI abnormality, the accuracy of this technique is dependent on numerous technical factors, which may make the targeting suboptimal. The limitations of this technique include the additional costs of the hardware and software, the accuracy of the merging software, the accuracy of the spatial localization of the TRUS probe, and the associated learning curve and training.

Conclusion

In-bore MRI-targeted prostate biopsy has become an established approach to safely and accurately sample suspicious prostate targets identified on mpMRI. The biopsy results are more likely to detect clinically significant PCa and correlate with the Gleason score of radical prostatectomy specimens when compared to TRUS-guided sPBx. Although more comparison data is needed, in-bore MRI-targeted prostate biopsy has reportedly resulted in comparable or slightly higher detection rates of PCa when compared to other MRI-guided techniques. The performance of in-bore MRI-targeted prostate biopsy specifically and MRI-guided prostate biopsy techniques in general can help address the current concerns of overdiagnosis and overtreatment of clinically indolent PCa, by allowing for more reliable risk stratification, patient selection, and monitoring for less aggressive and morbid treatment options such as watchful waiting, active surveillance, and focal therapy. Focal therapy will become more widely accepted and utilized, thanks in large part to the advent and optimization of mpMRI and subsequent MRI-guided prostate biopsy techniques.

References

1. Marko J, Gould CF, Bonavia GH, Wolfman DJ. State-of-the-art imaging of prostate cancer. Urol Oncol Semin Orig Investig. 2016;34(3):134–46.
2. Beyersdorff D, Winkel A, Hamm B, Lenk S, Loening SA, Taupitz M. MR imaging-guided prostate biopsy with a closed MR unit at 1.5 T: initial results. Radiology. 2005;234(2):576–81.
3. Hambrock T, Somford DM, Hoeks C, Bouwense SAW, Huisman H, Yakar D, et al. Magnetic resonance imaging guided prostate biopsy in men with repeat negative biopsies and increased prostate specific antigen. J Urol. 2010;183(2):520–7.
4. Roethke M, Anastasiadis AG, Lichy M, Werner M, Wagner P, Kruck S, et al. MRI-guided prostate biopsy detects clinically significant cancer: analysis of a cohort of 100 patients after previous negative TRUS biopsy. World J Urol. 2012;30(2):213–8.
5. Bjurlin MA, Meng X, Le Nobin J, Wysock JS, Lepor H, Rosenkrantz AB, et al. Optimization of prostate biopsy: the role of magnetic resonance imaging targeted biopsy in detection, localization and risk assessment. J Urol. 2014;192(3):648–58.
6. Moore CM, Robertson NL, Arsanious N, Middleton T, Villers A, Klotz L, et al. Image-guided prostate biopsy using magnetic resonance imaging-derived targets: a systematic review. Eur Urol. 2013;63(1):125–40.
7. Puech P, Rouvière O, Renard-Penna R, Villers A, Devos P, Colombel M, et al. Prostate cancer diagnosis: multiparametric MR-targeted biopsy with cognitive and transrectal US-MR fusion guidance versus systematic biopsy—prospective multicenter study. Radiology. 2013;268(2):461–9.
8. Le JD, Stephenson S, Brugger M, Lu DY, Lieu P, Sonn GA, et al. Magnetic resonance imaging-ultrasound fusion biopsy for prediction of final prostate pathology. J Urol. 2014;192(5):1367–73.
9. Siddiqui MM, Rais-Bahrami S, Turkbey B, George AK, Rothwax J, Shakir N, et al. Comparison of MR/ultrasound fusion-guided biopsy with ultrasound-guided biopsy for the diagnosis of prostate cancer. JAMA. 2015;313(4):390–7.
10. Siddiqui MM, Rais-Bahrami S, Truong H, Stamatakis L, Vourganti S, Nix J, et al. Magnetic resonance imaging/ultrasound-fusion biopsy significantly upgrades prostate cancer versus systematic 12-core transrectal ultrasound biopsy. Eur Urol. 2013;64(5):713–9.
11. Pokorny MR, de Rooij M, Duncan E, Schröder FH, Parkinson R, Barentsz JO, et al. Prospective study of diagnostic accuracy comparing prostate cancer detection by transrectal ultrasound-guided biopsy versus magnetic resonance (MR) imaging with subsequent MR-guided biopsy in men without previous prostate biopsies. Eur Urol. 2014;66(1):22–9.
12. de Rooij M, Crienen S, Witjes JA, Barentsz JO, Rovers MM, Grutters JPC. Cost-effectiveness of magnetic resonance (MR) imaging and MR-guided targeted biopsy versus systematic transrectal ultrasound-guided biopsy in diagnosing prostate cancer: a modelling study from a health care perspective. Eur Urol. 2014;66(3):430–6.
13. Lotan Y, AQ H, DN C, Pedrosa I, NM R, CG R. Decision analysis model comparing cost of multiparametric magnetic resonance imaging vs. repeat biopsy for detection of prostate cancer in men with prior negative findings on biopsy. Urol Oncol. 2015;33(6):266.e9–16.
14. Cormack RA, D'Amico AV, Hata N, Silverman S, Weinstein M, Tempany CM. Feasibility of transperineal prostate biopsy under interventional magnetic resonance guidance. Urology. 2000;56(4):663–4.
15. D'Amico AV, Tempany CM, Cormack R, Hata N, Jinzaki M, Tuncali K, et al. Transperineal magnetic resonance image guided prostate biopsy. J Urol. 2000;164(2):385–7.
16. D'Amico AV, Cormack RA, Tempany CM. MRI-guided diagnosis and treatment of prostate cancer. N Engl J Med. 2001;344(10):776–7.
17. Cantwell CP, Hahn PF, Gervais DA, Mueller PR. Prostate biopsy after ANO-rectal resection: value of CT-guided trans-gluteal biopsy. Eur Radiol. 2008;18(4):738–42.
18. Shinohara K, Gulati M, Koppie TM, Terris MK. Transperineal prostate biopsy after abdominoperineal resection. J Urol. 2003;169(1):141–4.
19. Seaman EK, Sawczuk IS, Fatal M, Olsson CA, Shabsigh R. Transperineal prostate needle biopsy guided by transurethral ultrasound in patients without a rectum. Urology. 1996;47(3):353–5.
20. Zangos S, Eichler K, Engelmann K, Ahmed M, Dettmer S, Herzog C, et al. MR-guided transgluteal biopsies with an open low-field system in patients with clinically suspected prostate cancer: technique and preliminary results. Eur Radiol. 2005;15(1):174–82.
21. Tokuda J, Tuncali K, Iordachita I, Song S-E, Fedorov A, Oguro S, et al. In-bore setup and software for 3 T MRI-guided transperineal prostate biopsy. Phys Med Biol. 2012;57(18):5823–40.
22. Sartor AO, Hricak H, Wheeler TM, Coleman J, Penson DF, Carroll PR, et al. Evaluating localized prostate cancer and identifying candidates for focal therapy. Urology. 2008;72(6 Suppl):S12–24.
23. Fischer GS, Iordachita I, Csoma C, Tokuda J, Dimaio SP, Tempany CM, et al. MRI-Compatible Pneumatic Robot for Transperineal Prostate Needle Placement. IEEE ASME Trans Mechatron. 2008;13(3):295–305.
24. Muntener M, Patriciu A, Petrisor D, Schär M, Ursu D, Song DY, et al. Transperineal prostate intervention: robot for fully automated MR imaging–system description and proof of principle in a canine model. Radiology. 2008;247(2):543–9.
25. van den Bosch MR, Moman MR, van Vulpen M, Battermann JJ, Duiveman E, van Schelven LJ, et al. MRI-guided robotic system for transperineal prostate interventions: proof of principle. Phys Med Biol. 2010;55(5):N133–40.
26. Cunha JA, Hsu I-C, Pouliot J, Roach Iii M, Shinohara K, Kurhanewicz J, et al. Toward adaptive stereotactic robotic brachytherapy for prostate cancer: demonstra-

tion of an adaptive workflow incorporating inverse planning and an MR stealth robot. Minim Invasive Ther Allied Technol. 2010;19(4):189–202.
27. Schimmöller L, Blondin D, Arsov C, Rabenalt R, Albers P, Antoch G, et al. MRI-Guided In-Bore biopsy: differences between prostate cancer detection and localization in primary and secondary biopsy settings. AJR Am J Roentgenol. 2016;206(1):92–9.
28. Engelhard K, Hollenbach HP, Kiefer B, Winkel A, Goeb K, Engehausen D. Prostate biopsy in the supine position in a standard 1.5-T scanner under real time MR-imaging control using a MR-compatible endorectal biopsy device. Eur Radiol. 2006;16(6):1237–43.
29. Hoeks CMA, Schouten MG, Bomers JGR, Hoogendoorn SP, de Kaa CA H-v, Hambrock T, et al. Three-Tesla magnetic resonance-guided prostate biopsy in men with increased prostate-specific antigen and repeated, negative, random, systematic, transrectal ultrasound biopsies: detection of clinically significant prostate cancers. Eur Urol. 2012;62(5):902–9.
30. Roehl KA, Antenor JAV, Catalona WJ. Serial biopsy results in prostate cancer screening study. J Urol. 2002;167(6):2435–9.
31. Campos-Fernandes J-L, Bastien L, Nicolaiew N, Robert G, Terry S, Vacherot F, et al. Prostate cancer detection rate in patients with repeated extended 21-sample needle biopsy. Eur Urol. 2009;55(3):600–6.
32. Roemeling S, Roobol MJ, Kattan MW, van der Kwast TH, Steyerberg EW, Schröder FH. Nomogram use for the prediction of indolent prostate cancer: impact on screen-detected populations. Cancer. 2007;110(10): 2218–21.
33. Lattouf J-B, Saad F. Gleason score on biopsy: is it reliable for predicting the final grade on pathology? BJU Int. 2002;90(7):694–8. discussion 698–9
34. Divrik RT, Eroglu A, Sahin A, Zorlu F, Ozen H. Increasing the number of biopsies increases the concordance of Gleason scores of needle biopsies and prostatectomy specimens. Urol Oncol. 2007;25(5):376–82.
35. Andriole GL, Crawford ED, Grubb RL, Buys SS, Chia D, Church TR, et al. Mortality results from a randomized prostate-cancer screening trial. N Engl J Med. 2009;360(13):1310–9.
36. Hambrock T, Hoeks C, de Kaa C H-v, Scheenen T, Fütterer J, Bouwense S, et al. Prospective assessment of prostate cancer aggressiveness using 3-T diffusion-weighted magnetic resonance imaging-guided biopsies versus a systematic 10-core transrectal ultrasound prostate biopsy cohort. Eur Urol. 2012;61(1):177–84.
37. Hambrock T, Somford DM, Huisman HJ, van Oort IM, Witjes JA, de Kaa CA H-v, et al. Relationship between apparent diffusion coefficients at 3.0-T MR imaging and Gleason grade in peripheral zone prostate cancer. Radiology. 2011;259(2):453–61.
38. Verma S, Rajesh A, Morales H, Lemen L, Bills G, Delworth M, et al. Assessment of aggressiveness of prostate cancer: correlation of apparent diffusion coefficient with histologic grade after radical prostatectomy. AJR Am J Roentgenol. 2011;196(2):374–81.
39. Arsov C, Rabenalt R, Blondin D, Quentin M, Hiester A, Godehardt E, et al. Prospective randomized trial comparing magnetic resonance imaging (MRI)-guided in-bore biopsy to MRI-ultrasound fusion and transrectal ultrasound-guided prostate biopsy in patients with prior negative biopsies. Eur Urol. 2015;68(4):713–20.
40. Quentin M, Blondin D, Arsov C, Schimmöller L, Hiester A, Godehardt E, et al. Prospective evaluation of magnetic resonance imaging guided in-bore prostate biopsy versus systematic transrectal ultrasound guided prostate biopsy in biopsy naïve men with elevated prostate specific antigen. J Urol. 2014;192(5):1374–9.
41. Bott SRJ, Young MPA, Kellett MJ, Parkinson MC, Contributors to the UCL Hospitals' Trust Radical Prostatectomy Database. Anterior prostate cancer: is it more difficult to diagnose? BJU Int. 2002;89(9):886–9.
42. Sivaraman A, Barret E. Focal therapy for prostate cancer: an "à la carte" approach. Eur Urol. 2016;69(6):973–5.
43. Turkbey B, Mani H, Aras O, Rastinehad AR, Shah V, Bernardo M, et al. Correlation of magnetic resonance imaging tumor volume with histopathology. J Urol. 2012;188(4):1157–63.
44. Valerio M, Ahmed HU. Tumor target volume for focal therapy of prostate cancer—does multiparametric magnetic resonance imaging allow for a reliable estimation? F. Cornud, G. Khoury, N. Bouazza, F. Beuvon, M. Peyromaure, T. Flam, M. Zerbib, P. Legmann and N. B. Delongchamps. J Urol 2014; 191: 1272–1279; J Urol 2014;192(4):1297–8.
45. Cornud F, Khoury G, Bouazza N, Beuvon F, Peyromaure M, Flam T, et al. Tumor target volume for focal therapy of prostate cancer-does multiparametric magnetic resonance imaging allow for a reliable estimation? J Urol. 2014;191(5):1272–9.
46. Numao N, Yoshida S, Komai Y, Ishii C, Kagawa M, Kijima T, et al. Usefulness of pre-biopsy multiparametric magnetic resonance imaging and clinical variables to reduce initial prostate biopsy in men with suspected clinically localized prostate cancer. J Urol. 2013;190(2):502–8.
47. Heidenreich A, Bastian PJ, Bellmunt J, Bolla M, Joniau S, van der Kwast T, et al. EAU guidelines on prostate cancer. part 1: screening, diagnosis, and local treatment with curative intent-update 2013. Eur Urol. 2014;65(1):124–37.
48. Serag H, Banerjee S, Saeb-Parsy K, Irving S, Wright K, Stearn S, et al. Risk profiles of prostate cancers identified from UK primary care using national referral guidelines. Br J Cancer. 2012;106(3):436–9.
49. Cormio L, Scattoni V, Lorusso F, Perrone A, Di Fino G, Selvaggio O, et al. Prostate cancer detection rates in different biopsy schemes. Which cores for which patients? World J Urol. 2014;32(2):341–6.
50. Nelson AW, Harvey RC, Parker RA, Kastner C, Doble A, Gnanapragasam VJ. Repeat prostate biopsy strategies after initial negative biopsy: meta-regression comparing cancer detection of transperineal, transrectal saturation and mri guided biopsy. PLoS One. 2013;8(2):e57480.
51. Komai Y, Numao N, Yoshida S, Matsuoka Y, Nakanishi Y, Ishii C, et al. High diagnostic ability of multiparametric magnetic resonance imaging to

detect anterior prostate cancer missed by transrectal 12-core biopsy. J Urol. 2013;190(3):867–73.
52. Volkin D, Turkbey B, Hoang AN, Rais-Bahrami S, Yerram N, Walton-Diaz A, et al. Multiparametric magnetic resonance imaging (MRI) and subsequent MRI/ultrasonography fusion-guided biopsy increase the detection of anteriorly located prostate cancers: MRI/US fusion biopsy for detection of anterior prostate cancer. BJU Int. 2014;114(6b):E43–9.
53. Resnick MJ, Lee DJ, Magerfleisch L, Vanarsdalen KN, Tomaszewski JE, Wein AJ, et al. Repeat prostate biopsy and the incremental risk of clinically insignificant prostate cancer. Urology. 2011;77(3):548–52.
54. Chodak GW, Thisted RA, Gerber GS, Johansson JE, Adolfsson J, Jones GW, et al. Results of conservative management of clinically localized prostate cancer. N Engl J Med. 1994;330(4):242–8.
55. Adolfsson J, Oksanen H, Salo JO, Steineck G. Localized prostate cancer and 30 years of follow-up in a population-based setting. Prostate Cancer Prostatic Dis. 2000;3(1):37–42.
56. Zietman AL, Thakral H, Wilson L, Schellhammer P. Conservative management of prostate cancer in the prostate specific antigen era: the incidence and time course of subsequent therapy. J Urol. 2001;166(5): 1702–6.
57. Johansson J-E, Andrén O, Andersson S-O, Dickman PW, Holmberg L, Magnuson A, et al. Natural history of early, localized prostate cancer. JAMA. 2004;291(22): 2713–9.
58. Bill-Axelson A, Holmberg L, Ruutu M, Häggman M, Andersson S-O, Bratell S, et al. Radical prostatectomy versus watchful waiting in early prostate cancer. N Engl J Med. 2005;352(19):1977–84.
59. Albertsen PC, Hanley JA, Barrows GH, Penson DF, Kowalczyk PDH, Sanders MM, et al. Prostate cancer and the Will Rogers phenomenon. J Natl Cancer Inst. 2005;97(17):1248–53.
60. Albertsen PC, Hanley JA, Fine J. 20-year outcomes following conservative management of clinically localized prostate cancer. JAMA. 2005;293(17):2095–101.
61. Popiolek M, Rider JR, Andrén O, Andersson S-O, Holmberg L, Adami H-O, et al. Natural history of early, localized prostate cancer: a final report from three decades of follow-up. Eur Urol. 2013;63(3):428–35.
62. Dall'Era MA, Konety BR, Cowan JE, Shinohara K, Stauf F, Cooperberg MR, et al. Active surveillance for the management of prostate cancer in a contemporary cohort. Cancer. 2008;112(12):2664–70.
63. Conti SL, Dall'era M, Fradet V, Cowan JE, Simko J, Carroll PR. Pathological outcomes of candidates for active surveillance of prostate cancer. J Urol. 2009;181(4):1628–33. discussion 1633–4
64. Krakowsky Y, Loblaw A, Klotz L. Prostate cancer death of men treated with initial active surveillance: clinical and biochemical characteristics. J Urol. 2010;184(1):131–5.
65. Klotz L, Zhang L, Lam A, Nam R, Mamedov A, Loblaw A. Clinical results of long-term follow-up of a large, active surveillance cohort with localized prostate cancer. J Clin Oncol. 2010;28(1):126–31.
66. Bul M, Zhu X, Valdagni R, Pickles T, Kakehi Y, Rannikko A, et al. Active surveillance for low-risk prostate cancer worldwide: the prias study. Eur Urol. 2013;63(4):597–603.
67. Godtman RA, Holmberg E, Khatami A, Stranne J, Hugosson J. Outcome following active surveillance of men with screen-detected prostate cancer. Results from the Göteborg randomised population-based prostate cancer screening trial. Eur Urol. 2013;63(1):101–7.
68. Venderbos LDF, Roobol MJ, Bangma CH, van den Bergh RCN, Bokhorst LP, Nieboer D, et al. Rule-based versus probabilistic selection for active surveillance using three definitions of insignificant prostate cancer. World J Urol. 2016;34(2):253–60.
69. Mohler JL, Armstrong AJ, Bahnson RR, Boston B, Busby JE, D'Amico AV, et al. Prostate cancer, Version 3.2012: featured updates to the NCCN guidelines. J Natl Compr Canc Netw. 2012;10(9):1081–7.
70. Heidegger I, Skradski V, Steiner E, Klocker H, Pichler R, Pircher A, et al. High risk of under-grading and -staging in prostate cancer patients eligible for active surveillance. PLoS One. 2015;10(2):e0115537.
71. Al Otaibi M, Ross P, Fahmy N, Jeyaganth S, Trottier H, Sircar K, et al. Role of repeated biopsy of the prostate in predicting disease progression in patients with prostate cancer on active surveillance. Cancer. 2008;113(2):286–92.
72. Ross AE, Loeb S, Landis P, Partin AW, Epstein JI, Kettermann A, et al. Prostate-specific antigen kinetics during follow-up are an unreliable trigger for intervention in a prostate cancer surveillance program. J Clin Oncol. 2010;28(17):2810–6.
73. Recabal P, Assel M, DD S, Lee D, VP L, Touijer K, et al. The efficacy of multiparametric magnetic resonance imaging and MRI-targeted biopsy in risk classification for patients with prostate cancer on active surveillance. J Urol. 2016;196(2):374–81.
74. Kitajima K, Murphy RC, Nathan MA, Froemming AT, Hagen CE, Takahashi N, et al. Detection of recurrent prostate cancer after radical prostatectomy: comparison of 11C-choline PET/CT with pelvic multiparametric MR imaging with endorectal coil. J Nucl Med. 2014;55(2):223–32.
75. Alfarone A, Panebianco V, Schillaci O, Salciccia S, Cattarino S, Mariotti G, et al. Comparative analysis of multiparametric magnetic resonance and PET-CT in the management of local recurrence after radical prostatectomy for prostate cancer. Crit Rev Oncol Hematol. 2012;84(1):109–21.
76. Roy C, Foudi F, Charton J, Jung M, Lang H, Saussine C, et al. Comparative sensitivities of functional MRI sequences in detection of local recurrence of prostate carcinoma after radical prostatectomy or external-beam radiotherapy. AJR Am J Roentgenol. 2013;200(4):W361–8.
77. Linder BJ, Kawashima A, Woodrum DA, Tollefson MK, Karnes J, Davis BJ, et al. Early localization of

recurrent prostate cancer after prostatectomy by endorectal coil magnetic resonance imaging. Can J Urol. 2014;21(3):7283–9.
78. Puech P, Potiron E, Lemaitre L, Leroy X, Haber G-P, Crouzet S, et al. Dynamic contrast-enhanced-magnetic resonance imaging evaluation of intraprostatic prostate cancer: correlation with radical prostatectomy specimens. Urology. 2009;74(5):1094–9.
79. Labanaris AP, Engelhard K, Zugor V, Nützel R, Kühn R. Prostate cancer detection using an extended prostate biopsy schema in combination with additional targeted cores from suspicious images in conventional and functional endorectal magnetic resonance imaging of the prostate. Prostate Cancer Prostatic Dis. 2010;13(1):65–70.
80. Moore CM, Kasivisvanathan V, Eggener S, Emberton M, Fütterer JJ, Gill IS, et al. Standards of reporting for MRI-targeted biopsy studies (START) of the prostate: recommendations from an International Working Group. Eur Urol. 2013;64(4):544–52.
81. Cerantola Y, Haberer E, Torres J, Alameldin M, Aronson S, Levental M, et al. Accuracy of cognitive MRI-targeted biopsy in hitting prostate cancer-positive regions of interest. World J Urol. 2016;34(1):75–82.
82. Puech P, Ouzzane A, Gaillard V, Betrouni N, Renard B, Villers A, et al. Multiparametric MRI-targeted TRUS prostate biopsies using visual registration. Biomed Res Int. 2014;2014:819360.

17 Multiparametric MRI/TRUS Fusion Biopsy, Outcomes, and Commercial Systems

Akhil Muthigi, Ardeshir R. Rastinehad, Arvin K. George, Masakatsu Oishi, Osamu Ukimura, and Peter A. Pinto

Introduction

In current practice, prostate cancer suspicion is confirmed with transrectal ultrasound (TRUS)-guided 12-core biopsy directed at various regions of the prostate in a systematic manner. These biopsies are, in essence, blinded and random by nature as they are not directed toward a specific target, but rather to various geographic regions of the prostate. The widespread use of prostate-specific antigen (PSA) screening and TRUS-guided prostate biopsy has resulted in the overdiagnosis and overtreatment of low-risk prostate cancers and the underdetection/undertreatment of high-risk cancers, leading to unwarranted interventions without definitive benefit. The introduction of multiparametric magnetic resonance imaging (mpMRI) has revolutionized the way we visualize prostate cancer, as it helps delineate and characterize specific lesions that are potentially malignant. Extending from mpMR imaging, a novel and potentially transformative technique, named MRI/TRUS fusion-guided biopsy, has recently emerged as an option for a more precise prostate biopsy.

TRUS offers the ability to acquire imaging in real time but is limited by poor spatial resolution and low sensitivity for prostate cancer, as lesions can often appear isoechoic on TRUS imaging, making them difficult to distinguish from background [1]. Conversely, MR imaging presents prostatic lesions with striking detail and possesses high sensitivity, yet does not offer the capability for real-time image acquisition and guidance for biopsy in a timely or cost-efficient manner. Developers have strategically created "fusion" platforms to combine MR and TRUS imaging, thus allowing individuals performing biopsy to take advantage of the essential information and features offered by both modalities [2]. Utilizing these fusion biopsy platforms, a targeted fusion biopsy allows for sampling of specific regions within the prostate with lesions

A. Muthigi • A.K. George
National Institutes of Health Clinical Center, Urologic Oncology Branch, National Cancer Institute, National Institutes of Health, Bethesda, MD, USA

A.R. Rastinehad (✉)
Department of Urology and Radiology, Mount Sinai Hospital, NY, New York, USA
e-mail: art.rastinehad@mountsinai.org

M. Oishi
Department of Urology, Kyoto Prefectural University of Medicine, Kyoto, Kyoto, Japan

O. Ukimura
Department of Urology, University of Southern California Institute of Urology, Los Angeles, CA, USA

P.A. Pinto
Prostate Cancer Section, National Institutes of Health Clinical Center, Urologic Oncology Branch, National Cancer Institute, National Institutes of Health, Bethesda, MD, USA

© Springer International Publishing AG 2017

T.J. Polascik (ed.), *Imaging and Focal Therapy of Early Prostate Cancer*, Current Clinical Urology, DOI 10.1007/978-3-319-49911-6_17

pre-identified on MRI, thus providing the future possibility of circumventing the need for random "blinded" biopsies throughout the gland.

Herein, we provide a comprehensive review of the current MRI/TRUS fusion-based targeting strategies, indications as well as general workflow for the fusion biopsy technique, and an overview of commercially available software-based registration platforms and their respective strengths, limitations, and patient outcomes.

Magnetic Resonance Imaging-Based Targeted Biopsy Techniques

Three methods of MRI guidance are currently utilized for performance of targeted prostate biopsy: cognitive fusion, direct MRI-guided biopsy ("in-bore" biopsy), and MRI/TRUS fusion-guided biopsy (software-based registration).

Cognitive Fusion

Cognitive fusion (visual targeted biopsy) is a technique in which the ultrasound operator simply aims the biopsy needle in the general region of the prostate where a prior MRI demonstrates a lesion [3]. Therefore, prostate MR imaging is acquired prior to a TRUS-guided biopsy procedure, and "cognitive registration" is performed using knowledge from the MRI to guide the biopsy needle to the appropriate area(s) of the prostate with MRI-identified cancer-suspicious lesions. This method is appealing as it is simple and time efficient and does not require any additional equipment beyond an MRI scanner and traditional TRUS biopsy setup. Furthermore, cognitive fusion does not necessitate significant upfront capital investment or additional training modules/sessions with unfamiliar hardware and software. Several studies have compared cognitive fusion to the conventional systematic biopsy technique and to software-based registration platforms. Haffner et al. showed, in a cohort of 555 patients with suspicion of prostate cancer, that cognitive fusion biopsy had higher detection accuracy of clinically significant prostate cancer relative to extended systematic biopsy involving 10–12 cores ($p < 0.001$) [4]. Furthermore, targeted biopsy with cognitive registration detected 16 % more grade 4/5 cancers and more accurately quantified tumor burden ($p = 0.002$). Similarly, Park et al. demonstrated in a prospective evaluation in patients with elevated PSA and no prior biopsy history that cognitive fusion had higher cancer detection rates (29.5 % vs. 9.8 %, OR 3.9, $p = 0.03$) relative to TRUS biopsy alone [5]. In the prospective PROFUS trial, Wysock et al. compared targeted biopsy outcomes between MRI/ultrasound fusion biopsy and cognitive fusion biopsy and found similar cancer detection rates (CDRs) for all cancers (32.0 % vs. 20.3 %, $p = 0.1374$) and Gleason sum ≥7 cancers (26.7 % vs. 15.1 %, $p = 0.0523$) [6]. Another study compared targeted MRI/TRUS fusion biopsy (both cognitive fusion and software based) to TRUS-guided systematic biopsy in a prospective trial of 95 patients who had suspicious images at mpMRI [7]; they found that positivity rates for prostate cancer (69 % vs. 59 %, $p = 0.033$) and sampling quality (maximum cancer length per core, Gleason grade) were superior with targeted biopsy relative to systematic biopsy, regardless of visual (cognitive)-based registration or software-assisted registration.

Nevertheless, it appears that results with cognitive fusion biopsy are mixed, as a few studies have shown cognitive fusion biopsy to be no better than systematic TRUS biopsy [8, 9]. Delongchamps et al. tested accuracy of visual targeted biopsy in 127 patients and found no difference when compared to systematic biopsy with respect to cancer detection rate ($p = 0.66$) [8]. In the only Level I evidence to date comparing cognitive fusion biopsy to systematic 10- to 12-core TRUS biopsy, Tonttila et al. found no difference in cancer detection rates for both overall (64 % vs. 57 %, $p = 0.5$) and clinically significant (55 % vs. 45 %, $p = 0.8$) cancers; therefore, the authors concluded that additional prostate MRI before prostate biopsy did not add significant value [9]. However, rather than inferring that no benefit is achieved from MRI, this study may signify that there is limited benefit in biopsy-naïve patients. Lastly, in direct comparison of MRI/

TRUS fusion versus cognitive registration, one study found cognitive registration to be inferior to software-based MRI/TRUS fusion, as fewer than 50 % of clinically significant prostate cancer lesions were successfully sampled with cognitive registration, regardless of experience level [10].

Cognitive fusion biopsy is heavily operator dependent and requires extensive knowledge of prostate anatomy in order to extrapolate lesion location from MRI to TRUS without an actual overlay and registration of imaging. One study highlights the difficulty in performing visual registration, as TRUS 2D images project in a fan-shaped pattern and can be markedly different from the axial imaging plane on MRI, making it difficult to accurately estimate lesion location during TRUS biopsy [11]. This imaging disparity is most evident in anterior base and anterior apical lesions. Inaccurate lesion location estimation can be partially overcome by utilization of anatomical landmarks, such as prostatic cysts, benign prostatic hyperplasia (BPH) nodules, and/or calcifications as internal reference points to help further guide the biopsy needle. However, these "internal fiducials" are not always present, and heterogeneous echogenicity on TRUS may falsely lead the reader to misregister images, small differences of which can dramatically alter the results. As a final limitation, cognitive fusion methods do not offer the ability to track and record biopsy coordinates for later reference.

In-Bore MRI-Guided Biopsy

In-bore MRI-guided biopsy entails acquiring biopsy samples within the MRI gantry under direct guidance after prostate lesions have been pre-identified with a prior diagnostic mpMRI. During biopsy, the patient is placed prone in the MRI apparatus, and biopsy needles are directed toward suspicious lesions via a transrectal or transperineal (TP) approach [12]. Core samples are obtained with serial MRI scans to confirm biopsy needle placement [13]. The primary advantages for this approach are precise lesion sampling due to elimination of registration error and less total number of cores relative to systematic 10–12-core biopsy, as only suspicious lesions are targeted [14].

In a study of 100 patients with prior negative TRUS biopsy, persistently elevated or rising serum PSA, and at least one suspicious lesion on MRI, Roethke et al. found a CDR of 52 % overall and 80.8 % for clinically significant prostate cancer utilizing the in-bore MRI-guided biopsy technique [15]. Similarly, another report demonstrated the utility of MRI-guided in-bore biopsy in patients with prior negative biopsies and biopsy-naïve patients, with overall CDRs of 43.1 % and 55.6 %, respectively [16]. Hambrock et al. compared the ability of in-bore mpMRI-guided biopsies versus 10-core TRUS biopsy to match true Gleason grade as determined by the gold standard of radical prostatectomy specimens; they showed that the highest Gleason grade from in-bore biopsy matched final pathology in 88 % (30 of 34) patients, whereas the highest Gleason grade from 10-core TRUS biopsy matched final pathology in only 55 % (35 of 64) of patients ($p = 0.001$) [17].

Despite initial success with several studies demonstrating its efficacy, in-bore MRI-guided biopsy has not been embraced clinically due to several limitations. Firstly, the procedure is relatively lengthy and often requires sedation as patients have to remain still for the duration of the procedure. Moreover, the technique is costly and requires trained personnel and specialized MR-safe equipment. Lastly, the biopsy is performed in the radiology department and thus interferes with normal day-to-day workflow. Its unique benefit would be in patients unable to undergo TRUS (e.g., abdominoperineal resection), where an in-gantry approach would provide reliable imaging and targeting [18]. Thus, although accurate and utilized in some centers, this technique has not been broadly adopted for clinical use [19].

Software-Based Registration

The next step in the evolution of MRI-targeted biopsy has involved "fusion" of mpMRI to TRUS imaging utilizing software-based platforms that

allow for digital overlay. MpMRI provides detailed lesion information such as size and location, while TRUS provides real-time guidance for biopsy. Thus, MRI/TRUS fusion technology allows the user to combine advantages provided by both for sampling, such that lesion(s) previously delineated on MRI can be brought into view via manipulation of the TRUS probe and directly targeted. Furthermore, these software-based strategies enable prostate biopsy to be performed in the clinical outpatient office-based setting, much like the cognitive technique. This strategy, although it requires users to become familiar with additional software and hardware, is quick, efficient, and cost-effective.

Henceforth in this chapter, we will focus on MRI/TRUS fusion-guided biopsy as it is currently the most widely utilized MRI-based targeted biopsy approach. Since the late 2000s, multiple MRI/TRUS fusion platforms have been developed and are currently utilized in clinical practice (Table 17.1). While the workflow begins similarly with MR image acquisition and analysis, biopsy planning, and MR/TRUS image fusion (registration), the available platforms primarily differ in the following ways: the image registration algorithm, method of needle tracking, the hardware and software interface to present fused MR/TRUS imaging, additional software functionality, and route of biopsy.

Additionally, the major commercially available software-based registration platforms, their similarities, and differences for targeted biopsy of the prostate as well as outcomes are reviewed.

Indications for Fusion Biopsy

As adoption of fusion biopsy has steadily increased over the last several years, the indications for its use have expanded [20–22]. Targeted biopsy currently has an established role in the following three scenarios: (1) patients with continued suspicion for prostate cancer despite prior negative systematic TRUS biopsies, (2) patients with apparent low-risk prostate cancer interested in active surveillance, and (3) patients with mpMRI-defined lesions in locations of the prostate that are traditionally missed with systematic 12-core biopsy.

In the context of rising PSA and continued cancer suspicion despite multiple negative standard TRUS biopsies, current standard of care is to perform saturation biopsy with >20 cores, which is often associated with increased patient discomfort and need for general anesthesia [23]. One

Table 17.1 Summary of commercially available MRI/ultrasound fusion-guided prostate biopsy platforms

Platform (manufacturer)	FDA approval year	US probe manipulation	Tracking method	Registration method	Route of biopsy
UroNav (Philips/Invivo)	2005	Freehand	Electromagnetic	Rigid or elastic	Transrectal or transperineal
Virtual Navigator (Esaote)	2014	Freehand	Electromagnetic	Rigid	Transrectal
Real-time Virtual Sonography (Hitachi)	2010	Freehand	Electromagnetic	Rigid	Transrectal or transperineal
Artemis (Eigen)	2008	Rotation of articulated arm	Mechanical arm with encoders	Elastic	Transrectal
BiopSee (Pi Medical/ MedCom)	–	Mechanical stepper movement in two planes	Stepper with encoders	Rigid	Transperineal
BioJet (D&K Technologies)	2012	Rotation of articulated arm	Mechanical arm with encoders	Rigid	Transrectal or transperineal
Urostation (Koelis)	2010	Freehand	TRUS-TRUS registration	Elastic	Transrectal

FDA Food and Drug Administration, *US* ultrasound, *TRUS* transrectal ultrasound

early study demonstrated the utility of targeted prostate biopsy in men with prior negative biopsy and elevated PSA, as fusion biopsy revealed prostate cancer in 34 % (36/105) of men, with 72 % of men with prostate cancer detected harboring clinically significant disease [24]. Similarly, Vourganti et al. showed in a prior negative TRUS biopsy cohort of 195 men that MRI/TRUS fusion biopsy picked up all high-grade cancers (21 men, 11 %), whereas standard TRUS biopsy missed 12 of these high-grade cancers (55 %) [25]. Furthermore, in a prospective study by Salami et al. in 140 patients with at least one prior negative biopsy, the CDRs for clinically significant prostate cancer utilizing MRI/TRUS fusion biopsy were significantly higher than that of 12-core biopsy (47.9 % vs. 30.7 %, $p < 0.001$) [26].

With respect to active surveillance (AS), mpMRI- and MR-targeted fusion biopsy has proven utility in confirmation of candidacy for AS and continued monitoring [27]. In a study of 113 men enrolled in an AS protocol, confirmatory fusion biopsy resulted in reclassification in 36 % of patients, including 26 (23 %) due to Gleason grade 6 or greater and 15 (13 %) due to high-volume Gleason 6 disease [28]. Similarly, Stamatakis et al. found 29 % of their cohort (25/85 men) no longer met AS criteria after a confirmatory MRI/TRUS fusion-guided prostate biopsy [29]. In this study, number of mpMRI lesions, lesion density, and highest MRI lesion suspicion score were the significant MRI predictors of patients who would be poor AS candidates. In addition, in a study of 111 patients on AS, researchers showed that the use of mpMRI with subsequent fusion biopsy significantly increased the rate of AS termination relative to standard template biopsy alone (27 vs. 10, $p = 0.015$) [30]. Furthermore, early work has shown successful monitoring of cancer in patients on AS using MRI to electronically track specific cancer sites within the prostate, allowing for the return to that specific site with subsequent targeted biopsies [31]. Repeat sampling of cancerous sites within MRI targets was more likely to show cancer than resampling of tumors at systematic sites (61 % vs. 29 %, $p = 0.005$), suggesting improved accuracy in MRI-aided resampling methods over TRUS-guided methods. Walton Diaz et al. illustrated the utility of serial mpMRI and MRI/TRUS fusion biopsy in monitoring patients on AS, as stable findings on mpMRI were associated with Gleason score stability [32]. In this study, the number needed to biopsy to detect one Gleason progression was 8.74 for systematic 12-core biopsy vs. 2.9 for MRI/TRUS fusion biopsy. While further work is necessary, these initial studies help validate the use of serial imaging and targeted fusion biopsy with limited number of cores as tools to monitor patients on AS.

Lastly, MRI/TRUS fusion biopsy has demonstrated utility in targeting regions of the prostate that are typically missed with systematic 12-core biopsy, such as the anterior prostate, distal apical, and subcapsular regions [33–35]. Therefore, MR-targeted fusion biopsy should potentially be employed in patients in which MR imaging illustrates the presence of lesions in regions that are traditionally outside the systematic 12-core biopsy template.

Workflow of MRI/TRUS Fusion-Guided Biopsy

The workflow of MRI/TRUS fusion-guided biopsy in general involves the following steps in a sequential manner: MR image acquisition, MR prostate and lesion segmentation, ultrasound prostate segmentation, and image registration, followed by fusion-guided biopsy (Fig. 17.1).

MR images of the prostate are acquired first, followed by prostate boundary surface rendering and tumor location marking by the radiologist. An mpMRI study typically consists of T2-weighted (T2W), diffusion-weighted imaging (DWI), and dynamic contrast-enhanced (DCE) sequences, with or without the use of an endorectal coil while acquiring images, as well as other sequences required for completion of a standard pelvic MRI. Utilizing T2W imaging, the prostate is semiautomatically contoured with imaging software and manually adjusted where necessary [36]. The MR slice with the largest lesion diameter is utilized to define biopsy targets as a centroid marker or alternatively can be segmented on multiple slices to produce a three-dimensional (3D)

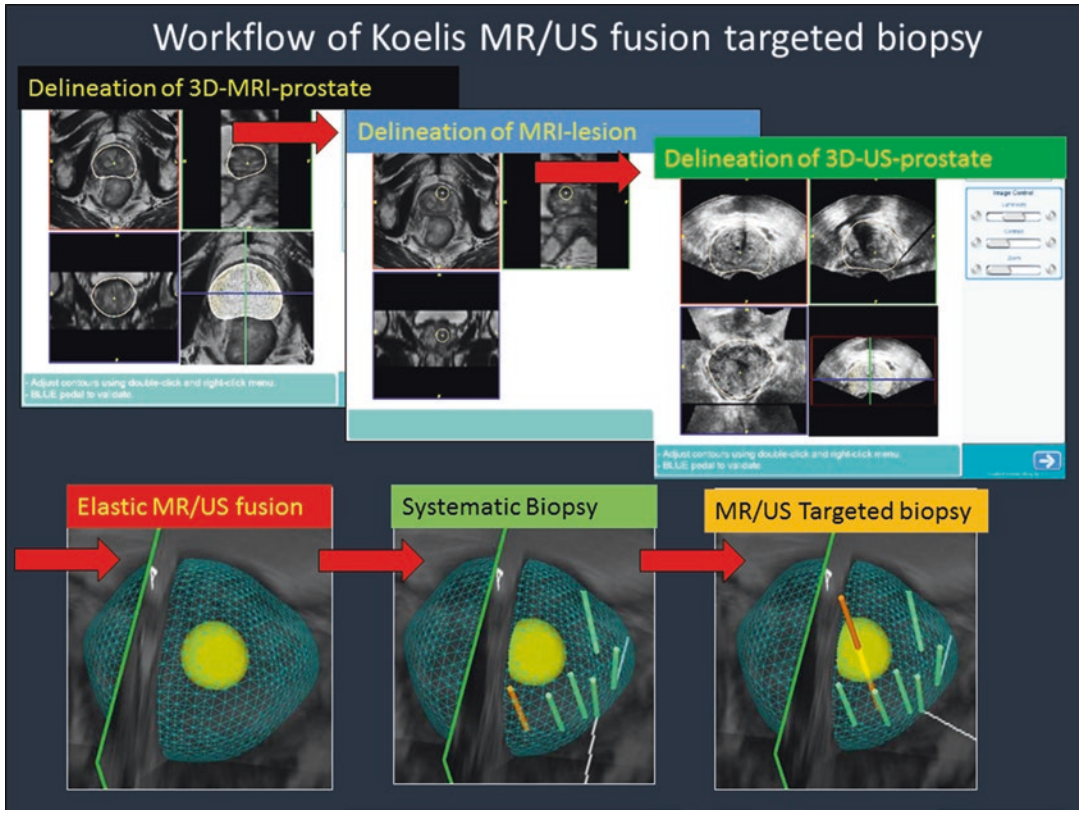

Fig. 17.1 Workflow of Urostation (Koelis) software-based registration platform

volume. This information is then sent electronically to the biopsy suite. Next, at the time of biopsy, a 3D TRUS volume model of the prostate is constructed from a series of two-dimensional (2D) TRUS images obtained via a sweep of the entire prostate with the TRUS probe. The TRUS 3D model is then segmented semiautomatically (with manual adjustments if necessary) and "fused" to the prostate MRI with registration software. This fusion or "registration" can be completed manually utilizing rigid registration; alternatively, the software can co-register the two prostate shapes to each other using a deformable or elastic registration algorithm depending on the fusion system being utilized (discussed in greater detail later). After registration of the two imaging modalities, the TRUS probe can be manipulated in real time, which allows the user to observe corresponding rotation or translation of the MR image. Thus, this technique enables the TRUS operator to guide a precise targeted biopsy of lesion(s) utilizing information from the previously acquired prostate MRI.

Registration Algorithms

The major technological challenge with MRI/TRUS fusion biopsy is the registration process that fuses MRI to the ultrasound image. Because the prostate on MRI (with an endorectal coil in place) often differs in shape from the same prostate on TRUS due to deformation, adjustments are necessary for optimal registration. This process can partly involve indirect alignment of prostate landmarks/internal fiducials (calcifications, cysts, BPH nodules, fixed bony points, etc.) that can be identified on both corresponding images and/or manual adjustment of probe pressure. Registration can be completed in one of two manners: rigid registration or elastic registration. In rigid registration, the surface rendering of the

prostate generated from MR and TRUS sweep is not altered in any manner; the prostate contours are simply manipulated to allow for rotational or translational alignment between images using a mathematical algorithm. Thus, with rigid registration, the internal anatomy of the prostate is preserved at the expense of prostate borders that may not appear to perfectly align. If images are suboptimally aligned during the procedure due to patient movement and/or prostate deformation, registration can be manually adjusted in real time by re-aligning the prostate contour edges or adjusting probe pressure. In elastic registration, the software algorithm stretches or "warps" the MR image prostate shape to match the TRUS prostate contour. Therefore, internal prostate anatomy is altered in an attempt to more properly match the two images with respect to surface contours. As the MR prostate contour is artificially altered to match the TRUS-generated 3D model of the prostate in elastic transformation, the quality of the ultrasound segmentation becomes highly critical. Robust US image acquisition helps to avoid misaligned or incorrectly warped registration.

After registration is completed, the graphical user interface of the different platforms vary and present fused MR-US images to the operator in different manners depending on the specific platform and user preference. Some platforms have the fused images displayed separately side by side in a "co-display" fashion, while others display a blended fusion image with MR and TRUS overlaid on top of each other in different color schemes. Lesions are typically marked with an indicator/"bullseye" or 3D region of interest to guide sampling.

A few fusion platforms currently are equipped with both rigid and elastic registration algorithms, allowing the user to potentially take advantage of both options depending on the specific circumstances encountered with a given patient. Regardless of the registration method, real-time operator input throughout the biopsy procedure and manual adjustments of the registration are of critical importance to fine-tune registration and optimize the targeting before and between core sampling.

Biopsy Needle Tracking

An additional functional aspect of several of the fusion platforms is the ability to track and record the position of the TRUS biopsy probe in real time in 3D space. This allows the user to track and navigate the needle to the appropriate slices with marked targets. There are currently three main methods for tracking: (1) electromagnetic (EM) tracking ("medical GPS"), (2) position-encoded joints in smart robotic arms, and (3) image-based software tracking.

Electromagnetic tracking (e.g., UroNav, Invivo Corp., Gainesville, FL, USA; Virtual Navigator, Esaote SpA, Genoa, Italy; Real-time Virtual Sonography, Hitachi Ltd., Tokyo, Japan) refers to a process by which the position of a small sensor attached to the TRUS biopsy probe within an external magnetic field (produced by a EM field generator) is relayed continuously to the computer. This form of tracking operates on Faraday's law of induction, which is the idea that a moving sensor located in the midst of an electromagnetic field emits an electrical current, which can then, in turn, be converted by software into a 3D position in space. This position in space can then be translated onto the fused imaging. The exact position of the TRUS probe is utilized to guide the operator toward the planned approach trajectory for each target as defined on pre-procedure mpMRI. The major advantage of this tracking technique is that it allows conventional freehand manipulation of the probe in multiple degrees of freedom, a process familiar to most urologists who routinely perform TRUS biopsy [37]. A potential disadvantage with this tracking method is the possibility for introduction of human error due to unsteady hands at time of needle deployment, leading to inaccurate sampling of the target lesion (mechanical error). Additional ferromagnetic interference from metallic objects can affect the accuracy of tracking, and care must be taken to minimize the proximity of these to the electromagnetic field.

Robotic fusion platforms (e.g., Artemis, Eigen, Grass Valley, CA, USA; BiopSee, Pi Medical, Athens, Greece; BioJet, BK Ultrasound, Analogic Corp., Peabody, MA, USA) operate

with mechanical devices that directly control the TRUS biopsy probe's movement. The probe is mounted on either a basic mechanical stepper with position sensors or a more complex self-articulating mechanical arm with built in angle-sensing encoders [38, 39]. Throughout the procedure, these sensors automatically relay angle and positional information to software that tracks the position of the probe and biopsy needle in 3D space. These robotic platforms allow for limited degrees of freedom along a fixed axis when manipulating the probe—mainly forward/backward and rotational. This technology offers improved probe stability during target acquisition, thereby reducing human mechanical error. However, the machine itself is bulkier relative to freehand devices and does not allow the user to review the MR images during procedure. Also, one is not able to turn off elastic deformation to review the raw MR image dataset and optimize the biopsy approach compared to other systems.

Image-based software tracking (Urostation, Koelis, Meylan, France) is unique in that it relies on TRUS-TRUS registration as the tracking mechanism and thus does not require additional hardware such as electromagnetic field generators or robotic arms. An initial 3D TRUS sweep of the prostate is performed, and then serial 3D TRUS images acquired after each biopsy are sequentially registered with the initial 3D TRUS panoramic volume to confirm needle position. Prior to the acquiring of targeted biopsies, elastic image fusion of real-time 3D TRUS volume from the sweep with previously acquired MR imaging is performed to allow for the identification of isoechoic lesions [40]. This technology was initially designed to map the 3D location of biopsy tracks within a 3D prostate model but then subsequently evolved to allow for prospective navigation of a TRUS probe to predefined suspicious areas within the prostate. This system offers potential advantages in that tracking can be achieved in a cost-effective manner without need for any additional hardware, and the use of the freehand biopsy technique is preserved, which should be familiar to most urologists. However, this technology is limited in that it does not offer "real-time" tracking, but rather allows for retrospective visualization of biopsy needle tracks relative to MRI-defined lesion locations. As an extension of this limitation, 3D TRUS imaging must be undertaken after every needle deployment to confirm location, with the needle held in exact place for 3–5 s.

Mapping and Navigation

Mapping and navigation are integral capabilities that are offered to varying degrees by the different fusion platforms. Mapping is the process by which software electronically tracks and records the location of a biopsy core in 3D space within a prostate model utilizing pre-procedure MRI as the reference "map." This information can be stored within the system for later use. Clinical applications of mapping include, but are not limited to, targeting cancer-positive-specific sites within the prostate on repeat biopsy (i.e., for patients on AS protocols) or planning the volumetric dimensions for focal therapy. Alternatively, a positive core from systematic sextant biopsy in a location not delineated by MRI ("MR invisible") can be mapped and subsequently targeted in a precise manner in a repeat fusion biopsy [31]. Navigation is the process by which the fusion biopsy system guides the operator with real-time imaging feedback to a specific lesion location for prospective placement of a biopsy needle. This is accomplished with utilization of a TRUS probe for real-time visualization and guidance toward a target pre-identified on MRI. Thus, a combination of tracking, navigation, and mapping allows for controlled and directed biopsies, accurate targeting, and accumulation of location data for future use in follow-up.

Biopsy Approach

Prostate biopsies are typically performed via a transrectal or transperineal approach, with transrectal being the most frequently used technique in the USA. Common, but transient, complications of prostate biopsy include hematuria, hematospermia, lower urinary tract symptoms (LUTS),

and pain [41]. With respect to post-biopsy, clinical outcomes, of particular concern and importance, are rates of infection and infectious complications following a biopsy procedure. Despite antimicrobial prophylaxis, infectious complications are increasing over time and are the most common reason for hospitalization post-biopsy [41]. In recent years, there has been a noticeable rise in the rate of TRUS biopsy sepsis, thought to be due to increasing prevalence of multiresistant (particularly fluoroquinolone resistance) causative bacteria in the rectal mucosa [42, 43]. Given that during a TRUS biopsy, the needle directly traverses the rectal mucosa, an increased risk of introducing rectal flora into the urinary tract and/or bloodstream is likely. In one study in which transperineal biopsy was performed in 245 patients, the rate of hospital readmission for infection was zero [44]. In a prospective, randomized, and controlled trial in 339 patients comparing TRUS biopsy to transperineal (TP) biopsy, the CDRs were equivalent (35.3 % vs. 31.9 %, $p > 0.05$). Importantly, the major complication rate was substantially lower in the TP biopsy group relative to the TRUS biopsy group (0.6 % vs. 4.3 %, $p < 0.05$). However, TP biopsy was more time-consuming (17.51 ± 3.33 min vs. 14.73 ± 3.25 min, $p < 0.05$), more painful (visual analogue scale score, 4.0 vs. 2.0; $p < 0.05$), and more often required additional anesthesia (15.0 % vs 1.2 %, $p < 0.05$). Therefore, TP biopsy may be a viable option in patients who have a history of sepsis on prior prostate biopsies or those who are at increased risk of developing infections along with infectious complications. Urologists should become increasingly aware of this rise in infectious complications post-biopsy and should consider appropriate antibiotic prophylaxis in all cases [45].

Commercial Systems

We devote the rest of this chapter to highlight the major fusion biopsy platforms currently available, including techniques, strengths, and weaknesses of each platform, as well as patient outcomes. It is important to note that these systems have and are continually evolving, with new features and applications constantly being added to adapt to various clinical scenarios and demands.

Electromagnetic Tracking

The **UroNav** platform (Invivo Corp., Gainesville, Florida, USA), which developed through a collaborative effort between the National Institutes of Health and Philips/Invivo Healthcare, began clinical trials in 2004 and was cleared by the US Food and Drug Administration (FDA) in 2006. This system is designed to be versatile, as it can operate with several different ultrasound vendors (Philips, General Electric, and BK Ultrasound systems) and can interface with readily available MR imaging software (DynaCad, Invivo). The UroNav platform has evolved, now incorporating both mapping capability and elastic registration. Furthermore, software has been developed to allow for the transperineal biopsy approach and is currently being prospectively evaluated. In 2015, the UroNav device was FDA cleared for guidance for focal therapy.

The workflow begins with the acquisition of mpMRI sequences (T2W imaging, DCE, and DWI) to identify suspicious lesions with the prostate. The radiologist segments the prostate and marks locations of target lesions and sends the MR imaging data to the UroNav workstation (Fig. 17.2). At the start of the procedure, the patient is placed in the left lateral decubitus position similarly to standard TRUS biopsy position, and an electromagnetic field generator box (~1 ft by 1 ft) is stationed directly above the patient's pelvis to allow for tracking of the TRUS probe in 3D space in real time. After attaching a sensor to the TRUS probe, the operator performs a "sweep" of the prostate in the axial plane from base to apex or apex to base. The sweep captures consecutive small slices of the prostate, which are then automatically compounded by the software to generate a working 3D TRUS volume prostate model. The borders of this 3D prostate model are then semiautomatically segmented (with manual corrections if necessary), followed by registration with MR imaging via rigid or elastic registration.

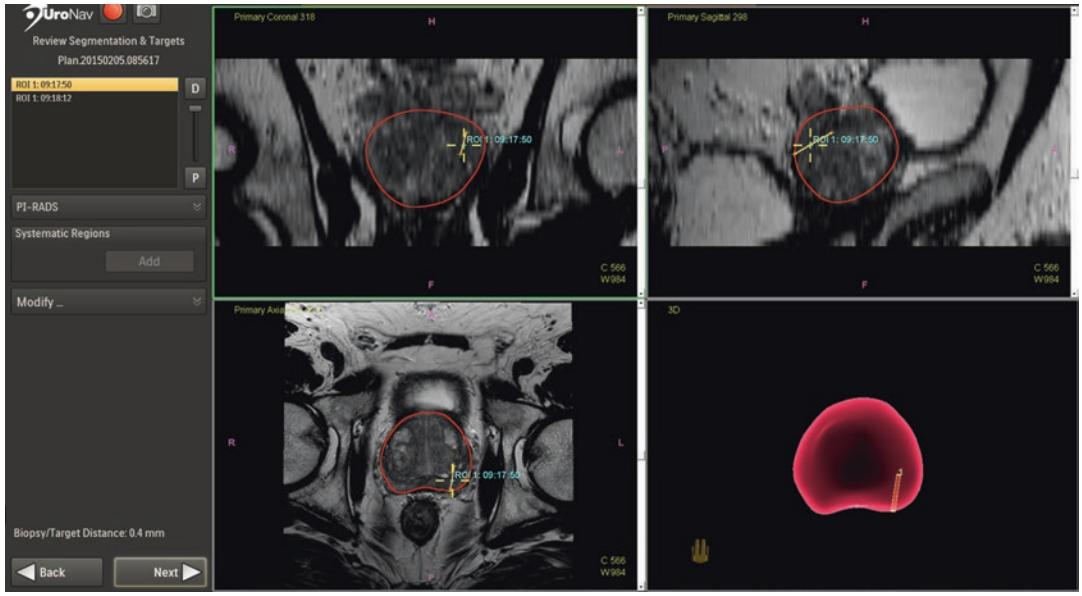

Fig. 17.2 UroNav screen capture of imported T2-weighted images demonstrating MR prostate segmentation and region of interest for targeted biopsy

Manual adjustments can be made to the registration throughout the procedure to account for patient and/or prostate motion, as well as differing degrees of prostate deformation due to variation in TRUS probe pressure applied.

After completion of registration, the operator can then proceed with targeted biopsies of the prostate utilizing a freehand TRUS approach. The UroNav system displays targets as a "bullseye" on the fused TRUS-MR image, which can appear side by side or overlaid on top of one another with a blending slider feature to adjust the relative transparencies of each image (Fig. 17.3). Through tracking of the TRUS probe, the navigation software guides the operator to the planned biopsy trajectory for each target. The TRUS probe is maneuvered until the bullseye is aligned onto a TRUS needle guide displayed on the screen; this is followed by insertion of the needle tip to the proximal edge of the lesion and spring biopsy deployment across the target, both in the axial and sagittal planes [46]. Mapping functionality documents the exact location of each core, which can be stored for later use.

Since its inception in 2006, several studies have been undertaken to test the functionality, accuracy, and utility of the UroNav system in clinical practice. Xu et al. illustrated the accuracy of the system to be 2.4 ± 1.2 mm in phantom studies [47]. In a landmark study in 1003 patients by Siddiqui et al. comparing MR/ultrasound fusion-guided biopsy utilizing the UroNav platform with standard 12-core TRUS biopsy, it was shown that targeted biopsy diagnosed 30 % more high-risk cancers vs. standard biopsy (173 vs. 122 cases, $p < 0.001$) and 17 % fewer low-risk cancers (213 vs. 258 cases, $p < 0.001$). This finding is highly critical, as a common critique of the standard systematic 12-core approach is that it tends to overdiagnose low-risk cancers, leading to unwarranted treatments, and underdiagnose high-risk cancers, resulting in lack of treatment and poor clinical outcomes. Furthermore, Rastinehad et al. illustrated in a propensity score-matched cohort (matched on age, PSA, MRI suspicion score, and prior negative biopsies) that improved detection of clinically significant cancer with mpMRI and fusion biopsy is reproducible across institutions [48]. In addition to this work, electromagnetic needle tracking capability has been validated by showing the software can accurately document the location of prior biop-

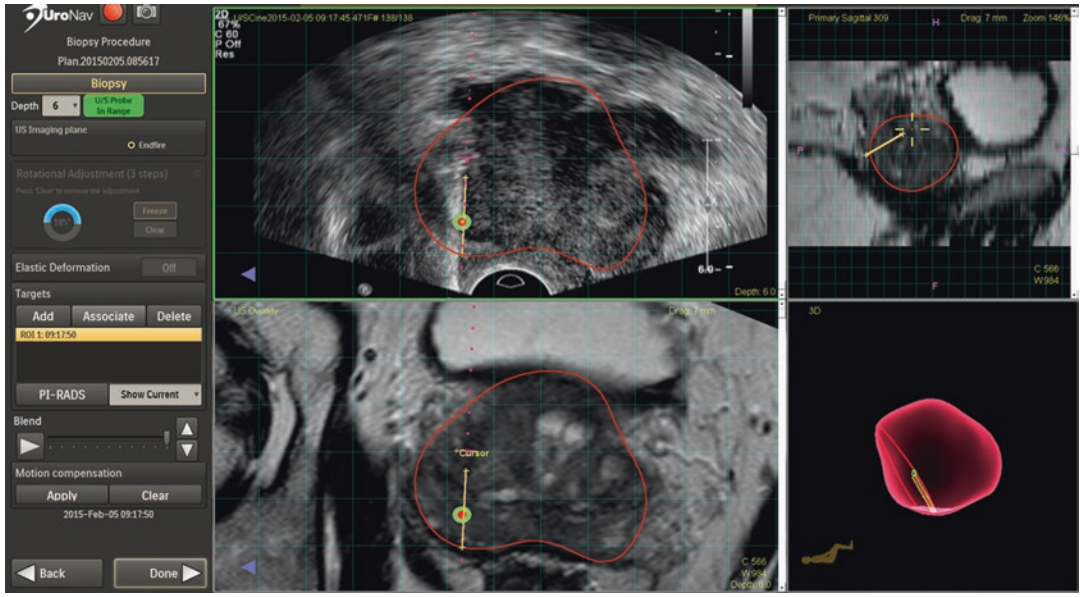

Fig. 17.3 UroNav screen capture demonstrating co-display of real-time TRUS and MR after registration. Bullseye demonstrates centroid point of a left peripheral zone lesion

sies, as well as direct subsequent biopsies to specific sites within the prostate [49].

Virtual Navigator (Esaote, Genoa, Italy) and **Real-time Virtual Sonography** (RVS) (Hitachi, Tokyo, Japan) are fusion platforms that were originally designed for percutaneous interventional guidance procedures and thereby had capabilities to fuse real-time TRUS with many different imaging modalities, such as computed tomography (CT), positron emission tomography (PET), or MRI [50–53]. The use of these systems in prostate biopsy has only recently been explored. The functionality is very similar to other fusion platforms, in which real-time TRUS imaging is fused with prior MR imaging via rigid registration. Both platforms employ electromagnetic tracking systems as well as freehand TRUS biopsy approach. Virtual Navigator primarily employs a transrectal biopsy approach, whereas RVS has capabilities for both transrectal and transperineal biopsies.

Studies with these systems with respect to prostate biopsy are limited. Puech et al. published results with the Virtual Navigator platform and found significant differences in overall cancer detection rate in favor of targeted biopsy over systematic biopsy (69 % vs. 59 %, $p = 0.033$), as well as higher detection of clinically significant prostate cancer (67 % vs. 52 %, $p = 0.0011$) [7]. However, these results must be interpreted cautiously as evaluation of targeted-core CDRs included results from combination of both cognitive targeting and targeting with the Virtual Navigator platform. A report using the Virtual Navigator platform in 78/131 (59.5 %) patients with a suspicious area found on MRI found this system to produce a significantly higher CDR relative to systematic 10–12-core biopsy ($p = 0.0065$) [8]. Targeted biopsy with this platform detected an additional 9 % (7/78) of patients missed by random biopsy with Gleason score >6, while random biopsy detected an additional 18 % (14/78) of low-risk patients with Gleason 6 disease. Miyagawa et al. evaluated transperineal biopsy with Real-time Virtual Sonography (RVS) in 85 patients with prior negative random biopsy and suspicious lesions found on MRI; overall, prostate cancer was detected in 52 patients (61 %), of which 87 % (45/52) were found via RVS-directed targeted cores [54]. On a per-core analysis, targeted cores with the RVS platform detected significantly more cancer than conventional

TRUS biopsy (32 % [62/192 cores] vs. 9 % [75/833 cores], $p < 0.01$).

Mechanical Position Encoders

The **Artemis** fusion biopsy platform (Eigen, Grass Valley, California, USA) was FDA approved in 2007, with patient recruitment and clinical trials beginning in 2009 at the University of California, Los Angeles (UCLA). As mentioned earlier, the Artemis device differs from the others in that it utilizes a robot-like self-articulating mechanical arm to sweep the prostate and perform targeted biopsies [3]. In this system, the needle and probe positions are tracked in 3D space with angle-sensing encoders built into each joint of the arm. Similar to other platforms, a high-quality MRI with T2W, DWI, and DCE sequences is obtained prior to biopsy to identify suspicious lesions within the prostate. Image registration is carried out by the Artemis software via elastic transformation algorithms. After image registration, navigation software guides the operator to the planned targets. The mechanical arm allows for 4 degrees of freedom, with biopsy limited by rotation of the arm along a fixed axis [55] (Fig. 17.4). Therefore, the learning curve with this system is more involved as users have to become acclimated to the software as well as TRUS biopsy using manual rotation of the mechanical arm as opposed to the freehand techniques commonly utilized by urologists during general TRUS biopsy.

Several studies have been carried out to test accuracy and utility of prostate biopsy with the Artemis system. Initial work showed a 33 % biopsy positive rate when suspicious lesions were targeted compared to a 7 % positivity rate for systematic nontargeted biopsy (19/57 cores vs. 9/124 cores, $p = 0.03$) [39]. MR fusion with subsequent targeted biopsy only added an additional 5 min on average to the overall biopsy procedural time. While testing the utility of the tracking mechanism, it was demonstrated that the Artemis system could return to prior biopsy sites within 1.2 ± 1.1 mm accuracy, which was independent of prostate volume or location of biopsy site. In a study with the Artemis system in 105 men with prior negative biopsy and elevated PSA, 21/23 men (91 %) with cancer detected on targeted biopsy had clinically significant cancer compared to 15 of 28 (54 %) with systematic biopsy; therefore, fusion biopsy yielded higher rates of clinically significant cancer [24]. The ability to eliminate mechanical error (e.g., hand unsteadiness during firing of the probe) is a unique and potential advantage of this robotic platform and may very well lead to higher accuracy while performing targeted prostate biopsy.

The **BiopSee** platform (Pi Medical, Athens, Greece) is similar to Artemis, yet utilizes a custom-made mechanical stepper fixed to the operating table to manipulate the TRUS probe as opposed to a self-articulating mechanical arm. Probe and needle motion are tracked via two built-in encoders; these encoders track motion of the probe in two dimensions: depth in/out and rotation. The workflow of this platform is very similar to many of the other platforms: pre-procedural MRI is obtained, and biopsy procedure consists of performing a sweep of the prostate with the TRUS probe from cranial to caudal, registering MRI data with real-time TRUS data via rigid registration, and carrying out targeted biopsies of specific regions within the prostate considered suspicious on MRI. Uniquely, this system is only equipped to perform biopsies via the transperineal route, in which biopsy needles are guided through a grid mounted to the mechanical stepper; however, ultrasound image guidance is still performed transrectally. As a potential limitation to this platform, users must familiarize themselves with not only the software but also the mechanics in handling the TRUS probe along fixed degrees of movement and rotation while simultaneously trying to align the needle with the virtual needle guide on the screen.

Most of the work with this system has been undertaken by Hadaschik et al. in Heidelberg, Germany. In an initial study with 106 men, the CDR was 59.4 % (63/106 patients), and MRI correlated positively with histopathology in 71 of 103 patients (68.9 %) [38]. On a per-core analysis, lesion-targeted cores had a significantly higher positivity rate than nontargeted cores

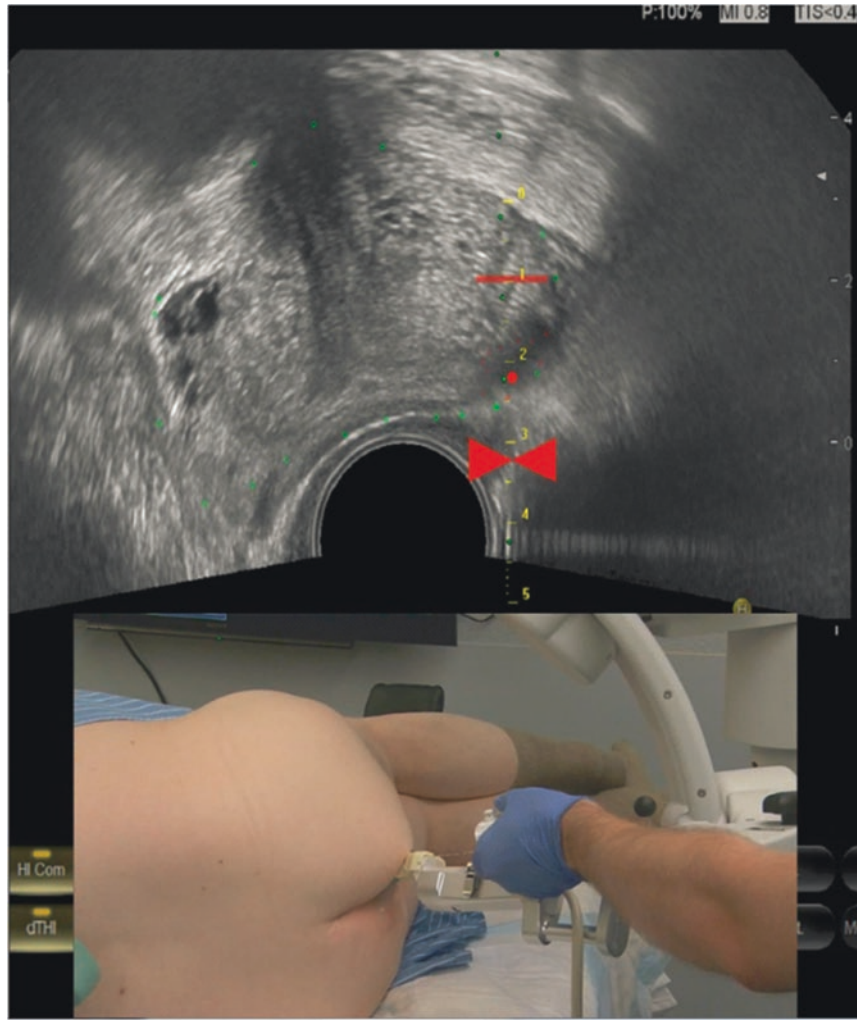

Fig. 17.4 (**a**) Artemis platform. The patient is placed in the lateral decubitus position. The US probe held securely by the robotic arm is placed transrectally to image the prostate. The needle biopsy guide is projected onto the US image to illustrate needle trajectory. The *red markings* assist in planning needle depth positioning and project the core sample to be taken. (Reprinted with permission from Eigen, Grass Valley, California, USA). (**b**) Artemis co-display of TRUS and T2W MRI of right peripheral zone lesion. Three-dimensional reconstruction demonstrates the acquired core location in the 3D volume. (Reprinted with permission from Eigen, Grass Valley, California, USA)

(101/410 [24.6 %] vs. 179/2051 [8.7 %], $p < 0.0001$). Lastly, the group reported an average procedural targeting error of 1.7 ± 1.7 mm for the first 2461 biopsy cores taken (comparing the virtually planned biopsy trajectory with the manually documented 3D needle positon of each biopsy core). Further work showed targeted biopsy CDRs of 82.6 % (86/104), 67 % (11/149), and 15 % (14/94) for patients with highly suspicious, questionably suspicious, and non-suspicious lesions detected on multiparametric 3 Tesla MRI, respectively [56]. On a core-by-core analysis, targeted cores detected significantly more cancer than systematic biopsies (386/1281 [30 %] vs. 523/6326 [8.2 %], $p < 0.01$). While initial work is promising, additional studies with this system are required to fully validate its accuracy and utility in clinical practice.

The **BioJet** platform (BK Ultrasound, Peabody, Massachusetts, USA; DK Technologies,

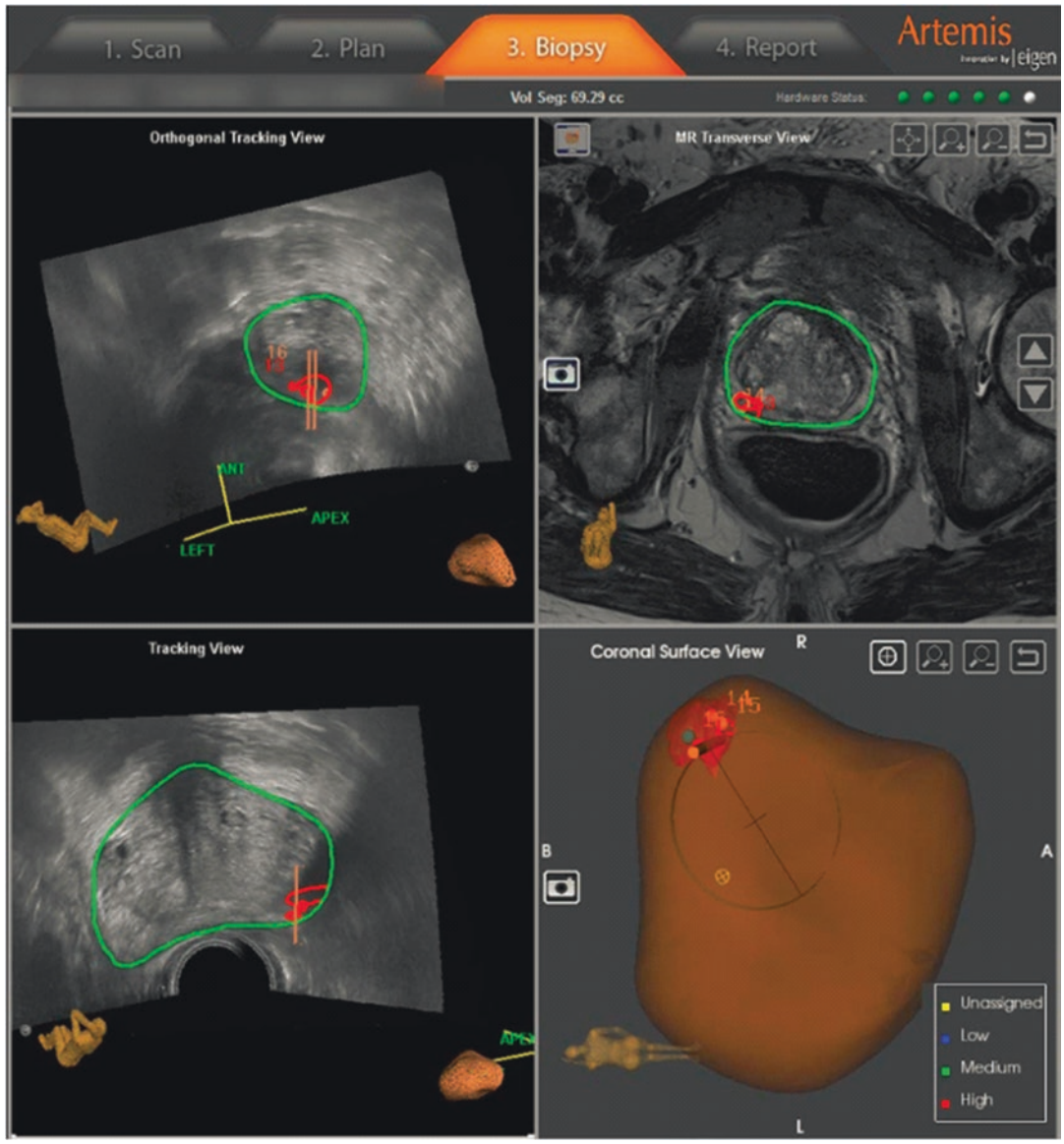

Fig. 17.4 (continued)

Barum, Germany), similar to Artemis, employs the use of a mechanical arm with angle-sensing encoders for tracking of the TRUS probe. Targeted biopsy can be performed via the transrectal or transperineal routes; however, the system is currently equipped with only rigid registration algorithms [57]. In a small proof-of-concept study consisting of 20 patients, Shoji et al. found an overall CDR of 70 % (14/20); the CDR was significantly higher for targeted biopsy cores utilizing the BioJet system relative to systematic biopsy (31.8 % vs. 6.7 %, $p < 0.0001$) [57]. However, the authors of the study pointed out that the shapes of the prostate contour on MRI and TRUS were pointedly different and contours had to be fused manually with several adjustments. In a study examining 72 total lesions in 39 men, one report found strong agreement between cancer detection via the BioJet platform and higher global Prostate Imaging Reporting

and Data System (PI-RADS) score for the dominant lesion found on mpMRI (positive cancer: 4.0 ± 1.3 vs. negative cancer: 2.6 ± 0.8, $p < 0.0006$) [58]. Using a global PI-RADS score cutoff ≥4, a sensitivity of 85 %, specificity of 82 %, and negative predictive value of 92 % were achieved. However, in a recent study in a prospective paired cohort of 50 patients with visible targets on MRI, Valerio et al. found similar CDRs on a per-patient level between cognitive fusion biopsy, directed targeted biopsies with the BioJet platform, and systematic transperineal template mapping biopsy (32 patients, 64 %; 34 patients, 68 %; and 38 patients, 76 %, respectively, $p > 0.05$) [59]. At a patient level, BioJet-based targeted biopsy did find more clinically significant disease relative to visually directed (cognitive) targeted biopsy, but this increased yield was not statistically significant (22 % vs. 14 %, $p = 0.48$). Therefore, more high-powered studies may be necessary to demonstrate significant differences in detection of clinically significant cancer with the BioJet platform relative to other biopsy methods.

Image-Based Tracking

The **Urostation** platform (Koelis, Grenoble, France), widely utilized across clinical centers in Europe, is an interesting platform in that tracking of the TRUS probe and needles is conducted with TRUS-TRUS registration. Thus, additional hardware such as an electromagnetic field generator or robotic arms is not necessary. The process begins with acquisition of prostate MRI as in other fusion platforms. At time of biopsy procedure, a 3D panorama TRUS volume is obtained via sweep of the prostate, and this model is fused to pre-procedural MRI data using elastic registration. Then, after each biopsy core is taken, a 3D TRUS image is acquired with the needle in place and registered to the original sweep TRUS volume to confirm proper needle placement. Similar to UroNav, this platform is advantageous as the biopsies are performed utilizing a standard freehand approach. However, one important drawback is that needles must be held in place without movement for 3–5 s to allow for 3D TRUS acquisition in order to acquire an accurate needle location. As technology improves, real-time 3D US image acquisition may make the process seamless.

Initial studies with phantom models conducted by Ukimura et al. at the University of Southern California (USC) in Los Angeles, California, USA, demonstrated an accuracy of 84 % (24/27 lesions hit) with this platform and a mean procedural targeting error of 2.09 ± 1.28 mm [40]. In a study of 80 patients with 115 MRI suspicious lesions, the hit rate for the Urostation platform was 97 % (112/115 lesions with confirmed biopsy inside target), and 60/115 (52 %) targets were positive for cancer [60]. Mozer et al., in a prospective study utilizing the Urostation platform in 152 biopsy-naïve men, found that the proportion of positive cores and proportion of men with clinically significant prostate cancer were significantly higher with the targeted-core protocol relative to a systematic 12-core protocol ($p < 0.001$ and $p = 0.03$, respectively). Therefore, initial work with this platform seems promising.

Discussion

MR/TRUS fusion technology has revolutionized the way we visualize, diagnose, and manage prostate cancer. To this day, the prostate remains the only solid-organ malignancy that is biopsied "blindly." The current standard of care is to direct 10–12 cores to various regions within the prostate, with the hope of identifying cancer, if present. Though systematic in fashion, the biopsies are in essence random as they are not directed toward specific targets within the prostate. Previously, imaging for prostate cancer has been a challenge due to its deep location within the pelvis, the complexity of prostatic zonal anatomy, and its multifocal nature. However, major strides in mpMRI capabilities over the last several years have allowed for precise characterization of cancerous lesions within the prostate; when this valuable information is integrated into fusion platforms, it allows the operator to perform targeted biopsies with high accuracy in the

specific location(s) in which there are image-identified lesions. Furthermore, this information can be stored and utilized in the future for various purposes, such as re-targeting the exact same location or planning focal therapy. Thus, fusion technology sheds light on the prostate and allows urologists to actually "see" malignancy with greater confidence, as opposed to grasping for cancer in the dark.

Software-based MRI/TRUS fusion-targeted biopsy, in general, detects more clinically significant cancers with fewer cores than standard biopsy [61–64]. A major criticism of systematic biopsy is the tendency to indiscriminately identify more clinically insignificant, low-risk cancers and less clinically relevant high-risk cancers. Therefore, targeted fusion biopsy may allow for more accurate risk stratification and subsequent treatment. Additionally, the clinical utility of fusion technology in various scenarios is apparent, such as in patients with history of prior negative TRUS biopsies yet continued prostate cancer suspicion, monitoring of patients on active surveillance, and targeting of lesions in areas of the prostate that are traditionally missed via systematic biopsy. Nevertheless, additional studies are warranted to further define the specific patient population that benefits the most from fusion biopsy [65].

Despite substantial progress in such a short time, there are many questions that still remain unanswered. At this time, most who have integrated fusion platforms into their practice perform systematic biopsy in addition to targeted biopsy. This is done, in part, to compare the two forms of biopsy head-to-head in the same patient, yet also because there still remain a small proportion of patients in which systematic biopsy reveals clinically significant disease missed by targeted fusion biopsy. Therefore, it is yet to be determined if targeted biopsy can be used alone primarily, or as an adjunctive strategy with systematic biopsy [26].

With respect to the available platforms, initial evidence suggests they offer clinical utility in one form or the other. However, there has been a paucity of clinical trials comparing the different platforms head-to-head. Retrospective analyses comparing the outcomes with each platform are quite difficult, as definitions, clinical parameters, workflow, and technique vary tremendously from institution to institution and study to study (for instance, variations in patient populations, mpMRI acquisition, MR imaging interpretation, fusion biopsy technique, definition of clinically significant cancer, etc.) [66].

Conclusion

Perhaps the most important question is how novel fusion technologies can be further integrated into mainstream urological practice. Due to proven success, the use of these commercially available fusion biopsy platforms seems to have taken off substantially in the last several years both in the USA and abroad. However, it is yet to be determined exactly what role fusion biopsy will play in the future. This office-based procedure empowers the urologist to specifically target lesions in the prostate; however, the entire process, from MR imaging interpretation to registration of a 3D ultrasound with MRI to accurate targeting of a "bullseye" displayed on the screen, requires several unique skillsets and a multidisciplinary team [67]. Though it remains to be seen whether this technology provides a favorable cost/benefit ratio, changes in the prostate cancer screening paradigm have forced clinicians to be more judicious in their approach to patient selection for biopsy. Improvements in imaging have facilitated this, and fusion technology will help integrate imaging findings to improve cancer diagnosis.

Acknowledgments This research was supported by the Intramural Research Program of the National Institutes of Health (NIH), National Cancer Institute, Center for Cancer Research, and the Center for Interventional Oncology. NIH and Philips Healthcare have a cooperative research and development agreement. NIH and Philips share intellectual property in the field.

This research was also made possible through the National Institutes of Health Medical Research Scholars Program, a public-private partnership supported jointly by the NIH and generous contributions to the Foundation for the NIH from Pfizer Inc.; the Doris Duke Charitable Foundation; the Alexandria Real Estate Equities, Inc., and Mr. and Mrs.

Joel S. Marcus; and the Howard Hughes Medical Institute, as well as other private donors. For a complete list, please visit the Foundation Website at http://fnih.org/work/education-training-0/medical-research-scholars-program.

References

1. Egawa S, Wheeler TM, Greene DR, Scardino PT. Unusual hyperechoic appearance of prostate cancer on transrectal ultrasonography. Br J Urol. 1992;69(2):169–74.
2. Kongnyuy M, George AK, Rastinehad AR, Pinto PA. Magnetic resonance imaging-ultrasound fusion-guided prostate biopsy: review of technology, techniques, and outcomes. Curr Urol Rep. 2016;17(4):32.
3. Marks L, Young S, Natarajan S. MRI-ultrasound fusion for guidance of targeted prostate biopsy. Curr Opin Urol. 2013;23(1):43–50.
4. Haffner J, Lemaitre L, Puech P, Haber GP, Leroy X, Jones JS, et al. Role of magnetic resonance imaging before initial biopsy: comparison of magnetic resonance imaging-targeted and systematic biopsy for significant prostate cancer detection. BJU Int. 2011;108(8 Pt 2):E171–8.
5. Park BK, Park JW, Park SY, Kim CK, Lee HM, Jeon SS, et al. Prospective evaluation of 3-T MRI performed before initial transrectal ultrasound-guided prostate biopsy in patients with high prostate-specific antigen and no previous biopsy. AJR Am J Roentgenol. 2011;197(5):W876–81.
6. Wysock JS, Rosenkrantz AB, Huang WC, Stifelman MD, Lepor H, Deng FM, et al. A prospective, blinded comparison of magnetic resonance (MR) imaging-ultrasound fusion and visual estimation in the performance of MR-targeted prostate biopsy: the PROFUS trial. Eur Urol. 2014;66(2):343–51.
7. Puech P, Rouviere O, Renard-Penna R, Villers A, Devos P, Colombel M, et al. Prostate cancer diagnosis: multiparametric MR-targeted biopsy with cognitive and transrectal US-MR fusion guidance versus systematic biopsy–prospective multicenter study. Radiology. 2013;268(2):461–9.
8. Delongchamps NB, Peyromaure M, Schull A, Beuvon F, Bouazza N, Flam T, et al. Prebiopsy magnetic resonance imaging and prostate cancer detection: comparison of random and targeted biopsies. J Urol. 2013;189(2):493–9.
9. Tonttila PP, Lantto J, Paakko E, Piippo U, Kauppila S, Lammentausta E, et al. Prebiopsy multiparametric magnetic resonance imaging for prostate cancer diagnosis in biopsy-naive men with suspected prostate cancer based on elevated prostate-specific antigen values: results from a randomized prospective blinded controlled trial. Eur Urol. 2015;69(3):419–25.
10. Cool DW, Zhang X, Romagnoli C, Izawa JI, Romano WM, Fenster A. Evaluation of MRI-TRUS fusion versus cognitive registration accuracy for MRI-targeted, TRUS-guided prostate biopsy. AJR Am J Roentgenol. 2015;204(1):83–91.
11. Kwak JT, Hong CW, Pinto PA, Williams M, Xu S, Kruecker J, et al. Is visual registration equivalent to semiautomated registration in prostate biopsy? Biomed Res Int. 2015;2015:394742.
12. Penzkofer T, Tuncali K, Fedorov A, Song SE, Tokuda J, Fennessy FM, et al. Transperineal in-bore 3-T MR imaging-guided prostate biopsy: a prospective clinical observational study. Radiology. 2015;274(1):170–80.
13. Robertson NL, Emberton M, Moore CM. MRI-targeted prostate biopsy: a review of technique and results. Nat Rev Urol. 2013;10(10):589–97.
14. Quentin M, Blondin D, Arsov C, Schimmoller L, Hiester A, Godehardt E, et al. Prospective evaluation of magnetic resonance imaging guided in-bore prostate biopsy versus systematic transrectal ultrasound guided prostate biopsy in biopsy naive men with elevated prostate specific antigen. J Urol. 2014;192(5):1374–9.
15. Roethke M, Anastasiadis AG, Lichy M, Werner M, Wagner P, Kruck S, et al. MRI-guided prostate biopsy detects clinically significant cancer: analysis of a cohort of 100 patients after previous negative TRUS biopsy. World J Urol. 2012;30(2):213–8.
16. Schimmoller L, Blondin D, Arsov C, Rabenalt R, Albers P, Antoch G, et al. MRI-guided in-bore biopsy: differences between prostate cancer detection and localization in primary and secondary biopsy settings. AJR Am J Roentgenol. 2016;206(1):92–9.
17. Hambrock T, Hoeks C, van de Kaa Hulsbergen- C, Scheenen T, Futterer J, Bouwense S, et al. Prospective assessment of prostate cancer aggressiveness using 3-T diffusion-weighted magnetic resonance imaging-guided biopsies versus a systematic 10-core transrectal ultrasound prostate biopsy cohort. Eur Urol. 2012;61(1):177–84.
18. Kongnyuy M, Frye T, George AK, Kilchevsky A, Iyer A, Kadakia M, et al. A case of in-bore transperineal MRI-guided prostate biopsy of a patient with ileal pouch-anal anastomosis. Case Rep Urol. 2015;2015:676930.
19. Pinto F, Totaro A, Palermo G, Calarco A, Sacco E, D'Addessi A, et al. Imaging in prostate cancer staging: present role and future perspectives. Urol Int. 2012;88(2):125–36.
20. Muller BG, Kaushal A, Sankineni S, Lita E, Hoang AN, George AK, et al. Multiparametric magnetic resonance imaging-transrectal ultrasound fusion-assisted biopsy for the diagnosis of local recurrence after radical prostatectomy. Urol Oncol. 2015;33(10):425.e1–6.
21. Okoro C, George AK, Siddiqui MM, Rais-Bahrami S, Walton-Diaz A, Shakir NA, et al. magnetic resonance imaging/transrectal ultrasonography fusion prostate biopsy significantly outperforms systematic 12-core biopsy for prediction of total magnetic resonance imaging tumor volume in active surveillance patients. J Endourol. 2015;29(10):1115–21.
22. Raskolnikov D, George AK, Rais-Bahrami S, Turkbey B, Shakir NA, Okoro C, et al. Multiparametric magnetic resonance imaging and image-guided biopsy to detect seminal vesicle invasion by prostate cancer. J Endourol. 2014;28(11):1283–9.

23. Shariat SF, Roehrborn CG. Using biopsy to detect prostate cancer. Rev Urol. 2008;10(4):262–80.
24. Sonn GA, Chang E, Natarajan S, Margolis DJ, Macairan M, Lieu P, et al. Value of targeted prostate biopsy using magnetic resonance-ultrasound fusion in men with prior negative biopsy and elevated prostate-specific antigen. Eur Urol. 2014;65(4):809–15.
25. Vourganti S, Rastinehad A, Yerram NK, Nix J, Volkin D, Hoang A, et al. Multiparametric magnetic resonance imaging and ultrasound fusion biopsy detect prostate cancer in patients with prior negative transrectal ultrasound biopsies. J Urol. 2012;188(6):2152–7.
26. Salami SS, Ben-Levi E, Yaskiv O, Ryniker L, Turkbey B, Kavoussi LR, et al. In patients with a previous negative prostate biopsy and a suspicious lesion on magnetic resonance imaging, is a 12-core biopsy still necessary in addition to a targeted biopsy? BJU Int. 2015;115(4):562–70.
27. Fascelli M, George AK, Frye T, Turkbey B, Choyke PL, Pinto PA. The role of MRI in active surveillance for prostate cancer. Curr Urol Rep. 2015;16(6):42.
28. Hu JC, Chang E, Natarajan S, Margolis DJ, Macairan M, Lieu P, et al. Targeted prostate biopsy in select men for active surveillance: do the Epstein criteria still apply? J Urol. 2014;192(2):385–90.
29. Stamatakis L, Siddiqui MM, Nix JW, Logan J, Rais-Bahrami S, Walton-Diaz A, et al. Accuracy of multiparametric magnetic resonance imaging in confirming eligibility for active surveillance for men with prostate cancer. Cancer. 2013;119(18):3359–66.
30. Abdi H, Pourmalek F, Zargar H, Walshe T, Harris AC, Chang SD, et al. Multiparametric magnetic resonance imaging enhances detection of significant tumor in patients on active surveillance for prostate cancer. Urology. 2015;85(2):423–8.
31. Sonn GA, Filson CP, Chang E, Natarajan S, Margolis DJ, Macairan M, et al. Initial experience with electronic tracking of specific tumor sites in men undergoing active surveillance of prostate cancer. Urol Oncol. 2014;32(7):952–7.
32. Walton Diaz A, Shakir NA, George AK, Rais-Bahrami S, Turkbey B, Rothwax JT, et al. Use of serial multiparametric magnetic resonance imaging in the management of patients with prostate cancer on active surveillance. Urol Oncol. 2015;33(5):202.e1–7.
33. Nix JW, Turkbey B, Hoang A, Volkin D, Yerram N, Chua C, et al. Very distal apical prostate tumours: identification on multiparametric MRI at 3 Tesla. BJU Int. 2012;110(11 Pt B):E694–700.
34. Sankineni S, George AK, Brown AM, Rais-Bahrami S, Wood BJ, Merino MJ, et al. Posterior subcapsular prostate cancer: identification with mpMRI and MRI/TRUS fusion-guided biopsy. Abdom Imaging. 2015;40(7):2557–65.
35. Kongnyuy M, Sidana A, AK G, Muthigi A, Iyer A, Fascelli M, et al. The significance of anterior prostate lesions on multiparametric magnetic resonance imaging in African-American men. Urol Oncol. 2016;34(6):254.e15–21.
36. Wang S, Burtt K, Turkbey B, Choyke P, Summers RM. Computer aided-diagnosis of prostate cancer on multiparametric MRI: a technical review of current research. Biomed Res Int. 2014;2014:789561.
37. Sonn GA, Margolis DJ, Marks LS. Target detection: magnetic resonance imaging-ultrasound fusion-guided prostate biopsy. Urol Oncol. 2014;32(6):903–11.
38. Hadaschik BA, Kuru TH, Tulea C, Rieker P, Popeneciu IV, Simpfendorfer T, et al. A novel stereotactic prostate biopsy system integrating pre-interventional magnetic resonance imaging and live ultrasound fusion. J Urol. 2011;186(6):2214–20.
39. Natarajan S, Marks LS, Margolis DJ, Huang J, Macairan ML, Lieu P, et al. Clinical application of a 3D ultrasound-guided prostate biopsy system. Urol Oncol. 2011;29(3):334–42.
40. Ukimura O, Desai MM, Palmer S, Valencerina S, Gross M, Abreu AL, et al. 3-Dimensional elastic registration system of prostate biopsy location by real-time 3-dimensional transrectal ultrasound guidance with magnetic resonance/transrectal ultrasound image fusion. J Urol. 2012;187(3):1080–6.
41. Loeb S, Vellekoop A, Ahmed HU, Catto J, Emberton M, Nam R, et al. Systematic review of complications of prostate biopsy. Eur Urol. 2013;64(6):876–92.
42. Wagenlehner FM, van Oostrum E, Tenke P, Tandogdu Z, Cek M, Grabe M, et al. Infective complications after prostate biopsy: outcome of the Global Prevalence Study of Infections in Urology (GPIU) 2010 and 2011, a prospective multinational multicentre prostate biopsy study. Eur Urol. 2013;63(3):521–7.
43. Nam RK, Saskin R, Lee Y, Liu Y, Law C, Klotz LH, et al. Increasing hospital admission rates for urological complications after transrectal ultrasound guided prostate biopsy. J Urol. 2013;189(1 Suppl):S12–7. discussion S7–8
44. Grummet JP, Weerakoon M, Huang S, Lawrentschuk N, Frydenberg M, Moon DA, et al. Sepsis and 'superbugs': should we favour the transperineal over the transrectal approach for prostate biopsy? BJU Int. 2014;114(3):384–8.
45. Womble PR, Linsell SM, Gao Y, Ye Z, Montie JE, Gandhi TN, et al. A statewide intervention to reduce hospitalizations after prostate biopsy. J Urol. 2015;194(2):403–9.
46. Hong CW, Rais-Bahrami S, Walton-Diaz A, Shakir N, Su D, George AK, et al. Comparison of magnetic resonance imaging and ultrasound (MRI-US) fusion-guided prostate biopsies obtained from axial and sagittal approaches. BJU Int. 2015;115(5):772–9.
47. Xu S, Kruecker J, Turkbey B, Glossop N, Singh AK, Choyke P, et al. Real-time MRI-TRUS fusion for guidance of targeted prostate biopsies. Comput Aided Surg. 2008;13(5):255–64.
48. Rastinehad AR, Abboud SF, George AK, Frye T, Ho R, Chelluri R, et al. Reproducibility of multiparametric MRI and fusion-guided prostate biopsy: multi-institutional external validation by a propensity score matched cohort. J Urol. 2016;193(4):e90–1.

49. Turkbey B, Xu S, Kruecker J, Locklin J, Pang Y, Bernardo M, et al. Documenting the location of prostate biopsies with image fusion. BJU Int. 2011;107(1):53–7.
50. Mauri G, De Beni S, Forzoni L, D'Onofrio S, Kolev V, Lagana MM, et al. Virtual navigator automatic registration technology in abdominal application. Conf Proc IEEE Eng Med Biol Soc. 2014;2014:5570–4.
51. Di Mauro E, Solbiati M, De Beni S, Forzoni L, D'Onofrio S, Solbiati L. Virtual navigator real-time ultrasound fusion imaging with positron emission tomography for liver interventions. Conf Proc IEEE Eng Med Biol Soc. 2013;2013:1406–9.
52. Uematsu T, Takahashi K, Nishimura S, Watanabe J, Yamasaki S, Sugino T, et al. Real-time virtual sonography examination and biopsy for suspicious breast lesions identified on MRI alone. Eur Radiol. 2015;26(4):1064–72.
53. Oshima T, Nakase J, Numata H, Takata Y, Tsuchiya H. Ultrasonography imaging of the anterolateral ligament using real-time virtual sonography. Knee. 2016;23(2):198–202.
54. Miyagawa T, Ishikawa S, Kimura T, Suetomi T, Tsutsumi M, Irie T, et al. Real-time Virtual Sonography for navigation during targeted prostate biopsy using magnetic resonance imaging data. Int J Urol. 2010;17(10):855–60.
55. Kaye DR, Stoianovici D, Han M. Robotic ultrasound and needle guidance for prostate cancer management: review of the contemporary literature. Curr Opin Urol. 2014;24(1):75–80.
56. Kuru TH, Roethke MC, Seidenader J, Simpfendorfer T, Boxler S, Alammar K, et al. Critical evaluation of magnetic resonance imaging targeted, transrectal ultrasound guided transperineal fusion biopsy for detection of prostate cancer. J Urol. 2013;190(4):1380–6.
57. Shoji S, Hiraiwa S, Endo J, Hashida K, Tomonaga T, Nakano M, et al. Manually controlled targeted prostate biopsy with real-time fusion imaging of multiparametric magnetic resonance imaging and transrectal ultrasound: an early experience. Int J Urol. 2015;22(2):173–8.
58. Tewes S, Hueper K, Hartung D, Imkamp F, Herrmann TR, Weidemann J, et al. Targeted MRI/TRUS fusion-guided biopsy in men with previous prostate biopsies using a novel registration software and multiparametric MRI PI-RADS scores: first results. World J Urol. 2015;33(11):1707–14.
59. Valerio M, McCartan N, Freeman A, Punwani S, Emberton M, Ahmed HU. Visually directed vs. software-based targeted biopsy compared to transperineal template mapping biopsy in the detection of clinically significant prostate cancer. Urol Oncol. 2015;33(10):424.e9–16.
60. Rud E, Baco E, Eggesbo HB. MRI and ultrasound-guided prostate biopsy using soft image fusion. Anticancer Res. 2012;32(8):3383–9.
61. Valerio M, Donaldson I, Emberton M, Ehdaie B, Hadaschik BA, Marks LS, et al. Detection of clinically significant prostate cancer using magnetic resonance imaging-ultrasound fusion targeted biopsy: a systematic review. Eur Urol. 2015;68(1):8–19.
62. Siddiqui MM, Rais-Bahrami S, Turkbey B, George AK, Rothwax J, Shakir N, et al. Comparison of MR/ultrasound fusion-guided biopsy with ultrasound-guided biopsy for the diagnosis of prostate cancer. JAMA. 2015;313(4):390–7.
63. Rastinehad AR, Turkbey B, Salami SS, Yaskiv O, George AK, Fakhoury M, et al. Improving detection of clinically significant prostate cancer: magnetic resonance imaging/transrectal ultrasound fusion guided prostate biopsy. J Urol. 2014;191(6):1749–54.
64. Salami SS, Vira MA, Turkbey B, Fakhoury M, Yaskiv O, Villani R, et al. Multiparametric magnetic resonance imaging outperforms the Prostate Cancer Prevention Trial risk calculator in predicting clinically significant prostate cancer. Cancer. 2014;120(18):2876–82.
65. Frye TP, Pinto PA, George AK. Optimizing Patient Population for MP-MRI and Fusion Biopsy for Prostate Cancer Detection. Curr Urol Rep. 2015;16(7):50.
66. Rastinehad AR, Durand M. A comparison of magnetic resonance imaging and ultrasonography (MRI/US)-fusion guided prostate biopsy devices: too many uncontrolled variables. BJU Int. 2016;117(3):392–400.
67. Tay KJ, Gupta RT, Rastinehad AR, Tsivian E, Freedland SJ, Moul JW, et al. Navigating MRI-TRUS fusion biopsy: optimizing the process and avoiding technical pitfalls. Expert Rev Anticancer Ther. 2016;16(3):303–11.

18 Detecting, Localizing, and Treating the Multiparametric Magnetic Resonance Imaging Invisible Lesion: Utilizing Three-Dimensional Transperineal Mapping

Nelson N. Stone and E. David Crawford

Introduction

Multiparametric magnetic resonance imaging (mpMRI) is quickly becoming the new "gold standard" to improve prostate cancer detection and to guide focal therapy. Combined with a targeted biopsy approach, it is beginning to replace transrectal ultrasound (TRUS)-guided prostate biopsy, which was introduced almost 30 years ago and had been the favored technique for the urologic community to diagnose prostate cancer [1]. Prostate-specific antigen (PSA) testing was also introduced almost simultaneously with the TRUS biopsy. PSA and TRUS biopsy combined with intense screening efforts tripled the detection rate of the disease and identified the majority of palpable and locally advanced prostate cancer lesions. In 1994 the Prostate Cancer Education Council (PCEC) reported the results of Prostate Cancer Awareness Week (PCAW) 1989–1992 [2]. A total of 14,900 men participated in the screening study in 1989, 150,000 in 1990, 400,000 in 1991, and >500,000 in 1992. The cancer detection rate by PSA rose from 4.98 % to 10 % in the first 2 years of the study and then fell to 6.48 % and 3.57 % for 1991 and 1992, respectively. Brawer reported a similar decrease from 2.6 % in year 1 to 2.0 % in year 2 and 1.8 % in year 3 [3]. The American Cancer Society (ACS) screening project also noted a decrease from 5.4 % to 1.0 % from the first to the third year of screening [4]. These efforts have resulted in a decrease of men presenting with an elevated PSA and a concomitant decrease in the volume of disease in the prostate. Today, most patients present with non-palpable disease (T1c).

When TRUS prostate biopsy was introduced, most prostate cancers were large and detectable by both digital rectal exam (DRE) and ultrasound. In addition, a positive diagnosis was readily available because these lesions were mostly peripheral and easily targeted by puncture through the anterior rectal wall. Over time, peripheral lesions have become smaller and more difficult to detect by TRUS and have in part been

N.N. Stone (✉)
Departments of Urology and Radiation Oncology, The Icahn School of Medicine at Sinai, Mount Sinai Medical Center, New York, NY, USA
e-mail: drnelsonstone@gmail.com

E.D. Crawford
Surgery, Urology and Radiation Oncology, Urologic Oncology, University of Colorado, Denver, CO, USA

The University of Colorado Anschutz Campus, Aurora, CO, USA

© Springer International Publishing AG 2017

T.J. Polascik (ed.), *Imaging and Focal Therapy of Early Prostate Cancer*, Current Clinical Urology, DOI 10.1007/978-3-319-49911-6_18

overshadowed by anterior lesions. Anteriorly located prostate cancer is not ideally suited for TRUS biopsy.

The decreasing volume of the lesions has also been associated with an increased interest in only treating the disease confined to the gland (pT2). A treatment methodology similar to that used for small-volume breast cancer, in essence the "male lumpectomy," has been proposed by Onik [5]. However, unlike breast cancer, where the solitary lesion is easily imaged, prostate cancer presents with small, mostly ultrasound-invisible multifocal disease [6]. The inability to image and detect all prostate cancers within the gland has generated interest in finding different imaging technologies and limiting detection and treatment to only the potentially lethal prostate cancers, thus the interest in multiparametric magnetic resonance imaging (mpMRI), which can reliably detect the larger and higher-grade prostate cancer, often termed the "index lesions." MRI-detected index lesions have also created interest in using focal ablative technologies to only treat these lesions as opposed to prostatectomy or whole-gland irradiation.

This chapter will make the argument that this approach may not be the best way to find and focally ablate isolated prostate cancer lesions. Multiparametric MRI, while an advance in prostate cancer detection compared to the "semi-blind" 12-core TRUS biopsy, is not ready to replace TRUS biopsy. We will review transperineal mapping biopsy (TPMB), which is a superior method to identify and select lesions for targeted focal therapy (TFT) because it improves intraprostatic staging. New technology, which corrects some of the deficiencies of the current TPMB technique, will also be discussed.

Multiparametric Magnetic Resonance Imaging and 12-Core Systematic Prostate Biopsy

The enhanced detection rate of clinically significant prostate cancer by mpMRI-targeted biopsy compared to the systematic 12-core technique is an accepted fact. Unfortunately, it is also now recognized that MRI alone does not have the necessary sensitivity, requiring most centers to add 12-core systematic biopsy after performing the targeted biopsy. Mendhiratta et al. compared targeted mpMRI biopsy with the additional 12-core systematic biopsy in 452 men undergoing prostate cancer detection [7]. Systematic biopsy detected more prostate cancer than the targeted biopsy (49.2 % vs. 43.5 %, $p = 0.006$). However MRI did have the advantage in detecting more Gleason score (GS) 7 lesions than did the 12-core procedure (88.6 % vs. 77.3 %, $p = 0.037$). Nassiri and others recently reported the experience from the University of California, Los Angeles (UCLA), in more than 1200 targeted biopsies and noted that 15–30 % of "potentially important prostate cancers" are MRI invisible [8, 9].

Several review studies have been published evaluating the utility of mpMRI in detecting significant prostate cancer. Fütterer et al. evaluated 12 articles using prostatectomy data as the reference standard [10]. The negative predictive value for the exclusion of clinically significant disease ranged from 63 to 98 %. Part of the difficulty is analyzing data from different institutions is the lack of a common definition of significant disease. These included maximum cancer core length, grade at biopsy, number of positive cores, and PSA.

Wysock investigated the use of 12-core biopsy in men with negative 3 T mpMRI [11]. In the 75 men studied, the negative predictive value (NPV) for all cancers was 82 % and for GS >7 was 98 %. While this study might provide some reassurance that a negative mpMRI does not require biopsy confirmation of lack of significant disease, it should be recognized that the confirmation in the Wysock study relied on the same technology that is being replaced by MRI: the 12-core semi-blind procured from the 1980s. To overcome this limitation, several centers have compared the MRI-detected lesions to prostatectomy specimens. Le et al. investigated 122 men who had mpMRI with prostate cancer detected and compared them to whole-mount histopathology [12]. Overall mpMRI sensitivity for tumor detection was 47 % (132/283) with increased sensitivity for larger (102/141 [72 %] >1.0 cm) and higher-grade

(96/134 [72 %] Gleason >7) and index tumors (98/122 [80 %]). One of the limitations in this study was that visual concordance was used by the uroradiologist and genitourinary pathologist to determine agreement between the MRI and prostatectomy specimens. The lack of digital co-registration adds additional error into their estimates of concordance.

Vargas et al. used the Prostate Imaging Reporting and Data System (PI-RADS) v2 for detection of clinically significant prostate cancer and compared the results in 150 prostatectomy specimens [13]. In this study the whole-mount specimens were digitized, but no information was provided about whether the images were co-registered to the MR images. PI-RADS correctly identified high-grade tumors >0.5 mL 94–95 % of the time. For lesions smaller than 0.5 mL, it was only successful in 20–26 %. It is important to recognize a lesion with a volume of 0.5 mL had a linear dimension of 8 mm in three planes (assuming a sphere). Missing high-grade lesions of this size in more than three-quarters of men who may be harboring them is worrisome.

Transperineal Prostate Mapping Biopsy

It is interesting to note that both the ultrasound-guided TRUS biopsy and TPMB were described in 1987 [14]. TPMB has emerged as an alternative to TRUS biopsy, but due to lack of proper instrumentation, the need for anesthesia other than local has stymied its development. Nonetheless, many investigators have published their results and compared them to TRUS and targeted MRI biopsy results and to prostatectomy specimens. Symons et al. performed TPMB on 409 men and found prostate cancer in 208 (50.9 %) of which 75 % were GS >7 [15]. In a study of 431 radical prostatectomy (RP) specimens, of which prostate cancer was diagnosed by TRUS (283) or TPMB (184), those men who had the latter were more likely to be assigned the actual clinical risk category [16]. Serrao et al. performed transperineal-targeted MRI biopsy followed by 24–36 sectoral mapping biopsies [17]. MRI-positive scans (mean 1.57 lesions/patient, median 2) had positive pathology in 75 %. Of the 220 positive biopsies, 46 (20.9 %) were in areas determined falsely negative on MRI.

Sivaraman et al. investigated the use of TPMB in men with negative mpMRI [18]; 27/75 (36 %) had prostate cancer. The detection of clinically significant cancer (depending on the definition) ranged from 22.7 to 30.7 %. Toner performed a MEDLINE and PubMed database search comparing mpMRI with RP or TPMB histology [19]. The analysis found that compared with RP and TPMB specimens, the sensitivity of mpMRI for prostate cancer detection was 80–90 % and the specificity for suspicious lesions is between 50 % and 90 %.

While it is clear that TPMB is superior to TRUS and perhaps targeted mpMRI biopsy, it is not without challenges. There is no standardized protocol on how many biopsies to obtain. While most agree that the 5 mm external template should be used, how thoroughly to sample the gland remains undefined. Pham et al. performed an investigation using two TPMB approaches [20]. The biopsy technique was based on a 24-core template with 12 anterior and 12 posterior cores or a template based on gland volume with 1 core per cc (median 62 cores). No significant difference was noted in upgrading or complications between the two techniques. Valerio et al. utilized different mapping zones when performing a 20-core TPMB approach. Strategy 1 involved excluding the anterior areas of the prostate representing the transition area, but not the anterior horns, which were sampled within the lateral zones. Strategy 2 and strategy 3 involved a reduced sampling density from 5 to 10 mm by omitting intervening areas. Strategies 1, 2, and 3 had sensitivities of 78 % (95 % confidence interval [CI] 73–84 %), 85 % (95 % CI 80–90 %), and 84 % (95 % CI 79–89 %), respectively. The NPVs of the three strategies were 73 % (95 % CI 67–80 %), 80 % (95 % CI 74–86 %), and 79 % (95 % CI 72–84 %), respectively. The authors stated that altering the TPMB sampling strategy by preferential sampling of certain locations or reducing the sampling density led to significant reductions in the ability of the test to exclude clinically significant cancers.

Focal Therapy Considerations Associated with Magnetic Resonance Imaging-Detected Lesions

The data presented herein has made it clear that the clinician cannot rely on MRI to exclude significant disease or to exclude disease in regions of the prostate not identified as regions of interest (ROI) for biopsy. However, even when an ROI is found to contain prostate cancer and targeted focal therapy is considered, how reliable is the MRI in demarcating the volume to be ablated? Cornud et al. evaluated 84 consecutive patients who underwent mpMRI before radical prostatectomy [21]. The volume of each suspicious area detected on magnetic resonance imaging and of all surgical histological foci was determined by planimetry. Histology revealed 99 significant tumors with a volume of greater than 0.2 cc and/or a Gleason score of greater than six. Of the tumors, 16 (16.2 %) were undetected by mpMRI. Linear regression analysis showed that tumor volume estimated by T2-weighted or diffusion-weighted imaging correlated significantly with pathological volume (r^2 = 0.82 and 0.83, respectively). Nevertheless, diffusion-weighted imaging underestimated pathological volume in 43 of 87 cases (49 %) by a mean of 0.56 cc (range 0.005–2.84). Multiparametric and target volumes significantly overestimated pathological volume by a mean of 16 % and 44 %, with underestimation in 28 (32 %) and 15 cases (17 %), respectively. Volume underestimation was significantly higher for tumor foci less than 0.5 cc.

Failure to identify all significant lesions, incorrect estimation of tumor size, and inability of creating a sufficiently accurate treatment map are some of the reasons focal prostate ablation remains an investigational exercise. Other issues also compromise the successful introduction of a focal ablation program. While mpMRI can identify larger high-grade disease with high sensitivity, its ability to find GS 6 cancer is very limited. The elimination from consideration of identifying and potentially treating these lesions could compromise any focal therapy program. Haffner et al. used whole-genome sequencing and molecular pathological analyses to characterize the lethal cell clone in a patient who died of prostate cancer [22]. The lethal clone arose from a small, relatively low-grade cancer focus in the primary tumor, and not from the bulk, higher-grade primary cancer or from a lymph node metastasis resected at prostatectomy. In an opposing view editorial, Gonzalgo summarized many of the concerns surrounding focal therapy for prostate cancer. Treating only the index lesion may compromise cancer control because of inadequate treatment of potentially lethal disease [23]. There is significant interfocal tumor heterogeneity in prostate cancer and, from a molecular standpoint, metastasis may arise from secondary tumor foci. To date, there remains no good scientific evidence to support the fundamental basis of the index lesion theory. In fact, recent data suggest that more aggressive and potentially lethal disease can be found outside of the index lesion [24]. These and other concerns prompted the US Food and Drug Administration (FDA) to hold a workshop at the 2015 American Urological Association (AUA), which culminated in a publication in 2016 stating: “The general consensus was that currently available technologies are capable of selective ablation with reasonable accuracy, but that criteria for patient selection remain debatable, and long term cancer control remains to be established in properly designed and well-performed prospective clinical trials. Concerns include the potential for excessive, unnecessary use in patients with low risk cancer and, conversely, that current diagnostic techniques may underestimate the extent and aggressiveness of some cancers, leading to inadequate treatment” [25].

The 3D Biopsy Approach

After nearly three decades of performing TRUS-guided biopsy, the diagnosis and treatment of prostate cancer has become very challenging. TRUS-guided biopsies identify many cancers that do not need to be treated while missing potentially lethal disease. Men who go on active surveillance are not appropriate candidates

because they were incorrectly identified as low risk based on the TRUS biopsy results. In order to improve the thorough sampling, Crawford described the use of computer simulation to map prostate transperineal biopsies [26]. This innovative approach could record lesion location but was limited because biopsy sites were annotated off-line. Stone, working with interactive software, developed a real-time computer-simulated prostate brachytherapy program [27]. 3DBiopsy, Inc., was formed in 2012 with the intention of refining the TPMB technique so its biopsy plan accurately finds all the disease within the prostate. The clinician would then decide what therapy is most appropriate and, in the case of focal therapy, which lesions (some or all) would need to be treated. In men with truly very-low-risk prostate cancer, active surveillance would become accurate surveillance as future biopsies, and frequent PSA testing could be eliminated.

In order to accomplish this goal, several components needed to be changed. First is a requirement that a biopsy plan needs to be created that had a high probability of sampling all lesions within the gland, regardless of Gleason score. Kepner discussed an approach to distributing transperineal prostate biopsy cores that yields data on the volume of a tumor that might be present when the biopsy is negative [28]. If the biopsy sites are parallel and spaced 5 mm apart and a 15-gauge biopsy needle is used, then the theoretical probability of encountering a lesion of 2.5 mm radius is 98 % (Fig. 18.1).

In order to put this approach into practice, three devices needed to be developed: First, a software program that generates a biopsy plan based on a reconstructed three-dimensional (3D) model of the prostate generated from the transrectal ultrasound images. Second, a variable biopsy needle apparatus that samples the prostate from apex to base as one core. And third, a pathology carrier system where the physician places the specimen after biopsy that preserves the integrity of the core and allows the pathologist to render a diagnosis that included location and length of cancer on the specimen.

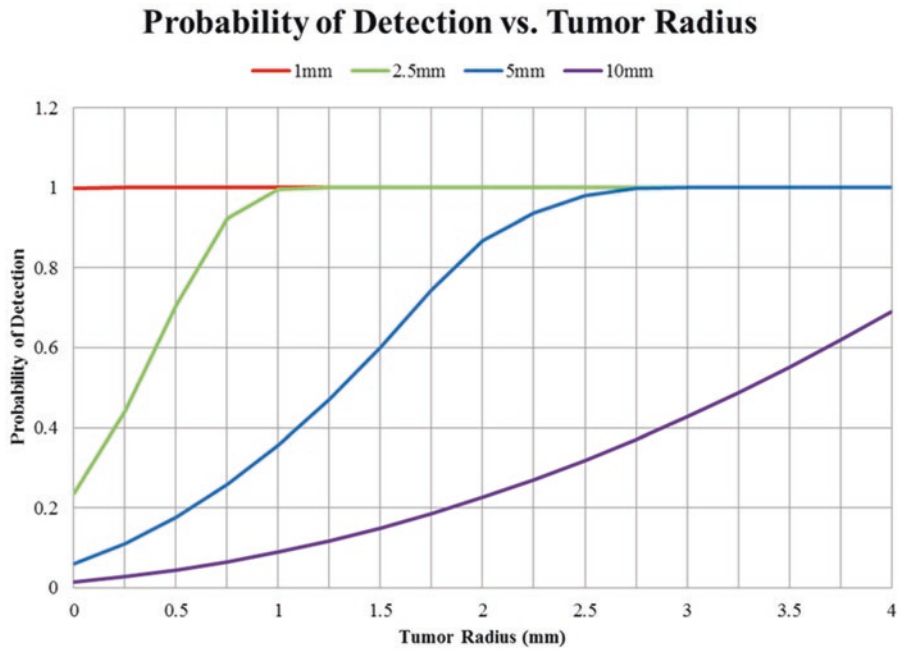

Fig. 18.1 The *blue line* represents 5 mm grid spacing utilizing a 15-gauge biopsy needle taking parallel cores as one specimen from apex to base

The results of these three are then integrated into a precise 3D model of the prostate and the areas of cancer.

3DBiopsy Digital Image-Guided Software

The requirements of the software are:

1. Generate 3D reconstruction of the prostate, seminal vesicles, bladder, urethra, and rectum from live ultrasound transverse images obtained in the operating room at time of biopsy (TPMB method).
2. Generate a biopsy plan specific to parameters set by user:
   (a) Distance from capsule and urethra
   (b) Size of biopsy needle
   (c) Full-length core or multiple in-line specimens
   (d) Virtual needle movement to align to actual biopsy needle in axial and sagittal planes
   (e) Probability score (necessary to make decisions to add or remove virtual needles as a result of needle and gland motion)
3. At the end of the biopsy procedure, generate a 3D record.
4. After pathology report, upload sites and locations of lesions and display in 3D (for patient and record).
5. Utilize 3D file to provide roadmap for focal therapy (output file in DICOM for treatment planning).
6. Incorporate MR images for targeted ROI biopsies.

Based on these requirements, a software program was designed utilizing prostate phantoms and a brachytherapy ultrasound setup (Fig. 18.2).

Each 5 mm axial US image of the prostate is segmented and the biopsy plan generated. When the biopsy needle passes through the template and enters the prostate, the virtual needle needs to move to match the actual needle. This maneuver aligns the needle in the axial plane. The inserted needle may reside up to one millimeter away from the virtual needle. There is no need to reinsert the needle (Fig. 18.3).

Figure 18.3 shows the biopsy-generated plan on prostate phantom. The prostate, urethra, and rectum have been contoured. The pointer is on needle #1, which is dragged to overlie the inserted needle.

Imaging is switched to sagittal and the two needles are lined up in this plane (Fig. 18.4).

The pathology report is returned to the urologist highlighting the positive cores with the Gleason sum. Each positive site is entered into the patient's file (Fig. 18.5).

The beta version of the 3DBiopsy software was completed at the end of 2014 and tested. To date 61 cases have been performed; 35/61

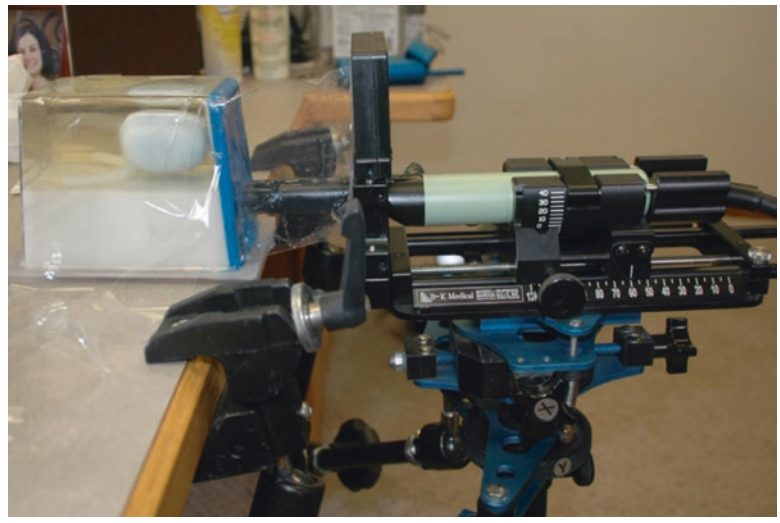

Fig. 18.2 Phantom setup for software design

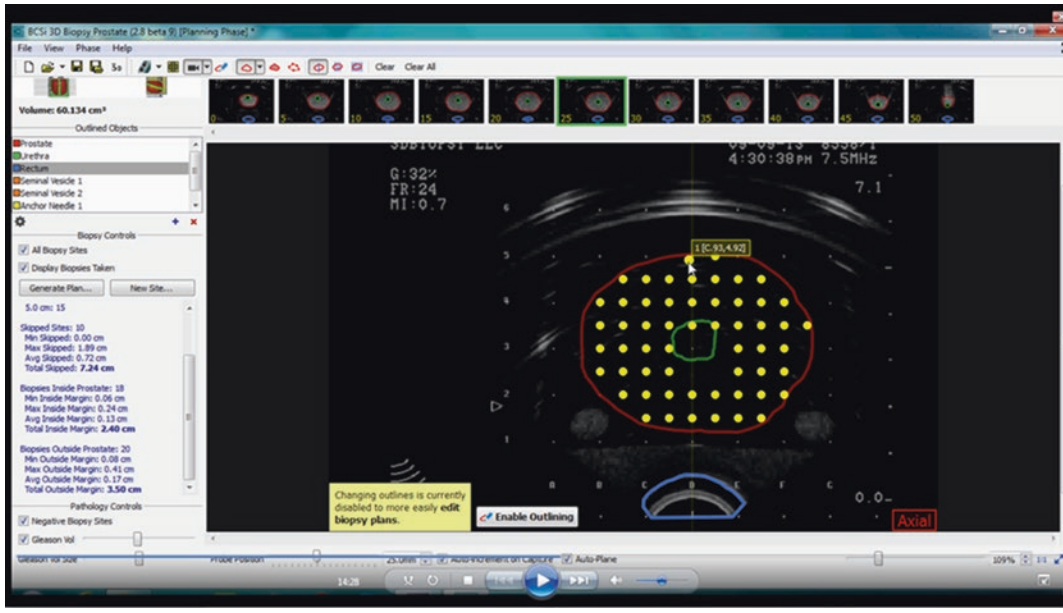

Fig. 18.3 Biopsy-generated plan on prostate phantom. The prostate, urethra, and rectum have been contoured. The pointer is on needle #1, which is dragged to overlie inserted needle

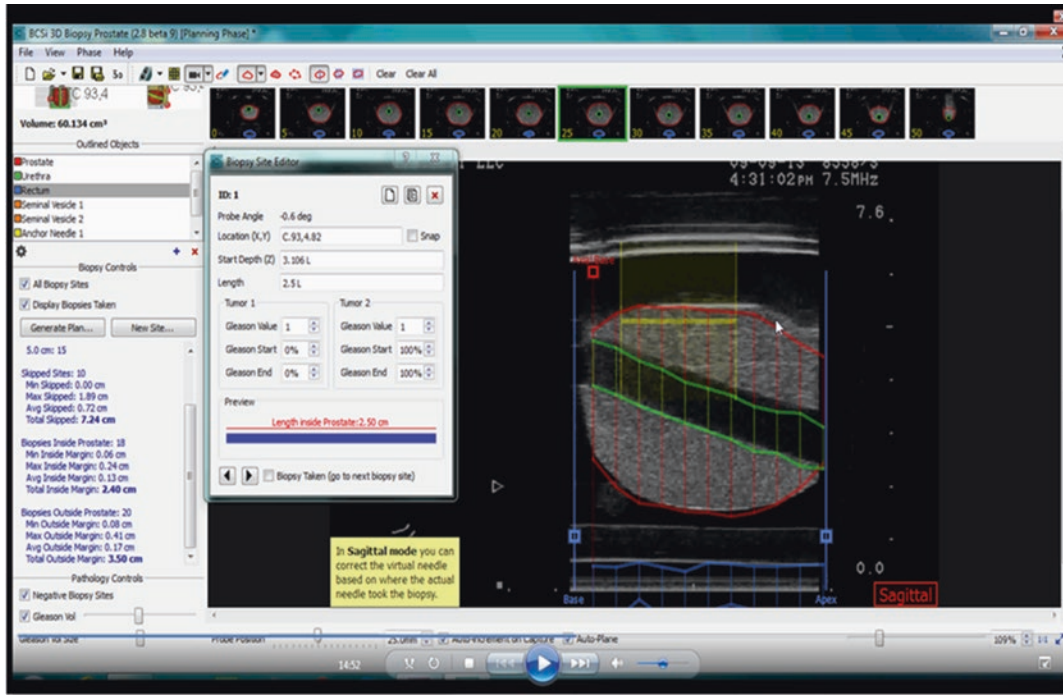

Fig. 18.4 Needle #1 in sagittal plane. Note that the dialogue box contains information on needle coordinates as well as needle length. The *yellow* virtual needle specimen length is 2.5 cm (not possible with current biopsy needle technology). As it appears too short to cover the entire length of the gland (apex to base), the user can add additional millimeters to specimen in the dialogue box so the core will span the full length of the gland

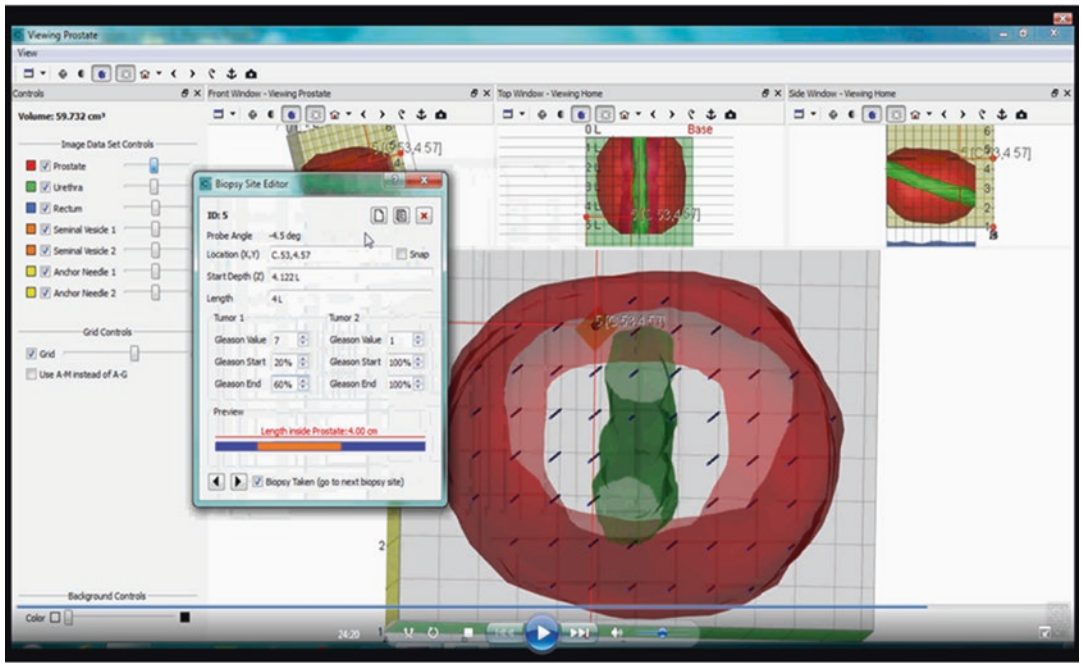

Fig. 18.5 Three-dimensional (3D) reconstruction with pathology entered at biopsy site 5. The GS 7 cancer is depicted in *orange*. The left side of the *blue specimen* represents the base of the gland at that site. Note that the *orange* lesion appears in the 3D prostate model, which can be rotated to different views

(57.3 %) had prior TRUS biopsy of which 23 were positive for one or two core minimal GS 6 or 7 disease. The purpose of the mapping biopsy was to perform intraprostatic staging for treatment selection. Of the 61 patients, 37 (60.7 %) were positive for prostate cancer with GS 6, 7, 8, and 9 in 12 (32.4 %), 22 (59.5 %), 1 (2.7 %), and 2 (5.4 %), respectively. There was a median 49.5 biopsies taken with a median of four positive cores (mean 5.8, range 1–23). Based on the 3DBiopsy results, treatment selection was accurate surveillance in 2 (5.4 %), radical prostatectomy in 7 (18.8 %), radiation therapy in 16 (43.2 %), targeted focal therapy in 10 (27 %), and undecided in 2 (5.4 %). The RP patients had a median of ten cores positive on 3DBiopsy, and the surgical specimens had GS 7 in 6 and GS 8 in 1; bilateral disease in 85.7 %; perineural invasion in 85.7 %; stage pT2b in 1, pT2c in 4, and pT3 in 2; and positive margins in 57.1 %. In contrast, of the ten men who had TFT with cryoablation, the number of positive cores was a median of three, GS was 6 or 7 in 5 each, and disease was bilateral in 6 (60 %). The 3DBiopsy file for the TFT patients provided the roadmap when performing the highly selective ablation in these ten patients even when bilateral disease was present. This initial study demonstrates the ability of a software-based TPMB program to improve patient treatment choice and guide focal ablation.

Improved Transperineal Mapping Biopsy Devices

The biopsy needle and actuator (gun) being used for TRUS biopsy (targeted or systematic) is the same one used for TPMB (including the aforementioned study). This needle, developed 30 years ago, is no longer appropriate for prostate biopsy, regardless of the approach. A properly designed biopsy needle would have no minimal deflection (entry and end points are in the same

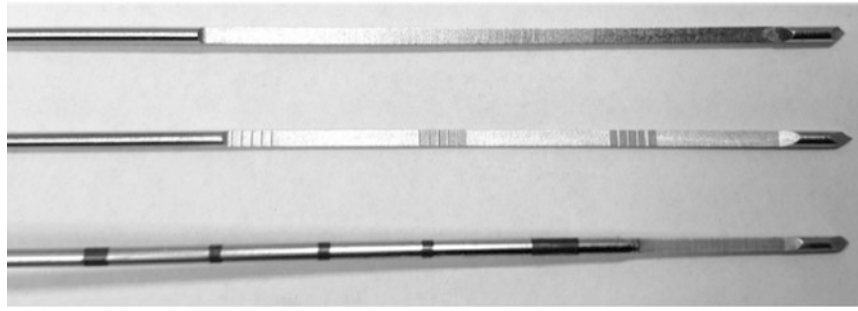

Fig. 18.6 Three needle types tested for deflection and core integrity. The *top* is a 15-G trocar tip, the middle is a 15-G trocar tip with "ridges" and the *lower* is the Bard lancet tip biopsy needle

plane), and the amount of tissue collected is consistent with the amount required (a 4 cm specimen length should be 4 cm). The biopsy needles used today suffer from significant deflection and marked core inconsistency. Nobody really cared previously because the focus was to make a diagnosis of cancer. Today with lesions substantially smaller (and in most cases microscopic) and when trying to reach an anterior ROI, needle deflection and core integrity are more critical. Brede and Jones examined needle defection using a 5 mm grid and found only 22 % shallow and 7 % deep precision [29]. The Bard MaxCore biopsy needle (C.R. Bard, Inc., Covington, Georgia, USA) was used for this study, which has a bevel or lancet tip design.

Satasivam et al. examined fragmentation of specimen cores taken by TRUS biopsy [30]. Although the biopsy needle type was not specified, substantial fragmentation was noted with the standard swipe technique, and core length and specimen length varied from 12.4 to 13.4 mm (73–79 % of full length). Öbek et al. performed a similar study and noted mean core length in patients with prostate cancer was 12.3 mm (72 %) vs. 11.4 mm (66 %) in those without ($p = 0.015$). Patients with a core length greater than 11.9 mm were 2.57 times more likely to be diagnosed with cancer [31].

In order to overcome these limitations, a new needle design and actuator have been under development. The needle tip was changed from lancet to trocar with various designs tested in gelatin matrix simulating prostate density (Fig. 18.6).

The Bard needle deflected a median of 0.9 mm (range 0.0–1.3), while the trocar tip needles deflected a median of 0 mm (range 0–1.7 mm, $p < 0.001$). Needle size (15-G vs. 18-G) did not affect deflection. Obtaining full intended length core length is also a necessary component of the needle design. When trying to obtain the entire length of the prostate in one sample, if the software designates 4 cm and only 2.8 cm is delivered, the remaining 1.2 cm is questionable. Testing of different needle designs demonstrated the 15-G trocar tip needle depicted in the top of Fig. 18.6 performed no better than the Bard needle. However, the addition of ridges to the core bed, which secures the specimen as the cutting portion of the cannula passes over it, resulted in a 92 % core consistency rate (over various lengths between 2 and 6 cm).

The new variable-length needle would not be useful without a companion actuator to fire it a variable distance. This device has also been developed and tested. The physician can dial the desired length of the specimen as dictated by the software. Each specimen length will vary depending on the length of the prostate when the probe is obliquely rotated away from the midline of the prostate. This actuator combined with the new needle would also be ideal for targeted MRI biopsies. When anterior lesions are present, the user can puncture the posterior capsule of the gland, dial the distance to the anterior capsule, and fire the gun to take a full-length specimen. The specimen will not only contain the entire cancer but also the noncancerous tissue on either side of it. Planning focal therapy with this additional information would be invaluable.

Integrated Pathology System

The process to handle tissue specimens has not substantially changed in more than 100 years. Take a specimen, drop it in formalin, and send it to the lab is the routine. In the past, there was not much concern because clinicians were only interested in knowing whether cancer was on the specimen and what type it was. The new biopsy system necessitates a substantial change in the carrier mechanism. The longer (up to 6 cm) cores need to be preserved intact so the pathologist can render an accurate diagnosis on cancer location and length on every positive core. In addition, staff have to manage an increased number of specimens (16–20 for MRI-targeted biopsy and 30 for the new 3DBiopsy). Specimen providence errors are not uncommon, and handling each core, in the OR and pathology lab, increases the risk of fragmentation [30]. Wojno et al. estimated a 2.5 % specimen providence error rate for prostate biopsies costing $879,900,000 per year in the USA [32]. Most of these cases were 12-core systematic TRUS biopsies. Increasing the number of specimens will likely increase the costs of managing these errors.

The solution to these problems was to develop a carrier system that secures the specimen, delivers it to the technicians intact, and eliminates the need to remove the specimen from the carrier. The specimen remains in the carrier through formalin fixation, processing, paraffin embedding, microtome sectioning, staining, and reading. The device is also under development (Fig. 18.7).

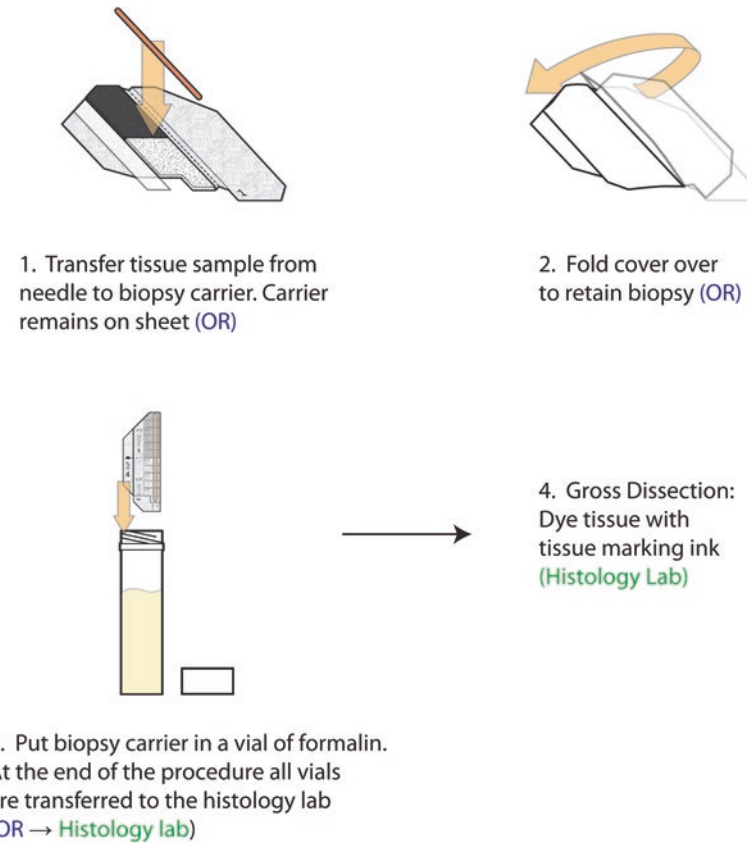

Fig. 18.7 The integrated pathology system (IPS) secures the specimen in the carrier device and preserves its integrity from the operating room (OR) or clinic through all of the required steps for final pathologic assessment

Conclusion

The diagnosis and management of prostate cancer is evolving rapidly. The current focus is to biopsy men at risk of harboring significant cancers. In most other cancers that we treat, whether it be lung, breast, or colorectal cancers, we stage them. We employ positron emission tomography (PET) scans, computed tomography (CT) scans, bone scans, and others to determine the extent of disease. In localized prostate cancer, these tests do not help. We want to know what is in the gland and where. Currently TRUS and even saturation biopsies do not help. Multiparametric MRI is much more helpful; however, as already reviewed, it can miss up to 20–30 % of potentially progressive and lethal cancers.

Having precise knowledge of the 3D location of the cancers is clearly going to change how we manage these patients and thereby reduce the current dominant roles of both radical prostatectomy and radiation therapy. Precise intraprostatic staging will afford some patients the opportunity to be followed without treatment because the fear of missing a lethal cancer will be greatly diminished. A large group of newly diagnosed men, perhaps as many as 1 in 3, will be candidates for targeted focal therapy because clinicians will have precise knowledge of the location of all lesions and be able to deliver the ablative treatment to the exact sites. Whether MRI or an improved biopsy strategy, as depicted here, will be the best means to achieve these results will need to be determined by prospective clinical trials.

References

1. Lee F. Transrectal ultrasound in the diagnosis, staging, guided needle biopsy, and screening for prostate cancer. Prog Clin Biol Res. 1987;237:73–109.
2. Stone NN, Crawford ED, DeAntoni EP, The Prostate Cancer Education Council. Screening for prostate cancer by digital rectal exam and prostate specific antigen: results of prostate cancer awareness week, 1989-1992. Urology. 1994;44:18–25.
3. Brawer MK. Screening for prostate cancer. Monogr Urol. 1994;15:1–24.
4. Metttin C. The status of prostate cancer early detection. Cancer. 1993;72:1050–5.
5. Onik G, Vaughan D, Lotenfoe R, Dineen M, Brady J. "Male lumpectomy": focal therapy for prostate cancer using cryoablation. Urology. 2007;70:16–21.
6. Meiers I, Waters DJ, Bostwick DG. Preoperative prediction of multifocal prostate cancer and application of focal therapy: review 2007. Urology. 2007;70:3–8.
7. Mendhiratta N, Rosenkrantz AB, Meng X, Wysock JS, Fenstermaker M, Huang R, et al. Magnetic resonance imaging-ultrasound fusion targeted prostate biopsy in a consecutive cohort of men with no previous biopsy: reduction of over detection through improved risk stratification. J Urol. 2015;194(6):1601–6.
8. Nassiri N, Natarajan S, Margolis DJ, Marks LS. Targeted prostate biopsy: lessons learned midst the evolution of a disruptive technology. Urology. 2015;86(3):432–8.
9. Filson CP, Natarajan S, Margolis DJ, Huang J, Lieu P, Dorey FJ, et al. Prostate cancer detection with magnetic resonance-ultrasound fusion biopsy: The role of systematic and targeted biopsies. Cancer. 2016;122(6):884–92.
10. Fütterer JJ, Briganti A, De Visschere P, Emberton M, Giannarini G, Kirkham A, et al. Can clinically significant prostate cancer be detected with multiparametric magnetic resonance imaging? A systematic review of the literature. Eur Urol. 2015;68(6):1045–53.
11. Wysock JS, Mendhiratta N, Zattoni F, Meng X, Bjurlin M, Huang WC, et al. Predictive value of negative 3 T multiparametric prostate MRI on 12 core biopsy results. BJU Int. 2016;118(4):515–20. doi:10.1111/bju.13427.
12. Le JD, Tan N, Shkolyar E, Lu DY, Kwan L, Marks LS, et al. Multifocality and prostate cancer detection by multiparametric magnetic resonance imaging: correlation with whole-mount histopathology. Eur Urol. 2015;67(3):569–76.
13. Vargas HA, Hötker AM, Goldman DA, Moskowitz CS, Gondo T, Matsumoto K, et al. Updated prostate imaging reporting and data system (PIRADS v2) recommendations for the detection of clinically significant prostate cancer using multiparametric MRI: critical evaluation using whole-mount pathology as standard of reference. Eur Radiol. 2016;26(6):1606–12.
14. Vallancien G, Leo JP, Brisset JM. Transperineal prostatic biopsy guided by transrectal ultrasonography. Prog Clin Biol Res. 1987;243B:25–7.
15. Symons JL, Huo A, Yuen CL, Haynes AM, Matthews J, Sutherland RL, et al. Outcomes of transperineal template-guided prostate biopsy in 409 patients. BJU Int. 2013;112(5):585–93.
16. Scott S, Samaratunga H, Chabert C, Breckenridge M, Gianduzzo T. Is transperineal prostate biopsy more accurate than transrectal biopsy in determining final Gleason score and clinical risk category? A comparative analysis. BJU Int. 2015;116(Suppl 3):26–30.
17. Serrao EM, Barrett T, Wadhwa K, Parashar D, Frey J, Koo BC, et al. Investigating the ability of multiparametric MRI to exclude significant prostate cancer prior to transperineal biopsy. Can Urol Assoc J. 2015;9(11–12):E853–8.

18. Sivaraman A, Sanchez-Salas R, Ahmed HU, Barret E, Cathala N, Mombet A, et al. Clinical utility of transperineal template-guided mapping biopsy of the prostate after negative magnetic resonance imaging-guided transrectal biopsy. Urol Oncol. 2015;33(7):329.e7–11.
19. Toner L, Weerakoon M, Bolton DM, Ryan A, Katelaris N, Lawrentschuk N. Magnetic resonance imaging for prostate cancer: comparative studies including radical prostatectomy specimens and template transperineal biopsy. Prostate Int. 2015;3(4):107–14.
20. Pham KN, Porter CR, Odem-Davis K, Wolff EM, Jeldres C, Wei JT, et al. Transperineal template guided prostate biopsy selects candidates for active surveillance–how many cores are enough? J Urol. 2015; 194(3):674–9.
21. Cornud F, Khoury G, Bouazza N, Beuvon F, Peyromaure M, Flam T, et al. Tumor target volume for focal therapy of prostate cancer-does multiparametric magnetic resonance imaging allow for a reliable estimation? J Urol. 2014;191(5):1272–9.
22. Haffner MC, Mosbruger T, Esopi DM, Fedor H, Heaphy CM, Walker DA, et al. Tracking the clonal origin of lethal prostate cancer. J Clin Invest. 2013;123(11):4918–22.
23. Gonzalgo ML. Focal therapy for prostate cancer: don't believe the hype. J Urol. 2015;194(4):876–7.
24. Boutros PC, Fraser M, Harding NJ, de Borja R, Trudel D, Lalonde E, et al. Spatial genomic heterogeneity within localized, multifocal prostate cancer. Nat Genet. 2015;47:736–45.
25. Jarow JP, Ahmed HU, Choyke PL, Taneja SS, Scardino PT. Partial gland ablation for prostate cancer: report of a Food and Drug Administration, American Urological Association, and Society of Urologic Oncology Public Workshop. Urology. 2016;88:8–13.
26. Crawford ED, Wilson SS, Torkko KC, Hirano D, Stewart JS, Brammell C, et al. Clinical staging of prostate cancer: a computer-simulated study of transperineal prostate biopsy. BJU Int. 2005;96:999–1004.
27. Stone NN, Hong S, Lo YC, Howard V, Stock RG. Comparison of intraoperative dosimetric implant representation to post-implant dosimetry in patients receiving prostate brachytherapy. Brachytherapy. 2003;2(1):17–25.
28. Kepner GR, Kepner JV. Transperineal prostate biopsy: analysis of a uniform core sampling pattern that yields data on tumor volume limits in negative biopsies. Theor Biol Med Model. 2010;7:23.
29. Brede CM, Douville NJ, Jones S. Variable correlation of grid coordinates to core location in template prostate biopsy. Curr Urol. 2013;6(4):194–8.
30. Satasivam P, Thomas R, Rao K, Jack GS, Lawrentschuk N, Bolton DM. Fragmentation of transrectal ultrasound-guided biopsy cores is influenced by the method of specimen retrieval. Urology. 2014; 83(3):622–5.
31. Öbek C, Doğanca T, Erdal S, Erdoğan S, Durak H. Core length in prostate biopsy: size matters. J Urol. 2012;187(6):2051–5.
32. Wojno K, Hornberger J, Schellhammer P, Dai M, Morgan T. The clinical and economic implications of specimen provenance complications in diagnostic prostate biopsies. J Urol. 2015;193(4):1170–7.

Multiparametric Transrectal Ultrasound Biopsy

19

Arnoud W. Postema, Jochen Walz, and Hessel Wijkstra

Introduction

Ultrasound (US) has been the standard method for prostate imaging for decades. Transrectal ultrasound (TRUS) is used for prostate volumetry, needle guidance during systematic prostate biopsies, brachytherapy guidance, and real-time monitoring during focal therapy. The widespread usage of US within prostate cancer diagnostic and therapeutic pathways relates to its many advantages: There are no harmful radiation or nephrotoxic contrast agents involved, making it safe and repeatable. Ultrasound equipment is mobile and less costly compared to that of other imaging modalities. Ultrasound imaging is real time, and there is a lot of experience with US within the urological community. From a technical standpoint, the close proximity between the US transducer during TRUS and the prostate combined with the technical characteristics of US allows imaging at much higher resolutions and frame rates than can be achieved with other imaging modalities [1]. Downsides of ultrasound are the user dependency and learning curve. Although three-dimensional (3D) imaging is available, ultrasound is still mostly performed in two dimensions (2D). TRUS allows detailed visualization of the prostate, but early prostate cancer (PCa) is hard to detect with standard grayscale TRUS. The sensitivity of grayscale TRUS reported in the literature varies but is often cited to be 11–35 % [2]. Some large modern series have reported sensitivities up to 59 %, reflecting the known distribution of echogenicity of prostate cancer [3, 4]. The positive predictive value of a hypoechoic lesion is only 17–57 % [5]. Several systems for computerized analysis of grayscale TRUS images exist that attempt to improve the diagnostic accuracy [6]. The artificial neural network analysis/computerized transrectal ultrasound (ANNA/C-TRUS) system has shown the best results in clinical testing thus far. TRUS images are sent to the ANNA/C-TRUS server through a secure connection; C-TRUS then uses an ANNA algorithm to analyze the ultrasound signals and highlight suspicious areas [7]. With a maximum of six targeted biopsies, PCa was found in 31/75 (41 %) patients without prior biopsy. An external validation study in 28 patients using radical prostatectomy (RP) specimens as a reference standard showed a sensitivity, specificity, positive predictive value (PPV), and negative predictive value (NPV) of 83 %,

A.W. Postema (✉) • H. Wijkstra
Department of Urology, Academic Medical Center (AMC) University Hospital, Amsterdam, The Netherlands
e-mail: a.w.postema@amc.uva.nl

J. Walz
EAU Section of Urological Imaging (ESUI), Department of Urology, Institut Paoli-Calmettes Cancer Centre, Marseille, France

© Springer International Publishing AG 2017

T.J. Polascik (ed.), *Imaging and Focal Therapy of Early Prostate Cancer*, Current Clinical Urology, DOI 10.1007/978-3-319-49911-6_19

64 %, 80 %, and 63 %, respectively [8]. Histoscanning is another system for computerized analysis of 3D grayscale TRUS images. The original article by Braeckmann et al. showed promising results, with all tumors larger than 0.5 mL being detected in 13 men [9]. Subsequent publications were not able to confirm these initial results, and a 2015 meta-analysis concluded that there is little evidence for the value of histoscanning in the larger patient cohorts [10]. The latest data coming from a cohort of 282 patients who underwent histoscanning prior to RP show a sensitivity of 16–54 % and a specificity of 59–92 % for the detection of lesions bigger than 0.5 mL [11]. In a separate development, preliminary results with a high-frequency "micro-ultrasound" TRUS system have been reported [12]. The system acquires TRUS images at 29 MHz, allowing anatomical imaging at a spatial resolution of about 70 microns. The ongoing development trial and external validation must prove whether it has a place in prostate cancer imaging. Similar to the functional sequences developed for MRI, two advanced US modalities are being developed that evaluate the changes in tissue stiffness and vascularity that are associated with PCa: (shear wave) elastography and contrast ultrasound. The remainder of this chapter will focus on these modalities and the advances made to combine the different US techniques into multiparametric ultrasound.

Elastography

Technical Aspects of Elastography

Elastography is an ultrasound-based technology for prostate cancer detection and treatment. The aim of this technology is to evaluate tissue stiffness by using ultrasound as information source. The rationale behind the use of elastography for prostate cancer management is the observation that prostate cancer tissue is harder or denser then benign prostate tissue. This observation is well known from the digital rectal exam (DRE), where indurations of the prostate are suspicious for prostate cancer, as well as from mechanical elasticity testing of prostate tissue. Such mechanical ex vivo tests showed an average elasticity for prostate cancer tissue of 40.4 ± SD 15.7 kPa and for benign prostate tissue of 15.9 ± SD 5.9 kPa and a ratio between the two tissue types of 2.6 ± SD 0.9 [13]. Several companies offer this technology for their ultrasound scanners, and several possibilities exist to generate the elastogram. In urology the most frequently used systems are the real-time elastography system and the shear wave elastography system. The real-time elastography system generates the elastogram of the prostate by an analysis of tissue strain generated by compression and decompression of the tissue with the help of the transrectal ultrasound probe. The rhythmic compression and decompression result in displacements inside the ultrasound picture where softer areas show higher amplitude of displacement and harder areas show lower amplitude. This information is transferred into an elastogram or cartography showing areas with relatively higher tissue stiffness (coded blue) or relatively lower tissue stiffness (coded red) [14, 15]. This analysis is provided in real time and can be repeated without limitation. The elastogram with the real-time elastography system gives information about relative tissue stiffness inside of the ultrasound picture but does not allow any objective measurements of tissue elasticity or density. Moreover, the quality of the tissue evaluation depends on the quality of the tissue compression and decompression. Visual indicators help to provide a reproducible and reliable quality. This system is most extensively evaluated for the use in the diagnosis of prostate cancer as well as for the use in treatment of prostate cancer. Most of the other elastography systems available on the market are based on a similar analysis, but their use in urology is limited [16]. The shear wave elastography system provides a different analysis. The system is based on an ultrafast analysis of the ultrasound picture using plane wave transmission instead of rapidly aligned individual sector sound wave emissions [17]. This analysis allows to capture the speed of acoustic shear waves in the tissue that are generated by push pulses from focused ultrasound beams (acoustic radiation force palpation). These

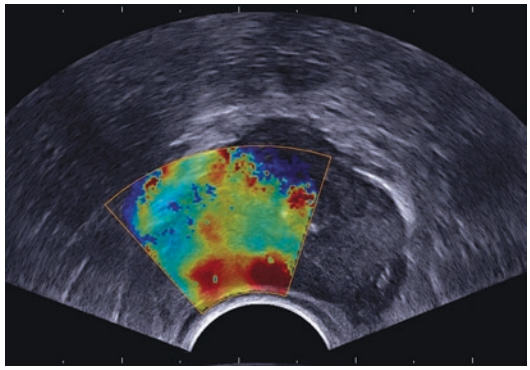

Fig. 19.1 Shear wave elastography of the prostate. A stiff (*red*) area is visible in the right peripheral zone. Prostate cancer was confirmed on whole mount section after radical prostatectomy

shear waves extend perpendicular to the sound waves in the tissue, and their extension speed depends on the tissue density. The speed is higher in dense tissue and lower in softer tissue. These differences in speed are used to generate an elastogram providing a color coding, where harder areas are coded red and softer areas are coded blue (Fig. 19.1) [18, 19]. On the other hand, the system provides absolute elasticity expressed either as speed of the shear waves in m/sec or as a true elasticity measurement in kPa. Similar to the real-time elastography system, the shear wave elastography system provides the analysis in real time with a frequency of 1 Hz = 1 frame/s. It is of note that several frames are necessary per analysis to achieve stable tissue elasticity measurements. The absolute elasticity measurements can be used as absolute numbers using regions of interest (ROI) inside of the ultrasound picture, providing maximum, minimum, mean, and standard deviation of elasticity. Moreover, ratios of the means inside of the region of interest can be calculated. These objective measurements render the analysis amenable to cutoff calculation as well as integration into algorithms. Measurements of tissue elasticity with this system showed an average elasticity of 65 ± SD 22 kPa for prostate cancer tissue and of 25 ± SD 7 kPa for benign prostate tissue with a ratio of 2.7 ± SD1.4 (Walz, unpublished data). Those numbers replicate the measurements obtained from mechanical testing with a systematic increase of tissue elasticity in the in vivo measurements with the shear wave elastography system but a stable ratio of 2.6 and 2.7 between the two tissue types (Walz, unpublished data) [13]. This increase is probably due to blood perfusion in vivo that is known to increase tissue stiffness and density relative to tissue that is not perfused, such as in the case in the ex vivo measurements. For the current time, the shear wave elastography system is the only system on the market offering such an analysis.

Use of Elastography to Identify Prostate Cancer Lesions

Several studies compared real-time elastography with whole mount sections after radical prostatectomy to evaluate its diagnostic performance in the localization of prostate cancer lesions inside the prostate (Table 19.1) [15, 19–35]. The sensitivity for correct cancer localization varied between 68–77 %, therefore ranging in a rather narrow range [15, 31–33]. Two studies showed different sensitivities of 87 % and 50 %, which could be considered as outliers [20, 34]. The specificity varied between 77 % and 92 %, again ranging in a relatively narrow range [15, 32–34]. Again one study showed a lower specificity of only 72 % [20]. Other studies used biopsy data for validation, an approach that does not provide reliable values on sensitivity and specificity due to under-sampling and sampling bias, and therefore those studies are not included in this overview. The aforementioned studies suggest that real-time elastography is a reliable tool to identify prostate cancer lesion inside the prostate. The fact that the diagnostic values of real-time elastography remain in a rather narrow range suggests user-friendliness and operator independency and confirms good reproducibility of the performance—all representing advantages of the system.

Currently there is only one study comparing shear wave elastography with whole mount sections after radical prostatectomy to evaluate its diagnostic performance in the localization of prostate cancer lesions inside the prostate [19].

Table 19.1 Diagnostic performance of elastography, shear wave elastography, contrast-enhanced Doppler (CE-Doppler), and dynamic contrast-enhanced ultrasound (DCE-US)

Tumor detection: SB vs TB (ref's)	Studies (*n*)	Total patients (*n*)	Per-patient detection rate: difference between TB and SB (range)	Per-patient detection rate: difference between overall and SB
Elastography [20–24]	5	1840	−18 % to +12 %	+7 % to +12 %
CE-Doppler [25–27]	3	2206	+1 % to +4 %	+2 % to +8 %
DCE-US [28–30]	3	397	−13 % to −5 %	+3 % to +4 %
Tumor localization: Imaging vs RP	**Studies (*n*)**	**Total patients (*n*)**	**Sensitivity (range)**	**Specificity (range)**
Elastography [15, 20, 31–34]	6	488	50–87 %	72–92 %
Shear wave [19]	1	28	81 %	69 %
DCE-US [35], [unpublished data][a]	2	66	58–71 %	50–95 %

[a]Unpublished data from AMC University Hospital, 2013

In this study, a cutoff of 50 kPa was identified to be the most informative to differentiate prostate cancer lesions from benign tissue. When using a cutoff of 50 kPa, the sensitivity for correct cancer localization was at 81 %, and the specificity was 69 % [19]. Similar to real-time elastography, other studies using the shear wave elastography system used biopsy data for validation; those were not included in this overview for the same reasons of under-sampling and sample bias. Further studies are necessary to confirm the reproducibility of shear wave elastography.

Use of Elastography to Identify the Prostate Cancer Index Lesion

Especially for focal therapy, there is a need to identify the prostate cancer index lesion inside the prostate. This index lesion is usually the lesion that comprises the highest Gleason grade or when several lesions have the same Gleason grade, it is the lesion that is associated with the highest cancer volume. Real-time elastography was used to identify the prostate cancer index lesion in two studies [20, 36]. In one study, the sensitivity and specificity to identify the index lesion were only at 59 % and 43 %, respectively [36]. In the second study, the sensitivity and specificity were 59 % and 92 %, respectively [20]. Both suggest that the performance of real-time elastography alone is not sufficient to be used for focal therapy guidance. However, when combining elastography and biopsy data together to identify the prostate cancer index lesion, the performance increased, and the sensitivity and specificity increased to 85 % and 48 %, respectively [36]. Using this combined approach might be interesting for treatment guidance of focal therapy and should be further explored.

Use of Elastography for Prostate Cancer Diagnosis

Elastography was also used for the diagnosis of prostate cancer with the aim to direct biopsies into suspicious lesions. In the following overview, only studies comparing the detection rates of targeted biopsies over systematic biopsies in a controlled fashion and in an appropriate patient cohort were included. Basically only two different study designs fulfilled these criteria [37]. In the first study design, targeted and systematic biopsies were performed in the same patient during the same session with separate analysis of the detection rate based on targeted cores and on systematic cores [25]. In such studies, each patient serves as his own control, and selection biases could be excluded. In the second

study design, a randomized approach was used by randomizing patients into two groups: the first group combining image-targeted and systematic biopsies and the second group doing only systematic biopsies without the use of targeted biopsies [38]. By comparing the prostate cancer detection rates between the groups, the effect of targeted biopsies could be estimated. The randomized approach should also exclude selection biases in favor of one of the approaches. In total, five studies including 94–1024 patients used such a study design [21–23, 38, 39]. Out of these, four studies used each patient as his own control, where two studies showed with a maximum of five elastography targeted cores a higher detection rate (detection rate, 21 % and 30 %) than with a 10-core systematic scheme (detection rate, 19 % and 25 %) [21, 22]. Two other studies showed with four elastography targeted cores a lower detection rate (detection rate, 11 % and 29 %) than with a 10-core systematic scheme (detection rate, 38 % and 39 %) [23, 39]. One study randomized patients into two groups: (1) 10-core biopsy including elastography targeted cores if suspicious lesion present and (2) 10-core systematic scheme without the use of elastography targeted cores [38]. This study showed a 12 % higher detection rate in the arm including elastography targeted cores in a 10-core biopsy scheme (detection rate, 51 %) over a standard systematic 10-core scheme (detection rate, 39 %). When looking at the overall detection rates in these studies, all studies showed an increase of the detection rate over the systematic biopsy scheme, when systematic and targeted biopsies were combined. This increase varied between 7–12 % absolute and 16–53 % relative [37] (Table 19.1). The aforementioned studies allow the conclusion that randomized biopsies cannot be safely replaced by elastography-targeted biopsies. However, combining randomized and targeted biopsies together provides the highest prostate cancer detection rate over randomized biopsy alone with, in some studies, a substantial increase in cancer detection.

To the best of our knowledge, there is currently no study evaluating shear wave elastography inside one of the aforementioned study designs. This needs to be explored in future studies.

Use of Elastography for Treatment Guidance and Monitoring

To the best of our knowledge, no study has used elastography for treatment guidance for focal therapy so far. Despite this, the ability of real-time elastography together with biopsy data to identify the prostate cancer index lesion is promising. Moreover, as most of the currently used ablative energies for prostate cancer focal therapy are guided by ultrasound, the use of ultrasound-based technologies such as elastography for treatment guidance is attractive, and a prospective evaluation in future trials seems to be interesting [40]. Moreover, the real-time evaluation and the possibility of unlimited repetition of the analysis render elastography an attractive choice for such an approach. The same applies to the use of elastography for treatment monitoring. A change in tissue elasticity is of interest, especially for ablative energies using heat for tissue destruction, such as focused ultrasound ablation, laser ablation, or microwave ablation. Similar to the cooking process of meat, where proteins are denaturalized by heat, rendering the meat harder and denser relative to its raw aspect, heat ablative energies will result in the same tissue changes inside of the prostate when used for focal therapy. Very preliminary experiences confirm this theory and suggest a correlation between the ablated area identified by elastography and later confirmed by magnetic resonance imaging (MRI) (personal communication, Rouvière O, 2012.). A combination of elastography and contrast-enhanced ultrasound for treatment monitoring might become a useful option to monitor and control tissue ablation in real time during focal therapy of prostate cancer. Only this approach would allow for correction of insufficiently treated areas in the same session without the need of re-intervention at distance of the initial treatment, a step currently necessary when using MRI or prostate biopsy for treatment control. Further research in this field is necessary.

Contrast Ultrasound

Technical Aspects of Contrast Ultrasound

Prostate tumors need angiogenesis to progress from small dormant lesions into clinically significant disease [41]. Microvascularization has been shown to correlate with tumor aggressiveness and prognosis. Therefore, visualization of the altered vascularity has the potential to aid in both detection and risk stratification of prostate cancers. The standard US techniques for imaging blood flow are Doppler and power Doppler. These techniques visualize blood flow through analysis of the frequency shift that occurs when the US signal is reflected from moving particles in the bloodstream. Doppler US is easily performed in conjunction with normal grayscale TRUS. Two biopsy-controlled studies report finding 11.7–15.8 % absolute more tumors with the addition of Doppler US to grayscale TRUS [42, 43]. It should be noted that these figures represent an increase in detection rate after retrospective analysis of imaging and biopsy results, not of targeted biopsy versus systematic biopsy. The largest prostatectomy controlled trial to date by Eisenberg et al. shows that in 620 preoperative patients, when Doppler is used to further characterize lesions found by grayscale ultrasound, sensitivity dropped from 59 % to 47 %, but specificity rose from 47 % to 74 %. Unfortunately, in this study, Doppler US findings did not correlate with tumor grade and stage or biochemical recurrence or secondary treatment after RP [4]. Contrast ultrasound was first used in PCa imaging as a technique to potentiate Doppler US. A contrast agent, consisting of a solution of gas-filled microbubbles that remain strictly intravascular for several minutes, is administered intravenously during or just prior to US scanning [41]. After use in thousands of patients, most adverse events of microbubble contrast media appear to be transient, mild, and rare [44]. The theory behind adding contrast ultrasound to Doppler US is to improve the sensitivity of Doppler US to detect slow flow in small vessels by adding more reflectors to the bloodstream. One of the drawbacks of this contrast-enhanced Doppler US is the relatively high-energy US pulses delivered, causing premature bursting of the microbubbles [45]. Dynamic contrast-enhanced ultrasound (DCE-US) uses much lower energy pulses overcoming this issue. DCE-US visualizes blood flow not through the Doppler effect but by detecting the nonlinear oscillations that occur when the microbubbles are incited by the US beam and differentiating these from the normal, linear tissue reflections [46]. This allows contrast-specific imaging that is sensitive enough to visualize a single microbubble with the size of an erythrocyte traveling through the microvasculature [41]. Typically, the user sets the ultrasound machine in a split-screen mode with normal grayscale imaging on one side and contrast only (DCE-US) on the other. Scanning is done using sweeps or plane by plane after the injection of an ultrasound contrast agent (UCA) bolus. The visual interpretation relies mostly on the identification of asymmetrical rapidly enhancing foci in the peripheral zone (PZ). Other cues of malignancy are increased focal peak enhancement and asymmetry of intraprostatic and capsular vessels (Fig. 19.2) [35]. Early enhancement can be assessed after bolus injection, requiring a bolus and outflow period for each successive plane. Some work has been done with so-called flash replenishment technique. This entails destroying the microbubbles in the US field of view using a strong US pulse. The ensuing inflow of fresh microbubbles from the surrounding circulation can then be assessed [28, 47]. At low volumes of circulating microbubbles, the flash replenishment technique combined with maximum intensity projection allows visualization of the trajectory of individual bubbles revealing the structure of single microvessels.

Use of Contrast Ultrasound to Identify Prostate Cancer Lesions

Few studies have compared contrast-specific DCE-US with radical prostatectomy specimens (Table 19.1). Halpern et al. mapped preoperative DCE-US and grayscale findings in 12

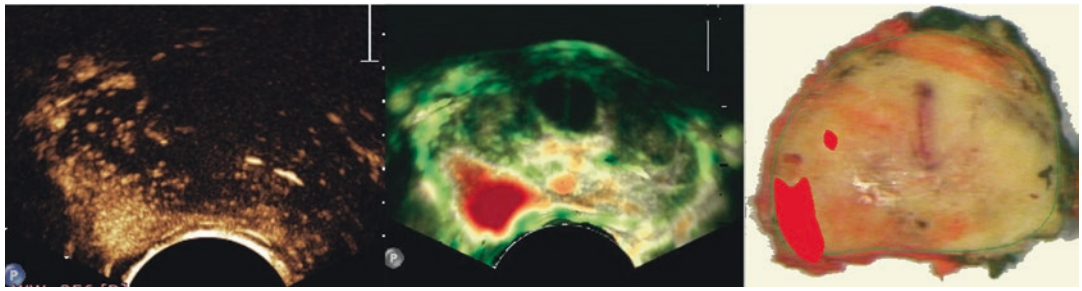

Fig. 19.2 Dynamic contrast-enhanced ultrasound (DCE-US) and parametric map of the prostate. *Left*: DCE-US of the prostate showing strong early enhancement suspicious for prostate cancer (PCa) in the right peripheral zone (lower left side in the image). *Middle*: contrast ultrasound dispersion imaging (CUDI) map showing high time-intensity curve similarity indicating low dispersion suspicious for PCa in the right peripheral zone (marked *red*). Pathology slice indicating Gleason 4+3 tumor in the right peripheral zone (marked *red*) (Courtesy of RJG van Sloun, Eindhoven University of Technology)

patients, finding 13 out of 31 PCa foci resulting in a sensitivity of 42 % [48]. Similar figures were subsequently found by Sano et al. who detected 10/26 cancerous foci in 13 prostates resulting in a sensitivity of 38 % [49]. Matsumoto et al. used DCE-US and grayscale US to evaluate the prostates of 50 patients scheduled for radical prostatectomy, locating 43 of 106 tumor foci resulting in a sensitivity of 41 % [47]. Unfortunately, the design of these three studies did not allow calculation of specificity. Better figures were reported by Seitz et al. who preoperatively scanned 35 patients scheduled for prostatectomy or cystoprostatectomy using DCE-US and were able to locate the tumor focus in 22/31 patients scheduled for prostatectomy [35]. On a per-patient basis, they calculated a sensitivity, specificity, PPV, and NPV of 71 %, 50 %, 92 %, and 18 %, respectively. Yet-to-be published data from the Academic Medical Center (AMC) university hospital compared preoperative DCE-US scanning of the prostate with radical prostatectomy specimens of 36 patients. Two observers achieved sensitivities of 58–69 % and specificities of 93–95 % for detecting lesions larger than 0.5 mL. The scarcity of the literature comparing RP specimens with contrast ultrasound calls for further studies to evaluate its performance in locating PCa.

Use of Contrast Ultrasound to Identify the Prostate Cancer Index Lesion

As outlined before, accurate localization of the dominant tumor focus is highly important for the application of contrast ultrasound within focal therapy. The aforementioned study by Seitz et al. evaluated to what extent the localization of DCE-US findings correlates with the localization of the index lesion [35]. In 17/22 patients with tumors detected by DCE-US, the index lesion was correctly localized. Excluding Gleason 6 index lesions, their dataset shows that 11/17 (65 %) index tumors could be located in the correct sextant, 5/17 (29 %) were missed altogether, and 1/17 (6 %) was placed at the opposite side. Qi et al. attempted to localize the index tumor in 83 patients scheduled for prostatectomy and were able to detect 51 %, 64 %, and 81 % of index lesions using grayscale US, DCE-US, and the combination, respectively [50]. Unfortunately the precise methodology of comparing imaging and pathology was not described. Based on these data, the use of DCE-US alone for index lesion targeting cannot be recommended, but again, data is scarce, and further investigation with accurate matching between imaging and pathology is necessary to definitively establish the performance in localizing the index lesion.

Use of Contrast Ultrasound for Prostate Cancer Diagnosis

For reasons explained before, the value of an imaging tool for prostate biopsy guidance can only truly be evaluated when the per-patient detection rates of targeted biopsies and systematic biopsies taken from the same patients or patients randomized to either protocol are compared [37] (Table 19.1). In the following section, we will therefore focus on studies that were designed in such a way. Two studies compared detection rates of ten systematic biopsy cores with five contrast-enhanced Doppler US targeted biopsy cores in 1776 and 230 patients, respectively [25, 26]. In both studies, 23 % of patients had positive systematic biopsies. In the larger study, 27 % of targeted cores were positive, in the smaller 24 %. This indicates contrast-enhanced targeted biopsies perform at least as well or better than systematic biopsies with fewer cores. Nevertheless, significant tumor foci were picked up by systematic biopsy and missed by targeted biopsy. Combining systematic and targeted biopsies showed a gain of 7–8 % absolute compared to only systematic biopsies. Taverna et al. randomized 300 patients to undergo either: 13-core systematic biopsy, 13-core systematic biopsy plus Doppler targeted biopsies, or 13-core systematic biopsy plus contrast-enhanced targeted biopsies [27]. They found a modest 2 % absolute increase in detection rate of systematic + contrast-enhanced Doppler targeted compared to systematic biopsies alone. Three studies compared detection rates of DCE-US targeted cores and systematic cores in the same patients, using cohorts of 272, 60, and 65 patients [28–30]. These studies report a lower detection rate using the 2–6 targeted cores compared to 10–12-core systematic biopsy, but an overall gain of 3–4 % absolute when the two are combined. Besides per-patient detection rate, tumor grading is important, and targeted cores are usually expected to yield larger tumor volumes and higher Gleason scores. Only two studies describe these figures: 31 % of patients were diagnosed with Gleason ≥7 with systematic biopsy only compared to 29 % for the systematic + contrast-enhanced Doppler US targeted cores in the study by Taverna et al. [27]. Frauscher et al. report finding equal numbers of Gleason 6 tumors with only systematic biopsy and only targeted biopsy (both 8/46 (17 %) Gleason 6 tumors) [25]. However, 5/13 (38 %) Gleason 7 tumors and 4/5 (80 %) of Gleason ≥8 tumors were found only by targeted biopsy, while none were found with systematic biopsy alone. The figures for both types of contrast-enhanced ultrasound illustrate that incorporating targeted cores improves detection but systematic biopsies remain necessary, as is the case with all other currently available imaging tools [37].

Use of Contrast Ultrasound for Treatment Guidance and Monitoring

Since DCE-US is highly sensitive to blood flow in the smallest capillaries, it is a suitable option for the monitoring of focal treatments in which the vascularity is destroyed. It provides high-resolution images that accurately depict whether tissue is perfused or not. Furthermore, the use of DCE-US is not limited by restrictions on ferromagnetic components of the ablation equipment as is the case with MRI-based monitoring. DCE-US is used for the real-time monitoring of lesion development during interstitial laser photothermal therapy by using a continuous UCA infusion [51, 52]. Rouviere and colleagues have shown that contrast ultrasound allows immediate visualization of HIFU-induced ablation zone by comparing postoperative biopsy results taken from areas showing residual enhancement and the non-enhancing ablation zone [53]. Based on these results, non-enhancing areas can safely be considered destroyed [54]. Some modern HIFU probes can be used to scan DCE-US volumes to check whether the ablation extent has progressed as planned intraoperatively. This allows immediate adjustment of the ablated zone by applying additional HIFU to any undertreated areas [54]. DCE-US has also been used to depict the ablation zone in the days or weeks after HIFU, interstitial laser phototherapy, and IRE, correlating well with MRI and histopathology findings [52, 54, 55].

Multiparametric Ultrasound

Prostate cancer is such a heterogenous disease that it is very conceivable that no single imaging modality will be able to detect all different tumor morphologies. In MRI imaging, it has been demonstrated that the diagnostic performance of single sequences is inadequate and multiparametric MRI is now the standard [56]. For US too, it may hold true that the best diagnostic performance will be reached by combining several modalities that each target different tissue characteristics that help differentiate benign from malignant prostate tissue. Available US modalities target anatomical morphology (grayscale US), altered vascularity (contrast ultrasound), and tissue density (elastography). The parallels to the T2 MRI, DCE-MRI, and DWI-MRI sequences—the combination of which was proven effective—are clear. Yet only modest steps have been undertaken to combine these US modalities into multiparametric ultrasound. Most notably, Brock and colleagues matched the preoperative elastography and DCE-US in 86 patients with RP specimen analysis [57]. They followed a two-step approach toward combining the US modalities: First, suspicious lesions were identified using elastography. Elastography alone showed a sensitivity of 49 % and a specificity of 74 %. Second, only the suspicious areas found by elastography were investigated further using DCE-US, raising the PPV from 65 % to 90 %. Clearly, further research into various combinations of multiparametric ultrasound is necessary to assess its full potential [58].

Future Perspectives

Currently ultrasound remains a dynamic and operator-dependent exam, rendering its standardization and reproducibility limited. Quantification and computer-aided interpretation are feasible for both DCE-US and shear wave elastography, and these developments should increase accuracy and decrease operator dependency. Especially for DCE-US, algorithms are being developed that analyze the inflow and outflow of the UCA by plotting per-pixel time-intensity curves (enhancement as function of time) that are used to extract various blood flow-related parameters. These parameters can be displayed as a color-coded map for further visual interpretation or used by a classifying algorithm to predict whether tissue is malignant [6]. In a study published in 2010, Zhu et al. performed DCE-US in 103 patients before prostate biopsies and then correlated biopsy results with several blood flow parameters extracted from the DCE-US recordings. They found that arrival time (AT) and time to peak (TTP) and peak intensity (PI) differed significantly between low-grade and high-grade PZ tumors and found significant correlations between these parameters and the Gleason score [59].

Jung et al. used a prototype of software under development by the UCA manufacturer Bracco (Bracco Suisse SA, Geneva, Switzerland) to analyze the preoperative DCE-US recordings of 20 men scheduled for RP [60]. They designated suspicious and unsuspicious sectors in each of the patients and evaluated the ability of several parameters to correctly classify the sectors as benign or malignant. Using the mean transit time (time between 50 % enhancement levels of the wash-in and wash-out phase) and rise time (time range of UCA influx), they were able to identify 29 and 25 of 34 tumor foci, respectively. Using early enhancement, 30/34 tumors were identified resulting in a sensitivity and specificity of 88 % and 100 %, respectively.

The current version of the aforementioned quantification software by Bracco includes a classifying algorithm that uses two statistical parameters (mode and standard deviation of wash-in rates) obtained from TIC analysis to predict whether the tissue is malignant or benign. Postema et al. correlated the PCa-probability maps generated by this software to the systematic biopsy results of 82 patients and reported classifying 63 % of 651 of biopsy locations as benign, resulting in 23 (5.6 %) missed biopsy cores with

significant PCa (Gleason ≥7 and ≥10 % core involvement) [61]. In 31/82, no lesions were apparent using DCE-US + quantification software, resulting in three missed diagnoses of significant PCa. Sensitivity, specificity, PPV, and NPV were calculated to be 91 %, 56 %, 57 %, and 90 %. An Eindhoven University of Technology research group is developing contrast ultrasound dispersion imaging (CUDI), a quantification method based on the analysis of UCA dispersion parameters that are also extracted from TICs [6, 62]. They validated their algorithms by using the preoperative DCE-US recordings and marked RP slices of up to 24 patients showing a gradual improvement of the CUDI method reaching an AUC of 0.92 in their last study [63–65]. Ideally, technologies such as elastography or contrast-enhanced ultrasound should be amenable to 3D or 4D imaging. Moreover, the 3D or 4D ultrasound loop should be systematically filed and amenable to post-acquisition processing and analysis. The first tests with commercially available contrast-ready 3D/4D endorectal US systems have shown that 4D DCE-US and quantification are feasible [66]. Besides allowing scanning of the whole prostate in 2 min after one single bolus, the authors hypothesize that with 3D/4D DCE-US accuracy of the quantification techniques could improve since the blood flow alterations they try to detect are fundamentally 3D phenomena.

Such improvements would substantially improve the usefulness of ultrasound-based technologies for diagnosis and treatment of prostate cancer. These improvements are under development but not yet commercially available. Moreover, the different ultrasound-based technologies are commercialized by different companies, each of them favoring one of the different technologies. Therefore, most scanners offer either elastography or contrast-enhanced ultrasound at the high-quality level that is necessary to render this pathway useful but not both in the same system. Despite these limitations, ultrasound-based imaging for diagnosis and treatment of prostate cancer harbors great potential for the future.

References

1. Bueschen AJ, Lockhart ME. Evolution of urological imaging. Int J Urol. 2011;18(2):102–12.
2. Schroder FH, Van der Maas P, Beemsterboer P, Boeken Kruger A, Hoedemaeker R, Rietbergen J, et al. Evaluation of the digital rectal examination as a screening test for prostate cancer. J Natl Canacer Inst. 1998;90(23):1817–23.
3. Shinohara K, Wheeler TM, Scardino PT. The appearance of prostate cancer on transrectal ultrasonography: correlation of imaging and pathological examinations. J Urol. 1989;142(1):76–82.
4. Eisenberg ML, Cowan JE, Carroll PR, Shinohara K. The adjunctive use of power Doppler imaging in the preoperative assessment of prostate cancer. BJU Int. 2010;105(9):1237–41.
5. Beerlage HP, Aarnink RG, Ruijter ET, Witjes JA, Wijkstra H, Van de Kaa CA, et al. Correlation of transrectal ultrasound, computer analysis of transrectal ultrasound and histopathology of radical prostatectomy specimen. Prostate Cancer Prostatic Dis. 2001;4(1):56–62.
6. Postema A, Idzenga T, Mischi M, Frinking P, de la Rosette J, Wijkstra H. Ultrasound modalities and quantification: developments of multiparametric ultrasonography, a new modality to detect, localize and target prostatic tumors. Curr Opin Urol. 2015; 25(3):191–7.
7. Loch T, Loch A, Grabski B, Baeurle L, Paul U, Tokas T. Computerized transrectal ultrasound targeted biopsies: preoperative prediction of the radical prostatectomy Gleason grade. J Urol. 2014 Apr;191(4):e470–1.
8. Walz J, Thomassin-Piana J, Poizat F, Brunelle S, Salem N, Gravis G. External validation of the Anna/C-trus system regarding the correct identification of prostate cancer lesions in the diagnosis of prostate cancer. J Urol. 2012;187(4):e820.
9. Braeckman J, Autier P, Garbar C, Marichal MP, Soviany C, Nir R, et al. Computer-aided ultrasonography (HistoScanning): a novel technology for locating and characterizing prostate cancer. BJU Int. 2008; 101(3):293–8.
10. Schiffmann J, Manka L, Boehm K, Leyh-Bannurah SR, Karakiewicz PI, Graefen M, et al. Controversial evidence for the use of HistoScanning™ in the detection of prostate cancer. World J Urol. 2015; 33(12):1993–9.
11. Porres D, Kuru TH, Epplen R, Eck A, Zugor V, Kennes LN, et al. Sextant-specific analysis of detection and tumor volume by HistoScanning™. Urol Int. 2015;194–201
12. Ghai S, Eure G, Hyndman ME, Fradet V, Mcgrath T, Wodlinger B, et al. Assessing cancer risk in 29 MHz micro-ultrasound images of the prostate: creation of the PRI-MUS (prostate risk identification using micro-ultrasound) protocol. J Urol. 2016;196(2):562–9.

13. Zhang M, Nigwekar P, Castaneda B, Hoyt K, Joseph J, di Sant'Agnese A, et al. Quantitative characterization of viscoelastic properties of human prostate correlated with histology. Ultrasound Med Biol. 2008;34(7):1033–42.
14. Pallwein L, Mitterberger M, Pinggera G, Aigner F, Pedross F, Gradl J, et al. Sonoelastography of the prostate: comparison with systematic biopsy findings in 492 patients. Eur J Radiol. 2008;65(2):304–10.
15. Salomon G, Köllerman J, Thederan I, Chun FKH, Budäus L, Schlomm T, et al. Evaluation of prostate cancer detection with ultrasound real-time elastography: a comparison with step section pathological analysis after radical prostatectomy. Eur Urol. 2008;54(6):1354–62.
16. König K, Scheipers U, Pesavento A, Lorenz A, Ermert H, Senge T. Initial experiences with real-time elastography guided biopsies of the prostate. J Urol. 2005;174(1):115–7.
17. Tanter M, Fink M. Ultrafast imaging in biomedical ultrasound. IEEE Trans Ultrason Ferroelectr Freq Control. 2014;61(1):102–19.
18. Barr RG, Memo R, CR S. Shear wave ultrasound elastography of the prostate: initial results. Ultrasound Q. 2012;28(1):13–20.
19. Boehm K, Salomon G, Beyer B, Schiffmann J, Simonis K, Graefen M, et al. Shear wave elastography for localization of prostate cancer lesions and assessment of elasticity thresholds: implications for targeted biopsies and active surveillance protocols. J Urol. 2015;193(3):794–800.
20. Brock M, von Bodman C, Sommerer F, Löppenberg B, Klein T, Deix T, et al. Comparison of real-time elastography with grey-scale ultrasonography for detection of organ-confined prostate cancer and extra capsular extension: a prospective analysis using whole mount sections after radical prostatectomy. BJU Int. 2011;108(8 Pt 2):E217–22.
21. Pallwein L, Mitterberger M, Struve P, Horninger W, Aigner F, Bartsch G, et al. Comparison of sonoelastography guided biopsy with systematic biopsy: impact on prostate cancer detection. Eur Radiol. 2007;17(9):2278–85.
22. Aigner F, Pallwein L, Junker D, Schäfer G, Mikuz G, Pedross F, et al. Value of real-time elastography targeted biopsy for prostate cancer detection in men with prostate specific antigen 1.25 ng/ml or greater and 4.00 ng/ml or less. J Urol. 2010;184(3):913–7.
23. Ganzer R, Brandtner A, Wieland WF, Fritsche H-M. Prospective blinded comparison of real-time sonoelastography targeted versus randomised biopsy of the prostate in the primary and re-biopsy setting. World J Urol. 2012;30(2):219–23.
24. Salomon G, Drews N, Autier P, Beckmann A, Heinzer H, Hansen J, et al. Incremental detection rate of prostate cancer by HI-real time elastography targeted biopsies in combination to a conventional 10 core biopsy in 1024 consecutive men. BJU Int. 2013:1–19.
25. Frauscher F, Klauser A, Volgger H, Halpern EJ, Pallwein L, Steiner H, et al. Comparison of contrast enhanced color Doppler targeted biopsy with conventional systematic biopsy: impact on prostate cancer detection. J Urol. 2002;167(4):1648–52.
26. Mitterberger MJ, Aigner F, Horninger W, Ulmer H, Cavuto S, Halpern EJ, et al. Comparative efficiency of contrast-enhanced colour Doppler ultrasound targeted versus systematic biopsy for prostate cancer detection. Eur Radiol. 2010;20(12):2791–6.
27. Taverna G, Morandi G, Seveso M, Giusti G, Benetti A, Colombo P, et al. Colour Doppler and microbubble contrast agent ultrasonography do not improve cancer detection rate in transrectal systematic prostate biopsy sampling. BJU Int. 2011;108(11):1723–7.
28. Linden RA, Trabulsi EJ, Forsberg F, Gittens PR, Gomella LG, Halpern EJ. Contrast enhanced ultrasound flash replenishment method for directed prostate biopsies. J Urol. 2007;178(6):2354–8.
29. Halpern EJ, Gomella LG, Forsberg F, McCue PA, Trabulsi EJ. Contrast enhanced transrectal ultrasound for the detection of prostate cancer: a randomized, double-blind trial of dutasteride pretreatment. J Urol. 2012;188(5):1739–45.
30. Zhao H-X, Xia C-X, Yin H-X, Guo N, Zhu Q. The value and limitations of contrast-enhanced transrectal ultrasonography for the detection of prostate cancer. Eur J Radiol. 2013;82(11):e641–7.
31. Tsutsumi M, Miyagawa T, Matsumura T, Kawazoe N, Ishikawa S, Shimokama T, et al. The impact of real-time tissue elasticity imaging (elastography) on the detection of prostate cancer: clinicopathological analysis. Int J Clin Oncol. 2007;12(4):250–5.
32. Walz J, Marcy M, Maubon T, Brunelle S, Laroche J, Gravis G, et al. Real time elastography in the diagnosis of prostate cancer: comparison of preoperative imaging and histology after radical prostatectomy. Prog Urol. 2011;21(13):925–31.
33. Zhu Y, Chen Y, Qi T, Jiang J, Qi J, Yu Y, et al. Prostate cancer detection with real-time elastography using a bi-plane transducer: comparison with step section radical prostatectomy pathology. World J Urol. 2014;32:329–33.
34. Pallwein L, Mitterberger M, Struve P, Pinggera G, Horninger W, Bartsch G, et al. Real-time elastography for detecting prostate cancer: preliminary experience. BJU Int. 2007;100(1):42–6.
35. Seitz M, Gratzke C, Schlenker B, Buchner A, Karl A, Roosen A, et al. Contrast-enhanced transrectal ultrasound (CE-TRUS) with cadence-contrast pulse sequence (CPS) technology for the identification of prostate cancer. Urol Oncol. 2011;29(3):295–301.
36. Walz J, Marcy M, Pianna JT, Brunelle S, Gravis G, Salem N, et al. Identification of the prostate cancer index lesion by real-time elastography: considerations for focal therapy of prostate cancer. World J Urol. 2011;29(5):589–94.
37. van Hove A, Savoie P-H, Maurin C, Brunelle S, Gravis G, Salem N, et al. Comparison of image-guided targeted biopsies versus systematic randomized biopsies in the detection of prostate cancer: a systematic literature review of well-designed studies. World J Urol. 2014;32(4):847–58.

38. Brock M, von Bodman C, Palisaar RJ, Löppenberg B, Sommerer F, Deix T, et al. The impact of real-time elastography guiding a systematic prostate biopsy to improve cancer detection rate: a prospective study of 353 patients. J Urol. 2012;187(6):2039–43.
39. Salomon G, Drews N, Autier P, Beckmann A, Heinzer H, Hansen J, et al. Incremental detection rate of prostate cancer by real-time elastography targeted biopsies in combination with a conventional 10-core biopsy in 1024 consecutive patients. BJU Int. 2014;113(4):548–53.
40. Eggener SE, Scardino PT, Carroll PR, Zelefsky MJ, Sartor O, Hricak H, et al. Focal therapy for localized prostate cancer: a critical appraisal of rationale and modalities. J Urol. 2007;178(6):2260–7.
41. Russo G, Mischi M, Scheepens W, De la Rosette JJ, Wijkstra H. Angiogenesis in prostate cancer: onset, progression and imaging. BJU Int. 2012;110(11 Pt C):E794–808.
42. Kuligowska E, Barish MA, Fenlon HM, Blake M. Predictors of prostate carcinoma: accuracy of gray-scale and color Doppler US and serum markers. Radiology. 2001;220(3):757–64.
43. Cheng S, Rifkin MD. Color Doppler imaging of the prostate: important adjunct to endorectal ultrasound of the prostate in the diagnosis of prostate cancer. Ultrasound Q. 2001;17(3)
44. Appis AW, Tracy MJ, Feinstein SB. Update on the safety and efficacy of commercial ultrasound contrast agents in cardiac applications. Echo Res Pract. 2015;2(2):R55–62.
45. Wink M, Frauscher F, Cosgrove D, Chapelon J-Y, Palwein L, Mitterberger M, et al. Contrast-enhanced ultrasound and prostate cancer; a multicentre European research coordination project. Eur Urol. 2008;54(5):982–92.
46. Heijmink SWTPJ, Barentsz JO. Contrast-enhanced versus systematic transrectal ultrasound-guided prostate cancer detection: an overview of techniques and a systematic review. Eur J Radiol. 2007;63(3):310–6.
47. Matsumoto K, Nakagawa K, Hashiguchi A, Kono H, Kikuchi E, Nagata H, et al. Contrast-enhanced ultrasonography of the prostate with Sonazoid. Jpn J Clin Oncol. 2010;40(11):1099–104.
48. Halpern EJ, McCue PA, Aksnes AK, Hagen EK, Frauscher F, Gomella LG. Contrast-enhanced US of the prostate with Sonazoid: comparison with whole-mount prostatectomy specimens in 12 patients. Radiology. 2002;222(2):361–6.
49. Sano F, Terao H, Kawahara T, Miyoshi Y, Sasaki T, Noguchi K, et al. Contrast-enhanced ultrasonography of the prostate: various imaging findings that indicate prostate cancer. BJU Int. 2011;107(9):1404–10.
50. Qi T, Chen Y, Zhu Y, Jiang J, Wang L, Qi J. Contrast-enhanced transrectal ultrasonography for detection and localization of prostate index tumor: correlation with radical prostatectomy findings. Urology. 2014:1–6.
51. Atri M, Gertner MR, Haider MA, Weersink RA, Trachtenberg J. Contrast-enhanced ultrasonography for real-time monitoring of interstitial laser thermal therapy in the focal treatment of prostate cancer. Can Urol Assoc J. 2009;3(2):125–30.
52. Lindner U, Weersink RA, Haider MA, Gertner MR, Davidson SRH, Atri M, et al. Image guided photothermal focal therapy for localized prostate cancer: phase I trial. J Urol. 2009;182(4):1371–7.
53. Rouvière O, Glas L, Girouin N, Mège-lechevallier F, Gelet A, Dantony E, et al. Prostate cancer ablation with transrectal high-intensity focused ultrasound: assessment of tissue destruction with contrast-enhanced us. Radiology. 2011;259(2):583–91.
54. Crouzet S, Rouviere O, Martin X, Gelet A. High-intensity focused ultrasound as focal therapy of prostate cancer. Curr Opin Urol. 2014;24(3):225–30.
55. van den Bos W, de Bruin DM, van Randen A, Engelbrecht MRW, Postema AW, Muller BG, et al. MRI and contrast-enhanced ultrasound imaging for evaluation of focal irreversible electroporation treatment: results from a phase I-II study in patients undergoing IRE followed by radical prostatectomy. Eur Radiol. 2015;26(7):2252–60.
56. Hoeks CCM, Barentsz JJO, Hambrock T, Yakar D, Somford DM, Heijmink SW, et al. Prostate cancer: multiparametric MR imaging for detection, localization, and staging. Radiology. 2011;261(1):46–66.
57. Brock M, Eggert T, Palisaar RJ, Roghmann F, Braun K, Löppenberg B, et al. Multiparametric ultrasound of the prostate: adding contrast enhanced ultrasound to real-time elastography to detect histopathologically confirmed cancer. J Urol. 2013;189(1):93–8.
58. Postema A, Mischi M, de la Rosette J, Wijkstra H. Multiparametric ultrasound in the detection of prostate cancer: a systematic review. World J Urol. 2015; doi:10.1007/s00345-015-1523-6.
59. Zhu Y, Chen Y, Jiang J, Wang R, Zhou Y, Zhang H. Contrast-enhanced harmonic ultrasonography for the assessment of prostate cancer aggressiveness: a preliminary study. Korean J Radiol. 2010;11(1):75–83.
60. Jung EM, Wiggermann P, Greis C, Eder F, Ehrich J, Jung W, et al. First results of endocavity evaluation of the microvascularization of malignant prostate tumors using contrast enhanced ultrasound (CEUS) including perfusion analysis: first results. Clin Hemorheol Microcirc. 2012;52(2–4):167–77.
61. Postema AW, Frinking PJA, Smeenge M, De Reijke TM, De la Rosette JJ, Tranquart F, et al. Dynamic contrast-enhanced ultrasound parametric imaging for the detection of prostate cancer. BJU Int. 2015; doi:10.1111/bju.13116.
62. Mischi M, Kuenen MPJ, Wijkstra H. Angiogenesis imaging by spatiotemporal analysis of ultrasound contrast agent dispersion kinetics. IEEE Trans Ultrason Ferroelectr Freq Control. 2012;59(4):621–9.
63. Mischi M, Kuenen MP, Beerlage HP, De La Rosette JJMCH, Wijkstra H. Prostate cancer localization by contrast-ultrasound-dispersion imaging: results from a pilot study. Eur Urol Suppl. 2014;13(1):e1054.

64. Kuenen MPJ, Saidov TA, Wijkstra H, Mischi M. Contrast-ultrasound dispersion imaging for prostate cancer localization by improved spatiotemporal similarity analysis. Ultrasound Med Biol. 2013; 39(9):1631–41.
65. Mischi M, Bouhouch N, Demi L, Kuenen MPJ, Postema A, de la Rosette JJ, et al. Contrast-ultrasound dispersion imaging of cancer neovascularization by mutual-information analysis. 2014 IEEE International Ultrasonics Symposium [Internet]. IEEE; 2014; 1148–1151. Available from: http://ieeexplore.ieee.org/lpdocs/epic03/wrapper.htm?arnumber=6931833
66. Schalk SG, Demi L, Smeenge M, Mills DM, Wallace KD, De La Rosette JJ, et al. 4-D spatiotemporal analysis of ultrasound contrast agent dispersion for prostate cancer localization: a feasibility study. IEEE Trans Ultrason Ferroelectr Freq Control. 2015; 62(5):839–51.

Robotic Magnetic Resonance Imaging Targeting for Biopsy and Therapy

20

Wesley W. Ludwig, Mohamad E. Allaf, and Dan Stoianovici

Introduction

More than 250,000 men in the United States are diagnosed with prostate cancer on a yearly basis [1]. With the advent of prostate-specific antigen (PSA) screening, many identified prostate cancers are indolent and nonlethal. Yet, they are frequently treated in an aggressive manner with extirpative surgery or radiation. Concern for overtreatment of low-risk prostate cancer in large part guided the United States Preventive Services Task Force's recommendation to no longer recommend PSA screening for men of any age [2]. PSA screening has decreased in the era of these recommendations, and prostate cancer diagnoses have decreased as well [3]. While the rate of prostate cancer detection has been declining, it is estimated that 400 in 100,000 men continue to be diagnosed with prostate cancer yearly [4]. The urological community now finds itself at a crossroads, in which prostate cancer continues to kill more than 28,000 men on a yearly basis, but diagnosis and treatment require increased sensitivity and accuracy. At this junction, accurate robotic targeting using magnetic resonance imaging (MRI) may serve as an important tool in permitting more accurate prostate cancer detection and focal treatments.

The Current State of Prostate Biopsy

Currently, prostate biopsies are performed freehand with the use of transrectal ultrasound (TRUS) to guide needle placement into the prostate in a systematic fashion. Prostate biopsy is one of the most common urological procedures, with well over a million biopsies performed on a yearly basis [5]. Standard TRUS infrequently identifies areas that are suspicious for malignancy, and abnormality on ultrasound is a poor predictor of prostate cancer [6]. More importantly, traditional TRUS-guided prostate biopsies frequently fail to detect prostate cancer. Simulations of random sextant biopsies have shown that up to 25 % of prostate cancers may be missed [7]. Even with an increasing number of biopsies, 10 % of cancers will not be detected, and these

W.W. Ludwig
Department of Urology, The James Buchanan Brady Urological Institute, The Johns Hopkins University School of Medicine, Baltimore, MD, USA

M.E. Allaf
Urology, Oncology, and Biomedical Engineering, Minimally Invasive and Robotic Surgery, Brady Urological Institute, Johns Hopkins Hospital, Baltimore, MD, USA

D. Stoianovici (✉)
Brady Urological Institute, Johns Hopkins University, Baltimore, MD, USA
e-mail: dss@jhu.edu

© Springer International Publishing AG 2017
T.J. Polascik (ed.), *Imaging and Focal Therapy of Early Prostate Cancer*, Current Clinical Urology, DOI 10.1007/978-3-319-49911-6_20

often represent high-risk disease [8]. Interestingly, freehand TRUS-guided biopsies are dependent on the individual performing the biopsy. A study using a biopsy simulation platform in pelvic mock-up accurately tracked the location and trajectory of prostate biopsies. Five urologists performed prostate biopsies in the standard fashion and were found to biopsy in a distinctive clustered pattern that significantly under-sampled the prostate. Human accuracy for targeting of particular lesions had a mean error of 9.0 mm. In the same study, robot-assisted biopsies had no clustering and a mean targeting error of 1.0 mm. Robotic assistance improved accuracy, precision, and increased the rate of prostate cancer detection [9]. An additional issue with TRUS-guided biopsy is the detection of low-grade cancers that are likely clinically insignificant. A number of series have investigated this and found the rate to range from 10 % to 49 % [10, 11]. Clearly, tools to improve lesion targeting may increase prostate biopsy yield and decrease the rate of incidental lesions.

Advances in Prostate Biopsy Using Magnetic Resonance Imaging

In contrast to ultrasound (US), which poorly differentiates benign from malignant prostatic tissue, MRI is an excellent tool for soft-tissue imaging. Multiparametric MRI (mpMRI) permits differentiation of prostate cancer from the surrounding prostatic stroma in a proven and reproducible manner. Multiple studies have shown that MRI detects clinically significant prostate cancer in 44–87 % of biopsy naïve or negative men and has a negative predictive value of 63–98 % [12].

Magnetic Resonance/Ultrasound Fusion-Guided Biopsy

There are a number of strategies to incorporate MRI into prostate biopsy; direct in-gantry guided biopsy, cognitive fusion, and MR/US fusion using a software platform. In recent years, MRI fusion with TRUS-guided biopsy has been gaining in popularity. Available platforms include UroNav (Invivo Corp., Gainesville, Florida), Artemis (Eigen, Grass Valley, California), and Urostation (Koelis, Meylan, France) among others [13]. For most platforms, a prostate MRI is acquired, and if a suspicious lesion is present, the MR image is registered to US during TRUS biopsy. A physician can thus visualize the approximate location of the lesion from MR on images acquired by US, and biopsies are performed in a directed manner. A recent study compared MR/US fusion-guided biopsies to standard TRUS-guided biopsies. The authors found that MR/US fusion-guided biopsies detected 30 % more high-risk cancers and 17 % fewer low-risk cancers than standard biopsies [14]. Clearly, MR imaging of the prostate adds a very important dimension to detecting clinically relevant prostate cancers.

MR/US fusion-guided prostate biopsy has areas that can be improved upon. It is prone to human error in regard to needle guidance and placement. Additionally, it relies on cross-modality imaging registration, which can introduce significant inaccuracy [15]. Prostate MRI is now typically done without an endorectal coil, and there is little tissue deformation. When TRUS is being performed, an ultrasound probe is inserted into the rectum with varying degrees of pressure and torque applied depending on the target location. Tissue deformity during TRUS biopsy can make cross-modality image registration difficult. Methods have been developed to improve contours in a deformable setting, but they remain imperfect [16]. For these reasons, there is interest in performing MR-guided biopsies.

Magnetic Resonance-Guided In-Gantry Biopsy

MR-guided in-gantry biopsies are performed directly during MRI, eliminating issues with cross-modality image registration. Initial studies found this technique to be feasible in men with an elevated PSA and previous negative TRUS-guided biopsies, with a prostate cancer detection rate of 37–38 % [17–19]. A recent study of

patients with an average of 2 previous negative TRUS-guided biopsies, rising PSA, and a suspicious lesion on MRI detected prostate cancer in 52 % of individuals [20]. A study by Hambrock et al. examined the efficacy of MRI-guided biopsy of suspicious lesions on mpMRI using a commercially available transrectal MR biopsy device compared to standard TRUS biopsy in a matched cohort. Prostate cancer detection was significantly greater (55 % vs. 88 %) in the MR-guided biopsy group [21]. These studies indicate that MR-guided biopsy can be efficacious in the setting of a previously failed TRUS-guided biopsy.

Robot-Assisted Magnetic Resonance-Guided Prostate Biopsy

Targeting a specific lesion on MRI can prove challenging, particularly if the lesion is small. Robotic assistance for accurate needle placement has the potential to both simplify and improve the biopsy yield. A number of groups have worked on developing this important tool.

In 2005, a small study of five patients showed feasibility of a custom-made, MR-compatible device that assisted in fiducial placement and prostate biopsy—with fairly accurate targeting to within 1.8 mm [22]. The device was composed entirely of Ultam plastic and utilized a pre-placed endorectal sheath containing a single-turn imaging coil and an anterior aperture for needle placement. The needle guide contained MR tracking microcoils that facilitated image registration.

Researchers at the Nijmegen Medical Center in the Netherlands developed a novel MR-compatible robotic system. Device energy was obtained via a pneumatic motor—in which air was compressed outside the MR room and delivered through MR-compatible tubing. The needle guide was placed transrectally, and a phased-array coil was positioned on the patient's buttocks. After a suspicious area was identified on MRI, needle trajectory was set. Prior to biopsy, the patient was removed from the MRI, and the biopsy was performed manually using the previously obtained coordinates. Following the biopsy, the patient was reimaged to confirm accuracy. This system was utilized in a prospective study of 9 patients with a PSA greater than 4, history of negative prostate biopsy, and an area on MRI suspicious for malignancy. Prostate cancer was detected in 4 of 9 patients, and 6 of 13 suspicious areas were found to have prostate cancer. This allowed a higher rate of prostate cancer detection than with traditional TRUS-guided biopsy and with fewer overall biopsies [23]. Clearly, there was room for improvement in terms of patient access during MRI and the necessity for movement of the MRI table. Fully MR-compatible robotic assistance is ideal to improve accuracy and ease of intra-MRI biopsy.

Construction of a Magnetic Resonance-Safe Robot

One of the greatest challenges to robotic assistance for MR-guided biopsy has been development of a fully MR-compatible robot. MRI utilizes high-density magnetic fields, with pulsed magnetic and radio frequency fields. A ferromagnetic object in close proximity to MRI would be subject to high magnetic interaction forces and can cause heating and movement within conductive objects. If critical robotic items are subject to a magnetic field, accuracy and functionality are compromised. Most available robotic devices require an electromagnetic motor, yet the use of electricity near MRI will cause interference of signal-to-noise attenuation, signal distortion, and artifact [24]. Therefore, when building a device, it is important that materials be nonmagnetic and nonconducting [25]. In order to be completely MR-safe and not merely MR-conditional, robotic components need to be built of rubber, glass, or plastic [26]. The primary challenge is providing non-electrical energy to the device, as electric currents generate electromagnetic waves and are not MR-safe. Available options are energy sources that are not coupled to electromagnetism, including pneumatic and light energy. Pneumatic actuation is MR-safe, and a number of organizations have attempted to create an MR-safe robot using pneumatic actuators. The PneuStep motor is one such example.

PneuStep Motor

The PneuStep motor (Johns Hopkins Urology Robotics Lab, Baltimore, Maryland) uses a novel pneumatic step motor. All motor components were constructed from nonmagnetic and nonconductive materials. Sensors within the device were constructed with fiber optics—obviating the need entirely for the use of electricity. The PneuStep motor has undergone thorough testing and is MR-safe. There is no image interference or disturbed motor function, even with the motor located at the image isocenter of a magnetic field imager [27].

Pneumatic actuation is employed in numerous applications due to its ease of use when an air supply is readily available. However, it has had limited use in medical applications due to its reduced precision in controlled motion from friction with various motor components. Step motors are able to bypass these issues. In simplified terms, end-to-end motion of a piston within its cylinder provides an exact quantity of energy. The step motor collects successive end-to-end motion strokes during a rotary motion, which provides simple and precise low-speed pneumatic actuation [28].

Robotic-Assisted Targeting Device

An endorectal robotic-assistance device was developed to achieve accurate prostatic targeting. The physician performing the biopsy selects an appropriate target on MR image, and the device provides assistance by orienting the needle guide and fixing target depth. A physician is required to insert the needle and execute the biopsy, but the targeting device guides biopsy performance. Similarly designed devices typically have 2 degrees of freedom, which requires the physician to control needle depth [22, 29, 30]. The currently described targeting device provides 3 degrees of freedom—allowing all needle motion to be guided robotically. The endorectal component has a series of registration markers, and the needle guide passes through the endorectal extension at an angle determined robotically. A needle spacer adjusts the depth of biopsy needle insertion [24].

Kinematic Structure

A downside of imaging fusion technology is the requirement for cross-modality image registration. This introduces the potential for significant error, particularly if a given target area is small. An ideal system avoids prostatic deformation, obviating the need for calibration. The endorectal extension for the MrBot (Johns Hopkins Urology Robotics Lab, Baltimore, Maryland) functions similarly to previously described TRUS probes, with a purely rotary motion that largely eliminates prostate deformation [24, 31]. Biopsy performance was tested using a computer-simulated design, and the endorectal probe and needle guide did not deform prostatic tissue significantly [24]. The 3 robotic degrees of freedom include (R1) rotation of the endorectal extension around its axis, (R2) rotation of the needle guide relative to the endorectal extension, and (T) insertion of the needle through the needle guide. A motor adjusts the angle of R1 and is supported by a revolute joint (R). A second motor performs a screw transmission and is supported by a prismatic joint (P). The bottom of the needle guide moves through a revolute (R) joint. The top of the needle guide slides through the revolute-cylindrical joint (RC). The needle is then inserted manually through the needle guide but will stop when it reaches the nut at the top of the needle guide [24]. This system is pictured in Fig. 20.1.

Magnetic Resonance-Guided Biopsy Results

After development of an MR-safe robot, its safety and feasibility were tested in a canine model. Image to robot registration was performed, and radiologists selected appropriate targets within the canine prostate for needle placement. Thirty targets in six dog prostates were sampled. The robot-guided biopsies were found to have an average precision of 1.31 mm and accuracy of 1.58. The greatest deviation was found to be 2.58, which is still within the 5 mm margin of acceptable error for targeting of

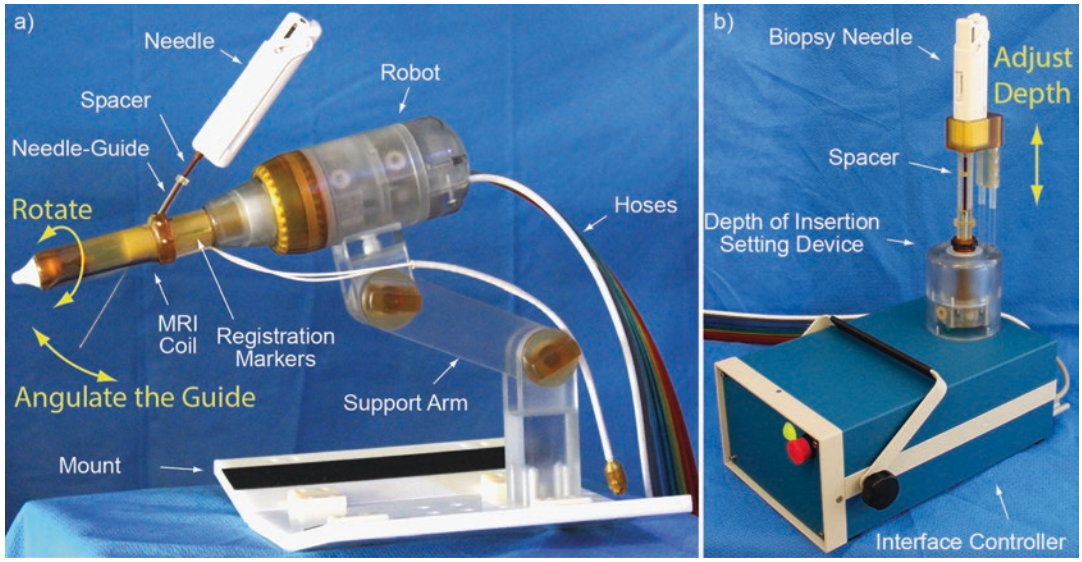

Fig. 20.1 (**a**) The needle guide is featured with 2 degrees of freedom (DoF), permitting accurate needle placement in three-dimensional space. (**b**) Displays the third DoF, which controls the depth of needle placement. (**c**) The 2 rotational DoF are depicted with *red arrows*, and the *black dotted line* represent the axis of rotation. Reprinted with permission from Srimathveeravalli G, Kim C, Petrisor D, Ezell P, Coleman J, Hricak H, Solomon SB, and Stoianovici D. MRI-safe robot for targeted transrectal prostate biopsy: Animal experiments. BJU Int. 2014;113(6):977–85

clinically significant tumors [32]. All 6 dogs recovered without complication. All needle placements were successful on the first attempt, and the time from targeting to biopsy was approximately 3 min [24].

Recently, the safety and feasibility of direct MRI-guided biopsy were assessed in a human cohort. Five men with elevated PSA, previous negative biopsy, and presence of a cancer suspicious region on MRI underwent transperineal direct MRI-guided biopsy using the MrBot. Figure 20.2 displays patient and robot setup. Biopsies targeting the cancer suspicious regions and sextant biopsies were obtained. Two men required post-procedural urethral catheter placement, but no complications occurred. There were 30 total biopsy sites, and clinically significant prostate cancer was detected in two patients. Overall, the targeting accuracy was 2.55 mm normal to the needle without trajectory corrections.

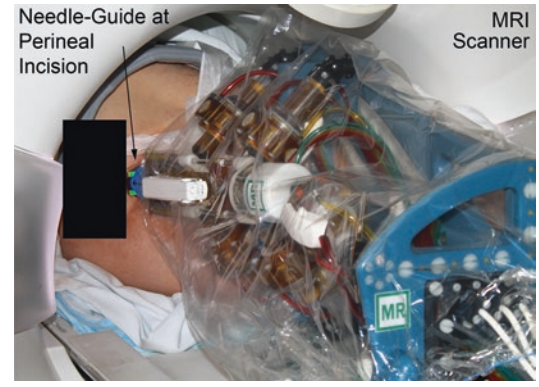

Fig. 20.2 Displays a patient in left lateral decubitus position within the MRI scanner. The MrBot is mounted to the MRI table and placed at the perineum

There were no unsuccessful biopsies targeting attempts [33]. Clearly, MR-guided biopsy can be performed with excellent accuracy for small lesions.

Magnetic Resonance-Guided Robotic Assistance for Prostate Cancer Therapy

Brachytherapy is a commonly used treatment modality for prostate cancer. It utilizes either permanent low-dose rate brachytherapy seeds or temporary high-dose rate brachytherapy seeds. Therapy is typically performed under US guidance according to a predesignated treatment map. The treatment map is usually template based and attempts to target areas of greater malignant risk and spare areas that may lead to poor continence or erectile function outcomes [34].

For properly selected men, some studies show that brachytherapy has similar oncologic outcomes to external beam radiation therapy (EBRT) and radical prostatectomy (RP) [34]. Compared with other treatment modalities, individuals undergoing brachytherapy also have shorter convalescence times and have lower risk of developing some treatment side effects that are more common with EBRT and RP [35].

To better target areas with the highest cancer risk, there is interest in applying MR imaging for placement and evaluation of brachytherapy seeds. MRI has been used in numerous areas of prostate brachytherapy—including real-time implantation guidance, high-dose rate optimization, and low-dose rate post-implant dosimetry [36]. These are areas under active investigation and are not utilized in a standard fashion.

The benefit of robotic-assisted MR-guided brachytherapy seed placement is accurate targeting of radiation doses to areas harboring aggressive disease while sparing critical nearby structures. Currently, brachytherapy is performed using a template, which restricts possible needle trajectories [37]. A benefit of robotic placement is that it is not template limited and seeds can be placed in areas that would not typically be possible to access. Additionally, treatment under MR guidance allows for dosimetric feedback, thus allowing additional seed placement to underdosed areas [38].

In order for brachytherapy seeds to be inserted robotically, 3 tasks must be performed: (1) needle orientation, (2) needle insertion, and (3) seed deployment. The previously described MrBot was utilized for this purpose. An MR-compatible needle seed injector was designed and is able to perform high-speed needle insertion to greatly decrease soft-tissue deflection [39]. Prior to biopsy, image-to-robot registration is performed. A fiducial marker is attached to the seed injector end-effector. The intersection of this marker with the planes of the MR image slices is utilized to perform image-to-robot registration. Two different algorithms are used to perform this feat, as detailed in Muntener et al. [40]. Accuracy of motion tests were performed, in which the robot was repeatedly positioned in extreme work space points. The MrBot was very accurate during basic motion capability tests, in which placement reliably had an error of only 0.076 ± 0.035 mm. After warm-up, the mean error value decreased to 0.060 ± 0.032 mm. When tested with the tissue mock-up, the mean error was somewhat higher at 0.72 ± 0.36 mm [40].

Conclusion

Prostate cancer is the most prevalent malignancy effecting males, with nearly 1 in 6 men receiving a prostate cancer diagnosis during their lifetime [41]. More than one million TRUS-guided biopsies are performed yearly, and it is one of the most common procedures performed by urologists. However, systematic TRUS-guided biopsies frequently miss aggressive tumors and due to their systematic nature frequently detect clinically insignificant tumors [7, 42]. Additionally, these biopsies are prone to human error and surgeons tend to cluster biopsies in an individualized pattern [9].

MRI is an excellent tool to detect prostatic lesions, and it is increasingly being used to inform prostate biopsy both in the form of cognitive fusion biopsies and MR/US fusion-guided biopsies [13]. Various groups have attempted MRI-guided in-gantry biopsy. Using this technique, prostate cancer is frequently detected in individuals with previous negative prostate biopsy and appears to have higher cancer detection rates than standard TRUS-guided biopsy [21].

In order to better target suspicious lesions identified on MRI, there has been interest in developing robotic-assisted MR-guided prostate biopsy. A few groups have developed MR-compatible robots capable of biopsy with successful results [23]. One such system is the MrBot, which is a fully MR-compatible robotic system, capable of precise lesion targeting without influence on acquisition of MR images [24]. Electric energy is not compatible with MRI, and thus the PneuStep motor was designed. This is a pneumatic step motor that utilizes energy from successive end-to-end motion strokes during rotary motion and is able to generate a consistent source of energy that is both MR-compatible and effective for the accuracy required for robotic targeting [28]. Additionally, a robotic-assisted targeting device was developed with 3 degrees of freedom. The endorectal component contains registration markers, and an associated needle guide sets the needle trajectory based on coordinates derived from the targeting device [24]. A unique kinematic structure, based on purely rotary motion, allows prostate scanning without significant tissue deformation [24]. MR-guided biopsies with robotic assistance improve accuracy and precision with a targeting error of approximately only 1.0 mm [9, 43].

There has also been considerable interest in the utilization of robotic assistance for treatment of prostate cancer—particularly in the form of brachytherapy. Currently, brachytherapy seeds are placed using a template. MRI guidance offers real-time implantation guidance, high-dose rate dose optimization, and low-dose rate post-implant dosimetry [36]. The MrBot with PneuStep motor has been used in brachytherapy simulations and shown to have a targeting error of only 0.72 mm [40].

While initial trials with robot-assisted MR-guided prostate biopsies have been promising, a number of questions remain. It is unknown how well these biopsies will compare to systematic TRUS-guided biopsies and MR/US fusion-guided biopsies. It is presumed that more accurate targeting discrete lesions would lead to increased diagnosis of higher-grade tumors and reduce incidentally found lower-grade cancers; however, this remains unverified. Moving forward, prospective randomized trials will be necessary to truly differentiate the diagnostic potentials between various biopsy methods.

References

1. Siegel R, Naishadham D, Jemal A. Cancer statistics, 2013. CA Cancer J Clin. 2013;63(1):11–30
2. Lin K, Croswell J, Koenig H, Lam C, Maltz A. Prostate-specific antigen-based screening for prostate cancer: an evidence update for the U.S. Preventive Services Task Force. Evid Synth. 2011;(90) 12–05160
3. Barocas DA, Mallin K, Graves AJ, Penson DF, Palis B, Winchester DP, et al. The effect of the United States Preventive Services Task Force grade D recommendation against screening for prostate cancer on incident prostate cancer diagnoses in the US. J Urol. 2015;194(6):1587–93.
4. Jemal A, Fedewa SA, Ma J, Siegel R, Lin CC, Brawley O, et al. Prostate cancer incidence and PSA testing patterns in relation to USPSTF screening recommendations. JAMA. 2015;314(19):2054–61.
5. Loeb S, Carter HB, Berndt SI, Ricker W, Schaeffer EM. Complications after prostate biopsy: data from SEER-medicare. J Urol. 2011;186(5):1830–4.
6. Ghai S, Eure G, Fradet V, Hyndman M, McGrath T, Wodlinger B, et al. Assessing cancer risk in novel 29 MHz micro-ultrasound images of the prostate: creation of the PRI-MUS (prostate risk identification using micro-ultrasound) protocol. J Urol. 2016; 16:22–53.
7. Daneshgari F, Taylor GD, Miller GJ, Crawford ED. Computer simulation of the probability of detecting low volume carcinoma of the prostate with six random systematic core biopsies. Urology. 1995;45(4): 604–9.
8. Fink KG, Hutarew G, Lumper W, Jungwirth A, Dietze O, Schmeller NT. Prostate cancer detection with two sets of ten-core compared with two sets of sextant biopsies. Urology. 2001;58(5):735–9.
9. Han M, Chang D, Kim C, Lee BJ, Zuo Y, Kim HJ, et al. Geometric evaluation of systematic transrectal ultrasound guided prostate biopsy. J Urol. 2012; 188(6):2404–9.
10. Goto Y, Ohori M, Arakawa A, MW K, TM W, PT S. Distinguishing clinically important from unimportant prostate cancers before treatment: value of systematic biopsies. J Urol. 1996;156(3):1059–63.
11. Steyerberg EW, Roobol MJ, Kattan MW, van der Kwast TH, de Koning HJ, Schröder FH. Prediction of indolent prostate cancer: validation and updating of a prognostic nomogram. J Urol. 2007;177(1):107–12.
12. Fütterer JJ, Briganti A, De Visschere P, Emberton M, Giannarini G, Kirkham A, et al. Can clinically significant prostate cancer be detected with multiparametric magnetic resonance imaging? a systematic review of the literature. Eur Urol. 2015;68(6):1045–53.

13. Logan JK, Rais-Bahrami S, Turkbey B, Gomella A, Amalou H, Choyke PL, et al. Current status of magnetic resonance imaging (MRI) and ultrasonography fusion software platforms for guidance of prostate biopsies. BJU Int. 2014;114(5):641–52.
14. Siddiqui M, Rais-Bahrami S, Turkbey B, George A, Rothwax J, Shakir N, et al. Comparison of MR/ultrasound fusion-guided biopsy with ultrasound-guided biopsy for the diagnosis of prostate cancer. JAMA. 2015;313(4):390–7.
15. Yang EY, Polsani VR, Washburn MJ, Zang W, Hall AL, Virani SS, et al. Real-time co-registration using novel ultrasound technology: ex vivo validation and in vivo applications. J Am Soc Echocardiogr. 2011; 24(7):720–8.
16. Cheung MR, Krishnan K. Using manual prostate contours to enhance deformable registration of endorectal MRI. Comput Methods Prog Biomed. 2012;108(1): 330–7.
17. Engelhard K, Hollenbach H, Kiefer B, Winkel A, Engehausen D. MRI-guided prostate biopsy in two different standard 1.5 T scanners using an endorectal biopsy device. Proc Intl Soc Mag Reson Med. 2006;14:1446. http://cds.ismrm.org/ismrm-2006/files/01446.pdf
18. Franiel T, Stephan C, Erbersdobler A, Dietz E, Maxeiner A, Hell N, et al. Areas suspicious for prostate cancer: MR-guided biopsy in patients with at least one transrectal US-guided biopsy with a negative finding–multiparametric MR imaging for detection and biopsy planning. Radiology. 2011;259(1):162–72.
19. Zangos S, Melzer A, Eichler K, Sadighi C, Thalhammer A, Bodelle B, et al. MR-compatible assistance system for biopsy in a high-field-strength system: initial results in patients with suspicious prostate lesions. Radiology. 2011;259(3):903–10.
20. Roethke M, Anastasiadis AG, Lichy M, Werner M, Wagner P, Kruck S, et al. MRI-guided prostate biopsy detects clinically significant cancer: analysis of a cohort of 100 patients after previous negative TRUS biopsy. World J Urol. 2012;30(2):213–8.
21. Hambrock T, Hoeks C, Hulsbergen-Van De Kaa C, Scheenen T, Fütterer J, Bouwense S, et al. Prospective assessment of prostate cancer aggressiveness using 3-T diffusion-weighted magnetic resonance imaging-guided biopsies versus a systematic 10-core transrectal ultrasound prostate biopsy cohort. Eur Urol. 2012;61(1):177–84.
22. Krieger A, Susil RC, Ménard C, Coleman JA, Fichtinger G, Atalar E, et al. Design of a novel MRI compatible manipulator for image guided prostate interventions. IEEE Trans Biomed Eng. 2005;52(2): 306–13.
23. Yakar D, Schouten MG, Bosboom DGH, Barentsz JO, Scheenen TWJ, Fütterer JJ. Feasibility of a pneumatically actuated MR-compatible robot for transrectal prostate biopsy guidance. Radiology. 2011;260(1): 241–7.
24. Stoianovici D, Kim C, Srimathveeravalli G, Sebrecht P, Petrisor D, Coleman J, et al. MRI-safe robot for endorectal prostate biopsy. IEEE/ASME Trans Mechatronics. 2014;19(4):1289–99.
25. Stoianovici D. Multi-imager compatible actuation principles in surgical robotics. Int J Med Robot. 2005;1(2):86–100.
26. Yu N, Gassert R, Riener R. Mutual interferences and design principles for mechatronic devices in magnetic resonance imaging. Int J Comput Assist Radiol Surg. 2011;6(4):473–88.
27. Stoianovici D, Song D, Petrisor D, Ursu D, Mazilu D, Mutener M, et al. "MRI Stealth" robot for prostate interventions. Minim Invasive Ther Allied Technol. 2007;16(4):241–8.
28. Stoianovici D, Patriciu A, Petrisor D, Mazilu D, Kavoussi L. A new type of motor: pneumatic step motor. IEEE/ASME Trans Mechatronics. 2007;12(1): 98–106.
29. Krieger A, Song SE, Bongjoon Cho N, Iordachita II, Guion P, Fichtinger G, et al. Development and evaluation of an actuated MRI-compatible robotic system for MRI-guided prostate intervention. IEEE/ASME Trans Mechatronics. 2013;18:273–84.
30. Krieger A, Csoma C, Iordachital II, Guion P, Singh AK, Fichtinger G, et al. Design and preliminary accuracy studies of an MRI-guided transrectal prostate intervention system. Med Image Comput Comput Assist Interv. 2007;10(Pt 2):59–67.
31. Han M, Kim C, Mozer P, Schfer F, Badaan S, Vigaru B, et al. Tandem-robot assisted laparoscopic radical prostatectomy to improve the neurovascular bundle visualization: a feasibility study. Urology. 2011;77(2): 502–7.
32. Ploussard G, Epstein JI, Montironi R, Carroll PR, Wirth M, Grimm MO, et al. The contemporary concept of significant versus insignificant prostate cancer. Eur Urol. 2011;60(2):291–303.
33. Stoianovici D, Kim C, Petrisor D, Jun C, Lim S, Ball M, Ross A, Macura K, Allaf M. MR safe robot, FDA clearance, safety and feasibility of prostate biopsy clinical trial. IEEE/ASME Trans Mechatron. 2016. doi:10.1109/TMECH.2016.2618362 [Epub ahead of print].
34. Chao MW, Grimm P, Yaxley J, Jagavkar R, Ng M, Lawrentschuk N. Brachytherapy—state of the art radiotherapy in prostate cancer. BJU Int. 2015;116(3): 80–8.
35. Ferrer M, Suárez JF, Guedea F, Fernández P, Macías V, Mariño A, et al. Multicentric Spanish Group of Clinically Localized Prostate Cancer. Health-related quality of life 2 years after treatment with radical prostatectomy, prostate brachytherapy, or external beam radiotherapy in patients with clinically localized prostate cancer. Int J Radiat Oncol Biol Phys. 2008;72(2):421–32.

36. Tanderup K, Viswanathan AN, Kirisits C, Frank SJ. Magnetic resonance image guided brachytherapy. Semin Radiat Oncol. 2014;24(3):181–91.
37. MPR G, Van MA M, JJ B, JJW L, Van MPR G. MRI-guided prostate brachytherapy with single needle method—a planning study. Radiother Oncol. 2004; 71(3):327–32.
38. Cormack RA, Tempany CM, D'Amico AV. Optimizing target coverage by dosimetric feedback during prostate brachytherapy. Int J Radiat Oncol Biol Phys. 2000;48(4):1245–9.
39. Lagerburg V, Moerland MA, Konings MK, van de Vosse RE, Lagendijk JJW, Battermann JJ. Development of a tapping device: a new needle insertion method for prostate brachytherapy. Phys Med Biol. 2006;51(4):891–902.
40. Muntener M, Patriciu A, Petrisor D, Mazilu D, Bagga H, Kavoussi L, et al. Magnetic resonance imaging compatible robotic system for fully automated brachytherapy seed placement. Urology. 2006;68(6):1313–7.
41. Li J, Djenaba JA, Soman A, Rim SH, Master VA. Recent trends in prostate cancer incidence by age, cancer stage, and grade, the United States, 2001–2007. Prostate Cancer. 2012;2012:691380.
42. Epstein JI, Walsh PC, Carmichael M, Brendler CB. Pathologic and clinical findings to predict tumor extent of nonpalpable (stage T1c) prostate cancer. JAMA. 1994;271(5):368–74.
43. Srimathveeravalli G, Kim C, Petrisor D, Ezell P, Coleman J, Hricak H, et al. MRI-safe robot for targeted transrectal prostate biopsy: animal experiments. BJU Int. 2014;113(6):977–85.

Part VI

Technologies for Focal Therapy: Transperineal Approach

In-Bore Transperineal Magnetic Resonance Imaging-Guided Laser Ablation

21

Nathan Perlis, John Trachtenberg, and Sangeet Ghai

Introduction

Localized Prostate Cancer Treatment and Morbidity

Prostate cancer continues to be the most commonly diagnosed non-cutaneous malignancy among North American men [1]. Prostate-specific antigen (PSA) screening is believed to have raised detection, thus causing increased treatment of low-grade, localized prostate cancer [2]. Despite a now common robotic approach to surgery and more advanced targeted external beam radiation therapy technologies, significant deterioration of urinary and sexual function remain prevalent side effects of radical therapies [3]. Conservative expectant management of localized prostate cancer is a response to this morbidity and attempts to prevent or defer complications in men with low risk of disease progression. This is confirmed by the minimal benefit for patients in a randomized trial of surgery versus active surveillance for low-risk tumors [4].

However, it is understood that even the diagnosis of prostate cancer causes substantial psychological and emotional burden, resulting in impairment of health-related quality of life [5]. Despite mounting evidence for active surveillance in localized low-risk prostate cancer, uptake of active surveillance remains limited and may be linked to a perceived concept that treating all cancers early is beneficial [6]. There may also be a cohort of men with intermediate-risk prostate cancer who may not be good candidates for active surveillance but for whom whole-gland therapies still constitute therapeutic overkill. Patients with Gleason score 7 (3 + 4) with low percent Gleason pattern 4, no cribriform or intraductal carcinoma, low PSA, and small-volume disease are known to have low rates of extraprostatic disease (non-organ confined rates) at prostatectomy and low rates of biochemical recurrence post-prostatectomy [7–9]. For this group of patients, focal ablation may be appropriate.

N. Perlis (✉)
Department of Urologic Oncology, University of Toronto, Toronto, ON, Canada

Division of Urology, Department of Surgical Oncology, University Health Network, Princess Margaret Cancer Centre, Toronto, ON, Canada
e-mail: nathan.perlis@utoronto.ca

J. Trachtenberg
Division of Urology, Department of Surgical Oncology, University Health Network, Princess Margaret Cancer Centre, Toronto, ON, Canada

S. Ghai
Department of Urologic Oncology, University of Toronto, Toronto, ON, Canada

Joint Department of Medical Imaging, University Health Network—Mount Sinai Hospital—Womens' College Hospital, Toronto General Hospital, Toronto, ON, Canada

© Springer International Publishing AG 2017

T.J. Polascik (ed.), *Imaging and Focal Therapy of Early Prostate Cancer*, Current Clinical Urology, DOI 10.1007/978-3-319-49911-6_21

Focal Ablation of Prostate Cancer

In focal ablation, an identified tumor is targeted for destruction, while the remainder of the prostate and surrounding vital structures (i.e., bladder, urethra, neurovascular bundles) are preserved [10]. Historically prostate cancer was deemed a "field defect" disease with presumed multifocality and thus treated solely with whole-gland therapies. With advent of multiparametric magnetic resonance imaging (mpMRI) and more accurate and thorough biopsy approaches, we are learning that there are occasionally solitary tumors in the prostate and other times there is a dominant tumor [11]. This dominant tumor, or index lesion, is generally the largest site of cancer with the highest Gleason score and is hypothesized to promote disease progression [12]. Grade also plays a key factor in pursuing less radical therapy for prostate cancer. Many genetic alterations and mutations associated with Gleason 6 cancer are separate from the changes in Gleason 7 tumors, suggesting that Gleason 6 tumors do not have metastatic potential [13]. There are almost no cases in the literature of metastatic Gleason 6 prostate cancer [14]. Thus, if we could reliably identify and isolate the large, higher-grade tumors and target them solely for destruction, patients will theoretically be afforded better quality of life and good oncologic outcomes.

Focal ablation can be applied by many unique energy sources and in a wide variety of manners. Cryotherapy, high-intensity focused ultrasound (HIFU), photothermal laser, radiofrequency ablation, and intracorporeal electroporation have all been studied for prostate ablation. The interstitial modalities can be applied transrectally or transperineally, while HIFU is predominantly a transrectal energy. Regardless of the route and energy used, the amount of tissue destroyed needs to be carefully planned [15]. This is a delicate balance. In the most focal approaches, the tumor and a margin of normal prostate are ablated so that vital structures are preserved and morbidity reduced. However, when less tissue is targeted, then persistent or recurrent cancer becomes more likely. For this reason, when attempting a targeted focal treatment of a lesion plus margin, one has to have excellent tumor localization and monitoring of tumor destruction. Both of these are afforded when performing transperieneal focal laser ablation.

Magnetic Resonance Imaging for Diagnosis and Targeting Therapy

Multiparametric MRI can precisely identify clinically significant adenocarcinoma of the prostate (PCa) [16, 17]. This targeted localization offers a unique opportunity to use mpMRI as a map for image-guided diagnosis and treatment [15, 18, 19]. Several groups have established that mpMRI-targeted prostate biopsies diagnose more clinically significant high- and intermediate-grade cancers while avoiding low-grade lesions when compared to traditional systematic sextant biopsy [20, 21]. This technology promises to identify high- and intermediate-grade tumors that were previously missed with systematic biopsy alone and avoid overdiagnosing low-grade cancer.

Multiparametric MRI also has been successfully employed in targeting lesions for focal ablative therapy [18]. In this targeted approach, clinically significant MRI-visible tumor or the index lesion is selectively ablated while sparing the remainder of the prostate gland [22, 23]. By targeting only the tumor and a margin of normal-appearing prostate, sensitive structures such as the neurovascular bundles, bladder neck, and urethra are generally spared, decreasing morbidity (i.e., erectile dysfunction) compared to radical extirpative surgery or radiotherapy [24]. Index lesions are commonly the largest and highest grade tumors visualized on MRI and confirmed on biopsy and are targeted in focal therapy because they are hypothesized to drive disease progression [12]. Multiparametric MRI can accurately detect 80–90 % of index lesions [25].

In-bore treatments are uniquely suited for focal interventions because the visualization of tumor on mpMRI can be harnessed for targeting a lesion and concurrent MRI-thermometry can detect treatment location and efficacy based on real-time temperature feedback [26, 27].

Temperature is used to determine if coagulative necrosis is likely in the selected ablation site but also confirms safety of vital structures (i.e., rectum, urethra, bladder neck) to avoid major morbidity. Finally, a contrast-enhanced scan at the end of the procedure demarcates the nonperfused treatment area to confirm adequate coverage before terminating the session. Supraphysiological hyperthermia (42–60 °C) may be visible as a thin rim (approximately 2 mm) of hyperemia or hemostasis around the necrotic zone. This is often seen only on immediate post-ablation contrast-enhanced scan. This rim eventually develops into coagulative necrosis within approximately 5 days [28, 29].

Laser interstitial prostate ablation can be performed via transperineal or transrectal fiber insertion. We believe that transperineal application has several theoretical advantages over the transrectal approach. Infection may be reduced by avoiding transrectal fiber insertion. Also transperineal application allows access to midline lesions anterior to the urethra that are only accessible in the transrectal approach by traversing the urethra. There is also potential to cause a rectourethral fistula when treating midline posterior tumors via the rectum. However, despite these theoretical advantages, Lepor et al. reported safe treatment with transrectal interstitial laser ablation on 25 consecutive patients [30]. Another trial is evaluating the safety of transrectal applied focal laser ablation in 100 patients [31].

Magnetic Resonance-Guided Transperineal Focal Laser Ablation

Transperineal, in-bore MR-guided focal laser ablation (FLA) is currently being evaluated as a novel approach for management of localized PCa in clinical trials. This technique relies on high-energy laser light emitted from laser fibers placed through the perineum into the lesion, causing rapid heating and coagulation. The amount of tissue destroyed relates to depth of light distribution and the amount of energy delivered to the surrounding tissue and is regulated by the wavelength of the laser fiber. The cylindrical diffuser tip varies in length from 10 mm to 40 mm, and optical fibers for light delivery range between 300 μm and 600 μm in diameter [32]. The 15 W fiber is generally 400 μm in diameter, and the 30 W fiber is 600 μm (Visualase® cooled laser applicator system, Medtronic, Dublin, Ireland). One advantage of laser compared with other energy sources is its MRI compatibility. In addition, because MRI is used for real-time guidance, inaccuracy inherent in image registration that may plague other modalities, such as HIFU, is avoided. Laser energy is predictable and precise and can be modulated in real time by the operator based on anatomic and temperature feedback from real-time MR thermography. With precision of both prostate lesion identification and laser energy delivery, in-bore FLA is well suited for targeted ablation (versus hemi-ablation or zonal ablation). For this reason, we suggest that this approach be reserved for MRI-visible lesions confirmed on biopsy.

The procedure is carried out in the MRI day surgery suite with deep sedation (intravenous propofol) and the patient in the supine position with a Foley urethral catheter placed for bladder drainage. Several unique MRI sequences are used throughout the treatment. Prior to needle insertion, T2-weighted and diffusion-weighted imaging (DWI) sequences are obtained to confirm anatomy and target location (Fig. 21.1a, b). To visualize needle placement intraoperatively, we use T1-weighted spoiled gradient echo, ultrafast gradient echo, and true fast imaging with steady-state precision (bSSFP) sequences (Fig. 21.1c) [33]. Our group has reported on identifying the catheter by instilling contrast in the catheter and visualizing it on spoiled gradient echo sequences. After confirming the cannula position, the obturator is exchanged for the optical fiber in the cooling sheath, and the laser source can then be activated for energy delivery. An initial low-power subtherapeutic test dose is generally applied to check the position of the fiber and to confirm MRI thermography. Real-time thermal maps can be gathered using the proton resonance frequency (PRF) shift, which is based on gradient echoes with long TE. With three-dimensional processing, the anatomic relation of the thermal map to the important

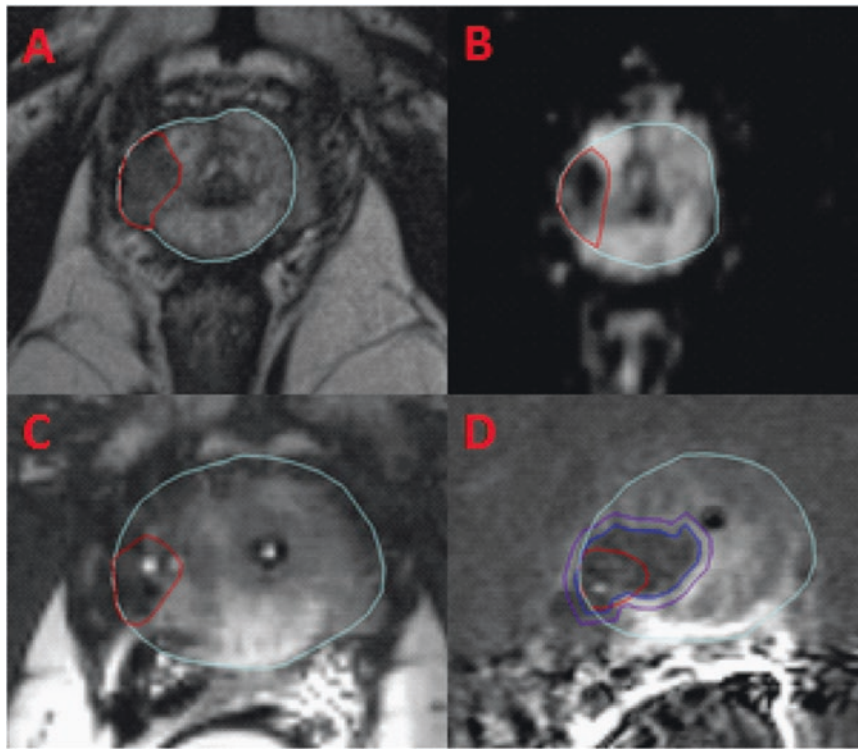

Fig. 21.1 A 65-year-old man with Gleason 3+4 prostate cancer. (**a**) Axial T2WI. (**b**) ADC showing the contoured tumor in right apical peripheral zone. (**c**) Axial bSSFP showing two transperineal cannulas in position. (**d**) Posttreatment contrast-enhanced images showing nonperfused ablated volume overlaid on the pretreatment tumor contour

surrounding structures can be identified. Contrast-enhanced sequence is used posttreatment to confirm ablation (Fig. 21.1d). A Foley catheter is generally left in place for 1–3 days.

Preclinical trials using 980 nm diode laser (Visualase) for thermal energy delivery for in-bore FLA have shown precise and predictable ablation zones [29]. In two separate phase I trials, efficacy was demonstrated in 47 patients who were treated using the transperineal approach with minimal or no side effects [34, 35]. Successful ablation at treatment site was reported in approximately 75 % of cases, and most of the patients with residual disease had low-risk disease, not visible on mpMRI at 4–6 months posttreatment. Ongoing phase II transperineal clinical trial results at our institute (University of Toronto) and the University of Chicago are due in 2016. Our group at University of Toronto is presently using an MR-compatible mechatronic device for needle guidance [36]. In 37 consecutive transperineal needle insertions using the mechatronic device in the course of 10 focal laser ablation treatments, we reported a median needle guidance error of 3.5 mm and needle delivery time of 9 min [37]. Woodrum et al. reported successful in-bore ablation of a 2.2 cm focus of recurrent tumor in the prostatectomy bed using interstitial laser via the transperineal route [38].

Initial results from 38 men treated with transperineal focal laser ablation were presented from University of Toronto with a median follow-up of 18 months [39]. Of the ablated tumors, 64 % were Gleason pattern 6 (3 + 3) with the remainder being Gleason pattern 7 (3 + 4). No cases had to be aborted and all were performed without requiring overnight hospitalization. There were no intraoperative complications, and postoperative complications were predominantly urinary retention (three patients) and transient stress urinary incontinence in one patient that resolved within 8 weeks. On follow-up biopsy, 47 % of

patients were completely cancer-free. An additional 26 % of patients were clear of disease at the ablated site but demonstrated cancer in the contralateral lobe, while another 26 % had persistent disease at the ablated zone. Erections were minimally impacted as 96 % of men with good erections pre-laser ablation maintained their function.

In these 38 men, PSA declined by a mean of 2.0 ng/ml from 5.6 to 3.6, and was inversely correlated to the ablation volume. Ablation volume as measured by immediate posttreatment gadolinium-enhanced MRI increased from 4.8 cm^3 for the first ten patients to 8 cm^3 in the last ten patients.

Medium- and long-term functional and oncologic control for transperineal focal laser ablation has yet to be established.

Conclusion

Multiparametric MRI is ideally suited for guiding targeted treatment of prostate cancer due to its spatial resolution, real-time temperature monitoring feedback, and ability to localize clinically significant tumors. In-bore therapy avoids multiple image co-registration—required for ultrasound-guided treatments—which has an inherent margin of error. In-bore FLA is particularly advantageous due to its precise, predictable, and easily monitored tissue destruction. Several drawbacks to in-bore therapy are the cost associated with MRI time, prolonged anesthesia, and the challenge of using MRI-compatible instruments. These limitations may deter uptake of MRI-guided in-bore FLA. Speeding up the procedure is vital to its cost-effectiveness and wider adoption. We believe that wider bore MRI machines, using MRI-compatible robots for needle insertion and generating more efficient workflow processes are important areas for improvement.

References

1. Siegel R, Miller K, Jemal A. Cancer statistics, 2015. CA Cancer J Clin. 2015;65:5–29.
2. Cooperberg MR, Lubeck DP, Meng MV, Mehta SS, Carroll PR. The changing face of low-risk prostate cancer: trends in clinical presentation and primary management. J Clin Oncol. 2004;22(11):2141–9.
3. Resnick MJ, Koyama T, Fan K-H, Albertsen PC, Goodman M, Hamilton AS, et al. Long-term functional outcomes after treatment for localized prostate cancer. N Engl J Med. 2013;368:436–45.
4. Wilt TJ, Brawer MK, Jones KM, Barry MJ, Aronson WJ, Fox S, et al., Prostate Cancer Intervention versus Observation Trial (PIVOT) Sotudy Group. Radical prostatectomy versus observation for localized prostate cancer. N Engl J Med. 2012;367:203–13.
5. Reeve BB, Stover AM, Jensen RE, Chen RC, Taylor KL, Clauser SB, et al. Impact of diagnosis and treatment of clinically localized prostate cancer on health related quality of life for older Americans. Cancer. 2012;118:5679–87.
6. Bul M, Zhu X, Valdagni R, Pickles T, Kakehi Y, Rannikko A, et al. Active surveillance for low-risk prostate cancer worldwide: the PRIAS study. Eur Urol. 2013;63(4):597–603.
7. Kweldam CF, Kümmerlin IP, Nieboer D, Verhoef EI, Steyerberg EW, Kwast TH, et al. Disease-specific survival of patients with invasive cribriform and intraductal prostate cancer at diagnostic biopsy. Mod Pathol. 2016;29(6):630–6.
8. Sauter G, Steurer S, Clauditz TS, Krech T, Wittmer C, Lutz F, et al. Clinical utility of quantitative Gleason grading in prostate biopsies and prostatectomy specimens. Eur Urol. 2016;69(4):592–8.
9. Cole AI, Morgan TM, Spratt DE, Palapattu GS, He C, Tomlins SA, et al. Prognostic value of percent Gleason grade 4 at prostate biopsy on predicting prostatectomy pathology and recurrence. J Urol. 2016; 196(2):405–11.
10. Marshall S, Taneja S. Focal therapy for prostate cancer: the current status. Prostate Int. 2015;3:35–41.
11. Murphy G, Haider M, Ghai S, Sreeharsha B. The expanding role of MRI in prostate cancer. Am J Roentgenol. 2013;201:1229–38.
12. Ahmed HU. The index lesion and the origin of prostate cancer. N Engl J Med. 2009;361(17):1704–6.
13. VanderWeele DJ, Brown CD, Taxy JB, Gillard M, Hatcher DM, Tom WR, et al. Low-grade prostate cancer diverges early from high grade and metastatic disease. Cancer Sci. 2014;105:1079–85.
14. Ross HM, Kryvenko ON, Cowan JE, Simko JP, Wheeler TM, Epstein JI. Do adenocarcinomas of the prostate with Gleason score (GS) ≤6 have the potential to metastasize to lymph nodes? Am J Surg Pathol. 2012;36(9):1346–52.
15. Nobin J, Rosenkrantz AB, Villers A, Orczyk C, Deng F-M, Melamed J, et al. Image guided focal therapy of MRI-visible prostate cancer: defining a 3D treatment margin based on MRI-histology co-registration analysis. J Urol. 2015;194:364–70.
16. Turkbey B, Pinto PA, Mani H, Bernardo M, Pang Y, McKinney YL, et al. Prostate cancer: value of multiparametric MR imaging at 3 T for detection—histopathologic correlation. Radiology. 2010;255:89–99. doi:10.1148/radiol.09090475.

17. Langer DL, Kwast TH, Evans AJ, Plotkin A, Trachtenberg J, Wilson BC, et al. Prostate tissue composition and MR measurements: investigating the relationships between ADC, T2, K(trans), v(e), and corresponding histologic features. Radiology. 2010;255:485–94. doi:10.1148/radiol.10091343.
18. Muller BG, Futterer JJ, Gupta RT, Katz A, Kirkham A, Kurhanewicz J, et al. The role of magnetic resonance imaging (MRI) in focal therapy for prostate cancer: recommendations from a consensus panel. BJU Int. 2014;113(2):218–27.
19. Cornud F, Khoury G, Bouazza N, Beuvon F, Peyromaure M, Flam T, et al. Tumor target volume for focal therapy of prostate cancer—does multiparametric magnetic resonance imaging allow for a reliable estimation? J Urol. 2014;191:1272–9.
20. Siddiqui MM, Rais-Bahrami S, Turkbey B, George AK, Rothwax J, Shakir N, et al. Comparison of MR/ultrasound fusion–guided biopsy with ultrasound-guided biopsy for the diagnosis of prostate cancer. JAMA. 2015;313(4):390–7.
21. Meng X, Rosenkrantz AB, Mendhiratta N, Fenstermaker M, Huang R, Wysock JS, et al. Relationship between prebiopsy multiparametric magnetic resonance imaging (MRI), biopsy indication, and MRI-ultrasound fusion–targeted prostate biopsy outcomes. Eur Urol. 2016;69(3):512–7.
22. Bott SRJ, Ahmed HU, Hindley RG, Abdul-Rahman A, Freeman A, Emberton M. The index lesion and focal therapy: an analysis of the pathological characteristics of prostate cancer. BJU Int. 2010;106:1607–11.
23. Rosenkrantz AB, Deng FM, Kim S, Lim RP, Hindman N, Mussi TC, et al. Prostate cancer: multiparametric MRI for index lesion localization—a multiple-reader study. Am J Roentgenol. 2012;199:830–7.
24. Yap T, Ahmed HU, Hindley RG, Guillaumier S, McCartan N, Dickinson L, et al. The effects of focal therapy for prostate cancer on sexual function: a combined analysis of three prospective trials. Eur Urol. 2016;69(5):844–51.
25. Le JD, Tan N, Shkolyar E, Lu DY, Kwan L, Marks LS, et al. Multifocality and prostate cancer detection by multiparametric magnetic resonance imaging: correlation with whole-mount histopathology. Eur Urol. 2014;67:1–8.
26. Raz O, Haider MA, Davidson SRH, Lindner U, Hlasny E, Weersink R, et al. Real-time magnetic resonance imaging-guided focal laser therapy in patients with low-risk prostate cancer. Eur Urol. 2010;58:173–7.
27. Lindner U, Lawrentschuk N, Weersink RA, Davidson SRH, Raz O, Hlasny E, et al. Focal laser ablation for prostate cancer followed by radical prostatectomy: validation of focal therapy and imaging accuracy. Eur Urol. 2010;57:1111–4.
28. Cheng HLM, Haider MA, Dill-Macky MJ, Sweet JM, Trachtenberg J, Gertner MR. MRI and contrast-enhanced ultrasound monitoring of prostate microwave focal thermal therapy: an in vivo canine study. J Magn Reson Imaging. 2008;28:136–43.
29. Colin P, Nevoux P, Marqa M, Auger F, Leroy X, Villers A, et al. Focal laser interstitial thermotherapy (LITT) at 980 nm for prostate cancer: treatment feasibility in Dunning R3327-AT2 rat prostate tumour. BJU Int. 2012;109:452–8.
30. Lepor H, Llukani E, Sperling D, Fütterer JJ. Complications, recovery, and early functional outcomes and oncologic control following in-bore focal laser ablation of prostate cancer. Eur Urol. 2015; 68(6):924–6.
31. Phase II laser focal therapy of prostate cancer (LITT or FLA). NCT02243033. Desert Medical Imaging. https://clinicaltrials.gov/ct2/show/NCT02243033.
32. Colin P, Mordon S, Nevoux P, Marqa MF, Ouzzane A, Puech P, et al. Focal laser ablation of prostate cancer: definition, needs, and future. Adv Urol. 2012;2012: 589160.
33. Sussman MS, Lindner U, Haider M, Kucharczyk W, Hlasny E, Trachtenberg J. Optimizing contrast agent concentration and spoiled gradient echo pulse sequence parameters for catheter visualization in MR-guided interventional procedures: an analytic solution. Magn Reson Med. 2013;70:333–40.
34. Linder U, Davidson S, Fleshner N, Finelli A, Zlotta A, Jewett MAS, et al. Initial results of MR guided laser focal therapy for prostate cancer. J Urol. 2013; 189:e227–8.
35. Oto A, Sethi I, Karczmar G, McNichols R, Ivancevic M, Stadler W, et al. MR imaging-guided focal laser ablation for prostate cancer: phase I trial. Radiology. 2013;267:932–40.
36. Cepek J, Lindner U, Davidson SR, Haider MA, Ghai S, Trachtenberg J, et al. Treatment planning for prostate focal laser ablation in the face of needle placement uncertainty. Med Phys. 2014;41:013301.
37. Cepek J, Lindner U, Ghai S, Louis AS, Davidson SRH, Gertner M, et al. Mechatronic system for in-bore MRI-guided insertion of needles to the prostate: an in vivo needle guidance accuracy study. J Magn Reson Imaging. 2015;42(1):48–55.
38. Woodrum DA, Mynderse LA, Gorny KR, Amrami KK, McNichols RJ, Callstrom MR. 3.0 T MR-guided laser ablation of a prostate cancer recurrence in the postsurgical prostate bed. J Vasc Interv Radiol. 2011;22:929–34.
39. Lindner U, Davidson SRH, Fleshner NE, Finelli A, Zlotta AR, Jewett MAS, et al. Initial results of MR guided laser focal therapy for prostate cancer. J Urol. 2013;189(4S):e227–8.

Focal Cryotherapy

22

Kae Jack Tay, Efrat Tsivian, and Thomas J. Polascik

Introduction

Prostate cancer is the second most common male cancer worldwide accounting for 15 % of cancers diagnosed in men [1]. Radical prostatectomy and whole-gland irradiation are considered traditional gold standards for cure. However, these modalities are associated with significant posttreatment functional impairment due to the intimate relationship between the prostate and the urethral sphincter mechanism and the cavernosal nerves that affect penile erection [2]. The widespread use of these therapies has led to concerns regarding overtreatment and unnecessary exposure of men to functional impairment. Studies of the natural history of untreated prostate cancer have shown that the risk of cancer progression and mortality are heavily influenced by the Gleason grade of the cancer [3, 4]. Focal therapy was initially conceived as a minimally invasive treatment with low morbidity for men with less aggressive prostate cancer, such as those with Gleason 3+3.

In the last decade, there has been increasing evidence that low-grade prostate cancer of the Gleason 3+3 or prognostic grade group (PGG) 1 variety are slow-growing and unlikely to result in prostate cancer mortality if left untreated [5]. Current surveillance cohorts show a metastatic cancer rate of 0.4–2.8 % and a cancer mortality rate of 0.15–1.5 % at 10–15-year follow-up [6, 7]. However, up to half of these men do eventually undergo treatment due to cancer progression [8]. The 12–18-month re-biopsy cancer upgrading rate can be as high as 21 %, suggesting that many of these men were undergraded as Gleason 3+3/PGG 1 in the first place [9]. This undergrading is likely due to undersampling of the prostate gland with random, 12-core transrectal ultrasound (TRUS) biopsy as the diagnostic test [10]. Multiparametric magnetic resonance imaging, or mpMRI, with its ability to detect clinically significant, or Gleason ≥3+4 cancer irrespective of location within the prostate gland, has transformed patient selection for active surveillance [11]. The large-scale adoption of mpMRI in early prostate cancer has also allowed urologists to detect small foci of clinically significant cancer that could potentially be focally treated. If these lesions could be successfully ablated, the remaining low-grade cancer could be safely monitored on active surveillance, thus sparing suitable men from the morbidity of radical treatment.

K.J. Tay (✉)
Department of Urology, Duke University, Durham, NC, USA
e-mail: Kaejack.tay@gmail.com

E. Tsivian
Division of Urology, Department of Surgery, Duke University Medical Center, Durham, NC, USA

T.J. Polascik, MD
Professor of Surgery, Division of Urology, Department of Surgery, Duke Cancer Institute, Duke University School of Medicine, Durham, NC, USA

© Springer International Publishing AG 2017

T.J. Polascik (ed.), *Imaging and Focal Therapy of Early Prostate Cancer*, Current Clinical Urology, DOI 10.1007/978-3-319-49911-6_22

There are many ablative modalities available today that can be delivered to prostate tissue. Herein, we discuss the principles and technology underpinning cryotherapy and how these synergize with the principles and aims of focal therapy.

Cryobiology and Technological Advances in Cryotherapy

Cryotherapy refers to the use of controlled local freezing to remove thermal heat and cause cellular death. The majority of initial cellular death arises from the physical effects of intracellular ice crystal formation that occurs initially at approximately −10 to 15 °C and maximally at −40 °C resulting in cell membrane rupture [12]. Extracellular ice removes water from cells that are not completely destroyed leading to an abnormally high solute concentration. Subsequently during the thaw phase, microcirculatory failure negatively impacts the viability of any surviving cells in which mitochondria-related apoptotic pathways are activated [13].

The use of ice for treating inflammation has been known since the time of ancient Egyptians. The first recorded use of a salt-ice "frigorific" solution to freeze cancers was described by Arnott in 1950 [14]. Subsequent advances in chemistry permitted the use of liquid oxygen and then liquid nitrogen for treatment of superficial organs. Delivery of freezing temperatures to deep-seated organs only became possible when Cooper and Lee designed the first cryosurgical probe in 1961 comprised of a dual-lumen cannula with a hollow tip allowing for circulation of liquid nitrogen [15]. In 1974, Megalli et al. reported the first transperineal percutaneous prostate cryotherapy procedure using such a cryoprobe [16]. These early probes were large and required prostate dilatation prior to placement, and the entire procedure was monitored with a finger in the rectum.

Modern prostate cryotherapy is vastly superior in terms of efficiency, accuracy, and safety compared to early efforts. The three key developments leading to modern cryotherapy since the 2000s are the development of (1) transrectal ultrasound (TRUS) guidance systems, (2) third-generation cryogenic systems utilizing argon gas, and (3) protective urethral warming catheters. The development of high-quality TRUS systems has allowed cryosurgeons to harness a unique quality of ice, its extremely high acoustic impedance, which results in reflection of up to 99 % of acoustic signals producing a characteristic appearance [17]. Direct visualization of the edge of the iceball allows the operator to control the extent of cryoablation and ensure that a good margin is achieved while avoiding the rectum, urethral sphincter, or the neurovascular bundles if so desired.

Argon gas cryotherapy probes operate on the Joule-Thompson effect whereby the rapidly decompressing argon within the needle tip loses heat rapidly to a nadir temperature of −186 °C. These needles also exchange for helium gas when the freeze phase is complete, resulting in a much faster thaw. Modern cryoprobes are smaller, easier to place, and through variable ice length adjustment allow the iceballs to be conformed to the shape of the intended ablation zone. Third, urethral warming devices protect the urethral mucosa from necrosis [18, 19]. When an effective warmer is used, the rates of incontinence and urinary retention are significantly reduced, and the use of a warmer has now become standard of care in prostate cryotherapy [20]. Additionally, thermocouples ensure that a lethal temperature of colder than −20 to −40 °C is achieved, while a safe temperature is maintained in the urethral sphincter and Denonvilliers' fascia [21].

Focal Therapy and the Application of Cryotechnology

Focal therapy is a concept whereby only the dangerous focus of cancer within the prostate is destroyed, while vital collateral structures such as the urethra, urethral sphincter, and neurovascular bundles are spared. This would result in better sexual and urinary function outcomes compared to traditional whole-gland treatments that are often associated with significant functional

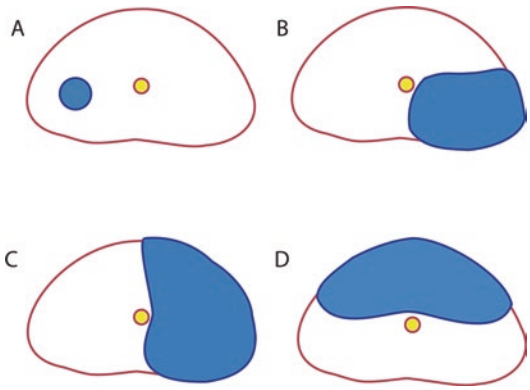

Fig. 22.1 Patterns of focal cryoablation. (**a**) Image-guided targeted/lesional ablation; (**b**) quadrant-ablation; (**c**) hemi-gland ablation; (**d**) anterior gland ablation

impairment. The pattern of ablation depends on the size of the lesion(s) to be treated, with the addition of an adequate margin, typically thought to be at least 5 mm from the edge of the known lesion [22]. Alternately, if the lesion is known to be isolated to one quadrant or hemi-gland, but the exact three-dimensional (3D) shape is unknown, a regional type of ablation can be administered (Fig. 22.1).

Cryotherapy is well suited for focal therapy for several reasons:

First, the transperineal approach allows excellent access to all regions of the prostate, including the anterior zone, where 20–30 % of prostate cancers arise.

Second, variable-length cryoprobes allow the shape of the iceball to be adjusted to create the desired ablation zone.

Third, the extent of ablation can be monitored in real time under TRUS guidance, allowing the operator precise control of margins.

Fourth, thermocouples allow real-time monitoring of nearby vital structures such as the urinary sphincter and neurovascular bundles, ensuring their safety, while monitoring of the ablation zone itself allows the operator to be certain of lethal ablation temperatures.

Fifth, the use of a urethral warming device prevents urethral injury and reduces urinary-related complications compared to other ablative modalities.

Finally, cryotherapy is a minimally invasive, often pain-free outpatient procedure and can be repeated if necessary with low morbidity.

The Focal Prostate Cryotherapy Procedure

Focal cryotherapy is usually performed in the operating room under general or spinal anesthesia, though there have been reports of doing it under local anesthesia (Fig. 22.2). The patient is placed in the lithotomy position. A biplanar TRUS probe, mounted on a holder and placed into the rectum, is used to visualize the prostate and measure its dimensions. The variable length cryoprobes are then adjusted to create the length of the iceballs according to the prostate measurements. They are placed into the prostate using a template biopsy grid as a holder. Cryoprobe positions are checked on ultrasound in both transverse and sagittal planes. Thermocouples are placed typically at the external sphincter and the Denonvilliers' fascia, though additional probes may be placed at the neurovascular bundles or at the margin of the planned ablation zone as needed. Flexible cystoscopy is then performed to check that the urethra has not been traversed by the cryoprobes. A urethral warmer is placed over a super-stiff guidewire. Freezing is performed under real-time ultrasound and temperature monitoring followed by an active thaw. Two freeze-thaw cycles are typically performed to ensure complete cell kill within the ablation zone. The cryoprobes are removed after the final thaw, and the urethral warmer is exchanged for a Foley catheter that will be usually kept for several days. The patient is usually discharged home on the same day.

Contemporary Focal Cryotherapy Series

Focal cryotherapy was first described by Onik et al. in 1997 as a form of hemi-ablative treatment and since then has been the most widely used modality for focal therapy in the United

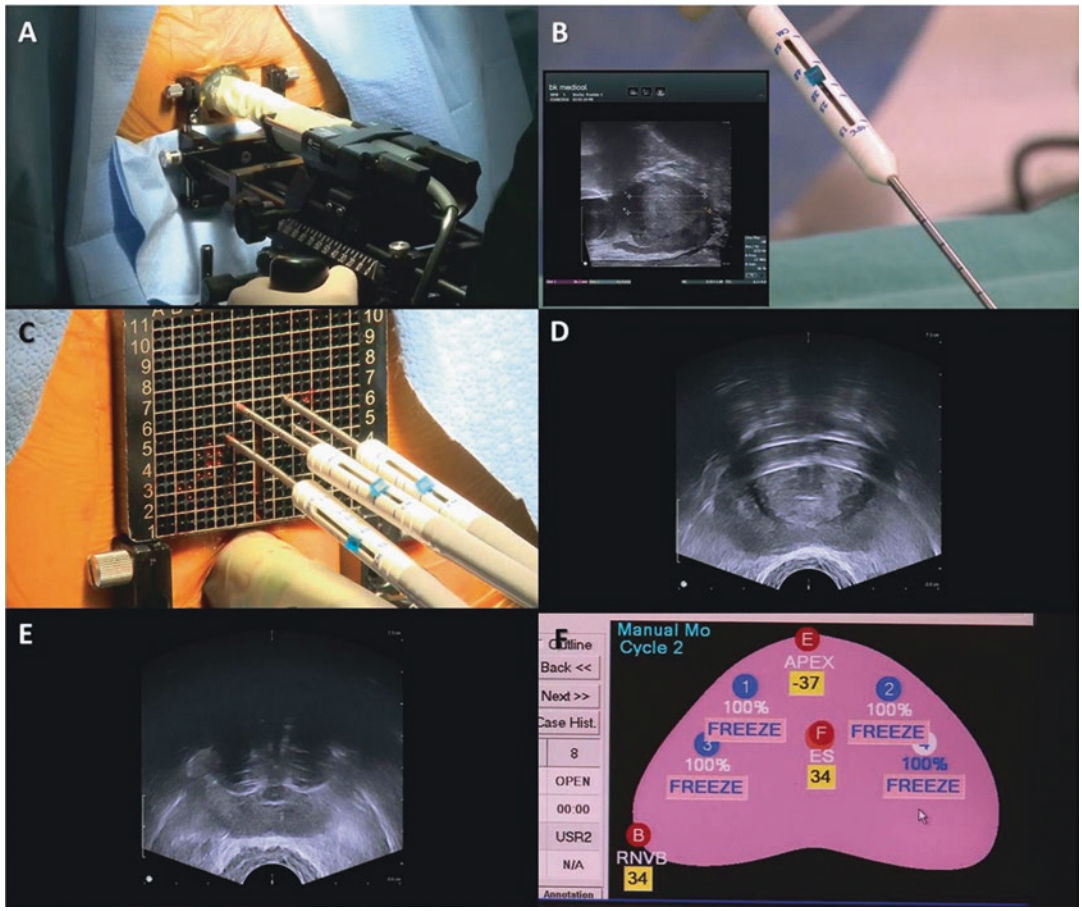

Fig. 22.2 Focal cryoablation procedure. (**a**) Biplanar ultrasound probe is placed in the rectum. (**b**) Variable length cryoprobes are set to prostate measurements. (**c**, **d**) An anterior ablation pattern is being used here with four probes in the anterior prostate. (**e**) The ice in the anterior prostate. The leading ice edge has a hyperechoic rim and can be easily monitored. (**f**) Console readout showing lethal temperature in the anterior apex and safe temperatures in the external sphincter (ES) and the right neurovascular bundle (RNVB). You may view the full video at: http://www.liebertpub.com/videourology. Used with permission from: Tay KJ, Polascik TJ. Anterior Prostate Cancer Cryoablation: A function-preserving technique. Journal of Endourology, Part B: Videourology

States. Several focal cryotherapy series have since been reported, mostly utilizing hemi-gland ablations. However, like the rest of the focal therapy literature, there is significant heterogeneity in patient selection, inclusion criteria, use of imaging, and follow-up. These factors play a significant role in interpreting the outcome of focal treatments. For example, many low-volume, low-grade cancers may do as well on surveillance as on treatment. On the other hand, high-grade cancers are more likely to exhibit local or systemic spread, and inclusion of such patients worsen the oncological outcomes of focal therapy. The use of mpMRI and the extent/intensity of the biopsy impact the accuracy of grading the cancer. The traditional definition of recurrence using prostate-specific antigen (PSA) is less reliable when a large portion of glandular tissue remains viable (i.e., the benign or untreated area) and PSA-producing after treatment. After focal therapy, a follow-up biopsy or imaging study may be much more informative with regard to cancer recurrence.

A recent systematic review of focal cryotherapy yielded eight cohort studies including a total of 435 men and one report from the Cryo On-Line

Data (COLD) registry of 1140 men [23]. Using the D'Amico risk criteria, 52 % of the men were low risk, 38 % intermediate risk, and 10 % high risk [24]. Three cohorts reported using transperineal template mapping biopsy (TTMB), one included mpMRI, and the remainder used conventional TRUS biopsy to select men for focal treatment. The reported biochemical recurrence-free survival rate ranged from 71 to 98 %. Among the five cohorts that stipulated a mandatory 6–12-month posttreatment biopsy, 216 of 272 men (79 %) did undergo biopsy, with 47 positive (21.8 %). Of these positive biopsies, approximately a third were infield or treatment zone recurrences, suggesting inadequate ablation. Overall, two men had metastatic disease and none died of prostate cancer. Posttreatment continence rates were excellent (96–100 %). The rate of posttreatment urinary retention ranged from 0 to 15 %, and the rate of rectourethral fistula was 0–0.1 %. A summary of contemporary focal cryotherapy studies are presented in Table 22.1 [25–32].

Cryotherapy used in a whole-gland setting is traditionally associated with high rates of erectile dysfunction. The majority of prostate focal cryotherapy has been applied in a hemi-ablative fashion, resulting in the sacrifice of at least 1 neurovascular bundle. In the reviewed focal cryotherapy cohorts, reported rates of potency ranged from 58 to 100 %. In a matched comparison of low-risk prostate cancer patients undergoing focal or whole-gland cryotherapy, Mendez et al. found that focal therapy was associated with significantly better erectile function rates compared to whole-gland therapy (68.8 % vs. 46.8 %) [33]. In another matched comparison of *intermediate-risk* prostate cancer patients, where more aggressive ablation is expected, the 12-month rate of successful sexual intercourse for men undergoing focal therapy was twice that of men undergoing whole-gland ablation [34]. Of course, if a patient undergoes a more targeted ablation of a specific lesion, or an anterior gland ablation whereby the lesion is located far from the neurovascular bundles, the potency rate is much higher.

Conclusion

Future Developments

Developments in image guidance have caused a paradigm shift in the application of focal therapies. Whereas the majority of focal cryotherapy series have used hemi-ablation, with the advent of mpMRI, it has become possible to visualize cancer foci, sample them with MRI-TRUS fusion biopsy, and define the exact target volume within the gland that needs to be treated. By defining the ablation target accurately in relation to collateral sphincter and neurovascular structures, better functional outcomes could be achieved. Furthermore, the same MRI-TRUS fusion platforms can be brought to the operating room to direct cryotherapy probes. While such MRI-directed therapies have been available in-bore, the ability to bring advanced imaging-based targeting into the operating room improves the accessibility of the procedure and reduces valuable magnet time. Multiparametric MRI is heavily equipment and reader dependent with wide variations in performance characteristics within the community [35]. MRI-TRUS fusion also comprises many moving parts and requires the operator to recognize and adjust for technical limitations in order to achieve successful fusion [36]. Currently, high-quality mpMRI and fusion biopsy are available at centers of excellence and may be less accessible to the wider community. However, these limitations will be overcome as experience in using this technology grows.

The development of MRI-fusion technology has laid the foundation for application of other advanced imaging technologies to better stratify prostate cancer and direct ablative therapies. While positron emission tomography/computed tomography (PET/CT) and MRI-fusion have been used mainly in identification of metastatic cancer, axial imaging fused with detection of novel small molecules linked to prostate-specific membrane antigen (PSMA) is able to identify intraprostatic cancer foci at high resolution [37]. Whether these tools add value to existing targeting methods remains to be elucidated.

Table 22.1 Contemporary focal cryotherapy series

Author	*N*	Pretreatment work-up	Demographic	Ablation pattern	Posttreatment re-biopsy	Median follow-up (months)	Oncological outcome	Sexual function outcomes	Complications
Onik 2008 [25]	48	TRUS biopsy (restaging TMB after 2001)	Low risk —48 % Int. risk—38 % High risk—14 %	Hemi-gland	Mandatory	54	92 % 1-year BRFS; 85 % absolute BRFS (ASTRO); 8.3 % (outfield) positive biopsy	90 % of those previously potent retained ability to penetrate	NR
Truesdale 2010 [26]	77	TRUS biopsy	Low risk—57 % Int. risk—40.3 % High risk—2.6 %	Hemi-gland	For cause	24	72.7 % BRFS (Phoenix); 3.9 % (infield) and 10.4 % (outfield) positive biopsy	1.9 point decrease in IIEF at 12 months	NR
Bahn 2012 [27]	73	TRUS biopsy	Low risk—33 % Int. risk—67 %	Hemi-gland	Mandatory	44	1.4 % (infield) and 15.1 % (outfield) positive biopsy	74 % had ability to penetrate at 1 year and 86 % in 2.4 year	Rectal injury—0 %
Ward 2012 [28]	1160	NR	Low risk—47 % Int. risk—41 % High risk—12 %	NR	NR	21	2-year BRFS 75.7 %	59 % had ability to penetrate at 1 year	Retention 1.2 % Rectourethral fistula 0.1 %
Hale 2013 [29]	26	Staging TTMB	Low risk—88.5 % Int. risk—11.5 %	Hemi-gland	For cause	19	88 % BRFS (using nadir +0.5); 7.7 % biopsy positive	73 % needed assistance No impotence reported	Retention needing TURP 4 %, UTI 4 % Rash 4 %
Barqawi 2014 [30]	62	TTMB	Low-risk—100 %	Targeted sectoral ablation	Mandatory	28	71 % BRFS (any post-op increase); 19.4 % positive biopsy	No change in IIEF at 24 months	NR

Durand 2014 [31]	48	12-core staging TRUS biopsy + mpMRI	Low risk—100 %	Hemi-gland	Mandatory	13	98 % BRFS (Phoenix); 12.5 % (infield) and 14.6 % (outfield) positive biopsy	Mild reduction in IIEF at 3 months then back to baseline at 6 months	Retention 15 % Rectourethral fistula 2 % Cavernous corpus necrosis 2 % Urethral stenosis 2 %
Lian 2015 [32]	41	Minimum 12-core biopsy	Low risk—56 % Int. risk—44 %	Hemi-gland	Mandatory	63	95 % BRFS (Phoenix); 4.9 % (infield) and 12.2 % (outfield) positive biopsy	76.9 % of those previously potent retained ability to penetrate	Retention 3.4 %

TRUS transrectal ultrasound; *TTMB* transperineal template mapping biopsy; *NR* not reported; *BRFS* biochemical recurrence-free survival; *IIEF* International Index for Erectile Function; *mpMRI* multiparametric magnetic resonance imaging; *infield* within the treatment field; *outfield* outside the treatment field; *ASTRO* American Society of Therapeutic Radiation Oncology; *TURP* transurethral resection of prostate; *UTI* urinary tract infection

Since the 2000s, the majority of cryotherapy devices employ the third-generation technology described in the second section of this chapter. Continued efforts to improve cryoprobes have led to prototypes that may allow for faster freeze and thaw times and more efficient use of gases that can potentially reduce procedure times and reduce costs. These benefits remain to be defined in clinical trials.

Last, multidisciplinary efforts have led the rapid growth in the field of prostate cancer oncology in the last decade. Trials exploring multimodality treatments have led to a better understanding of the optimal sequencing of radiation, surgery, and systemic modalities, which now occur in tandem rather than in isolation. The field of breast focal therapy, or "lumpectomy" as breast surgeons term it, began in the setting of adjuvant whole-gland treatment with irradiation, whereas prostate focal therapy stopped with "male lumpectomy" alone [38]. With better understanding of low-risk prostate cancer, focal surgeons have increasingly embraced the idea of treating just the focus of intermediate-/high-grade cancer within the prostate while placing the remainder of the gland with low-grade cancer on active surveillance. However, even in the active surveillance arena, there is great interest in the used of vaccines or other systemic therapies to reduce the risk of cancer progression. To complete its role as an active surveillance "extender," investigation in this area should encompass the use of adjunctive drugs, vaccines, or cold-ablation adjuvants in improving oncological outcomes of focal cryotherapy.

References

1. Ferlay J, Soerjomataram I, Ervik M, Dikshit R, Eser S, Mathers C, et al. Globocan 2012 v1.0, cancer incidence and mortality worldwide: IARC cancerbase no. 11 [internet]. Lyon: International Agency for Research on Cancer; 2013 .Available from: http://globocan.iarc.fr
2. Donovan JL, Hamdy FC, Lane JA, Mason M, Metcalfe C, Walsh E, et al. Patient-reported outcomes after monitoring, surgery, or radiotherapy for prostate cancer. N Engl J Med. 2016;375:1425–37.
3. Albertsen PC, Hanley JA, Fine J. 20-year outcomes following conservative management of clinically localized prostate cancer. JAMA. 2005;293(17): 2095–101.
4. Johansson JE, Andren O, Andersson SO, Dickman PW, Holmberg L, Magnuson A, et al. Natural history of early, localized prostate cancer. JAMA. 2004; 291(22):2713–9.
5. Wilt TJ, Brawer MK, Jones KM, Barry MJ, Aronson WJ, Fox S, et al. Radical prostatectomy versus observation for localized prostate cancer. New England J Med. 2012;367(3):203–13.
6. Klotz L, Vesprini D, Sethukavalan P, Jethava V, Zhang L, Jain S, et al. Long-term follow-up of a large active surveillance cohort of patients with prostate cancer. J Clin Oncol. 2015;33(3):272–7.
7. Tosoian JJ, Mamawala M, Epstein JI, Landis P, Wolf S, Trock BJ, et al. Intermediate and longer-term outcomes from a prospective active-surveillance program for favorable-risk prostate cancer. J Clin Oncol. 2015;33(30):3379–85.
8. Klotz L, Zhang L, Lam A, Nam R, Mamedov A, Loblaw A. Clinical results of long-term follow-up of a large, active surveillance cohort with localized prostate cancer. J Clin Oncol. 2010;28(1):126–31.
9. Dall'Era MA, Albertsen PC, Bangma C, Carroll PR, Carter HB, Cooperberg MR, et al. Active surveillance for prostate cancer: a systematic review of the literature. Eur Urol. 2012;62(6):976–83.
10. Tay KJ, Mendez M, Moul JW, Polascik TJ. Active surveillance for prostate cancer: can we modernize contemporary protocols to improve patient selection and outcomes in the focal therapy era? Curr Opin Urol. 2015;25(3):185–90.
11. Arumainayagam N, Ahmed HU, Moore CM, Freeman A, Allen C, Sohaib SA, et al. Multiparametric mr imaging for detection of clinically significant prostate cancer: a validation cohort study with transperineal template prostate mapping as the reference standard. Radiology. 2013;268(3):761–9.
12. Gage AA, Baust J. Mechanisms of tissue injury in cryosurgery. Cryobiology. 1998;37(3):171–86.
13. Robilotto AT, Baust JM, Van Buskirk RG, Gage AA, Baust JG. Temperature-dependent activation of differential apoptotic pathways during cryoablation in a human prostate cancer model. Prostate Cancer Prostatic Dis. 2013;16(1):41–9.
14. Arnott J. Practical illustrations of the remedial efficacy of a very low or anæsthetic temperature. I. In cancer. Lancet. 1850;56(1409):257–9.
15. Cooper IS, Lee AS. Cryostatic congelation: a system for producing a limited, controlled region of cooling or freezing of biologic tissues. J Nerv Ment Dis. 1961;133:259–63.
16. Megalli MR, Gursel EO, Veenema RJ. Closed perineal cryosurgery in prostatic cancer new probe and technique. Urology. 1974;4(2):220–2.

17. Onik G, Cobb C, Cohen J, Zabkar J, Porterfield B. Us characteristics of frozen prostate. Radiology. 1988; 168(3):629–31.
18. Donnelly BJ, Saliken JC, Ali-Ridha N, Rewcastle JC, White LJ. Histological findings in the prostate two years following cryosurgical ablation. Can J Urol. 2001;8(2):1237–9.
19. Vellet AD, Saliken J, Donnelly B, Raber E, McLaughlin RF, Wiseman D, et al. Prostatic cryosurgery: use of MR imaging in evaluation of success and technical modifications. Radiology. 1997;203(3): 653–9.
20. Cespedes RD, Pisters LL, Von Eschenbach AC, McGuire EJ. Long-term follow-up of incontinence and obstruction after salvage cryosurgical ablation of the prostate: results in 143 patients. J Urol. 1997; 157(1):237–40.
21. WS W, DO C, Chinn M, Chinn J, WL T, WL T. Cryosurgery as a treatment for prostate carcinoma. Results and complications. Cancer. 1997;79(5):963–74.
22. Donaldson IA, Alonzi R, Barratt D, Barret E, Berge V, Bott S, et al. Focal therapy: patients, interventions, and outcomes—a report from a consensus meeting. Eur Urol. 2015;67(4):771–7.
23. Tay KJ, Polascik TJ. Focal cryotherapy for localized prostate cancer. Arch Esp Urol. 2016;69(6):317–26.
24. D'Amico AV, Whittington R, Malkowicz SB, Schultz D, Blank K, Broderick GA, et al. Biochemical outcome after radical prostatectomy, external beam radiation therapy, or interstitial radiation therapy for clinically localized prostate cancer. JAMA. 1998; 280(11):969–74.
25. Onik G, Vaughan D, Lotenfoe R, Dineen M, Brady J. The "male lumpectomy": focal therapy for prostate cancer using cryoablation results in 48 patients with at least 2-year follow-up. Urol Oncol. 2008;26(5): 500–5.
26. Truesdale MD, Cheetham PJ, Hruby GW, Wenske S, Conforto AK, Cooper AB, et al. An evaluation of patient selection criteria on predicting progression-free survival after primary focal unilateral nerve-sparing cryoablation for prostate cancer: recommendations for follow up. Cancer J. 2010;16(5): 544–9.
27. Bahn D, de Castro Abreu AL, Gill IS, Hung AJ, Silverman P, Gross ME, et al. Focal cryotherapy for clinically unilateral, low-intermediate risk prostate cancer in 73 men with a median follow-up of 3.7 years. Eur Urol. 2012;62(1):55–63.
28. Ward JF, Jones JS. Focal cryotherapy for localized prostate cancer: a report from the national cryo online database (cold) registry. BJU Int. 2012;109(11): 1648–54.
29. Hale Z, Miyake M, Palacios DA, Rosser CJ. Focal cryosurgical ablation of the prostate: a single institute's perspective. BMC Urol. 2013;13:2.
30. Barqawi AB, Stoimenova D, Krughoff K, Eid K, O'Donnell C, Phillips JM, et al. Targeted focal therapy for the management of organ confined prostate cancer. J Urol. 2014;192(3):749–53.
31. Durand M, Barret E, Galiano M, Rozet F, Sanchez-Salas R, Ahallal Y, et al. Focal cryoablation: a treatment option for unilateral low-risk prostate cancer. BJU Int. 2014;113(1):56–64.
32. Lian H, Zhuang J, Yang R, Qu F, Wang W, Lin T, et al. Focal cryoablation for unilateral low-intermediate-risk prostate cancer: 63-month mean follow-up results of 41 patients. Int Urol Nephrol. 2016;48(1):85–90.
33. Mendez MH, Passoni NM, Pow-Sang J, Jones JS, Polascik TJ. Comparison of outcomes between preoperatively potent men treated with focal versus whole gland cryotherapy in a matched population. J Endourol. 2015;29(10):1193–8.
34. Tay KJ, Polascik T, Elshafei A, Tsivian E, Jones JS. Mp18-16 propensity score matched comparison of partial to whole gland cryotherapy for intermediate-risk prostate cancer: an analysis of the cold registry data. J Urol. 2016;195(4):e199.
35. Tay KJ, Gupta RT, Brown AF, Silverman RK, Polascik TJ. Defining the incremental utility of prostate multiparametric magnetic resonance imaging at standard and specialized read in predicting extracapsular extension of prostate cancer. Eur Urol. 2016;70(2): 211–3.
36. Tay KJ, Gupta RT, Rastinehad AR, Tsivian E, Freedland SJ, Moul JW, et al. Navigating MRI-TRUS fusion biopsy: optimizing the process and avoiding technical pitfalls. Expert Rev Anticancer Ther. 2016; 16(3):303–11.
37. Pillai MR, Nanabala R, Joy A, Sasikumar A, Russ Knapp FF. Radiolabeled enzyme inhibitors and binding agents targeting PSMA: effective theranostic tools for imaging and therapy of prostate cancer. Nucl Med Biol. 2016;43(11):692–720.
38. Newman LA, Mamounas EP. Review of breast cancer clinical trials conducted by the national surgical adjuvant breast project. Surg Clin North Am. 2007; 87(2):279–305. vii

Photodynamic Therapy for Early Prostate Cancer

23

Caroline M. Moore and Mark Emberton

Introduction

Photodynamic therapy (PDT) uses directed light of a specific wavelength to activate a photosensitizing drug. The activated drug then interacts with molecular oxygen to form reactive oxygen species, and it is these that are responsible for localized tissue destruction. Phototherapy, the use of light in treating disease, has been in use for many centuries, with heliotherapy (sun worship) reported by Hippocrates as a way of building up wasted muscles. Modern phototherapy includes the use of visible light to breakdown bilirubin in babies with neonatal jaundice.

Photochemotherapy involves the use of light and drug in combination. This was described in ancient India as a treatment for vitiligo. The leaves of the plant *Psoralea coryfolia* were eaten and the patient then sat in sunlight. These leaves are now known to contain furocoumarins, which are the active ingredient in contemporary agents used for the treatment of psoriasis.

Photodynamic therapy is a further subset of photochemotherapy, where oxygen is required for the effect to take place. The first modern scientific experiment was performed by a medical student, Oscar Raab, and his supervisor Hermann von Tappeiner [1]. They observed that paramecia given the biological dye acridine survived for ten times longer in a thunderstorm than in an identical experiment in light conditions. They concluded that the thunderstorm had reduced the light to the paramecium, reducing the photodynamic effect. Further work showed that oxygen was necessary for the effect to take place [1].

In 1903 Niels Rydberg Finsen, considered the father of modern photodynamic therapy, was awarded the Nobel Prize for his work on lupus vulgaris, a tubercular skin condition common in Nordic countries. He set up the Medical Light Institute in Copenhagen. Queen Alexandra brought Finsen's work to England and set up the Light Department in the London Hospital, Whitechapel.

While popular in the early 1900s, photodynamic therapy then fell out of practice somewhat until the early 1960s when Lipson showed that hematoporphyrin localized in tumors and gave a red fluorescence [2]. His initial report included the use of hematoporphyrin in both diagnosis and treatment of cancer, but a later report only mentioned the diagnostic aspects.

C.M. Moore (✉)
Division of Surgical and Interventional Sciences, University College London, London, UK

Division of Surgery, Urology Department, University College London Hospitals Trust, London, UK
e-mail: caroline.moore@ucl.ac.uk

M. Emberton
Faculty of Medical Sciences, University College London, London, UK

Division of Surgery, Urology Department, University College London Hospitals Trust, London, UK

© Springer International Publishing AG 2017
T.J. Polascik (ed.), *Imaging and Focal Therapy of Early Prostate Cancer*, Current Clinical Urology, DOI 10.1007/978-3-319-49911-6_23

In 1978 Thomas Dougherty, at Roswell Park, USA, reported the first clinical case series of PDT for cancer. Twenty-five patients with a range of skin or subcutaneous tumors were treated, including a prostate metastasis, and the authors "found no type to be unresponsive."[3].

The development of photosensitizers continued over the next decades, accompanied by developments in light delivery devices.

Photosensitizer Development

Hematoporphyrin, one of the photosensitizers popular from the 1960s onward, was derived from dried blood, which was treated with sulfuric acid. The difficulty in using dried blood lays in the variability of the concentration of the active ingredient. This problem led to a number of groups working to develop alternative photosensitizers, which could be manufactured in a more reliable form. These can be classified into a number of different groups, based on their chemical structure. The groups include hematoporphyrins, e.g., hematoporphyrin derivative (HpD); chlorins, e.g., meso-tetra hydroxyphenyl chlorin (mTHPC); phthalocyanines, e.g., aluminum phthalocyanine (AlS_2Pc); purpurins, e.g., tin ethyl etiopurin ($SnET_2$); and protoporphyrin IX pathway agents (including aminolevulinic acid [ALA], familiar to many urologists for its use in photodynamic diagnosis of bladder cancer).

Another way to classify the photosensitizers is by the timing and mechanism of activation. This can be used to divide photosensitizers into tissue-activated or vascular-activated photosensitizers. Tissue-activated photosensitizers used in prostate cancer, either in preclinical or clinical work, include tin ethyl etiopurin ($SnET_2$), aluminum phthalocyanine (AlS_2Pc), and meso-tetra hydroxyphenyl chlorin (mTHPC). These photosensitizers are activated when they have reached maximal concentration in the tissue to be treated. Some photosensitizers will be preferentially concentrated in tumor rather than benign tissue, but it is now recognized that tumor selectivity also can be achieved by selective activation of the photosensitizer by placement of light delivery fibers in the required treatment volume. Tissue-activated photosensitizers tend to require time to accumulate in the tissue where they are activated; this gives rise to a drug-light interval of hours to days. From a clinical perspective, this usually means two separate hospital visits—the first for the photosensitizer administration and the second for light dose administration to activate the photosensitizer. These tissue-activated photosensitizers are also associated with the activation of accumulated photosensitizer in the skin and eyes, by daylight or artificial indoor lighting. As these photosensitizers can take a number of weeks to clear completely, light protection measures need to be taken to avoid a sunburn-like reaction. While this may be acceptable for those with advanced cancer refractory to other treatment, for a man with early prostate cancer, the need for such precautions would preclude the use of these agents for photodynamic therapy.

The light dose for vascular-activated photosensitizers is given when the photosensitizer is at maximal concentration in the vasculature of the tissue to be treated—with a drug-light interval, which is typically a few minutes. This means that the entire treatment can be carried out in one clinical visit. In addition, these photosensitizers tend to be cleared rapidly from the circulation, so that light protection measures do not need to be continued once the patient has left hospital. The vascular-activated photosensitizers that have been used in preclinical and clinical work in prostate cancer are from the palladium bacteriopheophorbide family: Tookad® (WST-09) and Tookad® Soluble (WST-11).

The Ideal Photosensitizer

The ideal photosensitizer would be one that is inexpensive to manufacture, stable at a range of temperatures, and can be given easily as an intravenous or oral preparation. In addition, it would be able to be activated by different wavelengths of light, such that shorter wavelengths could be used to activate the drug at a short distance from the illuminating fiber (e.g., for the activation of ALA in the mucosa) and at a longer wavelength

for interstitial treatment (where the penetration depth of the light is likely to influence the depth of PDT effect that can be achieved).

Light Delivery Devices

The first light delivery devices for skin-based photodynamic therapy were simple lamps, delivering white light (a broad spectrum of wavelengths). A photosensitizer is generally able to absorb light at very specific wavelengths; while more than 1 wavelength may be practical for the activation of the drug (e.g., aminolevulinic acid can be activated by green or red light [4]), it is commonest for a single wavelength of light to have maximal photodynamic efficiency (e.g., to produce the most reactive oxygen species for a given drug dose.) This single wavelength can be given most efficiently using a laser that can be directed along optical fibers. These can be used as "bare-ended" fibers, where the light comes out at the end, like a flashlight. The light dose is usually given in joules per square meter (J/cm^2) for this sort of fiber as the light is distributed in all directions from the end of the fiber. The fibers also can be modified to allow light delivery along a given length (e.g., 1–5 cm) at the distal end of the fiber; the light delivery from a cylindrical diffuser is like a "strip light." The light dose for these fibers is most commonly given in J/cm of active fiber length. For the treatment of superficial lesions, either on the skin or within a hollow organ accessible by endoscopy, a bare-ended fiber can be used for light delivery. In solid organs, including the prostate, it is commoner for cylindrical diffusers to be used. It is important to note that the light dose for photodynamic therapy is not intended to have a thermal effect but to simply activate the photosensitizing drug. It is therefore a much lower light dose than would be used for other prostate applications such as potassium titanyl phosphate (KTP) laser for prostate ablation (green light laser), holmium laser enucleation of the prostate (HoLEP), or for stone destruction.

In preclinical studies of PDT for prostate cancer, light delivery was sometimes done by the insertion of fibers at laparotomy. This would be impractical in clinical use, and so to assess the clinical applicability of prostate photodynamic therapy, both transperineal and transurethral delivery were explored in the canine model. While each of the approaches could be used to cause prostatic ablation, transurethral light delivery was associated with an increase in urinary symptoms, and, particularly, urethral strictures, and has not been evaluated for the clinical treatment of prostate cancer [5]. It is, however, of interest in the treatment of benign prostate enlargement for the treatment of lower urinary tract symptoms [6]. While early clinical work in prostate photodynamic therapy used freehand transperineal placement of bare-ended optical fibers, the technique has now evolved, making use of developments in prostate brachytherapy delivery. It is now standard practice to use a stepper device to hold the transrectal ultrasound (TRUS) and a transperineal template to aid fiber placement, in a manner similar to that used for high-dose-rate brachytherapy (Fig. 23.1).

Vascular-Activated Photosensitizers for Prostate Cancer

Preclinical Animal Studies

The Tookad family of photosensitizers has been developed at the Weizmann Institute, Israel, where Avigdor Scherz led the preclinical work on the drug derived from a bacteriochlorophyll derivative. The addition of palladium gave photostability to the drug [7]. Once the in vitro work had established that Tookad resulted in cell death, the first animal studies using implanted gliomas were carried out by Yoram Solamon and his team [8]. This showed that not only was the photosensitizer effective at the local treatment of the implanted tumors but that it was also associated with a greater chance of cure than surgery. It is thought that this may be because of the immune reaction that can occur with PDT and allow sustained antitumor activity [9]. Further work was done assessing the effect of Tookad PDT in a human prostatic small-cell model [10].

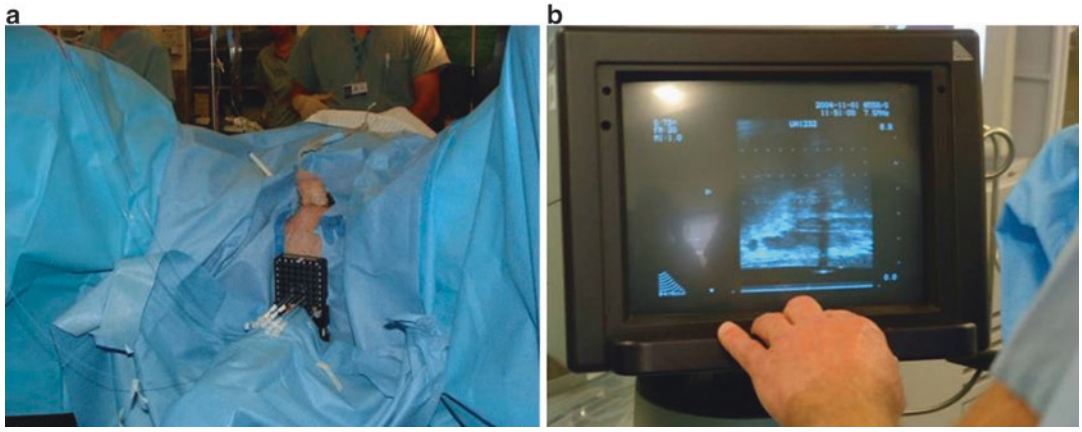

Fig. 23.1 Setup for vascular-targeted photodynamic therapy procedure. (**a**) Setup of the apparatus for vascular-targeted photodynamic therapy. The transrectal ultrasound is in position, with the transperineal template clearly seen. The optical fibers are placed within the hollow plastic needles, which are seen protruding from the template. (**b**) The needles are viewed on ultrasound, while they are being positioned in the prostate

When early work had shown promise in the use of Tookad as a treatment for cancer in small animal models, it was necessary to carry out studies in a larger animal model with prostate anatomy relevant to that in the human. The dog has the prostate structure closest to that seen in the human and is the commonest model used in the evaluation of prostate ablative techniques. The disadvantage of this model is that there is no prostate cancer model in the dog, so most groups use the benign prostate. There have been a few reports of prostate photodynamic therapy used to treat naturally occurring prostate cancer in the dog [11, 12], including one report of a vascular-activated photosensitizer [13].

The canine work with the palladium bacteriopheophorbide photosensitizers used a laparotomy approach to insert the optical fibers [14]. The first report used both superficial illumination and an interstitial approach to deliver light to the prostate; at the same time, light was delivered to the serosal surfaces of the colon and bladder in order to estimate the effect that unintended light delivery in these areas might have in the clinical setting. Temperature monitoring was done during treatment, and a maximum temperature rise of 0.9 °C was noted, confirming that the post-procedure effects seen were not due to a thermal laser effect. Sixteen dogs were studied, including one dog given drug only, one dog given the light dose only, and a third control dog receiving neither drug nor light. The drug dose was 2 mg/kg for all the dogs who received it, while the light dose varied from 50–200 J/cm for interstitial light delivery given using cylindrical diffusers and 100–200 J/cm^2 for superficial illumination using a bare-ended fiber [14].

None of the dogs had urinary retention, or any apparent urine symptoms following the procedure. No effect was seen in any of the control dogs. The treated prostates harvested at 1 week showed acute hemorrhagic necrosis with patchy subcapsular hyperemia and marked edema, with the volume of lesion correlating with the light dose given. One prostate was harvested at 4 weeks, when the volume of the lesion was seen to be smaller than for the same dose parameters when harvested at 1 week. In the two prostates harvested at 3 months, significant reduction in gland volume and scarring were seen, suggesting that healing of lesions occurs over time [14].

Direct illumination at 40 J/cm^2 to areas within the bladder showed mild hemorrhage and edema on histopathological examination, but without evidence of necrosis. The colon showed similar changes at the same direct light dose, while a dose of 80 J/cm^2 resulted in mucosal ulceration at 1 week, but without perforation. When the effects

of a scattered light dose to the colon or bladder, such as might occur from unintended light dose given at the time of light delivery to the prostate, no histopathological effect was seen [14].

This work then formed the basis of a number of other canine studies, prior to the initiation of a clinical program. Due to the interest in treating men with recurrent prostate cancer following radiotherapy, one of these studies pretreated dogs with ionizing radiation to the prostate prior to WST-09 PDT [15]. Four dogs were given a total of 70 Gy in 20 fractions over 4 weeks. After an interval of 20–23 weeks, WST-09 PDT was given, using a maximum of 1 cm diffuser fiber per lobe, at the same drug dose (2 mg/kg) and light doses of 50, 100, and 200 J/cm. Again, no dogs experienced urinary retention or evidence of urinary symptoms, although traces of blood were seen on urinalysis at 24 h.

The lesion size was seen to correlate with the light dose given, with diameters ranging from 12 to 28 mm, across the spectrum of light doses, with some variation within each light dose group. The length of lesion was longer than the diffuser fiber, particularly at the higher light doses (10–18 mm in length). Histopathological examination of all four animals at 1 week showed identical features to the lesions seen in the dogs that had not had previous radiotherapy. Chronic fibrosis, due to the radiotherapy, was clearly distinguishable from the acute PDT effect. Interestingly, even when the urethra was within the treatment zone, no urethral effect was seen [15]. This work formed the basis of the salvage PDT studies carried out in men with radiorecurrent prostate cancer in Canada and is discussed in detail in the next section.

Another aspect that was explored in the canine studies was the posttreatment assessment of vascular-targeted photodynamic therapy (VTP) effects with the use of imaging, in the form of magnetic resonance imaging (MRI) [16]. Five dogs had T2-weighted, dynamic contrast-enhanced (DCE), and diffusion-weighted (DWI) imaging performed prior to Tookad PDT and then at 2 days (one dog), 7 days (five dogs), and 1 month (one dog). For reasons that are not clear, a lower drug dose of 1 mg/kg was used in these animals, with light delivery at 50–300 J/cm, using a 1 cm cylindrical diffuser. Four of the prostates were harvested at 1 week, and one at 1 month, and 3 mm step-section whole-mount histopathological correlation with the MR images was performed. It was seen that the gadolinium-enhanced images gave the most accurate correlation with the histopathologically defined volume of effect, and this led to the use of a 1-week contrast-enhanced scan to define the volume of effect in the clinical studies. DCE-MRI showed a central zone of lack of uptake of gadolinium, surrounded by an outer zone of increased enhancement. This effect has also been reported in clinical MR studies following high-intensity focused ultrasound (HIFU) treatment [17]. The WST-09 canine study showed that the central non-enhancing area was an area of acute hemorrhagic necrosis with hyperemia and marked edema [14]. The outer ring, seen as enhancing tissue on DCE-MRI, was characterized by atrophic glandular tissue, patchy mononuclear cell infiltration, fibromuscular hyperplasia, neovascularization, edema, and dilated glandular structures. The histopathological changes seen at 1 month ($n = 1$) were partial resolution of necrosis with some fibrosis and atrophy, and these were seen as non-enhancing areas on MRI.

A concern in any treatment for prostate cancer is the potential effect on the nerves involved in erections. There had been some suggestions with other photosensitizers that PDT may be "nerve sparing," either because the drug or light dose may not be able to get into the nerves. This had been noted with both animal studies [18–20] and clinical studies [21]. A study looking at the effect of WST-09 PDT on peripheral nerves in a canine saphenous nerve model did, however, show a dose-dependent effect of PDT on the nerve, with effects seen using direct irradiation at a dose of 100–200 J/cm^2 in combination with a drug dose of 1–2 mg/kg [22]. The nerve changes were not seen immediately, but were apparent on both stimulation testing and histological examination at 1 week.

This substantial body of canine work enabled the introduction of WST-09 PDT into the clinical arena. The first studies were carried out in

radiorecurrent prostate cancer following definitive radiotherapy, and these will be discussed in detail in the following section.

Clinical Studies in Men with Radiorecurrent Prostate Cancer

The first in-man study using WST-09 for prostate cancer was carried out by Trachtenberg and colleagues in men with radiorecurrent prostate cancer in three centers in Canada [23]. Radiorecurrent prostate cancer was suspected on the basis of three consecutive rises in prostate-specific antigen (PSA) and confirmed on transrectal biopsy. Organ-confined disease status was assigned following digital rectal examination (DRE), computed tomography (CT), and bone scanning. The initial part of the study involved a drug dose escalation phase, where groups of three men were given a drug dose of 0.1, 0.25, 0.5, 1, and 2 mg/kg, respectively. Those in the first phase of study received a fixed light dose of 100 J/cm. The second part of the study, reported separately, involved a light dose escalation phase for men treated at the 2 mg/kg dose, with escalation to doses of 230 J/cm and 360 J/cm [24].

The VTP procedure was carried out under general anesthetic, with the patient in the lithotomy position. Prophylactic antibiotics were given prior to the procedure. A urinary catheter containing a light detector was inserted into the bladder. A transrectal ultrasound was placed in the rectum, and secured within a stepper, which allowed movement in the *x*, *y*, and *z* axes. After appropriate skin preparation, and with the use of a transperineal template designed for use in prostate brachytherapy, the light delivery catheters were inserted into the prostate. These catheters were again designed for use in prostate brachytherapy and required a track to be made in the prostate using a sharp metal needle. This sharp needle was then removed, and the hollow plastic catheter with a metal inner needle was inserted along the track. Once the positioning of the catheter was seen to be satisfactory on ultrasound, the inner needle was removed. Measurements of the catheter within the prostate allowed an appropriate length of cylindrically diffusing fiber to be selected from the available lengths of 1–4 cm, in 0.5 cm increments. A hydrodissection procedure was carried out to increase the space between the rectum and prostate, with the intention of reducing the light available in the rectum, and so reduce the risk of activation of any drug in the rectum, which could result in a rectourethral injury [23, 24].

Optical monitoring fibers were placed in the prostate and rectum, as well as the one in the urinary catheter. Once the planned fibers had been inserted, optical measurements were taken. If the light dose in the rectum was greater than 10 % of that in the prostate, then fibers would be removed or repositioned until the rectal fluence fell below this level. Once the fiber positioning was finalized, the drug infusion begun. The light dose was then given between 6 and 10 min after the end of the infusion [23, 24]. In the first studies, blood samples were taken to assess the peak concentration of the photosensitizer. These showed that the photosensitizer concentration peaked at the end of the infusion and then cleared with a half-life of about 20 min [23].

Skin sensitivity, previously a significant disadvantage to systemically administered photosensitizers, was formally assessed by Trachtenberg's group [25]. Men were kept in dimmed light for 24 h after photosensitizer administration, and skin photosensitivity testing was carried out using a solar simulator directed at small areas of skin, on the back of each patient, at 3, 12, and 24 h post-PDT. The areas were then assessed for photosensitivity reactions at 24, 48, and 72 h post-PDT. Patients were advised to wear dark clothing and wavelength-specific protective eyewear for 7 days after the photosensitizer infusion, although they were discharged from hospital at 24 h post-procedure. No skin response to ultraviolet (UV)-negative light was seen at any time point, for skin exposures of up to 128 J/cm^2 and the maximum drug dose of 2 mg/kg. An assessment was also made with UV-positive light, which, at a high enough dose, would cause a skin reaction in the absence of a photosensitizer. This was intended to see if the photosensitizer would potentiate the effect of the UV light and cause a greater extent of "sunburn"

reaction than would be expected from the light alone. This was not the case at any of the light activation doses, or time points tested [25]. This work allowed for the relaxation of the light protection rules in the clinical work that followed, so that patients could be discharged on the day of the procedure without restrictive light protection requirements being needed.

The outcomes of the post-radiotherapy studies were reported in a number of different publications [23–25]. The first report, of the first 24 men, reported the volume of effect as seen on 1 week gadolinium-enhanced MRI, as well as targeted transrectal biopsies to the lesion and serial PSA measurements [23]. They noted that those treated at the lower drug doses of 0.1, 0.25, and 0.5 mg/kg did not show any evident effect on any of the parameters. At both 1 and 2 mg/kg, effects were seen, with all six men in the 2 mg/kg group showing an effect at the highest light dose. No serious adverse events were noted, with only two men not regaining normal urination by day 7. In those men with more than a 20 % response on MR criteria, there was a significant decrease in urinary function as determined by the International Prostate Symptom Score (IPSS) and Patient-Oriented Prostate Utility Scale at 1 month, but this gradually returned to baseline by 6 months. A drop in blood pressure at 5 min after the infusion of the drug was seen in 12 men, but this responded promptly to fluids and/or vasopressors, and no adverse events related to hypotension were recorded [23].

Thermal recordings in this first in-man study confirmed that there was no significant temperature rise during treatment, and so intraprostatic temperature measurements were omitted from further clinical work [23].

The PSA response was seen to be negligible in those men who had less than a 20 % VTP effect at 1-week MRI. In those men who had the highest drug and light dose (six men) and had a greater than 20 % effect at 1-week MRI (five men, deemed responders), there was a PSA response where the PSA decreased to negligible levels following the procedure in four men, while the fifth man showed a significant but transient PSA response [23].

The next publication looked specifically at the MR imaging appearance following PDT for men within the light dose escalation phase [26]. Twenty-five men treated at 2 mg/kg were reported in this study, with three men excluded as they did not complete imaging follow-up, two of whom did not undergo the 6-month biopsy. The imaging analysis was therefore of 25 men, and the biopsy analysis of 26 men. Contrast-enhanced images were taken immediately after (dynamic contrast-enhanced) and at 10 min after the administration of the contrast agent gadopentetate dimeglumine (Magnevist). Confirming the results seen in the canine studies, the treatment effect on T2-weighted imaging was somewhat ill defined at 1 week, and contrast imaging gave the most useful information. A measurement of the percentage of VTP effect was calculated as the volume of non-enhancing tissue outlined from planimetry-based calculations of the region of interest on sequential MR images, divided by the whole prostate volume derived in a similar manner. The effect was noted to be between 0.9 % and 80 %, and varied with the light dose used. The maximal VTP effect was seen at 1 week in the majority of men [26].

Some of the men showed discontinuous effects, which were unexpected, with apparent preservation of tissue between treated areas. Urethral preservation was seen in ten men, when the treatment plan predicted a urethral effect in 24 of the 25 men. Fifteen men showed a lack of enhancement of the urethra at 1-week MRI—the reasons for the difference in responsiveness of the urethra in some men are not clear, although it may be related to the urethral blood supply [26].

Irregular treatment margins were noted, with the majority of men (22/25) showing some extraprostatic effects, which were not always contiguous with the intraprostatic effects. Involvement of the puborectalis or levator ani muscles was seen in 22 of 25 men, involvement of the obturator internus in three men, and involvement of the anterior rectal wall in nine men. These extraprostatic changes had resolved in over two-thirds of the men by the 6-month scan. Bone marrow changes in the pubic bone were seen in four men. These changes were not visible at 1 week, partially

visible at 4 weeks, and maximally visible at 6 months. There did not seem to be any association with clinical symptoms with these bone changes [26].

The rectal wall changes were seen on the 1-week MR scans as loss of enhancement of the outer rectal wall (muscularis propria) in seven men with partial involvement of the mucosa in two men. One of these men developed the clinical symptoms of a fistula, although none was specifically detected on MR imaging or cystoscopy. The symptoms resolved with conservative management. In those men in whom asymptomatic rectal wall involvement was noted on MR imaging at 1 week, these changes had resolved by the scan at 6 months, with associated scarring and reduction in volume of the prostate [26].

Assessment of VTP effect in fat was not possible, due to the poor enhancement of fat in the pre-VTP images. The neurovascular bundle was assessed on imaging criteria as spared in all men. In two patients, the 6-month scan showed a urine-filled cavity within the prostate. There was an attempt by the authors to correlate the volume of changes seen on the 1-week MRI with serial PSA changes post-procedure; however, only moderate correlation with change in PSA was seen with no definitive correlation with absolute PSA levels [26].

A subsequent paper assessed the clinical outcomes of the use of computer-aided treatment planning to get a complete response in the 28 men who received the optimal drug dose of 2 mg/kg WST-09 [24]. The treatment planning itself is described by Davidson in a later publication [27].

A complete response was attributed on the basis of a biopsy negative for cancer at 6 months. It was noted that a complete response required a delivered light dose of at least 23 J/cm^2 to at least 90 % of the prostate volume, but that, in the 13 patients who received this dose, only eight had negative biopsies. These eight men had a significant decrease in PSA, with negligible PSA levels in those men with a pretreatment PSA of less than 5 ng/ml. Three different measures of treatment efficacy were compared to the light dose received by the prostate: biopsy status at 6 months, volume of effect seen on dynamic contrast-enhanced MRI at 1 week, and PSA response. The light dose received by the prostate was determined by the fluence readings taken by the optical detectors during treatment and is measured in J/cm^2 rather than the more usual method of reporting the intended light dose, as determined by the dose per cm to the cylindrical diffusers and reported in J/cm of diffuser fiber. The fluence readings were then used to construct an optical model, based on the patient-specific optical properties and the exact positions of the optical fibers as taken from transrectal ultrasound measurements [27].

Variability in response at the same light dose was noted, although there was a trend to a larger MR effect and a reduction in tumor burden with an increase in the light dose in these men. Men were divided into three groups: (1) those who had a poor response, expected due to a low light dose in the early part of this light dose escalation study (<23 J/cm^2) (15 men); (2) those who had a light dose greater than 23 J/cm^2, but still had a poor response (5 men); and (3) those who had a light dose greater than 23 J/cm^2 and had a complete response. The reasons for this variability in response are not clear, although it is postulated that it may be due to heterogeneity of blood supply in the previously irradiated prostate. An analysis of the previous radiation dose was, however, not able to explain the variability in effect between men in this study [27].

The 1-week MRI was perhaps a better predictor of the final biopsy outcome than the derived light dose. In those men in whom >60 % VTP effect was seen at 1 week, a negative biopsy was always seen. However, some men who had a low percentage of effect at the 1-week MRI had negative biopsies. It is not clear whether this might have been due to variability in sampling that can result in men having a negative result after a positive result or if the treatment effect was not detected on MRI [27].

The side effects in this treatment group are also reported in this paper. The most significant toxicity was the two rectourethral fistulae. One of these, which became apparent at 2 months after the VTP procedure, occurred in a man who had had hemorrhagic proctitis following radiother-

apy, and it was felt that this may have contributed to an increased dose of photosensitizer in the rectum, leading to a greater VTP effect and subsequent fistula formation. No particular explanation for the second fistula was given [27].

Most patients had a deterioration in urinary function in the initial posttreatment phase, which had returned to baseline at 6 months. This was usually due to storage symptoms, which were controlled with medical therapy [27].

Safety concerns raised in other studies meant that WST-09 was not further explored in radiation recurrent cancer. These will be discussed in the following section.

Clinical Studies in Men with Previously Untreated Prostate Cancer

The first use of VTP using a palladium bacteriopheophorbide sensitizer was a single-center study of Tookad VTP at University College London Hospital, London, UK [28, 29]. This was conducted in two parts: part A, a single fiber per lobe escalation of the light dose per cm of diffusing fiber, and part B, where the number of fibers per patient was escalated.

Men with organ-confined histologically confirmed prostate cancer, who had decided not to undertake immediate radical treatment, were approached to take part. All men had a PSA of less than 20 ng/ml prior to informed consent, and multiparametric MRI had excluded locally advanced or nodal disease. For men with a Gleason score >6, or a PSA of >10 ng/ml, a bone scan was used to assess for metastatic disease and was negative in all included men [28, 29].

The procedure was very similar to that used in the radiorecurrent prostate cancer study. The only significant difference was that hydrodissection to develop the space between the prostate and Denonvilliers fascia was not used. It was felt that there was no evidence to suggest that it had a protective effect and, in the treatment-naïve prostate, might cause harm [28, 29].

Follow-up comprised both safety and efficacy measurements. The safety measurements included vital signs and electrocardiogram (ECG) recording, clinical assessment, serum biochemistry, adverse event recording, and patient-reported outcome measures for both urinary and erectile function. Efficacy measurements included assessment of the dynamic gadolinium-enhanced MRI at 1 week and 1, 3, 6, and 12 months post-procedure, PSA monitoring, and transperineal template-guided biopsy at 6 months [28, 29].

Based on the radiorecurrent prostate cancer study results, the photosensitizer dose used for the study was 2 mg/kg. As it was considered that the treatment-naïve prostate might be more sensitive than the previously irradiated prostate, the starting light dose was 50 J/cm, considerably lower than the doses being used in the radiorecurrent treatment group at the time (up to 360 J/cm). The first patient received 50 J/cm with a 2 cm diffuser in one lobe of the prostate. This did not result in any measurable effect, and the dose was increased to 100 J/cm in one lobe and 150 J/cm in the opposite lobe for the next patient. Only the 150 J/cm dose gave a measurable effect of 0.68 mls. Dose escalation continued, with the maximum light dose of 300 J/cm being seen to give noncontiguous effect and some extraprostatic areas lacking uptake of gadolinium at 1-week MRI. The largest volume of effect on the 1-week MRI scan in the single fiber part of the study was 4.06 mls in a lobe that received a total light dose of 300 J (2 cm at 150 J/cm) (Fig. 23.2). However, the most consistent effects had been with a dose of 200 J/cm given at a rate of 150 mW, and this dose was chosen to be further explored in the multifiber phase [28, 29].

The fiber escalation phase resulted in a maximum total dose of 3800 J per lobe. It was seen that a higher light dose correlated with a greater effect on 1-week MRI and a greater likelihood of a negative biopsy. However, there had been some unexpected toxicity in the study, thought to be related to the use of Cremophor® required to allow the lipophilic Tookad to be given intravenously. This comprised thrombotic effects, namely, one deep venous thrombosis in one man 5 days after VTP and two superficial venous thromboses in the arm into which the photosensitizer

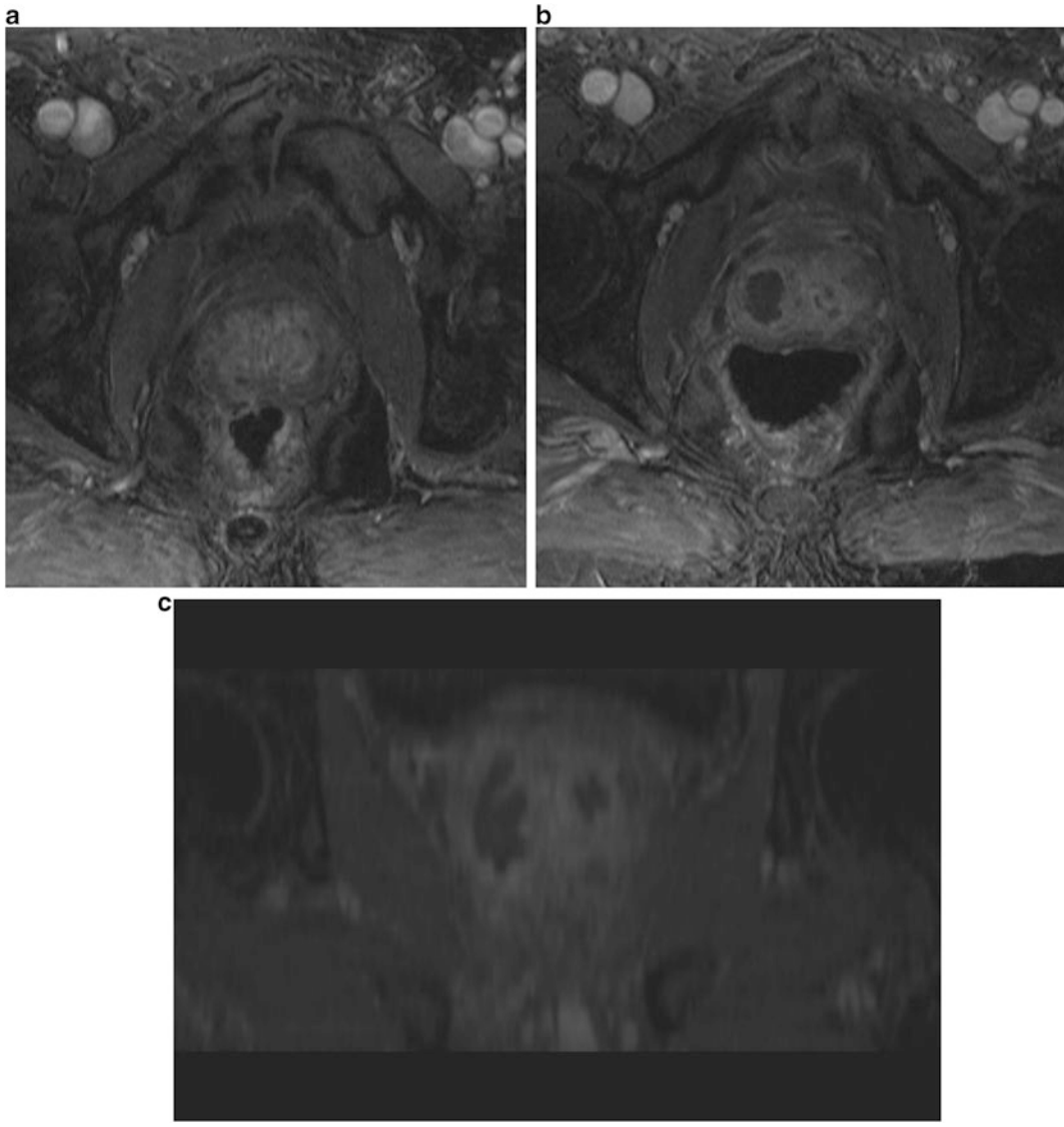

Fig. 23.2 Treatment effect in single fiber phase of WST-09 study. (**a**) Pretreatment MRI—post-gadolinium image. (**b**) Posttreatment MRI: 1 week post-gadolinium image (axial). (**c**) Posttreatment MRI: 1 week post-gadolinium image (coronal)

was infused. This happened in the first two men in the study and resolved without any serious sequelae. However, the protocol was then changed to allow a bolus of saline to be given after the infusion had finished, and a 24-h saline drip was then used [28, 29].

There were two men who experienced serious cardiac events in the study. The first was a man who had previously had a coronary artery bypass graft. He had some ischemic ECG changes during the procedure and awoke with some chest discomfort. He developed fast atrial fibrillation during the procedure and was cardioverted at the end of the procedure. This meant that markers of cardiac damage were unreliable, and acute coronary syndrome was diagnosed. He underwent

stent placement during the same hospital admission and made an excellent recovery [28, 29].

The second man was noted to have a myocardial infarction and a cerebrovascular accident (CVA) in the first 24 h after the procedure. He was found to have a patent foramen ovale, which was deemed to have contributed to the CVA. The study was halted pending a safety investigation, and it was decided that the lipophilic formulation would not continue in clinical use. A water-soluble formulation, Tookad® Soluble (WST-11; padeliporfin), was therefore used in the next stage of development, within multicenter European and US clinical trials.

WST-11 Clinical Work

There have been simultaneous programs in Europe and the USA to develop the evidence base for the use of WST-11 (Tookad Soluble) in men with low-risk prostate cancer. The first study in Europe included a dose escalation phase, where the optimal drug dose (calculated per kg) and the optimal light dose per cm of light diffusing fiber were determined (PCM 201) [30]. The first men were given a drug dose of 2 mg/kg, shown to be safe in men having VTP after radiotherapy. The drug dose was escalated to 4 mg/kg and then 6 mg/kg, and a constant light dose of 200 J/cm was used, based on the results for the WST-09 work. The maximal effect on 1-week MRI was seen in men having a drug dose of 4 mg/kg, 200 J/cm, and a light dose index (LDI) of >1. The light dose index was a new concept to express the light dose per ml of prostate and is calculated from length of illuminated fibers/volume of targeted prostate, where the volume was calculated from the pre-procedure MRI. As the number of light fibers was escalated during the study, only 12 of the 40 treated men had the optimal conditions of drug dose, light dose, and LDI. Of these 12 men, 10 men had negative biopsies in the treated lobe posttreatment.

A similar study design was used in the USA (PCM 202), although the treatment zone was limited to a hemi-ablation, while some men in the European study had bilateral treatment [31]. Another difference is that in the USA men had to have only unilateral disease, and no Gleason pattern 4 component, whereas in Europe bilateral disease was allowed, and secondary Gleason pattern 4 of low volume on transperineal template biopsy was permitted. Thirty men were enrolled, of which nine were included in the dose escalation phase. This comprised three men having single fiber 200 J/cm light dose to activate 2 mg/kg WST-11, followed by six men having 2 mg/kg WST-11 and 300 J/cm light dose. Due to the evidence from simultaneous dose escalation studies in Europe, it was determined that 4 mg/kg WST-11 and 200 J/cm energy was an appropriate dose. Twenty-one men underwent treatment to either the right or left lobe of the prostate using 4 mg/kg WST-11 and 200 J/cm energy. Biopsies were done of the treated and untreated lobes at 6 months following treatment. Overall, 15 of 21 men at the optimal dose had residual cancer after treatment: one in both lobes, four in the untreated lobe only, and ten in the treated lobe. The effect did depend on the light dose delivered with 13 of 17 men (73 %) having a light dose index of >1 having no cancer in the treated lobe at posttreatment biopsy [31].

A pooled analysis of men receiving treatment with 4 mg/kg Tookad Soluble, and light at 200 J/cm in either of the aforementioned two studies, or the further European study PCM 301 were analyzed together [32]. In total, 109 men received treatment according to the protocol, with 76 of those 109 receiving an LDI >1 (70 %), of which 67 had unilateral treatment. In this subset, there was an 80.6 % negative biopsy rate at 6 months. A slight improvement in urinary function and slight reduction in sexual function were noted on IPSS and International Index of Erectile Function (IIEF) questionnaires at 6 months, compared to baseline [32].

A European phase III study comparing WST-11 VTP to active surveillance has been completed and was presented at the European Association of Urology in 2016 [33]. Men were included if they had Gleason 3+3 disease, with one positive core on standard TRUS biopsy showing 3–5 mm Gleason 3+3 or two positive cores of up to 5 mm Gleason 3+3 in each core, with a PSA ≤10 ng/ml. Men were randomized to Tookad VTP or active surveillance. The primary

endpoint was 58/206 (28 %) men in the Tookad arm progressed to higher-risk disease compared to 120/207 (58 %) men in the active surveillance arm, and progression was closely related to subsequent radical therapy. At 24 months, 101 (49 %) men in the Tookad arm had a negative biopsy compared to 28 men (14 %) in the active surveillance arm [33]. This is a landmark study, as it is the first completed randomized study of focal therapy for prostate cancer. Formal publication is awaited. Some challenged the presentation suggesting that all men in the study would have been suitable for active surveillance and that further work is needed in men with intermediate-risk prostate cancer.

The question of radical treatment after focal therapy is of interest, both in terms of oncological and functional outcomes. Outcomes have been reported in 19 men [34]. Thirteen men (68 %) were completely continent at a median of 10 months with five needing a pad a day and one needing three pads per day. Eleven men had erectile function after VTP, but none after radical prostatectomy. Nine men had positive margins, and six had postoperative radiotherapy [34].

Future Directions

There are many who are interested in increasing the specificity of a photosensitizer so that it is only taken up by cancer cells. One of the ways of doing this is to attach the photosensitizer to a monoclonal antibody that is specific to a given cancer cell type [35]. One of the difficulties with this approach is that some tumor types may not consistently express a given antigen, and the antibody-photosensitizer conjugate may not therefore be taken up by all the cells of a given tumor. It has, however, been tried in small animal models and may be of use in the future. One study has shown the advantage of conjugating a chlorin photosensitizer to a monoclonal antibody in an ovarian cancer model [36]. Further work in this area has included the use of an antibody conjugated to a pheophorbide photosensitizer, albeit in an in vitro model [37]. One study has shown that use of antibody conjugation to prostate-specific membrane antigen (PMSA) allows a marked reduction in photosensitizer dose for the same effect [38].

Other advances may be seen in the use of different approaches to treatment planning for the photodynamic therapy procedure. At present, different groups have developed different approaches to the planning of prostate photodynamic therapy. One approach is to constantly modify the light dose given according to real-time feedback. This requires a "multitasking" probe, consisting of a fiber that can be used to deliver light and then, when the light is momentarily turned off, to take a light reading, which is then used within a complex feedback mechanism to determine the subsequent light dose. One such system has been used in a canine model and shown to result in treatment effect within 2 % of the value predicted [39]. It is also possible to incorporate available drug dose and oxygen readings into such a feedback system [40]. While such a system has been piloted in the clinical setting, formal results of this are not yet available.

Another way to plan treatment is to assign a given treatment effect to each light fiber, at a given drug and light dose, and to then calculate the number and distribution of fibers needed to give a treatment effect in a given prostate. This is the system that has been used in the Tookad studies, with both the Canadian group and the European group developing different treatment planning systems. In this situation the volume and shape of the prostate on MRI is used to determine the treatment plan, which is then delivered in the operating theater using ultrasound images [41, 42]. A further possibility would be to use a "rules-based" approach to plan directly based on ultrasound, putting in fibers to achieve a treatment plan that is based either on the sites of histological evidence of disease or on areas suspicious for disease on MRI.

Conclusion

Vascular targeted photodynamic therapy using palladium bacteriopheophorbide is a promising modality in the treatment of prostate cancer that

has been studied extensively in the canine model prior to clinical work. There have been studies assessing its use in radiorecurrent prostate cancer, but this is not under continued development at present. In men with previously untreated prostate cancer, WST-11 (Tookad Soluble, padeliporfin) has replaced WST-09 (Tookad), due to unexpected toxicity associated with the Cremophor-based preparation of WST-09. Tookad Soluble has been studied in European and North American phase II studies with promising results.

References

1. Ackroyd R, Kelty C, Brown N, Reed M. The history of photodetection and photodynamic therapy. Photochem Photobiol. 2001;74(5):656–69.
2. Lipson RL, Baldes EJ, Gray MJ. Hematoporphyrin derivative for detection and management of cancer. Cancer. 1967;20(12):2255–7.
3. Dougherty TJ, Kaufman JE, Goldfarb A, Weishaupt KR, Boyle D, Mittleman A. Photoradiation therapy for the treatment of malignant tumors. Cancer Res. 1978;38(8):2628–35.
4. Mackenzie GD, Dunn JM, Selvasekar CR, Mosse CA, Thorpe SM, Novelli MR, et al. Optimal conditions for successful ablation of high-grade dysplasia in barrett's oesophagus using aminolaevulinic acid photodynamic therapy. Lasers Med Sci. 2009;24(5):729–34.
5. Selman SH, Keck RW. The effect of transurethral light on the canine prostate after sensitization with the photosensitizer tin (II) etiopurpurin dichloride: a pilot study. J Urol. 1994;152(6 Pt 1):2129–32.
6. Tiwari A, Krishna NS, Nanda K, Chugh A. Benign prostatic hyperplasia: an insight into current investigational medical therapies. Expert Opin Investig Drugs. 2005;14(11):1359–72.
7. Fiedor J, Fiedor L, Kammhuber N, Scherz A, Scheer H. Photodynamics of the bacteriochlorophyll-carotenoid system. 2. Influence of central metal, solvent and beta-carotene on photobleaching of bacteriochlorophyll derivatives. Photochem Photobiol. 2002;76(2):145–52.
8. Schreiber S, Gross S, Brandis A, Harmelin A, Rosenbach-Belkin V, Scherz A, Salomon Y. Local photodynamic therapy (PDT) of rat C6 glioma xenografts with PD-bacteriopheophorbide leads to decreased metastases and increase of animal cure compared with surgery. Int J Cancer. 2002;99(2):279–85.
9. Preise D, Scherz A, Salomon Y. Antitumor immunity promoted by vascular occluding therapy: lessons from vascular-targeted photodynamic therapy (VTP). Photochem Photobiol Sci. 2011;10(5):681–8.
10. Koudinova NV, Pinthus JH, Brandis A, Brenner O, Bendel P, Ramon J, et al. Photodynamic therapy with Pd-bacteriopheophorbide (Tookad): successful in vivo treatment of human prostatic small cell carcinoma xenografts. Int J Cancer. 2003;104(6):782–9.
11. Lucroy MD, Bowles MH, Higbee RG, Blaik MA, Ritchey JW, Ridgway TD. Photodynamic therapy for prostatic carcinoma in a dog. J Vet Intern Med. 2003;17(2):235–7.
12. L'eplattenier HF, Klem B, Teske E, van Sluijs FJ, van Nimwegen SA, Kirpensteijn J. Preliminary results of intraoperative photodynamic therapy with 5-aminolevulinic acid in dogs with prostate carcinoma. Vet J. 2008;178(2):202–7.
13. Huang Z, Chen Q, Luck D, Beckers J, Wilson BC, Trncic N, et al. Studies of a vascular-acting photosensitizer, Pd-bacteriopheophorbide (Tookad), in normal canine prostate and spontaneous canine prostate cancer. Lasers Surg Med. 2005;36(5):390–7.
14. Chen Q, Huang Z, Luck D, Beckers J, Brun PH, Wilson BC, et al. Preclinical studies in normal canine prostate of a novel palladium-bacteriopheophorbide (WST09) photosensitizer for photodynamic therapy of prostate cancers. Photochem Photobiol. 2002;76(4):438–45.
15. Huang Z, Chen Q, Trncic N, LaRue SM, Brun PH, Wilson BC, et al. Effects of Pd-bacteriopheophorbide (Tookad)-mediated photodynamic therapy on canine prostate pretreated with ionizing radiation. Radiat Res. 2004;161(6):723–31.
16. Huang Z, Haider MA, Kraft S, Chen Q, Blanc D, Wilson BC, Hetzel FW. Magnetic resonance imaging correlated with the histopathological effect of Pd-bacteriopheophorbide (Tookad) photodynamic therapy on the normal canine prostate gland. Lasers Surg Med. 2006;38(7):672–81.
17. Kirkham AP, Emberton M, Hoh IM, Illing RO, Freeman AA, Allen C. MR imaging of prostate after treatment with high-intensity focused ultrasound. Radiology. 2008;246(3):833–44.
18. Chang SC, Chern IF, Hsu YH. Biological responses of dog prostate and adjacent structures after meso-tetra-(m-hydroxyphenyl) chlorin and aluminum disulfonated phthalocyanine based photodynamic therapy. Proc Natl Sci Counc Repub China B. 1999;23(4):158–66.
19. Kübler AC, Stenzel W, Rühling M, Meul B, Fischer JH. Experimental evaluation of possible side effects of intra-operative photodynamic therapy on rabbit blood vessels and nerves. Lasers Surg Med. 2003;33(4):247–55.
20. Christensen NR, Charabi S, Johansen LS, Rygaard J, Balle VH, Tos M, Thomsen J. Effect of photodynamic therapy on a heterotransplanted human parotid tumor. Auris Nasus Larynx. 2000;27(3):241–5.
21. Ris HB, Altermatt HJ, Nachbur B, Stewart CM, Wang Q, Lim CK, et al. Intraoperative photodynamic therapy with m-tetrahydroxyphenylchlorin for chest malignancies. Lasers Surg Med. 1996;18(1):39–45.
22. Dole KC, Chen Q, Hetzel FW, Whalen LR, Blanc D, Huang Z. Effects of photodynamic therapy on

peripheral nerve: in situ compound-action potentials study in a canine model. Photomed Laser Surg. 2005;23(2):172–6.
23. Trachtenberg J, Bogaards A, Weersink RA, Haider MA, Evans A, McCluskey SA, et al. Vascular targeted photodynamic therapy with palladium-bacteriopheophorbide photosensitizer for recurrent prostate cancer following definitive radiation therapy: assessment of safety and treatment response. J Urol. 2007;178(5):1974–9.
24. Trachtenberg J, Weersink RA, Davidson SR, Haider MA, Bogaards A, Gertner MR, et al. Vascular-targeted photodynamic therapy (padoporfin, WST09) for recurrent prostate cancer after failure of external beam radiotherapy: a study of escalating light doses. BJU Int. 2008;102(5):556–62.
25. Weersink RA, Forbes J, Bisland S, Trachtenberg J, Elhilali M, Brún PH, Wilson BC. Assessment of cutaneous photosensitivity of Tookad (WST09) in preclinical animal models and in patients. Photochem Photobiol. 2005;81(1):106–13.
26. Haider MA, Davidson SR, Kale AV, Weersink RA, Evans AJ, Toi A, et al. Prostate gland: MR imaging appearance after vascular targeted photodynamic therapy with palladium-bacteriopheophorbide. Radiology. 2007;244(1):196–204.
27. Davidson SR, Weersink RA, Haider MA, Gertner MR, Bogaards A, Giewercer D, et al. Treatment planning and dose analysis for interstitial photodynamic therapy of prostate cancer. Phys Med Biol. 2009;54(8):2293–313.
28. Moore CM, Hoh I, Mosse CA, Allen C, Freeman A, Bown SG, Emberton M. Vascular-targeted photodynamic therapy in organ confined prostate cancer – report of a novel photosensitiser. European Association of Urology 21st Annual Conference. 2006.
29. Pendse DA, Allen C, Kirkham A, Moore C, Bown S, Ahmed HU, et al. Dynamic contrast-enhanced magnetic resonance imaging after vascular-targeted photodynamic therapy (VTP) with Tookad (padoporfin) in primary prostate cancer. Eur Urol Suppl. 2008;7(3):233.
30. Moore CM, Azzouzi AR, Barret E, Villers A, Muir GH, Barber NJ, et al. Determination of optimal drug dose and light dose index to achieve minimally invasive focal ablation of localised prostate cancer using WST11-vascular-targeted photodynamic (VTP) therapy. BJU Int. 2015;116(6):888–96.
31. Taneja SS, Bennett J, Coleman J, Grubb R, Andriole G, Reiter RE, et al. Final results of a phase I/II multicenter trial of WST11 vascular targeted photodynamic therapy for hemi-ablation of the prostate in men with unilateral low risk prostate cancer performed in the United States. J Urol. 2016;196:1096–104.
32. Azzouzi AR, Barret E, Bennet J, Moore C, Taneja S, Muir G, et al. Tookad® Soluble focal therapy: pooled analysis of three phase II studies assessing the minimally invasive ablation of localized prostate cancer. World J Urol. 2015;33(7):945–53.
33. Azzouzi AR, Vincendeau S, Barret E, Cicco A, Kleinclauss F, Van der Pole H, et al. Tookad (padeliporfin) vascular targeted photodynamic therapy versus active surveillance in men with low risk prostate cancer. A randomized phase III clinical trial. Presented at the European Association of Urology Annual meeting 2016, http://eaumunich2016.uroweb.org/resource-centre/results/webcast/05901f06/ Accessed 24 July 2016.
34. Lebdai S, Villers A, Barret E, Nedelcu C, Bigot P, Azzouzi AR. Feasibility, safety, and efficacy of salvage radical prostatectomy after Tookad® Soluble focal treatment for localized prostate cancer. World J Urol. 2015;33(7):965–71.
35. Bullous AJ, Alonso CM, Boyle RW. Photosensitiser-antibody conjugates for photodynamic therapy. Photochem Photobiol Sci. 2011;10(5):721–50.
36. Goff BA, Blake J, Bamberg MP, Hasan T. Treatment of ovarian cancer with photodynamic therapy and immunoconjugates in a murine ovarian cancer model. Br J Cancer. 1996;74(8):1194–8.
37. Stamati I, Kuimova MK, Lion M, Yahioglu G, Phillips D, Deonarain MP. Novel photosensitisers derived from pyropheophorbide-a: uptake by cells and photodynamic efficiency in vitro. Photochem Photobiol Sci. 2010;9(7):1033–41.
38. Jankun J. Protein-based nanotechnology: antibody conjugated with photosensitizer in targeted anticancer photoimmunotherapy. Int J Oncol. 2011;39(4):949–53.
39. Jankun J, Keck RW, Skrzypczak-Jankun E, Lilge L, Selman SH. Diverse optical characteristic of the prostate and light delivery system: implications for computer modeling of prostatic photodynamic therapy. BJU Int. 2005;95(9):1237–44.
40. Johansson A, Axelsson J, Andersson-Engels S, Swartling J. Realtime light dosimetry software tools for interstitial photodynamic therapy of the human prostate. Med Phys. 2007;34(11):4309–21.
41. Betrouni N, Lopes R, Puech P, Colin P, Mordon S. A model to estimate the outcome of prostate cancer photodynamic therapy with Tookad soluble WST11. Phys Med Biol. 2011;56(15):4771–83.
42. Betrouni N, Colin P, Puech P, Villers A, Mordon S. An image guided treatment platform for prostate cancer photodynamic therapy. Conf Proc IEEE Eng Med Biol Soc. 2013;2013:370–3.

Part VII

Technologies for Focal Therapy: Transrectal Approach

High-Intensity Focused Ultrasound

24

Paolo Capogrosso and Eric Barret

Introduction

High-intensity focused ultrasound (HIFU) is a minimally invasive treatment option for localized prostate cancer (PCa). This technology was initially developed for whole-gland treatment with the possibility of repeated treatments in case of failure. The urologic community has shown a growing interest in HIFU because of its efficacy in destroying prostatic tissue and its limited side effects. HIFU induces coagulative necrosis of a tumor with sharp boundaries. It allows the accurate destruction of a small volume of tissue within the gland and has a limited impact at the level of the surrounding tissue. These advantages make it an ideal option for the focal treatment of localized PCa.

In this chapter, we summarize the principles, technical aspects, and indications of focal HIFU, and we review the evidence published thus far concerning the oncologic and functional outcomes of HIFU for the focal treatment of PCa.

P. Capogrosso
Department of Urology, IRCCS Ospedale San Raffaele/Università Vita-Salute San Raffaele, Milan, Italy

E. Barret (✉)
Department of Urology, Institut Montsouris, Paris-Descartes University, Paris, France
e-mail: eric.barret@imm.fr

Technique

Physics

HIFU converts energy from ultrasound (US) waves to heat, resulting in immediate and irreversible coagulation necrosis with sharply delineated boundaries at the level of the targeted area. The basic principles of HIFU rely on the creation of US waves emitted by a high-powered transducer capable of higher time-averaged intensities (100–10,000 W/cm^2) than conventional diagnostic US and targeted to a precise volume without affecting the surrounding tissues [1]. HIFU is generated by a piezoelectric transducer. This transducer has a parabolic configuration that focuses the sound waves into a fixed focal point (Fig. 24.1). The characteristics of the ablated area, in terms of size and shape, depend on a few variables: the geometric configuration of the transducer, the time-averaged acoustic intensity, the duration of sonication, and the absorption coefficient of the targeted tissue [1, 2]. HIFU allows for the deposition of a large amount of energy at the focal point. Temperature within the tissue rises significantly, resulting in an irreversible and precise ablative lesion without damaging the tissue in the path of the US beam.

The tissue ablation effect of HIFU is based on two main mechanisms: a thermal effect and a mechanical effect. Because the US beam is

© Springer International Publishing AG 2017

T.J. Polascik (ed.), *Imaging and Focal Therapy of Early Prostate Cancer*, Current Clinical Urology, DOI 10.1007/978-3-319-49911-6_24

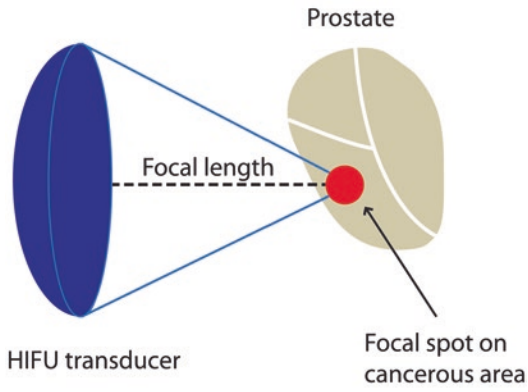

Fig. 24.1 Physics of high-intensity focused ultrasound (HIFU) treatment

concentrated in a small area of tissue, it results in maximum pressure at this focal point. This acoustic pressure creates tissue movement (dilatation and contraction), resulting in a loss of energy that is converted into heat, increasing the temperature to more than 60 °C and leading to protein denaturation and coagulation necrosis of tissues. Because of the significant drop in energy outside the focal zone, the thermal damage beyond the boundaries of treatment is minimized [1, 2]. At higher intensities of acoustic pulses, the mechanical effect could occur, characterized by the interaction of US waves with microbubbles of water that collapse as a result of alternating compression and expansion, finally resulting in a dispersion of energy with consequent tissue ablation [1, 2]. The aim of focal HIFU is to treat the cancer foci inside the gland by the juxtaposition of elementary lesions.

Procedure

HIFU treatment is administered transrectally, with the patient under general or spinal anesthesia. The procedure is performed in a dorsal lithotomic position or flank lateral position according to the characteristics of the treatment device. An enema is usually performed the night before the procedure, and no preoperative antibiotic prophylaxis is needed. A transrectal probe integrating a US probe and a piezoceramic transducer and endowed with a cooling balloon to avoid thermal injury of the rectal wall is inserted into the rectum. The prostate is scanned with the US probe. The probe provides images in both the coronal and sagittal planes of the prostate, allowing exact localization of the bladder neck, apex, and rectal wall. The treatment zone is then defined by the urologist and logged into the treatment computer. The integrated software allows precise contouring of the target zone, sparing the surrounding tissue from thermal ablation. After the treatment zone has been defined, the transducer moves the focal point of the US beams through the area to be ablated, with a treatment cycle including a heating period of the tissue followed by a cooling period during which the computer-controlled device moves to the next treatment zone, distant from the first. All selected areas are ablated as the transducer moves back and forth. A transurethral or suprapubic catheter is generally placed at the end of the procedure and will be removed at day 1 (Table 24.1).

Table 24.1 Practical steps for focal high-intensity focused ultrasound treatment

Before treatment
Prostate cancer diagnosis (either TRUS or TPM biopsy)
Preoperative mpMRI for precise localization of the tumor area
Procedure
Correct definition of the target zone with the integrated software device
Ablation of the tumor area
Possible check of the ablated area with CEUS
Urethral catheter placement at the end of the procedure
Posttreatment management
Catheter removal the day after the procedure and patient discharged
Follow-up
PSA level every 3 months
mpMRI at early (3–10 days) and late stage (6 months) after treatment
Prostate TRUS biopsy within the first year

CEUS contrast-enhanced ultrasound, *mpMRI* multiparametric magnetic resonance imaging, *PSA* prostate-specific antigen, *TPM* transperineal prostate mapping, *TRUS* transrectal ultrasound

Devices

Three devices for HIFU therapy are currently available: the Sonablate 500 (SonaCare Medical, Charlotte, NC, USA), Ablatherm Integrated Imaging (EDAP TMS SA, Vaulx-en-Velin, France), and the Focal One (EDAP TMS SA, Vaulx-en-Velin, France) [3]. All share the fundamental features of the HIFU system even if the evolution of the technique in the last two decades can be clearly recognized among the three devices. Newly developed technologies allowing HIFU treatment to be carried out directly with multiparametric magnetic resonance imaging (mpMRI) guidance are currently under evaluation.

Sonablate 500

The Sonablate 500 (Fig. 24.2) is characterized by a single transducer (4 MHz) for both imaging and treatment [3]. Probes with different focal lengths (25–45 mm) allow the treatment of prostate volumes with sagittal diameters up to 40 mm.

Fig. 24.2 Sonablate 500® (Courtesy of SonaCare, Charlotte, NC, USA)

The feature of tissue change monitoring gives visual confirmation of the treated volume, allowing the physician to monitor and eventually modify the treatment planning to cover the entire cancerous area. The procedure is conducted with the patient lying in a dorsal position on a conventional operating table. The system is also provided with a safety feature called a *reflectivity index measurement* that compares a stored B-mode image of the rectal wall taken before the start of the treatment with a real-time image of the rectum itself, analyzing any potential differences between the two and finally assigning a score that alerts the physician of any significant injury to the rectum and automatically stops the treatment over a certain threshold [3].

Ablatherm Integrated Imaging

The Ablatherm Integrated Imaging system (Fig. 24.3) is composed of imaging (7.5 MHz) and therapeutic (3 MHz) transducers, both incorporated in the same endorectal probe. The treatment crystal is focused at a maximum of 45 mm and allows the creation of an ablation area ranging from 0.05 to 0.08 mL.

The treatment is carried out with the patient in a lateral flank position requiring a specific operating table. The lateral treatment position allows gas bubbles that can be created by the heating of the prostatic tissue to rise with gravity into a position outside the field of treatment, reducing potential acoustic interference. The system includes four protocols of treatment with different parameters according to the clinical indications: standard treatment, HIFU re-treatment, post-external beam radiation therapy (post-EBRT), and post-brachytherapy (post-BT) [3].

Regarding the safety issue, the Ablatherm device allows the user to have a real-time visual monitoring of the treatment with the US probe. The treatment probe is robotically controlled: The system is capable of automatically adjusting the endorectal position of the transducer according to the real distance from the rectal wall and to eventual modifications of the patient position, consequently stopping the procedure in case of risk of injury [4].

Fig. 24.3 Ablatherm Integrated Imaging® (Courtesy of EDAP TMS SA, Vaulx-en-Velin, France)

Fig. 24.4 Focal One® (Courtesy of EDAP TMS SA, Vaulx-en-Velin, France)

Focal One

The Focal One (Fig. 24.4) is the most recently developed system and incorporates several useful features that allow more precise and safe localized treatment of the tumor foci within the prostate [3]. From a general perspective, the treatment protocol with the Focal One device can be divided into three steps: fusion of the real-time US image with magnetic resonance (MR) images acquired before the treatment; planning of the treatment with focal target definition; and application of precise ablative energy, checking the treated area.

The procedure is carried out with the patient in a lateral flank position on a standard operating table. The first step is the upload of the mpMR images. The operator defines contours of the prostate and delineates the suspected lesions to be treated on the MR images. The prostate boundaries are then defined on the US real-time image of the prostate obtained with the transrectal probe of the device. An "elastic fusion" of the two defined volumes is then automatically executed by the software, leading to a perfect three-dimensional (3D) match of the MR volume with the US volume of the prostate (Fig. 24.5). The same 3D fusion is applied to the suspicious area previously identified on the MRI that can thus be correctly identified on the live US image [3].

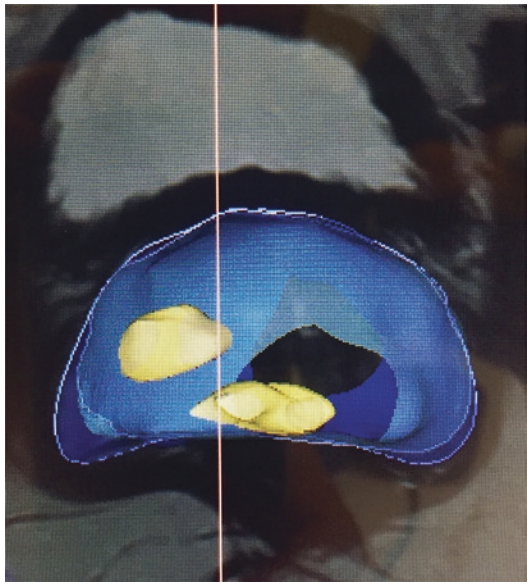

Fig. 24.5 Three-dimensional magnetic resonance imaging-ultrasound (MRI-US) fusion

The device is equipped with a dynamic focusing transducer for the HIFU treatment: This innovative probe is characterized by 16 isocentric rings driven by a dedicated electronic system allowing the user to drive the US beam, with the possibility of moving the focal point to a maximum of eight different points between 32 and 67 mm from the probe. The size of the ablated area is approximately 5 mm, and multiple unitary lesions can be stacked together to achieve a possible necrotic volume ranging from 5 to 40 mm, according to the defined area of treatment.

The treatment is planned for transversal slices, and the contours of the targeted area are defined for each slide by the operator using the MR-US fusion image. The software automatically adjusts the focus of the HIFU beams according to the planned volume of treatment, with a continuous shooting process of US pulses lasting 1 s each that allows a shortened treatment duration compared with the other devices. During treatment, the operator is able to check the HIFU energy delivery process in the treated area, with the possibility of stopping and modifying the treatment plan in case of an alteration in positioning.

Finally, at the end of the treatment, the system allows the physician to assess the final results of the process by performing contrast-enhanced US (CEUS). The image can be compared with the initial MRI to check for correct ablation of the cancer lesion [3].

Follow-Up After Treatment

Postoperative Evaluation

To increase the chance of focal therapy success, an assessment of treatment efficacy can be performed immediately after the procedure to detect residual viable cancer tissue, allowing the operator to eventually complete the treatment. In this context, CEUS, using a suspension of phospholipid-stabilized sulfur hexafluoride microbubbles (SonoVue, Bracco, Milan, Italy), has been demonstrated to be useful in detecting the volume and position of the treated zone after HIFU; the CEUS image appears nonenhanced and can be distinguished from the enhancement of the residual viable tissue [5]. Because of the intrinsic characteristics of the SonoVue contrast agent, the CEUS image can be acquired immediately after the intravenous injection with good spatial resolution and contrast/tissue ratio and can be immediately performed in the operating room after the HIFU procedure [6]. The accuracy of CEUS imaging was evaluated in a small population of 28 patients at 1 to 3 days and 30 to 45 days after HIFU and correlated with posttreatment biopsy findings [5]. The results clearly demonstrated that CEUS was able to accurately discern the ablated area of the prostate from the viable tissue, showing that the imaging findings were stable from day 1 to 45 and were associated with biopsy findings [5].

The gold standard for post-HIFU evaluation of the ablated area remains the gadolinium-enhanced MRI [7]. The initial results published by Rouviere et al. [8] demonstrated that at the MRI performed 2–5 days after HIFU, the treated area appeared as a hypointense zone surrounded by a peripheral rim of enhancement that has been

demonstrated to contain a variable amount of viable tissue [9]. Nevertheless, MRI is not a feasible option for the immediate evaluation of the treated volume inside the operating room.

Detection of Post-HIFU Failure

Because the prostatic parenchyma is incompletely destroyed, the post-focal HIFU evaluation is more challenging. From a general perspective, the assessment of potential failure after focal HIFU treatment should be based on the evaluation of biochemical parameters, imaging, and histologic assessment.

The assessment of prostate-specific antigen (PSA) serum level after whole-gland HIFU has been demonstrated to significantly predict clinical cancer recurrence during follow-up [10]. The focal treatment, however, is based on the destruction of the index lesion, keeping intact the rest of the gland. Therefore, biochemical recurrence (BCR) will be difficult to estimate, and then criteria such as American Society for Therapeutic Radiology and Oncology (ASTRO), Phoenix, or Stuttgart seem to be inappropriate for an adequate evaluation [11, 12]. After successful HIFU ablation of the index lesion, some authors reported a significant decrease in PSA compared with its initial value. Even if the exact percentage of the decrease is not currently known (approximately 50 %), this decrease should be observed within 3 months after treatment and, most important, should remain stable over time. Failure is strongly suspected if this does not occur after ablation [11–14].

In addition to the biochemical evaluation, the use of mpMRI has become essential in the context of follow-up after focal HIFU, playing an important role both at an early stage (within 3–10 days after treatment) and at 6 months after treatment and thereafter in case of a PSA rise. In the early postoperative setting, the MRI allows the determination of the extent of tissue damage and the analysis of the untreated prostatic parenchyma. On a fat-saturated gadolinium-enhanced nondynamic T1-weighted sequence, the ablated area appears as an unenhanced (devascularized) zone surrounded by a peripheral rim of enhancement representing an amount of viable inflamed tissue [7, 8]. Published data showed that the volume of enhancing prostate at the MRI performed within the first months after treatment correlates with PSA level nadir and with histologic evidence of residual cancer [7]; however, the correct timing for the posttreatment MRI evaluation has not yet been defined. Despite previous data that showed the area of nonenhancing tissue decreases by 50 % at 1 month compared with the immediate post-HIFU acquisition [8], no data show a correlation between parameters of immediate imaging findings and subsequent treatment outcomes [7]. At the late 6-month assessment, T2-weighted images show a decrease in volume of the gland. The prostate parenchyma usually appears as heterogeneously and diffusely hypointense with a loss of normal zonal anatomy, hampering easy detection of local recurrence. The peripheral enhanced rim is no longer detectable due to fibrosis and thickening of the tissue. To discriminate areas of recurrent malignant tumors correctly, the T2-weighted sequence has to be combined with dynamic contrast-enhanced (DCE) and diffusion-weighted sequences, allowing the differentiation of recurrent or residual cancer (hypervascular) from post-HIFU fibrosis (homogeneous and hypovascular). The combination of T2-weighted and DCE MRI can guide biopsies in case of biochemical relapse, improving the sensitivity of recurrent cancer detection. Follow-up imaging should be performed every year after the initial imaging or in the case of BCR [15].

Despite the promising results of imaging in the context of follow-up after HIFU, the altered anatomy following focal therapy limits the utility of MRI; therefore, the histologic assessment with prostate biopsies is crucial. In most published series, a postoperative systematic biopsy has been suggested at 3- to 6-month follow-up (within the first year). The use of a perineal template prostate biopsy would guarantee high accuracy in detecting clinical failure; however, because of the requirement of general anesthesia for perineal biopsies and the associated cost issues [16], a conventional transrectal US (TRUS)

sextant biopsy is normally applied that can also be combined with mpMRI and targeted to the detected suspicious areas.

According to an international multidisciplinary consensus project, sampling of both the treated and untreated part of the gland should be performed [15]. The treated area should be biopsied both at the margins and in the center of the ablation to verify the efficacy and completeness of the treatment. The interpretation of a post-HIFU biopsy should be accurate, and pathologists should be aware of common histologic findings of prostatic cores after HIFU including coagulation necrosis, stromal fibrosis, and edema [17]. Some areas of atypical cell hyperplasia and reactive atypia have been found in biopsy specimens after HIFU and should be carefully differentiated with immunohistochemical staining from recurrent cancer foci [17]. Finally, the untreated area of the gland should also always be biopsied for surveillance purposes. After the first year, rebiopsy of the treated and/or untreated area should be performed only when there is a suspicion of recurrence either on imaging or for a PSA rise [15].

Indications for Focal High-Intensity Focused Ultrasound

The current main indication for HIFU is the primary treatment of PCa in the context of focal therapy, and HIFU is considered one of the most effective treatment modalities in this field according to international clinical guidelines [18].

Despite the lack of both long-term follow-up data and evidence from prospective randomized trials, in most of the published retrospective series and current ongoing trials, HIFU therapy is considered for patients with low- to intermediate-risk disease [18, 19].

Along with oncologic risk, to carefully choose the best candidates for HIFU treatment, clinical and pathologic factors should be taken into account regarding prostate volume, the localization and dimensions of the index lesion, and anatomic and comorbid conditions that eventually hamper treatment [19, 20].

Although large prostate volume originally represented a real contraindication in the context of whole-gland HIFU treatment, this issue is no longer a limitation for focal HIFU, especially in the case of posterior or posterolateral lesions.

The localization of the tumor within the prostate should be taken into account before HIFU treatment for several reasons. It has been shown that the anterior prostate tissue, located beyond the focal point of the transducer, usually is not destroyed because most of the energy is absorbed by the posterior prostatic parenchyma [1]. Because prostate swelling and intraprostatic point shifts can occur during the treatment of the anterior area, a real-time intraoperative adjustment is recommended. The focal length of the HIFU machine also represents per se a limiting factor in reaching anterior lesions located beyond the focal point, thus potentially hampering the possibility to treat anterior lesions radically [21]. Consequently, focal therapy of an anterior lesion using HIFU cannot currently be recommended.

The treatment of the apex could also have a significant impact on urinary continence (UC), given the proximity of the external sphincter to the ablated tissue. A safety margin of 6 mm above the apex has to be considered, based on theoretical calculations and histologic findings [21, 22]. For these reasons, the apical lesions should be treated with caution to limit the risk of functional complications.

Finally, there are specific contraindications to HIFU treatment [23]. Anatomic or pathologic conditions, limiting the correct introduction of the probe through the rectum, represent an absolute contraindication to the treatment. Similarly, the procedure should not be performed in patients with a rectal fistula. The presence of major intraprostatic calcifications (>1 cm) should be seen as a relative contraindication.

In addition to the primary treatment of PCa, HIFU therapy has been applied for salvage treatment of PCa local recurrence after either EBRT or BT [24, 25]. The aim of focal HIFU is to achieve a complete ablation of the histologically proved recurrent lesion within the prostate, with minimal damage to critical surrounding structures [26, 27]. The biological changes that

occurred in prostate tissue after radiation therapy (RT) should be taken into account, given that the ability to ablate a lesion correctly with demarcated boundaries could be less efficient compared with the primary treatment setting [26]. The Ablatherm device currently incorporates parameters for treating radiorecurrent PCa, allowing the physician to obtain better ablation results in this specific setting.

Treatment Outcomes

Primary Treatment

Oncologic Outcomes

In the last 10 years, several studies have been published assessing the role of HIFU in the primary focal treatment of PCa and have shown encouraging results (Table 24.2) [28–33]. The first published series on focal HIFU for PCa treatment in the primary setting included 29 patients treated with the Sonablate 500 device with a "subtotal" protocol of ablation involving the total peripheral zone and a half portion of the transitional zone [28]. Patients with both low- and intermediate-risk unilateral cancer were included with a median follow-up of 34 months. The mean PSA level decreased from 5.35 to 1.53 ng/mL at a mean of 36 months. Overall, 10.7 % and 23.5 % of patients showed a residual cancer foci at control biopsy at 6- and 12-month follow-up, respectively. Interestingly, no significant difference was noted in terms of disease-free survival rates between patients treated with subtotal or whole-gland HIFU [28].

In a prospective phase 1/2 trial, Ahmed et al. assessed the outcomes of HIFU hemiablation in 20 patients with low to intermediate unilateral disease, all diagnosed with a preoperative mpMRI and template perineal biopsies [29]. At the time of the enrollment, 83 % of patients had a Gleason score (GS) of 3+3 and a mean PSA of 7.3 ng/mL. At 12-month follow-up, 89 % overall were disease-free as assessed with a TRUS control biopsy and showed a decreased PSA level to a mean of 1.5 ng/mL. No patient was diagnosed with a high volume or GS of 7 or higher cancer in the treated lobe [29]. Longer follow-up data were published on a series of 12 patients with three or fewer biopsies positive for PCa in one lobe, clinical stage T2a or lower, GS score of 7 or lower 7 (3+4), and PSA of 10 ng/mL or lower [30]. All patients were treated with HIFU hemiablation using the Ablatherm device. Recurrence-free survival was 90 % at 5-year and 38 % at 10-year follow-up, with an overall cancer-specific survival of 100 % at 10-year follow-up.

In 2012, Ahmed et al. published a prospective study aimed at assessing the feasibility of focal HIFU treatment localized to all cancer lesions with a margin of normal tissue [31]. A total of 41 men aged 45–80 years were eligible for the study, having a diagnosis of low-risk to high-risk PCa with a PSA of 15 ng/mL or lower, GS of 4+3 or lower, and stage T2 or lower. The patients underwent preoperative mpMRI and template prostate mapping biopsies. Of the treated patients, 49 % received unilateral single-area ablation, 37 % received bilateral two-area ablation, and 15 % received a midline single-area ablation. At the 6-month follow-up, 77 % of the patients were disease-free at control biopsy, and 92 % were free of clinically significant cancer, according to the Epstein criteria (Gleason >3+3, >2 positive cores, >2 mm involvement). Of patients with positive biopsies, five were placed on active surveillance; four received a second HIFU session. After re-treatment, 39 of 41 (95 %) had no evidence of disease on mpMRI at 12 months.

More recently, Feijoo et al. [32] published results of a prospective single-center study conducted on a population of 67 patients submitted to HIFU hemiablation. Inclusion criteria were unilateral disease, clinical stage T1c to T2a, maximum positive biopsies less than 33 %, Gleason score of 7 or lower (3+4), PSA lower than 15 ng/mL, and life expectancy longer than 10 years. The cancer localization was done with mpMRI and subsequent TRUS biopsy with at least 20 cores. The study included patients with longer median maximum cancer core length (CCL) and total CCL compared with other series. The results showed that at 12-month follow-up, 83.6 % of patients had a negative biopsy in the treated area, and the overall negative biopsy rate was 74.6 %,

Table 24.2 Oncologic and functional outcomes of currently published series on focal high-intensity focused ultrasound for the primary treatment of prostate cancer

Study	No. of patients	Type of ablation	Mean pretreatment PSA (ng/mL)	Cancer localization	Gleason score, no. (%)	Risk classification D'Amico or NCCN, no. (%)	Median follow-up	Biopsy recurrence,[a] no. (%)	Cancer-specific survival (%)	Continence (%)	Potency (%)
Muto et al. [28]	29	Subtotal (total peripheral zone and half transition zone)	5.4	mpMRI + TRUS biopsy	≤5: 2 (6.9) 6: 14 (48.3) 7: 6 (20.7) 8–10: 5 (17.2) Unknown: 2 (6.9)	NR	72 months	3 (10.7) 4 (23.5)	100	NR	NR
El Fegoun et al. [30]	12	Hemiablation	7.3	NR	≤3+3: 10 (83) 3+4: 2 (17)	NR	10.6 years	1 (10)[a] 7(62)[a]	100	100	NR
Ahmed et al. [29]	20	Hemiablation	7.3	mpMRI and TPM biopsy	NR	Low: 5 (25) Intermediate: 15 (75)	12 months	2 (11)	100	90	95
Ahmed et al. [31]	41	Unilateral, bilateral, or midline single-area ablation	6.6	mpMRI and TPM biopsy	3+3: 13 (32) 3+4: 24 (59) 4+3: 4 (10)	Low: 11 (27) Intermediate: 26 (63) High: 4 (10)	12 months	9 (23)	100	100	89
Feijoo et al. [32]	67	Hemiablation	6.1	mpMRI and TRUS biopsy	3+3: 58 (86.6) 3+4: 9 (13.4)	NR	12 months	11 (16.4)	100	100	Mean IIEF-5 decreased from 17.9 to 15.4 at 3-months follow-up
Ahmed et al. [33]	56	Index lesion ablation	7.4	mpMRI and TPM biopsy (60.7 %) or TRUS biopsy (39.3 %)	3+3: 20 (37) 3+4: 30 (54.3) 4+3 6 (8.7)	Low: 7 (12.5) Intermediate: 47 (83.9) High: 2 (3.6)	12 months	18 (34.6) in the treated area 6 (11.5) in the untreated area	100	92.6	76.9

IIEF-5 International Index of Erectile Function-5, *mpMRI* multiparametric magnetic resonance imaging, *NCCN* National Comprehensive Cancer Network guidelines, *NR* not reported, *PSA* prostate-specific antigen, *TPM* transperineal mapping, *TRUS* transrectal ultrasound

[a]Follow-up data at 5 and 10 years after treatment, respectively

[b]Follow-up biopsies were performed at 6 and 12 months after treatment

given that six patients presented positive biopsies in the nontreated lobe along with negative biopsies in the treated lobe [32]. Finally, the first prospective study testing the index lesion hypothesis was recently published [33]. A total of 56 men with low-risk (12.5 %), intermediate-risk (83.9 %), and high-risk (3.6 %) cancers were included in the study. Cancer localization was assessed with mpMRI and transperineal template prostate mapping. The index lesion was identified according to the presence of a significant visible lesion at mpMRI with histologic confirmation of the disease. In case of negative mpMRI, the index lesion was defined according to the histologic findings of the biopsies. The Sonablate 500 device was used exclusively to treat the index lesion in all patients, eventually leaving untreated small disease GS 3+3 and CCL of 5 mm or smaller. The PSA level decreased from a median baseline of 7.4–2.4 ng/mL at the 12-month follow-up. No residual cancer in the treated area was found in 65.4 %, and no histologic evidence of clinically significant cancer was found in the treated area in 84.6 % of patients at the 6-month follow-up. Only two patients showed the presence of a clinically significant cancer in the untreated area at follow-up, which could be reasonably explained by a possible misdiagnosis that occurred at baseline evaluation, given the 5 % rate of false-negative findings associated with mpMRI [33].

Functional Outcomes

Besides oncologic outcomes, the other goal of focal HIFU for PCa is to achieve good functional outcomes in terms of both UC and erectile function (EF). Focal HIFU was primarily investigated with the aim of demonstrating an advantage in terms of posttreatment side effects, with a limited impact on UC and EF and without compromising the oncologic results. All published series reported functional outcome data as assessed with international validated instruments, showing high rates of posttreatment UC and variable rates of posttreatment EF impairment (Table 24.2) [28–33].

After HIFU hemiablation, Ahmed et al. [29] evaluated urinary incontinence rates using the University of California, Los Angeles-Expanded Prostate Cancer Index Composite urinary incontinence scale, and they did not found any significant difference between baseline and 6-month follow-up evaluations. Overall, 90 % of patients were pad- and leak-free at 6 months. They assessed urinary function using the International Prostatic Symptom Score (IPSS), showing a significantly lower score at 6-month follow-up compared with the baseline evaluation. Interestingly, no difference was noted in terms of IPSS score between patients treated with ablation crossing the midline compared with the ablation up to the midline. EF was assessed with the International Index of Erectile Function (IIEF) questionnaire. The EF domain score significantly decreased from a mean baseline of 20.9 to 14.3 at the 1-month assessment; however, data showed a recovery of EF through follow-up, reporting no difference in IIEF-EF score at the 12-month follow-up. Similar results were also observed for the orgasmic function domain. Overall, the authors reported a trifecta status of pad-free, leak-free continence, erections sufficient for intercourse, and early cancer control in 89 % of the patients treated. Similar results in terms of UC rates after treatment were also reported in a series with a longer follow-up, showing a 100 % rate of UC at a median 10-year follow-up and 81 % of patients reporting an IPSS score equal or higher to the baseline score at 1 year after treatment [30].

The idea that tissue preservation leads to functional preservation was highlighted in a study involving 39 patients treated with focal unilateral or bilateral cancer ablation [31]. The authors reported an initial decrease of IIEF score after treatment, gradually returning to baseline at 12 months, with 89 % reporting successful penetration at 12-month follow-up. Moreover, 100 % of patients were pad-free and leak-free at 9-month follow-up, and the IPSS scores were significantly lower at 12 months compared with baseline, showing an improvement in lower urinary tract symptoms.

In a more recent prospective study of 67 patients treated with HIFU hemiablation, Feijoo et al. [32] reported similar results in terms of UC, but they observed a significant deterioration of

EF with the IIEF-5 mean score decreasing from 17.9 to 15.4. Only 11 of 21 preoperatively potent patients (defined as IIEF-5 ≥22) maintained potency 3 months after treatment, even if EF assessment at longer follow-up was not reported.

Similar lower rates of posttreatment EF were reported by Ahmed [33] in a recent series of 56 patients who received HIFU ablation localized only to the index lesion: 76.9 % of patients had erections allowing a penetration at 12-month follow-up. They also reported rates of phosphodiesterase type 5 inhibitor use increasing from 12.7 % to 42.6 %. Leak- and pad-free continence was 92.6 % at 12-month follow-up.

Salvage Treatment

The role of focal HIFU was first investigated in the setting of salvage PCa treatment because of the high morbidity associated with the standard whole-gland salvage treatment (Table 24.3) [24, 25, 34].

Oncologic Outcomes

Initial encouraging data came from a registry base analysis conducted on a total of 39 patients with locally recurrent PCa after EBRT [24]. Patients were assessed preoperatively with mpMRI in combination with transperineal template prostate mapping biopsies for localization of disease recurrence. Focal salvage treatment was either hemiablation or quadrant ablation (ablation of half the lobe anterior or posterior); in the case of multifocal recurrent foci, only the ablation of the index lesion was performed if the untreated areas had one or no cores with 3 mm or smaller GS 3+3 disease and/or no lesion on mpMRI. A PSA response to treatment was observed in 87 % of the treated patients with a mean PSA nadir of 0.57 ng/mL achieved at a mean time of 4.3-month follow-up. Overall, 44 % of the patients achieved a PSA nadir lower than 0.5 ng/mL, showing biochemical-free survival rates of 86 %, 75 %, and 63 % (Phoenix criteria) and 86 %, 76 %, and 42 % (Stuttgart criteria) at 1-, 2-, and 3-year follow-up, respectively. Posttreatment biopsy, however, was performed in only 23 % of the patients, and 44 % of them showed residual disease. Two patients developed bone metastases, and 40 % required subsequent androgen deprivation therapy. Considering both histologic and biochemical findings, the overall progression-free survival rates were 69 % and 49 % at 1 and 2 years, respectively, after salvage treatment, almost comparable with the previously published outcomes of whole-gland salvage ablation.

Similar results were published by Baco et al. [25] in a series of 48 patients with radiorecurrent PCa after either EBRT (77 %) or BT (23 %); all patients had BCR (defined according to the Phoenix criteria), unilateral MRI-detected cancer verified with prostate biopsies, and no metastases. Salvage treatment was performed with the Ablatherm device and consisted of salvage hemiablation with a 4-mm security distance from the sphincter (in case of negative apical biopsies). At a median follow-up of 16.3 months, the mean PSA nadir was 0.69 ng/mL, and the biochemical-free survival rate was 67 %. Disease progression, defined according to BCR (Phoenix criteria) and/or the need for adjuvant hormonal treatment, occurred in 33 % of the patients, with 13 % of them having confirmed metastases. The overall progression-free survival rates were 83 %, 64 %, and 52 % at 12, 18, and 24 months, respectively, after treatment. Local recurrence was identified with MRI and control biopsy in eight patients, with positive findings in the untreated lobe in four of them.

Salvage HIFU was also evaluated in the context of local recurrence after RP [34]. Asimakopoulos et al. analyzed data of a series of 19 patients with palpable TRUS- and biopsy-proven local recurrence of PCa after surgery. All patients underwent single-session HIFU targeted to the recurrent cancer area. Overall, 17 of 19 patients achieved a PSA nadir lower than 0.1 ng/mL after 3 months; of them, 47 % had proven histologic findings of disease recurrence or underwent other salvage treatments for BCR at a median follow-up of 48 months. A median pre-HIFU PSA value of 2 ng/mL was significantly associated with better oncologic outcomes.

Data of focal salvage HIFU appear promising in terms of oncologic outcomes, but distant dis-

Table 24.3 Oncologic and functional outcomes of currently published series on focal high-intensity focused ultrasound for prostate cancer salvage treatment

Study	No. of patients	Primary treatment (%)	Type of ablation	Mean pretreatment PSA (ng/mL)	Cancer localization	Median follow-up	Biopsy recurrence,[a] no. (%)	Progression-free survival	Cancer-specific survival	Continence (%)	Potency
Ahmed et al. [24]	39	EBRT	Hemiablation, quadrant ablation, or index lesion ablation	4.6	mpMRI and TPM biopsy	17 months	4/9 (44)	At 1 year: 69 % At 2 years: 49 %	NR	64	Mean IIEF-5 decreased from 18 to 13 at 6 months
Baco et al. [25]	48	EBRT (77) BT (23)	Hemiablation	14.2	mpMRI and TRUS biopsy	16.3 years	8/48 (17)	At 12 months: 37 (83) At 18 months: 23 (64) At 24 months: 11(52)	NR	75	Mean IIEF-5 decreased from 11.2 to 7
Asimakopoulos et al. [34]	19	RP	Ablation of local recurrent lesion	3.8	TRUS biopsy	48 months	1/8 (12.5)	At median FU: 9 (47.4)	94.7 %	78.9	NR

BT brachytherapy, *EBRT* external beam radiation therapy, *FU* follow-up, *IIEF-5* International Index of Erectile Function-5, *mpMRI* multiparametric magnetic resonance imaging, *NR* not reported, *PSA* prostate-specific antigen, *RP* radical prostatectomy, *TPM* transperineal mapping, *TRUS* transrectal ultrasound

[a]Data at median follow-up

ease must be ruled out, and intraprostatic disease must be accurately detected and localized. The Focal Recurrent Assessment and Salvage Treatment trial (FORECAST) is an ongoing study designed to evaluate the correct clinical pathway for patients with PCa recurrence by identifying the correct diagnostic tools (mpMRI, choline positron emission tomography/computed tomography, bone scan, and MRI transperineal prostate biopsy) and evaluating the outcomes of salvage treatment with either HIFU or cryotherapy [35].

Functional Outcomes

Very few data are reported in the literature regarding the functional assessment after salvage focal HIFU (Table 24.3) [24, 25, 34]. In a series of 39 patients with PCa recurrence after EBRT, Ahmed et al. [24] showed an overall rate of patients being pad-free and leak-free of 64 % at 17-month follow-up and median IIEF-5 scores that decreased from 18 to 13 at 6 months. Finally, Baco et al. [25] reported a pad-free, leak-free rate of 75 % in a series of 48 patients after salvage HIFU hemiablation.

Complications

Focal HIFU should lead to lower morbidity rates compared with radical treatments [19]. The most frequent complications reported in the literature were urinary retention, urethral stricture, and urinary tract infections (Table 24.4) [28–33]. In a prospective study comparing whole-gland and focal HIFU, the authors demonstrated lower rates of complications after focal treatment compared with the whole-gland treatment, especially in terms of both frequency of urethral strictures and symptomatic urinary tract infections (4 % and 4 % vs 8.6 % and 11.4 %, respectively). They also described a shorter period of an indwelling urethral catheter after focal therapy (15.2 vs 19.7 days) [28]. In a series of 20 men treated with HIFU hemiablation, a suprapubic catheter was systematically placed before treatment, and all patients were able to void on postoperative day 2 with the catheter clamped [29]. A total of 30 % experienced self-resolving mild to moderate intermittent dysuria lasting a mean of 6.5 days, and intermittent transient hematuria was also reported in 65 % overall. Similar rates of transient urinary troubles were recently reported by the same group in a larger series treated only at the level of the index lesion [33]. In the same study, urinary retention requiring a bladder neck incision was reported in 3.6 % of cases, and one patient was submitted to rigid cystoscopic resection of retained necrotic prostatic tissue causing recurrent urinary tract infections. Sivaraman and Barret [20] first reported the morbidity outcomes of focal treatment with different modalities as objectively assessed with the Clavien-Dindo system. Interestingly, they reported only minor-grade complications in the group of patients treated with HIFU. Similarly, in a more recently published series, only 14 % of patients treated with HIFU hemiablation had postoperative complications, of whom 11.2 % were scored Clavien grade 2 (urinary infections and urinary retention) and 2.8 % showed a Clavien grade 3b complication (urinary retention treated with transurethral resection of the prostate [TURP]), underscoring the possible impact of baseline prostate volume on the risk of post-HIFU urinary retention [32]. Finally, due to an efficient system ensuring the safety of the rectal wall during the procedure, rectal toxicity is poorly reported among published series, with only one study reporting the case of a patient showing postoperative diarrhea and mucous discharge 2 weeks after treatment, who was submitted to a mpMRI showing the affected serosal layer of the rectum without a sign of fistula [31].

In the context of salvage treatment, the morbidity prevalence of focal HIFU is lower compared with

Table 24.4 Reported complications after focal high-intensity focused ultrasound for primary treatment of prostate cancer

Short-term complications
Urinary retention: 3.6–4 % Intermittent dysuria: 30 % Intermittent hematuria: 65 %
Mid- to long-term complications
Symptomatic urinary tract infections: 4 % Urethral strictures: 4 % Rectal fistula: 0 %

other salvage therapy modalities. Ahmed et al. reported an overall rate of Clavien 3b complications as high as 23 % after focal salvage HIFU for radiorecurrent PCa [24]. One patient developed a rectourethral fistula that was managed with a suprapubic catheterization and a colostomy, leading to a spontaneous resolution after 6 months. The authors stated that the high energy levels of the pre-HIFU RT received, together with the small volume of the gland (17 mL) and the need to treat the seminal vesicles due to the cancer extension, were all contributing factors in the development of the rectal fistula in that specific case. Baco et al. [25] reported high-grade complications in two cases only: a delayed pubic osteitis at 6-month follow-up and a pubovesical fistula, diagnosed in a patient with diabetes several months after treatment that led to a cystoprostatectomy with urinary diversion.

Conclusion

Focal HIFU can be considered a feasible treatment in selected PCa patients according to currently published data. In the primary treatment setting, the oncologic outcomes of focal HIFU appear promising, even if strong evidence at long-term follow-up are currently lacking. Patients with low- to intermediate-risk disease can be safely treated with the selective ablation of the cancerous areas, ensuring both good functional outcomes and low morbidity rates. Focal salvage HIFU appears to be an effective treatment for recurrence after either EBRT or BT, ensuring comparable oncologic outcomes with other treatment modalities despite lower morbidity rates.

Above all, an à la carte approach, taking into account precise disease localization before treatment, is recommended for better efficiency and fewer side effects of focal HIFU.

References

1. Haar GT, Coussios C. High intensity focused ultrasound: physical principles and devices. Int J Hyperth. 2007;23(2):89–104.
2. Gelet A, Chapelon JY, Margonari J, Theillere Y, Gorry F, Cathignol D, et al. Prostatic tissue destruction by high-intensity focused ultrasound: experimentation on canine prostate. J Endourol. 1993;7(3):249–53.
3. Crouzet S, Lafond C, Chapelon JY, Gelet A. Focal high-intensity focused ultrasound (hifu). In: Barret EDM, editor. Technical aspects of focal therapy in localized prostate cancer. Paris: Springer; 2014. p. 137–51.
4. Chaussy CG, Thuroff S. Robot-assisted high-intensity focused ultrasound in focal therapy of prostate cancer. J Endourol. 2010;24(5):843–7.
5. Rouviere O, Glas L, Girouin N, Mege-Lechevallier F, Gelet A, Dantony E, et al. Prostate cancer ablation with transrectal high-intensity focused ultrasound: assessment of tissue destruction with contrast-enhanced us. Radiology. 2011;259(2):583–91.
6. Schneider M. Sonovue, a new ultrasound contrast agent. Eur Radiol. 1999;9(Suppl 3):S347–8.
7. Kirkham AP, Emberton M, Hoh IM, Illing RO, Freeman AA, Allen C. MR imaging of prostate after treatment with high-intensity focused ultrasound. Radiology. 2008;246(3):833–44.
8. Rouviere O, Lyonnet D, Raudrant A, Colin-Pangaud C, Chapelon JY, Bouvier R, et al. MRI appearance of prostate following transrectal hifu ablation of localized cancer. Eur Urol. 2001;40(3):265–74.
9. Illing RO, Kennedy JE, Wu F, ter Haar GR, Protheroe AS, Friend PJ, et al. The safety and feasibility of extracorporeal high-intensity focused ultrasound (HIFU) for the treatment of liver and kidney tumours in a western population. Br J Cancer. 2005;93(8):890–5.
10. Ganzer R, Rogenhofer S, Walter B, Lunz JC, Schostak M, Wieland WF, et al. Psa nadir is a significant predictor of treatment failure after high-intensity focussed ultrasound (HIFU) treatment of localised prostate cancer. Eur Urol. 2008;53(3):547–53.
11. Roach 3rd M, Hanks G, Thames Jr H, Schellhammer P, Shipley WU, Sokol GH, et al. Defining biochemical failure following radiotherapy with or without hormonal therapy in men with clinically localized prostate cancer: recommendations of the RTOG-astro phoenix consensus conference. Int J Radiat Oncol Biol Phys. 2006;65(4):965–74.
12. Blana A, Brown SC, Chaussy C, Conti GN, Eastham JA, Ganzer R, et al. High-intensity focused ultrasound for prostate cancer: comparative definitions of biochemical failure. BJU Int. 2009;104(8):1058–62.
13. Uchida T, Illing RO, Cathcart PJ, Emberton M. To what extent does the prostate-specific antigen nadir predict subsequent treatment failure after transrectal high-intensity focused ultrasound therapy for presumed localized adenocarcinoma of the prostate? BJU Int. 2006;98(3):537–9.
14. Ganzer R, Robertson CN, Ward JF, Brown SC, Conti GN, Murat FJ, et al. Correlation of prostate-specific antigen nadir and biochemical failure after high-intensity focused ultrasound of localized prostate cancer

based on the stuttgart failure criteria – analysis from the @-registry. BJU Int. 2011;108(8 Pt 2):E196–201.
15. Muller BG, van den Bos W, Brausi M, Futterer JJ, Ghai S, Pinto PA, et al. Follow-up modalities in focal therapy for prostate cancer: results from a Delphi consensus project. World J Urol. 2015;33(10):1503–9.
16. Delongchamps NB, Haas GP. Saturation biopsies for prostate cancer: current uses and future prospects. Nat Rev Urol. 2009;6(12):645–52.
17. Biermann K, Montironi R, Lopez-Beltran A, Zhang S, Cheng L. Histopathological findings after treatment of prostate cancer using high-intensity focused ultrasound (HIFU). Prostate. 2010;70(11):1196–200.
18. Heidenreich A, Bastian PJ, Bellmunt J, Bolla M, Joniau S, van der Kwast T, et al. Eau guidelines on prostate cancer. Part II: treatment of advanced, relapsing, and castration-resistant prostate cancer. Eur Urol. 2014;65(2):467–79.
19. Valerio M, Ahmed HU, Emberton M. Focal therapy of prostate cancer using irreversible electroporation. Tech Vasc Interv Radiol. 2015;18(3):147–52.
20. Sivaraman A, Barret E. Focal therapy for prostate cancer: an "a la carte" approach. Eur Urol. 2016;69(6):973–5.
21. Boutier R, Girouin N, Cheikh AB, Belot A, Rabilloud M, Gelet A, et al. Location of residual cancer after transrectal high-intensity focused ultrasound ablation for clinically localized prostate cancer. BJU Int. 2011;108(11):1776–81.
22. Beerlage HP, van Leenders GJ, Oosterhof GO, Witjes JA, Ruijter ET, van de Kaa CA, et al. High-intensity focused ultrasound (hifu) followed after one to two weeks by radical retropubic prostatectomy: results of a prospective study. Prostate. 1999;39(1):41–6.
23. Uchida T, Nakano M, Hongo S, Shoji S, Nagata Y, Satoh T, et al. High-intensity focused ultrasound therapy for prostate cancer. Int J Urol. 2012;19(3):187–201.
24. Ahmed HU, Cathcart P, McCartan N, Kirkham A, Allen C, Freeman A, et al. Focal salvage therapy for localized prostate cancer recurrence after external beam radiotherapy: a pilot study. Cancer. 2012;118(17):4148–55.
25. Baco E, Gelet A, Crouzet S, Rud E, Rouviere O, Tonoli-Catez H, et al. Hemi salvage high-intensity focused ultrasound (HIFU) in unilateral radiorecurrent prostate cancer: a prospective two-centre study. BJU Int. 2014;114(4):532–40.
26. Kanthabalan A, Arya M, Punwani S, Freeman A, Haroon A, Bomanji J, et al. Role of focal salvage ablative therapy in localised radiorecurrent prostate cancer. World J Urol. 2013;31(6):1361–8.
27. Leibovici D, Spiess PE, Heller L, Rodriguez-Bigas M, Chang G, Pisters LL. Salvage surgery for locally recurrent prostate cancer after radiation therapy: tricks of the trade. Urol Oncol. 2008;26(1):9–16.
28. Muto S, Yoshii T, Saito K, Kamiyama Y, Ide H, Horie S. Focal therapy with high-intensity-focused ultrasound in the treatment of localized prostate cancer. Jpn J Clin Oncol. 2008;38(3):192–9.
29. Ahmed HU, Freeman A, Kirkham A, Sahu M, Scott R, Allen C, et al. Focal therapy for localized prostate cancer: a phase I/II trial. J Urol. 2011;185(4):1246–54.
30. El Fegoun AB, Barret E, Prapotnich D, Soon S, Cathelineau X, Rozet F, et al. Focal therapy with high-intensity focused ultrasound for prostate cancer in the elderly. A feasibility study with 10 years follow-up. Int Braz J Urol. 2011;37(2):213–9. discussion 220-212
31. Ahmed HU, Hindley RG, Dickinson L, Freeman A, Kirkham AP, Sahu M, et al. Focal therapy for localised unifocal and multifocal prostate cancer: a prospective development study. Lancet Oncol. 2012;13(6):622–32.
32. Feijoo ER, Sivaraman A, Barret E, Sanchez-Salas R, Galiano M, Rozet F, et al. Focal high-intensity focused ultrasound targeted hemiablation for unilateral prostate cancer: a prospective evaluation of oncologic and functional outcomes. Eur Urol. 2016;69(2):214–20.
33. Ahmed HU, Dickinson L, Charman S, Weir S, McCartan N, Hindley RG, et al. Focal ablation targeted to the index lesion in multifocal localised prostate cancer: a prospective development study. Eur Urol. 2015;68(6):927–36.
34. Asimakopoulos AD, Miano R, Virgili G, Vespasiani G, Finazzi AE. Hifu as salvage first-line treatment for palpable, trus-evidenced, biopsy-proven locally recurrent prostate cancer after radical prostatectomy: a pilot study. Urol Oncol. 2012;30(5):577–83.
35. Kanthabalan A, Shah T, Arya M, Punwani S, Bomanji J, Haroon A, et al. The forecast study – focal recurrent assessment and salvage treatment for radiorecurrent prostate cancer. Contemp Clin Trials. 2015. doi:10.1016/j.cct.2015.07.004.

Transrectal Laser Focal Therapy of Prostate Cancer

25

John F. Feller, Bernadette M. Greenwood, and R. Jason Stafford

Introduction

The lower-stage migration of screen-detected prostate cancer, evolving understanding of the natural history of disease, and increased utilization of multiparametric magnetic resonance imaging (mpMRI) and targeted biopsies are fueling continued interest in focal ablative therapies for prostate cancer. Laser focal therapy (LFT) delivers thermal energy to a targeted region of the prostate to produce coagulative necrosis and destroy a focus of cancerous cells while sparing nonmalignant prostate tissue and nearby vital structures.

Clinical trial NCT02243033 is an ongoing trial investigating the safety and efficacy and oncologic outcomes of transrectal, MR-guided LFT with near real-time MR thermometry (MRT) in an outpatient setting [1]. This study involves the use of the Visualase Thermal Therapy System (Medtronic, Minneapolis, MN, USA) coupled with the DynaLOC software and DynaTRIM hardware for instrument placement planning and transrectal access. Each of these devices and their respective components are commercially available for use as indicated in US Food and Drug Administration (FDA) 510(k) clearance; however, until 2010 they had not been used in combination; thus, investigation and establishment of a rigorous review in the setting of an institutional review board (IRB)-approved clinical trial were warranted.

Procedures are performed in a closed-loop fashion within the MRI to facilitate the MR temperature imaging feedback for monitoring therapy progress. Laser ablation targeting via transrectal approach was utilized to bring a known, highly researched, and commercialized approach to targeting of MR-visible prostate lesions, thus minimizing uncertainties in this aspect of the investigation. While a simple percutaneous transgluteal approach could be used for placement, this approach could limit access to some lesions and exclude some larger patients due to limitations on the applicator length and requires a higher level of expertise for accurate placement. Transperineal approaches are also being explored in the MR environment using MR-conditional templates and software for guidance; however, there are no commercially available solutions for guidance at this time [2].

J.F. Feller, M.D. (✉)
Desert Medical Imaging, Indian Wells, CA, USA
e-mail: drfeltoid@gmail.com; drfeller@desertmedicalimaging.com

B.M. Greenwood, B.Sc.
Clinical Services, Desert Medical Imaging, Indian Wells, CA, USA

R.J. Stafford, Ph.D.
Department of Imaging Physics, The University of Texas MD Anderson Cancer Center, Houston, TX, USA

© Springer International Publishing AG 2017
T.J. Polascik (ed.), *Imaging and Focal Therapy of Early Prostate Cancer*, Current Clinical Urology, DOI 10.1007/978-3-319-49911-6_25

History

Preclinically, McNichols et al. originally investigated the use of the Visualase Thermal Therapy System in the prostate in porcine and canine models [3, 4]. The canine prostate most closely resembles the human prostate. A transperineal approach was pioneered by Barqawi et al. at the University of Colorado [5] and further investigated at the Mayo Clinic (NCT01743638) [6], the University of Toronto (NCT00448695) [7], and the University of Chicago (NCT01792024) [8]. Early results of Raz et al., Lindner et al., Woodrum et al., and Wenger et al. [9–12] demonstrated the safety and feasibility of the transperineal approach to focally ablate prostate cancer in human subjects. McNichols et al. applied laser interstitial thermal therapy in neurologic applications, further demonstrating the precision and control achieved with the MRI-guided, real-time MR-thermal mapping technique [13, 14]. The precision and control demonstrated in the neurologic setting were postulated to be reproducible in the prostate gland.

In 2009 an MRI-guided in-bore biopsy system [15] was FDA cleared for prostate biopsy using DynaLOC computer software (Fig. 25.1) for planning and DynaTRIM MRI-compatible positioning hardware (Fig. 25.2) for device delivery. This novel system was awarded the Medical Design Excellence Award (Gold) 2010 in the radiological and electromechanical devices category [16]. It was hypothesized that the same equipment that was used for planning the trajectory of the biopsy gun could possibly be useful for laser applicator placement and laser energy delivery with a transrectal approach. In 2008, McNichols, Greenwood, and Stafford conducted preclinical experiments with phantoms at MD Anderson Cancer Center. The objective was to simulate workflow for assembly of devices and delivery of treatment in-bore using existing, commercially available instruments and equipment. The components included:

- Visualase laser fiber
- Cooling catheter
- Introducer
- Trocar
- Needle guide

In 2010, Feller et al. established the first IRB-approved clinical trial for transrectally delivered, MRI-guided laser focal therapy of prostate cancer using real-time MR thermometry in an outpatient setting (NCT 02243033) with the first patient treated in May 2010 [1]. Initially the study was intended for treatment-naïve, organ-confined, low- and intermediate-risk prostate cancer; however, a protocol amendment was

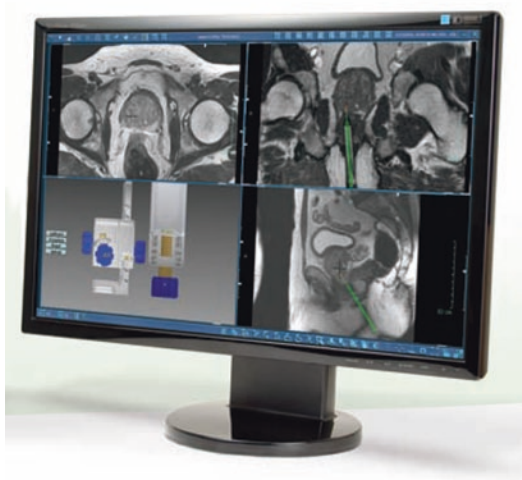

Fig. 25.1 DynaLOC module of DynaCAD software for interventional planning of trajectory for prostate biopsy or other intervention. Figure courtesy of Invivo Corporation, Orlando, FL, USA

Fig. 25.2 DynaTRIM hardware for positioning of needle guide prior to insertion of coaxial or applicator. Figure courtesy of Invivo Corporation, Orlando, FL, USA

approved by the institutional review board for salvage treatment in carefully selected research subjects [1].

Since focal therapy had become a topic of discussion and was evolving rapidly, an international consensus panel consisting of 15 expert members generated a report in 2014 [17] for the purpose of providing guidance to clinicians on focal therapy of localized disease in clinical practice and trial design from the perspective of experts in the field. Consensus was reached using the RAND/UCLA appropriateness methodology [18]. Topics addressed included patient selection, setting, outcomes measures, and retreatment. NCT02243033 pre-dated these guidelines (Table 25.1) [1].

Evidence has demonstrated that active surveillance can be used judiciously in men with low-risk Gleason score 3+3 low-volume disease [19]. Our study included Gleason score 3+3, 3+4, and 4+3 in the treatment-naïve group and carefully selected men of any Gleason score for the salvage limb [1].

Table 25.1 NCT02243033 study parameters [1]

Ages eligible for study	45 years to 90 years
Genders eligible for study	Male
Accepts healthy volunteers	No
Sampling method	Non-probability sample
Inclusion criteria (treatment naïve)	
Male, 45 years of age or older	
Diagnosis of prostate adenocarcinoma	
Clinical stage T1c or T2a	
Gleason score of 7 (3+4 or 4+3) or less	
Three or fewer TRUS biopsy cores with prostate cancer	
PSA density not exceeding 0.375 ng/ml/cc	
One, two, or three tumor-suspicious regions identified on multiparametric MRI	
Negative radiographic indication of extra-capsular extent	
A Karnofsky performance status of at least 70	
Estimated survival of 5 years or greater, as determined by treating physician	
Tolerance for anesthesia/sedation	
Ability to give informed consent	
At least 6 weeks since any previous prostate biopsy	
MR-guided biopsy confirmation of adenocarcinoma at one or more MRI-visible prostate lesion(s) with Gleason score of 7 (3+4 or 4+3) or less	
Inclusion criteria for salvage limb	
Previous prostate cancer treatment with biochemical recurrence	
MR-guided biopsy confirmation of locally recurrent adenocarcinoma at one or more MRI-visible prostate lesions	
Exclusion criteria	
Presence of any condition (e.g., metal implant, shrapnel) not compatible with MRI	
Severe lower urinary tract symptoms as measured by an International Prostate Symptom Score (IPSS) of 20 or greater	
History of other primary non-skin malignancy within previous 3 years	
Diabetes	
Smoker	

TRUS transrectal ultrasound, *PSA* prostate-specific antigen, *MRI* magnetic resonance imaging

Procedure Planning with MRI Guidance

At our institution, we rely heavily on MRI to detect, localize, biopsy, treat, and follow each focus of prostate cancer. Our multiparametric MRI (mpMRI) protocol consists of T2-weighted axial, sagittal, and coronal imaging, axial diffusion-weighted imaging (DWI), and dynamic contrast-enhanced (DCE) imaging. Apparent diffusion coefficient (ADC) maps and histograms are also generated. Scans are acquired with two 8-channel general-purpose "flex" coils (Invivo, Orlando, FL, USA), which operate as a 16-channel phased array on a Philips Achieva XR ramped to 1.5 T (Philips Healthcare, Best, the Netherlands). An important aspect of our MRI-based prostate program is the choice of equipment used for imaging and intervention. Many artifacts, such as motion, susceptibility, and metallic and dielectric signal losses, are linearly worse at higher field strengths, negatively impacting image quality. Additionally, some patients and implants contraindicated for 3 T can still be scanned safely and on label at 1.5 T. Therefore, we use a 1.5 Tesla system for continuity of care for imaging, biopsy, therapy delivery, and follow-up. For therapy it is particularly helpful to use 1.5 T as the thermal maps are gradient echo based and are less influenced

by bowel gas, motion, and other artifact-generating problems such as hip arthroplasty at 1.5 T. For our study [1], the same reader interprets each mpMRI, and the same interventional radiologist performs each in-bore MR-guided biopsy. The entire research team, which includes two radiologists, a researcher, and a registered MRI technologist, is present for all laser focal therapy treatments.

The published negative predictive value (NPV) of mpMRI for exclusion of clinically significant prostate cancer is 63–98 % [20, 21]. Using this relatively high negative predictive value, we can target the most aggressive appearing component of even a heterogeneous lesion for biopsy using the inverse linear relationship of apparent diffusion coefficient value and aggressiveness of disease [22–25]. Assigning a Prostate Imaging Reporting and Data System version 2 (PI-RADS v2) suspicion score [26] to each lesion helps to standardize lesion scoring, description, and follow-up, i.e., observation or biopsy. Figure 25.3 illustrates the workflow for performance of in-bore MRI-guided interventional planning for laser therapy delivery.

With intravenous access established, the patient lays prone on the MRI table with a dual-array 16-channel receive-only phased-array coil placed anteriorly and posteriorly over the pelvis. A transrectal needle guide is inserted in the rectum using viscous lidocaine as lubricant and anesthetic. The needle guide (Fig. 25.4) is mounted to the clamp stand (Fig. 25.5), which can be adjusted anterior-posterior, left-right, and head-foot. The needle guide functions two ways: It is both a receptacle for the biopsy gun or other instrument and also functions as a fiducial marker. When imaged in-plane, it appears as two bright, parallel white lines. Using the localization software, a cursor is placed at the tip of the needle guide on a sagittal T2-weighted image. The patient is scanned in the axial plane and that image is imported. A cursor is placed on the suspicious region, and the software calculates the delta between the needle guide starting position and the anticipated target location. The software displays coordinates to adjust the needle guide position to achieve the desired trajectory.

When performing laser therapy, the device trajectory is planned, and the device is adjusted to reach the lesion prior to device insertion; however, the z-depth of insertion is adjusted to subtract the pre-calculated throw of the biopsy gun. As of this writing, the software does not

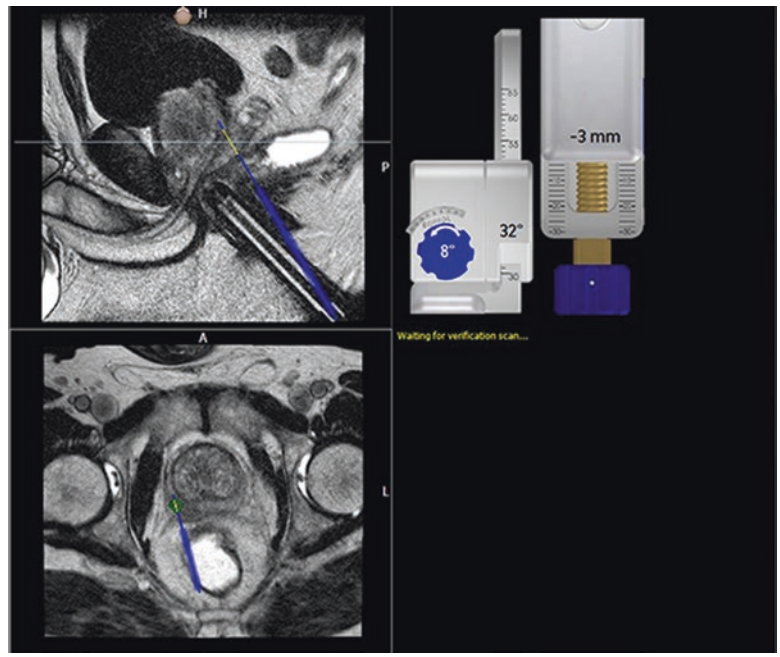

Fig. 25.3 DynaLOC user interface displaying sagittal calibration scan (*upper left*), adjustment coordinates (*upper right*), and axial planning image (*lower left*)

Fig. 25.4 Transrectal needle guide. Figure courtesy of Invivo Corporation, Orlando, FL, USA

Fig. 25.5 Clamp stand allows adjustment of the needle guide in the anterior-posterior. *Left-right* and head-foot directions to achieve planned trajectory. Figure courtesy of Invivo Corporation, Orlando, FL, USA

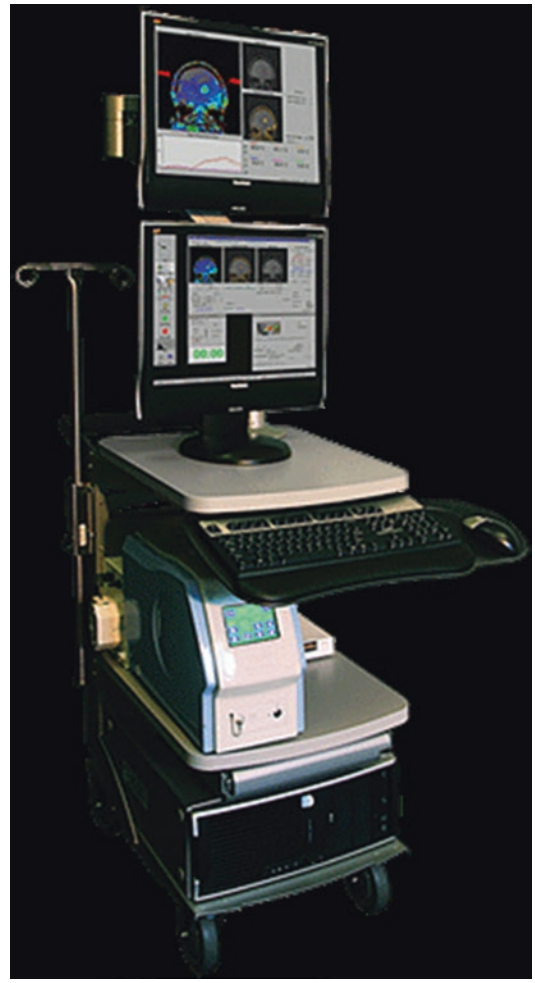

Fig. 25.6 Visualase Laser Therapy System (Medtronic, Minneapolis, MN, USA)

accommodate a throw-less introducer, so one must manually subtract the automatically generated recommend throw.

Procedure

Laser energy can be deposited into tissue at a range of power settings, leading to various rates of energy delivery. Higher powers deliver at faster rates and tend to use shorter exposure times. All procedures performed at our institution are conducted using an FDA-cleared 15 W Visualase Thermal Therapy System. This laser system is available in 15 W and 30 W models. While the system is listed by the vendor as MR conditional for use at magnetic field strengths up to 1.5 T at this time, investigators have reported findings at 3.0 T as well [11]. Per the manufacturer, "The catheter and fiber are MR compatible up to 1.5T, however the SMA connector on the proximal end of the LDF is not. Damage to imaging equipment or patients can occur if appropriate precautions are not taken" [27].

The 15 W laser system utilizes a 980 nm diode laser. The system is on a consolidated mobile cart with the laser, a computer, a dual monitor vertical display, and a water pump (Fig. 25.6). The laser

is powered by standard AC power, and the thermal mapping software is connected to the MRI scanner via an Ethernet cable.

The laser fiber is housed within a water-cooled applicator. Water cooling is helpful to facilitate use of higher laser powers being generated to create larger foci of coagulation necrosis (1.5–2.0 cm diameter) in a relatively short time (60–150 s) without charring the tissue adjacent to the applicator surface. Charring would result in increased absorption at this interface and an inability to generate a large focus of coagulation necrosis as well as potential damage to the applicator itself. To this end, a room temperature saline bag is hung from an intravenous (IV) pole on the Visualase cart, and tubing is run through a peristaltic pump that is part of the system to deliver normal saline through a cooling catheter to protect the heat-diffusing tip during heating. It is important to check to make sure there is flow and no leaks along the line prior to the start of heating. While the Visualase system uses MR temperature imaging to measure tissue temperature changes, it does not monitor absolute temperature. Therefore, it is important to pay careful attention to when the cooling pump is turned on and off. During real-time monitoring, generally the pump is turned on just prior to laser delivery, and the baseline reference image is set after the pump has started to avoid flow artifacts in the temperature maps and thermal damage images (Figs. 25.7 and 25.8).

Additionally, while cooling can assist in returning to baseline prior to the next ablation, the pump should be turned off after an ablation if a new baseline is to be acquired in the subsequent ablation site. Baseline reference images should always be as close to normal body temperature as possible with the Visualase system. This extends to urethral and rectal cooling scenarios as well, when employed.

Table 25.2 lists the tray setup for the procedure.

As part of the IRB-approved single institution clinical trial, the risks, benefits, and alternatives of MR-guided laser focal therapy of the prostate gland are explained to each patient and all questions answered. Both verbal and written informed consent are obtained. Each patient reviews and signs a California Human Subjects Bill of Rights. A formal documentation of the informed consent process is completed by research staff for every subject. Patients are informed that this procedure, regardless of complexity or time, may be associated with unforeseen problems, which may include but are not limited to the following, taken from our informed consent document:

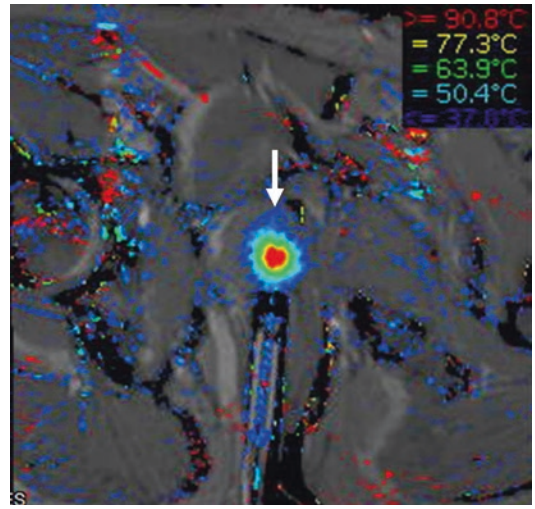

Fig. 25.7 Axial thermal map image

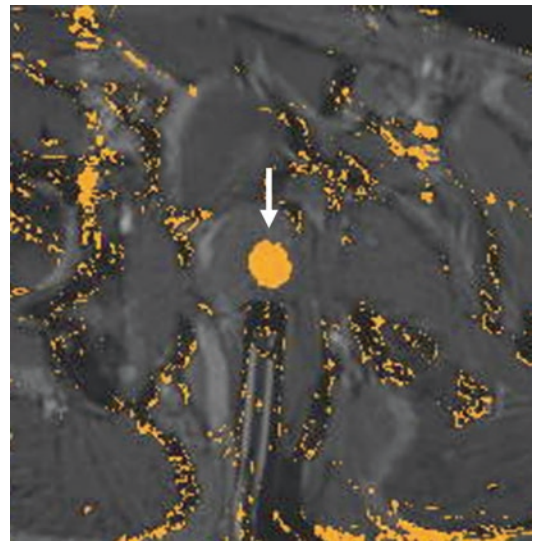

Fig. 25.8 Axial irreversible damage estimate image

Table 25.2 Tray setup for laser focal therapy

Urokit: 400 or 600
Laser fiber optic 980 nm diode
Cooling catheter
Titanium stiffener
13G introducer trocar
13G introducer catheter/sheath
Cooling fluid line set
Effluent collection bag
Steri-strips
NaCl: 1000 cc bag (cooling fluid)
TRIM needle guide
HurriCaine (benzocaine) gel or lidocaine gel
22 g titanium Bx needle set
0.5 % Marcaine—nerve block
Alcohol wipes
IV gentamicin 80 mg
IV midazolam (Versed)
IV fentanyl
IV hydromorphone hydrochloride (Dilaudid)
Oxygen/nasal cannula
IV Romazicon (flumazenil)
IV naloxone (Narcan)
IV ondansetron (Zofran)

- Pain and/or discomfort
- Excessive bleeding from the rectum/anus
- Hematuria
- Hematospermia
- Urinary retention
- Urinary tract infection or urosepsis
- Erectile dysfunction
- Urinary incontinence
- Numbness of the penis
- Residual prostate cancer
- Thermal injury to nearby organs
- Carbonization of laser applicator
- Rectal fistula

Regarding rectal fistula, a search of the US FDA MAUDE adverse event report database revealed a single report of an event dated April 17, 2015: Medtronic Navigation, Inc. (Louisville) SYSTEM 002-3100 30 W Thermal Therapy Powered Laser Surgical Instrument, Device Problems: Patient-Device incompatibility [28]. The report, submitted by the manufacturer, contains a manufacturer narrative that explains the nature of the rectourethral fistula experienced by the patient and ascribes the event to previous treatment of the patient with radiation therapy and subsequent weakening of the rectal wall. According to the report, it was hypothesized by the surgeon that this weakening prevented recovery in the way normal, healthy tissue would heal, thus causing the rectourethral fistula. The report also cites two occurrences of erectile dysfunction [28].

Conscious sedation is performed during the laser focal therapy procedure utilizing intravenously administered Versed (midazolam) and intravenously administered fentanyl. Prophylactic antibiotic therapy is also administered including 500 mg of orally administered ciprofloxacin twice a day the day before, the day of, and for 3 days following the laser focal therapy as well as intravenously administered gentamicin 80 mg given at the time of the laser focal therapy.

The patient is positioned prone in a 1.5 T Philips Achieva XR MR System (Best, the Netherlands). MR guidance for laser placement within the prostate is performed using the Invivo DynaTRIM hardware and DynaLOC software (Invivo, Orlando, FL, USA). An endorectal needle guide is placed in the rectum coated with benzocaine or lidocaine gel for topical anesthesia. Following calibration scanning, a periprostatic nerve block is performed bilaterally utilizing MR guidance and a 22-gauge MR-compatible titanium needle; 10 cc of 0.5 % Marcaine is injected into the periprostatic fat at the junction between the prostate gland and the seminal vesicle bilaterally—an anatomic feature referred to as the "Mt. Everest sign" (Fig. 25.9).

This technique of nerve block, referred to in the urologic literature as the "Mt. Everest technique," is usually performed for transrectal prostate biopsies under ultrasound guidance [29, 30]. While the "Mt. Everest technique" performed under MRI guidance has not yet been described in the literature, we have found the procedure easily performed and an important component of pain management in addition to conscious sedation during the laser focal therapy (Figs. 25.10, 25.11, 25.12, and 25.13).

The MR-visible index lesion is localized utilizing T2-weighted fast spin echo (FSE) imaging

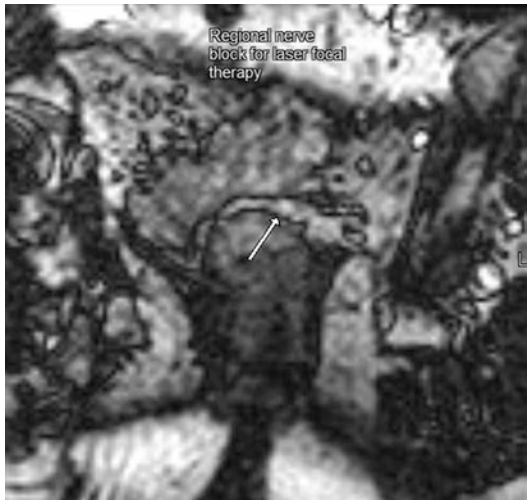

Fig. 25.9 Axial 2D bFFE image with the "Mt. Everest" peak of fat between the seminal vesicle, prostate, and rectum (*arrow*)

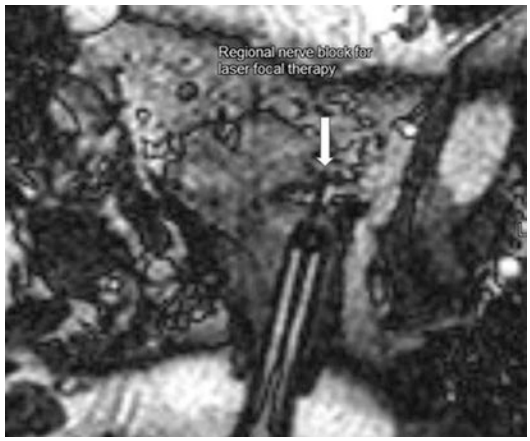

Fig. 25.10 Axial 2D bFFE image confirming the position of the 22 g needle in the apex of the "Mt Everest" peak of fat (*arrow*)

and diffusion-weighted imaging (DWI) with an apparent diffusion coefficient (ADC) map calculated. The laser fiber and cooling catheter are made of nonmetallic materials but are visible on MRI, making it superior to other energy sources for imaging while the device is in place. In particular, metal-based applicators create susceptibility artifacts, which are problematic for both MR temperature imaging as well as the echo-planar imaging sequence utilized for DWI lesion localization. While attempting to localize, these artifacts are most pronounced on DWI, often obscuring the tumor and much of the gland due to magnetic field inhomogeneity, susceptibility, and distortion. This problem is not encountered with the Visualase laser, which is imageable in vivo.

Le Nobin et al. examined the performance of mpMRI compared to whole-mount histology and noted underestimation of lesion volume with mpMRI [31]. This has led to the pursuit of a 1 cm margin around the MR-visible lesion as a goal of treatment planning.

The target is localized using the DynaLOC software designed to be used with the DynaTRIM hardware localization system. Following this, a 150 mm 13-gauge MR-conditional coaxial needle system is then inserted into the prostate gland through the endorectal needle guide into the target tumor. A confirmation scan of the needle position is obtained and adjustments made if needed. The needle trocar is then removed from the catheter sheath. A water-cooled laser applicator rated for a 15 W 980 nm laser source (Visualase Urokit 400) is introduced through the catheter sheath into the tumor using a titanium MR-conditional stiffener. For small tumors or those located in the apex near the external urethral sphincter, the smaller laser applicator with a 1 cm heat-diffusing tip (Visualase Urokit 400) is utilized. For larger tumors located elsewhere in the prostate gland, the larger laser applicator with a 1.5 cm heat-diffusing tip (Visualase Urokit 600) is utilized.

The placement of the tip of the laser applicator is verified via acquisition of a two-dimensional fast steady-state acquisition (2D bFFE) in the axial and sagittal planes. The stiffener in the cooling catheter is then replaced with the laser fiber.

The real-time biplane MR temperature imaging series (MR thermometry) is prescribed from the steady-state series and then transferred during acquisition real-time to the Visualase computer and is converted into temperature maps based upon the phase data from the fast gradient echo acquisition. The in-plane resolution of the MR thermometry is approximately 2.6 mm^2 with a 4 mm slice thickness acquired every 5–7 s. The temperature map is biplane, facilitating control and safety in the axial and sagittal planes

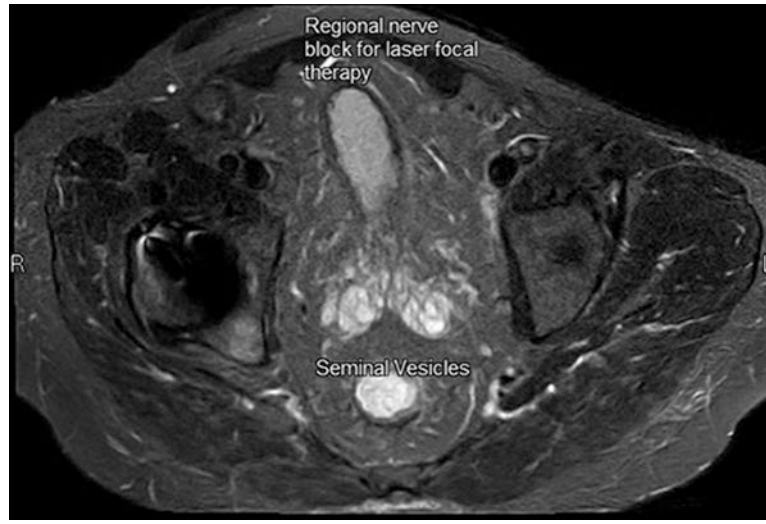

Fig. 25.11 Axial STIR image showing the normal perirectal fat and seminal vesicles before the bilateral periprostatic nerve block injections

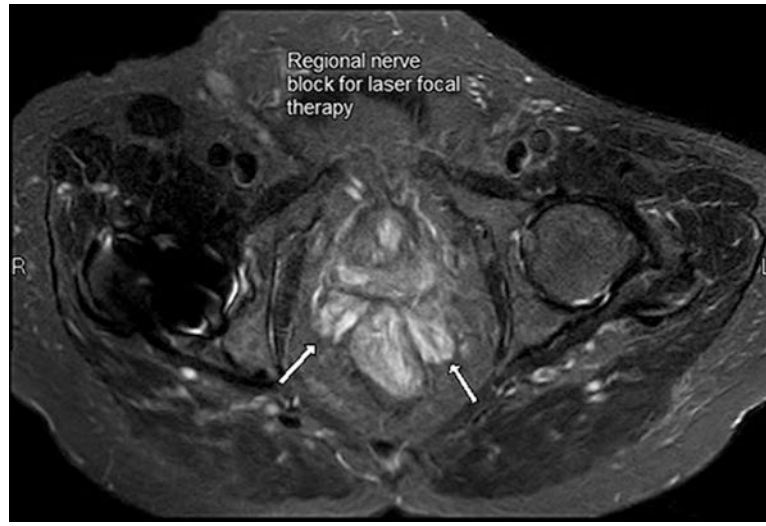

Fig. 25.12 Axial STIR image after bilateral periprostatic nerve block injections showing the bilateral infiltration of the fat in the rectoprostatic angles (*arrows*)

contemporaneously. The heat-diffusing laser applicator tip location and laser output and functionality are verified prior to therapy using a test dose of 4.5 W (30 % power on the 15 W system) monitored with MR thermometry. This is usually enough applied power to visualize the focus of heating on the Visualase system and compare to the anticipated location, but not enough power to cause thermal damage regardless of the exposure time; i.e., the temperature remains below 43 °C. With this information overlaid on the anatomical images, safety cursors can be programmed into the Visualase system. Generally, at least one high-temperature safety cursor is placed adjacent to the laser applicator and set to terminate power delivery if the estimated temperature on the MR temperature image exceeds 90 °C. Low-temperature safety cursors can be used to control the maximum temperature delivered to nearby, heat-sensitive critical structures such as the rectal wall or external urethral sphincter. Lastly, safety cursors may be used to monitor the return of the tissue temperature within the treatment volume, such as temperatures

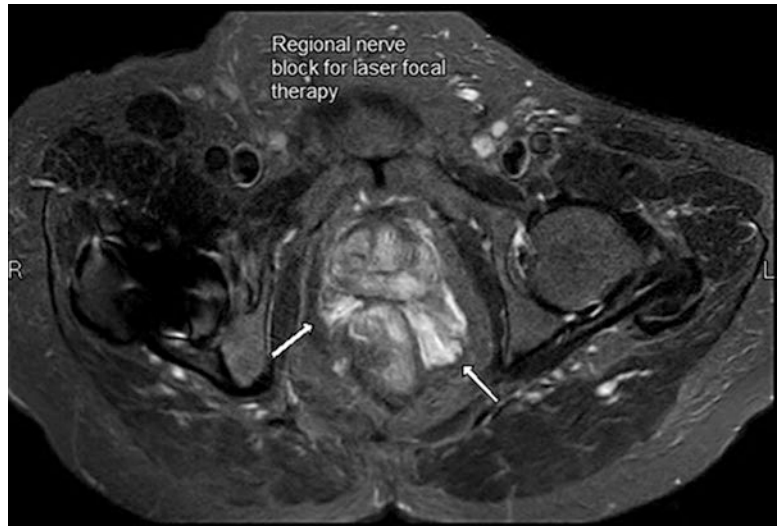

Fig. 25.13 Axial STIR image more inferiorly after bilateral periprostatic nerve block injections showing the bilateral infiltration of the fat in the rectoprostatic angles (*arrows*)

Table 25.3 Temperature limits for monitoring thermal therapy with MR thermometry

>100 °C: Vaporization of intra- and extracellular water. Rupture of cell membranes
60–100 °C: Instant denaturation of proteins and cellular components. Tissue coagulation
44–59 °C: Time-dependent thermal damage. Thermal denaturation of critical enzymes, cell death
~43 °C: Critical temperature below which thermal damage does not occur regardless of exposure time

achieved in the peri-ablational zone surrounding the visible irreversible damage estimate on the Visualase system.

Important temperature limits for monitoring thermal therapy with MR thermometry are summarized in Table 25.3 (Visualase) [32].

When the decision is made by the surgeon to deliver treatment, the patient is reminded to remain still during the therapy so temperature images do not suffer from motion-related artifacts. A 15 W laser operating at 980 nm is used to deliver therapy using 80–90 % of the maximum available power (12–13.5 W) with exposure times of 120–150 s. While 30 W lasers are available, applied power >15 W has not been found to be necessary to achieve the prescribed coagulation necrosis dimensions desired in the prostate. In our experience, the applied power range used provides a good tradeoff between the rate of coagulation necrosis formation and the ability to respond to and control the coagulation necrosis volume and location.

The laser applicator is inspected following each thermal ablation cycle whenever the applicator is removed to place in a new treatment location. Any charring or carbonization of the laser applicator should result in discontinued use because fiber damage increases rapidly with continued use. Materials become susceptible to failure with repeated treatments and heating. To prevent carbonization damage to the laser applicator, it is important to:

- Respect the heating-cooling cycle of no more than a 150-s treatment time at 80–90 % (12–13.5 W) followed by cooling below 40 °C between treatments.
- Make sure the cooling catheter water pump is functioning during treatments.
- Withdraw the laser fiber within the cooling catheter, avoiding too many treatments in one location.
- Clean the laser cooling catheter tip with alcohol wipes each time it is removed.

The 150 mm 13-gauge MR-compatible coaxial system is placed into the prostate gland

through the rectum strategically to minimize the number of rectal wall punctures required for adequate coverage of the tumor by the laser focal therapy. The laser applicator and coaxial needle system are removed from the endorectal needle guide upon confirmation of total tumor ablation with a 1 cm margin as measured by the Arrhenius damage integral (aka irreversible damage estimate) displayed by the Visualase system.

Immediately following therapy, a standard intravenous dose of gadolinium-based contrast agent is delivered, and 2D axial and sagittal T1-weighted gradient-recalled imaging is performed utilizing water excitation for fat suppression. These perfusion-weighted images are assessed providing a means for ablation zone/coagulation necrosis measurement and evaluation of evidence of periprostatic necrosis. They are also assessed for evidence of coagulation necrosis involving the rectal wall, neurovascular bundles, or external urethral sphincter.

After the endorectal needle guide is removed, the patient must demonstrate ability to void before leaving the outpatient facility. If the patient cannot void, a 14 Fr or 16 Fr coude urinary catheter is inserted and subsequently removed after his 48-h follow-up mpMRI. Rarely a suprapubic urinary catheter may be required. The patient is provided with post-procedure instructions and precautions, copies of informed consent document and California Human Subjects Bill of Rights, and a follow-up appointment schedule. The patient is instructed to return at 48 h for a diagnostic post-laser focal therapy multiparametric MRI of the prostate gland and an ultrasound of the urinary bladder pre- and post-void to exclude any significant post-void residual volume within the urinary bladder.

Mechanism of Action

As previously stated, laser energy can be deposited into tissue at various rates based on the power level used. Here we describe our technique. All procedures performed at our institution utilize a 15 W laser system incorporating a 980 nm interstitial diode laser inside a cooling catheter (Fig. 25.14).

The near real-time (5–7 s per update) MR thermometry acquired by the MRI and displayed on the Visualase utilizes the water proton resonance frequency (PRF) shift thermometry technique [33]. By looking at changes in the phase of a gradient-recalled echo sequence to estimate temperature-dependent frequency shifts, this technique provides a quantitative estimate of temperature change versus an initial reference image. The technique has been well characterized and is used in other FDA-cleared technology for thermal ablation, such as MRI-guided focused ultrasound (ExAblate 2100 l Insightec, Haifa, Israel). The temperature sensitivity coefficient (α[alpha]) for the PRF is approximately −0.01 ppm/°C in soft tissue and varies relatively little in different tissues, whether treated or untreated. A fairly rigorous technical review versus competing techniques can be found in Rieke et al. [34]. Briefly, the temperature dependence of the water resonance is due to temperature-dependent hydrogen bond lengths, which allow the protons to spend more or less time in close proximity to their parent oxygen, resulting in an approximately linear temperature-dependent change in the chemical shift (σ[sigma]). The chemical shift is usually given in parts per million with respect to the Larmor frequency (γ[gamma]B_0), where γ(gamma) is the proton gyromagnetic ratio and B_0 is the field strength. Knowing this, the phase

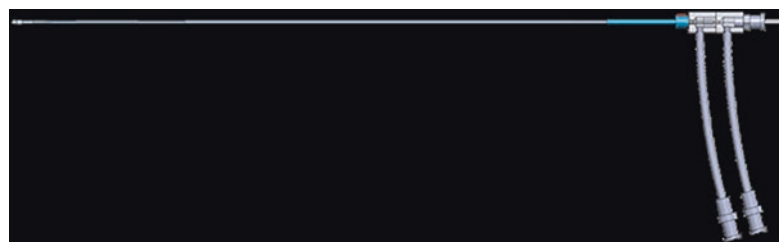

Fig. 25.14 Cooling catheter system (CCS) for protection of laser-diffusing fiber (LDF) during thermal ablation (Medtronic, Minneapolis, MN, USA)

change measured between two gradient-recalled echo images relates to the temperature change (Δ[Delta]T) as

$$\Delta(\text{Delta})\phi(phi) = -2\pi(pi)\gamma(\text{gamma})B_0 TE\,\alpha(\text{alpha})\Delta(\text{Delta})T,$$

where TE is the sequence echo time. From this relation, the temperature can be estimated.

It should be noted that since lipid tissue is covalently bonded, it has no temperature-dependent changes. Therefore, lipids should be suppressed or avoided to avoid errors unless more advanced techniques are employed. Also, all changes in the local magnetic field captured by this phase change are expected to come from temperature only during the measurement period. Changes from non-temperature-dependent sources, such as due to motion, particularly near susceptibility interfaces, or drift in the field over long periods of time, result in errors in the temperature measurement and should be considered if present in data.

Damage to tissue from rapid, high-temperature heating can be modeled as an Arrhenius rate process, whereby the damage (Ω[Omega]) is cumulative over the course of the exposure. This can be expressed as an integral over time (in seconds) as

$$\Omega = A \cdot \int_0^t e^{-E_a/RT(\tau)} d\tau,$$

where A is a frequency factor (3.1×10^{98} s^{-1}), E_a (6.25×10^5 J/mol) is the activation energy, R is the universal gas constant, and T(τ[tau]) is the absolute temperature in degree Kelvin as a function of time [35, 36]. The Visualase system uses the estimated temperature from the MR temperature images to calculate this integral discretely on a voxel-by-voxel basis to provide an estimate of damage (Ω[Omega] ≥1) [37].

During a patient treatment, an initial nontherapeutic dose is administered for acquisition of baseline images (body temperature $T_0 = 37.2$ °C). Once the laser-diffusing fiber (LDF) is localized in multiple planes and placement in the desired tissue is confirmed, the energy is increased, and cycles of energy are administered for 120–150 s at 80–90 % energy at 15 W until coagulation necrosis is achieved. On the Visualase platform, the colorized thermal map, temperature graph, and calculated irreversible damage estimate (orange color overlay on the anatomic image) are depicted on the user interface during treatment (Fig. 25.15).

Low-temperature control points are placed adjacent to sensitive structures such as the rectal wall, external urethral sphincter, and neurovascular bundles in order to avoid undesired tissue damage. Should the temperature exceed a preset threshold, the laser aborts automatically to protect the designated regions. Careful consideration must be given to the factors influencing energy delivery and lesion size including:

- Core fiber size (Urokit 400 vs. Urokit 600)—for small lesion or those near sensitive structures, a smaller fiber with more cycles of ablation may be preferred over the larger fiber to minimize risk of undesired damage.
- Duration and amplitude of energy—by increasing or decreasing laser energy power or exposure time.
- Cooling rate—thermal damage can be controlled by adjusting the flow rate of saline in the cooling catheter. If urethral or rectal cooling is used, this can also reduce the rate and extent of therapeutic thermal damage.
- Location of rectal wall punctures and therapy trajectory—strategic planning of tumor ablation will minimize number of rectal wall punctures and ensure contiguous volume ablation/coagulation necrosis to the desired 1 cm margin around the MRI-visible lesion.

During planning it is imperative to note the location of the rectal wall, external urethral sphincter, and neurovascular bundles and to assess their relationship and proximity to the target lesion in multiple planes. It may be desirable to plan multiple, low-energy, long-duration treatments in tissue close to sensitive structures to avoid unintended irreversible damage to those tissues. Another strategy is to increase the saline flow rate through the cooling catheter.

To reiterate, our institution uses a 15 W rather than 30 W laser system for the following reasons:

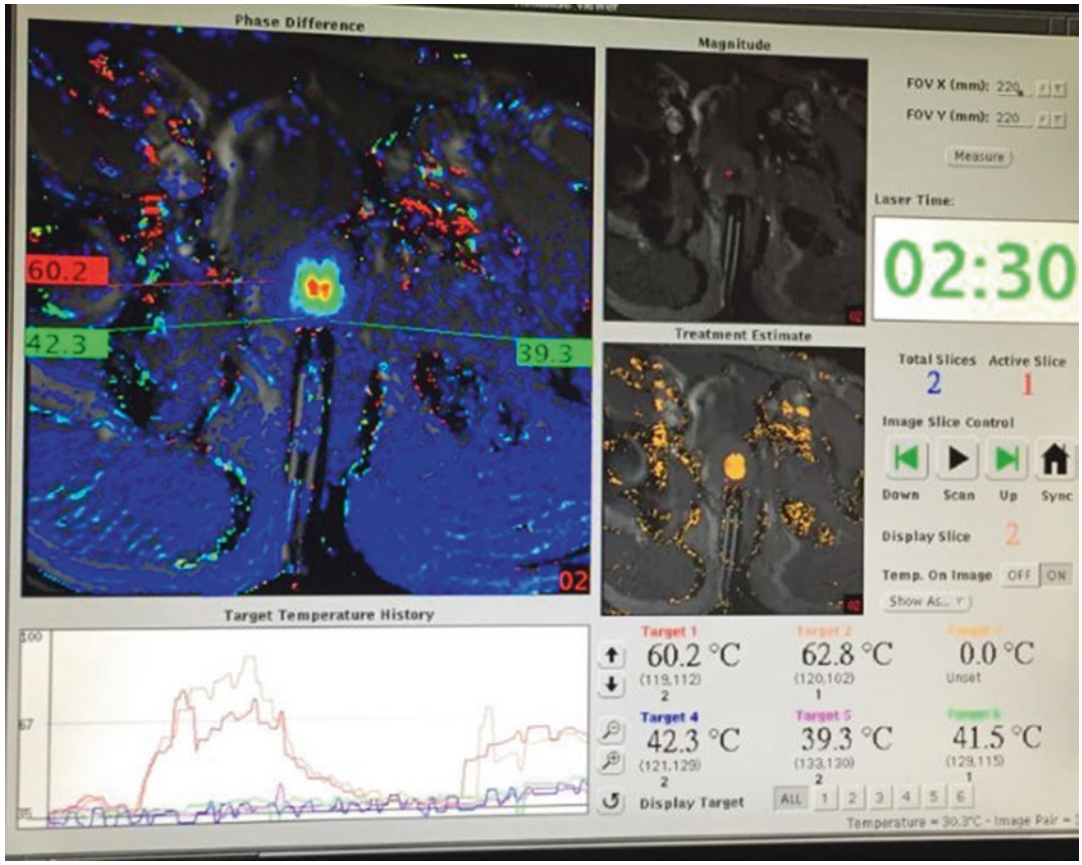

Fig. 25.15 Visualase user interface for planning and monitoring thermal dose

- The tumors requiring ablation can be in close proximity to anatomic structures that warrant careful monitoring and repeated cooling for an acceptable safety profile.
- Power greater than 12–13.5 W for greater than 150 s increases the risk of carbonization of the laser applicator.
- Power of 12–13.5 W for up to 150 s combined with multiple treatment sites can create adequate volumes of coagulation necrosis in a reasonable procedure time.
- Manufacturer maximum thresholds in indications for use are achievable with either system.

Case Study

Prior to each therapy, a tumor board is convened to review each case. This discussion includes review of the subject's clinical history, inclusion/exclusion criteria, and prior multiparametric MRI. Magnetic resonance-guided biopsy pathology is reviewed and correlated to imaging findings.

Presented as a case example is a 70-year-old patient with a serum PSA = 5.4 ng/mL and no history of a TRUS biopsy who underwent mpMRI of the prostate gland. Axial T2-weighted (T2 W) fast spin echo image (Fig. 25.16), apparent diffusion coefficient (ADC) map image (Fig. 25.17), high *b*-value (b = 1400) diffusion-weighted imaging (DWI) (Fig. 25.18), and dynamic contrast-enhanced (DCE) image (Fig. 25.19) demonstrate the tumor-suspicious region, PI-RADS 5, in the right transition zone anteriorly to the right of midline at the mid-gland level. MR-guided in-bore biopsy of this lesion demonstrated adenocarcinoma Gleason score 3+4 confined to the prostate gland. The patient underwent transrectal MR-guided laser focal therapy in an outpatient setting. Figure 25.20 demonstrates an axial

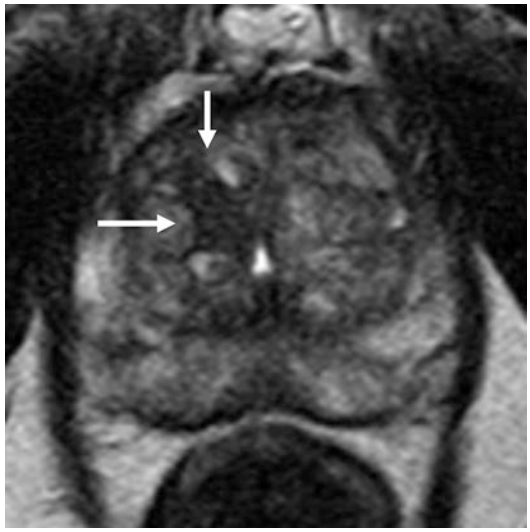

Fig. 25.16 Axial T2 FSE

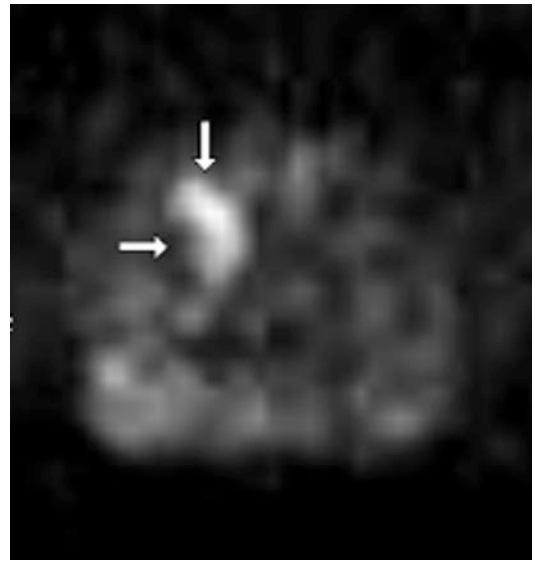

Fig. 25.18 Axial high *b*-value diffusion-weighted image (DWI)

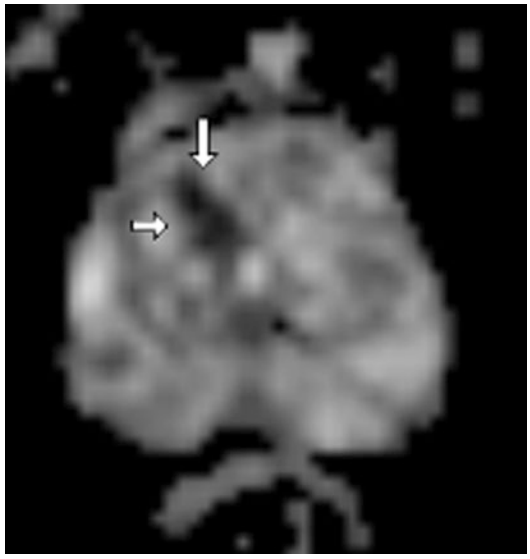

Fig. 25.17 Axial apparent diffusion coefficient (ADC) map image

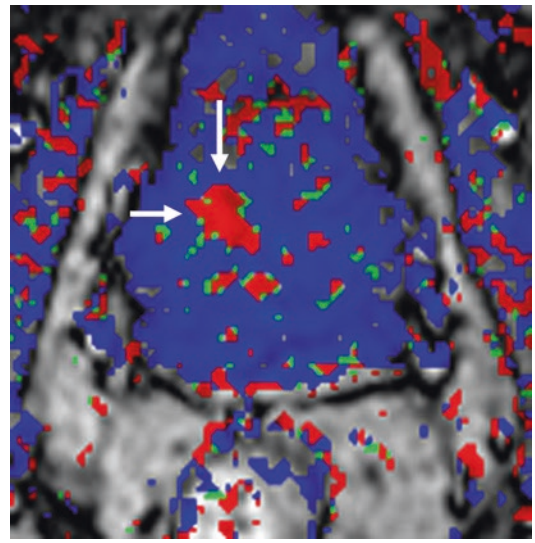

Fig. 25.19 Axial dynamic contrast-enhanced (DCE) image

gradient-recalled echo (GRE) image of the laser applicator in place. Figure 25.21 is a sagittal gradient-recalled echo (GRE) image of the applicator tip in position. The thermal map image (Fig. 25.22) demonstrates heating of the intended target area and temperature map. Anatomic imaging is used to guide placement of the laser applicator, and the user can monitor therapy delivery from irreversible damage estimate images (Fig. 25.23). The tumor was treated successfully with no com-

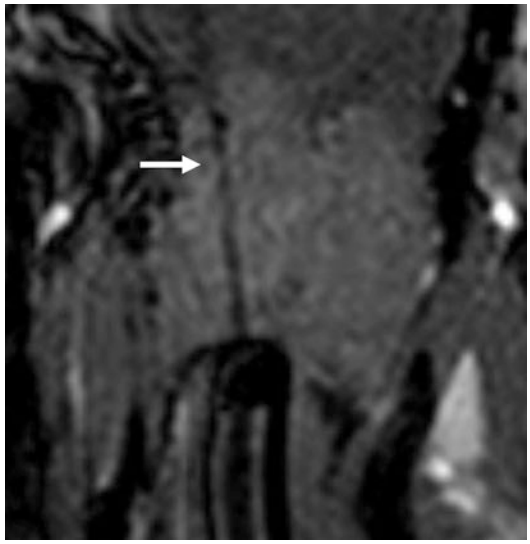

Fig. 25.20 Axial gradient-recalled echo (GRE) image of laser in place

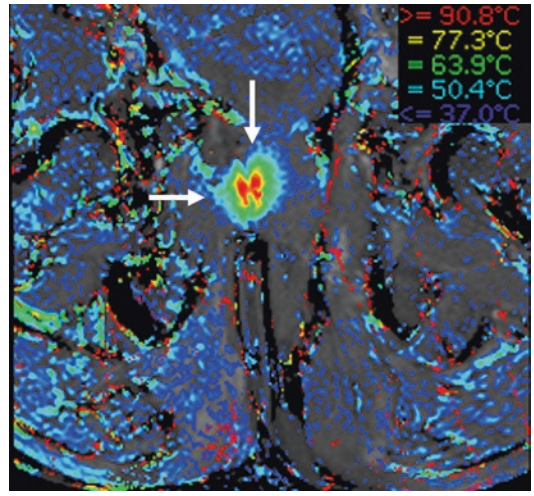

Fig. 25.22 Thermal map axial image

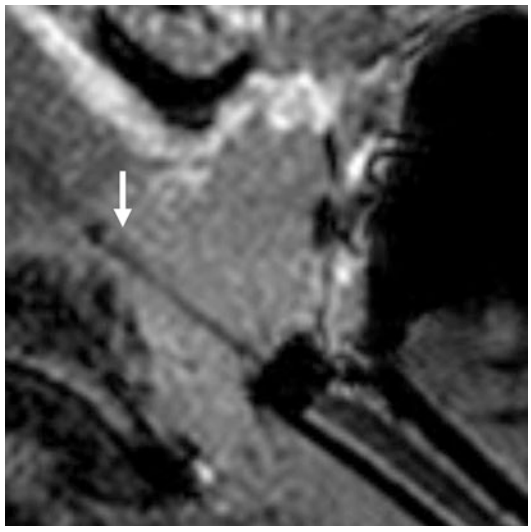

Fig. 25.21 Sagittal gradient-recalled echo (GRE) image of laser in place

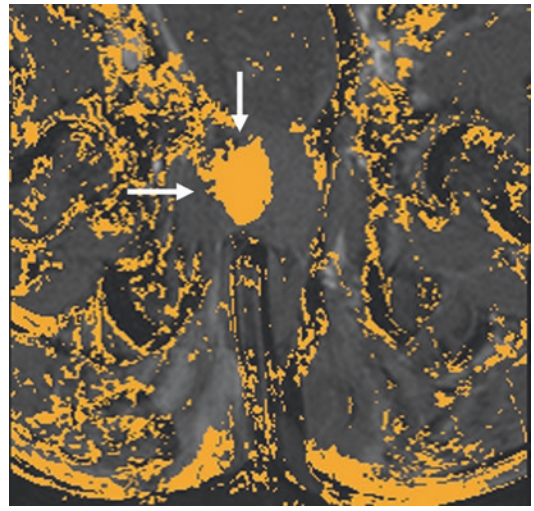

Fig. 25.23 Irreversible damage estimate axial image

plication as evidenced by 48-h posttreatment contrast-enhanced images (Fig. 25.24) and perfusion map (Fig. 25.25) images documenting nonenhancing coagulation necrosis completely replacing the mpMRI abnormalities associated with the focus of prostate cancer.

Preliminary Results

The technique for performing transrectally delivered, MRI-guided laser focal therapy has evolved into an outpatient procedure that can be safely

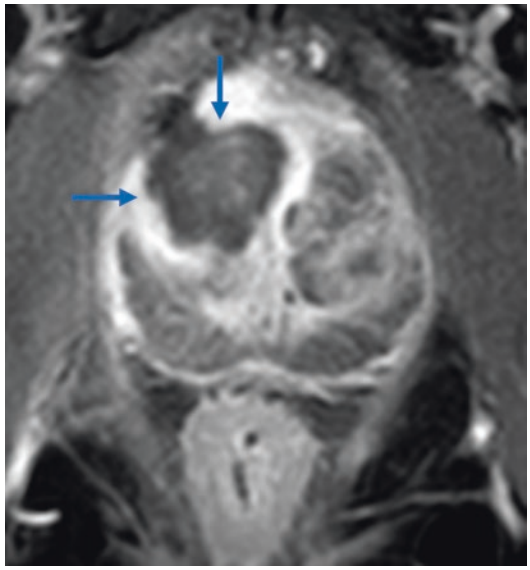

Fig. 25.24 Axial DCE image 48 h posttreatment

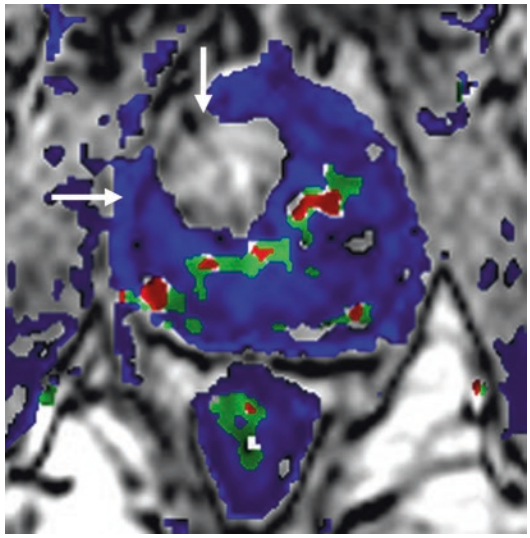

Fig. 25.25 Axial perfusion map 48 h posttreatment

performed in 1.5–4 h depending upon the size, shape, and geometry of the tumor(s). As of this writing, 87 prostate cancer foci have been treated with transrectal MRI-guided laser focal therapy in 62 men in our current IRB-approved Phase I clinical trial [1]. Outcome measures for the ongoing Phase I clinical trial are listed below:

Primary Outcome Measures:

- Safety. Time Frame: 1 year posttreatment reported as number of subjects reporting serious adverse events

Secondary Outcome Measures:

- Efficacy of treatment. Time Frame: 1 year posttreatment reported as MR-guided biopsy results of treated area and PSA

Other Outcome Measures:

- Damage estimate volume measurement. Time Frame: 24–96 h reported as measurement (in cc) of Visualase estimates of thermal damage compared to acute post contrast MR images
- Approach efficacy. Time Frame: 24–96 h reported as number of patients reporting inability to tolerate the procedure
- Quality of life. Time Frame: 1 year posttreatment reported as patient responses to International Prostate Symptom Score (IPSS), Sexual Health Inventory for Men (SHIM), and Patient Health Questionnaire (PHQ)-9 surveys

In the current Phase I clinical trial, no statistically significant change in IPSS or SHIM scores has been documented [1]. Mean PSA levels in our treatment-naïve cohort decreased 35 %, while the salvage population mean PSA decreased 47 %. Although no patient experienced a serious adverse event, one treatment resulted in carbonization of the laser applicator associated with a retained cooling catheter tip, which the patient spontaneously expelled while voiding without sequelae. During the 6 years since the clinical trial began, no patient has developed metastatic prostate cancer and no mortality from prostate cancer has occurred. Fifteen patients have successfully undergone repeat laser focal therapy for marginal recurrence of prostate cancer, and five patients have successfully undergone subsequent whole-gland therapy for incidence prostate cancer.

Discussion

In our Phase I clinical trial experience as of this writing, transrectally delivered, MRI-guided laser focal therapy of prostate cancer is safe and feasible for both treatment-naïve and salvage patients in an outpatient setting on a 1.5 Tesla MRI system [1]. This study has also documented that patients who have undergone transrectal MRI-guided laser focal therapy remain re-treatment viable, with either additional laser focal therapy or whole-gland therapy.

Conspicuously *absent* from the transrectal, outpatient approach to the MRI-guided laser focal therapy procedure are the following: (1) general anesthesia, (2) hospitalization, (3) anesthesiologist, (4) 3 Tesla MRI system, (5) endorectal MRI coil, and (6) MR spectroscopy. The addition of the newly modified "Mt. Everest" technique utilizing MRI guidance for the periprostatic nerve block, in particular, has favorably affected the anesthesia requirements and patient tolerance for this outpatient procedure.

By significantly reducing healthcare resources including staffing necessary to perform focal therapy for the treatment of prostate cancer, the cost-effectiveness and access compare favorably to other focal therapy strategies.

There are some additional advantages of laser energy over other energy sources for focal therapy of prostate cancer. First, laser therapy has the most precise temporal and spatial localizing control. Second, the transition zone between coagulation necrosis and viable tissue from laser thermal therapy measures 0.5–2.5 mm, producing a discrete, focused area of ablation. [4] Third, the biplane real-time feedback of MR thermometry and safety controls ensures the favorable safety profile of laser focal therapy. Several other energy sources are not MRI compatible, or the device cannot function with real-time MR thermometry because of susceptibility artifact or magnetic field inhomogeneity. Both the MR thermometry gradient echo sequence (GRE) and the diffusion-weighted imaging (DWI) are exquisitely sensitive to susceptibility and magnetic field inhomogeneity issues. Transrectal high-intensity focused ultrasound (HIFU) is limited to small glands (<40 cc), and many energy sources are used to perform hemiablation or "regional" ablation as opposed to true focal therapy.

Performing the procedure transrectally, using MRI guidance in-bore eliminates the misregistration errors that can be associated with procedures done using MRI-ultrasound fusion strategies outside of the MRI system "in office." The authors' experience also suggests a "continuity of imaging modality" advantage to using the same MR imaging technology to perform the diagnostic multiparametric MRI (pre- and post-laser focal therapy), the interventional MRI-guided in-bore biopsy, and the therapeutic MRI-guided laser focal therapy.

Currently, there is a paucity of peer-reviewed published outcomes for the transrectal approach to this procedure, which warrants further investigation and comparison to other approaches (e.g., transperineal) and other energy sources. In 2014 Lee et al. described their experience with successful in-bore, MR-guided laser ablation of prostate lesions [38]. They reported low morbidity and indicated that patients remained re-treatment viable post-procedure. Also in 2014, Lepor et al. demonstrated short-term oncologic control of biopsy-proven prostate cancer with minimal adverse events in a cohort of 25 men [39].

In our study the men who have undergone this treatment can be divided into two groups: treatment-naïve and salvage therapy. Treatment-naïve men can be further subdivided by Gleason score 3+3, 3+4, and 4+3. The salvage group can be divided into categories by primary treatment modality. Treatment-naïve men with low-risk, low-volume Gleason score 3+3 cancer can be followed with active surveillance. Clinically localized, larger-volume Gleason score 3+3 and Gleason score 3+4 and 4+3 cancers can be safely treated with transrectal laser focal therapy in an outpatient setting. It is our goal to study these men for the next two decades to better understand oncologic control and quality of life.

Most Phase I focal therapy studies have closed and moved to Phase II. Upon closure of our Phase I study, we will progress to a Phase II clinical trial and incorporate genomic assays in an effort study

the role of genomic pathways for risk stratification of men to active surveillance, focal treatment, or whole-gland therapy. Local control of disease following laser focal therapy will be monitored with 6-month posttreatment MR-guided in-bore biopsy.

In 2014, the International Laser Network was founded to share best practices and methodology for laser focal therapy among early adopters. The primary goal was to ensure patient safety. Other goals included harmonization of data collection intervals and patient-reported outcomes measures (PROMs). Ultimately an IRB-approved, Phase II, multicenter 20-year outcome study will be initiated to establish the efficacy of laser focal therapy. The intent is not to replace active surveillance in men with low-risk, low-volume disease. In our experience, laser focal therapy should be reserved for men with significant, clinically localized disease, except in the salvage setting. Assuming adequate cancer control can be documented, the vision of focal therapy research includes the possibility of converting low- and intermediate- risk, organ-confined, clinically significant prostate cancer into a chronic illness that is managed with an appropriate combination of active surveillance and outpatient laser focal therapy pro re nata (p.r.n.).

Conclusion

MR-guided, transrectal LFT has proven to be a precise, safe, and oncologically efficacious technique for the treatment of localized prostate cancer in Phase I trials.

Our technique compares favorably with other ablative therapies and is performed in a streamlined fashion to reduce patient discomfort and healthcare costs.

As the technology matures through clinical trials and focal therapy in the treatment of prostate cancer continues to expand, we believe this technique will become firmly established as a first-line therapy.

Acknowledgments The authors gratefully acknowledge the skill and expertise of our interventional radiologist, Stuart T. May, MD and our MRI technologist, Wes Jones, RT. We also acknowledge the early work of Roger J. McNichols, PhD, who saw the potential of light and harnessed it. Without him much of our work would have been impossible. We dedicate this chapter to him. BMG, JFF, and RJS.

References

1. Phase II Laser Focal Therapy of Prostate Cancer (LITT or FLA). NCT02243033. clinicaltrials.gov/ct2/show/NCT02243033. Accessed 14 Feb 2016.
2. Oto A, Sethi I, Karczmar G, McNichols R, Ivancevic MK, Stadler WM, et al. MR imaging-guided focal laser ablation for prostate cancer: phase I trial. Radiology. 2013;267(3):932–40.
3. Garcia-Medina O, Gorny K, McNichols R, Friese J, Misra S, Amrami K, et al. In vivo evaluation of a MR-guided 980 nm laser interstitial thermal therapy system for ablations in porcine liver. Lasers Surg Med. 2011;43(4):298–305.
4. Stafford RJ, Shetty A, Elliott AM, Klumpp SA, McNichols RJ, Gowda A, et al. Magnetic resonance guided, focal laser induced interstitial thermal therapy in a canine prostate model. J Urol. 2010;184(4):1514–20.
5. Neff T. First-ever targeted laser prostate surgery a success. UCH Insider. 2009;3(8). http://www3.uch.edu/uchinsider/laser%20prostate%20surgery.pdf
6. MR-Guided Laser Ablation of Prostate Bed Recurrences. NCT01743638. https://clinicaltrials.gov/ct2/show/NCT01743638. Accessed 15 Sept 2016.
7. MRI Targeted Focal Laser Thermal Therapy of Biopsy Confirmed Prostate Cancer. NCT00448695. https://clinicaltrials.gov/ct2/show/NCT00448695. Accessed 15 Sept 2016.
8. MR-Guided Laser Interstitial Thermal Therapy in Treating Patients with Prostate Cancer. NCT01792024. https://clinicaltrials.gov/ct2/show/NCT01792024. Accessed 15 Sept 2016.
9. Raz O, Haider MA, Davidson SR, Lindner U, Hlasny E, Weersink R, et al. Real-time magnetic resonance imaging-guided focal laser therapy in patients with low-risk prostate cancer. Eur Urol. 2010;58(1):173–7.
10. Lindner U, Lawrentschuk N, Weersink RA, Davidson SR, Raz O, Hlasny E, et al. Focal laser ablation for prostate cancer followed by radical prostatectomy: validation of focal therapy and imaging accuracy. Eur Urol. 2010;57(6):1111–4.
11. Woodrum DA, Mynderse LA, Gorny KR, Amrami KK, McNichols RJ, Callstrom MR. 3.0 T MR-guided laser ablation of a prostate cancer recurrence in the postsurgical prostate bed. J Vasc Interv Radiol. 2011;22(7):929–34.
12. Wenger H, Yousuf A, Oto A, Eggener S. Laser ablation as focal therapy for prostate cancer. Curr Opin Urol. 2014;24(3):236–40.

13. Curry DJ, Gowda A, McNichols RJ, Wilfong AA. MR-guided stereotactic laser ablation of epileptogenic foci in children. Epilepsy Behav. 2012;24(4):408–14.
14. Carpentier A, Chauvet D, Reina V, Beccaria K, Leclerq D, McNichols RJ, et al. MR-guided laser-induced thermal therapy (LITT) for recurrent glioblastomas. Lasers Surg Med. 2012;44(5):361–8.
15. Beyersdorff D, Winkel A, Hamm B, Lenk S, Loening SA, Taupitz M. MR imaging-guided prostate biopsy with a closed MR unit at 1.5 T: initial results. Radiology. 2005;234(2):576–81.
16. Schertz A. Advancements improve prostate exams. BizTimes. Aug 20, 2010.
17. Donaldson IA, Alonzi R, Barratt D, Barret E, Berge V, Bott S, et al. Focal therapy: patients, interventions, and outcomes–a report from a consensus meeting. Eur Urol. 2015;67(4):771–7.
18. Fitch K, Bernstein SJ, Aguilar MD, Burnand B, LaCalle JR, Lazaro P, et al. The RAND/UCLA appropriateness method user's manual. Santa Monica, CA: RAND Corporation; 2001 .http://www.rand.org/pubs/monograph_reports/MR1269.html
19. van der Poel H, Klotz L, Andriole G, Azzouzi AR, Bjartell A, Cussenot O, et al. Role of active surveillance and focal therapy in low- and intermediate-risk prostate cancers. World J Urol. 2015;33(7):907–16.
20. Abd-Alazeez M, Ahmed HU, Arya M, Charman SC, Anastasiadis E, Freeman A, et al. The accuracy of multiparametric MRI in men with negative biopsy and elevated PSA level–can it rule out clinically significant prostate cancer? Urol Oncol. 2014;32(1):45.e17–22.
21. Fütterer JJ, Briganti A, De Visschere P, Emberton M, Giannarini G, Kirkham A, et al. Can clinically significant prostate cancer be detected with multiparametric magnetic resonance imaging? A systematic review of the literature. Eur Urol. 2015;68(6):1045–53.
22. Shigemura K, Yamanaka N, Yamashita M. Can diffusion-weighted magnetic resonance imaging predict a high Gleason score of prostate cancer? Korean J Urol. 2013;54(4):234–8.
23. Nagarajan R, Margolis D, Raman S, Sheng K, King C, Reiter R, et al. Correlation of Gleason scores with diffusion-weighted imaging findings of prostate cancer. Adv Urol. 2012;2012:374805.
24. deSouza NM, Riches SF, Vanas NJ, Morgan VA, Ashley SA, Fisher C, et al. Diffusion-weighted magnetic resonance imaging: a potential non-invasive marker of tumour aggressiveness in localized prostate cancer. Clin Radiol. 2008;63(7):774–82.
25. Hambrock T, Somford DM, Huisman HJ, van Oort IM, Witjes JA, van de Hulsbergen Kaa CA, et al. Relationship between apparent diffusion coefficients at 3.0-T MR imaging and Gleason grade in peripheral zone prostate cancer. Radiology. 2011;259(2):453–61.
26. Weinreb JC, Barentsz JO, Choyke PL, Cornud F, Haider MA, Macura KJ, et al. PI-RADS prostate imaging – reporting and data system: 2015, Version 2. Eur Urol. 2016;69(1):16–40.
27. Medtronic Indications, Safety, and Warnings Visualase Thermal Therapy System. http://www.medtronic.com/for-healthcare-professionals/products-therapies/neurological/laser-ablation/visualase/indications-safety-warnings/index.htm. Accessed 5 Mar 2016.
28. U.S. Food and Drug Administration MAUDE Adverse Event Report Database. http://www.accessdata.fda.gov/scripts/cdrh/cfdocs/cfmaude/detail.cfm?mdrfoi__id=5101035. Accessed 8 Mar 2016.
29. Nash PA, Bruce JE, Indudhara R, Shinohara K. Transrectal ultrasound guided prostatic nerve blockade eases systematic needle biopsy of the prostate. J Urol. 1996;155(2):607–9.
30. Soloway MS, Obek C. Periprostatic local anesthesia before ultrasound guided prostate biopsy. J Urol. 2000163(1):172–3.
31. Le Nobin J, Orczyk C, Deng FM, Melamed J, Rusinek H, Taneja SS, et al. Prostate tumour volumes: evaluation of the agreement between magnetic resonance imaging and histology using novel co-registration software. BJU Int. 2014;114(6b):E105–12.
32. Whinnery JR, Ausubel J, Langford HD; National Academy of Engineering. Lasers: invention to application. Washington, DC: National Academy Press; 1987.
33. Ishihara Y, Calderon A, Watanabe H, Okamoto K, Suzuki Y, Kuroda K, et al. A precise and fast temperature mapping using water proton chemical shift. Magn Reson Med. 1995;34(6):814–23.
34. Rieke V, Butts Pauly K. MR thermometry. J Magn Reson Imaging. 2008;27(2):376–90.
35. Henriques FC. Studies of thermal injury, V. The predictability and significance of thermally induced rate processes leading to irreversible epidermal injury. Arch Pathol. 1947;43:489–502.
36. Pearce JA. Comparative analysis of mathematical models of cell death and thermal damage processes. Int J Hyperthermia. 2013;29(4):262–80.
37. McNichols RJ, Gowda A, Kangasniemi M, Bankson JA, Price RE, Hazle JD. MR thermometry-based feedback control of laser interstitial thermal therapy at 980 nm. Lasers Surg Med. 2004;34(1):48–55.
38. Lee T, Mendhiratta N, Sperling D, Lepor H. Focal laser ablation for localized prostate cancer: principles, clinical trials, and our initial experience. Rev Urol. 2014;16(2):55–66.
39. Lepor H, Llukani E, Sperling D, Fütterer JJ. Complications, recovery, and early functional outcomes and oncologic control following in-bore focal laser ablation of prostate cancer. Eur Urol. 2015;68(6):924–6.

Part VIII

New Approaches and Applications of Focal Therapy

Focal Therapy for Prostate Cancer: A Molecular Biology Approach with TRAIL

26

Vikram Narayan, Badrinath R. Konety, and Thomas S. Griffith

Introduction

Management of patients with prostate cancer remains challenging given the variability of its natural history—from indolent forms of disease that do not cause symptoms during a man's lifetime to very aggressive forms that metastasize rapidly, cause severe local symptoms and poor quality of life, and hasten death. Localized prostate cancer can be effectively treated with radical prostatectomy, external beam therapy, and brachytherapy, although a significant portion of these patients will have disease recurrence within 10 years of treatment [1, 2].

For years, prostate cancer (as well as other solid tumors) was treated in a manner that did not discriminate between normal healthy tissue and malignant cells. While radiation, surgery, and chemotherapy were able to have their intended effects on prostate cancer, these treatments also caused significant damage to normal cells in the surrounding (and sometimes distant) anatomical location. Additionally, whole-gland and systemic therapy is associated with various well-known short- and late-term morbidities that affect quality of life, including urinary complications and sexual dysfunction. The advent of more sophisticated and sensitive diagnostic and imaging techniques permitted the clinician to precisely know where the tumors were located within the prostate, allowing for targeted biopsies to identify clinically significant disease and for surgical and radiotherapy planning. The heterogeneity of prostate cancer, as well as determining the best treatment options based on the extent of the disease, mandated the development of other novel forms of treatment, including those that specifically target the malignant lesions, known as focal therapy. Among these novel therapeutics include molecular and immunotherapy options, which selectively target prostate cancer cells in vivo. The current era in oncology encouraging the use of personalized therapeutic approaches has led to an intense area of focus on immune system targets and other molecular pathways that may provide for a more tailored treatment strategy based on an individual's specific cancer biology. The information presented in this chapter will outline the implementation of gene transfer therapeutic approaches for treating prostate cancer. We will highlight our efforts in this area describing our use of a recombinant adenoviral vector encoding for a proapoptotic protein with intrinsic tumor specificity. More importantly, the ability to inject adenoviral vectors directly into organs such as the prostate to induce localized tumor cell death

V. Narayan • B.R. Konety • T.S. Griffith (✉)
Department of Urology, University of Minnesota Medical Center, Minneapolis, MN, USA
e-mail: tgriffit@umn.edu

© Springer International Publishing AG 2017
T.J. Polascik (ed.), *Imaging and Focal Therapy of Early Prostate Cancer*, Current Clinical Urology, DOI 10.1007/978-3-319-49911-6_26

through the elaboration of proteins, such as tumor necrosis factor (TNF)-related apoptosis-inducing ligand (TRAIL), allows us to consider this as a method of biologically induced focal ablation of prostate cancer.

Conventional Approaches to Focal Therapy for Prostate Cancer

Focal therapy for prostate cancer remains an emerging area of interest. Traditionally, this term encompasses treatment options that target the tumor within the prostate along with a margin of normal tissue. There is currently no consensus as to which patients are best suited for focal therapy as a primary treatment option for prostate cancer. Because most prostate cancer is multifocal [3], an ongoing challenge is whether it is adequate to selectively treat some parts of the prostate. Reliably identifying which lesion(s) or zone(s) warrants treatment is still a challenge if the whole gland is to be spared. The manner by which the target lesions are identified is also an area of debate, though imaging modalities are improving and most studies employ multiparametric magnetic resonance imaging (mpMRI) combined with transrectal ultrasound (TRUS) for localization [4]. For management of primary disease, among the options that have been evaluated for traditional focal therapy include brachytherapy, cryotherapy, high-intensity focused ultrasound (HIFU), photodynamic/photothermal therapy, laser ablation, and radiofrequency ablation (RFA). With the exception of brachytherapy (which uses ionizing radiation), these modalities predominantly work by modulating the thermal properties of the target lesion (either by freezing or heating) and eventually causing tissue necrosis. Currently, the largest and most frequently reported series in the literature involves patients receiving treatment with either HIFU (12 series) or cryotherapy (six series) [4]. There have not been head-to-head comparisons of these approaches with whole-gland therapy, either with the same ablative therapy or with radical prostatectomy and external beam radiation. Long-term data remains lacking for most ablative focal therapy approaches.

Targeting the Biology of Cancer to Fight Cancer

The increased use of genomics has played a tremendous role in understanding the biology of cancer, but it has also provided researchers with the information for developing a variety of agents that exploit the abnormal lifestyle of the tumor cell. Targeted biological molecules have already played a major role in treatment of several non-urologic cancers, such as trastuzumab for treatment of human epidermal growth factor receptor 2 (HER-2) positive breast cancer and rituximab for treatment of $CD20^+$ B-cell lymphoma, particularly when combined with conventional therapy. Within the confines of prostate cancer, several novel molecular pathways have been targets of therapy, including agents that target angiogenesis and cell cycle progression in prostate cancer [5, 6]. Targeted biological agents under investigation include PROSTVAC®-VF, which targets PSA; BEZ235, which is a PI3K/mTOR inhibitor; and the tyrosine kinase inhibitor cabozantinib (XL184), which targets c-Met [7–9].

In recent years, immunotherapy has become one of the most heavily investigated treatments for cancer. The concept that one of the many functions of the immune system is to detect and remove neoplastic cells before they can develop into a tumor dates back to the early 1900s. Recent years have seen the development of various immunological strategies as viable therapy for cancer such as Sipuleucel-T (Provenge®) for treating prostate cancer. Agents designed to block T-cell checkpoint inhibition have received the greatest publicity in recent years, largely based on their ability to restart the antitumor immune response. Though these and other immunotherapeutics all target different aspects of the canonical cellular immune response, the premise behind all of these therapies is that they leverage key traits of the adaptive immune system:

- *Specificity*: distinct tumor antigen will elicit responses that target cells that only express those antigen.
- *Diversity*: reactivity to a wide variety of tumor-specific and tumor-associated antigens.
- *Memory*: rapid and robust responses to multiple exposures to the same tumor antigens (tumor recurrence).
- *Clonal expansion*: increased number of tumor antigen-specific immune cells.
- *Self-nonreactivity*: prevention of off-target killing of normal cells.

TNF-Related Apoptosis-Inducing Ligand (TRAIL)/TRAIL Receptor System

The identification of TNF-related apoptosis-induced ligand (TRAIL) and its potential role in therapy to target cancer has been investigated in earnest since its discovery in 1995 [10], because of its ability to specifically induce apoptosis in tumor cells. Apoptotic cell death is a normal physiologic process that aids in regulation of cell reproduction and tissue growth, embryologic development, and immune regulation, among other cell hemostasis functions. Many mechanisms can result in cellular apoptosis, but some of the best characterized at the molecular level are those mediated by members of the TNF receptor (TNFR) superfamily and their cognate ligands [11, 12]. Of the death-inducing TNF superfamily ligands, induction of apoptosis by TNF, lymphotoxin (LT)-α(alpha), Fas ligand (FasL), and TRAIL has received the lion's share of attention and is thus the best characterized. In the cases of TNF, LT-α(alpha), and FasL, the induction of apoptosis is tightly regulated by limiting the expression of the ligand. TRAIL mRNA, in contrast, is constitutively expressed on a wide variety of cells and tissues [10]. TRAIL is a type II transmembrane protein that forms a homotrimer and cross-links specific receptors (discussed later) on the surface of target cells. The precise physiological role of TRAIL is not fully understood, although studies in genetically modified *Trail−/−* mice suggest that it plays a key role in the immune system. *Trail−/−* mice have impaired tumor immune surveillance and greater susceptibility to autoimmune diseases [13–16].

The TRAIL receptor system is the most diverse of the TNFR superfamily, with multiple closely related, but distinct, receptors that bind TRAIL at high affinity. The four TRAIL receptors are expressed as membrane-bound proteins and (with the exception of TRAIL-R3/DcR1) are constitutively expressed in a wide variety of human cells and tissues. TRAIL-R1/DR4 and TRAIL-R2/DR5 both contain "death domains" (DD) in the intracellular portions of the molecules, and ligation of either of these receptors induces apoptosis [17–19]. TRAIL-R3/DcR1 is expressed as a GPI-linked cell-surface protein with no known signaling properties [17, 20]. TRAIL-R4/DcR2 contains only a partial DD in the intracellular region of the molecule, and ligation of this receptor does not induce apoptosis [21–23]. Interestingly, the genes encoding these four receptors are all highly homologous (ranging from 54 to 70 % identical) and are tightly linked and map to human chromosome 8p21-23, suggesting that they arose by gene duplication in the recent evolutionary past [19–21]. Osteoprotegerin (OPG) has also been reported to bind TRAIL with reasonable affinity [24]. However, OPG is produced solely as a secreted protein—there is no cell-surface intermediate—and is found in serum of healthy normal adults at concentrations of approximately 1 ng/ml. There are limited data indicating that OPG mediates any physiologic function (either stimulatory or inhibitory) in the regulation of tumor sensitivity to TRAIL either in vitro or in vivo. In contrast, OPG and TRAIL may participate in cardiovascular disease [25].

As mentioned, TRAIL is unique compared to other death-inducing ligands of the TNF superfamily in that it has the ability to induce apoptosis specifically in transformed and tumorigenic cell lines, while leaving normal cell lines intact [10]. This has led to the investigation of TRAIL as a potential molecular therapy to target tumor cells. Injection of soluble recombinant TRAIL intravenously into mice and nonhuman primates demonstrated no detectable evidence of toxicity

[26, 27]. These (and other) preclinical data served as important stepping stones to clinical testing of recombinant TRAIL protein and agonistic mAb specific for TRAIL-R1/DR4 or TRAIL-R2/DR5 in patients with a variety of solid and hematologic tumors. Despite being well tolerated by the patients, there were few cases of clinical efficacy in the patients receiving soluble TRAIL. This lack of efficacy remains to be determined.

Regulating TRAIL-Induced Apoptosis

Many of the initial studies describing the mechanics of TRAIL-induced killing of tumor cells used established tumor cell lines, but as more work was done, it became clear that many tumor cell lines (and surprisingly most fresh tumor isolates) were not susceptible to TRAIL-mediated apoptosis [28–30]. For example, the human prostate cancer cell lines LNCaP and DU-145 are relatively resistant to TRAIL, even at higher concentrations [31, 32]. The exact mechanisms underlying cellular resistance to TRAIL have yet to be fully understood. As noted earlier, TRAIL functions by binding to four receptors, with TRAIL-R1/DR4 and TRAIL-R2/DR5 being responsible for the apoptotic cascade. Decreased expression of TRAIL-R1/DR4 and TRAIL-R2/DR5 may account for the resistance observed in certain cases [33, 34]. A second theory, and one that was initially touted as the definitive mechanism, was based on data showing that neither TRAIL-R3/DcR1 nor TRAIL-R4/DcR2 was capable of activating the apoptotic signaling pathway [17, 20–23]. Thus, it seemed possible that these receptors acted as "decoys" to functionally sequester TRAIL from the death-inducing TRAIL-R1/DR4 and TRAIL-R2/DR5. Indeed, early data were consistent with this hypothesis, including the observation that overexpression of TRAIL-R3/DcR1 in TRAIL-sensitive tumor cells conferred resistance to TRAIL [35, 36]. Additional support came from reports showing transcripts for TRAIL-R3/DcR1 were detected in many normal human tissues but not in tumor cells. In addition, treatment of cells with phospholipase C (to "strip" GPI-linked TRAIL-R3/DcR1) in the presence of cycloheximide (to prevent re-expression) resulted in the conversion of these cells from TRAIL resistant to TRAIL sensitive [36]. Similarly, overexpression of TRAIL-R4 in TRAIL-sensitive cells also inhibits TRAIL-induced apoptosis [9, 34, 37].

Development of Replication-Defective Ad5-TRAIL as a Gene Transfer Vector

Recombinant adenoviral vectors have been employed as attractive gene transfer vehicles because of their ability to be used in a variety of cell types with high levels of gene expression [38]. These adenoviral vectors can in turn be locally administered to provide concentrated amounts of biologically active proteins in vivo, thereby overcoming the previously described challenges in administering cytotoxic levels of recombinant TRAIL [39, 40]. This strategy could serve as a novel, biological method of localized solid tumor therapy, similar to other nonmolecular ablative intraprostatic treatment regimens such as cryotherapy, brachytherapy, and HIFU. The use of an adenoviral vector engineered to encode the cDNA for full-length TRAIL was first investigated in vitro with the human prostate tumor cell lines [41]. As with recombinant TRAIL protein, adenovirus type 5 (Ad5) TRAIL selectively induced apoptosis in the prostate tumor cells, while normal prostate epithelial cells were not killed. In fact, Ad5-TRAIL-infected normal prostate epithelial cells could effectively kill prostate tumor cells when mixed in culture, and the tumor cell death could be blocked with the addition of soluble TRAIL receptor:Fc. The tumor cells were noted to have undergone apoptotic death, with high levels of caspase activation and PARP cleavage. Further study investigated the efficacy of the Ad5-TRAIL) vector in vivo, by directly injecting Ad5-TRAIL into immunodeficient SCID mice bearing s.c. prostate tumors [42]. When compared with controls, Ad5-TRAIL-treated mice showed significantly reduced tumor growth. Importantly, TRAIL

expression was sustained up to 7 days after a single injection, thus overcoming the pharmacologic limitations of administering recombinant TRAIL protein alone [42]. It is important to emphasize that these initial in vivo studies could only evaluate the direct tumoricidal activity of the Ad5-TRAIL vector. Subsequent studies in syngeneic immunocompetent mouse tumor models have examined the ability of Ad5-TRAIL therapy to stimulate a systemic antitumor immune response, which not only leads to regression of distant tumors that have metastasized from the primary tumor but also affords the animal immunological memory to secondary tumor challenge [43, 44]. Efforts to improve the distribution of TRAIL within the prostate led to the use of Gelfoam® (Pharmacia and Upjohn Company, Kalamazoo, MI), a porous collagen-based matrix, as a drug delivery vehicle. Gelfoam is approved for use as a hemostatic agent when applied to bleeding surfaces. When Gelfoam was co-injected into benign dog prostates with a canarypox virus vector (ALVAC) carrying the gene for β(beta)-galactosidase (ALVAC-β [beta]-gal), expression levels were noted to be far greater than they had been when the vector had been co-injected with fluid alone (Figs. 26.1 and 26.2), which is consistent with data in mice [45]. Subsequent studies were able to replicate this delivery efficiency using Ad5-TRAIL combined with Gelfoam.

Clinical Testing of Ad5-TRAIL

As with any model that tests the efficacy of cancer therapy, the promising preclinical studies provided us the necessary data to design a study to test Ad5-TRAIL in humans. We conducted a phase I clinical trial to determine the toxicity profile, maximally tolerated dose, and the tumor treatment efficacy of Ad5-TRAIL in men with locally confined prostate cancer [33, 46]. Patients with histologically confirmed prostate cancer of clinical stages T1c, T2a, or T2b and scheduled to undergo radical prostatectomy within 10 days after study entry were enrolled. The Ad5-TRAIL vector was administered via ultrasound-guided intraprostatic injection in Gelfoam (30 mg/ml). Gelfoam served as a hemostatic agent, prevented backflow out of the prostate, and enhanced the distribution of adenovirus (Ad) vectors within the injected tissue while helping to "protect" the virus from anti-Ad neutralizing antibodies [47]. We were also surprised to see that the Gelfoam proved to be echogenic on the ultrasound imaging, permitting visualization at the time of injection.

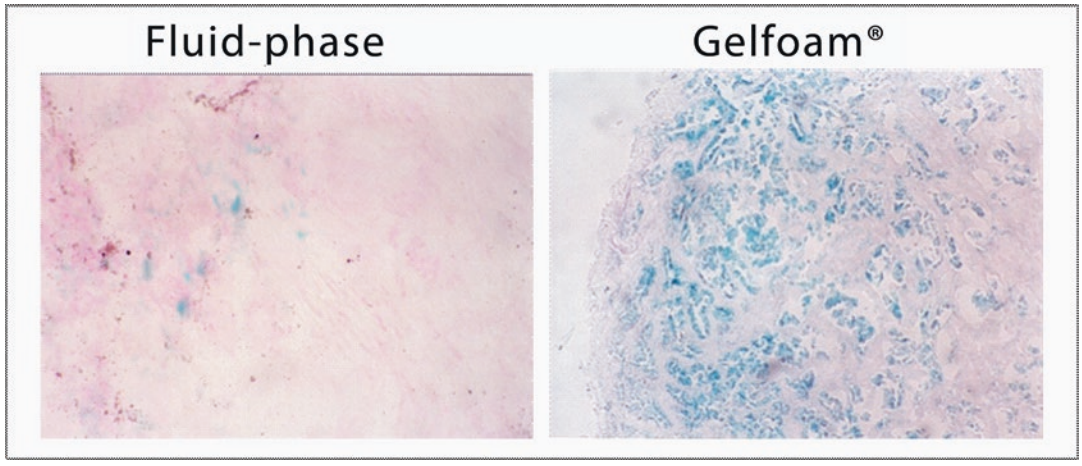

Fig. 26.1 Effect of Gelfoam® on the distribution of gene expression in benign dog prostate. ALVAC-β (beta)-gal (10^7 pfu) was injected transperineally with ultrasound guidance. Prostates were removed 24 h later, fixed, and stained for β (beta)-gal.

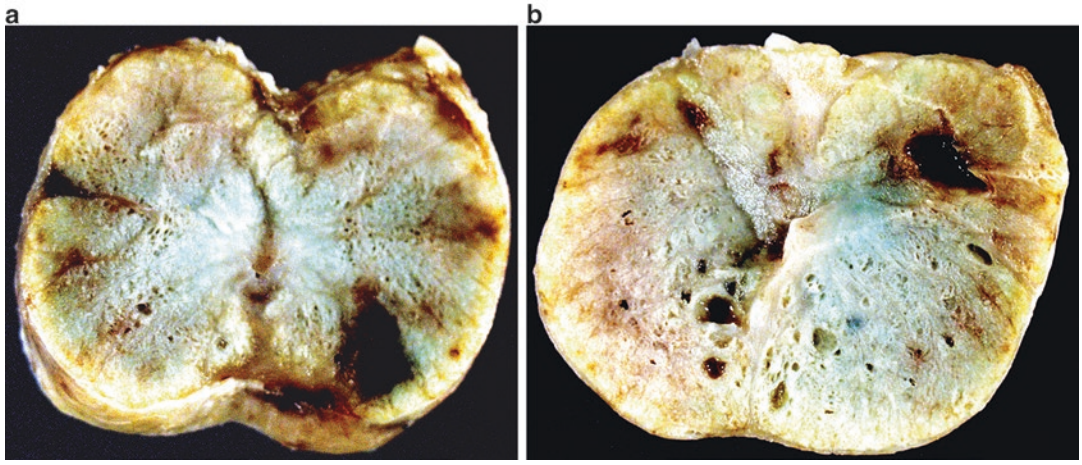

Fig. 26.2 (**a**, **b**) Gross specimen of benign dog prostate injected with Ad5-β (beta)-gal in Gelfoam®

Three levels of dose escalation were given to a total of 12 patients (four at each dose level), with equal volumes of injections into each lobe of the prostate, further divided into two injection points per lobe (four total injections per prostate). None of the patients developed adverse reactions and all tolerated the procedure well; additionally, there were no difficulties encountered at the time of surgery. Histological assessment of the injected prostate specimens following prostatectomy revealed inflammation in the areas where Gelfoam had been injected, as well as TUNEL-positive staining, indicative of DNA fragmentation resulting from apoptotic death. Every patient also had elevated levels of active caspase 3, an enzymatic marker of apoptosis.

Conclusion

The ability of TRAIL to trigger apoptosis specifically in tumor cells with minimal cytotoxicity in normal tissue makes it a potentially game-changing therapeutic. The unique ability to locally inject Ad5-TRAIL into the prostate and cause focal ablation and generate an immune reaction can potentially serve either as an adjunct to other ablative therapies or even as a standalone approach. The activation of TRAIL at higher temperatures is a feature that could be particularly exploited in this context wherein TRAIL could be injected following focal thermal ablation of prostate tissue. Additional understanding of both the downstream signaling pathway for TRAIL will be required before consistently efficacious therapies can be developed using TRAIL for the prostate, as we still remain unable to reliably predict the prostate tumor cell biology that is most susceptible to a TRAIL-based treatment regimen. Since its identification more than 20 years ago, significant advancements have already led to phase II clinical trials for a few non-urologic tumors, including for treatment of chondrosarcoma and non-small cell lung cancer [48]. Continued research is hoped to advance TRAIL into becoming a similarly exciting therapeutic option for clinically localized prostate cancer.

References

1. Coen JJ, Zietman AL, Thakral H, Shipley WU. Radical radiation for localized prostate cancer: local persistence of disease results in a late wave of metastases. J Clin Oncol. 2002;20(15):3199–205.
2. Han M, Partin AW, Pound CR, Epstein JI, Walsh PC. Long-term biochemical disease-free and cancer-specific survival following anatomic radical retropubic prostatectomy. The 15-year johns hopkins experience. Urol Clin North Am. 2001;28(3):555–65.
3. Humphrey PA. Complete histologic serial sectioning of a prostate gland with adenocarcinoma. Am J Surg Pathol. 1993;17(5):468–72.

4. Valerio M, Ahmed HU, Emberton M, Lawrentschuk N, Lazzeri M, Montironi R, et al. The role of focal therapy in the management of localised prostate cancer: a systematic review. Eur Urol. 2014;66(4): 732–51.
5. Kelly WK, Halabi S, Carducci M, George D, Mahoney JF, Stadler WM, et al. Randomized, double-blind, placebo-controlled phase III trial comparing docetaxel and prednisone with or without bevacizumab in men with metastatic castration-resistant prostate cancer: Calgb 90401. J Clin Oncol. 2012;30(13):1534–40.
6. Pili R, Haggman M, Stadler WM, Gingrich JR, Assikis VJ, Bjork A, et al. Phase II randomized, double-blind, placebo-controlled study of tasquinimod in men with minimally symptomatic metastatic castrate-resistant prostate cancer. J Clin Oncol. 2011;29(30):4022–8.
7. Bendell JC, Kurkjian C, Infante JR, Bauer TM, Burris 3rd HA, Greco FA, et al. A phase 1 study of the sachet formulation of the oral dual pi3k/mtor inhibitor bez235 given twice daily (bid) in patients with advanced solid tumors. Investig New Drugs. 2015;33(2):463–71.
8. Madan RA, Arlen PM, Mohebtash M, Hodge JW, Gulley JL. Prostvac-vf: a vector-based vaccine targeting psa in prostate cancer. Expert Opin Investig Drugs. 2009;18(7):1001–11.
9. Smith DC, Smith MR, Sweeney C, Elfiky AA, Logothetis C, Corn PG, et al. Cabozantinib in patients with advanced prostate cancer: results of a phase II randomized discontinuation trial. J Clin Oncol. 2013;31(4):412–9.
10. Wiley SR, Schooley K, Smolak PJ, Din WS, Huang CP, Nicholl JK, et al. Identification and characterization of a new member of the TNF family that induces apoptosis. Immunity. 1995;3(6):673–82.
11. Ashkenazi A, Dixit VM. Death receptors: signaling and modulation. Science. 1998;281(5381):1305–8.
12. Schulze-Osthoff K, Ferrari D, Los M, Wesselborg S, Peter ME. Apoptosis signaling by death receptors. Eur J Biochem. 1998;254(3):439–59.
13. Cretney E, McQualter JL, Kayagaki N, Yagita H, Bernard CC, Grewal IS, et al. TNF-related apoptosis-inducing ligand (trail)/apo2l suppresses experimental autoimmune encephalomyelitis in mice. Immunol Cell Biol. 2005;83(5):511–9.
14. Cretney E, Takeda K, Yagita H, Glaccum M, Peschon JJ, Smyth MJ. Increased susceptibility to tumor initiation and metastasis in TNF-related apoptosis-inducing ligand-deficient mice. J Immunol. 2002;168(3):1356–61.
15. Hilliard B, Wilmen A, Seidel C, Liu TS, Goke R, Chen Y. Roles of tnf-related apoptosis-inducing ligand in experimental autoimmune encephalomyelitis. J Immunol. 2001;166(2):1314–9.
16. Sedger LM, Glaccum MB, Schuh JC, Kanaly ST, Williamson E, Kayagaki N, et al. Characterization of the in vivo function of TNF-alpha-related apoptosis-inducing ligand, trail/apo2l, using trail/apo2l gene-deficient mice. Eur J Immunol. 2002;32(8):2246–54.
17. Pan G, Ni J, Wei YF, Yu G, Gentz R, Dixit VM. An antagonist decoy receptor and a death domain-containing receptor for trail. Science. 1997;277(5327):815–8.
18. Pan G, O'Rourke K, Chinnaiyan AM, Gentz R, Ebner R, Ni J, et al. The receptor for the cytotoxic ligand trail. Science. 1997;276(5309):111–3.
19. Walczak H, Degli-Esposti MA, Johnson RS, Smolak PJ, Waugh JY, Boiani N, et al. Trail-r2: A novel apoptosis-mediating receptor for trail. EMBO J. 1997;16(17):5386–97.
20. Degli-Esposti MA, Smolak PJ, Walczak H, Waugh J, Huang C-P, DuBose RF, et al. Cloning and characterization of trail-r3, a novel member of the emerging trail receptor family. J Exp Med. 1997;186:1165–70.
21. Degli-Esposti MA, Dougall WC, Smolak PJ, Waugh JY, Smith CA, Goodwin RG. The novel receptor trail-r4 induces nf-kappab and protects against trail-mediated apoptosis, yet retains an incomplete death domain. Immunity. 1997;7(6):813–20.
22. Marsters SA, Sheridan JP, Pitti RM, Huang A, Skubatch M, Baldwin D, et al. A novel receptor for apo2l/trail contains a truncated death domain. Curr Biol. 1997;7(12):1003–6.
23. Pan G, Ni J, Yu G, Wei YF, Dixit VM. Trundd, a new member of the trail receptor family that antagonizes trail signalling. FEBS Lett. 1998;424(1-2):41–5.
24. Emery JG, McDonnell P, Burke MB, Deen KC, Lyn S, Silverman C, et al. Osteoprotegerin is a receptor for the cytotoxic ligand trail. J Biol Chem. 1998;273(23): 14363–7.
25. Kavurma MM, Bennett MR. Expression, regulation and function of trail in atherosclerosis. Biochem Pharmacol. 2008;75(7):1441–50.
26. Ashkenazi A, Pai RC, Fong S, Leung S, Lawrence DA, Marsters SA, et al. Safety and antitumor activity of recombinant soluble apo2 ligand. J Clin Invest. 1999;104(2):155–62.
27. Walczak H, Miller RE, Ariail K, Gliniak B, Griffith TS, Kubin M, et al. Tumoricidal activity of tumor necrosis factor-related apoptosis-inducing ligand in vivo. Nat Med. 1999;5(2):157–63.
28. Kim K, Fisher MJ, Xu SQ, el-Deiry WS. Molecular determinants of response to trail in killing of normal and cancer cells. Clin Cancer Res. 2000;6(2):335–46.
29. Nesterov A, Lu X, Johnson M, Miller GJ, Ivashchenko Y, Kraft AS. Elevated akt activity protects the prostate cancer cell line lncap from trail-induced apoptosis. J Biol Chem. 2001;276(14):10767–74.
30. Nguyen T, Zhang XD, Hersey P. Relative resistance of fresh isolates of melanoma to tumor necrosis factor-related apoptosis-inducing ligand (trail)-induced apoptosis. Clin Cancer Res. 2001;7(3 Suppl):966s–73s.
31. Bonavida B, Ng CP, Jazirehi A, Schiller G, Mizutani Y. Selectivity of trail-mediated apoptosis of cancer cells and synergy with drugs: the trail to non-toxic cancer therapeutics (review). Int J Oncol. 1999;15(4):793–802.
32. Voelkel-Johnson C, King DL, Norris JS. Resistance of prostate cancer cells to soluble TNF-related apoptosis-

inducing ligand (trail/apo2l) can be overcome by doxorubicin or adenoviral delivery of full-length trail. Cancer Gene Ther. 2002;9(2):164–72.
33. Griffith TS, Stokes B, Kucaba TA, Earel Jr JK, VanOosten RL, Brincks EL, et al. Trail gene therapy: From preclinical development to clinical application. Curr Gene Ther. 2009;9(1):9–19.
34. Merino D, Lalaoui N, Morizot A, Solary E, Micheau O. Trail in cancer therapy: present and future challenges. Expert Opin Ther Targets. 2007;11(10):1299–314.
35. MacFarlane M, Ahmad M, Srinivasula SM, Fernandes-Alnemri T, Cohen GM, Alnemri ES. Identification and molecular cloning of two novel receptors for the cytotoxic ligand trail. J Biol Chem. 1997;272(41):25417–20.
36. Sheridan JP, Marsters SA, Pitti RM, Gurney A, Skubatch M, Baldwin D, et al. Control of trail-induced apoptosis by a family of signaling and decoy receptors. Science. 1997;277(5327):818–21.
37. Dai X, Zhang J, Arfuso F, Chinnathambi A, Zayed ME, Alharbi SA, et al. Targeting TNF-related apoptosis-inducing ligand (trail) receptor by natural products as a potential therapeutic approach for cancer therapy. Exp Biol Med. 2015;240:760–73.
38. Wold WS, Toth K. Adenovirus vectors for gene therapy, vaccination and cancer gene therapy. Curr Gene Ther. 2013;13(6):421–33.
39. Lee J, Hampl M, Albert P, Fine HA. Antitumor activity and prolonged expression from a trail-expressing adenoviral vector. Neoplasia. 2002;4(4):312–23.
40. Tanaka T, Manome Y, Wen P, Kufe DW, Fine HA. Viral vector-mediated transduction of a modified platelet factor 4 cdna inhibits angiogenesis and tumor growth. Nat Med. 1997;3(4):437–42.
41. Griffith TS, Anderson RD, Davidson BL, Williams RD, Ratliff TL. Adenoviral-mediated transfer of the tnf-related apoptosis-inducing ligand/apo-2 ligand gene induces tumor cell apoptosis. J Immunol. 2000;165(5):2886–94.
42. Griffith TS, Broghammer EL. Suppression of tumor growth following intralesional therapy with trail recombinant adenovirus. Mol Ther. 2001;4(3):257–66.
43. Norian LA, Kresowik TP, Rosevear HM, James BR, Rosean TR, Lightfoot AJ, et al. Eradication of metastatic renal cell carcinoma after adenovirus-encoded tnf-related apoptosis-inducing ligand (trail)/cpg immunotherapy. PLoS One. 2012;7(2):e31085.
44. VanOosten RL, Griffith TS. Activation of tumor-specific cd8$^+$ t cells after intratumoral Ad5-trail/cpg oligodeoxynucleotide combination therapy. Cancer Res. 2007;67(24):11980–90.
45. Siemens DR, Austin JC, Hedican SP, Tartaglia J, Ratliff TL. Viral vector delivery in solid-state vehicles: gene expression in a murine prostate cancer model. J Natl Cancer Inst. 2000;92(5):403–12.
46. Griffith TS, Konety BR, Joudi FN, Aubert H, Cohen MB, Ratliff TL, et al. Phase I study of Ad5-trail in men wih clinically organ confined prosate cancer. Cancer Res. 2007;67(9 Suppl):4870.
47. Siemens DR, Elzey BD, Lubaroff DM, Bohlken C, Jensen RJ, Swanson AK, et al. Cutting edge: restoration of the ability to generate CTL in mice immune to adenovirus by delivery of virus in a collagen-based matrix. J Immunol. 2001;166(2):731–5.
48. Mahalingam D, Szegezdi E, Keane M, de Jong S, Samali A. Trail receptor signalling and modulation: are we on the right trail? Cancer Treat Rev. 2009;35(3):280–8.

Focal Brachytherapy and Intensity-Modulated Radiation Therapy

27

R. Alex Hsi

Introduction

The use of radiation therapy for localized prostate cancer is well established. External beam radiation therapy, low-dose rate (LDR) brachytherapy, high-dose rate (HDR) brachytherapy, and combinations of these modalities have been shown to be effective in treating all stages of localized disease [1]. However, as with other whole-gland treatments, significant toxicities are associated with radiation therapy primarily involving urinary, rectal, and sexual function. Whole-gland external beam radiation using current doses (≥78 Gy) can result in late grade 2 and 3 urinary toxicity rates of up to 10 % and 3 %, with late grade 2 and 3 rectal toxicity rates of up to 19 % and 7 % [2, 3]. Loss of erectile function has been reported in up to 50 % of cases [3]. Whole-gland brachytherapy can result in late grade 2 and 3 urinary toxicity of 24 % and 6 % with grade 2 and 3 rectal toxicities occurring in 7 % and 1 % of patients [4, 5]. Loss of erectile function has been reported at approximately 25 % [6].

The rationale for partial-gland, or focal, radiation therapy does seem logical. It is clear that radiation therapy is effective at eradicating prostate cancer. With currently available radiation techniques, the accuracy and precision of dose delivery and the dose-shaping capabilities around irregular volumes make radiation an attractive modality to treat within the prostate gland. Brachytherapy techniques, in particular, would allow for very conformal treatments. Also, radiographic confirmation of the treated area is obvious and easily recreated if radioactive seeds or brachytherapy catheters are placed. With improved accuracy in localizing prostate cancer to a specific area within the gland, partial-gland radiation therapy should maintain a high rate of disease control while reducing urinary, rectal, and sexual toxicity compared to whole-gland therapy. The general techniques, equipment, and facilities needed to perform these radiation treatments are already in place at established radiation therapy centers and should be easy to adapt to a focal treatment approach.

The development of partial-gland radiation therapy as initial prostate cancer treatment is currently under investigation. Low-dose rate and high-dose rate brachytherapy techniques for partial-gland treatment are being evaluated throughout the world. Studies of focal external beam radiation (EBRT), most often using a technique known as intensity-modulated radiation therapy (IMRT), are more limited and have typically involved combined whole-gland therapy with partial-gland dose escalation or focal boost

R.A. Hsi (✉)
Department of Radiation Oncology, Peninsula Cancer Center, Poulsbo, WA, USA
e-mail: ralexhsi@gmail.com

© Springer International Publishing AG 2017

T.J. Polascik (ed.), *Imaging and Focal Therapy of Early Prostate Cancer*,
Current Clinical Urology, DOI 10.1007/978-3-319-49911-6_27

(also known as "focused" radiation therapy). A focused approach is also possible using brachytherapy alone.

Salvage radiation therapy for a local recurrence of prostate cancer after primary radiation therapy is also an area of significant interest. Normal tissues adjacent to the prostate such as bladder and rectum can show increased fibrosis and decreased vascularization after primary radiation therapy leading to impaired repair capacity [7, 8]. Although multiple studies of whole-gland salvage brachytherapy can result in good rates of tumor control [9], the normal tissue toxicities of such treatment can also be high [10]. A focal treatment approach presents an opportunity to decrease toxicity while still providing a second chance for tumor control.

The following review will summarize the technical considerations around partial-gland radiation as well as the existing literature describing the dosimetric and clinical outcomes for primary focal, primary focused, and focal salvage radiation therapy.

Technical Considerations

Determination of optimal technical and dosimetric parameters will be critical to the success of a partial-gland radiation therapy program. Issues that must be addressed include proper patient selection, delineation of the radiation treatment volume, brachytherapy technique (low-dose rate versus high-dose rate), isotopes, treatment planning system (preplan versus real-time method), and determination of dosimetric constraints for the target and normal tissues. Posttreatment evaluation and cancer monitoring, as with other treatment modalities, must also be addressed.

Patient Selection

As with other focal therapy treatments, proper patient selection is a prerequisite for good outcomes. Technical issues, such as prostate size ($\leq$60 cm^3), the absence of pubic arch interference, and the patient's ability to undergo anesthesia, are the same as for whole-gland brachytherapy. Ideal clinical characteristics for primary focal radiation therapy, such as life expectancy $\geq$10 years, low- to intermediate-grade disease (Gleason score 6–7), and unilateral disease, would be similar to other focal treatment modalities. For focal salvage brachytherapy, a negative metastatic workup would be a prerequisite. Even with a negative metastatic workup, the potential for microscopic metastatic disease still exists, and therefore, clinical factors such as prostate-specific antigen (PSA) level and PSA doubling time prior to salvage therapy and Gleason score should be considered. These parameters parallel the situation in choosing local prostate bed irradiation in the post-prostatectomy patient with a rising PSA [11]. Patients who have developed grade 3 or higher toxicities from initial radiation treatments would also not be ideal candidates for salvage brachytherapy, either whole gland or focal.

Determination of Radiation Treatment Volume

In 2012, a multidisciplinary international consensus group of prostate cancer experts proposed uniform definitions for partial-gland brachytherapy [12]. Treatment volume scenarios as defined by the consensus panel included (1) ultrafocal therapy, treatment of the target lesion with a margin; (2) hemi-gland therapy, treatment of half of the prostate gland containing the target lesion; and (3) focused therapy, treatment of the target lesion with a margin plus a lower dose of radiation applied to the rest of the prostate. However, it should be noted that the term "focal" is used throughout the literature when referring to any treatment involving partial-gland therapy. Accurate delineation of the target lesion was felt to be best achieved by template-guided transperineal three-dimensional (3D) mapping biopsy with 5 mm spacing of the biopsies. This method has been shown to identify bilateral disease in 39 % of cases that were found to be negative on transrectal ultrasound (TRUS)-guided biopsy [13, 14]. The addition of a pre-biopsy

multiparametric magnetic resonance imaging (mpMRI) can help to rule out extraprostatic disease and may further enhance the biopsy technique by providing additional biopsy targeting information within the prostate.

For treatment planning purposes, radiation oncologists use standardized definitions of treatment targets that take the aforementioned issues into consideration [15]. The GTV, or gross tumor volume, describes what can be seen or imaged. In the case of whole-gland therapy, the GTV is defined as the prostate itself. In the case of partial-gland therapy, the GTV can be defined as the lesion visualized on MRI and occasionally ultrasound. However, interpretation of these studies can be variable, and the sensitivity of these modalities to detect all tumors is not 100 %. Reliance on MRI and ultrasound may limit the number of patients eligible for partial-gland therapy. As a result, an alternative method using the grid locations of the positive biopsies defined during a transperineal 3D mapping biopsy procedure can be used. However, since the positions of the positive biopsies do not define the borders of the lesion, the *negative* biopsies adjacent to the positive areas could be used to delineate the border of target lesion. Using the template grid as an image registration tool, the location of the positive and adjacent negative biopsies can be reproduced on the TRUS images when performing partial-gland brachytherapy in the same manner as is done using a standard preplan brachytherapy procedure. The use of the biopsy information and the positions of the negative biopsies around the lesion makes good sense, but will obviously delineate a volume somewhat larger than the GTV, depending on the spacing between biopsies.

The CTV, or clinical target volume, describes the GTV plus a margin for subclinical or microscopic disease that cannot be imaged. In whole-gland brachytherapy, the CTV has been defined as the prostate plus a 3 mm margin [16]. In the partial-gland setting, it may make sense to define the CTV as the previously mentioned area demarcated by the negative biopsies immediately adjacent to and surrounding the positive biopsies on a transperineal 3D mapping plan, especially if 5 mm spacing is used between biopsies.

Finally, the PTV, or planning target volume, allows for uncertainties in planning and treatment delivery and is designed to ensure that the prescribed radiotherapy dose is actually delivered to the CTV. Image fusion error between the biopsy and brachytherapy plans is one such issue taken into consideration in designing the PTV. Variations in the planned and actual needle positions during brachytherapy are also taken into account in the PTV. Often the PTV expansion can result in treatment volumes that extend beyond the prostate or into normal structures such as bladder, urethra, and rectum. Adjustments to the treatment volumes as a normal course of the treatment planning process are necessary to account for these issues.

Another unique issue when using MRI information in planning both transperineal biopsy and brachytherapy is the differing patient position during MRI versus biopsy and brachytherapy. Patients lay supine for MRI scans and are in dorsal lithotomy position during biopsy and prostate brachytherapy. Fortunately, recent advancements in commercially available prostate brachytherapy planning software (MIM®, Variseed®) allow reorientation of the MRI images to match the angle of the prostate and surrounding anatomy in the dorsal lithotomy position, thus allowing accurate planning of biopsy positions and radiation source placement.

Brachytherapy Technique, Isotopes, and Treatment Planning

The two brachytherapy techniques generally available to perform partial-gland treatment are low-dose rate and high-dose rate. The LDR technique for whole-gland treatment has been employed in its current form since the late 1980s and HDR since the 1990s. LDR brachytherapy involves the permanent placement of low activity seeds through needles placed through the perineum and into the prostate. Isotopes used include iodine (I^{125}), palladium (Pd^{103}), and cesium (Cs^{131}). HDR brachytherapy utilizes a high activity radiation source, iridium (Ir^{192}), that is temporarily placed in catheters positioned in

the prostate. LDR brachytherapy has been shown to be an efficient, cost-effective procedure that can be completed in a single application usually in less than 1 h [17]. HDR brachytherapy can also be completed either in a single or multiple fractions but requires higher up-front capital costs for a remote after-loading machine with iridium source. Patients must also be transported with needles in place in the perineum from the operating room to a shielded vault in the radiation oncology department for treatment. An advantage to the HDR technique is that adjustments in dose can be made with the treatment planning software for suboptimal needle placement. In addition, there is less radiation exposure to staff as the source is delivered remotely. Ultimately, however, both techniques require experienced brachytherapists to optimize outcomes. If an institution already has an established HDR or LDR program, it would make the most sense to use the same technique to initiate a partial-gland brachytherapy program.

An LDR technique also raises several other methodological considerations including choice of isotope, loose versus stranded seeds, and which treatment planning system (preplan vs. real time) to use. Differences between the isotopes include half-lives (cesium 9.7 days, palladium 17 days, iodine 60 days) and energies (palladium 21 KeV, iodine 28 KeV, cesium 29 KeV). The use of isotopes with a shorter half-life, such as cesium, could potentially lead to lower delivered dose than intended due to post-procedure edema, which can take nearly 1 month to resolve [18]. Higher energy isotopes may be advantageous from a geographic coverage standpoint due to less acute dose fall off from each seed. However, lower energy isotopes can be useful in controlling dose if the treatment volume is in close proximity to sensitive structures such as urethra, bladder neck, or rectum. The use of stranded seeds can reduce the potential for source migration, which would be important when implanting smaller partial-gland therapy volumes, although misplacement of a single strand will lead to multiple misplaced seeds. Loose seeds offer the advantage of greater flexibility in geographic positioning of seeds, which may be of primary importance particularly in smaller volumes and proximity to organs at risk. The choice of both isotope and loose versus stranded seeds may ultimately depend on the treatment volume and location of the target lesion. With regard to treatment planning, both preplan and real-time systems can incorporate biopsy and MRI information to fuse with the intraoperative ultrasound images. Real-time systems can adjust for variations in patient positioning and allow intraoperative monitoring of dose deposition, although may take slightly more operating room time compared to a preplan approach. Again, the comfort and familiarity of the brachytherapist with the treatment planning system may be most important in this choice.

Dosimetric Outcomes

Dosimetric investigations have examined the feasibility of primary focal therapy, focused therapy, and focal salvage therapy using LDR and HDR brachytherapy techniques as well as EBRT/IMRT (in the focused scenario). Most studies compare doses to the tumor target, the whole prostate gland, and the surrounding normal tissues such as bladder, urethra, and rectum (organs at risk, or OAR). Table 27.1 is a compilation of published reports evaluating the dosimetric outcomes for all forms of partial-gland radiation therapy [19–37].

Primary Focal Therapy

Dosimetric evaluations in the primary focal therapy setting focus on comparisons of whole-gland versus partial-gland treatment. Banerjee et al. [19] compared various partial-gland HDR plans generated from five patients who had previously undergone whole-gland (WG) HDR monotherapy. Plans were generated to treat subvolumes of prostate (not actual target lesions) including hemi-gland (HG), one-third gland (1/3G), and one-sixth gland (1/6G). The planning strategy was to reach the same WG target dose objectives (D90 > 100 % or dose to 90 % of the target greater than 100 % of the prescription dose and

Table 27.1 Dosimetric outcomes of partial-gland radiation therapy

Author/year	No. pts	Approach	Modality	Tumor delineation	Dosimetric result (v. WG)
Banerjee et al. 2015 [19]	5	Primary focal WG vs. HG vs. 1/3 G vs. 1/6 G	HDR	CT	↑Tumor ↓OAR
Kamrava et al. 2013 [20]	10	Primary focal WG vs. HG	HDR	CT	↔ Tumor ↓OAR
Mason et al. 2014 [21]	9	Primary focal WG vs. HG vs. UF	HDR	MRI w/Bx	↑Tumor ↓OAR
Al-Qaisieh et al. 2015 [22]	9	Primary focal WG vs. HG vs. UF	LDR I^{125}	MRI w/Bx	↑Tumor ↓OAR
Polders et al. 2015 [23]	15	Primary focal WG vs. UF	LDR I^{125}	MRI	↔ Tumor ↓OAR
Ennis et al. 2015 [24]	13	Primary focused	LDR Pd^{103}	TTI US	↑Tumor ↔OAR
Gaudet et al. 2010 [25]	120	Primary focused	LDR I^{125}	Bx	↑Tumor ↓OAR
Todor et al. 2011 [26]	2	Primary focused	LDR I^{125}	MRI/MRS	↑Tumor ↓OAR
Mason et al. 2014 [27]	15	Primary focused	HDR	MRI	↑Tumor ↔OAR
Pouliot et al. 2004 [28]	10	Primary focused	HDR	MRI/MRS	↑Tumor ↔OAR
D'Alimonte et al. 2016 [29]	15	Primary focused	HDR	MRI	↑Tumor ↔OAR
Carlone et al. 2016 [30]	10	Primary focused	HDR	MRI	↑Tumor ↔OAR
	15	Primary focused	3D EBRT + HDR boost	MRI	↑Tumor ↔OAR
Dankulchai et al. 2014 [31]	16	Primary focused	HDR	MRI	↑Tumor ↔OAR
Housri et al. 2011 [32]	24	Primary focused	IMRT	MRI w/Bx	↑Tumor ↔OAR in 12/24
Van Lin et al. 2006 [33]	5	Primary focused	IMRT	MRI/MRS	↑Tumor ↓OAR
Ost et al. 2011 [34]	12	Primary focused	IMRT	MRI/MRS	↑Tumor ↔OAR
Peters et al. 2016 [35]	20	Focal salvage after EBRT or Brachy	LDR I^{125}	MRI w/Bx	↑Tumor ↓OAR
Guimas et al. 2016 [36]	18	Focal salvage after EBRT	LDR I^{125}	MRI or PET w/Bx	↑Tumor ↓OAR
Moman et al. 2010 [37]	3	Focal salvage after EBRT or Brachy	HDR	MRI w/Bx	↑Tumor ↓OAR

WG whole gland, *HG* hemi-gland, *UF* ultrafocal, *HDR* high-dose rate brachytherapy, *LDR* low-dose rate brachytherapy, *OAR* organs at risk, *Bx* biopsy, *MRI* magnetic resonance imaging, *MRS* magnetic resonance spectroscopy, *TTI* tissue-type imaging, *US* ultrasound, *PET* positron emission tomography

V100 > 97 % or volume of the target receiving 100 % of the prescription dose greater than 97 %) for each subvolume while decreasing the dose to OAR such as bladder, rectum, and urethra. Significant OAR dose reductions were achieved for all subvolume approaches, and as expected, the 1/6G plans resulted in the greatest reductions versus the WG plans (>50 % reduction in bladder, rectal, and urethral doses with 1/6G plan vs. WG plan).

Another study, by Mason et al. [21], examined HDR brachytherapy plans for nine patients in which actual tumor volumes were identified based on MRI and transperineal template-guided biopsies. Whole-gland, hemi-gland, and ultrafocal (UF) plans were generated to compare doses to the tumor volumes as well as the OAR. This comparison showed both an increase in dose to tumor volumes and a decrease to the OAR. The mean D90 of the tumor volumes were 20.4, 22.2, and 23.0 Gy for the WG, HG, and UF plans, respectively. The mean rectal D2 cm^3 (dose to 2 cm^3 of rectum) was 12.5, 9.8, and 4.6 Gy; the mean bladder D2 cm^3 (dose to 2 cm^3 of bladder)

was 9.8, 7.3, and 2.6 Gy; and the mean urethra D10 (dose to 10 % of the urethra) was 20.3, 19.7, and 9.2 Gy for the WG, HG, and UF plans.

A similar study by Al Qaisieh et al. [22] investigated the same WG, HG, and UF comparison using LDR I^{125} seeds in nine patients. Tumor volume was also determined by MRI and transperineal template-guided biopsies. As reported by Mason et al. [21], doses to the tumor volume could be increased, while doses to the OAR could be reduced with a focal approach. The mean D90 of the tumor volumes were 181.3, 195.7, and 218.3 Gy for the WG, HG, and UF plans. The mean rectal D2cc was 107.5, 77.0, and 42.7 Gy; the mean bladder D2cc was 80.5, 54.7, and 17.6 Gy; and the mean urethra D10 was 205.9, 191.4, and 92.4 Gy for the WG, HG, and UF plans.

Other issues that have been explored in this setting include image registration for target delineation within the prostate and influence on treatment margin by variability between planned and actual radioactive source placement. As noted previously, MRI plays an important role in target delineation within the prostate. However, both LDR and HDR brachytherapy implants are performed under ultrasound guidance and UF plans often utilize MRI registration to define the treatment volume. However, deformable registration algorithms have been developed for accurate fusion of the TRUS and MRI. Mayer et al. [38] performed a quantitative validation of the registration accuracy using either brachytherapy seeds or implanted fiducials as landmarks in ten patients showing an overall average registration error of 2.56 mm. In addition to image registration error, one must also consider variance in planned versus delivered dose due to source displacement when using preplanned LDR brachytherapy. Polders et al. [23] examined the differences between planned and delivered dose for focal plans developed in 15 patients by comparing isodose contours and quantifying the distances between them to account for variances in planned versus actual seed positions. They found the maximum distance needed to cover 95 % of the planned target volume with the prescribed dose (145 Gy using I^{125} seeds) was 0.48 cm. This uncertainty, however, could be partially mitigated by using a real-time dosimetry method in which needles are placed within the target volume and a plan is developed in the operating room based on those exact needle positions. However, care must still be taken to drop the seeds in their planned orientation within each needle to minimize the variability between the planned and delivered dose. Considering that the PTV would need to be expanded by approximately 2.5 mm for image registration error plus nearly 5 mm for source position error (making the total PTV expansion 0.75 mm), a real-time technique in which special attention is paid to limiting the PTV when adjacent to critical normal structures would be sensible.

Finally, the ability to perform salvage brachytherapy *after initial focal therapy* has been explored, at least from a theoretical standpoint. Several studies [19, 20, 39] have performed simulations in which a recurrence in an untreated area after HG or UF brachytherapy is treated with the same modality (HDR in these reports). Composite plans combining doses from both the initial partial-gland treatment and the salvage treatment are shown to still conform to typical dose constraints to the OAR for a single primary whole-gland treatment. Feasibility of this approach would likely be affected by the proximity of the recurrence to the OAR. For rectal protection, however, the introduction of hyaluronic acid gel between the prostate and rectum may make the possibility of salvage therapy more feasible [40] as use of the gel has been shown to reduce rectal radiation doses by as much as 75 %, with similar reductions in clinical rectal side effects [41]. Also, the time interval between these treatments can also influence salvageability. There is some time-dependent recovery of normal tissues after radiation therapy making a second treatment potentially less toxic if the interval between the initial and salvage therapy is longer [42].

Primary Focused Therapy

A range of studies utilizing HDR brachytherapy, LDR brachytherapy, and EBRT/IMRT have investigated the feasibility and outcomes for focused therapy. In the majority of studies, treatment plans

were created to treat the whole gland followed by a boost in which the target volumes received much higher doses and the OAR received the same or lower doses compared to standard whole-gland plans.

The feasibility of focused HDR brachytherapy boost versus whole-gland boost was investigated by Mason et al. [27]. The actual delivered therapy in 15 patients consisted of a 15 Gy single fraction WG HDR boost followed by external beam radiation therapy 37.5 Gy in 15 fractions to the prostate and seminal vesicles. The hypothetical intraprostatic tumor targets were delineated using mpMRI. Focused therapy plans were then created to study the ability to increase tumor target dose while maintaining dose constraints to the OAR similar to standard WG treatments. After plan optimization, the median boost volume D90 was increased by about 19 % from 17.6 to 20.9 Gy. The urethral D10 and rectal D2 cm^3 were essentially equivalent at 17.2 versus 17.4 Gy and 8.0 versus 9.0 Gy, respectively. In this study, the margin for tumor delineation was also evaluated. Based on intra- and interobserver variance in tumor contouring from mpMRI plus similar variances in MRI-TRUS image registration, uncertainty was estimated to be 4.5 mm. Another study by Pouliot et al. [28] used a unique MRI/MRSI (magnetic resonance spectroscopic imaging) technique to define dominant intraprostatic lesions (DILs) as targets for focused HDR monotherapy. Ten patients underwent HDR treatment planning optimization to determine the highest doses that could be delivered to the DIL while again maintaining normal WG dose constraints to the OAR. In this study, the DIL dose was escalated to 120–150 % of the WG dose without significantly increasing doses to the OAR. More recent reports using WG HDR monotherapy show similar ability boost the DIL to the same 120–150 % range [29–31] again while preserving dose constraints to the OAR.

The feasibility of focused LDR brachytherapy has also been evaluated in several studies. Ennis et al. [24] treated 13 patients successfully with what is described as a "dose-painting" strategy based on ultrasound spectrum analysis tissue-type imaging (TTI). TTI uses a neural network to process radiofrequency spectrum parameters associated with tumor tissue and creates a color image on ultrasound to represent cancerous regions within the prostate [43]. Focused LDR brachytherapy plans using Pd^{103} seeds were then developed in which the dose to the TTI identified lesions was increased to 200 % of the WG plan. The urethral and rectal doses were equivalent.

Another study by Gaudet et al. [25] treated a large number of patients (n = 120) employing a focused technique in which a boost volume was determined by sextant biopsies and received at least 150 % of the prescribed WG dose (144 Gy using I^{125} seeds). It should be noted that even with their standard WG LDR brachytherapy plans using real-time inverse planning algorithms, a mean of 86 % of the DIL was covered by the 150 % isodose line. However, by specifically optimizing the plan to limit the high-dose area to the DIL only, the mean DIL 150 % coverage was increased to 95 % while the bladder, urethral, and rectal doses were significantly decreased.

A final approach to focused LDR therapy was described by Todor et al. [26] in which dual isotope plans with various combinations of I^{125}, Pd^{103}, and Cs^{131} were compared using MRI-/MRSI-delineated boost volumes within the prostate. This study showed the feasibility of combining isotopes to create plans delivering very high doses to the boost volumes (80 % greater than the WG dose) while reducing urethral doses by 10 %. Dose calculations using more than one isotope, however, do require more complicated mathematical formulas to determine the biologically effective dose (BED) of a mixture of isotopes relative to a single isotope [44]. A similar approach has been proposed for primary focal brachytherapy plans [45].

Dosimetric investigations of focused external beam therapy using IMRT are somewhat more limited compared to brachytherapy. However, two studies [33, 34] have shown the feasibility of increasing IMRT dose from 76–78 Gy to 90–93 Gy or more when boosting a mpMRI- or MRSI-delineated DIL. Each showed doses to the OAR were similar or slightly decreased compared to the WG plans. A report from Housri et al. [32] attempted to deliver a more aggressive

focused therapy utilizing a simultaneous integrated boost to a MRI-delineated DIL. IMRT plans were generated in 24 patients in which 75.6 Gy in 42 fractions was delivered to the WG with an integrated boost to deliver a total dose of 151.2 Gy (200 % of the prescribed WG dose) to the DIL. Interestingly, only 12 of the 24 patients could be successfully planned without violating the normal tissue dose constraints to the OAR. The authors noted that distance between the DIL and the rectum was an important factor. Lesions located less than 0.42 cm from the rectum were significantly associated with infeasibility of the DIL boost ($p = 0.0002$).

Salvage Focal Therapy

Determining the optimal dosimetric parameters to the tumor target and surrounding normal tissues after prior prostate radiation therapy is critical to the efficacy and safety of salvage therapy. Well-defined recommendations on normal tissue dose constraints in this setting are still in development. Salvage focal brachytherapy dosimetry data are relatively limited, although there are a few reports utilizing both HDR and LDR techniques. Moman et al. [37] compared focal and whole-gland salvage HDR plans for four patients with biopsy-proven and MRI-identified locally recurrent prostate cancer after radiation therapy (external beam radiation $n = 2$, I^{125} brachytherapy $n = 5$). In each case, a single fraction dose of 15 Gy was delivered to the MRI-delineated recurrent lesion designated as the GTV while setting the maximal dose to the bladder and rectum at 6 Gy and the maximum urethral dose at 10 Gy [46]. In three of four cases, the focal salvage plans were able to achieve the dose to the GTV while maintaining the bladder, urethral, and rectal dose constraints. None of the whole-gland salvage HDR plans in those same four cases were able to meet their GTV target dose or normal tissue constraints.

Peters et al. [35] reported the dosimetric findings from 20 patients who actually underwent focal salvage I^{125} LDR brachytherapy for locally recurrent prostate cancer after primary radiation therapy and compared those results with another group of 28 patients who underwent whole-gland salvage I^{125} treatment. The recurrent lesion (GTV) for the focal treatment was delineated by mpMRI and correlative biopsy. A total dose of ≥145 Gy was delivered to either the GTV or the whole gland. Dosimetric analysis revealed significant reductions in rectal dose for the focal salvage group. Compared to the whole-gland salvage group, the median D0.1 cm^3, D1 cm^3, D2 cm^3, and V100 reductions to the rectum using a focal approach were 38 Gy, 46 Gy, 46 Gy, and 0.41 cm^3, respectively, all of which achieved statistical significance ($p \leq 0.002$). None of the 20 patients in the focal salvage group developed late severe gastrointestinal (GI) toxicity. By performing a receiver operating characteristic (ROC) analysis of the late GI toxicity data in the whole-gland salvage group, restrictions on rectal dose were determined for salvage therapy: D0.1 cm^3 < 160 Gy, D1 cm^3 < 120 Gy, D2 cm^3 < 100 Gy, and V100 < 0.35 cm^3. For comparison, restrictions for rectal dose for primary therapy are D0.1 cm^3 < 200 Gy, D2 cm^3 ≤ 145 Gy, and V100 < 1.0 cm^3 [5, 47, 48]. Another report from the same group of patients [49] performed another ROC analysis for restrictions on bladder and urethral doses to prevent late genitourinary (GU) toxicity. That analysis indicated a bladder D2 cm^3 < 70 Gy to prevent ≥ Grade 3 GU toxicity and a urethral V100 < 0.4 cm^3. The caveat to these results, however, would be that the prior radiation treatments varied in technique (including both primary I^{125} brachytherapy with loose or stranded seeds and EBRT) and dose (I^{125} 145Gy, EBRT 64.4–76 Gy). Also, the time between primary and salvage treatment was not reported for patients in either the focal or whole-gland group, which can affect normal tissue tolerance to retreatment as these tissues can recover to some degree depending on the time interval between treatments [42]. However, a report by Guimas et al. [36] analyzed cumulative doses in eight patients receiving focal salvage I^{125} brachytherapy and ten patients receiving whole-gland salvage I^{125} brachytherapy. Using a biologic effective dose (BED) calculation that allows comparison of combined doses from primary and salvage radiation regardless of modality

(EBRT or brachytherapy), they showed that the cumulative BED to the rectum could be reduced with focal versus whole-gland salvage therapy (172.6 Gy vs. 258.1 Gy, $p < 0.01$).

In summary, there are dosimetric studies demonstrating the feasibility and improved ability of all radiation therapy modalities to dose escalate the primary tumor and deescalate, or at least maintain, doses to OAR when delivering primary focal, focused, and focal salvage radiation therapy. As noted by Housri et al. [32], the proximity of the tumor target to critical organs may have significant impact on the ability to achieve the desired outcomes of increased tumor and decreased normal tissue doses. Newer technologies such as placement of hyaluronic acid gel between the prostate and the rectum may help to address that issue.

Clinical Outcomes

Clinical outcome investigations of primary focal, focused, and focal salvage therapy report mostly toxicity results with relatively limited long-term follow-up for treatment response. As with the dosimetric outcome reports, all forms of radiation therapy including HDR and LDR brachytherapy as well as external beam RT have been studied. Table 27.2 is a compilation of published reports evaluating the clinical outcomes for all forms of partial-gland radiation therapy. [50–60].

Primary Focal Therapy

Clinical outcomes in the primary focal therapy setting have been reported using I^{125} LDR brachytherapy. Cosset et al. [50] evaluated the early toxicity and disease response in 21 patients with low- to intermediate-risk prostate cancer treated with a real-time dosimetry I^{125} brachytherapy technique to a focal tumor volume within the prostate. The target volume was determined based on biopsy and MRI results indicating a unilateral localized tumor amenable to ultrafocal therapy. A "large safety margin" was also incorporated into the focal PTV, or F-PTV, such that the mean ultrafocal treatment volume still represented 34 % (range 20–48 %) of the whole prostate volume. The mean focal D90 was 183.2 Gy (range 176.4–188.1 Gy), and the mean V100 of the intraprostatic focal treatment volume was 99.3 % (range 98.8–100 %). The total number of needles used was 13–21 (mean 17), and the total number of seeds varied from 26 to 57 (mean 39). Patient follow-up included physical exam and PSA every 3 months for the first year and every 6 months thereafter with a post-implant biopsy performed 12–24 months after treatment. Urinary, rectal, and sexual toxicity scores were found to be excellent. Mean International Prostate Symptom Score (IPSS) at 6 and 12 months was 6.6 (range 2–17) and 6.1 (range 2–9) compared to a mean pretreatment score of 5.4 (range 0–15). Only one patient reported slight rectal discomfort at 2 months, and no rectal toxicity was reported at 6, 12, and 18 months. The mean pretreatment IIEF5 score was 20.1 (range 5–25) with mean scores at 6 and 12 months of 19.1 (range 5–25) and 19.8 (range 5–25). The mean initial PSA was 6.9 ng/ml (range 3.6–13.9). At 12 months, the mean value dropped to 2.6 ng/ml, and PSA dropped in almost all cases, although follow-up was too short to draw any definitive conclusions about tumor control. Biopsies were performed in six patients from 14 to 27 months after treatment (10–12 cores sampled from the whole prostate, including the treatment volume) with five negative results. One patient was found to have Gleason 6 (3+3) disease in an untreated area in the contralateral side from treatment.

Another unique study by Nguyen et al. [52] addressed the issue of posttreatment monitoring and definition of failure after focal therapy. The authors reported the results of partial I^{125} prostate brachytherapy in which only the peripheral zone (PZ) of the prostate was targeted. Sources were placed under intraoperative real-time MRI guidance such that a PZ V100 of 100 % was achieved while the anterior base and transition zone anterior to the urethra were kept to less than 100 %. Between 1997 and 2008, 318 patients were treated with this technique of which 280 had Gleason score 3+3 = 6 and 38 had Gleason score

Table 27.2 Clinical outcomes of partial-gland radiation therapy

Author/year	No. pts	Risk group	Median F/U (mos)	Approach	Modality	Toxicity	PSA DFS
Cosset et al. 2013 [50]	21	Low 19 Int 2	NR	Primary focal	LDR I^{125}	Initial vs. 12-mo IPSS 5.4 vs. 6.1 Initial vs. 12-mo IIEF 20.1 vs. 19.8	Initial vs. 12-mo PSA 6.9 vs. 2.6 Neg posttx bx 5/6
Barret et al. 2013 [51]	12	Low 12	9	Primary focal	LDR I^{125}	Initial vs.12-mo IPSS 3 vs. 7 Initial vs. 12-mo IIEF 21 vs. 14	Initial vs. 12-mo PSA 6.2 vs. 2.8
Nguyen et al. 2012 [52]	318	Low 280 Int 38	61	Primary focal to PZ	LDR I^{125}	NR	Phoenix 8 year 78.1 % Modified phoenix 8 year 90 %
Schick et al. 2011 [53]	77	High 77	69	Primary focused	3DCRT + WG HDR vs. 3DCRT + HG HDR ADT $n = 62$ pts	No diff in grade ≥3 GU/GI grade 4 late GI 8.8 % (WG) vs. 0 % (HG)	Phoenix 5 year 70.5 % (WG) vs. 79.7 % (HG) $p = 0.99$
Vigneault et al. 2016 [54]	20	Int 20	57	Primary focused	3D EBRT + WG HDR + UF HDR	Initial vs.12 mo IPSS 7.8 vs. 8.3 Grade ≥3late GI 0 %	Phoenix 5 year 95.7 %
Miralbell et al. 2010 [55]	50	Low 5 Int 12 High 33	63	Primary focused	IMRT + UF IMRT boost ADT $n = 33$ pts	Grade ≥3 late GU 0 % Grade ≥3 late GI $n = 5$ pts	Phoenix 5 year 98 %
Aluwini et al. 2013 [56]	50	Low 30 Int 20	23	Primary focused	SBRT + SBRT UF boost	Grade ≥3 late GU 6 % Grade ≥3 late GI 0 %	Phoenix 2 year 100 %
Hsu et al. 2013 [57]	15	Low 11 Int 4	69	Focal salvage after brachy	LDR I^{125}, Pd^{103} or IMRT + I^{125}	Grade ≥3 late GU 0 % Grade ≥3 late GI 0 % 100 % pretx vs. 87 % posttx w/erections	Phoenix 3 year 71.4 %
Peters et al. 2014 [58]	20	Low 5 Int 3 High 12	36	Focal salvage after brachy or EBRT	LDR I^{125}	Grade ≥3 late GU 5 % Grade ≥3 late GI 0 %	Phoenix 3 year 60 %
Chung et al. 2016 [59]	15	NR	12	Focal salvage after EBRT	HDR	Grade ≥3 late GU 0 % Grade ≥3 late GI 0 %	Initial PSA 3.96 vs. 12 mo PSA < 1.0 in 9/12 pts
Chung et al. 2016 [60]	15	Low 5 Int 8 High 2	18	Focal salvage after EBRT	HDR	Grade ≥3 late GU 0 % Grade ≥3 late GI 0 %	6/15 pts with PSA relapse at last f/u

WG whole gland, *HG* hemi-gland, *UF* ultrafocal, *HDR* high-dose rate brachytherapy, *LDR* low-dose rate brachytherapy, *IPSS* International Prostate Symptom Score, *IIEF* International Index of Erectile Function, *3D EBRT* 3-dimensional external beam radiation therapy, *IMRT* intensity-modulated radiation therapy, *SBRT* stereotactic body radiation therapy, *ADT* androgen deprivation therapy, *NR* not reported, *PZ* peripheral zone, *GI* gastrointestinal, *GU* genitourinary, *mo* month, *bx* biopsy, *pre tx* pretreatment, *post tx* post treatment, *f/u* follow-up

3+4 = 7 disease with a mean PSA of 5.0 ng/ml. Earlier reports [61, 62] of this treatment approach showed decreased need for alpha blocking medication and less intense 3-month urinary obstructive and irritative symptoms compared to whole-gland brachytherapy, while the current

report focused on tumor control. With a median follow-up of 5.1 years, biochemical failure-free survival was 91.5 % at 5 years and 78.1 % at 8 years using the Phoenix definition (nadir + 2). Given the majority of patients had low-risk prostate cancer, these outcomes were deemed inferior compared to standard whole-gland treatment. However, since the Phoenix definition assumes whole-gland treatment, this measure may not be appropriate for partial-gland therapy since benign causes such as benign prostatic hyperplasia (BPH), rather than true cancer recurrence, may cause a PSA elevation. Borrowing from PSA screening literature, the authors proposed incorporating a PSA velocity of greater than 0.75 ng/ml/year to improve the specificity of prostate cancer recurrence over the Phoenix definition alone. A total of 36 patients met the Phoenix definition alone of PSA failure, while only 26 met both the Phoenix and PSA velocity criteria (called the modified PSA failure definition). Sixteen of seventeen patients with biopsy-proven local recurrence were among the 26 meeting the modified PSA failure definition. Twenty-two of twenty-six patients also had posttreatment MRIs suspicious for recurrence. The use of the modified PSA failure definition improved the biochemical failure-free survival to 95.6 % and 90.0 % at 5 and 8 years. The authors concluded that although there is no consensus for the appropriate definition of failure after focal therapy, their modified PSA failure definition should be considered a starting point for further investigation.

Primary Focused Therapy

Clinical outcomes in the primary focused therapy setting have been reported using brachytherapy alone, combined brachytherapy and external beam RT, and external beam RT alone.

The previously mentioned study by Ennis et al. [24] utilizing a focused Pd^{103} LDR brachytherapy approach (WG brachytherapy followed by a brachytherapy boost to the identified intraprostatic tumor) not only evaluated the dosimetry of their ultrasound spectrum analysis tissue-type imaging (TTI) but also toxicity and tumor control outcomes. With a median follow-up of 31.5 months, none of the 13 treated patients developed acute or late grade 3 or higher GI or GU toxicities. Of six patients who underwent 24-month posttreatment biopsy, five (83 %) were negative, while one showed evidence of residual adenocarcinoma with treatment effect. No patients had a PSA failure by Phoenix definition, although the authors acknowledge, as did Nguyen et al. [52] that more posttreatment PSA production is expected in this situation as parts of the prostate gland were under dosed or not treated all.

Two studies of focused therapy combining whole-gland external beam RT and focal HDR boosts have also demonstrated low toxicity and good tumor control data compared to whole-gland treatment. Schick et al. [53] compared 77 patients undergoing 3D conformal EBRT (64–64.4 Gy) plus hemi- (n = 22) versus whole-gland (n = 57) HDR boost of 12–16 Gy in two fractions. With a median follow-up of 69 months, no differences were observed in late rectal toxicity, although late grade 4 urinary toxicity was exclusively observed in the whole-gland group (5/57, 8.8 %). No difference was noted in 5-year biochemical relapse-free survival by Phoenix definition, 79.7 % versus 70.5 % for the hemi- and whole-gland groups (p = 0.99). Vigneault et al. [54] examined 26 patients with intermediate-risk prostate cancer who underwent external beam pelvic radiation (40–44 Gy) followed by HDR brachytherapy boost consisting of 15 Gy single fraction to the whole gland with a simultaneous 3 Gy selective boost to the MRI/MRS or fluorocholine-positron emission tomography/computed tomography (PET/CT)-defined DIL (total of 18 Gy to the DIL). No acute or late grade 3 GI toxicities were noted with a median follow-up of 57 months. The average IPSS score at baseline, 12, 24, and 48 months, were 7.78, 8.3, 8.25, and 7.73, respectively. The 5-year PSA disease-free survival (Phoenix definition) was 95.7 %, which compared favorably with 93.4 % (p = 0.53) in a cohort of 685 intermediate-risk patients treated at the same institution without the DIL boost.

Finally, two studies reported the use of stereotactic radiation therapy in a focused therapy

approach. Miralbell et al. [55] performed a hypofractionated stereotactic IMRT boost to the DIL in combination with whole-gland standard fractionated 3D conformal EBRT (64–64.4 Gy). Due to the differing fractionation schedules between the whole-gland and boost treatments, a cumulative BED_{2Gy} (biologically effective dose if all treatment was given in 2 Gy fractions) was calculated in order to combine the 3D EBRT whole-gland and stereotactic IMRT boost doses. The MRI-defined DIL received two fractions of 5, 6, and 7 Gy (cumulative BED_{2Gy} 82, 88, and 96 Gy, 21 patients) or 8 Gy (cumulative BED_{2Gy} of 104 Gy, 29 patients). Comparisons were made between the 21 patients whose BED_{2Gy} was <100 Gy (low dose) and the 29 patients whose BED_{2Gy} was >100 Gy (high dose). With a median follow-up of 63 months, there was no correlation between dose and acute or late GI or GU toxicities. No patients developed late grade 3 or higher GU toxicities, although five did develop late grade 3 GI toxicity. The proximity of the boost volume to the rectum, as referenced by Housri et al. [32], was not delineated in this report, but a trend was noted between the proportion of rectum (≥30 %) receiving ≥3 Gy per fraction and grade ≥2 late GI toxicity. Five-year biochemical disease-free survival was 98 %, although interpretation of that result is difficult since the group included a mixture of low-, intermediate-, and high-risk patients in whom 66 % were also on 6–30 months of androgen deprivation therapy. Aluwini et al. [56] reported a study of hypofractionated stereotactic body radiation therapy (SBRT, Cyberknife®) for 50 patients with low- to intermediate-risk prostate cancer. A dose of 38 Gy in four fractions (9.5 Gy per fraction) was delivered to the whole gland with an integrated focal boost to 11 Gy per fraction applied to the DIL if identified on MRI. The whole-gland dose was consistent with current literature on prostate SBRT [63]. Median follow-up was 23 months. Urinary, bowel, and sexual domains on quality-of-life questionnaires showed no significant changes at 24 months after treatment. Late grade 2 GI toxicity was 2 % and late grade 2 and 3 GU toxicity was 10 % and 6 %. These rates were compared to a contemporary series of reports of prostate SBRT and found to be comparable. Prostate SBRT is rapidly becoming accepted as a standard treatment for early-stage prostate cancer, and as a result, treatment such as that proposed by Miralbell [55] and Aluwini [56] will likely become more common as improvement and availability of this technology become more widespread.

Focal Salvage Therapy

Focal salvage therapy for a local recurrence of prostate cancer is conceptually attractive as a treatment that could provide equivalent tumor control rates while reducing the toxicities of whole-gland salvage therapy. The 5-year biochemical control rates of whole-gland salvage have been reported in the 50–80 % range [9]. Grade 3–4 urinary toxicity, however, has been reported between 14 % and 47 % and grade 3–4 gastrointestinal toxicity between 2 % and 24 % [10]. Two focal salvage therapy reports have been published utilizing focal LDR brachytherapy while two others report results with HDR brachytherapy.

Hsu et al. [57] reported the outcomes for 15 patients with a biopsy-proven local recurrence after primary LDR brachytherapy. Areas of recurrence based on biopsy and MR/MRS as well as areas of undertreatment from the primary brachytherapy procedure as determined by a MR expansion algorithm were treated with full dose I^{125} seeds 144 Gy (n = 13), full dose Pd^{103} seeds 125 Gy (n = 1), or combined I^{125} seed boost 108 Gy and IMRT to the prostate and seminal vesicles 40 Gy/20 fractions (n = 1). Of note, the authors stated that limiting urethral and rectal toxicity was prioritized and patients with recurrence considered too close to the urethra or anterior rectal wall were not considered for this treatment protocol. The median interval between initial and salvage therapy was 69 months (range 28–132 months), and the median presalvage PSA was 3.5 ng/ml (range 0.9–5.6 ng/ml). The Gleason scores of the recurrence were 6 (66.7 %), 7 (13.3 %), 8 (13.3 %), or undefinable (6.7 %). With median follow-up of 23.3 months, 53 % of

patients achieved a PSA nadir of <0.10 ng/ml, and 73.3 % achieved a PSA nadir of <0.50 ng/ml. PSA disease-free survival by ASTRO definition (three consecutive rises) at 1, 2, and 3 years after salvage was 86.7 %, 78.4 %, and 63.7 %, respectively. PSA disease-free survival by Phoenix definition (nadir + 2 ng/ml) for the same time intervals was 100 %, 100 %, and 71.4 %. No patient developed urinary incontinence or grade ≥3 GI or GU toxicity. Presalvage, all patients had functional erections without (47 %) or with (53 %) medication, while 87 % of patients after salvage therapy had either intact erectile function (20.3 %) or medication-responsive ED (66.7 %).

Peters et al. [58] analyzed a similar cohort of 20 patients who underwent focal salvage I^{125} brachytherapy for biopsy-proven and MRI-localized local recurrences after primary radiation therapy (LDR brachytherapy 35 %, EBRT/IMRT 65 %). The recurrent tumor volumes received doses of ≥144 Gy. The median interval between initial and salvage therapy was 79 months (range 42–144), median presalvage PSA was 4.7 ng/ml (range 0.3–14.0), and the presalvage median PSA doubling time was 19 months (range 6.1–90.0). The Gleason scores of the recurrent disease were ≤6 (35 %), 7 (30 %), and undefinable (35 %). With a median follow-up of 36 months (range 10–45), the 3-year PSA disease-free survival (Phoenix definition) was 60 %. Three patients did not respond to treatment and developed metastatic disease. A single patient developed late grade 3 GU toxicity (urethral stricture), while no patients developed late grade ≥3 GI toxicity. The five patients who were potent prior to salvage therapy maintained potency at last follow-up.

Chung et al. [59] reported a series of 15 patients treated with focal salvage HDR brachytherapy for biopsy-proven local recurrence after EBRT. MR-guided transperineal mapping biopsy results were utilized to define the GTV, and focal HDR was delivered to a total dose of 26 Gy in two fractions. All patients had a PSA doubling time >6 months and an interval between initial and salvage therapy of at least 18 months. The mean presalvage PSA was 3.96 ng/ml (range 1.68–8.39). With median follow-up of 12 months (range 3–24), 14 of 15 (93.3 %) patients had a >50 % reduction in PSA after salvage brachytherapy. Nine of 12 (75 %) patients with ≥12 months follow-up had a PSA < 1.0 ng/ml. Only one patient developed grade 2 GU toxicity (urinary obstruction requiring temporary catheterization) with no patients experiencing grade ≥3 toxicities. A similar report by Chung et al. [60] described a series of 15 patients who also were treated with focal salvage HDR brachytherapy after EBRT. Biopsy confirmed local recurrences identifiable on mpMRI underwent HDR treatment to a total dose of 27 Gy in 2 fractions. The time interval between initial and salvage therapy was ≥30 months with presalvage PSA ≤ 10 ng/ml. The Gleason scores of the local recurrences were 6 (1 patient), 7 (7 patients), 8–10 (6 patients), and unassessable (1 patient), respectively. With median follow-up of 18 months (range 6–30), 9 of 15 (60 %) patients remained relapse-free by PSA. No acute or late grade ≥3 GU/GI toxicities or urinary retention were observed. There was no significant change in IPSS score or Expanded Prostate Cancer Index Composite (EPIC) urinary, bowel, and sexual domains from presalvage assessment through 18-month follow-up.

Each of these reports indicate that both focal salvage LDR and HDR brachytherapy are feasible after primary radiation therapy and can result in biochemical disease-free survival in the same range as whole-gland salvage therapy with minimal toxicity. However, given the small patient numbers and short follow-up, further study is needed to prove the utility of this approach.

In summary, the clinical outcomes in a small number of studies have shown that primary focal, primary focused, and focal salvage radiation therapy is feasible using varied techniques including LDR and HDR brachytherapy, as well as IMRT and SBRT. Low complication rates and good initial tumor control rates in the primary focal and focused setting show promise, but larger numbers of patients and longer follow-up will be needed to determine if these approaches can provide equal or better cancer control with lower complication rates compared to standard whole-gland radiation approaches. The definition

of cancer control still remains unclear in this situation, although it seems reasonable that standard ASTRO or Phoenix definitions of PSA failure may not be optimal and alternative measures may be necessary to define success. Toxicity outcomes compare favorably with whole-gland treatment, but future evaluations will be needed to measure toxicity outcomes between various focal and focused treatment techniques to determine the optimal approach. Relative to primary focal or focused approaches, focal salvage therapy has a lower bar to reach in terms of tumor control and toxicity outcomes. Early reports indicate that both focal salvage LDR and HDR brachytherapy are feasible after primary radiation therapy and can result in biochemical disease-free survival in the same range as whole-gland salvage therapy with less toxicity. However, the same issues remain with regard to the need for larger numbers of patients and longer follow-up as well as new studies to determine the optimal technique to deliver the treatment.

Conclusion

The accuracy and precision of treatment delivery along with its dose-shaping capability make radiation therapy an ideal modality for focal therapy. With advancements in the ability to localize tumor within the gland, there is interest in applying current HDR and LDR brachytherapy techniques as well as IMRT/SBRT to a partial-gland treatment approach. Early studies have shown the feasibility of using currently available planning and treatment technology to deliver focal radiation doses to the prostate. Higher tumor and lower normal tissue doses can be achieved when treating the smaller volumes of tissue with focal therapy, but location of these smaller volumes relative to normal structures such as bladder, urethra, and particularly rectum can still significantly influence the ability to achieve those dosimetric goals. Initial outcome studies appear promising for primary focal and focused radiation therapy as well as for focal salvage radiation, but larger numbers of patients and longer follow-up will be needed to determine the optimal radiation modalities, treatment planning techniques, dose constraints, and outcome measurements to make these approaches mainstream therapy.

References

1. Grimm P, Billiet I, Bostwick D, Dicker AP, Frank S, Immerzeel J, et al. Comparative analysis of prostate-specific antigen free survival outcomes for patients with low, intermediate and high risk prostate cancer treatment by radical therapy. Results from the prostate cancer results study group. BJU Int. 2012;109(Suppl 1):22–9.
2. Pollack A, Zagars GK, Starkschall G, Antolak JA, Lee JJ, Huang E, et al. Prostate cancer radiation dose response: results of the M. D. Anderson phase III randomized trial. Int J Radiat Oncol Biol Phys. 2002;53(5):1097–105.
3. Zelefsky MJ, Fuks Z, Hunt M, Yamada Y, Marion C, Ling CC, et al. High-dose intensity modulated radiation therapy for prostate cancer: early toxicity and biochemical outcome in 772 patients. Int J Radiat Oncol Biol Phys. 2002;53(5):1111–6.
4. Keyes M, Miller S, Moravan V, Pickles T, McKenzie M, Pai H, et al. Predictive factors for acute and late urinary toxicity after permanent prostate brachytherapy: long-term outcome in 712 consecutive patients. Int J Radiat Oncol Biol Phys. 2009;73(4):1023–32.
5. Keyes M, Spadinger I, Liu M, Pickles T, Pai H, Hayden A, et al. Rectal toxicity and rectal dosimetry in low-dose-rate (125) I permanent prostate implants: a long-term study in 1006 patients. Brachytherapy. 2012;11(3):199–208.
6. Crook J, Borg J, Evans A, Toi A, Saibishkumar EP, Fung S, et al. 10-Year experience with I-125 prostate brachytherapy at the princess Margaret hospital: results for 1100 patients. Int J Radiat Oncol Biol Phys. 2011;80(5):1323–9.
7. Marks LB, Carroll PR, Dugan TC, Anscher MS. The response of the urinary bladder, urethra, and ureter to radiation and chemotherapy. Int J Radiat Oncol Biol Phys. 1995;31(5):1257–80.
8. Grado GL, Collins JM, Kriegshauser JS, Balch CS, Grado MM, Swanson GP, et al. Salvage brachytherapy for localized prostate cancer after radiotherapy failure. Urology. 1999;53(1):2–10.
9. Nguyen PL, D'Amico AV, Lee AK, Suh WW. Patient selection, cancer control, and complications after salvage local therapy for postradiation prostate-specific antigen failure: a systematic review of the literature. Cancer. 2007;110(7):1417–28.
10. Kimura M, Mouraviev V, Tsivian M, Mayes JM, Satoh T, Polascik TJ. Current salvage methods for recurrent prostate cancer after failure of primary radiotherapy. BJU Int. 2010;105(2):191–201.
11. Stephenson AJ, Scardino PT, Kattan MW, Pisansky TM, Slawin KM, Klein EA, et al. Predicting the out-

come of salvage radiation therapy for recurrent prostate cancer after radical prostatectomy. J Clin Oncol. 2007;25(15):2035–41.
12. Langley S, Ahmed HU, Al-Qaisieh B, Bostwick D, Dickinson L, Veiga FG, et al. Report of a consensus meeting on focal low dose rate brachytherapy for prostate cancer. BJU Int. 2012;109(Suppl 1):7–16.
13. Onik G, Miessau M, Bostwick DG. Three-dimensional prostate mapping biopsy has a potentially significant impact on prostate cancer management. J Clin Oncol. 2009;27(26):4321–6.
14. Ahmed HU, Hu Y, Carter T, Arumainayagam N, Lecornet E, Freeman A, et al. Characterizing clinically significant prostate cancer using template prostate mapping biopsy. J Urol. 2011;186(2):458–64.
15. Burnet NG, Thomas SJ, Burton KE, Jefferies SJ. Defining the tumour and target volumes for radiotherapy. Cancer Imaging. 2004;4(2):153–61.
16. Salembier C, Lavagnini P, Nickers P, Mangili P, Rijnders A, Polo A, et al. Tumour and target volumes in permanent prostate brachytherapy: a supplement to the ESTRO/EAU/EORTC recommendations on prostate brachytherapy. Radiother Oncol. 2007;83(1):3–10.
17. Petereit DG, Frank SJ, Viswanathan AN, Erickson B, Eifel P, Nguyen PL, et al. Brachytherapy: where has it gone? J Clin Oncol. 2015;33(9):980–2.
18. Tejwani A, Bieniek E, Puckett L, Lavaf A, Guirguis A, Bennish A, et al. Case series analysis of post-brachytherapy prostate edema and its relevance to post-implant dosimetry. Post-implant prostate edema and dosimetry. J Contemp Brachytherapy. 2012;4(2):75–80.
19. Banerjee R, Park SJ, Anderson E, Demanes DJ, Wang J, Kamrava M. From whole gland to hemigland to ultrafocal high-dose-rate prostate brachytherapy: a dosimetric analysis. Brachytherapy. 2015;14(3):366–72.
20. Kamrava M, MP C, Kayode O, Wang J, Marks L, Kupelian P, et al. Focal high-dose-rate brachytherapy: a dosimetric comparison of hemigland vs. Conventional whole-gland treatment. Brachytherapy. 2013;12(5):434–41.
21. Mason J, Al-Qaisieh B, Bownes P, Thwaites D, Henry A. Dosimetry modeling for focal high-dose-rate prostate brachytherapy. Brachytherapy. 2014;13(6):611–7.
22. Al-Qaisieh B, Mason J, Bownes P, Henry A, Dickinson L, Ahmed HU, et al. Dosimetry modeling for focal low-dose-rate prostate brachytherapy. Int J Radiat Oncol Biol Phys. 2015;92(4):787–93.
23. Polders DL, Steggerda M, van Herk M, Nichol K, Witteveen T, Moonen L, et al. Establishing implantation uncertainties for focal brachytherapy with I-125 seeds for the treatment of localized prostate cancer. Acta Oncol. 2015;54(6):839–46.
24. Ennis RD, Quinn SA, Trichter F, Ryemon S, Jain A, Saigal K, et al. Phase I/II prospective trial of cancer-specific imaging using ultrasound spectrum analysis tissue-type imaging to guide dose-painting prostate brachytherapy. Brachytherapy. 2015;14(6):801–8.
25. Gaudet M, Vigneault E, Aubin S, Varfalvy N, Harel F, Beaulieu L, et al. Dose escalation to the dominant intraprostatic lesion defined by sextant biopsy in a permanent prostate I-125 implant: a prospective comparative toxicity analysis. Int J Radiat Oncol Biol Phys. 2010;77(1):153–9.
26. Todor DA, Barani IJ, Lin PS, Anscher MS. Moving toward focal therapy in prostate cancer: dual-isotope permanent seed implants as a possible solution. Int J Radiat Oncol Biol Phys. 2011;81(1):297–304.
27. Mason J, Al-Qaisieh B, Bownes P, Wilson D, Buckley DL, Thwaites D, et al. Multi-parametric MRI-guided focal tumor boost using HDR prostate brachytherapy: a feasibility study. Brachytherapy. 2014;13(2):137–45.
28. Pouliot J, Kim Y, Lessard E, Hsu IC, Vigneron DB, Kurhanewicz J. Inverse planning for HDR prostate brachytherapy used to boost dominant intraprostatic lesions defined by magnetic resonance spectroscopy imaging. Int J Radiat Oncol Biol Phys. 2004;59(4):1196–207.
29. D'Alimonte L, Helou J, Morton G, Ravi A, Chung H, McGuffin M, et al. Dosimetric analysis of an MRI assisted focal boost integrated with HDR monotherapy for low and intermediate risk prostate cancer. Brachytherapy. 2016;15:S200.
30. Carlone M, Rink A, Beiki-Ardakani A, Simeonov A, Lao B, Bayley A, et al. MR-guided high-dose-rate (HDR) brachytherapy: simultaneous integrated focal boost to intra-prostatic GTV(s). Brachytherapy. 2016;15:S51–2.
31. Dankulchai P, Alonzi R, Lowe GJ, Burnley J, Padhani AR, Hoskin PJ. Optimal source distribution for focal boosts using high dose rate (HDR) brachytherapy alone in prostate cancer. Radiother Oncol. 2014;113(1):121–5.
32. Housri N, Ning H, Ondos J, Choyke P, Camphausen K, Citrin D, et al. Parameters favorable to intraprostatic radiation dose escalation in men with localized prostate cancer. Int J Radiat Oncol Biol Phys. 2011;80(2):614–20.
33. van Lin EN, Fütterer JJ, Heijmink SW, van der Vight LP, Hoffmann AL, van Kollenburg P, et al. IMRT boost dose planning on dominant intraprostatic lesions: gold marker-based three-dimensional fusion of CT with dynamic contrast-enhanced and 1 h-spectroscopic MRI. Int J Radiat Oncol Biol Phys. 2006;65(1):291–303.
34. Ost P, Speleers B, De Meerleer G, De Neve W, Fonteyne V, Villeirs G, et al. Volumetric arc therapy and intensity-modulated radiotherapy for primary prostate radiotherapy with simultaneous integrated boost to intraprostatic lesion with 6 and 18 MV: a planning comparison study. Int J Radiat Oncol Biol Phys. 2011;79(3):920–6.
35. Peters M, Hoekstra CJ, van der Voort van Zyp JR, Westendorp H, van de Pol SM, Moerland MA, et al. Rectal dose constraints for salvage iodine-125 prostate brachytherapy. Brachytherapy. 2016;15(1):85–93.
36. Guimas V, Quivrin M, Bertaut A, Martin E, Chambade D, Maingon P, et al. Focal or whole-gland salvage prostate brachytherapy with iodine seeds with or

without a rectal spacer for postradiotherapy local failure: how best to spare the rectum? Brachytherapy. 2016;15(4):406–11.
37. Moman MR, van den Berg CA, Boeken Kruger AE, Battermann JJ, Moerland MA, van der Heide UA, et al. Focal salvage guided by t2-weighted and dynamic contrast-enhanced magnetic resonance imaging for prostate cancer recurrences. Int J Radiat Oncol Biol Phys. 2010;76(3):741–6.
38. Mayer A, Zholkover A, Portnoy O, Raviv G, Konen E, Symon Z. Deformable registration of trans-rectal ultrasound (TRUS) and magnetic resonance imaging (MRI) for focal prostate brachytherapy. Int J Comput Assist Radiol Surg. 2016;11(6):1015–23.
39. Peach MS, Trifiletti DM, Libby B. Systematic review of focal prostate brachytherapy and the future implementation of image-guided prostate HDR brachytherapy using MR-ultrasound fusion. Prostate Cancer. 2016;2016:4754031.
40. Nguyen PL, Devlin PM, Beard CJ, Orio PF, O'Leary MP, Wolfsberger LD, et al. High-dose-rate brachytherapy for prostate cancer in a previously radiated patient with polyethylene glycol hydrogel spacing to reduce rectal dose: case report and review of the literature. Brachytherapy. 2013;12(1):77–83.
41. Mariados N, Sylvester J, Shah D, Karsh L, Hudes R, Beyer D, et al. Hydrogel spacer prospective multicenter randomized controlled pivotal trial: dosimetric and clinical effects of perirectal spacer application in men undergoing prostate image guided intensity modulated radiation therapy. Int J Radiat Oncol Biol Phys. 2015;92(5):971–7.
42. Orton CG. Radiation dosimetry: physical and biological aspects. New York: Plenum; 1986.
43. Feleppa EJ, Ennis RD, Schiff PB, Wuu CS, Kalisz A, Ketterling J, et al. Spectrum-analysis and neural networks for imaging to detect and treat prostate cancer. Ultrason Imaging. 2001;23(3):135–46.
44. Chen Z, Nath R. Biologically effective dose (BED) for interstitial seed implants containing a mixture of radionuclides with different half-lives. Int J Radiat Oncol Biol Phys. 2003;55(3):825–34.
45. Mahdavi SS, Spadinger IT, Morris WJ, Salcudean SE, Chang SD, Kozlowski P, et al. Dual source strength planning for focal low-dose-rate brachytherapy of prostate cancer. Brachytherapy. 2015;14:S53–4.
46. Kovács G, Pötter R, Loch T, Hammer J, Kolkman-Deurloo IK, de la Rosette JJ, et al. GEC/ESTRO-EAU recommendations on temporary brachytherapy using stepping sources for localised prostate cancer. Radiother Oncol. 2005;74(2):137–48.
47. Davis BJ, Horwitz EM, Lee WR, Crook JM, Stock RG, Merrick GS, et al. American brachytherapy society consensus guidelines for transrectal ultrasound-guided permanent prostate brachytherapy. Brachytherapy. 2012;11(1):6–19.
48. Snyder KM, Stock RG, Hong SM, Lo YC, Stone NN. Defining the risk of developing grade 2 proctitis following 125I prostate brachytherapy using a rectal dose-volume histogram analysis. Int J Radiat Oncol Biol Phys. 2001;50(2):335–41.
49. Peters M, van der Voort van Zyp J, Hoekstra C, Westendorp H, van de Pol S, Moerland M, et al. Urethral and bladder dosimetry of total and focal salvage iodine-125 prostate brachytherapy: late toxicity and dose constraints. Radiother Oncol. 2015;117(2):262–9.
50. Cosset JM, Cathelineau X, Wakil G, Pierrat N, Quenzer O, Prapotnich D, et al. Focal brachytherapy for selected low-risk prostate cancers: a pilot study. Brachytherapy. 2013;12(4):331–7.
51. Barret E, Ahallal Y, Sanchez-Salas R, Galiano M, Cosset JM, Validire P, et al. Morbidity of focal therapy in the treatment of localized prostate cancer. Eur Urol. 2013;63(4):618–22.
52. Nguyen PL, Chen MH, Zhang Y, Tempany CM, Cormack RA, Beard CJ, et al. Updated results of magnetic resonance imaging guided partial prostate brachytherapy for favorable risk prostate cancer: implications for focal therapy. J Urol. 2012;188(4):1151–6.
53. Schick U, Popowski Y, Nouet P, Bieri S, Rouzaud M, Khan H, et al. High-dose-rate brachytherapy boost to the dominant intra-prostatic tumor region: hemi-irradiation of prostate cancer. Prostate. 2011;71(12):1309–16.
54. Vigneault E, Martin A-G, Lavallée M-C, Janelle M, Beaulieu L, Després P, et al. Clinical outcomes in patients treated with selective HDR image-guided boost to dominant intra-prostatic lesion. Brachytherapy. 2016;15:S52.
55. Miralbell R, Mollà M, Rouzaud M, Hidalgo A, Toscas JI, Lozano J, et al. Hypofractionated boost to the dominant tumor region with intensity modulated stereotactic radiotherapy for prostate cancer: a sequential dose escalation pilot study. Int J Radiat Oncol Biol Phys. 2010;78(1):50–7.
56. Aluwini S, van Rooij P, Hoogeman M, Kirkels W, Kolkman-Deurloo IK, Bangma C. Stereotactic body radiotherapy with a focal boost to the MRI-visible tumor as monotherapy for low- and intermediate-risk prostate cancer: early results. Radiat Oncol. 2013;8:84.
57. Hsu CC, Hsu H, Pickett B, Crehange G, Hsu IC, Dea R, et al. Feasibility of MR imaging/MR spectroscopy-planned focal partial salvage permanent prostate implant (PPI) for localized recurrence after initial PPI for prostate cancer. Int J Radiat Oncol Biol Phys. 2013;85(2):370–7.
58. Peters M, Maenhout M, van der Voort van Zyp JR, Moerland MA, Moman MR, Steuten LM, et al. Focal salvage iodine-125 brachytherapy for prostate cancer recurrences after primary radiotherapy: a retrospective study regarding toxicity, biochemical outcome and quality of life. Radiother Oncol. 2014;112(1):77–82.
59. Chung P, Berlin A, Rink A, Carlone M, Abed J, Simeonov A, et al. Preliminary results of MR-guided focal salvage HDR brachytherapy for locally recurrent prostate cancer after primary radiotherapy. Brachytherapy. 2016;15:S200.
60. Chung HT, Loblaw A, D'Alimonte L, Ravi A, Wronski M, Davidson M, et al. Toxicities, quality of life and

MRI response to focal salvage HDR prostate brachytherapy for locally recurrent prostate cancer after external-beam radiotherapy. Brachytherapy. 2016;15:S179–80.
61. Hurwitz MD, Cormack R, Tempany CM, Kumar S, D'Amico AV. Three-dimensional real-time magnetic resonance-guided interstitial prostate brachytherapy optimizes radiation dose distribution resulting in a favorable acute side effect profile in patients with clinically localized prostate cancer. Tech Urol. 2000;6(2):89–94.
62. Seo PH, D'Amico AV, Clark JA, Kaplan I, Manola JB, Mitchell SP, et al. Assessing a prostate cancer brachytherapy technique using early patient-reported symptoms: a potential early indicator for technology assessment? Clin Prostate Cancer. 2004;3(1):38–42.
63. Mantz C. A phase II trial of stereotactic ablative body radiotherapy for low-risk prostate cancer using a non-robotic linear accelerator and real-time target tracking: report of toxicity, quality of life, and disease control outcomes with 5-year minimum follow-up. Front Oncol. 2014;4:279.

Focal Therapy for Anterior Cancers (Originated from Transition Zone)

28

Arnauld Villers and Kae Jack Tay

Introduction

The concept of anterior cancer was recently defined as cancers located anterior to the posterior sectors/part of the prostate sampled by posterior systematic biopsies, i.e., at a distance of at least 17 mm (posterior biopsy core length) anterior to the rectal surface of the gland [1, 2]. Anterior cancers comprise peripheral zone (PZ) origin and transition zone (TZ) origin cancers [3]. Their pattern of spread differs according to their PZ or TZ origin [4, 5]. In this chapter we will discuss only TZ origin cancers. In the last decade, their detection, diagnosis, and treatment options were transformed by the emergence of multiparametric magnetic resonance imaging (mpMRI).

The prevalence of TZ cancers is 25 %. These cancers are located at the anterior part of the TZ, anterior to the distal urethra, on the midline. Due to this location, the detection and sampling of TZ origin, clinically significant cancers depend on MRI and targeted biopsies. Their clinical incidence in men with suspicious prostate-specific antigen (PSA) is close to 20 % [6]. Posterior extended 12-core systematic biopsies underdiagnosed and undersampled these TZ origin cancers, at least at early curable stage.

Specific approaches and applications of focal therapy (FT) should be considered for these anterior cancers originated from the TZ. Hence, partial therapy studies use various ablative methods delivering thermal energy, which should be adapted to the various intraprostatic locations of the targeted tumor or area such as the PZ, the TZ, or the anterior fibromuscular stroma (AFMS). An à la carte model for partial or focal therapy according to intraprostatic tumor location and size was therefore discussed [7]. In this chapter we will first review their prevalence, pattern of spread, and diagnostic pathways. Then the rationale for focal therapy and approaches including surgical partial excision, thermal ablation, and radiation therapy will be discussed.

Anatomic Definition

Current understanding of the anatomic subdivision of the adult prostate gland is secondary to two major studies successively published by Gil-Vernet in 1953 and by McNeal in 1968 [8]. McNeal defined *anterior cancers as TZ origin*

A. Villers (✉)
Department of Urology, Hôpital Huriez, Centre Hospitalier Regional Universitaire, Université Lille Nord de France, Lille, France
e-mail: arnauld.villers@univ-lille2.fr; arnauld.villers@wanadoo.fr

K.J. Tay
Department of Urology, Duke University, Durham, NC, USA

© Springer International Publishing AG 2017
T.J. Polascik (ed.), *Imaging and Focal Therapy of Early Prostate Cancer*, Current Clinical Urology, DOI 10.1007/978-3-319-49911-6_28

cancers only (part of the gland removed during benign prostatic hyperplasia [BPH] surgery, corresponding roughly to former stages A or T1a/T1b cancers) [5, 9]. Determination of zonal origin of prostate cancer (PCa) is possible only for small-volume cancers, <2–4 cc, and using detailed histological reconstruction of step sections of radical prostatectomy (RP) specimens with zonal histology and cancer contouring. Definition of zonal origin and focality was proposed by McNeal [5]. Cancer should entirely or mainly be confined to a zone. Two separate foci should be at least at 3 mm in all directions to be two different cancers.

In cases of larger cancer volumes, it is mostly not possible to determine their zone of origin, and authors refer to their anterior location, which could be either anterior PZ or TZ in origin [10]. This anterior location comprises the periurethral tissue, the anterior horns of the PZ, the TZ, and the anterior fibromuscular stroma (Fig. 28.1).

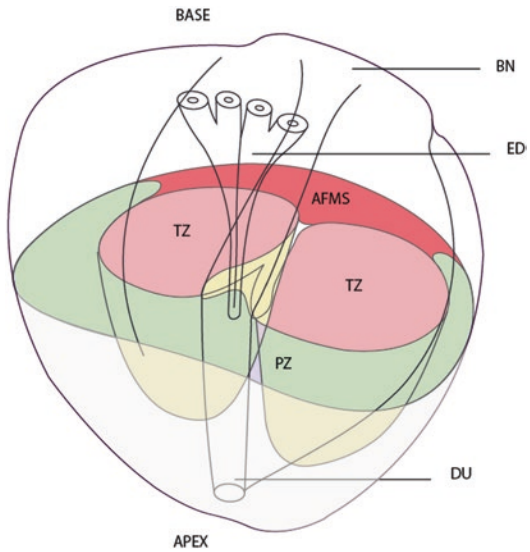

Fig. 28.1 From superior to inferior, the prostate consists of the base (just below the urinary bladder), the midgland, and the apex. It is divided into histologic zones: the anterior fibromuscular stroma (AFMS) contains no glandular tissue; the transition zone (TZ), surrounding the urethra proximal to the verumontanum; and the outer peripheral zone (PZ). When benign prostatic hyperplasia (BPH) develops, the TZ will account for an increasing percentage of the gland volume. *BN* bladder neck, *DU* distal urethra

Al-Ahmadie defined anterior predominant prostatic tumors as index tumor located anterior to a horizontal line drawn at the midpoint of the prostatic urethra on average at a 15 mm distance from the rectal surface [10]. The concept of "evasive" anterior tumors was also proposed, referring to the absence of evidence for zonal origin determination at MRI or pathology [11, 12].

Another definition of anterior cancer location is the part of the gland anterior to an area sampled by transrectal systematic 12-core posterior biopsies, at least 17 mm (average biopsy core length) from any part of the posterior prostate. This definition was first proposed by Villers et al. to help for imaging scheme reporting (Fig. 28.2) [1, 2, 6, 13]. This definition has the advantage of separating cancers that may be sampled by systematic 12-core posterior biopsies, which is the accepted standard from the others that require an anterior targeted biopsy. This definition was retained in the American College of Radiology (ACR) and European Society of Uroradiology (ESUR) Prostate Imaging Reporting and Data System version 2 (PI-RADS v2) guideline [14], in which a sector map is provided and employs 39 sectors/regions: 36 for the prostate, 2 for the seminal vesicles, and 1 for the external urethral sphincter. However, these anterior PZ and TZ zones are anatomically and histologically distinct. Their patterns of spread are different, and for these reasons, we will discuss in this chapter only TZ origin cancers [5].

Prevalence/Incidence

Histologic Prevalence

In a series of cystoprostatectomy specimens performed for bladder cancer from 345 consecutive patients without clinically manifest prostate cancer [3], in the 96 prostates with cancer, 215 cancer foci were identified (mean 2.24 cancers per prostate). Of the 215 cancers, 90 % were <0.5 cc and 79 % <0.2 cc. Overall, 88 % of cancer foci were clinically insignificant with a tumor volume <0.5 cc and no Gleason grades 4–5. It was possible to determine the zonal origin of these foci and

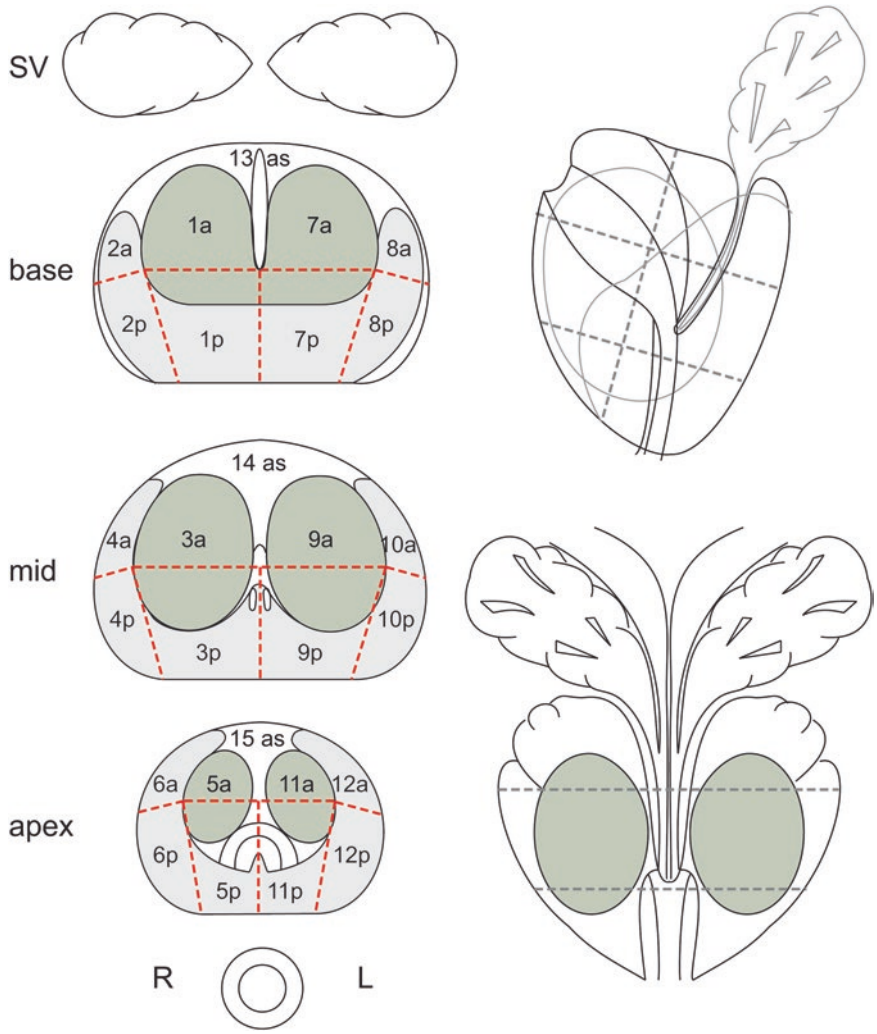

Fig. 28.2 Twenty-seven regions/sectors standardized MRI prostate reporting scheme. Posteriorly (p), average axial sections at prostate base, midgland, and apex are subdivided into four regions (midlobar and lateral). Anteriorly, the prostate is divided into four anterior regions (a) (midlobar and lateral) and three anterior stroma regions (as). The anterior region starts 17 mm from the prostatic posterior surface (biopsy core length). A 12-core extended biopsy scheme would be expected to sample the 12 posterior sectors. Adapted from [1]

small-volume cancers. Approximately 70–75 % of prostate cancers originate in the peripheral zone-central zone (PZ-CZ) and 20–30 % in the TZ (Fig. 28.3). In addition, 30 % of cancer foci were anteriorly located beyond the posterior area sampled by posterior biopsies, and 20 % foci were within 6 mm of the apex. These results created the rationale for hypothesizing that AFMS cancers originate from anterior and medial TZ but become excluded from the TZ, anteriorly into the AFMS, due to growth of BPH. The TZ anterior limit would then function as a barrier to their posterior extension (Fig. 28.4).

Clinical Incidence

In the last decade, MRI and targeted biopsies allowed better detection, depiction of location, and burden and diagnosis of anterior cancers originated from TZ. They account for 19 % of new cancers [6, 11, 15, 16].

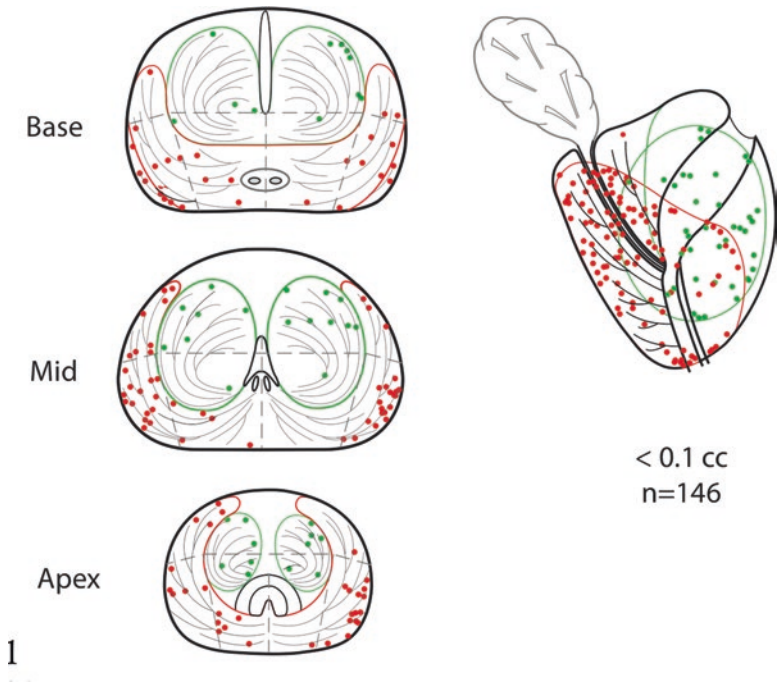

Fig. 28.3 Cancer originates at the distal part of glandular ducts: 75 % (*red dots*) from peripheral zone ducts, 25 % (*green dots*) from transition zone ducts. Series of 146 cancers <0.1 cc. Adapted from [3]

Origin and Pattern of Spread

Detailed studies of TZ cancers morphometry and pattern of spread showed that these cancers originate from anterior and medial TZ, anterior to the urethra on the midline at the distal part of TZ ducts [4]. Transition zone cancers are located at the anterior third of the TZ. AFMS cancers are medially located, anterior to the urethra. Because of this location, their detection by systematic biopsy scheme is minimal in comparison to detection by TB to MRI suspicious area.

Due to BPH enlargement, they become partly or totally excluded from the TZ, spreading anteriorly into the AFMS, the TZ anterior limit acting as a barrier to their posterior extension [6]. It was observed that above 1 cc of volume, spatial distribution of anterior cancers extended at histology from the apex, close to striated sphincter, to the bladder neck [4].

The role of spatial distribution of cancers according to the zone of origin and volume is discussed in Chap. 7.

Prognosis/Natural History

Before the MRI era, for TZ cancers, treated by RP in a series from Stanford, mean PSA was 31.1 ng/ml (1–270), and the percentage of patients with indetectable PSA after RP was 80 %. The same figures for PZ cancers were 11.1 ng/ml (1–23) and 56 %, respectively [17–19]. Does it mean that TZ cancers grow to a high volume, as well as differentiated cancers, differently from PZ cancers? Probably not. These results for TZ cancers should be viewed with caution due to a selection bias: only large TZ cancers sampled by posterior biopsies were diagnosed. In addition only the one with negative frozen section lymph node dissection had an RP. These results for TZ cancer do not reflect the whole spectrum of TZ cancers. Currently, TZ cancers should be similarly detected with MRI at an early stage, as with PZ cancers, by experienced radiologists [20–22].

After the MRI era, the association between TZ tumor origin and the risk of biochemical recur-

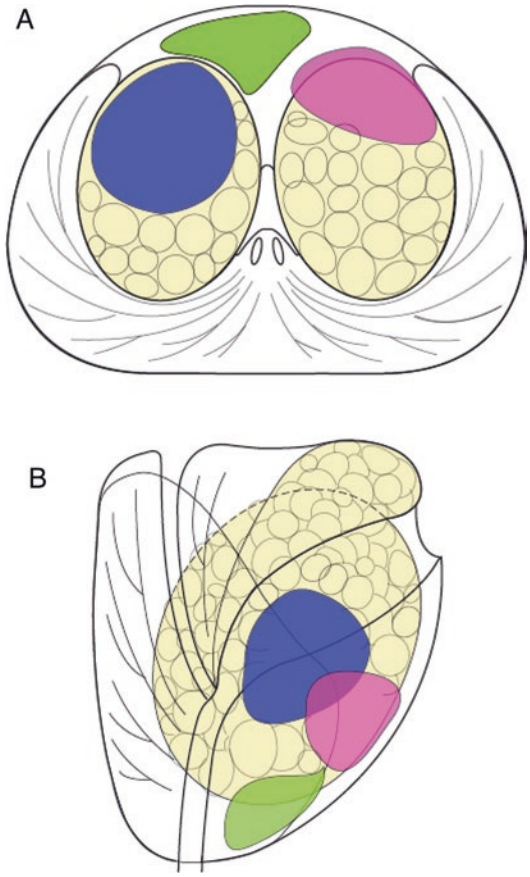

Fig. 28.4 Cancers originated in the transition zone are located at the anterior part of the transition zone or medially in the anterior fibromuscular stroma (AFMS) due to BPH growth. (**a**) Transverse section. (**b**) Sagittal section. Adapted with permission from Ouzzane A, Puech P, Lemaitre L, Leroy X, Nevoux P, and Betrouni N et al. Combined multiparametric MRI and targeted biopsies improve anterior prostate cancer detection, staging, and grading. Urology. 2011 Dec;78(6):1356–1362 [6]

rence does not add important predictive value to the standard prognostic factors. However, large series with MRI-detected cancers should be available to conclude.

Diagnosis Based on Magnetic Resonance Imaging and Targeted Biopsies

MR imaging can be used to detect, localize, and stage TZ origin prostate cancers, also described as "evasive" anterior tumors by Lawrentschuk et al. [6, 11, 13, 15, 16, 23–27].

While mpMRI is an excellent tool in the detection and staging of prostate cancer, there exists significant variability in hardware, scan protocols, and reader experience that affects accuracy. To ameliorate these limitations, reporting guidelines, such as the second version of PI-RADS, have emerged in order to standardize mpMRI acquisition and interpretation [14]. PI-RADS predicts the likelihood of clinically significant cancer, which increases as the scale moves from 1 to 5. In its latest iteration, the implementation of different criteria for interpreting findings in the transition and peripheral zones acknowledges the fact that the prostate is an inhomogeneous organ with differential distributions of glands and stroma. In determining the presence and extent of the anterior prostate tumor, which resides largely in the transition zone but may invade the AFMS or lateral horns of the peripheral zone, recognition of these nuances is critical.

Many urologists perform transrectal ultrasound (TRUS)-guided prostate biopsies in their clinics. While MRI-targeted biopsy was hitherto performed in-bore and considered the domain of radiologists, the advent of MRI-TRUS fusion biopsy has naturally extended the urologists' skills with ultrasound. The early implementations of MRI-TRUS fusions were cognitive or visual estimation (visual estimation targeting or VET). Ouzzane et al. reported that the addition of VET MRI-TRUS fusion biopsies almost doubled the cancer detection rate compared to random systematic cores in 46 men with anterior prostate cancers and upgraded cancer findings of the systematic cores by 44 % [6]. Current advances in MRI-ultrasound image fusion include software registration and probe tracking, which have led to a plethora of MRI-US fusion platforms [28]. These platforms have fostered a multidisciplinary approach to fusion biopsy with a radiologist marking a suspicious lesion and a urologist transferring this information to an ultrasound machine for a convenient office-based image-targeted biopsy [29].

In situations where mpMRI is not available, a transperineal biopsy better samples the anterior zone than a transrectal approach. Ong et al. found that of repeat transperineal biopsies, the diagnostic rate of exclusively anterior prostate cancers was 25 % [30]. However, transperineal biopsy

has to be performed under anesthesia and does have complications [31].

Rationale for Focal Therapy for Transition Zone Origin Cancers

Energy-based partial gland ablation is an emerging treatment for localized intermediate-risk prostate cancers aimed at reducing the morbidity associated with radical whole-gland therapy, while delivering cancer control [32, 33]. These focal therapies are adapted to PCa location, such as the peripheral zone, transitional zone, or anterior fibromuscular stroma [7].

Anterior cancer nodule can be isolated, mainly in the AFMS, at distance from the PZ, with no cancer in the PZ. In these cases, which may represent 3–5 % of new cancers [34], focal or partial treatment may be discussed in order to decrease morbidity associated with whole-gland therapy.

Anterior, apical cancer locations are suboptimal for ablative focal or partial therapy approaches because of issues with tumor location. Targeting such apical nodules located anterior to the prostatic urethra for ablative therapies is challenging due to interference of the anteroinferiorly located pubic symphysis, the potential of perforating the urethra and/or neurovascular bundles during transperineal approaches, and the risk of external striated sphincter damage by thermal treatment effect diffusion. These anterior cancers might be candidates for focal high-intensity focused ultrasound (HIFU) or cryotherapy or irreversible electroporation (IRE) [35]; however, no study results focusing on this specific location are yet published.

Anterior tumor contours in relation to prostate volume and zonal anatomy distortion by BPH are crucial for patient selection and success of the procedure. One challenge is at the anterior apex. Hence, focal ablative therapy is a suboptimal treatment option for PCa located in the anterior apex of the prostate because of potential thermal diffusion injury to the external striated sphincter, neurovascular bundles, and/or urethra, as well as interference from the pubic symphysis. In 11 out of 17 cases, anterior cancer was at the apex at systematic biopsies or MRI. Another challenge is at the anterior bladder neck, which should be treated due to its close location to the cancer limit if the volume is <1 cc [4].

Methods of Focal Therapy for Transition Zone Origin Cancers

The anterior prostate gland is more easily reached with a transperineal than a transrectal approach. The majority of anterior cancers occur in the mid and apical anterior gland with a fifth of them situated within 6 mm of the apex where the prostatic capsule tapers and meets the urethral sphincter [3, 6]. Delivering thermal energy to anterior cancer with apical extension may thus be undesirable [7], for fear of compromising the sphincteric unit.

Thus, any form of ablative energy should be directed carefully to avoid injury to collateral structures at the apical anterior gland. At this juncture in treatment planning, described anatomical variations of the prostatic apical shape should be kept in mind [36]. Some specific theoretical advantages or disadvantages of some of the currently available ablative technologies are discussed here, though the reader should be cautious that many of these are opinions and have not yet been supported by evidence [7].

Thermal Ablation

Cryotherapy

Prostate cryotherapy is most commonly performed as a transperineal procedure. Modern cryotherapy probes have an adjustable ice length, and this allows the ice balls to be conformed to the shape of the intended ablation zone. Having a characteristic ultrasound appearance due to its high-acoustic impedance, the ice ball margin can be carefully monitored and adjusted by the operator [37]. It is also a standard practice to use urethral warming devices, which have been shown to protect the urethral mucosa from necrosis and reduce the rates of incontinence and urinary retention [38–40]. Thermocouples can also be

deployed to aid in monitoring of temperature in critical areas.

High-Intensity Frequency Ultrasound

HIFU is typically applied to the prostate via a transrectal probe. This is effective in the ablation of posterior cancers but less so in the anterior gland due to energy dissipation over intervening prostate tissue as well as edema, causing it to be displaced further ventrally [7, 41, 42]. One interesting new development that has arisen due to miniaturization of HIFU probes is transurethral HIFU [43]. Being close to the anterior gland, transurethral HIFU has the potential to treat anterior cancers more effectively, though this has yet to be proven. Lastly, in-bore HIFU with MR thermometry could help ensure lethal temperatures in the ablation zone and safe temperatures in the urethra and sphincter.

Irreversible Electroporation

IRE refers to the irreversible creation of pores in cellular membranes using short pulses of direct current electricity resulting in cell death [44]. Being delivered via transperineal probes, good access to the anterior prostate can be achieved. One theoretical benefit of IRE is the preservation of connective tissue architecture, which could act as a scaffolding for new cells to grow and thus improve functional recovery after treatment. However, early studies show fibrinoid necrosis noted in the unilateral neurovascular bundle and denudation of the prostatic urethra [45].

Radiation Therapy

Brachytherapy

The majority of brachytherapy reports in the literature refer to whole-gland treatment. Simulation studies do show an adequate dose delivery using a focal planning approach [46, 47]. Being a transperineal procedure, access to the anterior prostate gland is good, and there is the theoretical benefit of a rapid dose drop-off of several millimeters using an alpha radiation source allowing for a highly conformal approach. While low-dose rate (LDR) brachytherapy urinary toxicity rates appear low, high-dose rate (HDR) brachytherapy is associated with a urethral stricture rate as high as 8.2 % with the majority occurring near prostatic apex or bulbous urethra [48, 49].

Surgery

Surgical partial excision of such anterior nodules may be a viable option for delivering partial therapy [50, 51]. It has the advantages of an accurate excision of the cancer due to the standardized anterior en bloc approach and of having a pathologic assessment of the cancer and specimen margins. As for any focal treatment, no known foci of significant cancer should be present in the rest of the gland, with the possibility to perform a salvage radical procedure in case of a recurrence or de novo cancer in the follow-up. Anterior to the urethra, in close physical proximity to the external sphincter or bladder neck, focal ablative therapy may be a suboptimal option for APC reaching the prostate apex due to concerns for thermal injury to the external sphincter.

Villers et al. reported their results of an en bloc template surgical excision of anterior part of the gland including TZ, AFMS, and anterior part of PZ (Fig. 28.5) [34]. This technique would:

1. Be effective for complete tumor ablation with a safety margin of benign tissue posteriorly
2. Be associated with functional results significantly better than after RP, with no stress incontinence or modification of erectile function, similar to those after simple prostatectomy procedure [52]
3. Allow pathological assessment of ablated tissue and PSA nadir. Would be accurate for oncological control and diagnosis of recurrence or of de novo PZ cancer
4. Allow completion radical prostatectomy or ablative therapies in case of cancer recurrence or de novo, with oncologic and functional outcomes similar to what would have been expected in case of RP as initial treatment

Objectives were to explore technical feasibility of anterior partial prostatectomy for isolated,

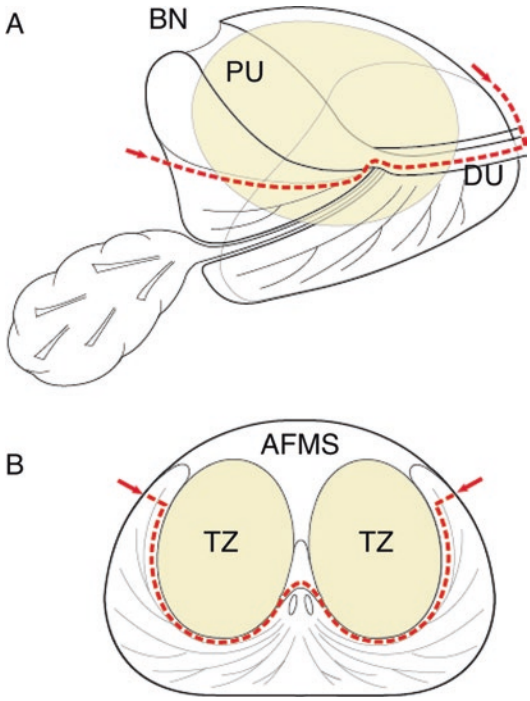

Fig. 28.5 Schematic view of the prostate: (**a**) sagittal and (**b**) transverse at midgland. *Red dotted line* shows dissection plane of anterior partial prostatectomy. Protocol comprises en bloc template excision of the anterior part of the prostate including anterior fibromuscular stroma (AFMS), prostate adenoma (transition zone (TZ) and median lobe) with the proximal urethra (PU), the anterior part of the distal (sub-montanal) urethra (DU), the most anterior apical parts of the peripheral zone (PZ), and anterior bladder neck (BN). Adapted from [34]

MRI-detected APC and to report oncological and functional outcomes [34]. Over an 8-year period, 17 consenting patients were enrolled in a prospective, single-arm, single-center, phase 2a study. Inclusion criteria comprised pre-urethral, low-intermediate-risk APC diagnosed by MRI and targeted biopsies. Robotic template anterior partial prostatectomy was performed; posterolateral aspect of sub-montanal urethra, peripheral zone, and periprostatic tissues were preserved intact. Technique was feasible in all cases. Perioperative complications included anastomotic leak (12 %, G2), urinary tract infection (6 %, G2), and transient intestinal ileus in one case (6 %, G2). At 3 months, continence and potency rates were 100 % and 83 %, respectively. Median nadir PSA was 0.4 ng/ml (IQR: 0.3–0.7). All margin and posterolateral margin rates were 55 % and 35 %, respectively. At a median follow-up of 30 months (range: 0.5–8), APC recurrence-free survival at 2 years was 0.86 (0.55–0.96). Four patients (24 %) who recurred underwent an uncomplicated completion robotic prostatectomy [34].

Positive margins at the site of PZ anterior aspect left in situ were observed in 6/17 cases and depend on tumor volume, location, and contour. The four cases who recurred were part of these six cases [34].

Positive margins along the anterior surface of the prostate should theoretically be similar to the risk during radical prostatectomy since the anterior aspect of the prostate is dissected similarly and to the same extent in both procedures. In a series of 189 patients who had MRI-detectable anterior tumors and RP, Al Edwan reported that 46 % had positive surgical margins [12]. Exposure of these cancers at the AFMS surface is limited by leaving as much as possible the periprostatic fat on the specimen, but may not be possible always by any technique. Biologic significance of these anterior margins is uncertain. In our series, anterior margin location was not associated to tumor recurrence in the prevesical space [34].

Partial prostatectomy may be a potential option for highly selected men with anterior cancers who are not candidates for focal ablative therapy. Additional criteria for selection should include whole-gland volume >40–45 cc. Technique should include frozen section assessment of PZ margin. Quality-of-life questionnaires should be added to assess overall benefits or harms of this technique before being recommended or not as a reasonable alternative to standard therapies.

Conclusion

Anterior prostate cancers often arise from the transition zone. Using modern diagnostic imaging with mpMRI and targeted biopsies, these may be detected at an organ-confined stage where they are suitable for focal treatment with less functional morbidity than traditional whole-gland methods.

References

1. Villers A, Lemaitre L, Haffner J, Puech P. Current status of mri for the diagnosis, staging and prognosis of prostate cancer: implications for focal therapy and active surveillance. Curr Opin Urol. 2009;19(3):274–82.
2. Dickinson L, Ahmed HU, Allen C, Barentsz JO, Carey B, Futterer JJ, et al. Magnetic resonance imaging for the detection, localisation, and characterisation of prostate cancer: recommendations from a European consensus meeting. Eur Urol. 2011;59(4):477–94.
3. Nevoux P, Ouzzane A, Ahmed HU, Emberton M, Montironi R, Presti Jr JC, et al. Quantitative tissue analyses of prostate cancer foci in an unselected cystoprostatectomy series. BJU Int. 2012;110(4):517–23.
4. Bouye S, Potiron E, Puech P, Leroy X, Lemaitre L, Villers A. Transition zone and anterior stromal prostate cancers: zone of origin and intraprostatic patterns of spread at histopathology. Prostate. 2009;69(1):105–13.
5. McNeal JE, Haillot O. Patterns of spread of adenocarcinoma in the prostate as related to cancer volume. Prostate. 2001;49(1):48–57.
6. Ouzzane A, Puech P, Lemaitre L, Leroy X, Nevoux P, Betrouni N, et al. Combined multiparametric MRI and targeted biopsies improve anterior prostate cancer detection, staging, and grading. Urology. 2011;78(6):1356–62.
7. Sivaraman A, Barret E. Focal therapy for prostate cancer: an "a la carte" approach. Eur Urol. 2016;69:972–5.
8. Villers A, Steg A, Boccon-Gibod L. Anatomy of the prostate: review of the different models. Eur Urol. 1991;20(4):261–8.
9. McNeal JE, Price HM, Redwine EA, Freiha FS, Stamey TA. Stage a versus stage b adenocarcinoma of the prostate: morphological comparison and biological significance. J Urol. 1988;139(1):61–5.
10. Al-Ahmadie HA, Tickoo SK, Olgac S, Gopalan A, Scardino PT, Reuter VE, et al. Anterior-predominant prostatic tumors: zone of origin and pathologic outcomes at radical prostatectomy. Am J Surg Pathol. 2008;32(2):229–35.
11. Lawrentschuk N, Haider MA, Daljeet N, Evans A, Toi A, Finelli A, et al. 'Prostatic evasive anterior tumours': the role of magnetic resonance imaging. BJU Int. 2010;105(9):1231–6.
12. Edwan GA, Ghai S, Margel D, Kulkarni G, Hamilton R, Toi A, et al. Magnetic resonance imaging detected prostate evasive anterior tumours: further insights. Can Urol Assoc J. 2015;9(5–6):E267–72.
13. Lemaitre L, Puech P, Poncelet E, Bouye S, Leroy X, Biserte J, et al. Dynamic contrast-enhanced MRI of anterior prostate cancer: morphometric assessment and correlation with radical prostatectomy findings. Eur Radiol. 2009;19(2):470–80.
14. Weinreb JC, Barentsz JO, Choyke PL, Cornud F, Haider MA, Macura KJ, et al. PI-RADS prostate imaging – reporting and data system: 2015, version 2. Eur Urol. 2016;69(1):16–40.
15. Vargas HA, Akin O, Franiel T, Goldman DA, Udo K, Touijer KA, et al. Normal central zone of the prostate and central zone involvement by prostate cancer: clinical and MR imaging implications. Radiology. 2012;262(3):894–902.
16. Hoeks CM, Hambrock T, Yakar D, de Kaa CA H-v, Feuth T, JA W, et al. Transition zone prostate cancer: detection and localization with 3-t multiparametric MR imaging. Radiology. 2013;266(1):207–17.
17. Stamey TA, Sozen TS, Yemoto CM, McNeal JE. Classification of localized untreated prostate cancer based on 791 men treated only with radical prostatectomy: common ground for therapeutic trials and TNM subgroups. J Urol. 1998;159(6):2009–12.
18. Stamey TA, Yemoto CM, McNeal JE, Sigal BM, Johnstone IM. Prostate cancer is highly predictable: a prognostic equation based on all morphological variables in radical prostatectomy specimens. J Urol. 2000;163(4):1155–60.
19. Noguchi M, Stamey TA, McNeal JE, Yemoto CE. Assessment of morphometric measurements of prostate carcinoma volume. Cancer. 2000;89(5):1056–64.
20. Erbersdobler A, Huhle S, Palisaar J, Graefen M, Hammerer P, Noldus J, et al. Pathological and clinical characteristics of large prostate cancers predominantly located in the transition zone. Prostate Cancer Prostatic Dis. 2002;5(4):279–84.
21. Augustin H, Hammerer PG, Blonski J, Graefen M, Palisaar J, Daghofer F, et al. Zonal location of prostate cancer: significance for disease-free survival after radical prostatectomy? Urology. 2003;62(1):79–85.
22. Iremashvili V, Pelaez L, Jorda M, Manoharan M, Rosenberg DL, Soloway MS. Prostate cancers of different zonal origin: clinicopathological characteristics and biochemical outcome after radical prostatectomy. Urology. 2012;80(5):1063–9.
23. Akin O, Sala E, Moskowitz CS, Kuroiwa K, Ishill NM, Pucar D, et al. Transition zone prostate cancers: features, detection, localization, and staging at endorectal MR imaging. Radiology. 2006;239(3):784–92.
24. Hambrock T, Somford DM, Hoeks C, Bouwense SA, Huisman H, Yakar D, et al. Magnetic resonance imaging guided prostate biopsy in men with repeat negative biopsies and increased prostate specific antigen. J Urol. 2010;183(2):520–7.
25. Komai Y, Numao N, Yoshida S, Matsuoka Y, Nakanishi Y, Ishii C, et al. High diagnostic ability of multiparametric magnetic resonance imaging to detect anterior prostate cancer missed by transrectal 12-core biopsy. J Urol. 2013;190(3):867–73.
26. Radtke JP, Boxler S, Kuru TH, Wolf MB, Alt CD, Popeneciu IV, et al. Improved detection of anterior fibromuscular stroma and transition zone prostate cancer using biparametric and multiparametric MRI with MRI-targeted biopsy and mri-us fusion guidance. Prostate Cancer Prostatic Dis. 2015;18(3):288–96.
27. Rosenkrantz AB, Kim S, Campbell N, Gaing B, Deng FM, Taneja SS. Transition zone prostate cancer: revisiting the role of multiparametric mri at 3 t. AJR Am J Roentgenol. 2015;204(3):W266–72.
28. Kongnyuy M, Sidana A, George AK, Muthigi A, Iyer A, Fascelli M, et al. The significance of anterior pros-

tate lesions on multiparametric magnetic resonance imaging in african-american men. Urol Oncol. 2016;34(6):254 e215–221.
29. Tay KJ, Mendez M, Moul JW, Polascik TJ. Active surveillance for prostate cancer: can we modernize contemporary protocols to improve patient selection and outcomes in the focal therapy era? Curr Opin Urol. 2015;25(3):185–90.
30. Ong WL, Weerakoon M, Huang S, Paul E, Lawrentschuk N, Frydenberg M, et al. Transperineal biopsy prostate cancer detection in first biopsy and repeat biopsy after negative transrectal ultrasound-guided biopsy: the victorian transperineal biopsy collaboration experience. BJU Int. 2015;116(4):568–76.
31. Tsivian M, Polascik TJ. Bilateral focal ablation of prostate tissue using low-energy direct current (ledc): a preclinical canine study. BJU Int. 2013;112(4):526–30.
32. Marien A, Gill I, Ukimura O, Betrouni N, Villers A. Target ablation–image-guided therapy in prostate cancer. Urol Oncol. 2014;32(6):912–23.
33. Orczyk C, Emberton M, Ahmed HU. What tumours should we treat with focal therapy based on risk category, grade, size and location? Curr Opin Urol. 2015;25(3):212–9.
34. Villers A, Puech P, Flamand V, Haber GP, Desai MM, Crouzet S, et al. Partial prostatectomy for anterior cancer: short-term oncologic and functional outcomes. Eur Urol. 2016; doi:10.1016/j.eururo.2016.08.057.
35. Marshall S, Taneja S. Focal therapy for prostate cancer: the current status. Prostate Int. 2015;3(2):35–41.
36. Myers RP, Goellner JR, Cahill DR. Prostate shape, external striated urethral sphincter and radical prostatectomy: the apical dissection. J Urol. 1987;138(3):543–50.
37. Onik G, Cobb C, Cohen J, Zabkar J, Porterfield B. Us characteristics of frozen prostate. Radiology. 1988;168(3):629–31.
38. Donnelly BJ, Saliken JC, Ali-Ridha N, Rewcastle JC, White LJ. Histological findings in the prostate two years following cryosurgical ablation. Can J Urol. 2001;8(2):1237–9.
39. Vellet AD, Saliken J, Donnelly B, Raber E, McLaughlin RF, Wiseman D, et al. Prostatic cryosurgery: use of MR imaging in evaluation of success and technical modifications. Radiology. 1997;203(3):653–9.
40. Cespedes RD, Pisters LL, von Eschenbach AC, McGuire EJ. Long-term followup of incontinence and obstruction after salvage cryosurgical ablation of the prostate: results in 143 patients. J Urol. 1997;157(1):237–40.
41. Clyne M. Prostate cancer: prostatic swelling and shift upon HIFU. Nat Rev Urol. 2013;10(6):306.
42. Shoji S, Uchida T, Nakamoto M, Kim H, de Castro Abreu AL, Leslie S, et al. Prostate swelling and shift during high intensity focused ultrasound: implication for targeted focal therapy. J Urol. 2013;190(4):1224–32.
43. Burtnyk M, Hill T, Cadieux-Pitre H, Welch I. Magnetic resonance image guided transurethral ultrasound prostate ablation: a preclinical safety and feasibility study with 28-day followup. J Urol. 2015;193(5):1669–75.
44. Onik G, Mikus P, Rubinsky B. Irreversible electroporation: implications for prostate ablation. Technol Cancer Res Treat. 2007;6(4):295–300.
45. van den Bos W, Jurhill RR, de Bruin DM, Savci-Heijink CD, Postema AW, Wagstaff PG, et al. Histopathological outcomes after irreversible electroporation for prostate cancer: results of an ablate and resect study. J Urol. 2016;196:552–9.
46. Haworth A. Which patients benefit from post-implant ct dosimetry after real-time intraoperative planning for ldr prostate brachytherapy: should intraoperatively planned patients be treated differently? J Med Imaging Radiat Oncol. 2016;60(2):244–6.
47. Butler WM, Merrick GS. Focal prostate brachytherapy with (103)Pd seeds. Phys Med. 2016;32(3):459–64.
48. Gutman S, Merrick GS, Butler WM, Wallner KE, Allen Z, Galbreath RW, et al. Severity categories of the international prostate symptom score before, and urinary morbidity after, permanent prostate brachytherapy. BJU Int. 2006;97(1):62–8.
49. Hindson BR, Millar JL, Matheson B. Urethral strictures following high-dose-rate brachytherapy for prostate cancer: analysis of risk factors. Brachytherapy. 2013;12(1):50–5.
50. Eggener S, Salomon G, Scardino PT, De la Rosette J, Polascik TJ, Brewster S. Focal therapy for prostate cancer: possibilities and limitations. Eur Urol. 2010;58(1):57–64.
51. Ahmed HU, Emberton M. Benchmarks for success in focal therapy of prostate cancer: cure or control? World J Urol. 2010;28(5):577–82.
52. Pokorny M, Novara G, Geurts N, Dovey Z, De Groote R, Ploumidis A, et al. Robot-assisted simple prostatectomy for treatment of lower urinary tract symptoms secondary to benign prostatic enlargement: surgical technique and outcomes in a high-volume robotic centre. Eur Urol. 2015;68(3):451–7.

Part IX

Manipulating the Microenvironment for Optimization

The Story of Adjuvants to Boost the Performance of Cryoablation

29

Kimberly L. Santucci, John M. Baust, Kristi K. Snyder, Anthony Robilotto, Robert G. VanBuskirk, and John G. Baust

Introduction

There is growing recognition that monotherapies infrequently yield the durable ("curative") outcome sought by patient and physician. Combinatorial strategies, especially with sequenced chemotherapy or radiation therapy, now represent the emerging standard of care for many cancers. Cryoablation, as an energy deprivation therapy, is unique in that it initiates distinct forms of cell death, including physical damage due to ice formation, activation of cellular stress responses that lead to the induction of gene-regulated apoptosis, vascular stasis, and likely activation of an ablative immune response. Each of these elements of the cell death cascade is separately influenced by the physical parameters of the freeze-thaw process (i.e., cooling rate, duration at nadir temperature, thawing rate, etc.). Also important to the ablative outcome are the distinct cancer cell sensitivities to freezing.

Efforts to find curative therapies for diverse cancers continue to be challenged by the complexity of each cancer's adaptive capabilities. A recent example of one such challenge is the apparent refractoriness of various cancers to repetitive chemotherapy with the ultimate outcome of the acquisition of treatment resistance and metastasis [1–3]. Similar observations have been reported following both radiotherapy [4–6] and hormonal ablation therapies [7–10]. These studies offer mechanistic insights into the incomplete clinical response in the treatment of nearly all forms of cancer over the past 50 years [11]. For advanced solid malignancies, "curative outcomes" seem limited to 5–10 % improving to approximately 60–80 % for locally confined disease. For metastatic prostate cancer posttreatment, the 5-year survival rate is 25 % with median survival 40 months [12].

Despite the emergence of a half century of divergent therapeutic regimens, no single therapy has challenged the norm of suppressive but not curative outcome. With monotherapies, cure is possible but not assured or predictable. We can gain insights into treatment alternatives, namely, combinatorial strategies, by considering the newly emerging concepts that describe the tumor microenvironment and the associated hallmarks of cancer that help define cancer cell plasticity and continued mutagenic potential, which

K.L. Santucci • A. Robilotto • R.G. VanBuskirk
Institute of Biomedical Technology, State University of New York at Binghamton, Binghamton, NY, USA

J.M. Baust • K.K. Snyder
CPSI Biotech, Owego, NY, USA

J.G. Baust (✉)
UNESCO, Institute of Biomedical Technology, State University of New York at Binghamton, Binghamton, NY, USA
e-mail: jgbaust@binghamton.edu

© Springer International Publishing AG 2017
T.J. Polascik (ed.), *Imaging and Focal Therapy of Early Prostate Cancer*, Current Clinical Urology, DOI 10.1007/978-3-319-49911-6_29

Table 29.1 Hallmarks of cancer

Hallmarks of cancer
Sustained proliferative signaling
Evasion of growth suppressors
Resisting programmed cell death—apoptosis
Induction of vasculogenesis and angiogenesis
Overcoming immune system defenses
Reprogramming cellular energetics
Cellular immortality
Mobilization and metastasis
Create tumor microenvironment through recruitment of stromal cells

together evoke substantial survival mechanisms [13, 14].

The adaptive strategies employed by cancers are variable in time and tumor location (Table 29.1) and yield a cohort of molecular cellular responses that often overcome therapeutic treatment strategies. This array of defensive tactics renders most first-line treatment standards transiently suppressive, of uncertain curative outcome and characterized by potential long-term metastatic involvement. In effect, efforts to manipulate the molecular schema of a cell are compromised by the highly evolved defenses of cancers [14]. We now recognize that a tumor is not simply a homogeneous mass of cancer cells growing without control that will often result in the structural disruption of the primary site of origin followed by tissue architectural destruction at secondary (metastatic) sites. Tumors are heterogeneous cell masses with complex structure, "neo-organ-like," that include (1) a cancer stem cell population; (2) a tumor microenvironment that recruits diverse non-cancerous, tumor-associated support cells; and (3) a tumor-developed immune cell population that compromises the body's natural immune surveillance functions.

Cancer cell growth is kept in check by tumor suppressor genes such as p53 until activating mutations downregulate or eliminate suppressor control. New blood vessel growth occurs in response to tumor-associated (recruited) endothelial cells and VEGF (vascular endothelial growth factor) signaling. Macrophages are recruited to the tumor environment and through an immune editing (desensitization) process compromise the immune system's ability to recognize cancer cells. Cellular immortality is accomplished by upregulation of telomerase to add DNA protective telomeres to dividing cancer cells. To support cancer cell mobilization, the wound healing epithelial-to-mesenchymal transition (EMT) process is co-opted to prepare cancer cells for movement out of the tumor. Metastatic cancer cells change structure, activate antiapoptotic pathways (i.e., Bcl-2 upregulation), and reprogram metabolism (aerobic glycolysis) to provide both adenosine triphosphate (ATP) and molecular intermediates to support cell growth. Taken together these characteristics or hallmarks result in a protective microenvironment designed to allow the tumor to function as an internal parasitic structure capable of self-management at both primary and secondary sites.

What then is a therapeutic course that would yield complete local control recognizing that the treatment must address the primary cancer cell, its associate cancer stem and circulating tumor cells, and tumor-associated support cells (i.e., epithelial cells, fibroblasts, etc.) when each demonstrates distinct responsiveness to standard treatments? Combinatorial strategies including multiplexed dosing of chemotherapeutic agents or chemotherapy-radiation sequencing are now widely applied. However, while these treatment variations may well yield improved short-term suppression, they are based on similar molecular strategies and appear not to kill cancer stem cells or even those cells in the G0 state of the cell cycle. Promising new developments in immune checkpoint blockade (i.e., PD-1 and CTLA-4) therapies warrant evaluation as an adjunctive strategy with freezing [15–17]. Tumor mutations at any stage of cancer development give rise to tumor-specific neoantigens. When recognized by the immune system, elimination of cancer cells is probable. However, tumors can employ a host of mechanisms including local immune suppression, induction of T-cell tolerance, and immune editing to defend themselves from destruction by the immune system. Since many previous cancer immunotherapies have likely been limited by these immunosuppressive mechanisms, and since

cryoablation is known to be an immune system activator [18, 19], evaluation of a possible combinatorial treatment strategy is warranted.

Needed is a combinatorial approach that includes the disruption of a cancer cell's defensive pathways (as with radiation and chemotherapy) but also amplification of stressor levels, thereby subjecting the cancer cell to additional defensive pathway disruption and even physical (damaging) challenges. Reports of such a treatment strategy have appeared recently from in vitro models that utilized staged combinations of cytotoxic agents and an energy deprivation event that would maximize free radical accumulation [20]. Freezing (cryoablation), when sequenced with cell stressors such as chemotherapeutic agents, initiates additional modes of cell death in all resident tumor cells with the additive benefit of physical disruption of >50–75 % of the total cell population. This occurs independent of cell cycle stage. The physical destruction is unrelated to molecular-based properties and pathways and related only to water-solute composition. In effect, if an appropriate nadir temperature is reached, intracellular freezing and complete cell death are unavoidable whether the cell is quiescent or dividing.

Cryosensitization: Combinatorial Strategies

Freeze zone imaging (ultrasound, computed tomography, or magnetic resonance imaging) is essential to ablative precision but fails to predict the outcome of the cryosurgical procedure [21–23]. This is caused by the uncertainty of tumor cells' exposure to lethal temperatures, especially at the margin of the freeze zone where only extracellular freezing is likely. Without exposure to an ablative nadir temperature, tumor recurrence may result from nonlethal freeze conditions and tissue morbidity associated with freezing adjacent anatomical structures [24–26]. These two limitations would be overcome if tissue sensitization was capable of "making ice lethal at 0 °C." The goal then with sensitization would be to make the boundary of the ice front completely lethal to cancer, thereby providing the physician with an unparalleled degree of precision. First attempts at sensitization have been accomplished by freeze-thaw cycling. Recent strategies rely on the use of cryoadjunctive agents in combination with freezing. These agents may either potentiate the physical effects of the freezing process and/or activate cellular stress responses that launch cell death cascades and/or inhibit cell survival/repair mechanisms. Cryosensitization studies in prostate cancer to date include activation of membrane death domain receptors using tumor necrosis factor-alpha (TNF-α[alpha]) [27–30] and tumor necrosis factor-related apoptosis-inducing ligand (TRAIL) [31] in combination with mild freezing (>−10 °C). The use of chemotherapeutic agents in combination with freezing has also shown benefit [28, 32–35]. Numerous other studies have reported similar outcomes with various adjuvants in cancers of the kidney, liver, skin, pancreas, lung, and colorectum [36–46]. Five categories of cryoadjuvants have been identified and include (1) thermophysical adjuvants, (2) chemotherapeutics, (3) pro-inflammatory cytokines or vascular-based agents, (4) immunomodulators, and (5) nutraceutical-based sensitization. The mechanism of action of these agents often overlaps and/or amplifies the molecular action of freezing thereby resulting in enhanced cell death.

Thermophysical Processes: Freeze-Thaw Cycling

Freeze-thaw cycling is a common practice [47–50]. Treatment protocols rely on repeated rapid freezing followed by slow (passive) thawing. Cryosurgical instruments typically provide a device-based maximum freeze rate related to cryoprobe diameter and cryogen type. The progress of the freeze is monitored by ultrasound to assure precise boundary control. Since a temperature gradient between the cryoprobe surface and freeze zone margin exists, freezing beyond the tumor margin is common and necessary to assure the delivery of the planned nadir temperature to the tumor margin. Herein lies a weakness of cryoablation: by relying on an "over-freeze"

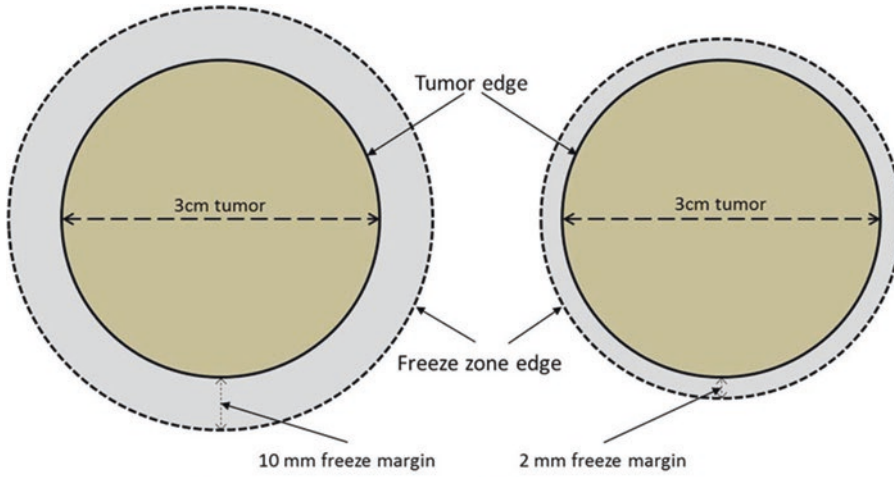

Impact of a Positive Freeze Margin on Targeted vs. Non-Targeted Frozen Tissue Volume (cm^3)

	Positive Freeze Margin (mm)			
	10 mm	5 mm	2 mm	1 mm
Tumor	14.13	14.13	14.13	14.13
Iceball	65.42	33.49	20.57	17.15
Margin	51.29	19.36	6.44	3.02
% Volume of Margin	78%	58%	31%	18%

Fig. 29.1 Volumetric analysis of freeze margins. The volume of the freeze margin, as a percentage of the total frozen volume, was calculated for a hypothetical tumor 3 cm in diameter (14.13 cm^3) with positive margins of 10 mm, 5 mm, 2 mm, and 1 mm. Note that all geometries were assumed to be spherical. For a 10 mm positive freeze margin, the ice ball had a total volume of 65.42 cm^3, but 78 % (51.29 cm^3) was comprised of nontargeted tissue. With a 2 mm positive margin, the nontargeted frozen tissue volume was 6.44 cm^3 or 31 % of the total frozen volume. Reducing the freeze margins greatly reduced the volume of nontargeted tissue ablation

beyond the tumor boundary, non-cancerous tissues may experience partial damage. Figure 29.1 provides a quantitative representation of the impact of freezing beyond the tumor margin. Since freezing typically creates a nearly spherical zone of destruction, the level of nontargeted tissue damage always exceeds in volume that of the target tissue when a 1 cm "over-freeze" is applied to a lesion, which equates to over 75 % of the total frozen mass in non-cancerous tissue.

The historical strategy for limiting the extent of peripheral damage has been the use of a double freeze-thaw cycle. Figure 29.2 illustrates the advantage of a double freeze-thaw cycle in a PC3 prostate cancer tissue-engineered model [39]. The −40 °C isotherm approximates the lethal temperature with the first freeze. When a second freeze is applied, the −40 °C isotherm extends distally, and the lethal temperature is elevated to approximately −30 °C, thereby permitting a reduction in the extent of the "over-freeze" necessary to ablate.

The cell death illustrated in Fig. 29.2 represents a combination of physical destruction from the ice, necrosis from partially damaged cells not able to self-repair and apoptosis or gene-regulated cell death. The observation that cell death unrelated to physical damage is significant [30]. Radiation, many forms of chemotherapy, and hormonal ablation each induce apoptosis as the primary mechanism of cancer cell destruction. However, repetitive dosing often results in long-term resistance to subsequent treatments following activation of defensive mutations [1–3, 51].

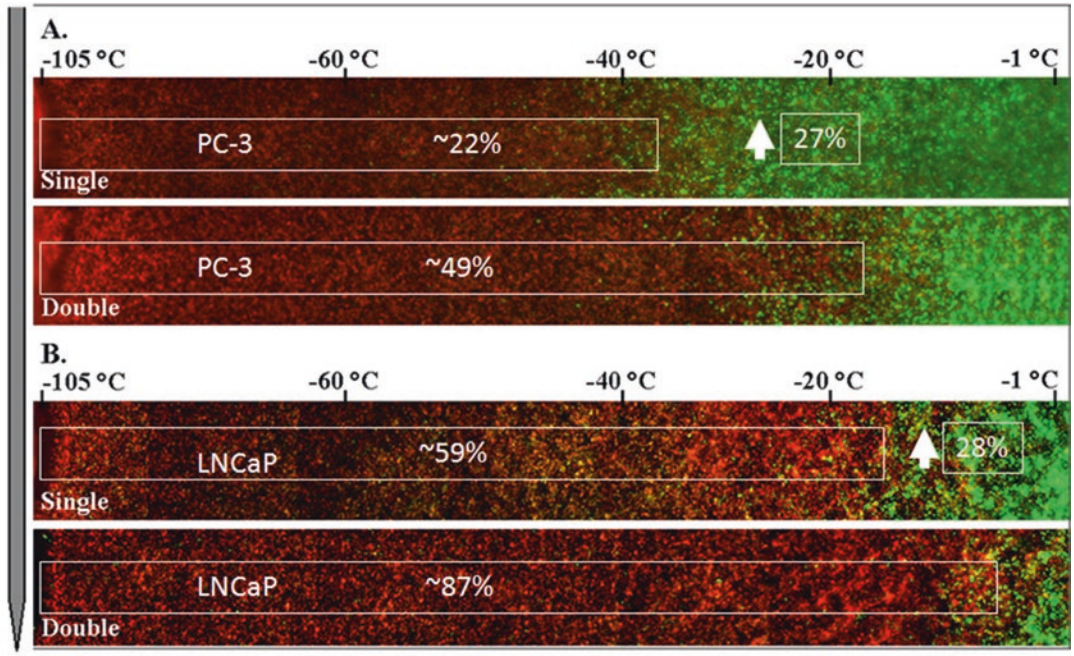

Fig. 29.2 Twenty-four hours post-freeze in a tissue-engineered prostate model (pTEM). A 17-gauge cryoprobe was used to freeze pTEM models seeded with (**a**) PC-3 cells or (**b**) LNCaP cells for either a single or double 10-min freeze event with thermocouple temperature monitoring. Samples were stained and visualized 24 h post-freeze with calcein AM (*green*) to assess live cells and propidium iodide (*red*) to assess dead cells. Fluorescent images were acquired using a Zeiss Axiovert 200 beginning at the center of the lesion (*left of image*) to the periphery of the lesion (*right of image*). In both androgen-insensitive PC-3 and androgen-sensitive LNCap, a double freeze cycle increases the percentage of cell death by 27 % and 28 %, respectively. Adapted with permission from Klossner DP, Robilotto AT, Clarke DM, VanBuskirk RG, Baust JM, Gage AA, Baust JG. Cryosurgical technique: Assessment of the fundamental variables using human prostate cancer model systems. Cryobiology. 2007;(55): 189–199

Cryoablation, as a single-setting therapy, may well eliminate a cancer cell's ability to launch its repertoire of defensive strategies thereby reducing the probability of disease recurrence.

Thermal responsiveness of prostate cancer cells can be distinct and related to androgen responsiveness. Figure 29.3 illustrates this distinction following a single freeze-thaw exposure. Androgen-sensitive LNCaP LP (low-passage) cells and PC-3 AR (PC-3 transfected with the androgen receptor) are fully ablated at temperatures lower than −20 °C. In contrast, LNCaP HP (high passage) and PC3, which are androgen insensitive, require exposure to nadir temperatures below −40 °C for full ablation. This differential response is linked to differences in "kill switch" activation and apoptotic signal pathway induction (Fig. 29.4). The intrinsic apoptotic pathway operating through the BCL_2/Bax mitochondrial axis is activated at elevated subfreezing temperatures (−15 °C) as illustrated by pro-caspase 9 cleavage. This contrasts with the Fas/Fas ligand membrane-mediated extrinsic pathway, which relies on caspase 8 activation. Pro-caspase 8 cleavage does not occur until exposure to lower temperatures approximating −30 °C. This dual temperature induction of different apoptotic signaling pathways [52] has been described as an apoptotic wave launched adjacent to the cryoprobe (extrinsic pathway) and radiating distally to the tumor margin (intrinsic pathway). This discovery is critical to optimizing cryoablation as it provides information on the design prospects on the use of adjuvants.

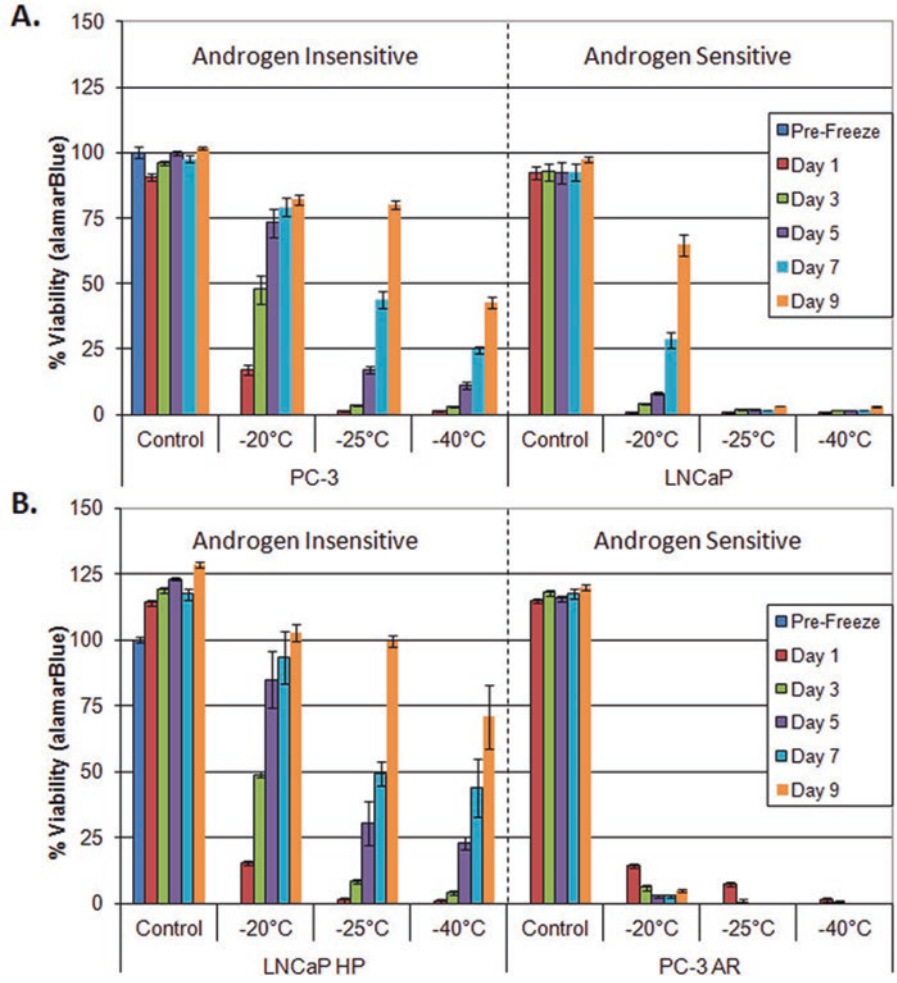

Fig. 29.3 Androgen responsiveness impacts cellular response to freezing. Prostate cancer cell lines (**a**) PC-3 (AI) and LNCaP (AS) or (**b**) LNCaP HP (AI) and PC-3 AR (AS) were seeded in costar strip well plates at 18,000 cells per well 2 days prior to experimentation. 2D monolayers were cooled to nadir temperatures of −20 °C, −25 °C, or −40 °C for 3 min and held for an additional 12 min prior to thawing and recovery incubation. Samples were assessed for post-freeze viability with the metabolic indicator assay alamarBlue every other day for 9 days. Results show that androgen-insensitive PC-3 cells and high passage (HP) LNCaP cells both recover after freezing excursions as low as −40 °C. However, androgen-sensitive cell lines LNCaP and PC-3 AR (PC-3 stably transfected with the androgen receptor) both yield complete ablation at temperatures below −20 °C. Adapted from Klossner DP, Baust JM, VanBuskirk RG, Gage AA, Baust JG. Cryoablative response of prostate cancer cells is influenced by androgen receptor expression. BJU Int. 2008;101(10):1310–6

Thermophysical Adjuvants

The addition of agents that affect the structure of ice with the intent of enhancing lethality constitutes the breadth of thermophysical adjuvants [53, 54]. These agents include antifreeze proteins, salts, and amino acids that when delivered in sufficient doses have elevated the injury threshold to −15 °C in vitro [41, 55–57].

Chemotherapeutics

There are many chemotherapy drugs used clinically that can be grouped by their mechanism of action. Alkylating agents cause damage to DNA; antimetabolites inhibit proper DNA/RNA synthesis by disrupting nucleotides; and mitotic inhibitors interfere with microtubules or spindle formation to prohibit cell division. Corticosteroids

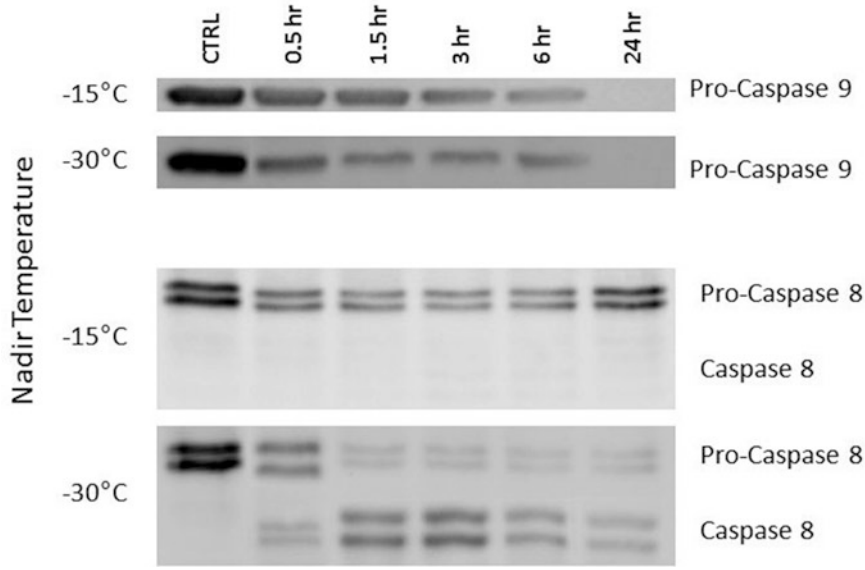

Fig. 29.4 Differential apoptotic protein levels for prostate cancer cells frozen to −15 °C and −30 °C. Cell cultures (PC3 cells) were frozen to nadir temperatures of −15 °C or −30 °C for 15 min in a refrigerated circulating bath. Total protein was extracted at 0.5, 1.5, 3, 6, and 24 h post-thaw and western blots performed with 30 μ(mu)g protein. Blots were assessed for the presence of β(beta)-tubulin (loading control, not shown), caspase-9, and caspase-8. Caspase-9 is associated with the intrinsic, or mitochondrial-mediated, apoptotic pathway, and its activation was found to occur by 3 h post-thaw for cells frozen to −15 °C and by 1.5 h post-thaw for cells frozen to −30 °C. Caspase-8 is associated with the extrinsic, or membrane-mediated, apoptotic pathway, and its activation was not observed following freezing to −15 °C, but for cells frozen to −30 °C, caspase-8 activation occurred by 0.5 h post-thaw. These data indicate that the mitochondrial and membrane-mediated apoptotic pathways are differentially activated following freezing based on the severity of the freeze insult. Adapted from Robilotto AT, Baust JM, Van Buskirk RG, Gage AA, Baust JG. Temperature-dependent activation of differential apoptotic pathways during cryoablation in a human prostate cancer model. Prostate Cancer Prostatic Dis. 2013;16(1): 41–49 [52]

are often given in conjunction with one or more chemo drugs to prevent adverse reactions and improve outcomes. Advances have been made in the dosing and selection of drugs best suited to various cancer types. However, one-size-fits-all cancer therapies have proven limited, and patients in advanced stages of cancer fail to respond to treatment except for modest survival benefits.

The systemic application of chemotherapy causes collateral damage to healthy cells in addition to the destruction of cancerous targets. Due to their high metabolic rate, cells of the bone marrow, hair follicles, mouth, digestive tract, and reproductive system are the most likely to be affected by chemotherapy [58]. Side effects vary but can often be severe. A major culprit is the standard approach to administering treatment with the maximum tolerated doses of cytotoxic cocktails, which leads to a compromised immune system and a poor quality of life. Additionally, clinical trials do not account for patients' different responses with the same cancer type (anatomical).

The challenge, then, is to determine which therapy or combination of therapies is/are the right therapy and optimal for every patient. Now that we have an initial understanding of the cell death pathways that initiate following a freeze-thaw excursion, a logical design for a secondary cell stressor use can be developed with the goal of making ice lethal at or near 0 °C thereby yielding complete cancer destruction as visualized by real-time ultrasound [59, 60].

Peplomycin and Adriamycin in combination with freezing were first reported in 1985 in a murine tumor model [61]. It was hypothesized

that freeze concentration of the anticancer drugs occurred, which resulted in increased cell death post-thaw. Following the identification of apoptosis as a significant mode of cell death in the periphery of the freeze zone [62], the concept of apoptotic enhancement emerged [28, 39]. When combined with cryosurgery, these agents (i.e., 5-fluorouracil, cisplatin, Taxotere, doxorubicin, mitomycin, bleomycin, vinorelbine, Navelbine, and TRAIL) function to directly activate apoptotic pathways at elevated subfreezing temperatures but not by freeze concentration [31, 33, 34, 37, 38, 63, 64]. Similar results have been reported with radiation/cryo combination [65, 66].

TNF-α(alpha), a pro-inflammatory cytokine, in combination with cryosurgery has been shown to destroy tumors up to the freeze zone edge (−0.5 °C) [27, 30, 67]. The mechanism(s) by which pro-inflammatory cytokines act in combination with freezing in vivo is uncertain as they have direct actions on the cancer cell, the tumor vasculature, and the immune response [44, 68–73].

Nutraceuticals

Unfortunately, the use of many cytotoxic agents as cryosensitizers results in problematic comorbidities common to chemotherapy alone. Successful cryosensitization strategies now focus on the use of nutraceuticals (natural anticancer agents) such as vitamin D_3 (VD_3). Prostate cancer sensitivity to freezing injury has been shown to increase with the application of calcitriol, the active metabolite of VD_3 [46, 74, 75]. Experimentally, exposure of prostate cancer to VD_3 prior to freezing results in complete cancer destruction at temperatures of ~−5° to −10 °C independent of the prostate cancer's androgen sensitivity status (Fig. 29.5). Given that a large number of cancer cell types retain the vitamin D_3 receptor (VDR), various in vitro studies have shown the promise of vitamin D_3 and analogues in the treatment of lung [76], prostate [46, 74, 75], colon [77, 78]), breast [79–81], and pancreatic [82] cancers. Many of the antiproliferative effects of calcitriol stem from its effects on cell cycle regulatory proteins. The upregulation of cyclin-dependent kinase (CDK) inhibitors p21 and p27 and upregulation of insulin-like growth factor-binding protein (IGFBP-3) lead to cell cycle arrest [83]. In MCF-7 breast cancer cells, calcitriol induces apoptosis through Bax translocation and subsequent mitochondrial-mediated caspase activation [84]. Calcitriol has been shown to decrease inflammation in several cancers through inhibition of prostaglandin synthesis [85], inhibition of nuclear factor-κ(kappa)B (NF-κ[kappa]B) signaling [86, 87], and inhibition of pro-inflammatory cytokine production [88].

When applied clinically, the dosage of calcitriol necessary to achieve a similar level of cell death to in vitro studies has proved problematic. High doses of calcitriol often lead to hypercalcemia, though it has been observed that this can be reduced when doses are given on a weekly basis rather than daily [89]. Calcitriol analogues have been developed that aim to minimize calcemic effects while maintaining antiproliferative actions, although reports have suggested that calcitriol and its analogues have little benefit unless combined with a second treatment modality [90]. Elevation of the vitamin D3 titer as a mechanism of cancer prevention has been an area of interest explored in recent clinical trials [91, 92], results of which should be available within the next year.

Another nutraceutical-based study involves the use of the potent free radical scavenger resveratrol, which showed that pretreatment of renal and prostate cancer cells yields freeze sensitization with complete cell death following exposure to temperatures below −10 °C [93]. In addition, several other studies have shown promise in increasing cancer cell sensitivity to freezing. These include (1) targeted activation of cell death pathways and inhibition of survival pathways [94], (2) the destructive effects of targeting cell attachment pathways (integrin inhibition) [95], (3) protein kinase B (AKT) pathway cell survival [96], (4) mitochondrial stress enhancement [32, 42, 97], (5) endoplasmic reticulum stress [98], (6) autophagy (or autophagocytosis), etc. These agents are designed to increase the lethality of mild freezing while having little or no negative side effects. This is especially true in prostate

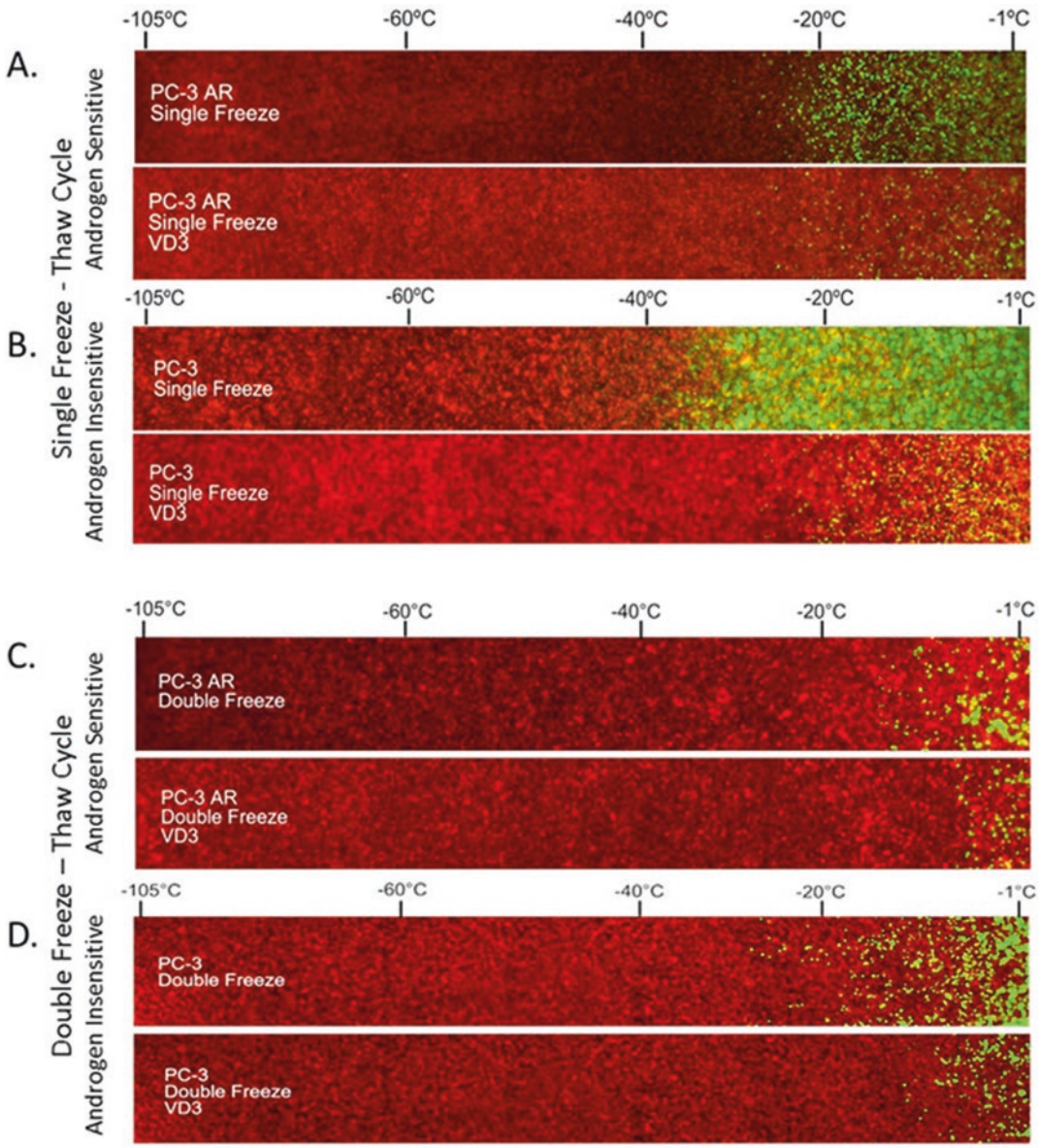

Fig. 29.5 Assessment of freeze-thaw cycling and VD3 treatment on androgen-sensitive and androgen-insensitive prostate cancer sensitivity to cryoablation. Tissue-engineered matrices containing untreated or VD_3-treated androgen-sensitive (PC-3 AR) and androgen-insensitive (PC-3) prostate cancer cells were subjected to 10-min freeze cycles applied in a single freezing cycle (**a** and **b**) or a double freezing cycle (**c** and **d**) followed by return to 37 °C. Twenty-four hours post-thaw matrices were probed with calcein AM (*green*, live cells) and propidium iodide (*red*, dead cells). A 50× panoramic series of fluorescent micrographs was taken extending from the center near the cryoprobe tip (*left of images*) to the periphery of the ice sphere (*right of image*). Compared to freeze alone, VD_3 treatment prior to freezing resulted in enhanced cell death following either a single of double freeze event in both the AS and AI populations

cancer cryoablation where avoidance of damage to adjacent structures (i.e., neurovascular bundles and rectal wall) is necessary to prevent postsurgical complications. Further, several studies have focused on tissue protective strategies while enhancing ablative outcome [99–101].

Conclusion

Cryoablation has been shown to provide long-term effectiveness in the treatment of prostatic and renal cancers with minimal morbidity [102–104]. As with any therapy, precision becomes essential to reduce damage to adjacent, nontargeted tissues. In today's clinical practice, the lethal temperature provides a complete ablative dose provided the <−40 °C isotherm is extended further into the tumor mass by a repetitive freeze-thaw cycle. To provide this dose, freezing is necessarily extended, an over-freeze, up to 1 cm beyond the tumor margin, or in the case of whole gland targeting, beyond the capsule margin. Numerous in vitro studies have demonstrated that tissue freeze sensitization can be accomplished through biophysical or molecular biological perturbations. While the presence of ice within the targeted tissue has been considered to be the mechanism by which tumor ablation is accomplished, it is now recognized that ice per se is lethal primarily at the intracellular level and less so when it is restricted to the extracellular environment within the tumor margin. It is this zone with nominal temperatures of −20 °C to 0 °C that is characterized by potential cell survival and is subject to adjuvant intervention by biophysical and/or molecular biological mechanisms. We describe a number, not all, of combinatorial strategies that offer promise to enhance the lethality of all cells within the tumor microenvironment.

References

1. Li Y, Zou L, Li Q, Haibe-Kains B, Tian R, Desmedt C, et al. Amplification of laptm4b and ywhaz contributes to chemotherapy resistance and recurrence of breast cancer. Nat Med. 2010;16(2):214–8.
2. Balko JM, Cook RS, Vaught DB, Kuba MG, Miller TW, Bhola NE, et al. Profiling of residual breast cancers after neoadjuvant chemotherapy identifies dusp4 deficiency as a mechanism of drug resistance. Nat Med. 2012;18(7):1052–9.
3. Sun Y, Campisi J, Higano C, Beer TM, Porter P, Coleman I, et al. Treatment-induced damage to the tumor microenvironment promotes prostate cancer therapy resistance through wnt16b. Nat Med. 2012;18(9):1359–68.
4. Gupta A, Yang Q, Pandita RK, Hunt CR, Xiang T, Misri S, et al. Cell cycle checkpoint defects contribute to genomic instability in pten deficient cells independent of DNA dsb repair. Cell Cycle. 2009;8(14):2198–210.
5. Pajonk F, Vlashi E, McBride WH. Radiation resistance of cancer stem cells: the 4 r's of radiobiology revisited. Stem Cells. 2010;28(4):639–48.
6. Rosser CJ, Gaar M, Porvasnik S. Molecular fingerprinting of radiation resistant tumors: can we apprehend and rehabilitate the suspects? BMC Cancer. 2009;9:225.
7. Tokunaga E, Kimura Y, Mashino K, Oki E, Kataoka A, Ohno S, et al. Activation of pi3k/akt signaling and hormone resistance in breast cancer. Breast Cancer. 2006;13(2):137–44.
8. Vesuna F, Lisok A, Kimble B, Domek J, Kato Y, Groep P, et al. Twist contributes to hormone resistance in breast cancer by downregulating estrogen receptor-alpha. Oncogene. 2012;31(27):3223–34.
9. Hoimes CJ, Kelly WK. Redefining hormone resistance in prostate cancer. Ther Adv Med Oncol. 2010;2(2):107–23.
10. Seruga B, Ocana A, Tannock IF. Drug resistance in metastatic castration-resistant prostate cancer. Nat Rev Clin Oncol. 2011;8(1):12–23.
11. Coventry BJ, Ashdown ML. Complete clinical responses to cancer therapy caused by multiple divergent approaches: a repeating theme lost in translation. Cancer Manag Res. 2012;4:137–49.
12. Sturge J, Caley MP, Waxman J. Bone metastasis in prostate cancer: emerging therapeutic strategies. Nat Rev Clin Oncol. 2011;8(6):357–68.
13. Baust JG, Bischof JC, Jiang-Hughes S, Polascik TJ, Rukstalis DB, Gage AA, et al. Re-purposing cryoablation: a combinatorial 'therapy' for the destruction of tissue. Prostate Cancer Prostatic Dis. 2015;18(2):87–95.
14. Hanahan D, Weinberg RA. Hallmarks of cancer: the next generation. Cell. 2011;144(5):646–74.
15. Quezada SA, Peggs KS. Exploiting ctla-4, pd-1 and pd-l1 to reactivate the host immune response against cancer. Br J Cancer. 2013;108(8):1560–5.
16. Mahoney KM, Freeman GJ, McDermott DF. The next immune-checkpoint inhibitors: Pd-1/pd-l1 blockade in melanoma. Clin Ther. 2015;37(4):764–82.
17. Postow MA, Callahan MK, Wolchok JD. Immune checkpoint blockade in cancer therapy. J Clin Oncol. 2015;33(17):1974–82.
18. Sabel MS, Arora A, Su G, Chang AE. Adoptive immunotherapy of breast cancer with lymph node cells primed by cryoablation of the primary tumor. Cryobiology. 2006;53(3):360–6.
19. Sabel MS, Su G, Griffith KA, Chang AE. Rate of freeze alters the immunologic response after cryoablation of breast cancer. Ann Surg Oncol. 2010;17(4):1187–93.
20. Bost F, Decoux-Poullot AG, Tanti JF, Clavel S. Energy disruptors: rising stars in anticancer therapy? Oncogenesis. 2016;5:e188.

21. Gilbert JC, Rubinsky B, Roos MS, Wong ST, Brennan KM. Mri-monitored cryosurgery in the rabbit brain. Magn Reson Imaging. 1993;11(8):1155–64.
22. Onik G, Rubinsky B, Zemel R, Weaver L, Diamond D, Cobb C, et al. Ultrasound-guided hepatic cryosurgery in the treatment of metastatic colon carcinoma. Preliminary Results Cancer. 1991;67(4):901–7.
23. Onik GM, Cohen JK, Reyes GD, Rubinsky B, Chang Z, Baust J. Transrectal ultrasound-guided percutaneous radical cryosurgical ablation of the prostate. Cancer. 1993;72(4):1291–9.
24. Caso JR, Tsivian M, Mouraviev V, Kimura M, Polascik TJ. Complications and postoperative events after cryosurgery for prostate cancer. BJU Int. 2012;109(6):840–5.
25. Pitman M, Shapiro EY, Hruby GW, Truesdale MD, Cheetham PJ, Saad S, et al. Comparison of biochemical failure definitions for predicting local cancer recurrence following cryoablation of the prostate. Prostate. 2012;72(16):1802–8.
26. Saliken JC, Donnelly BJ, Rewcastle JC. The evolution and state of modern technology for prostate cryosurgery. Urology. 2002;60(2 Suppl 1):26–33.
27. Goel R, Swanlund D, Coad J, Paciotti GF, Bischof JC. TNF-alpha-based accentuation in cryoinjury–dose, delivery, and response. Mol Cancer Ther. 2007;6(7):2039–47.
28. Goel R, Anderson K, Slaton J, Schmidlin F, Vercellotti G, Belcher J, et al. Adjuvant approaches to enhance cryosurgery. J Biomech Eng. 2009;131(7):074003.
29. Han B, Swanlund DJ, Bischof JC. Cryoinjury of mcf-7 human breast cancer cells and inhibition of post-thaw recovery using tnf-alpha. Technol Cancer Res Treat. 2007;6(6):625–34.
30. Jiang J, Goel R, Iftekhar MA, Visaria R, Belcher JD, Vercellotti GM, et al. Tumor necrosis factor-alpha-induced accentuation in cryoinjury: mechanisms in vitro and in vivo. Mol Cancer Ther. 2008;7(8):2547–55.
31. Clarke DM, Robilotto AT, VanBuskirk RG, Baust JG, Gage AA, Baust JM. Targeted induction of apoptosis via trail and cryoablation: a novel strategy for the treatment of prostate cancer. Prostate Cancer Prostatic Dis. 2007;10(2):175–84.
32. Clarke DM, Baust JM, Buskirk RG, Baust JG. Addition of anticancer agents enhances freezing-induced prostate cancer cell death: implications of mitochondrial involvement. Cryobiology. 2004;49(1):45–61.
33. Clarke DM, Baust JM, Van Buskirk RG, Baust JG. Chemo-cryo combination therapy: an adjunctive model for the treatment of prostate cancer. Cryobiology. 2001;42(4):274–85.
34. Pivert P, Haddad RS, Aller A, Titus K, Doulat J, Renard M, et al. Ultrasound guided combined cryoablation and microencapsulated 5-fluorouracil inhibits its growth of human prostate tumors in xenogenic mouse model assessed by luminescence imaging. Technol Cancer Res Treat. 2004;3(2):135–42.
35. Clarke DM, Hollister WR, Baust JG, Van Buskirk RG. Cryosurgical modeling: sequence of freezing and cytotoxic agent application affects cell death. Mol Urol. 1999;3(1):25–31.
36. Baust JG, Gage AA, Clarke D, Baust JM, Van Buskirk R. Cryosurgery-a putative approach to molecular-based optimization. Cryobiology. 2004;48(2):190–204.
37. Forest V, Peoc'h M, Campos L, Guyotat D, Vergnon JM. Effects of cryotherapy or chemotherapy on apoptosis in a non-small-cell lung cancer xenografted into scid mice. Cryobiology. 2005;50(1):29–37.
38. Forest V, Peoc'h M, Campos L, Guyotat D, Vergnon JM. Benefit of a combined treatment of cryotherapy and chemotherapy on tumour growth and late cryo-induced angiogenesis in a non-small-cell lung cancer model. Lung Cancer. 2006;54(1):79–86.
39. Baust JG, Gage AA, Robilottto AT, Baust JM. The pathophysiology of thermoablation: optimizing cryoablation. Curr Opin Urol. 2009;19(2):127–32.
40. Gu XY, Jiang Z, Fang W. Cryoablation combined with molecular target therapy improves the curative effect in patients with advanced non-small cell lung cancer. J Int Med Res. 2011;39(5):1736–43.
41. Han B, Iftekhar A, Bischof JC. Improved cryosurgery by use of thermophysical and inflammatory adjuvants. Technol Cancer Res Treat. 2004;3(2):103–11.
42. Hanai A, Yang WL, Ravikumar TS. Induction of apoptosis in human colon carcinoma cells ht29 by sublethal cryo-injury: mediation by cytochrome c release. Int J Cancer. 2001;93(4):526–33.
43. Kuflik EG. Cryosurgery for skin cancer: 30-year experience and cure rates. Dermatol Surg. 2004;30(2 Pt 2):297–300.
44. Redondo P, Olmo J, Lopez-Diaz de Cerio A, Inoges S, Marquina M, Melero I, et al. Imiquimod enhances the systemic immunity attained by local cryosurgery destruction of melanoma lesions. J Invest Dermatol. 2007;127(7):1673–80.
45. Rodriguez-Bigas MA, Klippenstein D, Meropol NJ, Weber TK, Petrelli NJ. A pilot study of cryochemotherapy for hepatic metastases from colorectal cancer. Cryobiology. 1996;33(6):600–6.
46. Santucci KL, Snyder KK, Baust JM, Van Buskirk RG, Mouraviev V, Polascik TJ, et al. The use of 1,25a dihydroxyvitamin D3 as a cryosensitizing agent in a murine prostate cancer model. Prostate Cancer Prostatic Dis. 2011;14(2):97–104.
47. Staren ED, Sabel MS, Gianakakis LM, Wiener GA, Hart VM, Gorski M, et al. Cryosurgery of breast cancer. Arch Surg. 1997;132(1):28–33. discussion 34
48. Neel 3rd HB, Ketcham AS, Hammond WG. Requisites for successful cryogenic surgery of cancer. Arch Surg. 1971;102(1):45–8.
49. Gill W, Fraser J, Carter DC. Repeated freeze-thaw cycles in cryosurgery. Nature. 1968;219(5152):410–3.
50. Gage AA, Augustynowicz S, Montes M, Caruana JA, Whalen Jr DA. Tissue impedance and temperature measurements in relation to necrosis in experimental cryosurgery. Cryobiology. 1985;22(3):282–8.

51. Ghisolfi L, Keates AC, Hu X, Lee DK, Li CJ. Ionizing radiation induces stemness in cancer cells. PLoS One. 2012;7(8):e43628.
52. Robilotto AT, Baust JM, Buskirk RG, Gage AA, Baust JG. Temperature-dependent activation of differential apoptotic pathways during cryoablation in a human prostate cancer model. Prostate Cancer Prostatic Dis. 2013;16(1):41–9.
53. Muldrew K, Rewcastle J, Donnelly BJ, Saliken JC, Liang S, Goldie S, et al. Flounder antifreeze peptides increase the efficacy of cryosurgery. Cryobiology. 2001;42(3):182–9.
54. Pham L, Dahiya R, Rubinsky B. An in vivo study of antifreeze protein adjuvant cryosurgery. Cryobiology. 1999;38(2):169–75.
55. Han B, Bischof JC. Direct cell injury associated with eutectic crystallization during freezing. Cryobiology. 2004;48(1):8–21.
56. Wang CL, Teo KY, Han B. An amino acidic adjuvant to augment cryoinjury of mcf-7 breast cancer cells. Cryobiology. 2008;57(1):52–9.
57. Koushafar H, Rubinsky B. Effect of antifreeze proteins on frozen primary prostatic adenocarcinoma cells. Urology. 1997;49(3):421–5.
58. Society AC. Chemotherapy basics. American Cancer Society: treatments and side effects; 2016. http://www.cancer.org/treatment/treatmentsandsideeffects/treatmenttypes/chemotherapy/index.
59. Baust JM, Robilotto AT, Gage AA, Baust JG, editors. Enhanced ablative methodologies. Singapore: World Scientific Publishing; 2016.
60. Soon-Shiong P. From small steps to a giant leap: defining the future of cancer medicine. AUA News. 2016;21(4):1–3.
61. Ikekawa S, Ishihara K, Tanaka S, Ikeda S. Basic studies of cryochemotherapy in a murine tumor system. Cryobiology. 1985;22(5):477–83.
62. Hollister WR, Mathew AJ, Baust JG, et al. The effects of freezing on cell viability and mechanisms of cell death in an in vitro human prostate cancer cell line. Mol Urol. 1998;2(1):13–8.
63. Mir LM, Rubinsky B. Treatment of cancer with cryochemotherapy. Br J Cancer. 2002;86(10):1658–60.
64. Yuan F, Zhou W, Zhang J, Zhang Z, Zou C, Huang L, et al. Anticancer drugs are synergistic with freezing in induction of apoptosis in hcc cells. Cryobiology. 2008;57(1):60–5.
65. Xu KC, Niu LZ, Hu YZ, He WB, He YS, Li YF, et al. A pilot study on combination of cryosurgery and (125)iodine seed implantation for treatment of locally advanced pancreatic cancer. World J Gastroenterol. 2008;14(10):1603–11.
66. Xu KC, Niu LZ, Hu YZ, He WB, He YS, Zuo JS. Cryosurgery with combination of (125)iodine seed implantation for the treatment of locally advanced pancreatic cancer. J Dig Dis. 2008;9(1):32–40.
67. Shenoi MM, ltis I I, Choi J, Koonce NA, Metzger GJ, Griffin RJ, et al. Nanoparticle delivered vascular disrupting agents (VDAS): use of tnf-alpha conjugated gold nanoparticles for multimodal cancer therapy. Mol Pharmaceutics. 2013;10(5):1683–94.
68. Udagawa M, Kudo-Saito C, Hasegawa G, Yano K, Yamamoto A, Yaguchi M, et al. Enhancement of immunologic tumor regression by intratumoral administration of dendritic cells in combination with cryoablative tumor pretreatment and bacillus calmette-guerin cell wall skeleton stimulation. Clin Cancer Res. 2006;12(24):7465–75.
69. Gazzaniga S, Bravo A, Goldszmid SR, Maschi F, Martinelli J, Mordoh J, et al. Inflammatory changes after cryosurgery-induced necrosis in human melanoma xenografted in nude mice. J Invest Dermatol. 2001;116(5):664–71.
70. Brok MH, Sutmuller RP, Nierkens S, Bennink EJ, Toonen LW, Figdor CG, et al. Synergy between in situ cryoablation and tlr9 stimulation results in a highly effective in vivo dendritic cell vaccine. Cancer Res. 2006;66(14):7285–92.
71. Sabel MS. Cryo-immunology: a review of the literature and proposed mechanisms for stimulatory versus suppressive immune responses. Cryobiology. 2009;58(1):1–11.
72. Waitz R, Solomon SB, Petre EN, Trumble AE, Fasso M, Norton L, et al. Potent induction of tumor immunity by combining tumor cryoablation with anti-ctla-4 therapy. Cancer Res. 2012;72(2):430–9.
73. Yuanying Y, Lizhi N, Feng M, Xiaohua W, Jianying Z, Fei Y, et al. Therapeutic outcomes of combining cryotherapy, chemotherapy and dc-cik immunotherapy in the treatment of metastatic non-small cell lung cancer. Cryobiology. 2013;67(2):235–40.
74. Baust JM, Klossner DP, Robilotto A, Vanbuskirk RG, Gage AA, Mouraviev V, et al. Vitamin D(3) cryosensitization increases prostate cancer susceptibility to cryoablation via mitochondrial-mediated apoptosis and necrosis. BJU Int. 2012;109(6):949–58.
75. Kimura M, Rabbani Z, Mouraviev V, Tsivian M, Caso J, Satoh T, et al. Role of vitamin D(3) as a sensitizer to cryoablation in a murine prostate cancer model: preliminary in vivo study. Urology. 2010;76(3):764.e14–20.
76. Verone-Boyle AR, hoemaker S S, Attwood K, Morrison CD, Makowski AJ, Battaglia S, et al. Diet-derived 25-hydroxyvitamin d3 activates vitamin D receptor target gene expression and suppresses EGFR mutant non-small cell lung cancer growth in vitro and in vivo. Oncotarget. 2016;7(1):995–1013.
77. Chen S, Zhu J, Zuo S, Ma J, Zhang J, Chen G, et al. 1,25(oh)2d3 attenuates tgf-beta1/beta2-induced increased migration and invasion via inhibiting epithelial-mesenchymal transition in colon cancer cells. Biochem Biophys Res Commun. 2015;468(1–2):130–5.
78. Wierzbicka JM, Binek A, Ahrends T, Nowacka JD, Szydlowska A, Turczyk L, et al. Differential antitumor effects of vitamin D analogues on colorectal carcinoma in culture. Int J Oncol. 2015;47(3):1084–96.

79. Garcia-Becerra R, Diaz L, Camacho J, Barrera D, Ordaz-Rosado D, Morales A, et al. Calcitriol inhibits ether-a go-go potassium channel expression and cell proliferation in human breast cancer cells. Exp Cell Res. 2010;316(3):433–42.
80. Ferronato MJ, Obiol DJ, Fermento ME, Gandini NA, Alonso EN, Salomon DG, et al. The alkynylphosphonate analogue of calcitriol em1 has potent anti-metastatic effects in breast cancer. J Steroid Biochem Mol Biol. 2015;154:285–93.
81. Johnson AL, Zinser GM, Waltz SE. Vitamin D3-dependent vdr signaling delays ron-mediated breast tumorigenesis through suppression of beta-catenin activity. Oncotarget. 2015;6(18):16304–20.
82. Kanemaru M, Maehara N, Chijiiwa K. Anti-proliferative effect of 1alpha,25-dihydroxyvitamin d3 involves upregulation of cyclin-dependent kinase inhibitor p21 in human pancreatic cancer cells. Hepatogastroenterology. 2013;60(125):1199–205.
83. Krishnan AV, Shinghal R, Raghavachari N, Brooks JD, Peehl DM, Feldman D. Analysis of vitamin D-regulated gene expression in lncap human prostate cancer cells using cdna microarrays. Prostate. 2004;59(3):243–51.
84. Narvaez CJ, Welsh J. Role of mitochondria and caspases in vitamin D-mediated apoptosis of mcf-7 breast cancer cells. J Biol Chem. 2001;276(12):9101–7.
85. Krishnan AV, Feldman D. Molecular pathways mediating the anti-inflammatory effects of calcitriol: implications for prostate cancer chemoprevention and treatment. Endocr Relat Cancer. 2010;17(1): R19–38.
86. Cohen-Lahav M, Shany S, Tobvin D, Chaimovitz C, Douvdevani A. Vitamin D decreases nfkappab activity by increasing ikappabalpha levels. Nephrol Dial Transplant. 2006;21(4):889–97.
87. Bao BY, Yao J, Lee YF. 1Alpha, 25-dihydroxyvitamin D3 suppresses interleukin-8-mediated prostate cancer cell angiogenesis. Carcinogenesis. 2006;27(9): 1883–93.
88. Nonn L, Peng L, Feldman D, Peehl DM. Inhibition of p38 by vitamin D reduces interleukin-6 production in normal prostate cells via mitogen-activated protein kinase phosphatase 5: implications for prostate cancer prevention by vitamin D. Cancer Res. 2006;66(8):4516–24.
89. Schwartz GG. Vitamin D and intervention trials in prostate cancer: from theory to therapy. Ann Epidemiol. 2009;19(2):96–102.
90. Christakos S, Dhawan P, Verstuyf A, Verlinden L, Carmeliet G. Vitamin D: metabolism, molecular mechanism of action, and pleiotropic effects. Physiol Rev. 2016;96(1):365–408.
91. Neale RE, Armstrong BK, Baxter C, Romero BD, Ebeling P, English DR, et al. The d-health trial: a randomized trial of vitamin D for prevention of mortality and cancer. Contemp Clin Trials. 2016;48:83–90.
92. Bassuk SS, Manson JE, Lee IM, Cook NR, Christen WG, Bubes VY, et al. Baseline characteristics of participants in the vitamin D and omega-3 trial (vital). Contemp Clin Trials. 2016;47:235–43.
93. Clarke DM, Robilotto AT, Rhee E, VanBuskirk RG, Baust JG, Gage AA, et al. Cryoablation of renal cancer: variables involved in freezing-induced cell death. Technol Cancer Res Treat. 2007;6(2):69–79.
94. Tian T, Olson S, Whitacre JM, Harding A. The origins of cancer robustness and evolvability. Integr Biol (Camb). 2011;3(1):17–30.
95. Baust JG, Klossner DP, Vanbuskirk RG, Gage AA, Mouraviev V, Polascik TJ, et al. Integrin involvement in freeze resistance of androgen-insensitive prostate cancer. Prostate Cancer Prostatic Dis. 2010;13(2):151–61.
96. Baust JM, Klossner D, Gage A, VanBuskirk RV, Baust JG Akt signaling mediates prostate cancer response to cryoablation. Cryobiology [Abstract]. 2013;67(3):427–428.
97. Yang WL, Addona T, Nair DG, Qi L, Ravikumar TS. Apoptosis induced by cryo-injury in human colorectal cancer cells is associated with mitochondrial dysfunction. Int J Cancer. 2003;103(3):360–9.
98. Corwin WL, Baust JM, Baust JG, Buskirk RG. The unfolded protein response in human corneal endothelial cells following hypothermic storage: implications of a novel stress pathway. Cryobiology. 2011;63(1):46–55.
99. Mouraviev VG, Chin JL, Downey DB, Moussa, M. Image-guided targeted cryoablation for canine prostate model using new cryopreservation cocktail for neurovascular bundle protection. Adv Cryomed. 2001:108–10.
100. Mouraviev VG, Prokhorov D., Prokhorov GA. Rectal and urethral sphincter protection during aggressive prostate cryosurgery: the possible clinical application of special antifreeze cocktail for an injection into anterior and posterior paraprostatic spaces. Adv Cryomed. 2001:111–3.
101. Rubinsky B, inventor Use of cryoprotective agent compounds during cryosurgery. United States patent 6,041,787. 2000 March 17, 1998.
102. Babaian RJ, Donnelly B, Bahn D, Baust JG, Dineen M, Ellis D, et al. Best practice statement on cryosurgery for the treatment of localized prostate cancer. J Urol. 2008;180(5):1993–2004.
103. Baust JG, Gage AA, Bjerklund Johansen TE, Baust JM. Mechanisms of cryoablation: clinical consequences on malignant tumors. Cryobiology. 2014;68(1):1–11.
104. Cohen JK, Miller RJJ, Ahmed S, Lotz MJ, Baust J, et al. Urology. 2008;71(3):515–8.

5-Alpha-Reductase Inhibition as a Secondary Preventive Strategy

30

Nathan Perlis and Antonio Finelli

Introduction

Active Surveillance for Prostate Cancer

Prostate cancer (PCa) is the most common non-skin malignancy in the USA and Canada [1], with approximately a 1-in-7 lifetime risk of diagnosis. Despite this, less than 3 % are estimated to die from prostate cancer [2]. With widespread prostate-specific antigen (PSA) testing, organ-confined, low-risk prostate cancer diagnosis is highly prevalent. Large population studies and clinical trials have emerged that highlight the indolent nature of low-risk prostate cancer and the high morbidity of radical prostatectomy and prostate radiation therapy [3–6]. As such, active surveillance (AS) has emerged as an alternative approach to definitive radiation or surgery in low-risk localized prostate cancer for select men [7].

N. Perlis
Department of Urologic Oncology,
University of Toronto, Toronto, ON, Canada

Division of Urology, Department of Surgical Oncology, University Health Network, Princess Margaret Cancer Centre, Toronto, ON, Canada

A. Finelli (✉)
Division of Urology/Uro-Oncology, Department of Surgical Oncology, Princess Margaret Cancer Centre, Toronto, ON, Canada
e-mail: Antonio.finelli@uhn.ca

In active surveillance protocols, patients are closely monitored with digital rectal examinations (DREs), PSA tests, repeat prostate biopsies, and other ancillary tests and offered definitive treatment should pathologic or clinical progression occur. The safe application of active surveillance relies on several assumptions [8]. First, indolent prostate cancer must have identifiable clinical and pathologic parameters that distinguish it from cancer with metastatic potential. Second, for those patients on active surveillance who are reclassified into a higher-risk category, implementing definitive treatment should not significantly decrease the chance of cure when compared to up-front therapy. Finally, detriment to health-related quality of life from the anxiety of living with prostate cancer and repeated blood tests and biopsies on active surveillance should be better than following surgery or radiation. Without 15-year follow-up, these assumptions are difficult to confirm, but several long-duration series exhibit impressive metastasis-free survival and quality of life for patients on active surveillance [7].

Accordingly, the National Comprehensive Cancer Network and the American Society of Clinical Oncology in the USA, the Canadian Urology Association in Canada, and the National Institute for Health and Clinical Excellence in the UK all suggest active surveillance as the first-line approach for men with low-risk prostate cancer [9–12]. For over a decade, this has translated to

© Springer International Publishing AG 2017

T.J. Polascik (ed.), *Imaging and Focal Therapy of Early Prostate Cancer*,
Current Clinical Urology, DOI 10.1007/978-3-319-49911-6_30

clinical practice evidenced by the fact that the proportion of patients with low-risk disease managed conservatively has increased from about 10 % in 2000 to 35 % in 2010 [13, 14].

5-Alpha-Reductase Inhibitors in Prostate Cancer

5-Alpha-reductase inhibitors (5-ARIs) block the enzyme responsible for generating dihydrotestosterone (DHT) from testosterone. DHT influences both benign and malignant prostate growth, and two medications (finasteride and dutasteride) are approved for medical management of benign prostatic hypertrophy. Dutasteride blocks both isoforms of 5-alpha reductase (types 1 and 2), while finasteride blocks solely type 1. It is hypothesized that by decreasing DHT in the prostate and altering the intraprostatic milieu, 5-ARIs may impair prostate tumor growth and progression. 5-ARIs have clearly been linked to reduction of serum DHT by at least 90 %. Prostate volume in the peripheral zone and transition zone can be reduced by approximately 25 %, and tumors can shrink as well [15, 16]. In fact, there have been two large randomized controlled trials (RCTs) investigating 5-ARIs for primary prostate cancer prevention in various at-risk populations demonstrating a 25 % relative risk reduction of PCa diagnosis compared to placebo [17, 18]. With this in mind, several investigators studied whether or not 5-ARIs could be used for patients already diagnosed with localized prostate cancer as a secondary prevention strategy. For example, could 5-ARIs limit men's pathologic progression and/or receipt of definitive treatment once already diagnosed with low-risk PCa?

In this chapter we review the clinical evidence for using 5-ARIs as secondary prevention for men with very low-, low-, and intermediate-risk PCa on active surveillance. Data from several observational studies and one high-quality randomized controlled trial will be presented. The data is relevant to focal therapy because in many cases, ablation is used to eradicate clinically significant prostate tumors while leaving indolent ones untouched [19]. In these scenarios, men are effectively converted into active surveillance patients and closely monitored as they otherwise would be in an AS cohort. Should patients be prescribed 5-ARIs post-focal ablation to prevent disease progression? Devoid of evidence for secondary prevention of PCa with 5-ARIs in the post-ablation setting, we rely on data from the non-focal literature.

Observational Studies

With PCa and benign prostatic hyperplasia (BPH) commonly coexisting, many men with PCa were taking 5-ARIs to control their voiding problems. This provided an excellent opportunity to evaluate association between 5-ARI use and PCa progression in patients on active surveillance in observational studies before randomized trials more formally addressed the question. To date, several series have been published and three will be explored in this chapter.

The first publication on secondary prevention using 5-ARIs in PCa described the outcomes of a cohort of 288 patients with very-low-risk prostate cancer on active surveillance, at Princess Margaret Hospital at the University of Toronto, who had no prior 5-ARI use [20]. Seventy patients in the group (24.3 %) had started using either finasteride or dutasteride during the study period from 1995 to 2010. The case and control groups were well matched at baseline except that the patients using 5-ARIs had slightly larger prostates (61 vs 41 cc) and higher PSA (5.4 vs 4.8). Median follow-up for the cohort was 38.5 months. Pathologic progression was defined by findings on repeat biopsy: increase overall Gleason grade to $\geq$7, $\geq$3 positive cores, or any core involvement >50 %. The main secondary endpoint was progression to active treatment with either surgery, radiation, or androgen deprivation. Overall, 33.3 % of patients in the group went on to active treatment at a median time of 32.3 months from initiation of active surveillance.

Pathologic progression was less frequent for patients using 5-ARIs (13/70 [18 %] vs 80/218 [36.7 %], $p = 0.004$). On Kaplan-Meier survival

analysis, median time to pathologic progression was 6 months longer for patients taking finasteride or dutasteride (41.3 months vs 35.1 months, $p = 0.013$). Patients who were not using a 5-ARI accumulated an almost double risk of undergoing active treatment during the study period with a shorter median time to active treatment (31.5 months vs 42.5 months, $p = 0.026$). The authors explored various predictors of time to pathologic progression on cox proportional hazards modeling. When taking into account 5-ARI use, age, PSA, maximum percent core involvement, and prostate volume, 5-ARI use was the most powerful predictor. Patients who did not use finasteride or dutasteride during the study period had a 2.9 increased hazard of pathologic progression. Age (HR 1.04) and PSA (HR 1.14) were also both independent predictors of pathologic progression in the model. In an attempt to balance the baseline characteristics of the groups slightly better, a sensitivity analysis limiting patients in the non-5-ARI group to prostate size ≥40 was performed, and no 5-ARI use continued to be strongly predictive of pathologic progression (HR 2.85, 95 % CI 1.5–5.4, $p = 0.001$).

Reasons for abandoning active surveillance and pursuing treatment were similar between the two groups. Approximately 50 % of men cited Gleason score upgrading as the reason for leaving surveillance. Rising PSA, higher number of positive cores, greater volume of disease, worsening voiding symptoms, and anxiety were other reasons that patients exited surveillance. Thus, men in both groups went on to active treatment for similar reasons, but fewer did so in the 5-ARI group.

This study provided a glimpse of the effect that 5-ARIs have in men on active surveillance for PCa. However, some contradictory data was also contemporarily published. Ross et al. presented the experience from Johns Hopkins Medicinal Institutions in Baltimore, Maryland, USA [21]. In their series of 587 men with very low-risk PCa on active surveillance without prior 5-ARI use, 5-ARIs were initiated by 47 men (all for BPH symptoms). They assessed 5-ARI use as a time-dependent variable and were able to explore pathologic progression depending if 5-ARI had been initiated at the time of re-biopsy (that led to progression).

Most men in their cohort initiated 5-ARIs at a median of 1.2 years after starting active surveillance for PCa, and the median duration of exposure of 5-ARIs was 2.4 years. All patients who started 5-ARIs remained on them for the duration of the study. For men using 5-ARIs, subsequent biopsy reclassified them as greater than very low risk less often as men not using 5-ARIs (17 % vs 31 %, $p = 0.04$). However, when taking into account age, PSA, PSA kinetics, volume of disease, and other predictors, 5-ARI use was associated with a nonstatistically significant 45 % increased hazard of disease reclassification (HR = 0.55, 95 % CI 0.23–1.28, $p = 0.16$). Based on these data, the authors concluded that treatment with 5-ARIs did not alter PCa progression for patients on active surveillance.

Although certain thought leaders in PCa felt that the time-dependent analysis provided strong evidence that 5-ARIs did not reduce progression [22], there were investigators who felt that the study from Johns Hopkins lacked statistical power to demonstrate an effect, evidenced by the fact that there were only eight tumors that demonstrated pathologic progression in their cohort [23]. Indeed, a reanalysis of the initial Princess Margaret cohort using time-dependent 5-ARI use persistently demonstrated protection with 5-ARIs [23].

Regardless of one's interpretation on the observational studies, the main limitation of these publications was inherent in their retrospective design. Despite a strong proposed biologic link between 5-ARIs, suppression of DHT, and regression of prostate cancer, causation cannot be ascertained without a prospective randomized trial.

Randomized Controlled Trials

The safety and efficacy of dutasteride for preventing prostate cancer progression in men aged 48–82 with low-risk prostate cancer was tested in a North American-wide randomized controlled trial [24]. Men were eligible for the Reduction by Dutasteride of Clinical Progression Events in Expectant Management (REDEEM) trial if they

had a clinical diagnosis within a year of screening. Only patients followed on active surveillance for low-risk disease with Gleason score ≤6 (no pattern 4), serum PSA ≤10, and life expectancy >5 years were included. All study entry biopsies were centrally reviewed by an expert genitourinary (GU) pathologist.

Between July 2006 and March 2007, 302 participants were accrued from 65 North American hospitals and clinics and treated with either 0.5 mg of dutasteride or matching placebo for 3 years. Patients, physicians, and study personnel were blinded to treatment allocation; however, PSA values were not adjusted to reflect the expected drop for patients treated with 5-ARI. Patients were monitored as per typical active surveillance protocol with visits every 3 months for the first year and every 6 months thereafter. Digital rectal exams were performed at baseline, 18 months, and study completion at 3 years. It was required of all participants to undergo repeat standard 12-core transrectal ultrasound (TRUS)-guided prostate biopsy at 18 and 36 months. A central pathologist blinded to the treatment group was responsible for reading and reporting the biopsies. Health-related quality-of-life outcomes were also measured. Memorial anxiety scale for prostate cancer (MAX-PC) was used to evaluate anxiety related to prostate cancer diagnosis and treatment.

The primary endpoint, prostate cancer progression, was a composite measure of disease progression that combined pathological progression (one of >3 cores positive on biopsy, ≥50 % PCa on any core or any Gleason pattern 4) and therapeutic progression (the institution of prostatectomy, radiation, or androgen deprivation). Several secondary endpoints were also explored including time to pathologic progression only and adverse event rate. Intention-to-treat analysis was carried out.

Treatment and control groups were well balanced at the baseline. Median age was approximately 65 years, body mass index (BMI) 28 kg/m^2, prostate volume 44 ml, PSA 5.7, and percent positive cancer cores 10 %. Patients were predominantly white (90 %) without a family history of prostate cancer (80 %). More men in the placebo group did not undergo on-trial biopsy (19/155 vs 7/147) suggesting lost to follow-up or study dropout.

Dutasteride significantly delayed composite prostate cancer progression compared to placebo over 3 years (HR 0.62, 95 % CI 0.43–0.89; p = 0.009) in time-to-event analysis. Overall, 10 % fewer cases of disease progression occurred in the treatment arm (38 % vs 48 %). When examining pathologic progression and therapeutic progression separately, there was a lower rate of pathologic progression for men on dutasteride, but the effect was not statistically significant (HR 0.7, 95 % CI 0.45–1.08). Prostate anxiety assessment demonstrated that anxiety for patients receiving dutasteride did not fluctuate during the trial but that patients receiving placebo decreased. This decrease was primarily driven by the "fear of recurrence" subscale.

There were no statistically significant differences between the incidence of adverse events, serious adverse event, and adverse events leading to study withdrawal between groups, although several nonstatistically significant events were seen. Breast tenderness or enlargement occurred in 13 patients on dutasteride versus six on placebo. Impotence was 9 % in both groups, and decreased libido was similar (7 % vs 4 %), but ejaculatory disorders were more common in the intervention arm (5 % vs 1 %). There were no differences in cardiovascular toxicity.

Interestingly, there was suggestion of tumor regression in the 5-ARI group. In final biopsy assessment, 50/140 (36 %) patients in the treatment arm had no cancer detected on biopsy versus 31/136 (23 %) in the placebo arm. However, the degree of upstaging was comparable between the groups. Two patients in the treatment group and three in the control group were upstaged to Gleason score 8. There were no cases of Gleason 9 or 10 in this study. The study authors suggest that the benefit of dutasteride is to reduce the amount of low-grade PCa (i.e., not reduce the likelihood of being diagnosed with a high-grade tumor) and thus reduce the overall number of interventions for patients on active surveillance.

This ultimately drops morbidity for a potential large cohort of patients with prostate cancer.

Although this was the first study to demonstrate secondary prevention in a randomized trial for men with low-risk prostate cancer on active surveillance, it was criticized for not being powered to detect a difference in pathologic progression alone and for its brief duration of follow-up. Thus, clinicians need to balance the benefits of preventing prostate cancer progression and reducing anxiety surrounding progression with the cost and side-effect profile of dutasteride.

A sub-analysis of the REDEEM study evaluating predictors of pathological progression was published by the study group [25]. Here the authors examined baseline variables and their ability to predict time to pathologic progression, defined by one of three findings on repeat biopsy during the 3-year study period (four or more cores positive, 50 % or greater of any core positive, or Gleason score 7 or greater). Age, ethnicity, prostate volume, PSA, PSA density, PSA velocity, number positive cores, International Prostate Symptom Score (IPSS), family history of prostate cancer, serum DHT, and serum testosterone were all evaluated as potential predictors of pathological progression.

For the entire cohort, 94 of 276 patients had pathologic progression. In more than half the cases of the 94 patients who progressed in both the control and placebo arms, pathologic progression was driven by volume progression alone (59 % in dutasteride and 56 % in the control arm). Pathologic progression was diagnosed in scheduled (18 and 36 month) biopsy for all patients receiving 5-ARI. In the placebo group, six patients were found to progress pathologically on unscheduled biopsies within the first 18 months and one further patient on an unscheduled biopsy after 18 months. Interestingly, only older age (HR 1.05, 95 % CI 1.01–1.08, $p = 0.009$) and higher baseline PSA density (HR 1.06, 95 % CI 1.04–1.09, $p < 0.001$) were associated with a statistically significant independent increased risk of pathological progression. PSA velocity did not predict for pathological progression.

Ongoing Trials in 5-Alpha-Reductase Inhibitors and Active Surveillance

With the advent and brisk uptake of multiparametric magnetic resonance imaging (mpMRI) in prostate cancer diagnosis and treatment, there is interest in exploring the changes to prostate tumors on mpMRI for patients using 5-ARIs in AS [26]. The MRI for Primary Prostate Cancer after Exposure to Dutasteride (MAPPED) study was designed by investigators at University College London in collaboration with physicians in the GlaxoSmithKline research and development group. In this double-blind, placebo-controlled randomized trial, patients will be offered daily dutasteride (0.5 mg) versus placebo and routine mpMRIs to assess relative tumor volume change on imaging. The changes in tumor characteristics using non-T2-weighted sequences will also be explored as secondary outcomes. Patients are also offered a cognitive fusion biopsy at the conclusion of the 6-month trial. The final analysis has not yet been reported, but if it demonstrates tumor shrinkage for patients taking active drug versus placebo, it would further support the biologic plausibility for using 5-ARIs in secondary prostate cancer prevention.

Guideline Suggestions for 5-Alpha-Reductase Inhibitor Use in Active Surveillance

There have been several published guidelines on active surveillance released since the publication of the aforementioned observational studies and randomized controlled trial on 5-ARI use for secondary prevention of prostate cancer progression on active surveillance. The American Society of Clinical Oncology (ASCO) and Cancer Care Ontario (CCO) published a combined guideline on AS [11]. (CCO's stance closely reflected a contemporary guideline from the Canadian Urological Association [10].) Interestingly, for the question, "In patients with localized prostate cancer undergoing AS, how does supplementation with 5-ARIs

compare with no supplementation?" ASCO did not endorse its use. It was, however, the opinion of the CCO panel that the benefits of 5-ARI use outweigh the risks and can be used as long as patients are counseled appropriately about the risks and benefits. Other guidelines on localized prostate cancer were released prior to the publication of REDEEM and will not be highlighted here.

Selectively Using 5-Alpha-Reductase Inhibitors for Secondary Prevention in Men with Larger Prostates

As previously outlined, there is data from observational studies and one well-designed RCT that 5-ARIs can prevent progression for men on active surveillance for prostate cancer. However, using 5-ARIs for men with prostate cancer is inherently controversial partly due to the risk of high-grade prostate cancer that was observed for 5-ARI versus placebo in the primary prevention trials [17, 18]. As mentioned earlier, this effect was not demonstrated when 5-ARIs were used for secondary prevention. Additionally, it is well established that 5-ARIs improved symptomatic BPH and BPH progression in men with larger prostates [27, 28]. Thus, one approach to personalize the use of 5-ARIs in secondary prevention is to reserve its use for men on active surveillance with concomitant lower urinary tract symptoms and BPH as an indication.

Conclusion

Although borrowed from BPH and primary PCa prevention literature, the biologic plausibility for using 5-ARIs in secondary prevention for AS patients is convincing. Furthermore, data from observational trials and the one randomized controlled trial addressing this question demonstrates decreased progression for men using 5-ARIs. There may be controversy over whether the improvement seen for the clinical progression outcome used in the REDEEM study offers sufficient evidence to use 5-ARIs for this population. However, all studies confirm that 5-ARIs are safe and carry minimal toxicity for patients. We believe that the relative benefits and harms of this strategy should be highlighted to patients so that a shared decision can be appropriately made. 5-ARIs should particularly be considered in men with concomitant, symptomatic BPH and large prostates, where cancer and BPH progression and symptomatic improvement can be targeted with a single medication.

References

1. Siegel R, Miller K, Jemal A. Cancer Statistics, 2015. CA Cancer J Clin. 2015;65:5–29.
2. American Cancer Society. Cancer facts and figures. https://cancerstatisticscenter.cancer.org/?_ga=1.221513048.1743771228.1460038038#/. Accessed 7 Apr 2016.
3. Bill-Axelson A, Holmberg L, Garmo H, Rider JR, Taari K, Busch C, et al. Radical prostatectomy or watchful waiting in early prostate cancer. N Engl J Med. 2014;370:932–42.
4. Andriole GL, Crawford ED, Grubb 3rd RL, Buys SS, Chia D, Church TR, et al. PLCO Project Team. Mortality results from a randomized prostate-cancer screening trial. N Engl J Med. 2009;360:1310–9.
5. Schröder FH, Hugosson J, Roobol MJ, Tammela TL, Ciatto S, Nelen V, ERSPC Investigators, et al. Screening and prostate-cancer mortality in a randomized European study. N Engl J Med. 2009;360:1320–8.
6. Resnick MJ, Koyama T, Fan KH, Albertsen PC, Goodman M, Hamilton AS, et al. Long-term functional outcomes after treatment for localized prostate cancer. N Engl J Med. 2013;368:436–45.
7. Klotz L, Vesprini D, Sethukavalan P, Jethava V, Zhang L, Jain S, et al. Long-term follow-up of a large active surveillance cohort of patients with prostate cancer. J Clin Oncol. 2014;33:272–7.
8. Dall'Era MA, Albertsen PC, Bangma C, Carroll PR, Carter HB, Cooperberg MR, et al. Active surveillance for prostate cancer: a systematic review of the literature. Eur Urol. 2012;62(6):976–83.
9. National Comprehensive Cancer Network. NCCN clinical practice guidelines in oncology 2015: prostate cancer. http://www.nccn.org/patients/guidelines/prostate/index.html#48. Accessed 7 Apr 2016.
10. Morash C, Tey R, Agbassi C, Klotz L, McGowan T, Srigley J, et al. Active surveillance for the management of localized prostate cancer: guideline recommendations. Can Urol Assoc J. 2015;9(5–6):171–8.
11. Chen RC, Rumble RB, Loblaw DA, Finelli A, Ehdaie B, Cooperberg MR, et al. Active surveillance for the management of localized prostate cancer (Cancer

Care Ontario Guideline): American Society of Clinical Oncology Clinical Practice Guideline Endorsement. J Clin Oncol. 2016;34(18):2182–90.
12. National Institute for Health and Clinical Excellence. Prostate cancer: diagnosis and management. https://www.nice.org.uk/guidance/cg175. Accessed 7 Apr 2016.
13. Cooperberg MR, Broering JM, Carroll PR. Time trends and local variation in primary treatment of localized prostate cancer. J Clin Oncol. 2010;28(7):1117–23.
14. Weiner AB, Patel SG, Etzioni R, Eggener SE. National trends in the management of low- and intermediate-risk prostate cancer in the United States. J Urol. 2015;193(1):95–102.
15. Gleave M, Qian J, Andreou C, Pommerville P, Chin J, Casey R, et al. The effects of the dual 5alpha-reductase inhibitor dutasteride on localized prostate cancer—results from a 4-month pre-radical prostatectomy study. Prostate. 2006;66:1674–85.
16. Marks LS, Roehrborn CG, Wolford E, Wilson TH. The effect of dutasteride on the peripheral and transition zones of the prostate and the value of the transition zone index in predicting treatment response. J Urol. 2007;177(4):1408–13.
17. Andriole GL, Bostwick DG, Brawley OW, Gomella LG, Marberger M, Montorsi F, REDUCE Study Group, et al. Effect of dutasteride on the risk of prostate cancer. N Engl J Med. 2010;362:1192–202.
18. Thompson IM, Goodman PJ, Tangen CM, Lucia MS, Miller GJ, Ford LG, et al. The influence of finasteride on the development of prostate cancer. N Engl J Med. 2003;349:215–24.
19. Feijoo ER, Sivaraman A, Barret E, Sanchez-Salas R, Galiano M, Rozet F, et al. Focal high-intensity focused ultrasound targeted hemiablation for unilateral prostate cancer: a prospective evaluation of oncologic and functional outcomes. Eur Urol. 2016;69(2):214–20.
20. Finelli A, Trottier G, Lawrentschuk N, Sowerby R, Zlotta AR, Radomski L, et al. Impact of 5α-reductase inhibitors on men followed by active surveillance for prostate cancer. Eur Urol. 2011;59:509–14.
21. Ross AE, Feng Z, Pierorazio PM, Landis P, Walsh PC, Carter HB, et al. Effect of treatment with 5-alpha reductase inhibitors on progression in monitored men with favourable-risk prostate cancer. BJUI. 2011;110:651–7.
22. Walsh PC. Re: Effect of treatment with 5-aplha reductase inhibitors on progression in monitored men with favourable-risk prostate cancer. J Urol. 2012;188:110–2.
23. Wong L, Fleshner N, Finelli A. Impact of 5-alpha reductase inhibitors on men followed by active surveillance for prostate cancer: a time-dependent covariate reanalysis. Eur Urol. 2013;64:343–5.
24. Fleshner NE, Lucia MS, Egerdie B, Aaron L, Eure G, Nandy I, et al. Dutasteride in localised prostate cancer management: the REDEEM randomised, double-blind, placebo-controlled trial. Lancet. 2012;379:1103–11.
25. Margel D, Nandy I, Wilson TH. Predictors of pathological progression among men with localized prostate cacner undergoing active surveillance: a sub-analysis of the REDEEM Study. J Urol. 2013;190:2039–46.
26. Robertson NL, Moore CM, Ambler G, Bott SR, Freeman A, Gambarota G, et al. MAPPED study design: A 6 month randomised controlled study to evaluate the effect of dutasteride on prostate cancer volume using magnetic resonance imaging. Contemp Clin Trials. 2013;34(1):80–9.
27. McConnell JD, Roehrborn CG, Bautista OM, Andriole Jr GL, Dixon CM, Kusek JW, et al. The long-term effect of doxazosin, finasteride, and combination therapy on the clinical progression of benign prostatic hyperplasia. N Engl J Med. 2003;349:2387–98.
28. Roehrborn CG, Siami P, Barkin J, Damião R, Major-Walker K, Nandy I, et al. The effects of combination therapy with dutasteride and tamsulosin on clinical outcomes in men with symptomatic benign prostatic hyperplasia: 4-year results from the CombAT study. Eur Urol. 2010;57:123–31.

Part X

Determining Outcomes of Focal Therapy

31 Measuring Patient-Based Outcomes: Setting Realistic Expectations When Balancing Functional Outcomes with Cancer Control

Behfar Ehdaie and Arjun Sivaraman

Introduction

Over the past decade, partial gland ablation or focal therapy for localized prostate cancer has emerged as a novel treatment balancing the improved quality of life associated with active surveillance and oncologic efficacy attributed to whole-gland treatments, including radical prostatectomy (RP) and external beam radiation therapy (EBRT). Focal therapy is based on identification and ablation of an "index lesion" while preserving the normal prostate parenchyma and maintaining baseline erectile and urinary function outcomes compared to whole-gland treatments. The index lesion is defined as the dominant cancer focus that determines the risk of malignancy and metastases [1, 2]. The wide adoption of prostate cancer screening using serum prostate-specific antigen (PSA) has led to a downward stage migration, and the majority of men diagnosed with prostate cancer harbor localized disease [3, 4]. As the population of men diagnosed with localized prostate cancer increases and the indications for focal therapy expand, more men are likely to seek these treatments in the future. In the absence of long-term studies with longitudinal data reporting functional outcomes, managing patients' expectations will be key for urologic oncologists who treat prostate cancer.

The decision of treatments for most diseases has historically centered on measuring outcomes associated with the elimination of the disease (e.g., oncologic outcomes, survival), while the effect of the disease and the subsequent treatment on the patient's quality of life were poorly understood. During the past two decades, several instruments have been developed to quantify patient's quality of life, and evidence suggests that systematic use of information from patient-reported outcome measures (PROMs) can aid in improving physician-patient communication and decision-making [5, 6]. However, several obstacles have restricted the routine use of PROMs in actual clinical practice. In this chapter, we emphasize the need for routine PROMs in focal therapy for treatment of prostate cancer, evaluate the current standard of care in PROM strategies, and suggest recommendations for future implementation in routine clinical practice to manage patients' expectations to improve decision-making.

Measuring Patient-Reported Outcomes in Focal Therapy for Prostate Cancer

Patient-reported outcome measures have emerged as a vital component of clinical care, and new instruments are being developed for

B. Ehdaie (✉) • A. Sivaraman
Urology Service, Department of Surgery, Memorial Sloan Kettering Cancer Center, New York, NY, USA
e-mail: EhdaieB@mskcc.org

© Springer International Publishing AG 2017
T.J. Polascik (ed.), *Imaging and Focal Therapy of Early Prostate Cancer*, Current Clinical Urology, DOI 10.1007/978-3-319-49911-6_31

various diseases and treatments [6]. Conventional management strategies are focused on measuring the radiographic or biochemical impact of the disease and treatment. PROMs are informative to traditional assessments of patients by physicians and have been shown to improve patient decision-making by providing individualized comparative data on various treatment options. According to the US Food and Drug Administration (FDA), "PROM is any report of the status of a patient's health condition that comes directly from the patient, without interpretation of the patient's response by a clinician or anyone else" [7]. A well-designed PROM questionnaire can address physical functions, symptoms, global judgments of health, psychological well-being, social well-being, cognitive functioning, role activities, personal constructs, satisfaction with care, health-related quality of life (HRQOL), adherence to medical regimens, and clinical trial outcomes.

The emergence of PROMs is notable in oncology and has been shown to provide accurate data on complications and adverse events for various treatments, and PROMs have been effectively incorporated into clinical trials for comparative effectiveness analyses [5, 8].

In addition to providing individualized data for comparative studies, PROMs have emerged as important tools in health policy. In the United States, there is a transition from the traditional fee-for-service to a value-based health model. Value-based healthcare can potentially be a unifying force aligning the patients, providers, and payers toward improved outcomes and cost control [9]. This model emphasizes bundled reimbursement covering the entire care cycle, and the providers are made accountable and rewarded for delivering better patient health outcomes. An essential tool for establishing a value-based healthcare system is to provide standardized outcome measures for the evaluation and comparison. A PROM can be a potential tool in this scenario mainly to address the outcomes, and this can be applied across different medical disciplines and can be customized according to specific diseases and treatments [10].

Overall, the essence of PROMs is to improve patient decision-making and provide physicians with better assessment tools to monitor treatment efficacy. In many diseases, patients are confronted with many options for management, and the only comparative data available is traditional outcome measures (e.g., survival or complication data collected by physicians). In most situations, the various treatments have similar survival or commonly assessed adverse events. Therefore, patients are asked to choose a treatment option without access to outcomes reported by similar patients and uncommon adverse events associated with a specific treatment. The management of localized prostate cancer is largely preference based, and comparative effectiveness studies have yet to demonstrate an advantage to a single treatment modality, highlighting the complexities of treatment decision-making for patients. Furthermore, studies have found biases or heuristics at work in patients' decision-making [11, 12]. In the case of prostate cancer, instruments to assess patient-reported outcomes were developed and validated for radical prostatectomy and radiation therapy [13, 14]. A key aspect to these tools was that they expanded the adverse outcomes initially reported by physicians, including erectile and urinary function, and added, for example, bowel-related dysfunction associated with radiation therapy. The incorporation of PROMs in localized prostate cancer set the stage for comparative effectiveness research for whole-gland treatments and added to the data available to help patients make decisions beyond only survival or cancer recurrence [15, 16].

The landscape of management options available for localized prostate is being constantly reviewed and novel treatments are developed. Our understanding of the biology of the cancer is continuously evolving, which opens opportunities for innovative technologies. Focal therapy has emerged as the newest treatment option for men with localized prostate cancer. Notably, the tissue ablation strategies developed to achieve focal therapy include a variety of thermal and nonthermal energy sources: cryotherapy, high-intensity focused ultrasound (HIFU), irreversible

Table 31.1 Potential use of PROMs in focal therapy treatments for prostate cancer

Health system	Performance assessment
	Cost-effectiveness
Healthcare provider organization	Benchmarking
	Quality assessment
Clinical trials	Treatment outcomes
Clinical practice	Diagnosis
	Monitoring progress
Information for patients or clinicians	Choosing between providers/treatments

electroporation, and photodynamic therapy [17]. Research efforts are still underway to improve patient selection and develop better techniques to identify the cancer within the prostate cancer. Despite the development of various energy sources and focal therapy techniques and adoption of focal therapy as a viable option for select men with prostate cancer, patient-centered outcomes are inconsistently collected and reported. The paucity of data limits comparative studies evaluating energy sources and techniques and providing patients with data to help select between focal therapy and standard whole-gland treatment options. The development and validation of standard PROM instruments will foster more robust comparative studies and enhance physician-patient counseling with individualized data to improve patient decision-making in localized prostate cancer treatment.

Focal therapy will likely have a major impact in the management of localized prostate cancer, and the effective implementation of uniform, validated PROM instruments in clinical practice will inform physician-patient counseling and improve patient decision-making. The potential uses of PROMs in focal therapy for localized prostate cancer are listed in Table 31.1.

PROM Reporting in Prostate Cancer Focal Therapy Studies

A key advantage of focal therapy for prostate cancer, discussed by its early adopters, is the lower rate of adverse events and improved quality-of-life outcomes compared to whole-gland treatment. However, a paucity of comparative data exists to support the quality-of-life advantages associated with focal therapy. A key step to building evidence to support focal therapy is designing a minimal set of patient-centered outcomes and developing a framework to standardize reporting of quality-of-life outcomes specific to focal therapy.

A systematic review of studies evaluating focal therapy demonstrates reporting of functional outcomes after treatment relies on PROM tools developed for whole-gland treatment [18]. Urinary symptoms are reported using the International Prostate Symptom Score (IPSS) and the Expanded Prostate Cancer Index Composite (EPIC) in most studies. In addition, the assessment of urinary incontinence is heterogeneous across most studies. For example, studies report only "pad-free" or "leak-free" rates, or both, as a measure of urinary incontinence, and the International Continence Society (ICS) questionnaire score was used sparsely.

Similarly, reporting of erectile function outcomes after focal therapy treatment was varied and there was no standard definition of "potency." Physical evaluation and need for assisted devices or medication were used rarely in studies to evaluate erectile function. Further, the International Index of Erectile Function (IIEF) and Brief Male Sexual Function Index were the instruments used most commonly in focal therapy studies. The methodology and PROMs used in focal therapy studies are described in Table 31.2 [19–32].

In the largest registry study for focal therapy in prostate cancer, Ward et al. examined the outcomes of focal therapy using cryotherapy in 1160 patients with prostate cancer [23]. Overall, 47 %, 41 %, and 12 % of patients were categorized into low-, intermediate-, and high-risk prostate cancer, respectively. The authors reported 58.1 % of patients were "potent" after treatment and they used a single question to measure erectile function, defined as preservation of spontaneous erections. Urinary continence was defined as "pad-free" and 98.4 % of patients were reported continent after treatment. In a separate study, Bahn et al. evaluated 73 patients treated with cryotherapy [22]. The authors defined "potency"

Table 31.2 Focal therapy reports and the method of PROM used

Author (year)	Number of patients	Energy	Mean follow-up	Continence (%)	Method	PROM	Potency	Method	PROM
Bahn et al. (2006) [19]	31	Cryotherapy	5.8 years	100	Leak-free, pad-free	None	88.9 %	None	Brief Male Sexual Function Index
Ellis et al. (2007) [20]	60	Cryotherapy	15.2 months	96	Leak-free, pad-free	None	70.5 %	Assisted devices or medication	None
Truesdale et al. (2010) [21]	77	Cryotherapy	24 months	100	Leak-free	IPSS	NA	None	IIEF
Bahn et al. (2012) [22]	70	Cryotherapy	3.7 years	100	Leak-free, pad-free	None	86 %	None	IIEF
Ward et al. (2012) [23]	1160	Cryotherapy	21 months	98	NA	NA	58 %	NA	NA
Muto et al. (2008) [24]	29	HIFU	32 months	100	Leak-free, pad-free	UCLA-EPIC, IPSS	NA	None	None
Ahmed et al. (2011) [25]	20	HIFU	12 months	90	Leak-free, pad-free	UCLA-EPIC, IPSS	95 %	None	IIEF-15
El Feguon et al. (2011) [26]	12	HIFU	10 years	100	Leak-free, pad-free	None	NA	None	None
Ahmed et al. (2012) [27]	41	HIFU	12 months	100	Leak-free, pad-free	UCLA-EPIC, IPSS	89 %	None	IIEF-15
Barret et al. (2013) [28]	21	HIFU	12 months	100	Leak-free	IPSS	Mean IIEF decreased from 20 to 19	None	IIEF-5
French Urology Association (2014) [29]	104	HIFU	12 months	100		IPSS, ICS, EORTC QLQ-C30	NA	None	IIEF 5
Feijoo et al. (2015) [30]	67	HIFU	12 months	100	Leak-free	IPSS, ICS	Mean IIEF decreased from 17.9 to 15.4	None	IIEF-5
Ahmed et al. (2015) [31]	56	HIFU	12 months	92		None	76.8 %	None	IIEF
Valerio et al. (2015) [32]	34	IRE	6 months	100	Pad-free	None	95 %	Physician evaluation	None

HIFU high-intensity focused ultrasound, *UCLA-EPIC* University of California, Los Angeles-Expanded Prostate Cancer Index Composite, *IPSS* International Prostate Symptom Score, *ICS* International Continence Society, *EORTC QLQ-C30* European Organisation for Research and Treatment of Cancer Quality of Life Questionnaire Core 30, *IIEF* International Index of Erectile Function

based on the IIEF questionnaire and reported 86 % of patients achieved erections after treatment. In addition, all patients were reported as continent after treatment based on the definition of "leak-free" outcome. Importantly, no study reported outcomes comparatively between various treatments, including focal therapy and whole-gland treatments.

In the most comprehensive prospective study of focal therapy for prostate cancer, Ahmed et al. reported outcomes of 42 patients treated with HIFU [27]. International Index of Erectile Function-15 (IIEF-15) scores were used for measuring erectile function and noted no significant differences in median IIEF scores at baseline and 12 months after treatment ($p = 0.060$). In addition, the authors reported categories of erectile function based on the IIEF questionnaire. The median IIEF-15 scores for intercourse satisfaction ($p = 0.454$), sexual desire ($p = 0.644$), and overall satisfaction ($p = 0.257$) were similar at baseline and 12 months after treatment. However, the median scores for IIEF-15 erectile ($p = 0.042$) and orgasmic ($p = 0.003$) function were reported to demonstrate significant deterioration after treatment. In regard to urinary function, no differences in median score for University of California, Los Angeles (UCLA)-EPIC were discovered at baseline and 12 months after treatment ($p = 0.045$). Lower urinary tract symptoms were assessed by International Prostate Symptom Score (IPSS) and demonstrated significant improvement from baseline at 12 months after treatment ($p = 0.026$). Importantly, the overall quality-of-life measures did not demonstrate significant differences after treatment.

In a study evaluating various techniques for focal therapy in localized prostate cancer, Barret et al. reported functional outcomes in 106 patients comparing HIFU, cryoablation, brachytherapy, and vascular-targeted photodynamic therapy [28]. The authors did not identify clinically significant differences in median IPSS at baseline and12 months after treatment. However, the authors concluded that patients experienced a clinically significant decline of erectile function based on changes in the median IIEF-5 score at baseline and 12 months after treatment. Finally, Valerio et al. treated 34 men with localized prostate cancer with focal therapy using irreversible electroporation [32]. Overall, 26 %, 71 %, and 3 % of men were classified as having low-, intermediate-, and high-risk prostate cancer, respectively. After a median follow-up of 6 months (range 1–24), all patients were reported potent based on physician-documented physical examination. In addition, all patients were reported to be "pad-free" at 6 months after treatment.

Future Directions and Recommendations to Measure Outcomes in Focal Therapy for Localized Prostate Cancer

Despite an increase in prostate cancer focal therapy studies that demonstrate it is safe based on complication data and short-term oncologic outcomes, there is a paucity of comparative data using PROM instruments. As focal therapy is being more adopted into the management of localized prostate cancer, the selection of who, how, and when to treat need to be elucidated with well-designed comparative studies. In addition, the clinical spectrum of disease considered suitable for focal therapy is expanding to include salvage therapy after radiation treatment. The heterogeneity of treatment techniques and selection of patients in focal therapy requires methods to standardize tools to measure outcomes and report patient-centered data. Notably, five international consensus meetings have convened to discuss key issues in focal therapy and prioritize standardized reporting of functional and oncologic outcomes [33–36].

Qualitative research methodology is well described in PROM instrument development [37–40]. We will briefly outline the key aspects of this research domain based upon a review of the published literature and apply these methods to focal therapy. Organizing a multidisciplinary working group is the key step to initiate the process. This group should involve the stakeholders in focal therapy, including surgeons, patients, patients' families, and nurses, in order to achieve a multidimensional perspective of the scope of

outcomes associated with focal therapy. The qualitative research interview is a scientifically described research process based on verbal communication aimed at gathering information in relation to a specific aim. The patient has considerable freedom to respond to open-ended questions within a framework of themes encompassing various aspects of treatment outcomes, including physical function, adverse events, and secondary therapies. Performing a qualitative interview requires experience and involves in-depth, open-ended questions, allowing patients to respond in their own words. Researchers should understand that the interview narratives must not be contaminated by biases from personal experiences, theoretical understanding, hypotheses, or assumptions.

A properly designed qualitative interview will result in a list of themes encompassing existing problems and concerns that is experienced by patients after focal therapy treatment. The qualitative research working group processes this information and develops meaningful close-ended questions specific to patients with prostate cancer. Importantly, prompt investigation should be initiated in cases in which symptoms not directly related to focal therapy occur at a higher-than-expected rate in these patients (examples: testicular pain or pelvic pain syndrome). These interviews generate extensive data and require robust statistical analyses to look for patterns in terms of demographics, cancer characteristics, and treatment parameters.

The newly developed close-ended questions as a result of qualitative interview constitute the PROM instrument. The PROM instrument aims to evaluate symptoms (impairments) and other aspects of well-being, functioning, health status, general health perceptions, and quality of life. The PROM tool must be validated and revised in a separate population of patients in a multi-institutional study [38]. Importantly, the successful implementation of PROMs in clinical practice requires a balance of collecting a minimal set of data and not overburdening the healthcare system with a survey that may take too much time to complete.

Conclusion

Focal therapy has emerged as a viable treatment option for select men with prostate cancer. Advancement in technology and refining techniques will expand the clinical indications for focal therapy in the future. However, counseling men about the functional outcomes, adverse events, and long-term risks for secondary therapy after treatment with focal therapy is difficult due to the paucity of patient-reported data. Subsequently, managing a patient's expectations after focal therapy is an unmet need for research. The development and incorporation into clinical care of a standard validated PROM specific for focal therapy is key for comparative research to define the role of focal therapy in the management of localized prostate cancer.

Acknowledgments

Attestation All authors attest to approving the final manuscript and reviewed the original study data and data analysis and attest to the integrity of the original data and the analysis reported in this manuscript.

Funding Support for this project is provided by the Sidney Kimmel Center for Prostate and Urologic Cancers and by NIH Cancer Center Support Grant P30 CA008748 to PI: Craig B. Thompson, MD.

References

1. Ahmed HU. The index lesion and the origin of prostate cancer. N Engl J Med. 2009;361(17):1704–6.
2. Ahmed HU. Introduction–targeting the lesion, not the organ. Urol Oncol. 2014;32(6):901–2.
3. Loeb S, Gonzalez CM, Roehl KA, Han M, Antenor JAV, Yap RL, et al. Pathological characteristics of prostate cancer detected through prostate specific antigen based screening. J Urol. 2006;175(3 Pt 1):902–6.
4. Mahmood U, Levy LB, Nguyen PL, Lee AK, Kuban DA, Hoffman KE. Current clinical presentation and treatment of localized prostate cancer in the United States. J Urol. 2014;192(6):1650–6.

5. Basch E, Snyder C, McNiff K, Brown R, Maddux S, Smith ML, et al. Patient-reported outcome performance measures in oncology. J Oncol Pract. 2014; 10(3):209–11.
6. Dawson J, Doll H, Fitzpatrick R, Jenkinson C, Carr AJ. The routine use of patient reported outcome measures in healthcare settings. BMJ. 2010;340:c186.
7. US Food and Drug Administration Guidance for Industry. Patient-reported outcome measures—use in medical development to support labeling claims. Silver Spring, MD: US Food and Drug Administration; 2009. Available from: http://www.fda.gov/downloads/Drugs/Guidances/UCM193282.pdf
8. Basch E, Torda P, Adams K. Standards for patient-reported outcome-based performance measures. JAMA. 2013;310(2):139–40.
9. Porter ME. A strategy for health care reform—toward a value-based system. N Engl J Med. 2009;361(2): 109–12.
10. Ehdaie B, Eastham JA. Standardization of patient-centered outcomes: less is more. Eur Urol. 2015;67(3): 468–9.
11. Fagerlin A, Zikmund-Fisher BJ, Ubel PA. Cure me even if it kills me: preferences for invasive cancer treatment. Med Decis Making. 2005;25(6):614–9.
12. Denberg TD, Melhado TV, Steiner JF. Patient treatment preferences in localized prostate carcinoma: the influence of emotion, misconception, and anecdote. Cancer. 2006;107(3):620–30.
13. Wagner AA, Cheng PJ, Carneiro A, Dovirak O, Khosla A, Taylor KN, et al. Clinical use of epic for clinical practice (EPIC-CP) to assess patient-reported prostate cancer quality-of-life following robot-assisted radical prostatectomy. J Urol. 2016; doi:10.1016/j.juro.2016.07.080.
14. Zelefsky MJ, Poon BY, Eastham J, Vickers A, Pei X, Scardino PT. Longitudinal assessment of quality of life after surgery, conformal brachytherapy, and intensity-modulated radiation therapy for prostate cancer. Radiother Oncol J Eur Soc Ther Radiol Oncol. 2016;118(1):85–91.
15. Martin NE, Massey L, Stowell C, Bangma C, Briganti A, Bill-Axelson A, et al. Defining a standard set of patient-centered outcomes for men with localized prostate cancer. Eur Urol. 2015;67(3):460–7.
16. Zelefsky MJ, Eastham JA, Cronin AM, Fuks Z, Zhang Z, Yamada Y, et al. Metastasis after radical prostatectomy or external beam radiotherapy for patients with clinically localized prostate cancer: a comparison of clinical cohorts adjusted for case mix. J Clin Oncol Off J Am Soc Clin Oncol. 2010;28(9):1508–13.
17. Bozzini G, Colin P, Nevoux P, Villers A, Mordon S, Betrouni N. Focal therapy of prostate cancer: energies and procedures. Urol Oncol. 2013;31(2):155–67.
18. Valerio M, Ahmed HU, Emberton M, Lawrentschuk N, Lazzeri M, Montironi R, et al. The role of focal therapy in the management of localised prostate cancer: a systematic review. Eur Urol. 2014;66(4):732–51.
19. Bahn DK, Silverman P, Lee F, Badalament R, Bahn ED, Rewcastle JC. Focal prostate cryoablation: initial results show cancer control and potency preservation. J Endourol Endourol Soc. 2006;20(9):688–92.
20. Ellis DS, Manny TB, Rewcastle JC. Cryoablation as primary treatment for localized prostate cancer followed by penile rehabilitation. Urology. 2007; 69(2):306–10.
21. Truesdale MD, Cheetham PJ, Hruby GW, Wenske S, Conforto AK, Cooper AB, et al. An evaluation of patient selection criteria on predicting progression-free survival after primary focal unilateral nerve-sparing cryoablation for prostate cancer: recommendations for follow up. Cancer J Sudbury Mass. 2010;16(5):544–9.
22. Bahn D, de Castro Abreu AL, Gill IS, Hung AJ, Silverman P, Gross ME, et al. Focal cryotherapy for clinically unilateral, low-intermediate risk prostate cancer in 73 men with a median follow-up of 3.7 years. Eur Urol. 2012;62(1):55–63.
23. Ward JF, Jones JS. Focal cryotherapy for localized prostate cancer: a report from the national Cryo On-Line Database (COLD) Registry. BJU Int. 2012;109(11):1648–54.
24. Muto S, Yoshii T, Saito K, Kamiyama Y, Ide H, Horie S. Focal therapy with high-intensity-focused ultrasound in the treatment of localized prostate cancer. Jpn J Clin Oncol. 2008;38(3):192–9.
25. Ahmed HU, Hu Y, Carter T, Arumainayagam N, Lecornet E, Freeman A, et al. Characterizing clinically significant prostate cancer using template prostate mapping biopsy. J Urol. 2011;186(2):458–64.
26. El Fegoun AB, Barret E, Prapotnich D, Soon S, Cathelineau X, Rozet F, et al. Focal therapy with high-intensity focused ultrasound for prostate cancer in the elderly: a feasibility study with 10 years follow-up. Int Braz J Urol. 2011;37(2):213–22.
27. Ahmed HU, Hindley RG, Dickinson L, Freeman A, Kirkham AP, Sahu M, et al. Focal therapy for localised unifocal and multifocal prostate cancer: a prospective development study. Lancet Oncol. 2012;13(6):622–32.
28. Barret E, Ahallal Y, Sanchez-Salas R, Galiano M, Cosset J-M, Validire P, et al. Morbidity of focal therapy in the treatment of localized prostate cancer. Eur Urol. 2013;63(4):618–22.
29. Crouzet S, Rouviere O, Martin X, Gelet A. High-intensity focused ultrasound as focal therapy of prostate cancer. Curr Opin Urol. 2014;24(3):225–30.
30. Feijoo ERC, Sivaraman A, Barret E, Sanchez-Salas R, Galiano M, Rozet F, et al. Focal high-intensity focused ultrasound targeted hemiablation for unilateral prostate cancer: a prospective evaluation of oncologic and functional outcomes. Eur Urol. 2016;69(2):214–20.
31. Ahmed HU, Dickinson L, Charman S, Weir S, McCartan N, Hindley RG, et al. Focal ablation targeted to the index lesion in multifocal localised prostate cancer: a prospective development study. Eur Urol. 2015;68(6):927–36.
32. Valerio M, Stricker PD, Ahmed HU, Dickinson L, Ponsky L, Shnier R, et al. Initial assessment of safety and clinical feasibility of irreversible electroporation

in the focal treatment of prostate cancer. Prostate Cancer Prostatic Dis. 2014;17(4):343–7.
33. de la Rosette J, Ahmed H, Barentsz J, Johansen TB, Brausi M, Emberton M, et al. Focal therapy in prostate cancer-report from a consensus panel. J Endourol Endourol Soc. 2010;24(5):775–80.
34. Eggener SE, Scardino PT, Carroll PR, Zelefsky MJ, Sartor O, Hricak H, et al. Focal therapy for localized prostate cancer: a critical appraisal of rationale and modalities. J Urol. 2007;178(6):2260–7.
35. van den Bos W, Muller BG, Ahmed H, Bangma CH, Barret E, Crouzet S, et al. Focal therapy in prostate cancer: international multidisciplinary consensus on trial design. Eur Urol. 2014;65(6):1078–83.
36. Donaldson IA, Alonzi R, Barratt D, Barret E, Berge V, Bott S, et al. Focal therapy: patients, interventions, and outcomes–a report from a consensus meeting. Eur Urol. 2015;67(4):771–7.
37. Mays N, Pope C. Qualitative research: observational methods in health care settings. BMJ. 1995; 311(6998):182–4.
38. Brod M, Tesler LE, Christensen TL. Qualitative research and content validity: developing best practices based on science and experience. Qual Life Res Int J Qual Life Asp Treat Care Rehabil. 2009;18(9):1263–78.
39. Brédart A, Marrel A, Abetz-Webb L, Lasch K, Acquadro C. Interviewing to develop Patient-Reported Outcome (PRO) measures for clinical research: eliciting patients' experience. Health Qual Life Outcomes. 2014;12:15.
40. Snyder CF, Aaronson NK, Choucair AK, Elliott TE, Greenhalgh J, Halyard MY, et al. Implementing patient-reported outcomes assessment in clinical practice: a review of the options and considerations. Qual Life Res Int J Qual Life Asp Treat Care Rehabil. 2012;21(8):1305–14.

32 Pathologic Assessment and Implications Following Focal Therapy of Prostate Cancer

Rafael E. Jimenez, Andrew Evans, James Kench, Rodolfo Montironi, and Mahul B. Amin

Introduction

Assessment of prostate tissue after focal therapy has resulted in novel challenges for the surgical pathologist. Independently of the modality used, the application of focal therapy results, by definition, in the division of the prostate into two distinct areas: a treated and an untreated zone. For each of these areas, therapy success from both the clinical and pathologic standpoints will be defined differently (Table 32.1). Ideally that portion of the prostate undergoing treatment should be completely free of residual high-grade cancer and is expected to show morphological changes associated with the specific treatment modality utilized. In principle, the persistence of aggressive tumor should be considered a failure of therapy, although for most modalities it is unknown to what degree persistent tumor manifests the same biological behavior as untreated disease. The untreated area should ideally be pathologically free of tumor or harbor exclusively low-grade tumor. Clinically, the untreated portion should be thoroughly investigated to exclude aggressive disease and monitored with active surveillance (AS) if low-grade disease is present.

R.E. Jimenez (✉)
Division of Anatomic Pathology, Mayo Clinic, Rochester, MN, USA
e-mail: jimenez.rafael@mayo.edu

A. Evans
Department of Laboratory Medicine and Pathology, University Health Network, Toronto General Hospital, Toronto, ON, Canada

J. Kench
Department of Tissue Pathology and Diagnostic Oncology, Royal Prince Alfred Hospital, Sydney, NSW, Australia

R. Montironi
Department of Pathology, Genitourinary Cancer Program, Institute of Pathological Anatomy and Histopathology, Polytechnic University of the Marche Region, Ancona, Italy

School of Medicine, United Hospitals, Torrette, Ancona, Italy

M.B. Amin
Department of Pathology and Laboratory Medicine, Cedars-Sinai Medical Center, UCLA David Geffen School of Medicine, Los Angeles, CA, USA

Assessment of Treated Area

All modalities of focal therapy create localized tissue necrosis by generating tissue damage upon the application of some type of energy or cellular insult. With the possible exception of radiation therapy, the insult does not discriminate between neoplastic and nonneoplastic tissue, and thus the mechanisms and morphologic changes in both components will be similar. Given that the desired endpoint is complete necrosis of aggressive tumor, the result is usually a discrete area of necrosis and tissue destruc-

© Springer International Publishing AG 2017

T.J. Polascik (ed.), *Imaging and Focal Therapy of Early Prostate Cancer*, Current Clinical Urology, DOI 10.1007/978-3-319-49911-6_32

Table 32.1 Desired oncologic/pathologic outcome in focal therapy

	Treated zone	Untreated zone
Desired oncologic outcome	Eradication of aggressive disease	Absence of aggressive disease
Expected pathologic findings	Specific therapy-related changes Absence of residual tumor	Absence of tumor or at most small Gleason 3+3 (grade group 1) tumors
Clinical follow-up	Imaging/biopsy interrogation for evidence of recurrent tumor	Active surveillance protocol

tion within the prostate and sometimes the immediately adjacent tissue, with the consequential inflammatory and reparative response. Each distinct technique results in subtle morphologic differences, and the surgical pathologist will likely be requested to not only determine the presence or absence of residual viable tumor but also to assess the degree of tissue damage as a method of providing feedback as to whether the technique was appropriately applied. Familiarity with the particular changes associated with each technique is thus necessary for proper evaluation of the treated area. Our knowledge of these changes is rather limited, as currently there are only a small number of published studies on the histopathological changes associated with newer partial therapy modalities, with most of these encompassing only a small number of cases.

Postradiation Treatment Changes

Changes associated with radiation have been well characterized in the prostate pathology literature, given the popularity of external beam radiation as a whole-gland treatment modality. The changes are similar whether the method of delivery is external beam radiation or brachytherapy, with the latter being the most likely form in which focal radiation therapy is currently applied.

In contrast to most other techniques, radiation can achieve tumor eradication without complete obliteration of the adjacent benign tissue. Thus, benign prostatic glands are usually seen in areas of radiation therapy, although their morphology is markedly altered by the radiation. Typical histologic changes in benign tissue include a decreased ratio of glands to stroma, atrophy, and squamous-like metaplasia of the nonneoplastic glands. Atrophy is predominant in the secretory cells, while the basal cells show atypical pleomorphic nuclei with smudged chromatin and cytoplasmic vacuolization. This cytologic atypia and pleomorphism tends to be marked, frequently resembling neoplastic changes to the inexperienced observer (Fig. 32.1a). The fact that prostatic adenocarcinoma is rarely a pleomorphic tumor should provide reassurance that the atypical cells are not neoplastic in nature [1]. Paneth-like cells and mucinous metaplasia may also be seen. Changes in the adjacent elements include stromal fibrosis, arterial luminal narrowing due to myointimal proliferation, foam cells within vessel walls, and fibrosis and atrophy of seminal vesicles [2]. Despite the striking cytological changes, low-power examination reveals a retention of the lobular architecture of the normal prostatic parenchyma. Changes in the benign glandular elements can persist for prolonged periods of time, up to 5 years postradiation [3].

Prostatic adenocarcinoma shows a spectrum of changes that vary in severity according to the degree of therapy effect in the tumor glands. The most affected tumor tissue shows infiltrative abortive glands and single cells with prominent cytoplasmic vacuolization, pyknotic nuclei, and disappearance of nucleoli (Fig. 32.1b–d). The least affected tumor tissue is indistinguishable from untreated tumor, with amphophilic cytoplasm, enlarged nuclei, and prominent nucleoli. A grading scale to assess the severity of the treatment effect has been proposed and correlated with chances of recurrence (in the setting of external beam radiation) (Table 32.2) [4]. According to the proponents of this grading scale, tumors with scores of 1 or 2 in biopsies taken at 24 months post-therapy biopsy show morphology almost identical to untreated tumors

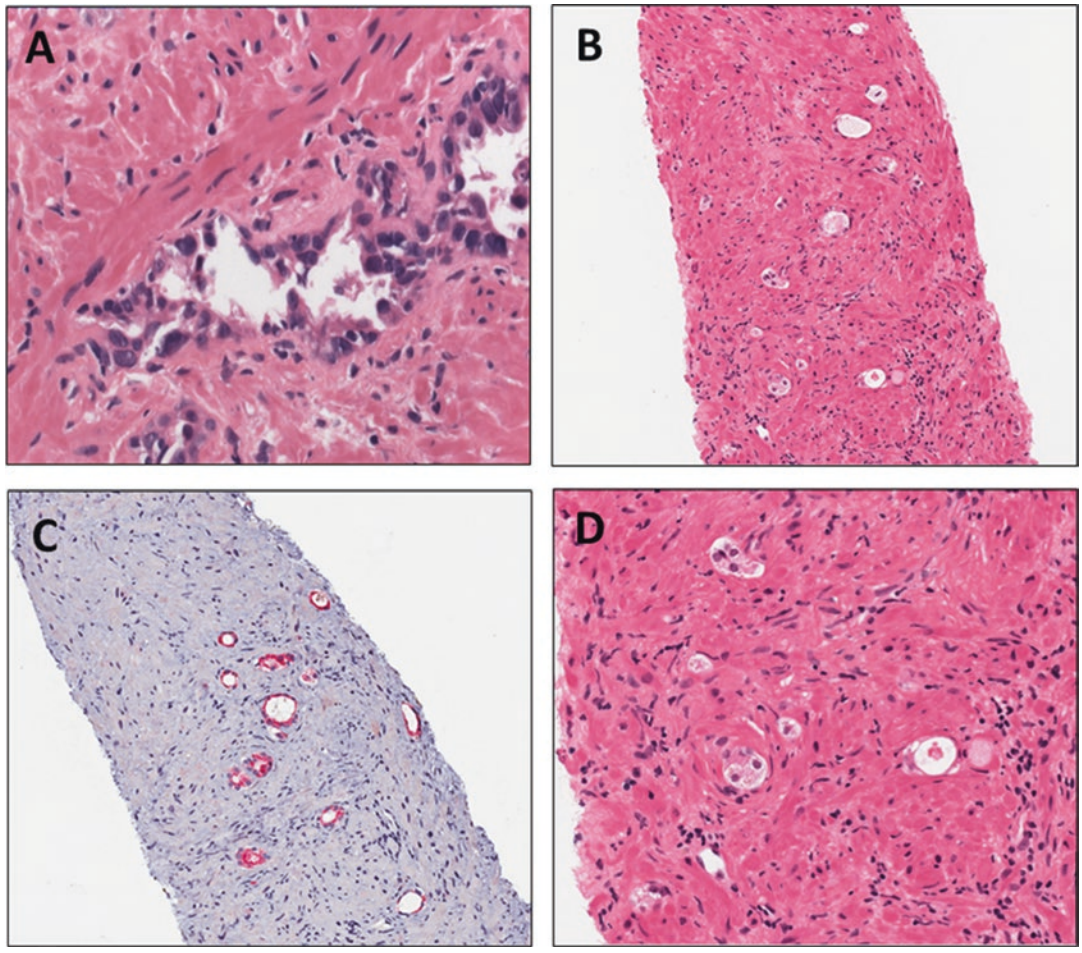

Fig. 32.1 Radiation induced changes in prostatic adenocarcinoma and benign prostatic glands. (**a**) Typical appearance of benign prostatic glands following radiation therapy, characterized by prominent, irregular basal cells with smudged dark chromatin. (**b**) Typical hematoxylin and eosin (H&E) stain appearance of prostatic adenocarcinoma on needle biopsy performed 18 months after external beam radiation therapy, showing malignant acini distributed in a haphazard manner within the prostatic stroma. (**c**) Immunohistochemical staining with a p63/high-molecular-weight keratin/alpha-methylacyl-CoA racemase (AMACR) cocktail showing the expected absence of basal cells (evidenced by a lack of *brown* staining with p63/high-molecular-weight keratin) and positive staining for AMACR (red staining). This profile provides additional support for the diagnosis of prostatic adenocarcinoma with radiation-induced treatment effects. (**d**) High-magnification H&E appearance of the malignant glands shown in (**b**), showing the typical degenerative nuclear changes and vacuolated clear cytoplasm seen following radiation therapy. Gleason grading is not applicable in this setting

and are associated with recurrence rates of 55 %. Tumors with scores in the intermediate range of 3–4 have local failure rates of around 30 %. Tumors showing severe treatment effects, with total treatment grades of 5 to 6, have five-year disease-free survival rates that are similar to negative biopsies and could be considered "indeterminate" for residual tumor [5]. However, in a recent study, no statistically significant difference in biochemical disease-free survival was found between the different degrees of therapy effect in patients undergoing high-dose rate brachytherapy boost for intermediate-risk prostate cancer (PCa) at routine two-year biopsy [6]. It is controversial

Table 32.2 Grading of postradiation treatment effect in prostate biopsies. Adapted from [3, 4]

Cytoplasmic	
0	No identifiable treatment effect
1	Swelling and microvesicular change
2	Vacuolization and voluminous cytoplasm, ruptured cytoplasm, lipofuscin accumulation
3	Single tumor cells or dilated glands
Nuclear	
0	No identifiable treatment effect
1	Nuclear enlargement with smudging and visible nucleoli
2	Large bizarre nuclei with smudging and rare or absent nucleoli
3	Pyknotic, small nuclei

whether Gleason scoring is applicable to radiation-treated tumors: Most institutions apply a Gleason score only to tumors with minimal therapy effect, while avoiding it for tumors with marked effect, given the severe alteration of the tumor's architecture [3, 7].

In general, identification of a haphazard, infiltrative distribution of the glandular elements at low-power microscopic examination is the best way to differentiate residual tumor from benign glandular elements. In difficult cases, immunohistochemical staining with basal cell markers (p63, keratin 34βE12, keratin 5/6) and alpha-methylacyl-CoA racemase (AMACR) is extremely useful, as the differences in immunophenotype between benign and malignant glands are maintained in the setting of radiation therapy. Some authors have investigated the use of proliferation markers such as Ki67 to provide an objective assessment of the viability of the tumor cells [8, 9], although this is not currently routinely recommended.

Post-High-Intensity Focused Ultrasound Treatment Changes

High-intensity focused ultrasound (HIFU) therapy uses highly energetic ultrasound waves that rapidly increase the temperature within the affected area causing tissue destruction and coagulation necrosis (Fig. 32.2). Early reports of the effects of HIFU on canine prostates found subtotal hemorrhagic liquefactive necrosis in 90 % of the gland [10, 11]. In human prostates, radical prostatectomy (RP) specimens at 2 weeks after HIFU treatment showed a spectrum of morphological changes from subtle ultrastructural cell damage to frank necrosis [12, 13]. Treated tumor was associated with loss of cytokeratin 8, signifying severe cellular damage [13]. In a 65-year-old man treated with radical cystoprostatectomy for a prostate-rectal fistula from postradiation salvage HIFU, histological changes of dense fibrosis, neuronal proliferation, and chronic inflammation were noted where prostatic tissue should have been located, with no evidence of residual cancer [14].

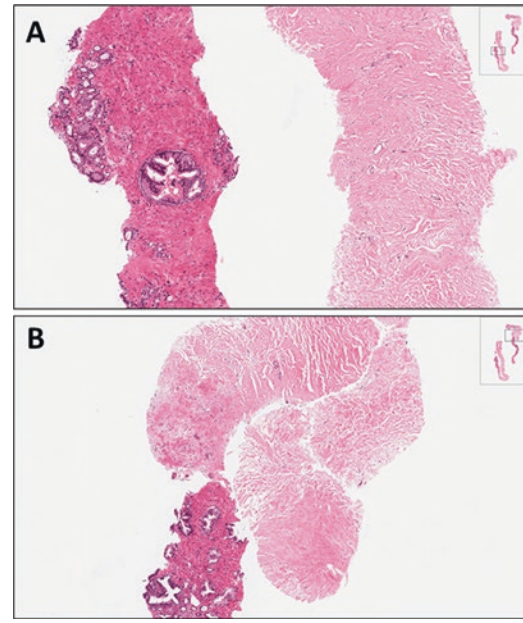

Fig. 32.2 Prostate biopsy following high-intensity focused ultrasound (HIFU) therapy. (**a**) Marked HIFU-induced fibrosis is seen in the core fragment on the right, in this biopsy performed 15 months after HIFU therapy for clinically low-risk prostate cancer. In contrast, the core fragment on the left shows residual prostatic adenocarcinoma and adjacent stroma showing no obvious effects of HIFU therapy. (**b**) Note the sharp interface between the HIFU-induced fibrosis and the unaffected prostate parenchyma

Changes in needle core biopsy are dependent on timing of the biopsy. In an examination of needle biopsies taken 6 months after HIFU treatment, necrosis—often accompanied by acute, chronic, or granulomatous inflammation—was noted in 72 % of the cases, with mild to moderate

fibrosis in all biopsies [15]. In 44 % of their cases, residual adenocarcinoma was present; little to no treatment changes were seen among the glands, raising the possibility of insufficient delivery of thermal energy. In another study of needle biopsies taken at a mean of 14 months after HIFU, coagulation necrosis was much less prevalent (only 4 of 30 cases), with well-developed fibrosis being more common, usually associated with hemosiderin deposition, granulation tissue, and corpora amylacea within spaces lacking epithelium [16]. Adenocarcinoma was present in 63 % of cases, and the authors found that it lacked any morphologic evidence of therapy effect and that Gleason grading could be easily performed. Most of the patients with positive post-HIFU biopsies had Gleason scores less than or equal to their pre-HIFU biopsies along with similar or lower percentage tissue involvement. Cases with higher posttreatment Gleason scores all showed biochemical failure. Additionally, the tumor immunophenotype was not altered by the therapy, and application of common markers yielded expected results. Similarly, both Dalfior et al. and Walter et al. found a preserved immunophenotype in residual tumors in patients who underwent post-HIFU biopsy [17, 18].

Post-Cryotherapy Treatment Changes

Cryotherapy induces tumor ablation through multiple pathways, including mechanical cell destruction by the formation of ice crystals, necrosis, and the induction of apoptosis through metabolic, vascular, and immune pathways [19]. Initial experience on six patients revealed coagulative necrosis in the proximity to the cryosurgery probe (Fig. 32.3a, b), with squamous metaplasia of glandular epithelium and hemorrhagic areas observed further away. A larger study of 30 biopsies performed on a man at 19 months post-cryotherapy revealed chronic inflammation, myxoid stromal change, and stromal hemosiderin [20]. Additional findings included stromal fibrosis, necrosis, calcifications, acute inflammation, granulomas, hemorrhage, vessel wall thickening with prominent endothelial cells, and squamous metaplasia (Fig. 32.3c, d). Residual benign glands, when present, did not show significant histopathologic changes. Recurrent or residual prostatic adenocarcinoma was present in 36 % of cases, almost half of them with a higher Gleason score compared to the pretreatment biopsy. The residual tumor glands did not show evidence of tumor effect [20]. Similarly, Koppie et al. found that of 111 biopsies in patients with 24 or more months of follow-up, 41 (37 %) displayed residual/recurrent prostate cancer [21]. Ellis et al. also found that of 35 patients who underwent biopsy, 14 (40.0 %) contained adenocarcinoma at a mean of 12.0 months posttreatment. However, they caution that 13 of these had been taken from the side of the prostate that was not initially treated [22].

Post-Laser Ablation Changes

Laser ablation induces tissue necrosis by thermal injury, and thus the findings are similar to those of HIFU, including a sharp interface between treated and untreated tissue, the former characterized by coagulative necrosis and "ghosts" of malignant glands (Fig. 32.4). Lindner et al. described four patients who underwent RP after laser ablation therapy and found that the ablation zone was characterized by homogeneous areas of coagulation necrosis, surrounded by a small hemorrhagic rim, devoid of vital glandular tissue [23]. Vitality of the residual glands was assessed by the use of cytokeratin 8, which demonstrated an abrupt transition of positive (vital) glandular tissue and negative (ablated) glands. The points of insertion of the laser fibers were easily identified in the whole-mount sections of the RP specimen, and the absence of residual tumor in between the two fibers was evident. The ablation zone extended all the way to the prostate capsule. Also, there was a good correlation between magnetic resonance imaging (MRI) and whole-mount hematoxylin and eosin (H&E) stain histological examination and an even better correlation with the loss of cytokeratin 8 immunohistochemical staining. Oto et al. published results on 6-month post-procedure biopsies for nine patients who

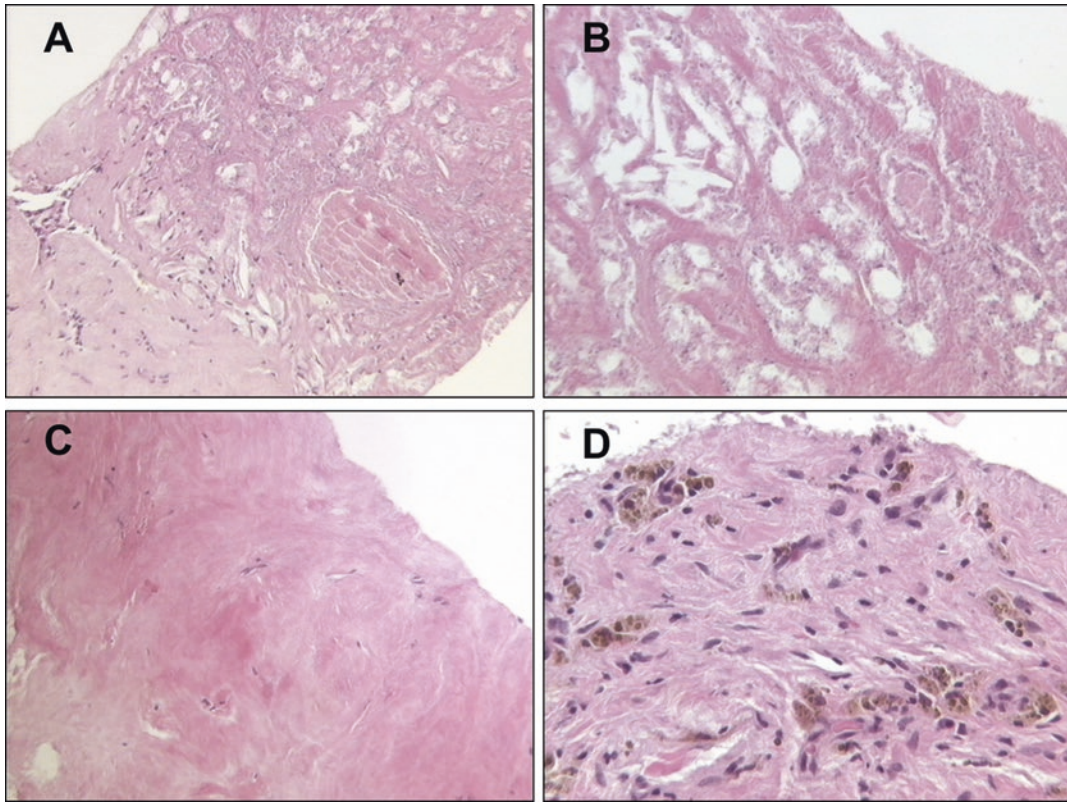

Fig. 32.3 Prostate biopsy following cryotherapy. (**a**) Cryotherapy induces extensive coagulative necrosis and adjacent fibrosis. (**b**) Necrotic tumor is characterized by "ghost" glands that maintain the architecture of the original glands, but lose all cytologic detail. (**c**) Area of hyalinized fibrosis, with minimal cellularity. (**d**) More cellular area of fibrosis, with fibroblasts and hemosiderin-laden macrophages, indicative of prior hemorrhage

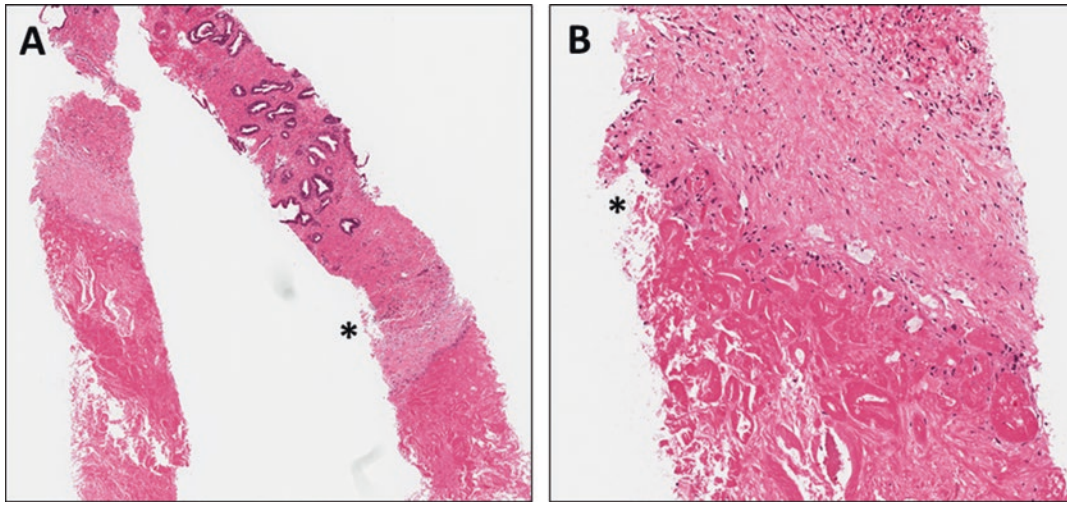

Fig. 32.4 Prostate biopsy following interstitial laser ablation therapy. (**a**) Low-magnification view of a prostate needle biopsy performed 5–6 months after primary interstitial laser ablation therapy. Note the core fragment on the right, where the sharp interface between treated and untreated tissue is readily apparent (denoted by the *asterisk*). (**b**) High-magnification view showing the ablation zone characterized by a peripheral rim of fibrosis between the unaffected parenchyma and the ablated tumor, which is characterized by coagulative necrosis and "ghosts" of malignant glands

underwent laser ablation: seven patients had no evidence of residual/recurrent disease, while two showed Gleason 3+3 adenocarcinoma [24]. Retrospective review of the ablation images revealed incomplete coverage of the lesion site by the ablation zone for the two patients with positive follow-up biopsies. Similarly, Lee et al. reported that 12 of their 13 patients who had laser ablation therapy had no residual cancer on follow-up biopsy [25]. The remaining patient had Gleason 3+4 adenocarcinoma. An additional patient developed a new multiparametric MRI (mpMRI) abnormality away from the treated area that upon biopsy revealed 3+3 adenocarcinoma. Both cases were subsequently reablated.

Post-Photodynamic Therapy Changes

Photodynamic therapy uses photosensitizing drugs that are pharmacologically inactive until they are exposed to light in the presence of oxygen. Once activated, the drug forms reactive oxygen species that are directly responsible for thrombosis and tissue destruction around the optical fiber. For prostate cancer, the photosensitizers are administered orally or intravenously and activated in the prostate by a low-power laser light delivered with optical fibers. Histopathologic changes associated with photodynamic therapy include hemorrhagic necrosis with inflammation, gland destruction, atrophy, and vascular thrombosis in the treated area, ultimately followed by dense fibrosis (Fig. 32.5a–d) [3, 26]. Eymerit-Morin et al. described the histopathologic findings in 6-month follow-up biopsies of 53 patients who underwent focal photodynamic therapy; these comprised sharply demarcated hyaline scars, rare atrophic glands, mild chronic inflammatory infiltrate, hemosiderin deposition, and coagulative necrosis [27]. Vascular lesions such as intimal hyaline fibrosis or organized thrombi were not prominent. Seventeen of the 53 patients had residual carcinoma in the treated lobe, all located outside the scarred area, usually close to the capsule (which was intentionally avoided). The Gleason score was upgraded in five patients. The viable carcinoma glands did not display any therapy-related changes and were easily recognized in most cases with routine histology.

Post-Irreversible Electroporation Changes

Irreversible electroporation (IRE), or electropermeabilization, is a nonthermal ablation technique by which cell membrane permeability to ions and macromolecules is increased by exposing the cell to short electric current pulses, creating permanent cellular and tissue damage. The electric current pulses are delivered by needle electrodes percutaneously placed in the tumor under ultrasound guidance [28]. A small study by Neal et al. describes the findings in two patients who underwent RP after IRE [29]. The treatment areas exhibited extensive necrosis with inflammatory neutrophilic infiltrate, surrounded by an area of reactive fibroblasts and hemorrhage. The adjacent viable ducts displayed squamous metaplasia. A recent study reported on 16 patients who underwent IRE 4 weeks prior to scheduled RP [30]. Microscopic assessment of the ablation zone showed areas of fibrosis, necrosis, and ghost tubuli with eosinophilic cytoplasm, surrounded by a hemorrhagic area corresponding with the location of the electrodes on ultrasound. Mild to moderate inflammation, basal cell hyperplasia, and urothelial metaplasia were also seen. No skip lesions (residual viable tissue) were identified in the ablated area. The prostate capsule was affected by the IRE treatment in most cases, showing invasion of adipocytes and lipophages in the capsule. IRE effects were observed extending into the neurovascular bundle in the majority of patients, where it was recognized as eosinophilic degeneration of the cytoplasm and pyknotic nuclei of the nerves. The prostatic urethra was affected in nine patients, showing denudation of the urothelium. Tissue outside the ablation zone contained multifocal adenocarcinoma in 15 patients with the diameter of the dominant tumor area ranging from 3 mm to 18 mm. Four tumors extended into the extraprostatic tissue. More recently, Ting et al. reported on 25 patients who underwent IRE; of

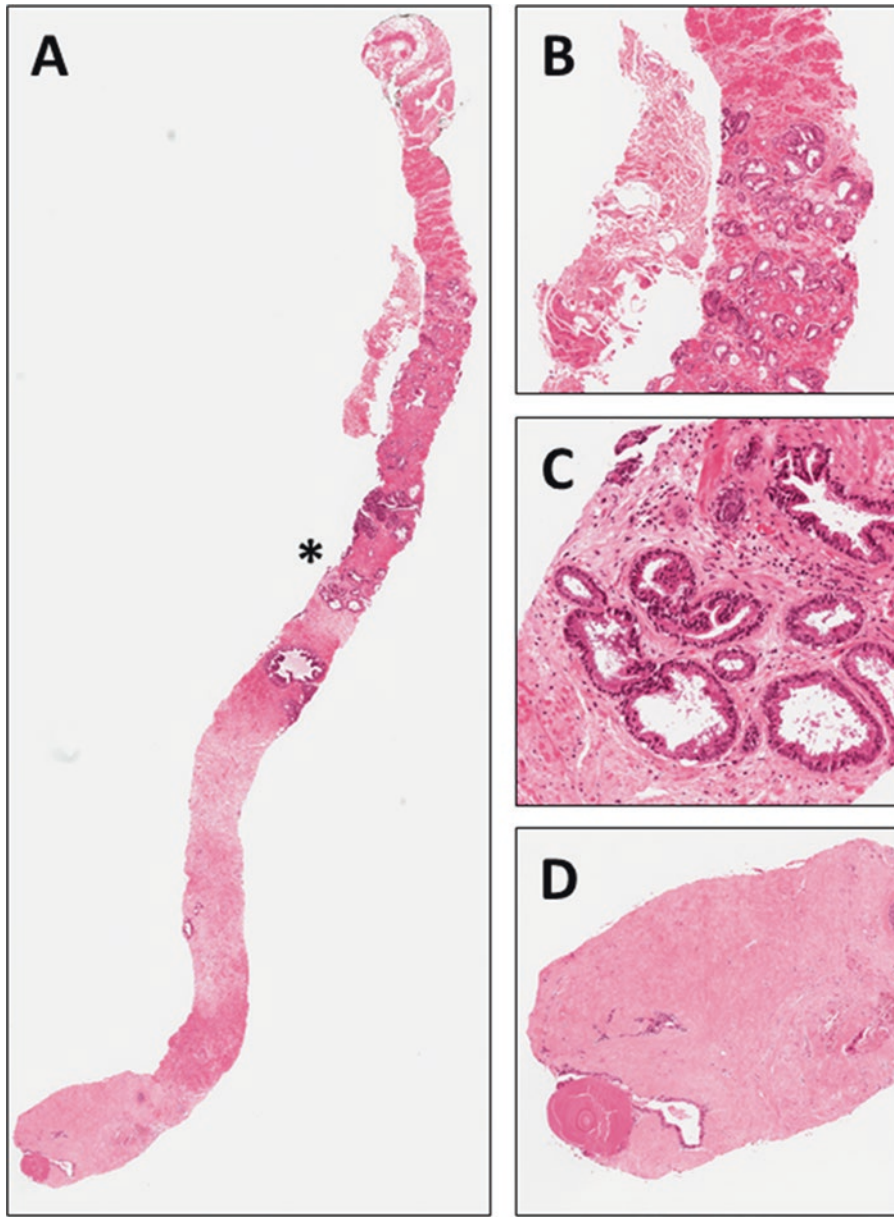

Fig. 32.5 Prostate biopsy following photodynamic therapy (PDT). (**a**) Low-magnification overview of a needle biopsy obtained 8 months following salvage PDT after incomplete primary radiotherapy. Tissue above the asterisk shows no appreciable treatment effect, while that below the asterisk shows a marked range of fibrosis. (**b**) High-magnification view of adenocarcinoma and stroma from the top of the core in (**a**) showing no treatment effect. (**c**) High-magnification view of tissue located at the asterisk in (**a**). The adenocarcinoma shows no appreciable treatment effects, while the adjacent stroma shows moderate fibrosis. (**d**) High-magnification view of the end of the core in (**a**) showing dense scarring resulting from the PDT therapy

the 21 who underwent follow-up biopsy, 5 (21 %) had significant disease on follow-up biopsy. However, four of these were located in the field adjacent to the ablation zone, suggesting that a wider margin around the area of concern is required to ensure adequate treatment [31].

Other Emerging Therapy Modalities

Other modalities of energy delivery to the prostate for purposes of focal therapy are in early stages of investigation, and relatively little information is available on the pathologic findings associated with these therapies.

Interstitial microwave thermal therapy (IMT) induces tissue damage by heating of tissue to cytotoxic levels of 55–70 °C. The electromagnetic energy, which increases kinetic energy by rotating cellular molecules, is delivered to the prostate by the insertion of microwave antennas through the perineum. Only a few studies have been published that include histopathologic analysis after IMT. In a report of findings in canine prostates, Cheng et al. described three discrete zones within hours of IMT, one characterized by its resemblance to untreated tissue, with the glandular and stromal architecture intact, but nuclei appearing pyknotic. The second zone had a ghostlike appearance due to disrupted cell membranes and vessels; extravasated red blood cells were present. The third zone had similar cellular changes with vascular dilatation and interstitial hemorrhage [32]. A study of five RP specimens, performed 1 week after IMT delivered transurethrally, revealed sharply circumscribed necrosis with the nonviable zone wider at the base, gradually decreasing toward the apex. The prostate cancer was generally localized in the peripheral zone at depths greater than microwave penetration, whereas the thermally damaged zone appeared in the transition zone circumferential to the prostatic urethra [33].

Radiofrequency interstitial tumor ablation (RITA) generates temperatures of around 100 °C and induces coagulative necrosis. The radiofrequency energy is delivered by precise placement of needle electrodes into the previously localized tumor. Zlotta et al. reported on 13 RP specimens removed immediately and after 1 week post-RITA. Macroscopically large hemorrhagic areas were visible; microscopically they were characterized by an intense interstitial edema and fading of the cell borders with cytoplasmic hypereosinophilia. Glandular retraction and desquamation of the epithelium in the glandular lumen were seen [34]. Another study reported on follow-up needle core biopsies on 11 patients who underwent RITA. Seven had negative biopsies at 6 months and six of nine at 12 months after RITA [35].

Monitoring of the Non-treated Area

As stated previously, in a successful partial therapy, the non-treated area should harbor no neoplastic disease or at worst low-grade, clinically insignificant tumors. It is well known that prostate cancer is a multifocal disease in 57–91 % of cases [36–40]. Despite this, Liu et al., by using a high-resolution genome-wide survey of single-nucleotide and copy-number polymorphisms, concluded that different, anatomically distinct metastases within the same patient originated from a single precursor cell [41]. This notion is central to the concept of index tumor, which proposes that the biologic behavior of PCa is determined, in multifocal tumors, by its most aggressive lesion, usually the one that has the largest size, highest grade, or highest stage within the prostate [42]. Index tumor determination by mpMRI or transperineal template-guided mapping biopsy is highly accurate. The largest tumors usually have the highest Gleason score—up to 98 % of patients in one study [43]. However, in a recent series of 122 men, 20 % had Gleason 7 non-index tumors, including 5 % with tumors >4+3, the majority of which were missed by MRI [44]. Further, non-index tumors have been reported to locally invade [39] and metastasize [45, 46]. Focal therapy series treating the index lesion only have reported detection of clinically significant disease arising in the outfield, or untreated, area at 6-month biopsy [47]. It remains unclear at present, whether outfield recurrence is due to disease progression as a result of field change or previously undetected small foci of cancer. Data on histological assessment of untreated zone is difficult to interpret as not all series that report residual adenocarcinoma post-focal therapy specify location or even grade of the positive cores [48]. Nonetheless, the published data provides evidence supporting active surveillance of the untreated area and having a

low threshold to intervene in case of suspicion of clinically significant tumor. Documentation of clinically significant disease in the untreated area should prompt further therapy, either whole-gland therapy or additional focal therapy.

Multiple active surveillance protocols have been employed, and the majority of series include clinical assessment with digital rectal examination, prostate-specific antigen (PSA)/PSA kinetics, and re-biopsy at 12–18 months, followed by trigger-based biopsies [49]. It is still unclear what the impact of mpMRI as a surveillance technique is in follow-up protocols [50]. Similarly, it is unclear whether histologic criteria for active surveillance defined for systematic blinded biopsy are applicable to surveillance protocols in the era of mpMRI and focal therapy [51].

Reporting Recommendations for Post-focal Therapy Treatment Biopsies

The following recommendations have been recently published by the Société Internationale d'Urologie and the International Consultation on Urologic Diseases [52]:

1. In biopsies from the treated area, it is important for the pathologist to report findings that confirm that the area biopsied is indeed the treated area. As stated above, these may include necrosis, hemorrhage, acute and chronic inflammation, stromal edema, glandular atrophy, hemosiderin deposition, reactive fibroblasts, and stromal fibrosis and should be consistent with the treatment modality employed.
2. In the treated area, a diagnostic menu for biopsy findings may include:
   (a) Benign prostatic tissue with posttreatment changes, no residual carcinoma
   (b) High-grade prostatic intraepithelial neoplasia (HGPIN)
   (c) Atypical small glands, suspicious for carcinoma, a diagnosis usually rendered after examination of multiple levels and/or immunohistochemical studies
   (d) Prostatic adenocarcinoma
3. If no treatment-induced changes are apparent, which is usually the case with focal therapy, a Gleason score should be assigned to the finding of prostatic carcinoma in the treated area.
4. A finding of HGPIN in the treated area following focal therapy is of uncertain but likely little significance, particularly if isolated.
5. The recent World Health Organization/International Society of Urologic Pathologists (WHO/ISUP) recommended prognostic grade groups (1 through 5), which group different combinations of Gleason grades according to prognosis, and should be reported in parallel with the Gleason grade [53].
6. In core and systematic biopsies outside of the treated areas, handling and reporting should occur in conjunction with established practices.
7. Judicious use of immunohistochemistry markers should be considered for the microscopic interpretation of treated glands in biopsy specimens. Basal cell markers, such as cytokeratin 34BE12, p63, or cytokeratin 5/6 selectively label basal cells in prostatic glands. These cells are present only in benign glands, and thus their detection is reassuring when the benignity of a group of atypical glands is questioned. The presence of alpha-methylacyl-coenzyme A racemase (AMACR), a well-known marker overexpressed in prostate cancer, has been found to facilitate or support decision-making in differentiating cancer from benign glands with atypia, such as those seen after radiation therapy [54]. Many modern pathology laboratories use a p63/high-molecular-weight cytokeratin/AMACR immunohistochemical stain, which has demonstrated utility in the setting of treated prostate [55].

Conclusion

In summary, focal therapy is associated with technique-dependent histopathologic changes that the surgical pathologist will encounter more frequently as these techniques gain popularity. Pathologists not only need to familiarize themselves with the effects of these new treatment modalities, but should actively participate in the

development of criteria for determining therapeutic success or failure and their appropriate reporting, as well as defining the optimal surveillance of both the treated and untreated areas of the prostate.

References

1. Gaudin PB, Zelefsky MJ, Leibel SA, Fuks Z, Reuter VE. Histopathologic effects of three-dimensional conformal external beam radiation therapy on benign and malignant prostate tissues. Am J Surg Pathol. 1999;23(9):1021–31.
2. Bostwick DG, Egbert BM, Fajardo LF. Radiation injury of the normal and neoplastic prostate. Am J Surg Pathol. 1982;6(6):541–51.
3. Evans AJ, Ryan P, Van derKwast T. Treatment effects in the prostate including those associated with traditional and emerging therapies. Adv Anat Pathol. 2011;18(4):281–93.
4. Crook JM, Bahadur YA, Robertson SJ, Perry GA, Esche BA. Evaluation of radiation effect, tumor differentiation, and prostate specific antigen staining in sequential prostate biopsies after external beam radiotherapy for patients with prostate carcinoma. Cancer. 1997;79(1):81–9.
5. Crook JM, Malone S, Perry G, Eapen L, Owen J, Robertson S, et al. Twenty-four-month postradiation prostate biopsies are strongly predictive of 7-year disease-free survival: results from a canadian randomized trial. Cancer. 2009;115(3):673–9.
6. D'Alimonte L, Helou J, Sherman C, Loblaw A, Chung HT, Ravi A, et al. The clinical significance of persistent cancer cells on prostate biopsy after high-dose-rate brachytherapy boost for intermediate-risk prostate cancer. Brachytherapy. 2015;14(3):309–14.
7. Epstein JI, Netto GJ. In: JI E, editor. Biopsy interpretation of the prostate. Philadelphia, PA: Wolters Kluwer Health; 2015.
8. Crook J, Robertson S, Esche B. Proliferative cell nuclear antigen in postradiotherapy prostate biopsies. Int J Radiat Oncol Biol Phys. 1994;30(2):303–8.
9. Scalzo DA, Kallakury BV, Gaddipati RV, Sheehan CE, Keys HM, Savage D, et al. Cell proliferation rate by mib-1 immunohistochemistry predicts postradiation recurrence in prostatic adenocarcinomas. Am J Clin Pathol. 1998;109(2):163–8.
10. Gelet A, Chapelon JY, Margonari J, Theillere Y, Gorry F, Cathignol D, et al. Prostatic tissue destruction by high-intensity focused ultrasound: experimentation on canine prostate. J Endourol. 1993;7(3):249–53.
11. Lu J, Ye Z, Wang W, Chen Z, Zhang Y, Hu W. Experimental study on the effect of high-intensity focused ultrasound (hifu) using sonablate-500 in the ablation of canine prostate. J Huazhong Univ Sci Technol Med Sci. 2007;27(2):193–6.
12. Napoli A, Anzidei M, De Nunzio C, Cartocci G, Panebianco V, De Dominicis C, et al. Real-time magnetic resonance-guided high-intensity focused ultrasound focal therapy for localised prostate cancer: preliminary experience. Eur Urol. 2013;63(2):395–8.
13. Van Leenders GJ, Beerlage HP, Ruijter ET, de la Rosette JJ, van de Kaa CA. Histopathological changes associated with high intensity focused ultrasound (hifu) treatment for localised adenocarcinoma of the prostate. J Clin Pathol. 2000;53(5):391–4.
14. Chalasani V, Martinez CH, Williams AK, Kwan K, Chin JL. Histological changes in the human prostate after radiotherapy and salvage high intensity focused ultrasound. Can Urol Assoc J. 2010;4(4):E100–2.
15. Biermann K, Montironi R, Lopez-Beltran A, Zhang S, Cheng L. Histopathological findings after treatment of prostate cancer using high-intensity focused ultrasound (hifu). Prostate. 2010;70(11):1196–200.
16. Ryan P, Finelli A, Lawrentschuk N, Fleshner N, Sweet J, Cheung C, et al. Prostatic needle biopsies following primary high intensity focused ultrasound (hifu) therapy for prostatic adenocarcinoma: histopathological features in tumour and non-tumour tissue. J Clin Pathol. 2012;65(8):729–34.
17. Dalfior D, Delahunt B, Brunelli M, Parisi A, Ficarra V, Novara G, et al. Utility of racemase and other immunomarkers in the detection of adenocarcinoma in prostatic tissue damaged by high intensity focused ultrasound therapy. Pathology. 2010;42(1):1–5.
18. Walter B, Weiss T, Hofstadter F, Gaumann A, Hartmann A, Rogenhofer S, et al. Utility of immunohistochemistry markers in the interpretation of post-high-intensive focussed ultrasound prostate biopsy cores. World J Urol. 2013;31(5):1129–33.
19. Baust JG, Bischof JC, Jiang-Hughes S, Polascik TJ, Rukstalis DB, Gage AA, et al. Re-purposing cryoablation: a combinatorial 'therapy' for the destruction of tissue. Prostate Cancer Prostatic Dis. 2015;18(2):87–95.
20. Gooden C, Nieh PT, Osunkoya AO. Histologic findings on prostate needle core biopsies following cryotherapy as monotherapy for prostatic adenocarcinoma. Hum Pathol. 2013;44(5):867–72.
21. Koppie TM, Shinohara K, Grossfeld GD, Presti Jr JC, Carroll PR. The efficacy of cryosurgical ablation of prostate cancer: the University of California, San Francisco experience. J Urol. 1999;162(2):427–32.
22. Ellis DS, Manny Jr TB, Rewcastle JC. Focal cryosurgery followed by penile rehabilitation as primary treatment for localized prostate cancer: initial results. Urology. 2007;70(6 Suppl):9–15.
23. Lindner U, Lawrentschuk N, Trachtenberg J. Focal laser ablation for localized prostate cancer. J Endourol. 2010;24(5):791–7.
24. Oto A, Sethi I, Karczmar G, McNichols R, Ivancevic MK, Stadler WM, et al. MR imaging-guided focal laser ablation for prostate cancer: phase I trial. Radiology. 2013;267(3):932–40.
25. Lee T, Mendhiratta N, Sperling D, Lepor H. Focal laser ablation for localized prostate cancer: principles, clinical trials, and our initial experience. Rev Urol. 2014;16(2):55–66.

26. Srigley JR, Delahunt B, Evans AJ. Therapy-associated effects in the prostate gland. Histopathology. 2012;60(1):153–65.
27. Eymerit-Morin C, Zidane M, Lebdai S, Triau S, Azzouzi AR, Rousselet MC. Histopathology of prostate tissue after vascular-targeted photodynamic therapy for localized prostate cancer. Virchows Arch. 2013;463(4):547–52.
28. van den Bos W, de Bruin DM, Muller BG, Varkarakis IM, Karagiannis AA, Zondervan PJ, et al. The safety and efficacy of irreversible electroporation for the ablation of prostate cancer: a multicentre prospective human in vivo pilot study protocol. BMJ Open. 2014;4(10):e006382.
29. Neal 2nd RE, Millar JL, Kavnoudias H, Royce P, Rosenfeldt F, Pham A, et al. In vivo characterization and numerical simulation of prostate properties for non-thermal irreversible electroporation ablation. Prostate. 2014;74(5):458–68.
30. van den Bos W, Jurhill RR, de Bruin DM, Savci-Heijink CD, Postema AW, Wagstaff PG, et al. Histopathological outcomes after irreversible electroporation in prostate cancer; results of an ablate-and-resect study. J Urol. 2016;196(2):552–9.
31. Ting F, Tran M, Bohm M, Siriwardana A, Van Leeuwen PJ, Haynes AM, et al. Focal irreversible electroporation for prostate cancer: functional outcomes and short-term oncological control. Prostate Cancer Prostatic Dis. 2016;19(1):46–52.
32. Cheng HL, Haider MA, Dill-Macky MJ, Sweet JM, Trachtenberg J, Gertner MR. MRI and contrast-enhanced ultrasound monitoring of prostate microwave focal thermal therapy: an in vivo canine study. J Magn Reson Imaging. 2008;28(1):136–43.
33. Huidobro C, Bolmsjo M, Larson T, de la Rosette J, Wagrell L, Schelin S, et al. Evaluation of microwave thermotherapy with histopathology, magnetic resonance imaging and temperature mapping. J Urol. 2004;171(2 Pt 1):672–8.
34. Zlotta AR, Djavan B, Matos C, Noel JC, Peny MO, Silverman DE, et al. Percutaneous transperineal radiofrequency ablation of prostate tumour: safety, feasibility and pathological effects on human prostate cancer. Br J Urol. 1998;81(2):265–75.
35. Shariat SF, Raptidis G, Masatoschi M, Bergamaschi F, Slawin KM. Pilot study of radiofrequency interstitial tumor ablation (RITA) for the treatment of radiorecurrent prostate cancer. Prostate. 2005;65(3):260–7.
36. Wise AM, Stamey TA, McNeal JE, Clayton JL. Morphologic and clinical significance of multifocal prostate cancers in radical prostatectomy specimens. Urology. 2002;60(2):264–9.
37. Karavitakis M, Winkler M, Abel P, Livni N, Beckley I, Ahmed HU. Histological characteristics of the index lesion in whole-mount radical prostatectomy specimens: implications for focal therapy. Prostate Cancer Prostatic Dis. 2011;14(1):46–52.
38. Delongchamps NB, Beuvon F, Eiss D, Flam T, Muradyan N, Zerbib M, et al. Multiparametric mri is helpful to predict tumor focality, stage, and size in patients diagnosed with unilateral low-risk prostate cancer. Prostate Cancer Prostatic Dis. 2011;14(3):232–7.
39. Ruijter ET, Van De Kaa CA, Schalken JA, Debruyne FM, Ruiter DJ. Histological grade heterogeneity in multifocal prostate cancer. Biological and clinical implications. J Pathol. 1996;180(3):295–9.
40. Noguchi M, Stamey TA, McNeal JE, Nolley R. Prognostic factors for multifocal prostate cancer in radical prostatectomy specimens: lack of significance of secondary cancers. J Urol. 2003;170(2 Pt 1):459–63.
41. Liu W, Laitinen S, Khan S, Vihinen M, Kowalski J, Yu G, et al. Copy number analysis indicates monoclonal origin of lethal metastatic prostate cancer. Nat Med. 2009;15(5):559–65.
42. Ahmed HU. The index lesion and the origin of prostate cancer. N Engl J Med. 2009;361(17):1704–6.
43. Baco E, Ukimura O, Rud E, Vlatkovic L, Svindland A, Aron M, et al. Magnetic resonance imaging-transectal ultrasound image-fusion biopsies accurately characterize the index tumor: correlation with step-sectioned radical prostatectomy specimens in 135 patients. Eur Urol. 2015;67(4):787–94.
44. Le JD, Tan N, Shkolyar E, Lu DY, Kwan L, Marks LS, et al. Multifocality and prostate cancer detection by multiparametric magnetic resonance imaging: correlation with whole-mount histopathology. Eur Urol. 2015;67(3):569–76.
45. Gburek BM, Kollmorgen TA, Qian J, D'Souza-Gburek SM, Lieber MM, Jenkins RB. Chromosomal anomalies in stage d1 prostate adenocarcinoma primary tumors and lymph node metastases detected by fluorescence in situ hybridization. J Urol. 1997;157(1):223–7.
46. Haffner MC, Mosbruger T, Esopi DM, Fedor H, Heaphy CM, Walker DA, et al. Tracking the clonal origin of lethal prostate cancer. J Clin Invest. 2013;123(11):4918–22.
47. Ahmed HU, Dickinson L, Charman S, Weir S, McCartan N, Hindley RG, et al. Focal ablation targeted to the index lesion in multifocal localised prostate cancer: a prospective development study. Eur Urol. 2015;68(6):927–36.
48. Shah TT, Kasivisvanathan V, Jameson C, Freeman A, Emberton M, Ahmed HU. Histological outcomes after focal high-intensity focused ultrasound and cryotherapy. World J Urol. 2015;33(7):955–64.
49. Dall'Era MA, Albertsen PC, Bangma C, Carroll PR, Carter HB, Cooperberg MR, et al. Active surveillance for prostate cancer: a systematic review of the literature. Eur Urol. 2012;62(6):976–83.
50. Tay KJ, Mendez M, Moul JW, Polascik TJ. Active surveillance for prostate cancer: can we modernize contemporary protocols to improve patient selection and outcomes in the focal therapy era? Curr Opin Urol. 2015;25(3):185–90.
51. Hu JC, Chang E, Natarajan S, Margolis DJ, Macairan M, Lieu P, et al. Targeted prostate biopsy in select

men for active surveillance: do the epstein criteria still apply? J Urol. 2014;192(2):385–90.
52. Polascik TJ, Tay KJ, Ghai S, Jimenez RE, Kench J, Klotz L, et al. Surveillance after prostate focal therapy. In: Sanchez-Salas R, Desai M, editors. Image-guided therapy in urology a joint SIU-ICUD international consultation. Montreal: Société Internationale d'Urologie; 2016.
53. Epstein JI, Egevad L, Amin MB, Delahunt B, Srigley JR, Humphrey PA, et al. The 2014 international society of urological pathology (ISUP) consensus conference on gleason grading of prostatic carcinoma: definition of grading patterns and proposal for a new grading system. Am J Surg Pathol. 2016;40(2):244–52.
54. Yang XJ, Laven B, Tretiakova M, Blute Jr RD, Woda BA, Steinberg GD, et al. Detection of alpha-methylacyl-coenzyme a racemase in postradiation prostatic adenocarcinoma. Urology. [Comparative Study Multicenter Study]2003;62(2):282–6.
55. Martens MB, Keller JH. Routine immunohistochemical staining for high-molecular weight cytokeratin 34-beta and alpha-methylacyl coa racemase (p504s) in postirradiation prostate biopsies. Mod Pathol. 2005;19(2):287–90.

Posttreatment Surveillance Using Multiparametric Magnetic Resonance Imaging

33

Alex Kirkham

Introduction

In the previous edition of this book, there was one chapter devoted to post-ablation follow-up, addressing both imaging and biopsy [1]. The subject is given more attention in the current volume, and for several reasons magnetic resonance imaging (MRI) in particular has the potential to play a vital role in the follow-up of focal therapies.

Firstly, all current technologies for ablating the prostate are subject to a degree of imprecision, and MRI provides early feedback about the size of the ablated zone and the likelihood of incomplete treatment, creating both an important feedback loop for the operator and an opportunity to detect early complications.

Second, all current focal treatment modalities, even if appropriately targeted, have a significant rate of incomplete treatment. In a recent analysis of high-intensity focused ultrasound (HIFU), one of the most mature technologies, the rate of failure of the primary treatment approaches 30 % at 5 years [2]. Follow-up is of vital importance, both for in-field residual tumor and for new or previously undetected synchronous disease [3]. While it is possible to reduce the morbidity of prostate biopsy by the transperineal approach [4], there is a growing body of evidence to suggest that biopsy is potentially more sensitive and less morbid if targeted to MRI findings [5]. In the long term, a follow-up strategy based on noninvasive tests is likely to be far better tolerated than repeated biopsy, with its risk of infection and functional morbidity [6].

This chapter will address the appearance of the prostate after several focal treatment techniques, both soon after treatment and over months or years.

Early Appearances

Assessing Necrosis

Almost all ablative techniques (whether by cold [7], heat [8], or electroporation [9]) produce confluent areas of tissue necrosis. The treated zone usually increases in volume in the days following treatment [10, 11], and although necrotic tissue shows changes in elasticity that can be seen with ultrasound [12] and MRI [13], techniques that assess perfusion have far greater spatial resolution [10]. Although ultrasound has been used to successfully delineate the perfusion defect after ablation with HIFU [14] and irreversible electroporation [15] and is potentially of high resolution [16], MRI allows a standardized technique in which all

A. Kirkham (✉)
Department of Radiology, University College Hospital, London, UK
e-mail: Alex.Kirkham@uclh.nhs.uk; alexkirkham@yahoo.com

© Springer International Publishing AG 2017
T.J. Polascik (ed.), *Imaging and Focal Therapy of Early Prostate Cancer*, Current Clinical Urology, DOI 10.1007/978-3-319-49911-6_33

areas of the prostate are easily imaged, and comparison can be made with preoperative appearances [14].

The effects of radiotherapy are likely to be much more gradual, although significant changes in prostate volume and tumor enhancement are seen at 2 months after stereotactic radiotherapy [17]. There are few studies of the earlier effects of radiotherapy on the prostate, so we will address the appearance of the prostate after radiotherapy, and the detection of residual disease, in the "Late Scans" section of this chapter.

Technique

The best time for imaging necrosis has yet to be determined. For some technologies the final amount of necrosis may not be apparent immediately (taking several hours to develop in the case of photodynamic therapy [18]), and we know that after whole-gland HIFU, the volume of the necrotic part of the prostate may shrink by around 50 % in the first month [19]. To accurately delineate the volume of necrosis, we therefore recommend scanning at 1–7 days after treatment.

T2 appearances are heterogeneous and cannot be used to assess necrosis, but a high-resolution T2 sequence is useful for correlation with preoperative imaging [19]. Diffusion is generally not assessed, and even if the diffusion findings correlated with necrosis, the spatial resolution of diffusion sequences is usually inferior to either spin or gradient echo T1-weighted sequences [20]. Pre-contrast imaging is vital because necrosis is often associated with hemorrhage, and it is possible to assess the prostate using pre- and post-contrast high-resolution (3 mm slices, in plane resolution <1 mm) T1 spin echo sequences. However, although potentially of lower resolution, dynamically enhanced scans are a mainstay of the assessment of tumor before treatment [21] and can be performed in addition with little time penalty. A protocol that conforms to the European Society of Urogenital Radiology (ESUR) guidelines on multiparametric prostate MRI [21], but omitting diffusion and including post-contrast spin echo images in several planes, will suffice.

Significance of Non-perfusion and Prognostic Value

Effective thermal ablation should produce an area of confluent non-enhancement, which is usually surrounded by a thin enhancing rim (Figs. 33.1 and 33.2) [10, 19]. This rim is also seen after thermal ablation of the liver [22] and kidney [23] and is likely to represent inflammation, granulation, and fibrosis [24], although after HIFU at least part of it appears necrotic at biopsy [8].

We are careful to use the term "non-enhancement" (others use "signal void" [7]) rather than fibrosis because we cannot be sure that lack of enhancement correlates with truly necrotic tissue. The early experience in cryotherapy suggested that if the volume of the tumor were non-enhancing after treatment, then recurrence was unlikely [25], but subsequent experience has shown that there is a significant rate of residual, viable tumor, even when treatment is apparently complete and margins are adequate [7]. The difference may well be due to inhomogeneous freezing [26], and a similar limit of sensitivity of MRI for small amounts of enhancement is likely to be present with thermal therapies. However, two small series (one in HIFU, of 13 patients [10], the other in photodynamic therapy, with ten patients [27]) have suggested that the completeness of early non-enhancement predicts the absence of tumor at 6 months. Both of these studies were in the era of whole-gland treatment, and similar studies for focal therapy are awaited.

What is the evidence that non-enhancement correlates with necrosis? To answer this question probably requires animal studies in which the MRI and histological appearances can be correlated accurately. One such study examined the effects of a prototype rotating HIFU probe that produced confluent necrosis extending out from the urethra. The line of non-enhancement on MRI lays *inside* the line drawn on histology to map the complete necrosis. In other words, non-enhancement always implied necrosis. However, such results must be interpreted with caution:

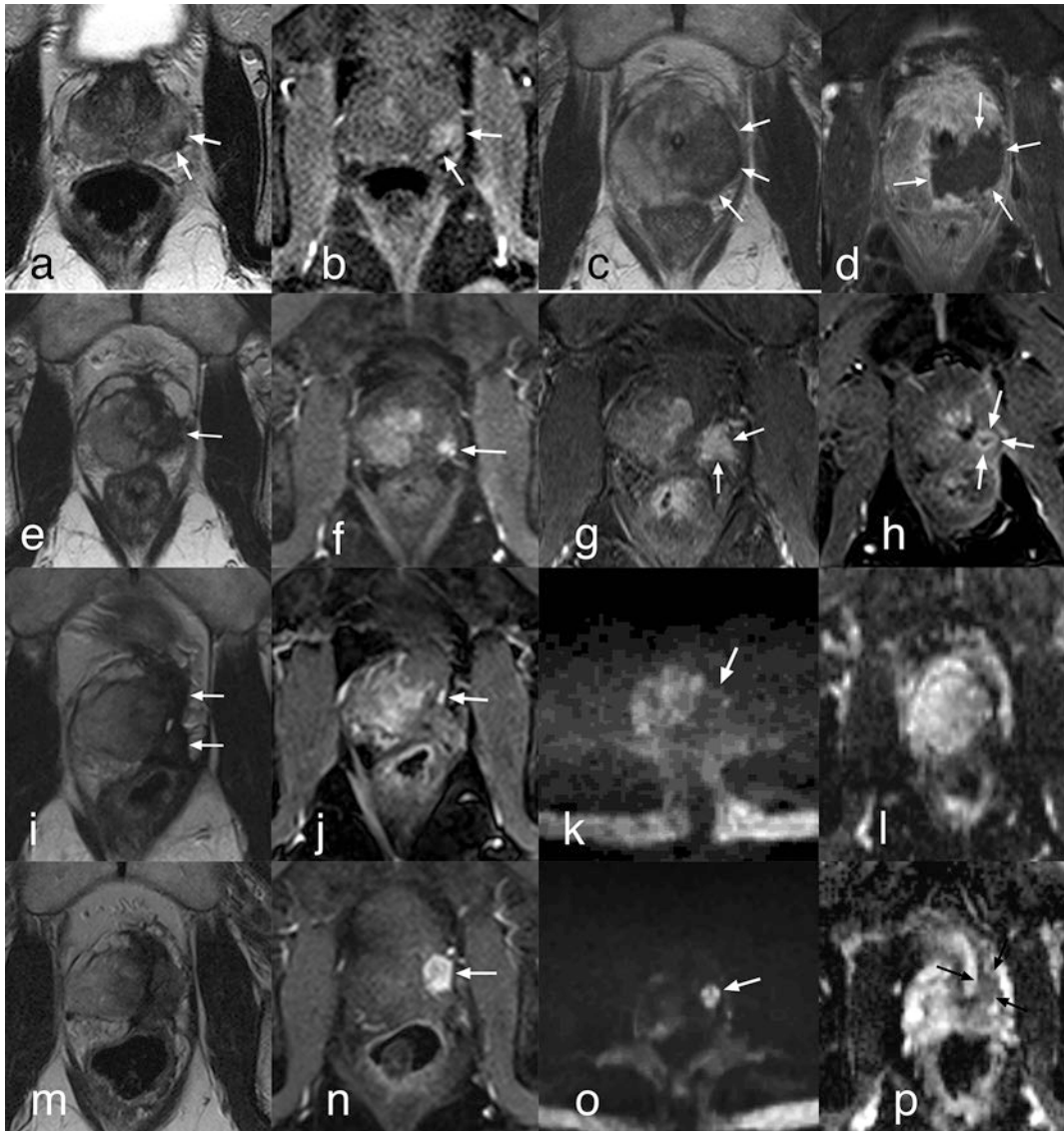

Fig. 33.1 A series of MRI scans in a 67-year-old man before and after focal ablation to a lesion in the left peripheral zone. (**a, b**) T2 and early dynamically enhanced sequences with arrows showing the original tumor (Gleason 3+4 on template transperineal biopsy) in the left posterolateral peripheral zone (PSA 5.7). (**c, d**) T2 and late enhanced sequences 1 week after treatment. The left hemiablation is easy to appreciate (*arrows*) on the enhanced sequences, but the margins of the ablation are very difficult to define on T2. A little patchy enhancement remains in against the posterior capsule. (**e, f**) T2 and early dynamically enhanced sequences 6 months after focal HIFU. The PSA has fallen to 0.7. The T2 sequence shows atrophy and low signal in the treated zone, but does not reveal a focal tumor. The dynamically enhanced image shows a 5 mm diameter focus of residual tumor (*arrow*) on the left, which was targeted at transrectal biopsy, but missed (atrophy only on biopsy). Note the diffuse enhancement on the opposite (*right*) side: a common finding after HIFU. (**g, h**) Shows the prostate 9 months later: the focal tumor has enlarged significantly. The PSA is now 1.5. Biopsy showed a maximum cancer core length of 10 mm of Gleason 4+3 tumor. (**i**) A late dynamic image showing the prostate 3 months after repeat HIFU. Note the enhancing rim (*arrows*), making it impossible to assess completeness of treatment. (**j–m**) T2, early dynamically enhanced, b1400 diffusion-weighted, and apparent diffusion coefficient (ADC) map 9 months after the second HIFU treatment. Note that neither the T2 sequence nor the diffusion images (either long b or ADC map) show the recurrent tumor: at this stage it is only seen as a small focus of enhancement (*arrow*) on the enhanced image. (**m–p**) T2, early dynamically enhanced, b1400 diffusion-weighted, and ADC map after a further year. The residual tumor has enlarged and is now seen on both enhanced and diffusion-weighted images (*arrows*). It is still difficult to define on T2

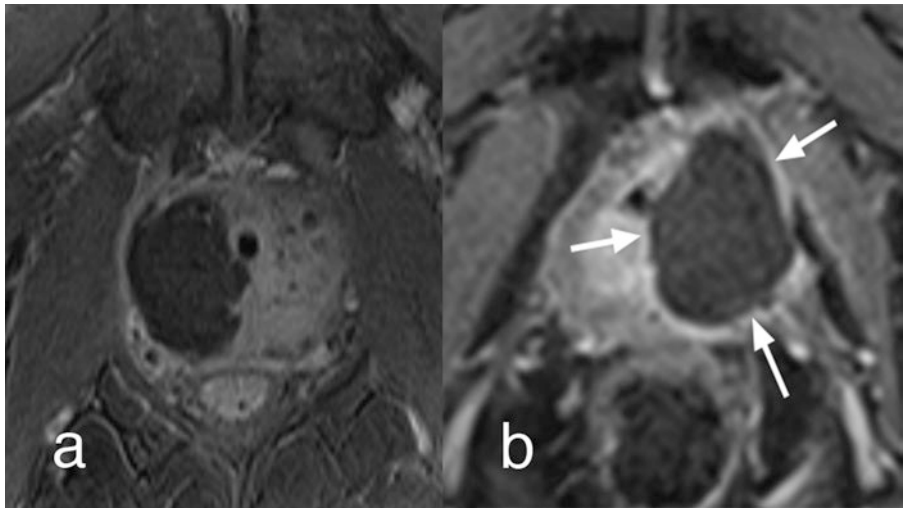

Fig. 33.2 Post-contrast scans 1 week after focal treatment with photodynamic therapy (**a**) and cryotherapy (**b**). The appearances of the necrosis at this stage are very similar to those seen with HIFU (Fig. 33.1)

they depend on MRI technique, the method of ablation, and the histological definition of necrosis [28].

Complications

Because the evidence that early imaging (at <1 month) can predict outcome is poor, many of those performing focal therapy wait for at least 6 months before performing MRI after treatment [29]. Nevertheless, where either the technique or the operator is new, MRI provides a powerful method for delineating the ablation lesion and optimizing treatment. In particular, it can help to detect damage to adjacent structures: the neurovascular bundles, external urethral sphincter, and rectum.

Several complications of ablation (whether by cooling or heating)—in particular incontinence and rectal injury leading to fistulation—are more common in patients who have previously undergone radiotherapy [30] ("salvage" cases), and indeed the incidence of incontinence after primary focal HIFU is low [31], and rectal fistulation almost unheard of in both primary HIFU [32] and cryotherapy [33]. A non-enhancing segment of rectal muscularis is common after HIFU and is usually of no consequence, but in patients who have undergone both brachytherapy and external beam radiotherapy, it is an ominous finding for fistulation (Fig. 33.3) [34].

Anterior treatments can also result in anterior fistulation, most commonly presenting with pain. In a small group of patients presenting after transurethral resection of the prostate (TURP) or prostate vaporization [35], this was diagnosed between 2 weeks and 11 months after treatment. In a group of 16 patients developing this complication after treatment for prostate cancer, all had undergone radiotherapy [36], and pain was the primary presentation, with extensive fistulous tracks extending to the adductor compartment or thigh in many. Three patients developed fistulation after cryotherapy, though in two cases there were complicating factors (a TURP and a traumatic catheterization). MRI can show fluid within the symphysis, adjacent bony inflammation (although this must be distinguished from post-radiotherapy changes and osteonecrosis [37]), and the fistulous tracks, and was used in all cases [36].

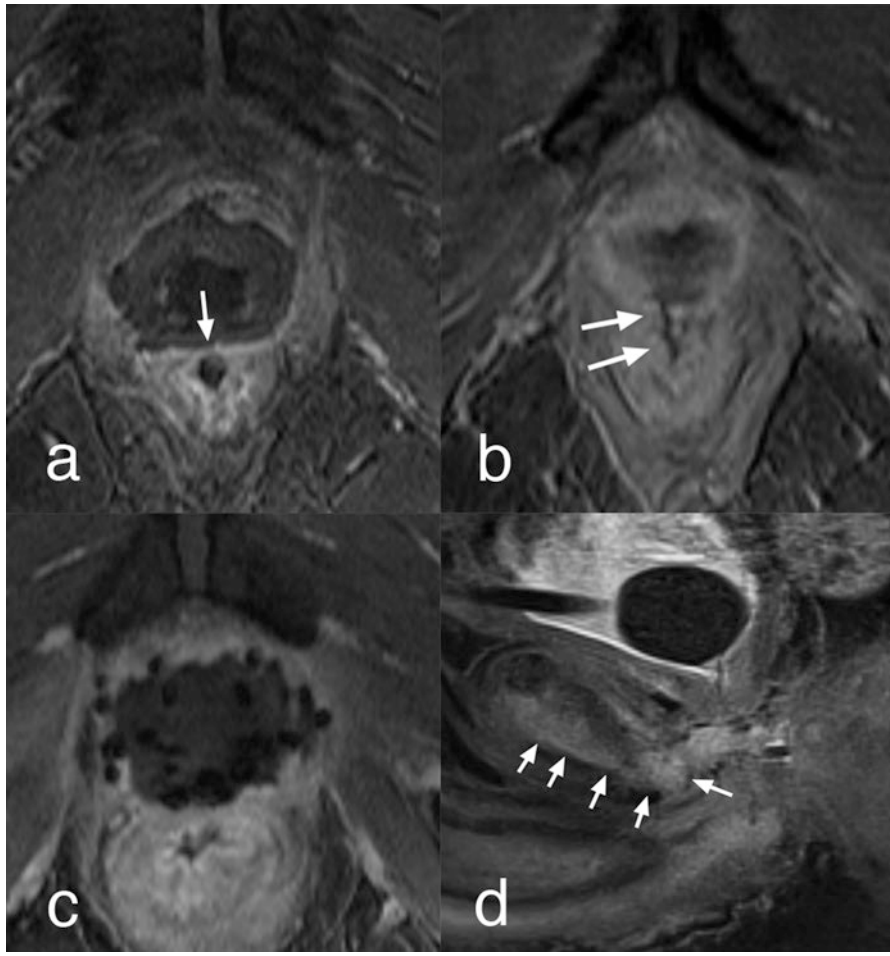

Fig. 33.3 Early and late scans showing fistulas in two patients. (**a, b**) 10-day and 6-week enhanced scans in a 67-year-old man undergoing whole-gland HIFU for recurrent tumor after external beam radiotherapy and cryotherapy. The early scan shows necrosis of the rectal muscularis but persisting mucosal enhancement. One month later (**b**) there were symptoms of fistula, and the enhanced images demonstrate the posterior fistulous tract between the prostate and rectum (*arrow*). (**c, d**) Two-month post-contrast and 1-year sagittal short tau inversion recovery (STIR) images in a 66-year-old man treated with whole-gland HIFU for recurrent tumor after low dose rate brachytherapy. The early scan shows good coverage: confluent necrosis occupying the whole prostate (note the low-signal defects from the brachytherapy seeds). A year later the STIR images show fluid tracking into the symphysis (*arrows*): an anterior fistula. Symptoms were minimal, possibly because urethral stricture meant long-term management with a urethral catheter

Appearances at 2–5 Months

Between 2 and 5 months, the appearances after ablation are variable, and the treated volume gradually becomes smaller and fibrotic; after HIFU there is often a double enhancing rim [10], but the changes may be different after cryotherapy or photodynamic therapy or if there has been previous radiotherapy, when the resorption of necrotic tissue is considerably slower.

Fistulation after salvage HIFU (in post-radiotherapy glands) usually presents between 4 and 8 months after treatment [34] and can be demonstrated most simply with a cystourethrogram. MRI is useful in planning the operative approach to repair, and for this we usually use a combination of small field of view T2 and short

tau inversion recovery (STIR) sequences, with dynamic gadolinium sequences in the axial plane; the latter may sometimes show the enhancing walls of a fistulous track when the other sequences do not.

Late Scans

Imaging After 6 Months

After thermal ablation, necrosis has usually resolved by 6 months [11], and the enhancing rim seen on imaging between 2 and 5 months is no longer visible [10, 19]. The treated volume will be replaced by low-signal, fibrous tissue that shows delayed, moderate enhancement after gadolinium (as with fibrosis elsewhere in the body [38, 39]). If there has been previous radiotherapy, the resorption will usually take longer, and we generally do not image until 1 year. Although there is little published data, we have observed that an inflammatory-type response is seen in the surrounding untreated prostate (often including the contralateral peripheral zone), with moderately prominent enhancement that may persist for several years after treatment.

Once the necrotic tissue has been resorbed, we are in a position to detect residual tumor, which has similar signal characteristics to before the treatment: T2 low signal, early-peaking enhancement, and restricted diffusion [40]. Because the fibrotic, treated part of the gland will also be of low signal, T2 sequences are of relatively reduced utility, and it is essential that a full multiparametric scan is performed. We will not go into detail on the protocol, except to say that T2-, diffusion-weighted, and dynamically enhanced scans should be obtained, with minimum standards for resolution recently described in the ESUR guidelines [21]. Restricted diffusion should be assessed on both the apparent diffusion coefficient (ADC) map and a long b image; the latter is crucial because fibrosis (similarly to the anterior fibromuscular stroma) may show apparent restriction on the ADC map. It will not, however, be cellular and will therefore not show the same high signal as tumor on long b images [41]. Similarly, tumor will stand out from its fibrotic surroundings early after contrast [40], though there is a problem at the margin that is especially acute in focal therapy: reactive enhancement is likely to be most intense close to the site of the treatment and may be very difficult to distinguish from tumor, so that diffusion sequences may be more specific, although less sensitive [40] (The voxel size for diffusion images is considerably higher than dynamically enhanced scans optimized for anatomical information [42].)

The most likely location of the residual tumor depends on the technique used. For HIFU, anterior tumors may be difficult to target accurately, and a margin of safety around the sphincter means that undertreatment of inferior lesions may be more likely [43]. For the same reason, to avoid rectal injury, posterior recurrence may be more likely after cryotherapy.

After whole-gland radiotherapy, there is a reduction in prostate volume and loss of zonal anatomy, with a general reduction in T2 signal in the peripheral zone [44] (Fig. 33.4); the changes after focal radiation therapy have not been described in detail, but are likely to be similar: focal atrophy and loss of T2 signal.

Published Results for Detection of Tumor After Ablation

Much of the data for detecting recurrent tumor after ablation comes from treatments of the whole prostate. These data should be extrapolated to the focal setting with caution, because the background may be almost universally “dark” or fibrotic, making tumor easier to see. There is little doubt that T2 sequences are of little utility alone, so that diffusion-weighted and dynamically enhanced scans both become useful. The relative contribution of each in the context of whole-gland HIFU was studied by Kim et al. in 2008 [40]. In 27 patients, with analysis by sextant, T2 and diffusion sequences had a sensitivity of 66 % and specificity of 76 % for residual tumor. Enhanced images detected more tumors but were less specific (sensitivity 83 %, specificity 66 %). This is not a surprising result, given the

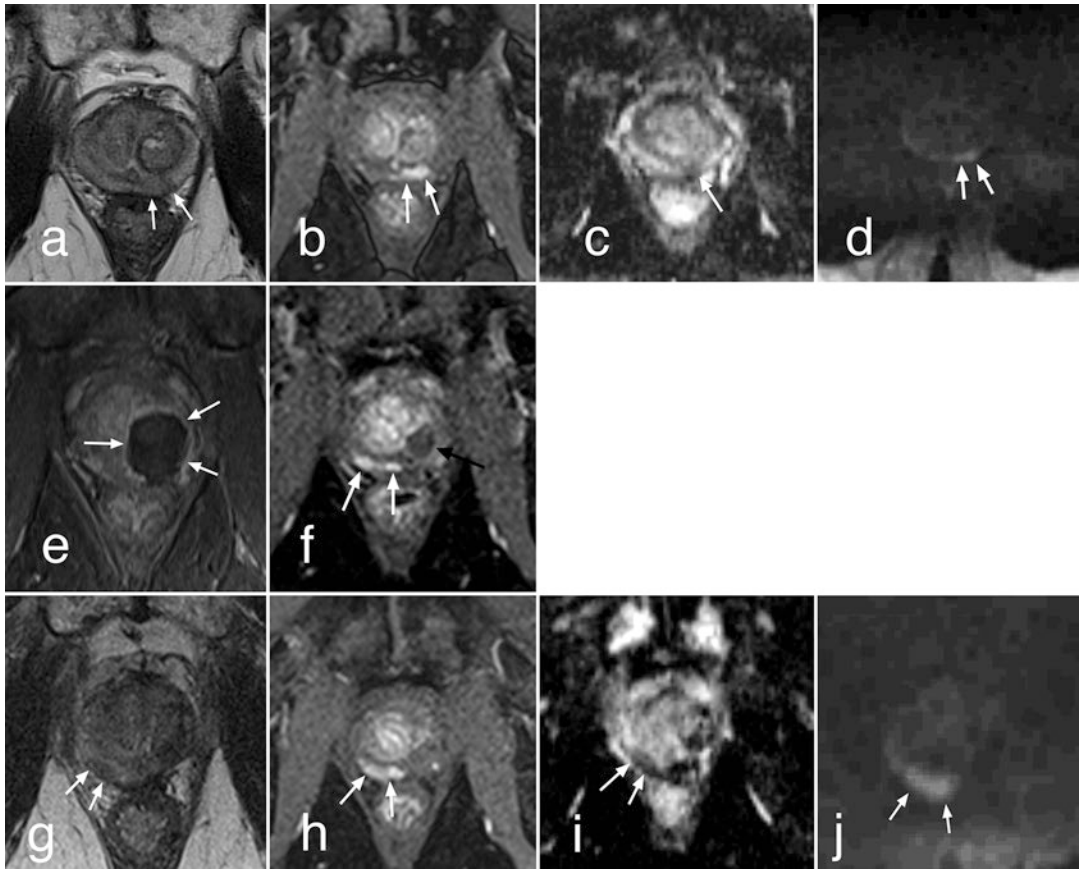

Fig. 33.4 Salvage HIFU in a 64-year-old man after radiotherapy. (**a–d**) T2, dynamically enhanced, ADC map, and b1400 diffusion-weighted images in a man with a rising PSA after radiotherapy. The tumor is hard to distinguish on T2 because of a generalized loss of signal and loss of zonal differentiation seen after radiotherapy. It is best seen (*arrow*) on the enhanced sequences and is moderately conspicuous on diffusion. (**e, f**) One-month and 6-month postcontrast images after radiotherapy. Note the persisting necrosis (*black arrow*) on the left at 6 months and new enhancement on the right. While some diffuse enhancement is common after HIFU (see Figure 33.1f), this is more focal and suspicious for tumor. (**g–j**) T2, dynamically enhanced, ADC map, and b1400 diffusion-weighted images 9 months later. The necrosis on the left has resolved, and no recurrent tumor is visible on this side (a small punctate focus of enhancement is vascular). The tumor on the right has enlarged and was Gleason 3+4 at biopsy

widespread enhancement that can persist for years after ablation in non-fibrotic prostate at the margin.

In another study of enhanced MRI after whole-gland HIFU, the performance of MRI was similar to absolute prostate-specific antigen (PSA) value for the detection of residual tumor (sensitivity 75 % and specificity 76 %) [45], and these figures are similar to the performance of PSA (with a criterion of nadir +1.2 ng/ml) in an online whole-gland HIFU registry (sensitivity 78 %, specificity 79 %) [46]. Finally, Rouviere et al. have shown that a strategy of MRI-targeted sampling is possible and effective, with cores directed to MR suspicious areas much more likely to be positive than systematic sampling, and 22 % of positive samples only found on MRI-directed cores [47]. This study serves to emphasize that surveillance biopsies can have false negatives too and that the use of biopsy as a gold standard to assess imaging techniques or PSA is problematic, especially if untargeted [5]. Spectroscopy has been studied in a

group of ten patients after HIFU and detected three out of four recurrences at 4 months, but the group was small and it is likely that, as elsewhere, spectroscopy is time-consuming and expensive and will not add significantly to a full multiparametric MRI [42, 48].

It is likely that the results for focal HIFU will favor MRI (with persisting, potentially inflamed residual prostate, the PSA may be less reliable and prone to increase with an enlarging gland), but there is currently little evidence for the performance of MRI in this context. In one small study of focal HIFU, multiparametric MRI showed "signs of residual cancer" in nine men, with biopsy confirmed residual tumor in seven; there were two false negatives [49]. These results are encouraging but preliminary.

There is no data for the performance of MRI after focal cryotherapy. In a study using T2 sequences and spectroscopy after whole-body cryotherapy, all eight patients with residual tumor on biopsy were identified, although there was a false-positive rate of 29 % [50]. We are skeptical that this high sensitivity would be replicated in an era of focal therapy for relatively small tumors, and a recent study comparing the effects of adding spectroscopy, diffusion imaging, and dynamic enhancement to T2 sequences after radiotherapy showed that spectroscopy was far inferior to diffusion and dynamic-

enhanced sequences and "needs to be improved" [51].

Changes After Radiotherapy

As with ablation, there is little data on the performance of MRI after focal radiotherapy techniques. We know that after whole-gland treatment, contrast markedly improves the detection of recurrent tumor, with one study showing sensitivity and specificity of 72 % and 85 % for dynamically enhanced MR compared to 38 % and 80 % for T2 sequences [52]. Another group has shown that the addition of diffusion-weighted images to standard T2 images markedly improved performance (with the area under curve [AUC] increasing from 0.61 to 0.88) [53], and a study of T2-, diffusion-weighted, and enhanced MRI in 13 patients analyzed by prostate quadrant showed AUCs for the detection of tumor of 0.77 and 0.89, improving considerably to 0.86 and 0.93 if only cancer core lengths ≥3 mm were considered positive [54]. These figures are at least as high as those for MRI in the pre-biopsy diagnostic setting [55], emphasizing that the low-signal background after radiotherapy can make tumors relatively conspicuous.

As with post-ablation imaging, it is clear that T2 images must be augmented with additional sequences, but is a full multiparametric MRI necessary? A recent study examined the effect on diagnostic performance after radiotherapy of adding ADC maps, long b diffusion images, and dynamically enhanced images to standard T2 sequences; only the long b images significantly improved performance [56]. This fits with our experience: long b images of good quality are an essential part of diffusion-weighted imaging [21]. Kim's group obtained the best accuracy using T2-, diffusion-weighted, and contrast-enhanced images [57], and it is likely that as in the primary diagnostic setting [21], dynamically enhanced scans add accuracy to the "bedrock" MR sequences of T2 and diffusion. This is confirmed by a recent study showing that the best sensitivity for residual tumor was obtained with T2-, diffusion-weighted, and enhanced imaging combined [51].

Although there is an early study of robotic stereotactic radiotherapy [17] showing changes in quantitative parameters, no results have yet been published for the performance of MRI in surveillance after focal forms of radiotherapy.

Ultrasound for Local Recurrence

As in the primary diagnostic setting, microbubble-enhanced ultrasound is less established and almost certainly less effective than MRI for the detection of cancer in the prostate [58], but there is one interesting study of its performance after prostatectomy, showing that in ten patients the addition of microbubble contrast improved the performance of ultrasound to the same level of

MRI [59]. This is, however, likely an effect of a relatively "dark" background after prostatectomy: we expect that ultrasound after focal therapy will be considerably more challenging.

Nuclear Medicine Studies

It is clear that fludeoxyglucose (FDG) positron emission tomography (PET) is of lower sensitivity than MRI for the detection of tumor after prostatectomy or radiotherapy, but choline PET improves performance (though not approaching MRI) [60], and prostate-specific membrane antigen-based agents are likely even better [61]. It may be that the addition of the newer PET agents to MRI improves performance, but it is unlikely to be to a degree that justifies the radiation exposure of PET in a surveillance protocol.

Conclusion

The number of directly relevant results (showing the utility of MRI in surveillance after focal therapy) is tiny, and the case for using it as a primary method of surveillance after focal treatment is based on its performance in the detection of tumor in the untreated prostate and after whole-gland therapy. Nevertheless, MRI is very attractive compared to the imprecision of PSA and the morbidity and cost of repeat biopsy, and it has the great potential advantage of enabling targeted biopsy of any recurrence. It is, therefore, an integral part of the recommended trial design in several recent international consensus projects [29, 62, 63]. Many of these trials will include routine posttreatment MRI and biopsy, and we hope that by the next edition of this book, we can replace "tiny" with "small."

References

1. Polascik TJ. Imaging and focal therapy of early prostate cancer. New York: Springer; 2012.
2. Dickinson L, Arya M, Afzal N, Cathcart P, SC C, Cornaby A, et al. Medium-term outcomes after whole-gland high-intensity focused ultrasound for the treatment of nonmetastatic prostate cancer from a multicentre registry cohort. Eur Urol. 2016; doi:10.1016/j.eururo.2016.02.054.
3. Shah TT, Kasivisvanathan V, Jameson C, Freeman A, Emberton M, Ahmed HU. Histological outcomes after focal high-intensity focused ultrasound and cryotherapy. World J Urol. 2015;33(7):955–64.
4. Merrick GS, Taubenslag W, Andreini H, Brammer S, Butler WM, Adamovich E, et al. The morbidity of transperineal template-guided prostate mapping biopsy. BJU Int. 2008;101(12):1524–9.
5. Moore CM, Robertson NL, Arsanious N, Middleton T, Villers A, Klotz L, et al. Image-guided prostate biopsy using magnetic resonance imaging–derived targets: a systematic review. Eur Urol. 2013;63(1):125–40.
6. Dowrick AS, Wootten AC, Howard N, Peters JS, Murphy DG. A prospective study of the short-term quality of life outcomes of patients undergoing transperineal prostate biopsy. BJU Int. 2016;118(1):60–7.
7. Donnelly SE, Donnelly BJ, Saliken JC, Raber EL, Vellet AD. Prostate cancer: gadolinium-enhanced MR imaging at 3 weeks compared with needle biopsy at 6 months after cryoablation. Radiology. 2004;232(3):830–3.
8. Rouvière O, Lyonnet D, Raudrant A, Colin-Pangaud C, Chapelon JY, Bouvier R, et al. MRI appearance of prostate following transrectal HIFU ablation of localized cancer. Eur Urol. 2001;40(3):265–74.
9. Ting F, Tran M, Böhm M, Siriwardana A, Van Leeuwen PJ, Haynes AM, et al. Focal irreversible electroporation for prostate cancer: functional outcomes and short-term oncological control. Prostate Cancer Prostatic Dis. 2016;19(1):46–52.
10. Kirkham AP, Emberton M, Hoh IM, Illing RO, Freeman AA, Allen C. MR imaging of prostate after treatment with high-intensity focused ultrasound. Radiology. 2008;246(3):833–44.
11. Natarajan S, Raman S, Priester AM, Garritano J, Margolis DJ, Lieu P, et al. Focal laser ablation of prostate cancer: phase I clinical trial. J Urol. 2016;196(1):68–75.
12. Lafon C, Bouchoux G, Souchon R, Chapelon J. Monitoring and follow up of HIFU lesions by ultrasound. Biomedical imaging: from nano to macro, 2007. ISBI 2007. 4th IEEE international symposium on biomedical imaging 068–1071 (2007).
13. Chen J, Daniel BL, Diederich CJ, Bouley DM, van den Bosch MA, Kinsey AM, et al. Monitoring prostate thermal therapy with diffusion-weighted MRI. Magn Reson Med. 2008;59(6):1365–72.
14. Rouvière O, Glas L, Girouin N, Mège-Lechevallier F, Gelet A, Dantony E, et al. Prostate cancer ablation with transrectal high-intensity focused ultrasound: assessment of tissue destruction with contrast-enhanced US. Radiology. 2011;259(2):583–91.
15. van den Bos W, de Bruin DM, van Randen A, Engelbrecht MR, Postema AW, Muller BG, et al. MRI and contrast-enhanced ultrasound imaging for evaluation of focal irreversible electroporation treatment: results from a phase I–II study in patients undergoing

IRE followed by radical prostatectomy. Eur Radiol. 2016;26(7):2252–60.
16. Arteaga-Marrero N, Rygh CB, Mainou-Gomez JF, Nylund K, Roehrich D, Heggdal J, et al. Multimodal approach to assess tumour vasculature and potential treatment effect with DCE-US and DCE-MRI quantification in CWR22 prostate tumour xenografts. Contrast Media Mol Imaging. 2015;10(6):428–37.
17. Low RN, Fuller DB, Muradyan N. Dynamic gadolinium-enhanced perfusion MRI of prostate cancer: assessment of response to hypofractionated robotic stereotactic body radiation therapy. AJR Am J Roentgenol. 2011;197(4):907–15.
18. Korbelik M. PDT-associated host response and its role in the therapy outcome. Lasers Surg Med. 2006;38:500–8.
19. Rouvière O, Souchon R, Salomir R, Gelet A, Chapelon JY, Lyonnet D. Transrectal high-intensity focused ultrasound ablation of prostate cancer: effective treatment requiring accurate imaging. Eur J Radiol. 2007;63(3):317–27.
20. Barentsz JO, Richenberg J, Clements R, Choyke P, Verma S, Villeirs G, et al. European Society of Urogenital Radiology. ESUR prostate MR guidelines 2012. Eur Radiol. 2012;22(4):746–57.
21. Weinreb JC, Barentsz JO, Choyke PL, Cornud F, Haider MA, Macura KJ, et al. PI-RADS prostate imaging – reporting and data system: 2015, version 2. Eur Urol. 2016;69(1):16–40.
22. Guan YS, Sun L, Zhou XP, Li X, Zheng XH. Hepatocellular carcinoma treated with interventional procedures: CT and MRI follow-up. World J Gastroenterol. 2004;10(24):3543–8.
23. Merkle EM, Nour SG, Lewin JS. MR imaging follow-up after percutaneous radiofrequency ablation of renal cell carcinoma: findings in 18 patients during first 6 months. Radiology. 2005;235(3):1065–71.
24. Raman SS, Lu DS, Vodopich DJ, Sayre J, Lassman C. Creation of radiofrequency lesions in a porcine model: correlation with sonography, CT, and histopathology. AJR Am J Roentgenol. 2000;175(5):1253–8.
25. Vellet AD, Saliken J, Donnelly B, Raber E, McLaughlin RF, Wiseman D, et al. Prostatic cryosurgery: use of MR imaging in evaluation of success and technical modifications. Radiology. 1997;203(3):653–9.
26. Zhu L, Xu LX. Evaluation of the effectiveness of transurethral radio frequency hyperthermia in the canine prostate: temperature distribution analysis. J Biomech Eng. 1999;121(6):584–90.
27. Barrett T, Davidson SR, Wilson BC, Weersink RA, Trachtenberg J, Haider MA. Dynamic contrast enhanced MRI as a predictor of vascular-targeted photodynamic focal ablation therapy outcome in prostate cancer post failed external beam radiation therapy. Can Urol Assoc J. 2014;8(9–10):E708–14.
28. Patriarca C, Bergamaschi F, Gazzano G, Corrada P, Ordesi G, Zanitzer L, et al. Histopathological findings after radiofrequency (RITA) treatment for prostate cancer. Prostate Cancer Prostatic Dis. 2006;9(3):266–9.
29. Muller BG, van den Bos W, Brausi M, Cornud F, Gontero P, Kirkham A, et al. Role of multiparametric magnetic resonance imaging (MRI) in focal therapy for prostate cancer: a Delphi consensus project. BJU Int. 2014;114(5):698–707.
30. Siddiqui KM, Billia M, Williams A, Alzahrani A, Chin JL. Comparative morbidity of ablative energy-based salvage treatments for radio-recurrent prostate cancer. Can Urol Assoc J. 2015;9(9–10):325–9.
31. Ahmed HU, Dickinson L, Charman S, Weir S, McCartan N, Hindley RG, et al. Focal ablation targeted to the index lesion in multifocal localised prostate cancer: a prospective development study. Eur Urol. 2015;68(6):927–36.
32. Rebillard X, Soulié M, Chartier-Kastler E, Davin JL, Mignard JP, Moreau JL, Association Francaise d'Urologie, et al. High-intensity focused ultrasound in prostate cancer; a systematic literature review of the French Association of Urology. BJU Int. 2008;101(10):1205–13.
33. Jones JS, Rewcastle JC, Donnelly BJ, Lugnani FM, Pisters LL, Katz AE. Whole gland primary prostate cryoablation: initial results from the cryo on-line data registry. J Urol. 2008;180(2):554–8.
34. Ahmed HU, Ishaq A, Zacharakis E, Shaw G, Illing R, Allen C, et al. Rectal fistulae after salvage high-intensity focused ultrasound for recurrent prostate cancer after combined brachytherapy and external beam radiotherapy. BJU Int. 2009;103(3):321–3.
35. Sanchez A, Rodríguez D, Cheng J-S, McGovern FJ, Tabatabaei S. Prostato-symphyseal fistula after photoselective vaporization of the prostate: case series and literature review of a rare complication. Urology. 2015;85:172–7.
36. Bugeja S, Andrich DE, Mundy AR. Fistulation into the pubic symphysis after treatment of prostate cancer: an important and surgically correctable complication. J Urol. 2016;195(2):391–8.
37. Addley HC, Vargas HA, Moyle PL, Crawford R, Sala E. Pelvic imaging following chemotherapy and radiation therapy for gynecologic malignancies. Radiographics. 2010;30(7):1843–56.
38. Khalifa F, Soliman A, El-Baz A, Abou El-Ghar M, El-Diasty T, Gimel'farb G, et al. Models and methods for analyzing DCE-MRI: a review. Med Phys. 2014;41(12):124301.
39. Lucht RE, Delorme S, Hei J, Knopp MV, Weber MA, Griebel J, et al. Classification of signal-time curves obtained by dynamic magnetic resonance mammography: statistical comparison of quantitative methods. Invest Radiol. 2005;40(7):442–7.
40. Kim CK, Park BK, Lee HM, Kim SS, Kim E. MRI techniques for prediction of local tumor progression after high-intensity focused ultrasonic ablation of prostate cancer. AJR Am J Roentgenol. 2008;190(5):1180–6.

41. Rosenkrantz AB, Hindman N, Lim RP, Das K, Babb JS, Mussi TC, et al. Diffusion-weighted imaging of the prostate: Comparison of b1000 and b2000 image sets for index lesion detection. J Magn Reson Imaging. 2013;38(3):694–700.
42. Kirkham AP, Haslam P, Keanie JY, McCafferty I, Padhani AR, Punwani S, et al. Prostate MRI: Who, when, and how? Report from a UK consensus meeting. Clin Radiol. 2013;68(10):1016–23.
43. Boutier R, Girouin N, Cheikh AB, Belot A, Rabilloud M, Gelet A, et al. Location of residual cancer after transrectal high-intensity focused ultrasound ablation for clinically localized prostate cancer. BJU Int. 2011;108(11):1776–81.
44. De Visschere PJ, Vargas HA, Ost P, De Meerleer GO, Villeirs GM. Imaging treated prostate cancer. Abdom Imaging. 2013;38(6):1431–46.
45. Punwani S, Emberton M, Walkden M, Sohaib A, Freeman A, Ahmed H, et al. Prostatic cancer surveillance following whole-gland high-intensity focused ultrasound: comparison of MRI and prostate-specific antigen for detection of residual or recurrent disease. Br J Radiol. 2012;85(1014):720–8.
46. Blana A, Brown SC, Chaussy C, Conti GN, Eastham JA, Ganzer R, et al. High-intensity focused ultrasound for prostate cancer: comparative definitions of biochemical failure. BJU Int. 2009;104(8):1058–62.
47. Rouvière O, Girouin N, Glas L, Ben Cheikh A, Gelet A, Mège-Lechevallier F, et al. Prostate cancer transrectal HIFU ablation: detection of local recurrences using T2-weighted and dynamic contrast-enhanced MRI. Eur Radiol. 2010;20(1):48–55.
48. Weinreb JC, Blume JD, Coakley FV, Wheeler TM, Cormack JB, Sotto CK, et al. Prostate cancer: sextant localization at MR imaging and MR spectroscopic imaging before prostatectomy–results of ACRIN prospective multi-institutional clinicopathologic study. Radiology. 2009;251(1):122–33.
49. Ahmed HU, Hindley RG, Dickinson L, Freeman A, Kirkham AP, Sahu M, et al. Focal therapy for localised unifocal and multifocal prostate cancer: a prospective development study. Lancet Oncol. 2012;13(6):622–32.
50. Parivar F, Hricak H, Shinohara K, Kurhanewicz J, Vigneron DB, Nelson SJ, et al. Detection of locally recurrent prostate cancer after cryosurgery: evaluation by transrectal ultrasound, magnetic resonance imaging, and three-dimensional proton magnetic resonance spectroscopy. Urology. 1996;48(4):594–9.
51. Roy C, Foudi F, Charton J, Jung M, Lang H, Saussine C, Jacqmin D. Comparative sensitivities of functional MRI sequences in detection of local recurrence of prostate carcinoma after radical prostatectomy or external-beam radiotherapy. AJR Am J Roentgenol. 2013;200(4):W361–8.
52. Haider MA, Chung P, Sweet J, Toi A, Jhaveri K, Ménard C, et al. Dynamic contrast-enhanced magnetic resonance imaging for localization of recurrent prostate cancer after external beam radiotherapy. Int J Radiat Oncol, Biol, Phys. 2008;70(2):425–30.
53. Kim CK, Park BK, Lee HM. Prediction of locally recurrent prostate cancer after radiation therapy: incremental value of 3 T diffusion-weighted MRI. J Magn Reson Imaging. 2009;29(2):391–7.
54. Arumainayagam N, Kumaar S, Ahmed HU, Moore CM, Payne H, Freeman A, et al. Accuracy of multiparametric magnetic resonance imaging in detecting recurrent prostate cancer after radiotherapy. BJU Int. 2010;106(7):991–7.
55. Fütterer JJ, Briganti A, De Visschere P, Emberton M, Giannarini G, Kirkham A, et al. Can clinically significant prostate cancer be detected with multiparametric magnetic resonance imaging? A systematic review of the literature. Eur Urol. 2015;68(6):1045–53.
56. Abd-Alazeez M, Ramachandran N, Dikaios N, Ahmed HU, Emberton M, Kirkham A, et al. Multiparametric MRI for detection of radiorecurrent prostate cancer: added value of apparent diffusion coefficient. Prostate Cancer Prostatic Dis. 2015;18(2):128–36.
57. Kim CK, Park BK, Park W, Kim SS. Prostate MR imaging at 3 T using a phased-arrayed coil in predicting locally recurrent prostate cancer after radiation therapy: preliminary experience. Abdom Imaging. 2010;35(2):246–52.
58. Pummer K, Rieken M, Augustin H, Gutschi T, Shariat SF. Innovations in diagnostic imaging of localized prostate cancer. World J Urol. 2014;32(4):881–90.
59. Drudi FM, Giovagnorio F, Carbone A, Ricci P, Petta S, Cantisani V, et al. Transrectal colour Doppler contrast sonography in the diagnosis of local recurrence after radical prostatectomy–comparison with MRI. Ultraschall Med. 2006;27(2):146–51.
60. Evangelista L, Cimitan M, Hodolič M, Baseric T, Fettich J, Borsatti E. The ability of 18F-choline PET/CT to identify local recurrence of prostate cancer. Abdom Imaging. 2015;40(8):3230–7.
61. Rowe SP, Gorin MA, Allaf ME, Pienta KJ, Tran PT, Pomper MG, et al. PET imaging of prostate-specific membrane antigen in prostate cancer: current state of the art and future challenges. Prostate Cancer Prostatic Dis. 2016;19(3):223–30.
62. Muller BG, van den Bos W, Brausi M, Fütterer JJ, Ghai S, Pinto PA, et al. Follow-up modalities in focal therapy for prostate cancer: results from a Delphi consensus project. World J Urol. 2015;33(10):1503–9.
63. van den Bos W, Muller BG, Ahmed H, Bangma CH, Barret E, Crouzet S, et al. Focal therapy in prostate cancer: international multidisciplinary consensus on trial design. Eur Urol. 2014;65(6):1078–83.

Determining Focal Therapy Failure and Salvage Options

34

Theo M. de Reijke, Arnoud W. Postema, and J. Stephen Jones

Introduction

The awareness for prostate cancer has increased during the last decades, and due to earlier detection and "screening" programs, a stage shift has been observed to earlier stages of prostate cancer. However, in the screening programs, it has been demonstrated that overtreatment of the prostate cancers detected at an earlier stage is of a major concern, and this has led to the concept of active surveillance [1, 2]. The ideal patient and optimal strategy for active surveillance are still under discussion. Most patients are selected for active surveillance based on prostate-specific antigen (PSA) level, number of positive biopsy cores (minimum of eight cores), and biopsy-based Gleason score. Since these three determinants are not representative for the true tumor volume and tumor aggressiveness, some advocate more extensive biopsy protocols and/or imaging using multiparametric magnetic resonance imaging (mpMRI), which could indicate if there is, in fact, a very low-risk prostate cancer. However, in case a small volume of intermediate-risk prostate cancer is found, the question of focal therapy arises, since whole-gland treatment can induce bothering side effects, e.g., incontinence, erectile dysfunction, or rectal problems. The question arises if focal therapy should only be offered to patients with a unifocal tumor and several consensus meetings have addressed this topic. Throughout the years, some consensus projects have advised widening the indication for focal therapy to treatment of the index lesion only, leaving insignificant tumors untreated [3, 4]. The approach for focal therapy applied has, of course, implications for the chance of recurrences and follow-up of the patients.

Focal therapy can be applied using several approaches, high-intensity focused ultrasound (HIFU), cryotherapy, irreversible electroporation (IRE), TOOKAD®, brachytherapy, etc. [5–9].

In these studies, follow-up after the procedures has not been long enough to determine which approach is optimal concerning side effects and oncological outcome. Therefore, it is of utmost importance that all focal therapy approaches are being registered and there should be close follow-up in order to determine the outcome of the different approaches not only oncological and functional but also to identify failures and the successive (salvage) treatments.

T.M. de Reijke (✉) • A.W. Postema
Department of Urology, Academic Medical Center, Amsterdam, The Netherlands
e-mail: t.m.dereyke@amc.uva.nl

J.S. Jones
Regional Hospitals & Family Health Centers, Cleveland, OH, USA

© Springer International Publishing AG 2017
T.J. Polascik (ed.), *Imaging and Focal Therapy of Early Prostate Cancer*, Current Clinical Urology, DOI 10.1007/978-3-319-49911-6_34

Consensus meetings on focal therapy have been organized in order to speak the same language in determining what is considered focal therapy, how the follow-up should be organized, and how treatment failure is defined. The different definitions will be discussed together with the possible treatment approaches in case a recurrence or persistence is found.

Focal Therapy

Approach

The definition of focal therapy and selection of patients is important in order to decide which salvage treatment could be instituted in case of failure.

The concept of focal therapy is not widely accepted for localized disease since prostate cancer is in the majority of cases multifocal and current imaging is not accurate enough to identify all lesions. Multiparametric MRI is believed to be able to identify the index lesion (driving the disease), but evidence is insufficient to completely rely on this enhanced imaging modality alone [10, 11].

Therefore, systematic biopsies are advised in order to identify the right candidate for focal therapy. Based on these data, different focal therapy protocols have been described: treatment of all identified lesions, hemiablation, subtotal ablation, and treatment of the index lesion alone even in case of multifocal disease [12]. Again, which approach is the best remains to be established. Based on the initial workup (imaging or systematic biopsies) and treatment protocol, failure rates can be different, because significant cancers can be missed.

Follow-Up Investigations

The surveillance following focal therapy is not uniform, although most of the clinicians dealing with focal therapy were part of consensus meetings. Ideally, most patients have strictly local disease, and the chance of identifying disease spread outside the prostate in the short-term after focal therapy should be negligible. PSA in the follow-up is not really helpful, since focal therapy by definition deliberately leaves PSA-producing prostatic tissue or even insignificant tumor foci untreated. Nevertheless, some series have reported the American Society for Therapeutic Radiation and Oncology (ASTRO) or Phoenix criteria to define success or failure [13].

However, these criteria have been developed for the follow-up after external beam radiotherapy (EBRT), and these were never validated for focal therapy. Others used the Stuttgart definition evaluated in patients who underwent HIFU [14].

The role of imaging during follow-up has not been clearly investigated, but in the consensus meeting it was proposed as standard follow-up investigation. Multiparametric MRI is the imaging modality of choice [15].

Suspicion for tumor persistence is based on an early enhancing area on the dynamic contrast sequence and residual restricted diffusion in the treated area. Contrast-enhanced ultrasound is not an established method to accurately identify local recurrence or failure, but the fusion of MRI and transrectal ultrasound (TRUS) is considered useful to target the suspicious site with confirmatory biopsies. A promising imaging tool for identifying local recurrences or persistent disease could possibly be the gallium (Ga) positron emission tomography(PET)/computed tomography (CT) scan [16].

According to the consensus meeting from 2015, suspicious areas on imaging should be confirmed by biopsies to identify failure or recurrence [15]. This was a modification from a previous consensus meeting where systematic biopsies were advised [17]. In the terminology derived from this consensus project, an important concept that needs to be appreciated during follow-up is “ablation failure,” which means that the applied technique did not eliminate the cancer [15].

Salvage Therapy

Salvage focal therapy was defined as a treatment following biochemical recurrence after whole-gland treatment with curative intent or in the same region of the prostate when a previous focal therapy had been performed [15]. This is a bit confusing since these are two different situations, but here we will focus on the situation where initial focal therapy failed. In case of the so-called selection failure, meaning focal therapy was indicated for a patient that showed locally advanced or even metastatic disease early during follow-up, it is obvious that invasive or systemic treatment is indicated.

There are currently no protocols and/or guidelines on how to treat failure of focal therapy within or outside the treated zone. It seems logical that these patients should be treated with whole-gland treatment (radical prostatectomy, repeat whole-gland ablation, or radiotherapy). However, there are many scenarios that could be applied to the individual patient depending on time to recurrence/failure, site of failure, grade and volume of recurrent disease found, and initial treatment. The whole range of treatment modalities could be applied:

1. Active surveillance in cases that would have been regarded as candidates for active surveillance had this been the initial presentation, i.e., low volume, low-risk disease
2. Re-focal therapy in or outside treated zone if only a few biopsies show prostate cancer of low or intermediate grade/risk (Gleason 3+3/4), with the same or different energy source
3. Radical treatment (radical prostatectomy, whole-gland repeat ablation, brachytherapy, or external beam radiotherapy)
4. Watchful waiting in case of comorbidity and thus short life expectancy

At this moment in time, there are no firm data on each of these second-line treatments, and also there is no recommendation from consensus meetings. This implies that salvage following focal therapy is based on individual parameters and patient and doctors' preference. Analogous to focal therapy for renal cancer, a second focal treatment seems possible [18].

The optimal salvage focal approach depends on the initial treatment and location of the tumor. Especially apical lesions pose a problem for HIFU, because the sphincter mechanism could be jeopardized. Repeat whole-gland HIFU has been reported to be feasible, although it may carry an increased risk of urinary side effects, specifically incontinence [19, 20].

Salvage EBRT and radical prostatectomy and active surveillance following focal therapy have been anecdotally described in the results of IRE and HIFU trial reports [7, 21, 22].

However, there is little data from larger series applying these salvage treatment options following focal therapy. Van den Bos et al. reported no significant increased morbidity or complications performing radical prostatectomy in 16 patients following IRE in a phase 2 study [23]. But at this moment there are not many reported data about oncological and/or functional outcome data for salvage therapy following focal therapy.

Discussion

It is clear that focal therapy for prostate cancer is still in its infancy and we need many more data about the selection criteria and follow-up procedures to determine if the treatment was successful. Important is registration and using uniform language in communicating the results of the different treatment modalities. The same applies for the second-line treatments following failure of the initial focal treatment; timing, approach, and, again, side effects of salvage treatment should be registered in order to determine which treatment results in the best outcome with the least number of side effects.

References

1. de Carvalho TM, Heijnsdijk EA, de Koning HJ. Estimating the individual benefit of immediate treatment or active surveillance for prostate cancer after screen detection in older (65+) men. Int J Cancer. 2016;138:2522–8.

2. Klotz L, Vesprini D, Sethukavalan P, Jethava V, Zhang L, Jain S, Yamamoto T, Mamedov A, Loblaw A. Long-term follow-up of a large active surveillance cohort of patients with prostate cancer. J Clin Oncol. 2015;33:272–7.
3. De la Rosette J, Ahmed H, Barentsz J, Johansen TB, Brausi M, Emberton M, et al. Focal therapy in prostate cancer – report from a consensus panel. J Endourol. 2010;24:775–80.
4. Donaldson IA, Alonzi R, Barratt D, Barret E, Berge V, Bott S, et al. Focal therapy: patients, interventions, and outcomes – a report from a consensus meeting. Eur Urol. 2015;67:771–7.
5. Feijoo ER, Sivaraman A, Barret E, Sanchez-Salas R, Galiano M, Rozet F, et al. Focal high-intensity focused ultrasound targeted hemiablation for unilateral prostate cancer: a prospective evaluation of oncologic and functional outcomes. Eur Urol. 2016;69:214–20.
6. Ward JF, Jones JS. Focal cryotherapy for localized prostate cancer: a report from the national Cryo On-Line Database (COLD) Registry. BJU Int. 2012;109:1648–54.
7. Ting F, Tran M, Böhm M, Siriwardana A, Van Leeuwen PJ, Haynes AM, et al. Focal irreversible electroporation for prostate cancer: functional outcomes and short-term oncological control. Prostate Cancer Prostatic Dis. 2016;19:46–52.
8. Azzouzi AR, Lebdai S, Benzaghou F, Stief C. Vascular-targeted photodynamic therapy with TOOKAD® Soluble in localized prostate cancer: standardization of the procedure. World J Urol. 2015; 33:937–44.
9. Al-Qaisieh B, Mason J, Bownes P, Henry A, Dickinson L, Ahmed HU, et al. Dosimetry modeling for focal low-dose-rate prostate brachytherapy. Int J Radiat Oncol Biol Phys. 2015;92:787–93.
10. Liu W, Laitinen S, Khan S, Vihinen M, Kowalski J, Yu G, et al. Copy number analysis indicates monoclonal origin of lethal metastatic prostate cancer. Nat Med. 2009;15:559–65.
11. Ahmed HU, Hindley RG, Abdul-Rahman A, Freeman A, Emberton M. The index lesion and focal therapy: an analysis of the pathological characteristics of prostate cancer. BJU Int. 2010;106:1607–11.
12. Tsivian M, Polascik TJ. Focal therapy for prostate cancer. Curr Urol Rep. 2010;11:147–51.
13. Roach 3rd M, Hanks G, Thames Jr H, Schellhammer P, Shipley WU, Sokol GH, et al. Defining biochemical failure following radiotherapy with or without hormonal therapy in men with clinically localized prostate cancer: recommendations of the RTOG-ASTRO Phoenix Consensus Conference. Int J Radiat Oncol Biol Phys. 2006;65:965–74.
14. Ganzer R, Robertson CN, Ward JF, Brown SC, Conti GN, Murat FJ, et al. Correlation of prostate-specific antigen nadir and biochemical failure after high-intensity focused ultrasound of localized prostate cancer based on the Stuttgart failure criteria—analysis from the @-Registry. BJU Int. 2011;108(8 Pt 2): E196–201.
15. Postema AW, De Reijke TM, Ukimura O, Van den Bos W, Azzouzi AR, Barret E, et al. Standardization of definitions in focal therapy of prostate cancer: report from a Delphi consensus project. World J Urol. 2016;34(10):1373–82.
16. Morigi JJ, Stricker PD, van Leeuwen PJ, Tang R, Ho B, Nguyen Q, et al. Prospective comparison of 18F-fluoromethylcholine versus 68Ga-PSMA PET/CT in prostate cancer patients who have rising PSA after curative treatment and are being considered for targeted therapy. J Nucl Med. 2015;56:1185–90.
17. Muller BG, van den Bos W, Brausi M, Fütterer JJ, Ghai S, Pinto PA, et al. Follow-up modalities in focal therapy for prostate cancer: results from a Delphi consensus project. World J Urol. 2015;33:1503–9.
18. Breda A, Anterasian C, Belldegrun A. Management and outcomes of tumor recurrence after focal ablation renal therapy. J Endourol. 2010;24:749–52.
19. Berge V, Dickinson L, McCartan N, Hindley RG, Diep LM, Emberton M, et al. Morbidity associated with primary high intensity focused ultrasound and redo high intensity focused ultrasound for localized prostate cancer. J Urol. 2014;191:1764–9.
20. Crouzet S, Rebillard X, Chevallier D, Rischmann P, Pasticier G, Garcia G, et al. Multicentric oncologic outcomes of high-intensity focused ultrasound for localized prostate cancer in 803 patients. Eur Urol. 2010;58:559–66.
21. Crouzet S, Rouviere O, Martin X, Gelet A. High-intensity focused ultrasound as focal therapy of prostate cancer. Curr Opin Urol. 2014;24:225–30.
22. Ahmed HU, Dickinson L, Charman S, Weir S, McCartan N, Hindley RG, et al. Focal ablation targeted to the index lesion in multifocal localised prostate cancer: a prospective development study. Eur Urol. 2015;68:927–36.
23. Van den Bos W, De Bruin DM, Veelo DP, Postema AW, Muller BG, Varkarakis IM, et al. Quality of life and safety outcomes following irreversible electroporation treatment for prostate cancer: results from a phase I–II study. J Cancer Sci Ther. 2015; 7:312–21.

Positioning Focal Therapy from Consensus to Guidelines

35

Matthijs J.V. Scheltema, Anouk E. Hentschel, and Jean J.M.C.H. de la Rosette

Introduction

Focal therapy (FT) in prostate cancer (PCa) has gained increasing popularity due to the minimally invasive procedure, low patient morbidity, function preservation, and good oncological control. The evidence behind focal therapy is growing exponentially with already more than 60 ongoing trials in 2014 [1], exploring the opportunities for FT in treatment-naïve localized PCa and salvage therapy for recurrent or residual PCa.

This chapter focuses on the development and the current status of PCa therapy guidelines and tries to position focal therapy for localized PCa by answering the following questions:

- What is needed for a prostate cancer therapy to be included into guidelines?
- How do current treatment options meet these requirements?
- Do focal therapy studies proceed according to these requirements?
- Are we there yet?
- Are randomized controlled trials really needed to get into the guidelines?

What Is Needed for a Prostate Cancer Therapy to Be Included into Guidelines?

The ideal PCa therapy is defined by effective and complete PCa elimination at low morbidity. The treatment modality needs to spare important anatomical prostate-related structures (e.g., neurovascular bundle, urinary sphincter, rectal wall, and urethra), preserving urinary, rectal, and erectile function. Consequently, the treatment would not impair patients' quality of life. The procedure needs to be easily and safely executed with a low risk of complications, a short length of hospital stay, and low economical costs. Lastly, the therapy should be applicable and appropriate for a large patient population.

For new prostate cancer treatments, data regarding treatment safety, efficacy, and long-term oncological and functional outcomes needs to be validated in large (multicenter) comparative randomized controlled trials (RCTs), comparing the accepted segments of prostate cancer therapies (e.g., radical prostatectomy, radiotherapy) with this new treatment. Due to the indolent nature of most PCas, follow-up would preferably be 10 years and over.

M.J.V. Scheltema (✉)
A.E. Hentschel • J.J.M.C.H. de la Rosette
Department of Urology, Academic Medical Center (AMC) University Hospital, Amsterdam, The Netherlands
e-mail: m.j.scheltema@amc.nl

© Springer International Publishing AG 2017
T.J. Polascik (ed.), *Imaging and Focal Therapy of Early Prostate Cancer*, Current Clinical Urology, DOI 10.1007/978-3-319-49911-6_35

How Do Current Treatment Options Meet These Requirements?

Current curative treatments by guideline are surgical radical prostatectomy (RP), external beam radiation therapy (EBRT), and brachytherapy—all proven to be effective and safe treatment options for localized PCa [2, 3]. The other treatment option is active surveillance (AS), postponing and selecting definitive treatment for patients who are in need of curative treatment [3, 4]. These treatments will be evaluated on the aforementioned (ideal) requirements for a PCa therapy to get into international guidelines.

Radical Prostatectomy

Traditionally surgical radical prostatectomy (RP) has been performed for low- to high-risk PCa, ranging from early, organ-confined PCa to extracapsular extended PCa. At present it is one of the recommended treatments with curative intent for all PCa risk groups, and salvage RP has been performed in recurrent PCa following radiotherapy [5].

Procedure Execution and Complications

Surgical RP can be performed through open, laparoscopic, or robot-assisted surgery. For robot-assisted laparoscopy, the mean operative time is 210 min, whereas for conventional radical prostatectomy, this is 163 min [6]. The length of hospital stay varies remarkably among different countries and ranges from 3 to 7 days [3, 6]. Among the intraoperative and perioperative complications of RP are anastomotic leakage, damage to adjacent structures/organs, ileus, bleeding, and infection [7].

Oncological Results, Functional Outcomes, and Quality of Life

Since FT is nowadays recommended for low- and intermediate-risk PCa, the following results will focus on low and intermediate PCa only. The Scandinavian Prostate Cancer Group Study Number 4 (SPCG-4) and Prostate Cancer Intervention Versus Observation Trial (PIVOT) show important evidence concerning the potential benefit for survival. Between 1989 and 1999, the SPCG-4 study randomly assigned 695 men with localized PCa to either watchful waiting or RP, and mean follow-up was 13.4 years (range 3 weeks to 23.2 years). For low-risk PCa the SPCG-4 study showed a significant decrease in all-cause mortality and distant metastasis at 18 years. Yet, this was not the case for PCa-specific mortality [8]. The PIVOT trial randomly assigned 731 men with localized PCa to watchful waiting or RP between 1994 and 2002, and mean follow-up was 10.0 years (range 7.3–12.6 years). For low-risk PCa the PIVOT trial found comparable results on PCa-specific mortality at 10 years and found no significant decrease in all-cause mortality after RP [9].

In intermediate-risk PCa, the SPCG-4 study found a significant decrease in all-cause mortality, PCa-specific mortality, and distant metastases at 18 years after RP [8]. However, the PIVOT trial did not show a significant decrease in PCa-specific mortality at 10 years after RP [9]. In a prospective non-comparative longitudinal trial, Mendhiratta et al. included 1864 men with low-risk (55.5 %), intermediate-risk (35.3 %), and high-risk (9.2 %) localized PCa treated with RP between 2000 and 2013 to investigate the effect of RP on PCa-specific mortality (mean follow-up 9.1 years, range 9 months to 13.2 years). These authors found a relative risk for PCa-specific mortality at 10 years of 0.9 % for low-risk and 1.0 % for intermediate-risk PCa [10].

Erectile dysfunction, urinary toxicity, and bowel dysfunction are common side effects after RP, all progressing over time. In a long-term follow-up study after RP, urinary incontinence was seen in 18.3 % of all men at 15 years after their RP (n = 1164), urinary dripping or leakage was seen in 17.3 % whereas the rate of erections insufficient for intercourse increased to 87 % [11]. Of all men studied, 21.9 % reported rectal toxicity (bowel urgency, pain, frequent bowel movements) after 15 years [11]. Understandably these side effects have a detrimental impact on a patient's quality of life [12].

Follow-Up Regimen

Follow-up consists of regular prostate-specific antigen (PSA) monitoring and digital rectal examination (DRE). The American Urological Association (AUA) guideline determines two sequential PSA levels ≥0.2 ng/mL as recurrent disease after RP [13]. However, Antonarakis et al. illustrate that biochemical recurrence is not always associated with the development of distant metastases [14]. They performed a retrospective analysis of 450 men treated with RP between 1981 and 2010 that developed biochemical recurrence (PSA ≥ 0.2 ng/mL) and received no treatment before developing metastases (median follow-up 8.0 years after RP and 4.0 years after biochemical recurrence). At the end of follow-up, 29.8 % had metastatic disease and the median metastasis-free survival was 10.0 years. PSA doubling time and pretreatment Gleason score were independent risk factors for disease progression [14].

Applicable to Large Patient Population and Economic Analysis

Li et al. showed that there were 1,310,373 newly diagnosed cases of PCa in the USA from 2001 to 2007 of which 81 % presented with localized PCa—all possible candidates for RP [15].

From 2003 to 2013, Leow et al. performed a cohort study of 629,593 men undergoing RP for localized PCa in the USA. They concluded that direct hospital costs in the first 90 days after treatment were higher for robot-assisted RP than for open RP: $14,897 vs. $9558 [16]. In addition, Hughes et al. retrospectively analyzed the postoperative health resource and secondary care costs in 10,565 patients at 1080 days after their RP in the UK, comparing robot-assisted laparoscopy to conventional laparoscopy and open surgery. Median total costs for patients after open surgery were $5972 at 1080 days after the intervention, $4912 for patients after robot-assisted laparoscopy, and $5374 for patients after conventional laparoscopy [17].

External Beam Radiation Therapy

External beam radiation therapy (EBRT) is one of the treatment options for localized PCa and is performed by using intensity-modulated radiotherapy (IMRT) alone or in combination with image-guided radiotherapy (IGRT). IMRT enables the distribution of radiation doses around complex and irregular target volumes. IGRT visualizes organ movement, aiming to improve tumor control and reduce treatment toxicity [7].

Procedure Execution and Complications

Anatomical data of the tumor, prostate, and surrounding tissues need to be collected in a three-dimensional (3D) treatment planning system in order to determine the clinical target volume and the required safety margin. Dose-volume histograms maximize the doses to the areas at highest risk [7].

Acute gastrointestinal grade ≥2 toxicity is present in approximately 29 % of patients after conformal techniques (combining IMRT and IGRT) for the treatment of PCa and acute genitourinary grade ≥2 toxicity in 38 %. Gastrointestinal toxicity most frequently involves painful defecation, cramps, tenesmus, and mucous discharge; genitourinary toxicity is most often presented as painful urination, straining, incontinence, and increased frequency (≥12/day) [18]. Among general complications, fatigue is the most common complaint with a peak level at the end of treatment.

Oncological Results, Functional Outcomes, and Quality of Life

The Prostate Testing for Cancer and Treatment (ProtecT) trial will present randomized data comparing radiotherapy to radical prostatectomy and active surveillance in the future, but results are not yet available [19]. Randomizing patients for radiation therapy with conventional dose (60–70 Gy) or dose escalation (range 74–80 Gy) has

shown a significant superiority on 5-year biochemical disease-free survival rates for the dose escalation cohort [20]. From 1994 to 2001, 1979 patients with T1b-T2b PCa and PSA ≤ 20 ng/mL were included (36 % low risk, 53 % intermediate risk, and 11 % high risk) and randomly assigned to radiotherapy plus short-term androgen deprivation therapy (ADT) (987 patients) or radiotherapy alone (992 patients) with a mean follow-up of 9.1 years. The PCa-specific mortality was 8 % in the radiotherapy alone group, while this was 4 % in the radiotherapy plus short-term ADT group. The 10-year overall survival rate was more favorable in the radiotherapy plus short-term ADT group (62 % vs. 57 %). However, the reductions in overall and disease-specific mortality were only significant in intermediate-risk patients [21]. A study by Bolla et al. has shown that in high-risk localized PCa long-term ADT is required for optimal disease control [22].

Zelefsky et al. included 561 patients between 1996 and 2000 with localized PCa (36 % low risk, 46 % intermediate risk, and 18 % high risk) who were receiving IMRT with a dose of 81 Gy (mean follow-up 7 years, range 5–9 years), and 53 % of cases received neoadjuvant short-term ADT. The National Cancer Institute Common Terminology Criteria for Adverse Events toxicity scale was used to score late toxicity. The 8-year actuarial likelihood of late grade ≥2 urinary toxicities was 15 %, and for rectal toxicities this was 1.6 %. In this cohort 72 % had erections sufficient for intercourse before IMRT. Erectile dysfunction developed in 49 % of these men [23] but has been reported to be up to 60.8 % 2 years after RT [11]. Another series by the same authors on the incidence of late rectal and urinary toxicities after conformal radiation therapy and IMRT for localized PCa found that the presence of acute symptoms was a significant risk factor for experiencing late toxicity. Late rectal and urinary toxicity was seen in 42 % of the patients with a history of acute symptoms (10-year incidence) versus 9 % in patients without a history of acute symptoms [24]. The prospective longitudinal study of Sanda et al., published in the *New England Journal of Medicine*, shows that EBRT significantly affects health-related quality of life (HRQoL). From 2003 to 2006, they included 202 patients receiving EBRT alone and 90 patients receiving a combination of EBRT and ADT. At 1 year after EBRT, 11 % of patients had moderate or worse distress due to urinary toxicity whereas for rectal toxicity this percentage was 9 % [12]. Furthermore, ADT is associated with negative effects on multiple QoL domains [12].

Follow-Up Regimen

The follow-up after EBRT consists of PSA testing at 3, 6, and 12 months after treatment, continuing every 6 months until 3 years and then once per year [7]. PSA levels decrease slowly after EBRT. Evidence showed that a PSA nadir <0.5 ng/mL is associated with a beneficial outcome [25], although there is no consensus about the optimal posttreatment PSA level. According to the Phoenix criteria, biochemical failure occurs when PSA levels rise >2 ng/mL above the nadir [26].

Zumsteg et al. performed a retrospective analysis of 2694 patients with low-risk (21.9 %), intermediate-risk (47.8 %), and high-risk (30.3 %) localized PCa treated with EBRT (in 53.8 % combined with ADT) from 1991 to 2008. During follow-up, 609 patients (22.6 %) experienced biochemical failure (9.5 % low risk and 37.8 % intermediate risk), and median time to biochemical failure was 57 months. Interestingly, of these patients only 47 % developed clinical metastases 5 years after biochemical failure (no risk groups reported), and the median period to PCa-specific mortality was 10.5 years since biochemical failure. PCa-specific mortality after biochemical failure was 18 %; however, no risk groups were reported [27].

Applicable to Large Patient Population and Economic Analysis

EBRT can be offered to all different risk groups in localized PCa. IMRT is an expensive radical treatment for localized PCa. Yong et al. developed a Markov model for the economic evaluation of IMRT for localized PCa, conducted from the perspective of the Canadian health care system. The costs of radiation treatment using IMRT were Can$14,520 (2009; US $12,800).

However, total costs increased to Can$60,138 (2009; US$53,400) after addition of radiotherapy toxicity costs and other costs (diagnostic tests, surgical procedures, long-term care, etc.) [28]. However, in patients with intermediate- and high-risk PCa, EBRT is combined with, respectively, short- and long-term ADT, expanding costs even more.

Brachytherapy

Guided by ultrasound, brachytherapy implants a radioactive source into the prostate using a transperineal approach. The tumor receives the maximum dose of radiation while radiation exposure to normal structures is minimized. Brachytherapy can be divided into low-dose rate (LDR) and high-dose rate (HDR) brachytherapy.

Procedure Execution and Complications

Patients with low-risk and favorable intermediate-risk localized PCa are most qualified for LDR monotherapy. In patients with intermediate- or high-risk localized PCa, both LDR and HDR brachytherapy can be administered [7]. LDR brachytherapy will then be combined with supplemental EBRT [7] or neoadjuvant ADT [29]. HDR brachytherapy can be used as monotherapy or as a boost in combination with EBRT [30]. Genitourinary and gastrointestinal toxicity are the most common complications after brachytherapy. Baseline sexual, bowel, and urinary functional levels significantly influence the severity of complications [31]. The majority of patients experience acute urinary toxicity after brachytherapy, although these complaints resolve slowly in most men [32, 33].

Oncological Results, Functional Outcomes, and Quality of Life

There are no randomized controlled trials (RCTs) available comparing brachytherapy as monotherapy for localized PCa to other treatment options. Taira et al. included 1656 men with low-risk (34.7 %), intermediate-risk (36.7 %), and high-risk (28.6 %) localized PCa who underwent LDR brachytherapy monotherapy or a combination with ADT (37.6 %) or EBRT (49.8 %) from 1995 to 2006, followed during a mean period of 7 years [34]. Cause-specific survival (CSS) at 12 years was 99.8 % for low-risk, 99.3 % for intermediate-risk, and 95.2 % for high-risk PCa. Tumor grade appeared to be the strongest predictor of CSS [34]. Two smaller trials combining HDR brachytherapy with EBRT for the treatment of localized PCa found a CSS of 98 % (n = 309, 67 patients low risk, 109 intermediate risk, 133 high risk) after a mean follow-up of 5 years [35] and a CSS of 97 % (209 patients, 33.5 % low risk, 44 % intermediate risk, and 22.5 % high risk) after a mean follow-up of 7.25 years [36]; however, follow-up in both trials was short.

Kittel et al. included 1989 men with low-risk (61.3 %), intermediate-risk (29.8 %), high-intermediate-risk (4.5 %), and high-risk (4.4 %) PCa treated with LDR brachytherapy as monotherapy between 1996 and 2007 and followed them prospectively (mean follow-up 6.8 years) [37]. Severe late genitourinary toxicities were present in 7.6 % of patients, while gastrointestinal toxicities were present in 0.8 % [37]. Sanda et al. performed a prospective multicenter analysis of 1201 localized PCa survivors, included between 2003 and 2006 (median follow-up 30 months) [12]. Of the patients, 306 men were treated with brachytherapy, of whom 59 % had low-risk, 39 % intermediate-risk, and 1 % high-risk localized PCa. Rates of poor sexual function were 47 % at 2 months and remained high at 2 years (46 %); 30 % of patients reported sexual functions as a moderate to big problem. Urinary toxicity caused moderate to worse distress in 18 % of patients at 1 year after brachytherapy. Moderate to worse distress rates for rectal toxicity were 9 % at 1 year after treatment [12]. Functional outcomes after LDR and HDR brachytherapy have been shown to be comparable [30].

Follow-Up Regimen

PSA testing after brachytherapy is complex since benign prostate tissue remains and therefore it is uncommon that PSA levels will decrease to zero. The appearance of benign “PSA bounces” complicates the diagnosis of biochemical recurrence

even more. Interestingly, Stone et al. performed post-brachytherapy prostate biopsies in 185 patients 2 years after LDR mono-brachytherapy (inclusion period from 1990 to 1998) [38]. Patients were offered repeat prostate biopsies annually if the first set of prostate biopsies was positive or if PSA progression occurred. Negative biopsy rates increased over time: 82.2 % at 2 years rising to 92.4 % at 8 years. This study is performed in a small patient population, but these data implicate that the interpretation of PSA levels 2 years after treatment may be unreliable to evaluate the actual effect of brachytherapy on PCa [38].

According to the Phoenix criteria, biochemical failure is defined by a PSA rise of ≥2 ng/mL above the nadir PSA [26]. However, repeat biopsies are generally performed to evaluate the possibility of a PSA bounce. There is no consensus about the cause and clinical consequences of PSA bounces, but the main concern is that they are diagnosed and treated as biochemical failure. The time of appearance can be helpful in distinguishing PSA bounces from treatment failure since often they occur significantly earlier (15–17 months vs. 34 months) [39].

Applicable to Large Patient Population and Economic Analysis

Brachytherapy is applicable to a large patient population, although treatment for intermediate- and high-risk PCa requires a combination of brachytherapy with either hormonal treatment or EBRT, affecting patient morbidity and treatment costs. Furthermore it is important to pay careful attention to appropriate patient selection based on preoperative characteristics. A large prostate gland (>60 cm^3) is a relative contraindication to LDR and HDR brachytherapy [30, 40, 41] since it is associated with a higher treatment-related morbidity (especially acute urinary retention). However contraindicative evidence for HDR brachytherapy is less convincing [42]. Other factors that may constitute a relative contraindication for both LDR and HDR brachytherapy include preexisting urinary symptoms, prior rectal or prostatic surgery, pelvic radiotherapy, and inflammatory bowel disease [30, 43].

Average cumulative direct costs during the first 6 months of treatment were $7588 for brachytherapy monotherapy. Calculated accumulated costs over 5.5 years for men across all risk groups were $35,143 using a hypothetic model. According to the hypothetic model used by these authors, all other radical treatments were more expensive than brachytherapy [44].

Active Surveillance

Active surveillance (AS) is an alternative option to radical treatments, focusing mainly on low-risk PCa. By stratifying the risk for PCa-specific mortality, patients with a low mortality risk are prevented from overtreatment and treatment-related morbidity or complications. Patients are strictly monitored by serial PSA testing and repeat prostate biopsies, differentiating patients with latent PCa from patients with disease progression who are in need of treatment with curative intent.

Procedure Execution and Complications

Eligible patients have low-risk PCa, defined by a clinical stage T1/2, PSA < 10 mg/L, or PSA density <0.2 mg/L and one or two positive prostate biopsy cores (<50 % involvement) with sum Gleason score of 6 [45]. Different follow-up regimens exist, with the Prostate Cancer Research International Active Surveillance (PRIAS) study performing PSA measurements every 3–6 months and repeat biopsies at 1, 4, and 7 years after diagnosis [45]. Since AS is not active or invasive therapy, patient morbidity or treatment-related complications are very low. The most frequent complications are related to repeat biopsies and include prostatitis, bleeding, and urinary retention [2]. In the SPCG-4 trial, patients were evaluated on psychological distress during watchful waiting by use of a standardized questionnaire every 6 months for 2 years followed annually up to 8 years. Anxiety and worrying for the future was less common in the RP cohort compared to the watchful waiting cohort (OR: 0.60; 95 % CI, 0.38–0.96) [46]. However, another Dutch series

showed that anxiety and distress scores were favorable in AS compared to other PCa treatments, whereas poor shared decision-making and a neurotic personality were negatively correlated with anxiety and distress [47].

Oncological Results, Functional Outcomes, and Quality of Life

At present, only data is available from premature randomized controlled trials comparing AS with radical treatment. However, long-term data exist on PCa-specific mortality of low-risk PCa when comparing watchful waiting with RP. The SPCG-4 trial [8] included 695 men with low-grade (61 %), intermediate-grade (23 %), and high-grade (5 %) PCa (11 % unknown), follow-up was up to 23.2 years (median 13.4 years). PCa-specific mortality was 99/348 (28 %) in the watchful waiting cohort, compared to 63/347 (18 %) in the RP cohort with a relative risk of 0.56. Eight men needed to be treated in order to prevent one death, but this ratio improved with age <65 years and higher tumor grade. Another series in the PIVOT study [48] randomized low-risk (40 %), intermediate-risk (34 %), and high-risk (21 %) PCa patients (5 % missing data) to either RP or observation, follow-up was 10 years. Of the 364 men assigned to RP, 21 died from PCa (5.8 %), and in the observation group, PCa-specific mortality was 31/367 (8.4 %), showing no significant difference in PCa-specific mortality between RP and observation after 10 to 12 years of follow-up.

A patient on AS has improved functional outcomes when compared to either radiotherapy or RP, with lower rates of urinary incontinence, erectile dysfunction, and bowel complaints. Overall health-related quality of life was similar for AS and radical treatments [49–51].

Follow-Up Regimen

Follow-up consists of serial PSA testing and repeat biopsies. A major pitfall for AS is the inherent understaging and undergrading of current PCa diagnostics. In a study by Heidegger et al., 197 patients diagnosed with low-grade PCa by 10 or 15 scheme systematic transrectal ultrasound (TRUS)-guided prostate biopsies received a RP [52]. These patients were eligible for AS (according to the European Association of Urology guidelines for PCa) [2]. Whole-mount pathology showed upgrading in 41.1 % (40.1 % Gleason sum score 7 and 1 % Gleason sum score 8) [52]. Sub-analysis showed that the number of prostate biopsies taken did not influence undergrading. In a bigger series, constituting 10,287 patients receiving a prostatectomy for low-risk PCa (Gleason sum score 6), tumor grade was upgraded in 44 % of the cases to Gleason sum score 7 or higher [53].

In a study by Guzzo et al., 172 patients who met the criteria for AS and were scheduled for RP, preoperative endorectal magnetic resonance imaging (MRI) with T2-weighted sequences (from 1991 to 2007) was performed [54]. Of the patients, 49 % had a suspected lesion on MRI, but this was not predictive for upgrading or staging on whole-mount pathology [54]. However, no dynamic contrast-enhanced imaging was performed (no multiparametric MRI [mpMRI]), and the image quality of current mpMRI has drastically improved. Yerram and colleagues performed an mpMRI of the prostate in 800 patients (from 2007 to 2011) and identified suspicious lesions in 125 patients [55]. TRUS/MRI fusion-guided prostate biopsies were performed and showed no cancer (62 %), Gleason sum score 6 (30 %), and Gleason score 3 + 4 = 7 (8 %). No Gleason 4 + 3 or higher was found. Of the 48 patients with PCa, 30 were eligible for AS. Fifteen patients opted for surgical intervention (eligible for AS and non-eligible for AS), and final histopathology did not show any upgrading or extracapsular extension nor seminal vesicle invasion [55]. This may indicate the potential of TRUS/MRI fusion-guided prostate biopsies to reduce PCa understaging or undergrading; however, the current negative predictive value of mpMRI is suboptimal, and even in expert centers, clinical significant disease may be missed [56].

Applicable to Large Patient Population and Economic Analysis

In a sub-analysis of the Surveillance, Epidemiology, and End Results (SEER) database, 132,606 men with newly diagnosed (2004–2006,

non-metastatic) PCa were evaluated on clinical T-score, PSA, and Gleason score to classify this cohort according to the D'Amico risk classification; 44,071 (33 %) were excluded from analysis due to unavailable data (either cT-score, PSA, or Gleason score). In total 32,566 (37 %) men were classified to have low-risk PCa (eligible for AS), whereas 28,961 (33 %) and 27,011 (30 %) had intermediate- and high-risk PCa, respectively [57]. It has been estimated (SEER database) that 220,800 new cases of PCa were diagnosed in the USA in 2015, resulting in a total of 81.696 (33 %) potential AS candidates in the USA only.

The economic analysis of AS is complicated due to the prolongation of treatment due to the indolent nature of PCa in a significant amount of AS patients. The cumulative direct costs for the first 6 months were $2586 for watchful waiting, which is far below the direct costs of radical treatment. However, when a hypothetical model was used, including the costs for (repeat) prostate biopsies and a follow-up period, total costs at 5 years were estimated to be $22,000 and lifetime costs between $25,000 and $30,000, which is comparable to brachytherapy or RP [58].

Do Focal Therapy Studies Proceed According to These Requirements?

Focal therapy (FT) for PCa emerged as alternative minimally invasive treatment with curative intent for primary localized PCa. The rationale of focal (ablative) treatment derived from impaired functional outcomes after whole-gland treatment (RT or RP). The aim of FT is to spare important adjacent anatomical structures to preserve erectile, urinary, and rectal function while maintaining oncological control by eradicating PCa lesions. FT can be performed on either a target or zonal basis (quadrant, hemi-, or hockey-stick ablation). Techniques used for ablative therapy include cryosurgery, high-intensity focused ultrasound (HIFU), irreversible electroporation (IRE), vascular-targeted photodynamic therapy (VTP), radiofrequency ablation (RFA), (interstitial) laser ablation, and microwave ablation. In order to objectively position FT to the guidelines, FT will be evaluated on the same aforementioned (ideal) requirements for a PCa therapy to get into the international guidelines, and outcomes will be compared to the accepted segments in the PCa Guidelines.

Procedure Execution and Complications

Prior to the FT procedure, it has been recommended that patients will undergo mpMRI (with MR-guided biopsies) and/or transperineal template-mapping biopsies for patient selection and to obtain disease topography for adequate treatment planning [59, 60]. TRUS, TRUS-mpMRI (cognitive) fusion, and in-bore MRI are imaging modalities used for FT treatment guidance. The actual procedure is different for respective ablative modalities, which have been described in detail and standardized elsewhere [61–64], but total procedure time generally lasts about 1 h and is usually performed during a 1–2 day admittance. The most frequent complications seen after FT are urinary retention (from 0 to 17 %), urethral stricture (from 0 to 5 %), and urinary tract infections (from 0 to 17 %), although many of the available phase I–II trials reported these complications inconsistently [65].

Oncological Results, Functional Outcomes, and Quality of Life

In a systematic review on primary and salvage focal therapy, including 30 nonrandomized controlled trials (25 primary FT) with a total of 2350 cases, current available evidence and ongoing trials were assessed on study quality, patient selection, and functional and disease control outcomes [65]. Primary FT for localized PCa was performed with cryosurgery (n = 6), HIFU (n = 12), VTP (n = 1), photothermal therapy (n = 3), RFA (n = 1), and focal brachytherapy (n = 1), and one trial performed FT with different ablative modalities. Patient characteristics (n = 2232) include median age of 56.5–73 years, PSA levels of 3.76–24 μ(mu)g/L, Gleason sum score of ≤6

($n = 1503$), 7 ($n = 521$), and ≥8 ($n = 82$) resulting in low-risk ($n = 1109$), intermediate-risk ($n = 704$), and high-risk ($n = 164$) PCa (some trials did not mention Gleason score or risk stratification). When post-FT biopsies were performed in the treated zone and/or contralateral side, positive biopsies with clinical significant disease were found in 0–17 %, and clinical insignificant disease was found in 4–50 % of patients. Since in the majority of these trials, follow-up was too short for metastatic PCa to develop (if mentioned at all), it was very low (0–0.3 %), and consequently no PCa-specific mortality was found [65]. The Cryo On-Line Database (COLD) registry (1997–2007) included 1160 patients who were treated with partial cryotherapy. Prostate biopsies were performed when clinical suspicion arose; in 43/164 patients (26.3 %), recurrent or residual disease was found, but this only comprised a small portion of focally treated patients 43/1160 (3.7 %) [66]. Although some studies report biochemical recurrence by use of the American Society for Radiation Oncology (ASTRO) or Phoenix definition, it must be stressed that this has not yet been validated after FT and insufficient data are available on PSA velocity of untreated prostatic tissue and the risk of residual/recurrent PCa.

Excellent pad-free continence rates were found after FT (95–100 %), measured with the use of standardized questionnaires, whereas leak-free continence was found in 83–100 % of these patients [65]. Promising rates of erectile functioning are found after FT when compared to radical whole-gland therapies. Erectile function was preserved in 54–100 % of the patients who had an erectile function (with or without the use of medication) sufficient for intercourse before FT [65]. In a combined analysis of three prospective trials ($n = 118$) on FT with HIFU for localized PCa (T1/2, low to intermediate PCa), erectile function was assessed by use of the International Index of Erectile Function (IIEF-5) score. Although a significant drop was seen at 1 and 3 months after FT, erectile function improved so that after 6, 9, and 12 months after FT no significant changes in individual sexual domain scores were found compared to baseline [67]. The overall quality of life after FT showed no significant difference at 12 months when compared to baseline [68]; however, data is lacking.

Follow-Up Regimen

Oncological follow-up after FT is more challenging due to the remnants of untreated prostatic tissue producing PSA with unknown velocity. Factors of influence include the diminished unknown fraction of PSA produced by the treated tumor lesion(s), local inflammation, and progression of benign prostatic hyperplasia (BPH) [69]. However, it is important to perform serial PSA testing every 3 months for the first year and every 6 months for the remaining follow-up. It is recommended to perform repeat prostate biopsies (e.g., TRUS-guided biopsies, MRI/TRUS fusion biopsies, transperineal template-mapping biopsies, in-bore MR-guided biopsies) at 6 or 12 months after FT or if clinical suspicion arises [59]. It has been shown in several studies that the extent of the focal ablation can be visualized with mpMRI after FT, with ablation-induced changes on T1- and T2-weighted images as well as non-enhancement during the contrast phase. Normally residual or recurrent disease will appear as an enhanced lesion within or adjacent to the ablation zone. However, it may be difficult to distinguish post-FT effects on mpMRI with recurrent lesions and likewise non-enhanced recurrent lesions may be missed as well [70–74].

Applicable to Large Patient Population and Economic Analysis

When the previous mentioned sub-analysis of the SEER database is translated to FT, 70 % of all patients will have low- or intermediate-risk PCa (154,500 patients in the USA, 2015) [57]. In a consensus meeting on patient selection for FT, it has been agreed that FT should ideally be performed in patients with cT1c-T2a, Gleason sum score ≤7, and PSA < 15 μ(mu)g/L [75]. Therefore, patient suited for FT should have unilateral, organ-confined PCa. In an analysis on radical

prostatectomy specimen ($n = 1184$; 1106 patients had Gleason sum score ≤7 on preoperative biopsy), unilateral PCa was found in 19.2 % of all patients ($n = 227$) [76]. This is in line with more recent findings, showing unilateral tumors in 22.5 % of all patients suitable for hemiablation on histopathological analysis after RP [77]. When extrapolating this data to the SEER data, still a significant part of these patients are potential candidates for FT. Especially when taking recent understandings of tumor behavior and natural history of PCa into account, suggesting that only the index lesion should be treated and clinically insignificant (satellite) lesions are unlikely to metastasize [78]. Nowadays bilateral ablative therapy is performed using bilateral focal ablation or hockey-stick ablation extending the indication for FT.

To our best knowledge, no study exists on the cost-effectiveness of different ablative modalities used for FT, and cost analysis studies are lacking. In a structured literature analysis on the clinical effectiveness, safety, and cost-effectiveness (total costs and quality-adjusted life-years) of current PCa treatment, HIFU was reported to cost £19,860 (or $28,291) and was less costly than other ablative modalities. In terms of quality-adjusted life-years, which is used for the economical assessment for medical interventions and include both the quality and quantity of life after the respective intervention, it is more effective (3.86) than EBRT (3.63) [79]. However, it is expected that increased experience and use of FT will reduce these costs significantly.

Are We There Yet?

In Table 35.1 comparative outcomes are presented for FT and current PCa treatments [8–11, 18, 21, 24, 34, 48, 50, 51, 65]. There are different ways to approach this variety of available data to position FT to current PCa treatment in the guidelines (Fig. 35.1).

When focusing on functional outcomes, FT can be positioned as a therapeutic option with excellent urinary, rectal, and erectile functional preservation compared to radical treatments. If evaluating the impact of a therapy on the functional domain is the primary objective of a trial, short- and medium-term data is evident. Therefore it could be argued that distinctive and mature data are published on the functional outcomes after FT. Similar to AS, FT can spare genitourinary functioning, however, with curative intent and applicable to a bigger patient populations (low- and intermediate-risk PCa). Focal therapy potentially saves the majority of PCa patients from impaired outcomes and complications (e.g., urinary incontinence and erectile dysfunction) associated with radical treatment. Ablative therapy is executed within 1–2 h and has a low complication rate, and patients are usually discharged the day after the procedure with no or minimal physical complaints.

If oncological control is the main objective for FT in low- to intermediate-risk PCa, mature and distinctive data are more complicated to obtain. As seen in the SPCG-4, surgical intervention was only shown beneficial (PCa-specific mortality) after 18 years in the intermediate-risk PCa cohort, whereas no significance was found in the low-risk group at 18 years or in neither risk groups at 10 years (PIVOT). Consequently follow-up after FT should be more than 15–20 years before any firm statements regarding oncological control can be made. An interesting study design is the so-called ablate and resect design, in which an ablative procedure is performed prior to a radical prostatectomy to compare ablative configurations with ablation zone dimensions and effective PCa eradication. Complete PCa ablation without skip lesions have been published [80], advocating safe and effective tissue ablation. The relative low risk of PCa-specific mortality in low- and intermediate-risk PCa serves as the main rationale behind AS, reserving radical treatment only for patients who show upgrading or upstaging—both increasing the risk for PCa-specific mortality. It may be difficult to comprehend that it is acceptable (according to the guidelines) to undergrade or understage 41.1 % of AS candidates due to the inherent errors of current PCa diagnostics, but not accept any residual (satellite) lesions after FT due to these same inherent errors of current PCa diagnostics. Especially since all radical

Table 35.1 Eligible patients, outcomes, and complications of different treatment options for localized prostate cancer

Treatment (reference)	Number of patients	Eligible patients	Oncological control	Urinary functioning	Erectile dysfunction	Rectal toxicity
Radical prostatectomy SPCG-4 trial (18 years) [8] PIVOT (10 years) [9] Mendhiratta (10 years) [10] SPCG-4 trial (18 years) [8] PIVOT (10 years) [48] Mendhiratta (10 years) [10]	108 (347) 148 (364) 1034 (1864) 159 (347) 129 (364) 658 (1864)	T1/2, all risk groups	*Low risk* 10.2 % PSM 4.1 % PSM 0.9 % PSM *Intermediate risk* 15.1 % PSM 4.7 % PSM 1.0 % PSM	*Urinary incontinence*: 18.3 % [11] *Dripping or leakage*: 17.3 % [11]	78.8 %, 2 years after RP [11]	21.9 % [11]
EBRT [21] RT + ADT (10 years) RT (10 years) RT + ADT (10 years) RT (10 years)	351 (1979) 334 (1979) 524 (1979) 544 (1979)	T1/2, all risk groups	*Low risk* 2.3 % PSM 1.5 % PSM *Intermediate risk* 4.0 % PSM 9.6 % PSM	*Acute toxicity*: 38 % [18] *Late toxicity*: 11 % [12]	60.8 % [11] 49 % [24]	*Acute toxicity*: 29 % [21] *Late toxicity*: 9 % [12, 24]
Brachytherapy Taira (12 years) [34] Taira (12 years) [34]	575 (1656) 608 (1656)	T1/2, low, intermediate risk	*Low risk* 0.2 % PSM *Intermediate risk* 0.7 % PSM	*Late toxicity*: 18 % [12]	46 % [12]	*Late toxicity*: 9 % [12]
Active surveillance SPCG-4 trial (18 years) [8] PIVOT (10 years) [48] SPCG-4 trial (18 years) [8] PIVOT (10 years) [48]	143 (348) 148 (367) 127 (348) 120 (367)	T1/2, low risk, PSA <10, ≤2 positive biopsies	*Low risk* 14.0 % PSM 2.7 % PSM *Intermediate risk* 39.3 % PSM 10.8 % PSM	No statistical difference [50]	30 % [51]	No statistical difference [50]
Focal therapy Valerio [65]	1109 (2350) 704 (2350)	T1/2, low, intermediate risk	*Low risk* 0 % PSM[a] *Intermediate risk* 0 % PSM[a]	Urinary incontinence: 0–5 % Dripping or leakage: 0–17 %	0–46 % No significant change after FT	0–1 %

[a]No long-term follow-up

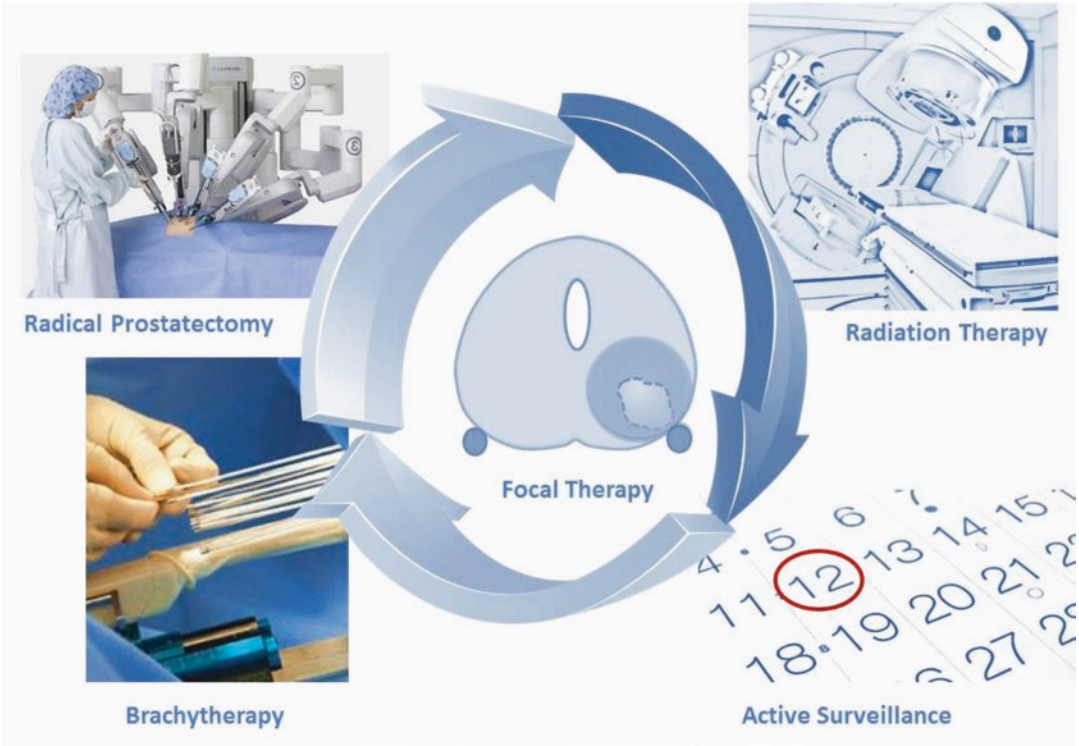

Fig. 35.1 Positioning focal therapy to current prostate cancer treatments

treatment options are still possible after FT as well as salvage FT on the untreated prostatic tissue outside the ablation zone. Moreover, residual/satellite lesions may not be of any clinical significance, as discussed extensively in Chap. 8 on Identifying and Characterizing the Index Lesion.

What is the trigger in the history of the PCa guidelines that defines the moment that a new therapy or imaging modality is included into the guidelines? One of the most recent active treatments is brachytherapy and one may ask: What brought brachytherapy to that point? Brachytherapy has been accepted as a standard segment of PCa therapy without any head-to-head RCTs. Although it had been shown that brachytherapy is effective in biochemical elimination of PCa and the biochemical recurrence rates were low within the first years, no long-term (comparative) data were available on functional outcomes and oncological control. Excellent 10-year post-brachytherapy PCa-specific survival was presented and used for the implementation of brachytherapy in the 2007 AUA guidelines, based on a study by Stock et al. [81]. However this study included 1561 patients of which 69 % (n = 1073) had low-grade, 21 % (n = 330) intermediate-grade, and only 10 % (n = 158) high-grade PCa, and of all patients 71 % (n = 1111) had PSA levels ≤10 μ(mu) g/L. Consequently the results of this study may not be reflective for all PCa risk groups. Interestingly, the 2007 AUA guideline states that interstitial brachytherapy is an option for the management of high-risk PCa [3]. In line, AS has been included in the international guidelines without any comparative RCT, although one might argue that long-term oncological outcomes were available from the watchful waiting cohorts in the SPCG-4 and PIVOT trials. Since patients do not actually undergo any intervention, side effects and complications are consequently low.

In the same train of thoughts, one might be critical to the embracement of robot-assisted RP without evident clinical benefit compared to conventional laparoscopic or open RP or the recent

utilization of mpMRI and MR-targeted biopsies in clinical practice in which some centers even propagate that no more systematic TRUS-guided biopsies should be taken. It is intriguing how some technological advancements are so easily accepted when, for example, there is also a significant proportion of patients where clinical significant disease is missed (for an overview on mpMRI PCa detection, see [1] and Chap. 13 of this book).

Are Randomized Controlled Trials Really Needed to Get into the Guidelines?

Data from the first phase I/II trials are being pooled into database registries (e.g., COLD registry for cryosurgery, Clinical Research Office of the Endourological Society [CROES] database for IRE), providing large datasets on long-term functional, oncological, and quality of life outcomes. At present, the initial experience is already >15 years ago, and these datasets are evolving into the first long-term data available, despite early technology and the absence of mpMRI for PCa lesion localization or treatment guidance. In a recent review by Mendez et al., these authors stated that there is a need for head-to-head (long-term) randomized controlled trials to provide the highest evidence for or against a position for FT in the international guidelines [1].

Previous comparative RCTs in early PCa have had difficulty recruiting patients due to a strong patient preference. Consequently many attempts resulted in early closure due to poor recruitment. Examples of these comparative RCTs are the LopeRA feasibility trial (laparoscopic vs. open vs. robot-assisted RP), START trial (AS vs. RP), SPIRIT trial (RP vs. brachytherapy), and SABRE-1 feasibility trial (brachytherapy vs. RP) [82]. Only the ProtecT trials (AS vs. RP vs. EBRT) included sufficient patients for their target by the use of intensive recruitment training and is at present in follow-up [82, 83]. Due to the inherent difficulty in recruiting patients, there is no comparative RCT available showing which therapy is best for low- and intermediate-risk PCa. Therefore one might argue it to be arbitrary to demand comparative RCTs on FT for the implementation into the current guidelines. Nevertheless, the first phase III trials on FT commenced, with VTP vs. AS, HIFU vs. brachytherapy, hemiablation vs. whole-gland ablation using brachytherapy, and focal vs. extended ablation with IRE [1].

In 2014 the Prostate Cancer RCT consensus group gathered to appoint the aforementioned difficulties in patient recruitment for comparative RCT on primary PCa treatment [84]. This expert panel proposed an alternative trial design, the so-called cohort-embedded RCT, which involves an observational cohort (with prospective follow-up) that meet the inclusion criteria for FT. This cohort receives a focal intervention and will be compared with a cohort (also meeting the inclusion criteria for FT) that receives the standard of care (AS, RP, or radiotherapy). By use of this design, various ablative modalities can be evaluated against the same standard of care and vice versa, accelerating the availability of positioning data for or against FT. The panel recommended that primary comparative objectives could be obtained within midterm follow-up and validity should be strengthened by the utilization of available long-term data of the existing database registries (e.g., COLD or CROES) [1, 84].

Conclusion

The main objective of the PCa international guidelines is to provide clinicians with safe and effective PCa treatment options based on the best evidence available. The implementation of new therapies should include the recommendations of expert panels based on consensus projects, pooled data from available database registries, grade III–IV evidence, and systematic reviews. Based on the present literature, FT proves to be a safe and effective therapeutic option for low to intermediate PCa. Promising rates of functional preservation and short-term oncological control are found when data is compared with the accepted segment of PCa treatments. Data from the first phase I/II trials are being pooled into

databases, providing large datasets on long-term functional, oncological, and quality of life outcomes.

Recent developments and understanding of PCa behavior have revolutionized our approach toward lesion-specific risk assessment. Due to the advancements made in mpMRI technology, lesion characteristics can be assessed on lesion size/volume, topography, and morphology aiding both risk stratification and treatment planning. In an editorial, Emberton [85] signals a shift toward prostate-specific risk factors that can well be compared to the same risk assessment in AS evaluating patient-specific risk factors. By treating the prostate-specific risk factors (e.g., the index lesion or clinical significant lesions), the relative risk of prostate-specific mortality may be reduced.

To position FT in the guidelines, one might position FT as a mediating treatment option between AS and radical treatment, reducing prostate-specific risk factors while sparing patient-specific functioning. Hence the burning question is: Should patients have the option by guidelines to choose for lesion-based risk assessment and treatment, potentially saving them from overtreatment or radical treatment-related toxicity?

References

1. Mendez MH, Joh DY, Gupta R, Polascik TJ. Current trends and new frontiers in focal therapy for localized prostate cancer. Curr Urol Rep. 2015;16(6):1–11.
2. Mottet N, Bellmunt J, Briers E, van den Bergh RCN, Bolla M, van Casteren NJ, et al. Guidelines on prostate cancer. Eur Assoc Urol Guid. 2015:1–156.
3. Thompson I, Thrasher J, Gunnar Aus M, Burnett A, Canby-Hagino E, Cookson M, et al. Guideline for the management of clinically localized prostate cancer: 2007 update. J Urol. 2007;177(6):2106–31.
4. Johansson J, Andren O, Andersson S, Dickman PW, Holmberg L, Magnuson A, et al. Natural history of early, localized prostate cancer. JAMA. 2004;291(22): 2713–9.
5. Chade DC, Eastham J, Graefen M, Hu JC, Karnes RJ, Klotz L, et al. Cancer control and functional outcomes of salvage radical prostatectomy for radiation-recurrent prostate cancer: a systematic review of the literature. Eur Urol. 2012;61(5):961–71.
6. Wood DP, Schulte R, Dunn RL, Hollenbeck BK, Saur R, Wolf JS, et al. Short-term health outcome differences between robotic and conventional radical prostatectomy. Urology. 2007;70(5):945–9.
7. Mottet N, Bellmunt J, Briers E, Bergh R, Bolla M, Casteren N, et al. EAU guidelines on prostate cancer. 2014. https://uroweb.org/wp-content/uploads/1607-Prostate-Cancer_LRV3.pdf. Accessed 24 July 2016.
8. Bill-Axelson A, Holmberg L, Garmo H, Rider JR, Taari K, Busch C, et al. Radical prostatectomy or watchful waiting in early prostate cancer. N Engl J Med. 2014;370(10):932–42.
9. Wilt TJ. The prostate cancer intervention versus observation trial: VA/NCI/AHRQ cooperative studies program #407 (PIVOT): design and baseline results of a randomized controlled trial comparing radical prostatectomy with watchful waiting for men with clinically loc. J Natl Cancer Inst Monogr. 2012; 407(45):184–90.
10. Mendhiratta N, Lee T, Prabhu V, Llukani E, Lepor H. 10-year mortality after radical prostatectomy for localized prostate cancer in the prostate-specific antigen screening era. Urology. 2015;86(4):783–8.
11. Resnick MJ, Koyama T, Fan K-H, Albertsen PC, Goodman M, Hamilton AS, et al. Long-term functional outcomes after treatment for localized prostate cancer. N Engl J Med. 2013;368(5):436–45.
12. Sanda MG, Dunn RL, Michalaski J, et al. Quality of life and satisfaction with outcome among prostate cancer survivors. N Engl J Med. 2008;358:1250–61.
13. Cookson MS, Aus G, Burnett AL, Canby-Hagino ED, D'Amico AV, Dmochowski RR, et al. Variation in the definition of biochemical recurrence in patients treated for localized prostate cancer: the American Urological Association Prostate Guidelines for localized prostate cancer update panel report and recommendations for a standard in the re. J Urol. 2007; 177(2):540–5.
14. Antonarakis ES, Feng Z, Trock BJ, Humphreys EB, Carducci MA, Partin AW, et al. The natural history of metastatic progression in men with prostate-specific antigen recurrence after radical prostatectomy: long-term follow-up. BJU Int. 2012;109(1):32–9.
15. Li J, Djenaba JA, Soman A, Rim SH, Master VA. Recent trends in prostate cancer incidence by age, cancer stage, and grade, the United States, 2001–2007. Prostate Cancer. 2012;2012:691380.
16. Leow JJ, Chang SL, Meyer CP, Wang Y, Hanske J, Sammon JD, et al. Robot-assisted versus open radical prostatectomy: a contemporary analysis of an all-payer discharge database. Eur Urol. 2016:1–9.
17. Hughes D, Camp C, O'Hara J, Adshead J. Health resource use following robot-assisted surgery versus open and conventional laparoscopic techniques in oncology: analysis of English secondary care data for radical prostatectomy and partial nephrectomy. BJU Int. 2016;117(6):940–7.
18. Wortel RC, Incrocci L, Pos FJ, Lebesque JV, Witte MG, Van Der Heide UA, et al. Acute toxicity after image-guided intensity modulated radiation therapy compared to 3D conformal radiation therapy in prostate cancer patients. Int J Radiat Oncol Biol Phys. 2015;91(4):737–44.

19. Lane JA, Donovan JL, Davis M, Walsh E, Dedman D, Down L, et al. Active monitoring, radical prostatectomy, or radiotherapy for localised prostate cancer: study design and diagnostic and baseline results of the ProtecT randomised phase 3 trial. Lancet Oncol. 2014;15(10):1109–18.
20. Viani GA, Stefano EJ, Afonso SL. Higher-than-conventional radiation doses in localized prostate cancer treatment: a meta-analysis of randomized, controlled trials. Int J Radiat Oncol Biol Phys. 2009; 74(5):1405–18.
21. Jones C, Hunt D, McGowan D, Amin M, Chetner M, Bruner D, et al. Radiotherapy and short-term androgen deprivation for localized prostate cancer. N Engl J Med. 2011;365(2):107–18.
22. Bolla M, Van Tienhoven G, Warde P, Dubois JB, Mirimanoff RO, Storme G, et al. External irradiation with or without long-term androgen suppression for prostate cancer with high metastatic risk: 10-year results of an EORTC randomised study. Lancet Oncol. 2010;11(11):1066–73.
23. Zelefsky MJ, Chan H, Hunt M, Yamada Y, Shippy AM, Amols H. Long-term outcome of high dose intensity modulated radiation therapy for patients with clinically localized prostate cancer. J Urol. 2006;176:1415–9.
24. Zelefsky MJ, Levin EJ, Hunt M, Yamada Y, Shippy AM, Jackson A, et al. Incidence of late rectal and urinary toxicities after three-dimensional conformal radiotherapy and intensity-modulated radiotherapy for localized prostate cancer. Int J Radiat Oncol Biol Phys. 2008;70(4):1124–9.
25. Ray ME, Thames HD, Levy LB, Horwitz EM, Kupelian PA, Martinez AA, et al. PSA nadir predicts biochemical and distant failures after external beam radiotherapy for prostate cancer: a multi-institutional analysis. Int J Radiat Oncol Biol Phys. 2006;64(4): 1140–50.
26. Roach M, Hanks G, Thames H, Schellhammer P, Shipley WU, Sokol GH, et al. Defining biochemical failure following radiotherapy with or without hormonal therapy in men with clinically localized prostate cancer: recommendations of the RTOG-ASTRO Phoenix Consensus Conference. Int J Radiat Oncol Biol Phys. 2006;65(4):965–74.
27. Zumsteg ZS, Spratt DE, Romesser PB, Pei X, Zhang Z, Polkinghorn W, et al. The natural history and predictors of outcome following biochemical relapse in the dose escalation era for prostate cancer patients undergoing definitive external beam radiotherapy. Eur Urol. 2014;194(6):1624–30.
28. Yong JHE, Beca J, McGowan T, Bremner KE, Warde P, Hoch JS. Cost-effectiveness of intensity-modulated radiotherapy in prostate cancer. Clin Oncol. 2012; 24(7):521–31.
29. Lee LN, Stock RG, Stone NN. intermediate- to high-risk prostate cancer treated with permanent radioactive seed implantation. Int J Radiat Oncol Biol Phys. 2002;52(2):444–52.
30. Yamada Y, Rogers L, Demanes DJ, Morton G, Prestidge BR, Pouliot J, et al. American Brachytherapy Society consensus guidelines for high-dose-rate prostate brachytherapy. Brachytherapy. 2012;11(1): 20–32.
31. Chen AB, D'Amico AV, Neville BA, Earle CC. Patient and treatment factors associated with complications after prostate brachytherapy. J Clin Oncol. 2006; 24(33):5298–304.
32. Merrick GS, Butler WM, Wallner KE, Galbreath RW, Murray B, Zeroski D, et al. Dysuria after permanent prostate brachytherapy. Int J Radiat Oncol Biol Phys. 2003;55(4):979–85.
33. Keyes M, Miller S, Moravan V, Pickles T, McKenzie M, Pai H, et al. Predictive factors for acute and late urinary toxicity after permanent prostate brachytherapy: long-term outcome in 712 consecutive patients. Int J Radiat Oncol Biol Phys. 2009;73(4):1023–32.
34. Taira AV, Merrick GS, Butler WM, Galbreath RW, Lief J, Adamovich E, et al. Long-term outcome for clinically localized prostate cancer treated with permanent interstitial brachytherapy. Int J Radiat Oncol Biol Phys. 2011;79(5):1336–42.
35. Phan TP, Syed MN, Puthawala A, Sharma A, Khan F. High dose rate brachytherapy as a boost for the treatment of localized prostate cancer. J Urol. 2007; 177(1):123–127; discussion 127.
36. Demanes DJ, Rodriguez RR, Schour L, Brandt D, Altieri G. High-dose-rate intensity-modulated brachytherapy with external beam radiotherapy for prostate cancer: California endocurietherapy's 10-year results. Int J Radiat Oncol Biol Phys. 2005;61(5): 1306–16.
37. Kittel JA, Reddy CA, Smith KL, Stephans KL, Tendulkar RD, Ulchaker J, et al. Long-term efficacy and toxicity of low-dose-rate (1)(2)(5)I prostate brachytherapy as monotherapy in low-, intermediate-, and high-risk prostate cancer. Int J Radiat Oncol Biol Phys. 2015;92(4):884–93.
38. Stone N, Stock R, Unger P. Intermediate term biochemical-free progression and local control following 125Iodine brachytherapy for prostate cancer. J Urol. 2005;173(3):803–7.
39. Caloglu M, Ciezki JP, Reddy CA, Angermeier K, Ulchaker J, Chehade N, et al. PSA bounce and biochemical failure after brachytherapy for prostate cancer: a study of 820 patients with a minimum of 3 years of follow-up. Int J Radiat Oncol Biol Phys. 2011;80(3):735–41.
40. Niehaus A, Merrick GS, Butler WM, Wallner KE, Allen ZA, Galbreath RW, et al. The influence of isotope and prostate volume on urinary morbidity after prostate brachytherapy. Int J Radiat Oncol Biol Phys. 2006;64(1):136–43.
41. Nag S, Beyer D, Friedland J, Grimm P, Nath R. American brachytherapy society (ABS) recommendations for transperineal permanent brachytherapy of prostate cancer. Int J Radiat Oncol Biol Phys. 1999;44(4):789–99.

42. Monroe AT, Faricy PO, Jennings SB, Biggers RD, Gibbs GL, Peddada AV. High-dose-rate brachytherapy for large prostate volumes (> or = 50 cc)-Uncompromised dosimetric coverage and acceptable toxicity. Brachytherapy. 2008;7(1):7–11.
43. Davis BJ, Horwitz EM, Lee WR, Crook JM, Stock RG, Merrick GS, et al. American Brachytherapy Society consensus guidelines for transrectal ultrasound-guided permanent prostate brachytherapy. Brachytherapy. 2012;11(1):6–19.
44. Wilson LS, Tesoro R, Elkin EP, Sadetsky N, Broering JM, Latini DM, et al. Cumulative cost pattern comparison of prostate cancer treatments. Cancer. 2007; 109(3):518–27.
45. Bul M, Zhu X, Valdagni R, Pickles T, Kakehi Y, Rannikko A, et al. Active surveillance for low-risk prostate cancer worldwide: the PRIAS study. Eur Urol. 2013;63(4):597–603.
46. Bill-Axelson A, Garmo H, Holmberg L, Johansson JE, Adami HO, Steineck G, et al. Long-term distress after radical prostatectomy versus watchful waiting in prostate cancer: a longitudinal study from the Scandinavian Prostate Cancer Group-4 randomized clinical trial. Eur Urol. 2013;64(6):920–8.
47. Van Den Bergh RCN, Essink-Bot ML, Roobol MJ, Wolters T, Schröder FH, Bangma CH, et al. Anxiety and distress during active surveillance for early prostate cancer. Cancer. 2009;115(17):3868–78.
48. Wilt TJ, Brawer MK, Jones KM, Barry MJ, Aronson WJ, Fox S, et al. Radical prostatectomy versus observation for localized prostate cancer. N Engl J Med. 2012;367(3):203–13.
49. Bergman J, Litwin MS. Quality of life in men undergoing active surveillance for localized prostate cancer. J Natl Cancer Inst Monogr. 2012;45:242–9.
50. Acar C, Schoffelmeer CC, Tillier C, de Blok W, van Muilekom E, van der Poel HG. Quality of life in patients with low-risk prostate cancer. A comparative retrospective study: brachytherapy versus robot-assisted laparoscopic prostatectomy versus active surveillance. J Endourol. 2014;28(1):117–24.
51. Van Den Bergh RCN, Korfage IJ, Roobol MJ, Bangma CH, De Koning HJ, Steyerberg EW, et al. Sexual function with localized prostate cancer: active surveillance vs radical therapy. BJU Int. 2012;110(7): 1032–9.
52. Heidegger I, Skradski V, Steiner E, Klocker H, Pichler R, Pircher A, et al. High risk of under-grading and -staging in prostate cancer patients eligible for active surveillance. PLoS One. 2015;10(2):1–12.
53. Dinh KT, Mahal BA, Ziehr DR, Muralidhar V, Chen Y-W, Viswanathan VB, et al. Incidence and predictors of upgrading and up staging among 10,000 contemporary patients with low risk prostate cancer. J Urol. 2015;194(2):343–9.
54. Guzzo TJ, Resnick MJ, Canter DJ, Bivalacqua TJ, Rosen MA, Bergey MR, et al. Endorectal T2-weighted MRI does not differentiate between favorable and adverse pathologic features in men with prostate cancer who would qualify for active surveillance. Urol Oncol Semin Orig Investig. 2012;30(3):301–5.
55. Yerram NK, Volkin D, Turkbey B, Nix J, Hoang AN, Vourganti S, et al. Low suspicion lesions on multiparametric magnetic resonance imaging predict for the absence of high-risk prostate cancer. BJU Int. 2012;110(11 B):783–8.
56. Turkbey B, Mani H, Shah V, Rastinehad AR, Bernardo M, Pohida T, et al. Multiparametric 3 T prostate magnetic resonance imaging to detect cancer: histopathological correlation using prostatectomy specimens processed in customized magnetic resonance imaging based molds. J Urol. 2011;186(5):1818–24.
57. Elliott SP, Johnson DP, Jarosek SL, Konety BR, Adejoro OO, Virnig BA. Bias due to missing SEER data in D'Amico risk stratification of prostate cancer. J Urol. 2012;187(6):2026–31.
58. Kim S, Dall'Era MA, Evans CP. Economic analysis of active surveillance for localized prostate cancer. Curr Opin Urol. 2012;22(3):247–53.
59. de la Rosette J, Ahmed H, Barentsz J, Johansen TB, Brausi M, Emberton M, et al. Focal therapy in prostate cancer-report from a consensus panel. J Endourol. 2010;24(5):775–80.
60. Muller BG, van den Bos W, Pinto PA, la Rosette JJ d. Imaging modalities in focal therapy: patient selection, treatment guidance, and follow-up. Curr Opin Urol. 2014;24(3):218–24.
61. Illing RO, Leslie TA, Kennedy JE, Calleary JG, Ogden CW, Emberton M. Visually directed high-intensity focused ultrasound for organ-confined prostate cancer: a proposed standard for the conduct of therapy. BJU Int. 2006;98(6):1187–92.
62. Onik GM, Cohen JK, Reyes GD, Rubinsky B, Chang Z, Baust J. Transrectal ultrasound-guided percutaneous radical cryosurgical ablation of the prostate. Cancer. 1993;72(4):1291–9.
63. Azzouzi AR, Lebdai S, Benzaghou F, Stief C. Vascular-targeted photodynamic therapy with TOOKAD® Soluble in localized prostate cancer: standardization of the procedure. World J Urol. 2015: 937–44.
64. Valerio M, Dickinson L, Ali A, Ramachandran N, Donaldson I, Freeman A, et al. A prospective development study investigating focal irreversible electroporation in men with localised prostate cancer: Nanoknife electroporation ablation trial (NEAT). Control Clin Trials. 2014;39(1):57–65.
65. Valerio M, Ahmed HU, Emberton M, Lawrentschuk N, Lazzeri M, Montironi R, et al. The role of focal therapy in the management of localised prostate cancer: a systematic review. Eur Urol. 2013;66(4): 732–51.
66. Ward JF, Jones JS. Focal cryotherapy for localized prostate cancer: a report from the national Cryo On-Line Database (COLD) Registry. BJU Int. 2012; 109(11):1648–54.
67. Yap T, Ahmed HU, Hindley RG, Guillaumier S, McCartan N, Dickinson L, et al. The effects of focal

therapy for prostate cancer on sexual function: a combined analysis of three prospective trials. Eur Urol. 2015:1–8.
68. Ahmed HU, Hindley RG, Dickinson L, Freeman A, Kirkham AP, Sahu M, et al. Focal therapy for localised unifocal and multifocal prostate cancer: a prospective development study. Lancet Oncol. 2012; 13(6):622–32.
69. Kasivisvanathan V, Emberton M, Ahmed HU. Focal therapy for prostate cancer: rationale and treatment opportunities. Clin Oncol. 2013;25(8):461–73.
70. Muller BG, Fütterer JJ, Gupta RT, Katz A, Kirkham A, Kurhanewicz J, et al. The role of magnetic resonance imaging (MRI) in focal therapy for prostate cancer: recommendations from a consensus panel. BJU Int. 2014;113(2):218–27.
71. Kalbhen CL, Hricak H, Shinohara K, Chen M, Parivar F, Kurhanewicz J, et al. Prostate carcinoma: MR imaging findings after cryosurgery. Radiology. 1996; 198(3):807–11.
72. Rouvière O, Lyonnet D, Raudrant A, Colin-Pangaud C, Chapelon JY, Bouvier R, et al. MRI appearance of prostate following transrectal HIFU ablation of localized cancer. Eur Urol. 2001;40(3):265–74.
73. van den Bos W, de Bruin DM, van Randen A, Engelbrecht MRW, Postema AW, Muller BG, et al. MRI and contrast-enhanced ultrasound imaging for evaluation of focal irreversible electroporation treatment: results from a phase I-II study in patients undergoing IRE followed by radical prostatectomy. Eur Radiol. 2016;26(7):2252–60.
74. Kirkham APS, Emberton M, Hoh IM, Illing RO, Freeman AA, Allen C. MR imaging of prostate after treatment with high-intensity focused ultrasound. Radiology. 2008;246(3):833–44.
75. Van Den Bos W, Muller BG, Ahmed H, Bangma CH, Barret E, Crouzet S, et al. Focal therapy in prostate cancer: international multidisciplinary consensus on trial design. Eur Urol. 2014;65(6):1078–83.
76. Mouraviev V, Mayes JM, Sun L, Madden JF, Moul JW, Polascik TJ. Prostate cancer laterality as a rationale of focal ablative therapy for the treatment of clinically localized prostate cancer. Cancer. 2007;110(4):906–10.
77. Polascik TJ, Mayes JM, Schroeck FR, Sun L, Madden JF, Moul JW, et al. Patient selection for hemiablative focal therapy of prostate cancer: variables predictive of tumor unilaterality based upon radical prostatectomy. Cancer. 2009;115(10): 2104–10.
78. Ahmed HU. The index lesion and the origin of prostate cancer. N Engl J Med. 2009;361(17):1704–6.
79. Ramsay CR, Adewuyi TE, Gray J, Hislop J, Shirley MD, Jayakody S, et al. Ablative therapy for people with localised prostate cancer: a systematic review and economic evaluation. Health Technol Assess. 2015;19(49):1–490.
80. van den Bos W, de Bruin DM, Jurhill RR, Savci-Heijink CD, Muller BG, Varkarakis IM, et al. The correlation between the electrode configuration and histopathology of irreversible electroporation ablations in prostate cancer patients. World J Urol. 2016;34(5):657–64.
81. Stock RG, Cesaretti JA, Stone NN. Disease-specific survival following the brachytherapy management of prostate cancer. Int J Radiat Oncol Biol Phys. 2006;64(3):810–6.
82. Eccles BK, Cross W, Rosario DJ, Doble A, Parker C, Logue J, et al. SABRE 1 (Surgery Against Brachytherapy—a Randomised Evaluation): feasibility Randomised Controlled Trial (RCT) of brachytherapy vs radical prostatectomy in low-intermediate risk clinically localised prostate cancer. BJU Int. 2013;112(3):330–7.
83. Donovan J, Mills N, Smith M, Brindle L, Jacoby A, Peters T, et al. Quality improvement report: Improving design and conduct of randomised trials by embedding them in qualitative research: ProtecT (prostate testing for cancer and treatment) study. Br Med J. 2002;325(7367):766–9.
84. Ahmed HU, Berge V, Bottomley D, Cross W, Heer R, Kaplan R, et al. Can we deliver randomized trials of focal therapy in prostate cancer? Nat Rev Clin Oncol. 2014;11(8):1–10.
85. Emberton M. Why focal therapy is a legitimate and necessary response to a changing world. J Urol. 2015;194(4):875–6.

Index

© Springer International Publishing AG 2017

T.J. Polascik (ed.), *Imaging and Focal Therapy of Early Prostate Cancer*,
Current Clinical Urology, DOI 10.1007/978-3-319-49911-6